Publication Date (Web): October 13, 2015 | doi: 10.1021/bk-2015-1200.fw001

Oxidative Stress: Diagnostics, Prevention, and Therapy Volume 2

In Oxidative Stress: Diagnostics, Prevention, and Therapy Volume 2; Hepel, et al.;
ACS Symposium Series; American Chemical Society: Washington, DC, 2015.

Publication Date (Web): October 13, 2015 | doi: 10.1021/bk-2015-1200.fw001

In Oxidative Stress: Diagnostics, Prevention, and Therapy Volume 2; Hepel, et al.;
ACS Symposium Series; American Chemical Society: Washington, DC, 2015.

ACS SYMPOSIUM SERIES **1200**

Oxidative Stress: Diagnostics, Prevention, and Therapy Volume 2

Maria Hepel, Editor
SUNY Potsdam
Potsdam, New York

Silvana Andreescu, Editor
Clarkson University
Potsdam, New York

Publication Date (Web): October 13, 2015 | doi: 10.1021/bk-2015-1200.fw001

Sponsored by the
ACS Division of Analytical Chemistry

American Chemical Society, Washington, DC

Distributed in print by Oxford University Press

In Oxidative Stress: Diagnostics, Prevention, and Therapy Volume 2; Hepel, et al.;
ACS Symposium Series; American Chemical Society: Washington, DC, 2015.

Library of Congress Cataloging-in-Publication Data

Oxidative stress : diagnostics, prevention, and therapy / Silvana Andreescu, Maria Hepel, editor[s] ;
sponsored by the ACS Division of Analytical Chemistry.
p. cm.
Includes bibliographical references and index.
ISBN 978-0-8412-3100-9 (acid-free paper) 1. Oxidative stress--Physiological effect. 2. Antioxidants. I.
Andreescu, Silvana. II. Hepel, Maria. III. American Chemical Society. Division of Analytical Chemistry.
RB170.O943 2011
616.3'9--dc23

2011042499

The paper used in this publication meets the minimum requirements of American National Standard for Information Sciences—Permanence of Paper for Printed Library Materials, ANSI Z39.48n1984.

Distributed in print by Oxford University Press

PRINTED IN THE UNITED STATES OF AMERICA

In Oxidative Stress: Diagnostics, Prevention, and Therapy Volume 2; Hepel, et al.;
ACS Symposium Series; American Chemical Society: Washington, DC, 2015.

Publication Date (Web): October 13, 2015 | doi: 10.1021/bk-2015-1200.fw001

Publication Date (Web): October 13, 2015 | doi: 10.1021/bk-2015-1200.fw001

Foreword

The ACS Symposium Series was first published in 1974 to provide a mechanism for publishing symposia quickly in book form. The purpose of the series is to publish timely, comprehensive books developed from the ACS sponsored symposia based on current scientific research. Occasionally, books are developed from symposia sponsored by other organizations when the topic is of keen interest to the chemistry audience.

Before agreeing to publish a book, the proposed table of contents is reviewed for appropriate and comprehensive coverage and for interest to the audience. Some papers may be excluded to better focus the book; others may be added to provide comprehensiveness. When appropriate, overview or introductory chapters are added. Drafts of chapters are peer-reviewed prior to final acceptance or rejection, and manuscripts are prepared in camera-ready format.

As a rule, only original research papers and original review papers are included in the volumes. Verbatim reproductions of previous published papers are not accepted.

ACS Books Department

In Oxidative Stress: Diagnostics, Prevention, and Therapy Volume 2; Hepel, et al.;
ACS Symposium Series; American Chemical Society: Washington, DC, 2015.

Publication Date (Web): October 13, 2015 | doi: 10.1021/bk-2015-1200.pr001

Preface

Following the edition of the first volume of *Oxidative Stress: Diagnostics, Prevention, and Therapy*, which was met with great interest, Volume 2 of this series covers the latest achievements in diagnosis, prevention, and therapy of oxidative stress and related diseases. The book provides a comprehensive overview of the oxidative stress related mechanisms in biological systems and the involvement of reactive oxygen and nitrogen species (ROS and RNS), the damage of DNA, proteins, and lipids caused by oxidative stress, the protection of cells and tissues against free radicals, the relation of the oxidative stress to aging and human diseases including cancer and neurological disorders, and the development of new therapeutic approaches to modulate oxidative stress. The current state-of-the-art methodologies including the development of sensors and biosensors for the detection of ROS/RNS and of biomarkers of oxidative stress are also discussed. The book is organized in three overlapping parts, starting with general considerations of the oxidative stress, homeostasis pathways, and ROS mechanisms, followed by chapters discussing the involvement of ROS in particular diseases and concluding with analytical aspects of oxidative stress monitoring. The book provides a solid background on oxidative stress and ROS/RNS generation for novice learners while also offering scientists and practitioners already involved in this field a wealth of information covering the most recent developments in the study of oxidative stress, the role of radical species, novel antioxidant therapies, and methods for assessing free radicals and oxidative stress. We sincerely hope that this book will find a wide audience of scientists searching for a useful collection of critical reviews related to the expanding field of oxidative stress.

Maria Hepel
SUNY Potsdam
Potsdam, New York

Silvana Andreescu
Clarkson University
Potsdam, New York

In Oxidative Stress: Diagnostics, Prevention, and Therapy Volume 2; Hepel, et al.;
ACS Symposium Series; American Chemical Society: Washington, DC, 2015.

Publication Date (Web): October 13, 2015 | doi: 10.1021/bk-2015-1200.ot001

Editors' Biographies

Maria Hepel

Maria Hepel received her M.S. and Ph.D. in chemistry from Jagellonian University in Krakow, Poland. Beginning in 1985, she worked as part of the faculty at the State University of New York at Potsdam where she is now a professor and Chair of the Department of Chemistry. She has published more than 160 papers and 44 chapters in books, and she has made more than 400 presentations at national and international symposia. Her current research interests are multidisciplinary and include DNA intercalation sensors, piezoimmunosensors, sensors for biomarkers of oxidative stress and cancer, fluorescence energy transfer (FRET and NSET), DNA-hybridization biosensors, microsensor arrays, controlled drug release systems, nanotechnology, dye pollutant degradation, supercapacitors and electrochromic devices. She won the SUNY Potsdam President's Award for Excellence in Research and Creative Endeavor in 1995 and 2001, the SUNY Chancellor's Award for Excellence in Teaching in 1998, and the SUNY Chancellor's Award for Research in 2003. She was also awarded the 2012 Northeast Region ACS Award for Achievements in the Chemical Science. In 2013, she was named a SUNY Distinguished Professor and became a member of the SUNY Distinguished Academy and SUNY Excellence Network.

Silvana Andreescu

Silvana Andreescu is the Egon Matijević Endowed Chair in Chemistry in the Department of Chemistry and Biomolecular Science at Clarkson University. Her research interests include biosensors, bioanalytical applications of metal and metal oxide nanoparticles, and the development of microelectrochemical probes for studying physiological mechanisms in biological systems. Her recent work involved study of the nanoceria chemistry, the mechanism of the antioxidant activity of these particles, and the development of probes for monitoring reactive oxygen species and oxidative stress in biological model systems.

In Oxidative Stress: Diagnostics, Prevention, and Therapy Volume 2; Hepel, et al.;
ACS Symposium Series; American Chemical Society: Washington, DC, 2015.

Publication Date (Web): October 13, 2015 | doi: 10.1021/bk-2015-1200.ch001

Chapter 1

Oxidative Stress and Human Health

Maria Hepel[1,*] and Silvana Andreescu[2,*]

[1]Department of Chemistry, State University of New York at Potsdam, Potsdam, New York 13676
[2]Department of Chemistry and Biomolecular Science, Clarkson University, Potsdam, New York 13699-5810
[*]E-mail: hepelmr@potsdam.edu (M.H.), eandrees@clarkson.edu (S.A.)

Evidence from experimental and clinical studies indicates that oxidative stress plays a critical role in the initiation and progression of many diseases. In this Chapter, we provide an overview of the processes and consequences of oxidative stress within cells, tissues, organs and whole organisms. We consider processes involving the release of Reactive Oxygen and Nitrogen Species (ROS/RNS), ROS/RNS toxicity and the imbalance between the ROS/RNS production and the antioxidant defense system. We discuss changes in DNA, proteins and lipids as a result of oxidative stress and their consequences in the development of diseases of the central nervous system, heart, lungs, kidneys, liver, reproductive organs, joints, skin, and blood. Diseases that spread over multiple organs and systemic diseases in which oxidative stress has been implicated, such as cancer and diabetes are also discussed.

Introduction

Extensive studies carried out in the field of pathogenesis indicate the involvement of oxidative stress and reactive oxygen species (ROS) in a wide range of diseases. Many illnesses caused by *inflammation* may in fact be induced by oxidative stress (*1–4*). Oxidative stress has also been implicated in many other diseases, for instance, those developing in the brain (*5–7*) or those without any pathogenic origin (*8*, *9*). New experimental tools are aiding now in discoveries of ROS present in cells and blood during disease onset and progression, and even

In Oxidative Stress: Diagnostics, Prevention, and Therapy Volume 2; Hepel, et al.;
ACS Symposium Series; American Chemical Society: Washington, DC, 2015.

long before the appearance of disease symptoms. In this review, we have analyzed the mechanism of release of ROS/RNS species, means of their neutralization, and the contribution of the oxidative stress to the pathogenesis of common diseases developing in all organs of the human body.

The excess amounts of ROS are either produced in the organism on call for pathogenic defenses or generated at normal levels but not neutralized due to the insufficient anti-oxidant capacity of the redox homeostasis system. ROS species are formed as intermediates and by-products in the energy production cycle in mitochondria in the electron transfer chain reactions (*10*, *11*) and in endoplasmic reticulum (*12*). The generation of ROS takes also place in neutrophils (*13*) and macrophages (*14*) during inflammation and in other processes of normal cellular metabolic activities. ROS are produced in response to environmental conditions, such as ultraviolet radiation, cigarette smoking, alcohol, or drugs. The enzymes involved in protecting cells from the damaging effects of ROS include superoxide dismutase, glutathione peroxidase, catalase and others.

Prolonged exposure to environmental pollutants (strong oxidizing agents, heavy metal ions, herbicides and pesticides, photosensitizers, etc.) (*15–17*), UV light or ionizing radiation (*18*), as well as the internal ROS generation in physiological processes may contribute to the damage of DNA, lipids, and proteins (*19*). To avert the propagation of mutations, various DNA repair mechanisms (*20*) and pathways to initiate apoptosis (*21*), if DNA is unrepairable, have been developed in cells. The short-term oxidative stress (or "oxidative shock") may also be beneficial in deterrence of aging by inducing natural anti-oxidative responses in a process called hormesis (*22*, *23*). For instance, to reduce the chronic oxidative stress in elderly patients with cardiovascular disease, an ozone therapy has been applied showing some improvement in redox status (*24*). However, such cases are not without controversy since even a low dose of ozone may induce cancer. The increase in ROS stressor levels in elderly, suffering from chronic oxidative stress, by exercises is generally beneficial for improving cellular antioxidant responses (*25*).

Whether antibiotics kill bacteria by an oxidative stress mechanism is also subject to controversy. While some believe that antibiotics kill bacteria by inducing ROS (*26*, *27*), others (*28*, *29*) have shown that there is no increased generation of ROS or Fe(II) during the pathogen attack suggesting that lethality is likely caused by inhibition of protein synthesis, DNA replication, and other life processes.

Unraveling the signaling mechanisms involving oxidative stress messengers at the cellular level is essential to gain better understanding of the pathogenesis of many diseases and to develop new therapies to help managing the conditions for which currently there is no cure or the present treatments are obscured with serious side effects.

Redox Homeostasis

Under sustainable redox conditions, the generation of ROS must be balanced by the antioxidant power of ROS scavengers, as illustrated in Fig. 1.

In Oxidative Stress: Diagnostics, Prevention, and Therapy Volume 2; Hepel, et al.;
ACS Symposium Series; American Chemical Society: Washington, DC, 2015.

Publication Date (Web): October 13, 2015 | doi: 10.1021/bk-2015-1200.ch001

Publication Date (Web): October 13, 2015 | doi: 10.1021/bk-2015-1200.ch001

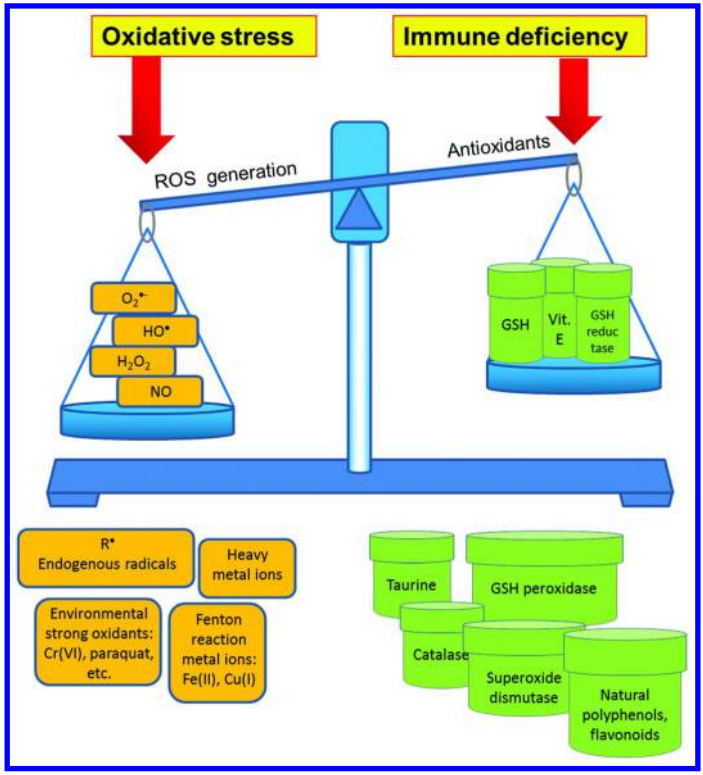

Figure 1. Schematic representation of balancing the ROS generation and antioxidant protection against damage to DNA, protein and lipids. (see color insert)

Any change in ROS production must be met with the respective adjustment of the antioxidant counterbalance to prevent slipping into an oxidative stress or immune deficiency state. This means that an active redox-potential homeostasis system must be established in any healthy organism. Since such homeostasis systems are found in all living organisms, one can say that the ROS generation is generally a balanced process. The actual mechanism of operation of the redox-potential homeostasis is a complex one and it consists of many pathways of autonomous replenishment of antioxidants stored and synthesized (expressed) in different tissues, cells, and organelles. Many proteins that contain sulfhydryl groups or dislphide bonds can act as the *redox sensors* and *effectors* since redox state of the biological environment can readily modify those proteins and these modifications are critically important for the control of protein functions. Small biomolecule antioxidants, such as glutathione, tocopherol, and ascorbic acid, are redox buffers that interact with various cellular components influencing the organization of defense, enzymatic activity, as well as the growth and development by modulating processes from mitosis to senescence and death. These cellular antioxidants can also influence gene expression associated with stress responses to optimize cellular defenses. The major components playing important roles in

In Oxidative Stress: Diagnostics, Prevention, and Therapy Volume 2; Hepel, et al.;
ACS Symposium Series; American Chemical Society: Washington, DC, 2015.

balancing the ROS production and the antioxidant countermeasures, are listed in Figure 1. Further discussion of ROS reactivities, their generation, and scavenging is presented in the next two sections.

Oxidative Power of Exogenous Oxidants and Endogenous ROS

The reactions involved in energy production generate a multitude of oxidative intermediates including ROS which are capable of inflicting damage to nucleic acids, proteins and lipids. Therefore, both the external strong oxidants and the internally generated ROS can cause oxidative stress which must be managed by the organism in order to survive. The prolonged oxidative stress leads to serious diseases and accelerated aging process. Table I presents common oxidants and radicals (*30*) that can be formed in aqueous solutions and their oxidizing power as characterized by the standard reduction potential E^o versus the *normal hydrogen electrode* (NHE) reference. The redox electrode (half-cell) reactions are included as well, presented as the reduction reactions, according to the Stockholm Convention.

There are many powerful exogenous oxidants, produced or used in various industrial processes, which are subsequently dumped into the environment creating challenging environmental pollution problems. These include chromium(VI), chlorine, ozone, nitrogen oxides, paraquat, and others.

For instance, strongly oxidizing chromate and dichromate species (Cr(VI)), now banned in Europe and USA, are mutagenic and carcinogenic and cause DNA damage (*39*, *40*). So are the perchlorates and common compounds such as hypochlorites and chlorine used ordinarily as a bleach and for water disinfection. Some of the pesticides and herbicides are also strong oxidants, for instance, paraquat (methyl viologen) causing serious health threat, depending on the type of exposure. In USA, a license is required to use paraquat products since paraquat is listed for "restricted commercial use". Its acute syndromes are: respiratory distress (lung failure), holes in esophagus, kidney failure, and pulmonary fibrosis (*41*). Even at low concentrations, paraquat can cause DNA damage in the presence of H_2O_2 (*16*).

Common Reactions of ROS Formation, Conversion, and Neutralization

The reactive oxygen species are formed as a byproduct of various reactions of exogenous oxidants (mainly inhaled molecular oxygen from atmosphere) and fuels (ingested foodstaf and nutrients). Under normal conditions, the generation of ROS remains well balanced. This means that the ROS level is regulated by homeostasis systems and well controlled by enzyme-catalyzed reactions. The full reduction of molecular oxygen requires four electrons to be tranferred and this process is carried out by enzymes step by step producing a variety of intermediates. In the first step, dioxygen O_2 is reduced to a radical superoxide anion $O_2^{\bullet-}$ which has one unpaired electron and carries one negative charge:

$$O_2 + e^- = O_2^{\bullet-} \quad (1)$$

In Oxidative Stress: Diagnostics, Prevention, and Therapy Volume 2; Hepel, et al.;
ACS Symposium Series; American Chemical Society: Washington, DC, 2015.

Publication Date (Web): October 13, 2015 | doi: 10.1021/bk-2015-1200.ch001

Publication Date (Web): October 13, 2015 | doi: 10.1021/bk-2015-1200.ch001

Table I. Electrode Reactions and Standard Potentials for Powerful Oxidants Formed in Aqueous Sulfate and Chloride Solutions (*30*)

Oxidant	Reaction	E^o, V vs. NHE	Ref.
ozonide radical anion	$O^{\bullet-}_{3(aq)} + 6H^+ + 5e = 3H_2O$	1.575	a
hydroxyl radical	$OH^{\bullet}_{(g)} + H^+ + e = H_2O$ $OH^{\bullet}_{(aq)} + H^+ + e = H_2O$ $O^{\bullet-}_{(aq)} + 2H^+ + e = H_2O$	2.82 2.722 3.426	g b c
atomic oxygen	$O_{(g)} + 2H^+ + e = H_2O$	2.421	(*31*)
ozone	$O_{3(g)} + 2H^+ + 2e = O_2 + H_2O$ $O_{3(g)} + 6H^+ + 6e = 3H_2O$	2.076 1.511	(*31*)
hydrogen peroxyl radical	$HO_2^{\bullet} + 3H^+ + 3e = 2H_2O$	1.684	h
hydrogen peroxide	$H_2O_2 + 2H^+ + 2e = 2H_2O$ $HO_2^- + 3H^+ + 2e = 2H_2O$	1.776 2.119	(*31*)
oxygen	$O_2 + 4H^+ + 4e = 2H_2O$	1.228	(*31*)
atomic chlorine	$Cl^{\bullet} + e = Cl^-$	2.410	(*32-33*),d
dichlorine radical anion	$Cl_2^{\bullet-} + e = 2Cl^-$	2.090	(*32*)
hydroxyl chloride radical anion	$ClOH^{\bullet-} + H^+ + e = Cl^- + H_2O$ $ClOH^{\bullet-} + e = Cl^- + OH^-$	2.729 1.90	e (*32*)
chlorine monoxide	$Cl_2O + 2H^+ + 2e = 2Cl^- + H_2O$	2.153	(*31*)
chlorine dioxide	$ClO_2 + 4H^+ + 5e = Cl^- + 2H_2O$	1.511	(*31*)
hypochlorous acid	$HClO + H^+ + e = Cl^- + H_2O$ $ClO^- + 2H^+ + e = Cl^- + H_2O$	1.494 1.715	(*31*)
chlorine	$Cl_2 + 2e = 2Cl^-$	1.395	(*31*)
persulfate radical	$HSO_4^{\bullet} + e = HSO_4^-$	2.60	(*34*)
peroxysulfate	$S_2O_8^{-2} + 2e = 2SO_4^{-2}$	1.940	(*34*),f

a - calcd on the basis of $\Delta G^0_f(O_3^{\bullet-}(aq)) = 11.25$ obtained from $E^0(O_2/O_3^{\bullet-})$ (*35*);

b - calcd using $\Delta G(OH^{\bullet}_{aq}) = +6.0$ (*33*); Koppenol-Liebman (*35*) obtained 2.59 V; calcd from Pourbaix data (*31*): 2.832 V;

c - calcd on the basis of pK of $OH^{\bullet}$: pK = 11.9 [53]; $E^0 = 3.308$ calcd from (*35*);

d - Berdnikov and Bazhin (*36*) obtained 2.55 V; Gratzel: 2.55 V (*34*);

e - calcd using $\Delta G(ClOH^{\bullet-}_{aq}) = -25.18$ kcal/mol obtained from data of Ref. (*32*);

f - 2.01 V given by Pourbaix (*31*);

g - calcd from (*37-38*);

h - calcd from (*31*).

The formal oxidation state of oxygen atoms in $O_2^{\bullet-}$ is -1/2. Superoxide is generated in phagocytes by enzyme NADPH oxidase and in mitochondria by NADH dehydrogenase (Complex I) and coenzyme Q (Complex III). Superoxide is

In Oxidative Stress: Diagnostics, Prevention, and Therapy Volume 2; Hepel, et al.;
ACS Symposium Series; American Chemical Society: Washington, DC, 2015.

neutralized by antioxidants, GSH and superoxide-scavenger, enzyme superoxide dismutase (SOD). SOD deficiency leads to mutagenicity and a variety of pathologies, including neurodegeneration, lactic acidosis, cardiomyopathy, muscle atrophy, cataracts, reduced lifespan, decline in fertility, liver cancer, and others. The superoxide scavenging by GSH is represented by the reaction:

$$2O_2^{\bullet-} + 2GSH + 2H^+ = 2H_2O_2 + GSSG \quad (2)$$

$$H_2O_2 + 2GSH = 2H_2O + GSSG \quad (3)$$

where GSSG is the glutathione disulfide (oxidized glutathione). Superoxide has a short half-life and disproportionates in aqueous media according to the reaction:

$$4O_2^{\bullet-} + 2\ H_2O \rightarrow 3O_2 + 4\ OH^- \quad (4)$$

On the other hand, SOD promotes the disproportionation of superoxide into hydrogen peroxide and oxygen:

$$2O_2^{\bullet-} + 2\ H^+ \rightarrow H_2O_2 + O_2 \quad (5)$$

Hydrogen peroxide is formed also in organelles, peroxisomes, during the reduction of dioxygen with fatty acids, polyamines, and other compunds, catalyzed by flavin adenine dinucleotide (FAD). The important source of hydrogen peroxide is the degradation of adenosine monophosphate (AMP), which is converted to hypoxanthine and then further oxidzed to xanthine and uric acid by an enzyme xanthine oxidase (XO):

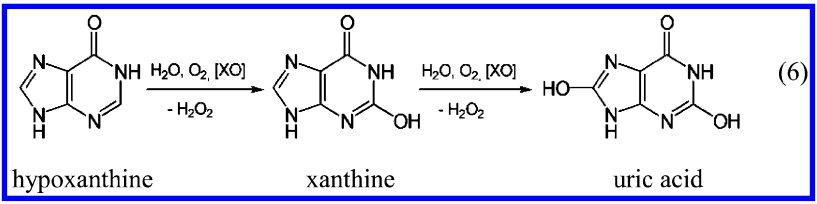

(6)

The peroxisomal enzyme, catalase, utilizes H_2O_2 to oxidize alcohols, phenols, acetaldehyde, formaldehyde, and formic acid in reactions:

$$RH_2 + H_2O_2 = R + 2\ H_2O \quad (7)$$

The excess of hydrogen peroxide is removed by peroxiredoxins or by the enzyme catalase through the formation of dioxygen:

$$H_2O_2 = ½\ O_2 + H_2O \quad (8)$$

In the presence of Fe^{2+} or Cu^+, hydrogen peroxide decomposes forming a highly reactive hydroxyl radical $HO^\bullet$ via Fenton reaction:

$$H_2O_2 + Me^{z+} = OH^- + HO^\bullet + Me^{z+1} \quad (9)$$

where Me^{z+} is Fe^{2+} or Cu^+ ion. Organic peroxides R-OO-R′ are subject to homolytic cleavage generating two highly reactive radicals:

$$R\text{-}O\text{-}O\text{-}R' = R\text{-}O^\bullet + R'\text{-}O^\bullet \quad (10)$$

In Oxidative Stress: Diagnostics, Prevention, and Therapy Volume 2; Hepel, et al.;
ACS Symposium Series; American Chemical Society: Washington, DC, 2015.

Publication Date (Web): October 13, 2015 | doi: 10.1021/bk-2015-1200.ch001

Publication Date (Web): October 13, 2015 | doi: 10.1021/bk-2015-1200.ch001

The last two reactions are facilitated by the weak bonding between oxygen atoms in the -O-O- group which means that a low energy is required for their breakage. The formation of HO• and RO• is activated by UV-Vis irradiation, chemical processes, or heating.

The hydroxyl radical HO• is the strongest oxidant of the ROS group with the redox standard potential E^{o} = +2.722 V *vs.* NHE (see: Table I). It is capable of causing damage to nucleic acids (*19*), proteins and lipids. In DNA, it can cause strand breaks, base oxidation, formation of abasic sites, etc. The DNA lesions caused by HO• radicals may be irreparable and may result in mutations and carcinogenesis. The generation of HO• radicals serves the defensive roles when the purpose of it is to combat pathogens but it may be detrimental to the host organism if HO• radicals are not neutralized quickly. Fortunately, the lifetime of HO• radicals is very short ($\tau_{1/2} \approx 4.5\times10^{-9}$ s (*42*)) so they cannot diffuse far from the point of their formation ($\delta \approx 3.2$ nm (*19*), assuming $D_{HO} = 2.3\times10^{-5}$ cm^{2}s^{-1} (*43*)).

Effects of Oxidative Stress on Human Health

There is an overwhelming body of evidence that oxidative stress affects virtually all aspects of human health. This includes all organs and the system as a whole. The scope of the problem is illustrated in Figure 2 showing major groups of common diseases in which oxidative stress has been implicated. There are also many other diseases which are either induced by the oxidative stress or in which the ROS/RNS play a role in the disease progression.

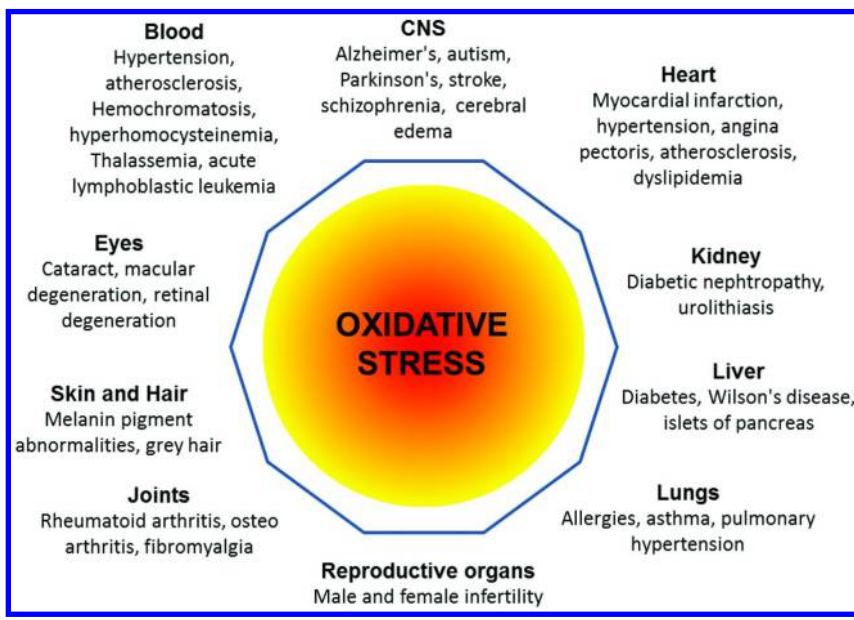

Figure 2. Major diseases in which ROS involvement has been found.

In Oxidative Stress: Diagnostics, Prevention, and Therapy Volume 2; Hepel, et al.;
ACS Symposium Series; American Chemical Society: Washington, DC, 2015.

Publication Date (Web): October 13, 2015 | doi: 10.1021/bk-2015-1200.ch001

ROS Involvement in Localized Diseases

Central Nervous System

Brain Damage

ROS generated in the brain can cause severe damage to neurons and result in memory loss and cognitive impairment. The oxidative stress due to ROS in brain has been implicated in several debilitating diseases, including Parkinson's, Alzheimer's, autism, and Down syndrome, which are discussed below. It has been found in experiments *in vitro* that the brain astrocytes exhibit considerably higher sensitivity to H_2O_2 than neurons (*44*). Hence, during the ROS attack, astrocytes suffer a greater loss. Astrocytes play an important role in the brain, supporting neurons with glucose, nutrients, and neurotransmitters, including glutamate and ATP. They also absorb excess potassium released by neurons into the extracellular space (*45*). Abnormal accumulation of extracellular potassium causes epileptic response of neurons. Astrocytes also modulate synaptic transmission between neurons by releasing ATP which is hydrolyzed to adenosine that binds to adenosine receptors in neurons, thereby inhibiting synaptic transmission (*46*, *47*). Astrocytes perform also a repair service upon neuronal injury by transforming into neurons (*48*) and replacing the injured neurons which cannot regenerate. Therefore, severe loss of astrocytes due to oxidative stress impairs functions of the brain and its ability to regenerate injured neurons.

Parkinson's Disease (PD)

PD is a progressive movement disorder caused by neurodegenerative processes in the substantia nigra pars compacta in the brain which lead to selective death of dopaminergic neurons and the degeneration of nerve fibers in the striatum (*7*, *49–51*). Currently, there is no cure for PD and no therapy capable to delay the neurodegenerative process. Extensive research studies have been carried out to uncover mechanisms of PD and understand cellular processes rendering the substantia nigra neurons particularly susceptible (*52*). There is a need to develop a neuroprotective therapy to be able to control the progression of the disease. Growing evidence indicates that oxidative stress plays a key part. Detailed investigations of dopamine metabolism have shown that it generates ROS in a process of the catecholic Fenton-like $HO^{\bullet}$ radicals formation (*19*):

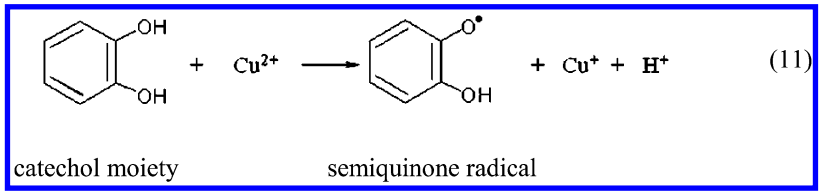

In Oxidative Stress: Diagnostics, Prevention, and Therapy Volume 2; Hepel, et al.;
ACS Symposium Series; American Chemical Society: Washington, DC, 2015.

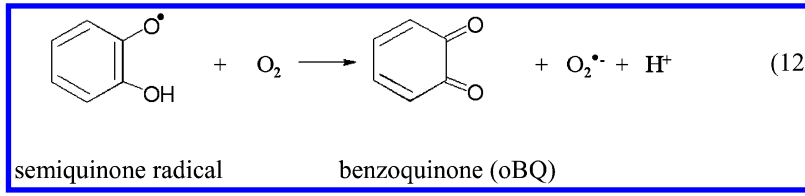

(12)

$$2O_2^{\bullet-} + 2H^+ = H_2O_2 + O_2 \quad (13)$$

$$H_2O_2 + Cu^+ = HO^\bullet + OH^- + Cu^{2+} \quad (14)$$

This reaction sequence is most likely to proceed in substantia nigra since metal ions, including Fe and Cu cations, are stored in melanin which accumulates there over the years. Melanin itself is a polymer of dopamine residues. It is probable that it is formed by the attachment of dopamine oxidation intermediate which is a semiquinone radical. These reactions make substantia nigra particularly vulnerable to the development of PD. In addition to this, mitochondrial dysfunction may lead to the increased ROS production, triggering pathways leading to cell demise. On the other hand, nitric oxide and superoxide are generated in microglia, activated in neuroinflammatory responses, and this is aggravated by α-synuclein, neuromelanin, and matrix metalloproteinase-3, which are released by damaged dopaminergic neurons. The released nitric oxide reacts with superoxide to form peroxynitrite, a powerful oxidizing agent which can be converted to hydroxyl radical. There is no doubt that the oxidative stress dominates in PD and cause oxidative damage to lipids, proteins, and DNA. Highly toxic products of oxidative damage, such as 4-hydroxynonenal (HNE), react with proteins which impair the cell viability (*53*). The degradation of proteins by oxidative stress and altered ubiquitination have been implicated as key to dopaminergic cell death in PD. Oxidative damage to α-synuclein, a protein of the synaptic area interacting with lipids and controlling dopamine release, has been observed in PD. It results in the formation of Lewy bodies which are protein clumps in the brain mainly composed of α-synuclein. Nuber et al. (*54*) have studied the effects of exogenous toxins on the induction of PD, including a strong oxidant, herbicide paraquat. In experiments with paraquat-exposed mice, they observed an increased calpain activity and an induced pathological cascade leading to the accumulation of calpain-cleaved insoluble α-synuclein. At the same time, the autophagy clearance of α-synuclein was inhibited. Recent reports point to the mutation as the cause of α-synuclein induction of glucose-related protein (GRP78) which forms clusters in the neuronal plasma membrane, found in PD patients (*55*). Therefore, the therapeutic strategy for PD should be based on the means of reducing the oxidative stress and removal of damaged α-synuclein (*56*). Hwang et al. (*57*) have found that the enzyme NAD(P)H quinone oxidoreductase (NQO1) provides protection for substantia nigra neurons and they have reported on the development of a novel drug KMS04014 capable of inducing NQO1 gene expression. NQO1 and also other antioxidant enzymes, regulated by the transcription factor Nrf2, can serve as target proteins to enable novel therapies for PD (*7*).

Publication Date (Web): October 13, 2015 | doi: 10.1021/bk-2015-1200.ch001

Publication Date (Web): October 13, 2015 | doi: 10.1021/bk-2015-1200.ch001

Alzheimer's Disease (AD)

This chronic neurodegenerative disease is characterized with a gradual deterioration of memory and impairment of brain functions due to the formation of protein plug in the brain and death of neurons and synapses in the cerebral cortex and subcortical regions (*58–61*). While the etiology of AD is poorly understood, two main mechanisms are usually considered: (i) genetic predisposition and (ii) environmental effects including oxidative stress (*5*, *62*, *63*). Recent studies have demonstrated compelling evidence of the involvement of oxidative stress in AD pathogenesis (*64*). The biochemical mechanisms of plaque formation are complex and only recently some deeper insights have been gained (*62*, *65*). The plaques formed in AD are dense insoluble deposits of beta-amyloid peptide A_β and cellular material surrounding neurons. There are also tangles (fibrils) which are protein tau aggregates associated with microtubules that accumulate inside the neurons. It is generally assumed that AD plaque accumulation is caused by misfolded amyloid beta protein and tau protein (*66*) and there is growing evidence that the immunological mechanisms play a critical role in neuronal damage (*63*, *67*). According to Ehrlich et al. (*6*), oxidative stress plays a major role in the impaired clearance of A_β at the blood-brain barrier. It has been found that platelets contain high levels of the amyloid precursor protein (APP). In AD, abnormally high expression of platelet APP fragments (A_β) is observed (*6*). Moreover, the injection of H_2O_2 affects the fragmentation of APP. Thus, in combination with an impaired A_β clearance, the changed APP fragmentation under oxidative stress plays an important part in the development of AD and β-amyloid angiopathy (*6*). Although, there is no cure for AD, many drugs are under development to slow down the progrssion of AD. In view of the oxidative stress involvement in AD, treatments with specific antioxidant may prove to be of some value. In fact, the use of GSH has been shown to counteract APP abnormal fragmentation induced by H_2O_2 (*6*).

Amyotrophic Lateral Sclerosis (ALS) and Frontotemporal Lobar Degeneration (FTLD)

One common feature of neurodegenerative diseases is the deposition of protein aggregates in the brain. In the case of ALS and FTLD, the main agglomerating bodies are RNA-binding proteins (*68*, *69*). ALS is a devastating neurodegenerative disorder characterized by loss of motor neurons leading to muscle deterioration, paralysis, and death. There is no cure for ALS and prognosis is usually limited to 2-3 years. The causes of ALS are not well understood since diverse processes are involved in the progression of the disease. There is a growing evidence indicating that oxidative stress is the key mechanism of the demise of motor neurons, comprising of prominent levels of oxidative damage markers in spinal cord and cerebrospinal fluid in ALS patients. A mutation of the antioxidant enzyme Cu/Zn superoxide dismutase 1 (SOD1) has been found in ca. 20% of ALS cases. However, an exact mechanism by which mutant SOD1 would cause the motor neuron degradation has not been elucidated. The antioxidant

therapies have been tested in animal models with some success (*70–72*), for instance, treatment of ALS in mouse with Withaferin A (*72*), an inhibitor of nuclear factor-kappa B activity, was effective in relieving inflammation in neurons, reducing the concentrations of misfolded SOD1 proteins in the spinal cord, and diminishing the losses of motor neurons. This resulted in slowing down the progress of the disease. However, the clinical trials of human ALS have shown no benefits of antioxidants tested (*70*). Several mutations in the sequestosome 1 (SQSTM1) gene have recently been reported in ALS patients (*73*). This gene encodes p62 protein which is a multifunctional adapter protein mainly involved in selective autophagy, oxidative stress response, and cell signaling pathways. Thus, mutation of the SQSTM1 gene can modulate the oxidative stress response on motoneurons. Similar mutations of SQSTM1 have been found in FTLD patients (*74*).

Publication Date (Web): October 13, 2015 | doi: 10.1021/bk-2015-1200.ch001

Autism Spectrum Disorder (ASD)

ASD is a pervasive neurological disorder which develops in early childhood and results in mental retardation, impaired social interaction, strongly diminished communication skills, and repetitive behavior at young age. The cause of ASD is poorly understood (*75*). Recent studies have shown that oxidative stress is involved in the development of autism in children (*76–79*). Because of the increasing occurrence of this disease, it is highly desirable to diagnose the environmental conditions requiring preventive or medical intervention to control the development and spreading of the disease. As a solution to this problem, applying a widespread screening of the biomarkers of oxidative stress has been considered with the utilization of simple and inexpensive analytical platforms in field and the points-of-care.

The results of studies performed by different groups suggest that oxidative stress and impaired antioxidant defenses are the main causes of ASD (*76*, *77*). While the source of the increased oxidative state may be due to internal problems including mitochondrial dysfunction and compromised energy metabolism involving NAD+, NADH, ATP, pyruvate, and lactate, it may also originate from exogenous oxidants, heavy meatal ions, pesticides and herbicides, and industrial pollutants. The lipid peroxidation process has been recognized as one of the major processes leading to highly cytotoxic products. In the reaction of polyunsaturated fatty acids with ROS, nonenal and malonyldialdehyde are formed. They have been found in plasma of autistic subjects (*78*) consistent with the hypothesis of oxidative stress-induced mechanism of ASD. The increased excretion of 8-isoprostane F_2alpha has been observed in the urine of autistic children (*80*). Isoprostanes are known to form during the radical attack on arachidonic acid in cell membrane lipids. Therefore, 8-isoprostane F_2alpha can also be utilized as a marker of oxidative stress. It has been found that the increased oxidative stress in children with autism is associated with decreased concentrations of non-enzymatic endogenous antioxidants leading to the deterioration of the organism ability to counter the oxidative stress. Thus, the levels of glutathione (GSH), vitamin E, and ascorbic acid have all been found lower in autistic children.

Also, the concentration ratio of reduced GSH to oxidized glutathione (GSSG) (*77*) and SOD activity in erythrocytes (*81*) were substantially reduced.

Downs Syndrome

Down syndrome (DS) is a chromosomal abnormality of the trisomy 21 leading to developmental brain disorders and mental retardation (*82–84*). Oxidative stress has been implicated in the progression and pathology of DS (*82–84*). The imbalance of ROS in DS has been related to overexpression of the copper-zinc superoxide dismutase (SOD1) enzyme, encoded by trisomic chromosome 21, as well as to oxidative stress in genes located at other chromosones (*85*). The increased H_2O_2 generated by SOD, in levels higher than catalase and glutathione peroxidase can convert results in oxidative stress. Increased ROS levels in the brain may generate subsequent mitochondrial dysfunctions (*86*), neurodegeneration and an increased oxidative stress in trisomic cells. Cells try to compensate this effect by increasing glutathione peroxidase levels. The increased ROS was also found to contribute to formation of allantoin and uric acid. Therefore, allantoin and uric acid have been suggested as biomarkers of oxidative stress in neurological diseases and DS (*84*). The same study indicated that antioxidants can modulate production of xanthine and hypoxanthine and modulate the accumulation of uric acid in DS (*84*).

Multiple Sclerosis

Multiple sclerosis is a chronic inflammatory disease of the central nervous system characetrized by focal demyelinating lesions and axonal damage. Inflammatory processes with infiltrating leucocytes and excessive ROS production, leading to oxidative stress have been involved in the pathogenesis of MS (*87*). ROS species generated in excess by macrophages and activated mycroglia can induce damage to cellular components including lipids, proteins and nucleic acids, further weakening the antioxidant defense system, affecting the blood-brain barrier and causing cell death and tissue injury in processes underlying MS pathology. The source of free radicals in MS depends on the stage of disease. Enzymes such as myeloperoxidase, xanthine oxidase and NADPH oxidase have been involved in oxidative pathways leading to oxidative damage (*88*). Inflammation derived ROS and mitochondrial ROS production have both been suggested to contribute to increased ROS production and initiation of a cascade of events leading to axonal neurodegeneration in MS. Treatment with antioxidants such as flavonoids might in principle prevent damage caused by oxidative stress (*89*). However, few natural antioxidants showed efficacy in the treatment of MS and despite progress, evidence of a successful antioxidant treatment in MS patients is limited. This has been linked with the narrow therapeutic window and the inability of exogenous antioxidants to cross the blood-brain barrier (*88*). More recently artificial antioxidants possessing superoxide dismutase and catalase like activity have been proposed as therapeutic antioxidants for the treatment of MS.

Publication Date (Web): October 13, 2015 | doi: 10.1021/bk-2015-1200.ch001

For example, cerium oxide nanoparticles, or nanoceria have received a great deal of attention as neuroprotective agents due to their free radical scavenging activity and regenerative capability (*90*). Recent studies in animal models have shown that nanoceria particles (1-5 nm) can cross the blood-brain and act as potent antioxidants, inactivating free radicals and alleviate clinical symptoms in neurodegenerative diseases including MS (*91*).

Cardiovascular Diseases

Oxidative stress may lead to cardiomyopathy, coronary heart disease (*92*, *93*), and cardiovascular disease by inducing inflammation of heart muscle and blood vessels (*92–95*). Vascular complications are often due to the oxidative stress induced by hyperglycemia in diabetes (*96*). NAD(P)H oxidase has been associated with the formation of ROS in the vasculature when the levels of glucose and advanced glycation end-products (AGE) are high. This results in the depletion of intracellular NADPH which is a cofactor for NO synthase (NOS). The antioxidant treatments of diminished levels of NADPH and NOS, and overproduced ROS, have largely been ineffective.

The oxidative stress may appear as a secondary effect, for instance moderate hyperhomocysteinemia known to cause dysfunction of cardiovascular autonomic system has been found to induce liver oxidative stress in rats (*97*).

Kidney

Urolithiasis

The lipid peroxidation caused by ROS has been associated with urolithiasis (renal calculus) (*98*). An increased oxidative stress has been observed during the renal stone formation (*99*). The lipid peroxidation is mediated by oxalate anions under oxidative stress and has been found to induce membrane disruption (*100*). Very effective against membrane disruption are SOD, α-tocopherol, and plasma ascorbate ions (*101*).

Diabetic End-Stage Kidney Disease

The explosion of diabetes mellitus cases in recent years has led to the dramatic increase in the end-stage kidney disease, sending hundreds of thousands of patients for routine dialyses to detoxify their blood. The mechanism of the development of diabetic end-stage kidney disease (or: diabetic nephropathy) is not well understood. However, the oxidative stress is a common link for all pathways involved in diabetes-related complications in microvasculature (*102*). Several macromolecules have been involved in the increased ROS production, including NADPH oxidase, advanced glycation end products (AGE), defects in polyol pathway, nitric oxide synthase (NOS) and mitochondrial Complex I and III (*102*, *103*). The unbalanced ROS generation influences the activation of protein kinase C, different cytokines, and transcription factors which induce enhanced

In Oxidative Stress: Diagnostics, Prevention, and Therapy Volume 2; Hepel, et al.;
ACS Symposium Series; American Chemical Society: Washington, DC, 2015.

Publication Date (Web): October 13, 2015 | doi: 10.1021/bk-2015-1200.ch001

expression of genes for extracellular matrix (ECM) resulting in the development of fibrosis and nephropathy. An early feature of diabetic nephropathy is glomerular hyperfiltration. The damage to the kidney inflicted by ROS is followed by the activation of renin-angiotensin system (RAS) which deteriorates the kidney function beyond repair. Although screening of the ROS generation seems to be a rational strategy to protect against renal damage, recent reports indicate that antioxidants do not offer any effective treatments (*102*). Therefore, the development of new kinds of nephropathy-specific antioxidants able to diminish reno-vascular impediments in diabetes would save many lives. Nephropathy in non-diabetic patients can be caused by ROS attack induced by pathogen invasion, e.g. during *Staphylococcus aureus* sepsis (*104*). The role of oxidative stress in critically ill patients with acute renal failure has been emphasized by Galle et al. (*105*) and Himmelfarb et al. (*106*).

Publication Date (Web): October 13, 2015 | doi: 10.1021/bk-2015-1200.ch001

Liver

The pathophysiology of oxidative stress in liver in small animals with liver disease has been reviewed and various antioxidant treatment options discussed by Webb and Twedt (*107*).

Liver facilitates breakdown of many poisons by inducing the ROS generation. The unbalanced ROS often cause injury to the liver itself. Thus, the oxidative stress in liver is often associated with poison digestion. There are some antioxidants that ameliorate the oxidative stress in liver in various cases. On the other hand, there are substances that intensify the existing oxidative stress. For instance, iron ions have been found to induce hepatic oxidative stress in rats (*108*) and to aggravate liver injury in diabetic rats through oxidative/nitrative stress (*109*). The administration of hesperidin provides shielding against iron-induced oxidative stress (*108*). There are many antioxidants that can attenuate hepatic oxidative stress but because of the complex processes involved in digestion processes, each type of liver poisoning requires different antioxidants to be effective. The specific antioxidants reported in various hepatic oxidative stress range from selenium (*110*), through less known astaxanthin (*111*), hesperidin (*108*), morin (*112*), jinlida (*113*), and berberin (*114*), to more common and widely used ones, including: olive oil (*115*), colocynth oil (*115*), quercetin (*116*), curcumin (*117*), emblica officinalis (*118*), and cynnamoyloctopamine antioxidants from garlic skin (*119*), as well as vitamins K, B, and others.

Among poisons that induce oxidative stress in liver are: heavy metal ions (*115*), such as Cd(II), Pb(II) and others; arsenic (*110*); nicotine (*120*); ethanol (*114*, *118*); cocaine and morphine (*121*); biomarker of cardiovascular disease homocysteine (*97*); chemotherapeutic drugs: doxorubicin, paclitaxel, and docetaxel (*122*); other drugs, e.g. acetaminophen (brand name: Tylenol) (*123*), methionine (*124*), etc.; natural carcinogens, e.g. aflatoxin-contaminated food (*116*); and industrial pollutants, such as polychlorinated biphenyls (PCB) (*125*) and chromates/dichromates (*39*).

The incresed oxidative stress during pathogen invasion often results in DNA damage. The most common is the oxidation of guanine into 7,8-oxoguanine which causes the base pair mismatch GC → GA during DNA replication. The

In Oxidative Stress: Diagnostics, Prevention, and Therapy Volume 2; Hepel, et al.;
ACS Symposium Series; American Chemical Society: Washington, DC, 2015.

8-oxoguanine DNA glycosylase 1 (OGG-1), a base-excision DNA-repair enzyme, is strongly expressed after pathogen encounter, e.g. during *Staphylococcus aureus* sepsis (*126*) resulting in severe mitochondrial DNA damage caused by ROS upsurge.

Gastrointestinal (GI) Tract

It is generaly accepted that ROS are produced in the GI tract, though the pathogenetic mechanisms of these processes have not been elucidated. Under normal conditions, the GI tract is well protected against ROS by a shielding film of mucosa. However, the ingested food and microbial pathogens can cause an oxidative damage to the GI tract followed by an inflammation. According to Bhattaharyya et al. (*127*), oxidative stress plays the main role in pathogenesis of GI diseases, such as: gastrointestinal cancers, peptic ulcers, and inflammatory bowel disease. An oxidative damage to the GI mucosa can also be done by drugs (*128*). For instance, the nonsteroidal anti-inflammatory drugs (NSAIDs), which are widely used in clinical medicine, such as ibuprofen, ketoprofen, and naproxen, can cause oxidative damage to the GI epithelial cells and to kidney membrane, including bleeding and perforation, leading to the dramatic decrease of the glomerular filtration rate (GFR). Cheng et al. (*128*) have studied the effect of several antioxidants on the activity of antioxidant enzymes in human intestinal cells (Int-407) treated with ketoprofen. It was found that catechin substantially diminished lipid peroxidation (by 40.5%), decreased ROS level by 30.0% and increased the activity of glutathione peroxidase, glutathione reductase and total sulfhydryl groups. Thus, catechin may offer a protection against gastrointestinal ulcers caused by oxidative stress.

Lungs

Asthma

Asthma is a chronic disease characterized by allergic airway inflammation, hyper-responsiveness, reversible airflow obstruction, and bronchospasm. The pathogenesis of recuring symptoms of asthma is complex (*129*, *130*) and involves multiple pathways, Th2 cytokines, oxidative stress, and other factors. There is evidence that oxidative stress may be a crucial contributor to the progression of airway inflammation, induction of mucin secretion, and enhanced airway hyper-responsiveness. Surprisingly, the increased levels of oxidative stress are found in asthma patients, not only in their lungs but also in the blood (*131*). It has been shown that the oxidative stress can induce allergic inflammation but it can also result from inflammation (*132*). The swift generation of ROS in response to the exposure to allergens causes airway inflammation. Here, ROS act as messengers inducing NF-κB activator that induces pro-inflammatory cytokines (*133*). Also, the generation of ROS in cells enhances the expression of gene of Th2 cytokine IL-4 which is associated with asthma (*134*). It has been found that 8-oxoguanine DNA glycosylase 1 (OGG-1), which is a base-excision DNA-repair enzyme, increases the oxidative stress in lungs and induces inflammation of

In Oxidative Stress: Diagnostics, Prevention, and Therapy Volume 2; Hepel, et al.;
ACS Symposium Series; American Chemical Society: Washington, DC, 2015.

Publication Date (Web): October 13, 2015 | doi: 10.1021/bk-2015-1200.ch001

allergic airways by regulating STAT6 and IL-4 in cells and in murine model (*135*). Thus, OGG-1 may be involved in modulation of the levels of oxidative stress and pro-inflammatory cytokines in the course of asthma attacks. The association of OGG1 with incresed oxidative stress is well known, for instance, OGG1 is strongly expressed during *Staphylococcus aureus* sepsis resulting in mitochondrial DNA damage inflicted by oxidative stress (*126*).

Reproductive Organs

A clear link between oxidative stress and fertility status has been established. The increased oxidative stress in tobacco smokers has been found to cause fragmentation of DNA in sperm and reduced sperm count (*136–139*). Several studies report on the association of spontaneous abortion to oxidative stress (*140–142*). The premature rupture of fetal membranes has been attributed to elevated oxidative stress (*143*). It has been found that mitochondrial superoxide regulates endothelial dysfunction in pre-eclampsia (*144*). The observed increase in PGC-1α expression is thought to induce a protective response to mitochondrial ROS overproduction by stimulating the release of protein antioxidants.

According to recent studies by Rudov et al. (*145*), the oxidative stress is involved in mediation of placental alterations by miRNAs. The increased oxidative stress-induced DNA damage in fetal cells, evidenced by elevated levels of 8-oxoG, is expected to persevere due to low levels of OGG1 repair enzyme and lead to complications in pregnancy (*146*).

Joints

Rheumatoid Arthritis (RA)

RA is a debilitating disease affecting millions of people, especially at an older age. An elevated oxidative stress is commonly found in patients with RA (*8*). However, since the oxidative stress increases with age, detailed mechanisms associating RA with oxidative stress need to be investigated. There is a growing evidence of the involvement of oxidative stress in the development of arthritis, for instance, the increase in vascular oxidative stress in RA-induced rats has been implicated in the endothelial dysfunction (*147*). In model RA rats, the oxidative stress was triggered by NAD(P)H oxidase and uncoupled endothelial nitric oxide synthase (eNOS). In the arthritic rat aortas, the levels of nitrotyrosine and lipid peroxidation product, 4-hydroxy-2-nonenal (HNE), were higher than in healthy rats, clearly showing the overproduction of reactive oxygen species. Also, the eNOS was highly expressed in RA rat aortas. The oxidative stress measurements can be based on the albumin-thiol redox state (*8*). Interestingly, the collagen-induced arthritis, studies by Yu et al. (*148*), can be ameliorated by fibroblast growth factor 21 (FGF21) through a modulation of the oxidative stress and suppression of nuclear factor-kappa B pathway.

Publication Date (Web): October 13, 2015 | doi: 10.1021/bk-2015-1200.ch001

Publication Date (Web): October 13, 2015 | doi: 10.1021/bk-2015-1200.ch001

Atherosclerosis

Atheroschlerosis is a disease of the arteries involving diffusion and retention of lipids and proteins into the subendothelial space of the vascular wall (*149*). The pathology of atheroschlerosis involves a series of complex cellular events including endothelial dysfunction, inflammation and neovascularization.

Overproduction of ROS in the vascular wall and the vascular oxidative stress plays a critical role in artherosclerosis. ROS is produced in the vascular wall by NADPH oxidase, xanthine oxidase, endothelial nitric oxide synthase (eNOS) and the mitochondrial electron transport chain (*150*). Overproduction of ROS was involved in vascular inflammation and oxidative modifications in the artery wall from the initial stage through lesion progression (*151*). Protective antioxidant enzymes in the vascular wall include SOD, catalase, glutathione peroxidases and paraoxonases. The imbalance between the ROS producing enzymes and the ROS-detoxifying systems can result in oxidative damage and promote atherogenesis through a number of events including mitochondrial and DNA damage, endoplasmic stress and pro-inflammatory effects leading to endothelial cell activation, vascular smooth muscle cell proliferation and immune cell activation (Figure 3). The link between the vascular oxidative stress, nitric oxide and atherosclerosis has been described in a recent review (*82*).

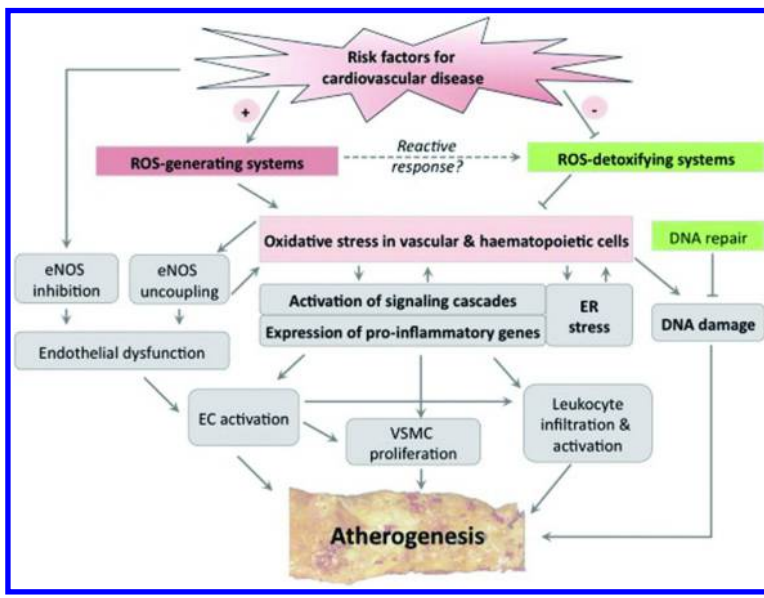

Figure 3. The role of oxidative stress in atherosclerosis showing the contribution of both ROS-generating and ROS-detoxifying systems and their consequences leading to atherogenesis. Reproduced with permission from Reference (150). Copyright 2014 Elsevier. (see color insert)

Publication Date (Web): October 13, 2015 | doi: 10.1021/bk-2015-1200.ch001

Skin

Human skin, in general, is very well protecting the organism against damaging solar UV radiation. A biopolymer, melanin, which is a pigment of yellow, red, or black color, is present in the skin and absorbs most of the dangerous UV-B light (wavelength range 280-320 nm) and neutralizes it via radiationless quenching processes (*152*). The melanin protection is supported by another natural sunscreen, *trans*-urocanic acid (UCA) which is a metabolite of the amino acid histidine formed from the protein filaggrin in the upper layer of epidermis. The *trans*-UCA absorbs UV-B and and is converted to *cis*-UCA. It also exhibits immunosuppressive properties and is an excellent antioxidant and a scavenger of $HO^{\bullet}$ radicals (up to 4 $HO^{\bullet}$ per UCA molecule) (*153*, *154*). In cases of inadequate melanin and UCA protection, e.g. in light skin complexion (Caucasians) or during sun exposure after long period of no exposure or illness, skin cancer may develop. There are three main types of skin cancers: basal cell cancer, squamous cell cancer, and melanoma. Virtually all skin cancer cases are caused by UV irradiation, either from the sun or the tanning beds, and they account for ca. 40% of all cancer cases. The mechanism of carcinogenesis is not well understood. According to one concept (*155*), UV radiation is absorbed by endogenous photosensitizers, such as flavins, porphyrins, and quinones, or some drugs or bioactive molecules, and it excites these molecules leading to the generation of ROS and highly reactive radicals able to disrupt biochemical processes and cause oxidation of DNA, lipids, and proteins. According to another hypothesis, the inflammation caused by local oxidative stress induces, upon UV irradiation, the development of skin cancer (*156*). It has been shown that while melanin is shielding against UV-B radiation, it can also act as a photo sensitizer due to the presence of catecholic groups and may contribute to the formation of ROS and DNA damage (*157*). The energy of UV absorbed by hydrogen peroxide and organic peroxides is likely to generate $HO^{\bullet}$ radicals which can damage DNA (*19*) inducing carcinogenesis. Therefore, the oxidative stress is involved in skin cancer development, either as a prerequisite condition or as a secondary cause, with intermediate ROS generation.

Eyes

Cataract

A powerful antioxidant system protects the eyes from oxidative stress and damaging effects of constant exposure to factors producing ROS. The major component of the antioxidant system in eyes is the enzyme superoxide dismutase (SOD). Three isoforms of SOD: cytosolic copper/zinc–dependent Cu/Zn-SOD (or SOD1), mitochondrial manganese-dependent Mn-SOD (or SOD2), and an extracellular Cu/Zn-dependent EC-SOD (or SOD3), catalyze the conversion of highly reactive superoxide radical anion $O_2^{\bullet-}$ to H_2O_2 which is further reduced to water by glutathione peroxidase or catalase. Cataract impairs vision due to lens opacification and is the leading cause of blindness in elderly over the age of 50. The development of cataract parallels the increase of oxidative stress and

In Oxidative Stress: Diagnostics, Prevention, and Therapy Volume 2; Hepel, et al.;
ACS Symposium Series; American Chemical Society: Washington, DC, 2015.

decrease of antioxidant defences with age (*158*). The pathophysiology of the cataract is based on biochemical reactions in which the oxidative stress plays a central part in both the onset and the progression of a cataract (*159*). In the cataractogenous process, proteins contained in the lens become cross-linked by disulfide bonds forming insoluble aggregates which affect the lens transparency (*160*). Increased levels of serum malondialdehyde and decreased levels of SOD and glutathione peroxidase were also observed. The measurements of the level of lipid peroxidation products such as the Thiobarbituric Acid Reactive Substances (TBARS), malondialdehyde and the levels of antioxidant enzymes in the blood are suggested for the assessment of the oxidative stress and as biomarkers of the degeneration in the lens (*161*).

Publication Date (Web): October 13, 2015 | doi: 10.1021/bk-2015-1200.ch001

Age-Related Macular Degeneration (AMD)

AMD is a medical condition affecting elderly which results in deterioration and even loss of vision in the center of the view, called macula. AMD does not lead to a total blindness since the peripheral vision remains unaffected. AMD is caused by damage to the retina associated with oxidative stress. Although the exposure to sun light has been implicated, *in vitro* experiments do not support any evidence of direct damage to the retina by normal light levels. It has been found that hydrogen peroxide causes a considerable damage to retinal pigment epithelial ARPE-19 cells *in vitro* (*162*). Treatments with lutein and zeaxanthin, have shown that these carotenoid pigments completely protect the cells and also they can partially reverse the H_2O_2 damage (*162*). The observed degradative processes in melanosomes and lysosomes in the retinal pigment epithelium have been attributed to the age-related incease in oxidative stress associated with the accumulation of phototoxic short melanin oligomers in lysosomes (*163*). These oligomers are rich in catechol moieties capable of mediating ROS generation via Fenton cascade (*19*). Genetic predispositions for AMD have also been identified (*164*, *165*).

Other Eye Diseases

Other serious eye conditions attributed to the oxidative stress in inflammatory processes include: retinitis pigmentosa, diabetic retinopathy, autoimune uveitis, and keratoconus (*166–169*).

Blood

Metabolic changes as a result of oxidative stress can be detected in blood. High levels of ROS can induce biochemical alterations in red blood cells (RBC) (*170*). RBC's oxidative stress affects oxygen delivery which is linked to the pathology of many diseases (*171*). The cells are continuously exposed to endogenous and exogenous sources of ROS including superoxide and hydrogen peroxide. For the most part, ROS is neutralized by the antioxidant system (e.g. catalase, glutathione peroxidase); however, excess ROS can react with

In Oxidative Stress: Diagnostics, Prevention, and Therapy Volume 2; Hepel, et al.;
ACS Symposium Series; American Chemical Society: Washington, DC, 2015.

the heme producing heme degradation products that can contribute to RBC's oxidative stress, deformability, and cellular stiffness (*171*). Recent technological innovations have enabled development of blood tests to assess the body's oxidative stress status and evaluate the antioxidant defense system in an individual. Such tests provide a general 'oxidative stress index' regarding the balance between the oxidative stress (pro-oxidant) and antioxidants; as and indication of early disease, or disease progression. Several oxidative stress biomarkers can be monitored in blood including: glutathione, cysteine, glutathione peroxidase, lipid peroxides, superoxide dismutase and the Total Antioxidant Capacity (TAC). Such blood tests may be used in disease monitoring and in epidemiological studies. For example, increased levels of lipid peroxidation were found in blood on Alzheimer's disease patients, and dysregulation in copper metabolism were found in mild cognitive impairment. In the same time, non-enzymatic antioxidants (e.g. uric acid, vitamins A and E, α and β carotene) were significantly decreased. Significant oxidative damage was found in peripheral blood early in the process of neurodegeneration (*172*). However, several challenges should be considered in developing a blood based biomarker tests for disease monitoring that can influence interpretation of oxidative biomarker assays results including: 1) specificity of measurements as plasma components and oxidative stress markers can be affected by a series of pathologies, 2) the lack of standardization and sample heterogeneity with a degree of variability between samples and individuals, 3) the requirement for validation. An overview of blood based biomarkers for Alzheimer's disease has been reviewed by Henriksen et al. which include development challenges and opportunities (*173*).

Publication Date (Web): October 13, 2015 | doi: 10.1021/bk-2015-1200.ch001

Systemic Diseases

Carcinogenesis

Cancer can form initially in a local tissue but later on spread over to various distant tissues. The matastasis occurs via circulating cancer cells which separate themselves from the initial tumor and travel with the blood stream and in lymphatic system, making cancer a systemic disease.

The pathogenesis of cancer depends on the type of cancer and the host tissue but it is largely unknown. Different theories point to the genetic roots of cancer, random mutations, environmental factors, or oxidative stress. The concept of the involvement of the oxidative stress in development of cancer has been recently considered by many scientists and clinicians (*174*, *175*). Since ROS is capable of damaging DNA, proteins and lipids (*19*), it is rational to expect that under an oxidative stress, many mutations are created and some of them may switch oncogenes, such as p53, and the many transcription factors, such as NF-κB, AP-1, PPAR-γ, Nrf2, β-catenin/Wnt, and HIF-1α, and induce the development of a cancer. For instance, Nrf2 plays a key role in the regulation of oxidative stress and inflammation. It has been found that loss of Nrf2 promotes intestinal tumorigenesis in mice (*176*). It is commonly assumed that more than one mutation is necessary to cause cancer. The ways the oxidative stress can activate inflammatory pathways

In Oxidative Stress: Diagnostics, Prevention, and Therapy Volume 2; Hepel, et al.;
ACS Symposium Series; American Chemical Society: Washington, DC, 2015.

and induce cancer have been reviewed by Reuter et al. (*3*). Schematic view is presented in Figure 4.

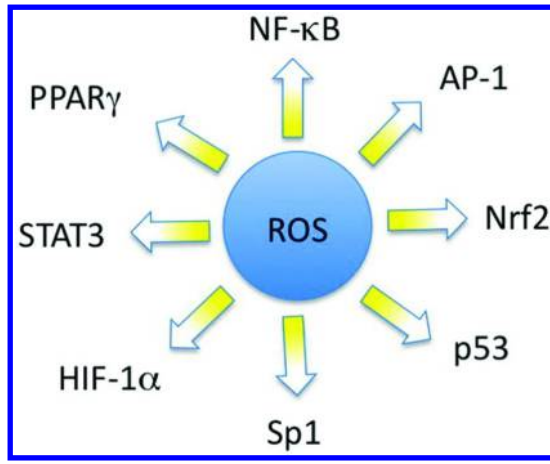

Figure 4. Schematic representation of various activators and inhibitors of reactive oxygen species production. Reproduced with permission from Reference (3). Copyright 2010 Elsevier.

While normal cells are sensitive to oxidative stress and may be easily damaged by ROS, the cancer cells, once formed, have inhibited apoptosis pathways and upregulated antioxidant defense mechanisms based on glutathione, SOD, catalase, and others which protect them against ROS, UV radiation, and lethal drugs (chemotherapy). These defense mechanisms of cancer cells, leading to multi-drug resistance, pose major challenges in cancer therapy. In order to sustain the high energy demand of cancer cells to support their high proliferation rate, alternate metabolic pathways to minimize ROS production have also been developed by cancer cells. For instance, the glycolytic pathway is guided into the pentose phosphate pathway (PPP) (*177*). Also, the aerobic respiration in mitochondria is in part replaced with the generation of lactate.

In summary, all recent observations and detailed studies indicate that prolonged oxidative stress, inflammation, and cancinogenesis are interrelated.

ROS in Cancer Treatment

Due to the increased metabolic activity caused by oncogenic stimulation, cancer cells exhibit a high inherent ROS stress. The main source of ROS generation in cells is the respiratory electron transfer chain of Complexes I-V in mitochondria, from where the ROS emanates. In response to the increased ROS production, the redox signaling induces swift natural cellular defences by increasing HIF-1α and HIF-2α expression and producing elevated levels of GSH which protects cancer cells against ROS inflicted damages. The superactive defence forces create a challenge in cancer therapy because of the developed immunity of cancer cells and multiple drug resistance (*178*). The antioxidant

Publication Date (Web): October 13, 2015 | doi: 10.1021/bk-2015-1200.ch001

pathway acts in parallel with other factors such as the expression of antiapoptotic and proliferation-inducing proteins (*179*) and the inhibition of mitochondrial permeability transition pore (mPTP) (*180*).

The photodynamic therapy (PDT) is a cancer treatment based on the laser light excitation of a photosensitizer drug to create highly reactive singlet oxygen which indiscriminately attacks and destroys cells (*181*). PDT is a potentially curative therapy for cancers which can be irradiated by power laser beams either directly from outside or via endoscopes and fiber optic catheters when located deep inside the body (*182*). Recently tested targeted drug delivery enables reducing damage done by singlet oxygen to healthy cells. Significant suppression of tumor growth in murine model has been attained using passive delivery of a photosensitizer, 3-devinyl-3-(1′-hexyloxyethyl)pyropheophorbide (HPPH), noncovalently entrapped in a polyethylene glycol (PEG) shell on gold nanocages (*183*). The PDT can be augmented by a photothermal therapy (PTT) and enhanced tumor localization with theranostic photoacoustic (PA) and near-infrared fluorescent (NIRF) imaging (*184*). In these studies, cyanine dye photosensitizer-loaded micelle nanocarriers were employed. Graphene oxide (GO) carriers have also been used for photosensitizer delivery (*185–188*). GO modified with PEG has been loaded with a photosensitizer, 2-(1-hexyloxyethyl)-2-devinyl pyropheophorbide-alpha (HPPH, branded under the name Photochlor®), by π-π stacking interactions with unoxidized portions of GO (*185*). After labeling of HPPH with ^{64}Cu, the carrier delivery was traced by fluorescence and positron emission tomography (PET) showing high drug internalization. On the other hand, low-oxygen graphene carriers, modified with PEG, polypropylenimine dendrimer polyelectrolyte, and phthalocyanine photosensitizer (*186*), were delivered to tumors guided by LHRH peptide. Near-IR irradiation caused a synergistic PDT/PTT damage to cancer cells.

Yan et al. (*187*) have designed a PEG-modified GO carriers loaded with a photosensitizer sinoporphyrin sodium (DVDMS). The fluorescence of DVDMS was enhanced by intramolecular charge-transfer which prevented the usual quenching by GO. The carriers were delivered *in vivo*, intravenously, showing 100% tumor destruction in the theranostic imaging-guided PDT. Lin et al. (*189*) have found that PDT with DVDMS causes phototoxic effects including skin swelling, ulceration, blood coagulation, and other side effects at doses higher than 1 mg/kg which was safe.

High PDT efficiency has been achieved by depositing semiconducting TiO_2 nanoparticles on GO directly from $Ti(OC_4H_9)_4$ (*190*). The GO@TiO_2 nanosheets upon illumination with blue light have shown considerable ROS generation, diminution of cell viability, decreased mitochondrial membrane potential, and significantly lowered activities of superoxide dismutase, catalase and glutathione peroxidase. The formation of malondialdehyde has also been observed. Cell death was attributed to the induction of caspase-3. Without irradiation, GO@TiO_2 were not cytotoxic.

The PDT has achieved great success in killing tumor cells and appeared to be very efficient, especially in the initial treatment. However, it often suffers from challenging immunity of cancer cells and an increased defence against singlet oxygen in the following treatments rendering them ineffective.

In Oxidative Stress: Diagnostics, Prevention, and Therapy Volume 2; Hepel, et al.;
ACS Symposium Series; American Chemical Society: Washington, DC, 2015.

Publication Date (Web): October 13, 2015 | doi: 10.1021/bk-2015-1200.ch001

Despite the challenges caused by increased ROS levels in cancer cells, it is still promising to exploit the pathways inducing the ROS generation to develop new approaches to selectively destroy cancer cells via ROS based killing mechanisms.

Diabetes

Diabetes is a complex disorder that affects the body's abilty to control glucose levels. Oxidative stress has been identified as a major contributing factor in the development of both types of diabetes (*191*) and diabetic complications (*192*, *193*). Oxidative stress has been linked with the insulin signaling and can potentially lead to insulin resistance and diabetes. Figure 5 shows the role of oxidative stress and the complex interrelated mechanisms involved in the insulin signalic pathway.

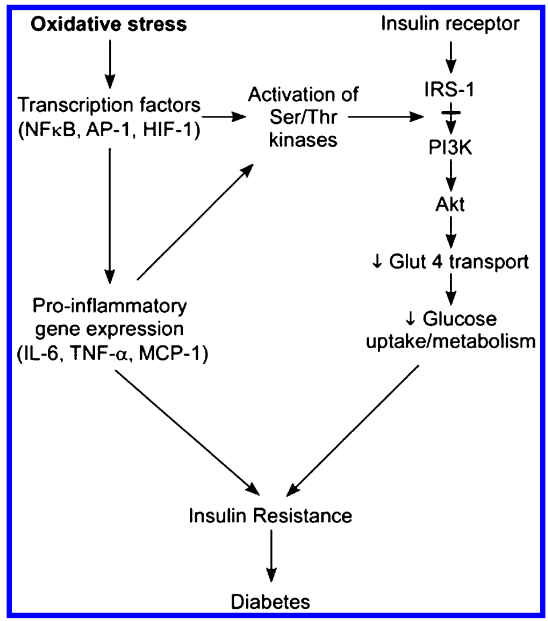

Figure 5. The role of oxidative stress in the insulin signaling pathway. Reproduced with permission from Reference (194). Copyright 2011 Elsevier.

Studies have shown an increase in ROS production and oxidative stress markers in diabetic subjects, associated with a decrease in antioxidant levels (*194*). Free radicals can be formed in diabetes by glucose oxidation, nonenzymatic glycation of proteins and the oxidative degradation products of glycated proteins (*191*). Excessive release of ROS have been related to insulin resistance, β-cell dysfunction, impaired glucose resistance and type 2 diabetes mellitus (*195*). Hyperglycemia, shared by both Type 1 and 2 diabetics can induce an increase in oxidative stress markers. Changes in oxidative stress biomarkers including superoxide dismutase, catalase, glutathione reductase, glutathione peroxidase, glutathionelevels, vitamin, lipid peroxidation and their involvement in the development of diabetic complications have been reviewed (*191*). The role of

Publication Date (Web): October 13, 2015 | doi: 10.1021/bk-2015-1200.ch001

mitochondria in the pathogenesis of type 2 diabetes has been discussed by Patti and Corvera (*11*). Mitochondrial dysfunction can also lead to insulin resistance (*195*). Some studies have suggested the use of antioxidants to prevent the generation of free radicals (*196*) and provide protective effects to reverse or normalize diabetic effects. However, there is wide discrepancy among studies (*191*) and further evidence is needed to demonstrate the effectiveness of antioxidant therapies.

Aging

Aging is a biological process of living organisms that is driven by irreversible processes inadvertently leading to the deterioration of functionality beyond the system's capacity for self-repair. Detailed analysis of the basic cause of aging points to the generation of ROS (*4*, *9*) and the damage done by the unbalanced ROS to the DNA, proteins and lipids. The excess ROS and the subsequent oxidative stress created induce a range of degenerative diseases that contribute to the aging process. These diseases can include different organs, such as kidney, liver of cardiovascular system. But aging is not only a disease. It is mainly a gradual decrease of the organism's functionality due the continual depletion of irreplaceable resources. For instance, skin is being gradually damaged, both by internal and external oxidative stress. In this case, the external stress is stronger, as seen in the damaged skin on hands and the face, as compared to the skin on other parts of the body (*197*). Clearly, the aging rate of a tissue is determined by the ratio of the tissue degeneration to its regeneration. The aging of an organism is more complex than the aging mechanism of any single tissue and there are many theories of aging spanning from telomere shortening, accumulation of genetic code errors, to component (organ) failure statistics. It is likely that different aging mechanisms are superimposd on each other. The involvement of the oxidative stress in aging and in age-related illnesses is well documented. The oxidative stress plays an important role in accelerating the aging process (*4*).

Conclusions

In summary, there is increasing evidence that oxidative stress is central to the initiation, development and progression of many diseases. The mechanism of oxidative stress is complex and involves many interrelated processes and cell signaling patways that vary significantly with the disease model. This chapter provided a general overview of the oxidative stress related mechanisms in diseases such as: diseases of the central nervous system, cardiovascular, kidney, liver, skin and eyes diseases, cancer and aging. Despite significant progress in the study of oxidative stress, there is still a need to explore the relationship between free radicals, consequences of free radicals production and the mechanism by which oxidative stress affects development of disease and its relationship with human health. Further studies to evaluate the role of antioxidants and other therapeutic approaches to prevent overproduction of ROS, and regulate the balance between free radicals and the antioxidant defense system are also needed to develop more potent therapeutic strategies to prevent oxidative stress, and reduce further damage

Publication Date (Web): October 13, 2015 | doi: 10.1021/bk-2015-1200.ch001

In Oxidative Stress: Diagnostics, Prevention, and Therapy Volume 2; Hepel, et al.;
ACS Symposium Series; American Chemical Society: Washington, DC, 2015.

to DNA, proteins, cells and tissues. In vitro, in vivo and clinical studies may be helpful to further evaluate the role of oxidative stress and antioxidants in the prevention and development of the wide variety of diseases connected to ROS.

Acknowledgments

This work was partially supported by the SUNY Research Foundation Collaborative Grant No. 66507.

References

1. Srivastava, A.; Shinn, A. S.; Lee, P. J.; Mannam, P. *Free Radical Biol. Med.* **2015**, *83*, 139–148.
2. Fernández-Sánchez, A.; Madrigal-Santillán, E.; Bautista, M.; Esquivel-Soto, J.; Morales-González, Á.; Esquivel-Chirino, C.; Durante-Montiel, I.; Sánchez-Rivera, G.; Valadez-Vega, C.; Morales-González, J. A. *Int. J. Mol. Sci.* **2011**, *12*, 3117–3132.
3. Reuter, S.; Gupta, S. C.; Chaturvedi, M. M.; Aggarwal, B. B. *Free Radical Biol. Med.* **2010**, *49*, 1603–1616.
4. Poljsak, B. *Decreasing Oxidative Stress and Retarding the Aging Process*; Nova Science Publishers: New York, 2010.
5. Pohanka, M. *Curr. Med. Chem.* **2013**, *21*, 356–364.
6. Ehrlich, D.; Hochstrasser, T.; Humpel, C. *Platelets* **2013**, *24*, 26–36.
7. Hwang, O. *Exp. Neurobiol.* **2013**, *22*, 11–17.
8. Kizaki, K.; Yoshizumi, Y.; Takahashi, T.; Era, S. *Clin. Lab.* **2015**, *61*, 175–178.
9. Finkel, T.; Holbrook, N. J. *Nature* **2000**, *408*, 239–247.
10. Indo, H. P.; Davidson, M.; Yen, H. C.; Suenaga, S.; Tomita, K.; Nishii, T.; Higuchi, M.; Koga, Y.; Ozawa, T.; Majima, H. J. *Mitochondrion* **2007**, *7*, 106–118.
11. Patti, M. E.; Corvera, S. *Endocr. Rev.* **2010**, *31*, 364–395.
12. Alfadda, A. A.; Sallam, R. M. *J. Biomed. Biotechnol.* **2012**, *2012*, 936486.
13. Razumovitch, J. A.; Semenkova, G. N.; Fuchs, D.; Cherenkevich, S. N. *FEBS Lett.* **2003**, *549*, 83–86.
14. Kraaij, M. D.; Savage, N. D. L.; Kooij, S. W. v. d.; Koekkoek, K.; Wang, J.; Berg, J. M. v. d.; Ottenhoff, T. H. M.; Kuijpers, T. W.; Holmdahl, R.; Kooten, C. v.; Gelderman, K. A. *Proc. Natl. Acad. Sci. U. S. A.* **2010**, *107*, 17686–17691.
15. Møller, P.; Danielsen, P. H.; Karottki, D. G.; Jantzen, K.; Roursgaard, M.; Klingberg, H.; Jensen, D. M.; Christophersen, D. V.; Hemmingsen, J. G.; Cao, Y.; Loft, S. *Mutat. Res. Rev. Mutat. Res.* **2014**, *762*, 133–166.
16. Stobiecka, M.; Prance, A.; Coopersmith, K.; Hepel, M., Antioxidant effectiveness in preventing paraquat-mediated oxidative DNA damage in the presence of H_2O_2. In *Oxidative Stress: Diagnostics, Prevention and Therapy*; Andreescu, S., Hepel, M., Eds.; Oxford University Press: Oxford, 2012; Vol. 1083, pp 211−233.

In Oxidative Stress: Diagnostics, Prevention, and Therapy Volume 2; Hepel, et al.;
ACS Symposium Series; American Chemical Society: Washington, DC, 2015.

Publication Date (Web): October 13, 2015 | doi: 10.1021/bk-2015-1200.ch001

17. Hepel, M.; Stobiecka, M. *Interactions of Atrazine with DNA*; Nova Science Publishers: New York, 2010.
18. Ma, H.; Wallis, L. K.; Diamond, S.; Li, S.; Canas-Carrell, J.; Parra, A. *Environ. Pollut.* **2014**, *193*, 165–172.
19. Hepel, M.; Stobiecka, M.; Peachey, J.; Miller, J. *Mutat. Res.* **2012**, *735*, 1–11.
20. Yan, S.; Sorrell, M.; Berman, Z. *Cell. Mol. Life Sci.* **2014**, *71*, 3951–3967.
21. Oyinloye, B. E.; Adenowo, A. F.; Kappo, A. P. *Pharmaceuticals (Basel)* **2015**, *8*, 151–175.
22. Kaiser, J. *Science* **2003**, *302*, 376–379.
23. Radak, Z.; Chung, H. Y.; Koltai, E.; Taylor, A. W.; Goto, S. *Ageing Res. Rev.* **2008**, *7*, 34–42.
24. Wilkins-Perez, I.; Delgado-Roche, L.; Barrios, J. M.; Fabregas-Popoco, G. B. *Oxid. Antioxid. Med. Sci.* **2015**, *4*, 1–5.
25. Ristow, M.; Zarse, K. *Exp. Gerontol.* **2010**, *45*, 410–418.
26. Foti, J. J.; Devadoss, B.; Winkler, J. A.; Colins, J. J.; Walker, G. C. *Science* **2012**, *336*, 315–319.
27. Grant, S. S.; Kaufmann, B. B.; Chand, N. S.; Haseley, N.; Hung, D. T. *Proc. Natl. Acad. Sci. U. S. A.* **2012**, *109*, 121147–121152.
28. Liu, Y.; Imlay, J. A. *Science* **2013**, *339*, 1210–1213.
29. Keren, I.; Wu, Y.; Inocencio, J.; Mulcahy, L. R.; Lewis, K. *Science* **2013**, *339*, 1213–1216.
30. Hepel, M.; Luo, J. *Electrochim. Acta* **2001**, *47*, 729–740.
31. Pourbaix, M. *Atlas of Electrochemical Equilibria in Aqueous Solutions*; Pergamon Press: Brussels, 1966.
32. Jayson, G. G.; Parsons, B. J.; Swallow, A. J. *J. Chem. Soc., Faraday Soc. Trans.* **1973**, *69*, 1597–1607.
33. Schwarz, H. A.; Dodson, R. W. *J. Phys. Chem.* **1984**, *88*, 3643–3647.
34. Desilvestro, J.; Gratzel, M. *J. Electroanal. Chem.* **1987**, *238*, 129–150.
35. Koppenol, W. H.; Liebman, J. F. *J. Phys. Chem.* **1984**, *88*, 99–101.
36. Berdnikov, V. M.; Bazin, N. M. *Russ. J. Phys. Chem.* **1970**, *44*, 395–398.
37. *JANAF Thermochemical Tables*, 2nd ed.; U.S. Natl. Bur. Stand.: Washington DC, 1971; Vol. 37.
38. Wagman, D. D.; Evans, W. H.; Parker, V. B.; Schum, R. H.; Halow, I.; Bailey, S. M.; Churney, K. L.; Nuttall, R. N. *J. Phys. Chem. Ref. Data Suppl.* **1982**, *2*.
39. Nowicka, A.; Stojek, Z.; Hepel, M. *J. Phys. Chem. B* **2013**, *117*, 1021–1030.
40. Nowicka, A. M.; Kowalczyk, A.; Stojek, Z.; Hepel, M. *Biophys. Chem.* **2010**, *146*, 42–53.
41. Rhee, J. W. Pesticides. In *Rosen's Emergency Medicine: Concepts and Clinical Practice*; Marx, J. A., Hockberger, R. S., Walls, R., Eds.; Elsevier Mosby: Philadelphia, PA, 2013.
42. Roots, R.; Okada, S. *Radiat. Res.* **1975**, *64*, 306–320.
43. Baxton, G. V.; Greenstock, C. L.; Helman, W. P.; Ross, A. B. *J. Phys. Chem. Ref. Data Suppl.* **1988**, *17*, 513–886.
44. Feeney, C. J.; Frantseva, M. V.; Carlen, P. L.; Pennefather, P. S.; Shulyakova, N.; Shniffer, C.; Mills, L. R. *Brain Res.* **2008**, *1198*, 1–15.

45. Walz, W. *Neurochem. Int.* **2000**, *36*, 291–300.
46. Piet, R.; Vargová, L.; Syková, E.; Poulain, D.; Oliet, S. *Proc. Natl. Acad. Sci. U. S. A.* **2004**, *101*, 2151–2155.
47. Pascual, O.; Casper, K. B.; Kubera, C.; Zhang, J.; Revilla-Sanchez, R.; Sul, J. Y.; Takano, H.; Moss, S. J.; McCarthy, K.; Haydon, P. G. *Science* **2005**, *310*, 113–116.
48. Su, Z.; Niu, W.; Liu, M. L.; Zou, Y.; Zhang, C. L. *Nat. Commun.* **2014**, *5*, 3338.
49. Krishnan, C. V.; Garnett, M.; Chu, B. *Int. J. Electrochem. Sci.* **2008**, *3*, 1348–1363.
50. Nikam, S.; Nikam, P.; Ahaley, S. K.; Sontakke, A. V. *Indian J. Clin. Biochem.* **2009**, *24*, 98–101.
51. Singh, R. P.; Sharad, S.; Kapur, S. *JIACM* **2004**, *5*, 218–225.
52. Obeso, J. A.; Rodriguez-Oroz, M. C.; Goetz, C. G.; Marin, C.; Kordower, J. H.; Rodriguez, M.; Hirsch, E. C.; Farrer, M.; Schapira, A. H.; Halliday, G. *Nat. Med.* **2010**, *16*, 653–661.
53. Bosco, D. A.; Fowler, D. M.; Zhang, Q.; Nieva, J.; Powers, E. T. *Nat. Chem. Biol.* **2006**, *2*, 249–253.
54. Nuber, S.; Tadros, D.; Fields, J.; Overk, C. R.; Ettle, B.; Kosberg, K.; Mante, M.; Rockenstein, E.; Trejo, M.; Masliah, E. *Acta Neuropathol.* **2014**, *127*, 477–494.
55. Bellani, S.; Mescola, A.; Ronzitti, G.; Tsushima, H.; Tilve, S.; Canale, C.; Valtorta, F.; Chieregatti, E. *Cell Death Differ.* **2014**, *21*, 1971–1983.
56. Morshedi, D.; Aliakbari, F. *Modares J. Med. Sci.: Pathobiol.* **2012**, *15*, 45–60.
57. Son, H. J.; Choi, J. H.; Lee, J. A.; Kim, D. J.; Shin, K. J.; Hwang, O. *J. Mol. Neurosci.* **2015**, *56*, 263–272.
58. Wenk, G. L. *J. Clin. Psychiatry* **2003**, *64*, 7–10.
59. Markesbery, W. R. *Free Radical Biol. Med.* **1997**, *23*, 134–147.
60. Perry, G.; Cash, A. D.; Smith, M. A. *J. Biomed. Biotechnol.* **2002**, *2* (3), 120–123.
61. Yves, C. *Am. J. Clin. Nutr.* **2000**, *71*, 621S–629S.
62. Zhao, Y.; Zhao, B. *Oxid. Med. Cell. Longevity* **2013**, *2013*, 316523.
63. Ansari, M. A.; Scheff, S. W. *J. Neuropathol. Exp. Neurol.* **2010**, *69*, 155–167.
64. Perry, G.; Cash, A. D.; Smith, M. A. *J. Biomed. Biotechnol.* **2002**, *2*, 120–123.
65. Tiraboschi, P.; Hansen, L. A.; Thal, L. J.; Corey-Bloom, J. *Neurology* **2004**, *62*, 1984–1989.
66. Hashimoto, M.; Rockenstein, E.; Crews, L.; Masliah, E. *Neuromol. Med.* **2003**, *4*, 21–36.
67. Greig, N. H.; Mattson, M. P.; Perry, T.; Chan, S. L.; Giordano, T.; Sambamurti, K.; Rogers, J. T.; Ovadia, H.; Lahiri, D. K. *Ann. N. Y. Acad. Sci.* **2004**, *1035*, 290–315.
68. Ash, P. E.; Vanderweyde, T. E.; Youmans, K. L.; Apicco, D. J.; Wolozin, B. *Brain Res.* **2014**, *1584*, 52–58.
69. Wolozin, B. *Discov. Med.* **2014**, *17*, 47–52.

Publication Date (Web): October 13, 2015 | doi: 10.1021/bk-2015-1200.ch001

70. Barber, S. C.; Shaw, P. J. *Free Radical Biol. Med.* **2010**, *48*, 629–641.
71. Milanese, M.; Giribaldi, F.; Melone, M.; Bonifacino, T.; Musante, I.; Carminati, E.; Rossi, P. I.; Vergani, L.; Voci, A.; Conti, F.; Puliti, A.; Bonanno, G. *Neurobiol. Dis.* **2014**, *64*, 48–59.
72. Patel, P.; Julien, J. P.; Kriz, J. *Neurotherapeutics* **2015**, *12*, 217–233.
73. Rubino, E.; Rainero, I.; Chiò, A.; Rogaeva, E.; Galimberti, D.; Fenoglio, P.; Grinberg, Y.; Isaia, G.; Calvo, A.; Gentile, S.; Bruni, A. C.; StGeorge-Hyslop, P. H.; Scarpini, E.; Gallone, S.; Pinessi, L. *Neurology* **2012**, *79*, 1556–1562.
74. Ber, I. L.; Camuzat, A.; Guerreiro, R.; Bouya-Ahmed, K.; Bras, J.; Nicolas, G.; Gabelle, A.; Didic, M.; Septenville, A. D.; Millecamps, S.; Lenglet, T.; Latouche, M.; Kabashi, E.; Campion, D.; Hannequin, D.; Hardy, J.; Brice, A. *JAMA Neurol.* **2013**, *70*, 1403–1410.
75. Essa, M. M.; Subash, S.; Braidy, N.; Al-Adawi, S.; Lim, C. K.; Manivasagam, T.; Guillemin, G. J. *Int. J. Trypt. Res.* **2013**, *6*, 15–28.
76. James, S. J.; Cutler, P.; Melnyk, S.; Jernigan, S.; Janak, L.; Gaylor, D. W.; Neubrander, J. A. *Am. J. Clin. Nutr.* **2004**, *80*, 1611–1617.
77. James, S. J.; Melnyk, S.; Jernigan, S.; Cleves, M. A.; Halsted, C. H.; Wong, D. H.; Cutler, P.; Bock, K.; Boris, M.; Bradstreet, J. J.; Baker, S. M.; Gaylor, D. W. *Am. J. Med. Genet. B Neuropsychiatr. Genet.* **2006**, *141B*, 947–956.
78. Chauhan, A.; Chauhan, V.; Brown, W. T.; Cohen, I. *Life Sci.* **2004**, *75*, 2539–2549.
79. Essa, M. M.; Guillemin, G. J.; Waly, M. I.; et al. *Biol. Trace Elem. Res.* **2012**, *147*, 25–27.
80. Ming, X.; Stein, T. P.; Brimacombe, M.; Johnson, W. G.; Lamber, G. H.; Wagner, G. C. *Prostaglandins Leukot Essent Fatty Acids* **2005**, *73*, 379–384.
81. Zoroglu, S. S.; Armutcu, F.; Ozen, S.; et al. *Eur. Arch. Psychiatry Clin. Neurosci.* **2004**, *254*, 143–147.
82. Perluigi, M.; Butterfield, D. A. *Expert Rev. Proteomics* **2011**, *8*, 427–429.
83. Zana, M.; Janka, Z.; Kalman, J. *Neurobiol. Aging* **2007**, *28*, 648–676.
84. Zitnanova, I.; Korytar, P.; Aruoma, O. I.; Sustrova, M.; Garaiova, I.; Muchova, J.; Kalnovicova, T.; Pueschel, S.; Durackova, Z. *Clin. Chim. Acta* **2004**, *341*, 139–146.
85. Garlet, T. R.; Parisotto, E. B.; de Medeiros, G. D.; Pereira, L. C. R.; Moreira, E. A. D. M.; Dalmarco, E. M.; Dalmarco, J. B.; Wilhelm, D. *Life Sci.* **2013**, *93*, 558–563.
86. Pagano, G.; Castello, G. *Adv. Exp. Med. Biol.* **2012**, *724*, 291–299.
87. Gilgun-Sherki, Y.; Melamed, E.; Offen, D. *J. Neurol.* **2004**, *251*, 261–268.
88. van Horssen, J.; Witte, M. E.; Schreibelt, G.; de Vries, H. E. *Biochim. Biophys. Acta, Mol. Basis Dis.* **2011**, *1812*, 141–150.
89. Mirshafiey, A.; Mohsenzadegan, M. *Immunopharmacol. Immunotoxicol.* **2009**, *31*, 13–29.
90. Estevez, A. Y.; Pritchard, S.; Harper, K.; Aston, J. W.; Lynch, A.; Lucky, J. J.; Ludington, J. S.; Chatani, P.; Mosenthal, W. P.; Leiter, J. C.; Andreescu, S.; Erlichman, J. S. *Free Radical Biol. Med.* **2011**, *51*, 1155–1163.

Publication Date (Web): October 13, 2015 | doi: 10.1021/bk-2015-1200.ch001

91. Heckman, K. L.; DeCoteau, W.; Estevez, A.; Reed, K. J.; Costanzo, W.; Sanford, D.; Leiter, J. C.; Clauss, J.; Knapp, K.; Gomez, C.; Mullen, P.; Rathbun, E.; Prime, K.; Marini, J.; Patchefsky, J.; Patchefsky, A. S.; Hailstone, R. K.; Erlichman, J. S. *ACS Nano* **2013**, *7*, 10582–10596.
92. Tardif, J.-C. *Cardiol. Rounds* **2003**, *7*, 1–6.
93. Lakshmi, S. V. V.; Padmija, G.; Kuppusamy, P.; Kutala, V. K. *Indian J. Biochem. Biophys.* **2009**, *46*, 421–440.
94. Hamilton, C. A.; H. Miller, W. H.; Al-Benna, S.; Brosnan, M. J.; Drummond, R. D.; McBride, M. W.; Dominiczak, A. F. *Clin. Sci.* **2004**, *106*, 219–234.
95. Madamanchi, N. R.; Vendrov, A.; Runge, M. S. *Arterioscler. Thromb. Vasc. Biol.* **2005**, *25*, 29–38.
96. Gao, L.; Mann, G. E. *Cardiovasc. Res.* **2009**, *82*, 9–20.
97. Mendes, R. H.; Mostarda, C.; Candido, G. O.; Moraes-Silva, I. C.; D'Almeida, V.; Belló-Klein, A.; Irigoyen, M. C.; Rigatto, K. *Autonomic Neurosci.* **2014**, *180*, 43–47.
98. Selvam, R.; Kalaiselvi, P. *Nephron* **2001**, *88*, 163–167.
99. Singh, P. P.; Barjatia, M. K. *Indian J. Nephrol.* **2002**, *12*, 10–15.
100. Thamilselvan, S.; Hackett, R. L.; Khan, S. R. *J. Urology* **1997**, *157*, 1059–1063.
101. Pillai, C. K.; Pillai, K. S. *Indian J. Physiol. Pharmacol.* **2002**, *46*, 1–5.
102. Kashihara, N.; Haruna, Y.; Kondeti, V. K.; Kanwar, Y. S. *Curr. Med. Chem.* **2010**, *17*, 4256–4269.
103. Satoh, M.; Fujimoto, S.; Haruna, Y.; Arakawa, S.; Horike, H.; Komai, N.; Sasaki, T.; Tsujioka, K.; Makino, H.; Kashihara, N. *Am. J. Physiol. Renal Physiol.* **2005**, *288*, F1144–F1152.
104. Bartz, R. R.; Fu, P.; Suliman, H. B.; Crowley, S. D.; MacGarvey, N. C.; Welty-Wolf, K.; Piantadosi, C. A. *PLoS One* **2014**, *9*, e100912.
105. Galle, J. *Nephrol. Dial. Transplant.* **2001**, *16*, 2135–2137.
106. Himmelfarb, J.; McMonagle, E.; Freedman, S.; Klenzak, J.; McMenamin, E.; Le, P.; Pupim, L. B.; Ikizler, T. A.; The Picard Group. *J. Am. Soc. Nephrol.* **2004**, *15*, 2449−2456.
107. Webb, C.; Twedt, D. *Vet. Clin. North Am.: Small Anim. Pract.* **2008**, *38*, 125–135.
108. Pari, L.; Karthikeyan, A.; Karthika, P.; Rathinam, A. *Toxicol. Rep.* **2015**, *2*, 46–55.
109. Li, X.; Li, H.; Lu, N.; Feng, Y.; Huang, Y.; Gao, Z. *Biochimie* **2012**, *94*, 2620–2627.
110. Xu, Z.; Wang, Z.; Li, J. J.; Chen, C.; Zhang, P. C.; Dong, L.; Chen, J. H.; Chen, Q.; Zhang, X. T.; Wang, Z. L. *Food Chem. Toxicol.* **2013**, *58*, 1–7.
111. Sila, A.; Kamoun, Z.; Ghlissi, Z.; Makni, M.; Nasri, M.; Sahnoun, Z.; Nedjar-Arroume, N.; Bougatef, A. *Pharmacol. Rep.* **2015**, *67*, 310–316.
112. Heeba, G. H.; Mahmoud, M. E. *Environ. Toxicol. Pharmacol.* **2014**, *37*, 662–671.
113. Liu, Y.; Song, A.; Zang, S.; Wang, C.; Song, G.; Li, X.; Zhu, Y.; Yu, X.; Li, L.; Wang, Y.; Duan, L. *J. Ethnopharmacol.* **2015**, *162*, 244–252.

114. Zhang, P.; Ma, D.; Wang, Y.; Zhang, M.; Qiang, X.; Liao, M.; Liu, X.; Wu, H.; Zhang, Y. *Food Chem. Toxicol.* **2014**, *74*, 225–232.
115. Amamou, F.; Nemmiche, S.; Meziane, R. k.; Didi, A.; Yazit, S. M.; Chabane-Sari, D. *Food Chem. Toxicol.* **2015**, *78*, 177–184.
116. El-Nekeety, A. A.; Abdel-Azeim, S. H.; Hassan, A. M.; Hassan, N. S.; Aly, S. E.; Abdel-Wahhab, M. A. *Toxicol. Rep.* **2014**, *1*, 319–329.
117. Tokaç, M.; Taner, G.; Aydın, S.; Özkardeş, A. B.; Dündar, H. Z.; Taşlıpınar, M. Y.; Arıkök, A. T.; Kılıç, M.; Başaran, A. A.; Basaran, N. *Food Chem. Toxicol.* **2013**, *61*, 28–35.
118. Reddy, V. D.; Padmavathi, P.; Hymavathi, R.; Maturu, P.; Varadacharyulu, N. C. *Pathophysiology* **2014**, *21*, 153–159.
119. Wu, Z. R.; Yang-Li, P. C.; Li, J. Y.; Yong-Wang, X. W.; Guo, D. D.; Cui, L.; Guan, Q. G.; Li, H. Y. *Phytomedicine* **2015**, *22*, 178–182.
120. Conceição, E. P.; Peixoto-Silva, N.; Pinheiro, C. R.; Oliveira, E.; Moura, E. G.; Lisboa, P. C. *Food Chem. Toxicol.* **2015**, *78*, 52–59.
121. Cunha-Oliveira, T.; Silva, L.; Silva, A. M.; Moreno, A. J.; Oliveira, C. R.; Santos, M. S. *Life Sci.* **2013**, *92*, 1157–1164.
122. Pieniążek, A.; Czepas, J.; Piasecka-Zelga, J.; Gwoździński, K.; Koceva-Chyła, A. *Adv. Med. Sci.* **2013**, *58*, 104–111.
123. Urrunaga, N. H.; Jadeja, R. N.; Rachakonda, V.; Ahmad, D.; McLean, L. P.; Cheng, K.; Shah, V.; Twaddell, W. S.; Raufman, J. P.; Khurana, S. *Free Radical Biol. Med.* **2015**, *78*, 66–81.
124. Ying, Y.; Yun, J.; Guoyao, W.; Kaiji, S.; Zhaolai, D.; Zhenlong, W. *Exp. Gerontol.* **2015**, *65*, 35–41.
125. Buha, A.; Antonijević, B.; Milovanović, V.; Janković, S.; Bulat, Z.; Matović, V. *Environ. Res.* **2015**, *136*, 309–317.
126. Bartz, R. R.; Suliman, H. B.; Fu, P.; Welty-Wolf, K.; Carraway, M. S.; MacGarvey, N. C.; Withers, C. M.; Sweeney, T. E.; Piantadosi, C. A. *Am. J. Respir. Crit. Care Med.* **2011**, *183*, 226–233.
127. Bhattacharyya, A.; Chattopadhyay, R.; Mitra, S.; Crowe, S. E. *Physiol. Rev.* **2014**, *94*, 329–354.
128. Cheng, Y. T.; Wu, C. H.; Ho, C. Y.; Yen, G. C. *J. Nutr. Biochem.* **2013**, *24*, 475–483.
129. Broide, D. H. *J. Allergy Clin. Immunol.* **2001**, *108*, S65–S71.
130. Agrawal, D. K.; Shao, Z. *Curr. Allergy Asthma Rep.* **2010**, *10*, 39–48.
131. Nadeem, A.; Chhabra, S. K.; Masood, A.; Raj, H. G. *J. Allergy Clin. Immunol.* **2003**, *111*, 72–78.
132. Dozor, A. J. *Ann. N. Y. Acad. Sci.* **2010**, *1203*, 133–137.
133. Gomez-Mejiba, S. E.; Zhai, Z.; Akram, H.; Pye, Q. N.; Hensley, K.; Kurien, B. T.; Scofield, R. H.; Ramirez, D. C. *Mutat. Res.* **2009**, *674*, 62–72.
134. Wu, Z.; Turner, D. R.; Oliveira, D. B. *Int. Immunol.* **2001**, *13*, 297–304.
135. Li, G.; Yuan, K.; Yan, C.; Fox, J.; Gaid, M.; Breitwieser, W.; Bansal, A. K.; Zeng, H.; Gao, H.; Wu, M. *Free Radical Biol. Med.* **2012**, *52*, 392–401.
136. Potts, R. J.; Newbury, C. J.; Smith, G.; Notarianni, L. J.; Jefferies, T. M. *Mutat. Res.* **1999**, *423*, 103–111.
137. Vine, M. F.; Tse, C. K.; Hu, P.; Truong, K. Y. *Fertility Sterility* **1996**, *65*, 835–842.

Publication Date (Web): October 13, 2015 | doi: 10.1021/bk-2015-1200.ch001

138. Makker, K.; Agarwal, A.; Sharma, R. *Ind. J. Med. Res.* **2009**, *129*, 357–367.
139. Sun, J. G.; Jurisicova, A.; Casper, R. F. *Biol. Reprod.* **1997**, *56*, 602–607.
140. Al-Gubory, K. H.; Krawiec, A.; Grange, S.; Faure, P.; Garrel, C. *Free Radical Res.* **2014**, *48*, 1505–1513.
141. Vural, P.; Akgul, C.; Yildirim, A.; Canbaz, M. *Clin. Chim. Acta* **2000**, *295*, 169–177.
142. Ishii, T.; Miyazawa, M.; Takanashi, Y.; Tanigawa, M.; Yasuda, K.; Onouchi, H.; Kawabe, N.; Mitsushita, J.; Hartman, P. S.; Ishii, N. *Redox Biol.* **2014**, *2*, 679–685.
143. Menon, R.; Boldogh, I.; Hawkins, H. K.; Woodson, M.; Polettini, J.; Syed, T. A.; Fortunato, S. J.; Saade, G. R.; Papaconstantinou, J.; Taylor, R. N. *Am. J. Pathol.* **2014**, *184*, 1740–1751.
144. McCarthy, C.; Kenny, L. C. *Pregnancy Hypertens.* **2015**, *5*, 8.
145. Rudov, A.; Balduini, W.; Carloni, S.; Perrone, S.; Buonocore, G.; Albertini, M. C. *Oxid. Med. Cell Longev.* **2014**, *2014*, 103068.
146. Menon, R.; Polettini, J.; Syed, T. A.; Saade, G. R.; Boldogh, I. *Am. J. Reprod. Immunol.* **2014**, *72*, 75–84.
147. Haruna, Y.; Morita, Y.; Komai, N.; Yada, T.; Sakuta, T.; Tomita, N.; Fox, D. A.; Kashihara, N. *Arthritis Rheum.* **2006**, *54*, 1847–1855.
148. Yu, Y.; Li, S.; Liu, Y.; Tian, G.; Yuan, Q.; Bai, F.; Wang, W.; Zhang, Z.; Ren, G.; Zhang, Y.; Li, D. *Int. Immunopharmacol.* **2015**, *25*, 74–82.
149. Perrotta, I.; Aquila, S. *Oxid. Med. Cell. Longev.* **2015**, *2015*, 1–10.
150. Li, H. G.; Horke, S.; Forstermann, U. *Atherosclerosis* **2014**, *237*, 208–219.
151. Bonomini, F.; Tengattini, S.; Fabiano, A.; Bianchi, R.; Rezzani, R. *Histol. Histopathol.* **2008**, *23*, 381–390.
152. Brenner, M.; Hearing, V. J. *Photochem. Photobiol.* **2008**, *84*, 539–549.
153. Tiwari, S.; Mishra, P. C. *J. Mol. Model.* **2011**, *17*, 59–72.
154. Kammeyer, A.; Eggelte, T. A.; Overmars, H.; Bootsma, A.; Bos, J. D.; Teunissen, M. B. *Biochim. Biophys. Acta* **2001**, *1526*, 277–285.
155. Narendhirakannan, R. T.; Hannah, M. A. C. *Indian J. Clin. Biochem.* **2013**, *28*, 110–115.
156. Jomova, K.; Valko, M. *Toxicology* **2011**, *283*, 65–87.
157. Takeuchi, S.; Zhang, W.; Wakamatsu, K.; Ito, S.; Hearing, V. J.; Kraemer, K. H.; Brash, D. E. *Proc. Natl. Acad. Sci. U. S. A.* **2004**, *101*, 15076–15081.
158. Rajkumar, S.; Vasavada, A. R.; Praveen, M. R.; Ananthan, R.; Reddy, G. B. *Inv. Ophthalmol. Vis. Sci.* **2013**, *54*, 6224–6233.
159. Babizhayev, M. A.; Yegorov, Y. E. *Curr. Drug Delivery* **2014**, *11*, 24–61.
160. Ho, M. C.; Peng, Y. J.; Chen, S. J.; Chiou, S. H. *J. Clin. Gerontol. Geriatrics* **2010**, *1*, 17–21.
161. Kaur, J.; Kukreja, S.; Kaur, A.; Malhotra, N.; Kaur, R. *J. Clin. Diagn. Res.* **2012**, *6*, 1629–1632.
162. Xu, X.; Hang, L.; Huang, B.; Wei, Y.; Zheng, S.; Li, W. *J. Ophthalmol.* **2013**, *2013*, 862806.
163. Sarangarajan, R.; Apte, S. P. *Ophth. Res.* **2005**, *37*, 136–141.
164. Yang, Z.; Camp, N. J.; Sun, H.; Tong, Z.; Gibbs, D.; Cameron, D. J.; Chen, H.; Zhao, Y.; Pearson, E.; et al. *Science* **2006**, *314*, 992–993.
165. Dewan, A.; Liu, M.; Hartman, S.; et al. *Science* **2006**, *314*, 989–992.

Publication Date (Web): October 13, 2015 | doi: 10.1021/bk-2015-1200.ch001

166. Williams, D. L. *Vet. Clin. North Am.: Small Anim. Pract.* **2008**, *38*, 179–192.
167. Pinazo-Durán, M. D.; Gallego-Pinazo, R.; García-Medina, J. J.; Zanón-Moreno, V.; Nucci, C.; Dolz-Marco, R.; Martínez-Castillo, S.; Galbis-Estrada, C.; Marco-Ramírez, C.; López-Gálvez, M. I.; Galarreta, D. J.; Díaz-Llópis, M. *Clin. Interv. Aging* **2014**, *9*, 637–652.
168. Toprak, I.; Kucukatay, V.; Yildirim, C.; Kilic-Toprak, E.; Kilic-Erkek, O. *Eye* **2014**, *28*, 285–289.
169. Cejka, C.; Cejkova, J. *Oxid. Med. Cell. Longev.* **2015**, *2015*, 591530.
170. Pandey, K. B.; Rizvi, S. I. *Biomed. Pap.* **2011**, *155*, 131–136.
171. Mohanty, J. G.; Nagababu, E.; Rifkind, J. M. *Front Physiol* **2014**, *5* (84), 1–6.
172. Schrag, M.; Mueller, C.; Zabel, M.; Crofton, A.; Kirsch, W. M.; Ghribi, O.; Squitti, R.; Perry, G. *Neurobiol. Dis.* **2013**, *59*, 100–110.
173. Henriksen, K.; O'Bryant, S. E.; Hamper, H.; Trojanowski, J. Q.; Montine, T. J.; Jeromin, A.; Blennow, K.; Lonneborg, A.; Wyss-Coray, T.; Soares, H.; Bazenet, C.; Sjogren, M.; Hu, W.; Lovestone, S.; Karsdal, M. A.; Weiner, M. W.; Grp, B.-B. B. I. *Alzheimers Dement* **.2014**, *10*, 115–131.
174. Halliwell, B. *Biochem. J.* **2007**, *401*, 1–11.
175. Tandon, V. R.; Sharma, S.; Mahajan, A.; Bardi, G. H. *JK Science* **2005**, *7*, 1–3.
176. Cheung, K. L.; Lee, J. H.; Khor, T. O.; Wu, T. Y.; Li, G. X.; Chan, J.; Yang, C. S.; Kong, A. N. *Mol. Carcinog.* **2014**, *53*, 77–84.
177. Sosa, V.; Moliné, T.; Somoza, R.; Paciucci, R.; Kondoh, H.; Leonart, M. E. *Ageing Res. Rev.* **2013**, *12*, 376–390.
178. Pelicano, H.; Carney, D.; Huang, P. *Drug Resist. Updates* **2004**, *7*, 97–110.
179. Ralph, S. J.; Rodríguez-Enríquez, S.; Neuzil, J.; Saavedra, E.; Moreno-Sánchez, R. *Mol. Aspects Med.* **2010**, *31*, 145–170.
180. Bonora, M.; Pinton, P. *Front. Oncol.* **2014**, *4* (302), 1–12.
181. Usacheva, M.; Swaminathan, S. K.; Kirtane, A. R.; Panyam, J. *Mol. Pharm.* **2014**, *11*, 3186–3195.
182. Wang, S. S.; Chen, J.; Keltner, L.; Christophersen, J.; Zheng, F.; Krouse, M.; Singhal, A. *Cancer J.* **2002**, *8*, 154–163.
183. Srivatsan, A.; Jenkins, S. V.; Jeon, M.; Wu, Z.; Kim, C.; Chen, J.; Pandey, R. K. *Theranostics* **2014**, *4*, 163–174.
184. Guo, M.; Mao, H.; Li, Y.; Zhu, A.; He, H.; Yang, H.; Wang, Y.; Tian, X.; Ge, C.; Peng, Q.; Wang, X.; Yang, X.; Chen, X.; Liu, G.; Chen, H. *Biomaterials* **2014**, *35*, 4656–4666.
185. Rong, P.; Yang, K.; Srivastan, A.; Kiesewetter, D. O.; Yue, X.; Wang, F.; Nie, L.; Bhirde, A.; Wang, Z.; Liu, Z.; Niu, G.; Wang, W.; Chen, X. *Theranostics* **2014**, *4*, 229–239.
186. Taratula, O.; Patel, M.; Schumann, C.; Naleway, M. A.; Pang, A. J.; He, H.; Taratula, O. *Int. J. Nanomed.* **2015**, *10*, 2347–2362.
187. Yan, X.; Niu, G.; Lin, J.; Jin, A. J.; Hu, H.; Tang, Y.; Zhang, Y.; Wu, A.; Lu, J.; Zhang, S.; Huang, P.; Shen, B.; Chen, X. *Biomaterials* **2015**, *42*, 94–102.
188. Li, Y.; Dong, H.; Li, Y.; Shi, D. *Int. J. Nanomed.* **2015**, *10*, 2451–2459.
189. Lin, N.; Li, C.; Wang, Z.; Zhang, J.; Ye, X.; Gao, W.; Wang, A.; Jin, H.; Wei, J. *Photochem. Photobiol. Sci.* **2015**, *14*, 815–832.

Publication Date (Web): October 13, 2015 | doi: 10.1021/bk-2015-1200.ch001

190. Hu, Z.; Huang, Y.; Sun, S.; Guan, W.; Yao, Y.; Tang, P.; Li, C. *Carbon* **2012**, *50*, 994–1004.
191. Maritim, A. C.; Sanders, R. A.; Watkins, J. B. *J. Biochem. Mol. Toxicol.* **2003**, *17*, 24–38.
192. Moussa, S. A. *Romanian J. Biophys.* **2008**, *18*, 225–236.
193. Wiernsperger, N. F. *Diabetes Metab.* **2003**, *29*, 579–585.
194. Rains, J. L.; Jain, S. K. *Free Radical Biol. Med.* **2011**, *50*, 567–575.
195. Wright, E.; Scism-Bacon, J. L.; Glass, L. C. *Int. J. Clin. Pract.* **2006**, *60*, 308–314.
196. Johansen, J. S.; Harris, A. K.; Rychly, D. J.; Ergul, A. *Cardiovasc. Diabetol.* **2005**, *4* (5), 1–11.
197. Kammeyer, A.; Luiten, R. M. *Ageing Res. Rev.* **2015**, *21*, 16–29.

Publication Date (Web): October 13, 2015 | doi: 10.1021/bk-2015-1200.ch001

Publication Date (Web): October 13, 2015 | doi: 10.1021/bk-2015-1200.ch002

Chapter 2

Oxidative Metabolism of Estrogens in Cancer Initiation and Prevention

Eleanor G. Rogan[1,2,*] and Ercole L. Cavalieri[1,2]

[1]Department of Environmental, Agricultural and Occupational Health, College of Public Health, University of Nebraska Medical Center, 984388 Nebraska Medical Center, Omaha, Nebraska 68198-4388
[2]Eppley Institute for Research in Cancer and Allied Diseases, University of Nebraska Medical Center, 986805 Nebraska Medical Center, Omaha, Nebraska 68198-6805
[*]E-mail: egrogan@unmc.edu

Oxidative metabolism of the estrogens estrone (E_1) and estradiol (E_2) is the critical event in the initiation of cancer by estrogens. E_1 and E_2 are oxidized by cytochrome P450 (CYP) to the catechol estrogens 2-$OHE_1(E_2)$ and 4-$OHE_1(E_2)$ and then to the catechol estrogen quinones, which react with DNA to form estrogen-DNA adducts. The $E_1(E_2)$-3,4-quinones [$E_1(E_2)$-3,4-Q] react predominantly with DNA to form the depurinating adducts 4-$OHE_1(E_2)$-1-N3Ade and 4-$OHE_1(E_2)$-1-N7Gua. Loss of these adducts forms apurinic sites in the DNA that can generate mutations leading to the initiation of cancer. When estrogen metabolism becomes unbalanced toward oxidation, larger amounts of adducts are formed, and the risk of initiating cancer is greater. Women at high risk of developing breast cancer, or diagnosed with the disease, have higher levels of estrogen-DNA adducts than women at normal risk. With unbalanced estrogen metabolism, women are six-times more likely to be diagnosed with ovarian cancer. These results and others in humans and cell culture indicate that unbalanced oxidative metabolism of estrogens with formation of estrogen-DNA adducts is a critical event in the initiation of cancer. Two compounds, *N*-acetylcysteine and resveratrol, efficiently block formation of estrogen-DNA adducts and, thus, are promising agents to prevent cancer.

In Oxidative Stress: Diagnostics, Prevention, and Therapy Volume 2; Hepel, et al.; ACS Symposium Series; American Chemical Society: Washington, DC, 2015.

A large body of evidence for oxidative metabolism of estrogens as a mechanism of carcinogenesis has been derived from experiments on estrogen metabolism, formation of DNA adducts, mutagenicity, cell transformation and carcinogenicity (*1–3*). In fact, unbalanced oxidative metabolism of the natural estrogens estrone (E_1) and estradiol (E_2) has been shown to be the factor that renders the estrogens weak carcinogenic compounds. The predominant pathway that leads to the initiation of cancer is formation of $E_1(E_2)$-3,4-quinones [$E_1(E_2)$-3,4-Q] and reaction of these electrophilic compounds with DNA to form the depurinating 4-$OHE_1(E_2)$-1-N3Ade and 4-$OHE_1(E_2)$-1-N7Gua adducts (Figure 1) (*1–3*). Error-prone repair of the resulting apurinic sites leads to mutations that can initiate cancer (*4*, *5*).

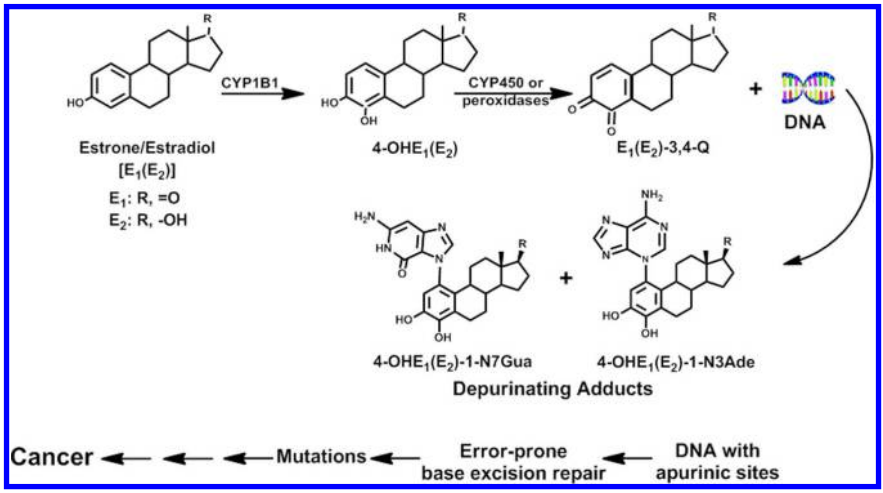

Figure 1. Major metabolic pathway in cancer initiation by estrogens. (Reproduced with permission from reference (2). Copyright 2011 Pergamon.)

Evidence for Genotoxicity Pathway in Estrogen Carcinogenesis

The most direct evidence for this pathway of genotoxicity leading to cancer initiation can be summarized as follows. Evidence that depurinating DNA adducts play a major role in cancer initiation derives from the correlation between the levels of depurinating aromatic hydrocarbon-DNA adducts and oncogenic Harvey (H)-*ras* mutations in mouse skin papillomas (*1–3*). A similar correlation between the sites of formation of depurinating DNA adducts and H-*ras* mutations was observed in mouse skin and rat mammary gland treated with E_2-3,4-Q (*4*, *5*).

Studies with cultured breast epithelial cells from humans or mice have provided evidence that initiation of cancer occurs by formation of estrogen-DNA adducts. The MCF-10F cell line is an immortalized non-transformed estrogen receptor-α (ER-α)-negative human cell line. When these cells are treated with E_2 or 4-OHE_2, the depurinating estrogen-DNA adducts are formed (*6–9*). Treatment

In Oxidative Stress: Diagnostics, Prevention, and Therapy Volume 2; Hepel, et al.;
ACS Symposium Series; American Chemical Society: Washington, DC, 2015.

Publication Date (Web): October 13, 2015 | doi: 10.1021/bk-2015-1200.ch002

with E_2 or 4-OHE_2 at doses of 0.007-3.5 nM produces transformation of these cells as detected by their ability to form colonies in soft agar (*6*, *9–11*). The presence of the antiestrogen tamoxifen or ICI-182,780 does not prevent this transformation (*10*). These changes are induced to a much smaller extent by 2-OHE_2. These results indicate that transformation is determined by genotoxic effects of estrogens. When estrogen-transformed MCF-10F cells, which were selected by their invasiveness, were implanted into severely compromised immune-deficient mice, the cells induced tumors (*12*). These results demonstrate that human breast epithelial cells lacking ER-α are transformed by the genotoxic effects of estrogen metabolites. Thus, these results support the hypothesis that formation of depurinating estrogen-DNA adducts is the critical event in the initiation of cancer by estrogens.

Similarly, the immortalized, normal mouse mammary cell line E6 also forms depurinating estrogen-DNA adducts and is transformed to grow in soft agar by a single treatment with 4-OHE_2 or E_2-3,4-Q (*13*). These results demonstrate that transformation of breast cells by estrogen genotoxicity occurs in both humans and animals.

Studies of transgenic mice with ER-α knocked out, ERKO/*wnt-1* mice, provide further important evidence demonstrating the role of estrogen genotoxicity in the initiation of cancer. Despite the absence of ER-α, mammary tumors develop in 100% of female ERKO/*wnt-1* mice, driven by the *wnt-1* transgene (*14*, *15*). The protective methoxyestrogen conjugates were not found in the mammary tissue of female ERKO/*wnt-1* mice, but 4-$OHE_1(E_2)$ and estrogen-glutathione (GSH) conjugates, which are formed by the catechol estrogen quinones, were detected (*16*). These results indicate that estrogen metabolism in these mice is unbalanced toward an excess of activating pathways and limited protective pathways. When the mice were implanted with E_2 following ovariectomy at 15 days of age to remove their major source of estrogens, the E_2-treated mice developed mammary tumors in a dose-dependent manner (*17*, *18*). The mammary tumors developed even in the presence of the implanted anti-estrogen ICI-182,780 (*19*). These results provide strong evidence for the critical role of estrogen genotoxicity in tumor initiation.

The "mainstream" proposed pathway for estrogen carcinogenesis is that ER-α-mediated events increase the rate of cell proliferation, giving cells less time to repair random mutations induced by unknown causes. This unproven hypothesis is belied by a variety of evidence, most directly by the difference in carcinogenicity of the 2- and 4- catechol estrogen metabolites.

The catechol estrogens 4-$OHE_1(E_2)$ and 2-$OHE_1(E_2)$ were tested for carcinogenic activity by subcutaneous implantation into male Syrian golden hamsters. The 4-$OHE_1(E_2)$ were carcinogenic, while the 2-$OHE_1(E_2)$ were not (*20*, *21*). The two catechol estrogens were also tested in CD-1 mice by injection of the compound into newborns. Once again, the 4-catechol estrogen induced uterine adenocarcinomas, whereas the 2-catechol estrogen was borderline active (*22*). These results are consistent with the structure of the two catechols. The 4-catechol estrogens, when oxidized to their quinones, produce an electrophilic species that reacts very strongly with DNA by protonated 1,4-Michael addition (*23*), whereas the catechol estrogen-2,3-quinones react with DNA by 1,6-Michael

Publication Date (Web): October 13, 2015 | doi: 10.1021/bk-2015-1200.ch002

addition via an intermediate quinone methide (*24*). For this reason, $E_1(E_2)$-3,4-Q react with DNA to a much greater extent than the $E_1(E_2)$-2,3-Q (*25*), forming 97% of the depurinating adducts found in humans (*26*).

In summary, evidence from studies of carcinogenesis in animal models and malignant transformation of human and mouse mammary cells supports the hypothesis that estrogens initiate cancer by a genotoxic mechanism.

Imbalances in Estrogen Metabolism

Initiation of cancer by estrogens occurs when a relatively large amount of $E_1(E_2)$-3,4-Q reacts with DNA, contributing about 97% of the adducts. A large amount of quinone reacting with DNA is due to oxidative stress, namely, the oxidative events that give rise to the catechol quinones in great abundance. These oxidative events start with the formation of the estrogens E_1 and E_2 from androgens, catalyzed by CYP19 (aromatase) (Figure 2). When this enzyme is over-expressed, a large amount of estrogen is produced. The estrogens are metabolized via two major pathways: 16α-hydroxylation (not shown in Figure 2) and formation of the catechol estrogens, 2-$OHE_1(E_2)$ and 4-$OHE_1(E_2)$. The formation of 4-$OHE_1(E_2)$, catalyzed by CYP1B1, is of critical importance.

The catechol estrogens are oxidized through estrogen semiquinones to the reactive catechol estrogen quinones. Molecular oxygen can oxidize the semiquinones to quinones (Figure 2). In turn, the estrogen quinones can be reduced to semiquinones by CYP reductase. This reaction completes the redox cycle. In this process, the molecular oxygen is reduced to superoxide anion radical, which is converted to H_2O_2. In the presence of Fe^{2+}, H_2O_2 yields the reactive hydroxyl radicals. Formation of lipid hydroperoxides can occur as the first damage by hydroxyl radicals. The lipid hydroperoxides can act as unregulated cofactors of cytochrome P450; this lack of regulation can generate an abnormal increase in the oxidation of catechol estrogens to quinones. Thus, efficient redox cycling can generate abundant catechol estrogen quinones, the ultimate carcinogenic metabolites of estrogens.

Conjugation of the catechols to form glucuronides, sulfates or methoxyestrogens is very abundant in the liver, but in extrahepatic tissues the major conjugation is formation of methoxyestrogens, catalyzed by the protective enzyme catechol-*O*-methyltransferase (COMT). If the activity of COMT is insufficient, the oxidation of catechols to semiquinones and quinones becomes competitive (Figure 2). The quinones, $E_1(E_2)$-2,3-Q and $E_1(E_2)$-3,4-Q, can be conjugated with GSH or reduced back to catechols by the enzyme quinone reductase (NQO1 and NQO2) (*27*, *28*). Once again, if these two protective events are insufficient, the quinones can react with DNA (Figure 2). A relatively large amount of the depurinating 4-$OHE_1(E_2)$-1-N3Ade and 4-$OHE_1(E_2)$-1 N7Gua adducts indicates unbalanced estrogen metabolism. This occurs only when the oxidative events overcome the protective events. Inhibition of adduct formation can be achieved by increased activity of the protective enzymes COMT and NQO1 and/or NQO2, or decreased activity of the oxidative enzymes CYP19 and CYP1B1.

Publication Date (Web): October 13, 2015 | doi: 10.1021/bk-2015-1200.ch002

In Oxidative Stress: Diagnostics, Prevention, and Therapy Volume 2; Hepel, et al.;
ACS Symposium Series; American Chemical Society: Washington, DC, 2015.

Publication Date (Web): October 13, 2015 | doi: 10.1021/bk-2015-1200.ch002

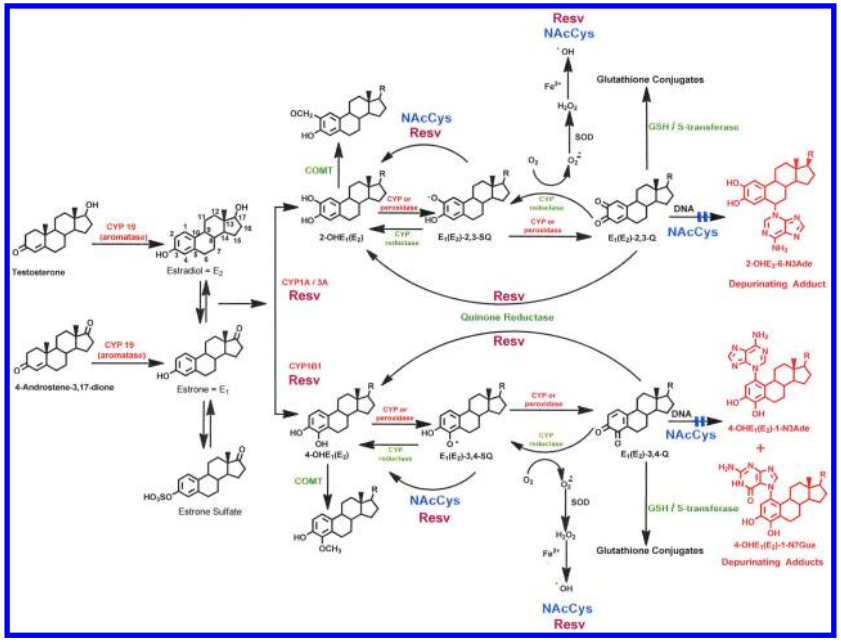

Figure 2. Formation, metabolism and DNA adducts of estrogens. Activating enzymes and depurinating DNA adducts are in red and protective enzymes are in Green. N-acetylcysteine (NAcCys, shown in blue) and resveratrol (Resv, burgundy) indicate the various points where NAcCys and Resv could improve the balance of estrogen metabolism and minimize formation of depurinating estrogen-DNA adducts. (Reproduced with permission from reference (2). Copyright 2011 Pergamon.) (see color insert)

Levels of Estrogen-DNA Adducts in Humans with and without Cancer

While most of us metabolize estrogens to products that are easily excreted from the body, people at risk for cancer metabolize estrogens to increased levels of $E_1(E_2)$-3,4-Q, which can react with DNA to form the depurinating adducts 4-$OHE_1(E_2)$-1-N3Ade and 4-$OHE_1(E_2)$-1 N7Gua. These adducts are shed from DNA, and the resulting apurinic sites can be unfaithfully repaired to generate mutations leading to cancer (*1–5*). After the depurinating adducts are released from DNA, they travel out of cells and tissues into the bloodstream and are excreted in urine. Thus, they can be identified and quantified as biomarkers of risk of developing cancer (*26*, *29–34*). Higher levels of depurinating estrogen-DNA adducts have been detected in analyses of urine or serum from women and men who have been diagnosed with cancer, compared to healthy controls who have never had cancer: breast, ovarian and thyroid cancer in women (*26*, *29*, *32–34*) and prostate cancer and non-Hodgkin lymphoma in men (*30*, *31*).

In Oxidative Stress: Diagnostics, Prevention, and Therapy Volume 2; Hepel, et al.;
ACS Symposium Series; American Chemical Society: Washington, DC, 2015.

Publication Date (Web): October 13, 2015 | doi: 10.1021/bk-2015-1200.ch002

Breast Cancer

In addition to women diagnosed with breast cancer, women that are at high risk for breast cancer have higher levels of these adducts (Figure 3) (*26*, *29*, *32*). In the largest of three such studies (*32*) (approximately 80 women per group), a serum sample was obtained from women at normal or high risk for breast cancer (Gail Model score >1.66% (*35*) and women diagnosed with breast cancer. After partial purification of an aliquot by solid phase extraction, each sample was analyzed for 40 estrogen metabolites, conjugates and depurinating DNA adducts by using ultraperformance liquid chromatography/tandem mass spectrometry (UPLC-MS/MS).

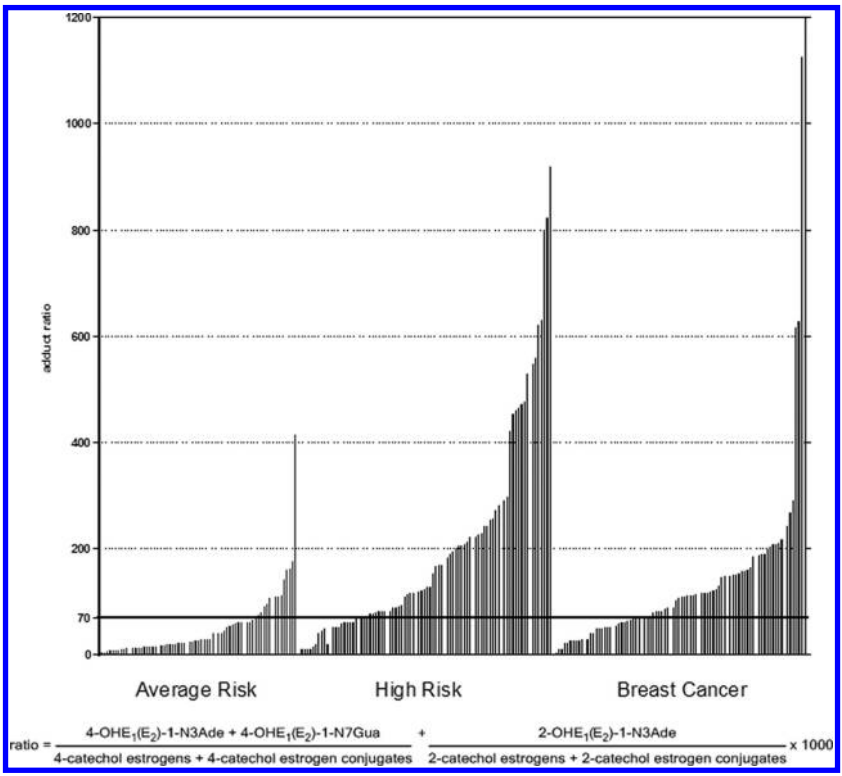

Figure 3. Ratio of depurinating estrogen-DNA adducts to estrogen metabolites and conjugates in serum of healthy women, high-risk women and women with breast cancer. (Reproduced with permission from reference (32). Copyright 2012 Pergamon.)

The risk of developing breast cancer was measured as the ratio of depurinating estrogen-DNA adducts to their respective estrogen metabolites and conjugates (Figure 3) because this ratio indicates the degree of imbalance in a person's estrogen metabolism. The DNA adducts formed by $E_1(E_2)$-3,4-Q are predominant (97%) in this ratio, whereas the adducts formed by $E_1(E_2)$-2,3-Q are minimal (3%)

In Oxidative Stress: Diagnostics, Prevention, and Therapy Volume 2; Hepel, et al.;
ACS Symposium Series; American Chemical Society: Washington, DC, 2015.

(*26*, *29*, *32*). The typically low ratio in women at normal risk for breast cancer indicates that their estrogen metabolism is balanced and they form relatively few estrogen-DNA adducts.

Subject characteristics did not affect the highly significant differences observed between the normal risk women and the women at high risk for breast cancer or diagnosed with it. Thus, these studies demonstrate that unbalanced estrogen metabolism leading to increased levels of estrogen-DNA adducts is associated with high risk of developing breast cancer. This study (*32*), as well as the other two studies of women with and without breast cancer (*26*, *29*), provide strong evidence that formation of estrogen-DNA adducts is a critical factor in the etiology of breast cancer.

Publication Date (Web): October 13, 2015 | doi: 10.1021/bk-2015-1200.ch002

Thyroid Cancer

Well-differentiated thyroid cancer most frequently occurs in premenopausal women, and greater exposure to estrogens may be a risk factor for this type of cancer. To investigate the role of estrogens in thyroid cancer, a spot urine sample was obtained from 40 women with thyroid cancer and 40 age-matched controls (*33*). Thirty-eight estrogen metabolites, conjugates and DNA adducts were analyzed by using UPLC-MS/MS, and the ratio of adducts to metabolites and conjugates was calculated for each sample. The ratio of depurinating estrogen-DNA adducts to estrogen metabolites and conjugates significantly differed between cases and controls ($p<0.0001$, Figure 4), demonstrating high specificity and sensitivity (*33*). These findings indicate that estrogen metabolism is unbalanced in thyroid cancer and suggest that formation of estrogen-DNA adducts might play a role in the initiation of thyroid cancer, as well as breast cancer.

Ovarian Cancer

Greater exposure to estrogens is a risk factor for ovarian cancer. To investigate the role of estrogens in ovarian cancer, a spot urine sample and a saliva sample were obtained from 33 women with ovarian cancer and 34 age-matched controls (*34*). Thirty-eight estrogen metabolites, conjugates and DNA adducts were analyzed in the urine samples by using UPLC-MS/MS, and the ratio of adducts to metabolites and conjugates was calculated for each sample. The ratio of depurinating estrogen-DNA adducts to estrogen metabolites and conjugates was significantly higher in cases compared to controls ($p<0.0001$, Figure 5), demonstrating high specificity and sensitivity. DNA was purified from the saliva samples and analyzed for genetic polymorphisms in the genes for two estrogen-metabolizing enzymes. Women with one or two high-activity alleles of CYP1B1 and two low-activity alleles of COMT had higher levels of estrogen-DNA adducts and were more likely to have ovarian cancer (Table 1) (*34*). In fact, women with two low-activity alleles of COMT plus two high-activity alleles of CYP1B1 were six times more likely to have ovarian cancer. These findings indicate that unbalanced estrogen metabolism leading to formation of estrogen-DNA adducts plays a critical role in the initiation of ovarian cancer.

In Oxidative Stress: Diagnostics, Prevention, and Therapy Volume 2; Hepel, et al.;
ACS Symposium Series; American Chemical Society: Washington, DC, 2015.

Publication Date (Web): October 13, 2015 | doi: 10.1021/bk-2015-1200.ch002

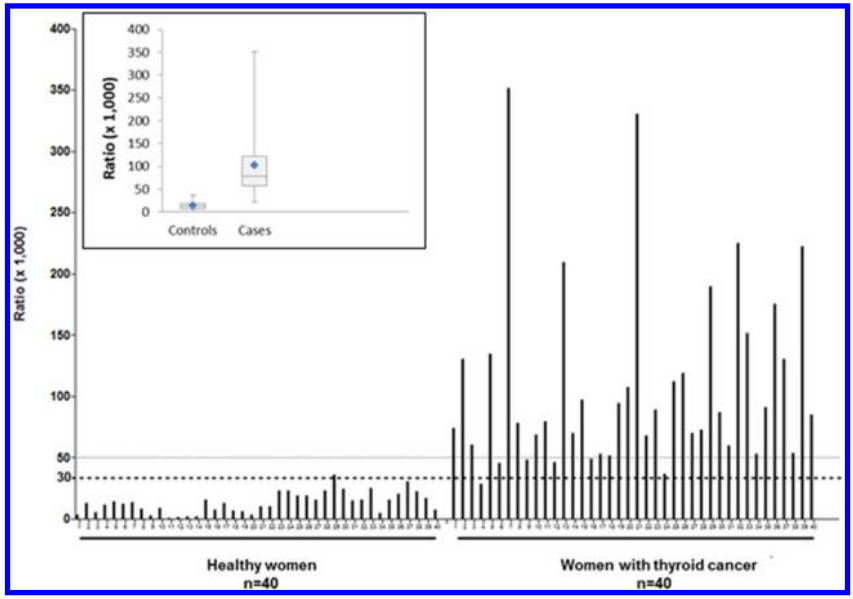

Figure 4. Ratio of urinary depurinating estrogen-DNA adducts to estrogen metabolites and conjugates for women diagnosed with thyroid cancer (cases) or not diagnosed with cancer (controls). The dotted line representing a ratio of 30 is the cross-over point for sensitivity and specificity of the ratio. Insert: Ratios presented as median values and ranges (min to max). The diamonds represent the mean values. (Reproduced with permission from reference (33). Copyright 2013 John/Wiley & Sons, Inc.)

In summary, the observation that women at high risk for breast cancer have significantly higher levels of estrogen-DNA adducts, coupled with the finding that women with unbalanced estrogen metabolism due to polymorphisms in COMT and CYP1B1 are more likely to have ovarian cancer, strongly supports the hypothesis that formation of estrogen-DNA adducts plays a critical role in the etiology of certain types of human cancer. These approaches can be used with other types of cancer to ascertain the role of unbalanced estrogen metabolism and formation of estrogen-DNA adducts in their etiology.

Publication Date (Web): October 13, 2015 | doi: 10.1021/bk-2015-1200.ch002

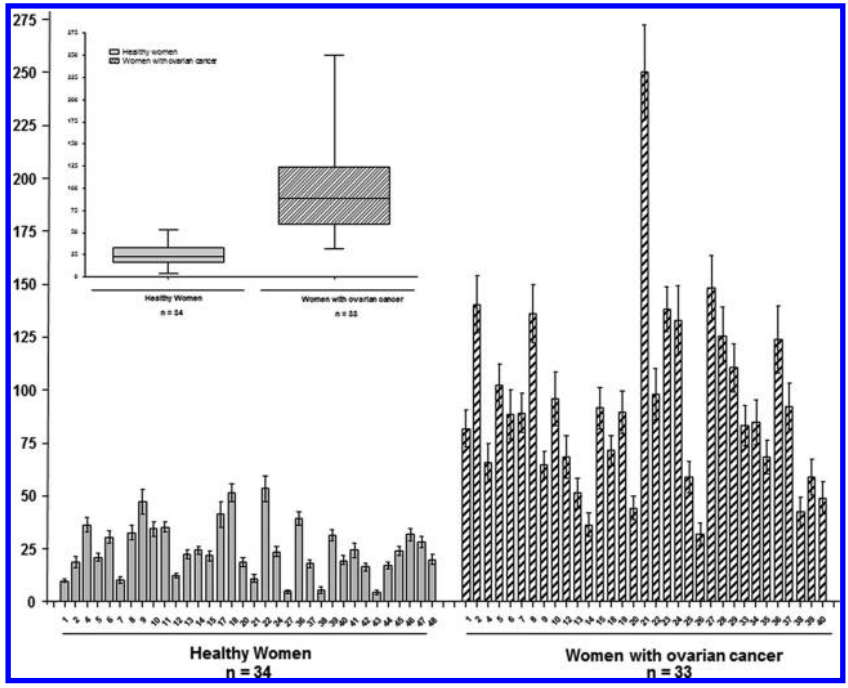

Figure 5. Ratio of urinary depurinating estrogen-DNA adducts to estrogen metabolites and conjugates for women diagnosed with ovarian cancer (cases) or not diagnosed with cancer (controls). The dotted line representing a ratio of 43 is the cross-over point for sensitivity and specificity of the ratio. Insert: Ratios presented as median values and ranges (min to max). The diamonds represent the mean values. (Reproduced with permission from reference (34). Copyright 2014 John/Wiley & Sons, Inc.)

Cancer Prevention by *N*-Acetylcysteine and Resveratrol

In the catechol estrogen pathway of metabolism, E_1 and E_2 are oxidized to 2-OHE_1(E_2) and 4-OHE_1(E_2) (Figure 2). CYP1B1 catalyzes the formation of 4-OHE_1(E_2) almost exclusively. The compounds that we have selected for cancer prevention exert their influence at various levels of oxidation of 4-OHE_1(E_2), namely, formation of semiquinones and then quinones, followed by reaction of E_1(E_2)-3,4-Q with DNA to form depurinating adducts. Ninety-seven percent of the adducts arise from the reaction of E_1(E_2)-3,4-Q with DNA (*26*).

In Oxidative Stress: Diagnostics, Prevention, and Therapy Volume 2; Hepel, et al.;
ACS Symposium Series; American Chemical Society: Washington, DC, 2015.

Table 1. Descriptions and t-tests for association between the DNA adduct ratio and having one or two high activity CYP1B1 alleles in the presence of being homozygous for the mutant allele resulting in low COMT activity. (Reproduced with permission from reference (*34*). Copyright 2014 John/Wiley & Sons, Inc.)

Risk combination	*n*	*Mean adduct ratio (SD)*	*T-test (p-value)*	*Ovarian Cancer OR (95% CI)*
CYP1B1 GC or GG + COMT AA				
No	52	49.7 (36.8)	-2.43	Reference
Yes	13	91.4 (64.9)	(0.018)	2.84 (0.77-10.4)
CYP1B1 GG + COMT AA				
No	59	51.9 (37.6)	-2.43	Reference
Yes	6	118.5 (79.5)	(0.018)	5.93 (0.65-53.9)

Publication Date (Web): October 13, 2015 | doi: 10.1021/bk-2015-1200.ch002

We have selected compounds for keeping the metabolism of estrogens in balance, resulting in minimal amounts of formation of catechol estrogen quinones and their reaction with DNA. Two compounds have demonstrated great efficiency in keeping the catechol estrogen oxidative pathway balanced in the MCF-10F human breast epithelial cell line and in the E6 mouse mammary cell line (*9*, *13*, *36–38*). The effect of *N*-acetylcysteine (NAcCys) in reducing formation of estrogen-DNA adducts in MCF-10F cells treated with 4-OHE_2 (*37*) is due to the reaction of NAcCys with E_2-3,4-Q and the reduction of E_2-3,4-semiquinone to 4-OHE_2 (Figure 2) (*39*). Resveratrol also reduces E_2-3,4-semiquinone to 4-OHE_2 (Figure 2) (*9*, *36*). In addition, resveratrol induces NQO1, which catalyzes the reduction of E_2-3,4-Q to 4-OHE_2 (*27*), thereby limiting reaction of the quinone with DNA (Figure 2). Resveratrol displays another important effect by modulating the action of CYP1B1 (*9*). When MCF-10F cells are treated with 4-OHE_2 plus NAcCys and resveratrol mixed together, the two compounds display an additive effect in reducing the formation of estrogen-DNA adducts by the cells (Figure 6) (*38*). At low concentrations, the two antioxidants inhibit formation of estrogen-DNA adducts similarly, but at higher concentrations, the effect of resveratrol is 50% greater than that of NAcCys (*38*).

Resveratrol was also found to inhibit the malignant transformation of MCF-10F cells, which do not contain ER-α, treated with E_2 (*9*). This was seen in a set of experiments in which MCF-10F cells were treated with E_2 plus the CYP1B1-inducer dioxin (TCDD) (*9*). When the cells were treated with TCDD plus E_2, higher levels of estrogen-DNA adducts were formed than when E_2 alone was used (Figure 7A). Similarly, with E_2 plus TCDD, more transformed cells were detected than with E_2 alone (Figure 7B). In either case, inclusion of Resv in the culture

medium resulted in undetectable levels of estrogen-DNA adducts and significantly lower numbers of transformed cells (Figure 7) (*9*). NAcCys was also found to inhibit not only formation of estrogen-DNA adducts, but also transformation of E6 mouse mammary cells treated with 4-OHE_2 or E_2-3,4-Q (*13*).

Thus, the use of these two compounds serves to re-establish and/or maintain balanced estrogen metabolism. This effect reduces DNA damage and the resulting mutations that can lead to the initiation of cancer. Therefore, NAcCys and resveratrol are promising candidates for the prevention of estrogen-initiated cancers in people.

In fact, in a pilot study with 21 healthy women treated for 90 days with a protocol that reduced oxidative stress and provided NAcCys and resveratrol, 16 of the women showed significant reduction in their level of urinary estrogen-DNA adducts, four women showed no significant change and one woman showed an increase (Figure 8) (*40*).

Publication Date (Web): October 13, 2015 | doi: 10.1021/bk-2015-1200.ch002

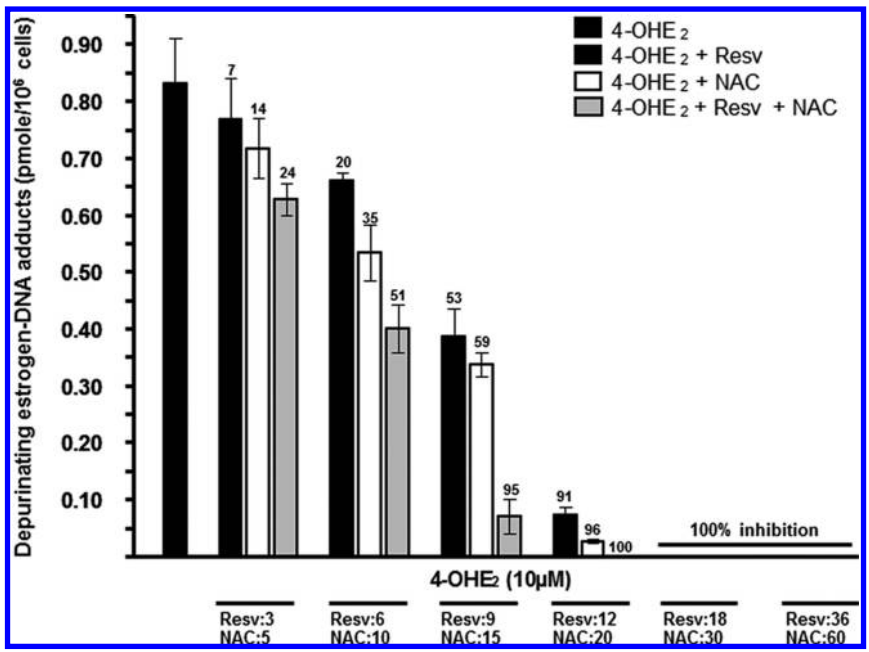

Figure 6. Effects of NAC, Resv, or NAC + Resv on the formation of depurinating estrogen-DNA adducts in MCF-10F cells treated with 4-OHE_2. The number above each bar indicates the percent inhibition compared to treatment with 4-OHE_2 alone. (Reproduced with permission from reference (38). Copyright 2011 Elsevier Inc.)

Publication Date (Web): October 13, 2015 | doi: 10.1021/bk-2015-1200.ch002

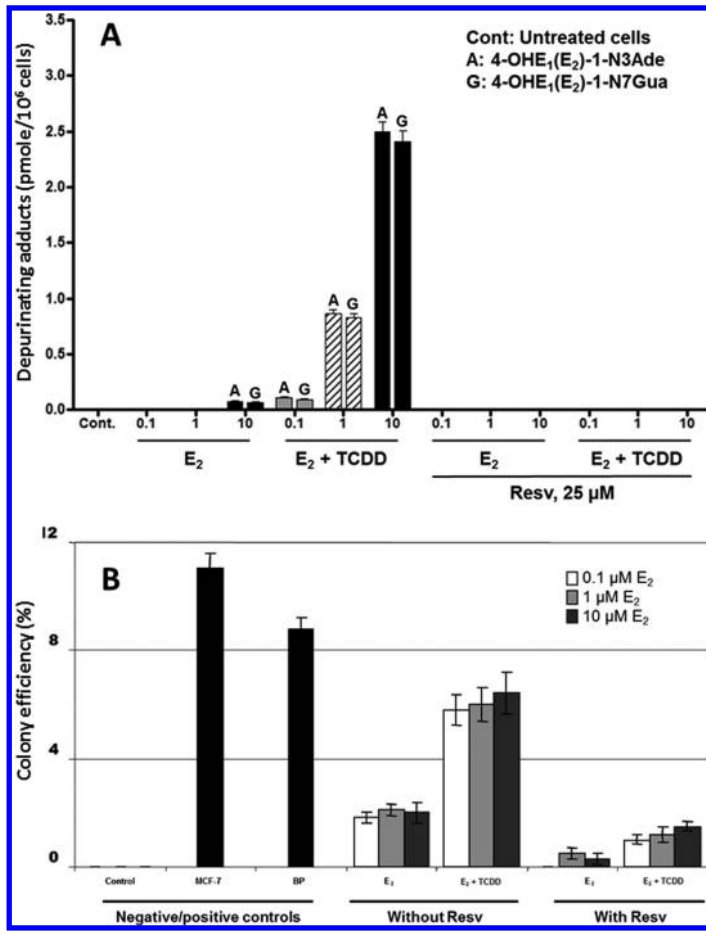

Figure 7. (A) Levels of depurinating DNA adducts in MCF-10F cells pretreated with TCDD with and without Resv and treated with increasing concentrations of E_2 for 24 h. The levels of DNA adducts in Resv pretreated cells are significantly lower than those in the cells not pretreated with Resv, $p < 0.05$ as determined by ANOVA. The DNA adduct levels were corrected for recovery and normalized to cell numbers. Columns, mean of triplicate cultures from three experiments; bars, SD. (B) Antitransformation effects of Resv on E_2-induced transformation of MCF-10F cells. MCF-10F cells were pretreated with TCDD with and without Resv, then treated with E_2. The results are expressed as colony efficiency (%): The number of colonies formed per number of cells plated x 100. Columns, mean of assays from triplicate experiments; bars, SD: $p < 0.05$. A negative control was conducted with MCF-10F cells cultured without any treatment. Two positive controls were included. One was cultured MCF-7 cells, which are a transformed cell line. In the other, MCF-10F cells were transformed with benzo[a]pyrene (BP). (A and B reproduced with permission from reference (9). Copyright 2008 American Association for Cancer Research.)

Publication Date (Web): October 13, 2015 | doi: 10.1021/bk-2015-1200.ch002

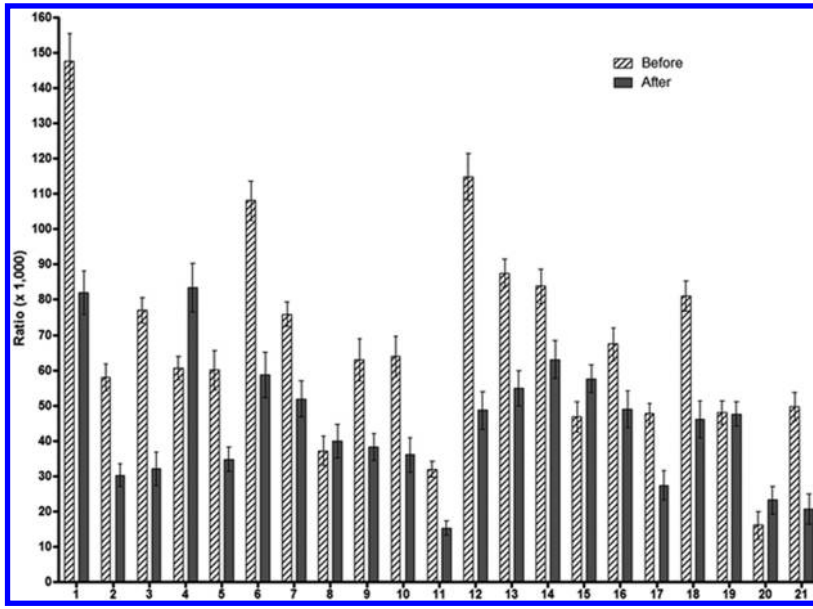

Figure 8. Assessment of DNA adduct ratios (n=21) before women began daily self-administration of NAcCys and Resv and after three months of the dietary supplements. (Reproduced with permission from reference (40).)

Conclusions

Oxidative metabolism of the natural estrogens E_1 and E_2 results in the formation of catechol estrogen quinones. With unbalanced metabolism, excessive amounts of $E_1(E_2)$-3,4-Q are formed and react with DNA to generate depurinating estrogen-DNA adducts and apurinic sites. Error-prone repair of the apurinic sites can lead to mutations that initiate cancer. This pathway of cancer initiation has been studied in cell culture, laboratory animals and humans.

The depurinating estrogen-DNA adducts 4-$OHE_1(E_2)$-1-N3Ade and 4-$OHE_1(E_2)$-1-N7Gua have been detected in human urine and serum by using UPLC-MS/MS. The observation of high ratios of estrogen-DNA adducts to estrogen metabolites and conjugates in women at high risk for breast cancer, as well as woman diagnosed with the disease, provides strong evidence that formation of these adducts is a critical factor in the initiation of breast cancer. Similarly, women with ovarian cancer are more likely to have a genetic polymorphism in the estrogen-activating CYP1B1 that has higher than normal and a polymorphism in the estrogen-protective enzyme COMT that has lower activity than normal. These genetic polymorphisms result in unbalanced estrogen metabolism leading to cancer initiation. This finding also provides evidence on the role of estrogen-DNA adducts in the initiation of ovarian cancer.

Dietary supplements that inhibit the formation of catechol estrogen quinones and/or inhibit their reaction with DNA reduce the levels of estrogen-DNA adducts

In Oxidative Stress: Diagnostics, Prevention, and Therapy Volume 2; Hepel, et al.;
ACS Symposium Series; American Chemical Society: Washington, DC, 2015.

in women who take these supplements on a daily basis. All of these findings suggest that these dietary supplements are prime candidates to block formation of the oxidative metabolism of estrogens leading to adduct formation and, thus, cancer initiation.

Acknowledgments

The progress in research on the etiology and prevention of cancer is due to the efforts, dedication, accomplishments and creativity of the many fine scientists with whom we have worked over the years. We particularly acknowledge our long-term collaboration with Dr. Muhammad Zahid. Preparation of this article was supported by Prevention LLC. Core support at the Eppley Institute was supported by grant P30 36727 from the National Cancer Institute.

Publication Date (Web): October 13, 2015 | doi: 10.1021/bk-2015-1200.ch002

References

1. Cavalieri, E.; Chakravarti, D.; Guttenplan, J.; Hart, E.; Ingle, J.; Jankowiak, R.; Muti, P.; Rogan, E.; Russo, J.; Santen, R.; Sutter, T. Catechol estrogen quinones as initiators of breast and other human cancers. Implications for biomarkers of susceptibility and cancer prevention. *BBA-Rev. Cancer* **2006**, *1766*, 63–78.
2. Cavalieri, E.; Rogan, E. Unbalanced metabolism of endogenous estrogens in the etiology and prevention of human cancer. *J. Steroid Biochem. Mol. Biol.* **2011**, *125*, 169–180.
3. Cavalieri, E.; Rogan, E. The molecular etiology and prevention of estrogen-initiated cancers. *Mol. Aspects Med.* **2014**, *36*, 1–55.
4. Chakravarti, D.; Mailander, P.; Li, K.-M.; Higginbotham, S.; Zhang, H.; Gross, M. L.; Cavalieri, E.; Rogan, E. Evidence that a burst of DNA depurination in SENCAR mouse skin induces error-prone repair and form mutations in the H-*ras* gene. *Oncogene* **2001**, *20*, 7945–7953.
5. Mailander, P. C.; Meza, J. L.; Higginbotham, S.; Chakravarti, D. Induction of A.T to G.C mutations by erroneous repair of depurinated DNA following estrogen treatment of the mammary gland of ACI rats. *J. Steroid Biochem.* **2006**, *101*, 204–215.
6. Russo, J.; Hasan Lareef, M.; Balogh, G.; Guo, S.; Russo, I. H. Estrogen and its metabolites are carcinogenic agents in human breast epithelial cells. *J. Steroid Biochem. Mol. Biol.* **2003**, *87*, 1–25.
7. Lu, F.; Zahid, M.; Saeed, M.; Cavalieri, E. L.; Rogan, E. G. Estrogen metabolism and formation of estrogen-DNA adducts in estradiol-treated MCF-10F cells. The effects of 2,3,7,8-tetrachlorodibenzo-*p*-dioxin induction and catechol-*O*-methyltransferase inhibition. *J. Steroid Biochem. Mol. Biol.* **2007**, *105*, 150–158.
8. Saeed, M.; Rogan, E.; Fernandez, S. V.; Sheriff, F.; Russo, J.; Cavalieri, E. Formation of depurinating N3Adenine and N7Guanine adducts by MCF-10F cells cultured in the presence of 4-hydroxyestradiol. *Int. J. Cancer* **2007**, *120*, 1821–1824.

9. Lu, F.; Zahid, M.; Wang, C.; Saeed, M.; Cavalieri, E.; Rogan, E. Resveratrol prevents estrogen-DNA adduct formation and neoplastic transformation in MCF-10F cells. *Cancer Prev. Res.* **2008**, *1*, 135–145.
10. Russo, J.; Russo, I. H. Genotoxicity of steroidal estrogens. *Trends Endocrinol. Metab.* **2004**, *15*, 211–214.
11. Lareef, M. H.; Garber, J.; Russo, P. A.; Russo, I. H.; Heulings, R.; Russo, J. The estrogen antagonist ICI-182-780 does not inhibit the transformation phenotypes induced by 17-beta-estradiol and 4-OH estradiol in human breast epithelial cells. *Int. J. Oncol.* **2005**, *26*, 423–429.
12. Russo, J.; Fernandez, S. V.; Russo, P. A.; Fernbaugh, R.; Sheriff, F. S.; Lareef, H. M.; Garber, J.; Russo, I. H. 17β-Estradiol induces transformations and tumorigenesis in human breast epithelial cells. *FASEB J.* **2006**, *20*, 1622–1634.
13. Venugopal, D.; Zahid, M.; Mailander, P.C.; Meza, J. L.; Rogan, E. G.; Cavalieri, E. L.; Chakravarti, D. Reduction of estrogen-induced transformation of mouse mammary epithelial cell by N-acetylcysteine. *J. Steroid Biochem. Mol. Biol.* **2008**, *109*, 22–30.
14. Bocchinfuso, W. P.; Korach, K. S. Mammary gland development and tumorigenesis in estrogen receptor knockout mice. *J. Mammary Gland Biol. Neoplasia* **1997**, *2*, 323–334.
15. Bocchinfuso, W. P.; Hively, W. P.; Couse, J. F.; Varmus, H. E.; Korach, K. S. A mouse mammary tumor virus-wnt-1 transgene induces mammary gland hyperplasia and tumorigenesis in mice lacking estrogen receptor-alpha. *Cancer Res.* **1999**, *59*, 1869–1876.
16. Devanesan, P.; Santen, R.J.; Bocchinfuso, W. P.; Korach, K. S.; Rogan, E. G.; Cavalieri, E. L. Catechol estrogen metabolites and conjugates in mammary tumors and hyperplastic tissue from estrogen receptor alpha knock out (ERKO)/Wnt 1 mice; implications for initiation of mammary tumors. *Carcinogenesis* **2001**, *22*, 1573–1576.
17. Yue, W.; Santen, R. J.; Wang, J. P.; Li, Y.; Verderame, M. F.; Bocchinfuso, W. P.; Korach, K. S.; Devanesan, P.; Todorovic, R.; Rogan, E. G.; Cavalieri, E. L. Genotoxic metabolites of estradiol in breast: Potential mechanism of estradiol induced carcinogenesis. *J. Steroid Biochem. Mol. Biol.* **2003**, *86*, 477–486.
18. Santen, R. J.; Yue, W.; Bocchinfuso, W.; et al. Estradiol-induced carcinogenesis via formation of genotoxic metabolites. In *Advances in Endocrine Therapy of Breast Cancer*; Ingle, J. N., Dowsett, M., Eds.; Marcel Dekker: 2003; pp 13−177.
19. Santen, R.; Cavalieri, E.; Rogan, E.; Russo, J.; Guttenplan, J.; Ingle, J.; Yue, W. Estrogen mediation of breast tumor formation involves estrogen receptor-dependent, as well as independent, genotoxic effects. *Ann. N. Y. Acad. Sci.* **2009**, *1155*, 132–140.
20. Liehr, J. G.; Fang, W. F.; Sirbasku, D. A.; Ari-Ulubelen, A. Carcinogenicity of catechol estrogens in Syrian hamsters. *J. Steroid Biochem.* **1986**, *24*, 353–356.
21. Li, J. J.; Li, S. A. Estrogen carcinogenesis in Syrian hamster tissues: Role of metabolism. *Fed. Proc.* **1987**, *46*, 1858–1863.

Publication Date (Web): October 13, 2015 | doi: 10.1021/bk-2015-1200.ch002

22. Newbold, R. R.; Liehr, J. G. Induction of uterine adenocarcinoma in CD-1 mice by catechol estrogens. *Cancer Res.* **2000**, *60*, 235–237.
23. Stack, D.; Byun, J.; Gross, M. L.; Rogan, E. G.; Cavalieri, E. Molecular characteristics of catechol estrogen quinones in reactions with deoxyribonucleosides. *Chem. Res. Toxicol.* **1996**, *9*, 851–859.
24. Bolton, J. L.; Shen, L. *p*-Quinone methides are the major decomposition products of catechol estrogen *o*-quinones. *Carcinogenesis* **1998**, *17*, 925–929.
25. Zahid, M.; Kohli, E; Saeed, M.; Rogan, E.; Cavalieri, E. The greater reactivity of estradiol-3,4-quinone versus estradiol-2,3-quinone with DNA in the formation of depurinating adducts. Implications for tumor-initiating activity. *Chem. Res. Toxicol.* **2006**, *19*, 164–172.
26. Gaikwad, N.W.; Yang, L.; Muti, P.; Meza, J. L.; Pruthi, S.; Ingle, J. N.; Rogan, E. G.; Cavalieri, E. L. The molecular etiology of breast cancer: evidence from biomarkers of risk. *Int. J. Cancer* **2008**, *122*, 1949–1957.
27. Gaikwad, N. W.; Rogan, E. G.; Cavalieri, E. L. Evidence from ESI-MS for NQO1-catalyzed reduction of estrogen *ortho*-quinones. *Free Radical Biol. Med.* **2007**, *43*, 1289–1298.
28. Gaikwad, N. W.; Yang, L.; Rogan, E. G.; Cavalieri, E. L. Evidence for NQO2-mediated reduction of the carcinogenic estrogen *ortho*-quinones. *Free Radical Biol. Med.* **2009**, *46*, 253–262.
29. Gaikwad, N. W.; Yang, L.; Pruthi, S.; Ingle, J. N.; Sandhu, N.; Rogan, E.; Cavalieri, E. Urine biomarkers of risk in the molecular etiology of breast cancer. *Breast Cancer: Basic Clin. Res.* **2009**, *3*, 1–8.
30. Yang, L.; Gaikwad, N.; Meza, J.; Cavalieri, E.; Muti, P.; Trock, B.; Rogan, E. Novel biomarkers for risk of prostate cancer. Results from a case-control study. *Prostate* **2009**, *69*, 41–48.
31. Gaikwad, N.; Yang, L.; Weisenburger, D. D.; Vose, J.; Beseler, C.; Rogan, E.; Cavalieri, E. Urinary biomarkers suggest that estrogen-DNA adducts may play a role in the etiology of non-Hodgkin lymphoma. *Biomarkers* **2009**, *14*, 502–512.
32. Pruthi, S.; Yang, L.; Sandhu, N. P.; Ingle, J. N.; Beseler, C. L.; Suman, V. J.; Cavalieri, E. L.; Rogan, E. G. Evaluation of serum estrogen-DNA adducts as potential biomarkers for breast cancer risk. *J. Steroid Biochem. Mol. Biol.* **2012**, *132*, 73–79.
33. Zahid, M.; Goldner, W.; Beseler, C. L.; Rogan, E. G.; Cavalieri, E. L. Unbalanced estrogen metabolism in thyroid cancer. *Int. J. Cancer* **2013**, *133*, 2642–2649.
34. Zahid, M.; Beseler, C. L.; Hall, J. B.; LeVan, T.; Cavalieri, E. L.; Rogan, E. G. Unbalanced estrogen metabolism in ovarian cancer. *Int. J. Cancer* **2014**, *134*, 2414–2423.
35. Gail, M. H.; Brinton, L. A.; Byar, D. P.; Corle, D. K.; Green, S. B.; Schairer, C.; Mulvihill, J. J. Protecting individualized probabilities of developing breast cancer for white females who are being examined annually. *J. Natl. Cancer Inst.* **1989**, *81*, 1879–1886.

Publication Date (Web): October 13, 2015 | doi: 10.1021/bk-2015-1200.ch002

36. Zahid, M.; Gaikwad, N. W.; Ali, M. F.; Lu, F.; Saeed, M.; Yang, L.; Rogan, E. G.; Cavalieri, E. L. Prevention of estrogen-DNA adduct formation in MCF-10F cells by resveratrol. *Free Radical Biol. Med.* **2008**, *45*, 136–145.
37. Zahid, M.; Saeed, M.; Ali, M. F.; Rogan, E. G.; Cavalieri, E. L. *N*-Acetylcysteine blocks formation of cancer-initiating estrogen-DNA adducts in cells. *Free Radical Biol. Med.* **2010**, *49*, 392–400.
38. Zahid, M.; Saeed, M.; Beseler, C.; Rogan, E. G.; Cavalieri, E. L. Resveratrol and *N*-acetylcysteine block the cancer-initiating step in MCF-10F cells. *Free Radical Biol. Med.* **2011**, *50*, 78–85.
39. Samuni, A. M.; Chuang, E. Y.; Krishna, M. C.; Stein, W.; DeGraff, W.; Russo, A.; Mitchell, J. B. Semiquinone radical intermediate in catecholic estrogen-mediated cytotoxicity and mutagenesis: Chemoprevention strategies with antioxidants. *Proc. Natl. Acad. Sci. U.S.A.* **2003**, *100*, 5390–5395.
40. Muran, P.; Muran, S.; Beseler, C. L.; Cavalieri, E. L.; Rogan, E. G; Zahid, M. Validating tools for the prevention of breast cancer. **2015**, in preparation.

Publication Date (Web): October 13, 2015 | doi: 10.1021/bk-2015-1200.ch002

Publication Date (Web): October 13, 2015 | doi: 10.1021/bk-2015-1200.ch003

Chapter 3

Oxidative Stress, Redox Homeostasis and NF-κB Signaling in Neurodegeneration

Annadurai Anandhan, Pablo Hernandez-Franco, and Rodrigo Franco*

Redox Biology Center and School of Veterinary Medicine and Biomedical Sciences, University of Nebraska-Lincoln, Lincoln, Nebraska 68583, United States

***E-mail: rfrancocruz2@unl.edu**

NF-κB is a multifunctional redox sensitive transcription factor. In neurodegenerative disorders such as Alzheimer's, Huntington's, Parkinson's disease and amyotrophic lateral sclerosis (ALS), inducible NF-κB activation is observed in glial cells (astrocytes and microglia) as an inflammatory response that regulates the expression of cytokines, chemokines and adhesion molecules as well as the generation of reactive oxygen (ROS) and nitrogen species (RNS). As such, NF-κB activation is thought to contribute to neuronal loss. However, there is strong evidence demonstrating that in neurons, NF-κB protects against cell death progression by regulation of anti-apoptotic genes. Understanding the molecular pathways involved in NF-κB activation during neurodegeneration and its downstream signaling mediating pro-survival, pro-death and inflammatory responses will provide novel targets for therapeutic intervention. In this chapter we revise the role of NF-κB in neurodegeneration, its role in oxidative stress and antioxidant defense in the brain, and its regulation by redox homeostasis and oxidative stress.

Introduction

Inducible regulation of gene expression allows organisms to respond and adapt to stress conditions. Signal transduction mediated by the nuclear factor

In Oxidative Stress: Diagnostics, Prevention, and Therapy Volume 2; Hepel, et al.; ACS Symposium Series; American Chemical Society: Washington, DC, 2015.

Publication Date (Web): October 13, 2015 | doi: 10.1021/bk-2015-1200.ch003

kappa-light-chain-enhancer of activated B cells (NF-κB) family of transcription factors plays a pivotal role in a myriad of cellular responses to stress conditions including host immune and inflammatory responses, regulation of cell death and survival signals and antioxidant defenses. Stimulation of the NF-κB pathway is mediated by diverse signal transduction cascades. Dysregulation of NF-κB signaling can contribute to human diseases such as cancer, chronic inflammatory diseases, heart disease, autoimmune and neurodegenerative disorders (*1*).

NF-κB activation has involved in neurodegenerative disorders where inflammation has been proposed as a causative mechanisms contributing to neuronal cell death (*2*, *3*). Interestingly, there is also strong evidence demonstrating that in neurons, NF-κB signaling primarily protects them from cell death progression (*4*, *5*). It is still poorly understood the exact role of NF-κB signaling in neuronal cell loss linked to neurodegeneration. Furthermore, the molecular mechanisms involved in its regulation/activation and downstream effects are still unclear. However, evidence so far highlights the potential for targeted therapeutic intervention of NF-κB signaling in neurodegeneration. In the present chapter, we discuss the role of oxidative stress / redox homeostasis on NF-κB signaling and its implications in neurodegeneration.

The NF-κB Signalosome: A Brief Summary

Mammalian NF-κB signaling is mediated by dimeric transcription factors from the Rel homology domain or region (RHD or RHR)-containing protein family that includes RelA (p65), RelB, c-Rel, p50 and p52. p50 and p52 are processed via the ubiquitin-proteasome system (UPS) from the p105 (NF-κB1) and p100 (NF-κB2) precursor proteins, respectively. The RHD is a structurally conserved 300 amino acid sequence, which contains the dimerization, nuclear localization, and DNA binding domains. NF-κB refers to homo- and heterodimeric DNA binding complexes as the result of dimerization of the five monomers. From the 15 possible dimer combinations only 9 have potential transcriptional activity (p50 and p52 only dimers lack transcriptional activity and RelB and RelA, c-Rel or RelB only dimmers do not bind DNA). NF-κB dimer availability is regulated transcriptionally and homeostaticaly in a cell type and stimulus (environment) specific manner (Figure 1) (*6*–*8*).

NF-κB dimers are negatively and stochiometrically regulated by IκB inhibitors via binding through IκBs' ankyrin repeat domain (ARD). IκB proteins identified include IκBα, IκBβ, IκBε, and the precursor proteins p100 (IκBγ) and p105 (IκBδ), this last two with non-classical IκB activity as high molecular weight complexes (IκBsome). NF-κB dimers bound to IκBs are sequestered in the cytoplasm. Two major general signaling pathways lead to the activation of NF-κB that relies on inducible phosphorylation of IκBs, leading to nuclear translocation of NF-κB complexes. Canonical NF-κB activation is mediated by IκB kinase (IKK) trimeric complexes composed of two catalytic subunits, IKKα (IKK1) and/or IKKβ (IKK2), and the NF-κB essential modulator (NEMO, also known as IKKγ) (*6*), which act on IκBα, IκBβ, IκBε and p105 (IκBγ). Noncanonical NF-κB is mediated by complexes requiring IKKα and the NF-κB inducing kinase (NIK)

In Oxidative Stress: Diagnostics, Prevention, and Therapy Volume 2; Hepel, et al.;
ACS Symposium Series; American Chemical Society: Washington, DC, 2015.

acting on p100 (IκBδ). NIK activates IKKα, whereas IKKβ can be activated by multiple kinases (*9*). Phosphorylated IκBs are subsequently degraded by the UPS, or in the case of p100 and p105 processed to p52 or p50 monomers (Figure 1) (*6*, *7*). Nuclear IκB proteins Blc-3, IκBζ and IκBNS are primarily localized in the nucleus and bind specifically homodimers also regulating gene expression. IκB proteins are thought to associate preferentially with a specific subset of NF-κB dimmers (*6*–*8*). However, the specific role of each IκB protein in regulating NF-κB signaling is still not understood completely.

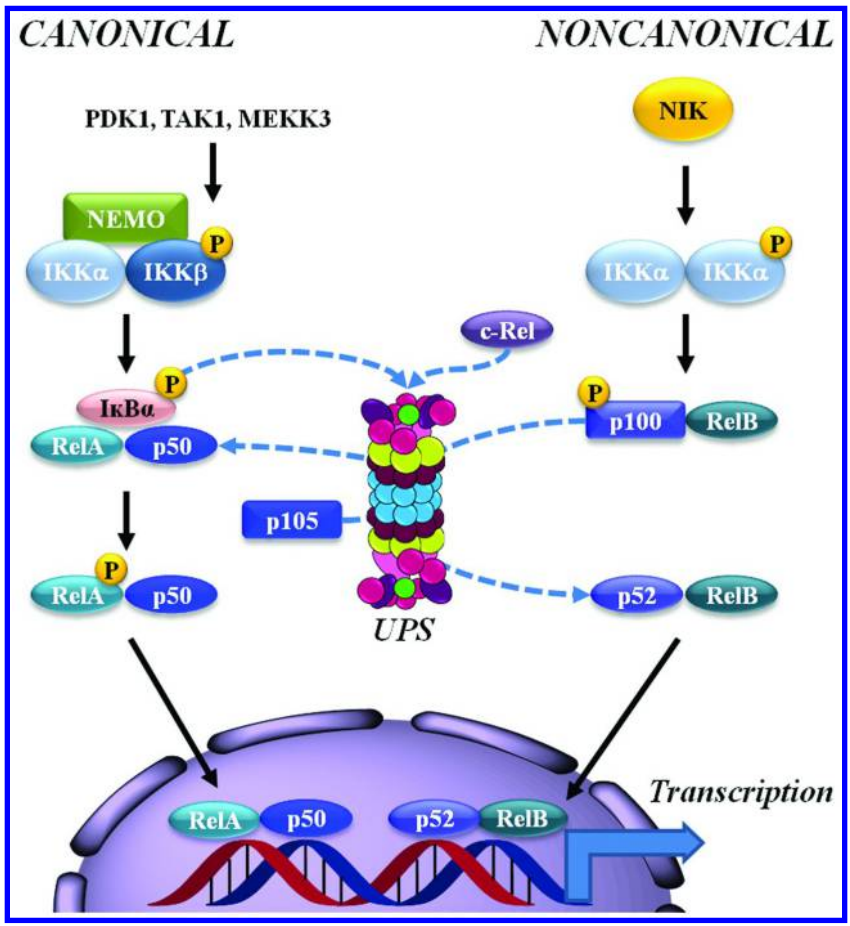

Figure 1. NF-κB dimers are sequestered in the cytosol when bound to IκB proteins, including the IκB-like function of p100 and p105. Stimulus-induced phosphorylation of IκB by IKK complexes induces its degradation or processing via the UPS. Canonical activation of NF-κB is mediated by the trimeric complex: IKKα and/or IKKβ, and NEMO. Noncanonical activation involves IKKα dimers. While a number of kinases activate canonical complexes, NIK is primarily involved in noncanonical activation of NF-κB signaling. Released NF-κB dimers translocate to the nucleus to mediate transcription. MEKK3, MAP/ERK kinase kinase 3.

In Oxidative Stress: Diagnostics, Prevention, and Therapy Volume 2; Hepel, et al.;
ACS Symposium Series; American Chemical Society: Washington, DC, 2015.

Publication Date (Web): October 13, 2015 | doi: 10.1021/bk-2015-1200.ch003

NF-κB signaling is controlled by a number of additional mechanisms. In the nucleus NF-κB dimers bind to κB sites within the promoters/enhancers of target genes and regulate transcription through the recruitment of co-activators and co-repressors. The C-terminal regions of RelA, RelB and c-Rel contain a transactivating domain that is important for NF-κB-mediated gene transactivation. Acetylation of NF-κB is important for its activation and resistance to the inhibitory effects of IκB binding. RelA degradation via nuclear proteasomes has also been proposed as a mechanism to terminate NF-κB signaling. NF-κB signaling is modified and modulated at every single step in its signaling cascade by distinct signaling pathways (*6–8*). In addition, NF-κB signaling system components such as IKKα or IKKβ, affect the function of many other signaling pathways and transcription systems in a NF-κB-independent manner (*1*).

Publication Date (Web): October 13, 2015 | doi: 10.1021/bk-2015-1200.ch003

Oxidative Stress and Neurodegeneration

Oxidative stress is defined as the increase in the steady-state levels of reactive species of oxygen (ROS) or nitrogen (RNS) and their oxidative byproducts, as a result of increased production or impaired antioxidant mechanisms. Oxidative damage arises when oxidative modifications in biomolecules (proteins, lipids and nucleic acids) cannot be repaired or efficiently turned over and thus, cellular dysfunction persists. ROS, primarily superoxide anion ($O_2^{\bullet-}$), are generated as either a byproduct of metabolism, mitochondrial dysfunction, or activation of ROS generating systems such as the nicotinamide adenine dinucleotide phosphate (NADPH)-oxidases (NOX). In general it is considered that generation of one ROS has the potential to convey a cascade that generates distinct and more reactive species. $O_2^{\bullet-}$ can be dismutated by $O_2^{\bullet-}$ dismutases (SODs) generating hydrogen peroxide (H_2O_2), which in the presence of metals (Fenton-like reactions) can produce the highly reactive hydroxyl radical ($OH^{\bullet}$) (Figure 2) (*10–12*). RNS are primarily derived from the formation of nitric oxide ($NO^{\bullet}$) by nitric oxide synthases (NOS). In the presence of $O_2^{\bullet-}$, $NO^{\bullet}$ generates peroxynitrite ($ONOO^-$) (Figure 2) (*13*). Additional sources of reactive species exist. In glial cells, myeloperoxidases (MPOs) are peroxidase enzymes that produce hypochlorous acid (HOCl) from H_2O_2 using heme as a cofactor (*14*) (Figure 2). Cyclooxygenases (COXs) are also known to generate ROS as a byproduct of the metabolism of arachidonic acid. COXs metabolize arachidonic to prostaglandin G2 (PGG_2) and produce peroxyl radicals. COXs also possess a heme-containing active site that provides peroxidase activity that may oxidize various co-substrates and produce $O_2^{\bullet-}$ (*15*).

Intrinsic cellular antioxidant mechanisms maintain a tight homeostatic control of ROS/RNS generated under physiological conditions, and help detoxify their excessive accumulation in pathological conditions (Figure 2). Catalase enzymatically decomposes H_2O_2 to H_2O and O_2 and is primarily localized in the peroxisomes (*10–12*). Glutathione (L-γ-glutamyl-L-cysteinyl-glycine, GSH) is the most abundant non-protein thiol in mammalian cells acting as a major reducing

In Oxidative Stress: Diagnostics, Prevention, and Therapy Volume 2; Hepel, et al.;
ACS Symposium Series; American Chemical Society: Washington, DC, 2015.

agent for antioxidant defense against peroxides via the enzymatic activity of GSH peroxidases (Gpxs) and peroxiredoxin 6, and the detoxification of electrophiles via the action of GSH-S-transferases (GSTs) (*16*). Heme-oxygenase (HO) is a microsomal enzyme that catalyzes heme degradation playing an important role in Fe^{2+} recycling. HO activity results in decreased oxidative stress by removal of heme, a potent pro-oxidant (Figure 2) (*17*). NF-κB signaling has been reported to directly regulate the transcription of both ROS/RNS generating enzymes (NOXs, NOS, COX-2) and antioxidant defenses (GCLC, GCLM, SOD1 [CuZnSOD], SOD2 [MnSOD], HO-1). A seemingly complete list of genes regulated by NF-κB is found in (http://www.bu.edu/nf-kb/).

Neurodegenerative diseases are defined as hereditary or sporadic conditions characterized by progressive and selective neuronal cell loss, which include: Alzheimer's Disease (AD) and other dementias, Parkinson's Disease (PD), Huntington's Disease (HD), Amyotrophic Lateral Sclerosis (ALS or Lou Gehrig's Disease), and others. Solid evidence has demonstrated that oxidative stress plays a central role in the initiation of neuronal damage in neurodegeneration. We next briefly summarize the main proposed mechanisms involved in oxidative stress in neurodegenerative disorders (Figure 2), but more detailed information can be found elsewhere (*18–21*).

Publication Date (Web): October 13, 2015 | doi: 10.1021/bk-2015-1200.ch003

Alzheimer's Disease (AD)

AD primarily affects neuronal populations in the cerebral cortex and hippocampus. Among the characteristics found in postmortem brains of AD patients are senile plaques, which contain amyloid-β peptide (Aβ) derived from the amyloid precursor protein (APP). Neurofibrillary tangles are also found in postmortem brains of AD patients containing pathologically aggregates of hyperphosphorylated tau protein (*22*). Accumulation of byproducts of biomolecule oxidative damage has been found in brains from AD and mild cognitive-impairment (MCI) patients (*23*, *24*), as well as in transgenic AD mouse models (*25*). Previous studies implicate Aβ as the mediator of oxidative stress (*26*). AD pathogenesis may be influenced by early life exposures to toxic metals (*27*). Aβ interacts with several metal ions such as Fe^{+2} and Cu^{+2} to mediate the production of H_2O_2 and $OH^{\bullet}$ (*28*) (Figure 2). Mitochondrial dysfunction in AD has been related to the accumulation of Aβ within mitochondria (*29*). The receptor for advanced glycation end products (RAGE) and perturbations in neuronal Ca^{2+} homeostasis have also been proposed to mediate mitochondrial dysfunction and ROS formation (*30*, *31*). MPO levels have been found increased in AD brains (*32*), while COX-2 inhibition is reported to improve the memory and synaptic plasticity in AD models (*33*, *34*). Aβ and ApoE epsilon 4 allele (*ApoE4*), a risk factor for AD, induce an increase in NOS expression and $NO^{\bullet}/ONOO^{-}$ generation in glial cells. However, whether NOS activation depends on cytokine release and/or canonical or noncanonical NF-κB signaling remains unclear (*35–39*). Aβ has also been shown to induce COX-2 upregulation via NF-κB in catecholaminergic cells (*34*).

In Oxidative Stress: Diagnostics, Prevention, and Therapy Volume 2; Hepel, et al.;
ACS Symposium Series; American Chemical Society: Washington, DC, 2015.

Publication Date (Web): October 13, 2015 | doi: 10.1021/bk-2015-1200.ch003

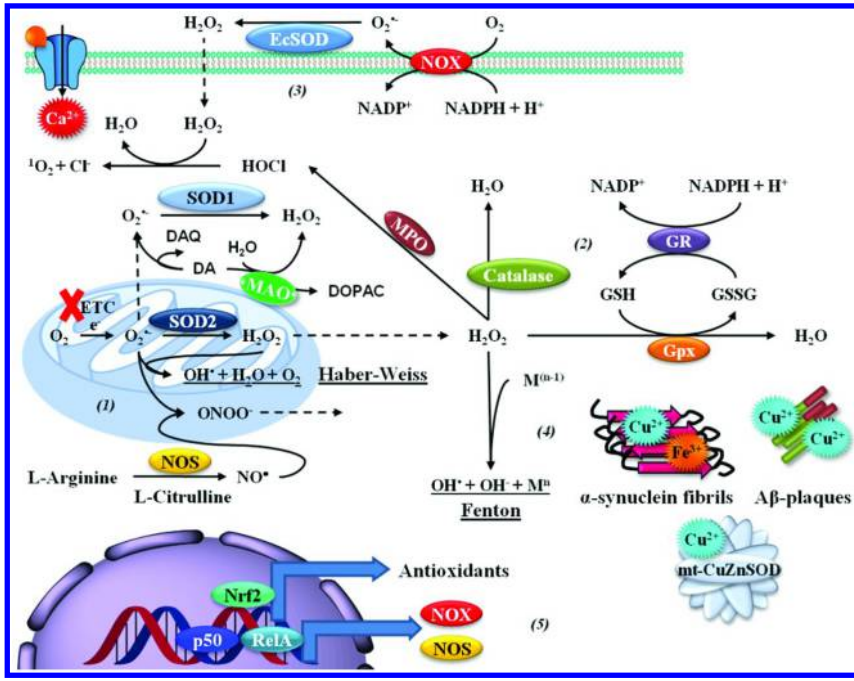

Figure 2. ***Oxidative stress in neurodegenerative diseases.*** ***(1)*** *Mitochondrial dysfunction is the primary source for ROS in neurodegenerative disorders.* $O_2^{\bullet-}$ *can lead to the generation of a number of reactive species including* $ONOO^-$ *and* $^{\bullet}OH$. ***(2)*** *Antioxidant defenses maintain a tight control in the redox balance of the cell. Catalase and Gpxs catalyzes the decomposition of peroxides and also regulate redox signaling mediated by oxidative post-translational modifications.* ***(3)*** *In the brain, the extracellular environment is a major contributor to oxidative stress. Activation of glial cells by cytokines or misfolded protein aggregates (Aβ-plaques) leads to the production of reactive species that can target neuronal populations.* Ca^{2+} *increase by excitatory amino acids also mediates mitochondrial dysfunction and activation of ROS/RNS generating systems.* ***(4)*** *Misfolded protein aggregates also contribute to oxidative damage by aberrant redox chemistry involving their interaction with metals.* ***(5)*** *Transcriptional regulation of NOX and NOS upon activation of the NF-κB by (oxidative) stress or cytokines contributes to ROS/RNS formation. Both NF-κB and Nrf2 activation regulates the expression of antioxidant defenses.GR, GSH-reductase; EcSOD, extracellular SOD.*

Parkinson's Disease (PD)

PD is a neurodegenerative disorder characterized by the selective loss of A9 dopaminergic neurons of the substantia nigra pars compacta (SNpc). The accumulation of α-synuclein in intraneuronal proteinaceous inclusions known as Lewy bodies is the pathological hallmark of PD (*40*, *41*). A fraction of PD occurrence is related to mutations in genes such as α-synuclein (*SNCA*), DJ-1

In Oxidative Stress: Diagnostics, Prevention, and Therapy Volume 2; Hepel, et al.;
ACS Symposium Series; American Chemical Society: Washington, DC, 2015.

(PARK7), PTEN-induced putative kinase 1 (*PINK1*), leucine rich repeat kinase 2 (*LRRK2*) and parkin (*PARK2*). However, 90% of PD cases occur in a sporadic (idiopathic) form without a defined genetic basis. The major risk factor identified for PD is aging as its occurrence increases exponentially from ages 60 to 90 (*42*, *43*). Epidemiological evidence shows an increase in the risk of developing PD upon the exposure to environmental toxicants and inflammatory processes (*44*). Oxidative damage to biomolecules including lipids, proteins and DNA is found in the cerebrospinal fluid (CSF) of PD patients and post-mortem PD brains (*45–51*). SNpc dopaminergic cells have high levels of basal oxidative stress compared to other dopaminergic neuronal populations (*52*). In addition, a decrease in the activity of the mitochondrial ETC is found in the SNpc of patients with PD (*53–55*) suggesting that oxidative stress is linked to mitochondrial dysfunction. PD-associated genes have also been shown to modulate or induce oxidative stress in dopaminergic cells. Accumulation of α-synuclein has been suggested to trigger mitochondrial oxidative stress (*56*). DJ-1, PINK1 and Parkin deficiency or mutations render cells more susceptible to oxidative stress and mitochondrial dysfunction (*57–60*). Gain-of-function of LRRK2 mutations disturb mitochondrial dynamics leading to increased ROS formation (*61*).

Metal-induced ROS generation has also been postulated to contribute to oxidative damage in PD (*62*). Metal ions bind to α-synuclein to induce ROS formation and dopamine (DA) oxidation (*63*, *64*). Increased Fe^{+2} deposition and increased free Fe^{+2} concentrations have been found in the SNpc of PD brains, which may lead to increased generation of $OH^{\bullet}$ (*65*). Oxidative stress in PD is also associated with the pro-oxidant properties of DA. which is either metabolized by monoamine oxidase (MAO) to generate H_2O_2, or auto-oxidized in the presence of Fe^{+2} generating $O_2^{\bullet-}$, H_2O_2 and DA-quinone species (DAQ) (*66*). NOX, NOS, MPO and COX-2 also mediate ROS generation in dopaminergic and microglial cells upon treatment with PD-related toxicants (*67–76*), which seems to involve NF-κB signaling (*77*).

Huntington's Disease (HD)

HD is an autosomal dominant neurodegenerative disorder caused by CAG trinucleotide repeat expansion in the exon-1 of the huntingtin (Htt) gene (*IT15*). Mutant (mt)-Htt containing polyglutamine repeats becomes misfolded, aggregates and resists degradation (*78–80*). Several biomarkers of oxidative stress including lipid peroxidation, nucleic acid and protein oxidation byproducts, are increased in HD brains, and in the serum and leukocytes of patients diagnosed with HD (*81–90*). Mt-Htt selectively affects medium spiny striatal neurons, and oxidative stress together with mitochondrial dysfunction have been implicated in the pathology of HD (*91*). Transgenic mice expressing mt-Htt gene develop a progressive neurologic disorder and present increased levels of oxidative stress (*92*). Striatal cells expressing mt-Htt show higher levels of mitochondrial-generated ROS and mitochondrial DNA damage (*93*). Impaired activity of the electron transport chain (ETC) and tricarboxylic acid cycle enzymes has been found in brains of HD patients (*94–96*). Succinate dehydrogenase (SDH) or complex II subunits Fp (FAD) and Ip (iron–sulphur cluster) are found reduced

In Oxidative Stress: Diagnostics, Prevention, and Therapy Volume 2; Hepel, et al.;
ACS Symposium Series; American Chemical Society: Washington, DC, 2015.

Publication Date (Web): October 13, 2015 | doi: 10.1021/bk-2015-1200.ch003

in HD brains and in striatal neurons overexpressing the N-terminal fragment of mt-Htt. Accordingly, administration of complex II inhibitors such as malonate and 3-nitropropionic acid (3-NP) *in vivo* induce both biochemical and clinical alterations that resemble those in HD. The iron–sulphur containing dehydratase aconitase, is one of the most affected tricarboxylic acid cycle enzymes in HD (*94*). 3-NP toxicity is enhanced by DA (*97*, *98*). In addition, 3-NP induces a decrease in ATP levels and the activation of excitatory amino acid receptors, which mediate ROS formation (*99*). A recent report demonstrates that aggregation of a polyglutamine Htt fragment directly causes ROS formation (*100*).

Amyotrophic Lateral Sclerosis (ALS)

ALS is characterized by the progressive degeneration of motor neurons in the motor cortex and lower motor neurons connecting the spinal cord and brain stem to muscle fibers. ALS typically develops between 50 and 60 years of age as a relentless progressive neuromuscular failure leading to muscle denervation and atrophy. Only ~10% of ALS cases have a clear inherited genetic component, while the majority are sporadic. Approximately 10-20% of the familial ALS cases are caused by dominant mutations in the copper-zinc SOD (CuZnSOD) gene (*SOD1*). Increased oxidative stress biomarkers are found in ALS postmortem tissues, such as brain and spinal cord as well as in cerebrospinal fluid and *in vivo* models (*101–105*). It is now widely accepted that loss of SOD1 dismutase activity is not sufficient to cause ALS (*106*). SOD1 mutants induce NOX-dependent ROS production in microglia, and neuronal death (*107*). Dysregulation of proteins involved in Fe^{+2} homeostasis has also been shown in mouse overexpressing mutant SOD1. Similarly, aberrant coordination of Cu^{2+} by mutant SOD1 has also been demonstrated to mediate oxidative stress (*108*). Mutations in the fused in sarcoma (FUS/TLS) and the TAR DNA-binding protein (TDP-43) are responsible for 5-10% of familial and 1% of sporadic cases. FUS and TDP-43 are DNA- and RNA- binding proteins involved in transcriptional regulation, pre-RNA slicing and micro-RNA processing. Cytoplasmic inclusions of TDP-43 and FUS are pathological hallmarks of most non-SOD1 sporadic ALS cases, in frontotemporal lobar degeneration (FTLD) and in 25-50% of AD cases. TDP-43 overexpression induces mitochondrial dysfunction and oxidative stress (*109*).

Oxidative Stress, Redox Homeostasis and NF-κB Signaling

NF-κB signaling is shown to respond directly to oxidative stress or to a large number of conditions and agents that induce ROS formation such as inflammatory cytokines, mitogens, bacterial products, protein synthesis inhibitors and ultraviolet (UV) radiation. H_2O_2 directly activates NF-κB signaling in some cells (*110*). In addition, overexpression of superoxide dismutase (SOD) enhances activation of NF-κB (*111*). Inducers of NF-κB signaling, including lipopolysaccharides (LPS), tumor necorsis-alpha (TNFα), and interleukin-1 (IL-1), produce oxidative stress in cells. Accordingly, treatment with several antioxidants such as N-acetylcysteine (NAC), α-lipoic acid, free-radical scavengers and metal chelators block NF-κB

Publication Date (Web): October 13, 2015 | doi: 10.1021/bk-2015-1200.ch003

activation. However, it is important to consider that the effects of these compounds are not always related to their antioxidant properties. Overexpression of catalase and Gpxs also inhibit NF-κB activation (*112*). Recent reports have demonstrated that H_2O_2 activates NIK (*113*). Thus, it is clear that ROS mediate/regulate NF-κB activation (*114*). While the exact mechanisms are still unclear, evidence so far suggests a large degree of specificity depending on the pro-oxidant stimuli involved. We next summarize the possible mechanisms by which NF-κB signaling can be directly or indirectly regulated by oxidative stress and redox homeostasis (Figure 3).

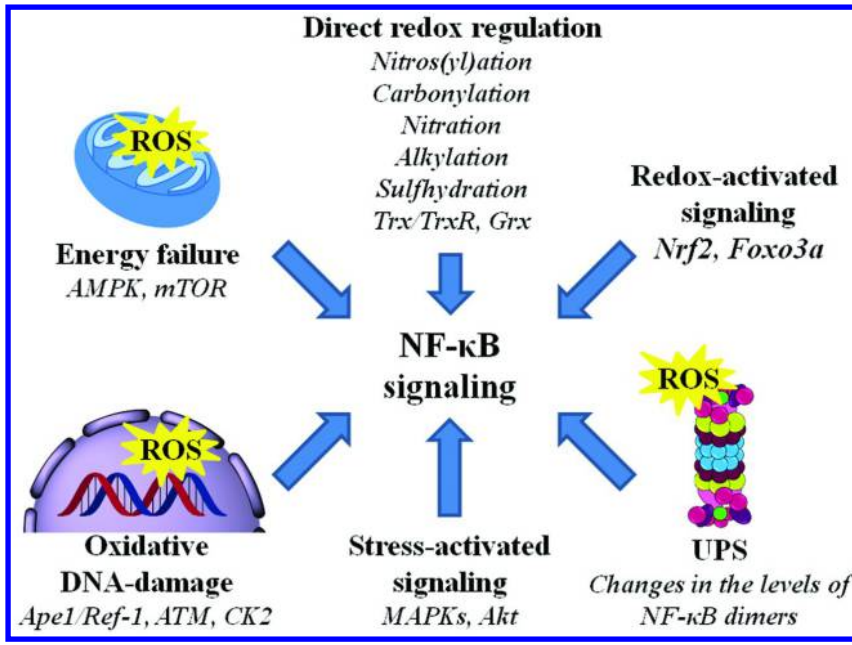

Figure 3. ***Redox regulation of NF-κB.*** *Proposed mechanisms by which oxidative stress and changes in the redox environment can regulate NF-κB signaling directly or indirectly.*

Publication Date (Web): October 13, 2015 | doi: 10.1021/bk-2015-1200.ch003

Redox Regulation of NF-κB Signaling

Oxidative protein modifications mediate the integration of redox changes and the activation of signal transduction pathways (*115–117*). Redox-sensitive thiols in cysteines undergo reversible and irreversible modifications in response to ROS or RNS, thereby modulating protein function, activity, or localization. Almost all physiological oxidants react with thiols (*118*, *119*). $O_2^{\bullet-}$ and peroxides mediate one- and two-electron oxidation of protein cysteines respectively, leading to the formation of reactive intermediates including protein sulfenic acids (PSOH) and protein thiyl radicals (PS•). PSOH can lead to the formation of additional oxidative modifications that act as signaling events regulating protein function.

The reaction of PSOH with either a neighboring cysteine or GSH will generate a disulfide bond or a glutathionylated residue (PSSG) respectively, which is reversed primarily by the activity of the oxidoreductases thioredoxin (Trx) and glutaredoxin (Grx), respectively. A similar outcome will be obtained by reaction of a PS• with another thyil radical. PSOH can undergo further oxidation to irreversibly generate protein sulfinic (PSO_2H), and sulfonic (PSO_3H) acids (*115–117*). Cysteine nitros(yl)ation (PSNO) refers to the reversible covalent adduction of a nitroso group to a protein cysteine thiol. PSNO formation is mediated by nitros(yl)ating agents such as dinitrogen trioxide (N_2O_3) or by transition metal catalyzed addition of a nitroso group. Nitroso-GSH (GSNO) is formed during the oxidation of nitric oxide (NO•) in the presence of GSH, and as a minor byproduct from the oxidation of GSH by $ONOO^-$. Transfer of NO groups between PSNO and GSNO (transnitros(yl)ation) has been reported as one of the major mechanisms mediating PSNO (*120*). Trxs also reduce PSNOs. The Trx redox system depends on thiol-disulfide exchange reactions at the active site. Trx reductase (TrxR), a homodimeric selenium containing flavoprotein, transfers reducing equivalents from NADPH to Trxs reducing them (*121*).

NF-κB signaling is directly modulated by reversible oxidative modifications (Figure 3) (*122*, *123*). Cysteine (Cys) residue 62, located in the N-terminal DNA-binding region, is highly conserved in NF-κB proteins and its oxidation (including nitros(yl)ation or glutathionylation) or alkylation modification decreases their ability to bind DNA (*124–129*). Oxidation (nitros(yl)ation and glutathionylation) of IKKβ (Cys179) also inhibit its activity (*130–132*). Accordingly, Grx and Trx/TrxR restore NF-κB signaling (*131*, *133–138*). Hydrogen sulfide (H_2S) is a reactive species generated by the activity of cystathionine γ-lyase (cystathionase; CSE) and cystathionine β-synthase (CBS). H_2S has the ability to sulfhydrate Cys thereby altering and enzymes function or activity. Cys38 sulhydration of RelA increases its DNA-binding activity and anti-apoptotic signaling (*139*). For the most part, previous studies have demonstrated the protective role of Grx, Trx/TrxR and H_2S against neurodegeneration (*140–147*), but whether their effects are ascribed to maintenance of NF-κB signaling has not been explored. Irreversible oxidative modifications also regulate NF-κB signaling (Figure 3). Carbonylation and tyrosine (Tyr) nitration (Tyr66 and Tyr152) of RelA inhibits its activation (*148*, *149*). In contrast nitration of IκBα (Tyr181) has been shown to activate NF-κB (*150*).

Due to its highly regulated nature and crosstalk with a number of signal transduction pathways, NF-κB signaling can be activated / regulated by oxidative stress and ROS/RNS through a number of mechanisms, again, with a high degree of crosstalk between them (Figure 3).

Oxidative DNA-Damage and NF-κB Signaling

DNA damage can be induced directly by the interaction of DNA with various ROS or indirectly as the result of alterations in DNA repair. DNA lesions that usually arise from persistent endogenous oxidative stress are apurinic / apyrimidinic (abasic; AP) DNA sites, oxidized purines and pyrimidines, single

In Oxidative Stress: Diagnostics, Prevention, and Therapy Volume 2; Hepel, et al.;
ACS Symposium Series; American Chemical Society: Washington, DC, 2015.

Publication Date (Web): October 13, 2015 | doi: 10.1021/bk-2015-1200.ch003

stranded DNA breaks (SSBs) and double stranded DNA breaks. DNA damage response in cells can effectively detect DNA lesions, signal their presence and promote their repair (*151*). The base excision repair pathway (BER) repairs oxidized bases by their excision via DNA glycosylases generating AP sites, which are subsequently processed by AP-endonucleases (Ape1/Ref-1). Ape1 promotes the reduction and activation of NF-κB via glutathione, Grxs and Trx, exerting a protective effect against dopamine-induced neuronal cell death (*152*, *153*).

The response to genotoxic stress starts with the detection of the DNA damage and activation of transcription factors involved in DNA repair, cell cycle arrest, and if DNA repair fails, activation cell death. Different sensors for DNA damage repair and for the regulation of cell cycle checkpoints have been identified including members of the phosphoinositide 3-kinase-like kinase family: ataxia telangiectesia mutated (ATM), ATM and Rad3 related (ATR), and DNA-dependent protein kinases (DNA-PK) (*154*, *155*). NF-κB signaling is activated as part of the DNA-damage response to promote primarily cell survival, but in some circumstances it can contribute to cell death progression (*156*) (Figure 3). Interestingly, NF-κB activation has also been shown to promote DNA repair (*157*). Activation of NF-κB signaling by DNA damage seems to require functional IKK canonical complexes (IKKα, IKKβ and NEMO). ATM-induced activation of NF-κB signaling has been proposed to involve direct phosphorylation of IκBα by ATM, regulation of NEMO sumoylation/phosphorylation, and/or ubiquitination / phosphorylatipon of the transforming growth factor β-activated kinase 1 (TAK1) (*156*, *158–160*). ATM also mediates the activation and stabilization of p53 in response to DNA damage, which exerts an antagonistic role for NF-κB signaling (*156*, *161*, *162*). Importantly, ATM can be directly activated by oxidative stress (*163*). No evidence exists so far regarding the activation of NF-κB signaling via ATR. However, an antagonistic effect of ATR on ATM-NF-κB signaling was recently described (*164*). DNA-PK mediated activation of NF-κB signaling has also been reported, which seems to depend on the IKK canonical complex or phosphorylation of p50 (*165*, *166*). Interestingly, activation of NF-κB signaling by UV radiation, a major promoter of oxidative DNA-damage, is independent from the canonical IKK complex, and involves casein kinase 2 (CK2) activation (*156*), which is required for assemble and activity of DNA repair protein complexes (*167*).

Aging, the major risk factor for most neurodegenerative disorders, is paralleled by the accumulation of byproducts of oxidative DNA-damage (*168*, *169*). Post-mitotic terminally differentiated brain cells lack robust replication-associated DNA damage detection and DNA repair machinery as evidenced by the accumulation of oxidative DNA damage with age. Recent studies suggest that deficiencies in oxidative DNA-damage repair contribute to the neurodegenerative process (*170*). Consistently, AD and HD post-mortem brain samples show accumulation of DNA-damage. ATM is activated in mouse models of HD, AD and in neuronal cell death induced by the PD-related toxicants. Knockdown or inhibition of ATM prevents mt-Htt and toxicant (PD)-induced toxicity (*171*, *172*). In contrast, CK2 has been shown to be protective against mt-Htt (*173*). CK2-mediated phosphorylation of α-synuclein contributes to its degradation and aggregation (*174*) and Aβ has been reported to inhibit DNA-PK

Publication Date (Web): October 13, 2015 | doi: 10.1021/bk-2015-1200.ch003

activity (*175*). However, none of these effects have been related so far to the regulation of NF-κB signaling.

Energy Dysfunction and NF-κB Signaling

As the major source for ROS formation, mitochondrial oxidative damage is well recognized to mediate energy dysfunction in neurodegeneration. Neurons primarily metabolize glucose via the pentose phosphate pathway (PPP) to provide reducing equivalents required to maintain antioxidant defenses via the production of NADPH (*176*). In contrast, to glial cells, neurons cannot upregulate glycolysis in response to stress, and astrocytes are thought to shuttle lactate to neurons as supplementary energy fuel (*177*) (Figure 4). Cellular energy status is monitored by specific signaling mechanisms. The adenosine monophosphate (AMP)-activated protein kinase (AMPK) is a cellular energy sensor and signal transducer regulated by a wide array of metabolic stresses. AMPK activation requires phosphorylation of their activation loop by upstream kinases such as the liver kinase B1 (LKB1). The activity of AMPK is allosterically enhanced by AMP binding, and because cellular concentrations of AMP (or ADP, which also plays a regulatory role) are much lower than those of ATP, a small decrease in ATP can be effectively sensed by AMPK (*178*). Recently, AMPKα1 has been shown to interact and regulate TAK1 activation, and thereby NF-κB signaling (Figure 3) (*179*). The mammalian target of rapamycin (mTOR) is regulated by metabolic signals such as growth factors, amino acids, and cellular energy. mTOR forms two distinct complexes, mTOR complex 1 (mTORC1) and mTORC2. mTORC1 is regulated by cellular energy and nutrient status (*178*). mTOR has also been recently suggested to regulate NF-κB signaling (*180*, *181*) (Figure 3). Conversely, NF-κB signaling has been shown to regulate mitochondrial respiration (*182*, *183*), but the mechanisms involved remain unclear.

Mitochondrial dysfunction and energy failure are central events in the etiology of neurodegenerative disorders (*19*, *184*, *185*). Despite the importance of both AMPK and mTOR signaling cascades in the regulation of energy metabolism and adaptation, their role in neurodegeneration is largely unclear. Mt-Htt was shown to stimulate mTORC1 signaling and contribute to striatal neuronal neurodegeneration (*186*). However, recent reports have demonstrated that mTORC1 activity is actually impaired in HD patients and when restored, it exerts protective effects against mt-Htt (*187*). mTOR regulates Tau phosphorylation and aggregation (*188*). Rapamycin, an allosteric inhibitor of mTOR protects neurons from PD-related toxin insults (*189*), enhances clearance of TDP-43 aggregates linked to ALS (*190*), and rescues cognitive deficits by ameliorating Aβ and Tau pathology in an AD mouse model (*191*). AMPK has been shown to phosphorylate Tau as well (*192*), and its knockdown reduced Aβ deposits and rescues memory deficits in an AD mouse models (*193*). In contrast, other studies report that AMPK activation decreases the extracellular accumulation of Aβ (*194*, *195*). AMPK mediates motor neuron death in ALS models (*196*, *197*) and striatal neurodegeneration induced by mt-Htt (*198*). Contradictory results exist regarding the role of AMPK in dopaminergic cell death. A protective role for AMPK against mitochondrial dysfunction induced by parkin-, α-synuclein,

Publication Date (Web): October 13, 2015 | doi: 10.1021/bk-2015-1200.ch003

leucine-rich repeat kinase 2 (LRRK2)-mutations, and PD-related toxicants has been reported (*199–201*). In contrast, AMPK activation has been shown to facilitate α-synuclein aggregation (*202*) and the toxicity of DA analogs, as well as mitochondrial toxins (*203*, *204*). We have observed that AMPK exerts a protective role against dopaminergic cell death induced mitochondrial toxins and by the pesticide paraquat, a major risk factor in PD (*unpublished data*). These contradictory findings are likely related to the number of homeostatic signals regulated by mTOR and AMPK including NF-κB signaling, autophagy, energy balance, mitochondrial biogenesis and survival signals, and unfortunately, to the use of non-specific pharmacological agents to modulate mTOR and AMPK signaling.

Publication Date (Web): October 13, 2015 | doi: 10.1021/bk-2015-1200.ch003

Alterations in the Ubiquitin-Proteasome System (UPS) and NF-κB Signaling

If not properly degraded, misfolded protein aggregates can cause cellular toxicity and disease. Protein degradation pathways such as the ubiquitin (Ub)-proteasome-system (UPS) and autophagy degrade misfolded or aggregated proteins to avoid proteotoxic stress (*205*). Dysfunction in protein quality control mechanisms is a hallmark in neurodegenerative diseases (*205–207*). A number of mechanisms have been proposed to impair the degradation of misfolded protein aggregates by the UPS in neurodegeneration which include: 1) energy failure linked to mitochondrial dysfunction; 2) inability of the UPS to recognize misfolded / oxidized / mutant proteins and large aggregates; 3) direct impairment of the proteasome by the same misfolded / oxidized / mutant / aggregated proteins involved in neurodegeneration; and 4) oxidative damage to UPS components (*205–208*). Several components of the UPS can present different sensitivities to oxidative damage/modulation (*209*, *210*). Deubiquitinating enzymes are also inhibited by oxidation of their catalytic Cys residue (*211*, *212*). The proteasome is more susceptible to oxidative inhibition than the Ub–conjugating enzymes (*210*, *213*). Mild to moderate oxidative stress upregulates Ub and the Ub–conjugating system promoting the formation of Ub-conjugates, and reduces proteasomal activity. In contrast, extensive but no lethal oxidative stress reduces the formation of Ub-conjugates by inactivating Ub–conjugating enzymes promoting the accumulation / aggregation of damaged / abnormal proteins (*210*). We have recently found that mitochondrial dysfunction and oxidative stress impair ubiquitin protein synthesis at the post-translational level (*unpublished data*).

As mentioned above, NF-κB signaling is tightly regulated by the activity of the proteasome (Figure 1). Processing of p105 to p50 and p100 to p52, switches their IκB-like action to NF-κB functional monomers. Furthermore, c-Rel and IκBs are actively degraded by the proteasome (*214*), suggesting that proteasome activity has the potential to regulate the specificity of NF-κB signaling by modulation of available monomers and IκBs (Figure 3). Previous reports have demonstrated that while transient oxidative stress activates NF-κB signaling, sustained oxidative conditions impair proteasomal activity, IκBα degradation, and TNFα-induced NF-κB activation (*215*).

In Oxidative Stress: Diagnostics, Prevention, and Therapy Volume 2; Hepel, et al.;
ACS Symposium Series; American Chemical Society: Washington, DC, 2015.

Publication Date (Web): October 13, 2015 | doi: 10.1021/bk-2015-1200.ch003

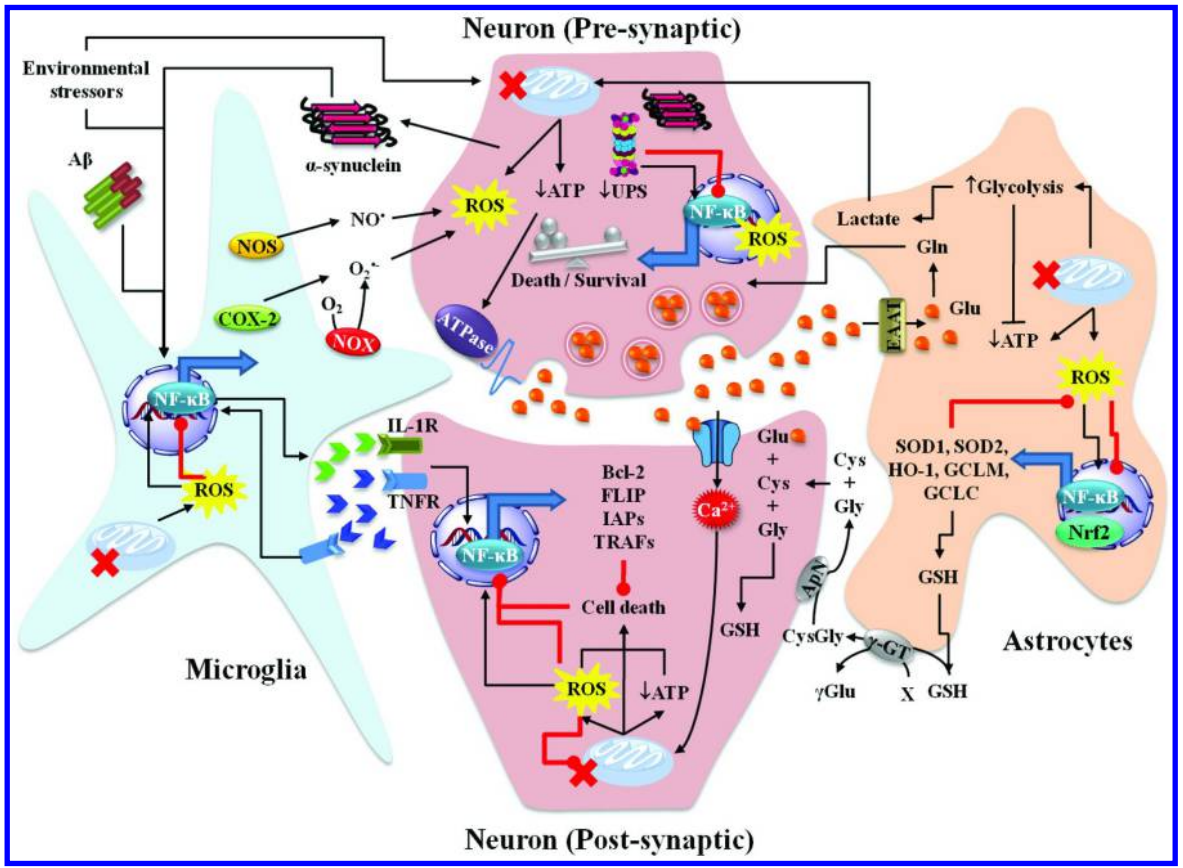

In Oxidative Stress: Diagnostics, Prevention, and Therapy Volume 2; Hepel, et al.;
ACS Symposium Series; American Chemical Society: Washington, DC, 2015.

Publication Date (Web): October 13, 2015 | doi: 10.1021/bk-2015-1200.ch003

Figure 4. ***Integrated overview of the interrelationship between oxidative stress and NF-κB signaling in neurodegenerative diseases.*** *Environmental toxicants, misfolded protein aggregates, and oxidative stress associated with neurodegeneration induce a NF-κB-dependent inflammatory response that mediates the increased expression of cytokines and ROS/RNS generating enzymes. Reactive species, released cytokines and neuronal damage-associated molecules potentiate the inflammatory response in both neurons and glial cells (see Microglia). While mitochondrial dysfunction in neurodegeneration can induce neuronal injury, glial cells have the ability to increase glycolysis to counteract energy failure. Activation of NF-κB and Nrf2 induced by oxidative stress also regulate antioxidant defenses. Astrocytes contribute to neuronal survival by active uptake of excitatory amino acids (Glu), and by supplying neurons with lactate as an alternative energy source, and precursors for de novo GSH synthesis (see Astrocyte). Activation of NF-κB signaling in neurons exerts neuroprotective effects by transcription of anti-apoptotic genes (see post-synaptic neuron). In neurons, energy failure leads to neuronal depolarization via impaired ATPase activity that leads to increase excitability (excitatory amino acid release) that contributes to neuronal cell death. Energy failure and oxidative stress impair the UPS and as a consequence the degradation of misfolded protein aggregates, as well as the processing/degradation of NF-κB monomers, which can re-direct/impair NF-κB signaling "tilting" the balance to neuronal dysfunction (see pre-synaptic neuron). ROS/RNS can both activate (black arrows) and inhibit (red dot lines) the NF-κB signaling. ApN, aminopeptidase N; ATPase, Na^+/K^+-ATPase; GCL(C or M), glutamate-cysteine ligase (C, catalytic or M, modifier subunit); γ-GT, gamma-glutamyl transferase; EAAT, excitatory amino acid transporter; IL-1R, interleukin-1 receptor; TNFR, tumor necrosis factor receptor; TRAF, TNF receptor associated factor.*

Publication Date (Web): October 13, 2015 | doi: 10.1021/bk-2015-1200.ch003

Redox-Activated Signaling and NF-κB

Inducible transcription of antioxidant genes is an important cellular defense against oxidative stress. Nuclear factor (erythroid-derived 2)-like 1 (Nrf1) and 2 (Nrf2), members of the Cap-N-Collar family of transcription factors, bind cis-acting sequences known as antioxidant response elements (ARE) or electrophile-responsive elements (EpRE) to regulate the expression of antioxidant proteins and proteins that mediate GSH synthesis or recycling (*216*). Nrf2 is kept in a cytosolic complex with the kelch-like ECH-associated protein 1 (Keap1), where it is subjected to proteasomal degradation. Oxidants or electrophiles induce a conformational change in Keap1 that allow the translocation of Nrf2 to the nucleus (*216*). Similarly, the forkhead homeobox type O (Foxo) transcription factors are critical mediators of the cellular responses to oxidative stress, but whether they are directly regulated by redox homeostasis or indirectly by stress-activated signaling remains unclear (*217*). Under certain conditions, Nrf2 regulates the GSH synthesis pathway in a NF-κB-dependent pathway (*218*). Foxo3a also promotes NF-κB signaling (*219*).

Nrf2 deficiency exacerbates dopaminergic degeneration induced by α-synuclein (*220*) and PD-related toxicants (*221–223*), as well as 3-NP/malonate-induced striatal cell loss (HD model) (*224*). The selective overexpression of Nrf2 in astrocytes protects against dopaminergic cell death induced by mitochondrial oxidative stress (*225*), and increases the survival of mutant SOD1 ALS mice (*226*). Viral-mediated delivery of Nrf2 also improves cognitive function but not Aβ burden in an AD mouse model (*227*).

Stress-Activated Signaling and NF-κB

It is widely recognized that oxidative stress induces the activation of a myriad of signaling cascades that mediate cell death progression or cell stress response. Activation of signal transduction pathways by redox changes has been shown to be mediated by direct regulation of kinases of phosphatases (*16*, *115*, *228–234*). Signaling cascades mediated by mitogen-activated protein kinases (MAPKs: p38, c-jun kinase [JNK] and the extracellular signal-regulated kinases [ERKs]), the phosphoinoisitide 3-kinase (PI3K) / 3-phosphoinositide-dependent protein kinase-1 (PDK1) / Akt (protein kinase B) axis, and protein kinase C (PKC) are well known to become activated upon oxidative stress (*232*, *233*). Furthermore, these signaling cascades are involved in either cell death progression or survival during neurodegeneration (*235–242*). Crosstalk between these signaling pathways and NF-κB suggests that under certain circumstances NF-κB activation might be the actual result from the indirect induction of any of these signaling cascades (Figure 3). A number of kinases including Akt, PDK1 and PKCζ, θ and λ, have been suggested to phosphorylate and activate IKKs acting as IKK-kinases or IKKKs (*1*, *243*). Phosphorylation of RelA by MSK-1 or MSK-2, which are activated by ERKs and p38, as well as CK2, and PKCζ, also regulate NF-κB signaling and represent potential crosstalk mechanisms induced by oxidative stress. Apoptotic signaling cascades are also regulated by redox changes and are known to regulate

In Oxidative Stress: Diagnostics, Prevention, and Therapy Volume 2; Hepel, et al.;
ACS Symposium Series; American Chemical Society: Washington, DC, 2015.

NF-κB signaling. For example, caspases have been reported to cleave IKKs and NEMO (*16*, *228*, *229*).

NF-kB and Neurodegeneration

In the central nervous system (CNS), two heterogeneous classes of cells exist, neurons and glia. Neurons receive, transmit and store information. Communication between neurons occurs via specialized cellular domains called synapses, consisting of a pre- and a postsynaptic cell. Glia cells, astrocytes, microglial and oligodendrocytes, contribute to neuronal homeostasis and function by participating in a number of metabolic and stress related responses and regulating synaptic communication (Figure 4). Constitutive NF-κB activity is found in neuronal cells, which is associated to a high metabolic and synaptic activity involving activation of glutamate (Glu) and growth factor receptors, and Ca^{2+} influx. Constitutive NF-κB signaling is primarily involved in the regulation of neurophysiological activities, such as spatial memory formation, synaptic transmission, and neuroplasticity. Neurons also possess an inducible NF-κB pathway that is activated in response to pro-inflammatory stimuli, and activity-dependent neuron-specific inducers to regulate neural stem cell proliferation (*4*). In glial cells, only inducible NF-κB activity is found. NF-κB signaling is found activated in both neurons and glial cells treated with Aβ, transgenic ApoE4 mice, and in post-mortem brains from AD patients (*244–246*). Similarly, increased nuclear localization of NF-κB is found in dopaminergic neurons from PD brains (*247*). We have observed that overexpression of α-synuclein in dopaminergic cells *in vivo* and *in vitro* stimulates NF-κB phosphorylation (unpublished data). Mutant SOD1 (ALS model) also activates NF-κB (*248*).

Neuronal Survival and NF-κB Signaling

In neurons, NF-κB regulates the expression of anti-apoptotic genes (Bcl-2 [B-cell lymphoma 2], FLICE (FADD-like IL-1β-converting enzyme)-inhibitory protein (FLIP), and inhibitors of apoptosis proteins (IAPs) (Figure 4) (*4*, *249*). Constitutive NF-κB signaling protects neurons against neurotoxic stimuli including oxidative stress (*250*, *251*). NF-κB exerts an inhibitory effect in neuronal cell death that occurs during normal development (*4*). NF-κB activation has also been implicated in neurodegenerative disorders, but contradictory results exist regarding its role in cell survival or cell death progression. NF-κB signaling exerts a protective effect against Aβ-induced toxicity (*252*, *253*) and 3-nitropropionic acid (HD model) (*254*). In contrast, inhibition of NF-κB protects against the toxicity of DA (*255*) and mt-Htt (*256*). Neuroprotection of parkin has been linked to activation of NF-κB, which is reduced by overexpression of PD-related parkin mutants (*257*). Inducible NF-κB in neurons has been primarily linked to p50 and/or RelA dimers and IκBα complexes. However, our poor understanding regarding the existence of diverse NF-κB signaling complexes in distinct neuronal cell types (NF-κB signalosome), their specificity regarding

Publication Date (Web): October 13, 2015 | doi: 10.1021/bk-2015-1200.ch003

the transcriptional regulation of genes, and their selective regulation by specific stimuli, might explain the contradictory findings on the role of NF-κB in neuronal death or survival. Accordingly, recent reports suggest that the neuroprotective effects of NF-κB signaling might be primarily ascribed to c-Rel (*258*, *259*).

Neuroinflammation

NF-κB is a well established regulator of inflammation (*260*). Astrocytes and microglia are activated in response to neurodegenerative and neuroinflammatory conditions. In contrast to neurons, NF-κB signaling in microglia and astrocytes induces large amounts of ROS, RNS, cytokines, and excitotoxins that indirectly promote neuronal death (Figure 4). Neurodegenerative diseases are strongly linked to inflammatory processes as evidenced by the enhanced expression of iNOS, COX-2, TNF-α, and interleukins (IL-1, IL-6) (*3*, *261*, *262*). In contrast to the protective effects of neuronal NF-κB signaling against Aβ-induced toxicity, in microglia, Aβ-induced activation of NF-κB contributes to neuronal cell death (*263*). NF-κB signaling also promotes HD pathogenesis (*264*). Contradictory results exist regarding the role of inflammatory NF-κB signaling in experimental PD models (*265*, *266*). α-synuclein has also been shown to activate NF-κB signaling in microglia (*267*). Accordingly, activation of anti-inflammatory signaling such as that mediated by the peroxisome proliferator-activated receptor (PPAR) and anti-inflammatory drugs exerts a protective effect against neurodegeneration (*77*, *268–270*).

Perspectives

NF-κB signaling plays an important role in the brain response to injury in neurodegenerative conditions. Oxidative stress is increased in neurodegenerative disorders as a result of mitochondrial dysfunction and inflammatory processes. NF-κB signaling can be regulated directly by oxidative modifications, which primarily exert an inhibitory effect on its transcriptional activity. Furthermore, NF-κB can be activated indirectly by oxidative stress/damage and the resultant stress response. In general it is well established that activation of NF-κB in glia promotes neuronal degeneration, while in neurons there is still controversy regarding the exact role that NF-κB plays in neuronal survival or death. Anti-inflammatory therapies have the potential to be used to target neuronal injury in neurodegeneration and are currently being studied in clinical trials. However, the use of such agents is complicated by the possibility that inhibition of NF-κB in neurons may exacerbate the neurodegenerative process. Alterations in NF-κB activation/signaling have been widely reported to occur during neurodegeneration (clinics) and in experimental models of neurodegeneration. However, very poor mechanistic information has been generated to delineate its exact role in neuronal dysfunction. More research is required to characterize the existence of diverse NF-κB signaling complexes in distinct neuronal and glial cell types (NF-κB signalosome), their specificity regarding the transcriptional regulation of genes, and their regulation by specific stimuli. This knowledge can then be efficiently

Publication Date (Web): October 13, 2015 | doi: 10.1021/bk-2015-1200.ch003

translated to a more targeted approach to selectively regulate NF-κB signaling in neuronal and glial populations.

Acknowledgments

Research in Dr. Franco's lab is supported by the National Institutes of Health Grant P20RR17675, Centers of Biomedical Research Excellence (COBRE), the Scientist Development Grant of the American Heart Association (12SDG12090015), and the Office of Research of the University of Nebraska-Lincoln. P.H-F. was supported by a Postdoctoral Fellowship (238703) from the National Council of Science and Technology (CONACYT, Mexico)

Publication Date (Web): October 13, 2015 | doi: 10.1021/bk-2015-1200.ch003

References

1. Oeckinghaus, A.; Hayden, M. S.; Ghosh, S. Crosstalk in NF-kappaB signaling pathways. *Nat. Immunol.* **2011**, *12*, 695–708.
2. Block, M. L.; Zecca, L.; Hong, J. S. Microglia-mediated neurotoxicity: uncovering the molecular mechanisms. *Nat. Rev. Neurosci.* **2007**, *8*, 57–69.
3. Khandelwal, P. J.; Herman, A. M.; Moussa, C. E. Inflammation in the early stages of neurodegenerative pathology. *J. Neuroimmunol.* **2011**, *238*, 1–11.
4. Kaltschmidt, B.; Kaltschmidt, C. NF-kappaB in the nervous system. *Cold Spring Harbor Perspect. Biol.* **2009**, *1*, a001271.
5. Mincheva-Tasheva, S.; Soler, R. M. NF-kappaB signaling pathways: role in nervous system physiology and pathology. *Neuroscientist* **2013**, *19*, 175–194.
6. O'Dea, E.; Hoffmann, A. The regulatory logic of the NF-kappaB signaling system. *Cold Spring Harbor Perspect. Biol.* **2010**, *2*, a000216.
7. Sethi, G.; Tergaonkar, V. Potential pharmacological control of the NF-kappaB pathway. *Trends Pharmacol. Sci.* **2009**, *30*, 313–321.
8. Oeckinghaus, A.; Ghosh, S. The NF-kappaB family of transcription factors and its regulation. *Cold Spring Harbor Perspect. Biol.* **2009**, *1*, a000034.
9. Hinz, M.; Scheidereit, C. The IkappaB kinase complex in NF-kappaB regulation and beyond. *EMBO Rep.* **2014**, *15*, 46–61.
10. Kalyanaraman, B. Teaching the basics of redox biology to medical and graduate students: Oxidants, antioxidants and disease mechanisms. *Redox Biol.* **2013**, *1*, 244–257.
11. Janssen-Heininger, Y. M.; Mossman, B. T.; Heintz, N. H.; Forman, H. J.; Kalyanaraman, B.; Finkel, T.; Stamler, J. S.; Rhee, S. G.; van der Vliet, A. Redox-based regulation of signal transduction: principles, pitfalls, and promises. *Free Radical Biol. Med.* **2008**, *45*, 1–17.
12. Halliwell, B. Biochemistry of oxidative stress. *Biochem. Soc. Trans.* **2007**, *35*, 1147–1150.
13. Martinez-Ruiz, A.; Cadenas, S.; Lamas, S. Nitric oxide signaling: classical, less classical, and nonclassical mechanisms. *Free Radical Biol. Med.* **2011**, *51*, 17–29.

14. van der Veen, B. S.; de Winther, M. P.; Heeringa, P. Myeloperoxidase: molecular mechanisms of action and their relevance to human health and disease. *Antioxid. Redox Signalling* **2009**, *11*, 2899–2937.
15. Im, J. Y.; Kim, D.; Paik, S. G.; Han, P. L. Cyclooxygenase-2-dependent neuronal death proceeds via superoxide anion generation. *Free Radical Biol. Med.* **2006**, *41*, 960–972.
16. Franco, R.; Cidlowski, J. A. Apoptosis and glutathione: beyond an antioxidant. *Cell Death Differ.* **2009**, *16*, 1303–1314.
17. Jozkowicz, A.; Was, H.; Dulak, J. Heme oxygenase-1 in tumors: is it a false friend? *Antioxid. Redox Signalling* **2007**, *9*, 2099–2117.
18. Navarro-Yepes, J.; Zavala-Flores, L.; Anandhan, A.; Wang, F.; Skotak, M.; Chandra, N.; Li, M.; Pappa, A.; Martinez-Fong, D.; Del Razo, L. M.; Quintanilla-Vega, B.; Franco, R. Antioxidant gene therapy against neuronal cell death. *Pharmacol. Ther.* **2014**, *142*, 206–230.
19. Yin, F.; Boveris, A.; Cadenas, E. Mitochondrial energy metabolism and redox signaling in brain aging and neurodegeneration. *Antioxid. Redox Signalling* **2014**, *20*, 353–371.
20. Halliwell, B. Oxidative stress and neurodegeneration: where are we now? *J. Neurochem.* **2006**, *97*, 1634–1658.
21. Fukui, H.; Moraes, C. T. The mitochondrial impairment, oxidative stress and neurodegeneration connection: reality or just an attractive hypothesis? *Trends Neurosci.* **2008**, *31*, 251–256.
22. Mena, R.; Edwards, P.; Perez-Olvera, O.; Wischik, C. M. Monitoring pathological assembly of tau and beta-amyloid proteins in Alzheimer's disease. *Acta Neuropathol.* **1995**, *89*, 50–56.
23. Pratico, D. Oxidative stress hypothesis in Alzheimer's disease: a reappraisal. *Trends Pharmacol. Sci.* **2008**, *29*, 609–615.
24. Good, P. F.; Werner, P.; Hsu, A.; Olanow, C. W.; Perl, D. P. Evidence of neuronal oxidative damage in Alzheimer's disease. *Am. J. Pathol.* **1996**, *149*, 21–28.
25. Belkacemi, A.; Ramassamy, C. Time sequence of oxidative stress in the brain from transgenic mouse models of Alzheimer's disease related to the amyloid-beta cascade. *Free Radical Biol. Med.* **2012**, *52*, 593–600.
26. Xie, H.; Hou, S.; Jiang, J.; Sekutowicz, M.; Kelly, J.; Bacskai, B. J. Rapid cell death is preceded by amyloid plaque-mediated oxidative stress. *Proc. Natl. Acad. Sci. U. S. A.* **2013**, *110*, 7904–7909.
27. Wu, J.; Basha, M. R.; Brock, B.; Cox, D. P.; Cardozo-Pelaez, F.; McPherson, C. A.; Harry, J.; Rice, D. C.; Maloney, B.; Chen, D.; Lahiri, D. K.; Zawia, N. H. Alzheimer's disease (AD)-like pathology in aged monkeys after infantile exposure to environmental metal lead (Pb): evidence for a developmental origin and environmental link for AD. *J. Neurosci.* **2008**, *28*, 3–9.
28. Su, B.; Wang, X.; Nunomura, A.; Moreira, P. I.; Lee, H. G.; Perry, G.; Smith, M. A.; Zhu, X. Oxidative stress signaling in Alzheimer's disease. *Curr. Alzheimer Res.* **2008**, *5*, 525–532.
29. Hansson Petersen, C. A.; Alikhani, N.; Behbahani, H.; Wiehager, B.; Pavlov, P. F.; Alafuzoff, I.; Leinonen, V.; Ito, A.; Winblad, B.; Glaser, E.;

Publication Date (Web): October 13, 2015 | doi: 10.1021/bk-2015-1200.ch003

Ankarcrona, M. The Amyloid b-peptide is imported into mitochondria via the TOM import machinery and localized to mitochondrial cristae. *Proc. Natl. Acad. Sci. U. S. A.* **2008**, *105*, 13145–13150.
30. Yan, S. D.; Chen, X.; Fu, J.; Chen, M.; Zhu, H.; Roher, A.; Slattery, T.; Zhao, L.; Nagashima, M.; Morser, J.; Migheli, A.; Nawroth, P.; Stern, D.; Schmidt, A. M. RAGE and amyloid-beta peptide neurotoxicity in Alzheimer's disease. *Nature* **1996**, *382*, 685–691.
31. Bezprozvanny, I.; Mattson, M. P. Neuronal calcium mishandling and the pathogenesis of Alzheimer's disease. *Trends Neurosci.* **2008**, *31*, 454–463.
32. Green, P. S.; Mendez, A. J.; Jacob, J. S.; Crowley, J. R.; Growdon, W.; Hyman, B. T.; Heinecke, J. W. Neuronal expression of myeloperoxidase is increased in Alzheimer's disease. *J. Neurochem.* **2004**, *90*, 724–733.
33. Kotilinek, L. A.; Westerman, M. A.; Wang, Q.; Panizzon, K.; Lim, G. P.; Simonyi, A.; Lesne, S.; Falinska, A.; Younkin, L. H.; Younkin, S. G.; Rowan, M.; Cleary, J.; Wallis, R. A.; Sun, G. Y.; Cole, G.; Frautschy, S.; Anwyl, R.; Ashe, K. H. Cyclooxygenase-2 inhibition improves amyloid-beta-mediated suppression of memory and synaptic plasticity. *Brain* **2008**, *131*, 651–664.
34. Jang, J. H.; Surh, Y. J. Beta-amyloid-induced apoptosis is associated with cyclooxygenase-2 up-regulation via the mitogen-activated protein kinase-NF-kappaB signaling pathway. *Free Radical Biol. Med.* **2005**, *38*, 1604–1613.
35. Akama, K. T.; Van Eldik, L. J. Beta-amyloid stimulation of inducible nitric-oxide synthase in astrocytes is interleukin-1beta- and tumor necrosis factor-alpha (TNFalpha)-dependent, and involves a TNFalpha receptor-associated factor- and NFkappaB-inducing kinase-dependent signaling mechanism. *J. Biol. Chem.* **2000**, *275*, 7918–7924.
36. Combs, C. K.; Karlo, J. C.; Kao, S. C.; Landreth, G. E. beta-Amyloid stimulation of microglia and monocytes results in TNFalpha-dependent expression of inducible nitric oxide synthase and neuronal apoptosis. *J. Neurosci.* **2001**, *21*, 1179–1188.
37. Xie, Z.; Wei, M.; Morgan, T. E.; Fabrizio, P.; Han, D.; Finch, C. E.; Longo, V. D. Peroxynitrite mediates neurotoxicity of amyloid beta-peptide1-42- and lipopolysaccharide-activated microglia. *J. Neurosci.* **2002**, *22*, 3484–3492.
38. Colton, C. A.; Brown, C. M.; Cook, D.; Needham, L. K.; Xu, Q.; Czapiga, M.; Saunders, A. M.; Schmechel, D. E.; Rasheed, K.; Vitek, M. P. APOE and the regulation of microglial nitric oxide production: a link between genetic risk and oxidative stress. *Neurobiol. Aging* **2002**, *23*, 777–785.
39. Brown, C. M.; Wright, E.; Colton, C. A.; Sullivan, P. M.; Laskowitz, D. T.; Vitek, M. P. Apolipoprotein E isoform mediated regulation of nitric oxide release. *Free Radical Biol. Med.* **2002**, *32*, 1071–1075.
40. Yao, Z.; Wood, N. W. Cell death pathways in Parkinson's disease: role of mitochondria. *Antioxid. Redox Signalling* **2009**, *11*, 2135–2149.
41. Levy, O. A.; Malagelada, C.; Greene, L. A. Cell death pathways in Parkinson's disease: proximal triggers, distal effectors, and final steps. *Apoptosis* **2009**, *14*, 478–500.

Publication Date (Web): October 13, 2015 | doi: 10.1021/bk-2015-1200.ch003

42. Driver, J. A.; Logroscino, G.; Gaziano, J. M.; Kurth, T. Incidence and remaining lifetime risk of Parkinson disease in advanced age. *Neurology* **2009**, *72*, 432–438.
43. Reeve, A.; Simcox, E.; Turnbull, D. Ageing and Parkinson's disease: why is advancing age the biggest risk factor? *Ageing Res. Rev.* **2014**, *14*, 19–30.
44. Gao, H. M.; Hong, J. S. Gene-environment interactions: key to unraveling the mystery of Parkinson's disease. *Prog. Neurobiol.* **2011**, *94*, 1–19.
45. Alam, Z. I.; Daniel, S. E.; Lees, A. J.; Marsden, D. C.; Jenner, P.; Halliwell, B. A generalised increase in protein carbonyls in the brain in Parkinson's but not incidental Lewy body disease. *J. Neurochem.* **1997**, *69*, 1326–1329.
46. Sian, J.; Dexter, D. T.; Lees, A. J.; Daniel, S.; Agid, Y.; Javoy-Agid, F.; Jenner, P.; Marsden, C. D. Alterations in glutathione levels in Parkinson's disease and other neurodegenerative disorders affecting basal ganglia. *Ann. Neurol.* **1994**, *36*, 348–355.
47. Yoritaka, A.; Hattori, N.; Uchida, K.; Tanaka, M.; Stadtman, E. R.; Mizuno, Y. Immunohistochemical detection of 4-hydroxynonenal protein adducts in Parkinson disease. *Proc. Natl. Acad. Sci. U. S. A.* **1996**, *93*, 2696–2701.
48. Jimenez-Jimenez, F. J.; Alonso-Navarro, H.; Garcia-Martin, E.; Agundez, J. A. Cerebrospinal fluid biochemical studies in patients with Parkinson's disease: toward a potential search for biomarkers for this disease. *Front. Cell. Neurosci.* **2014**, *8*, 369.
49. Buhmann, C.; Arlt, S.; Kontush, A.; Moller-Bertram, T.; Sperber, S.; Oechsner, M.; Stuerenburg, H. J.; Beisiegel, U. Plasma and CSF markers of oxidative stress are increased in Parkinson's disease and influenced by antiparkinsonian medication. *Neurobiol. Dis.* **2004**, *15*, 160–170.
50. Garcia-Moreno, J. M.; Martin de Pablos, A.; Garcia-Sanchez, M. I.; Mendez-Lucena, C.; Damas-Hermoso, F.; Rus, M.; Chacon, J.; Fernandez, E. May serum levels of advanced oxidized protein products serve as a prognostic marker of disease duration in patients with idiopathic Parkinson's disease? *Antioxid. Redox Signalling* **2013**, *18*, 1296–1302.
51. Dexter, D. T.; Sian, J.; Rose, S.; Hindmarsh, J. G.; Mann, V. M.; Cooper, J. M.; Wells, F. R.; Daniel, S. E.; Lees, A. J.; Schapira, A. H.; Jenner, P.; Marsden, C. D. Indices of oxidative stress and mitochondrial function in individuals with incidental Lewy body disease. *Ann. Neurol.* **1994**, *35*, 38–44.
52. Guzman, J. N.; Sanchez-Padilla, J.; Wokosin, D.; Kondapalli, J.; Ilijic, E.; Schumacker, P. T.; Surmeier, D. J. Oxidant stress evoked by pacemaking in dopaminergic neurons is attenuated by DJ-1. *Nature* **2010**, *468*, 696–700.
53. Schapira, A. H. Mitochondria in the aetiology and pathogenesis of Parkinson's disease. *Lancet Neurol.* **2008**, *7*, 97–109.
54. Henchcliffe, C.; Beal, M. F. Mitochondrial biology and oxidative stress in Parkinson disease pathogenesis. *Nat. Clin. Pract. Neurol.* **2008**, *4*, 600–609.
55. Schapira, A. H.; Cooper, J. M.; Dexter, D.; Jenner, P.; Clark, J. B.; Marsden, C. D. Mitochondrial complex I deficiency in Parkinson's disease. *Lancet* **1989**, *1*, 1269.

Publication Date (Web): October 13, 2015 | doi: 10.1021/bk-2015-1200.ch003

56. Devi, L.; Raghavendran, V.; Prabhu, B. M.; Avadhani, N. G.; Anandatheerthavarada, H. K. Mitochondrial import and accumulation of alpha-synuclein impair complex I in human dopaminergic neuronal cultures and Parkinson disease brain. *J. Biol. Chem.* **2008**, *283*, 9089–9100.
57. Taira, T.; Saito, Y.; Niki, T.; Iguchi-Ariga, S. M.; Takahashi, K.; Ariga, H. DJ-1 has a role in antioxidative stress to prevent cell death. *EMBO Rep.* **2004**, *5*, 213–218.
58. Morais, V. A.; Verstreken, P.; Roethig, A.; Smet, J.; Snellinx, A.; Vanbrabant, M.; Haddad, D.; Frezza, C.; Mandemakers, W.; Vogt-Weisenhorn, D.; Van Coster, R.; Wurst, W.; Scorrano, L.; De Strooper, B. Parkinson's disease mutations in PINK1 result in decreased Complex I activity and deficient synaptic function. *EMBO Mol. Med.* **2009**, *1*, 99–111.
59. Palacino, J. J.; Sagi, D.; Goldberg, M. S.; Krauss, S.; Motz, C.; Wacker, M.; Klose, J.; Shen, J. Mitochondrial dysfunction and oxidative damage in parkin-deficient mice. *J. Biol. Chem.* **2004**, *279*, 18614–18622.
60. Jiang, H.; Ren, Y.; Zhao, J.; Feng, J. Parkin protects human dopaminergic neuroblastoma cells against dopamine-induced apoptosis. *Hum. Mol. Genet.* **2004**, *13*, 1745–1754.
61. Niu, J.; Yu, M.; Wang, C.; Xu, Z. Leucine-rich repeat kinase 2 disturbs mitochondrial dynamics via Dynamin-like protein. *J. Neurochem.* **2012**, *122*, 650–658.
62. Mariani, S.; Ventriglia, M.; Simonelli, I.; Donno, S.; Bucossi, S.; Vernieri, F.; Melgari, J. M.; Pasqualetti, P.; Rossini, P. M.; Squitti, R. Fe and Cu do not differ in Parkinson's disease: a replication study plus meta-analysis. *Neurobiol. Aging* **2013**, *34*, 632–633.
63. Wang, C.; Liu, L.; Zhang, L.; Peng, Y.; Zhou, F. Redox reactions of the alpha-synuclein-Cu(2+) complex and their effects on neuronal cell viability. *Biochemistry* **2010**, *49*, 8134–8142.
64. Meloni, G.; Vasak, M. Redox activity of alpha-synuclein-Cu is silenced by Zn(7)-metallothionein-3. *Free Radical Biol. Med.* **2011**, *50*, 1471–1479.
65. Sian-Hulsmann, J.; Mandel, S.; Youdim, M. B.; Riederer, P. The relevance of iron in the pathogenesis of Parkinson's disease. *J. Neurochem.* **2011**, *118*, 939–957.
66. Abou-Sleiman, P. M.; Muqit, M. M.; Wood, N. W. Expanding insights of mitochondrial dysfunction in Parkinson's disease. *Nat. Rev. Neurosci.* **2006**, *7*, 207–219.
67. Wu, D. C.; Teismann, P.; Tieu, K.; Vila, M.; Jackson-Lewis, V.; Ischiropoulos, H.; Przedborski, S. NADPH oxidase mediates oxidative stress in the 1-methyl-4-phenyl-1,2,3,6-tetrahydropyridine model of Parkinson's disease. *Proc. Natl. Acad. Sci. U. S. A.* **2003**, *100*, 6145–6150.
68. Gao, H. M.; Liu, B.; Hong, J. S. Critical role for microglial NADPH oxidase in rotenone-induced degeneration of dopaminergic neurons. *J. Neurosci.* **2003**, *23*, 6181–6187.
69. Cristovao, A. C.; Choi, D. H.; Baltazar, G.; Beal, M. F.; Kim, Y. S. The role of NADPH oxidase 1-derived reactive oxygen species in paraquat-mediated dopaminergic cell death. *Antioxid. Redox Signalling* **2009**, *11*, 2105–2118.

Publication Date (Web): October 13, 2015 | doi: 10.1021/bk-2015-1200.ch003

70. Choi, D. K.; Pennathur, S.; Perier, C.; Tieu, K.; Teismann, P.; Wu, D. C.; Jackson-Lewis, V.; Vila, M.; Vonsattel, J. P.; Heinecke, J. W.; Przedborski, S. Ablation of the inflammatory enzyme myeloperoxidase mitigates features of Parkinson's disease in mice. *J. Neurosci.* **2005**, *25*, 6594–6600.
71. Teismann, P.; Tieu, K.; Choi, D. K.; Wu, D. C.; Naini, A.; Hunot, S.; Vila, M.; Jackson-Lewis, V.; Przedborski, S. Cyclooxygenase-2 is instrumental in Parkinson's disease neurodegeneration. *Proc. Natl. Acad. Sci. U. S. A.* **2003**, *100*, 5473–5478.
72. Wang, T.; Pei, Z.; Zhang, W.; Liu, B.; Langenbach, R.; Lee, C.; Wilson, B.; Reece, J. M.; Miller, D. S.; Hong, J. S. MPP+-induced COX-2 activation and subsequent dopaminergic neurodegeneration. *FASEB J.* **2005**, *19*, 1134–1136.
73. Przedborski, S.; Jackson-Lewis, V.; Yokoyama, R.; Shibata, T.; Dawson, V. L.; Dawson, T. M. Role of neuronal nitric oxide in 1-methyl-4-phenyl-1,2,3,6-tetrahydropyridine (MPTP)-induced dopaminergic neurotoxicity. *Proc. Natl. Acad. Sci. U. S. A.* **1996**, *93*, 4565–4571.
74. Liberatore, G. T.; Jackson-Lewis, V.; Vukosavic, S.; Mandir, A. S.; Vila, M.; McAuliffe, W. G.; Dawson, V. L.; Dawson, T. M.; Przedborski, S. Inducible nitric oxide synthase stimulates dopaminergic neurodegeneration in the MPTP model of Parkinson disease. *Nat. Med.* **1999**, *5*, 1403–1409.
75. LaVoie, M. J.; Hastings, T. G. Peroxynitrite- and nitrite-induced oxidation of dopamine: implications for nitric oxide in dopaminergic cell loss. *J. Neurochem.* **1999**, *73*, 2546–2554.
76. Ara, J.; Przedborski, S.; Naini, A. B.; Jackson-Lewis, V.; Trifiletti, R. R.; Horwitz, J.; Ischiropoulos, H. Inactivation of tyrosine hydroxylase by nitration following exposure to peroxynitrite and 1-methyl-4-phenyl-1,2,3,6-tetrahydropyridine (MPTP). *Proc. Natl. Acad. Sci. U. S. A.* **1998**, *95*, 7659–7663.
77. Dehmer, T.; Heneka, M. T.; Sastre, M.; Dichgans, J.; Schulz, J. B. Protection by pioglitazone in the MPTP model of Parkinson's disease correlates with I kappa B alpha induction and block of NF kappa B and iNOS activation. *J. Neurochem.* **2004**, *88*, 494–501.
78. Zuccato, C.; Valenza, M.; Cattaneo, E. Molecular mechanisms and potential therapeutical targets in Huntington's disease. *Physiol. Rev.* **2010**, *90*, 905–981.
79. Oliveira, J. M. Nature and cause of mitochondrial dysfunction in Huntington's disease: focusing on huntingtin and the striatum. *J. Neurochem.* **2010**, *114*, 1–12.
80. Finkbeiner, S. Huntington's Disease. *Cold Spring Harbor Perspect. Biol.* **2011**, *3*, 1–24.
81. Long, J. D.; Matson, W. R.; Juhl, A. R.; Leavitt, B. R.; Paulsen, J. S. 8OHdG as a marker for Huntington disease progression. *Neurobiol. Dis.* **2012**, *46*, 625–634.
82. Weir, D. W.; Sturrock, A.; Leavitt, B. R. Development of biomarkers for Huntington's disease. *Lancet Neurol.* **2011**, *10*, 573–590.
83. Sorolla, M. A.; Rodriguez-Colman, M. J.; Tamarit, J.; Ortega, Z.; Lucas, J. J.; Ferrer, I.; Ros, J.; Cabiscol, E. Protein oxidation in Huntington disease

Publication Date (Web): October 13, 2015 | doi: 10.1021/bk-2015-1200.ch003

affects energy production and vitamin B6 metabolism. *Free Radical Biol. Med.* **2010**, *49*, 612–621.
84. Sorolla, M. A.; Reverter-Branchat, G.; Tamarit, J.; Ferrer, I.; Ros, J.; Cabiscol, E. Proteomic and oxidative stress analysis in human brain samples of Huntington disease. *Free Radical Biol. Med.* **2008**, *45*, 667–678.
85. Browne, S. E.; Beal, M. F. Oxidative damage in Huntington's disease pathogenesis. *Antioxid. Redox Signalling* **2006**, *8*, 2061–2073.
86. Klepac, N.; Relja, M.; Klepac, R.; Hecimovic, S.; Babic, T.; Trkulja, V. Oxidative stress parameters in plasma of Huntington's disease patients, asymptomatic Huntington's disease gene carriers and healthy subjects : a cross-sectional study. *J. Neurol.* **2007**, *254*, 1676–1683.
87. Polidori, M. C.; Mecocci, P.; Browne, S. E.; Senin, U.; Beal, M. F. Oxidative damage to mitochondrial DNA in Huntington's disease parietal cortex. *Neurosci. Lett.* **1999**, *272*, 53–56.
88. Hersch, S. M.; Gevorkian, S.; Marder, K.; Moskowitz, C.; Feigin, A.; Cox, M.; Como, P.; Zimmerman, C.; Lin, M.; Zhang, L.; Ulug, A. M.; Beal, M. F.; Matson, W.; Bogdanov, M.; Ebbel, E.; Zaleta, A.; Kaneko, Y.; Jenkins, B.; Hevelone, N.; Zhang, H.; Yu, H.; Schoenfeld, D.; Ferrante, R.; Rosas, H. D. Creatine in Huntington disease is safe, tolerable, bioavailable in brain and reduces serum 8OH2′dG. *Neurology* **2006**, *66*, 250–252.
89. Chen, C. M.; Wu, Y. R.; Cheng, M. L.; Liu, J. L.; Lee, Y. M.; Lee, P. W.; Soong, B. W.; Chiu, D. T. Increased oxidative damage and mitochondrial abnormalities in the peripheral blood of Huntington's disease patients. *Biochem. Biophys. Res. Commun.* **2007**, *359*, 335–340.
90. Browne, S. E.; Bowling, A. C.; MacGarvey, U.; Baik, M. J.; Berger, S. C.; Muqit, M. M.; Bird, E. D.; Beal, M. F. Oxidative damage and metabolic dysfunction in Huntington's disease: selective vulnerability of the basal ganglia. *Ann. Neurol.* **1997**, *41*, 646–653.
91. Bano, D.; Zanetti, F.; Mende, Y.; Nicotera, P. Neurodegenerative processes in Huntington's disease. *Cell Death Dis.* **2011**, *2*, e228.
92. Bogdanov, M. B.; Andreassen, O. A.; Dedeoglu, A.; Ferrante, R. J.; Beal, M. F. Increased oxidative damage to DNA in a transgenic mouse model of Huntington's disease. *J. Neurochem.* **2001**, *79*, 1246–1249.
93. Siddiqui, A.; Rivera-Sanchez, S.; Castro Mdel, R.; Acevedo-Torres, K.; Rane, A.; Torres-Ramos, C. A.; Nicholls, D. G.; Andersen, J. K.; Ayala-Torres, S. Mitochondrial DNA damage is associated with reduced mitochondrial bioenergetics in Huntington's disease. *Free Radical Biol. Med.* **2012**, *53*, 1478–1488.
94. Costa, V.; Scorrano, L. Shaping the role of mitochondria in the pathogenesis of Huntington's disease. *EMBO J.* **2012**, *31*, 1853–1864.
95. Shirendeb, U.; Reddy, A. P.; Manczak, M.; Calkins, M. J.; Mao, P.; Tagle, D. A.; Reddy, P. H. Abnormal mitochondrial dynamics, mitochondrial loss and mutant huntingtin oligomers in Huntington's disease: implications for selective neuronal damage. *Hum. Mol. Genet.* **2011**, *20*, 1438–1455.
96. Mochel, F.; Haller, R. G. Energy deficit in Huntington disease: why it matters. *J. Clin. Invest.* **2011**, *121*, 493–499.

Publication Date (Web): October 13, 2015 | doi: 10.1021/bk-2015-1200.ch003

97. Benchoua, A.; Trioulier, Y.; Diguet, E.; Malgorn, C.; Gaillard, M. C.; Dufour, N.; Elalouf, J. M.; Krajewski, S.; Hantraye, P.; Deglon, N.; Brouillet, E. Dopamine determines the vulnerability of striatal neurons to the N-terminal fragment of mutant huntingtin through the regulation of mitochondrial complex II. *Hum. Mol. Genet.* **2008**, *17*, 1446–1456.
98. Charvin, D.; Vanhoutte, P.; Pages, C.; Borrelli, E.; Caboche, J. Unraveling a role for dopamine in Huntington's disease: the dual role of reactive oxygen species and D2 receptor stimulation. *Proc. Natl. Acad. Sci. U. S. A.* **2005**, *102*, 12218–12223.
99. Liot, G.; Bossy, B.; Lubitz, S.; Kushnareva, Y.; Sejbuk, N.; Bossy-Wetzel, E. Complex II inhibition by 3-NP causes mitochondrial fragmentation and neuronal cell death via an NMDA- and ROS-dependent pathway. *Cell Death Differ.* **2009**, *16*, 899–909.
100. Hands, S.; Sajjad, M. U.; Newton, M. J.; Wyttenbach, A. In vitro and in vivo aggregation of a fragment of huntingtin protein directly causes free radical production. *J. Biol. Chem.* **2011**, *286*, 44512–44520.
101. Liu, R.; Althaus, J. S.; Ellerbrock, B. R.; Becker, D. A.; Gurney, M. E. Enhanced oxygen radical production in a transgenic mouse model of familial amyotrophic lateral sclerosis. *Ann. Neurol.* **1998**, *44*, 763–770.
102. Ferrante, R. J.; Shinobu, L. A.; Schulz, J. B.; Matthews, R. T.; Thomas, C. E.; Kowall, N. W.; Gurney, M. E.; Beal, M. F. Increased 3-nitrotyrosine and oxidative damage in mice with a human copper/zinc superoxide dismutase mutation. *Ann. Neurol.* **1997**, *42*, 326–334.
103. Beal, M. F.; Ferrante, R. J.; Browne, S. E.; Matthews, R. T.; Kowall, N. W.; Brown, R. H., Jr. Increased 3-nitrotyrosine in both sporadic and familial amyotrophic lateral sclerosis. *Ann. Neurol.* **1997**, *42*, 644–654.
104. Bogdanov, M.; Brown, R. H.; Matson, W.; Smart, R.; Hayden, D.; O'Donnell, H.; Flint Beal, M.; Cudkowicz, M. Increased oxidative damage to DNA in ALS patients. *Free Radical Biol. Med.* **2000**, *29*, 652–658.
105. Smith, R. G.; Henry, Y. K.; Mattson, M. P.; Appel, S. H. Presence of 4-hydroxynonenal in cerebrospinal fluid of patients with sporadic amyotrophic lateral sclerosis. *Ann. Neurol.* **1998**, *44*, 696–699.
106. Barber, S. C.; Shaw, P. J. Oxidative stress in ALS: key role in motor neuron injury and therapeutic target. *Free Radical Biol. Med.* **2010**, *48*, 629–641.
107. Li, Q.; Spencer, N. Y.; Pantazis, N. J.; Engelhardt, J. F. Alsin and SOD1(G93A) proteins regulate endosomal reactive oxygen species production by glial cells and proinflammatory pathways responsible for neurotoxicity. *J. Biol. Chem.* **2011**, *286*, 40151–40162.
108. Kishigami, H.; Nagano, S.; Bush, A. I.; Sakoda, S. Monomerized Cu, Zn-superoxide dismutase induces oxidative stress through aberrant Cu binding. *Free Radical Biol. Med.* **2010**, *48*, 945–952.
109. Braun, R. J.; Sommer, C.; Carmona-Gutierrez, D.; Khoury, C. M.; Ring, J.; Buttner, S.; Madeo, F. Neurotoxic 43-kDa TAR DNA-binding protein (TDP-43) triggers mitochondrion-dependent programmed cell death in yeast. *J. Biol. Chem.* **2011**, *286*, 19958–19972.

Publication Date (Web): October 13, 2015 | doi: 10.1021/bk-2015-1200.ch003

110. Oliveira-Marques, V.; Marinho, H. S.; Cyrne, L.; Antunes, F. Role of hydrogen peroxide in NF-kappaB activation: from inducer to modulator. *Antioxid. Redox Signalling* **2009**, *11*, 2223–2243.
111. Schmidt, K. N.; Amstad, P.; Cerutti, P.; Baeuerle, P. A. The roles of hydrogen peroxide and superoxide as messengers in the activation of transcription factor NF-kappa B. *Chem Biol.* **1995**, *2*, 13–22.
112. Schreck, R.; Albermann, K.; Baeuerle, P. A. Nuclear factor kappa B: an oxidative stress-responsive transcription factor of eukaryotic cells (a review). *Free Radic. Res. Commun.* **1992**, *17*, 221–237.
113. Zhang, J.; Johnston, G.; Stebler, B.; Keller, E. T. Hydrogen peroxide activates NFkappaB and the interleukin-6 promoter through NFkappaB-inducing kinase. *Antioxid. Redox Signalling* **2001**, *3*, 493–504.
114. Morgan, M. J.; Liu, Z. G. Crosstalk of reactive oxygen species and NF-kappaB signaling. *Cell Res.* **2011**, *21*, 103–115.
115. Garcia-Garcia, A.; Zavala-Flores, L.; Rodriguez-Rocha, H.; Franco, R. Thiol-redox signaling, dopaminergic cell death, and Parkinson's disease. *Antioxid. Redox Signalling* **2012**, *17*, 1764–1784.
116. Go, Y. M.; Jones, D. P. Thiol/disulfide redox states in signaling and sensing. *Crit. Rev. Biochem. Mol. Biol.* **2013**, *48*, 173–181.
117. Paulsen, C. E.; Carroll, K. S. Cysteine-mediated redox signaling: chemistry, biology, and tools for discovery. *Chem. Rev.* **2013**, *113*, 4633–4679.
118. Winterbourn, C. C.; Hampton, M. B. Thiol chemistry and specificity in redox signaling. *Free Radical Biol. Med.* **2008**, *45*, 549–561.
119. Poole, L. B.; Nelson, K. J. Discovering mechanisms of signaling-mediated cysteine oxidation. *Curr. Opin. Chem. Biol.* **2008**, *12*, 18–24.
120. Foster, M. W.; Hess, D. T.; Stamler, J. S. Protein S-nitrosylation in health and disease: a current perspective. *Trends Mol. Med.* **2009**, *15*, 391–404.
121. Benhar, M.; Forrester, M. T.; Stamler, J. S. Protein denitrosylation: enzymatic mechanisms and cellular functions. *Nat. Rev. Mol. Cell Biol.* **2009**, *10*, 721–732.
122. Gloire, G.; Piette, J. Redox regulation of nuclear post-translational modifications during NF-kappaB activation. *Antioxid. Redox Signalling* **2009**, *11*, 2209–2222.
123. Pantano, C.; Reynaert, N. L.; van der Vliet, A.; Janssen-Heininger, Y. M. Redox-sensitive kinases of the nuclear factor-kappaB signaling pathway. *Antioxid. Redox Signalling* **2006**, *8*, 1791–1806.
124. Toledano, M. B.; Ghosh, D.; Trinh, F.; Leonard, W. J. N-terminal DNA-binding domains contribute to differential DNA-binding specificities of NF-kappa B p50 and p65. *Mol. Cell Biol.* **1993**, *13*, 852–860.
125. Glineur, C.; Davioud-Charvet, E.; Vandenbunder, B. The conserved redox-sensitive cysteine residue of the DNA-binding region in the c-Rel protein is involved in the regulation of the phosphorylation of the protein. *Biochem. J.* **2000**, *352* (Pt 2), 583–591.
126. Marshall, H. E.; Stamler, J. S. Inhibition of NF-kappa B by S-nitrosylation. *Biochemistry* **2001**, *40*, 1688–1693.
127. Cernuda-Morollon, E.; Pineda-Molina, E.; Canada, F. J.; Perez-Sala, D. 15-Deoxy-Delta 12,14-prostaglandin J2 inhibition of NF-kappaB-DNA binding

Publication Date (Web): October 13, 2015 | doi: 10.1021/bk-2015-1200.ch003

through covalent modification of the p50 subunit. *J. Biol. Chem.* **2001**, *276*, 35530–35536.
128. Pineda-Molina, E.; Klatt, P.; Vazquez, J.; Marina, A.; Garcia de Lacoba, M.; Perez-Sala, D.; Lamas, S. Glutathionylation of the p50 subunit of NF-kappaB: a mechanism for redox-induced inhibition of DNA binding. *Biochemistry* **2001**, *40*, 14134–14142.
129. Lambert, C.; Li, J.; Jonscher, K.; Yang, T. C.; Reigan, P.; Quintana, M.; Harvey, J.; Freed, B. M. Acrolein inhibits cytokine gene expression by alkylating cysteine and arginine residues in the NF-kappaB1 DNA binding domain. *J. Biol. Chem.* **2007**, *282*, 19666–19675.
130. Reynaert, N. L.; Ckless, K.; Korn, S. H.; Vos, N.; Guala, A. S.; Wouters, E. F.; van der Vliet, A.; Janssen-Heininger, Y. M. Nitric oxide represses inhibitory kappaB kinase through S-nitrosylation. *Proc. Natl. Acad. Sci. U. S. A.* **2004**, *101*, 8945–8950.
131. Reynaert, N. L.; van der Vliet, A.; Guala, A. S.; McGovern, T.; Hristova, M.; Pantano, C.; Heintz, N. H.; Heim, J.; Ho, Y. S.; Matthews, D. E.; Wouters, E. F.; Janssen-Heininger, Y. M. Dynamic redox control of NF-kappaB through glutaredoxin-regulated S-glutathionylation of inhibitory kappaB kinase beta. *Proc. Natl. Acad. Sci. U. S. A.* **2006**, *103*, 13086–13091.
132. Korn, S. H.; Wouters, E. F.; Vos, N.; Janssen-Heininger, Y. M. Cytokine-induced activation of nuclear factor-kappa B is inhibited by hydrogen peroxide through oxidative inactivation of IkappaB kinase. *J. Biol. Chem.* **2001**, *276*, 35693–35700.
133. Nolin, J. D.; Tully, J. E.; Hoffman, S. M.; Guala, A. S.; van der Velden, J. L.; Poynter, M. E.; van der Vliet, A.; Anathy, V.; Janssen-Heininger, Y. M. The glutaredoxin/S-glutathionylation axis regulates interleukin-17A-induced proinflammatory responses in lung epithelial cells in association with S-glutathionylation of nuclear factor kappaB family proteins. *Free Radical Biol. Med.* **2014**, *73*, 143–153.
134. Qanungo, S.; Starke, D. W.; Pai, H. V.; Mieyal, J. J.; Nieminen, A. L. Glutathione supplementation potentiates hypoxic apoptosis by S-glutathionylation of p65-NFkappaB. *J. Biol. Chem.* **2007**, *282*, 18427–18436.
135. Matthews, J. R.; Wakasugi, N.; Virelizier, J. L.; Yodoi, J.; Hay, R. T. Thioredoxin regulates the DNA binding activity of NF-kappa B by reduction of a disulphide bond involving cysteine 62. *Nucleic Acids Res.* **1992**, *20*, 3821–3830.
136. Mitomo, K.; Nakayama, K.; Fujimoto, K.; Sun, X.; Seki, S.; Yamamoto, K. Two different cellular redox systems regulate the DNA-binding activity of the p50 subunit of NF-kappa B in vitro. *Gene* **1994**, *145*, 197–203.
137. Sakurai, A.; Yuasa, K.; Shoji, Y.; Himeno, S.; Tsujimoto, M.; Kunimoto, M.; Imura, N.; Hara, S. Overexpression of thioredoxin reductase 1 regulates NF-kappa B activation. *J. Cell Physiol.* **2004**, *198*, 22–30.
138. Kelleher, Z. T.; Sha, Y.; Foster, M. W.; Foster, W. M.; Forrester, M. T.; Marshall, H. E. Thioredoxin-mediated denitrosylation regulates cytokine-induced nuclear factor kappaB (NF-kappaB) activation. *J. Biol. Chem.* **2014**, *289*, 3066–3072.

Publication Date (Web): October 13, 2015 | doi: 10.1021/bk-2015-1200.ch003

139. Sen, N.; Paul, B. D.; Gadalla, M. M.; Mustafa, A. K.; Sen, T.; Xu, R.; Kim, S.; Snyder, S. H. Hydrogen sulfide-linked sulfhydration of NF-kappaB mediates its antiapoptotic actions. *Mol. Cell.* **2012**, *45*, 13–24.
140. Kenchappa, R. S.; Ravindranath, V. Glutaredoxin is essential for maintenance of brain mitochondrial complex I: studies with MPTP. *FASEB J.* **2003**, *17*, 717–719.
141. Rodriguez-Rocha, H.; Garcia Garcia, A.; Zavala-Flores, L.; Li, S.; Madayiputhiya, N.; Franco, R. Glutaredoxin 1 protects dopaminergic cells by increased protein glutathionylation in experimental Parkinson's disease. *Antioxid. Redox Signalling* **2012**, *17*, 1676–1693.
142. Akterin, S.; Cowburn, R. F.; Miranda-Vizuete, A.; Jimenez, A.; Bogdanovic, N.; Winblad, B.; Cedazo-Minguez, A. Involvement of glutaredoxin-1 and thioredoxin-1 in beta-amyloid toxicity and Alzheimer's disease. *Cell Death Differ.* **2006**, *13*, 1454–1465.
143. Carroll, M. C.; Outten, C. E.; Proescher, J. B.; Rosenfeld, L.; Watson, W. H.; Whitson, L. J.; Hart, P. J.; Jensen, L. T.; Cizewski Culotta, V. The effects of glutaredoxin and copper activation pathways on the disulfide and stability of Cu,Zn superoxide dismutase. *J. Biol. Chem.* **2006**, *281*, 28648–28656.
144. Johnson, W. M.; Yao, C.; Siedlak, S. L.; Wang, W.; Zhu, X.; Caldwell, G. A.; Wilson-Delfosse, A. L.; Mieyal, J. J.; Chen, S. G. Glutaredoxin deficiency exacerbates neurodegeneration in C. elegans models of Parkinson's disease. *Hum. Mol. Genet.* **2015**, *24*, 1322–1335.
145. Kida, K.; Yamada, M.; Tokuda, K.; Marutani, E.; Kakinohana, M.; Kaneki, M.; Ichinose, F. Inhaled hydrogen sulfide prevents neurodegeneration and movement disorder in a mouse model of Parkinson's disease. *Antioxid. Redox Signalling* **2011**, *15*, 343–352.
146. Lu, M.; Zhao, F. F.; Tang, J. J.; Su, C. J.; Fan, Y.; Ding, J. H.; Bian, J. S.; Hu, G. The neuroprotection of hydrogen sulfide against MPTP-induced dopaminergic neuron degeneration involves uncoupling protein 2 rather than ATP-sensitive potassium channels. *Antioxid. Redox Signalling* **2012**, *17*, 849–859.
147. Xuan, A.; Long, D.; Li, J.; Ji, W.; Zhang, M.; Hong, L.; Liu, J. Hydrogen sulfide attenuates spatial memory impairment and hippocampal neuroinflammation in beta-amyloid rat model of Alzheimer's disease. *J. Neuroinflammation* **2012**, *9*, 202.
148. Muroya, T.; Ihara, Y.; Ikeda, S.; Yasuoka, C.; Miyahara, Y.; Urata, Y.; Kondo, T.; Kohno, S. Oxidative modulation of NF-kappaB signaling by oxidized low-density lipoprotein. *Biochem. Biophys. Res. Commun.* **2003**, *309*, 900–905.
149. Park, S. W.; Huq, M. D.; Hu, X.; Wei, L. N. Tyrosine nitration on p65: a novel mechanism to rapidly inactivate nuclear factor-kappaB. *Mol. Cell Proteomics* **2005**, *4*, 300–309.
150. Yakovlev, V. A.; Barani, I. J.; Rabender, C. S.; Black, S. M.; Leach, J. K.; Graves, P. R.; Kellogg, G. E.; Mikkelsen, R. B. Tyrosine nitration of IkappaBalpha: a novel mechanism for NF-kappaB activation. *Biochemistry* **2007**, *46*, 11671–11683.

Publication Date (Web): October 13, 2015 | doi: 10.1021/bk-2015-1200.ch003

151. Hakem, R. DNA-damage repair; the good, the bad, and the ugly. *EMBO J.* **2008**, *27*, 589–605.
152. Ando, K.; Hirao, S.; Kabe, Y.; Ogura, Y.; Sato, I.; Yamaguchi, Y.; Wada, T.; Handa, H. A new APE1/Ref-1-dependent pathway leading to reduction of NF-kappaB and AP-1, and activation of their DNA-binding activity. *Nucleic Acids Res.* **2008**, *36*, 4327–4336.
153. Daily, D.; Vlamis-Gardikas, A.; Offen, D.; Mittelman, L.; Melamed, E.; Holmgren, A.; Barzilai, A. Glutaredoxin protects cerebellar granule neurons from dopamine-induced apoptosis by activating NF-kappa B via Ref-1. *J. Biol. Chem.* **2001**, *276*, 1335–1344.
154. Jette, N.; Lees-Miller, S. P. The DNA-dependent protein kinase: A multifunctional protein kinase with roles in DNA double strand break repair and mitosis. *Prog. Biophys. Mol. Biol.* **2015**, *117*, 194–205.
155. Sancar, A.; Lindsey-Boltz, L. A.; Unsal-Kacmaz, K.; Linn, S. Molecular mechanisms of mammalian DNA repair and the DNA damage checkpoints. *Annu. Rev. Biochem.* **2004**, *73*, 39–85.
156. Janssens, S.; Tschopp, J. Signals from within: the DNA-damage-induced NF-kappaB response. *Cell Death Differ.* **2006**, *13*, 773–784.
157. Lavon, I.; Fuchs, D.; Zrihan, D.; Efroni, G.; Zelikovitch, B.; Fellig, Y.; Siegal, T. Novel mechanism whereby nuclear factor kappaB mediates DNA damage repair through regulation of O(6)-methylguanine-DNA-methyltransferase. *Cancer Res.* **2007**, *67*, 8952–8959.
158. McCool, K. W.; Miyamoto, S. DNA damage-dependent NF-kappaB activation: NEMO turns nuclear signaling inside out. *Immunol Rev.* **2012**, *246*, 311–326.
159. Mabb, A. M.; Wuerzberger-Davis, S. M.; Miyamoto, S. PIASy mediates NEMO sumoylation and NF-kappaB activation in response to genotoxic stress. *Nat. Cell Biol.* **2006**, *8*, 986–993.
160. Hadian, K.; Krappmann, D. Signals from the nucleus: activation of NF-kappaB by cytosolic ATM in the DNA damage response. *Sci. Signal.* **2011**, *4*, pe2.
161. Shiloh, Y.; Ziv, Y. The ATM protein kinase: regulating the cellular response to genotoxic stress, and more. *Nat. Rev. Mol. Cell Biol.* **2013**, *14*, 197–210.
162. Ak, P.; Levine, A. J. p53 and NF-kappaB: different strategies for responding to stress lead to a functional antagonism. *FASEB J.* **2010**, *24*, 3643–3652.
163. Guo, Z.; Kozlov, S.; Lavin, M. F.; Person, M. D.; Paull, T. T. ATM activation by oxidative stress. *Science* **2010**, *330*, 517–521.
164. Wu, Z. H.; Miyamoto, S. Induction of a pro-apoptotic ATM-NF-kappaB pathway and its repression by ATR in response to replication stress. *EMBO J.* **2008**, *27*, 1963–1973.
165. Liu, L.; Kwak, Y. T.; Bex, F.; Garcia-Martinez, L. F.; Li, X. H.; Meek, K.; Lane, W. S.; Gaynor, R. B. DNA-dependent protein kinase phosphorylation of IkappaB alpha and IkappaB beta regulates NF-kappaB DNA binding properties. *Mol. Cell Biol.* **1998**, *18*, 4221–4234.
166. Ju, J.; Naura, A. S.; Errami, Y.; Zerfaoui, M.; Kim, H.; Kim, J. G.; Abd Elmageed, Z. Y.; Abdel-Mageed, A. B.; Giardina, C.; Beg, A. A.; Smulson, M. E.; Boulares, A. H. Phosphorylation of p50 NF-kappaB at

Publication Date (Web): October 13, 2015 | doi: 10.1021/bk-2015-1200.ch003

a single serine residue by DNA-dependent protein kinase is critical for VCAM-1 expression upon TNF treatment. *J. Biol. Chem.* **2010**, *285*, 41152–41160.
167. Loizou, J. I.; El-Khamisy, S. F.; Zlatanou, A.; Moore, D. J.; Chan, D. W.; Qin, J.; Sarno, S.; Meggio, F.; Pinna, L. A.; Caldecott, K. W. The protein kinase CK2 facilitates repair of chromosomal DNA single-strand breaks. *Cell* **2004**, *117*, 17–28.
168. Moller, P.; Lohr, M.; Folkmann, J. K.; Mikkelsen, L.; Loft, S. Aging and oxidatively damaged nuclear DNA in animal organs. *Free Radical Biol. Med.* **2010**, *48*, 1275–1285.
169. Larsson, N. G. Somatic mitochondrial DNA mutations in mammalian aging. *Annu. Rev. Biochem.* **2010**, *79*, 683–706.
170. Canugovi, C.; Misiak, M.; Ferrarelli, L. K.; Croteau, D. L.; Bohr, V. A. The role of DNA repair in brain related disease pathology. *DNA Repair (Amsterdam)* **2013**, *12*, 578–587.
171. Lu, X. H.; Mattis, V. B.; Wang, N.; Al-Ramahi, I.; van den Berg, N.; Fratantoni, S. A.; Waldvogel, H.; Greiner, E.; Osmand, A.; Elzein, K.; Xiao, J.; Dijkstra, S.; de Pril, R.; Vinters, H. V.; Faull, R.; Signer, E.; Kwak, S.; Marugan, J. J.; Botas, J.; Fischer, D. F.; Svendsen, C. N.; Munoz-Sanjuan, I.; Yang, X. W. Targeting ATM ameliorates mutant Huntingtin toxicity in cell and animal models of Huntington's disease. *Sci. Transl. Med.* **2014**, *6*, 268ra178.
172. Camins, A.; Pizarro, J. G.; Alvira, D.; Gutierrez-Cuesta, J.; de la Torre, A. V.; Folch, J.; Sureda, F. X.; Verdaguer, E.; Junyent, F.; Jordan, J.; Ferrer, I.; Pallas, M. Activation of ataxia telangiectasia muted under experimental models and human Parkinson's disease. *Cell Mol. Life Sci.* **2010**, *67*, 3865–3882.
173. Fan, M. M.; Zhang, H.; Hayden, M. R.; Pelech, S. L.; Raymond, L. A. Protective up-regulation of CK2 by mutant huntingtin in cells co-expressing NMDA receptors. *J. Neurochem.* **2008**, *104*, 790–805.
174. Takahashi, M.; Ko, L. W.; Kulathingal, J.; Jiang, P.; Sevlever, D.; Yen, S. H. Oxidative stress-induced phosphorylation, degradation and aggregation of alpha-synuclein are linked to upregulated CK2 and cathepsin D. *Eur J. Neurosci.* **2007**, *26*, 863–874.
175. Cardinale, A.; Racaniello, M.; Saladini, S.; De Chiara, G.; Mollinari, C.; de Stefano, M. C.; Pocchiari, M.; Garaci, E.; Merlo, D. Sublethal doses of beta-amyloid peptide abrogate DNA-dependent protein kinase activity. *J. Biol. Chem.* **2012**, *287*, 2618–2631.
176. Brekke, E. M.; Walls, A. B.; Schousboe, A.; Waagepetersen, H. S.; Sonnewald, U. Quantitative importance of the pentose phosphate pathway determined by incorporation of 13C from [2-13C]- and [3-13C]glucose into TCA cycle intermediates and neurotransmitter amino acids in functionally intact neurons. *J. Cereb. Blood Flow Metab.* **2012**, *32*, 1788–1799.
177. Fernandez-Fernandez, S.; Almeida, A.; Bolanos, J. P. Antioxidant and bioenergetic coupling between neurons and astrocytes. *Biochem. J.* **2012**, *443*, 3–11.

Publication Date (Web): October 13, 2015 | doi: 10.1021/bk-2015-1200.ch003

178. Inoki, K.; Kim, J.; Guan, K. L. AMPK and mTOR in cellular energy homeostasis and drug targets. *Annu. Rev. Pharmacol. Toxicol.* **2012**, *52*, 381–400.
179. Kim, S. Y.; Jeong, S.; Jung, E.; Baik, K. H.; Chang, M. H.; Kim, S. A.; Shim, J. H.; Chun, E.; Lee, K. Y. AMP-activated protein kinase-alpha1 as an activating kinase of TGF-beta-activated kinase 1 has a key role in inflammatory signals. *Cell Death Dis.* **2012**, *3*, e357.
180. Ghosh, S.; Tergaonkar, V.; Rothlin, C. V.; Correa, R. G.; Bottero, V.; Bist, P.; Verma, I. M.; Hunter, T. Essential role of tuberous sclerosis genes TSC1 and TSC2 in NF-kappaB activation and cell survival. *Cancer Cell.* **2006**, *10*, 215–226.
181. Carling, D.; Mayer, F. V.; Sanders, M. J.; Gamblin, S. J. AMP-activated protein kinase: nature's energy sensor. *Nat. Chem Biol.* **2011**, *7*, 512–518.
182. Mauro, C.; Leow, S. C.; Anso, E.; Rocha, S.; Thotakura, A. K.; Tornatore, L.; Moretti, M.; De Smaele, E.; Beg, A. A.; Tergaonkar, V.; Chandel, N. S.; Franzoso, G. NF-kappaB controls energy homeostasis and metabolic adaptation by upregulating mitochondrial respiration. *Nat. Cell Biol.* **2011**, *13*, 1272–1279.
183. Johnson, R. F.; Witzel, II; Perkins, N. D. p53-dependent regulation of mitochondrial energy production by the RelA subunit of NF-kappaB. *Cancer Res.* **2011**, *71*, 5588–5597.
184. Pathak, D.; Berthet, A.; Nakamura, K. Energy failure: does it contribute to neurodegeneration? *Ann. Neurol.* **2013**, *74*, 506–516.
185. Soane, L.; Kahraman, S.; Kristian, T.; Fiskum, G. Mechanisms of impaired mitochondrial energy metabolism in acute and chronic neurodegenerative disorders. *J. Neurosci. Res.* **2007**, *85*, 3407–3415.
186. Pryor, W. M.; Biagioli, M.; Shahani, N.; Swarnkar, S.; Huang, W. C.; Page, D. T.; MacDonald, M. E.; Subramaniam, S. Huntingtin promotes mTORC1 signaling in the pathogenesis of Huntington's disease. *Sci. Signal.* **2014**, *7*, ra103.
187. Lee, J. H.; Tecedor, L.; Chen, Y. H.; Monteys, A. M.; Sowada, M. J.; Thompson, L. M.; Davidson, B. L. Reinstating aberrant mTORC1 activity in Huntington's disease mice improves disease phenotypes. *Neuron* **2015**, *85*, 303–315.
188. Tang, Z.; Bereczki, E.; Zhang, H.; Wang, S.; Li, C.; Ji, X.; Branca, R. M.; Lehtio, J.; Guan, Z.; Filipcik, P.; Xu, S.; Winblad, B.; Pei, J. J. Mammalian target of rapamycin (mTor) mediates tau protein dyshomeostasis: implication for Alzheimer disease. *J. Biol. Chem.* **2013**, *288*, 15556–15570.
189. Malagelada, C.; Jin, Z. H.; Jackson-Lewis, V.; Przedborski, S.; Greene, L. A. Rapamycin protects against neuron death in in vitro and in vivo models of Parkinson's disease. *J. Neurosci.* **2010**, *30*, 1166–1175.
190. Caccamo, A.; Majumder, S.; Deng, J. J.; Bai, Y.; Thornton, F. B.; Oddo, S. Rapamycin rescues TDP-43 mislocalization and the associated low molecular mass neurofilament instability. *J. Biol. Chem.* **2009**, *284*, 27416–27424.
191. Caccamo, A.; Majumder, S.; Richardson, A.; Strong, R.; Oddo, S. Molecular interplay between mammalian target of rapamycin (mTOR), amyloid-beta,

Publication Date (Web): October 13, 2015 | doi: 10.1021/bk-2015-1200.ch003

and Tau: effects on cognitive impairments. *J. Biol. Chem.* **2010**, *285*, 13107–13120.
192. Mairet-Coello, G.; Courchet, J.; Pieraut, S.; Courchet, V.; Maximov, A.; Polleux, F. The CAMKK2-AMPK kinase pathway mediates the synaptotoxic effects of Abeta oligomers through Tau phosphorylation. *Neuron* **2013**, *78*, 94–108.
193. Caccamo, A.; De Pinto, V.; Messina, A.; Branca, C.; Oddo, S. Genetic reduction of mammalian target of rapamycin ameliorates Alzheimer's disease-like cognitive and pathological deficits by restoring hippocampal gene expression signature. *J. Neurosci.* **2014**, *34*, 7988–7998.
194. Vingtdeux, V.; Giliberto, L.; Zhao, H.; Chandakkar, P.; Wu, Q.; Simon, J. E.; Janle, E. M.; Lobo, J.; Ferruzzi, M. G.; Davies, P.; Marambaud, P. AMP-activated protein kinase signaling activation by resveratrol modulates amyloid-beta peptide metabolism. *J. Biol. Chem.* **2010**, *285*, 9100–9113.
195. Vingtdeux, V.; Chandakkar, P.; Zhao, H.; d'Abramo, C.; Davies, P.; Marambaud, P. Novel synthetic small-molecule activators of AMPK as enhancers of autophagy and amyloid-beta peptide degradation. *FASEB J.* **2011**, *25*, 219–231.
196. Lim, M. A.; Selak, M. A.; Xiang, Z.; Krainc, D.; Neve, R. L.; Kraemer, B. C.; Watts, J. L.; Kalb, R. G. Reduced activity of AMP-activated protein kinase protects against genetic models of motor neuron disease. *J. Neurosci.* **2012**, *32*, 1123–1141.
197. Liu, Y. J.; Ju, T. C.; Chen, H. M.; Jang, Y. S.; Lee, L. M.; Lai, H. L.; Tai, H. C.; Fang, J. M.; Lin, Y. L.; Tu, P. H.; Chern, Y. Activation of AMP-activated protein kinase alpha1 mediates mislocalization of TDP-43 in amyotrophic lateral sclerosis. *Hum. Mol. Genet.* **2015**, *24*, 787–801.
198. Ju, T. C.; Chen, H. M.; Lin, J. T.; Chang, C. P.; Chang, W. C.; Kang, J. J.; Sun, C. P.; Tao, M. H.; Tu, P. H.; Chang, C.; Dickson, D. W.; Chern, Y. Nuclear translocation of AMPK-alpha1 potentiates striatal neurodegeneration in Huntington's disease. *J. Cell Biol.* **2011**, *194*, 209–227.
199. Ng, C. H.; Guan, M. S.; Koh, C.; Ouyang, X.; Yu, F.; Tan, E. K.; O'Neill, S. P.; Zhang, X.; Chung, J.; Lim, K. L. AMP kinase activation mitigates dopaminergic dysfunction and mitochondrial abnormalities in Drosophila models of Parkinson's disease. *J. Neurosci.* **2012**, *32*, 14311–14317.
200. Choi, J. S.; Park, C.; Jeong, J. W. AMP-activated protein kinase is activated in Parkinson's disease models mediated by 1-methyl-4-phenyl-1,2,3,6-tetrahydropyridine. *Biochem. Biophys. Res. Commun.* **2010**, *391*, 147–151.
201. Dulovic, M.; Jovanovic, M.; Xilouri, M.; Stefanis, L.; Harhaji-Trajkovic, L.; Kravic-Stevovic, T.; Paunovic, V.; Ardah, M. T.; El-Agnaf, O. M.; Kostic, V.; Markovic, I.; Trajkovic, V. The protective role of AMP-activated protein kinase in alpha-synuclein neurotoxicity in vitro. *Neurobiol. Dis.* **2014**, *63*, 1–11.
202. Jiang, P.; Gan, M.; Ebrahim, A. S.; Castanedes-Casey, M.; Dickson, D. W.; Yen, S. H. Adenosine monophosphate-activated protein kinase overactivation leads to accumulation of alpha-synuclein oligomers and decrease of neurites. *Neurobiol. Aging* **2013**, *34*, 1504–1515.

Publication Date (Web): October 13, 2015 | doi: 10.1021/bk-2015-1200.ch003

203. Xu, Y.; Liu, C.; Chen, S.; Ye, Y.; Guo, M.; Ren, Q.; Liu, L.; Zhang, H.; Xu, C.; Zhou, Q.; Huang, S.; Chen, L. Activation of AMPK and inactivation of Akt result in suppression of mTOR-mediated S6K1 and 4E-BP1 pathways leading to neuronal cell death in in vitro models of Parkinson's disease. *Cell Signal.* **2014**, *26*, 1680–1689.
204. Kim, T. W.; Cho, H. M.; Choi, S. Y.; Suguira, Y.; Hayasaka, T.; Setou, M.; Koh, H. C.; Hwang, E. M.; Park, J. Y.; Kang, S. J.; Kim, H. S.; Kim, H.; Sun, W. (ADP-ribose) polymerase 1 and AMP-activated protein kinase mediate progressive dopaminergic neuronal degeneration in a mouse model of Parkinson's disease. *Cell Death Dis.* **2013**, *4*, e919.
205. Tanaka, K.; Matsuda, N. Proteostasis and neurodegeneration: the roles of proteasomal degradation and autophagy. *Biochim Biophys Acta.* **2014**, *1843*, 197–204.
206. Cook, C.; Stetler, C.; Petrucelli, L. Disruption of protein quality control in Parkinson's disease. *Cold Spring Harb Perspect Med.* **2012**, *2*, a009423.
207. Dennissen, F. J.; Kholod, N.; van Leeuwen, F. W. The ubiquitin proteasome system in neurodegenerative diseases: culprit, accomplice or victim? *Prog Neurobiol.* **2012**, *96*, 190–207.
208. Dahl, J. U.; Gray, M. J.; Jakob, U. Protein Quality Control under Oxidative Stress Conditions. *J. Mol. Biol.* **2015**, *427*, 1549–1563.
209. Grimm, S.; Hohn, A.; Grune, T. Oxidative protein damage and the proteasome. *Amino Acids* **2012**, *42*, 23–38.
210. Shang, F.; Taylor, A. Ubiquitin-proteasome pathway and cellular responses to oxidative stress. *Free Radical Biol. Med.* **2011**, *51*, 5–16.
211. Cotto-Rios, X. M.; Bekes, M.; Chapman, J.; Ueberheide, B.; Huang, T. T. Deubiquitinases as a signaling target of oxidative stress. *Cell Rep.* **2012**, *2*, 1475–1484.
212. Lee, J. G.; Baek, K.; Soetandyo, N.; Ye, Y. Reversible inactivation of deubiquitinases by reactive oxygen species in vitro and in cells. *Nat. Commun.* **2013**, *4*, 1568.
213. Shang, F.; Gong, X.; Taylor, A. Activity of ubiquitin-dependent pathway in response to oxidative stress. Ubiquitin-activating enzyme is transiently up-regulated. *J. Biol. Chem.* **1997**, *272*, 23086–23093.
214. Chen, E.; Hrdlickova, R.; Nehyba, J.; Longo, D. L.; Bose, H. R., Jr.; Li, C. C. Degradation of proto-oncoprotein c-Rel by the ubiquitin-proteasome pathway. *J. Biol. Chem.* **1998**, *273*, 35201–35207.
215. Wu, M.; Bian, Q.; Liu, Y.; Fernandes, A. F.; Taylor, A.; Pereira, P.; Shang, F. Sustained oxidative stress inhibits NF-kappaB activation partially via inactivating the proteasome. *Free Radical Biol. Med.* **2009**, *46*, 62–69.
216. Brigelius-Flohe, R.; Flohe, L. Basic principles and emerging concepts in the redox control of transcription factors. *Antioxid. Redox Signalling* **2011**, *15*, 2335–2381.
217. Storz, P. Forkhead homeobox type O transcription factors in the responses to oxidative stress. *Antioxid. Redox Signalling* **2011**, *14*, 593–605.
218. Yang, H.; Magilnick, N.; Lee, C.; Kalmaz, D.; Ou, X.; Chan, J. Y.; Lu, S. C. Nrf1 and Nrf2 regulate rat glutamate-cysteine ligase catalytic subunit

Publication Date (Web): October 13, 2015 | doi: 10.1021/bk-2015-1200.ch003

transcription indirectly via NF-kappaB and AP-1. *Mol. Cell Biol.* **2005**, *25*, 5933–5946.
219. Li, Z.; Zhang, H.; Chen, Y.; Fan, L.; Fang, J. Forkhead transcription factor FOXO3a protein activates nuclear factor kappaB through B-cell lymphoma/leukemia 10 (BCL10) protein and promotes tumor cell survival in serum deprivation. *J. Biol. Chem.* **2012**, *287*, 17737–17745.
220. Lastres-Becker, I.; Ulusoy, A.; Innamorato, N. G.; Sahin, G.; Rabano, A.; Kirik, D.; Cuadrado, A. alpha-Synuclein expression and Nrf2 deficiency cooperate to aggravate protein aggregation, neuronal death and inflammation in early-stage Parkinson's disease. *Hum. Mol. Genet.* **2012**, *21*, 3173–3192.
221. Innamorato, N. G.; Jazwa, A.; Rojo, A. I.; Garcia, C.; Fernandez-Ruiz, J.; Grochot-Przeczek, A.; Stachurska, A.; Jozkowicz, A.; Dulak, J.; Cuadrado, A. Different susceptibility to the Parkinson's toxin MPTP in mice lacking the redox master regulator Nrf2 or its target gene heme oxygenase-1. *PLoS One* **2010**, *5*, e11838.
222. Rojo, A. I.; Innamorato, N. G.; Martin-Moreno, A. M.; De Ceballos, M. L.; Yamamoto, M.; Cuadrado, A. Nrf2 regulates microglial dynamics and neuroinflammation in experimental Parkinson's disease. *Glia* **2010**, *58*, 588–598.
223. Burton, N. C.; Kensler, T. W.; Guilarte, T. R. In vivo modulation of the Parkinsonian phenotype by Nrf2. *Neurotoxicology* **2006**, *27*, 1094–1100.
224. Calkins, M. J.; Jakel, R. J.; Johnson, D. A.; Chan, K.; Kan, Y. W.; Johnson, J. A. Protection from mitochondrial complex II inhibition in vitro and in vivo by Nrf2-mediated transcription. *Proc. Natl. Acad. Sci. U. S. A.* **2005**, *102*, 244–249.
225. Chen, P. C.; Vargas, M. R.; Pani, A. K.; Smeyne, R. J.; Johnson, D. A.; Kan, Y. W.; Johnson, J. A. Nrf2-mediated neuroprotection in the MPTP mouse model of Parkinson's disease: Critical role for the astrocyte. *Proc. Natl. Acad. Sci. U. S. A.* **2009**, *106*, 2933–2938.
226. Vargas, M. R.; Johnson, D. A.; Sirkis, D. W.; Messing, A.; Johnson, J. A. Nrf2 activation in astrocytes protects against neurodegeneration in mouse models of familial amyotrophic lateral sclerosis. *J. Neurosci.* **2008**, *28*, 13574–13581.
227. Kanninen, K.; Heikkinen, R.; Malm, T.; Rolova, T.; Kuhmonen, S.; Leinonen, H.; Yla-Herttuala, S.; Tanila, H.; Levonen, A. L.; Koistinaho, M.; Koistinaho, J. Intrahippocampal injection of a lentiviral vector expressing Nrf2 improves spatial learning in a mouse model of Alzheimer's disease. *Proc. Natl. Acad. Sci. U. S. A.* **2009**, *106*, 16505–16510.
228. Circu, M. L.; Aw, T. Y. Reactive oxygen species, cellular redox systems, and apoptosis. *Free Radical Biol. Med.* **2010**, *48*, 749–762.
229. Filomeni, G.; Ciriolo, M. R. Redox control of apoptosis: an update. *Antioxid. Redox Signalling* **2006**, *8*, 2187–2192.
230. Franklin, R. A.; Rodriguez-Mora, O. G.; Lahair, M. M.; McCubrey, J. A. Activation of the calcium/calmodulin-dependent protein kinases as a consequence of oxidative stress. *Antioxid. Redox Signalling* **2006**, *8*, 1807–1817.

Publication Date (Web): October 13, 2015 | doi: 10.1021/bk-2015-1200.ch003

231. Giorgi, C.; Agnoletto, C.; Baldini, C.; Bononi, A.; Bonora, M.; Marchi, S.; Missiroli, S.; Patergnani, S.; Poletti, F.; Rimessi, A.; Zavan, B.; Pinton, P. Redox control of protein kinase C: cell- and disease-specific aspects. *Antioxid. Redox Signalling* **2010**, *13*, 1051–1085.
232. Leslie, N. R. The redox regulation of PI 3-kinase-dependent signaling. *Antioxid. Redox Signalling* **2006**, *8*, 1765–1774.
233. Runchel, C.; Matsuzawa, A.; Ichijo, H. Mitogen-activated protein kinases in mammalian oxidative stress responses. *Antioxid. Redox Signalling* **2011**, *15*, 205–218.
234. Truong, T. H.; Carroll, K. S. Redox regulation of protein kinases. *Crit. Rev. Biochem. Mol. Biol.* **2013**, *48*, 332–356.
235. Miloso, M.; Scuteri, A.; Foudah, D.; Tredici, G. MAPKs as mediators of cell fate determination: an approach to neurodegenerative diseases. *Curr. Med Chem.* **2008**, *15*, 538–548.
236. Alkon, D. L.; Sun, M. K.; Nelson, T. J. PKC signaling deficits: a mechanistic hypothesis for the origins of Alzheimer's disease. *Trends Pharmacol. Sci.* **2007**, *28*, 51–60.
237. Giraldo, E.; Lloret, A.; Fuchsberger, T.; Vina, J. Abeta and tau toxicities in Alzheimer's are linked via oxidative stress-induced p38 activation: protective role of vitamin E. *Redox Biol.* **2014**, *2*, 873–877.
238. Hensley, K.; Floyd, R. A.; Zheng, N. Y.; Nael, R.; Robinson, K. A.; Nguyen, X.; Pye, Q. N.; Stewart, C. A.; Geddes, J.; Markesbery, W. R.; Patel, E.; Johnson, G. V.; Bing, G. p38 kinase is activated in the Alzheimer's disease brain. *J. Neurochem.* **1999**, *72*, 2053–2058.
239. Karunakaran, S.; Ravindranath, V. Activation of p38 MAPK in the substantia nigra leads to nuclear translocation of NF-kappaB in MPTP-treated mice: implication in Parkinson's disease. *J. Neurochem.* **2009**, *109*, 1791–1799.
240. Lievens, J. C.; Iche, M.; Laval, M.; Faivre-Sarrailh, C.; Birman, S. AKT-sensitive or insensitive pathways of toxicity in glial cells and neurons in Drosophila models of Huntington's disease. *Hum. Mol. Genet.* **2008**, *17*, 882–894.
241. Ries, V.; Henchcliffe, C.; Kareva, T.; Rzhetskaya, M.; Bland, R.; During, M. J.; Kholodilov, N.; Burke, R. E. Oncoprotein Akt/PKB induces trophic effects in murine models of Parkinson's disease. *Proc. Natl. Acad. Sci. U. S. A.* **2006**, *103*, 18757–18762.
242. Zhan, L.; Xie, Q.; Tibbetts, R. S. Opposing roles of p38 and JNK in a Drosophila model of TDP-43 proteinopathy reveal oxidative stress and innate immunity as pathogenic components of neurodegeneration. *Hum. Mol. Genet.* **2015**, *24*, 757–772.
243. Tanaka, H.; Fujita, N.; Tsuruo, T. 3-Phosphoinositide-dependent protein kinase-1-mediated IkappaB kinase beta (IkkB) phosphorylation activates NF-kappaB signaling. *J. Biol. Chem.* **2005**, *280*, 40965–40973.
244. Kaltschmidt, B.; Uherek, M.; Volk, B.; Baeuerle, P. A.; Kaltschmidt, C. Transcription factor NF-kappaB is activated in primary neurons by amyloid beta peptides and in neurons surrounding early plaques from patients with Alzheimer disease. *Proc. Natl. Acad. Sci. U. S. A.* **1997**, *94*, 2642–2647.

Publication Date (Web): October 13, 2015 | doi: 10.1021/bk-2015-1200.ch003

245. Bonaiuto, C.; McDonald, P. P.; Rossi, F.; Cassatella, M. A. Activation of nuclear factor-kappa B by beta-amyloid peptides and interferon-gamma in murine microglia. *J. Neuroimmunol.* **1997**, *77*, 51–56.
246. Ophir, G.; Amariglio, N.; Jacob-Hirsch, J.; Elkon, R.; Rechavi, G.; Michaelson, D. M. Apolipoprotein E4 enhances brain inflammation by modulation of the NF-kappaB signaling cascade. *Neurobiol. Dis.* **2005**, *20*, 709–718.
247. Hunot, S.; Brugg, B.; Ricard, D.; Michel, P. P.; Muriel, M. P.; Ruberg, M.; Faucheux, B. A.; Agid, Y.; Hirsch, E. C. Nuclear translocation of NF-kappaB is increased in dopaminergic neurons of patients with parkinson disease. *Proc. Natl. Acad. Sci. U. S. A.* **1997**, *94*, 7531–7536.
248. Casciati, A.; Ferri, A.; Cozzolino, M.; Celsi, F.; Nencini, M.; Rotilio, G.; Carri, M. T. Oxidative modulation of nuclear factor-kappaB in human cells expressing mutant fALS-typical superoxide dismutases. *J. Neurochem.* **2002**, *83*, 1019–1029.
249. Papa, S.; Bubici, C.; Zazzeroni, F.; Pham, C. G.; Kuntzen, C.; Knabb, J. R.; Dean, K.; Franzoso, G. The NF-kappaB-mediated control of the JNK cascade in the antagonism of programmed cell death in health and disease. *Cell Death Differ.* **2006**, *13*, 712–729.
250. Lezoualc'h, F.; Sagara, Y.; Holsboer, F.; Behl, C. High constitutive NF-kappaB activity mediates resistance to oxidative stress in neuronal cells. *J. Neurosci.* **1998**, *18*, 3224–3232.
251. Fridmacher, V.; Kaltschmidt, B.; Goudeau, B.; Ndiaye, D.; Rossi, F. M.; Pfeiffer, J.; Kaltschmidt, C.; Israel, A.; Memet, S. Forebrain-specific neuronal inhibition of nuclear factor-kappaB activity leads to loss of neuroprotection. *J. Neurosci.* **2003**, *23*, 9403–9408.
252. Mattson, M. P.; Goodman, Y.; Luo, H.; Fu, W.; Furukawa, K. Activation of NF-kappaB protects hippocampal neurons against oxidative stress-induced apoptosis: evidence for induction of manganese superoxide dismutase and suppression of peroxynitrite production and protein tyrosine nitration. *J. Neurosci. Res.* **1997**, *49*, 681–697.
253. Kaltschmidt, B.; Uherek, M.; Wellmann, H.; Volk, B.; Kaltschmidt, C. Inhibition of NF-kappaB potentiates amyloid beta-mediated neuronal apoptosis. *Proc. Natl. Acad. Sci. U. S. A.* **1999**, *96*, 9409–9414.
254. Yu, Z.; Zhou, D.; Cheng, G.; Mattson, M. P. Neuroprotective role for the p50 subunit of NF-kappaB in an experimental model of Huntington's disease. *J. Mol. Neurosci.* **2000**, *15*, 31–44.
255. Panet, H.; Barzilai, A.; Daily, D.; Melamed, E.; Offen, D. Activation of nuclear transcription factor kappa B (NF-kappaB) is essential for dopamine-induced apoptosis in PC12 cells. *J. Neurochem.* **2001**, *77*, 391–398.
256. Khoshnan, A.; Ko, J.; Watkin, E. E.; Paige, L. A.; Reinhart, P. H.; Patterson, P. H. Activation of the IkappaB kinase complex and nuclear factor-kappaB contributes to mutant huntingtin neurotoxicity. *J. Neurosci.* **2004**, *24*, 7999–8008.
257. Henn, I. H.; Bouman, L.; Schlehe, J. S.; Schlierf, A.; Schramm, J. E.; Wegener, E.; Nakaso, K.; Culmsee, C.; Berninger, B.; Krappmann, D.; Tatzelt, J.; Winklhofer, K. F. Parkin mediates neuroprotection through

Publication Date (Web): October 13, 2015 | doi: 10.1021/bk-2015-1200.ch003

activation of IkappaB kinase/nuclear factor-kappaB signaling. *J. Neurosci.* **2007**, *27*, 1868–1878.
258. Pizzi, M.; Sarnico, I.; Boroni, F.; Benarese, M.; Steimberg, N.; Mazzoleni, G.; Dietz, G. P.; Bahr, M.; Liou, H. C.; Spano, P. F. NF-kappaB factor c-Rel mediates neuroprotection elicited by mGlu5 receptor agonists against amyloid beta-peptide toxicity. *Cell Death Differ.* **2005**, *12*, 761–772.
259. Baiguera, C.; Alghisi, M.; Pinna, A.; Bellucci, A.; De Luca, M. A.; Frau, L.; Morelli, M.; Ingrassia, R.; Benarese, M.; Porrini, V.; Pellitteri, M.; Bertini, G.; Fabene, P. F.; Sigala, S.; Spillantini, M. G.; Liou, H. C.; Spano, P. F.; Pizzi, M. Late-onset Parkinsonism in NFkappaB/c-Rel-deficient mice. *Brain* **2012**, *135*, 2750–2765.
260. Lawrence, T. The nuclear factor NF-kappaB pathway in inflammation. *Cold Spring Harbor Perspect. Biol.* **2009**, *1*, a001651.
261. Cunningham, C. Microglia and neurodegeneration: the role of systemic inflammation. *Glia* **2013**, *61*, 71–90.
262. Brown, G. C.; Neher, J. J. Inflammatory neurodegeneration and mechanisms of microglial killing of neurons. *Mol. Neurobiol.* **2010**, *41*, 242–247.
263. Chen, J.; Zhou, Y.; Mueller-Steiner, S.; Chen, L. F.; Kwon, H.; Yi, S.; Mucke, L.; Gan, L. SIRT1 protects against microglia-dependent amyloid-beta toxicity through inhibiting NF-kappaB signaling. *J. Biol. Chem.* **2005**, *280*, 40364–40374.
264. Hsiao, H. Y.; Chen, Y. C.; Chen, H. M.; Tu, P. H.; Chern, Y. A critical role of astrocyte-mediated nuclear factor-kappaB-dependent inflammation in Huntington's disease. *Hum. Mol. Genet.* **2013**, *22*, 1826–1842.
265. Ghosh, A.; Roy, A.; Liu, X.; Kordower, J. H.; Mufson, E. J.; Hartley, D. M.; Ghosh, S.; Mosley, R. L.; Gendelman, H. E.; Pahan, K. Selective inhibition of NF-kappaB activation prevents dopaminergic neuronal loss in a mouse model of Parkinson's disease. *Proc. Natl. Acad. Sci. U. S. A.* **2007**, *104*, 18754–18759.
266. Teismann, P.; Schwaninger, M.; Weih, F.; Ferger, B. Nuclear factor-kappaB activation is not involved in a MPTP model of Parkinson's disease. *Neuroreport.* **2001**, *12*, 1049–1053.
267. Cao, J. P.; Wang, H. J.; Yu, J. K.; Liu, H. M.; Gao, D. S. The involvement of NF-kappaB p65/p52 in the effects of GDNF on DA neurons in early PD rats. *Brain Res Bull.* **2008**, *76*, 505–511.
268. Asanuma, M.; Miyazaki, I. Common anti-inflammatory drugs are potentially therapeutic for Parkinson's disease? *Exp Neurol.* **2007**, *206*, 172–178.
269. Napolitano, M.; Costa, L.; Palermo, R.; Giovenco, A.; Vacca, A.; Gulino, A. Protective effect of pioglitazone, a PPARgamma ligand, in a 3 nitropropionic acid model of Huntington's disease. *Brain Res Bull.* **2011**, *85*, 231–237.
270. Grilli, M.; Pizzi, M.; Memo, M.; Spano, P. Neuroprotection by aspirin and sodium salicylate through blockade of NF-kappaB activation. *Science* **1996**, *274*, 1383–1385.

Publication Date (Web): October 13, 2015 | doi: 10.1021/bk-2015-1200.ch003

Publication Date (Web): October 13, 2015 | doi: 10.1021/bk-2015-1200.ch004

Chapter 4

Oxidative Inactivation of Nitric Oxide and Peroxynitrite Formation in the Vasculature

N. Subelzu,[1] S. Bartesaghi,[1] A. de Bem,[2] and R. Radi[1,*]

[1]Departamento de Bioquímica and Center for Free Radical and Biomedical Research (CEINBIO), Facultad de Medicina, Universidad de la República, Montevideo, 11800 Uruguay

[2]Departamento de Bioquímica, Centro de Ciências Biológicas, Universidade Federal de Santa Catarina, Florianópolis, SC, 88040900 Brazil

[*]E-mail: rradi@fmed.edu.uy

The free radical nitric oxide (•NO) is a vasodilatory compound released by healthy vascular endothelium. Under conditions leading to endothelial dysfunction, •NO bioavailability is compromised partly due to its "oxidative inactivation". Indeed, the vascular wall challenged by hypercholesterolemia, hyperglycemia, turbulent blood flow, inflammatory mediators and cigarette smoke components facilitate the release of superoxide radical anion ($O_2^{\bullet-}$) which participates in the fast consumption of •NO. In turn, this radical-radical combination reaction leads to the generation of peroxynitrite ($ONOO^-$), a potent oxidizing, cytotoxic and proinflammatory species that mediates vascular degeneration. Alternatively, under vascular inflammatory conditions, endothelial-derived •NO can be also consumed by myeloperoxidase (MPO) released by activated neutrophils; in this case, •NO is consumed by oxidation acting as a substrate of MPO Compounds I and II (oxo-ferryl heme radical and oxo-ferryl heme respectively). The oxidative inactivation of •NO comes along with the formation of secondary oxidants that influence vascular responses in a condition defined as ¨nitroxidative stress¨. In this chapter, we provide an overview of the biological chemistry of •NO with a focus on its reactions with $O_2^{\bullet-}$ and other redox partners. In addition, we will provide evidence of the vascular formation of peroxynitrite under conditions of endothelial dysfunction

In Oxidative Stress: Diagnostics, Prevention, and Therapy Volume 2; Hepel, et al.; ACS Symposium Series; American Chemical Society: Washington, DC, 2015.

and vascular degeneration and aging. Among the oxidative modifications induced by peroxynitrite, we will closely address the nitration of tyrosine redisues in key proteins of the vascular system and how this process may participate in pathogenesis and be a predictor of vascular disease severity and evolution. Finally, we will analyze endogenous antioxidant mechanisms and successful pharmacological strategies in pre-clinical and clinical settings that modulate vascular nitroxidative stress that open possibilities for future therapeutics in vascular pathology.

Publication Date (Web): October 13, 2015 | doi: 10.1021/bk-2015-1200.ch004

Nitric Oxide as a Signal Transducing Free Radical Species in the Vasculature: Unique Biochemical Properties and Molecular Targets

Nitric oxide is synthesized in endothelial cells by the endothelial nitric oxide synthase (eNOS) from NADPH, O_2 and L-arginine. In the vasculature, •NO is responsible for different physiological processes such as vessel relaxation, inhibition of platelet aggregation, inhibition of cell proliferation and inhibition of the expression of pro-inflammatory genes (*1*). Endothelial cells are able to detect changes in hemodynamic forces on the vascular wall by releasing •NO which diffuses to the smooth muscle cells and promotes relaxation.

In the smooth muscle cells, •NO promotes the production of cytosolic cGMP by the soluble cytosolic enzyme guanylate cyclase (sGC). cGMP is a second messenger which directly or indirectly modulates different targets, such as protein kinases including protein kinase G (PKG), phosphodiesterases, phospholipase C (PLC), tyrosine phosphodiesterases and ion channels (*2*). The vasorelaxation is produced after the activation of PKG, which activates the myosin light chain phosphatase (MLCP) and dephosphorylates the smooth muscle myosin, resulting in vasorelaxation (*3*, *4*). This effect is potentiated by the effect of MLCP inducing insensitivity of smooth muscle to calcium (*2*). On the other hand, there are calcium pumps named sarco/endoplasmic reticulum Ca^{2+}-ATPase (SERCA) that decrease the cytosolic Ca^{2+} concentration and pump it back to the reticulum, allowing vasorelaxation (*5*). In addition to the action in the smooth muscle cells, •NO can activate the sGC in platelets, reducing the intra-platelet concentration of calcium and regulating several functions, such as interaction of the glycoproteins IIb/IIIa which are essential for platelet aggregation and activation (*2*).

There are two isoforms of the GC enzyme: the soluble and the transmembrane bound enzyme. Both contain two subunits, one regulatory (alpha of 73 kDa) and another catalytic (beta of 70 kDa). The amino terminal of the alpha subunit contains a heme group while the catalytic functions, reside on the carboxyl terminal domain. The heme group contains a ferrous-penta coordinated atom,

In Oxidative Stress: Diagnostics, Prevention, and Therapy Volume 2; Hepel, et al.;
ACS Symposium Series; American Chemical Society: Washington, DC, 2015.

which interacts with high affinity with •NO, becoming the sixth ligand of the heme group, and finally promoting the increase in its activity; there is a shift of the iron atom out of the porphyrin ring, leading to an allosteric activation of the dimer of sGC. Although the heme group of sGC is similar to other heme proteins with axil histidines such as deoxy-mioglobin or deoxy-hemoglobin, sGC is not able to bind O_2 (*6*). Other ligands that can bind to the heme group of the enzyme, such as carbon monoxide (CO), are unable to break the histidine-heme group and cannot activate the enzyme (*4*).

Publication Date (Web): October 13, 2015 | doi: 10.1021/bk-2015-1200.ch004

Nitric Oxide Biochemistry

Nitric oxide is a free radical which contains fifteen electrons, seven of which are located in the outer shell, and with an electronic configuration $(Be)^2$ $(2p\sigma)^2$ $(2p\pi)^4$ $(2\ p\pi^*)^1$ being the last electron in a π^* antibonding molecular orbital. Moreover, it is an non-polar molecule, which is able to freely diffuse through membranes and its biological half-life is about 1 to 10 s (*7*).

Nitric oxide can be oxidized in a third order process with O_2, leading to the formation of nitrogen dioxide ($^{\bullet}NO_2$) (Eq. 1), another free radical species (*8*). In addition, •NO can also react with $^{\bullet}NO_2$ leading to the production of dinitrogen trioxide (N_2O_3) and nitrite (NO_2^-) (Eqs. 2 and 3). In aqueous solutions, $^{\bullet}NO_2$ produces dinitrogen tetroxide (N_2O_4) and this goes to NO_2^- and, to a lesser extent, nitrate (NO_3^-) (Eqs. 4 and 5).

$$2\ ^{\bullet}NO + O_2 \rightarrow 2\ ^{\bullet}NO_2 \qquad \text{(Eq. 1)}$$

$$^{\bullet}NO + {}^{\bullet}NO_2 \rightarrow N_2O_3 \qquad \text{(Eq. 2)}$$

$$N_2O_3 + H_2O \rightarrow 2\ NO_2^- + 2H^+ \qquad \text{(Eq. 3)}$$

$$2\ ^{\bullet}NO_2 \rightarrow N_2O_4 \qquad \text{(Eq. 4)}$$

$$N_2O_4 + H_2O \rightarrow NO_3^- + NO_2^- + 2H^+ \qquad \text{(Eq. 5)}$$

In a biological environment, •NO can also react with metalloproteins leading to a variety of events including signal transduction, modulation of free radical chemistry or cytotoxicity (*9*).

Reaction with Iron-Containing Proteins: Heme Proteins

In the reaction with a heme group, •NO can react with iron in both oxidation states (ferric or ferrous) but it is a better ligand for a ferrous iron since it has an

In Oxidative Stress: Diagnostics, Prevention, and Therapy Volume 2; Hepel, et al.;
ACS Symposium Series; American Chemical Society: Washington, DC, 2015.

Publication Date (Web): October 13, 2015 | doi: 10.1021/bk-2015-1200.ch004

additional electron in the d orbital (d^6) compared to the ferric iron (d^5), increasing the interaction between iron d-orbitals and the antibonding $2p\pi^*$ electron in •NO. By this mechanism, a nitrogen-metal σ-bond is formed by using an unpaired electron pair in the nitrogen atom and a significant degree of π-bond is formed by backbonding between metal d-electrons and the $p\pi^*$ orbitals of •NO. Albeit high constant rates of association of •NO with ferrous iron, it could be a good ligand for ferric state due to its polarity (*10*). Kinetic studies showed that the reaction of •NO with the ferrous state of heme proteins is typically faster (10^7 M^{-1} s^{-1}) than with the ferric state (10^2-10^7 M^{-1} s^{-1}) (*11*). Once formed, the heme nitrosyl complex slowly dissociates but this process is usually faster for the ferric-heme nitrosyl complex (*12*). Moreover, •NO can react with a higher oxidation state of iron of heme-proteins such as the ferryl form (Fe^{4+}=O) (*13–17*); this last process becomes highly relevant in the vasculature in the context of the oxidative inactivation of •NO (*see below*).

Heme proteins with an unoccupied 6th coordination position (*i.e.* hemoglobin, myoglobin, catalase and guanylate cyclase) tend to react faster with •NO than proteins with an occupied 6th position (*i.e.* cytochrome *c*), because •NO requires the displacement of this ligand (usually an amino acid). For the ferric states of proteins with a free 6th coordination position, the presence of a histidine residue coordinated to the heme, stabilizes the binding of water at 6th position, making it more difficult for •NO to bind to the ferric heme compared to ferrous form. The protein-backbone makes the reaction of iron heme with •NO more difficult than with free heme but more selective, because the apolar environment of heme makes the diffusion of •NO much more favorable than that of •NO-derived oxidants such as NO_2^- (*7*).

Heme nitrosyl complexes can be either stable or transient. In some proteins the heme-nitrosyl complexes in equilibrium with free •NO do not result in a net redox change at iron heme. In some cases there is a formation of a transient complex as an intermediate step during heme-•NO interaction and the net formation of NO_2^- or NO_3^-. A classic example of these complexes, which is highly relevant in the vasculature, is represented by the interaction of •NO with the hemoglobin (Hb) heme. Firstly, •NO reacts with oxyhemoglobin (Hb^{2+}-O_2) with a second order rate constant of 3 x 10^7 M^{-1} s^{-1} (*18*), leading to the formation of metahemoglobin (Hb^{3+}) and NO_3^-. Hb^{3+} can also react with •NO yielding deoxy-Hb and nitrosylating species. Finally, •NO reacts with deoxy-Hb (Hb^{2+}) with rate constant above 10^7 M^{-1} s^{-1} leading to the formation of nitrosyl-Hb (Hb^{2+}-•NO, Figure 1). Due to large quantity of Hb^{2+}-O_2 in red blood cells, intravascular reactions between •NO and Hb mainly lead to the formation of Hb^{3+}, therefore being a sink for •NO produced in tissues. Only at low oxygen tensions and in the presence of deoxy-Hb, the formation of Hb^{2+}-NO can occur (*7*).

Some of the cytotoxic effects of •NO are related to its interaction with cytochromes P450 that result in the inhibition of enzymatic activities toward organic substrates. This effect is reversible but prevents O_2 binding to cytochrome P450 and blunts its monooxygenase activity (*18–20*). As •NO and O_2 compete for the same binding site, the efficiency of the inhibition is greater at lower oxygen tensions (*21*). In any case, the binding constant for •NO is significantly larger than that for O_2 (*20*).

In Oxidative Stress: Diagnostics, Prevention, and Therapy Volume 2; Hepel, et al.;
ACS Symposium Series; American Chemical Society: Washington, DC, 2015.

Publication Date (Web): October 13, 2015 | doi: 10.1021/bk-2015-1200.ch004

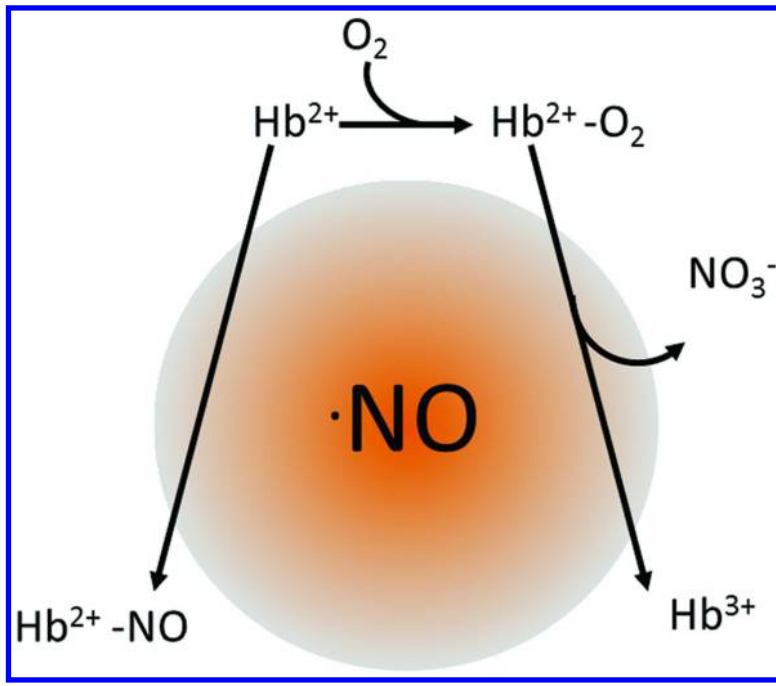

Figure 1. Main reactions of ·NO reaction with hemoglobin in the vascular system

Reaction with Iron-Containing Proteins: Non Heme Proteins

Nitric oxide binds to iron-sulfur clusters leading to the formation of iron-nitrosyl complexes (*22*). This mechanism involves the interaction of the unpaired electron that binds to Fe^{2+} giving iron-nitrosyl complexes that may be stable and reversible. Mitochondrial aconitase is an iron-sulfur complex (4Fe-4S)-containing protein that participates in the Krebs cycle. One Fe of the cluster (Feα) has a free uncoordinated position to sulfur, making it prone to be attacked by different oxidizing electrophiles such as molecular oxygen, peroxynitrite, ferricyanide and superoxide ($O_2^{\bullet-}$). In spite of initial proposals, •NO does not readily disrupt the aconitase iron-sulfur cluster, while peroxynitrite readily does (*23*). Persistently high concentrations of •NO in an oxidative environment lead to protein nitrosylation, cluster disruption and enzyme inhibition (*24–30*).

Mitochondrial electron transport complex I is characterized by several 4Fe-4S and 2Fe-2S cluster groups, while complex II is characterized with numerous clusters 2Fe-2S, 3Fe-4S and 4Fe-4S. Complex IV has 2 heme groups in cytochrome *a* and cytochrome a_3 and also 2 copper cluster groups, Cu_A and Cu_B. The 4Fe-4S groups are ligated to proteins *via* L-cysteine amino acids. Nitric oxide binds to one solvent accessible iron atom and displaces the hydroxyl previously bound, leading to the inhibition (*31*). The mitochondrial •NO concentrations necessary to promote the inhibition in these complexes are below micromolar level. The interactions of •NO with cytochrome *c* oxidase lead to the inhibition of

In Oxidative Stress: Diagnostics, Prevention, and Therapy Volume 2; Hepel, et al.;
ACS Symposium Series; American Chemical Society: Washington, DC, 2015.

the electron transport chain, O_2 consumption and cellular respiration, resulting on a fine regulation of the mitochondrial function as a consequence of the interplay between $^{\bullet}NO$ and O_2 levels. In these cases, the $^{\bullet}NO$-promoted depletion of ATP leads to a passive vasorelaxation (*32*, *33*).

Nitric oxide-mediated disruption of iron homeostasis has been postulated for many years as one important cytotoxic mechanism. Indeed, target cells loose a major fraction of cell and mitochondrial iron during co-incubation with $^{\bullet}NO$ produced *in vitro*. For instance, ferritin is an iron storage protein containing up to 4500 atoms of iron per molecule, mostly in the ferric form. Most of the non heme iron is stored as ferritin and participates in the formation of non heme iron-nitrosyl complexes in cells. Nitric oxide facilitates the release of Fe^{2+} from ferritin, reducing the ferric form to ferrous iron and later the complex dissociates with the iron release (*34*, *35*).

Publication Date (Web): October 13, 2015 | doi: 10.1021/bk-2015-1200.ch004

Reaction with Zinc-Containing Proteins

Zinc is the second most abundant transition metal in higher mammals and is usually complexed with protein ligands known as "zinc fingers" domains, where a zinc atom is coordinated with a thiol group of a cysteine residue or the imidazole nitrogen of an histidine residue. In some enzymes, such as alcohol dehydrogenase, the zinc finger is critical for their activity and some transcription factors proteins require the zinc finger for specific DNA binding (*7*).

It has been shown that the zinc complexing protein metallothionein, which contains 20 thiols per molecule and 7 Zn^{2+}, reacts with $^{\bullet}NO$ leading to the S-nitrosylation and later disulfide bond formation and Zn^{2+} release. Nitric oxide disruption of zinc-clusters represent another mechanism of cytotoxicity and cytotasis, which may previously require the intermediate formation of $^{\bullet}NO_2$ or peroxynitrite-promoted thiol oxidation (*7*).

Reaction with Copper-Containing Proteins

Several copper-containing proteins such as ceruloplasmin, ascorbate oxidase and laccase have been shown to react with $^{\bullet}NO$ (*36–38*). As in iron-containing proteins, the reaction can lead both to the formation of copper-nitrosyl complexes or redox chemistry. However, in some cases is difficult to discriminate between both mechanisms. The reactivity is largely dictated by the structural and geometric characteristics of the copper-protein complex site. There are three different copper types described in proteins (1, 2 and 3). Moreover, some proteins can contain more than one type of copper. Nitric oxide reacts with proteins that contains copper type 1 or 3, but not with type 2. Copper containing proteins type 1 (*i.e.* plastocyanin, azurin, stellacyanin) have the copper atom ligated to two nitrogen of histidine residues, one sulfur from a methionine and one sulfur from a cysteine, leading to the formation of copper-nitrosyl complexes (Eq. 6)

$$Cu^{2+} + {}^{\bullet}NO \rightleftharpoons Cu^{+}\text{-}NO^{+} \qquad \text{(Eq. 6)}$$

In Oxidative Stress: Diagnostics, Prevention, and Therapy Volume 2; Hepel, et al.;
ACS Symposium Series; American Chemical Society: Washington, DC, 2015.

Type 3 copper containing-proteins (*i.e.* hemocyanin, tyrosinase and blue oxidases) have one or more binuclear copper sites. One of them, Cu_B, is coordinated by three histidine residues, located in a highly conserved homology sequence of 56 amino acid. The protein sequence containing the Cu_A is not conserved except for the presence of two or three histidines involved in copper coordination. Type 3 copper-protein complexes can react with •NO in both the oxidized or reduced state.

Cytochrome *c* oxidase contains two copper atoms known as Cu_A and Cu_B in its structure. While Cu_A does not react with •NO, resembling type 2 copper, Cu_B binds to •NO leading to the formation of a photo-dissociable copper-nitrosyl complex described for type 1 copper (*39*). Although, •NO can bind to two different metal centers in cytochrome *c* oxidase, the biological consequences of the reaction between cytochrome a_3 and •NO are better understood (*7*).

Publication Date (Web): October 13, 2015 | doi: 10.1021/bk-2015-1200.ch004

Reactions of NO with Biomolecule-Derived Radicals: Termination Reactions and Formation of Nitrosated Derivatives

Due to the radical character of •NO, it can usually react at diffusion-controlled rates with other radical species derived from lipids, amino acids, DNA bases or sugars resulting in termination reactions and formation of nitrosated species (Eq. 7).

$$^{\bullet}NO + R^{\bullet} \rightarrow RNO \qquad \text{(Eq. 7)}$$

These reactions serve to stop free radical-dependent processs and have been viewed as antioxidant processes mediated by •NO. Indeed, •NO inhibits oxidative damage in numerous *in vitro* and *in vivo* models.

Nitric Oxide-Dependent Inhibition of Lipid Peroxidation

The inhibition of lipid peroxidation by •NO has been proposed to contribute in part to these protective actions (*40–43*).

The reaction of •NO with peroxidizing lipid mixtures leads to inhibition of oxidation (*40*, *41*, *43–45*) by terminating lipid radical-mediated chain propagation reactions (*46*). In biological systems, •NO-dependent inhibition of peroxidation could be due to a number of processes in addition to radical-radical chain termination. At high concentrations, •NO is able to inhibit enzymatic initiators of lipid peroxidation, such as lipoxygenase (*47*) and cyclooxygenase (*48*). Kinetic reaction between lipid peroxyl radicals (LOO•) and •NO lead to immediate termination of oxidation and occurr at a high rate constants (2-11 $\times$ 10^9 M^{-1} s^{-1} (*42*)) respect to other termination reactions (5×10^7 M^{-1} s^{-1} alkyl (L•)-LOO• (*49*); LOO•-LOO• 10^7 M^{-1} s^{-1} (*49*)).

The mechanism of the reaction was proposed as a multiple step-mechanism, in which LOO• reacts with •NO to give an unstable intermediate ROONO (Eq. 8)

In Oxidative Stress: Diagnostics, Prevention, and Therapy Volume 2; Hepel, et al.;
ACS Symposium Series; American Chemical Society: Washington, DC, 2015.

that decomposes very fast (k = 0.1-0.3 s^{-1} (*42*)) yelding free alkoxyl radical ($LO^{\bullet}$) and nitrogen dioxide ($^{\bullet}NO_2$) *via* a caged radical pair ($LO^{\bullet}$ $^{\bullet}NO_2$) (Eq. 9). Reaction between $RO^{\bullet}$ and $^{\bullet}NO$ to form RONO with a rate constant of 3×10^9 M^{-1} s^{-1} (*18*), an nitro-alkyl, has been suggested to account for removal of a second molecule of $^{\bullet}NO$, leading to the formation of nitro-lipids (Eq. 10). The reaction of $ROO^{\bullet}$ with $^{\bullet}NO_2$ leads the formation of $ROONO_2$ (k = $3\text{-}6 \times 10^9$ M^{-1} s^{-1}, Eq. 11) (*50*).

$$^{\bullet}NO + LOO^{\bullet} \rightarrow LOONO \quad \text{(Eq. 8)}$$

$$LOONO \rightarrow {}^{\bullet}NO_2 + LO^{\bullet} \quad \text{(Eq. 9)}$$

$$^{\bullet}NO_2 + LO^{\bullet} \rightarrow LONO_2 \quad \text{(Eq. 10)}$$

$$^{\bullet}NO + LO^{\bullet} \rightarrow LONO \quad \text{(Eq. 11)}$$

Effective antioxidant activity of $^{\bullet}NO$ against lipid peroxidation *in vivo* is influenced by different factors, including the rates of $^{\bullet}NO$ synthesis by vascular cells and the presence of other lipophilic antioxidants. On the other hand, the simultaneous production of $O_2^{\bullet-}$ will reduce the antioxidant capacity of $^{\bullet}NO$, leading to the formation of peroxynitrite (see below) and a consequente reduction in $^{\bullet}NO$ bioavailability to react with lipid radicals. Interestingly, many of the nitrosated and nitrated fatty acids arising from the reactions with $^{\bullet}NO$ and $^{\bullet}NO$-derived species have been revealed as electrophiles which participate in a series of cytoprotective and anti-inflammatory actions through a variety of reaction mechanisms (*51*). These processes are relevant in the vasculature, in particular in what refers to the modulation of lipoprotein oxidation by $^{\bullet}NO$, which typically exerts anti-atherogenic actions (*52*).

S-Nitrosation of Thiols

Thiols are critical sites of interaction for $^{\bullet}NO$ and $O_2^{\bullet-}$ in biological systems, and thiol S-nitrosation as well as oxidation can modulate cellular functions (*53*). In spite of the fact that cellular protein thiols can be nitrosated associated to $^{\bullet}NO$ production, $^{\bullet}NO$ does not react directly with thiol residues. The reaction of $^{\bullet}NO$ with thiyl radicals, the latter being the one-electron oxidation product of thiols (*54*), leads to S-nitrosothiol formation and can be one of the operating mechanisms under nitroxidative stress conditions.

Several groups studied proteins in cell culture that have been reported to be S-nitrosated, such as tissue plasminogen activator (*55*), cathepsin B (*55*), bovine serum albumin (BSA) (*55*), glyceraldehyde-3-phosphate dehydrogenase (GAPDH) (*56*, *57*), and hemoglobin (*57*, *58*). Furthermore, S-nitrosation of thiols has been proposed to be a mechanism for signal transduction in cells (*59*). From this point of view, it is important to understand the biological conditions under which S-nitrosation occur, since this will provide clues as to whether this is a physiological step or may already be a response to stress (*60*). Moncada et al proposed that the mechanism of S-nitrosation requires a previous step in wich

In Oxidative Stress: Diagnostics, Prevention, and Therapy Volume 2; Hepel, et al.;
ACS Symposium Series; American Chemical Society: Washington, DC, 2015.

Publication Date (Web): October 13, 2015 | doi: 10.1021/bk-2015-1200.ch004

the sulfur atom of the cysteine residue is oxidized, or the cellular environment becomes more oxidized, for example reduced gluthatione decreasing from 20 or 40% in 1 hr (*60*).

Of particular relevance in the vascular system is the presence of nitroso-hemoglobin (SNO-Hb), a modification found *in vivo* where a specific and conserved residue β93cys is modified (*61*). Nitroso-Hb has been proposed to participate in the regulation of •NO and O_2 dynamics in blood vessels.

S-Nitroso human serum albumin (SNO-HSA) has been found in human plasma (*62*, *63*). HSA is the most abundant plasma protein and contains 35 cysteine residues, 34 of which are forming disulfide bonds. Only Cys^{34} is free corresponding to the major fraction of free thiol in plasma (*64*) and prone to oxidation and nitrosation reactions.

It has been reported that SNO-HSA may serve *in vivo* as a circulating reservoir for •NO produced by the endothelial cells (*55*). For example, this function was meaningful in animals suffering from ischemia/reperfusion, where administration of SNO-HSA minimized the extent of tissue damage associated with reperfusion (*65*).

Publication Date (Web): October 13, 2015 | doi: 10.1021/bk-2015-1200.ch004

Early Evidences of the Nitric Oxide Reaction with Superoxide: Oxidative Inactivation of EDRF

Furchgott and Zawadzki used isolated aortas that were relaxed *in vitro* when exposed to acetylcholine (*66*), a known vasodilator *in vivo* when injected to patients. It was proposed that the treatment of endothelial cells with acetylcholine released a diffusible factor that was able to relax the smooth muscle and activate the guanylate cyclase, namely an endothelial-derived relaxing factor (EDRF). This EDRF was an agonist released by vascular endothelium in response to several substances including acetylcholine and bradykinin (*66*, *67*). It was found to be inactivated by hemoglobin, myoglobin or methylene blue, highly unstable in perfusion cascades used in vasorelaxation studies and with a short half-life (*34*, *68*, *69*). The chemical structure of EDRF was unknown at the moment but suggested to be a hydroperoxyl or a free radical derivative of arachidonic acid or an unstable aldehyde, ketone or lactone (*70*). In 1987, •NO was identified as EDRF by Moncada *et al* and Ignarro *et al* (*71*, *72*).

Other studies showed that the presence of L-arginine increased EDRF production while methylarginine inhibited it. Importantly, studies performed by Moncada and collaborators showed that the addition of superoxide dismutase (SOD, 5-30 U/mL) to the perfusion buffer used to study rabbit aorta´s vasorelaxation increased the half-life of the EDRF. Superoxide dismutase catalyzes the dismutation of superoxide ($O_2^{\bullet -}$) at near diffusion-controlled rates (eq. 12) (*73*).

$$2\ O_2^{\bullet -} + 2\ H^+ \rightarrow O_2 + H_2O_2 \qquad \text{(Eq. 12)}$$

In Oxidative Stress: Diagnostics, Prevention, and Therapy Volume 2; Hepel, et al.;
ACS Symposium Series; American Chemical Society: Washington, DC, 2015.

In contrast, the addition of catalase to the perfusion buffer did not influence the half-life of EDRF, indicating that H_2O_2 did not affect its stability. These studies demonstrated that the action of EDRF could be modulated by $O_2^{\bullet-}$ present in the vasculature and it was hypothesized that $O_2^{\bullet-}$ might destroy EDRF (*74*). Moreover, agents that produce ($O_2^{\bullet-}$) added to the buffer, decreased the activity of the EDRF. The reactivity of the EDRF with $O_2^{\bullet-}$ was then appreciated before determining the chemical nature of the EDRF, that was difficult due to the low amounts produced by the endothelium (*75–77*).

Studies by Ignarro *et al* showed that vasorelaxation of segments of bovine intrapulmonary artery was compromised in the presence of pyrogallol, an organic polyphenol compound that produces $O_2^{\bullet-}$ upon autooxidation in a cellular system mediating the monovalent reduction of O_2 (Figure 2). The effect of pyrogallol was partially reversed by the presence of SOD (Figure 2). Overall, the data reported in (*71*) indicated that $O_2^{\bullet-}$ could decrease the bioavailability and half-life of $^{\bullet}NO$ causing its oxidative inactivation.

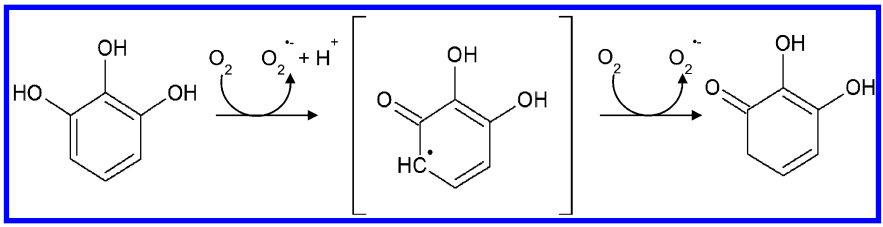

Figure 2. Pyrogallol autoxidation and $O_2^{\bullet-}$ formation

An Alternative Mechanism of Oxidative Inactivation of $^{\bullet}NO$ in the Vasculature: Myeloperoxidase plus Hydrogen Peroxide

Under vascular inflammatory conditions, myeloperoxidase released by activated neutrophils may decrease $^{\bullet}NO$ bioavailability. The mechanism requires the presence of H_2O_2 (typically arising from $O_2^{\bullet-}$ dismutation), which acts as the first substrate of MPO leading to the formation of compound I, an oxo-ferryl species associated to porphyrin cation radical. Elegant work by Abu-Soud and Hazen (*17*) demonstrated that $^{\bullet}NO$ can react with compound I, and subsequently with compound II, in one-electron oxidation reactions to yield NO_2^-. In this way, endothelial-derived $^{\bullet}NO$ acting as the second MPO substrate can be "inactivated" by oxidative reactions (Figure 3). Interestingly, nitrite can also serve as a compound I and II substrate to yield nitrogen dioxide $^{\bullet}NO_2$, a proximal nitrating species (*see below*).

Publication Date (Web): October 13, 2015 | doi: 10.1021/bk-2015-1200.ch004

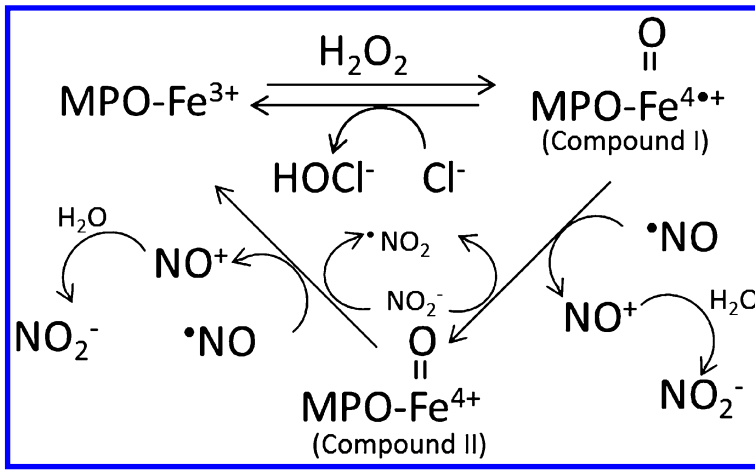

Figure 3. Oxidative inactivation of nitric oxide by MPO. In the vasculature, myeloperoxidase (MPO) is secreted by activated neutrophils. During its normal catalysis of MPO, the ferric heme is oxidized by H_2O_2 to Compound I. The catalytic cycle is normally completed by reaction of compound I with chloride to produce hypoclorite. In the presence of $^{\bullet}NO$, a small proportion of MPO-Compound I can react with it leading to the production of Compound II (oxo-ferryl heme) and yielding nitrite. Nitric oxide can be also consumed in a second reaction to restore the enzyme to the ferric state. In a vascular environment, the realease of MPO represents a $O_2^{\bullet-}$ independent mechanism of oxidative inactivation of $^{\bullet}NO$. In addition, once nitrite is formed, it can also be substrate of Compounds I and II to yield $^{\bullet}NO_2$ and promote tyrosine nitration reactions. Modified from (17).

Conditions and Sources That Enhance the Vascular Formation of Superoxide Radicals

Several physiopathological conditions in the vascular system such as hypercholesterolemia, hyperglycemia, turbulent blood flow, inflammatory mediators and cigarette smoke increase the formation of reactive oxygen species (ROS), in particular $O_2^{\bullet-}$. Superoxide radical anion decreases $^{\bullet}NO$ bioavailability by a radical-radical combination reaction that yields peroxynitrite anion (eq. 13).

$$^{\bullet}NO + O_2^{\bullet-} \rightarrow ONOO^- \qquad \text{(Eq. 13)}$$

In vascular tissues, $O_2^{\bullet-}$ can be produced by several enzymatic sources, that are described below.

In Oxidative Stress: Diagnostics, Prevention, and Therapy Volume 2; Hepel, et al.;
ACS Symposium Series; American Chemical Society: Washington, DC, 2015.

Publication Date (Web): October 13, 2015 | doi: 10.1021/bk-2015-1200.ch004

Publication Date (Web): October 13, 2015 | doi: 10.1021/bk-2015-1200.ch004

NOXs

The NADPH (β-Nicotinamide adenine dinucleotide 2′-phosphate) oxidases (NOXs) enzymes are expressed mainly in immune cells (polymorphonuclear cells and macrophages) but these are not exclusive for phagocytes mature cells (*78*). Therefore, these are expressed in many different cells in the vasculature including endothelial cells, smooth muscle cells and adventitia (*79*). The NOXs enzymes in these tissues have a basal activity that could be enhanced by physiopathological mediators, such as angiotensin II, physical stress and pro-inflammatory cytokines (*80*, *81*).

The structure and function of the NOXs enzymes were firstly described in neutrophils. The phagocytic NADPH is a multicomplex-enzyme which contains the domain $p22^{phox}$ and NOX2 (also known as $gp91^{phox}$), besides four cytoplasmatic subunits: $p47^{phox}$, the activator subunit $p67^{phox}$, $p40^{phox}$ and a small G protein called Rac. When monocytes and macrophages are in the resting state, the multienzymatic complex is disassembled and inactive. However, in conditions that promote activation of the phagocytic system, NOX is phosphorylated and the cytoplasmic subunits are translocated to the phagosomal membrane where the catalytic subunits are located. The monovalent reduction of O_2 is produced through an electron transport chain from the NADPH cofactor; this process is highly dependent on the phosphorylation and activation of the $p47^{phox}$ subunit. Different variants of the catalytic subunit of NOX have been identified in humans and classified under three groups dependent on their structure. The first group contein the isoforms NOX1, NOX3 and NOX4, which have a similar structure with NOX2. The second group includes the dual oxidases 1 and 2 (DUOX1 and DUOX2), which have an extracellular peroxidase domain and an intracellular EF hand motifs (protein domains that bind Ca^{2+}) necessary for enzyme activation. Finally, the third group is composed by NOX5-enzymes which contain an amino terminal with four EF hand motifs groups and a catalytically group similar to NOX2. All these variants of NOXs differ on the tissue expression specificity, subcellular localization and physiological activities.

NOX4 is the most relevant in the vasculature and smooth muscle cells. This isoform does not require the subunits $p47^{phox}$ and $p67^{phox}$ or other homologues for its activation because it is a constitutive enzyme and its activity is regulated by cytosolic subunits that are not well studied yet (*82*). In endothelial cells $O_2^{\bullet-}$ is produced towards the extracellular environment while in smooth muscle cells the $O_2^{\bullet-}$ is produced towards the cytoplasm (*83*, *84*).

Patients with coronary disease have an increase in the expression of the subunit $p22^{phox}$ of NOX in the vasculature (*85*). EPR studies showed that the NOX activity is significantly increased in coronary arteries of patients with coronary disease compared to non-atherosclerotic arteries, suggesting that NOX activity is affected during coronary illness (*85*). Several physiopathological conditions, such as smoking, diabetes or hypertension, can promote an increase in $O_2^{\bullet-}$ production leading to an increase in peroxynitrite formation (*86*, *87*).

Publication Date (Web): October 13, 2015 | doi: 10.1021/bk-2015-1200.ch004

Xantine Oxidase

Another vascular source of $O_2^{\bullet-}$ is the enzyme xanthine oxidase, responsible of the oxidation of hypoxanthine to uric acid with the concomitant production of $O_2^{\bullet-}$ and H_2O_2. Xanthine oxidase is activated in the cytosol by limited proteolysis of xanthine dehydrogenase (*88*). Also, xanthine oxidase is released to the circulation and bind to glycosaminoglycans of extracellular matrix of endothelial cells (*89*). The activity of this enzyme has been studied and characterized extensively as a major source of $O_2^{\bullet-}$ during cycles of ischemia-reperfusion. Several clinical studies performed in hypercholesterolemic patients showed high levels of intravascular xanthine oxidase activity compared with control patients (*85*, *90–92*).

Mitochondria

Mitochondria are another source of $O_2^{\bullet-}$ production in the vasculature and several tissues, due to electron leakage from the electron transport chain directly to O_2 (*93*). The standard reduction potential of O_2 by one electron is -0.160 V (*1*). The respiratory electron transport chain contains several redox cofactors with standard reduction potential between -0.32 V (NAD(P)H) and +0.39 V (cytochrome a_3 in complex IV). The electron transport chain includes several components such as flavoproteins, iron-sulfur clusters and ubiquinone groups that are capable to reduce O_2 *via* one electron and yield $O_2^{\bullet-}$ (*92*). The major sites of generation of $O_2^{\bullet-}$ within the mitochondria are complexes I and III of the mitochondrial respiratory chain (*94–96*). Several metabolic disorders lead to an increase of the mitochondrial $O_2^{\bullet-}$ like hyperglycemia (*87*) or exposure to tobacco smoke (*86*).

eNOS

The endothelial isoform of nitric oxide synthase (eNOS) consists in a homodimer of 135 kDa each subunit, which remain linked by a cluster zinc-thiolate (4Cys-Zn). Each monomer contains a reductase and an oxygenase domain. The reductase domain contains the cofactors NADPH, flavin adenine dinucleotide (FAD) and riboflavin 5′-monophosphate (FMN) while the oxygenase domain contains a heme group, a (5,6,7,8-Tetrahydrobiopterin) BH_4 cofactor and the cysteines of the cluster. Also eNOS binds Ca^{2+}/calmodulin which activates the ≪enzyme. The mechanism of catalysis consists in an electron transfer chain from the NADPH at the reductase domain to the O_2 attached at the heme group, which is then linked to the L-arginine, leading to N-hydroxy-arginine. A second electron transfer leads to the generation of $^{\bullet}NO$ and L-citrulline (eq. 14) (*1*).

$$2\ \text{L-arginine} + 4\ O_2 + 3\ \text{NADPH} \rightarrow 2\ ^{\bullet}NO + 2\ \text{L-citrulline} + 3\ NADP^{+} + 2\ H_2O \quad \text{(Eq. 14)}$$

In Oxidative Stress: Diagnostics, Prevention, and Therapy Volume 2; Hepel, et al.;
ACS Symposium Series; American Chemical Society: Washington, DC, 2015.

Publication Date (Web): October 13, 2015 | doi: 10.1021/bk-2015-1200.ch004

Some studies have shown that under depletion of the substrate L-arginine or oxidative stress (promoted by reactive oxygen species (ROS) and peroxynitrite that oxidizes the enzyme or the BH_4 cofactor) eNOS could become a new source of $O_2^{\bullet-}$ in the vasculature, therefore consuming $^{\bullet}NO$ (*97*, *98*). This process is known as eNOS uncoupling (Figure 4).

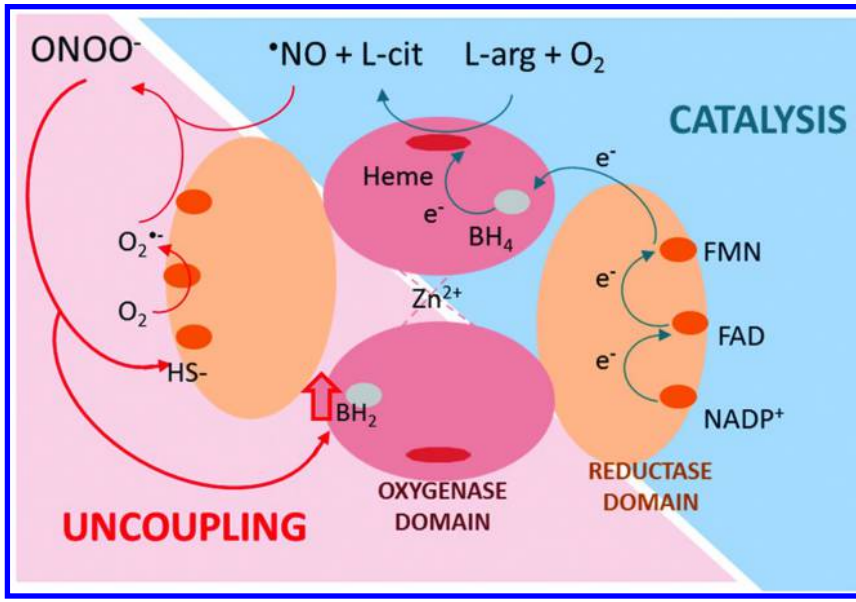

Figure 4. Peroxynitrite inhibits $^{\bullet}NO$ generation by eNOS and promotes its uncoupling. The endothelial isoform of NOS consists in a homodimer in which both monomers bind through zinc-thiolate cluster. Each monomer of the enzyme contains a reductase domain with the cofactors NADPH, FAD and FMN, and an oxygenase domain with the heme group and BH_4. During normal catalysis (1), electrons are transfered from NADPH, FAD and FMN through the reductase domain of one monomer of the enzyme, to (2) the oxygenase domain of the other monomer. The electrons are then transfered to BH_4, the heme group and finally to the guanidinium group of L-arginine to promote the synthesis of $^{\bullet}NO$. In the presence of peroxynitrite (and peroxynitrite-derived radicals) (3), BH_4 in the oxygenase domain and (4) thiols of the reductase domain can be oxidized, facilitating the uncoupling of the enzyme. As a consequence, oxygen becomes the final acceptor of electrons to yield $O_2^{\bullet-}$, which can react with $^{\bullet}NO$. As a consequence, the output of $^{\bullet}NO$ by eNOS is decreased, becaming a source of peroxynitrite source in the vascular wall.

In 2006 Marletta and collaborators performed EPR studies of the recombinant bovine eNOS, which is highly homologous with the human isoform. In the absence of the cofactor BH_4, the formation of $O_2^{\bullet-}$ was stimulated (*99*). Other

study in endothelial cells, showed that peroxynitrite promoted the monomerization of eNOS as a possible mechanism of eNOS uncoupling (*100*). Recent studies of Zweier´s group (*101*) showed that oxidation and S-glutathionylation of Cys910 in the reductase domain of eNOS promoted eNOS uncoupling. This modification has been demonstrated in hypertensive mice models (*101*). However, the $O_2^{\bullet-}$ dependent thiol oxidation and consequent mechanism of S-glutathionylation is not clear. On the other hand, recent publications indicated that oxidation of Cys910 is not enough to promote eNOS uncoupling, and oxidation of the thiol in Cys691 was also necessary to promote eNOS-dependent $O_2^{\bullet-}$production (*102*). This group continued studying the eNOS uncoupling mechanism in an endothelial cell model under hypoxia/reoxygenation and observed that, in addition to thiol S-glutathionylation, BH_4 oxidation can also be involved.

The $O_2^{\bullet-}$ produced by eNOS would react with $^{\bullet}NO$, leading to peroxynitrite formation that would oxidize new molecules of eNOS promoting further uncoupling. In consequence of this vicious cycle (Figure 4), there would be a decrease in $^{\bullet}NO$ levels in the vasculature, promoting endothelial dysfunction. Although the mechanism of the reaction between peroxynitrite and eNOS is still not well understood, there is strong evidence that peroxynitrite affects eNOS activity.

Publication Date (Web): October 13, 2015 | doi: 10.1021/bk-2015-1200.ch004

Redox Cycling of Xenobiotics

An additional mechanism of enhanced $O_2^{\bullet-}$ production in the vasculature involves the redox cycling of xenobiotics. Usually, the xenobiotic undergoes a reduction step by endogenous systems (e.g. P450 system, mitochondrial electron transport chain, flavoproteins) and then the reduced form yields $O_2^{\bullet-}$ upon reaction with molecular oxygen. A notable example of this is represented by smoke-associated quinonoid compounds present in plasma and vascular tissues as a result of smoking that lead to decreased $^{\bullet}NO$ levels, endothelial dysfunction and formation of (3-nitrotyrosine) 3NT *in vitro* and *in vivo* (*86*).

Detoxification $O_2^{\bullet-}$ in the Vasculature

The presence of $O_2^{\bullet-}$ in the vasculature largely depends in the velocity of its formation and dismutation mediated by the superoxide dismutases (SODs), which catalyze the dismutation of $O_2^{\bullet-}$ to H_2O_2. In mammals there are three different isoforms of SODs which differ in the cellular localization and the metal ion of the catalytic center. Two isoforms are located inside the cells. While the cytosolic isoform contains a copper-zinc (Cu,Zn-SOD) in the active site, the mitochondrial matrix isoform contains manganese (Mn-SOD). There is also an extracellular isoform of Cu,Zn-SOD (EC-SOD) which is expressed and excreted by smooth muscle cells in healthy vessels and is the predominant isoform on the vasculature (*103*). Nitric oxide increases EC-SOD expression *via* cGMP, consequently,

In Oxidative Stress: Diagnostics, Prevention, and Therapy Volume 2; Hepel, et al.;
ACS Symposium Series; American Chemical Society: Washington, DC, 2015.

Publication Date (Web): October 13, 2015 | doi: 10.1021/bk-2015-1200.ch004

pathologies that compromise •NO bioavailability also jeopardize $O_2^{\bullet-}$ dismutation. SOD reacts with $O_2^{\bullet-}$ with a second order rate constant reaction of 1-2x10^9 M^{-1} s^{-1} while the reaction between •NO and $O_2^{\bullet-}$ has a 10 times faster second order rate constant. For this reason, the local concentration of SOD is essential to prevent peroxynitrite formation and increase •NO bioavailability (*104*). Mn-SOD was one of the first nitrated proteins identified in renal allograft rejection in humans (*105*). Further studies demonstrated that Mn-SOD is inactivated due to nitration by peroxynitrite at Tyr^{34} (*106*). Moreover, nitrated Mn-SOD and reduction of its activity was identified in a vascular aging rat model, indicating a relationship between nitration and inactivation of the protein function (*107*, *108*). In another example, the addition of cyclosporin A (an immunosuppressant used in renal transplant with known vascular side effects) promoted peroxynitrite formation and nitration of MnSOD in vascular endothelial cells (*108*).

To note, african-american hypertensive patients have decreased EC SOD activity and increased nitrated plasma proteins compared to normotensive patients (*109*), underscoring the interplay of •NO and $O_2^{\bullet-}$ in the modulation of vasodilatory responses *in vivo*.

Peroxynitrite: Kinetic and Biochemical Evidence of Its Formation in the Vasculature

Nitric oxide reacts very fast with $O_2^{\bullet-}$ with a second order rate constant of ~10^{10} M^{-1} s^{-1} (*110*) to yield peroxynitrite anion ($ONOO^-$) (the term peroxynitrite refers to the sum of peroxynitrite anion and peroxynitrous acid, $ONOO^-$ and ONOOH, respectively). Peroxynitrite is a relative stable molecule in alkaline solutions but at biological pH, the acid form of peroxynitrite (peroxynitrous acid, ONOOH, pKa 6.8 (*111*), Eq. 15) quickly decomposes with a half life at pH 7.4 and 25ºC or 37ºC of 2.7 and 0.7 s, respectively (*111*). The products of the decomposition are hydroxyl and nitrogen dioxide radicals (•OH and $•NO_2$) in about 30 % yield (Eq. 16), with the rest isomerizing directly to nitrate. Peroxynitrite is a strong oxidant. In addition, peroxynitrite anion is a good nucleophile that reacts with CO_2 with a rate constant of 4.6 x 10^4 M^{-1} s^{-1} yielding an unstable adduct that evolves to $•NO_2$ and carbonate ($CO_3^{\bullet-}$) radicals in about 35 % yields (Eqs. 17 and 18) (*112*).

$$ONOO^- + H^+ \rightleftharpoons ONOOH \qquad \text{(Eq. 15)}$$

$$ONOOH \rightarrow {}^{\bullet}OH + {}^{\bullet}NO_2 \qquad \text{(Eq. 16)}$$

$$ONOO^- + CO_2 \rightarrow ONOOCO_2^- \qquad \text{(Eq. 17)}$$

$$ONOOCO_2^- \rightarrow {}^{\bullet}NO_2 + CO_3^{\bullet-} \qquad \text{(Eq. 18)}$$

In Oxidative Stress: Diagnostics, Prevention, and Therapy Volume 2; Hepel, et al.;
ACS Symposium Series; American Chemical Society: Washington, DC, 2015.

Publication Date (Web): October 13, 2015 | doi: 10.1021/bk-2015-1200.ch004

In biological systems, peroxynitrite half-life is ~10-20 ms because of the fast reaction of this oxidant with different molecular targets (*113*). Peroxynitrite formed inside a cell or a cell compartment can diffuse through the membrane. Although at biological pH $ONOO^-$ is the predominant species (*ca.* 80 % $ONOO^-$ at pH 7.4), part of protonated form, can diffuse outside. In addition, peroxynitrite anion can permeate through biological membranes by anionic channels (*114*, *115*).

Peroxynitrite formation in the vasculature promotes oxidative modifications in several proteins, which may affect their activity; the oxidative reactions can occur in plasma, in the blood cells and in the vascular tissue (*i.e.* endothelium, sub-endothelial smooth muscle, cardiac muscle and extracellular matrix (*116*). Several amino acid residues can be modified by peroxynitrite or peroxynitrite-derived oxidants. We will mention two key modifications in the context of the current chapter, namely thiol oxidation and tyrosine nitration. Other relevant modifications include methionine oxidation and tryptophan oxidation and nitration (*117*).

Peroxynitrite reaction with thiols is typically *ca.* 1,000 times faster than with H_2O_2 (*eg.* 1,000-5,000 M^{-1} s^{-1} vs. 1-10M^{-1} s^{-1} (*54*)). Moreover, certain thiol-containing proteins such as the peroxiredoxins can react very fast with peroxynitrite (1x 10^6 M^{-1} s^{-1} to 7 x 10^7 M^{-1} s^{-1}) (*118*). The overall process of the reaction of a thiol with peroxynitrite is a two-electron oxidation of the thiol to the sulfenic acid derivative, which is usually a transient species (*117*). Alternatively, peroxynitrite-derived radicals (*i.e.* $^{\bullet}OH$, $^{\bullet}NO_2$, $CO_3^{\bullet-}$) can mediate the one-electron oxidation of thiols to thiyl radicals which can then react with oxygen and yield overoxidized thiols such as sulfinic and sulfonic acids (*117*). Thiol oxidation in vascular proteins has been studied, including human serum albumin, SERCA and creatine kinase (*117*, *119*).

One of the most studied oxidative postranslational modifications in vascular proteins is the nitration of tyrosine residues. This modification can promote several biologically-relevant consequences such as gain or loss of protein function, induction of immunological responses by the formation of antigenic epitopes or affect signal transduction pathways, mainly phosphorylation cascades (*120*). The protein nitration by peroxynitrite promotes the formation of a tyrosyl radical ($^{\bullet}$Tyr) and the addition of a nitro group ($-NO_2$) in the adjacent position of the hydroxyl group of the aromatic ring, yielding 3-nitrotyrosine (3NT). Consequently, the protein may suffer structural and functional changes (figure 5).

Protein tyrosine nitration by peroxynitrite takes places through a free radical mechanism which implies the intermediate formation of •Tyr, and a subsequent reaction with $^{\bullet}NO_2$. A subtle kinetic, and sometimes puzzling, issue, is that there is no direct bimolecular reaction of tyrosine with peroxynitrite; indeed, tyrosine nitration reactions are due to peroxynitrite-derived radicals (*121*, *122*). The mechanism of peroxynitrite-mediated protein tyrosine nitration, involves a free radical mechanism in which first, a hydrogen atom is abstracted leading to the formation of a $^{\bullet}$Tyr radical. This reaction can be achieved by several oxidants such as hydroxyl radical ($^{\bullet}OH$), that reacts with tyrosine in a fast reaction (1.3x10^{10} M^{-1} s^{-1}) with a high efficiency, leading the initial addition of the hydroxyl to the phenyl group followed by dehydration to the $^{\bullet}$Tyr. Nitrogen dioxide can also react with tyrosine yielding $^{\bullet}$Tyr radical, but with a smaller constant rate (3.2 x 10^5 M^{-1}

In Oxidative Stress: Diagnostics, Prevention, and Therapy Volume 2; Hepel, et al.;
ACS Symposium Series; American Chemical Society: Washington, DC, 2015.

s^{-1}) at pH 7.5 (*123*). Carbonate radical, $CO_3^{\bullet-}$ (3×10^7 M^{-1} s^{-1}) can also efficiently promote tyrosine oxidation (*123*). Moreover, in the context of other concomitant oxidations mediated by peroxynitrite in the vasculature such as lipid peroxidation (*e.g.* low density lipoprotein (LDL) oxidation (*116*)), lipid-derived radicals such as peroxyl ($LOO^{\bullet}$) and alkoxyl ($LO^{\bullet}$) radicals, can promote one-electron oxidation of tyrosine yielding to the formation of $^{\bullet}$Tyr, which in the presence of $^{\bullet}NO_2$ can lead to tyrosine nitration (*124*). The second order rate constants for the reaction with tyrosine, are $5x10^3$ and $5x10^5$ M^{-1} s^{-1}, for $LOO^{\bullet}$ and $LO^{\bullet}$ respectively (*125*, *126*). These reactions have particular relevance in lipid-enriched biostructures such as lipoproteins and membranes, where lipid-derived radicals can be formed, fueling protein tyrosine nitration pathways within these compartments in proteins such as apoA-1 or apo-B-100 (*127*, *128*).

An alternative biologically-relevant mechanism for the formation of 3NT is through the action of heme-peroxidases (myeloperoxidase (MPO) eosinophil peroxidase (EPO)) in its reaction with hydrogen peroxide and NO_2^- (*129*). The process involves the peroxidase-catalyzed oxidation of NO_2^- yielding $^{\bullet}NO_2$ (Figure 3), which in the presence of $^{\bullet}$Tyr leads to the formation of 3NT. MPO compounds I and II can oxidize by one-electron NO_2^- to $^{\bullet}NO_2$ and tyrosine to tyrosyl radical, providing the two radical precursors necessary for tyrosine nitration. In any case, both the peroxynitrite-dependent and independent mechanisms of tyrosine nitration require the evolution of $^{\bullet}$NO to secondary oxidants and involving free radicals reactions. In addition to 3NT, other products can be formed once $^{\bullet}$Tyr is formed, such as di-tyrosine, by the combination reaction between to $^{\bullet}$Tyr radicals and 3-hydroxytyrosine (DOPA) (Figure 5).

Tyrosine nitration usually drops the pKa of the phenolic group from ~ 10 to ~ 7.2-7.5, which has important consequences in the structure and the function of the protein (*121*). Nitration of several proteins has been identified in vivo in different pathological conditions.

Protein nitration also generates oxidative posttranslational modifications that activate the immune response against these epitopes. Patients with conditions of chronic inflammation, rheumatoid arthritis, osteoarthritis or lupus showed high levels of anti 3NT antibodies (*130*). Recently, its has been reported that the levels of immunoglobulins against 3NT are higher in patients with coronary artery disease (CAD) (*131*). These data show that nitration of tyrosine residues are able to activate immunological responses against own proteins and therefore generating inflammatory and degenerative processes in the vasculature.

Albeit tyrosine nitrated proteins are widely distributed in the cardiovascular system (CV) in normal or disease conditions, there is a strong association between the formation of 3NT in the CAD correlated with CV risk factors. Proteins of different compartments of the CV can be modified, including intravascular space, vessel wall and myocardium (Table 1). We will describe the modified proteins found in these compartments.

Publication Date (Web): October 13, 2015 | doi: 10.1021/bk-2015-1200.ch004

Publication Date (Web): October 13, 2015 | doi: 10.1021/bk-2015-1200.ch004

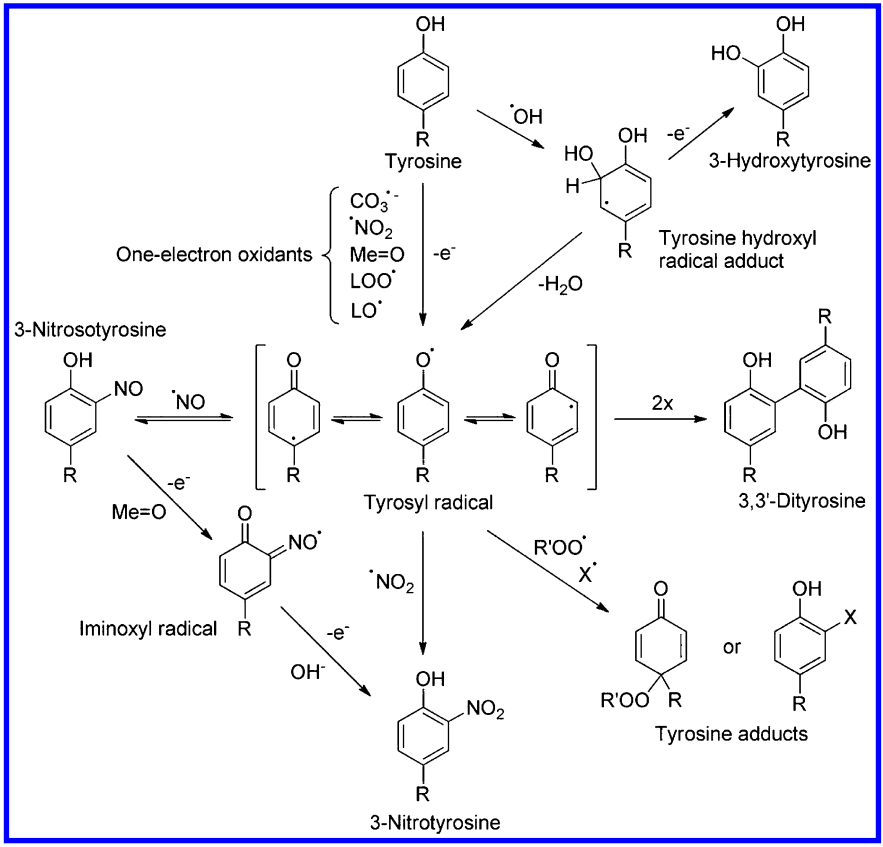

Figure 5. Pathways of tyrosine oxidation and nitration via one electron processes. Reproduced with permission from ref (121). Copyright 2012 American Chemical Society.

Nitration of Plasma Proteins

Identification of circulating nitrated proteins is extremely relevant because it shows a strong relationship between nitroxidative stress and human pathological conditions. Though the vascular proteins have a great turnover rate, the finding of nitrated proteins marks its importance in several pathologies. In this way, there is equilibrium between circulating nitrated proteins and modified proteins in other compartments which makes difficult to assess in which exact compartment the protein was modified (*132*).

In Oxidative Stress: Diagnostics, Prevention, and Therapy Volume 2; Hepel, et al.;
ACS Symposium Series; American Chemical Society: Washington, DC, 2015.

Table 1. Evidence of nitrated proteins in vasculature[a]

Nitrated protein	*Methodology*	*Observations*	*Ref.*
	Plasma proteins		
Fibrinogen	IP of fibrinogen, 3-NO_2-Tyr determination by HPLC-ESI-MS-MS, electron microscopy	30% increase on 3-NO_2-Tyr in CAD, accelerated clot formation, fragile clot.	(*136*, *184*, *185*)
Plasmin	IP with 3-NO_2-Tyr antibody of plasma proteins, WB of major plasma proteins.	Increase of nitration in plasmin and fibrinogen in smokers, in vitro inactivation of plasminogen by nitration	(*137*, *138*)
Apo-A1	IP with 3-NO_2-Tyr antibody from plasma and isolation of Apo-A1 from biopsies, HPLC-ESI-MS-MS for 3-NO_2-Tyr determination.	Apo-A1 MPO interaction, nitration and chlorination of Tyr^{192}, two-fold increase of Apo-A1 in CAD, preferential nitration of Apo-A1 in plasma when compared to other nitrated plasmatic proteins.	(*141*, *142*, *186*)
	Vessel wall		
Apo-B	LDL purification by ultracentrifugation of human plasma and aortic lesion, 3-NO_2-Tyr was determined after hydrolysis and derivatization by GC-MS.	90-fold increase of nitrated LDL compared to circulating plasma nitrated LDL.	(*149*, *187*)
COX	IP of COX-1 from smooth muscle cells and from human atheroma plaques, WB and spectrophotometrical determination of nitrated COX-1, COX-1 EPR studies, trypsin digestion with HPLC purification and amino acid sequencing.	*In vitro* inactivation by nitration of COX-1, identification of nitrated COX-1in smooth muscle cells and in human atheroma plaques, identification of NO2-Tyr^{385} by NO and Tyr·.	(*158*, *187*, *188*)
PGIS	IP with 3-NO_2-Tyr against endothelial proteins, WB, immunohistochemistry, thermolysin digestion of nitrated PGIS and high resolution MS (FT-ICR) of nitrated peptides.	Nitration of PGIS at low peroxynitrite concentrations (1 μM), IC_{50} for inactivation 100 nM, colocalization of nitrated proteins and PGIS in the endothelium of bovine coronary artery, specific nitration at Tyr^{430}.	(*159*, *160*)

Continued on next page.

Publication Date (Web): October 13, 2015 | doi: 10.1021/bk-2015-1200.ch004

Table 1. (Continued). Evidence of nitrated proteins in vasculature[a]

Nitrated protein	*Methodology*	*Observations*	*Ref.*
Mn-SOD	*In vitro* nitration of human Mn-SOD by peroxynitrite, ESI-MS analysis of digested SOD, amino acid sequencing, IP of aged rat aorta, WB, immunoelectron microscopy anti-3-NO_2-Tyr, development of specific antibody against nitrated SOD at Tyr^{34}, angiotensin II induced hypertension in rats.	Identification of specific nitration at Tyr^{34}, distribution of nitrated SOD in rat aorta, age-increase in nitrated SOD, distribution of nitrated SOD at Tyr^{34} in the kidney mainly in cortical collecting ducts.	(*106*, *107*, *185*)
Perlecan	Human coronary artery endothelial cells (HCAECs) and puri isolated protein treated with peroxynitrite. Immunofluorescence of human atherosclerotic lesions.	Nitration and aggregation of isolated protein. Changes in its function in cell culture studies. Nitrated protein in intima.	(*162*, *163*)
	Myocardium		
MM-CK	IP of CK from heart failure in rats, WB and immunohistochemistry, human biopsy of atrial fibrillation	Nitration and inactivation of MM-CK in heart, in vitro inactivation of MM-CK by peroxynitrite but not myosine ATPase, increase nitration and carbonyl formation of MM-CK in atrial fibrillation.	(*172*, *174*, *189*)
α-actinin	IP of α-actinin from human cardiomyocytes and WB against 3-NO_2-Tyr.	Contractile dysfunction of cardiomyocytes after exposure to peroxynitrite, detection of nitrated α-actinin as the only nitrated protein at the concentration used.	(*174*, *185*)
SERCA	IP of nitrated proteins from SR of age rat skeletal muscle, WB, protease digestion and HPLC-ESI-MS, amino acid analysis, IP of SERCA 2_a and WB against 3-NO_2-Tyr.	Nitration of $Tyr^{294,295}$ in the M4-M8 transmembrane domain of SERCA 2_a, nitration of $Tyr^{294,295}$ in SERCA 2_a in rat heart, nitration of SERCA 2_a in patients with idiopathic dilated cardiomyopathy.	(*177*, *179*, *180*)

[a] IP = immunoprecipitation, WB = western blot, HPLC = high performance liquid chromatography, ESI = electro spray ionization, MS = mass spectrometry, GC = gas chromatography, FT-ICR = Fourier transformed-ion cyclotron resonance, Apo = apolipoprotein, COX = cyclooxygenase, PGIS = prostacyclin synthase, SOD = superoxide dismutase, MM-CK = myofibrillar creatine kinase, SERCA = sarcoplasmic reticulum Ca^{2+}-ATPase, MPO = myeloperoxidase, CAD = coronary artery disease, LDL = low density lipoprotein, Tyr = tyrosine, Tyr· = tyrosil radical, 3-NO_2-Tyr = 3-nitrotyrosine and 3-Cl-Tyr = 3-chlorotyrosine.

Publication Date (Web): October 13, 2015 | doi: 10.1021/bk-2015-1200.ch004

Publication Date (Web): October 13, 2015 | doi: 10.1021/bk-2015-1200.ch004

Fibrinogen, a soluble plasma protein involved in clot formation, has been reported as an independent risk factor in CAD and stroke (*133*). Additionally it has been demonstrated a correlation between nitroxidative stress and an increase (~30%) in the fibrinogen nitration in CAD patients (*134*, *135*). Studies *in vitro* showed that nitro-fibrinogen polymerized faster than normal fibrinogen. Moreover the structure of the clot changed showing stable viscoelastic properties of nitro-fibrinogen compared with less stable clot of normal fibrinogen, increasing the risk of microemboli. The fibrinolytic system, which hydrolyzed the clot, composed by plasmin does not differentiate between fibrin clots or nitro-fibrin clots (*135*, *136*). However, plasmin can be nitrated *in vivo* an has been already detected nitro-plasmin in plasma of smokers (*137*). Moreover, *in vitro* studies showed that peroxynitrite is able to nitrate and inhibit plasmin activity (*138*).

On the other hand, lipoproteins can be nitrated by peroxynitrite. In the 90´ Beckman found nitrated proteins in the atheroma plaques of patients with CAD (*139*). After that high density lipoprotein (HDL) dysfunction was linked to nitroxidative stress in CV pathology (*140*). Apo A-1, the major apo lipoprotein of HDL, is susceptible to chlorination or nitration mediated by myeloperoxidase (*141*). Nitrated circulating HDL in plasma of CAD patients is two fold higher than control patients (*142*). Moreover HDL appears to be a preferential target among circulating proteins for nitration since nitro-A-1 is enriched 7 to 70 fold compared with total plasma nitro-proteins (*141*, *142*). Hazen *et al* discovered that nitration on the apoA-I Tyr^{166} was present in atherosclerotic human coronary arteries but this modification was undetectable in non-atherosclerotic artheries. Nitration of this Tyr was correlated with an 88% of decrease in lecithin-cholesterol acyltransferase activity, making HDL dysfunctional (*143*). When HDL is chlorinated at Tyr^{192} residue, the reverse cholesterol transport mediated by ABCA-1 receptor is affected while nitration in the same residues has minimal effects (*127*, *141*, *144*). Apolipoprotein A-1 binds with high efficiency myeloperoxidase facilitating the modification of the tyrosine.

Nitration in the Vessel Wall

The vessel wall is the major site for protein nitration in several physiopathological conditions such as hypertension or atheromatosis, where endothelial cells, smooth muscle cells and fibroblasts are activated by cytokines and angiotensin II to produce $O_2^{\bullet-}$ (*145*, *146*). Moreover, the attraction of macrophages and neutrophils generates an inflammatory site, promoting the increase in the release of $O_2^{\bullet-}$, $^{\bullet}NO$ and myeloperoxidase (*147*). Each of the individual major risk factors of atheromatosis (hyperglycemia, hypercholesterolemia, smoking and hypertension) produces endothelial dysfunction and promotes nitroxidative stress (*148*). Atheromatosis is an inflammatory condition in the vascular wall in which pro-atherogenic LDL is located in the neointima, promoting an inflammatory response with leucocyte infiltration (*120*).

LDL can be oxidized in the apo lipoprotein or lipids by either peroxynitrite or by myeloperoxidase system *in vitro* and *in vivo* (*129*, *149*). Nitrated LDL promotes

In Oxidative Stress: Diagnostics, Prevention, and Therapy Volume 2; Hepel, et al.;
ACS Symposium Series; American Chemical Society: Washington, DC, 2015.

inflammation by recruiting monocytes and thus releasing tumor necrosis factor alpha (TNF-α) (*150*). Oxidized LDL is endocyted by macrophages *via* scavenger receptor (SR-A and CD 36) (*151*).

Vascular hemostasis is also maintained by the regulation of clot/formation degradation. Certainly, eicosanoids are important for this role. In platelets, cyclooxygenase I (COX-1) transforms arachidonic acid (AA) to thromboxane-A_2 (TxA_2) a potent agonist of platelet aggregation, thrombus formation and vasoconstriction (*152*). Arachidonic acid also leads to the formation of prostacyclin 2 (PGI_2) mediated by cyclooxygenase 2 (COX-2) and prostacyclin synthase (PGIS), that increases cyclic AMP (cAMP) (*153*), which acts deactivating platelets, and inhibiting clot formation. Hence, PGI_2 and $^{\bullet}NO$ act synergistically to maintain endothelium homoestasis (*154*). Atheromatosis disrupts this balance, enhancing TxA_2 and peroxynitrite formation, generating as a result a pro thrombotic state. Intermediates derived from $^{\bullet}NO$ pathway can both activate or inactivate COX depending on their nature and concentration (*153–155*). Low levels of peroxynitrite or other peroxides and AA can activate COX, but higher levels nitrate and inactivate COX (*156*). COX catalysis requires the formation of a tyrosyl radical on Tyr^{385} (*157*). *In vitro* studies showed nitration of this Tyr and inactivation of the enzyme. Human atheroma plaques also demonstrated enzyme nitration and inactivation (*158*). On the other hand, peroxynitrite nitrates and inactivates PGIS (*159*) *via* nitration on Tyr^{430} (*160*). This enzyme depends on a heme-thiolate prosthetic group for its activity, thus peroxynitrite reacts with this group similarly as with other heme-peroxidases, but in a faster kinetic reaction (*161*). The nitroxidative stress that takes place in atheromatosis profoundly affects the artery wall leading not only to a decrease in $^{\bullet}NO$ bioavailability but also to a decline on PGI_2 levels due to nitration and inactivation of several enzymes (*120*). On the other hand, aging is also responsible for an increase of vascular $O_2^{\bullet-}$ formation. In parallel with this result, a seven fold increase in eNOS expression have been shown. All these data suggest that aging promotes vascular increase of peroxynitrite formation, promoted by the $O_2^{\bullet-}$ reaction with $^{\bullet}NO$, in parallel with a compensatory eNOS overexpression which, however, is not sufficient to maintain normal $^{\bullet}NO$ levels. As a consequence, peroxynitrite derived from aging process promotes the nitration of several cellular proteins, most notably in mitochondria (*107*).

It is interesting to note, that during $^{\bullet}NO$ and $O_2^{\bullet-}$ interactions in vascular tissues, peroxynitrite can also exert relevant effects in the extracellular matrix that may influence vascular structure, including the nitration of the key matrix protein perlacan (*162*). Indeed, perlecan, also known as basement membrane-specific heparan sulfate proteoglycan protein (HSPG) or heparan sulfate proteoglycan 2 (HSPG2), is synthesized by both vascular endothelial and smooth muscle cells and deposited in the extracellular matrix. Perlecan binds to extracellular matrix and cell-surface molecules, interacts with growth factors and adhesion molecules and also regulates the adhesion, differentiation and proliferation of vascular cells. After peroxynitrite exposure of perlecan, the protein agregated and was found nitrated. Moreover, changes in its activity were shown. Perlecan decreased its binding of human coronary artery endothelial cells (*163*).

Publication Date (Web): October 13, 2015 | doi: 10.1021/bk-2015-1200.ch004

Nitroxidative stress participates in conditions such as myocardial infarction, infectious processes such as myocarditis or contractile dysfunction of failing heart (*164*, *165*).

Creatine kinase is an enzyme that produces phospho creatine (pCr) a heart energy reserve source. Myofibrillar CK exists as a homodimer (MM-CK) or as a heterodimer (MB-CK), both expressed in cardiac and skeletal muscle. MM-CK is responsible for major proportion of pCr in the myocardium. In heart failure models, depletion of ~60% of pCr has been reported (*165*, *166*) and this observation was confirmed in humans by proton nuclear magnetic resonance studies (H NMR) (*167*). Nowadays, probabilities of total and cardiovascular mortality is determined by the ratio pCr/ATP and its correlation with severity of heart failure (*168*). Moreover experiments with either acute (*169*) or chronic (*170*) inhibition of CK have revealed a loss in contractile reserve of the heart (*171*). Animal models of pharmacological induced (*165*) and post ischemic heart failure (*172*) are associated with nitrated and inactivated MM-CK (*173*).

α-actinin is also susceptible to peroxynitrite-mediated nitration and inhibition of myofibrillar protein. In humans, this protein was isolated nitrated from cardiomyocytes, and this is associated with contractile dysfunction as measured by maximal Ca^{2+} activated isometric force generated by peroxynitrite-treated cardiomyocytes (*174*).

Myocardium contraction and relaxation are under strict control of calcium metabolism. During relaxation cytosolic Ca^{2+} is pumped back to sarcoplasmic reticulum by sarco/endoplasmic reticulum Ca^{2+}-ATPase **(**SERCA). If this metabolism is altered it can lead to a long term heart failure being that cardiac contractility is modulated by SERCA levels (*175*). There are several isoforms of SERCA, being sensitive to nitration and peroxynitrate-mediated inactivation, the one predominant on slow twitch skeletal muscle, vessel smooth muscle and cardiac muscle SERCA-2a. Studies of sarcoplasmatic reticulum (*63*) vesicles exposed to peroxynitrite showed SERCA inactivation by sulfhydryl oxidation that could be reverted by disulfide-reducing agents (*176*). *In vivo* nitration of Tyr^{294} and Tyr^{295} from SERCA-2a of skeletal muscle has been demonstrated during aging (*177*). Immunoprecipitation of SERCA from human coronary artery atheroma was found, and corroborated the previous used model of aging rats (*178*). In humans, nitrated SERCA was also found in idiopathic dilated cardiomyopathy but not in normal coronaries patients. Cardiomyocytes showed a correlation between half time relaxation and nitrated SERCA, suggesting that SERCA nitration can contribute to cardiac dysfunction in heart failure (*179*). The nitration of two consecutive tyrosines (Tyr^{294} and Tyr^{295}) in membrane-spanning helix-M4 was determined in senescent heart (*180*), while another nitrated tyrosine (Tyr^{122}) was detected by *in vitro* studies. For these discrepancies, some authors proposed that SERCA can be degraded by the proteasome or 3-nitro-Tyr^{122} might be reduced by accessory proteins, such as putative denitrase activity (*105*, *181–183*).

In Oxidative Stress: Diagnostics, Prevention, and Therapy Volume 2; Hepel, et al.;
ACS Symposium Series; American Chemical Society: Washington, DC, 2015.

Publication Date (Web): October 13, 2015 | doi: 10.1021/bk-2015-1200.ch004

Modulation of Vascular Nitroxidative Stress

A decreased •NO bioavailability and nitroxidative stress are associated with a myriad of cardiovascular disease conditions, including atherosclerosis, CAD, hypertension, stroke, heart failure, sepsis, and myocardial infarction, among others (*120*). The extent of vascular nitroxidative damage is determined by several factors, including the concentration and exposure time to peroxynitrite and its derived radicals, the contribution of other oxidizing and nitrating processes (including MPO-dependent reactions) and the ability of the vascular cells to face the oxidative challenge by means of its endogenous antioxidant mechanisms. It has become clear that basal level of antioxidant enzyme systems and its modulation by diet, exercise or drugs can influence •NO bioavailability, peroxynitrite formation and vascular health (*190*). On a related point, several redox-based pharmacological agents with peroxynitrite-detoxification activity could be useful in the treatment of vascular diseases (*191*). The pharmacological modulation of nitroxidative stress as a therapeutic tool includes the use of: i) antioxidant compounds that directly react with peroxynitrite and related oxidant species, ii) compounds that inhibit peroxynitrite formation either by preventing the formation or diminishing the steady-state concentrations of •NO or superoxide, iii) compounds that catalytically decompose peroxynitrite once it has formed (catalytic antioxidants), iv) compounds that upregulate the endogenous antioxidant mechanisms. It is becoming apparent that some compounds exert their effect by more than one mechanism of action.

In the following sections, we will discuss selected peroxynitrite detoxification systems including endogenous enzyme systems and pharmacologically-active organic and bioinorganic compounds.

Endogenous Antioxidant Mechanisms against Peroxynitrite in the Vasculature

Extracellular Superoxide Dismutase (EC-SOD)

Superoxide levels are increased in blood vessels in many vascular disease including hypercholesterolemia, atherosclerosis, hypertension, diabetes and cigarette smoking. This abnormal generation of $O_2^{\bullet-}$ markedly influences the bioactivity of •NO by favouring the formation of peroxynitrite. Besides the rate constant of peroxynitrite formation is approximately five times higher than the reaction between $O_2^{\bullet-}$ and superoxide dismutase (SODs), these enzymes are unique in regulating $O_2^{\bullet-}$ levels, therefore SODs play a critical role in inhibiting oxidative inactivation of •NO in the vasculature (*192*, *193*).

As mentioned previously, mammals have three different isoforms of SOD: the cytosolic or copper-zinc SOD (SOD-1), the mitochondrial manganese SOD (SOD-2), and an extracellular form of copper-zinc-SOD (EC-SOD or SOD-3). A major isoform of SOD, in the vasculature is the EC-SOD, which plays a critical role in regulating the vascular redox state in the extracellular space (*193*). EC-SOD is a 135kDa homotetramer composed of three functional domains: the amino-terminal residue, which allows secretion from the cell by an increase in the solubility of the

In Oxidative Stress: Diagnostics, Prevention, and Therapy Volume 2; Hepel, et al.;
ACS Symposium Series; American Chemical Society: Washington, DC, 2015.

protein; the active domain which binds copper and zinc and a carboxy-terminal region with a positively charged cluster which provides affinity for heparan sulfate proteoglycans on cell surfaces (*192*). EC-SOD is mainly synthesized by vascular smooth muscle cells in healthy vessels (*103*), however it can be internalized by endothelial cells through binding the heparan sulfates or a small portion can be displaced with heparin, increasing the circulating levels of the enzyme (*194*). In fact, immunohistochemical studies have shown that vascular EC-SOD is localized in high concentrations between the endothelium and the smooth muscle (*195*). The expression of EC-SOD in vascular cells and within the vessel wall confers to EC-SOD a critical role in the preservation the •NO bioavailability and endothelial function.

Recent evidence strongly suggests the involvement of endothelium-derived •NO in EC-SOD expression. Another study from 2000 showed that the expression of EC-SOD was up regulated by exogenous •NO in human aortic smooth muscle cells. They also demonstrated an intense decrease in EC-SOD expression in eNOS-deficient mice, while treadmill exercise training increased eNOS and EC-SOD expression in aorta of wild-type mice but not in mice lacking eNOS. Afterwards, the modulation of EC-SOD by •NO represents an important feed-forward mechanism whereby endothelial •NO stimulates EC-SOD expression in adjacent smooth muscle cells, thus preventing $O_2^{\bullet-}$-mediated degradation of endothelium-derived •NO (*104*).

The role of EC-SOD in redox signaling is another relevant approach of SOD protective effects in the vasculature, since various biological effects of SOD can be mediated by $O_2^{\bullet-}$ dismutation product, H_2O_2, which also works as a signaling molecule (*196*). A number of studies suggest that EC-SOD-derived H_2O_2 stimulates various redox signaling pathways to promote angiogenesis, cell proliferation and tissue repair (*197–199*). At the beginning of the 90s, another study showed the efficacy of vascular bound EC-SOD in protecting arterial relaxation mediated by EDRF against the inhibitory effects of $O_2^{\bullet-}$ (*200*). The vascular role of EC-SOD was also demonstrated in different experimental models of hypertension. EC-SOD plays a critical role in modulating blood pressure and vascular function in resistance vessels during angiotensin II-induced hypertension in EC-SOD deficient mice, while the gene transfer of in a genetic model of hypertension (*201*).

Findings of clinical and experimental studies suggest a critical role of EC-SOD in atherosclerosis Low plasma circulating EC-SOD was independently associated with an increased likelihood of a history of myocardial infarction (*202*). Moreover, the activity of EC-SOD, but not SOD-1 or SOD-2, was reduced in coronary artery segments of patients with coronary artery disease compared with normal subjects (*203*). The reduction of EC-SOD in the vascular wall could be attributed as a result of the decreased affinity of EC-SOD to endothelial surface verified in atherosclerotic patients (*204*). Despite the abundant expression of EC-SOD in the vascular wall, oxidized products of lipoproteins and nitrotyrosine residues were detected in iNOS-positive, macrophage-rich human and rabbit atherosclerotic lesions (*203*). In a rabbit balloon injury model, the sustained low vascular EC-SOD activity induced nitroxidative stress and impaired iNOS-derived •NO bioavailability, while EC-SOD administration attenuated tyrosine nitration

Publication Date (Web): October 13, 2015 | doi: 10.1021/bk-2015-1200.ch004

and enhances NO_2^- formation (*205*). Thus, it is conceivable that high EC-SOD expression in the arterial wall may prevent not only deleterious effects of $O_2^{\bullet -}$ but also peroxynitrite formation. As discussed previously in the chapter, decrease in EC-SOD activity produces hypertension in humans (*109*).

Peroxiredoxins-Prx

The cytotoxic effect of peroxynitrite is a consequence of cellular $^{\bullet}NO$ production within a oxidant-producing environment; thus, mammalian cells contain physiological mechanisms for peroxynitrite detoxification. The antioxidant enzyme family of peroxiredoxins (Prxs) is considered the most efficient enzymatic system to neutralize peroxynitrite in tissues (*206*).

Peroxiredoxins are thiol-containing enzymes widely distributed in nature from bacteria to man and found abundantly in various tissues and cells. In general, Prxs are able to reduce peroxides by an enzymatic substitution (ping-pong) mechanism, using electrons provided by a physiological thiol such as thioredoxin (*206*, *207*). The mammalian genome encodes six subclasses of Prxs (Prx 1 to 6), which are classified into three subgroups (2-Cys, atypical 2-Cys, and 1-Cys) according to the number of Cys residues required for catalysis (*208*).

The first evidence of peroxynitrite reductase activity of Prxs was reported by Bryk and collegues in 2000. The authors showed that three Prxs from phylogenetic different pathogens react extremely fast with peroxynitrite. The typical 2-Cys Prx of bacteria evaluated in this study, alkyl hydroperoxide reductase C (AhpC), completely decomposed peroxynitrite with a second-order rate constant of 1 x 10^6 M^{-1} s^{-1} (at pH 7.0 and room temperature) (*209*, *210*). After that, several other Prxs were reported to react with peroxynitrite with similar, or even higher second-order rate constants (*206*). The reaction of peroxynitrite with the catalytic peroxiredoxin thiol can be represented as follow (Eq. 19).

$$Prx\text{-}S^- + ONOOH \rightarrow Prx\text{-}SOH + NO_2^- \qquad \text{(Eq. 19)}$$

1x 10^6 M^{-1} s^{-1} to 7 x 10^7 M^{-1} s^{-1}) (*118*). The catalysis in this group of enzymes start with the reaction of the peroxide with the "peroxidatic" cysteine residue (fast reacting cysteine), to a sulfenic acid derivative, with the concomitant formation of nitrite. Then, in the typical two-cysteine peroxiredoxins, the sulfenic acid reacts with the "resolving" cysteine thiol to form a protein disulfide (*118*, *206*), which is the re-reduced to the native protein reduce state at the expense of substrates such us thioredoxin.

Two-electron reduction rates of peroxynitrite by peroxiredoxins have been established. An extremely rapid reaction has been reported for Prx5 with a k = 7 x 10^7 $M^{-1}s^{-1}$, which is two times higher than that of peroxynitrite with Mn^{3+} porphyrin, 20 times that with ebselen, and 5 times that with reduced glutathione peroxidase 1 (*211*). Independently of the actual reaction rate constants (k), it is critical to consider the concentration of the peroxynitrite targets to predict the biological relevance of a give reaction. Considering these two parameters, peroxiredoxins are recognized as the most efficient peroxynitrite scavengers

In Oxidative Stress: Diagnostics, Prevention, and Therapy Volume 2; Hepel, et al.;
ACS Symposium Series; American Chemical Society: Washington, DC, 2015.

Publication Date (Web): October 13, 2015 | doi: 10.1021/bk-2015-1200.ch004

known to date. For instance, assuming a concentration of Prx5 above 1 μM, the calculated apparent pseudo-first-order constant (obtained as k times the concentration of target, k(T)) is > 70 s^{-1}, *i.e;* higher than that with CO_2 (*211*).

Another relevant example of efficiency of Prx as a peroxynitrite scavenger in the vascular system, is the antioxidant activity of Prx2 in red blood cells. Even though intravascularly formed peroxynitrite can react with plasma components, a considerable portion diffuses into erythrocyte (*114*). Considering the large rate constant of Prx2 and peroxynitrite (1.7 x 10^7 M^{-1} s^{-1}) (*212*) and its abundant concentration in the erythrocyte ((*240*) μM; (*213*)), the calculated reaction constant is superior to 4000 s^{-1} (*211*), largely exceeding the detoxification capacity of oxyHb against peroxynitrite.

The relative abundance of Prxs enzymes in mammals appears to protect vascular environment by removing different peroxides produced as a result of normal cellular metabolism. Peroxiredoxins are widespread in biological compartments and are located mainly in the cytosol, but also within mitochondria and peroxisomes and associated with nuclei and membranes (*211*, *214*). The pharmacologic modulation of peroxiredoxin expression could represent an important protective response against vascular oxidants. In this way, we recently reported that the organoselenium compound, diphenyl diselenide efficiently protects endothelial cells from nitroxidative stress and mitochondrial dysfunction induced by the peroxynitrite donor SIN-1, by upregulating the expression of Prx1 and 3 (*215*) (see also below).

Publication Date (Web): October 13, 2015 | doi: 10.1021/bk-2015-1200.ch004

Oxy-Hemoglobin

Oxy-hemoglobin reacts with peroxynitrite with a high second order constant of (k_2 = 2 x 10^4 M^{-1} s^{-1} at 37 °C and pH 7.4 (*114*, *115*) yielding metHb and stoichiometric formation of NO_3^- as the final oxidation products. Taking into account the relatively high rate constant for this reaction as well as the facilitated diffusion of peroxynitrite across the membrane by the large abundance of anion channels, oxyhemoglobin is an important route of peroxynitrite decay in the vasculature (*216*).

The mechanism of the reaction implies the isomerization of peroxynitrite to NO_3^- in several steps. Firstly, peroxynitrite reacts with oxyHb (best described as an intermediate form between iron(II)-dioxygen and an Fe^{3+}-$O_2^{\bullet-}$ complex, (Eq. 20)) to yield $O_2^{\bullet-}$ and metHb-peroxynitrite intermediate (Eq. 21), followed by a rapid heme catalyzed peroxynitrite decomposition of O-O bond hemolysis to ferrylHb and $^{\bullet}NO_2$ (Eq. 22). The recombination of $^{\bullet}NO_2$ with ferrylHb within heme cavity produces metHb and NO_3^- (Eq. 23) (*217*).

$$Hb(Fe^{2+})O_2 \rightleftharpoons Hb(Fe^{3+})O_2^{\bullet-} \quad \text{(Eq. 20)}$$

$$Hb(Fe^{3+})O_2^{\bullet-} + ONOO^- \rightarrow Hb(Fe^{3+})\text{-}\ ONOO^- \quad \text{(Eq. 21)}$$

$$Hb(Fe^{3+})\text{-}\ ONOO^- \rightarrow Hb(Fe^{3+}\text{-O-ONO}) \quad \text{(Eq. 22)}$$

In Oxidative Stress: Diagnostics, Prevention, and Therapy Volume 2; Hepel, et al.;
ACS Symposium Series; American Chemical Society: Washington, DC, 2015.

$$Hb(Fe^{3+}\text{-}O\text{-}ONO) \rightarrow Hb(Fe^{3+}) + NO_3^- \quad \text{(Eq. 23)}$$

Until this moment, oxy-Hb acts as the major peroxynitrite scavenger in the vasculature, preventing oxidizing reactions against other proteins. However, red blood cells contain high levels of peroxiredoxin two, that reacts very fast with peroxynitrite 1.4 x 10^7 M-1 s^{-1} at 25 ºC and pH 7.4 (*212*).

Peroxynitrite-derived oxidative modifications have been demonstrated in hemoglobin, such as formation of protein radicals (cysteinyl and •Tyr derived radicals) and covalently-linked hemoglobin chains. Recent studies showed that several modification were identified from fresh isolated human hemoglobin, such as nitration of Tyr^{24} and Tyr^{42} in the α-globin chains, and Tyr^{130} in β-globin chains. Moreover, oxidation of methionine residues as well as cysteine residues were identified (α-Met^{32}, α-Met^{76}, and β-Met^{55}; α-Cys^{104}, β-Cys^{93}, and β-Cys^{112}) (*218*). Although these mechanisms occur in a very low yield *in vivo*, the identification of these oxidative modifications in human isolated hemoglobin implies that oxy-Hb is one important intravascular target of peroxynitrite; these reactions may contribute to RBC aging, amont other mechanisms, by favoring intermolecular cross links in hemoglobin and facilitating the formation of protein aggregates (*217*).

Notably, in spite of the presence of strong peroxynitrite detoxifying systems in RBC, namely Hb^{2+}-O_2 and Prx 2, basal 3NT levels are detectable, indicating that nitrating species are continuously formed or reaching RBC even in healthy individuals and that antioxidant systems are not completely efficient to cope against peroxynitrite (*219*).

Pharmacological Compounds That Attenuate Peroxynitrite-Dependent Damage in the Vascular System

According to several studies, organic and bioinorganic compounds added to celular systems are able to detoxify peroxynitrite. We will discuss some of them that have been reported to work successfully in the vascular system.

Metalloporphyrins - MnP

Metalloporphyrins (most notably manganese porphyrins, MnPs) can directly react with peroxynitrite, catalyzing its decomposition. There is great interest in these molecules because of the well-known ability of peroxynitrite to promote fast one- and two-electron oxidation processes with transition metals. Indeed, metalloporphyrins have shown to attenuate the toxic effects of peroxynitrite and prevent nitroxidative stress in several *in vitro* and *in vivo* models (*191*, *220*, *221*).

MnPs, depending on its redox state Mn^{+3} or Mn^{+2}, can reduce peroxynitrite uni or divalently, resulting the oxidizing radical $•NO_2$ or NO_2^-, respectively (*220*, *221*). While MnP are administered in the Mn^{3+} redox state, the most redox active form for cytoprotection is the fully reduced state, Mn^{2+}, which is obtained by reaction with cellular reductants such as ascorbate or glutathione or flavoenzymes,

In Oxidative Stress: Diagnostics, Prevention, and Therapy Volume 2; Hepel, et al.;
ACS Symposium Series; American Chemical Society: Washington, DC, 2015.

Publication Date (Web): October 13, 2015 | doi: 10.1021/bk-2015-1200.ch004

including mitochondrial respiratory complexes I and II. Indeed, Mn^{2+}Ps are able to promote the two-electron reduction of peroxynitrite yielding nitrite and the oxidized Mn^{+4}P. The oxidized Mn^{+4}Ps species, would then be reduced back to the Mn^{3+} state by cellular reductants ascorbate, glutathione and, most notably, uric acid. The redox transtions complete a catalytic redox cycle of peroxynitrite detoxification. For example, it has been shown that MnPs efficiently limited peroxynitrite-mediated oxidative damage in low-density lipoproteins (LDLs) by using uric acid as a reductant. This protective effect should predominate under *in vivo* vascular conditions having plasma uric acid concentrations ranging between 150 and 500 μM (*222*, *223*). The reactivity of different MnPs toward peroxynitrite is diverse, with rate constants ranging from 10^5 to 10^7 M^{-1} s^{-1} at 37°C (*206*) (Table 2). The mechanism of the reaction between the MnPorphyrin and peroxynitrite is outlined below (Eqs. 24 and 25) (*224*).

$$Mn^{2+}\text{-Porphyrin} + ONOO^- \rightarrow ONOO\text{-}\ Mn^{2+}\text{-Porphyrin} \qquad \text{(Eq. 24)}$$

$$ONOO\text{-}\ Mn^{2+}\text{-Porphyrin} \rightarrow O{=}Mn^{4+}\text{-Porphyrin} \qquad \text{(Eq. 25)}$$

Some of the Mn compunds have been used in several studies as SOD mimmics, but the main activity of these Mn-compounds is actually peroxynitrite decomposition (*226*).

An additional pharmacological aspect of MnPs is their ability to act as catalytic antioxidants in mitochondria (*220*, *227*). The mitochondria represents the prime *locus* of formation and actions of peroxynitrite (*228*). Indeed, mitochondria are central intracellular sources of $O_2^{\bullet -}$, and peroxynitrite formation is favoured by the $^{\bullet}NO$ diffusion from the cytosol. Peroxynitrite irreversibly affects the activity of electron transport chain complexes and enzymes of the Krebs cycle (*229*), altering mitochondrial bioenergetics and further increasing mitochondrial $O_2^{\bullet -}$ formation rate (*230*, *231*). In line with this, it has been recently demonstrated that MnP can undergo a catalytic redox cycle to neutralize peroxynitrite-dependent mitochondrial oxidative damage at the expense of reducing equivalents from the electron transport chain (*227*).

Publication Date (Web): October 13, 2015 | doi: 10.1021/bk-2015-1200.ch004

Selenium Compounds

The selenium-containing enzyme, glutathione peroxidase (GPx), can act as a peroxynitrite reductase (*232*). The second-order rate constant for the reaction of GPx with peroxynitrite is 8 X 10^6 M^{-1} s^{-1} (*233*). In fact, the reaction of GPx with peroxynitrite is considered a biologically efficient peroxynitrite detoxification pathway *in vivo*. Thus, as a way to mimic the peroxidase activity of the GPx, several synthetic organoselenium compounds have been designed (*234*). The first and most studied molecule has been ebselen (2-phenyl-1,2-benzoisoselenazol-3(2H)-one), whose peroxidase activity has been measured on various oxidants substrates, including peroxynitrite. In fact, ebselen reacts with peroxynitrite efficiently, exhibiting a high second-order rate constant

($k_2 \sim 10^6$ $M^{-1}s^{-1}$) for a low-molecular-weight compound with peroxynitrite (*235*, *236*). Considering an overall catalytic mechanism of action, ebselen reduces peroxynitrite to nitrite forming the corresponding selenoxide (Eq. 26), which is then reduced back to selenol either by glutathione or by the NADPH-selenoprotein thioredoxin reductase (*236–238*).

$$\text{Eb-Se}^- + \text{ONOOH} \rightarrow \text{Eb-SeOH} + \text{NO}_2^- \qquad \text{(Eq. 26)}$$

The protective effect of ebselen has been demonstrated in several *in vivo* and *in vitro* models where peroxynitrite is formed. As an example, ebselen prevented the premature endothelial cell senescence and vasculopathy in obesity-induced diabetic rats (*239*) and reduced the atherosclerotic lesions in diabetic apolipoprotein E–deficient mice through modulating vascular nitroxidative stress (*240*). Ebselen was also evaluated in clinical studies for the treatment of stroke and subarachnoid haemorrhage (*241*, *242*) pointing to the potential therapeutic significance of the organoselenides in vascular pathology.

Apart from ebselen, various organoselenium compounds have been synthesized and studied over the years aiming to mimic the peroxidase activity of the GPx. In particular, we would like to focus as a relevant example in the context of peroxynitrite pharmacology in properties of the simple diaryldiselenide, diphenyl diselenide $(PhSe)_2$. In fact, the GPx-mimetic activity of diphenyl diselenide is higher than that of ebselen; however, the biological properties of organoselenium compounds are much more complex and go far beyond their GPx mimetic activity (*243*). In line with this, diphenyl diselenide, as ebselen, is a good substrate of hepatic and cerebral thioredoxin reductase (TrxR) enzyme, which contributes to its potent antioxidant action (*244*, *245*). Some *in vitro* and *in vivo* studies propose diphenyl diselenide as a potent modulator of nitroxidative stress in the vasculature; however, the second order rate constant for peroxynitrite-mediated diphenyl diselenide/selenophenol oxidation (2.7×10^5 $M^{-1}s^{-1}$; (*246*)) was smaller than that reported by ebselen, indicating that a more complex mechanism is involved in the pharmacological properties of diphenyl diselenide against peroxynitrite.

The treatment with diphenyl diselenide efficiently prevented atherosclerosis, decreased nitroxidative stress in arterial wall and improved the endothelial function in LDL receptor knockout mice (*247*). In addition, diphenyl diselenide accurately inhibited *in vitro* human LDL oxidation (*242*). The neuroprotective effect of diphenyl diselenide was also demonstrated in an experimental model of stroke by preventing mitochondrial damage caused by ischemia and reperfusion (*248*).

Oxidative and inflammatory disturbances induced by LDL in the vasculature represent a relevant step in the development of cardiovascular disease. The protective effects of diphenyl diselenide could be attributed to its ability to modulate intracellular signaling pathways related to antioxidant and anti-inflammatory responses. In this way, the redox signaling effects of diphenyl diselenide down-regulated the NF-kB activation induced by LDLox in macrophages, thus preventing the reactive species generation, disturbance of •NO homeostasis, foam cell formation, and mitochondrial dysfunction (*249*).

In Oxidative Stress: Diagnostics, Prevention, and Therapy Volume 2; Hepel, et al.;
ACS Symposium Series; American Chemical Society: Washington, DC, 2015.

Publication Date (Web): October 13, 2015 | doi: 10.1021/bk-2015-1200.ch004

Table 2. Kinetic constant reaction of Mn-Porphyrins with peroxynitrite[a]

Mn Porphyrin	k_2 M^{-1} s^{-1}
Mn^{3+} TM 2-PyP	1.9 x 10^7
Mn^{3+} TnPr-2-PyP	1.4 x 10^7
Mn^{3+} TnBu-2-PyP	1.3 x 10^7
Mn^{3+} TnHex-2-PyP	1.3 x 10^7
Mn^{3+} TnOct-2-PyP	1.4 x 10^7
Mn^{3+} TM-3-PyP	4.2 x 10^6
Mn^{3+} TM-4-PyP	4.3 x 10^6
Mn^{3+} TSPP	3.4 x 10^5
Mn^{3+} TCPP	1 x 10^5
Mn^{2+} TE 2-PyP	>7 x 10^6

[a] MnIIITM-2-PyP, manganese(III)mesotetrakis((N-methyl)pyridinium-2-yl)porphyrin; MnIIITnPr-2-PyP, manganese(III)mesotetrakis((N-n-propyl)pyridinium-2-yl)porphyrin; MnIIITnBu-2-PyP, manganese(III)mesotetrakis((N-n-butyl)pyridinium-2-yl)porphyrin; MnIIITnHex-2-PyP, manganese(III)mesotetrakis((N-n-hexyl)pyridinium-2-yl)porphyrin; MnIIITnOct-2-PyP, manganese(III)mesotetrakis((N-n-octyl)pyridinium-2-yl)porphyrin; MnIIITM-3-PyP, manganese(III)mesotetrakis((N-methyl)pyridinium-3-yl)porphyrin; MnIIITM-4-PyP, manganese(III)mesotetrakis((N-methyl)pyridinium-4-yl)porphyrin; MnIIITSPP, manganese(III)mesotetrakis(4-sulfonatophenyl)-porphyrin; MnIIITCPP, manganese(III)mesotetrakis(4-carboxylatophenyl)porphyrin; manganese (*201*) mesotetrakis((N-ethyl)pyridinium-2-yl)porphyrin (MnTE-2-PyP). Note that the last example indicates the MnP in the reduced (+2) state. Modified from (*220*, *225*).

Publication Date (Web): October 13, 2015 | doi: 10.1021/bk-2015-1200.ch004

Another mechanism involved in the pharmacological actions of organoselenium compounds is its ability to react with redox-sensitive cysteines, as a "thiol reagent" (*243*). Recently we reported that diphenyl diselenide, (as already reported with ebselen), can activate the Keap1/Nrf2 signalling pathway through oxidation of critical cysteines in Keap1, which in turn, allows Nrf2 transcriptionally activate the expression of antioxidant systems and detoxification enzymes (*246*, *250*). In this way, diphenyl diselenide protected endothelial cells against peroxynitrite-induced nitration and apoptosis by improving the redox status of endothelium through increasing the general activity of glutathione and peroxiredoxin antioxidant system (*246*). During an oxidative challenge, mitochondrial and endothelial function can be protected by selenium compounds through a mechanism by which Prx expression is upregulated *via* transcriptional and translational mechanisms regulated by both Nrf2 and FOXO 3 (*215*).

As already described, endothelial dysfunction is characterized by a reduced bioavailability of •NO (*251*). In endothelial cells, the nitroxidative stress mediated by peroxynitrite flux compromises the mitochondrial function which in turn leads to additional intracellular production of peroxynitrite, amplifying the process, finally reducing the •NO bioavailability. In this situation, diphenyl diselenide

was able to prevent the endothelium dysfunction induced by a peroxynitrite flux generated by 1,3 morpholinosydnonimine (SIN-1) (*215*).

The impairment in mitochondrial function induced by nitroxidative stress is closely related to endothelial dysfunction, whereas targeting mitochondria pharmacology is actually a promising therapeutic strategy for vascular disease (*252*). Besides the upgrade of the glutathione antioxidant system through Nrf2 activation (*215*, *246*), diphenyl diselenide improved the intracellular redox state by also increasing the expression of different isoforms of peroxiredoxins (cytosolic Prx1 and mitochondrial Prx3), efficient enzymes in peroxynitrite detoxification (*215*). The profound impact mediated by peroxynitrite in endothelial mitochondria lead to an impairment in cellular respiration, a compromise in ATP generation, mitochondrial uncoupling and the reduction in mitochondria reserve capacity. These alterations in respiratory parameters were prevented by diphenyl diselenide *via* the amelioration of cellular redox capacity and the consequent improvements in the mitochondrial network (*215*).

Publication Date (Web): October 13, 2015 | doi: 10.1021/bk-2015-1200.ch004

Statins

Statins (3-hydroxy-3-methylgulutaryl-coenzyme A reductase inhibitors) are a group of lipid-lowering drugs used in the prevention and treatment of cardiovascular disease. However, there is increasing evidence that statins may also exert effects beyond cholesterol lowering. Indeed, many of cholesterol-independent or "pleiotropic" vascular effects of statins appear to involve restorative or improving endothelial function through increasing the bioavailability of •NO enhancing the stability of atherosclerotic plaques, reducing oxidative stress and inflammation, and decreasing the thrombogenic responses (*253–255*). The ability of statins to increase eNOS expression and activation may be an important mechanism by which statins improve endothelial function (*256*). By inhibiting HMG-CoA reductase, statins can also inhibit the synthesis of isoprenoids, which are important lipid attachments for intracellular signaling molecules such as Rho GTPases (*257*). A decrease in Rho GTPase responses, as a consequence of statin treatment, increases the expression and stabilization of eNOS by a post- transcriptional mechanism which finally increases the production and bioavailability of endothelium-derived •NO (*256*, *258*). Furthermore, Kureishi *et al.* reported that statins can activate protein kinase Akt. The serine-threonine kinase Akt is an important regulator of various cellular processes, including cell metabolism and apoptosis targets, such as caspase-9 and eNOS (*259*). For example, the Akt activation induced by statins, inhibits apoptosis and increases •NO production in cultured endothelial cells (*260*).

Another potential mechanism by which statins may improve endothelial function is through their antioxidant effects. Several statins inhibit endothelial $O_2^{\bullet -}$ formation by reducing the expression and/or activity of NADPH oxidase by preventing the isoprenylation of p21 Rac, which is critical for the assembly of NADPH oxidase (*261–263*). Because •NO is scavenged by ROS, these findings indicate that the antioxidant properties of statins may also contribute to their ability to improve endothelial function (*264*).

Hazen *et al* measured the relationship between 3NT systemic levels with patients with prevalence of CAD. In these cases, patients with CAD showed a significant increase of plasma 3NT levels respect to control patients. In addition, patients that were under Statin therapy, reduced nitrotyrosine levels significantly (*265*).

Conclusions and Perspectives

In this chapter we have highlighted the oxidative mechanisms by which the biological half-life and bioavailability of •NO is controlled (Figure 6); these reactions are particularly relevant under pathophysiological conditions where the vascular system is exposed or generates high rates of oxidants such as $O_2^{\bullet-}$ and H_2O_2. The so-called "oxidative inactivation" of •NO leads, in turn, to the generation of secondary •NO-derived oxidants that cause nitroxidative damage in the vasculature. As vascular nitroxidative stress is one of the mechanisms participating in vascular dysfunction and degeneration, early detection of biomarkers of this process can help for early prevention or treatment of disease conditions. Moreover, dietary habits, physical activity and pharmacological strategies can assist to optimize vascular •NO physiology while minimizing toxic effects of peroxynitrite and related •NO -derived oxidants in the cardiovascular system.

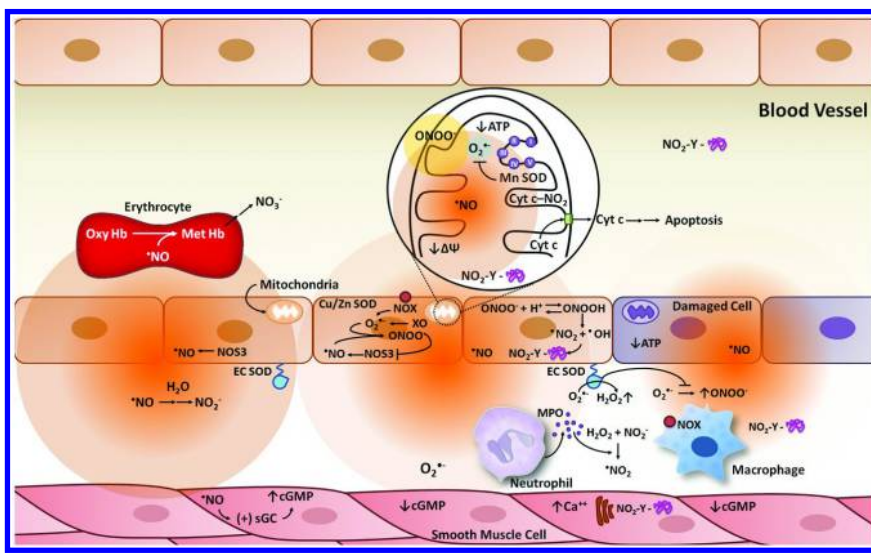

Figure 6. Impaired •NO bioavailability during vascular oxidant formation: formation of peroxynitrite and protein 3-nitrotyrosine

In Oxidative Stress: Diagnostics, Prevention, and Therapy Volume 2; Hepel, et al.;
ACS Symposium Series; American Chemical Society: Washington, DC, 2015.

Publication Date (Web): October 13, 2015 | doi: 10.1021/bk-2015-1200.ch004

Publication Date (Web): October 13, 2015 | doi: 10.1021/bk-2015-1200.ch004

Healthy endothelial cells regulate blood flow by controlling the smooth muscle cells tone in the medial layer of the vessel wall. Nitric oxide (•NO) is a major contributor to the normal homeostasis of the cardiovascular system. Produced by endothelial nitric oxide synthase (eNOS, NOS3), •NO can diffuse towards the surrounding smooth muscle cells where it activates soluble guanylate cyclase (sGC) to induce cGMP-dependent vessel relaxation. Endothelial dysfunction is characterized by a decrease in •NO bioavailability. The main pathway of •NO inactivation in the vasculature is its diffusion-controlled reaction with superoxide ($O_2^{\bullet-}$) producing the powerful oxidant peroxynitrite anion ($ONOO^-$). Sources of $O_2^{\bullet-}$ include NADPH oxidases (NOX), xanthine oxidase (XO) mitochondria and uncoupled eNOS. The vascular infiltration of inflammatory cells (neutrophils and macrophages) also contributes to reactive species generation. The neutrophil enzyme myeloperoxidase (MPO) can promote, in presence of H_2O_2 (generated by SOD-catalyzed dismutation of $O_2^{\bullet-}$), the one electron oxidation of •NO to NO_2^- and of NO_2^- to $^{\bullet}NO_2$, which can lead to the oxidative inactivation and protein tyrosine nitration, respectively.

The inset represents peroxynitrite formation and actions in mitochondria. Superoxide radical is mainly formed towards the matrix via the one-electron reduction of molecular oxygen by electron-transport chain components. While •NO has a half-life in the range of seconds and readily diffuses across membranes, $O_2^{\bullet-}$ is much shorter-lived and has restricted diffusion, so peroxynitrite formation is spatially associated to the sites of $O_2^{\bullet-}$ formation (The circles provide and approximation of relative diffusion distances). Peroxynitrite-dependent nitration of mitochondrial proteins such as Mn SOD, and cytochrome *c* amplify the cellular oxidative damage through either increase $O_2^{\bullet-}$ steady-state levels and enhanced peroxidase activity (NO_2-Cyt *c*).Mitochondrial enzymes, such as electron transport complexes I and II and ATP synthase (complex V), are particularly vulnerable to attacks by peroxynitrite, leading to reduced ATP formation and induction of mitochondrial permeability transition by opening of the permeability transition pore, which dissipates the mitochondrial membrane potential (Ψ) and allow the efflux of several pro-apoptotic molecules, including cytochrome *c*.

Superoxide dismutases (SOD) constitute an important defensive line, diverting $O_2^{\bullet-}$ to H_2O_2 and thus preventing peroxynitrite formation. Blood vessels express 3 isoforms of superoxide dismutase: cytosolic or Cu/Zn SOD, Mn SOD localized in mitochondria, and an extracellular form of Cu/Zn SOD (EC-SOD).

Peroxynitrite anion ($ONOO^-$) and peroxynitrous acid (ONOOH; pKa 6.8) can evolve to secondary radicals that can readily oxidize and nitrate tyrosine residues in proteins leading to NO_2-Y-proteins. This effect is represented in the Figure by nitration SERCA, inducing an increase of cytoplasmic Ca^{2+} concentration that affects the vascular tone. In aqueous phase •NO can be mainly converted in nitrite (NO_2^-) and both •NO and NO_2^- can react with oxyhemoglobin (Oxy Hb) to produce methemoglobin (Met Hb) and NO_3^-.

When the endothelial dysfunction is established *via* an enhancement of vascular $O_2^{\bullet-}$ levels, the half-life and levels of •NO are compromised, affecting cGMP-dependent relaxation at the smooth muscle cells. In parallel, $ONOO^-$ formation becomes relevant and tyrosine nitrated proteins increase in plasma and the vascular wall.

In Oxidative Stress: Diagnostics, Prevention, and Therapy Volume 2; Hepel, et al.;
ACS Symposium Series; American Chemical Society: Washington, DC, 2015.

Publication Date (Web): October 13, 2015 | doi: 10.1021/bk-2015-1200.ch004

Acknowledgments

This manuscript is dedicated to the memory of our friend and coinvestigator Prof. Dr. Gonzalo Peluffo.

NS was partially supported by fellowships from Universidad de la República (CSIC), Agencia Nacional de Investigación e Innovación (ANII) and the International Union of Biochemistry and Molecular Biology (IUBMB). This work was funded by grants from Fondo Clemente Estable (FCE _2_2011_1_6605) to SB, Conselho Nacional de Desenvolvimento Científico e Tecnológico (CNPq-PVE 401065/2014-6) and Coordenação de Aperfeiçoamento de Pessoal de Nível Superior (CAPES-UDELAR 017/2012) to AB and Universidad de la República (CSIC Grupos) and National Institutes of Health (1R01AI095173) to RR. Additional funding was obtained from CAPES-UDELAR, PEDECIBA and RIDALINE.

References

1. Ignarro, L. J.; Byrns, R. E.; Buga, G. M.; Wood, K. S.; Chaudhuri, G. Pharmacological evidence that endothelium-derived relaxing factor is nitric oxide: use of pyrogallol and superoxide dismutase to study endothelium-dependent and nitric oxide-elicited vascular smooth muscle relaxation. *J. Pharmacol. Exp. Ther.* **1988**, *244*, 181–189.
2. Gewaltig, M. T.; Kojda, G. Vasoprotection by nitric oxide: mechanisms and therapeutic potential. *Cardiovasc. Res.* **2002**, *55*, 250–260.
3. Etter, E. F.; Eto, M.; Wardle, R. L.; Brautigan, D. L.; Murphy, R. A. Activation of myosin light chain phosphatase in intact arterial smooth muscle during nitric oxide-induced relaxation. *J. Biol. Chem.* **2001**, *276*, 34681–34685.
4. Dudzinski, D. M.; Igarashi, J.; Greif, D.; Michel, T. The regulation and pharmacology of endothelial nitric oxide synthase. *Annu. Rev. Pharmacol. Toxicol.* **2006**, *46*, 235–276.
5. Amrani, Y.; Magnier, C.; Enouf, J.; Wuytack, F.; Bronner, C. Ca2+ increase and Ca(2+)-influx in human tracheal smooth muscle cells: role of Ca2+ pools controlled by sarco-endoplasmic reticulum Ca(2+)-ATPase 2 isoform. *Br. J. Pharmacol.* **1995**, *115*, 1204–1210.
6. Denninger, J. W.; Marletta, M. A. Guanylate cyclase and the .NO/cGMP signaling pathway. *Biochim. Biophys. Acta* **1999**, *1411*, 334–350.
7. Radi, R. Reactions of nitric oxide with metalloproteins. *Chem. Res. Toxicol.* **1996**, *9*, 828–835.
8. Espey, M. G.; Xavier, S.; Thomas, D. D.; Miranda, K. M.; Wink, D. A. Direct real-time evaluation of nitration with green fluorescent protein in solution and within human cells reveals the impact of nitrogen dioxide vs. peroxynitrite mechanisms. *Proc. Natl. Acad. Sci. U. S. A.* **2002**, *99*, 3481–3486.
9. Szabo, C.; Ischiropoulos, H.; Radi, R. Peroxynitrite: biochemistry, pathophysiology and development of therapeutics. *Nat. Rev. Drug Discov.* **2007**, *6*, 662–680.

10. Tsai, A. How does NO activate hemeproteins? *FEBS Lett.* **1994**, *341*, 141–145.
11. Cooper, C. E. Nitric oxide and iron proteins. *Biochim. Biophys. Acta* **1999**, *1411*, 290–309.
12. Sharma, V. S.; Traylor, T. G.; Gardiner, R.; Mizukami, H. Reaction of nitric oxide with heme proteins and model compounds of hemoglobin. *Biochemistry* **1987**, *26*, 3837–3843.
13. Herold, S.; Rehmann, F. J. Kinetics of the reactions of nitrogen monoxide and nitrite with ferryl hemoglobin. *Free Radic. Biol. Med.* **2003**, *34*, 531–545.
14. Galijasevic, S.; Proteasa, G.; Abdulhamid, I.; Abu-Soud, H. M. The potential role of nitric oxide in substrate switching in eosinophil peroxidase. *Biochemistry* **2007**, *46*, 406–415.
15. Galijasevic, S.; Saed, G. M.; Diamond, M. P.; Abu-Soud, H. M. Myeloperoxidase up-regulates the catalytic activity of inducible nitric oxide synthase by preventing nitric oxide feedback inhibition. *Proc. Natl. Acad. Sci. U. S. A.* **2003**, *100*, 14766–14771.
16. Abu-Soud, H. M.; Hazen, S. L. Nitric oxide is a physiological substrate for mammalian peroxidases. *J. Biol. Chem.* **2000**, *275*, 37524–37532.
17. Abu-Soud, H. M.; Hazen, S. L. Nitric oxide modulates the catalytic activity of myeloperoxidase. *J. Biol. Chem.* **2000**, *275*, 5425–5430.
18. Stadler, J.; Trockfeld, J.; Schmalix, W. A.; Brill, T.; Siewert, J. R.; Greim, H.; Doehmer, J. Inhibition of cytochromes P4501A by nitric oxide. *Proc. Natl. Acad. Sci. U. S. A.* **1994**, *91*, 3559–3563.
19. Wink, D. A.; Osawa, Y.; Darbyshire, J. F.; Jones, C. R.; Eshenaur, S. C.; Nims, R. W. Inhibition of cytochromes P450 by nitric oxide and a nitric oxide-releasing agent. *Arch. Biochem. Biophys.* **1993**, *300*, 115–123.
20. Brown, G. C.; Cooper, C. E. Nanomolar concentrations of nitric oxide reversibly inhibit synaptosomal respiration by competing with oxygen at cytochrome oxidase. *FEBS Lett.* **1994**, *356*, 295–298.
21. Cassina, A.; Radi, R. Differential inhibitory action of nitric oxide and peroxynitrite on mitochondrial electron transport. *Arch. Biochem. Biophys.* **1996**, *328*, 309–316.
22. Henry, Y.; Ducrocq, C.; Drapier, J. C.; Servent, D.; Pellat, C.; Guissani, A. Nitric oxide, a biological effector. Electron paramagnetic resonance detection of nitrosyl-iron-protein complexes in whole cells. *Eur. Biophys. J.* **1991**, *20*, 1–15.
23. Castro, L. A.; Robalinho, R. L.; Cayota, A.; Meneghini, R.; Radi, R. Nitric oxide and peroxynitrite-dependent aconitase inactivation and iron-regulatory protein-1 activation in mammalian fibroblasts. *Arch. Biochem. Biophys.* **1998**, *359*, 215–224.
24. Kennedy, M. C.; Emptage, M. H.; Dreyer, J. L.; Beinert, H. The role of iron in the activation-inactivation of aconitase. *J. Biol. Chem.* **1983**, *258*, 11098–11105.
25. Beinert, H.; Kennedy, M. C. Aconitase, a two-faced protein: enzyme and iron regulatory factor. *FASEB J.* **1993**, *7*, 1442–1449.
26. Gardner, P. R.; Fridovich, I. Superoxide sensitivity of the Escherichia coli aconitase. *J. Biol. Chem.* **1991**, *266*, 19328–19333.

In Oxidative Stress: Diagnostics, Prevention, and Therapy Volume 2; Hepel, et al.;
ACS Symposium Series; American Chemical Society: Washington, DC, 2015.

Publication Date (Web): October 13, 2015 | doi: 10.1021/bk-2015-1200.ch004

27. Gardner, P. R.; Fridovich, I. Inactivation-reactivation of aconitase in Escherichia coli. A sensitive measure of superoxide radical. *J. Biol. Chem.* **1992**, *267*, 8757–8763.
28. Flint, D. H.; Tuminello, J. F.; Emptage, M. H. The inactivation of Fe-S cluster containing hydro-lyases by superoxide. *J. Biol. Chem.* **1993**, *268*, 22369–22376.
29. Castro,, L.; Rodriguez,, M.; Radi, R. Aconitase is readily inactivated by peroxynitrite, but not by its precursor, nitric oxide. *J. Biol. Chem.* **1994**, *269*, 29409–29415.
30. Kennedy, M. C.; Antholine, W. E.; Beinert, H. An EPR investigation of the products of the reaction of cytosolic and mitochondrial aconitases with nitric oxide. *J. Biol. Chem.* **1997**, *272*, 20340–20347.
31. Piantadosi, C. A. Regulation of mitochondrial processes by protein S-nitrosylation. *Biochim. Biophys. Acta* **2012**, *1820*, 712–721.
32. Forfia, P. R.; Hintze, T. H.; Wolin, M. S.; Kaley, G. Role of nitric oxide in the control of mitochondrial function. *Adv. Exp. Med. Biol.* **1999**, *471*, 381–388.
33. Henry, Y.; Guissani, A. Interactions of nitric oxide with hemoproteins: roles of nitric oxide in mitochondria. *Cell. Mol. Life Sci.* **1999**, *55*, 1003–1014.
34. Martin, W.; Villani, G. M.; Jothianandan, D.; Furchgott, R. F. Blockade of endothelium-dependent and glyceryl trinitrate-induced relaxation of rabbit aorta by certain ferrous hemoproteins. *J. Pharmacol. Exp. Ther.* **1985**, *233*, 679–685.
35. Watts, R. N.; Richardson, D. R. Differential effects on cellular iron metabolism of the physiologically relevant diatomic effector molecules, NO and CO, that bind iron. *Biochim. Biophys. Acta* **2004**, *1692*, 1–15.
36. Wever, R.; van Leeuwen, F. X.; van Gelder, B. F. The reaction of nitric oxide with ceruloplasmin. *Biochim. Biophys. Acta* **1973**, *302*, 236–239.
37. Uiterkamp, A. J.; Mason, H. S. Magnetic dipole-dipole coupled Cu(II) pairs in nitric oxide-treated tyrosinase: a structural relationship between the active sites of tyrosinase and hemocyanin. *Proc. Natl. Acad. Sci. U. S. A.* **1973**, *70*, 993–996.
38. Gorren, A. C.; de Boer, E.; Wever, R. The reaction of nitric oxide with copper proteins and the photodissociation of copper-NO complexes. *Biochim. Biophys. Acta* **1987**, *916*, 38–47.
39. Brudvig, G. W.; Stevens, T. H.; Chan, S. I. Reactions of nitric oxide with cytochrome c oxidase. *Biochemistry* **1980**, *19*, 5275–5285.
40. Hayashi, K.; Noguchi, N.; Niki, E. Action of nitric oxide as an antioxidant against oxidation of soybean phosphatidylcholine liposomal membranes. *FEBS Lett.* **1995**, *370*, 37–40.
41. Hogg, N.; Kalyanaraman, B.; Joseph, J.; Struck, A.; Parthasarathy, S. Inhibition of low-density lipoprotein oxidation by nitric oxide. Potential role in atherogenesis. *FEBS Lett.* **1993**, *334*, 170–174.
42. Padmaja, S.; Huie, R. E. The reaction of nitric oxide with organic peroxyl radicals. *Biochem. Biophys. Res. Commun.* **1993**, *195*, 539–544.
43. Rubbo, H.; Radi, R.; Trujillo, M.; Telleri, R.; Kalyanaraman, B.; Barnes, S.; Kirk, M.; Freeman, B. A. Nitric oxide regulation of superoxide

Publication Date (Web): October 13, 2015 | doi: 10.1021/bk-2015-1200.ch004

and peroxynitrite-dependent lipid peroxidation. Formation of novel nitrogen-containing oxidized lipid derivatives. *J. Biol. Chem.* **1994**, *269*, 26066–26075.
44. Yates, M. T.; Lambert, L. E.; Whitten, J. P.; McDonald, I.; Mano, M.; Ku, G.; Mao, S. J. A protective role for nitric oxide in the oxidative modification of low density lipoproteins by mouse macrophages. *FEBS Lett.* **1992**, *309*, 135–138.
45. Wink, D. A.; Cook, J. A.; Pacelli, R.; DeGraff, W.; Gamson, J.; Liebmann, J.; Krishna, M. C.; Mitchell, J. B. The effect of various nitric oxide-donor agents on hydrogen peroxide-mediated toxicity: a direct correlation between nitric oxide formation and protection. *Arch. Biochem. Biophys.* **1996**, *331*, 241–248.
46. Pfeiffer, S.; Gorren, A. C.; Schmidt, K.; Werner, E. R.; Hansert, B.; Bohle, D. S.; Mayer, B. Metabolic fate of peroxynitrite in aqueous solution. Reaction with nitric oxide and pH-dependent decomposition to nitrite and oxygen in a 2:1 stoichiometry. *J. Biol. Chem.* **1997**, *272*, 3465–3470.
47. Kanner, J.; Harel, S.; Granit, R. Nitric oxide, an inhibitor of lipid oxidation by lipoxygenase, cyclooxygenase and hemoglobin. *Lipids* **1992**, *27*, 46–49.
48. Farb, M. G.; Tiwari, S.; Karki, S.; Ngo, D. T.; Carmine, B.; Hess, D. T.; Zuriaga, M. A.; Walsh, K.; Fetterman, J. L.; Hamburg, N. M.; Vita, J. A.; Apovian, C. M.; Gokce, N. Cyclooxygenase inhibition improves endothelial vasomotor dysfunction of visceral adipose arterioles in human obesity. *Obesity* **2014**, *22*, 349–355.
49. Pancake, S. J.; Mora, P. T. Limitations and utility of a cytolytic assay for measuring simian virus 40-induced cell surface antigens. *Cancer Res.* **1976**, *36*, 88–94.
50. Malo-Ranta, U.; Yla-Herttuala, S.; Metsa-Ketela, T.; Jaakkola, O.; Moilanen, E.; Vuorinen, P.; Nikkari, T. Nitric oxide donor GEA 3162 inhibits endothelial cell-mediated oxidation of low density lipoprotein. *FEBS Lett.* **1994**, *337*, 179–183.
51. Schopfer, F. J.; Baker, P. R.; Freeman, B. A. NO-dependent protein nitration: a cell signaling event or an oxidative inflammatory response? *Trends Biochem. Sci.* **2003**, *28*, 646–654.
52. O'Donnell, V. B.; Freeman, B. A. Interactions between nitric oxide and lipid oxidation pathways: implications for vascular disease. *Circ. Res.* **2001**, *88*, 12–21.
53. Wink, D. A.; Cook, J. A.; Kim, S. Y.; Vodovotz, Y.; Pacelli, R.; Krishna, M. C.; Russo, A.; Mitchell, J. B.; Jourd'heuil, D.; Miles, A. M.; Grisham, M. B. Superoxide modulates the oxidation and nitrosation of thiols by nitric oxide-derived reactive intermediates. Chemical aspects involved in the balance between oxidative and nitrosative stress. *J. Biol. Chem.* **1997**, *272*, 11147–11151.
54. Quijano, C.; Alvarez, B.; Gatti, R. M.; Augusto, O.; Radi, R. Pathways of peroxynitrite oxidation of thiol groups. *Biochem. J.* **1997**, *322* (Pt 1), 167–173.
55. Stamler, J. S.; Simon, D. I.; Osborne, J. A.; Mullins, M. E.; Jaraki, O.; Michel, T.; Singel, D. J.; Loscalzo, J. S-nitrosylation of proteins with nitric

Publication Date (Web): October 13, 2015 | doi: 10.1021/bk-2015-1200.ch004

oxide: synthesis and characterization of biologically active compounds. *Proc. Natl. Acad. Sci. U. S. A.* **1992**, *89*, 444–448.
56. Molina y Vedia, L.; McDonald, B.; Reep, B.; Brune, B.; Di Silvio, M.; Billiar, T. R.; Lapetina, E. G. Nitric oxide-induced S-nitrosylation of glyceraldehyde-3-phosphate dehydrogenase inhibits enzymatic activity and increases endogenous ADP-ribosylation. *J. Biol. Chem.* **1992**, *267*, 24929–24932.
57. Padgett, C. M.; Whorton, A. R. S-nitrosoglutathione reversibly inhibits GAPDH by S-nitrosylation. *Am. J. Physiol.* **1995**, *269*, C739–749.
58. Jia, L.; Bonaventura, C.; Bonaventura, J.; Stamler, J. S. S-nitrosohaemoglobin: a dynamic activity of blood involved in vascular control. *Nature* **1996**, *380*, 221–226.
59. Stamler, J. S. Redox signaling: nitrosylation and related target interactions of nitric oxide. *Cell* **1994**, *78*, 931–936.
60. Beltran, B.; Orsi, A.; Clementi, E.; Moncada, S. Oxidative stress and S-nitrosylation of proteins in cells. *Br. J. Pharmacol.* **2000**, *129*, 953–960.
61. Isbell, T. S.; Sun, C. W.; Wu, L. C.; Teng, X.; Vitturi, D. A.; Branch, B. G.; Kevil, C. G.; Peng, N.; Wyss, J. M.; Ambalavanan, N.; Schwiebert, L.; Ren, J.; Pawlik, K. M.; Renfrow, M. B.; Patel, R. P.; Townes, T. M. SNO-hemoglobin is not essential for red blood cell-dependent hypoxic vasodilation. *Nat. Med.* **2008**, *14*, 773–777.
62. Ishima, Y.; Akaike, T.; Kragh-Hansen, U.; Hiroyama, S.; Sawa, T.; Maruyama, T.; Kai, T.; Otagiri, M. Effects of endogenous ligands on the biological role of human serum albumin in S-nitrosylation. *Biochem. Biophys. Res. Commun.* **2007**, *364*, 790–795.
63. Dworschak, M.; Franz, M.; Hallstrom, S.; Semsroth, S.; Gasser, H.; Haisjackl, M.; Podesser, B. K.; Malinski, T. S-nitroso human serum albumin improves oxygen metabolism during reperfusion after severe myocardial ischemia. *Pharmacology* **2004**, *72*, 106–112.
64. Li, L.; Hitchcock, A. P.; Cornelius, R.; Brash, J. L.; Scholl, A.; Doran, A. X-ray microscopy studies of protein adsorption on a phase segregated polystyrene/polymethylmethacrylate surface. 2. Effect of pH on site preference. *J. Phys. Chem. B* **2008**, *112*, 2150–2158.
65. Hallstrom, S.; Gasser, H.; Neumayer, C.; Fugl, A.; Nanobashvili, J.; Jakubowski, A.; Huk, I.; Schlag, G.; Malinski, T. S-nitroso human serum albumin treatment reduces ischemia/reperfusion injury in skeletal muscle via nitric oxide release. *Circulation* **2002**, *105*, 3032–3038.
66. Furchgott, R. F.; Zawadzki, J. V. The obligatory role of endothelial cells in the relaxation of arterial smooth muscle by acetylcholine. *Nature* **1980**, *288*, 373–376.
67. Furchgott, R. F. The role of endothelium in the responses of vascular smooth muscle to drugs. *Annu. Rev. Pharmacol. Toxicol.* **1984**, *24*, 175–197.
68. Ignarro, L. J.; Burke, T. M.; Wood, K. S.; Wolin, M. S.; Kadowitz, P. J. Association between cyclic GMP accumulation and acetylcholine-elicited relaxation of bovine intrapulmonary artery. *J. Pharmacol. Exp. Ther.* **1984**, *228*, 682–690.

Publication Date (Web): October 13, 2015 | doi: 10.1021/bk-2015-1200.ch004

69. Martin, W.; Villani, G. M.; Jothianandan, D.; Furchgott, R. F. Selective blockade of endothelium-dependent and glyceryl trinitrate-induced relaxation by hemoglobin and by methylene blue in the rabbit aorta. *J. Pharmacol. Exp. Ther.* **1985**, *232*, 708–716.
70. Griffith, T. M.; Edwards, D. H.; Lewis, M. J.; Newby, A. C.; Henderson, A. H. The nature of endothelium-derived vascular relaxant factor. *Nature* **1984**, *308*, 645–647.
71. Ignarro, L. J.; Byrns, R. E.; Buga, G. M.; Wood, K. S. Endothelium-derived relaxing factor from pulmonary artery and vein possesses pharmacologic and chemical properties identical to those of nitric oxide radical. *Circ. Res.* **1987**, *61*, 866–879.
72. Palmer, R. M.; Ferrige, A. G.; Moncada, S. Nitric oxide release accounts for the biological activity of endothelium-derived relaxing factor. *Nature* **1987**, *327*, 524–526.
73. McCord, J. M.; Fridovich, I. Superoxide dismutase. An enzymic function for erythrocuprein (hemocuprein). *J. Biol. Chem.* **1969**, *244*, 6049–6055.
74. Gryglewski, R. J.; Palmer, R. M.; Moncada, S. Superoxide anion is involved in the breakdown of endothelium-derived vascular relaxing factor. *Nature* **1986**, *320*, 454–456.
75. Moncada, S.; Higgs, E. A. The discovery of nitric oxide and its role in vascular biology. *Br. J. Pharmacol.* **2006**, *147* (Suppl. 1), S193–201.
76. Moncada, S.; Palmer, R. M.; Higgs, E. A. The discovery of nitric oxide as the endogenous nitrovasodilator. *Hypertension* **1988**, *12*, 365–372.
77. Ignarro, L. J.; Wood, K. S.; Wolin, M. S. Activation of purified soluble guanylate cyclase by protoporphyrin IX. *Proc. Natl. Acad. Sci. U. S. A.* **1982**, *79*, 2870–2873.
78. Babior, B. M.; Lambeth, J. D.; Nauseef, W. The neutrophil NADPH oxidase. *Arch. Biochem. Biophys.* **2002**, *397*, 342–344.
79. Babior, B. M. The NADPH oxidase of endothelial cells. *IUBMB Life* **2000**, *50*, 267–269.
80. Lassegue, B.; Clempus, R. E. Vascular NAD(P)H oxidases: specific features, expression, and regulation. *Am. J. Physiol. Regul. Integr. Comp. Physiol.* **2003**, *285*, R277–297.
81. Li, J. M.; Shah, A. M. Mechanism of endothelial cell NADPH oxidase activation by angiotensin II. Role of the p47phox subunit. *J. Biol. Chem.* **2003**, *278*, 12094–12100.
82. Lyle, A. N.; Deshpande, N. N.; Taniyama, Y.; Seidel-Rogol, B.; Pounkova, L.; Du, P.; Papaharalambus, C.; Lassegue, B.; Griendling, K. K. Poldip2, a novel regulator of Nox4 and cytoskeletal integrity in vascular smooth muscle cells. *Circ. Res.* **2009**, *105*, 249–259.
83. Meier, B.; Cross, A. R.; Hancock, J. T.; Kaup, F. J.; Jones, O. T. Identification of a superoxide-generating NADPH oxidase system in human fibroblasts. *Biochem. J.* **1991**, *275* (Pt 1), 241–245.
84. Zulueta, J. J.; Yu, F. S.; Hertig, I. A.; Thannickal, V. J.; Hassoun, P. M. Release of hydrogen peroxide in response to hypoxia-reoxygenation: role of an NAD(P)H oxidase-like enzyme in endothelial cell plasma membrane. *Am. J. Respir. Cell Mol. Biol.* **1995**, *12*, 41–49.

Publication Date (Web): October 13, 2015 | doi: 10.1021/bk-2015-1200.ch004

85. Spiekermann, S.; Landmesser, U.; Dikalov, S.; Bredt, M.; Gamez, G.; Tatge, H.; Reepschlager, N.; Hornig, B.; Drexler, H.; Harrison, D. G. Electron spin resonance characterization of vascular xanthine and NAD(P)H oxidase activity in patients with coronary artery disease: relation to endothelium-dependent vasodilation. *Circulation* **2003**, *107*, 1383–1389.
86. Peluffo, G.; Calcerrada, P.; Piacenza, L.; Pizzano, N.; Radi, R. Superoxide-mediated inactivation of nitric oxide and peroxynitrite formation by tobacco smoke in vascular endothelium: studies in cultured cells and smokers. *Am. J. Physiol. Heart Circ. Physiol.* **2009**, *296*, H1781–1792.
87. Quijano, C.; Castro, L.; Peluffo, G.; Valez, V.; Radi, R. Enhanced mitochondrial superoxide in hyperglycemic endothelial cells: direct measurements and formation of hydrogen peroxide and peroxynitrite. *Am. J. Physiol. Heart Circ. Physiol.* **2007**, *293*, H3404–3414.
88. Nishino, T.; Okamoto, K.; Kawaguchi, Y.; Matsumura, T.; Eger, B. T.; Pai, E. F.; Nishino, T. The C-terminal peptide plays a role in the formation of an intermediate form during the transition between xanthine dehydrogenase and xanthine oxidase. *FEBS J.* **2015**.
89. Kelley, E. E.; Khoo, N. K.; Hundley, N. J.; Malik, U. Z.; Freeman, B. A.; Tarpey, M. M. Hydrogen peroxide is the major oxidant product of xanthine oxidase. *Free Radic. Biol. Med.* **2010**, *48*, 493–498.
90. Landmesser, U.; Spiekermann, S.; Dikalov, S.; Tatge, H.; Wilke, R.; Kohler, C.; Harrison, D. G.; Hornig, B.; Drexler, H. Vascular oxidative stress and endothelial dysfunction in patients with chronic heart failure: role of xanthine-oxidase and extracellular superoxide dismutase. *Circulation* **2002**, *106*, 3073–3078.
91. White, C. R.; Darley-Usmar, V.; Berrington, W. R.; McAdams, M.; Gore, J. Z.; Thompson, J. A.; Parks, D. A.; Tarpey, M. M.; Freeman, B. A. Circulating plasma xanthine oxidase contributes to vascular dysfunction in hypercholesterolemic rabbits. *Proc. Natl. Acad. Sci. U. S. A.* **1996**, *93*, 8745–8749.
92. Yokoyama, Y.; Beckman, J. S.; Beckman, T. K.; Wheat, J. K.; Cash, T. G.; Freeman, B. A.; Parks, D. A. Circulating xanthine oxidase: potential mediator of ischemic injury. *Am. J. Physiol.* **1990**, *258*, 564–570.
93. Turrens, J. F.; Alexandre, A.; Lehninger, A. L. Ubisemiquinone is the electron donor for superoxide formation by complex III of heart mitochondria. *Arch. Biochem. Biophys.* **1985**, *237*, 408–414.
94. Turrens, J. F.; Boveris, A. Generation of superoxide anion by the NADH dehydrogenase of bovine heart mitochondria. *Biochem. J.* **1980**, *191*, 421–427.
95. Zhang, L.; Yu, L.; Yu, C. A. Generation of superoxide anion by succinate-cytochrome c reductase from bovine heart mitochondria. *J. Biol. Chem.* **1998**, *273*, 33972–33976.
96. Kwong, L. K.; Sohal, R. S. Substrate and site specificity of hydrogen peroxide generation in mouse mitochondria. *Arch. Biochem. Biophys.* **1998**, *350*, 118–126.
97. Forstermann, U.; Munzel, T. Endothelial nitric oxide synthase in vascular disease: from marvel to menace. *Circulation* **2006**, *113*, 1708–1714.

Publication Date (Web): October 13, 2015 | doi: 10.1021/bk-2015-1200.ch004

98. Gautier, C.; Negrerie, M.; Wang, Z. Q.; Lambry, J. C.; Stuehr, D. J.; Collin, F.; Martin, J. L.; Slama-Schwok, A. Dynamic regulation of the inducible nitric-oxide synthase by NO: comparison with the endothelial isoform. *J. Biol. Chem.* **2004**, *279*, 4358–4365.
99. Hurshman, A. R.; Krebs, C.; Edmondson, D. E.; Huynh, B. H.; Marletta, M. A. Formation of a pterin radical in the reaction of the heme domain of inducible nitric oxide synthase with oxygen. *Biochemistry* **1999**, *38*, 15689–15696.
100. Zou, M. H.; Shi, C.; Cohen, R. A. Oxidation of the zinc-thiolate complex and uncoupling of endothelial nitric oxide synthase by peroxynitrite. *J. Clin. Invest.* **2002**, *109*, 817–826.
101. Chen, C. A.; Wang, T. Y.; Varadharaj, S.; Reyes, L. A.; Hemann, C.; Talukder, M. A.; Chen, Y. R.; Druhan, L. J.; Zweier, J. L. S-glutathionylation uncouples eNOS and regulates its cellular and vascular function. *Nature* **2010**, *468*, 1115–1118.
102. Crabtree, M. J.; Brixey, R.; Batchelor, H.; Hale, A. B.; Channon, K. M. Integrated redox sensor and effector functions for tetrahydrobiopterin- and glutathionylation-dependent endothelial nitric-oxide synthase uncoupling. *J. Biol. Chem.* **2013**, *288*, 561–569.
103. Stralin, P.; Karlsson, K.; Johansson, B. O.; Marklund, S. L. The interstitium of the human arterial wall contains very large amounts of extracellular superoxide dismutase. *Arterioscler. Thromb. Vasc. Biol.* **1995**, *15*, 2032–2036.
104. Fukai, T.; Siegfried, M. R.; Ushio-Fukai, M.; Cheng, Y.; Kojda, G.; Harrison, D. G. Regulation of the vascular extracellular superoxide dismutase by nitric oxide and exercise training. *J. Clin. Invest.* **2000**, *105*, 1631–1639.
105. MacMillan-Crow, L. A.; Crow, J. P.; Kerby, J. D.; Beckman, J. S.; Thompson, J. A. Nitration and inactivation of manganese superoxide dismutase in chronic rejection of human renal allografts. *Proc. Natl. Acad. Sci. U. S. A.* **1996**, *93*, 11853–11858.
106. Yamakura, F.; Taka, H.; Fujimura, T.; Murayama, K. Inactivation of human manganese-superoxide dismutase by peroxynitrite is caused by exclusive nitration of tyrosine 34 to 3-nitrotyrosine. *J. Biol. Chem.* **1998**, *273*, 14085–14089.
107. van der Loo, B.; Labugger, R.; Skepper, J. N.; Bachschmid, M.; Kilo, J.; Powell, J. M.; Palacios-Callender, M.; Erusalimsky, J. D.; Quaschning, T.; Malinski, T.; Gygi, D.; Ullrich, V.; Luscher, T. F. Enhanced peroxynitrite formation is associated with vascular aging. *J. Exp. Med.* **2000**, *192*, 1731–1744.
108. Navarro-Antolin, J.; Redondo-Horcajo, M.; Zaragoza, C.; Alvarez-Barrientos, A.; Fernandez, A. P.; Leon-Gomez, E.; Rodrigo, J.; Lamas, S. Role of peroxynitrite in endothelial damage mediated by Cyclosporine A. *Free Radic. Biol. Med.* **2007**, *42*, 394–403.
109. Zhou, L.; Xiang, W.; Potts, J.; Floyd, M.; Sharan, C.; Yang, H.; Ross, J.; Nyanda, A. M.; Guo, Z. Reduction in extracellular superoxide dismutase

Publication Date (Web): October 13, 2015 | doi: 10.1021/bk-2015-1200.ch004

activity in African-American patients with hypertension. *Free Radic. Biol. Med.* **2006**, *41*, 1384–1391.
110. Kissner, R.; Nauser, T.; Bugnon, P.; Lye, P. G.; Koppenol, W. H. Formation and properties of peroxynitrite as studied by laser flash photolysis, high-pressure stopped-flow technique, and pulse radiolysis. *Chem. Res. Toxicol.* **1997**, *10*, 1285–1292.
111. Radi, R.; Beckman, J. S.; Bush, K. M.; Freeman, B. A. Peroxynitrite-induced membrane lipid peroxidation: the cytotoxic potential of superoxide and nitric oxide. *Arch. Biochem. Biophys.* **1991**, *288*, 481–487.
112. Denicola, A.; Freeman, B. A.; Trujillo, M.; Radi, R. Peroxynitrite reaction with carbon dioxide/bicarbonate: kinetics and influence on peroxynitrite-mediated oxidations. *Arch. Biochem. Biophys.* **1996**, *333*, 49–58.
113. Radi, R.; Peluffo, G.; Alvarez, M. N.; Naviliat, M.; Cayota, A. Unraveling peroxynitrite formation in biological systems. *Free Radic. Biol. Med.* **2001**, *30*, 463–488.
114. Denicola, A.; Souza, J. M.; Radi, R. Diffusion of peroxynitrite across erythrocyte membranes. *Proc. Natl. Acad. Sci. U. S. A.* **1998**, *95*, 3566–3571.
115. Romero, N.; Denicola, A.; Souza, J. M.; Radi, R. Diffusion of peroxynitrite in the presence of carbon dioxide. *Arch. Biochem. Biophys.* **1999**, *368*, 23–30.
116. Hamilton, R. T.; Asatryan, L.; Nilsen, J. T.; Isas, J. M.; Gallaher, T. K.; Sawamura, T.; Hsiai, T. K. LDL protein nitration: implication for LDL protein unfolding. *Arch. Biochem. Biophys.* **2008**, *479*, 1–14.
117. Alvarez, B.; Radi, R. Peroxynitrite reactivity with amino acids and proteins. *Amino Acids* **2003**, *25*, 295–311.
118. Trujillo, M.; Ferrer-Sueta, G.; Thomson, L.; Flohe, L.; Radi, R. Kinetics of peroxiredoxins and their role in the decomposition of peroxynitrite. *Subcell. Biochem.* **2007**, *44*, 83–113.
119. Evangelista, A. M.; Thompson, M. D.; Weisbrod, R. M.; Pimental, D. R.; Tong, X.; Bolotina, V. M.; Cohen, R. A. Redox regulation of SERCA2 is required for vascular endothelial growth factor-induced signaling and endothelial cell migration. *Antioxid. Redox Signal.* **2012**, *17*, 1099–1108.
120. Peluffo, G.; Radi, R. Biochemistry of protein tyrosine nitration in cardiovascular pathology. *Cardiovasc. Res.* **2007**, *75*, 291–302.
121. Radi, R. Protein tyrosine nitration: biochemical mechanisms and structural basis of functional effects. *Acc. Chem. Res.* **2013**, *46*, 550–559.
122. Alvarez, B.; Ferrer-Sueta, G.; Freeman, B. A.; Radi, R. Kinetics of peroxynitrite reaction with amino acids and human serum albumin. *J. Biol. Chem.* **1999**, *274*, 842–848.
123. Prutz, W. A.; Monig, H.; Butler, J.; Land, E. J. Reactions of nitrogen dioxide in aqueous model systems: oxidation of tyrosine units in peptides and proteins. *Arch. Biochem. Biophys.* **1985**, *243*, 125–134.
124. Bartesaghi, S.; Ferrer-Sueta, G.; Peluffo, G.; Valez, V.; Zhang, H.; Kalyanaraman, B.; Radi, R. Protein tyrosine nitration in hydrophilic and hydrophobic environments. *Amino Acids* **2007**, *32*, 501–515.

Publication Date (Web): October 13, 2015 | doi: 10.1021/bk-2015-1200.ch004

125. Bartesaghi, S.; Wenzel, J.; Trujillo, M.; Lopez, M.; Joseph, J.; Kalyanaraman, B.; Radi, R. Lipid peroxyl radicals mediate tyrosine dimerization and nitration in membranes. *Chem. Res. Toxicol.* **2010**, *23*, 821–835.
126. Folkes, L. K.; Bartesaghi, S.; Trujillo, M.; Radi, R.; Wardman, P. Kinetics of oxidation of tyrosine by a model alkoxyl radical. *Free Radic. Res.* **2012**, *46*, 1150–1156.
127. Shao, B.; Bergt, C.; Fu, X.; Green, P.; Voss, J. C.; Oda, M. N.; Oram, J. F.; Heinecke, J. W. Tyrosine 192 in apolipoprotein A-I is the major site of nitration and chlorination by myeloperoxidase, but only chlorination markedly impairs ABCA1-dependent cholesterol transport. *J. Biol. Chem.* **2005**, *280*, 5983–5993.
128. Yamaguchi, Y.; Haginaka, J.; Morimoto, S.; Fujioka, Y.; Kunitomo, M. Facilitated nitration and oxidation of LDL in cigarette smokers. *Eur. J. Clin. Invest.* **2005**, *35*, 186–193.
129. Hazen, S. L.; Zhang, R.; Shen, Z.; Wu, W.; Podrez, E. A.; MacPherson, J. C.; Schmitt, D.; Mitra, S. N.; Mukhopadhyay, C.; Chen, Y.; Cohen, P. A.; Hoff, H. F.; Abu-Soud, H. M. Formation of nitric oxide-derived oxidants by myeloperoxidase in monocytes: pathways for monocyte-mediated protein nitration and lipid peroxidation In vivo. *Circ. Res.* **1999**, *85*, 950–958.
130. Khan, F.; Siddiqui, A. A. Prevalence of anti-3-nitrotyrosine antibodies in the joint synovial fluid of patients with rheumatoid arthritis, osteoarthritis and systemic lupus erythematosus. *Clin. Chim. Acta* **2006**, *370*, 100–107.
131. Thomson, L.; Tenopoulou, M.; Lightfoot, R.; Tsika, E.; Parastatidis, I.; Martinez, M.; Greco, T. M.; Doulias, P. T.; Wu, Y.; Tang, W. H.; Hazen, S. L.; Ischiropoulos, H. Immunoglobulins against tyrosine-nitrated epitopes in coronary artery disease. *Circulation* **2012**, *126*, 2392–2401.
132. Predescu, D.; Predescu, S.; Malik, A. B. Transport of nitrated albumin across continuous vascular endothelium. *Proc. Natl. Acad. Sci. U. S. A.* **2002**, *99*, 13932–13937.
133. Rudnicka, A. R.; Mt-Isa, S.; Meade, T. W. Associations of plasma fibrinogen and factor VII clotting activity with coronary heart disease and stroke: prospective cohort study from the screening phase of the Thrombosis Prevention Trial. *J. Thromb. Haemost.* **2006**, *4*, 2405–2410.
134. Koh, K. K.; Son, J. W.; Ahn, J. Y.; Jin, D. K.; Kim, H. S.; Choi, Y. M.; Ahn, T. H.; Kim, D. S.; Shin, E. K. Vascular effects of diet and statin in hypercholesterolemic patients. *Int. J. Cardiol.* **2004**, *95*, 185–191.
135. Kotur-Stevuljevic, J.; Memon, L.; Stefanovic, A.; Spasic, S.; Spasojevic-Kalimanovska, V.; Bogavac-Stanojevic, N.; Kalimanovska-Ostric, D.; Jelic-Ivanovic, Z.; Zunic, G. Correlation of oxidative stress parameters and inflammatory markers in coronary artery disease patients. *Clin. Biochem.* **2007**, *40*, 181–187.
136. Vadseth, C.; Souza, J. M.; Thomson, L.; Seagraves, A.; Nagaswami, C.; Scheiner, T.; Torbet, J.; Vilaire, G.; Bennett, J. S.; Murciano, J. C.; Muzykantov, V.; Penn, M. S.; Hazen, S. L.; Weisel, J. W.; Ischiropoulos, H. Pro-thrombotic state induced by post-translational modification of fibrinogen by reactive nitrogen species. *J. Biol. Chem.* **2004**, *279*, 8820–8826.

Publication Date (Web): October 13, 2015 | doi: 10.1021/bk-2015-1200.ch004

137. Pignatelli, B.; Li, C. Q.; Boffetta, P.; Chen, Q.; Ahrens, W.; Nyberg, F.; Mukeria, A.; Bruske-Hohlfeld, I.; Fortes, C.; Constantinescu, V.; Ischiropoulos, H.; Ohshima, H. Nitrated and oxidized plasma proteins in smokers and lung cancer patients. *Cancer Res.* **2001**, *61*, 778–784.
138. Nowak, P.; Kolodziejczyk, J.; Wachowicz, B. Peroxynitrite and fibrinolytic system: the effect of peroxynitrite on plasmin activity. *Mol. Cell. Biochem.* **2004**, *267*, 141–146.
139. Beckmann, J. S.; Ye, Y. Z.; Anderson, P. G.; Chen, J.; Accavitti, M. A.; Tarpey, M. M.; White, C. R. Extensive nitration of protein tyrosines in human atherosclerosis detected by immunohistochemistry. *Biol. Chem. Hoppe-Seyler* **1994**, *375*, 81–88.
140. Nicholls, S. J.; Zheng, L.; Hazen, S. L. Formation of dysfunctional high-density lipoprotein by myeloperoxidase. *Trends Cardiovasc. Med.* **2005**, *15*, 212–219.
141. Zheng, L.; Nukuna, B.; Brennan, M. L.; Sun, M.; Goormastic, M.; Settle, M.; Schmitt, D.; Fu, X.; Thomson, L.; Fox, P. L.; Ischiropoulos, H.; Smith, J. D.; Kinter, M.; Hazen, S. L. Apolipoprotein A-I is a selective target for myeloperoxidase-catalyzed oxidation and functional impairment in subjects with cardiovascular disease. *J. Clin. Invest.* **2004**, *114*, 529–541.
142. Pennathur, S.; Bergt, C.; Shao, B.; Byun, J.; Kassim, S. Y.; Singh, P.; Green, P. S.; McDonald, T. O.; Brunzell, J.; Chait, A.; Oram, J. F.; O'Brien, K.; Geary, R. L.; Heinecke, J. W. Human atherosclerotic intima and blood of patients with established coronary artery disease contain high density lipoprotein damaged by reactive nitrogen species. *J. Biol. Chem.* **2004**, *279*, 42977–42983.
143. DiDonato, J. A.; Aulak, K.; Huang, Y.; Wagner, M.; Gerstenecker, G.; Topbas, C.; Gogonea, V.; DiDonato, A. J.; Tang, W. H.; Mehl, R. A.; Fox, P. L.; Plow, E. F.; Smith, J. D.; Fisher, E. A.; Hazen, S. L. Site-specific nitration of apolipoprotein A-I at tyrosine 166 is both abundant within human atherosclerotic plaque and dysfunctional. *J. Biol. Chem.* **2014**, *289*, 10276–10292.
144. Zheng, L.; Settle, M.; Brubaker, G.; Schmitt, D.; Hazen, S. L.; Smith, J. D.; Kinter, M. Localization of nitration and chlorination sites on apolipoprotein A-I catalyzed by myeloperoxidase in human atheroma and associated oxidative impairment in ABCA1-dependent cholesterol efflux from macrophages. *J. Biol. Chem.* **2005**, *280*, 38–47.
145. Pueyo, M. E.; Arnal, J. F.; Rami, J.; Michel, J. B. Angiotensin II stimulates the production of NO and peroxynitrite in endothelial cells. *Am. J. Physiol.* **1998**, *274*, C214–220.
146. Touyz, R. M.; Schiffrin, E. L. Ang II-stimulated superoxide production is mediated via phospholipase D in human vascular smooth muscle cells. *Hypertension* **1999**, *34*, 976–982.
147. Guzik, T. J.; Harrison, D. G. Vascular NADPH oxidases as drug targets for novel antioxidant strategies. *Drug Discov. Today* **2006**, *11*, 524–533.
148. Widlansky, M. E.; Gokce, N.; Keaney, J. F., Jr.; Vita, J. A. The clinical implications of endothelial dysfunction. *J. Am. Coll. Cardiol.* **2003**, *42*, 1149–1160.

In Oxidative Stress: Diagnostics, Prevention, and Therapy Volume 2; Hepel, et al.;
ACS Symposium Series; American Chemical Society: Washington, DC, 2015.

149. Leeuwenburgh, C.; Hardy, M. M.; Hazen, S. L.; Wagner, P.; Oh-ishi, S.; Steinbrecher, U. P.; Heinecke, J. W. Reactive nitrogen intermediates promote low density lipoprotein oxidation in human atherosclerotic intima. *J. Biol. Chem.* **1997**, *272*, 1433–1436.
150. Smythe, C. D.; Skinner, V. O.; Bruckdorfer, K. R.; Haskard, D. O.; Landis, R. C. The state of macrophage differentiation determines the TNF alpha response to nitrated lipoprotein uptake. *Atherosclerosis* **2003**, *170*, 213–221.
151. Graham, A.; Hogg, N.; Kalyanaraman, B.; O'Leary, V.; Darley-Usmar, V.; Moncada, S. Peroxynitrite modification of low-density lipoprotein leads to recognition by the macrophage scavenger receptor. *FEBS Lett.* **1993**, *330*, 181–185.
152. Upmacis, R. K.; Deeb, R. S.; Hajjar, D. P. Oxidative alterations of cyclooxygenase during atherogenesis. *Prostaglandins Other Lipid Mediators* **2006**, *80*, 1–14.
153. Vane, J. R.; Anggard, E. E.; Botting, R. M. Regulatory functions of the vascular endothelium. *N. Engl. J. Med.* **1990**, *323*, 27–36.
154. Bachschmid, M.; Schildknecht, S.; Ullrich, V. Redox regulation of vascular prostanoid synthesis by the nitric oxide-superoxide system. *Biochem. Biophys. Res. Commun.* **2005**, *338*, 536–542.
155. Frein, D.; Schildknecht, S.; Bachschmid, M.; Ullrich, V. Redox regulation: a new challenge for pharmacology. *Biochem. Pharmacol.* **2005**, *70*, 811–823.
156. Trostchansky, A.; O'Donnell, V. B.; Goodwin, D. C.; Landino, L. M.; Marnett, L. J.; Radi, R.; Rubbo, H. Interactions between nitric oxide and peroxynitrite during prostaglandin endoperoxide H synthase-1 catalysis: a free radical mechanism of inactivation. *Free Radic. Biol. Med.* **2007**, *42*, 1029–1038.
157. Shimokawa, T.; Kulmacz, R. J.; DeWitt, D. L.; Smith, W. L. Tyrosine 385 of prostaglandin endoperoxide synthase is required for cyclooxygenase catalysis. *J. Biol. Chem.* **1990**, *265*, 20073–20076.
158. Deeb, R. S.; Resnick, M. J.; Mittar, D.; McCaffrey, T.; Hajjar, D. P.; Upmacis, R. K. Tyrosine nitration in prostaglandin H(2) synthase. *J. Lipid Res.* **2002**, *43*, 1718–1726.
159. Zou, M.; Jendral, M.; Ullrich, V. Prostaglandin endoperoxide-dependent vasospasm in bovine coronary arteries after nitration of prostacyclin synthase. *Br. J. Pharmacol.* **1999**, *126*, 1283–1292.
160. Schmidt, P.; Youhnovski, N.; Daiber, A.; Balan, A.; Arsic, M.; Bachschmid, M.; Przybylski, M.; Ullrich, V. Specific nitration at tyrosine 430 revealed by high resolution mass spectrometry as basis for redox regulation of bovine prostacyclin synthase. *J. Biol. Chem.* **2003**, *278*, 12813–12819.
161. Zou, M. H.; Daiber, A.; Peterson, J. A.; Shoun, H.; Ullrich, V. Rapid reactions of peroxynitrite with heme-thiolate proteins as the basis for protection of prostacyclin synthase from inactivation by nitration. *Arch. Biochem. Biophys.* **2000**, *376*, 149–155.
162. Chuang, C. Y.; Degendorfer, G.; Hammer, A.; Whitelock, J. M.; Malle, E.; Davies, M. J. Oxidation modifies the structure and function of the

Publication Date (Web): October 13, 2015 | doi: 10.1021/bk-2015-1200.ch004

extracellular matrix generated by human coronary artery endothelial cells. *Biochem. J.* **2014**, *459*, 313–322.
163. Kennett, E. C.; Rees, M. D.; Malle, E.; Hammer, A.; Whitelock, J. M.; Davies, M. J. Peroxynitrite modifies the structure and function of the extracellular matrix proteoglycan perlecan by reaction with both the protein core and the heparan sulfate chains. *Free Radic. Biol. Med.* **2010**, *49*, 282–293.
164. Kooy, N. W.; Lewis, S. J.; Royall, J. A.; Ye, Y. Z.; Kelly, D. R.; Beckman, J. S. Extensive tyrosine nitration in human myocardial inflammation: evidence for the presence of peroxynitrite. *Crit. Care Med.* **1997**, *25*, 812–819.
165. Weinstein, D. M.; Mihm, M. J.; Bauer, J. A. Cardiac peroxynitrite formation and left ventricular dysfunction following doxorubicin treatment in mice. *J. Pharmacol. Exp. Ther.* **2000**, *294*, 396–401.
166. Neubauer, S.; Remkes, H.; Spindler, M.; Horn, M.; Wiesmann, F.; Prestle, J.; Walzel, B.; Ertl, G.; Hasenfuss, G.; Wallimann, T. Downregulation of the Na(+)-creatine cotransporter in failing human myocardium and in experimental heart failure. *Circulation* **1999**, *100*, 1847–1850.
167. Nakae, I.; Mitsunami, K.; Omura, T.; Yabe, T.; Tsutamoto, T.; Matsuo, S.; Takahashi, M.; Morikawa, S.; Inubushi, T.; Nakamura, Y.; Kinoshita, M.; Horie, M. Proton magnetic resonance spectroscopy can detect creatine depletion associated with the progression of heart failure in cardiomyopathy. *J. Am. Coll. Cardiol.* **2003**, *42*, 1587–1593.
168. Neubauer, S.; Horn, M.; Cramer, M.; Harre, K.; Newell, J. B.; Peters, W.; Pabst, T.; Ertl, G.; Hahn, D.; Ingwall, J. S.; Kochsiek, K. Myocardial phosphocreatine-to-ATP ratio is a predictor of mortality in patients with dilated cardiomyopathy. *Circulation* **1997**, *96*, 2190–2196.
169. Hamman, B. L.; Bittl, J. A.; Jacobus, W. E.; Allen, P. D.; Spencer, R. S.; Tian, R.; Ingwall, J. S. Inhibition of the creatine kinase reaction decreases the contractile reserve of isolated rat hearts. *Am. J. Physiol.* **1995**, *269*, H1030–1036.
170. Zweier, J. L.; Jacobus, W. E.; Korecky, B.; Brandejs-Barry, Y. Bioenergetic consequences of cardiac phosphocreatine depletion induced by creatine analogue feeding. *J. Biol. Chem.* **1991**, *266*, 20296–20304.
171. Saupe, K. W.; Spindler, M.; Tian, R.; Ingwall, J. S. Impaired cardiac energetics in mice lacking muscle-specific isoenzymes of creatine kinase. *Circ. Res.* **1998**, *82*, 898–907.
172. Mihm, M. J.; Coyle, C. M.; Schanbacher, B. L.; Weinstein, D. M.; Bauer, J. A. Peroxynitrite induced nitration and inactivation of myofibrillar creatine kinase in experimental heart failure. *Cardiovasc. Res.* **2001**, *49*, 798–807.
173. Stachowiak, O.; Dolder, M.; Wallimann, T.; Richter, C. Mitochondrial creatine kinase is a prime target of peroxynitrite-induced modification and inactivation. *J. Biol. Chem.* **1998**, *273*, 16694–16699.
174. Borbely, A.; Toth, A.; Edes, I.; Virag, L.; Papp, J. G.; Varro, A.; Paulus, W. J.; van der Velden, J.; Stienen, G. J.; Papp, Z. Peroxynitrite-induced alpha-actinin nitration and contractile alterations in isolated human myocardial cells. *Cardiovasc. Res.* **2005**, *67*, 225–233.

Publication Date (Web): October 13, 2015 | doi: 10.1021/bk-2015-1200.ch004

175. Periasamy, M.; Huke, S. SERCA pump level is a critical determinant of Ca(2+)homeostasis and cardiac contractility. *J. Mol. Cell. Cardiol.* **2001**, *33*, 1053–1063.
176. Viner, R. I.; Huhmer, A. F.; Bigelow, D. J.; Schoneich, C. The oxidative inactivation of sarcoplasmic reticulum Ca(2+)-ATPase by peroxynitrite. *Free Radic. Res.* **1996**, *24*, 243–259.
177. Viner, R. I.; Ferrington, D. A.; Williams, T. D.; Bigelow, D. J.; Schoneich, C. Protein modification during biological aging: selective tyrosine nitration of the SERCA2a isoform of the sarcoplasmic reticulum Ca2+-ATPase in skeletal muscle. *Biochem. J.* **1999**, *340* (Pt 3), 657–669.
178. Adachi, T.; Matsui, R.; Xu, S.; Kirber, M.; Lazar, H. L.; Sharov, V. S.; Schoneich, C.; Cohen, R. A. Antioxidant improves smooth muscle sarco/endoplasmic reticulum Ca(2+)-ATPase function and lowers tyrosine nitration in hypercholesterolemia and improves nitric oxide-induced relaxation. *Circ. Res.* **2002**, *90*, 1114–1121.
179. Lokuta, A. J.; Maertz, N. A.; Meethal, S. V.; Potter, K. T.; Kamp, T. J.; Valdivia, H. H.; Haworth, R. A. Increased nitration of sarcoplasmic reticulum Ca2+-ATPase in human heart failure. *Circulation* **2005**, *111*, 988–995.
180. Knyushko, T. V.; Sharov, V. S.; Williams, T. D.; Schoneich, C.; Bigelow, D. J. 3-Nitrotyrosine modification of SERCA2a in the aging heart: a distinct signature of the cellular redox environment. *Biochemistry* **2005**, *44*, 13071–13081.
181. Irie, Y.; Saeki, M.; Kamisaki, Y.; Martin, E.; Murad, F. Histone H1.2 is a substrate for denitrase, an activity that reduces nitrotyrosine immunoreactivity in proteins. *Proc. Natl. Acad. Sci. U. S. A.* **2003**, *100*, 5634–5639.
182. Kamisaki, Y.; Wada, K.; Bian, K.; Balabanli, B.; Davis, K.; Martin, E.; Behbod, F.; Lee, Y. C.; Murad, F. An activity in rat tissues that modifies nitrotyrosine-containing proteins. *Proc. Natl. Acad. Sci. U. S. A.* **1998**, *95*, 11584–11589.
183. Souza, J. M.; Choi, I.; Chen, Q.; Weisse, M.; Daikhin, E.; Yudkoff, M.; Obin, M.; Ara, J.; Horwitz, J.; Ischiropoulos, H. Proteolytic degradation of tyrosine nitrated proteins. *Arch. Biochem. Biophys.* **2000**, *380*, 360–366.
184. Ding, Y.; Luo, Y.; Fu, J. Effects of Mn (II) on peroxynitrite nitrifying fibrinogen. *Biomed. Mater. Eng.* **2014**, *24*, 901–907.
185. Aslan, M.; Dogan, S. Proteomic detection of nitroproteins as potential biomarkers for cardiovascular disease. *J. Proteomics* **2011**, *74*, 2274–2288.
186. Lu, N.; Xie, S.; Li, J.; Tian, R.; Peng, Y. Y. Myeloperoxidase-mediated oxidation targets serum apolipoprotein A-I in diabetic patients and represents a potential mechanism leading to impaired anti-apoptotic activity of high density lipoprotein. *Clin. Chim. Acta* **2015**, *441C*, 163–170.
187. Goodwin, D. C.; Gunther, M. R.; Hsi, L. C.; Crews, B. C.; Eling, T. E.; Mason, R. P.; Marnett, L. J. Nitric oxide trapping of tyrosyl radicals generated during prostaglandin endoperoxide synthase turnover. Detection of the radical derivative of tyrosine 385. *J. Biol. Chem.* **1998**, *273*, 8903–8909.

Publication Date (Web): October 13, 2015 | doi: 10.1021/bk-2015-1200.ch004

188. Deeb, R. S.; Shen, H.; Gamss, C.; Gavrilova, T.; Summers, B. D.; Kraemer, R.; Hao, G.; Gross, S. S.; Laine, M.; Maeda, N.; Hajjar, D. P.; Upmacis, R. K. Inducible nitric oxide synthase mediates prostaglandin h2 synthase nitration and suppresses eicosanoid production. *Am J. Pathol.* **2006**, *168*, 349–362.
189. Mihm, M. J.; Yu, F.; Carnes, C. A.; Reiser, P. J.; McCarthy, P. M.; Van Wagoner, D. R.; Bauer, J. A. Impaired myofibrillar energetics and oxidative injury during human atrial fibrillation. *Circulation* **2001**, *104*, 174–180.
190. Ignarro, L. J.; Balestrieri, M. L.; Napoli, C. Nutrition, physical activity, and cardiovascular disease: an update. *Cardiovasc. Res.* **2007**, *73*, 326–340.
191. Calcerrada, P.; Peluffo, G.; Radi, R. Nitric oxide-derived oxidants with a focus on peroxynitrite: molecular targets, cellular responses and therapeutic implications. *Curr. Pharm. Des.* **2011**, *17*, 3905–3932.
192. Fukai, T.; Folz, R. J.; Landmesser, U.; Harrison, D. G. Extracellular superoxide dismutase and cardiovascular disease. *Cardiovasc. Res.* **2002**, *55*, 239–249.
193. Hink, H. U.; Fukai, T. Extracellular superoxide dismutase, uric acid, and atherosclerosis. *Cold Spring Harbor Symp. Quant. Biol.* **2002**, *67*, 483–490.
194. Ohta, H.; Adachi, T.; Hirano, K. Internalization of human extracellular-superoxide dismutase by bovine aortic endothelial cells. *Free Radic. Biol. Med.* **1994**, *16*, 501–507.
195. Oury, T. D.; Day, B. J.; Crapo, J. D. Extracellular superoxide dismutase: a regulator of nitric oxide bioavailability. *Lab Invest.* **1996**, *75*, 617–636.
196. Rhee, S. G. Cell signaling. H2O2, a necessary evil for cell signaling. *Science* **2006**, *312*, 1882–1883.
197. Oshikawa, J.; Urao, N.; Kim, H. W.; Kaplan, N.; Razvi, M.; McKinney, R.; Poole, L. B.; Fukai, T.; Ushio-Fukai, M. Extracellular SOD-derived H2O2 promotes VEGF signaling in caveolae/lipid rafts and post-ischemic angiogenesis in mice. *PLoS One* **2010**, *5*, e10189.
198. Kim, H. W.; Lin, A.; Guldberg, R. E.; Ushio-Fukai, M.; Fukai, T. Essential role of extracellular SOD in reparative neovascularization induced by hindlimb ischemia. *Circ. Res.* **2007**, *101*, 409–419.
199. Laurila, J. P.; Laatikainen, L. E.; Castellone, M. D.; Laukkanen, M. O. SOD3 reduces inflammatory cell migration by regulating adhesion molecule and cytokine expression. *PLoS One* **2009**, *4*, e5786.
200. Abrahamsson, T.; Brandt, U.; Marklund, S. L.; Sjoqvist, P. O. Vascular bound recombinant extracellular superoxide dismutase type C protects against the detrimental effects of superoxide radicals on endothelium-dependent arterial relaxation. *Circ. Res.* **1992**, *70*, 264–271.
201. Chu, Y.; Iida, S.; Lund, D. D.; Weiss, R. M.; DiBona, G. F.; Watanabe, Y.; Faraci, F. M.; Heistad, D. D. Gene transfer of extracellular superoxide dismutase reduces arterial pressure in spontaneously hypertensive rats: role of heparin-binding domain. *Circ. Res.* **2003**, *92*, 461–468.
202. Wang, W.; Yan, X.; Han, L. The clinical meaning and determination of the superoxid dismutase activity and malondialehyde content in the serum of the patients suffering from chronic tonsillitis. *Lin Chuang Er Bi Yan Hou Ke Za Zhi* **1998**, *12*, 156–157.

Publication Date (Web): October 13, 2015 | doi: 10.1021/bk-2015-1200.ch004

203. Luoma, J. S.; Stralin, P.; Marklund, S. L.; Hiltunen, T. P.; Sarkioja, T.; Yla-Herttuala, S. Expression of extracellular SOD and iNOS in macrophages and smooth muscle cells in human and rabbit atherosclerotic lesions: colocalization with epitopes characteristic of oxidized LDL and peroxynitrite-modified proteins. *Arterioscler. Thromb. Vasc. Biol.* **1998**, *18*, 157–167.
204. Adachi, T.; Wang, X. L. Association of extracellular-superoxide dismutase phenotype with the endothelial constitutive nitric oxide synthase polymorphism. *FEBS Lett.* **1998**, *433*, 166–168.
205. Leite, P. F.; Liberman, M.; Sandoli de Brito, F.; Laurindo, F. R. Redox processes underlying the vascular repair reaction. *World J. Surg.* **2004**, *28*, 331–336.
206. Trujillo, M.; Ferrer-Sueta, G.; Radi, R. Kinetic studies on peroxynitrite reduction by peroxiredoxins. *Methods Enzymol.* **2008**, *441*, 173–196.
207. Hofmann, B.; Hecht, H. J.; Flohe, L. Peroxiredoxins. *Biol. Chem.* **2002**, *383*, 347–364.
208. Rhee, S. G.; Chae, H. Z.; Kim, K. Peroxiredoxins: a historical overview and speculative preview of novel mechanisms and emerging concepts in cell signaling. *Free Radic. Biol. Med.* **2005**, *38*, 1543–1552.
209. Zvetina, J. R.; Nathan, N.; Facen, H. Pulmonary tuberculosis following successful treatment of pulmonary infection with Mycobacterium kansasii. *Chest* **1976**, *70*, 786–788.
210. Bryk, R.; Griffin, P.; Nathan, C. Peroxynitrite reductase activity of bacterial peroxiredoxins. *Nature* **2000**, *407*, 211–215.
211. Ferrer-Sueta, G.; Radi, R. Chemical biology of peroxynitrite: kinetics, diffusion, and radicals. *ACS Chem. Biol.* **2009**, *4*, 161–177.
212. Manta, B.; Hugo, M.; Ortiz, C.; Ferrer-Sueta, G.; Trujillo, M.; Denicola, A. The peroxidase and peroxynitrite reductase activity of human erythrocyte peroxiredoxin 2. *Arch. Biochem. Biophys.* **2009**, *484*, 146–154.
213. Moore, R. B.; Mankad, M. V.; Shriver, S. K.; Mankad, V. N.; Plishker, G. A. Reconstitution of Ca(2+)-dependent K+ transport in erythrocyte membrane vesicles requires a cytoplasmic protein. *J. Biol. Chem.* **1991**, *266*, 18964–18968.
214. Wood, Z. A.; Schroder, E.; Robin Harris, J.; Poole, L. B. Structure, mechanism and regulation of peroxiredoxins. *Trends Biochem. Sci.* **2003**, *28*, 32–40.
215. Fiuza, B.; Subelzu, N.; Calcerrada, P.; Straliotto, M. R.; Piacenza, L.; Cassina, A.; Rocha, J. B.; Radi, R.; de Bem, A. F.; Peluffo, G. Impact of SIN-1-derived peroxynitrite flux on endothelial cell redox homeostasis and bioenergetics: protective role of diphenyl diselenide via induction of peroxiredoxins. *Free Radic. Res.* **2015**, *49*, 122–132.
216. Romero, N.; Radi, R. Hemoglobin and red blood cells as tools for studying peroxynitrite biochemistry. *Methods Enzymol.* **2005**, *396*, 229–245.
217. Romero, N.; Radi, R.; Linares, E.; Augusto, O.; Detweiler, C. D.; Mason, R. P.; Denicola, A. Reaction of human hemoglobin with peroxynitrite. Isomerization to nitrate and secondary formation of protein radicals. *J. Biol. Chem.* **2003**, *278*, 44049–44057.

Publication Date (Web): October 13, 2015 | doi: 10.1021/bk-2015-1200.ch004

218. Chen, H. J.; Chen, Y. C. Reactive nitrogen oxide species-induced post-translational modifications in human hemoglobin and the association with cigarette smoking. *Anal. Chem.* **2012**, *84*, 7881–7890.
219. Heijnen, H. F.; van Donselaar, E.; Slot, J. W.; Fries, D. M.; Blachard-Fillion, B.; Hodara, R.; Lightfoot, R.; Polydoro, M.; Spielberg, D.; Thomson, L.; Regan, E. A.; Crapo, J.; Ischiropoulos, H. Subcellular localization of tyrosine-nitrated proteins is dictated by reactive oxygen species generating enzymes and by proximity to nitric oxide synthase. *Free Radic. Biol. Med.* **2006**, *40*, 1903–1913.
220. Ferrer-Sueta, G.; Hannibal, L.; Batinic-Haberle, I.; Radi, R. Reduction of manganese porphyrins by flavoenzymes and submitochondrial particles: a catalytic cycle for the reduction of peroxynitrite. *Free Radic. Biol. Med.* **2006**, *41*, 503–512.
221. Trujillo, M.; Ferrer-Sueta, G.; Radi, R. Peroxynitrite detoxification and its biologic implications. *Antioxid. Redox Signal.* **2008**, *10*, 1607–1620.
222. Trostchansky, A.; Ferrer-Sueta, G.; Batthyany, C.; Botti, H.; Batinic-Haberle, I.; Radi, R.; Rubbo, H. Peroxynitrite flux-mediated LDL oxidation is inhibited by manganese porphyrins in the presence of uric acid. *Free Radic. Biol. Med.* **2003**, *35*, 1293–1300.
223. Batinic-Haberle, I.; Reboucas, J. S.; Spasojevic, I. Superoxide dismutase mimics: chemistry, pharmacology, and therapeutic potential. *Antioxid. Redox Signal.* **2010**, *13*, 877–918.
224. Arteel, G. E.; Schroeder, P.; Sies, H. Reactions of peroxynitrite with cocoa procyanidin oligomers. *J. Nutr.* **2000**, *130*, 2100S–2104S.
225. Ferrer-Sueta, G.; Vitturi, D.; Batinic-Haberle, I.; Fridovich, I.; Goldstein, S.; Czapski, G.; Radi, R. Reactions of manganese porphyrins with peroxynitrite and carbonate radical anion. *J. Biol. Chem.* **2003**, *278*, 27432–27438.
226. Batinic-Haberle, I.; Cuzzocrea, S.; Reboucas, J. S.; Ferrer-Sueta, G.; Mazzon, E.; Di Paola, R.; Radi, R.; Spasojevic, I.; Benov, L.; Salvemini, D. Pure MnTBAP selectively scavenges peroxynitrite over superoxide: comparison of pure and commercial MnTBAP samples to MnTE-2-PyP in two models of oxidative stress injury, an SOD-specific Escherichia coli model and carrageenan-induced pleurisy. *Free Radic. Biol. Med.* **2009**, *46*, 192–201.
227. Valez, V.; Cassina, A.; Batinic-Haberle, I.; Kalyanaraman, B.; Ferrer-Sueta, G.; Radi, R. Peroxynitrite formation in nitric oxide-exposed submitochondrial particles: detection, oxidative damage and catalytic removal by Mn-porphyrins. *Arch. Biochem. Biophys.* **2013**, *529*, 45–54.
228. Radi, R.; Cassina, A.; Hodara, R.; Quijano, C.; Castro, L. Peroxynitrite reactions and formation in mitochondria. *Free Radic. Biol. Med.* **2002**, *33*, 1451–1464.
229. Castro, L.; Rodriguez, M.; Radi, R. Aconitase is readily inactivated by peroxynitrite, but not by its precursor, nitric oxide. *J. Biol. Chem.* **1994**, *269*, 29409–29415.
230. Radi, R.; Rodriguez, M.; Castro, L.; Telleri, R. Inhibition of mitochondrial electron transport by peroxynitrite. *Arch. Biochem. Biophys.* **1994**, *308*, 89–95.

Publication Date (Web): October 13, 2015 | doi: 10.1021/bk-2015-1200.ch004

231. Radi, R. Peroxynitrite, a stealthy biological oxidant. *J. Biol. Chem.* **2013**, *288*, 26464–26472.
232. Sies, H.; Sharov, V. S.; Klotz, L. O.; Briviba, K. Glutathione peroxidase protects against peroxynitrite-mediated oxidations. A new function for selenoproteins as peroxynitrite reductase. *J. Biol. Chem.* **1997**, *272*, 27812–27817.
233. Briviba, K.; Kissner, R.; Koppenol, W. H.; Sies, H. Kinetic study of the reaction of glutathione peroxidase with peroxynitrite. *Chem. Res. Toxicol.* **1998**, *11*, 1398–1401.
234. Nogueira, C. W.; Rocha, J. B. Toxicology and pharmacology of selenium: emphasis on synthetic organoselenium compounds. *Arch. Toxicol.* **2011**, *85*, 1313–1359.
235. Masumoto, H.; Kissner, R.; Koppenol, W. H.; Sies, H. Kinetic study of the reaction of ebselen with peroxynitrite. *FEBS Lett.* **1996**, *398*, 179–182.
236. Masumoto, H.; Sies, H. The reaction of ebselen with peroxynitrite. *Chem. Res. Toxicol.* **1996**, *9*, 262–267.
237. Chen, C.; Zhao, J.; Zhang, P.; Chai, Z. Speciation and subcellular location of se-containing proteins in human liver studied by sodium dodecyl sulfate-polyacrylamide gel electrophoresis and hydride generation-atomic fluorescence spectrometric detection. *Anal. Bioanal. Chem.* **2002**, *372*, 426–430.
238. Bhabak, K. P.; Vernekar, A. A.; Jakka, S. R.; Roy, G.; Mugesh, G. Mechanistic investigations on the efficient catalytic decomposition of peroxynitrite by ebselen analogues. *Org. Biomol. Chem.* **2011**, *9*, 5193–5200.
239. Brodsky, S. V.; Gealekman, O.; Chen, J.; Zhang, F.; Togashi, N.; Crabtree, M.; Gross, S. S.; Nasjletti, A.; Goligorsky, M. S. Prevention and reversal of premature endothelial cell senescence and vasculopathy in obesity-induced diabetes by ebselen. *Circ. Res.* **2004**, *94*, 377–384.
240. Chew, P.; Yuen, D. Y.; Koh, P.; Stefanovic, N.; Febbraio, M. A.; Kola, I.; Cooper, M. E.; de Haan, J. B. Site-specific antiatherogenic effect of the antioxidant ebselen in the diabetic apolipoprotein E-deficient mouse. *Arterioscler. Thromb. Vasc. Biol.* **2009**, *29*, 823–830.
241. Saito, I.; Asano, T.; Sano, K.; Takakura, K.; Abe, H.; Yoshimoto, T.; Kikuchi, H.; Ohta, T.; Ishibashi, S. Neuroprotective effect of an antioxidant, ebselen, in patients with delayed neurological deficits after aneurysmal subarachnoid hemorrhage. *Neurosurgery* **1998**, *42*, 269–277; discussion 277−268.
242. Yamaguchi, T.; Sano, K.; Takakura, K.; Saito, I.; Shinohara, Y.; Asano, T.; Yasuhara, H. Ebselen in acute ischemic stroke: a placebo-controlled, double-blind clinical trial. *Stroke* **1998**, *29*, 12–17.
243. Orian, L.; Toppo, S. Organochalcogen peroxidase mimetics as potential drugs: a long story of a promise still unfulfilled. *Free Radic. Biol. Med.* **2014**, *66*, 65–74.
244. Sakurai, T.; Kanayama, M.; Shibata, T.; Itoh, K.; Kobayashi, A.; Yamamoto, M.; Uchida, K. Ebselen, a seleno-organic antioxidant, as an electrophile. *Chem. Res. Toxicol.* **2006**, *19*, 1196–1204.

Publication Date (Web): October 13, 2015 | doi: 10.1021/bk-2015-1200.ch004

245. de Freitas, A. S.; Rocha, J. B. Diphenyl diselenide and analogs are substrates of cerebral rat thioredoxin reductase: a pathway for their neuroprotective effects. *Neurosci. Lett.* **2014**, *503*, 1–5.
246. de Bem, A. F.; Fiuza, B.; Calcerrada, P.; Brito, P. M.; Peluffo, G.; Dinis, T. C.; Trujillo, M.; Rocha, J. B.; Radi, R.; Almeida, L. M. Protective effect of diphenyl diselenide against peroxynitrite-mediated endothelial cell death: a comparison with ebselen. *Nitric Oxide* **2013**, *31*, 20–30.
247. Hort, M. A.; Straliotto, M. R.; Netto, P. M.; da Rocha, J. B.; de Bem, A. F.; Ribeiro-do-Valle, R. M. Diphenyl diselenide effectively reduces atherosclerotic lesions in LDLr -/- mice by attenuation of oxidative stress and inflammation. *J. Cardiovasc. Pharmacol.* **2011**, *58*, 91–101.
248. Dobrachinski, F.; da Silva, M. H.; Tassi, C. L.; de Carvalho, N. R.; Dias, G. R.; Golombieski, R. M.; da Silva Loreto, E. L.; da Rocha, J. B.; Fighera, M. R.; Soares, F. A. Neuroprotective effect of diphenyl diselenide in a experimental stroke model: maintenance of redox system in mitochondria of brain regions. *Neurotox. Res.* **2014**, *26*, 317–330.
249. Straliotto, M. R.; Hort, M. A.; Fiuza, B.; Rocha, J. B.; Farina, M.; Chiabrando, G.; de Bem, A. F. Diphenyl diselenide modulates oxLDL-induced cytotoxicity in macrophage by improving the redox signaling. *Biochimie* **2013**, *95*, 1544–1551.
250. Tamasi, V.; Jeffries, J. M.; Arteel, G. E.; Falkner, K. C. Ebselen augments its peroxidase activity by inducing nrf-2-dependent transcription. *Arch. Biochem. Biophys.* **2004**, *431*, 161–168.
251. Pober, J. S.; Sessa, W. C. Evolving functions of endothelial cells in inflammation. *Nat. Rev. Immunol.* **2007**, *7*, 803–815.
252. Smith, R. A.; Hartley, R. C.; Cocheme, H. M.; Murphy, M. P. Mitochondrial pharmacology. *Trends Pharmacol Sci.* **2012**, *33*, 341–352.
253. Liao, J. K. Beyond lipid lowering: the role of statins in vascular protection. *Int. J.Cardiol.* **2002**, *86*, 5–18.
254. Liao, J. K.; Laufs, U. Pleiotropic effects of statins. *Annu. Rev. Pharmacol. Toxicol.* **2005**, *45*, 89–118.
255. Wolfrum, S.; Jensen, K. S.; Liao, J. K. Endothelium-dependent effects of statins. *Arterioscler. Thromb. Vasc. Biol.* **2003**, *23*, 729–736.
256. Laufs, U.; La Fata, V.; Plutzky, J.; Liao, J. K. Upregulation of endothelial nitric oxide synthase by HMG CoA reductase inhibitors. *Circulation* **1998**, *97*, 1129–1135.
257. Rikitake, Y.; Liao, J. K. Rho GTPases, statins, and nitric oxide. *Circ. Res.* **2005**, *97*, 1232–1235.
258. Laufs, U.; Liao, J. K. Post-transcriptional regulation of endothelial nitric oxide synthase mRNA stability by Rho GTPase. *J. Biol. Chem.* **1998**, *273*, 24266–24271.
259. Coffer, P. J.; Jin, J.; Woodgett, J. R. Protein kinase B (c-Akt): a multifunctional mediator of phosphatidylinositol 3-kinase activation. *Biochem. J.* **1998**, *335* (Pt 1), 1–13.
260. Kureishi, Y.; Luo, Z.; Shiojima, I.; Bialik, A.; Fulton, D.; Lefer, D. J.; Sessa, W. C.; Walsh, K. The HMG-CoA reductase inhibitor

Publication Date (Web): October 13, 2015 | doi: 10.1021/bk-2015-1200.ch004

simvastatin activates the protein kinase Akt and promotes angiogenesis in normocholesterolemic animals. *Nat. Med.* **2000**, *6*, 1004–1010.
261. Wagner, A. H.; Kohler, T.; Ruckschloss, U.; Just, I.; Hecker, M. Improvement of nitric oxide-dependent vasodilatation by HMG-CoA reductase inhibitors through attenuation of endothelial superoxide anion formation. *Arterioscler. Thromb. Vasc. Biol.* **2000**, *20*, 61–69.
262. Rikitake, Y.; Kawashima, S.; Takeshita, S.; Yamashita, T.; Azumi, H.; Yasuhara, M.; Nishi, H.; Inoue, N.; Yokoyama, M. Anti-oxidative properties of fluvastatin, an HMG-CoA reductase inhibitor, contribute to prevention of atherosclerosis in cholesterol-fed rabbits. *Atherosclerosis* **2001**, *154*, 87–96.
263. Wassmann, S.; Laufs, U.; Baumer, A. T.; Muller, K.; Ahlbory, K.; Linz, W.; Itter, G.; Rosen, R.; Bohm, M.; Nickenig, G. HMG-CoA reductase inhibitors improve endothelial dysfunction in normocholesterolemic hypertension via reduced production of reactive oxygen species. *Hypertension* **2001**, *37*, 1450–1457.
264. Forstermann, U.; Li, H. Therapeutic effect of enhancing endothelial nitric oxide synthase (eNOS) expression and preventing eNOS uncoupling. *Br. J. Pharmacol.* **2011**, *164*, 213–223.
265. Shishehbor, M. H.; Aviles, R. J.; Brennan, M. L.; Fu, X.; Goormastic, M.; Pearce, G. L.; Gokce, N.; Keaney, J. F., Jr.; Penn, M. S.; Sprecher, D. L.; Vita, J. A.; Hazen, S. L. Association of nitrotyrosine levels with cardiovascular disease and modulation by statin therapy. *JAMA* **2003**, *289*, 1675–1680.

Publication Date (Web): October 13, 2015 | doi: 10.1021/bk-2015-1200.ch004

Publication Date (Web): October 13, 2015 | doi: 10.1021/bk-2015-1200.ch005

Chapter 5

Oxidative Stress in Parkinson's Disease: Role in Neurodegeneration and Targets for Therapeutics

Rebecca Banerjee,[1,2] Navneet Ammal Kaidery,[3] and Bobby Thomas[3,4,*]

[1]Laboratory of Clinical & Experimental Neuroscience, CSIR-Indian Institute of Chemical Biology, 4, Raja SC Mullick Road, Kolkata, India 700032
[2]Parkinson's Disease and Movement Disorders Program, Institute of Neurosciences Kolkata, 185/1 AJC Bose Road, Kolkata, India 700017
[3]Departments of Pharmacology and Toxicology & Georgia Regents University, 1459 Laney Walker Blvd, CB-3618, Augusta, Georgia 30912, United States
[4]Departments of Neurology Medical College of Georgia, Georgia Regents University, 1459 Laney Walker Blvd, CB-3618, Augusta, Georgia 30912, United States
[*]E-mail: bthomas1@gru.edu

Parkinson's disease (PD) is a prevalent neurodegenerative movement disorder affecting millions of predominantly elderly people worldwide and remains essentially untreatable. The underlying mechanisms of selective dopaminergic neurodegeneration in the substantia nigra pars compacta in PD are still poorly understood and the sufferings of the victims of the disease are unimaginable. Intense research endeavors have been directed in delineating the molecular events in the etiopathogenesis of PD. Oxidative stress stands at the forefront amongst several plausible hypotheses of PD pathogenesis in terms of the volume and substantiality of evidence acquired through controlled technologically advanced studies of the human disease and the experimental models of PD. Despite ample evidence in support of the involvement of oxidative stress in PD pathogenesis, traditional antioxidant-based therapeutic

In Oxidative Stress: Diagnostics, Prevention, and Therapy Volume 2; Hepel, et al.; ACS Symposium Series; American Chemical Society: Washington, DC, 2015.

strategies have failed in the clinic. Here we discuss lessons learnt from these failed clinical trials and new promising antioxidant-based neuroprotective strategies for therapeutic approaches that may usher hope to win the battle against this debilitating disease.

Publication Date (Web): October 13, 2015 | doi: 10.1021/bk-2015-1200.ch005

Introduction

Parkinson's disease (PD) is the second most common neurodegenerative disorder that affects the aging population worldwide. Characterized by selective loss of neuromelanin rich dopaminergic neurons in the substantia nigra pars compacta (SNpc) with resultant loss of dopamine (DA) in the striatum, PD clinically manifests in motor dysfunction. Resting tremor, muscle rigidity, bradykinesia and postural instability are the cardinal clinical symptoms of PD (*1*, *2*). The underlying molecular mechanisms that lead to neurodegeneration in PD remain elusive and hence there is no effective therapy that could halt or retard the progressive loss of dopaminergic neurons (*3*). Intensive research in PD spanning over several decades provides clues to the complexity and interplay of multiple factors in the etiopathology of the disease. The oxidative stress hypothesis of PD (*4*, *5*) could serve as one of the most plausible explanations to understand the key molecular events in PD etiopathogenesis. Further investigations to reveal the core mechanisms of oxidative stress in PD are warranted in order to nail down the cause of this relentless disease and relieve the sufferings of millions of PD victims globally. This chapter provides an overview of the involvement of oxidative stress in PD pathogenesis by evaluating the failure of conventional antioxidant-based treatments in clinical trials and also highlights the possibilities of new and promising antioxidant-based neuroprotective strategies for therapeutic interventions.

Reactive Oxygen Species: How Are They Generated in Dopaminergic Neurons?

Oxidative stress is a cytotoxic condition that occurs when there is an increased intracellular overproduction, or accumulation of reactive oxygen species (ROS) in conjunction with reduced antioxidant capacity within the cell. The most common species of ROS include molecules such as superoxide (O2•−) and hydrogen peroxide (H_2O_2). Additionally, H_2O_2 is associated with the production of reactive nitric oxide (NO•) species, which can also react with O2•- to produce highly reactive peroxynitrite ($ONOO^-$) (*6*). In general, ROS are continuously formed by chemical reactions via direct interactions between redox-active metals and oxygen species, or by indirect routes involving the activation of enzymes such as nitric oxide synthase (NOS) or NADPH oxidases (*7*). Univalent reduction of molecular oxygen leads to production of O2•−, OH• and H_2O_2. Superoxide dismutase (SOD) enzyme converts O2•− to H_2O_2 (*equation 1*). Hydroxyl radicals are also generated by Fenton chemistry (*equation 2*) and Haber-Weiss reaction (*equation 3*) involving redox-active metals, namely iron and copper. The NOS

In Oxidative Stress: Diagnostics, Prevention, and Therapy Volume 2; Hepel, et al.;
ACS Symposium Series; American Chemical Society: Washington, DC, 2015.

enzyme activity converts arginine to citrulline producing NO•, which further reacts with O2•− and forms peroxynitrite (*equation 4*). Peroxynitrite can get decomposed to OH• and NO2• (*equation 5*).

ROS Generating Chemical Equations within the Cell

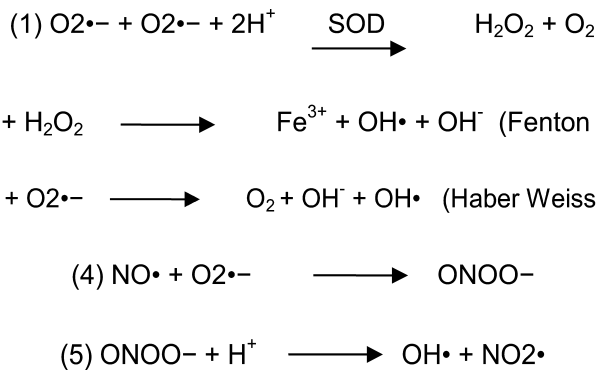

Generation of ROS under normal physiological conditions seems to facilitate numerous beneficial effects such as defense from infectious agents, cellular proliferations and survival (*8*). Under healthy conditions, O_2 and H_2O_2 are normal byproducts of oxygen metabolism by the mitochondria. The generation of O_2 from mitochondrial complexes I and III of the electron transport chain can result in H_2O_2 that can be decomposed by catalase and glutathione peroxidase. However, in both acute and chronic conditions where there are reduced levels of enzymatic antioxidants, the generation of oxidative stress occurs via the release of H_2O_2 into the cytosol. Furthermore, extracellular and environmental insults can stimulate generation of ROS and oxidative stress which leads to inactivation or damage of numerous proteins known to modulate key signaling pathways, ultimately leading to cellular dysfunction and death.

The nigrostriatal dopaminergic neurons that degenerate in PD are highly vulnerable to oxidative stress, due to high O_2 consumption of this brain region along with the low levels of antioxidant enzymes, such as SOD, glutathione, and catalase (*9*). In addition these neurons are intrinsically equipped with high levels of ROS generation machinery by virtue of their enrichment of the essential neurotransmitter DA, neuromelanin and iron content. The generation of ROS can also be increased in PD brain due to synthesis and storage of DA. DA is stable inside synaptic vesicles inside the cell, however, once DA exits the vesicle in a damaged neuron, it is easily metabolized by the enzyme monoamine oxidase B (MAO-B) to produce 3,4-dihydroxyphenylacetic acid (DOPAC) and H_2O_2. The DA redox chemistry engages a series of reactions producing ROS (*10*). DA metabolism by the enzyme MAO-B into DOPAC produces reactive H_2O_2 (*equation 6*).

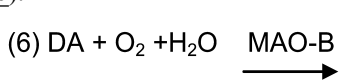

In Oxidative Stress: Diagnostics, Prevention, and Therapy Volume 2; Hepel, et al.;
ACS Symposium Series; American Chemical Society: Washington, DC, 2015.

Publication Date (Web): October 13, 2015 | doi: 10.1021/bk-2015-1200.ch005

Publication Date (Web): October 13, 2015 | doi: 10.1021/bk-2015-1200.ch005

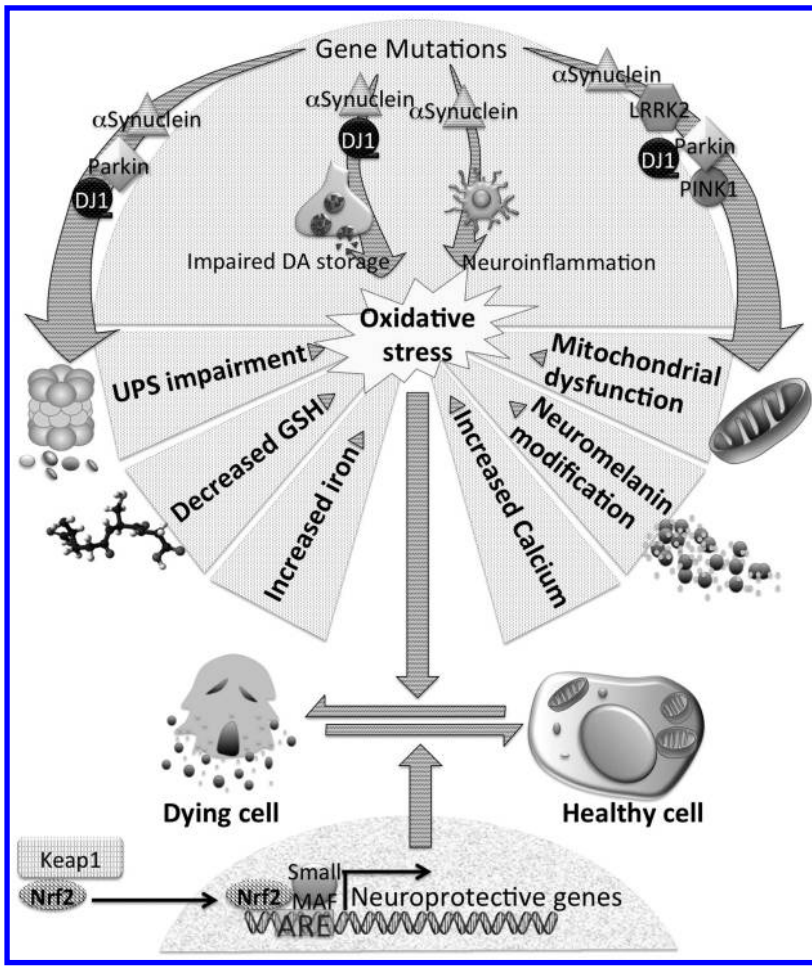

Figure 1. Oxidative Stress in Parkinson's disease: Various mechanisms are known to contribute to oxidative stress in dopaminergic neurons, such as impaired handling of dopamine, mitochondrial dysfunction, and neuroinflammation all of which leads to neurodegeneration. Alterations in PD-linked proteins can contribute and potentiate the impact of oxidative stress in dopaminergic neurons by various mechanisms leading to neurodegeneration. Nrf2 signaling is a promising pathway that can prevent oxidative stress buildup by activating the endogenous antioxidant, anti-inflammatory, and cytoprotective pathways to block dopaminergic neurodegeneration in PD. Abbreviations: DA: dopamine; Keap1: kelch-like ECH associated protein1; Nrf2: nuclear factor erythroid 2 (NF-E2)-related factor 2; UPS: Ubiquitin proteasome pathway; GSH: glutathione.

Moreover, DA undergoes spontaneous auto-oxidation in O_2 and iron rich environment to produce toxic DA quinones, O2•− and H_2O_2 (*equation 7*). Highly reactive OH• are produced from O2•− and H_2O_2, see *equation 3* above.

Publication Date (Web): October 13, 2015 | doi: 10.1021/bk-2015-1200.ch005

(7) DA $\xrightarrow{Fe^{2+} + O_2}$ dopa semiquinone + O2•− + H^+

$\xrightarrow{Fe^{2+} + O_2}$ dopaquinone + Fe^{2+} + H_2O_2

Normally, DA is sequestered in storage vesicles through an active transport process that requires vesicular monoamine transporter 2 (VMAT2) in preparation for its release after neuronal depolarization. Thus, VMAT2 keeps cytoplasmic DA levels under control, preventing ROS generation. As a result, over-expression of VMAT2 confers protection, while dopaminergic neurons with genetic or pharmacological blockade of VMAT2 are more susceptible against toxic insults (*11*). In addition, the reuptake of synaptically released DA into nigrostriatal terminals requires DA transporters (DAT). Perturbations in this reuptake mechanism impact the levels of cytoplasmic free DA that is susceptible to be oxidized (*12*).

Dopaminergic neurons are unique in containing neuromelanin pigment that imparts the dark brown color to the nigral neurons (*13*). DA quinones can cyclize to form a highly reactive aminochrome that polymerizes with neuromelanin. This process also involves O2•− generation and depletion of cellular NADPH. Neuromelanin accumulates iron, copper and other transition metal ions over the years and hence these neurons become fields for high reactivity with OH• and ROS generation. Neuromelanin contributes to H_2O_2 production by catalyzing dismutation of O2•− (*equation 8*).

(8) O2•− + $2H^+$ ⟶ H_2O_2

The Fenton chemistry for OH• generation is dependent on iron (Fe^{2+}) either cytosolic or compartmentalized as in the neuromelanin. Analysis of neuromelanin in the SN of PD patients has shown an early accumulation and overload of iron (Figure 1), which can lead to increased oxidative stress (*14*, *15*). Finally, neuromelanin that leaks from degenerating nigral neurons may contribute to the neurodegenerative process of the healthy cells by activating the neighboring microglia (*16*). Enzymatic antioxidant service against ROS in the brain is mainly served by SOD, catalase, and glutathione peroxidase (GPx). Reduced antioxidant potential of the antioxidant battalion in the brain correlate with neurodegenerative pathology in the brain. Downregulation of the catalase enzyme activity causes cytosolic H_2O_2 accumulation. Reduced glutathione (GSH) is a prominent determinant of the oxidative status in the brain. Localized exclusively in glial cells, GPx enzyme participates in the detoxification of H_2O_2 by converting GSH into oxidized glutathione (GS-SG) (*equation 9*).

(9) H_2O_2 + GSH $\xrightarrow{GPx}$ GS-SG + $2H_2O$

Reduction of GS-SG by glutathione reductase enzyme retrieves GSH and thereby, restores the antioxidant program.

The midbrain dopaminergic neurons are surrounded by extremely high numbers of resident microglia. It is estimated that the midbrain has about 4.5 fold more microglia than any other brain regions, suggesting that microglial

Publication Date (Web): October 13, 2015 | doi: 10.1021/bk-2015-1200.ch005

function is pivotal in the overall health of nigrostriatal dopaminergic neurons (*17*). Microglia are the major resident immune cells in the brain, providing innate immunity, however, astrocytes and oligodendrocytes are also involved in the neuroinflammatory response (*18*). The brain homeostasis is maintained by microglia by the production of various neurotrophic and anti-inflammatory factors that influences the neighboring astrocytes and neurons (*19*). In the healthy brain the resident microglia exhibits a resting phenotype. However, under stress conditions such as invasion of pathogens, injury, or during toxic protein accumulation microglia become activated to initiate an immune response to promote tissue repair and clearance of debris (*20*). This innate immune response eventually resolves in a controlled fashion once the injury is cured. However, persistence or a failure to resolve this inflammatory response leads to the uncontrolled release of neurotoxic factors such as ROS, pro-inflammatory cytokines, chemokines and prostaglandins and decreased secretion of trophic factors accumulating oxidative stress in the microenvironment. The heightened neuroinflammatory microglial response can be amplified by distress signals from damaged neurons thus leading to a self-perpetuating vicious cycle incurring further neuronal destruction (*21*). In PD, reactive microgliosis may be triggered by oxidized or nitrated molecules released by dying or damaged dopaminergic neurons that include aggregated α-synuclein, neuromelanin, histones, lipids, DNA and ATP. Indeed, studies have reported the presence of activated microglia, upregulation of inducible NOS, and presence of pro-inflammatory mediators released from these microglia in the brain and cerebrospinal fluid (*22*). Further evidence to the role of inflammation in PD comes from the findings of human leukocyte antigen (HLA) as a risk factor in Genome-Wide Association Studies (GWAS), which again raises the possibility for general pro-inflammatory state in this disease as a primary cause of neurodegeneration, or serves as a disease modifier to increase the risk of PD (*23*). All these observations suggest that ROS can initiate pro-inflammatory pathways, further perpetuating the deleterious environment for vulnerable neuronal populations such as the midbrain dopaminergic neurons (Figure 1).

It is suggested that the bioenergetic cost of both maintaining the large number of synapses and propagating action potentials is vast in long, unmyelinated nigrostriatal dopaminergic neurons (*24*, *25*). Theoretical calculations based on existing experimental data suggest that a single midbrain dopaminergic neuron may form over one million synapses and that the energy cost of maintaining these synapses and the cellular membrane potential increases with a non-linear relationship. Mitochondria are dynamic organelles serving these energy demands besides being closely involved in calcium homeostasis, stress response and cell death pathways. Indeed, mitochondrial dysfunction leads to oxidative stress and is associated with the pathogenesis of PD (*5*, *26*). The electron transport chain in mitochondria is a major source of ROS in dopaminergic neurons. As O_2 is sequentially reduced to H_2O by the electron transport chain complexes, a small percentage of O2•– is produced by complexes I and III. Once produced inside the mitochondria, O2•– may be converted to H_2O_2 by the enzyme manganese superoxide dismutase (MnSOD). Numerous other enzymes namely glutathione peroxidase 4 (GPx4), peroxiredoxins (PRDX) 3 and 5 that are localized in the

Publication Date (Web): October 13, 2015 | doi: 10.1021/bk-2015-1200.ch005

mitochondria catalyze further reduction of H_2O_2 to H_2O and O_2. Under normal conditions, ROS participate in signaling events mediated by select thiol residues in proteins that have the potential to control large scale changes in transcription amongst other things (*27*). However, certain situations can cause ROS production to surpass the antioxidant capacity of a cell to cause irreversible damage to cellular macromolecules ultimately leading to cell death. A significant reduction in the activity of mitochondrial complex I, a defective assembly process of its protein subunits, and increased oxidative damage to these protein subunits are reported in SN and other brain regions of PD patients (*26*). There is also evidence from multiple independent studies of a systemic reduction in complex I activity in blood platelets and muscle biopsies. Mitochondrial DNA encoded defects have been demonstrated where complex I defect from PD platelets are transferable into mitochondrial deficient cell lines known as "cybrids" (*28*). A major question that arises is whether impaired complex I activity represents a primary defect contributing to PD pathogenesis or whether it is secondary to disease, or due to related issues, such as medication. The former seems to be true since complex I activity does not correlate with levodopa (L-DOPA) dosage, and is normal in other neurodegenerative diseases, such as multiple system atrophy, suggesting that it is not a nonspecific consequence of neurodegeneration (*29*). There is also genetic evidence that abnormality in the mitochondrial DNA (mtDNA) may contribute to PD pathogenesis. These involve the point mutation in mitochondrial 12S rRNA found in a pedigree with parkinsonism, deafness and neuropathy, a marked age-dependent increase in mtDNA deletions in laser-captured dopaminergic neurons that are clonally expanded and associated with respiratory chain deficiencies (*30*). More extensive mtDNA deletions, which are associated with cytochrome c oxidase deficiency, occur in patients with PD compared with age-matched controls, and oxidative damage leading to double-strand breaks in mtDNA might be instrumental in the acquisition of these somatic mutations (*31*). A major source of mitochondrial deficits during aging is mutations in mtDNA, which is accelerated by oxidative stress. Individuals carrying polymerase gamma (POLG) mutations, the polymerase responsible for mtDNA maintenance and replication, acquire mtDNA deletions at an accelerated rate in the nigral dopaminergic neurons (*32*). In addition, gene expression profiling in dopaminergic neurons from PD patients showed down-regulation of genes encoding mitochondrial proteins, among others, providing further evidence for mitochondrial dysfunction in PD which may result in increased ROS generation (Figure 1) (*33*). Additionally, many of the PD-associated genes identified by both GWAS and Mendelian inheritance patterns encode proteins that have been shown to either directly or indirectly play a role in mitochondrial homeostasis (*34*). More on how these PD genes influence mitochondrial biology in PD pathogenesis is reviewed below.

Oxidative Stress in Idiopathic Parkinson's Disease

Oxidative stress has been proposed to play a major role in aging and neurodegenerative disorders such as PD (*4*). Although causal relationships

In Oxidative Stress: Diagnostics, Prevention, and Therapy Volume 2; Hepel, et al.;
ACS Symposium Series; American Chemical Society: Washington, DC, 2015.

between oxidative damage and PD remain to be defined fully, evidence to date has shown that oxidative damage occurs in PD, as judged by markers of lipid, protein and DNA oxidation in postmortem tissues. Increased lipid peroxidation was initially demonstrated in SN through measurement of increased levels of polyunsaturated fatty acids (*35*). Subsequently, an increase in lipid hydroperoxides was also demonstrated, confirming that free radical attack on lipid membranes is enhanced in PD (*36*). An immunohistochemical study demonstrated increased immunoreactivity to 4-hydroxynonenal (HNE) in the dopaminergic neurons in SN (*37*). This latter change is very important since HNE is a highly reactive product of lipid peroxidation that in turn may be able to interact with a variety of protein molecules. Indeed, HNE adducts are present in Lewy bodies in PD (*38*). *In vitro* studies have shown that HNE can cause cell death associated with increased oxidative or nitrosative stress, impaired mitochondrial function and decreased proteasomal activity (Figure 1) (*39*). There is also evidence for increased levels of isoflurans, another marker of lipid peroxidation, in SN in PD (*40*). Increased protein oxidation occurs in SN in PD, as demonstrated by enhanced levels of reactive protein carbonyls (*41*). However, higher amounts were also found in other brain regions examined both within and outside the basal ganglia. It is likely that oxidative stress is more widespread in the brain in PD and the pathogenic process is more extensive than currently thought and extends to many different brain areas. In fact studies reveal the existence of oxidative stress markers in peripheral blood lymphocytes and plasma of PD patients highlighting systemic oxidative stress involvement in PD (*42–45*). Moreover, reduced mitochondrial complex I activity in the platelets of PD patients has been reported previously (*46*, *47*). Interestingly, in PD, the dopaminergic neurons of the SNpc when compared to the nearby dopaminergic neurons of the ventral tegmental area are more vulnerable to oxidative stress. However, the precise mechanisms related to this differential vulnerability to oxidative stress between these neuronal populations remains unclear. The selective vulnerability of the SNpc dopaminergic neurons probably depends on their unique molecular and electrophysiological determinants (*48*). Alterations in DNA oxidation are also suggested to occur in PD as measured by increased levels of 8-hydroxyguanine or 8-hydroxy-deoxyguanosine (*41*, *49*), which are accompanied by alterations in DNA repair enzymes (*50*, *51*). A detailed study of alterations in a range of DNA bases and products of oxidation in PD showed only guanine was affected (*41*). However, whereas the levels of 8-hydroxyguanine were increased, these were balanced by a decrease in the levels of Fapy-guanine, another product of oxidative damage to guanine. 8-hydroxyguanine and Fapy-guanine are alternative products arising from the initial oxidation product of OH• attack on guanine bases. Since the subsequent formation of 8-hydroxyguanine or Fapy-guanine is determined by pH, these findings may reflect an alteration in the redox potential of nigral cells rather than an increase in overall DNA damage. Altered redox potential may itself enhance free radical production through a variety of mechanisms (*39*). It is also worth noting that L-DOPA may contribute to oxidative damage to DNA, particularly in the presence of divalent metal ions (*52*).

The potential for iron-mediated free radical formation initiated a range of assessments of the iron content in PD (Figure 1) (*53–57*). Overall there is

Publication Date (Web): October 13, 2015 | doi: 10.1021/bk-2015-1200.ch005

Publication Date (Web): October 13, 2015 | doi: 10.1021/bk-2015-1200.ch005

agreement that iron levels are increased in SN however, there does not seem to be agreement about the state of ionization of iron, whether it is present in a free or reactive form or whether it is inactivated by binding to proteins such as ferritin (*14*, *53–56*, *58–60*). The origin of excess iron remains unresolved and whether it has a glial or neuronal origin remains a question mark. There is also some evidence for alterations in proteins associated with the transport of iron, and their receptors in brain and in the periphery, but again this is an area that lacks consensus (*61*). It is clear, however, that changes in iron levels in the SN are not specific to PD since they occur in other neurodegenerative diseases affecting this brain region, such as multiple system atrophy, progressive supranuclear palsy, and also in neurodegenerative diseases affecting other areas of the brain, such as Huntington's disease and Alzheimer's disease (*39*). Despite these discrepancies related to a selective role of iron in the loss of nigral dopaminergic neurons in PD, evidence seem to favor towards iron chelation regimen as a tractable therapeutic opportunity (*62*). However, investigation into the cases of incidental Lewy body disease (ILBD) (these are normal individuals who at postmortem are found to have some nigral cell degeneration and the presence of Lewy bodies in SN) that may represent pre-symptomatic PD do not seem to support iron accumulation as an early pathogenic event, suggesting that iron accumulation occurs secondary to neurodegeneration (*63*). Similar to iron, levels of mitochondrial complex I in ILBD are not statistically different from age-matched controls, but are intermediate between those found in the normal cases and those found in PD (*57*). Consequently, it remains unknown whether mitochondrial dysfunction occurs at an early point in the illness. In contrast, the levels of the tripeptide antioxidant GSH in ILBD are significantly lower than those found in age-matched control and are decreased almost to the levels seen in advanced PD (*63*). This suggests that loss of this major antioxidant serves as an initial trigger for neuronal loss and may relate to the vulnerability of SN to subsequent oxidative mechanisms (Figure 1). The exact cause for the loss of GSH in PD is unclear and it is not associated with an impairment of the synthesis of GSH or in the enzyme systems associated with its oxidation-reduction cycle (*64*). Whatever, the cause of depletion of GSH, it renders cells more sensitive to toxic actions of ongoing oxidative mechanisms prevailing in the dopaminergic neurons of SN and also potentiate the toxic effects of glial activation towards dopaminergic neurons. Overall, these observations thus far suggest that markers of oxidative stress may serve as a pathologic trigger in the onset of PD pathophysiology. However, the origins of the oxidative stress, factors that determine their vulnerability, and its relationship with the progression of neuronal loss in PD are not immediately apparent.

Oxidative Stress in Toxin and Genetic Models of Parkinson's Disease

A better understanding of the pathophysiology of PD is only possible with the development of reliable experimental models, which can mimic disease processes with good fidelity. Hints that environmental toxins might play a role in the molecular pathology of PD first appeared after the accidental

In Oxidative Stress: Diagnostics, Prevention, and Therapy Volume 2; Hepel, et al.;
ACS Symposium Series; American Chemical Society: Washington, DC, 2015.

Publication Date (Web): October 13, 2015 | doi: 10.1021/bk-2015-1200.ch005

administration of 1-methyl-4-phenyl-1,2,3,6-tetrahydropyridine (MPTP) in a group of young intravenous drug users, who eventually developed a clinical phenotype reminiscent of late-stage PD (*65*). MPTP was subsequently identified as a potent neurotoxin that can easily cross the blood-brain barrier (BBB), being metabolized to 1-methyl-4-phenylpyridinium ion (MPP^+) in astrocytes, a potent mitochondrial complex I inhibitor (*66*). In addition to MPTP, other environmental toxins, such as the herbicide paraquat and rotenone have been identified as contributors to dopaminergic neuronal cell death and parkinsonism, supporting further the link between environmental exposure to pesticides and a risk of developing PD. Interestingly, a meta-analysis of 19 studies on the involvement of environmental pesticides in the pathogenesis of PD found an estimated doubling of the risk to develop PD (*67*). Four individual pesticides were found to increase the risk of PD: dieldrin, maneb, paraquat, and rotenone, the latter two behaving as mitochondrial toxins, in a similar manner to MPTP. Paraquat is also known to cause dopaminergic neurodegeneration by oxidative stress via O2•−, redox cycling with cellular diaphorase such as NOS (*68*). Oxidative stress is also the basis for dopaminergic neuronal damage inflicted upon by toxins like manganese, kainate, methamphetamine and isoquinoline. A neurotoxic analogue of DA, 6-hydroxydopamine (6-OHDA) has also been used to induce nigrostriatal degeneration in rodents. Unlike MPTP, it does not efficiently cross the BBB and therefore it must be injected directly into the nigrostriatal tract. The ability of 6-OHDA to induce DA degeneration has been linked to oxidative stress mechanisms, mitochondrial dysfunction and neuroinflammation (*69*). Interestingly, activation of microglia has been documented to be associated with dopaminergic neurodegeneration induced by almost all of the toxin models of PD releasing abundant ROS and pro-inflammatory mediators (*70*).

The discovery of genes linked to familial forms of PD also bonds the linkage of oxidative stress to PD pathogenesis (Figure 1) (*71*). Studies utilizing cell lines, autopsied patient samples, and genetically manipulated animal models have revealed a plethora of information on how oxidative stress is linked to PD pathophysiology by impacting normal functions of the proteins whose genes are linked to familial PD. Amongst these five genes that are studied extensively including- α-synuclein, parkin, PTEN-induced putative kinase 1 (PINK1), DJ-1, and Leucine-rich repeat kinase 2 (LRRK2) (*72*) will remain the main focus of this section.

α-Synuclein is a natively unfolded presynaptic protein believed to play a role in synaptic vesicle recycling, storage and compartmentalization of neurotransmitters and associates with vesicular and membranous structures. Both PD-linked pathogenic mutations and elevated concentrations will give α-synuclein a propensity to develop a β-sheet structure that readily polymerizes into oligomers and higher order aggregates such as fibrils (*71*). Although α-synuclein aggregates are a common feature of PD and alpha-synucleinopathies, little is known of the mechanism by which α-synuclein promotes neuronal loss or the factors that regulate α-synuclein toxicity. Several studies suggested direct pathologic relationships between oxidative stress/damage and α-synucleinopathies. Specifically, Lewy bodies and Lewy neurites in human α-synucleinopathies are associated with the accumulation of oxidatively modified form of α-synuclein,

Publication Date (Web): October 13, 2015 | doi: 10.1021/bk-2015-1200.ch005

including nitrated α-synuclein (*73*). Oxidative damage to α-synuclein, particularly dityrosine cross-linking of α-synuclein, is associated with increased aggregation (*74*, *75*). Moreover, α-synuclein can catalyze formation of H_2O_2 *in vitro* (*76*). The transition of α-synuclein from protofibrils to mature fibrils is inhibited by oxidative modification of α-synuclein by DA that results in accumulation of cytotoxic protofibrils in dopaminergic neurons suggesting that catechol oxidation may contribute to the accumulation of α-synuclein (*77*). It is suggested that pore forming α-synuclein protofibrils can disrupt the integrity of vesicular membranes thereby increasing cytosolic catecholamine concentrations further exacerbating toxicity of oxidized catechols (*78*, *79*). Dysregulated vesicle recycling could also result from interaction of misfolded or mutant α-synuclein with membrane-associated enzyme phospholipase D2 (PLD2), whereby it limits the number of vesicles to store DA (*80*). In addition, α-synuclein can cause clustering of DAT leading to increased reuptake of extracellular DA into the pre-synaptic neurons to increase cytosolic DA that may further exacerbate neurodegeneration (*81*). Several lines of studies demonstrate a direct role of α-synuclein in oxidative stress-induced neurodegeneration by influencing mitochondrial dysfunction. In this regard, α-synuclein is known to associate with the inner mitochondrial membrane where it is known to associate with the complex I of the mitochondrial electron transport chain thereby decreasing its activity (*82*, *83*). This notion gains support from the demonstration of the presence of α-synuclein in the mitochondrial membrane of dopaminergic neurons in control mice (*84*) and in the degenerating mitochondria of the human A53T α-synuclein transgenic mice (*85*). The phospholipid cardiolipin is an integral component of the mitochondrial inner membrane, which is externalized on mitochondria after stress where it acts as a "self destructive" signal that is recognized and destroyed by the mitochondrial degradation machinery known as mitophagy (*86*). Interestingly, α-synuclein has been demonstrated to interact with cardiolipin on vesicles mimicking mitochondrial inner membranes and the A30P substitution inhibits this interaction (*87*, *88*). Functional studies have shown that α-synuclein binding to mitochondria leads to cytochrome c release, increased calcium, and ROS levels culminating in cell death. Consistent to these findings genetic ablation of cyclophilin D, the modulator of the mitochondrial permeability transition delayed disease onset and extended lifespan in a mutant α-synuclein transgenic mice (*89*) implicating the role of ROS and mitochondrial calcium capacity in PD. Additionally, excessive ROS generation is also known to impact mitochondrial metabolism indirectly. Under conditions of oxidative stress α-synuclein is known to localize in the nucleus where it binds to the promoter of peroxisome proliferator-activated receptor gamma-coactivator-1 alpha (PGC1 α) gene that results in downregulation of PGC1 α target genes that are involved in modulating mitochondrial biogenesis, and oxidative stress (*90*). Other exogenous factors that link oxidative stress and mitochondrial dysfunction via α-synuclein are also suggested. For instance *in vivo* studies using rats demonstrate formation of α-synuclein aggregates following systemic exposure to mitochondrial toxins such as rotenone (*91*) or dichlorvos (*92*). Similarly, α-synuclein transgenic mice exhibit increased proteinase-K-resistant α-synuclein inclusions (*93*) and demonstrate increased sensitivity to neurodegeneration to

MPTP (*94–96*). Conversely, mice lacking α-synuclein are resistant to MPTP and other mitochondrial toxins such as malonate and 3-nitropropionic acid (*97*, *98*). Collectively, these studies suggest a direct reciprocal relationship between ROS, α-synuclein aggregation and mitochondrial dysfunction that can create a vicious cycle to set the stage for neurodegeneration.

α-synuclein-induced neurodegeneration can also be mediated through the activation of microglia that leads to increased ROS generation (*99–103*). It has been demonstrated that microglial cells can produce more pro-inflammatory cytokines such as tumor necrosis factor (TNF)-α, and interleukin-6 (*104*, *105*) when conditioned media from neuronal cells that overexpress mutant or wild-type α-synuclein is incubated with microglial cells. This is consistent with increased ROS production and microglial activation accompanied by increased secretion of TNF-α and interleukin-6 by microglial cells when incubated with α-synuclein aggregates, or mutant α-synuclein (*100*, *106*, *107*). The ability of α-synuclein to activate microglia is further enhanced when α-synuclein is nitrated, which renders it to aggregate and become resistant to proteolysis (*107–109*). In addition to its influence on microglia, nitrated α-synuclein is also known to activate adaptive immune response that leads to increased leukocyte infiltration in the brain (*110*). This is consistent with the accumulation of nitrated α-synuclein and subsequent loss of dopaminergic neurons in human α-synuclein transgenic mice administered with systemic lipopolysaccharide (LPS) when compared to wild-type mice (*111*). A proposed mechanism of excessive microglial activation and subsequent pro-inflammatory state in the brain is suggested by the release of misfolded α-synuclein from dying dopaminergic neurons. Notably, oligomeric α-synuclein has been shown to be an agonist for toll-like receptor (TLR)-2 resulting in microglial activation (*112*) which is consistent with increased microglial expression of TLR2 in ILBD indicative of an early microglial activation in response to PD pathology (*113*). Interestingly, activation of microglia by α-synuclein is attenuated in microglia from mice that lack CD36, the scavenger receptor further suggesting a direct role of α-synuclein and inflammation in PD pathogenesis (*100*). Taken together, it appears that genetic abnormalities in α-synuclein leads to increased oxidative stress, whereas oxidative stress itself is sufficient to impart a toxic phenotype to α-synuclein causing its aggregation which could then lead to mitochondrial dysfunction and exaggerated inflammation culminating in dopaminergic neurodegeneration.

Mutations in the parkin gene are a major cause of autosomal recessive early onset PD (*114*). Parkin functions as an E3 ubiquitin protein ligase similar to other RING finger containing proteins by targeting misfolded proteins to the ubiquitin proteasome pathway for degradation. Parkin functions as a multipurpose neuroprotective protein in a variety of toxic insults crucial for DA neuronal survival (*115*). Several lines of studies suggest that parkin's neuroprotective action could be mediated via modulation of oxidative stress. Neuroblastoma cells overexpressing wild-type parkin have low levels of ROS and are protected against apoptosis caused by DA and 6-OHDA (*116*). Contrary to this expression of mutant parkin is associated with increased oxidative stress markers such as protein carbonyls, lipid peroxidation and nitrated proteins (*117*). Importantly, the E3 ligase activity of parkin is known to be impaired by post-translational

Publication Date (Web): October 13, 2015 | doi: 10.1021/bk-2015-1200.ch005

modifications induced by oxidative and nitrosative stress (*118*, *119*). Especially treatment of cells expressing human parkin with DA has been shown to modify parkin by decreasing its solubility and inactivating its E3 ligase action (*118*). This observation is consistent with the presence of DA quinone modified parkin in the SN of PD patients compared to controls (*118*). Similarly, treatment of neurotoxins both *in vitro* and *in vivo* that causes oxidative stress-induced neurodegeneration could affect the native structure of parkin to compromise its solubility and protective functions (*120*). Moreover, parkin's protective function is compromised by S-nitrosylation in postmortem PD brains, and MPTP treated mice *in vivo* and by administering nitric oxide donors *in vitro* (*119*). More recently, parkin has been implicated in exerting its protective action against oxidative stress by the clearance of damaged mitochondria that results in increased ROS generation. It has been demonstrated that under physiological conditions, the majority of parkin is localized to the cytosol, but upon oxidative stress parkin translocates to depolarized mitochondria whereby it clears the depolarized/damaged mitochondria by an autophagic process commonly known as mitophagy (*121*, *122*). Taken together these studies suggest a direct relationship between parkin dysfunction and oxidative stress via regulation of misfolded protein clearance through the ubiquitin proteasome system and mitochondrial quality control in PD pathogenesis.

PINK1 is a mitochondrial targeted, highly conserved serine-threonine protein kinase of the Ca^{2+} calmodulin family, whose mutations are linked to autosomal recessive PD (*123*). Mutations in PINK1 are associated with loss of its kinase function and proper functioning of its kinase activity seems to be crucial for its neuroprotective actions. PINK1 has been suggested to be a key regulator of mitochondrial quality control, preserving mitochondrial respiration, and involved in mitochondrial transport and cell death possibly via phosphorylation of its substrates (*124*). Importantly, mitochondrial protein phosphorylation is involved in cell stress-induced programmed cell death such as apoptosis, which also contributes to the regulation of mitochondrial dynamics and mitophagy to ensure cellular homeostasis. The link between oxidative stress and PINK1 is potentially attributed to the actions of PINK1 on mitochondria, which serves as a major source of ROS. Loss of PINK1 function has been attributed to mitochondrial dysfunction and increased susceptibility to cell death (*125*). Mice lacking the PINK1 gene exhibit an increase in the number of larger mitochondria in the striatum with no change in total mitochondria numbers. These morphological changes are associated with impaired mitochondrial respiration in the striatum but not in the cerebral cortex, suggesting specificity of this defect for the nigrostriatal dopaminergic circuitry. PINK1 knockout mice also show increased sensitivity to oxidative stress, since mitochondria isolated from the brains of these animals exhibit increased cellular stress induced by H_2O_2 compared with mitochondria isolated from wild-type mice (*126*). PINK1 deficiency results in shortening, swelling and fragmentation of mitochondria in cultured cells (*127–131*) associated with loss of mitochondrial enzyme activity, particularly that of complex I (*126*, *132*, *133*). In addition, knocking down PINK1 in SH-SY5Y cells results in decreased mtDNA synthesis followed by loss of mitochondrial membrane potential and decreased ATP production (*132*). Neurophysiologically, it has been

Publication Date (Web): October 13, 2015 | doi: 10.1021/bk-2015-1200.ch005

demonstrated that the nigral dopaminergic neurons use Ca^{2+} for their pacemaking activity via $Ca_V1.3$ channels and that such pacemaking using these L-type Ca^{2+} channels increases mitochondrial oxidative stress (Figure 1) (*134*, *135*). This link between Ca^{2+} fluxes and mitochondria is enhanced by previous demonstration that loss of PINK1 sensitizes cells to Ca^{2+}-induced cytotoxicity (*136*). The result of these fluxes, if not buffered, is disruption of mitochondrial membrane potential and increased oxidative stress. On the other hand, overexpressing wild-type PINK1 in neuronal cell lines protects against staurosporine-induced mitochondrial cytochrome-c release and subsequent apoptosis through caspase 3 activation, while PINK1 mutants lack this protective effect (*123*) and enhance oxidative stress-induced cell death (*137*). Further, induced pluripotent stem cells (iPSC) from PINK1 mutant human subjects have increased vulnerability to MPP+ and H_2O_2 (*138*). Importantly, treatment of antioxidants can mitigate abnormalities associated with PINK1 deficiency.

Mutations in DJ-1 gene are linked to autosomal recessive early onset PD (*139*). Several studies have demonstrated that DJ-1 protects against oxidative stress through distinct cellular pathways (*140–148*). DJ-1 can eliminate H_2O_2 by becoming oxidized itself and thus functioning as a scavenger of ROS (*108*, *140*, *141*). DJ-1 is known to confer protective actions via transcriptional regulation. DJ-1 binds to PIAS proteins, a family of SUMO-1 ligases that modulate the activity of various transcription factors (*149*). Wild-type DJ-1 sequesters the death protein Daxx in the nucleus, preventing it from binding and activating its effector kinase, apoptosis signal-regulating kinase 1 (ASK1) in the cytoplasm (*150*). Other studies have shown that DJ-1 is a transcriptional co-activator that interacts with the nuclear proteins p54nrb and PSF to protect against apoptosis (*151*). DJ-1 also stabilizes the antioxidant transcriptional master regulator nuclear factor erythroid-2 related factor 2 (Nrf2) by preventing association with its inhibitor protein Keap1 (*152*, *153*). DJ-1 can also increase the expression of VMAT2 (*154*, *155*). Since VMAT2 keeps cytoplasmic DA levels in check by storing the neurotransmitter in synaptic vesicles, DJ-1 decreases intracellular ROS levels and enhances the resistance of cells against DA toxicity. Therefore, DJ-1 may act as a transcriptional co-factor that regulates the response to oxidative stress. DJ-1 has also been reported to confer protection against endoplasmic reticulum (ER) stress, proteasomal inhibition, and toxicity induced by overexpression of Pael-R (*156*). A pleiotropic role of DJ-1 seems to be related to the single function of binding multiple mRNA transcripts with a GG/CC-rich sequence (*157*). In addition, DJ-1 plays a role in maintenance of mitochondrial structure by counteracting the mitochondrial impairment induced by the tumor suppressor protein p53 (*158*). Moreover, overexpression of the gene encoding DJ-1 protects against oxidative injury whereas knocking down the expression by RNAi enhances susceptibility to oxidative stress (*141*, *156*, *159–163*). Thus, DJ-1 may play a crucial role both in sensing and conferring protection against a range of oxidative stressors, through multiple mechanisms.

LRRK2 is an autosomal dominant gene whose mutations cause familial PD. The LRRK2 protein contains a functional kinase and a GTPase domain. Disease associated mutations are common in its kinase domain leading to increased kinase activity and plays a role in PD pathogenesis (*164–169*). A proposed

In Oxidative Stress: Diagnostics, Prevention, and Therapy Volume 2; Hepel, et al.;
ACS Symposium Series; American Chemical Society: Washington, DC, 2015.

Publication Date (Web): October 13, 2015 | doi: 10.1021/bk-2015-1200.ch005

mechanism for the increased vulnerability of LRRK2 mutant cells to oxidative stress is via the kinase-dependent interaction between LRRK2 and dynamin-like protein (DLP1), which facilitates DLP1 translocation to mitochondria and subsequent mitochondrial fission (*170*, *171*). Overexpression of wild-type or mutant LRRK2 with enhanced kinase activity in various cell lines or primary neurons leads to mitochondrial fragmentation and dysfunction associated with increased ROS generation and increased susceptibility to H_2O_2 (*170*, *172*, *173*). Another mechanism is through the interaction of LRRK2 with PRDX3, which is a mitochondrial member of the antioxidant family of thioredoxin peroxidases. Mutations in the LRRK2 kinase domain increase phosphorylation of PRDX3 leading to decreased peroxidase activity, increased ROS production, and increased cell death. Notably, postmortem analyses of brains from PD patients carrying the G2019S mutation in the kinase domain of LRRK2 has shown marked increase in phosphorylated PRDX3 compared to normal brains (*174*). How LRRK2 might regulate oxidative stress in PD pathogenesis remains elusive, however, given its role in vesicular trafficking (*175*, *176*), cytoskeletal dynamics (*177*, *178*), mitochondrial function (*170*, *179*), and regulation of autophagy (*180–183*) it appears to play important role in the maintenance of cellular homeostasis. Dysfunction in any of these mechanisms might lead to increased oxidative stress and subsequent neurodegeneration due to LRRK2 mutations. More recently, LRRK2 has been shown to have a major function in the immune cells with its expression shown in microglia, astrocytes, peripheral blood mononuclear cells, mainly in B cells, dendritic cells, and macrophages (*184*). In a murine model of neuroinflammation, a robust induction of LRRK2 in microglia was observed. Experiments with TLR-4 stimulated rat primary microglia show that inflammation increases LRRK2 activity and expression, while inhibition of LRRK2 kinase activity or knockdown of LRRK2 attenuates TNFα secretion and inducible NOS induction (*185*). Notably, LRRK2 knockdown microglia exhibited a significant reduction of nuclear factor kappa B (NF-κB) transcriptional activity following TLR-mediated immune signaling induced by LPS, and an increase of DNA-binding activity of the NF-κB p50 inhibitor subunit. Taken together, these data suggest that LRRK2 expression and enzymatic activity are required during an inflammatory response, however, the specific pathways and signaling cascades that LRRK2 orchestrates have not been characterized. LRRK2 mutations might sensitize microglial cells and other immune cells toward a pro-inflammatory state, which in turn results in exacerbated inflammation, oxidative stress and subsequent neurodegeneration (*186*).

Publication Date (Web): October 13, 2015 | doi: 10.1021/bk-2015-1200.ch005

Targeting Oxidative Stress: A Promising Route to Therapeutic Intervention?

It is now generally accepted that PD pathogenesis is closely related to oxidative stress due to ROS generated by DA metabolism, mitochondrial dysfunction and neuroinflammation. Based on this observation, several antioxidants have been studied in clinical trials, including selegiline, vitamin E, and rasagiline. Selegiline is known to reduce autooxidation of DA by inhibiting

MAO-B and is the antioxidant drug most studied in clinical trials. The Deprenyl And Tocopherol Antioxidative Therapy Of Parkinsonism (DATATOP) trial was the largest clinical trial to investigate the neuroprotective potential of selegiline, along with vitamin E, in patients with early PD (*187*). The primary outcome was to time the clinical decision to begin L-DOPA treatment in PD patients. Although selegiline significantly delayed the time of onset of L-DOPA treatment, patients treated with vitamin E showed no benefits nor did the vitamin E added any benefit to selegiline. This study suggests that selegiline may delay disease progression, through mild symptomatic effects known to improve motor symptoms in PD. Rasagiline is a MAO-B inhibitor that is more potent than selegiline and has metabolites with potential antioxidant properties. It has been studied using a delayed-start clinical trial design intended to reduce the confounding effect of symptomatic efficacy. The outcomes of the TEMPO study suggest that early treatment confers a long-lasting improvement, but the overall duration of this study was relatively short, and the group sizes were modest (*188*). However, the ADAGIO trial designed to verify the TEMPO study in a larger sample and over a longer time course failed to demonstrate disease-modifying effects of the drug at 2 mg dose which was observed with 1 mg. Moreover, small change in Unified Parkinson Disease Rating Scale (UPDRS) scores made the results difficult to interpret (*189*). Coenzyme Q10 (CoQ10) is a cofactor in the electron transport chain in mitochondria and an antioxidant that has been shown to reduce dopaminergic neurodegeneration in mouse PD models (*190*). A decade ago one of the first clinical trials of CoQ10 showed that dosages of up to 1200 mg daily were safe for people with early stage PD, and also suggested that it helped symptoms. However, the large multicenter QE3 study evaluating the efficacy of two different doses of CoQ10 (1200 and 2400 mg daily) in early PD patients showed no significant benefits (*191*). Creatine is an antioxidant and improves mitochondrial bioenergetics and has been shown to be neuroprotective in preclinical animal models (*192*). The NIH Exploratory trials in Parkinson Long term study -1 (NET-PD LS-1) that tested a highly purified form of creatine 5 g twice a day failed to show any difference in UPDRS scores between the control and creatine groups (*193*). Mitoquinone (MitoQ) is a mitochondrial targeted antioxidant known to enhance mitochondrial bioenergetics and demonstrated neuroprotective effects in animal models (*194*) also failed to show any benefit in human PD (*195*). Failure of this study was attributed to small sample size and lack of adequate brain penetrance of MitoQ. While none of these clinical studies convincingly showed that these antioxidant therapies slow disease progression, several of these trials indicate that selegiline, rasagiline, and CoQ10 may be promising. Essentially, all of these antioxidant approaches possess good safety record, which is desirable in neuroprotective therapeutic design required for sustained long-term benefit in patients.

In addition to antioxidants several anti-inflammatory agents, including non-steroidal anti-inflammatory drugs (NSAIDS) have been pursued as therapeutic agents. Numerous studies, both in cell culture and in animal models have shown that certain NSAIDs, such as aspirin, have neuroprotective properties (*196*). Epidemiological studies examining the association of regular NSAID use with the risk of PD have provided conflicting results with only ibuprofen

Publication Date (Web): October 13, 2015 | doi: 10.1021/bk-2015-1200.ch005

showing a neuroprotective effect (*196*, *197*). An alternative approach to target inflammation may be the use of statins. In addition to cholesterol lowering properties, these drugs have anti-inflammatory effects and are known to scavenge free radicals to block dopaminergic neurodegeneration in an animal model of PD (*198*). Epidemiological studies showed that statin use, particularly simvastatin, is associated with lower incidence of PD (*199*, *200*). A limitation of these studies is that the use of statins was not randomized. Other studies have suggested low low-density lipoprotein (LDL) cholesterol levels increased PD risk (*201*, *202*), so that the increased use of statins among controls may just reflect high LDL levels that would be protective against PD. These issues need to be explored in a prospective, randomized study.

An emerging target for PD involves drug-induced activation of a coordinated antioxidant genetic program to maintain redox equilibrium by means of expression of pro-survival proteins and cytoprotective enzymes (*203–205*). A key transcription factor orchestrating this process is Nrf2, a member of the cap'n'collar family of basic leucine zipper transcription factors. In addition to its role in protection from oxidative stress, Nrf2 triggers expression of genes responsible for drug detoxification, iron metabolism, excretion transporters, immunomodulation, calcium homeostasis, growth factors, intracellular signaling, and neurotransmitter receptors (Figure 1). The breadth of this endogenous response suggests that its activation might counterbalance many of the large number of pathways implicated in PD pathogenesis. Uric acid has been shown to render neuroprotective effects in cell culture and animal models of PD by virtue of its ability to activate the Nrf2 pathway (*206*, *207*). Interestingly, epidemiological studies have shown a decreased incidence of PD among subjects with high serum urate levels (*208*, *209*) and among subjects with gout (*210*). In patients with early PD, higher plasma urate levels correlate with slower disease progression (*211*). A recent study showed that subjects on diets that promote high urate levels have a reduced risk of developing PD (*212*). Such a urate-rich diet could serve as a neuroprotective therapy in PD. However, the potential benefits of a urate-rich diet have to be weighed against the risk of developing gout and cardiovascular disease. A large-scale clinical trial of the effectiveness of elevating urate in patients with PD is in the planning stages. The Safety of Urate Elevation in Parkinson's Disease (SURE-PD) study was conducted to test the precursor of urate, inosine and was found to be safe and effective in increasing serum urate levels of PD patients and may prove to be a disease modifying therapy for PD (*213*). Dimethylfumarate (Tecfidera) is a new drug known to activate the Nrf2 pathway to induce, anti-inflammatory and antioxidant pathways and display neuroprotective properties in animal and *in vitro* studies. Clinical trials provide compelling evidence for the clinical efficacy of dimethylfumarate in the treatment of relapsing–remitting multiple sclerosis, and have demonstrated that oral administration is well tolerated and markedly reduced the annualized relapse rate, the numbers of gadolinium-enhancing lesions (*214*, *215*). Based on its favorable safety, tolerability and neuroprotective properties, dimethylfumarate represents an excellent oral disease-modifying drug in the treatment of various neurodegenerative disorders where oxidative stress and neuroinflammation play a significant role in disease pathogenesis. Preclinical studies demonstrate that

Publication Date (Web): October 13, 2015 | doi: 10.1021/bk-2015-1200.ch005

dimethylfumarate shows protective effects against 6-OHDA (*216*) and MPTP model of PD (our unpublished results). Positive outcomes of these preclinical works combined with promising safety profile of dimethylfumarate warrants it's testing in human PD. In addition to the neuroprotective strategies discussed here there are several other promising therapeutic agents that are currently being tested in human PD and many others that are being studied in preclinical models. For a detailed overview of these neuroprotective agents the readers are advised to refer to a recent review by Athauda and Foltynie (*217*).

Despite the obvious need for neuroprotective or disease-modifying agents for PD, and the great promise that many potential therapies have shown in preclinical studies, no treatments has so far been licensed as a neuroprotective agent in PD. Despite strong *in vitro* and *in vivo* data, several notable candidate neuroprotective drugs have failed to show benefits in recent high profile clinical trials (*217*). In PD clinical studies, a major confounding methodological issue has surfaced in determining whether a therapy is neuroprotective in a live patient. Traditionally, clinical measures based on neurological examination have been used to assess disease progression of PD. The UPDRS scale involves clinical examination of motor functions combined with scales rating patients' subjective view of function in daily activities. Much of the disability associated with PD is not considered in the UPDRS scale, such as those related to autonomic dysfunction. A new version of the UPDRS has been developed and may address some of these limitations (*218*). There are also no validated and sensitive biomarker for the diagnosis and monitoring of treatment response in PD that would replace clinical endpoints or symptomatic markers to assess disease progression. Another reason for the failure of potential neuroprotective therapies could also be explained by the limitations of the current preclinical models. Currently, there is no one animal model for PD that mimics the full pathology and clinical symptomology of the illness. Traditionally, preclinical studies have focused on toxin-based models. These toxin models show degeneration of nigrostriatal dopaminergic neurons, but the time course and pathological features of these models are different from human disease (*219*). In the last decade, discovery of PD-linked genes led to the development of genetic-based models as alternatives to toxin-based models. These genetic-models incorporate some additional features of the disease, but still fall short of the cardinal feature of PD that is nigrostriatal dopaminergic neurodegeneration (*219*). The predictive power of animal models of PD will be confirmed only if there is success in demonstrating neuroprotection in humans. In the meantime, most in the field rely on examining effectiveness of potential treatments in several different animal models, with the hope that treatments exhibiting a broad effect in these diverse models are the ones most likely to exhibit effectiveness against human disease. Lastly, our knowledge about the underlying molecular pathways involved in the pathogenesis of PD is still limited despite the voluminous research efforts invested in this field. We believe that this comprehensive discussion addressing many of these crucial issues on antioxidant treatment modalities shall provide new ideas and scope for future development of novel neuroprotective therapies in PD.

Publication Date (Web): October 13, 2015 | doi: 10.1021/bk-2015-1200.ch005

Conclusions and Future Perspective

To date PD remains incurable due to our limited understanding of the underlying molecular mechanisms. Ample neuropathological evidence from human and experimental PD strongly suggests a central role of oxidative stress in PD pathophysiology. It is unclear at this stage to determine what might be the primary source of oxidative stress, since these may originate from abnormal DA metabolism, mitochondrial dysfunction, and exaggerated neuroinflammation. Despite this uncertainty oxidative stress remains a promising target for therapeutic intervention in PD. Neuroprotective targets such as the Nrf2 signaling that can enhance antioxidant status, anti-inflammatory pathways, and induction of cytoprotective genes currently holds promise amongst other potential mechanisms to mitigate the oxidative stress buildup in PD. The ability to selectively induce a battery of cytoprotective and antioxidative enzymes that are directly under the genetic control of a single transcription factor such as Nrf2 may have significant advantages over conventional strategies. One can potentially induce multiple antioxidant pathways and associated neuroprotective responses, which would not be dependent on the antioxidant effects of a single molecule or combination of molecules that are frequently consumed while scavenging toxic-free radical species in a diseased brain. Failures in clinical trials with antioxidant therapy should not undermine the importance of oxidative stress in PD. Instead failures should be taken up as lessons to rectify the therapeutic design. Advances in our understanding of disease pathogenesis, a robust pipeline of rational treatments, and the advent of valid and reliable biomarkers holds promise in the coming decade for developing and achieving neuroprotective therapies for PD. Overall, the activity aimed at understanding and treating PD has grown exponentially and should ultimately result in better therapies for PD.

Publication Date (Web): October 13, 2015 | doi: 10.1021/bk-2015-1200.ch005

Acknowledgments

This work is supported in part by grants from the National Institutes of Health NS060885 (BT), and Michael J Fox Foundation for Parkinson's disease, National Parkinson Foundation CSRA Chapter (BT), Par fore Parkinson (BT). Department of Science & Technology, India, Women Scientist A Fellowship supports RB. NAK is a Parkinson's Disease Foundation postdoctoral fellow.

References

1. Lang, A. E.; Lozano, A. M. *N. Engl. J. Med.* **1998**, *339*, 1044–1053.
2. Lang, A. E.; Lozano, A. M. *N. Engl. J. Med.* **1998**, *339*, 1130–1143.
3. Savitt, J. M.; Dawson, V. L.; Dawson, T. M. *J. Clin. Invest.* **2006**, *116*, 744–754.
4. Jenner, P. *Ann. Neurol.* **2003**, *53* (Suppl. 3), S26–36; discussion S36−38.
5. Lin, M. T.; Beal, M. F. *Nature* **2006**, *443*, 787–795.
6. Chinta, S. J.; Andersen, J. K. *Free Radical Res.* **2011**, *45*, 53–58.
7. Halliwell, B. *J Neurochem* **2006**, *97*, 1634–1658.

8. Valko, M.; Leibfritz, D.; Moncol, J.; Cronin, M. T.; Mazur, M.; Telser, J. *Int. J. Biochem. Cell Biol.* **2007**, *39*, 44–84.
9. Floyd, R. A. *Proc. Soc. Exp. Biol. Med.* **1999**, *222*, 236–245.
10. Cadet, J. L.; Brannock, C. *Neurochem. Int.* **1998**, *32*, 117–1131.
11. Bernstein, A. I.; Stout, K. A.; Miller, G. W. *Neurochem. Int.* **2014**, *73*, 89–97.
12. Vaughan, R. A.; Foster, J. D. *Trends Pharmacol. Sci.* **2013**, *34*, 489–496.
13. Double, K. L.; Ben-Schachar, D.; Youdim, M. B.; Zecca, L.; Riederer, P.; Gerlach, M. *Neurotoxicol. Teratol.* **2002**, *24*, 621–628.
14. Faucheux, B. A.; Martin, M. E.; Beaumont, C.; Hauw, J. J.; Agid, Y.; Hirsch, E. C. *J. Neurochem.* **2003**, *86*, 1142–1148.
15. Double, K. L.; Gerlach, M.; Schunemann, V.; Trautwein, A. X.; Zecca, L.; Gallorini, M.; Youdim, M. B.; Riederer, P.; Ben-Shachar, D. *Biochem. Pharmacol.* **2003**, *66*, 489–494.
16. Karlsson, O.; Lindquist, N. G. *J. Neural Transm.* **2013**, *120*, 1623–1630.
17. Lawson, L. J.; Perry, V. H.; Dri, P.; Gordon, S. *Neuroscience* **1990**, *39*, 151–170.
18. Tansey, M. G.; McCoy, M. K.; Frank-Cannon, T. C. *Exp. Neurol.* **2007**, *208*, 1–25.
19. Schwartz, M.; Kipnis, J.; Rivest, S.; Prat, A. *J. Neurosci.* **2013**, *33*, 17587–17596.
20. Aloisi, F. *Adv. Exp. Med. Biol.* **1999**, *468*, 123–133.
21. Qian, L.; Flood, P. M.; Hong, J. S. *J. Neural Transm.* **2010**, *117*, 971–979.
22. Hirsch, E. C.; Breidert, T.; Rousselet, E.; Hunot, S.; Hartmann, A.; Michel, P. *Ann. N. Y. Acad. Sci.* **2003**, *991*, 214–228.
23. Hamza, T. H.; Zabetian, C. P.; Tenesa, A.; Laederach, A.; Montimurro, J.; Yearout, D.; Kay, D. M.; Doheny, K. F.; Paschall, J.; Pugh, E.; Kusel, V. I.; Collura, R.; Roberts, J.; Griffith, A.; Samii, A.; Scott, W. K.; Nutt, J.; Factor, S. A.; Payami, H. *Nat. Genet.* **2010**, *42*, 781–785.
24. Bolam, J. P.; Pissadaki, E. K. *Mov. Disord.* **2012**, *27*, 1478–1483.
25. Pissadaki, E. K.; Bolam, J. P. *Front. Comput. Neurosci.* **2013**, *7*, 13.
26. Banerjee, R.; Starkov, A. A.; Beal, M. F.; Thomas, B. *Biochim. Biophys. Acta* **2009**, *1792*, 651–663.
27. Fomenko, D. E.; Koc, A.; Agisheva, N.; Jacobsen, M.; Kaya, A.; Malinouski, M.; Rutherford, J. C.; Siu, K. L.; Jin, D. Y.; Winge, D. R.; Gladyshev, V. N. *Proc. Natl. Acad. Sci. U. S. A.* **2011**, *108*, 2729–2734.
28. Swerdlow, R. H.; Parks, J. K.; Miller, S. W.; Tuttle, J. B.; Trimmer, P. A.; Sheehan, J. P.; Bennett, J. P., Jr.; Davis, R. E.; Parker, W. D., Jr. *Ann. Neurol.* **1996**, *40*, 663–671.
29. Thomas, B.; Beal, M. F. *Mov. Disord.* **2010**, *25* (Suppl. 1), S155–S160.
30. Bender, A.; Krishnan, K. J.; Morris, C. M.; Taylor, G. A.; Reeve, A. K.; Perry, R. H.; Jaros, E.; Hersheson, J. S.; Betts, J; Klopstock, T.; Taylor, R. W.; Turnbull, D. M. *Nat. Genet.* **2006**, *38*, 515–517.
31. Srivastava, S.; Moraes, C. T. *Hum. Mol. Genet.* **2005**, *14*, 893–902.
32. Sanders, L. H.; McCoy, J.; Hu, X.; Mastroberardino, P. G.; Dickinson, B. C.; Chang, C. J.; Chu, C. T.; Van Houten, B.; Greenamyre, J. T. *Neurobiol. Dis.* **2014**, *70*, 214–223.

Publication Date (Web): October 13, 2015 | doi: 10.1021/bk-2015-1200.ch005

33. Elstner, M.; Muller, S. K.; Leidolt, L.; Laub, C.; Krieg, L.; Schlaudraff, F.; Liss, B.; Morris, C.; Turnbull, D. M.; Masliah, E.; Prokisch, H.; Klopstock, T.; Bender, A. *Mol. Brain* **2011**, *4*, 43.
34. Ryan, B. J.; Hoek, S.; Fon, E. A.; Wade-Martins, R. *Trends Biochem. Sci.* **2015**, *40*, 200–210.
35. Dexter, D. T.; Carter, C. J.; Wells, F. R.; Javoy-Agid, F.; Agid, Y.; Lees, A.; Jenner, P.; Marsden, C. D. *J. Neurochem.* **1989**, *52*, 381–389.
36. Dexter, D. T.; Holley, A. E.; Fitter, W. D.; Slater, T. F.; Wells, F. R.; Daniel, S. E.; Lees, A. J.; Jenner, P.; Marsden, C. D. *Mov. Disord.* **1994**, *9*, 92–97.
37. Yoritaka, A.; Hattori, N.; Uchida, K.; Tanaka, M.; Stadtman, E. R. *Proc. Natl. Acad. Sci. U. S. A.* **1996**, *93*, 2696–2701.
38. Castellani, R. J.; Perry, G.; Siedlak, S. L.; Nunomura, A.; Shimohama, S.; Zhang, J.; Montine, T.; Sayre, L. M.; Smith, M. A. *Neurosci. Lett.* **2002**, *319*, 25–28.
39. Jenner, P. *Handb. Clin. Neurol.* **2007**, *83*, 507–520.
40. Fessel, J. P.; Hulette, C.; Powell, S.; Roberts, L. J., 2nd; Zhang, J. *J. Neurochem.* **2003**, *85*, 645–650.
41. Alam, Z. I.; Jenner, A.; Daniel, S. E.; Lees, A. J.; Cairns, N.; Marsden, C. D.; Jenner, P.; Halliwell, B. *J. Neurochem.* **1997**, *69*, 1196–1203.
42. Migliore, L.; Petrozzi, L.; Lucetti, C.; Gambaccini, G.; Bernardini, S.; Scarpato, R.; Trippi, F.; Barale, R.; Frenzilli, G.; Rodilla, V.; Bonuccelli, U. *Int. J. Hyg. Environ. Health* **2001**, *204*, 61–66.
43. Migliore, L.; Petrozzi, L.; Lucetti, C.; Gambaccini, G.; Bernardini, S.; Scarpato, R.; Trippi, F.; Barale, R.; Frenzilli, G.; Rodilla, V.; Bonuccelli, U. *Neurology* **2002**, *58*, 1809–1815.
44. Prigione, A.; Isaias, I. U.; Galbussera, A.; Brighina, L.; Begni, B.; Andreoni, S.; Pezzoli, G.; Antonini, A.; Ferrarese, C. *Parkinsonism Relat. Disord.* **2009**, *15*, 327–328.
45. Bogdanov, M.; Matson, W. R.; Wang, L.; Matson, T.; Saunders-Pullman, R.; Bressman, S. S.; Flint Beal, M. *Brain* **2008**, *131*, 389–396.
46. Haas, R. H.; Nasirian, F.; Nakano, K.; Ward, D.; Pay, M.; Hill, R.; Shults, C. W. *Ann. Neurol.* **1995**, *37*, 714–722.
47. Parker, W. D., Jr.; Boyson, S. J.; Parks, J. K. *Ann. Neurol.* **1989**, *26*, 719–723.
48. Brichta, L.; Greengard, P. *Front. Neuroanat.* **2014**, *8*, 152.
49. Zhang, J.; Perry, G.; Smith, M. A.; Robertson, D.; Olson, S. J.; Graham, D. G.; Montine, T. J. *Am. J. Pathol.* **1999**, *154*, 1423–1429.
50. Shimura-Miura, H.; Hattori, N.; Kang, D.; Miyako, D.; Nakabeppu, Y.; Mizuno, Y. *Ann. Neurol.* **1999**, *46*, 920–924.
51. Fukae, J.; Takanashi, M.; Kubo, S.; Nishioka, K.; Nakabeppu, Y.; Mori, H.; Mizuno, Y.; Hattori, N. *Acta Neuropathol.* **2005**, *109*, 256–262.
52. Spencer, J. P.; Jenner, A.; Aruoma, O. I.; Evans, P. J.; Kaur, H.; Dexter, D. T.; Jenner, P.; Lees, A. J.; Marsden, C. D.; Halliwell, B. *FEBS Lett.* **1994**, *353*, 246–250.
53. Dexter, D. T.; Holley, A. E.; Flitter, W. D.; Slater, T. F.; Wells, F. R.; Daniel, S. E.; Lees, A. J.; Jenner, P.; Marsden, C. D. *Lancet* **1987**, *2*, 1219–1220.
54. Dexter, D. T.; Jenner, P; Marsden, C. D. *Mov. Disord.* **1989**, *4*, 176–182.

Publication Date (Web): October 13, 2015 | doi: 10.1021/bk-2015-1200.ch005

55. Sofic, E.; Riederer, P.; Heinsen, H.; Beckmann, H.; Reynolds, G. P.; Hebenstreit, G.; Youdim, M. B. *J. Neural Transm.* **1988**, *74*, 199–205.
56. Riederer, P.; Sofic, E.; Rausch, W. D.; Schmidt, B.; Reynolds, G. P.; Jellinger, K.; Youdim, M. B. *J. Neurochem.* **1989**, *52*, 515–520.
57. Good, P. F.; Olanow, C. W.; Perl, D. P. *Brain Res.* **1992**, *593*, 343–346.
58. Mann, V. M.; Cooper, J. M.; Daniel, S. E.; Srai, K.; Jenner, P.; Marsden, C. D.; Schapira, A. H. *Ann. Neurol.* **1994**, *36*, 876–881.
59. Gu, M.; Owen, A. D.; Toffa, S. E.; Cooper, J. M.; Dexter, D. T.; Jenner, P.; Marsden, C. D.; Schapira, A. H. *J. Neurol. Sci.* **1998**, *158*, 24–29.
60. Faucheux, B. A.; Martin, M. E.; Beaumont, C.; Hunot, S.; Hauw, J. J.; Agid, Y.; Hirsch, E. C. *J. Neurochem.* **2002**, *83*, 320–330.
61. Ayton, S.; Lei, P. *Biomed. Res. Int.* **2014**, *2014*, 581256.
62. Devos, D.; Moreau, C.; Devedjian, J. C.; Kluza, J.; Petrault, M.; Laloux, C.; Jonneaux, A.; Ryckewaert, G.; Garcon, G.; Rouaix, N.; Duhamel, A.; Jissendi, P.; Dujardin, K.; Auger, F.; Ravasi, L.; Hopes, L.; Grolez, G.; Firdaus, W.; Sablonniere, B.; Strubi-Vuillaume, I.; Zahr, N.; Destee, A.; Corvol, J. C.; Poltl, D.; Leist, M.; Rose, C.; Defebvre, L.; Marchetti, P.; Cabantchik, Z. I.; Bordet, R. *Antioxid. Redox Signal.* **2014**, *21*, 195–210.
63. Dexter, D. T.; Sian, J.; Rose, S.; Hindmarsh, J. G.; Mann, V. M.; Wells, F. R.; Daniel, S. E.; Lees, A. J.; Schapira, A. H. *Ann. Neurol.* **1994**, *35*, 38–44.
64. Smeyne, M.; Smeyne, R. J. *Free Radical Biol. Med.* **2013**, *62*, 13–25.
65. Langston, J. W.; Ballard, P.; Tetrud, J. W.; Irwin, I. *Science* **1983**, *219*, 979–980.
66. Ramsay, R. R.; Kowal, A. T.; Johnson, M. K.; Salach, J. I.; Singer, T. P. *Arch. Biochem. Biophys.* **1987**, *259*, 645–649.
67. Priyadarshi, A.; Khuder, S. A.; Schaub, E. A.; Shrivastava, S. *Neurotoxicology* **2000**, *21*, 435–440.
68. Day, B. J.; Patel, M.; Calavetta, L.; Chang, L. Y.; Stamler, J. S. *Proc. Natl. Acad. Sci. U. S. A.* **1999**, *96*, 12760–12765.
69. Barnum, C. J.; Tansey, M. G. *Prog. Brain Res.* **2010**, *184*, 113–132.
70. Litteljohn, D.; Mangano, E.; Clarke, M.; Bobyn, J.; Moloney, K.; Hayley, S. *Parkinsons Dis.* **2010**, *2011*, 713517.
71. Thomas, B.; Beal, M. F. *F1000 Med. Rep.* **2011**, *3*, 7.
72. Thomas, B.; Beal, M. F. *Hum. Mol. Genet.* **2007**, *16*, R183–194.
73. Giasson, B. I.; Duda, J. E.; Murray, I. V.; Chen, Q.; Souza, J. M.; Hurtig, H. I.; Ischiropoulos, H.; Trojanowski, J. Q.; Lee, V. M. *Science* **2000**, *290*, 985–989.
74. Souza, J. M.; Giasson, B. I.; Chen, Q.; Lee, V. M.; Ischiropoulos, H. *J. Biol. Chem.* **2000**, *275*, 18344–18349.
75. Paxinou, E.; Chen, Q.; Weisse, M.; Giasson, B. I.; Norris, E. H.; Rueter, S. M.; Trojanowski, J. Q.; Lee, V. M.; Ischiropoulos, H. *J. Neurosci.* **2001**, *21*, 8053–8061.
76. Turnbull, S.; Tabner, B. J.; El-Agnaf, O. M.; Moore, S.; Davies, Y.; Allsop, D. *Free Radical Biol. Med.* **2001**, *30*, 1163–1170.
77. Conway, K. A.; Rochet, J. C.; Bieganski, R. M.; Lansbury, P. T., Jr. *Science* **2001**, *294*, 1346–1349.

Publication Date (Web): October 13, 2015 | doi: 10.1021/bk-2015-1200.ch005

78. Mosharov, E. V.; Staal, R. G.; Bove, J.; Prou, D.; Hananiya, A.; Markov, D.; Poulsen, N.; Larsen, K. E.; Moore, C. M.; Troyer, M. D.; Edwards, R. H.; Przedborski, S.; Sulzer, D. *J. Neurosci.* **2006**, *26*, 9304–9311.
79. Hasegawa, T.; Matsuzaki-Kobayashi, M.; Takeda, A.; Sugeno, N.; Kikuchi, A.; Furukawa, K.; Perry, G.; Smith, M. A.; Itoyama, Y. *FEBS Lett.* **2006**, *580*, 2147–2152.
80. Lotharius, J.; Brundin, P. *Hum. Mol. Genet.* **2002**, *11*, 2395–2407.
81. Lee, F. J.; Liu, F.; Pristupa, Z. B. *FASEB J.* **2001**, *15*, 916–926.
82. Devi, L.; Raghavendran, V.; Prabhu, B. M.; Avadhani, N. G.; Anandatheerthavarada, H. K. *J. Biol. Chem.* **2008**, *283*, 9089–9100.
83. Nakamura, K. *Neurotherapeutics* **2013**, *10*, 391–399.
84. Li, W. W.; Yang, R.; Guo, J. C.; Ren, H. M.; Zha, X. L.; Cheng, J. S.; Cai, D. F. *Neuroreport* **2007**, *18*, 1543–1546.
85. Martin, L. J.; Pan, Y.; Price, A. C.; Sterling, W.; Copeland, N. G.; Jenkins, N. A.; Price, D. L.; Lee, M. K. *J. Neurosci.* **2006**, *26*, 41–50.
86. Chu, C. T.; Ji, J.; Dagda, R. K.; Jiang, J. F.; Tyurina, Y. Y.; Kapralov, A. A.; Tyurin, V. A.; Yanamala, N.; Shrivastava, I. H.; Mohammadyani, D.; Qiang Wang, K. Z.; Zhu, J.; Klein-Seetharaman, J.; Balasubramanian, K.; Amoscato, A. A.; Borisenko, G.; Huang, Z.; Gusdon, A. M.; Cheikhi, A.; Steer, E. K.; Wang, R.; Baty, C.; Watkins, S.; Bahar, I.; Bayir, H.; Kagan, V. E. *Nat. Cell Biol.* **2013**, *15*, 1197–1205.
87. Zigoneanu, I. G.; Yang, Y. J.; Krois, A. S.; Haque, E.; Pielak, G. J. *Biochim. Biophys. Acta* **2012**, *1818*, 512–519.
88. Robotta, M.; Gerding, H. R.; Vogel, A.; Hauser, K.; Schildknecht, S.; Karreman, C.; Leist, M.; Subramaniam, V.; Drescher, M. *ChemBioChem* **2014**, *15*, 2499–2502.
89. Martin, L. J.; Semenkow, S.; Hanaford, A.; Wong, M. *Neurobiol. Aging* **2014**, *35*, 1132–1152.
90. Siddiqui, A.; Chinta, S. J.; Mallajosyula, J. K.; Rajagopolan, S.; Hanson, I.; Rane, A.; Melov, S.; Andersen, J. K. *Free Radical Bio.l Med.* **2012**, *53*, 993–1003.
91. Sherer, T. B.; Kim, J. H.; Betarbet, R.; Greenamyre, J. T. *Exp. Neurol.* **2003**, *179*, 9–16.
92. Binukumar, B. K.; Bal, A.; Kandimalla, R. J.; Gill, K. D. *Mol. Brain* **2010**, *3*, 35.
93. Fernagut, P. O.; Hutson, C. B.; Fleming, S. M.; Tetreaut, N. A.; Salcedo, J.; Masliah, E.; Chesselet, M. F. *Synapse* **2007**, *61*, 991–1001.
94. Nieto, M.; Gil-Bea, F. J.; Dalfo, E.; Cuadrado, M.; Cabodevilla, F.; Sanchez, B.; Catena, S.; Sesma, T; Ribe, E.; Ferrer, I.; Ramirez, M. J.; Gomez-Isla, T. *Neurobiol. Aging* **2006**, *27*, 848–856.
95. Piltonen, M.; Savolainen, M.; Patrikainen, S.; Baekelandt, V.; Myohanen, T. T.; Mannisto, P. T. *Neuroscience* **2013**, *231*, 157–168.
96. Song, D. D.; Shults, C. W.; Sisk, A.; Rockenstein, E.; Masliah, E. *Exp. Neurol.* **2004**, *186*, 158–172.
97. Thomas, B.; Mandir, A. S.; West, N.; Liu, Y.; Andrabi, S. A.; Stirling, W.; Dawson, V. L.; Dawson, T. M.; Lee, M. K. *PLoS One* **2011**, *6*, e16706.

Publication Date (Web): October 13, 2015 | doi: 10.1021/bk-2015-1200.ch005

98. Klivenyi, P.; Siwek, D.; Gardian, G.; Yang, L.; Starkov, A.; Cleren, C.; Ferrante, R. J.; Kowall, N. W.; Abeliovich, A.; Beal, M. F. *Neurobiol. Dis.* **2006**, *21*, 541–548.
99. Wilkaniec, A.; Strosznajder, J. B.; Adamczyk, A. *Neurochem. Int.* **2013**, *62*, 776–783.
100. Su, X.; Maguire-Zeiss, K. A.; Giuliano, R.; Prifti, L.; Federoff, H. J. *Neurobiol. Aging* **2008**, *29*, 1690–1701.
101. Croisier, E.; Moran, L. B.; Dexter, D. T.; Pearce, R. K.; Graeber, M. B. *J. Neuroinflammation* **2005**, *2*, 14.
102. Kim, Y. S.; Joh, T. H. *Exp. Mol. Med.* **2006**, *38*, 333–347.
103. Beraud, D.; Hathaway, H. A.; Trecki, J.; Chasavskikh, S.; Johnson, D. A.; Johnson, J. A.; Federogg, H. J.; Shimoji, M.; Maguire-Zeiss, K. A. *J. Neuroimmune Pharmacol.* **2013**, *8*, 94–117.
104. Beraud, D.; Twomey, M.; Bloom, B.; Mittereder, A.; Ton, V.; Neitzke, K.; Chasovskikh, S.; Mhyre, T. R.; Maguire-Zeiss, K. A. *Front Neurosci.* **2011**, *5*, 80.
105. Couch, Y.; Alvarez-Erviti, L.; Sibson, N. R.; Wood, M. J.; Anthony, D. C. *J Neuroinflammation* **2011**, *8*, 166.
106. Klegeris, A.; Pelech, S.; Giasson, B. I.; Maguire, J.; Zhang, H.; McGeer, E. G.; McGeer, P. L. *Neurobiol. Aging* **2008**, *29*, 739–752.
107. Thomas, M. P.; Chartrand, K.; Reynolds, A.; Vitvitsky, V.; Banerjee, R.; Gendelman, H. E. *J. Neurochem.* **2007**, *100*, 503–519.
108. Zhou, W.; Freed, C. R. *J. Biol. Chem.* **2005**, *280*, 43150–43158.
109. Roodveldt, C.; Christodoulou, J.; Dobson, C. M. *J. Cell Mol. Med.* **2008**, *12*, 1820–1829.
110. Benner, E. J.; Banerjee, R.; Reynolds, A. D.; Sherman, S.; Pisarev, V. M.; Tsiperson, V.; Nemachek, C.; Ciborowski, P.; Przedborski, S.; Mosley, R. L.; Gendelman, H. E. *PLoS One* **2008**, *3*, e1376.
111. Gao, H. M.; Zhang, F.; Zhou, H.; Kam, W.; Wilson, B.; Hong, J. S. *Environ. Health Perspect.* **2011**, *119*, 807–814.
112. Kim, C.; Ho, D. H.; Suk, J. E.; You, S.; Michael, S.; Kang, J.; Joong Lee, S.; Masliah, E.; Lee, H. J.; Lee, S. J. *Nat. Commun.* **2013**, *4*, 1562.
113. Doorn, K. J.; Moors, T.; Drukarch, B.; van de Berg, WDj.; Lucassen, P. J.; van Dam, A. M. *Acta Neuropathol. Commun.* **2014**, *2*, 90.
114. Kitada, T.; Asakawa, S.; Hattori, N.; Matsumine, H.; Yamamura, Y.; Minoshima, S.; Yokochi, M.; Mizuno, Y.; Shimizu, N. *Nature* **1998**, *392*, 605–608.
115. Feany, M. B.; Pallanck, L. J. *Neuron* **2003**, *38*, 13–16.
116. Jiang, H.; Ren, Y.; Zhao, J.; Feng, J. *Hum. Mol. Genet.* **2004**, *13*, 1745–1754.
117. Hyun, D. H.; Lee, M.; Hattori, N.; Kubo, S.; Mizuno, Y.; Halliwell, B.; Jenner, P. *J. Biol. Chem.* **2002**, *277*, 28572–28577.
118. LaVoie, M. J.; Ostaszewski, B. L.; Weihofen, A.; Schlossmacher, M. G.; Selkoe, D. J. *Nat. Med.* **2005**, *11*, 1214–21.
119. Chung, K. K.; Thomas, B.; Li, X.; Pletnikova, O.; Troncoso, J. C.; Marsh, L.; Dawson, V. L.; Dason, T. M. *Science* **2004**, *304*, 1328–1331.

Publication Date (Web): October 13, 2015 | doi: 10.1021/bk-2015-1200.ch005

120. Wang, C.; Ko, H. S.; Thomas, B.; Tsang, F.; Chew, K. C.; Tay, S. P.; Ho, M. W.; Lim, T. M.; Soong, T. W.; Pletnokova, O.; Troncoso, J.; Dawson, V. L.; Dawson, T. M. *Hum. Mol. Genet.* **2005**, *14*, 3885–3897.
121. Lim, K. L.; Ng, X. H.; Grace, L. G.; Yao, T. P. *Antioxid. Redox Signal.* **2012**, *16*, 935–949.
122. Youle, R. J.; Narendra, D. R. *Nat. Rev. Mol. Cell Biol.* **2011**, *12*, 9–14.
123. Valente, E. M.; Abou-Sleiman, P. M.; Caputo, V.; Muqit, M. M.; Harvey, K.; Gispert, S.; Ali, Z.; Del Truco, D.; Bentivoglio, A. R.; Healy, D. G.; Albanese, A.; Nussbaum, R.; Gonzalez-Maldonado, R.; Deller, T.; Salvi, S.; Cortelli, P.; Gilks, W. P.; Latchman, D. S.; Harvey, R. J.; Dallapiccola, B.; Auburger, G.; Wood, N. W. *Science* **2004**, *304*, 1158–1160.
124. Cookson, M. R. *Cold Spring Harb. Perspect. Med.* **2012**, *2*, a009415.
125. Rojas-Charry, L.; Cookson, M. R.; Nino, A.; Arboleda, H.; Arboleda, G. *Neurotoxicology* **2014**, *44*, 140–148.
126. Gautier, C. A.; Kitada, T; Shen, J. *Proc. Natl. Acad. Sci. U. S. A.* **2008**, *105*, 11364–11369.
127. Wood-Kaczmar, A.; Gandhi, S.; Yao, Z.; Abramov, A. Y.; Milijan, E. A.; Keen, G.; Stanyer, L.; Hargreaves, I.; Klupsch, K.; Deas, E.; Downward, J.; Mansfield, L.; Jat, P.; Taylor, J.; Heales, S.; Duchen, M. R.; Latchman, D.; Tabrizi, S. J.; Wood, N. W. *PLoS One* **2008**, *3*, e2455.
128. Dagda, R. K.; Cherra, S. J., 3rd; Kulich, S. M.; Tandon, A.; Park, D.; Chu, C. T. *J. Biol. Chem.* **2009**, *284*, 13843–13855.
129. Cui, M.; Tang, X.; Christian, W. V.; Yoon, Y.; Tieu, K. *J. Biol. Chem.* **2010**, *285*, 11740–11752.
130. Lutz, A. K.; Exner, N.; Fett, M. E.; Schlehe, J. S.; Kloos, K.; Lammermann, K.; Brunner, B.; Kurz-Drexler, A.; Vogel, F.; Reichert, A. S.; Bouman, L.; Vogt-Weisenhorn, D.; Wirst, W.; Tatzelt, J.; Haas, C.; Winklhofer, K. F. *J. Biol. Chem.* **2009**, *284*, 22938–22951.
131. Sandebring, A.; Thomas, K. J.; Bellina, A.; van der Brug, M.; Cleland, M. M.; Ahmad, R.; Miller, D. W.; Zambrano, I.; Cowburn, R. F.; Behbahani, H.; Cedazo-Minguez, A.; Cookson, M. R. *PLoS One* **2009**, *4*, e5701.
132. Gegg, M. E.; Cooper, J. M.; Schapira, A. H.; Taanman, J. W. *PLoS One* **2009**, *4*, e4756.
133. Morais, V. A.; Verstreken, P.; Roethig, A.; Smet, J.; Snellinx, A.; Vanbrabant, M.; Haddad, D.; Frezza, C.; Mandemakers, W.; Vogt-Weisenhorn, D.; Van Coster, R.; Wurst, W.; Scorrano, L.; De Stropper, B. *EMBO Mol Med.* **2009**, *1*, 99–111.
134. Chan, C. S.; Guzman, J. N.; Illijic, E.; Mercer, J. N.; Rick, C.; Tkatch, T.; Meredith, G. E.; Surmeier, D. J. *Nature* **2007**, *447*, 1081–1086.
135. Guzman, J. N.; Sanchez- Padilla, J.; Wokosin, D.; Kondapalli, J.; Illijic, E.; Schumacker, P. T.; Surmeier, D. J. *Nature* **2010**, *468*, 696–700.
136. Gandhi, S.; Wood-Kaczmar, A.; Yao, Z.; Plun-Favreau, H.; Deas, E.; Klupsch, K.; Downward, J.; Latchman, D. S.; Tabrizi, S. J.; Wood, N. W.; Duchen, M. R.; Abramov, A. Y. *Mol Cell.* **2009**, *33*, 627–638.
137. Chien, W. L.; Lee, T. R.; Hung, S. Y.; Kang, K. H.; Wu, R. M.; Lee, M. J.; Fu, W. M. *Free Radical Biol. Med.* **2013**, *58*, 160–169.

Publication Date (Web): October 13, 2015 | doi: 10.1021/bk-2015-1200.ch005

Publication Date (Web): October 13, 2015 | doi: 10.1021/bk-2015-1200.ch005

138. Cooper, O.; Seo, H.; Andrabi, S.; Guardia-Laguarta, C.; Graziotto, J.; Sundberg, M.; McLean, J. R.; Carrilo-Reid, L.; Xie, Z.; Osborn, T.; Hargus, G.; Deleidi, M.; Lawson, T.; Bogetofte, H.; Perez-Torres, E.; Clark, L.; Moskowitz, C.; Mazzulli, J.; Chen, L.; Volpicelli-Daley, L.; Romero, N.; Jiang, H.; Uitti, R. J.; Huang, Z.; Opala, G.; Scarffe, L. A.; Dawson, V. L.; Klein, C.; Feng, J.; Ross, O. A.; Trojanowski, J. Q.; Lee, V. M.; Marder, K.; Surmeier, D. J.; Wszolek, Z. K.; Przedborski, S.; Krainc, D.; Dawson, T. M T. M.; Isacson, O. *Sci. Transl. Med.* **2012**, *4*, 141ra90.
139. Bonifati, V.; Rizzu, P.; van Baren, M. J.; Schaap, O.; Breedveld, G. J.; Krieger, E.; Dekker, M. C.; Squitieri, F.; Ibanez, P.; Josse, M.; van Dongen, J. W.; Vanacore, N.; van Swieten, J. C.; Brice, A.; Meco, G.; van Dujin, C. M.; Oostra, B. A.; Heutink, P. *Science* **2003**, *299*, 256–259.
140. Mitsumoto, A.; Nakagawa, Y. *Free Radical Res.* **2001**, *35*, 885–93.
141. Taira, T.; Saito, Y.; Niki, T.; Iguchi-Ariga, S. M.; Takahashi, K.; Ariga, H. *EMBO Rep.* **2004**, *5*, 213–218.
142. Martinat, C.; Shendelman, S.; Jonason, A.; Leete, T.; Beal, M. F.; Yang, L.; Floss, T.; Abeliovich, A. *PLoS Biol.* **2004**, *2*, e327.
143. Canet-Aviles, R. M.; Wilson, M. A.; Ahmad, R.; McLendon, C.; Bandyopadhyay, S.; Baptista, M. J.; Ringe, D.; Petsko, G. A.; Cookson, M. R. *Proc. Natl. Acad. Sci. U. S. A.* **2004**, *101*, 9103–9108.
144. Takahashi-Niki, K.; Niki, T.; Taira, T.; Iguchi-Ariga, S. M.; Ariga, H. *Biochem. Biophys. Res. Commun.* **2004**, *320*, 389–397.
145. Kim, R. H.; Peters, M.; Jang, Y.; Shi, W.; Pintille, M.; Fletcher, G. C.; DeLuca, C.; Liepa, J.; Zhou, L.; Snow, B.; Binari, R. C.; Manoukian, A. S.; Bray, M. R.; Liu, F. F.; Tsao, M. S.; Mak, T. W. *Cancer Cell* **2005**, *7*, 263–273.
146. Park, J.; Kim, S. Y.; Cha, G. H.; Lee, S. B.; Kim, S.; Chung, J. *Gene* **2005**, *361*, 133–139.
147. Meulener, M. C.; Xu, K.; Thomson, L.; Ischiropoulos, H.; Bonini, N. M. *Proc. Natl. Acad. Sci. U. S. A.* **2006**, *103*, 12517–12522.
148. Kahle, P. J.; Waak, J.; Gasser, T. *Free Radical Biol. Med.* **2009**, *47*, 1354–1361.
149. Takahashi, K.; Taira, T.; Niki, T; Seino, C.; Iguchi-Ariga, S. M.; Ariga, H. *J. Biol. Chem.* **2001**, *276*, 37556–37563.
150. Junn, E.; Taniguchi, H.; Jeong, B. S.; Zhao, X.; Ichijo, H.; Mouradian, M. M. *Proc. Natl. Acad. Sci. U. S. A.* **2005**, *102*, 9691–9696.
151. Xu, J.; Zhong, N.; Wang, H.; Elias, J. E.; Kim, C. Y.; Woldman, I.; Pifi, C.; Gygi, S. P.; Geula, C.; Yankner, B. A. *Hum. Mol. Genet.* **2005**, *14*, 1231–41.
152. Clements, C. M.; McNally, R. S.; Conti, B. J.; Mak, T. W.; Ting, J. P. *Proc. Natl. Acad. Sci. U. S. A.* **2006**, *103*, 15091–6.
153. Malhotra, D.; Thimmulappa, R.; Navas-Acien, A.; Sandford, A.; Elliott, M.; Singh, A.; Chen, L.; Zhuang, X.; Hogg, J.; Pare, P.; Tuder, R. M.; Biswal, S. *Am. J. Respir. Crit. Care Med.* **2008**, *178*, 592–604.
154. Lev, N.; Ickowicz, D.; Barhum, Y.; Lev, S.; Melamed, E.; Offen, D. *J. Gerontol., Ser. A* **2013**, *68*, 215–225.
155. Ishikawa, S.; Tanaka, Y.; Takahashi-Niki, K.; Niki, T.; Ariga, H.; Iguchi-Ariga, S. M. *Biochem. Biophys. Res. Commun.* **2012**, *421*, 813–818.

156. Yokota, T.; Sugawara, K.; Ito, K.; Takahashi, R.; Ariga, H.; Mizusawa, H. *Biochem. Biophys. Res. Commun.* **2003**, *312*, 1342–1348.
157. van der Brug, M. P.; Blackinton, J.; Chandran, J.; Hao, L. Y.; Lal, A.; Mazan-Mamczarz, K.; Martindale, J.; Xie, C.; Ahmad, R.; Thomas, K. J.; Beilina, A.; Gibbs, J. R.; Ding, J.; Myers, A. J.; Zhan, M.; Cai, H.; Bonini, N. M.; Gorospe, M.; Cookson, M. R. *Proc. Natl. Acad. Sci. U. S. A.* **2008**, *105*, 10244–10249.
158. Ottolini, D.; Cali, T.; Negro, A.; Brini, M. *Hum. Mol. Genet.* **2013**, *22*, 2152–2168.
159. Larsen, N. J.; Ambrosi, G.; Mullett, S. J.; Berman, S. B.; Hinkle, D. A. *Neuroscience* **2011**, *196*, 251–264.
160. Mullett, S. J.; Hinkle, D. A. *J. Neurochem.* **2011**, *117*, 375–387.
161. Gonzalez-Polo, R.; Niso-Santano, M.; Moran, J. M.; Ortiz-Ortiz, M. A.; Bravo-San Pedro, J. M.; Soler, G.; Fuentes, J. M. *J. Neurochem.* **2009**, *109*, 889–898.
162. Yamashita, S.; Mori, A.; Kimura, E.; Mita, S.; Maeda, Y.; Hirano, T.; Uchino, M. *J. Neurochem.* **2010**, *113*, 860–870.
163. Lev, N.; Ickowicz, D.; Barhum, Y.; Lev, S.; Melamed, E.; Offen, D. *J. Neural Transm.* **2009**, *116*, 151–160.
164. West, A. B.; Moore, D. J.; Biskup, S.; Bugayenko, A.; Smith, W. W.; Ross, C. A.; Dawson, V. L.; Dawson, T. M. *Proc. Natl. Acad. Sci. U. S. A.* **2005**, *102*, 16842–16847.
165. West, A. B.; Moore, D. J.; Choi, C.; Andrabi, S. A.; Li, X.; Dikeman, D.; Biskup, S.; Zhang, Z.; Lim, K. L.; Dawson, V. L.; Dawson, T. M. *Hum. Mol. Genet.* **2007**, *16*, 223–232.
166. White, L. R.; Toft, M.; Kvam, S. N.; Farrer, M. J.; Aasly, J. O. *J. Neurosci. Res.* **2007**, *85*, 1288–1294.
167. Jaleel, M.; Nichols, R. J.; Deak, M.; Campbell, D. G.; Gillardon, F.; Knebel, A.; Alessi, D. R. *Biochem J.* **2007**, *405*, 307–317.
168. Guo, L.; Gandhi, P. N.; Wang, W.; Petersen, R. B.; Wilson-Delfosse, A. L.; Chen, S. G. *Exp. Cell Res.* **2007**, *313*, 3658–3670.
169. Zimprich, A.; Biskup, S.; Leitner, P.; Lichtner, P.; Farrer, M.; Lincoln, S.; Kachergus, J.; Hulihan, M.; Uitti, R. J.; Calne, D. B.; Stoessl, A. J.; Pfeiffer, R. F.; Patenge, N.; Carbajal, I. C.; Vieregge, P.; Asmus, F.; Muller-Myhsok, B.; Dickson, D. W.; Meitinger, T.; Strom, T. M.; Wszolek, Z. K.; Gasser, T. *Neuron.* **2004**, *44*, 601–607.
170. Wang, X.; Yan, M. H.; Fujioka, H.; Liu, J.; Wilson-Delfosse, A.; Chen, G.; Perry, G.; Casadesus, G.; Zhu, X. *Hum. Mol. Genet.* **2012**, *21*, 1931–1944.
171. Niu, J.; Yu, M.; Wang, C.; Xu, Z. *J. Neurochem.* **2012**, *122*, 650–658.
172. Heo, H. Y.; Park, J. M.; Kim, C. H.; Han, B. S.; Kim, K. S.; Seol, W. *Exp. Cell Res.* **2010**, *316*, 649–656.
173. Nguyen, H. N.; Byers, B.; Cord, B.; Shcheglovitov, A.; Byrne, J.; Gujar, P.; Kee, L.; Schule, B.; Dolmetsch, R. E.; Langston, W.; Palmer, T. D.; Pera, R. R. *Cell Stem Cell* **2011**, *8*, 267–280.
174. Angeles, D. C.; Gan, B. H.; Onstead, L.; Zhao, Y.; Lim, K. L.; Daschel, J.; Melrose, H.; Farrer, M.; Wszolek, Z. K.; Dickson, D. W.; Tan, E. K. *Hum. Mutat.* **2011**, *32*, 1390–1397.

In Oxidative Stress: Diagnostics, Prevention, and Therapy Volume 2; Hepel, et al.;
ACS Symposium Series; American Chemical Society: Washington, DC, 2015.

Publication Date (Web): October 13, 2015 | doi: 10.1021/bk-2015-1200.ch005

175. Piccoli, G.; Condiliffe, S. B.; Bauer, M.; Giesert, F.; Boldt, K.; De Astis, S.; Meixner, A.; Sarioglu, H.; Vogt-Weisenhorn, D. M.; Wurst, W.; Gloeckner, C. J.; Matteoli, M.; Sala, C.; Ueffing, M. *J. Neurosci.* **2011**, *31*, 2225–2237.
176. Matta, S.; Van Kolen, K.; da Cunha, R.; van den Bogaart, G.; Mandemakers, W.; Miskiewicz, K.; De Bock, P. J.; Morais, V. A.; Vilain, S.; Haddad, D.; Delbroek, L.; Swerts, J.; Chavez-Guitierrez, L.; Esposito, G.; Daneels, G.; Karran, E; Holt, M.; Gevaert, K.; Moeschars, D. W.; De Strooper, B.; Verstreken, P. *Neuron* **2012**, *75*, 1008–1021.
177. Kett, L. R.; Boassa, D.; Ho, C. C.; Rideout, H. J.; Hu, J.; Terada, M.; Ellisman, M.; Dauer, W. T. *Hum. Mol. Genet.* **2012**, *21*, 890–899.
178. Law, B. M.; Spain, V. A.; Leinster, V. H.; Chia, R.; Beilina, A.; Cho, H. J.; Taymans, J. M.; Urban, M. K.; Sancho, R. M.; Blanca Ramirez, M.; Biskup, S.; Baekelandt, V.; Cai, H.; Cookson, M. R.; Berwick, D. C.; Harvey, K. *J. Biol. Chem.* **2014**, *289*, 895–908.
179. Papkovskaia, T. D.; Chau, K. Y.; Inesta-Vaquera, F.; Papkovsky, D. B.; Healy, D. G.; Nishio, K.; Staddon, J.; Duchen, M. R.; Hardy, J.; Schapira, A. H.; Cooper, J. M. *Hum. Mol. Genet.* **2012**, *21*, 4201–4213.
180. Plowey, E. D.; Cherra, S. J., 3rd; Liu, Y. J.; Chu, C. T. *J. Neurochem.* **2008**, *105*, 1048–1056.
181. Gomez-Suaga, P.; Luzon-Toro, B; Churamani, D.; Zhang, L.; Bloor-Young, D.; Patel, S.; Woodman, P. G.; Churchill, G. C.; Hilfiker, S. *Hum. Mol. Genet.* **2012**, *21*, 511–525.
182. Manzoni, C.; Lewis, P. A. *FASEB J.* **2013**, *27*, 3424–3429.
183. Orenstein, S. J.; Kuo, S. H.; Tasset, I.; Arias, E.; Koga, H.; Fernandez-Carasa, I.; Cortes, E.; Honig, L. S.; Dauer, W.; Consiglio, A.; Raya, A.; Sulzer, D.; Cuervo, A. M. *Nat. Neurosci.* **2013**, *16*, 394–406.
184. Russo, I.; Bubacco, L.; Greggio, E. *J. Neuroinflammation* **2014**, *11*, 52.
185. Moehle, M. S.; Webber, P. J.; Tse, T.; Sukar, N.; Standaert, D. G.; DeSilva, T. M.; Cowell, R. M.; West, A. B. *J. Neurosci.* **2012**, *32*, 1602–1611.
186. Daher, J. P.; Volpicelli-Daley, L. A.; Blackburn, J. P.; Moehle, M. S.; West, A. B. *Proc. Natl. Acad. Sci. U. S. A.* **2014**, *111*, 9289–9294.
187. Parkinson Study Group. *N. Engl. J. Med.* **1993**, *328*, 176–183.
188. Parkinson Study Group. *Arch Neurol.* **2002**, *59*, 1937–1943.
189. Olanow, C. W.; Rascol, O.; Hauser, R.; Feigin, P. D.; Jankovic, J.; Lang, A.; Langston, J. W.; Melamed, E.; Poewe, W.; Stocchi, F.; Tolosa, E. *N. Engl. J. Med.* **2009**, *361*, 1268–1278 (Adagio Study Investigators).
190. Beal, M. F. *Free Radical Res.* **2002**, *36*, 455–460.
191. Parkinson Study Group. *JAMA Neurol* **2014**, *71*, 543–552.
192. Beal, M. F. *Amino Acids* **2011**, *40*, 1305–1313.
193. Writing Group for the N.E.T.i.P.D.I. *JAMA* **2015**, *313*, 584–593.
194. Tauskela, J. S. *IDrugs* **2007**, *10*, 399–412.
195. Snow, B. J.; Rolfe, F. L.; Lockhart, M. M.; Frampton, C. M.; O'Sullivan, J. D.; Fung, V.; Smith, R. A.; Murphy, M. P.; Taylor, K. M. *Mov. Disord.* **2010**, *25*, 1670–1674 (Protect Study Group).
196. Asanuma, M.; Miyazaki, I. *Curr. Pharm. Des.* **2008**, *14*, 1428–1434.

Publication Date (Web): October 13, 2015 | doi: 10.1021/bk-2015-1200.ch005

197. Gao, X.; Chen, X.; Schwarzschild, M. A.; Ascherio, A. *Neurology* **2011**, *76*, 863–869.
198. Selley, M. L. *Brain Res.* **2005**, *1037*, 1–6.
199. Wolozin, B.; Wang, S. W.; Li, N. C.; Lee, A.; Lee, T. A.; Kazis, L. E. *BMC Med.* **2007**, *5*, 20.
200. Wahner, A. D.; Bronstein, J. M.; Bordelon, Y. M.; Ritz, B. *Neurology* **2008**, *70*, 1418–1422.
201. de Lau, L. M.; Koudstaal, P. J.; Hofman, A.; Breteler, M. M. *Am. J. Epidemiol.* **2006**, *164*, 998–1002.
202. Huang, X.; Chen, H.; Miller, W. C.; Mailman, R. B.; Woodard, J. L.; Chen, P. C.; Xiang, D.; Murrow, R. W.; Wang, Y. Z.; Poole, C. *Mov. Disord.* **2007**, *22*, 377–381.
203. Moi, P.; Chan, K.; Asunis, I.; Cao, A.; Kan, Y. W. *Proc. Natl. Acad. Sci. U. S. A.* **1994**, *91*, 9926–9930.
204. Gan, L.; Vargas, M. R.; Johnson, D. A.; Johnson, J. A. *J. Neurosci.* **2012**, *32*, 17775–17787.
205. Kaidery, N. A.; Banerjee, R.; Yang, L.; Smirnova, N. A.; Hushpulian, D. M.; Liby, K. T.; Williams, C. R.; Yamamoto, M.; Kensler, T. W.; Ratan, R. R.; Sporn, M. B.; Beal, M. F.; Gazaryan, I. G.; Thomas, B. *Antioxid. Redox Signal.* **2013**, *18*, 139–57.
206. Zhang, N.; Shu, H. Y.; Huang, T.; Zhang, Q. L.; Li, D.; Zhang, G. Q.; Peng, X. Y.; Liu, C. F.; Luo, W. F.; Hu, L. F. *PLoS One* **2014**, *9*, e100286.
207. Jhang, J. J.; Cheng, Y. T.; Ho, C. Y.; Yen, G. C. *Cell. Mol. Immunol.* **2014**, *12*, 424–434.
208. Davis, J. W.; Grandinetti, A.; Waslien, C. I.; Ross, G. W.; White, L. R.; Morens, D. M.; Grandinetti, A.; Waslien, C. I.; White, L. R.; Morens, D. M. *Am. J. Epidemiol.* **1996**, *144*, 480–484.
209. Weisskopf, M. G.; O'Reilly, E.; Chen, H.; Schwarzchild, M. A.; Ascherio, A. *Am. J. Epidemiol.* **2007**, *166*, 561–567.
210. Alonso, A.; Rodriguez, L. A.; Logroscino, G.; Hernan, M. A. *Neurology* **2007**, *69*, 1696–700.
211. Schwarzschild, M. A.; Schwid, S. R.; Marek, K.; Watts, A.; Lang, A. E.; Oakes, D.; Shoulson, I.; Ascherio, A. *Arch Neurol.* **2008**, *65*, 716–723 (Parkinson Study Group, Precept Investigators).
212. Gao, X.; Chen, X.; Choi, H. K.; Curhan, G.; Schwarzschild, M. A.; Ascherio, A. *Am J Epidemiol.* **2008**, *167*, 831–838.
213. Parkinson Study Group, S.-P.D.I. *JAMA Neurol* **2014**, *71*, 141–50.
214. Gold, R.; Kappos, L.; Arnold, D. L.; Bar-Or, A.; Giovannoni, G.; Selmaj, K.; Tornatore, C.; Sweetser, M. T.; Yang, M.; Sheikh, S. I.; Dawson, K. T. *N. Engl. J. Med.* **2012**, *367*, 1098–1107 (Define Study Investigators).
215. Fox, R. J.; Miller, D. H.; Phillips, J. T.; Hutchinson, M.; Havrdova, E.; Kita, M.; Yang, M.; Raghupathi, K.; Novas, M.; Sweetser, M. T.; Viglietta, V.; Dawson, K. T. *N. Engl. J. Med.* **2012**, *367*, 1087–1097 (Confirm Study Investigators).
216. Jing, X.; Shi, H.; Zhang, C.; Ren, M.; Han, M.; Wei, X.; Zhang, X.; Lou, H. *Neuroscience* **2015**, *286*, 131–140.
217. Athauda, D.; Foltynie, T. *Nat. Rev. Neurol.* **2015**, *11*, 25–40.

Publication Date (Web): October 13, 2015 | doi: 10.1021/bk-2015-1200.ch005

218. Goetz, C. G.; Tilley, B. C.; Shaftman, S. R.; Stebbins, G. T.; Fahn, S.; Martinez-Martin, P.; Poewe, W.; Sampaio, C.; Stern, M. B.; Dodel, R.; Dubois, B.; Holloway, R.; Jankovic, J.; Kulisevsky, J.; Lang, A. E.; Lees, A.; Leurgans, S.; LeWitt, P. A.; Nyenhuis, D.; Olanow, C. W.; Rascol, O.; Schrag, A.; Teresi, J. A.; van Hilten, J. J.; LaPelle, N. *Mov. Disord.* **2008**, *23*, 2129–2170 (Movement Disorder Society, UPDRS Revision Task Force).
219. Beal, M. F. *Nature* **2010**, *466*, S8–S10.

Publication Date (Web): October 13, 2015 | doi: 10.1021/bk-2015-1200.ch005

Publication Date (Web): October 13, 2015 | doi: 10.1021/bk-2015-1200.ch006

Chapter 6

Oxidative Stress in the Aging Process: Fundamental Aspects and New Insights

Lizette Gil del Valle,[1,*] Rosario Gravier Hernández,[1] Livan Delgado Roche,[2] and Olga Sonia León Fernández[2]

[1]Institute of Tropical Medicine "Pedro Kourí" (IPK), La Habana, Cuba
[2]Institute of Pharmacy and Food, Havana University, Cuba
[*]E-mail: lgil@ipk.sld.cu

Aging researches have experienced an unprecedented advance over recent years. The comprehension of process leading to age-associated alterations is at moment of the highest relevance for the development of new treatments for age-associated diseases, such as cancer, diabetes, Alzheimer and cardiovascular accidents but also to encourage healthy gain of years with high standard of quality of life. It is widely considered that the accumulation of molecular and cellular damage influenced by reactive oxygen species might orchestrate the progressive loss of control over biological homeostasis and the functional impairment typical of aged tissues. Here, we review how resulting oxidative stress-redox disruption signal took part in the mechanisms of ageing physiology and physiopathology. The discovery that the rate of aging is controlled, at least to some extent, by genetic pathways and biochemical processes conserved in evolution is discussed and integrate to common denominators of aging in different organisms, with special emphasis on mammalian aging. The aspects considered in revision are: genomic instability, telomere attrition, epigenetic alterations, loss of proteostasis, deregulated nutrient sensing, mitochondrial dysfunction, cellular senescence, stem cell exhaustion, and altered intercellular communication. Based on these critical aspects the revisited aging associated mechanisms causing damage, the compensatory responses leading to homeostasis reestablishment and the interconnection between them are analyzed and explore with the final goal of identifying

In Oxidative Stress: Diagnostics, Prevention, and Therapy Volume 2; Hepel, et al.;
ACS Symposium Series; American Chemical Society: Washington, DC, 2015.

pharmaceutical targets to improve human health during aging, with minimal side effects.

Introduction

Aging have been defined as the process of physiological integrity -progressive detrimental with age leading to dysfunction, homeostasis impairment and also to increased vulnerability to death, and it could be defined as a complex chronological and multifactor (*1*, *2*). Accumulating findings indicate that longevity depends on the ability of the organism to cope with extrinsic or intrinsic stressors (*3*). Indeed, compromised stress responses are linked to the onset of many age related diseases. 'Stress' is broadly defined as a noxious factor (physical, chemical or biological), which triggers a series of cellular and systemic events, resulting in restoration of cellular and organismal homeostasis. To cope with conditions of stress, organisms have developed a wide range of sophisticated stress response mechanisms, acting at the cellular or organelle-specific level. Notably, exposure to mild stress activates cellular homeodynamic mechanisms, without mounting a comprehensive stress response, which better prepare the organism against stronger insults and promote long-term survival (*4*, *5*). There are several hypotheses to explain how aging occurs, considering complex physiological alteration in the organism described as: genomic instability, telomere attrition, epigenetic alterations, loss of proteostasis, deregulated nutrient sensing, mitochondrial dysfunction, cellular senescence, stem cell exhaustion, and altered intercellular communication. Historically, theories of aging have been divided into two general categories: stochastic and developmental-genetic. In stochastic theories investigators grouped in: somatic mutation and DNA repair, error-catastrophe, protein modification and free radical (oxidative stress/ mitochondrial DNA) theories. In developmental-genetic theories are defined ones that recognized the aging process to be part of the genetically programmed and controlled continuum of development and maturation. Longevity genes, accelerated aging syndromes, neuroendocrine, immunologic, cellular senescence and cell death theories are among them (*6–8*). These categories are not mutually exclusive. Indeed there is probably that maturation reflects a spectrum of changes from decreasing influence of active genetic factors and an increasing effect of stochastic events (*9*).

No theory has been generally accepted. The early observations on the rate-of-living theory by Max Rubner and the report by Gershman (*10*) that oxygen free radicals exist in vivo culminated in the seminal proposal in the 1954 by Denham Harman that reactive oxygen species (ROS) are a cause of aging (free radical theory of aging). This hypothesis of Free Radicals Theory of Aging (*11*) was after modified in 1972 (*12*) and the modern version of this tenet is the oxidative stress (OS) theory. The OS hypothesis offers the best mechanistic elucidation of the aging process and other age-related phenomena such as age-related diseases.

The OS hypothesis of aging postulates that accrual of macromolecular damage accumulation is due to the redox imbalance, i.e. the net effect of disparity between the amount of ROS generation and the counter-acting antioxidative

In Oxidative Stress: Diagnostics, Prevention, and Therapy Volume 2; Hepel, et al.;
ACS Symposium Series; American Chemical Society: Washington, DC, 2015.

Publication Date (Web): October 13, 2015 | doi: 10.1021/bk-2015-1200.ch006

forces. Mild OS is the result of normal metabolism; the resulting biomolecular damage cannot be totally repaired or removed by cellular degradation systems, like lysosomes, proteasomes, and cytosolic and mitochondrial proteases. The contemporary definition of OS has been refined (*13*, *14*) to account for two different mechanistic outcomes, macromolecular damage, and disruption of thiol redox circuits, which leads to aberrant cell signaling and dysfunctional redox control (*15*, *16*). The imbalance and disruption is induced by ROS increased generation of different organelle origin (mainly from endopslamatic reticulum and mitochondria). ROS are oxygen derived metabolites that have higher reactivity than molecular oxygen. ROS include unstable oxygen radicals such as superoxide radical ($O_2^{\cdot-}$) and hydroxyl radical (·OH) and nonradical molecules like hydrogen peroxide (H_2O_2) and peroxynitrite ($ONOO^-$). These reactive species and others, with nitrogen and sulphur atom in the chemical composition, are continually produced through diverse metabolic pathways as consequences of normal aerobic metabolism as well as taken up from the external environment (*17–19*). Thus all living organisms in an aerobic ambient are exposed to ROS on a continual basis.

ROS serve as specific signalling molecules in both, normal and pathological conditions, and their transient generation, within boundaries is essential to maintain homeostasis. ROS can inflict oxidative molecular damage to lipids, proteins and DNA when their production overwhelms the capacity of antioxidant systems (*16*, *20*, *21*). Biological effects initiated by ROS can elicit a wide range of phenotypic responses that vary from activation of gene expression, proliferation to growth arrest, to senescence or cell death (*22–24*).

Thiol-containing proteins that function in redox signaling and physiological regulation are susceptible to two-electron oxidation by nonradical oxidants, including H_2O_2, lipid hydroperoxides, aldehydes, quinones, and disulfides. Either abnormal oxidation or irreversible modification can interfere with reversible oxidation-reduction reactions of thiols that physiologically function in receptor signaling, transcriptional regulation, cell proliferation, angiogenesis, and apoptosis. Thus the contemporary refinement in definition of OS (*13*, *14*) represents a shift to include both nonradical oxidants and reversible oxidative reactions of redox signalling and control as key components of OS and the most recent studies support the idea that OS is a significant marker of senescence in different species. Resistance to OS is a common trait of long-lived genetic variations in mammals and lower organisms.

The OS theory does not limit the source of detrimental metabolites moreover its scope extends beyond oxidant damage to include roles for oxidants in physiological process. The resulting OS including biomolecule oxidation processes is suggested to be the central cause factor promoting aging process (*25*).

Age-related diseases are often considered to be distinct pathologies, rather than inevitable part of aging and a consequence of redox deregulation. Indeed a chronic inflammatory process is crucial associated with degenerative conditions during aging (*15*, *26*). The OS connotation to aging has been elucidated through previous research in animal's models (*27*, *28*).

Diverse molecular aspects are considering as essential and remark criteria that OS ideally involve three important connotations. 1. Its manifestation during aging process, 2. Its augmentation should accelerate aging process and, 3. Its

In Oxidative Stress: Diagnostics, Prevention, and Therapy Volume 2; Hepel, et al.;
ACS Symposium Series; American Chemical Society: Washington, DC, 2015.

Publication Date (Web): October 13, 2015 | doi: 10.1021/bk-2015-1200.ch006

amelioration should influence the normal aging and could influence also healthy span of life. Extensive experiments on caloric or dietary restriction (CR) have clearly shown that is possible retard the rate of aging and also extend both the life expectancy and maximum life span. Possible molecular mechanisms involve reduction on ROS production and the damage it cause (*29*, *30*). At the same time CR delays the occurrence of a wide range of age dependent disease and disabilities and slows down the rate of aging.

The functional consequence of an age related modifications in such biochemical's markers of OS has been little studied and remains therefore largely unknown. In recent years several related theories containing ROS have also been proposed. The Telomere shortening hypothesis, The Reproductive-cell cycle, The Wear and tear theory, Error accumulation and Accumulative waste theories, Mitohormesis, and the Disposable soma theory are among extensively studied all of them contributing to aging (*31–33*). Evidence implies that an important theme linking several different kinds of cellular damage is the consequence of exposure to ROS. The overall aim of this paper is a current review of the main aspects related to molecular mechanisms underlying aging and connects biological at molecular, cellular and organism level. Recent clinical evidences in humans of OS alterations are finally compared and maintaining efficient mechanisms for counterbalancing stress emerging as a potential strategy towards ameliorating age-associated pathologies is discussed.

Publication Date (Web): October 13, 2015 | doi: 10.1021/bk-2015-1200.ch006

Biological System Related to ROS Generation

For better comprehension of OS process, it is first important to understand ROS generation -biological systems. It is generally accepted that the respiratory chain is one of the most important if not the first source of ROS generation in animal and human body. Interrelationships between ROS generation and effects in mitochondria have been studied in detail (*20*, *34*).

This organelle produces ATP through a series of oxidative phosphorylation sequences that ultimately involve a four electron reduction of molecular oxygen to water. During these events one- or two-electron reductions of molecular oxygen can occur, generating ROS as anion superoxide radical and non radical metabolites as hydrogen peroxide (*18*, *35*). The oxygen metabolites can be converted to others ROS as carbonate radical. This modification occurs in presence of peroxynitrite mixtures. In mitochondria peroxynitrite are produced from reaction of anion superoxide radical and nitric oxide. This last are generated enzymatically by a family of nitric oxide synthases (NOS) (*36*). Indeed mitochondria generate and are in contact with different oxidants of diverse strength, reactive properties and ability to diffuse and to be removed. This last action occurs by interaction with specific antioxidants such as: catalase (CAT), peroxiredoxins and theirs associated reductases (glutathione peroxidase (GPx)/ glutathione reductase (GRx) system and thioredoxin peroxidase (TrxP)/ thioredoxin reductase (TRxR) system), NADH/NADP transhydrogenase, matrix Mn superoxide dismutase (SOD) and Cu / Zn SOD in intermembrane spaces. Responses to the ROS presence depend

In Oxidative Stress: Diagnostics, Prevention, and Therapy Volume 2; Hepel, et al.;
ACS Symposium Series; American Chemical Society: Washington, DC, 2015.

on the species, rate, quantity, accumulation, and microenvironment of generation (*18*, *37*).

Progressive decline in mitochondrial function with age associated to OS have been demonstrated in a variety of tissues (*19*, *38*, *39*). This decline is related to impairment of electron transport chain, elicited by respiratory inhibitors, mitochondrial DNA (mtDNA) mutation, or gene knock-out (*40*). The five enzyme complexes in the respiratory chain are composed of more than 100 polypeptides, most of which are encoded by genes in the nuclear genome. However the 13 polypeptides involved in oxidative phosphorylation are encoded by mtDNA (*36*, *37*). Mitochondrial biogenesis and respiration of the humans cells are controlled by nuclear factors NRF-1 and NRF-2, mitochondrial factor A, and the thermogenic coactivator PGC-1 (*21*, *24*). Thus, any molecular defects that lead to altered expressions of the mt DNA encoded genes or impairment in the biogenesis of mitochondria would cause a defective in energy metabolism of the affected tissue cells (*29*, *39*, *41*, *42*). Three major evidences lead to the conclusions that bioenergetic function declines with age. First Citochrome C oxidase-negative fibers are increased with age. Second the respiratory functions of isolated mitochondria and electron transfer activities of complexes gradually decline with age in human cells from different tissues associated to reduced steady state levels of mitochondrial transcripts. And third mitochondrial membrane potential, the driving force of oxidative phosphorylation is decreased in tissues aged cells of mammalians (*43*).

It is expected, in turns, that mitochondrial disorders be primarily manifested in the organs or tissues that have a high demand for energy.

A number of large-scale deletions, point mutations, and tandem duplications of mtDNA have been found in various mammalians aged tissues. mtDNA are present in 2 to 10 copies in mitochondria. Each mammalians cell contains several hundred to more than one thousand mitochondrias. The mutant mtDNA (s), possible due to exposure to elevated OS, usually coexist with the wild type mtDNA termed heteroplasmy, the degree of which often varies in different tissues of the same individuals. Mt DNA should be more susceptible to oxidative damage because is attached to the ROS-generating sites in the mitochondrial inner membrane (*44*). The frequency of occurrence and the type of mtDNA mutation are determined by the interaction between mtDNA polymerase that bear the ROS-induced oxidative damage during DNA replication (*19*, *43*, *45*).

Several recent studies also demonstrated that aged human cells harbouring mutated mtDNA and or defective mitochondria had lower respiratory functions. They exhibited higher rate of ROS production as superoxide anions, hydroxyl radicals and hydrogen peroxide. Genotoxic intermediates of lipid peroxidation may play a role in eliciting age associated DNA mutation. The researchers suggest that accumulation of age dependent mtDNA mutations would results from damage by ROS, effects which in turn may provide an extra source of oxidants (*2*, *18*, *19*, *41*, *46*).

These finding and others evidences have been support the notion that OS is an important contributor to decline of mitochondria functions during aging (*47*).

ROS are produced from others endogenous sources too and serve as specific signalling molecules under both physiological and pathophysiological conditions.

Publication Date (Web): October 13, 2015 | doi: 10.1021/bk-2015-1200.ch006

These others sources are: conversion of xanthine dehydrogenase (XDH) to xanthine oxidase (XOD), dopamine oxidation in the nervous central systems, reactions involving peroxisomal oxidases, cytochrome P-450 enzymes, NAD(P)H oxidases (NOX), Haber Weiss and Fenton reactions, NADH dehydrogenases, glucose oxidase, monoamine oxidase, cyclooxygenases, lipoxygenases, dehydrogenases, peroxidases, amino acid oxidases and NOS family (*16*, *22*, *25*, *35*).

The reactive species are involved in: modulation of transcription factors as AP-1, p53, Forkhead transcription factors and NF-κB, modulation of kinases (protein kinase C, MAP, ERK), phosphorylation (protein tyrosine, protein ser/thr) adenylyl and guanylyl cyclases activation, modulation of cell adhesion molecules expression, endonucleases and proteases activation, DNA synthesis and repair, modulation of apoptosis, telomere shortening, autophagy and cellular senescence (*15*, *35*, *48–50*).

Several specific types of environmental stress and exogenous stimuli can lead to production of ROS. This generation can be specific for particular tissues, cells and organelles.

The importance of mitochondria in both aging and age related disease is testified by research from Tanaka 1998 (*51*). They showed that two-tends of Japanese centenarians have a mitochondrial gene variant known as Mt5178A. This variant codes for a subunit of NADH dehydrogenase, at complex I of the respiratory chain and it is associated with a low leakage of ROS generation. These people not only survive to hundred but they were half as likely to be hospitalized for any age –related disease as people without the variant: a strong link between aging and age related disease (*52*).

However these findings it remains unclear whether the decline in mitochondrial functions during aging mainly results from OS or consequences of synergistic effects of many factors associated.

Endoplasmic reticulum (ER) is a cardinal membrane-bound organelle comprising of interconnected highly branched tubules, vesicles, and cisternae. It is found in all eukaryote cells and is the organelle where newly synthesized proteins destined for secretion, integration into the plasma membrane or distribution to various organelles, are folded and posttranslationally modified. It is crucially involved also in lipid synthesis, glycogen production and storage, and calcium metabolism (*53*). ER structure can be categorized as domains like nuclear envelope domain (array of proteins that are synthesized on rough ER and concentrated within the inner membrane), the rough and smooth ER domain (due to presence and absence of bound ribosomes respectively), and the regions that contact other organelles. The environment within the ER is highly crowded with chaperones, processing enzymes and client proteins (*54*). In this cluttered and aggregation-prone environment, complex ER quality control mechanisms ensure the proper translation and folding of nascent proteins as well as the degradation of improperly folded polypeptides. ER provides an exclusive oxidizing-folding environment to the proteins to facilitate disulfide bond formation and this process is believed to contribute to 25% of ROS generated by cell.

Chronic ER stress and activation of the unfolded-protein response (UPR) through endogenous or exogenous insults may result in impaired calcium and

In Oxidative Stress: Diagnostics, Prevention, and Therapy Volume 2; Hepel, et al.;
ACS Symposium Series; American Chemical Society: Washington, DC, 2015.

Publication Date (Web): October 13, 2015 | doi: 10.1021/bk-2015-1200.ch006

redox homeostasis, OS via protein overload thereby also influencing vital mitochondrial functions (*55*, *56*). Calcium released from the ER augments the production of mitochondrial ROS. Toxic accumulation of ROS within ER and mitochondria disturbs fundamental organelle functions. Sustained ER stress is known to potentially elicit inflammatory responses via UPR pathways. Additionally, ROS generated through inflammation or mitochondrial dysfunction could accelerate ER malfunction. Age-dependent decline of protein folding efficiency and dysfunctional UPR pathways creates an unstable ER environment, not capable of sustaining homeostasis under steady-state or elevated stress conditions and have been associated with a wide range of diseases including several neurodegenerative diseases, stroke, metabolic disorders, cancer, inflammatory disease, diabetes mellitus, cardiovascular disease, and others (*53*).

ER stress activates both the ubiquitin–proteasome and the macroautophagy–lysosome proteolytic system (*57*, *58*). Whether ageing hinders the activation of these degradation systems, leading to overflow of damaged proteins remains to be seen (*59*).

Autophagy is one of the main processes mediating both bulk and specific degradation of cellular components, including whole organelles and protein aggregates. Cargoes destined for degradation are delivered to lysosomes, where they are recycled. Three main types of autophagy have been defined on the basis of lysosomal delivery mechanisms: macroautophagy, microautophagy and chaperone-mediate autophagy (CMA) (*60*, *61*).

Macroautophagy entails the sequestration of portions of the cytoplasm within a double-membrane autophagic vacuole,called autophagosome. The autophagosome fuses with secondary lysosomes to form an autolysosome, where hydrolases degrade the sequestered material (*62*). In microautophagy, which is less well characterized, the lysosomal membrane itself invaginates to engulf cytosolic components. CMA is a highly selective form of autophagy that requires unfolding of the protein before internalization into the lysosome for degradation (*60*, *63*). In addition to turnover of cellular material, autophagy is involved in development, differentiation and tissue remodelling. Although a basal level of macroautophagy and CMA is observed in various cell types, these pathways are maximally activated under conditions of stress.

Analysis of mice harbouring tissue-specific, conditional knockout alleles of autophagy genes demonstrates that the capacity to modulate the rate of intracellular content degradation in response to stress or a nutrient-depleted environment is vital both for cell and organismal survival (*64–66*).

The importance of maintaining an efficient autophagic response is also demonstrated by the fact that all longlived *C. elegans* mutants display increased macroautophagy (*67*, *68*). Nonetheless, excessive activation of autophagy may lead to depletion of the essential autophagic components and failure of proper response to stress.

Activation of autophagy above a crucial threshold, may also lead to cell demise due to interference with pro-survival mechanisms and digestion of anti-apoptotic molecules (*69*).

Evaluation of the degradation capacity of cells through lifespan, and genetic manipulation of autophagic processes in model organisms during ageing will

In Oxidative Stress: Diagnostics, Prevention, and Therapy Volume 2; Hepel, et al.;
ACS Symposium Series; American Chemical Society: Washington, DC, 2015.

Publication Date (Web): October 13, 2015 | doi: 10.1021/bk-2015-1200.ch006

provide significant insights into the role of autophagy in senescent decline, and may contribute to the development of intervention strategies targeting age-associated neurodegenerative disorders.

Antioxidant Defense

During lifetime, an antioxidant sophisticated network counteracts the deleterious action of ROS on macromolecules (*25*, *35*). Cells synthesize some of their antioxidants, as the enzymes SOD, CAT and GPx, as well as the peptides with thiols groups, as glutathione (GSH) and thioredoxin (TRX) family. Other antioxidants are obtained from nature through nutrition, as vitamin C, vitamin E, and carotenoids. Several repair systems contribute to recovery the damaged molecules. Together these systems play an important role in the ability of the body to respond to the oxidant challenge of using molecular oxygen to drive reactions that yield the necessary energy (*2*, *7*).

These all are strategically compartmentalized in subcellular organelles within the cell to provide maximum protection. Generally almost are specialized in removing or react with certain ROS. Considerable overlap and cooperation are demonstrated among antioxidants. As we mentioned it previously some antioxidants are obtained from diet. Others from endogenous origin are heavily influenced by nutritional factors. Some are mandatory in the diet, and trace elements (as selenium) for the biosynthesis, or other functions which require special aminoacids (*22*, *35*).

In eukaryotic organism, several ubiquitous primary antioxidant enzymes, such as SOD, CAT, and different forms of peroxidases work in a complex series of integrated reactions to convert ROS to more stable molecules, such as water and molecular oxygen. Secondary enzymes act in concert with small molecular-weight antioxidants to form redox cycles that provides necessary cofactors for primary antioxidant enzymes functions. The small molecular weight antioxidants (e.g. GSH, NADPH, TRX, vitamins E and C, trace metals, such as selenium) can also function as direct scavengers of ROS. This complex system has the ability to both maintain an intracellular redox balance and prevent or reduce molecular damage by ROS (*35*, *70*).

Longevity has been associated with higher rate of antioxidants capacity. Humans show the highest lifespan among mammals. It is generally accepted that the activities and capacities of antioxidant systems are declined with age, leading to the gradual loss of prooxidant/ antioxidant balance and accumulation of oxidative damage in the aging process (*2*, *71*). Evidences from populations' studies are contradictory. Previous works showed plasma and red blood cell SOD activity and plasma GPx activity increased or not change or decline with increasing age. Simultaneously a decline in nutritional antioxidants was observed. Mn SOD located in the mitochondria is most significantly elevated during aging in various human tissues (*72*). The modifications of antioxidants activities could be associated with dysfunctional shift, oxidative DNA damage of specific genes, protein altered expression, post transcriptional oxidative damage and consumption of basic pools (*73*). Different animals model have been developed to argue the functional consequence of decreased antioxidant capacities for aged cells (*27*).

Publication Date (Web): October 13, 2015 | doi: 10.1021/bk-2015-1200.ch006

In others, overexpressions of specific antioxidant enzymes were evaluated. The constructs modified or not the life span overall, although there were gender and genotypes specific effects. Pharmacological treatment can also used in appraisal investigation. Repair antioxidant system is influenced of age too (*6*, *35*). This system has received less attention than ROS scavenging or respiration efficiency. Some research explored the ability to repair oxidized proteins in animals' models. Results drive observation that an age related decrease expression of the system involves short life span (*27*).

Oxidative Stress and Biomolecules Damage

ROS could react with lipids, proteins, peptides, carbohydrates and nucleic acids. Oxidative damage to macromolecules is detectable under normal physiological conditions in healthy individuals suggesting that the efficiency of antioxidant and repair mechanisms cannot avoid completely the oxidation reaction mediated by ROS (*7*, *25*, *35*). The accrual "redox hypothesis" remarks four postulates: *1*) All biological systems contain redox elements [e.g., redox-sensitive cysteine, Cys, residues] that function in cell signalling, macromolecular trafficking, and physiological regulation. *2*) Organization and coordination of the redox activity of these elements occurs through redox circuits dependent on common control nodes (e.g., TRX, GSH). *3*) The redox-sensitive elements are spatially and kinetically insulated so that "gated" redox circuits can be activated by translocation/aggregation and/or catalytic mechanisms. *4*) OS is a disruption of the function of these redox circuits caused by specific reaction with the redox-sensitive thiol elements, altered pathways of electron transfer, or interruption of the gating mechanisms controlling the flux through these pathways (*14*).

During aging increased DNA damage accumulation have been reported. Some of them known as somatic mutations, chromosomal aneuploides, copy number variations, increased clonal mosaicism for large chromosomal anormalies and others. The integrity and stability of DNA are continuously challenged by endogenous threats, including DNA replication errors, spontaneous hydrolytic reactions, and ROS (*74*).

The genetic lesions arising include point mutations, translocations, chromosomal gains and losses, telomere shortening, and gene disruption caused by the integration of viruses or transposons. To avoid these damages a complex network of DNA repair mechanisms that are collectively capable of dealing with most of the damages have been evolved including specific mechanisms for maintaining the appropriate length and functionality of telomeres. Also defects in the nuclear architecture, known as laminopathies, can cause genome instability and result in premature aging syndromes (*75*).

DNA alterations may affect essential genes and transcriptional pathways, resulting in dysfunctional cells that, if not eliminated by apoptosis or senescence, may jeopardize tissue and organismal homeostasis. This is especially relevant when DNA damage impacts the functional competence of stem cells, thus compromising their role in tissue renewal (*76*).

In Oxidative Stress: Diagnostics, Prevention, and Therapy Volume 2; Hepel, et al.;
ACS Symposium Series; American Chemical Society: Washington, DC, 2015.

Publication Date (Web): October 13, 2015 | doi: 10.1021/bk-2015-1200.ch006

MtDNA has been considered a major target for aging-associated somatic mutations due to the oxidative microenvironment of the mitochondria. Multiplicity of mitochondrial genomes leads to the coexistence of mutant and wild-type genomes within the same cell, a phenomenon that is referred to as "heteroplasmy." However, single-cell analyses have revealed that, despite the low overall level of mtDNA mutations, the mutational load of individual aging cells becomes significant and may attain a state of homoplasmy in which one mutant genome prevails. Interestingly, contrary to previous expectations, most mtDNA mutations in adult or aged cells appear to be caused by replication errors early in life, rather than by oxidative damage. These mutations may undergo polyclonal expansion and cause respiratory chain dysfunction in different tissues (*77*).

Nuclear lamins participate in genome maintenance by providing a scaffold for tethering chromatin and protein complexes that regulate genomic. Mutations in genes encoding protein components of this structure, or factors affecting their maturation and dynamics, also a production of an aberrant prelamin A isoform called progerin have also been detected in normal aged cells (*76*).

DNA oxidative damage is a common mediator for both replicative senescence, which is triggered by telomere shortening, and premature cellular senescence induced by various stressors such as oncogenic stress and OS (*77*, *78*). Extensive observations suggest that DNA damage accumulates with age and this may be due to an increase in ROS production and a decline in DNA repair capacity with age. Mutation or disrupted expression of genes that increase DNA damage often result in premature aging. Different methods and parameters have been used in animal models producing variety of ranging concentrations and contradictory data. As a consequence it was assumed that same patron could occur also in humans (*79*).

Protein homeostasis or proteostasis impair during life involving mechanisms for stabilization of correctly folded proteins—most prominently, the heat shock family of proteins—and mechanisms for the degradation of proteins by the proteasome or the lysosome. Also regulators of age-related proteotoxicity have been identified, such as MOAG-4, which acts through an alternative pathway distinct from molecular chaperones and proteases. All of these systems function in a coordinated fashion to restore the structure of misfolded polypeptides or to remove and degrade them completely, thus preventing the accumulation of damaged components and assuring the continuous renewal of intracellular proteins (*78*).

Proteins contain two common functional groups [thiol of Cys and thioether of methionine, Met] that undergo reversible oxidation-reduction through metabolic pathways. The relevant oxidation states are the thiol (-SH), disulfide (-SS-), sulfenate ($-SO^-$), sulfinate ($-SO_2^-$), and sulfonate ($-SO_3^-$), of which the thiol and disulfide are most common. Thiyl radicals ($-RS\cdot$) generated from thiols in the presence of oxygen-centered radicals (*80*), as well as other reactive sulfur species (*81*), have also been considered as toxic species involved in oxidative stress. Thiyl radicals rapidly react to form disulfides (*80*), and this may serve as a convergence point between one-electron and two-electron events. Sulfenates are relatively unstable and are converted to disulfides in the presence of thiols. In certain protein structures, they can be stabilized as sulfenamides (*82*). The higher oxidation states (sulfinates and sulfonates) are typically not reversible

Publication Date (Web): October 13, 2015 | doi: 10.1021/bk-2015-1200.ch006

in mammalian systems, although a yeast enzyme (sulfiredoxin) was recently discovered, which reduces sulfinate in peroxiredoxin (*82*).

Reversible oxidations of Met residues and the less common amino acid selenocysteine (Sec) also occur. Oxidation of Met to methionine sulfoxide occurs in association with oxidative stress and aging (*83*). Such oxidation affects biological activity as shown by loss of α_1-antitrypsin inhibitor activity upon Met oxidation (*82*). Two types of methionine sulfoxide reductases act on the structurally distinct *S*- and *R*-sulfoxides; methionine sulfoxide reductases activities are dependent on thioredoxins (Trx) and have been associated with longevity (*83*). The less common selenol of Sec undergoes reversible oxidation-reduction during catalytic functions of Trx reductases and Se-dependent GSH peroxidases (*84*). These Se-dependent enzymes are present at key positions in both Trx and GSH pathways. Although the present review is focused on Cys oxidation, both Met and Sec oxidation are relevant to the redox hypothesis because of their relationships to the thiol systems and because of their individual functions in control of protein structure and activity.

Reversible oxidation of thiols to disulfides or sulfenic acid residues controls biological functions in three general ways, by chemically altering active site cysteines, by altering macromolecular interactions, and by regulating activity through modification of allosteric Cys. Cys residues are present in active sites of detoxification enzymes such as glutathione transferases, cytochromes *P*-450, Trxs, and peroxiredoxins. Cys is a component of active sites of iron-sulfur clusters of electron transfer proteins. Cys is a component of zinc fingers in transcription factors and zinc-binding domains of metallothioneins. Cys residues are conserved in structural proteins such as actin and docking proteins. Also Oxidation of Cys residues in αIIbβ3 integrin controls platelet activation (*85*). Cys-rich regions are present in plasma membrane receptors and ion channels, including the NMDA receptors, EGF receptor, and others. Thus reversible oxidation of active site thiols can provide a common and central "on-off" mechanism for control of cell functions. Such changes in protein structure and interaction due to reversible oxidation can provide a central mechanism for specificity in redox signalling (*85*).

Oxidation of the active site therefore functions as an "on-off" switch for apoptosis. In addition to these active-site thiols, the nonactive site Cys residues are also subject to redox regulation and provide orthogonal mechanisms for control. Modification of these residues can result in allosteric changes that affect the active site or structural changes, which affect macromolecular interactions.

These are likely to include enzyme, transporter, receptor, or transcription factor "active sites" as well as allosteric and macromolecular interaction sites. Accumulating evidence indicates that dozens, and perhaps hundreds, of proteins undergo *S*-nitrosylation and GS-ylation (*80*). The potential significance of a large number of redox-sensitive sites is apparent when one considers the nonequilibrium conditions of thiol-disulfide couples within cells and subcellular compartments. Together, the available data show that there are a large number of redox-sensitive thiols within the Cys proteome. These are widely distributed among signalling, structural, and regulatory proteins. Thus there is a secure basis for the first postulate of the redox hypothesis.

Publication Date (Web): October 13, 2015 | doi: 10.1021/bk-2015-1200.ch006

The other postulates that redox-sensitive elements are organized into redox pathways and control networks are related to both GSH and Trx support enzyme systems for elimination of peroxides, but each system has other distinct functions.

Several lines of evidence support the interpretation that critical thiol-disulfide redox couples are maintained under stable, nonequilibrium conditions in biological systems. One of the most unequivocal pieces of evidence is the disequilibrium of the cysteine/cystine (Cys/CySS) and GSH/GSSG couples in human plasma (*85*, *86*).

During aging the cellular homeostatic machinery becomes progressively impaired. Those increase vulnerability to oxidative damage. Oxidative process cause reversible or irreversible alteration to macromolecules (*87*). Accumulation of oxidative and deleterious change overtime is associated to senescence (*87*, *88*).

Validation of this hypothesis depends not only on the strength of supportive evidence, but in the absence of evidence of alternative, contradictory ideas. A major obstacle to accept the OS hypothesis has been the poor record of antioxidants in prolonging the life span of animals and humans during intervention trials. Nevertheless, in those trials parameters of life quality could be improved (*27*, *35*).

Many other variables, such as genetic factors, temperature, activity and nutrition can affect life span, making it a highly complex multi-factorial process (*50*, *88–90*). All the effective interventions in prolonged life span of different species and animals are related to oxidative damage reduction (*29*, *30*, *91*, *92*).

ROS mediated damage to proteins is particularly important in aging, as seen by the accumulation of oxidized proteins (ox-Prot) in a relation to reduced proteolysis, elimination or both (*15*, *22*, *93*, *94*). Generally oxidation of various aminoacids or side chains often leading to structural change and/or a loss of functions makes them susceptible to degradation. This process prevents the formation of large aggregates or potentially toxic fragments. Mammalian cells pose three major proteolytic systems: the lysosomal cathepsin, calcium activated calpains and the 20S and 26S proteasomes (*94–97*). Many investigators have found an accumulation of protein oxidation products and a concomitant impairment in proteolytic pathways with increasing age (*21*, *88*, *94*, *98*).

A conspicuous pro oxidative shift in the plasma thiol/disulfide redox couples such as GSH, cysteine and albumin have been observed in humans between 3r and 10^{th} decades of life (*99–101*).

This may have systemic consequences because several of the redox sensitive cascades respond not only to direct exposure to ROS but also to changes in the thiol redox state. At last this may produce changes in cellular functions controlled by these signalling cascades (*71*).

Diverse parameters of lipid peroxidation products are characterized like malondialdhyde (MDA), hidroxinonenal (HNE) and F_2-isoprostanes (*102–106*). Substantially higher levels of them have been observed in aged compared with young organism in tissues, such as kidney, brain, liver, lung and muscle (*102*).

It is important to note that the oxidative damage to macromolecule varies greatly among different tissues, species and detection methods.

It is possible that the concentration of this cumulative damage reported with age may fall below the threshold that a cell or tissue may tolerate with little or not

In Oxidative Stress: Diagnostics, Prevention, and Therapy Volume 2; Hepel, et al.;
ACS Symposium Series; American Chemical Society: Washington, DC, 2015.

Publication Date (Web): October 13, 2015 | doi: 10.1021/bk-2015-1200.ch006

direct impact on functional efficiency. Conversely oxidative damage to key genes and proteins may results in the efficiency of cell functioning (*15*, *73*, *97*).

Proteasome Regulation

It is well established that ox-Prot levels increase during aging. However, accumulation of ox-Prot is a complex process, which depends on the rates and kinds of modification, the efficiency of antioxidant systems, and the rates of ox-Prot degradation by a multiplicity of proteases that decline in aged organisms (*107*). Thus, protein degradation and its regulation are critical processes during aging.

The activities of the two principal proteolytic systems implicated in protein quality control—namely, the autophagy-lysosomal system and the ubiquitin-proteasome system—decline with aging.

Proteasome is involved in the degradation of both normal short-lived ubiquitinated proteins and mutated or damaged proteins, thereby regulating diverse cellular functions. The 26S proteasome consists of a 20S core particle bound to 19S regulatory particles. The 20S eukaryotic proteasome comprises of four stacked heptameric rings (two α type surrounding two of β type) that form a barrel-like structure (*108*). The 26S proteasome performs the ATP-dependent degradation of short-lived ubiquitinated proteins, whereas the 20S proteasome mediates the degradation of damaged polypeptides, in a manner that is mostly ATP- and ubiquitin-independent (*109*).

Proteasome activity and functionality declines with age (*110–113*). It has been demonstrated that proteasomal degradation increases due to mild oxidation, whereas at higher oxidant levels proteasomal degradation decreases. Moreover, the proteasome itself is affected by OS. Consequently, alterations of proteasome have dramatic effects on cellular viability and aging (*114*).

Proteasome control also depends on the activity of networks that regulate cellular responses to oxidative and electrophilic stress. The NFE2-related factor 2 (Nrf2)/Kelch-like ECH-associated protein 1 (Keap1) signaling pathway appears to be a central player (*115*). By mean a RNA interference (RNAi) screen in Drosophila cells, a Nrf2 isoform was identified as a possible transcriptional regulator of proteasome components' expression (*116*). Thus, it has been postulated that there may be a cross talk between the network of antioxidant responses and the proteasome-mediated protein quality control during aging. Furthermore, the signals between proteasome dysfunction and proteasome genes' up-regulation are severely compromised in aged somatic tissues (most likely, due to disruption of ROS signaling from damaged mitochondria or due to a decline in the functionality of the Nrf2/Keap1 signaling pathway), resulting in impaired de novo proteasome biogenesis after a proteasome damage (*113*).

Nevertheless, and despite the fact that proteasome function seems to be tightly regulated under conditions of increased OS including aging and disease, the molecular mechanisms of in vivo basal and stress-related proteasome regulation in tissues of higher organisms remain poorly understood.

Publication Date (Web): October 13, 2015 | doi: 10.1021/bk-2015-1200.ch006

All of these systems function in a coordinated fashion to restore the structure of misfolded polypeptides or to remove and degrade them completely, thus preventing the accumulation of damaged components and assuring the continuous renewal of intracellular proteins. Accordingly, many studies have demonstrated that proteostasis is altered with aging (*78*). Additionally, chronic expression of unfolded, misfolded, or aggregated proteins contributes to the development of some age-related pathologies. A number of animal models support a causative impact of chaperone decline on longevity, and on the master regulator of the heat-shock response, the transcription factor HSF-1. Deacetylation of HSF-1 by SIRT1 potentiates the transactivation of heat-shock genes such as Hsp70, whereas downregulation of SIRT1 attenuates the heat-shock response (*117*).

Publication Date (Web): October 13, 2015 | doi: 10.1021/bk-2015-1200.ch006

Genetic and Epigenetic Aspect

As previous mentioned in OXIDATIVE STRESS AND BIOMOLECULES DAMAGE subchapter DNA damage accumulation inflicting genetic consequence throughout life is an aspect to be considered.

Telomere maintenance has been shown to be linked to aging (*118*, *119*). Telomeres are required to protect chromosome ends, to provide chromosome stability, and to ensure faithful segregation of genetic material into daughter cells upon cell division (*120*).

Telomeres are bound by a group of telomere-associated proteins known as the “shelterin” complex. These proteins function as the protection for the loop structure of telomere, which prevents the chromosome ends uncapped; resemble a DNA break and activates DNA repair mechanism (*119*, *121*).

Telomeres are a G-rich repetitive DNA maintained by a specialized reverse transcriptase enzyme called telomerase (*120*). When telomere-associated proteins are no longer protecting telomeres and in the absence of telomerase, continued cell division results in telomere shortening and loss of ‘capping’ function, making telomeres recognized as single and lead to the breaking of the double-strand DNA (*119*, *122*, *123*). Damaged telomeres may provide a reservoir of persistent DNA damage signals and consequent sustained p53 activation with senescent quelae (*124*).

Also increased ROS levels would set in motion a detrimental cycle of genotoxic damage with rapid erosion and damage of G-rich telomeres, sustained p53 activation and progressive mitochondrial decline (*122*, *125*, *126*).

Under conditions of low oxidative stress, p53 activation preferentially induces expression of antioxidant genes; however, when ROS production is high, p53 instead activates pro-oxidant genes (*124*, *127*). This contrasting action of p53 might allow both cell-cycle arrest and repair under conditions of modest DNA damage or more robust cellular responses of senescence or apoptosis and/or mitochondrial dysfunction in cells with more substantial DNA damage, thus leading to tissue atrophy and functional decline (*124*, *128*, *129*).

In addition, alteration of epigenetic mechanisms may lead to accumulation of functional errors and to ageing-associated diseases. Aged organisms present a peculiarly modified epigenome. Alteration in micro-RNA expression, DNA

methylation patterns, post translational modifications of histones and chromatin remodelling may be involved in the age-associated impairment of organ function often seen in elderly people (*130*).

Members of the sirtuin family of NAD-dependent protein deacetylases and ADP ribosyltransferases have been studied extensively as potential anti-aging factors. Regarding mammals, several of the seven mammalian sirtuin paralogs can ameliorate various aspects of aging in mice. In particular, transgenic overexpression of mammalian SIRT1, which is the closest homolog to invertebrate SIRT2, improves aspects of health during aging but does not increase longevity. SIRT1 antagonization is involved in senescence of mouse fibroblasts, human cancer cells and endothelial cells (*130*, *131*). SIRT1 inhibition determines an increase of p53 acetylation which impact on endothelial cells growth arrest. During ageing, OS accumulates, paralleled with a decrease in NO production, which might be responsible for SIRT1 inactivation. This negative loop facilitates the senescence-like phenotype of endothelial cells (*130*).

More compelling evidence for a sirtuin-mediated prolongevity role in mammals has been obtained for SIRT6, which regulates genomic stability, NF-kB signaling, and glucose homeostasis through histone H3K9 deacetylation. Interestingly, the mitochondria-located sirtuin SIRT3 has been reported to mediate some of the CR beneficial effects in longevity, though its effects are not due to histone modifications but, rather, due to the deacetylation of mitochondrial proteins (*131*).

Also the accumulation of ROS directly impairs the function of lung cells, determining posttranslational modifications of histones and non-histone proteins, as well as that of chromatin remodelling enzymes (*130*, *132*).

The most frequent oxidative DNA lesion is the oxidation of guanine, which alters transcription factors binding to DNA because a deranged epigenetic signalling (*130*, *133*). The presence of oxidized guanosine is often associated with cytosine methylation when they are arrayed in a linear sequence forms the so-called “CpG island” in specific DNA regions. This array could lead to the formation of methylated and oxidized CG stretches. These regions might represent sites of interplay between epigenetic and OS signals potentially relevant in Alzheimer’s disease physiopathology (*130*, *134*). Oxidized guanosine cannot be repaired when it is preceded by a methylcytosine. Thus, in the presence of cytosines methylated early in life and belonging to CpG islands, the correction of adjacent guanines in the case of an oxidation event occurring late in life will be prevented, leading to accumulation of oxidative DNA damage in ageing brains (*130*, *134*). Then methylation imprinting hits both gene expression and susceptibility to oxidative DNA damage in the late stages of Alzheimer’s disease (*130*).

All of these epigenetic defects or epimutations accumulated throughout life may specifically affect the behavior and functionality of stem cells. Actually there is no direct experimental demonstration thus far that organismal lifespan can be extended by altering patterns of DNA methylation.

DNA- and histone-modifying enzymes act in concert with key chromosomal proteins, such as the heterochromatin protein 1a (HP1a), and chromatin remodeling factors, such as Polycomb group proteins or the NuRD complex,

In Oxidative Stress: Diagnostics, Prevention, and Therapy Volume 2; Hepel, et al.;
ACS Symposium Series; American Chemical Society: Washington, DC, 2015.

Publication Date (Web): October 13, 2015 | doi: 10.1021/bk-2015-1200.ch006

whose levels are diminished in both normally and pathologically aged cells. Supporting the functional relevance of epigenetically mediated chromatin alterations in aging, there is a notable connection between heterochromatin formation at repeated DNA domains and chromosomal stability. Mammalian telomeric repeats are also enriched for these chromatin modifications, indicating that chromosome ends are assembled into heterochromatin domains (*135*, *136*).

Microarray-based comparisons of young and old tissues from several species have identified age-related transcriptional changes in genes encoding key components of inflammatory, mitochondrial, and lysosomal degradation pathways. Also affect noncoding RNAs, including a class of miRNAs (gero-miRs) that is associated with the aging process and influences lifespan by targeting components of longevity networks or by regulating stem cell behavior (*137*).

Hence, the epigenetic machinery may represent an OS sensor that orchestrates the progressive homeostasis impairment typical of ageing, thus shaping the cellular senescence often observed during cardiovascular, respiratory and nervous system degeneration (*130*).

Publication Date (Web): October 13, 2015 | doi: 10.1021/bk-2015-1200.ch006

Mitochondrial Dysfunction

As previous mentioned in OXIDATIVE STRESS AND BIOMOLECULES DAMAGE subchapter the efficacy of the respiratory chain with age tends to diminish, thus increasing electron leakage and reducing ATP generation. The mitochondrial free radical theory of aging proposes that the progressive mitochondrial dysfunction that occurs with aging results in increased production of ROS, which in turn causes further mitochondrial deterioration and global cellular damage.

The reduced efficiency of mitochondrial bioenergetics with aging may result from multiple converging mechanisms, including reduced biogenesis of mitochondria—for instance, as a consequence of telomere attrition in telomerase-deficient mice, with subsequent p53-mediated repression of PGC-1a and PGC-1b. Also independently of increased ROS generation, DNA polymerase γ deficiency during age could also contribute to dysfunction (*138*).

Other mechanisms causing defective bioenergetics include accumulation of mutations and deletions in mtDNA, oxidation of mitochondrial proteins, destabilization of the macromolecular organization of respiratory chain (super)complexes, changes in the lipid composition of mitochondrial membranes, alterations in mitochondrial dynamics resulting from imbalance of fission and fusion events, and defective quality control by mitophagy, an organelle-specific form of macroautophagy that targets deficient mitochondria for proteolytic degradation (*139*).

Mitochondrial dysfunctions during aging are also connected with hormesis, a concept on which a number of aging research lines have recently converged. Although severe mitochondrial dysfunction is pathogenic, mild respiratory deficiencies may increase lifespan, perhaps due to a hormetic response. Importantly, metformin extends lifespan in *C. elegans* through the induction of a compensatory stress response mediated by AMPK and the master antioxidant

regulator NRF2. Recent studies have also shown that metformin retards aging in worms by impairing folate and methionine metabolism of their intestinal microbiome (*140*).

Accrual revision of parallel and separate works on the damaging effects of ROS, show related to intracellular signaling accumulated solid evidence for the role of ROS in triggering proliferation and survival in response to physiological signals and stress conditions). The two lines of evidence can be harmonized if ROS is regarded as a stress-elicited survival signal conceptually similar to AMP or NAD+. In this sense, the primary effect of ROS will be the activation of compensatory homeostatic responses. As chronological age advances, cellular stress and damage increase and the levels of ROS increase in parallel in an attempt to maintain survival. Beyond a certain threshold, ROS levels betray their original homeostatic purpose and eventually aggravate, rather than alleviate, the age-associated damage (*59*).

Publication Date (Web): October 13, 2015 | doi: 10.1021/bk-2015-1200.ch006

Nutrient Sensing and Caloric Restriction

The somatotrophic axis in mammals comprises the growth hormone (GH), which is produced by the anterior pituitary, and its secondary mediator, insulin-like growth factor 1 (IGF-1), produced in response to GH by many cell types, most notably hepatocytes. The intracellular signaling pathway of IGF-1 is the same as that elicited by insulin, which informs cells of the presence of glucose. IGF-1 and insulin signaling are known as the "insulin and IGF-1 signaling" (IIS) pathway. Remarkably, the IIS pathway is the most conserved aging-controlling pathway in evolution, and among its multiple targets are the FOXO family of transcription factors and the mTOR complexes, which are also involved in aging and conserved through evolution (*141*). Mutations that reduce the functions of GH,IGF-1 receptor, insulin receptor, or downstream intracellular effectors such as AKT, mTOR, and FOXO have been linked to longevity, both in humans and in model organisms, further illustrating the major impact of trophic and bioenergetic pathways on longevity. In addition to the IIS pathway that participates in glucose sensing, three additional related and interconnected nutrient sensing systems are the focus of intense investigation: mTOR, for the sensing of high amino acid concentrations; AMPK, which senses low-energy states by detecting high AMP levels; and sirtuins, which sense low-energy states by detecting high NAD+ levels (*142*).

Collectively, current available evidence strongly supports the idea that anabolic signaling accelerates aging and decreased nutrient signaling extends longevity. Further, CR and pharmacological manipulation that mimics a state of limited nutrient availability, such as rapamycin, can extend longevity in animal models (*143*).

Numerous experimental interventions designed to regulate the aging process have been attempted. To date, an established intervention that has been consistently shown to slow the rate of aging and to increase lifespan in various species is CR. CR is designed to induce "undernutrition" state without malnutrition. Usually in CR food intake is reduced to 20%-50% less than *ad*

libitum levels (*144*). Mechanisms responsible for the antiaging effects of CR remain uncertain, but reduction of mitochondrial OS and the activation of cell survival mechanisms are major aspects accounting for the antiaging effects of CR (*145*, *146*).

One of the hallmarks of CR is the increase of functional respiratory units (mitochondrial biogenesis) and the promotion of changes in dynamics and composition of this organelle (*147*). In fact, CR reduces OS at the same time that it stimulates mitochondrial proliferation through a peroxisome proliferation-activated receptor coactivator alpha (PPARα) signalling pathway. Mitochondria under CR conditions show less oxygen consumption, reduce membrane potential, and generate less ROS, but remarkably, they are able to maintain their critical ATP production (*148*). Moreover, CR increases ATP concentration, oxygen consumption and mtDNA when compared with *add libitum* fed mice. In addition, CR alters mitochondrial membrane fatty acid composition, allowing for increased mitochondrial functions (*149*). Thereby, the improvement of mitochondrial efficiency by CR maintains cellular metabolism with a lower OS damage accumulation and, ultimately, a decreased cellular and organism aging.

In mammals, the mitochondrial biogenesis is complex and a highly regulated process that coordinates the activity of numerous genes involved in mitochondrial function. In particular, the transcriptional coactivator PGC-1α is expressed and activated during aging in animal models of CR, leading to an increase of mitochondrial mass (*150*). PGC-1α modulates the activity of several transcription factors and coactivators involved in mitochondrial respiration and biogenesis such as NRF-1, NRF-2, PPARγ, steroid receptor coactivator-1, and mitochondrial transcription factor A. NRF-1 and NRF-2 coordinate the expression of nuclear and mitochondrial genes that encode most of the subunits of mitochondrial complexes (*151*). In the same sense, PGC-1α activates the shift of substrate utilization from carbohydrates to fatty acids through co-regulation of PPARγ. The PCG-1α signal includes the up-regulation of antioxidant and repair system, as well as a boost in energy metabolism (*152*).

It has been demonstrated that CR also impacts some growth signals, such as insulin-like growth factor 1 (IGF-1) and vascular endothelial growth factor (VEGF), regulating the occurrence of diabetes, chronic inflammation and some types of cancers. CR improves insulin sensitivity and normalizes glucose levels, which results in lowered serum insulin and IGF-1, and increased IGF-binding proteins (IGFBP) production (*153*).

On the other hand, the need for nutrients and oxygen triggers tumor cells to produce VEGF, leading to the formation of new blood vessels (angiogenesis) to allow the growth of tumors and facilitate the metastatic spread of malignant cells (*154*). Data from several experimental tumor models (*155*, *156*) suggest that CR decreases systemic and tissue VEGF and has anti-angiogenic effects. Moreover, CR can prevent the inflammation associated with preneoplasia or neoplasia (*157*). In fact, CR decreases the number of tumor-infiltrating macrophages, levels of circulating and tissue cytokines, NF-κB signaling pathway and COX-2 expression in many tissues and tumor types (*158*).

In summary, the mechanisms responsible for the antiaging effects of CR and age-related diseases remain unclear. Nonetheless, up to now, CR is the most

In Oxidative Stress: Diagnostics, Prevention, and Therapy Volume 2; Hepel, et al.;
ACS Symposium Series; American Chemical Society: Washington, DC, 2015.

Publication Date (Web): October 13, 2015 | doi: 10.1021/bk-2015-1200.ch006

robust, nongenetic intervention that increases lifespan and reduces the rate of aging in a variety of species.

The rate of mitochondrial ROS production is significantly influenced by the availability of energy substrate (*20*, *35*). Considering previous observation dietary restriction is well investigated and most promising experimental strategy to increase life span and to improve quality of life in old age (*159*, *160*). Molecular explanation for CR' ability to regulate age-related OS is provided by evidences. CR enhances stress resistance or tolerance over the lifespan by selective modulation of stress-related genes (*159*). This is much greater than its ability to enhance proliferation (*44*, *161*). This is consistent with diverse reports indicating that restrict caloric intake attenuates the regenerative process preserving the capacity to proliferate over long term (*160*). Certain manifestations of OS have been ameliorated during CR and suppression of pro-inflammatory cytokines in several animal species studies is well documented (*19*, *22*, *28*, *47*, *162*). Among its diverse effects CR have anti inflammatory action at molecular level through the modulation or reduction of ROS mitochondrial generation (*163*). It can also promote mitochondrial biogenesis through a pathway signalled by lower insulin levels, enhanced nitric oxide, and the activation of the transcriptional coactivator PCG-1α (*164*). Production of Glucocorticoids (GC) one of the most potent suppressors of NF-κB are enhanced during CR. Both mechanisms are implicated in the molecular effect (*7*, *165*).

GC is an antinflammatory agent which modulates biological activities in cell by activating their cognate GC receptor. Regarding the putative adverse action of GC with the aging process, GC cascade hypothesis was proposed by Sapolsky et al 1985 (*166*). GC elevated CR are relevant because its antinflammatory action at molecular levels (*23*, *71*). From a stand point of molecular inflammatory process, controlling NF-κB activation through the suppression of OS should be more effective way to manage the process than GC, as shown by CR action (*160*).

Inflammatory Process and Disease

Aging also involves changes in the levels of intercellular communication manifested meanly as increases of inflammatory reactions, immunosurveillance against pathogen and premalignant cells decline and the composition of the peri- and extracellular environment changes.

The inflammatory response is a complex cascade of cellular and molecular events designed to limit infection or tissue damage. Under physiological conditions, the resolution phase of inflammation restores tissue homeostasis. On the contrary, if inflammaging occurs for multiple causes as noxious stimulus persists (accumulation of proinflammatory tissue damage, the failure of an ever more dysfunctional immune system to effectively clear pathogens and dysfunctional host cells, the propensity of senescent cells to secrete proinflammatory cytokines, the enhanced activation of the NFkB transcription factor, or the occurrence of a defective autophagy response), conduce to alterations as an enhanced activation of the NLRP3 inflammasome and other proinflammatory pathways, finally leading to increased production of cytokines

In Oxidative Stress: Diagnostics, Prevention, and Therapy Volume 2; Hepel, et al.;
ACS Symposium Series; American Chemical Society: Washington, DC, 2015.

Publication Date (Web): October 13, 2015 | doi: 10.1021/bk-2015-1200.ch006

(IL-1b), tumor necrosis factor, interferons and ROS by cells of the innate and adaptive immunity which can result in disease (*167*).

Pathologic inflammation has diverse origins and causes. In one setting, there is an acute or subacute inflammatory reaction in response to pathogens or debris from damaged host cells. In another type of pathologic inflammation, a primary defect in the regulation of an inflammatory pathway triggers chronic disease. In a third class, the inflammatory response does not eradicate the primary stimulus, as would normally occur in most cases of infection or injury, and thus a chronic form of inflammation ensues that ultimately contributes to tissue damage (*168*).

Aging is characterized by a chronic low-grade inflammation, which is associated with increased risk for diseases, such as malignant tumors, atherosclerosis, diabetes, metabolic syndrome, ischemia-reperfusion (I/R) injury, neurodegenerative diseases, and rheumatoid arthritis. The elevation of circulating pro-inflammatory cytokines such as interleukin-1beta (IL-1β), IL-6, and tumor necrosis factor alpha (TNF-α), and acute phase proteins such as C-reactive protein (CRP) and serum amyloid A (SAA), are typical in aged persons when compared to the young, even in the absence of chronic diseases (*169*, *170*). Moreover, a decreased production of anti-inflammatory cytokines such as tumor growth factor-beta 1 (TGF-β1) and IL-10, contributes to the establishment of an inflammatory state (*171*).

Many studies have shown that OS can contribute to the development of chronic inflammation and disease during aging (*172*). There are potential mechanisms linking OS to inflammation, one of them is the emerging criteria that ROS-induced activation of toll-like receptors (TLR) of immune cells play an important role in activating the inflammatory cascade (*173*). Multiple studies have shown the in vivo requirement of TLR signaling in mediating injury from OS in I/R events (*174–177*). Furthermore, ROS act as endogenous agonists for TLR2, which stimulates blood vessel growth and inflammation during atherogenesis, through a mechanism that is independent of vascular endothelial growth factor (VEGF) (*178*, *179*).

In aged organisms, ROS and pro-inflammatory cytokines trigger common signal transduction pathways, mainly through activation of mitogen-activated protein kinases (MAPK), the nuclear factor-kappa B (NF-κB) and the activator protein-1 (AP-1). These activated transcription factors up-regulate gene expression of various pro-inflammatory molecules, including adhesion molecules for circulating monocytes, chemotactic proteins, pro-coagulant tissue factors, and smooth muscle cells (SMC) mitogenic factors (*180*, *181*). It was reported that redox imbalance increases the levels of TNF-α, which is able to impair the synthesis of glutathione (GSH), affecting the antioxidant status in aging (*182*). Pro-inflammatory cytokines contain redox-sensitive NF-κB, specific, DNA binding sites in the promoter regions and their production is influenced by oxidative status. In addition, cytokines can exacerbate the redox imbalance, leading to further activation of NF-κB (*183*). In this scenario, a positive feedback loop is activated, whereas additional ROS generation potentiates the inflammatory response-induced cellular and tissue damage.

In evaluating the Free Radical theory of aging and its possible link to numerous age related maladies, investigators have focused attention on the

Publication Date (Web): October 13, 2015 | doi: 10.1021/bk-2015-1200.ch006

possibility that an increase in ROS generation, along with a concomitant disruption in redox balance, leads to a state of chronic inflammation (*15*, *23*, *26*, *96*, *184*, *185*).

By enhancing the intracellular signalling pathways of lymphocytes, ROS from activated macrophages and neutrophils may contribute decisively to the activation of the antigen-specific immune response and may allow immune system to respond to minute amounts of invading pathogens (*184*, *185*). Signalling pathways involving JNK, p38 MAPK, and the transcription factors as AP-1 and NF-κB are particularly responsive to redox regulation (*7*, *22*, *186*, *187*). During physiological, redox regulation is implicated in gain or loss of functions or outright destruction, but an excessive stimulation by inflammatory mediator's increasingly relevant ROS production. Both acute and chronic inflammations are physiological protective mechanism that acts in response to cellular injury or tissue destruction (*89*, *188*, *189*). Inflammatory reactions are well-orchestrated events, known to be extremely complex but essential designed to limit insult and promote repair. Expressions of certain genes that encode several inflammatory proteins, including IL-1, IL-6, IL-8, and TNFα are enhanced in these conditions (*44*).

In aged organism, inflammatory reactions combined with the disruption of the organism's control could lead to a persistent pro-inflammatory state as, evidenced in a wide range of diseases that involve no-resolving or re-occurring reactivities (*190*, *191*). Consistent changes in redox responsive cascades and in the expressions of corresponding target genes may have a similar or even greater impact on senescence as the direct radical inflicted damage of cellular constituents (*22*, *72*, *96*).

There is a growing awareness that OS plays a role in various clinical conditions (*184*). Malignant diseases, diabetes, atherosclerosis, chronic inflammation, human immunodeficiency virus infection, I/R injury, neurodegenerative disease, rheumatoid arthritis, dengue and sleep apnea are important examples. These diseases fall into two major categories. In the first, diabetes mellitus and cancer show commonly a pro-oxidative shift in the systemic thiol/disulfide redox state and impaired glucose clearance, suggesting mitochondria may be the major site of elevated ROS production. Referred as mitochondrial OS without therapeutic interventions or modification the conditions lead to massive muscle wasting, reminiscent of aging related wasting (*71*). The second category may be referred to as inflammatory oxidative conditions because it is typically associated with an excessive stimulation of NOX activity by cytokines or other agents. Pathological changes indicative of a deregulation of signal cascades and/or gene expression, exemplified by altered expression of cell adhesion molecules were finding.

During inflammatory and aging process some events are recognized as common. Redox imbalance characterized by increased ROS generation and decreased antioxidant counteract system represented by reduced enzymatic activities and non enzymatic products reductions were found. Pro inflammatory enzymes as cyclooxygenase and hemeoxygenase are increased as well as pro inflammatory cytokines productions (IL-1β, IL-6, TNFα). NF-κB activation that include related phosphorylation cascade are involved too, those activation include

Publication Date (Web): October 13, 2015 | doi: 10.1021/bk-2015-1200.ch006

Erk, JNK, p38 MAPK pathways. During CR experiments all these events are blunted (*164*). Different laboratories reported regulation of gene expression of diverse factors as enzymes and cytokines (*191*). NF-κB are markedly suppress in parallel to diminish ROS generation (*105*, *159*).

In all cited studies benefits of this depended on the prevention of malnutrition and a reduction in total caloric intake rather than in any particular nutrient. CR protects homeostatic integrity by prioritizing energy allocation to increase the resistance capacity against both intrinsic and extrinsic insults.

There is compelling evidence that aging is not an exclusively cell biological phenomenon and that it is coupled to a general alteration in intercellular communication.

Publication Date (Web): October 13, 2015 | doi: 10.1021/bk-2015-1200.ch006

OS' Clinical Evidences during Aging

A large amount of data about OS implications in tissues damage, diseases, biological variables and life habits has been shown (*1*, *16*, *25*, *27*, *87*, *93*). The oxidative cumulative values in healthy humans related with aging and sex have been shown in biological fluids too (*192*, *193*). There exist some reports on human erythrocytic, blood and plasmatic GSH, GSSG MDA, protein carbonyls, HNE, glutathione disulfide (GSSH), uric acid (UA), SOD, CAT and GPx values and others redox indexes in blood and plasma samples of healthy women and men of ages ranging from 9 to 99 years and centenarians (*99*, *194–200*). In 2000 data from Italy (*194*), in 2002 data of USA (*195*), and Turkey (*99*, *196*), in 2004 data from Brazil (*197*), in 2006 from Germany (*198*), in 2007 data from USA (*199*) and Mexico (*200*), in 2008 data from Germany (*201*), in 2009 data from India (*202*), in 2010 data from Bulgaria (*203*) and in 2014 data from India (*204*) healthy populations have been published. In those investigations tendencies for some parameters also significant correlations were established showing an increase of prooxidative capacities and a decrease of antioxidant capacities (*99*, *195*, *197*, *198*, *201*, *202*, *204*). Further studies which were carried out previously present conflicting and contradictory results, e.g. concerning total antioxidative capacity of human blood plasma, which increased in one study, but decreased with age in another study (*102*, *192*, *200*, *203*). All these studies were arranged in Table 1 in order to compare in some aspects.

Authors carried out in general cross sectional and comparative studies. In order to test whether the age dependence of redox parameter are gradually or seems to be a continuous process, authors divided cohorts of healthy subjects in smaller groups (decenniums preferentially) according to their ages.

The results indicate that the balance of oxidant and antioxidant systems in plasma shifts in favour of accelerating oxidation during aging. One of the characteristic of aging is that the levels of nonenzymatic antioxidant components decline during senescence.

That is demonstrated by increases of plasma MDA and HNE, erythrocytic GSSG, CysCys and by the slight decrease of erythrocytic GSH with age (*99*, *194–198*). The plasma protein carbonyls means value, however, reach a lowest

In Oxidative Stress: Diagnostics, Prevention, and Therapy Volume 2; Hepel, et al.;
ACS Symposium Series; American Chemical Society: Washington, DC, 2015.

value in aged individuals (*198*) but others authors found invariable data in the age course (*197*). The age-dependent course of plasma UA is more determined by metabolic and nutritional influences than by the balance between prooxidants and antioxidants (*198*). Carotenoid and tocopherols values are reported increased in some studies as well as ascorbic acid are found decreased in age course (*194*, *197*). Plasmatic, blood and intracellular activity of SOD, GPx and CAT show discrepancy but generally erytrocytic activity of SOD and GPx increase and plasmatic are invariable (*99*, *194–200*). Others oxidative indexes such as isoprostanes in urine are recently reported with unchanged values respect age analyses (*199*). Evaluations of DNA damage by comet assay and Flare method are contradictory finding unchanged values and increased respectively (*199*). Total antioxidant capacity showed decreased values in correspondence with others results and increased lipoperoxides with age course were assessed too (*200*).

Association of oxidative stress indexes measured in males and females respect age are likely to be small in almost presenting results (*197–199*).

Linear dependence with age of some variables was considered reflecting a positive and significant correlation for E-GPx, P-SOD, E-SOD, MDA, HNE, PCO, and GSSG. A negative and significant correlation was found in GSH, Se (*99*, *194*, *198*, *199*). In some studies data were transformed for statistical analyses. Correlation between some parameters is few reported .In that cases association were found between HNE:MDA, MDA:GSH and HNE:MDA (*198*).

Analyses show general trends of oxidation as functions of age related to decreased antioxidant capacity.

Cross sectionals study design lend itself to limitations because it is not possible to know who from the individuals recruited in each group of age will live beyond 80 years or more. In the articles refereed authors did not directly measured free radical production so it is not possible to determine if older persons produce more free radicals but also have an enhanced capacity to defend against them.

Centenarians represent a highly selected group of successfully aged people. They apparently escaped the age-related disease during their lives and show some distinct immunologic or metabolic features. It would conceivable to expect their antioxidant status to be better than that of normally aged subjects (*194*). As results of different studies a quite peculiar antioxidant profile was finding. It is probably that this is not linked only to their antioxidants properties but also to their functions in other homeostatic mechanism such as immunomodulation.

Identified Pharmaceutical Targets

Evidences about molecular aspects contributing to aging permit to grouping identified elements in three groups (Figure 1). First are negative primary elements as: DNA damage, including chromosomal aneuploidies; mitochondrial DNA mutations; and telomere loss, epigenetic drift, and defective proteostasis which in terms impact on negative form on general process.

Publication Date (Web): October 13, 2015 | doi: 10.1021/bk-2015-1200.ch006

Publication Date (Web): October 13, 2015 | doi: 10.1021/bk-2015-1200.ch006

Table 1. Comparison of studies that evaluated the oxidative stress indexes in healthy individuals related to age.[a]

Study	*Design*	*Sample size*	*Age range (years)*	*OSI*	*Outcomes with age*
Meccoci Italy- 2000 (*194*)	Cross sectional and comparative study	107	60-99	Vit C, E, A, thiols, α-carotene, β-carotene, P-SOD, E-SOD, P-GPx	↓ Vit C, β-carotene, thiols, ↑ Vit E, A α-carotene, P-SOD, E-SOD, ↔ P-GPx
Jones USA- 2002 (*195*)	Cross sectional and comparative study	122	19-85	GSH, GSSG, Cys, CySS, CySSG, Eh GSH/GSSG, Eh Cys/cySS, Eh CSH-Cys/CySSG	↓ GSH, Cys, ↑ GSSG, CySS, CySSG, Eh GSH/GSSG, Eh Cys/cySS, Eh CSH-Cys/CySSG
Erden-Inal Turkey- 2002 (*99*)	Cross sectional and comparative study	176	0.2-69	GSH, GSSG, E-GSSGR, E-GPx, Se	↓ GSH, E-GSSGR, Se ↑ GSSG, E-GPx
Ozbay Turkey- 2002 (*196*)	Cross sectional and comparative study	257	9-71	MDA, E-SOD, E-GPx	↑ MDA, E-SOD, E-GPx
Junqueira Brazil – 2004 (*197*)	Cross sectional and comparative study	503	20->70	TBARS, E-SOD, E-CAT, E-GPx	↑ TBARS, E-GPx ↔ E-SOD, E-CAT
Gil Germany- 2006 (*198*)	Cross sectional and comparative study	194	18 - 84	MDA, PCO, HNE, GSH, GSH, GSSG, UA	↓ GSH, ↑ MDA, PCO, HNE, GSSG ↔ UA
Frisard USA-2007 (*199*)	Cross sectional and comparative study	170	20-90	U-IsoPs, PCO, DNA damage (Comet assay, FLARE)	↑ DNA damage FLARE ↔ U-IsoPs, PCO, DNA damage Comet assay

Publication Date (Web): October 13, 2015 | doi: 10.1021/bk-2015-1200.ch006

Study	*Design*	*Sample size*	*Age range (years)*	*OSI*	*Outcomes with age*
Mendoza Mexico-2007 (*200*)	Cross sectional and comparative study	249	25-70	LPO, TAS, E-GPx, E-SOD	↓ TAS, E-GPx,↑ LPO, ↔ E-SOD
Ditmar Germany 2008 (*201*)	Cross sectional and comparative study	40	24-79	DNA, P-SOD, GPx, LPO, GSH/GSSG, Vit C, β-carotene, Zn	↑ GPx, GSH/GSSG, Zn,DNA, LPO ↔ Vit C, P-SOD, β-carotene
Singh India- 2009 (*202*)	Cross sectional and comparative study	300	15-65	LPO,SOD, GSH, GPx, XOD	↓ GSH, GPx ↑ XOD, LPO,SOD,
Alexandrova Bulgaria 2010 (*203*)	Cross sectional and comparative study	45	40-80	E-SOD	↓ E-SOD < 70 years old ↔ E-SOD ≥ years old
Banerjee India-2014 (*204*)	Cross sectional and comparative study	80	35-90	TBARS, P-SOD, PCO	↑ PCO, TBARS ↓ P-SOD

[a] Legend: ↑ increased, ↓ decreased, ↔ unchanged; OSI: oxidative stress indexes, Vit : vitamin, P-: plasmatic, E-: erytrocytic, U- urine, SOD: superoxide dismutase, GPx: gluthatione peroxidase, GSH: glutathione, Cys: cisteine, Se: selenium, MDA: malonildialdehyde, TBARS: thiobarbituric acid –reactive species, CAT: catalase, PCO: protein carbonyls, HNE:hidroxinonenal, IsoPs: isoprotanes, UA: uric acid, LPO: lipoperoxide, TAS: total antioxidant status, DNA: oxidative DNA damage, XOD: xanthine oxidase, Zn: zinc

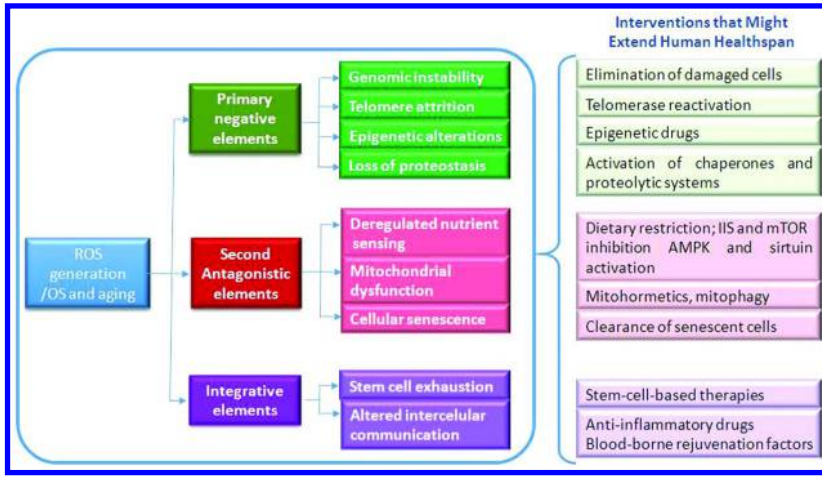

Figure 1. Hierarchical Elements related to ROS generation, OS and aging connected to interventions that might influence on human healthspan all of them described in the chapter.

In second place antagonistic elements have opposite effects depending on their intensity. At low levels, they mediate beneficial effects, but at high levels, they become deleterious. This is the case for senescence, which protects the organism from cancer but which, in excess, can promote aging. Similarly, ROS mediate cell signaling and survival but, at chronic high levels, can produce cellular damage; likewise, optimal nutrient sensing and anabolism are obviously important for survival but, in excess and during time, can become pathological. Al third place integrative elements —stem cell exhaustion and altered intercellular communication— that directly affect tissue homeostasis and function.

The interconnectedness between different elements confers some degree of hierarchical relation between them. First could be the initiating triggers whose damaging consequences progressively accumulate with time. The antagonistic, being in principle beneficial, become progressively negative in a process that is partly promoted or accelerated by the first elements. At last, the integrative elements arise when the accumulated damage caused by the first and antagonistic cannot be compensated by homeostatic mechanisms on cell or tissues. This appraisal proposed by López-Otin et. al (*143*) permit a better analysis and comprehension of experimental design, results and pharmaceutical interventions.

Developing natural or pharmacological agents capable of increasing the antioxidative protection and/or modulating the endogenous defense and repair mechanisms may potentially improve health, increase longevity and contribute to treatment of degenerative age-related diseases.

Actually some authors stated that the best strategy to enhance endogenous antioxidant levels may be the OS itself, based on the classical physiological concept of hormesis. It was observed that a wide variety of stressor (pro-oxidant) as ozone, aldehydes, CR, and other can have potential impact on redox status and in diverse pathways. The benefit of this adaptive response is protect molecules

In Oxidative Stress: Diagnostics, Prevention, and Therapy Volume 2; Hepel, et al.;
ACS Symposium Series; American Chemical Society: Washington, DC, 2015.

Publication Date (Web): October 13, 2015 | doi: 10.1021/bk-2015-1200.ch006

and tissues from moderate doses of toxic agents. In turn the enhanced defense and repair and even cross protection against multiple stressors could have clinical or public health use (*31*).

Enzymatic and non-enzymatic antioxidants protect against deleterious metal-mediated free radical attacks to some extent; e.g., vitamin E and melatonin can prevent the majority of metal-mediated (iron, copper, cadmium) damage both in *in vitro* systems and in metal-loaded animals.

A chelator is a molecule that has the ability to bind to metal ions, e.g. iron molecules, in order to remove heavy metals from the body. According to Halliwell and Gutteridge (*205*) chelators act by multiple mechanisms; mainly to i) alter the reduction potential or accessibility of metal ions to stop them catalysing $OH^{\cdot}$ production (e.g. transferrin or lactoferrin) ii) prevent the escape of the free radical into solution (e.g. albumin). In this case the free radicals are formed at the biding site of the metal ions to chelating agent. Chelators can be manmade or be produced naturally, e.g. plant phenols. Because the iron catalyzes ROS generation, sequestering iron by chelating agents is thought to be an effective approach toward preventing intracellular oxidative damage. Many chelating agents have been used to inhibit iron- or copper-mediated ROS formation, such as ethylenediaminetetraacetic acid (EDTA), diethylenetriaminepenta-acetic acid (DETAPAC), N,n′-Bis- (2-Hydroxybenzyl)ethylenediamine-N,n′-diacetic acid (HBED), 2-3-Dihydroxybenzoate, Desferrioxamine B (DFO), deferasirox (ICL 670), N,N′-bis-(3,4,5-trimethoxybenzyl) ethylenediamine N,N,-diacetic acid dihydrochloride (OR10141), phytic acid, PYSer and others (*205*, *206*).

The generation of excess superoxide due to abundance of energy substrates after the meal may be a predominate factor resulting in oxidative stress and a decrease in nitric oxide. A mixture of antioxidant compounds is required to provide protection from the oxidative effects of postprandial fats and sugars. No specific antioxidant can be claimed to be the most important, as consumption of food varies enormously in humans. However, a variety of polyphenolic compounds derived from plants appear to be effective dietary antioxidants, especially when consumed with high-fat meals (*206*).

Recent evidence also indicates that aging can be reverted by telomerase activation (Figure 1). In humans, recent meta-analyses have supported the existence of a strong relation between short telomeres and mortality risk, particularly at younger ages (*207*).

Restoration of physiological H4 acetylation through administration of histone deacetylase inhibitors avoids the manifestation of age-associated memory impairment in mice. Inhibitors of histone acetyltransferases also ameliorate the premature aging phenotypes of progeroid mice and extend their lifespan Conceptually similar to histone acetyltransferase inhibitors, histone deacetylase activators may conceivably promote longevity. Resveratrol has been extensively studied in relation to aging, and among its multiple mechanisms of action are the upregulation of SIRT1 activity, as well as other effects associated with energetic deficits (*208*).

Several approaches for maintaining or enhancing proteostasis aim at activating protein folding and stability mediated by chaperones. Pharmacological induction of the heat-shock protein Hsp72 preserves muscle function and delays

Publication Date (Web): October 13, 2015 | doi: 10.1021/bk-2015-1200.ch006

progression of dystrophic pathology in mouse models of muscular dystrophy (*209*). Small molecules may be also employed as pharmacological chaperones to assure the refolding of damaged proteins and to improve age-related phenotypes in model organisms. Interventions using chemical inducers of macroautophagy (another type of autophagy different than chaperone mediated autophagy) (Figure 1) have spurred extraordinary interest after the discovery that constant or intermittent administration of the mTOR inhibitor rapamycin can increase the lifespan of middle aged mice (*210*).

However, similar evidence does not yet exist for the effects of rapamycin on mammalian aging, and other mechanisms, such as inhibition of the ribosomal S6 protein kinase 1 (S6K1) implicated in protein synthesis. Spermidine, another macroautophagy inducer that, in contrast to rapamycin, has no immunosuppressive side effects, also promotes longevity in yeast, flies, and worms via the induction of autophagy (*211*). Similarly, nutrient supplementation with polyamine preparations containing spermidine or provision of a polyamine-producing gut flora increases longevity in mice. Dietary supplementation with u-6 polyunsaturated fatty acids also extends lifespan in nematodes through autophagy activation. Likewise, the enhancement of proteasome activity by deubiquitylase inhibitors or proteasome activators accelerates the clearance of toxic proteins in human cultured cells (*212*) and extends replicative lifespan in yeast.

Current available evidence strongly supports the idea that anabolic signaling accelerates aging and decreased nutrient signaling extends longevity (*213*). Further, a pharmacological manipulation that mimics a state of limited nutrient availability, such as rapamycin, can extend longevity in mice. Also results support the idea that telomeres and sirtuins may control mitochondrial function and thus play a protective role against age-associated diseases. endurance training and alternate-day fasting may improve healthspan through their capacity to avoid mitochondrial degeneration It is tempting to speculate that these beneficial effects are mediated, at least in part, through the induction of autophagy, for which both endurance training and fasting constitute potent triggers.

There is compelling evidence that compounds such as metformin and resveratrol are mild mitochondrial poisons that induce a low energy state characterized by increased AMP levels and activation of AMPK. senescence, the activation of p53 and INK4a/ARF can be regarded as a beneficial compensatory response aimed at avoiding the propagation of damaged cells and its consequences on aging and cáncer. Pharmacological interventions are also being explored to improve stem cell function in particular, mTORC1 inhibition with rapamycin, which can postpone aging by improving proteostasis. Some evidences attend that is possible to rejuvenate human senescent cells by pharmacological inhibition of the GTPase CDC42, whose activity is increased in aged HSCs. Recent promising studies suggest that stem cell rejuvenation may reverse the aging phenotype at the organismal level.

Genetic and pharmacological inhibition of NF-kB signaling prevents age-associated features in different mouse models of accelerated aging. A similar situation occurs with sirtuins, which may also have an impact on inflammatory responses associated with aging.

Publication Date (Web): October 13, 2015 | doi: 10.1021/bk-2015-1200.ch006

Several studies have revealed that, by deacetylating histones and components of inflammatory signaling pathways such as NF-kB, SIRT1 can downregulate inflammation-related genes. Pharmacologic activation of SIRT1 may prevent inflammatory responses in mice (*214*, *215*). SIRT2 and SIRT6 may also downregulate the inflammatory response through deacetylation of NF-kB subunits and transcriptional repression of their target genes. Conversely, lifespan-extending manipulations targeting one single tissue can retard the aging process in other tissues (*216*, *217*).

Additionally, given that the gut microbiome shapes the function of the host immune system and exerts systemic metabolic effects, it appears possible to extend lifespan by manipulating the composition and functionality of the complex and dynamic intestinal bacterial ecosystem of the human body (*218*, *219*).

All molecular aspects implying in detrimental aging process tempered by extensive interconnectedness between diverse elements should resound on one particular with impinge on others. The lifestyle changes, e.g. regular physical activity, increased intake of fruits and vegetables, and reduced calorie intake may improve health and increase cellular resistance to stress.

Publication Date (Web): October 13, 2015 | doi: 10.1021/bk-2015-1200.ch006

Conclusions

Taking into account that causes of ageing are complex and multifaceted, the recognition of molecular and cellular concert involved are crucial. A causal relationship between some elements such as oxidative macromolecules modifications, mutations of mtDNA, mitochondrial dysfunction and aging has emerged but the mechanism by which these molecular and biochemical events occur remain to be established. Contribution of elements and basic mechanistic aspect should be research for more comprehensive understanding of in vivo metabolism and repercussion to human health. Despite these concerns, substantial progress has been made toward an integrative understanding of living senescence and attempts to delineate mechanism considering OS and ROS as potential key participants. The process of ageing is influenced by cellular stress responses and produced an overlop which influences also on this reponse. Studies in different organisms converge to illustrate the multifaceted nature of this bi-directional crosstalk. Gaining in knowledge of specific aging pathway, investigators will be provided with additional opportunities to impact both life span and age related diseases in humans and others species. Nevertheless a strong possibility is previously suggested that the wasting process related to aging and diseases, at least to some extent, may not be irreversible in principle.

Available evidence indicates that redox-sensitive thiol elements function in signalling and control of virtually all aspects of life, including energy regulation, cytoskeletal structure, transport, proliferation, differentiation, and apoptosis. Consequently, disruption of thiol redox signalling and control by nonradical, two-electron oxidants could underlie much of the pathology linked to OS. To test this hypothesis, research is needed to identify critical redox elements and understand their physiology. Such knowledge can be expected to provide the

basis for novel therapeutic approaches to restore normal signalling and control and, thereby, prevent pathological and toxicological consequences of OS.

References

1. Muller, F.; Lustgarten, M. S.; Jang, Y.; Richardson, A.; Van Remmen, H. Trends in oxidative aging theories. *Free Radical Biol. Med.* **2007**, *43*, 477–503.
2. Block, G.; Dietrich, M.; Norkus, E. P.; Packer, L. Oxidative stress in human's populations. In *Critical Reviews of oxidative stress and Aging: Advances in Basic science, Diagnostic and Interventions*; Cutler, R., Rodriguez, H., Eds.; World Scientific Publishing: Singapore; 2003; pp 870−80.
3. Kirkwood, T.; Austad, S. Why do we age? *Nature* **2000**, *408*, 233–8.
4. Calabrese, E. Hormesis: from marginalization to mainstream: a case for hormesis as the default dose-response model in risk assessment. *Toxicol. Appl. Pharmacol.* **2004**, *197*, 125–36.
5. Rattan, S. Hormesis in aging. *Ageing Res. Rev.* **2008**, *7*, 63–78.
6. Sohal, R. Oxidative stress hypothesis of aging. *Free Radical Biol. Med.* **2002**, *33*, 573–4.
7. Troen, R. The biology of aging. *Mt. Sinai J. Med.* **2003**, *70* (1), 3–22.
8. Hughes, K.; Reynolds, R. M. Evolutionary and Mechanistic Theories of Aging. *Annu. Rev. Entomol.* **2005**, *50*, 421–5.
9. Petropoulou, C.; Chondrogianni, N.; Simoes, D.; Agiostratidou, G.; Drosopoulou, N.; Kotsota, V.; Gonos, E. S. Ageing and longevity: a paradigm of complementation between homeostatic mechanisms and genetic control? *Ann. N. Y. Acad. Sci.* **2000**, *9008*, 133–42.
10. Gerschman, R.; Gilbert, D.; Nye, S. W.; Dwyer, P.; Fenn, W. o Oxygen poisoning and X-ray toxicity.: a mechanism in common. *Science* **1954**, *119*, 623–6.
11. Harman, D. Ageing: a theory based on free radical and radiation chemistry. *J. Gerontol.* **1956**, *11*, 298–300.
12. Harman, D. The biological clock : the mitochondria? *J. Am. Geriartr. Soc.* **1972**, *20*, 145–7.
13. Jones, D. Redefining oxidative stress. *Antioxid. Redox Signaling* **2006**, *8*, 1865–79.
14. Jones, D. Radical-free biology of oxidative stress. *Am. J. Physiol. Cell Physiol.* **2008**, *295* (4), C849–C68.
15. Stadtman, E. Role of oxidant species in aging. *Curr. Med. Chem.* **2004**, *11* (9), 1105–12.
16. Barja, G. Free radicals and ageing. *Trends Neurosci.* **2004**, *27* (10), 595–600.
17. Buffenstein, R.; Edrey, Y. H.; Yang, T.; Mele, J. The oxidative stress theory of aging: embattled or invincible? Insights from non-traditional model organisms. *Age (Dordrecht, Netherlands)* **2008**, *30* (2−3), 99–109.
18. Xu, J. Radical metabolism is partner to energy metabolism in mitochondria. *Ann. N. Y. Acad. Sci.* **2004**, *1011*, 57–60.

Publication Date (Web): October 13, 2015 | doi: 10.1021/bk-2015-1200.ch006

19. Genova, M.; Pich, M. M.; Bernacchia, A.; Bianchi, C.; Biondi, A.; Bovina, C.; Falasca, A. I.; Formiggini, G.; Castelli, G. P.; Lenaz, G. The mitochondrial production of reactive oxygen species in relation to aging and pathology. *Ann. N. Y. Acad. Sci.* **2004**, *1011*, 86–100.
20. Boveris, A. Biochemistry of free radicals: from electrons to tissues. Shock 1998: Oxygen, nitric oxide and therapeutic perspectives. *Medicina* **1998**, *58*, 350–6.
21. Lenaz, G. The mitochondrial production of reactive oxygen species: mechanism and implications in human pathology. *IUBMB Life* **2000**, *152*, 159–64.
22. Droge, W. Free radicals in the physiological control of cell function. *Physiol. Rev.* **2002**, *82* (1), 47–95.
23. Hensley, K.; Robinson, K. A.; Gabbita, S. P.; Salsman, S.; Floyd, R. A. Reactive oxygen species, cell signalling, and cell injury. *Free Radical Biol. Med.* **2000**, *28*, 1456–62.
24. Finkel, T. Reactive oxygen species and signal transduction. *IUBMB Life* **2001**, *52*, 3–6.
25. Özben, T. Oxidative stress and antioxidants in ageing. In *Frontiers in Neurodegenerative Disorder and Ageing: Fundamental Aspects, Clinical perspectives and new insights*; Özben, T., Chevion, M., Eds.; IOS press: 2004, pp 99−115.
26. Lane, N. A unifying view of ageing and disease: the double-agent theory. *J. Theor. Biol.* **2003**, *225*, 531–40.
27. Nystrom T.; Osiewacz, H. D. *Model systems in aging*; Springer: Germany, 2004.
28. Kohn, R. Aging of animals: possible mechanism. In *Principles of mammalian aging*; Kohn, R., Ed.; Prentice-Hall: Englewood Cliffs, NJ: 1978.
29. Sohal, R.; Ku, H. H.; Agarwal, S.; Forster, M. J.; Lal, H. Oxidative damage, mitochondrial oxidant generation and antioxidant defenses during aging and in response to food restriction in the mouse. *Mech. Ageing Dev.* **1994**, *94*, 121–33.
30. Young, H.; Jeen, H.; Won, K.; Sue, J.; Pal, B. Molecular inflammation hypothesis of aging based on the anti-aging mechanism of caloric restriction. *Microsc. Res. Technol.* **2002**, *159*, 264–72.
31. Finkel, T.; Holbrook, N. Oxidants, oxidative stress and the biology of ageing. *Nature* **2000**, *408*, 239–47.
32. Schulz, T.; Zarse, K.; Voigt, A.; Urban, N.; Birringer, M.; Ristow, M. Glucose Restriction Extends Caenorhabditis elegans Lifespan by Inducing Mitochondrial Respiration and Increasing Oxidative Stress. *Cell Metab.* **2007**, *6*, 280–93.
33. Navratil V. *Health, Ageing and Entropy*; Masarykova Univerzita, Health Literacy Through Education: 2011.
34. Kowaltowski, A.; de Souza-Pinto, N. C.; Castilho, R.; Vercesi, A. E. Mitochondria and reactive oxygen species. *Free Radical Biol. Med.* **2009**, *47*, 333–43.

35. Tilman G. *Oxidants and antioxidants defense systems. The handbook of Enviromental Chemistry 2.0*; Springer: Berlin, Heidelberg, New York, 2005.
36. Cadenas, E.; Davies, K. J. Mitochondrial free radical generation, oxidative and aging. *Free Radical Biol. Med.* **2000**, *29*, 222–30.
37. Staniek, K.; Nohl, H. Are mitochondria a permanent source of reactive oxygen species? *Biochim. Biophys. Acta* **2000**, *1460*, 268–75.
38. Wei, Y.; Lee, H. C. Oxidative stress, mitochondrial DNA mutation and impairment of antioxidant enzymes in aging. *Exp. Biol. Med.* **2002**, *227*, 671–82.
39. Schapira, A. Primary and secondary defects of the mitochondrial respiratory chain. *J. Inherited Metab. Dis.* **2002**, *25* (3), 207–14.
40. Dillin, A.; Hsu, A. L.; Arantes-Oliveira, N.; Lehler-Graiwer, J.; Hsin, H.; Fraser, A. G.; Kamath, R. S.; Ahringer, J.; Kenyon, C. Rates of behaviour and aging specified by mitochondrial function during development. *Science* **2002**, *298*, 2398–401.
41. Golden, T.; Melov, S. Mitochondrial DNA mutations, oxidative stress and aging. *Mech. Ageing Dev.* **2001**, *122*, 1577–89.
42. Harper, M.; Bevilacqua, L.; Hagopian, K.; Weindruch, R.; Ramsey, J. J. Ageing, oxidative stress, and mitochondrial uncoupling. *Acta Physiol. Scand.* **2004**, *182* (4), 321–3.
43. Cadenas, E. Mitochondrial free radical production and cell signalling. *Mol. Aspects Med.* **2004**, *25*, 17–26.
44. Judge, S.; Jang, Y. M.; Smith, A.; Hagen, T.; Leeuwenburgh, C. Age-associated increases in oxidative stress and antioxidant enzyme activities in cardiac interfibrillar mitochondria: implications for the mitochondrial theory of aging. *FASEB J.* **2005**, *19*, 419–21.
45. Melov, S. Mitochondrial oxidative stress. Physiologic consequences and potential for a role in aging. *Ann. N. Y. Acad. Sci.* **2000**, *908*, 219–25.
46. de Souza-Pinto, N.; Bohr, V. A. The mitochondrial theory of aging: involvement of mitochondrial DNA damage and repair. *Int. Rev. Neurobiol.* **2002**, *53*, 519–34.
47. Scheckhuber, C. Impact of mitochondrial dynamics on organismic aging. *Sci. World J.* **2009**, *9*, 250–4.
48. Rodríguez, Y.; Vázquez, R.; Lavernia, L.; Robles, Y. Aging and Oxidative Stress. *Correo Cientifico Médico* **2009**, *13* (2).
49. Karlseder, J.; Smogorzewska, A.; de Lange, T. Senescente induced by altered telomerese state, not telomere loss. *Science* **2002**, *295*, 2446–9.
50. Saretzki, G.; Von Zglinicki, T. Replicative aging, telomeres, and oxidative stress. *Ann. N. Y. Acad. Sci.* **2002**, *959*, 24–9.
51. Tanaka, M.; Gong, J. S.; Zhang, J.; Yaneda, M.; Yagi, K. Mitochondrial genotype associated with longevity. *Lancet* **1998**, *351*, 185–6.
52. Camougrand, N.; Rigoulet, M. Aging and oxidative stress: studies of some genes involved both in aging and in response to oxidative stress. *Respir. Physiol.* **2001**, *128* (3), 393–401.
53. Szegezdi, E.; Logue, S.; Gorman, A.; Samali, A. Mediators of endoplasmic reticulum stress-induced apoptosis. *EMBO Rep.* **2006**, *7*, 880–5.

Publication Date (Web): October 13, 2015 | doi: 10.1021/bk-2015-1200.ch006

54. Stevens, F.; Argon, Y. Protein folding in the ER. *Semin. Cell Dev. Biol. Chem.* **1999**, *10*, 443–54.
55. Zhang, C.; Cuervo, A. Restoration of chaperone-mediated autophagy in aging liver improves cellular maintenance and hepatic function. *Nat. Med.* **2008**, *14*, 959–65.
56. Zhang, K.; Kaufman, R. Protein folding in the endoplasmic reticulum and the unfolded protein response. *Handb. Exp. Pharmacol.* **2006**, *172*, 69–91.
57. Yorimitsu, T.; Nair, U.; Yang, Z.; Klionsky, D. Endoplasmic reticulum stress triggers autophagy. *J. Biol. Chem.* **2006**, *281*, 30299–304.
58. Ding, W.; Yin, X. Sorting, recognition and activation of the misfolded protein degradation pathways through macroautophagy and the proteasome. *Autophagy* **2008**, *4*, 141–50.
59. Kourtis, N.; Tavernarakis, N. Cellular stress response pathways and ageing: intricate molecular relationships. *The EMBO Journal.* **2011**, *30*, 2520–31.
60. Cuervo, A. Chaperone-mediated autophagy: selectivity pays off. *Trends Endocrinol Metab* **2010**, *21*, 142–50.
61. Mizushima, N.; Levine, B.; Cuervo, A.; Klionsky, D. Autophagy fights disease through cellular self-digestion. *Nature* **2008**, *451*, 1069–75.
62. Yorimitsu, T.; Klionsky, D. Autophagy: molecular machinery for self-eating. *Cell Death Differ.* **2005**, *12* (2), 1542–52.
63. Dice, J. Chaperone-mediated autophagy. *Autophagy* **2007**, *3*, 295–9.
64. Komatsu, M.; Waguri, S.; Chiba, T.; Murata, S.; Iwata, J.; Tanida, I.; et al. Loss of autophagy in the central nervous system causes neurodegeneration in mice. *Nature* **2006**, *441*, 880–4.
65. Komatsu, M.; Waguri, S.; Ueno, T.; Iwata, J.; Murata, S.; Tanida, I.; et al. Impairment of starvation-induced and constitutive autophagy in Atg7-deficient mice. *J. Cell Biol.* **2005**, *169*, 425–34.
66. Nakai, A.; Yamaguchi, O.; Takeda, T.; Higuchi, Y.; Hikoso, S.; Taniike, M.; et al. The role of autophagy in cardiomyocytes in the basal state and in response to hemodynamic stress. *Nat. Med.* **2007**, *13*, 619–24.
67. Hars, E.; Qi, H.; Ryazanov, A.; Jin, S.; Cai, L.; Hu, C.; et al. Autophagy regulates ageing in C. elegans. *Autophagy* **2007**, *3*, 93–5.
68. Toth, M.; Sigmond, T.; Borsos, E.; Barna, J.; Erdelyi, P.; Takacs-Vellai, K.; et al. Longevity pathways converge on autophagy genes to regulate life span in Caenorhabditis elegans. *Autophagy* **2008**, *4*, 330–8.
69. Kourtis, N.; Tavernarakis, N. Autophagy and cell death in model organisms. *Cell Death Differ.* **2009**, *16*, 21–30.
70. Bonnefont-Rousselot, D.; Therond, P.; Beaudeux, J. L.; Peynet, J.; Legrand, A.; Delatrade, J. Aging and oxidative stress. Which potential markers? *Ann. Biol. Clin.* **2001**, *59* (4), 453–9.
71. Kregel, K.; Zhang, H. J. An integrated view of oxidative stress in aging: basic mechanisms, functional effects, and pathological considerations. *Am. J. Physiol. Regul. Integr. Comp. Physiol.* **2007**, *292*, R18–R36.
72. Richard, M.; Roussel, A. M. Micronutrients and ageing: intakes and requirements. *Proc. Nutr. Soc.* **1999**, *58* (3), 573–8.

Publication Date (Web): October 13, 2015 | doi: 10.1021/bk-2015-1200.ch006

73. Holbrook, N.; Ikeyama, S. Age-related decline in cellular response to oxidative stress: links to growth factor signaling pathways with common defects. *Biochem. Pharmacol.* **2002**, *64* (5−6), 999–1005.
74. De Bont, R.; van Larebeke, N. Endogenous DNA damage in humans: a review of quantitative data. *Mutagenesis* **2004**, *19*, 169–85.
75. Hoeijmakers, J. DNA damage, aging, and cancer. *N. Engl. J. Med.* **2009**, *361*, 1475–148.
76. Jones, D.; Rando, T. Emerging models and paradigms for stem cell ageing. *Nat. Cell Biol.* **2011**, *13*, 506–12.
77. Park, C.; Larsson, N. Mitochondrial DNA mutations in disease and aging. *J. Cell Biol.* **2011**, *193*, 809–18.
78. Koga, H.; Kaushik, S.; Cuervo, A. Protein homeostasis and aging: The importance of exquisite quality control. *Ageing Res. Rev.* **2011**, *10*, 205–15.
79. Gregg, S.; Gutierrez, V.; Robinson, A.; Woodell, T.; Nakao, A.; Ross, M.; et al. A mouse model of accelerated liver aging caused by a defect in DNA repair. *Hepatology* **2012**, *55*, 609–21.
80. Gilbert, H. Molecular and cellular aspects of thiol-disulfide exchange. *Adv. Enzymol. Relat. Areas Mol. Biol.* **1990**, *63*, 69–172.
81. Kemp, M.; Go, Y.; Jones, D. Nonequilibrium thermodynamics of thiol/disulfide redox systems: a perspective on redox systems biology. *Free Radical Biol. Med.* **2008**, *44*, 921–37.
82. Stadtman, E.; Levine, R. Free radical-mediated oxidation of free amino acids and amino acid residues in proteins. *Amino Acids* **2003**, *25*, 207–18.
83. Stadtman, E.; Van Remmen, H.; Richardson, A.; Wehr, N.; Levine, R. Methionine oxidation and aging. *Biochim. Biophys. Acta* **2005**, *1703*, 135–40.
84. Lillig, C.; Holmgren, A. Thioredoxin and related molecules–from biology to health and disease. *Antioxid. Redox Signaling* **2007**, *9*, 25–47.
85. Jones, D.; Go, Y.; Anderson, C.; Ziegler, T.; Kinkade, J. J.; Kirlin, W. Cysteine/cystine couple is a newly recognized node in the circuitry for biologic redox signaling and control. *FASEB J.* **2004**, *18*, 1246–8.
86. Jones, D. Redox potential of GSH/GSSG couple: assay and biological significance. *Methods Enzymol.* **2002**, *348*, 93–112.
87. Block, G.; Dietrich, M.; Norkus, E. P.; Morrow, J. D.; Hudes, M.; Caan, B.; Packer, L. Factors associated with oxidative stress in human populations. *Am. J. Epidemiol.* **2002**, *156*, 274–85.
88. Hack, V.; Breitkreutz, R.; Kinscherf, R.; Rohrer, H.; Bartsch, P.; Taut, F.; Benner, A.; Droge, W. The redox state as a correlate of senescence and wasting as a target for therapeutic intervention. *Blood.* **1998**, *92*, 59–67.
89. Florini, J. *Composition and function of cells and tissues. Handbook of biochemistry in aging*; CRC Press: Boca Raton, FL, 1981.
90. Browner, W.; Kahn, A. J.; Ziv, E.; Reiner, A. P.; Oshima, J.; Cawthon, R. M.; Hsueh, W. C.; Cummings, S. R. The genetics of human longevity. *Am. J. Med.* **2004**, *117* (11), 851–60.
91. Stadtman, E. Importance of individuality in oxidative stress and aging. *Free Radical Biol. Med.* **2002**, *33* (5), 597–604.

Publication Date (Web): October 13, 2015 | doi: 10.1021/bk-2015-1200.ch006

92. Masaaki, K.; Masatoshi, S.; Nihal, S. A. Antioxidant systems and erythrocyte life span in mammals. *Comp. Biochem. Physiol.* **1987**, *39*, 13–6.
93. Chomyn, A.; Attardi, G. MtDNA mutations in aging and apoptosis. *Biochem. Biophys. Res. Commun.* **2003**, *304* (3), 519–29.
94. Levine, R.; Stadtman, E. Protein modifications with aging. In *Handbook of the biology of aging*; Schneider, E., Rowe, J. W., Eds.; Academic Press: San Diego, CA, 1996; pp 184−197.
95. Grune, T.; Shringarpure, R.; Sitte, N.; Davies, K. J. A. Age related changes in protein oxidation and proteolysis in mammalian cells. *J. Gerontol., Series A* **2001**, *56*, B459–67.
96. Dean, R.; Shanlin, F.; Stocker, R.; Davies, M. J. Biochemistry and pathology of radical-mediated protein oxidation. *Biochem. J.* **1997**, *324*, 1–18.
97. Stadtman, E. Protein oxidation in aging and age-related diseases. *Ann. N. Y. Acad. Sci.* **2001**, *928*, 22–38.
98. Yang, C.; Chou, S. T.; Liu, L.; Tsai, P. J.; Kuo, J. S. Effect of ageing on human plasma glutathione concentrations as determined by high-perfornance liquid chromatography with fluorimetric detection. *J. Chromatogr. B: Biomed. Sci. Appl.* **1995**, *674* (1), 23–30.
99. Erden-Inal, M.; Sunal, E.; Kanbak, G. Age-related changes in the glutathione redox system. *Cell Biochem. Funct.* **2002**, *20* (1), 61–6.
100. Yoshida, T.; Oka, S. I.; Masutani, H.; Nakamura, H.; Yodi, J. The role of thioredoxin in the aging process: involvement of oxidative stress. *Antioxid. Redox Signaling* **2003**, *5*, 563–70.
101. Inal, M.; Kanbak, G.; Sunal, E. Antioxidant enzyme activities and malondialdehyde levels related to aging. *Clin. Chim. Acta* **2001**, *305*, 75–80.
102. Poubelle, P.; Chaintreuil, J.; Bensadoun, J.; Blotman, F.; Simon, L.; Crastes de Paulet, A. Plasma lipoperoxides and aging. *Biomedicine* **1982**, *36*, 164–7.
103. Esterbauer, H.; Cheeseman, K. H.; Dianzani, M. U.; Poli, G.; Slater, T. F. Separation and characterization of the aldehydic products of lipd peroxidation stimulated by ADP-Fe2+ in rat liver microsomes. *J. Biochem.* **1982**, *208*, 129–40.
104. Grune, T.; Siems, W. G.; Zollner, H.; Esterbauer, H. Metabolism of 4-hydroxynonenl, a cytotoxic lipid peroxidation product, in Ehrlich mouse ascites cells at different proliferation stages. *Cancer Res.* **1994**, *54*, 5231–5.
105. Esterbauer, H.; Cheeseman, K. H. Lipid peroxidation: pathological implications. *Chem. Phys. Lipids* **1987**, *45*, 103–7.
106. Feillet-Coudray, C.; Tourtauchaux, R.; Niculescu, M.; Rock, E.; Tauveron, I.; Alexandre-Gouabau, M. C.; Rayssiguier, Y.; Jalenques, I.; Mazur, A. Plasma levels of 8-epiPGF2 alpha, an in vivo marker of oxidative stress are not affected by aging or Alzheimer´s disease. *Free Radical Biol. Med.* **1999**, *27* (3−4), 463–9.
107. Stadtman, E. Protein oxidation and aging. *Free Radical Res.* **2006**, *40*, 1250–8.
108. Navon, A.; Ciechanover, A. The 26 S proteasome: from basic mechanisms to drug targeting. *J. Biol. Chem.* **2009**, *284*, 33713–8.

Publication Date (Web): October 13, 2015 | doi: 10.1021/bk-2015-1200.ch006

109. Kastle, M.; Grune, T. Protein oxidative modification in the aging organism and the role of the ubiquitin proteasomal system. *Curr. Pharm. Des.* **2011**, *17*, 4007–22.
110. Chondrogianni, N.; Stratford, F. L.; Trougakos, I. P.; Friguet, B.; Rivett, A. J.; Gonos, E. S. Central role of the proteasome in senescence and survival of human fibroblasts: induction of a senescence-like phenotype upon its inhibition and resistance to stress upon its activation. *J. Biol. Chem.* **2003**, *278*, 28026–37.
111. Fredriksson, A.; Johansson-Krogh, E.; Hernebring, M.; Pettersson, E.; Javadi, A.; Almstedt, A.; et al. Effects of aging and reproduction on protein quality control in soma and gametes of Drosophila melanogaster. *Aging Cell* **2012**, *11*, 634–43.
112. Tsakiri, E.; Sykiotis, G. P.; Papassideri, I. S.; Gorgoulis, V. G.; Bohmann, D.; Trougakos, I. P. Differential regulation of proteasome functionality in reproductive vs. somatic tissues of Drosophila during aging or oxidative stress. *FASEB J.* **2013**, *27*, 2407–20.
113. Tsakiri, E.; Sykiotis, G. P.; Papassideri, I. S.; Terpos, E.; Dimopoulos, M. A.; Gorgoulis, V. G.; et al. Proteasome dysfunction in Drosophila signals to an Nrf2-dependent regulatory circuit aiming to restore proteostasis and prevent premature aging. *Aging Cell* **2013**, *12*, 802–13.
114. Breusing, N.; Grune, T. Regulation of proteasome-mediated protein degradation during oxidative stress and aging. *Biol. Chem.* **2008**, *389*, 203–9.
115. Sykiotis, G.; Bohmann, D. Stress-activated cap'n'collar transcription factors in aging and human disease. *Sci. Signal* **2010**, *3*, re3.
116. Grimberg, K.; Beskow, A.; Lundin, D.; Davis, M. M.; Young, P. Basic Leucine zipper protein Cnc-C is a substrate and transcriptional regulator of the Drosophila 26S proteasome. *Mol. Cell Biol.* **2011**, *31*, 897–909.
117. Westerheide, S.; Anckar, J.; Stevens, S.; Sistonen, L.; Morimoto, R. Stress-inducible regulation of heat shock factor 1 by the deacetylase SIRT1. *Science* **2009**, *323*, 1063–6.
118. Sahin, E.; DePinho, R. A. Linking functional decline of telomeres, mitochondria and stem cells during ageing. *Nature* **2010**, *464* (7288), 520–8.
119. Mohamad, N.; Ponnuraj, T.; Amrah, S.; Shamsuddin, S.; Ahmad, S.; Stangaciu, S. Age and Disease Related Telomere Manifestations - A Review. *IOSR J. Dental Med. Sci.* **2014**, *13* (6), 63–8.
120. Aubert, G.; Lansdorp, P. M. Telomeres and Aging. *Physiol. Rev.* **2008**, *88*, 557–79.
121. Khan, S.; Chuturgoon, A. A.; Naidoo, D. P. Telomeres and atherosclerosis. *Cardiovasc. J. Africa* **2012**, *23* (10), 563–71.
122. Sahin, E.; Colla, S.; Liesa, M.; Moslehi, J.; Müller, F. L.; Guo, M.; Cooper, M.; Kotton, D.; Fabian, A. J.; Walkey, C.; Maser, R. S.; Tonon, G.; Foerster, F.; Xiong, R.; Wang, Y. A.; Shukla, S. A.; Jaskelioff, M.; Martin, E. S.; Heffernan, T. P.; Protopopov, A.; Ivanova, E.; Mahoney, J. E.; Kost-Alimova, M.; Perry, S. R.; Bronson, R.; Liao, R.; Mulligan, R.; Shirihai, O. S.; Chin, L.; DePinho, R. A. Telomere dysfunction induces metabolic and mitochondrial compromise. *Nature* **2011**, *470*, 359–65.

Publication Date (Web): October 13, 2015 | doi: 10.1021/bk-2015-1200.ch006

123. Shay, J.; Wright Hallmarks of telomeres in ageing research. *J. Pathol.* **2007**, *211* (2), 114–23.
124. Sahin, E.; DePinho, R. A. Linking functional decline of telomeres, mitochondria and stem cells during ageing. *Nature* **2010**, *464*, 520–8.
125. Liu, L.; Trimarchi, J. R.; Smith, P. J.; Keefe, D. L. Mitochondrial dysfunction leads to telomere attrition and genomic instability. *Aging Cell.* **2002**, *1*, 40–6.
126. Passos, J.; von Zglinicki, T. Mitochondria, telomeres and cell senescence. *Exp. Gerontol.* **2005**, *40*, 466–72.
127. Sablina, A. The antioxidant function of the p53 tumor suppressor. *Nat. Med.* **2005**, *11*, 1306–13.
128. Vousden, K.; Lane, D. P. p53 in health and disease. *Nat. Rev. Mol. Cell Biol.* **2007**, *8*, 275–83.
129. Rufini, A.; Tucci, P.; Celardo, I.; Melino, G. Senescence and aging: the critical roles of p53. *Oncogene* **2013**, *32*, 5129–43.
130. Cencioni, C. S. F.; Martelli, F.; Valente, S.; Mai, A.; Zeiher, A. M.; Gaetano, C. Oxidative Stress and Epigenetic Regulation in Ageing and Age-Related Diseases. *Int. J. Mol. Sci.* **2013**, *14*, 17643–63.
131. Ota, H.; Tokunaga, E.; Chang, K.; Hikasa, M.; Iijima, K.; Eto, M.; Kozaki, K.; Akishita, M.; Ouchi, Y.; Kaneki, M. SIRT1 inhibitor, Sirtinol, induces senescence-like growth arrest with attenuated Ras-MAPK signaling in human cancer cells. *Oncogene* **2006**, *25*, 176–85.
132. Rahman, I.; Marwick, J.; Kirkham, P. Redox modulation of chromatin remodeling: Impact on histone acetylation and deacetylation, NF-kappaB and pro-inflammatory gene expression. *Biochem. Pharmacol.* **2004**, *68*, 1255–67.
133. Dizdaroglu, M.; Jaruga, P.; Birincioglu, M.; Rodriguez, H. Free radical-induced damage to DNA: Mechanisms and measurement. *Free Radical Biol. Med.* **2002**, *32*, 1102–15.
134. Zawia, N.; Lahiri, D. K.; Cardozo-Pelaez, F. Epigenetics, oxidative stress, and Alzheimer disease. *Free Radical Biol. Med.* **2009**, *46*, 1241–9.
135. Pollina, E.; Brunet, A. Epigenetic regulation of aging stem cells. *Oncogene* **2011**, *30*, 3105–26.
136. Tsurumi, A.; Li, W. Global heterochromatin loss: a unifying theory of aging? *Epigenetics* **2012**, *7*, 680–8.
137. Ugalde, A.; Español, Y.; Lopez-Otın, C. Micromanaging aging with miRNAs: new messages from the nuclear envelope. *Nucleus* **2011**, *2*, 549–55.
138. Hiona, A.; Sanz, A.; Kujoth, G.; Pamplona, R.; Seo, A.; Hofer, T.; et al. Mitochondrial DNA mutations induce mitochondrial dysfunction, apoptosis and sarcopenia in skeletal muscle of mitochondrial DNA mutator mice. *PLoS ONE* **2010**, *5*, e11468.
139. Wang, K.; Klionsky, D. Mitochondria removal by autophagy. *Autophagy* **2011**, *7*, 297–300.
140. Cabreiro, F.; Au, C.; Leung, K.; Vergara-Irigaray, N.; Cocheme, H.; Noori, T.; et al. Metformin retards aging in C. elegans by altering microbial folate and methionine metabolism. *Cell* **2013**, *153*, 228–39.

Publication Date (Web): October 13, 2015 | doi: 10.1021/bk-2015-1200.ch006

141. Barzilai, N.; Huffman, D.; Muzumdar, R.; Bartke, A. The critical role of metabolic pathways in aging. *Diabetes* **2012**, *61*, 1315–22.
142. Price, N.; Gomes, A.; Ling, A.; Duarte, F.; Martin-Montalvo, A.; North, B.; et al. SIRT1 is required for AMPK activation and the beneficial effects of resveratrol on mitochondrial function. *Cell Metab.* **2012**, *15*, 675–90.
143. Lopez-Otın, C.; Blasco, M.; Partridge, L.; Serrano, M.; Kroemer, G. The Hallmarks of Aging. *Cell* **2013**, *153*, 1194–217.
144. Hou, C.; Bolt, K.; Bergman, A. A general life history theory for effects of caloric restriction on health maintenance. *BMC Systems Biol.* **2011**, *5*, 78.
145. Vendelbo, M.; Nair, K. S. Mitochondrial longevity pathways. *Biochim. Biophys. Acta* **2011**, *1813*, 634–44.
146. Shinmura, K. Effects of caloric restriction on cardiac oxidative stress and mitochondrial bioenergetics: Potential role of cardiac sirtuins. *Oxid. Med. Cell Longevity* **2013**, *2013*, 528935.
147. Civitarese, A.; Carling, S.; Heilbronn, L. K.; Hulver, M. H.; Ukropcova, B.; Deutsch, W. A.; Smith, S. R.; Ravussin, E. Calorie restriction increases muscle mitochondrial biogenesis in healthy humans. *PLoS Med* **2007**, *4*, e76.
148. Lopez-Lluch, G.; Hunt, N.; Jones, B.; Zhu, M.; Jamieson, H.; Hilmer, S.; et al. Calorie restriction induces mitochondrial biogenesis and bioenergetic efficiency. *Proc. Natl. Acad. Sci. U.S.A.* **2006**, *103*, 1768–73.
149. Faulks, S.; Turner, N.; Else, P. L.; Hulbert, A. J. Calorie restriction in mice: effects on body composition, daily activity, metabolic rate, mitochondrial reactive oxygen species production, and membrane fatty acid composition. *J. Gerontol.* **2006**, *61*, 781–94.
150. Martin-Montalvo, A.; de Cabo, R. Mitochondrial metabolic reprogramming induced by calorie restriction. *Antioxid. Redox Signaling* **2013**, *19* (3), 310–20.
151. Wu, Z.; Puigserver, P.; Andersson, U.; Zhang, C.; Adelmant, G.; Mootha, V.; et al. Mechanisms controlling mitochondrial biogenesis and respiration through the thermogenic coactivator PGC-1. *Cell* **1999**, *98*, 115–24.
152. Rodgers, J.; Lerin, C.; Haas, W.; Gygi, S. P.; Spiegelman, B. M.; Puigserver, P. Nutrient control of glucose homeostasis through a complex of PGC-1alpha and SIRT1. *Nature* **2005**, *434*, 113–8.
153. Hursting, S.; Dunlap, S. M.; Ford, N. A.; Hursting, M. J.; Lashinger, L. M. Calorie restriction and cancer prevention: a mechanistic perspective. *Cancer Metab.* **2013**, *1*, 10–20.
154. Saharinen, P.; Eklund, L.; Pulkki, K.; Bono, P.; Alitalo, K. VEGF and angiopoietin signaling in tumor angiogenesis and metastasis. *Trends Mol. Med.* **2011**, *17*, 347–62.
155. Powolny, A.; Wang, S.; Carlton, P. S.; Hoot, D. R.; Clinton, S. K. Interrelationships between dietary restriction, the IGF-1 axis, and expression of vascular endothelial growth factor by prostate adenocarcinoma in rats. *Mol. Carcinog.* **2008**, *47*, 458–76.
156. Lashinger, L.; Malone, L. M.; MacArthur, M. J.; Goldberg, J. A.; Daniels, E. A.; Pavone, A.; et al. Genetic reduction of insulin-like growth factor-1 mimics the anticancer effects of calorie restriction on

Publication Date (Web): October 13, 2015 | doi: 10.1021/bk-2015-1200.ch006

cyclooxygenase-2-driven pancreatic neoplasia. *Cancer Prev. Res.* **2011**, *4*, 1030–40.
157. Harvey, A.; Lashinger, L. M.; Hursting, S. D. The growing challenge of obesity and cancer: an inflammatory subject. *Ann. N. Y. Acad. Sci.* **2011**, *1229*, 45–52.
158. Harvey, A.; Lashinger, L.; Otto, G.; Malone, L.; Hursting, S. D. Decreased systemic insulin-like growth factor-1 in response to calorie restriction modulates tumor growth, NF-κB activation, and inflammation-related gene expression. *Mol. Carcinog.* **2012**, *52*, 997–1006.
159. Merry, B. Oxidative stress and mitochondrial function with aging-the effects of calorie restriction. *Ageing Cell.* **2004**, *3*, 7–12.
160. Masoro, E. Dietary restriction: an experimental approach to the study of the biology of aging. In *Handbook of the biology of aging*; Masoro, E., Austad, S. N., Eds.; New York Academy Press: 2001; pp 396−420.
161. Lee, C.; Klopp, R. G.; Weindruch, R.; Prolla, T. A. Gene expression profile of aging and its retardation by caloric restriction. *Science* **1999**, *285*, 1390–3.
162. Nisoli, E.; Tonello, C.; Cardile, A.; Cozzi, V.; Bracale, R.; Tedescvo, L.; Falcone, S.; Valerio, A.; Cantoni, O.; Clementi, E.; Moncada, S.; Carruba, M. O. Calorie restriction promotes mitochondrial biogenesis by inducing the expression of eNOS. *Science* **2005**, *310*, 314–7.
163. Chung, H.; Kim, H. J.; Kim, J. W.; Yu, B. P. The inflammation hypothesis of aging: molecular modulation by caloric restriction. *Ann. N. Y. Acad. Sci.* **2001**, *928*, 327–35.
164. Barja, G. Endogenous oxidative stress: relationship to ageing, longevity and caloric restriction. *Ageing Res. Rev.* **2002**, *1*, 397–411.
165. St-Pierre, J.; Drori, S.; Uldry, M.; Silvaggi, J. M.; Rhee, J.; Jager, S.; Handschin, C. F.; Zheng, K.; Lin, J.; Yang, W. E.; Simon, D. K.; Bachoo, R.; Spiegelman, B. M. Suppression of reactive oxygen species and neurodegeneration by the PGC-1 transcriptional coactivators. *Cell* **2006**, *127*, 397–408.
166. Sapolsky, R.; Krey, L.; McEwen, B. Prolonged glucocorticoid exposure reduces hippocampal neuron number: implications for aging. *J. Neurosci.* **1985**, *5*, 1221–7.
167. Medzhitov, R. Origin and physiological roles of inflammation. *Nature* **2008**, *454*, 428–35.
168. Tabas, I.; Glass, C. K. Anti-inflammatory therapy in chronic disease: Challenges and opportunities. *Science* **2013**, *339*, 166–72.
169. Woods, J.; Wilund, K. R.; Martin, S. A.; Kistler, B. M. Exercise, inflammation and aging. *Aging Dis.* **2012**, *3*, 130–40.
170. Libby, P.; Tabas, I.; Fredman, G.; Fisher, E. Inflammation and its resolution as determinants of acute coronary syndromes. *Circ. Res.* **2014**, *114* (12), 1867–79.
171. Walston, J.; Xue, Q.; Semba, R. D.; Ferrucci, L.; Cappola, A. R.; Ricks, M.; et al. Serum antioxidants, inflammation and total mortality in older women. *Am. J. Epidemiol.* **2006**, *163*, 18–26.

Publication Date (Web): October 13, 2015 | doi: 10.1021/bk-2015-1200.ch006

172. Salmon, A.; Richardson, A.; Pérez, V. I. Update on the oxidative stress theory of aging: Does oxidative stress play a role in aging or healthy aging? *Free Radical Biol. Med.* **2010**, *48*, 642–55.
173. Gill, R.; Tsung, A.; Billiar, T. Linking oxidative stress to inflammation: Toll-like receptors. *Free Radical Biol. Med.* **2010**, *48*, 1121–32.
174. Favre, J.; Musette, P.; Douin-Echinard, V.; Laude, K.; Henry, J. P.; Arnal, J. F.; et al. Toll-like receptors 2-deficient mice are protected against postischemic coronary endothelial dysfunction. *Arterioscler. Thromb. Vasc. Biol.* **2007**, *27*, 1064–71.
175. Tsung, A.; Stang, M. T.; Ikeda, A.; Critchlow, N. D.; Izuishi, K.; Nakao, A.; et al. The transcription factor interferon regulatory factor-1 mediates liver damage during ischemia–reperfusion injury. *Am. J. Physiol. Gastrointest. Liver Physiol.* **2006**, *290*, G1261–G8.
176. Chao, W. Toll-like receptor signaling: a critical modulator of cell survival and ischemic injury in the heart. *Am. J. Physiol. Heart Circ. Physiol.* **2009**, *296*, H1–H12.
177. Kuwahata, S.; Fujita, S.; Orihara, K.; Hamasaki, S.; Oba, R.; Hirai, H.; et al. High expression level of Toll-like receptor 2 on monocytes is an important risk factor for arteriosclerotic disease. *Atherosclerosis* **2010**, *209*, 248–54.
178. Iwasaki, A.; Medzhitov, R. Regulation of adaptive immunity by the innate immune system. *Science* **2010**, *327*, 291–5.
179. Karki, K.; Negi, R.; Pande, D.; Khanna, R. S.; Khanna, H. D. Expression of soluble Toll-like receptors and its correlation with the oxidative damage in disease conditions. *Webmed Central Cancer* **2011**, *2*, 001480.
180. Salvioli, S.; Olivieri, F.; Marchegiani, F.; Cardelli, M.; Santoro, A.; Bellavista, E.; et al. Genes, ageing and longevity in humans: Problems, advantages, and perspectives. *Free Radical Res.* **2006**, *40*, 1303–23.
181. Garrido-Urbani, S.; Meguenani, M.; Montecucco, F.; Imhof, B. A. Immunological aspects of atherosclerosis. *Semin. Immunopathol.* **2014**, *36*, 73–91.
182. Lee, H.; Yu, M. R.; Yang, Y.; Jiang, Z.; Ha, H. Reactive oxygen species-regulated signaling pathways in diabetic nephropathy. *J. Am. Soc. Nephrol.* **2003**, *14*, S241–S5.
183. Maziére, C.; Trécherel, E.; Ausseil, J.; Louandre, C.; Maziére, J. C. Oxidized low density lipoprotein induces cyclin a synthesis. Involvement of ERK, JNK and NFkappaB. *Atherosclerosis* **2011**, *218*, 308–11.
184. Kuor-o, M. Disease model: human aging. *Trends Mol. Med.* **2001**, *7*, 179–81.
185. Walfromg, R. Inmunologic theory of aging: current status. *Fed. Proc.* **1974**, *33*, 2020–7.
186. Phillips, M.; Cataneo, R. N.; Greenberg, J.; Gunawardena, R.; Rahbari-Oskoui, F. Increased oxidative stress in younger as well as in older humans. *Clin. Chim. Acta* **2003**, *328* (1-2), 83–6.
187. Van den Berg, R.; Haenen, G. R. M. M.; van den Berg, H.; Bast, A. Transcription factor NF- B as a potential biomarker for oxidative stress. *Brit. J. Nutr.* **2001**, *86* (1), 121–7.

Publication Date (Web): October 13, 2015 | doi: 10.1021/bk-2015-1200.ch006

188. Miller, R. The aging immune system: primer and prospectus. *Science* **1996**, *273*, 70–4.
189. Bodamyali, T., Stevens, C. R., Blake, D. R., Winyard, P. G. Reactive oxygen/nitrogen species and acute inflammation: A physiological process. In *Free Radicals and Inflammation*; Winyard, P., Blake, D. R., Evans, C. H., Eds.; Birkhauser Verlag: Basel, 2000; pp 11−6.
190. Wallace, D. Mitochondrial DNA mutations and bioenergetic defects in aging and degenerative diseases. In *Molecular and Genetics basis of neurologic disease*; Rosenburg, D., Ed.; Butterworth Heinemann: Boston, 1996; pp 237−69.
191. Raha, S.; Robinson, B. H. Mitochondria, oxygen free radicals, disease and ageing. *Trends Biochem. Sci.* **2000**, *25*, 502–8.
192. Kim, J.; No, J. K.; Yu, B. P.; Chung, H. Y. Analysis of redox status in serum during aging. *Ann. N. Y. Acad. Sci.* **2001**, *928*, 298–350.
193. Aejemelaeus, R.; Holm, P.; Kaukinen, U.; Metsa-Ketela, T. J.; Laippala, P.; Hervonen, A. L.; Alho, H. E. Age related changes in the peroxyl radical scavenging capacity of human plasma. *Free Radical Biol. Med.* **1997**, *23* (1), 69–75.
194. Meccoci, P.; Polidori, C. M.; Troiano, L.; Cherubini, A.; Cechetti, R.; Pini, G.; Stratman, M.; Monti, D.; Stahl, W.; Sies, H.; Franceschi, C.; Seni, U. Plasma antioxidants and longevity: a study on healthy centenarians. *Free Radical Biol. Med.* **2000**, *28* (8), 1243–8.
195. Jones, D.; Mody, V. C.; Carlson, J. L.; Lynn, M. J.; Sternberg, P. Redox analysis of human plasma allows separation of pro-oxidant events of aging from decline in antioxidant defenses. *Free Radical Biol. Med.* **2002**, *33* (1), 1290–300.
196. Ozbay, B.; Dulger, H. Lipid peroxidation and antioxidant enzymes in Turkish population: relation to age, gender, exercise, and smoking. *Tohoku J. Exp. Med.* **2002**, *197* (2), 119–24.
197. Junqueira, V.; Barros, S. B.; Chan, S. S.; Rodriguez, L.; Giavarotti, L.; Abud, R. L.; Deucher, G. P. Aging and oxidative stress. *Mol. Aspects Med.* **2004**, *25* (1−2), 5–16.
198. Gil, L.; Siems, W.; Mazurek, B.; Gross, J.; Schroeder, P.; Voss, P.; Grune, T. Age-associated analysis of oxidative stress parameters in human plasma and erythrocytes. *Free Radical Res.* **2006**, *40* (5), 495–505.
199. Frisard, M.; Broussand, A.; Davies, S. S.; Roberts, L. J.; Rood, J.; de Jonge, L.; Fang, X.; Jazwinski, S. M.; Deutsch, W. A.; Ravussin, E. Aging, resting metabolic rate, and oxidative stress damage: results from Louisiana healthy aging study. *J. Gerontol., Ser. A* **2007**, *62* (7), 752–9.
200. Mendoza, V.; Ruiz, M.; Sanchez, M. A.; Retana, R.; Muñoz, J. L. Aging-related oxidative stress in healthy humans. *Tohoku J. Exp. Med.* **2007**, *213*, 261–8.
201. Dittmar, M.; Knuth, M.; Beineke, M.; Epe, B. Role of Oxidative DNA Damage and Antioxidative Enzymatic Defence Systems in Human Aging. *The Open Anthropology J.* **2008**, *1*, 38–45.

Publication Date (Web): October 13, 2015 | doi: 10.1021/bk-2015-1200.ch006

202. Singh, K.; Kaur, S.; Kumari, K.; Singh, G.; Kaur, A. Alterations in Lipid Peroxidation and Certain Antioxidant Enzymes in Different Age Groups under Physiological Conditions. *J. Hum. Ecol.* **2009**, *27* (2), 143–7.
203. Alexandrova, M.; Bochev, P. Phagocyte mitochondrial superoxide production and erythrocyte Cu-Zn superoxide dismutase activity decline in very old age. *J. Biomed. Clin. Res.* **2010**, *3* (1), 27–32.
204. Banerjee, S.; Ghosh, C. Evaluation of oxidative stress between middle aged and elderly population of Kolkata and Suburbs. *IJPCBS* **2014**, *4* (3), 569–75.
205. Halliwell, B., Gutteridge, J. *Free radicals in biology and medicine*, 4th ed.; University Press: Oxford, 2007.
206. Valko, M.; Morris, H.; Cronin, M. Metals, toxicity and oxidative stress. *Curr. Med. Chem.* **2005**, *12* (10), 1161–208.
207. Boonekamp, J.; Simons, M.; Hemerik, L.; Verhulst, S. Telomere length behaves as biomarker of somatic redundancy rather than biological age. *Aging Cell* **2013**, *12*, 330–2.
208. Green, D.; Galluzzi, L.; Kroemer, G. Mitochondria and the autophagy-inflammation-cell death axis in organismal aging. *Science* **2011**, *333*, 1109–12.
209. Gehrig, S.; van der Poel, C.; Sayer, T.; Schertzer, J.; Henstridge, D.; Church, J.; et al. Hsp72 preserves muscle function and slows progression of severe muscular dystrophy. *Nature* **2012**, *484*, 394–8.
210. Wilkinson, J.; Burmeister, L.; Brooks, S.; Chan, C.; Friedline, S.; Harrison, D.; et al. Rapamycin slows aging in mice. *Aging Cell.* **2012**, *11*, 675–82.
211. Eisenberg, T.; Knauer, H.; Schauer, A.; Buttner, S.; Ruckenstuhl, C.; Carmona-Gutierrez, D.; et al. Induction of autophagy by spermidine promotes longevity. *Nat. Cell Biol.* **2009**, *11*, 1305–14.
212. Lee, I.; Cao, L.; Mostoslavsky, R.; Lombard, D.; Liu, J.; Bruns, N.; et al. A role for the NAD-dependent deacetylase Sirt1 in the regulation of autophagy. *Proc. Natl. Acad. Sci. U.S.A.* **2008**, *105*, 3374–9.
213. Fontana, L.; Partridge, L.; Longo, V. Extending healthy life span—from yeast to humans. *Science* **2010**, *328*, 321–6.
214. Gillum, M.; Kotas, M.; Erion, D.; Kursawe, R.; Chatterjee, P.; Nead, K.; et al. SirT1 regulates adipose tissue inflammation. *Diabetes* **2011**, *60*, 3235–45.
215. Yao, H.; Chung, S.; Hwang, J.; Rajendrasozhan, S.; Sundar, I.; Dean, D.; et al. SIRT1 protects against emphysema via FOXO3-mediated reduction of premature senescence in mice. *J. Clin. Invest.* **2012**, *122*, 2032–45.
216. Lavasani, M.; Robinson, A.; Lu, A.; Song, M.; Feduska, J.; Ahani, B.; et al. Muscle-derived stem/progenitor cell dysfunction limits healthspan and lifespan in a murine progeria model. *Nat. Commun.* **2012**, *3*, 608.
217. Tomás-Loba, A.; Flores, I.; Fernández-Marcos, P.; Cayuela, M.; Maraver, A.; Tejera, A.; et al. Telomerase reverse transcriptase delays aging in cancer-resistant mice. *Cell* **2008**, *135*, 609–22.
218. Claesson, M.; Jeffery, I.; Conde, S.; Power, S.; O'Connor, E.; Cusack, S.; et al. Gut microbiota composition correlates with diet and health in the elderly. *Nature* **2012**, *488*, 178–84.

Publication Date (Web): October 13, 2015 | doi: 10.1021/bk-2015-1200.ch006

219. Ottaviani, E.; Ventura, N.; Mandrioli, M.; Candela, M.; Franchini, A.; Franceschi, C. Gut microbiota as a candidate for lifespan extension: an ecological/evolutionary perspective targeted on living organisms as metaorganisms. *Biogerontology* **2011**, *12*, 599–609.

Publication Date (Web): October 13, 2015 | doi: 10.1021/bk-2015-1200.ch006

Publication Date (Web): October 13, 2015 | doi: 10.1021/bk-2015-1200.ch007

Chapter 7

Unifying Mechanism of Antiviral Drug Action Based on Electron Transfer and Reactive Oxygen Species

Peter Kovacic[1,*] and Ratnasamy Somanathan[2]

[1]Department of Chemistry and Biochemistry, San Diego State University, San Diego, California 92182-1030, United States
[2]Centro de Graduados e Investigación del Instituto Tecnológico de Tijuana, Apdo postal 1166, Tijuana, B.C. Mexico
[*]E-mail: pkovacic@mail.sdsu.edu

Viral infections are a major health problem, including hepatitis C. An adverse factor comprises serious side effects brought about by conventional therapy. A generally accepted mechanism for drug action involves interference with viral RNA replication. Since physiological effects are often multifaceted, it is reasonable to consider other plausible modes of action. A 1990 article presents a unifying mechanism based on electron transfer-reactive oxygen species-oxidative stress. The present study updates this approach with focus mostly on conjugated imine-iminium ET species. Related ET agents are quinones, aromatic nitro compounds and metal substances.

Keywords: antiviral; mechanism; imine-iminium; electron transfer; radicals; simeprevir; faldaprevir; sofosbuvir; daclatasivir; ribavirin

Introduction

The antiviral drug area, particularly pertaining to hepatitis C virus (HCV), has attracted much recent attention (*1*). HCV infects many millions of people throughout the world, including about 5 million in the USA, of which 12,000 died. In the search for more effective and less toxic antiviral drugs, the mechanistic focus has been on inhibition of protease function of RNA polymerase activity. Since the

In Oxidative Stress: Diagnostics, Prevention, and Therapy Volume 2; Hepel, et al.;
ACS Symposium Series; American Chemical Society: Washington, DC, 2015.

Publication Date (Web): October 13, 2015 | doi: 10.1021/bk-2015-1200.ch007

virus does not replicate outside the host cells, the drugs face daunting challenges. Drug screening usually involves inhibition in vitro of viral protein or inhibition of viral cellular replication, of which the latter is broader.

The mechanistic basis of this article is provided in a recent review (*2*) as follows. "The preponderance of bioactive substances or their metabolites incorporate ET functionality, which we believe, play an important role in physiological responses. These main groups include quinones (or phenolic precursors), metal complexes (or complexors), aromatic nitro compounds (or related hydroxylamine and nitroso derivatives), and conjugated imines (or iminium species) (*3*). In vivo cycling with oxygen can occur giving rise to oxidative stress (OS) through generation of reactive oxygen species (ROS), such as hydrogen peroxide, hydroperoxides, alkyl peroxides, and diverse radicals (hydroxyl, alkoxyl, hydroperoxyl, and superoxide). In some cases, electron transfer (ET) results in interference with normal electrical effects, for example, in respiration or neurochemistry. Generally, active entities possessing ET groups display reduction potentials in the physiologically responsive range, that is, more positive than -0.5V. ET, ROS, and OS have been increasingly implicated in the mode of action of drugs and toxins (toxicants), for example, anti-infective agents (*4*), anticancer drugs (*5*, *6*), carcinogens (*7*), reproductive toxins (*8*), nephrotoxins (*9*), hepatotoxins (*10*), cardiovascular toxins (*11*), nerve toxins (*12*), mitochondrial toxins (*13*), abused drugs (*14*), immunotoxins (*15*), pulmonary toxins (*16*), dermal toxins (*17*), ototoxins (*18*), eye toxins (*19*), thyroid toxins (*20*), and various other categories (*21*).

There is a plethora of experimental evidence supporting the OS theoretical framework, including generation of the common ROS, lipid peroxidation, degradation products of oxidation, depletion of antioxidants (AOs), effects of exogenous AOs, DNA oxidation and cleavage products, as well as electrochemical data. This comprehensive, unifying mechanism is in keeping with the frequent observations that many ET substances display a variety of activities, for example, multiple drug properties, as well as toxic effects."

Scheme 1 illustrates ET leading to generation of superoxide. The radical anion must not be too stable or too unstable. In Scheme 2, superoxide functions as precursor of other ROS. There are various sources of superoxide, such as mitochondria and the immune system. Electron uptake by conjugated iminium is depicted in Scheme 3, including delocalization. Conjugation is required for stabilization. This category is not as well recognized as the other three.

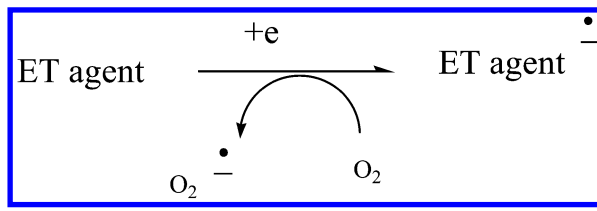

Scheme 1. Superoxide via ET

In Oxidative Stress: Diagnostics, Prevention, and Therapy Volume 2; Hepel, et al.;
ACS Symposium Series; American Chemical Society: Washington, DC, 2015.

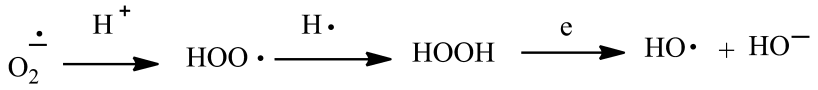

Scheme 2. ROS from superoxide

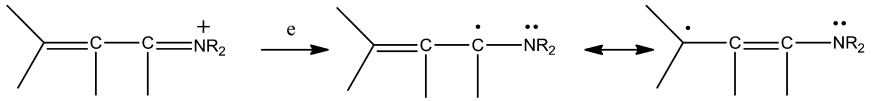

Scheme 3. Resonance stabilization of conjugated iminium after electron uptake

Publication Date (Web): October 13, 2015 | doi: 10.1021/bk-2015-1200.ch007

Although our mechanistic emphasis is on ET-ROS-OS, it should be stressed that bioactivation is often multifaceted. Emphasis in this review is on the more recent literature.

Oximes

A 1990 report presented a unifying mechanistic theme for antiviral action based on ET-ROS-OS (*22*). The members most relevant to the present study are the oximes (Fig. 1) containing a conjugated imine-type unit. Other ET agents were quinones and metal complexes, mostly of iron and copper. Reduction potentials were in the range amenable to ET in vivo. All of the organic agents are similar in possessing conjugated systems of different types, needed for radical anion stabilization. The inorganic metals must be large in order to provide requisite delocalization. Positive charge in either category acts to enhance electron attraction.

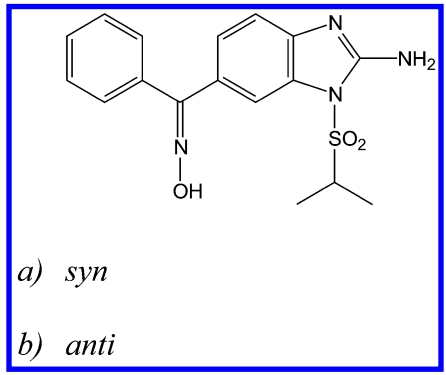

Figure 1. Zinviroxime (a) and enviroxime (b)

A factor hindering drug action is penetration of the cell by the virus making for difficulty of drug attack.

In Oxidative Stress: Diagnostics, Prevention, and Therapy Volume 2; Hepel, et al.;
ACS Symposium Series; American Chemical Society: Washington, DC, 2015.

Telaprevir

Telaprevir (Fig. 2) is used for treatment of HCV. The drug inhibits the virus protease which plays a role in replication.

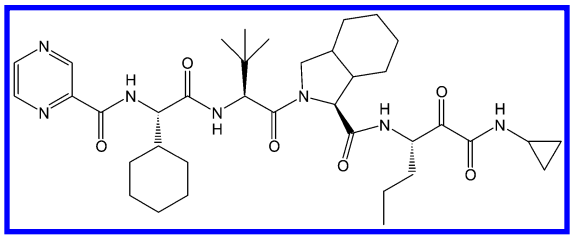

Figure 2. Telaprevir

Mechanistically, it is significant that the imine structure resembles related ones described herein, which may participate in ET-ROS-OS. The simple parent models and their ET properties are elucidated for imine and iminium derivatives of diacetyl (*23*, *24*). The reduction potentials of these imine and diimine derivatives fall within the physiological active range. Analogous bioactive imines are described (*24*).

Aromatic fused ring related compounds are found in the phenazine and quinoxaline classes including therapeutic effects (*25*). Phenazine methosulfate (Fig. 3) performs as an ET agent in biological systems (sigma product P9625). It acts as an electron carrier involving enzymes and oxygen. The iminium form usually possesses more favorable reduction potential than imine. The imine function can be converted to iminium by protonation in vivo.

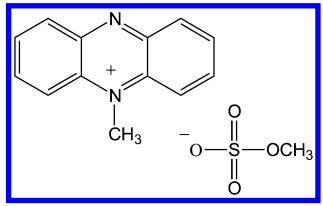

Figure 3. Phenazine methosulfate

Simeprevir

This antiviral drug (Fig. 4) is aimed mainly at treatment of hepatitis C (*26–28*). The commonly invoked mechanism involves viral protease inhibition resulting in interference with protein synthesis. An important aspect is the lower level of toxic response in infected patients (*27*, *29*).

In Oxidative Stress: Diagnostics, Prevention, and Therapy Volume 2; Hepel, et al.;
ACS Symposium Series; American Chemical Society: Washington, DC, 2015.

Publication Date (Web): October 13, 2015 | doi: 10.1021/bk-2015-1200.ch007

Publication Date (Web): October 13, 2015 | doi: 10.1021/bk-2015-1200.ch007

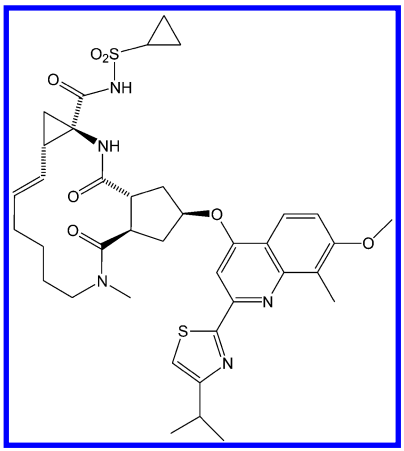

Figure 4. Simeprevir

Apparently, there has not been recognition of the structural presence of a potential ET segment, namely the 2-arylquinoline. A closely related analog is the anticancer drug Dup 785 (Fig. 5) containing a 2-phenyl substituent (*3*). A structurally related drug is camptothecin (Fig. 6). In both cases, the quinolinium forms (iminium type) display reduction potentials favorable for in vivo ET. The thiazole unit in simeprevir possesses heteroaromatic character including a highly conjugated imine-type group also present in quinoline. Mechanistic implications are elaborated in the Introduction. The ET property can result in generation of ROS which can give rise to OS leading to toxic effects.

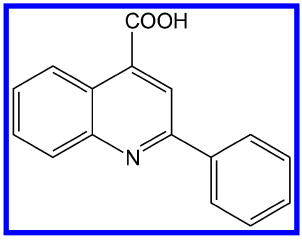

Figure 5. Dup 785

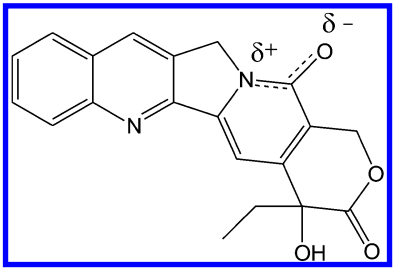

Figure 6. Camptothecin

In Oxidative Stress: Diagnostics, Prevention, and Therapy Volume 2; Hepel, et al.;
ACS Symposium Series; American Chemical Society: Washington, DC, 2015.

Publication Date (Web): October 13, 2015 | doi: 10.1021/bk-2015-1200.ch007

Faldaprevir

The drug (Fig. 7), being tested for treatment of hepatitis C, functions as protease inhibitor of the virus. An important point is structural similarity to simeprevir, particularly in relation to the 2-thiazylquinoline portion. Therefore, the mechanistic discussion for the related drug involving ET-ROS-OS would also be applicable for faldaprevir.

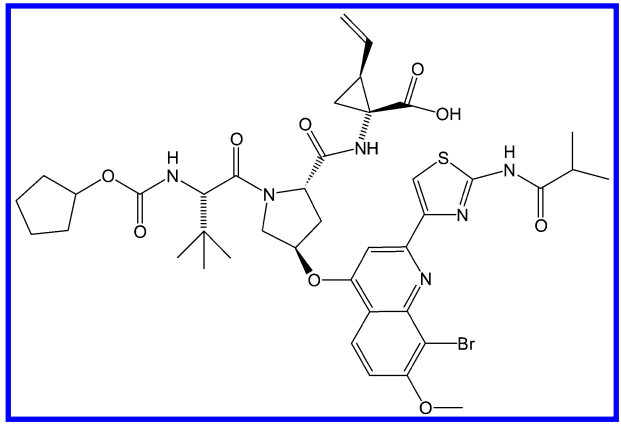

Figure 7. Faldaprevir

Sofosbuvir

The drug (Fig. 8), also designated PSI-78512 and PSI-7977, is used in mixtures for treatment of hepatitis C virus. It is rather effective and provides few adverse side effects. In relation to mode of action, the usual approach was proposed, namely inhibition of a polymerase enzyme that is needed for replication of viral RNA.

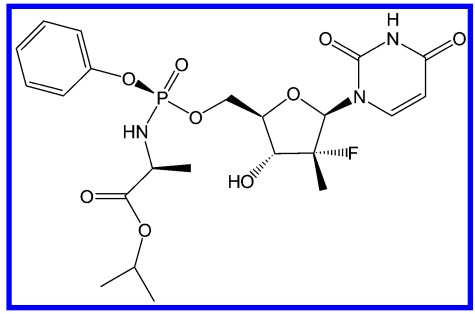

Figure 8. Sofosbuvir

Of particular interest in connection with the unifying mechanistic approach is a study involving metabolism of the drug (*30*). The initial step comprises enzymatic hydrolysis of the carboxylate ester moiety with formation of a carboxyl

group which, in turn, undergoes intramolecular attack on oxygen attached to benzene resulting in release of phenol. A significant aspect comprises evidence for involvement of phenol as an ET-ROS-OS agent. Facile oxidation occurs resulting in generation of catechol, hydroquinone and 1,2,4-trihydroxybenzene, followed by oxidation to the respective quinone products (*7*, *31*) (Scheme 4). This pathway is followed by benzene, a precursor of phenol, which exhibits carcinogenic properties (*7*). The 1,2,4-treihydroxybenzene segment is found in certain natural products, such as cannabinoids, in which there is action as precursor ET quinones (*32*). The other fragment from metabolism is a nucleoside analog which can participate in the usual manner interfering with RNA replication.

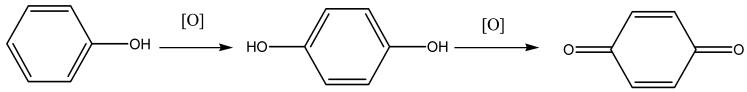

Scheme 4. Phenol metabolism to p-benzoquinone

Daclatasvir

This antiviral drug, also known as BMS-790052 (Fig. 9) (*33*), is electronically similar to simeprevir, but not as closely related as faldaprvir, with potential for ET-ROS-OS. Structurally, the highly conjugated biphenyl portion, related to quinoline, and the heteroaromatic imidazole segment is similar to thiazole. The two segments are connected in a highly conjugated structure, permitting favorable delocalization of the radical formed from electron uptake. Note that all of the drugs possess an imine nitrogen susceptible to protonation forming an iminium species that is more favorable to ET. Data show that daclatasvir interferes with viral replication and inhibits nonstructural protein in HCV.

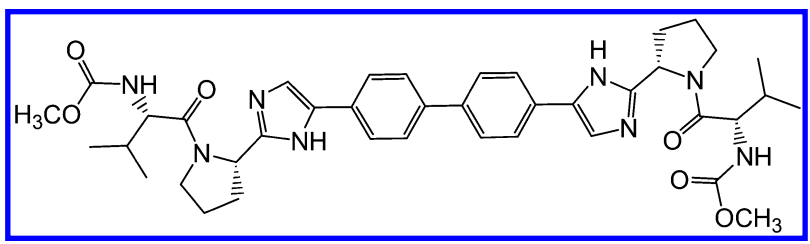

Figure 9. Daclatasvir

Ribavirin

Ribavirin (Fig. 10) is an aromatic triazole incorporating two conjugated imine groups, one of which is also conjugated with amide carbonyl. Numerous reports deal with mechanism of the antiviral drug. In vitro and in vivo investigations demonstrated genotoxicity which is associated with the generation of ROS (*34*). Cytotoxicity was also induced. Decreased toxicity was observed in the presence of silymarin, a phenolic, flavonoid AO (see AO section). No mutations occurred

In Oxidative Stress: Diagnostics, Prevention, and Therapy Volume 2; Hepel, et al.;
ACS Symposium Series; American Chemical Society: Washington, DC, 2015.

Publication Date (Web): October 13, 2015 | doi: 10.1021/bk-2015-1200.ch007

during silymarin treatment, evidence for attenuation of ROS by AO. The drug is reported to be a teratogen in rodents (*35*).

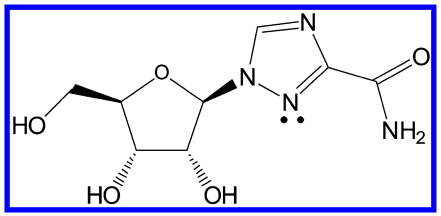

Figure 10. Ribavirin

Related Imine-Iminium Species

There is scant recognition of the importance of this ET class in the areas of biochemistry, medicine, and toxicology. A recent review (*17*), which places focus on this class, documents an abundance of members, from which representatives are selected in the following list: paraquat (herbicide) (Fig. 11), benzodiazepine diazepam (tranquilizer) (Fig.12), myosmine (tobacco alkaloid) (Fig. 13), retinal iminium (vision) (Fig. 14), and isoalloxazine (part of FAD redox enzymes) (Fig. 15).

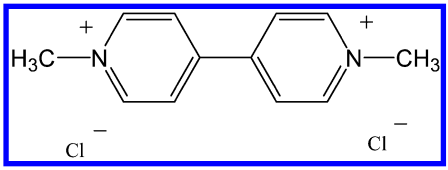

Figure 11. Paraquat

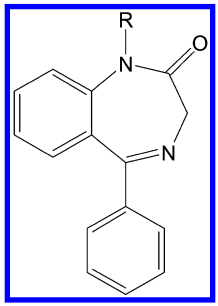

Figure 12. Benzodiazepine

Publication Date (Web): October 13, 2015 | doi: 10.1021/bk-2015-1200.ch007

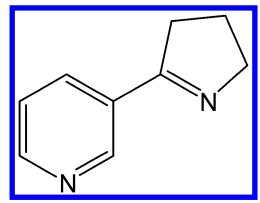

Figure 13. Myosmine

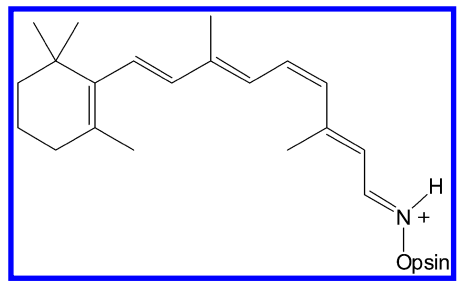

Figure 14. Retinal iminium

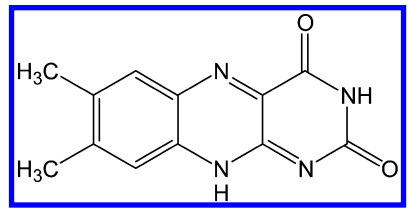

Figure 15. Isoalloxazine

Reactive Oxygen Species and Oxidative Stress

There is extensive literature (see Introduction) implicating ROS and OS in toxicity and therapeutic action. OS is a response to the generation of ROS. The ability of cells to cope with ROS-OS is hindered in patients infected with viruses (*36*). The liver plays an important role in dealing with toxic materials. Response of the liver includes additional production of ROS and reactive nitrogen species (RNS) as well as activation of many kinases. Lipid oxidation is an adverse effect, in addition to less protection as a result of decreased levels of AO GSH with increase in DNA strand breaks. Other adverse effects comprise cirrhosis and liver cancer. Various conditions accompany HCV infection, including OS, inflammation, excess iron and liver insult (*37*). Enhanced production of ROS and RNS, accompanied by lower AO levels, leads to damage involving liver and other organs. HCV gene expression has been associated with increased ROS and enhanced lipid peroxidation. HCV protein is known to perturb redox status. These adverse effects are accompanied by more subtle influences entailing cell signaling. Increased ROS/RNS levels have been associated with enhanced liver cancer via DNA damage. There are related reports involving HCV, OS and the liver (*38*, *39*).

In Oxidative Stress: Diagnostics, Prevention, and Therapy Volume 2; Hepel, et al.;
ACS Symposium Series; American Chemical Society: Washington, DC, 2015.

Publication Date (Web): October 13, 2015 | doi: 10.1021/bk-2015-1200.ch007

HIV/HCV co-infection involves enhanced OS and lower AO concentration compared with HIV mono-infection (*40*, *41*) in addition to production of ROS, HIV infection is characterized by lowering of mitochondrial membrane potential (*42*). A thiol AO prevented the change in potential. Results indicate that the mitochondrial insult was mediated by ROS and NO. Increased levels of lipid peroxidation occurred, in addition to DNA damage. A study showed decrease in GSH and total AO levels with significant increase in NO and malondialdehyde (indication of OS) (*43*). The patients received ribavirin and pegylated interferon. A related review addresses HCV illness in relation to mitochondrial dysfunction and changes in metal homeostasis (*44*). The dysfunction plays an important role in the metal imbalance. These aspects are importantly involved in the occurrence of OS. HCV core protein causes damage to DNA via oxidation, but apoptosis is hindered although associated with ROS generation (*45*). Thus, the mechanisms of the two pathways are different. There are other studies related to core protein. HCV core protein stimulates Ca activity resulting in enhancement of ROS generation via mitochondria (*46*, *47*). An article deals with pathology of HCV in relation to the impact of OS (*48*). A similar review deals with OS in HCV in relation to liver cancer (*49*). An investigation supports the multifaceted nature of drugs. Artemisinin, an important antimalarial agent (*50*) was found to be a powerful inhibitor of HCV (*51*). The mechanism was also addressed for the peroxide containing drug. In the antimalarial case, carbon-centered radicals are known to play an important role, in contrast to the HCV case. For the HCV situation, ROS appear to be the critical entities, as is often the case with peroxides. Considerable literature involves the role of AOs, which is the main topic of the following section. OS stress, associated with lower levels of AOs, is a well-established phenomenon in HCV patients (*52*). The adverse effect is overcome by administration of ribavirin and pegylated interferon. Although these agents are not recognized as AOs, it may be that they operate indirectly, e.g., by decreasing inflammation. Another investigation deals with AOs as beneficial in countering OS (*53*).

Publication Date (Web): October 13, 2015 | doi: 10.1021/bk-2015-1200.ch007

Antioxidants and Reactive Oxygen Species-Oxidative Stress

Extensive literature demonstrates important involvement of ROS-OS in drug and viral action. It is not surprising that numerous reports deal with beneficial effects bestowed by AOs. Excess ROS play a role in HCV infection (*54*). The study monitored the AO blood level. AO supplementation bestowed protection, thereby ameliorating harmful oxidative reactions in the illness. Clastrogenic factors (CFs), present in hepatitis C patients, are generated as a result of enhanced superoxide production (*55*). The CFs give rise to harmful effects on DNA, probably involving ROS. Use of a potent AO which destroys superoxide resulted in decreased levels of CFs. Exposure to AOs may enhance favorable results in interferon/ribavirin treatment. HCV infection is characterized by increased OS and mitochondrial insult, accompanied by harm to the liver (*56*). Application of

AO proved beneficial. The AO silymarin is often employed as therapy for HCV patients (*57*). OS accompanies HCV infection. Haem oxygenase-1 is an AO enzyme that demonstrates a beneficial influence in countering the OS. In a related vein, supplementation with AOs, iron and B vitamins (*58*), as well as silymarin (*59*), N-acetylcysteine (*60*, *61*), ascorbic acid and SOD (*62*), may be useful in hepatitis C therapy. A recent article on silymarin, a milk thistle food supplement, deals with effectiveness in treatment of HCV (*63*). The AO is a polyphenol, a class known for destruction of toxic radicals. Addition of ascorbic acid and alpha-tocopherol decreased oxidative damage by ribavirin on the membrane (*64*). Since OS could be involved in HCV infection, a study was performed on oxidant/AO status of infected patients (*52*). OS in anemia induced by ribavirin is accompanied by decrease in AO sulfhydryl levels in the membrane (*65*). OS is well established as an adverse factor in HCV infected patients. A study was performed with supplementation by flavonoid AOs which exhibited favorable effects (*66*). Thiol AO produced appreciable benefits in mice having influenza virus (*61*).

Redox imbalance was examined with HCV patients (*67*). MDA, a product of OS, was at lower concentration in responders vs nonresponders. Hence, MDA may serve as a medical marker for treatment. A study deals with oxidative and nitrosative stress mechanisms in HCV (*68*), OS appears to accelerate fibrosis. Contradictory results have been obtained in some reports on AOs (*53*). Toxic effects from high doses have been noted. Data indicated a beneficial effect from use of multi AOs, with favorable tolerance drugs (*69*). Combination therapy based on antiviral and AOs may be a beneficial approach. This recommendation was made in a related investigation involving children (*70*). An article addresses the influence of viusid, a dietary supplement in HCV patients (*71*). There were pronounced favorable effects on OS and the immune system. A 2012 review presents a comprehensive approach to various aspects of HCV infection (*72*). Included were the usual features concerning involvement of ROS, OS and nitrosative stress from various sources. There is decrease in AO potential and in levels of various AOs. The adverse effects are enhanced by even low quantities of alcohol. Redox interactions are addressed. A study in India was in accord with others in reporting enhanced OS and decreased levels of AOs, such as vitamins A,C and E (*73*). It is well known that ROS are generated in HCV, which are countered by AOs (*74*). HCV replication was inhibited by peroxidation of polyunsaturated fatty acids with restoration by vitamin E. Other therapies of HCV have been reported. An example is food supplementation by herbal medicines (*75*). There was moderate improvements in an appreciable number of patients. Egypt has been the prominent center for use of herbal medicines since ancient times (*75*). About 13-23% of American patients use alteranative medicines with silymarin, a flavonoid AO, being the preferred one. Treatment of patients with Phyllanthus amarus, a flowering plant constituent, increased AO levels, reduced lipoperoxidation and protected the liver from free radical attack (*76*). An investigation revealed that HCV proteins are involved in various effects on AO defense (*77*). Since redox balance is vital for cellular homeostasis, the effects of HCV on AO systems and cell signaling may play an important part in liver carcinogenesis (*78*). Related AO data can be found in the ROS-OS section.

Publication Date (Web): October 13, 2015 | doi: 10.1021/bk-2015-1200.ch007

Summary

There is widespread knowledge that ROS play an important role in both therapy and toxicity. However, there appears to be less recognition for ET agents as a source for ROS. The known drugs Zinivoxime, Simeprevir, Telaprevir, Dup 785, Camptothecin, Faldaprevir, Sofosbuvir, Daclatasvir and Ribavirin all have structures in which an imine functionality is involved. These imine and iminium functionalities are well established ET agents, which can transport the radical species to the virus. The present review is another example of the imine-iminium type as a source of ROS via ET, primarily as antiviral agents. Related structures are also addressed.

Publication Date (Web): October 13, 2015 | doi: 10.1021/bk-2015-1200.ch007

Abbreviations

ET= electron transfer; ROS= reactive oxygen species; OS= oxidative stress; AO= antioxidant; GSH= glutathione; HCV= hepatitis C virus; RNS= reactive nitrogen species

Acknowledgments

Editorial assistance by Thelma Chavez is acknowledged.

References

1. Bell, T. W. *Chem. Med. Chem.* **2010**, *5*, 1663–1665.
2. Kovacic, P.; Somanathan, R. *Nat. Prod. J.* **2014**, *4*, 47–53.
3. Kovacic, P.; Somanathan, R. *Curr. Bioactive Compd.* **2010**, *6*, 46–59.
4. Kovacic, P.; Becvar, L. E. *Curr. Pharm. Des.* **2000**, *6*, 143–167.
5. Kovacic, P.; Osuna, J. A. *Curr. Pharm. Des.* **2000**, *6*, 277–309.
6. Kovacic, P.; Osuna, J. A. *Med. Hypotheses* **2007**, *69*, 510–516.
7. Kovacic, P.; Jacintho, J. D. *Curr. Med. Chem.* **2001**, *8*, 773–796.
8. Kovacic, P.; Jacintho, J. D. *Curr. Med. Chem.* **2001**, *8*, 863–892.
9. Kovacic, P.; Sacman, A.; Wu-Weis, M. *Curr. Med. Chem.* **2002**, *9*, 823–847.
10. Poli, G.; Cheeseman, G. H.; Dianzani, M. U.; Slater, T. F. *Free Radicals in the Pathogenesis of Liver Injury*; Pergamon: 1989; pp 1−330.
11. Kovacic, P.; Thurn, L. A. *Curr. Vasc. Pharmacol.* **2005**, *3*, 107–117.
12. Kovacic, P.; Somanathan, R. *Curr. Med. Chem.-CNS Agents* **2005**, *5*, 249–258.
13. Kovacic, P.; Pozos, R. S.; Somanathan, R.; Shangari, R.; O'Brien, P. J. *Curr. Med. Chem.* **2005**, *5*, 2601–2623.
14. Kovacic, P.; Cooksy, A. L. *Med. Hypotheses* **2005**, *64*, 366–367.
15. Kovacic, P.; Somanathan, R. *J. Recept. Signal Transduct.* **2003**, *28*, 323–346.
16. Kovacic, P.; Somanathan, R. In *Reviews of Environmental Contamination and Toxicology*; Whitacre, D. M., Ed.; Springer: New York, 2009; Vol. 201, pp 41−69.

17. Kovacic, P.; Somanathan, R. In *Reviews of Environmental Contaminations and Toxicology*; Whitacre, D. M., Ed.; Springer: New York, 2010; Vol. 203, pp 119−138.
18. Kovacic, P.; Somanathan, R. *Med. Hypotheses* **2009**, *70*, 914–923.
19. Kovacic, P.; Somanathan, R. *Cell Membr. Free Radical Res.* **2008**, *1*, 56–69.
20. Kovacic, P.; Edwards, C. *J. Recept. Signal Transduct.* **2010**, *30*, 133–142.
21. Halliwell, B.; Gutteridge, J. M. C. *Free Radicals in Biology and Medicine*; Oxford University Press: New York, 1999; pp 1−897.
22. Kovacic, P.; Kassel, M. A.; Popp, W. J.; Feinberg, B. A. *J. Biopharm. Sci.* **1990**, *1*, 315–330.
23. Niufar, N. N.; Haycock, F. L.; Wesemann, J. L.; MacStay, J. A.; Heasley, V. L.; Kovacic, P. *J. Mex. Chem. Soc.* **2002**, *46*, 307–312.
24. Kovacic, P.; Cooksy, A. L. *Contam. Toxicol.* **2010**, *204*, 133–148.
25. Crawford, P. W.; Scamehorn, R. G.; Hollstein, U.; Ryan, M. D.; Kovacic, P. *Chem. Biol. Interface* **1986**, *60*, 67–84.
26. Flisiak, R.; Jaroszwicz, J.; Parfieniuk-Kowerda, A. *Expert Opin. Emerging Drugs* **2013**, *18*, 461–475.
27. You, D. M.; Pockros, P. J. *Expert Opin. Pharmacother.* **2013**, *14*, 2581–2589.
28. Fried, M. W.; Buti, M.; Dore, G. J.; Flisiak, R.; Ferenci, P.; Jacobson, I.; Marcellin, P.; Manns, M.; Nikitin, I.; Poordad, F.; Sherman, M.; Zeuzem, S.; Scott, J.; Gilles, L.; Lenz, O.; Peeters, M.; Sekar, V.; De Smedt, G.; Beumont-Mauviel, M. *Hepatology* **2013**, *58*, 1918–1929.
29. Barreiro, P.; Vispo, E.; Poveda, E.; Fernández-Montero, J. V.; Soriano, V. *Clin. Infect. Dis.* **2013**, *56*, 560–566.
30. Murakami, E.; Tolstykh, T.; Bao, H.; Niu, C.; Holly, M.; Steuer, M.; Bao, D.; Chang, W.; Espiritu, C.; Bansal, S.; Lam, A. M.; Otto, M. J.; Sofia, M. J.; Furman, P. A. *J. Biol. Chem.* **2010**, *285*, 34337–34347.
31. Kerina, H. J.; Trudgill, P. W.; Hooper, D. J. *Arch. Microbiol.* **1995**, *163*, 176–181.
32. Kovacic, P.; Somanathan, R. *J. Appl. Toxicol.* **2014**, *34*, 810–824; DOI:10.1002/jat.2980.
33. Gao, M.; Nettles, R. E.; Belema, M.; Snyder, L. B.; Nguyen, V. N.; Fridell, R. A.; Serrano-Wu, M. H.; Langley, D. R.; Sun, J.-H.; O'Boyle, D. R.; Lemm, J. A.; Wang, C.; Knipe, J. O.; Chien, C.; Colonno, R. J.; Grasela, D. M.; Meanwell, N. A.; Hamann, L. G. *Nature* **2010**, *456*, 96–100.
34. Noshy, M. M.; Hussien, N. A.; El-Ghor, A. A. *Mutat. Res.* **2012**, *752*, 14–20.
35. Lim, W. S.; Gong, H.; Anderson, K. R.; Clark, K. W.; Shamoo, D. A. *Arch. Environ. Health* **1995**, *50*, 445–451.
36. Parcha, U. Z.; Fatima, K.; Alqahtani, M.; Chaudhary, A.; Abuzenadah, A.; Damanhouri, G.; Qadri, I. *Virology J.* **2013**, *10*, 251; http://www.virologyj.com/content/10/1/251.
37. Choi, J.; James Ou, J.-H. *Am. J. Gastrointest. Liver Physiol.* **2006**, *290*, G847–G851.
38. Ivanov, A. V.; Bartosch, B.; Smirova, O. A.; Isaguliants, M. G.; Kochetkov, S. N. *Viruses* **2013**, *5*, 439–469.
39. Koike, K.; Miyoshi, J. *Hepatol. Res.* **2006**, *34*, 65–73.

Publication Date (Web): October 13, 2015 | doi: 10.1021/bk-2015-1200.ch007

40. Baum, M. K.; Sales, S.; Jayaweera, D. T.; Bradwin, G.; Rafire, C.; Page, J. B.; Campa, A. *HIV Med.* **2011**, *12*, 78–86.
41. Shin, D.-H.; Martinez, S. S.; Parsons, M.; Jayaweera, D. T.; Campa, A.; Baum, M. K. *Int. J. Biosci. Biochem. Bioinform.* **2012**, *2*, 217–223.
42. Machida, K.; Cheng, K. T.-H.; Lai, C.-K.; Jeng, K.-S.; Sung, V. M.-H.; Lai, M. M. C. *J. Virol.* **2006**, *80*, 7199–7207.
43. Ahmed, M. M.; Abdel-Salam, O. M. E.; Mohammed, N. A.; Habib, D. F.; Ez-eldin Goma, H. *EXCL1 J.* **2013**, *12*, 605–615.
44. Arciello, M.; Gori, M.; Balsnao, C. *Oxid. Med. Cell. Longevity* **2013**, *2013*, 971024; DOI: dx.doi.org/10.1155/2013/971024.
45. Hara, Y.; Hino, K.; Okuda, M.; Furutani, T.; Hidaka, I.; Yamaguchi, Y.; Korenaga, M.; Li, K.; Weinman, S. A.; Lemon, S. M.; Okita, K. *J. Gastroentol.* **2006**, *41*, 257–268.
46. Li, Y.; Boehning, D. F.; Qian, T.; Popov, V. L.; Weinman, S. A. *FASEB J* **2007**, *21*, 2474–2485.
47. Dionisio, N.; Garcia-Mediavilla, M. V.; Sanchez-Campos, S.; Majano, P. L.; Benedicto, I.; Rosado, J. A.; Salido, G. M.; Gonzalez-Gallego, J. *J. Hepatol.* **2009**, *50*, 872–882.
48. Fierbinţeanu-Braticevici, C.; Mohora, M.; Creţoiu, D.; Creţoiu, S.; Petrişor, A.; Usvat, R.; Adriana Ion, D. *Romanian J. Morphol. Embryol.* **2009**, *50*, 407–412.
49. Marra, M.; Sordelli, I.; Lombardi, A.; Lamberti, M.; Tarantino, L.; Giudice, A.; Stiuso, P.; Abbruzzese, A.; Sperlongano, R.; Accardo, M.; Agresti, M.; Caraglia, M.; Sperlongano, P. *J. Translat. Med.* **2011**, *9*, 171; http://www.translational-medicine.com/content/9/1/171.
50. Ames, J. R.; Ryan, M. D.; Klayman, D. L.; Kovacic, P. *J. Free Radical Biol. Med.* **1985**, *1*, 353–361.
51. Obeid, S.; Alen, J.; Nguyen, V. H.; Pham, V. C.; Mauleman, P.; Pannecouque, C.; Le, T. N.; Neyts, J.; Dehaen, W.; Paeshuyse, J. *PLoS ONE* **2013**, *8* (12), e81783; DOI: 10.1371/journal.pone.0081783.
52. Levent, G.; Ali, A.; Ahmet, A.; Polat, E. C.; Aytaç, C.; Ayşe, E.; Ahmet, S. *J. Translat. Med.* **2006**, *4*, 25; DOI: 10.1186/1479-5876-4-25.
53. Esrefoglu, M. *Hepatitis Mon.* **2012**, *12*, 160–167.
54. Farias, M. S.; Budini, P.; Ribeiro, C. M.; Parisotto, E. B.; Santos, C. E.; Dias, J. F.; Dalmarco, E. M.; Frode, T. S.; Pedrosa, R. C.; Wilhelm Filho, D. *Gastroentol. Hepatol.* **2012**, *35*, 386–394.
55. Emerit, I. *Hepatitis Mon.* **2011**, *11*, 434–439.
56. Gane, E. J.; Weilert, F.; Orr, D. W.; Keogh, G. F.; Gibson, M.; Lockhart, M. M.; Framton, C. M.; Taylor, K. M.; Smith, R. A. J.; Murphy, P. *Liver Int.* **2010**, *30*, 1019–1026.
57. Bonifaz, V.; Shan, Y.; Lambrecht, R. W.; Donohue, S. E.; Moschenross, D.; Bonkovsky, H. L. *Liver Int.* **2009**, *29*, 366–373.
58. Lin, C.-C.; Yin, M.-C. *Clin. Nutr.* **2009**, *28*, 34–38.
59. Par, A.; Roth, E.; Miseta, A.; Hegedus, G.; Par, G.; Hunyady, B.; Vincze, A. *Orv. Hetil.* **2009**, *150*, 73–79.
60. Garozzo, A.; Tempera, G.; Ungheri, D.; Timpanaro, R.; Castro, A. *Int. J. Immunopathol. Pharmacol.* **2007**, *20*, 349–354.

Publication Date (Web): October 13, 2015 | doi: 10.1021/bk-2015-1200.ch007

61. Ghezzi, P.; Ungheri, D. *Int. J. Immunophathol. Pharmacol.* **2004**, *17*, 99–102.
62. Duan, S.; Gu, L.; Wang, Y.; Zheng, R.; Lu, J.; Yin, J.; Guli, L.; Ball, M. *Am. J. Chinese Med.* **2009**, *37*, 1167–1177.
63. Anthony, K.; Subramanya, G.; Uprichard, S.; Hammoud, F.; Saleh, M. *Antioxidants* **2013**, *2*, 23–36.
64. Hino, K.; Murakami, Y.; Yasuko, N.; Ayako, K.; Kitase, A.; Hara, Y.; Furutani, T.; Ren, F.; Yamaguchi, Y.; Yutoku, K.; Yamashita, S.; Okuda, M.; Okita, M.; Okita, K. *J. Gastroentol. Hepatolol.* **2006**, *21*, 1269–1275.
65. Gattagliano, I.; Russmann, S.; Palmieri, V. O.; Portincasa, P.; Palasciano, G.; Lauterburgh, B. H. *Clin. Pharmacol. Ther.* **2005**, *78*, 422–432.
66. Emerit, I.; Huang, C. Y.; Serjo, F.; Filipe, P.; Fernandes, A.; Costa, A.; Freitas, J.; Baptisa, A.; Carneiro de Moura, M. *Hepato-Gatroentol.* **2005**, *52*, 530–536.
67. El-Kannishy, G.; Arafa, M.; Abdelaal, I.; Elarman, M.; El-Mahdy, R. *Saudi J. Gastroentrol.* **2012**, *18*, 375–379.
68. Moreno-Otero, R.; Trapero-Marugán, M. *World J. Gastroentrol.* **2010**, *16*, 1937–1938.
69. Melhem, A.; Stern, M.; Shibolet, O.; Israeli, E.; Ackerman, Z.; Pappo, O.; Hemed, N.; Rowe, M.; Ohana, H.; Zabrecky, G.; Cohen, R.; IIan, Y. *J. Clin. Gastroentrol.* **2005**, *39*, 737–742.
70. Ismail, N. A.; Okasha, S. H.; Dhawan, A.; Abdel Rahman, A. M. O.; Hamid, N. A.; Shaker, O. *Adv. Biosci. Biotechnol.* **2012**, *3*, 972–977.
71. Gomez, E. V.; Perez, Y. M.; Sanchez, H. V.; Forment, G. R.; Soler, E. A.; Bertot, L. C.; Garcia, A. Y.; Vasquez, M. R. A.; Fabian, L. G. *World J. Gastroentrol.* **2010**, *16*, 2638–2647.
72. Choi, J. *Free Radical Biol. Med.* **2012**, *52*, 1135–1150.
73. Sharma, S. K.; Sharma, A. K.; Sood, S. *J. Clin. Diagnostic Res.* **2012**, *6*, 358–360; Sigma, Product number P 9625, Saint Louis, MO, USA.
74. Huang, H.; Chen, Y.; Ye, J. *Proc. Natl. Acad. Sci. U.S.A.* **2007**, *104*, 18666–18770.
75. Younes, A. K. H. *J. Antivir. Antiretrovir.* **2012**, S15; DOI: 10.4172/jaa.s15-002.
76. Nikam, P. S.; Nikam, S. V.; Sontakke, A. V.; Khanwelkar, C. C. *Biomed. Res.* **2011**, *22*, 319–322.
77. Abdalla, M. Y.; Ahmad, I. M.; Spitz, D. R.; Schmidt, W. N.; Britigan, B. E. *J. Med. Virol.* **2005**, *76*, 489–497.
78. Wang, Q.; Na, B.; James Ou, J-H.; Pulliam, L.; Benedict Yen, T. S. *PLoS One* **2012**, *7* (5), e36818; DOI: 10.1371/journal.pone.0036818.

Publication Date (Web): October 13, 2015 | doi: 10.1021/bk-2015-1200.ch007

Publication Date (Web): October 13, 2015 | doi: 10.1021/bk-2015-1200.ch008

Chapter 8

Triclosan (Mechanism of Bactericidal Action and Toxicity): Metabolism, Electron Transfer and Reactive Oxygen Species

Peter Kovacic[1,*] and Ratnasamy Somanathan[1,2]

[1]Department of Chemistry and Biochemistry, San Diego State University, San Diego, California 92182-1030, United States
[2]Centro de Graduados e Investigación del Instituto Tecnológico de Tijuana, Apdo postal 1166, Tijuana, B.C. Mexico
[*]E-mail: pkovacic@mail.sdsu.edu

Triclosan, a widely used bactericide, has been the object recently of increased attention by the media and scientists in relation to safety and usefulness. This chapter deals with a unifying mechanism for antibacterial action and toxicity based on electron transfer (ET), reactive oxygen species (ROS) and oxidative stress (OS). The phenolic compound can be oxidatively converted to diols (catachol and hydroquinone types) which are then oxidized to o-or p-quinones. The quinones are ET agents capable of generating ROS which can act as either beneficial or toxic agents. Toxicity is associated with higher levels of ROS leading to OS. Mechanistic relationship to many physiologically active phenols is also addressed. This unifying action mode can be applied to other physiologically active ET agents.

Keywords: Triclosan; bactericide; toxicity; metabolism; electron transfer; reactive oxygen species; phenols

Introduction

In recent years, there has been increasing focus on triclosan (TCS) (Fig. 1), a bactericide, by the media and researchers. The agent has enjoyed widespread use, with recent enhanced attention to toxicity. Of relevance is a 2000 review

In Oxidative Stress: Diagnostics, Prevention, and Therapy Volume 2; Hepel, et al.;
ACS Symposium Series; American Chemical Society: Washington, DC, 2015.

that deals with a unifying mechanism for anti-infective agents including TCS (*1*). The fundamental aspect involves electron transfer (ET), reactive oxygen species (ROS) and oxidative stress (OS). Although widespread discussion of ROS exists in the literature, there is less recognition of the role played by ET agents. The main categories of ET agents are quinones (or phenolic precursors), aromatic nitro compounds, metals (or complexors) and imine (or iminium) species. The focus of the present review is the quinone class as applied to TCS. Generation of superoxide by ET is depicted in Scheme 1. In Scheme 2, superoxide is shown as precursor of other ROS.

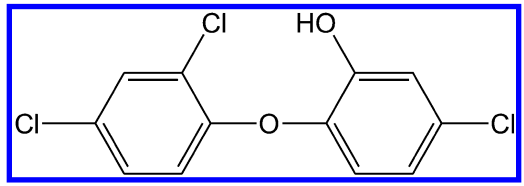

Figure 1. Triclosan (TCS)

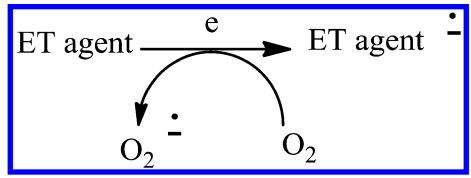

Scheme 1. Redox cycling with superoxide formation

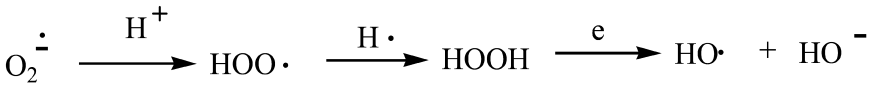

Scheme 2. Superoxide precursor of other ROS

There has been extensive literature supporting the ET-ROS-OS approach, including anti-infective agents (*1*), anticancer drugs (*2*), carcinogens (*3*) and many toxins (toxicants) (*4–17*). It is prudent to adopt a multifaceted approach to mechanism of physiological action, with operation of pathways in addition to ET-ROS-OS.

In the present report, mode of antibacterial action for TCS is addressed with emphasis on ET-ROS-OS. It is noteworthy that the unifying mechanism was first proposed as an hypothesis with scant supporting evidence (*1*). Since then, studies provide evidence for hydroxylation to diols (Fig 2 and 3) followed by formation of possible quinones (Fig 4 and 5). Numerous examples are provided of other phenols possessing various physiological activation in accord with the ET-ROS-OS approach. The mechanism can be applied to both therapy and toxicity. The beneficial route for anti-infective agent has been termed phagomimetic (*18*). Toxicity is limited to high and persistent levels of ROS and is commonly an undesirable effect that accompanies therapy.

In Oxidative Stress: Diagnostics, Prevention, and Therapy Volume 2; Hepel, et al.;
ACS Symposium Series; American Chemical Society: Washington, DC, 2015.

Publication Date (Web): October 13, 2015 | doi: 10.1021/bk-2015-1200.ch008

Publication Date (Web): October 13, 2015 | doi: 10.1021/bk-2015-1200.ch008

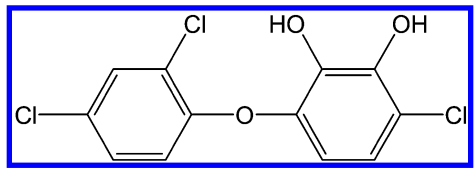

Figure 2. Catechol derivative of TCS

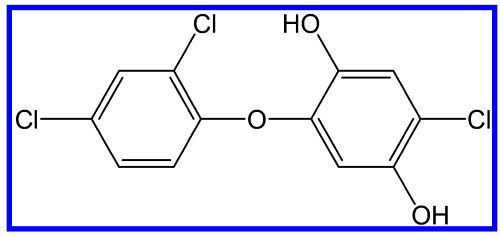

Figure 3. Hydroquinone derivative of TCS

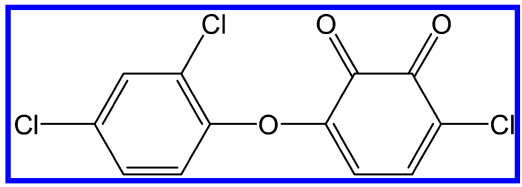

Figure 4. o-Quinone derivative of TCS

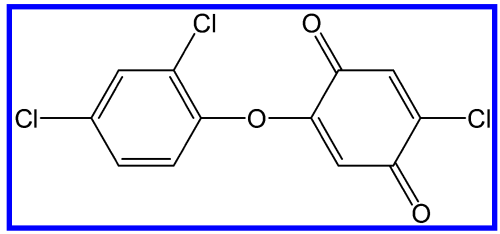

Figure 5. 5 p-Quinone derivative of TCS

Modes of Action

Triclosan, a widely used antibacterial agent, has been the object of attention in research and the media. There is controversy concerning safety of the product. Considerable research has been devoted to the mode of action in relation to therapy and toxicity (*19*). Mechanisms proposed include muscle contraction, and inhibition involving enzymes , such as a protein reductase. Disruption of the endocrine system occurs via signaling, entailing action of androgens, estrogens and thyroid hormones.

However, there has been little discussion of ET-ROS-OS which was addressed in 2000. The agent is a member of the phenolic class, many of which are

In Oxidative Stress: Diagnostics, Prevention, and Therapy Volume 2; Hepel, et al.;
ACS Symposium Series; American Chemical Society: Washington, DC, 2015.

therapeutic agents, e.g., hexylresorcinol (Fig. 6) a related bactericide. According to the therapeutic approach, conversion to the active agents entails oxidation to diols (catechols and hydroquinones), followed by oxidative conversion to o- and p- quinones (Fig. 3 and 4) which are well known ET agents capable of generating ROS.

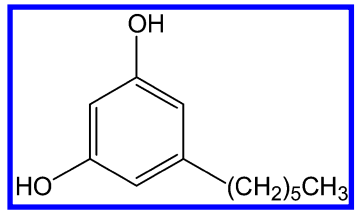

Figure 6. Hexylresorcinol

The proposed metabolism for TCS in 2000 (*1*) has been supported by subsequent reports dealing with hydroxylation and quinone formation. In one case, hydroxylation occurred by treatment with the Fenton reagent yielding a p-hydroquinone (*20*). The system resembles in vivo metabolism since the hydroxyl radical serves as oxidant. The reaction was found to be highly efficient. When exposed to a bacterial strain, the drug underwent both mono- and di-hydroxylation (*21*). The authors describe the drug as a "persistent environmental pollutant." A report deals with oxidation by manganese oxides found in the soil which operate as facile oxidants (*22*). One of the main products is the p-hydroquinone, formed via involvement of phenoxy radicals. The most significant investigation was performed with TiO_2 and hydrogen peroxide under irradiation by UV light (*23*). Oxidation took place at the phenol ring with generation of hydroquinone and quinone products. Possible quinones are indicated in Fig. 4 and 5, arising from 1,2-or 1,4-diols. A possible 1,3-dihydroxy (resorcinol) metabolite could also serve as a quinone precursor, as noted in a prior review (*24*).

An alternative metabolic pathway entails degradation via cleavage of the diphenyl ether backbone (*2*, *20–22*). A product is 2,4-dichlorophenol which might also display physiological activity by conversion to ET quinone with subsequent ROS generation. Bactericidal properties of the degraded phenol are reported (*2*). There is evidence from other phenols that supports the unifying mechanistic approach. Pentachlorophenol (PCP), 50 times more active than phenol, generates lipid peroxidation and enzyme deactivation by way of OS (*1*). Oxidative metabolites of PCP produce DNA cleavage via formation of ROS from redox cycling by tetrachlorosemiquinone radicals. Chlorine substituents facilitate the radical oxidation, as would be the case or triclosan. Closely related analogs in structure with various activities are hexylresorcinol (Fig. 6) (*23*), tetrahydrocannabinol (Fig. 7) (*24*), dopamine (Fig. 8) (*10*), 5-hydroxytryptamine (Fig. 9) (*10*), morphine (Fig. 10) (*10*), and salicylic acid (Fig. 11) (*10*) from aspirin. In many cases, benzenoid rings undergo oxidation to phenols with subsequent conversion to quinones, as for benzene (*25*) and phenolberbital (Fig. 12) (*10*).

Publication Date (Web): October 13, 2015 | doi: 10.1021/bk-2015-1200.ch008

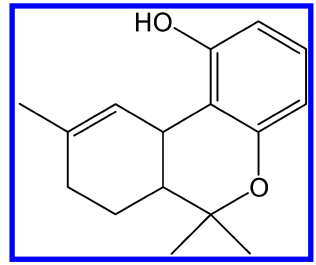

Figure 7. Tetrahydrocannbinol

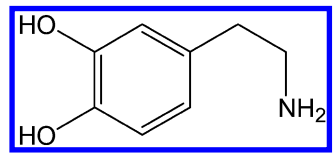

Figure 8. Dopamine

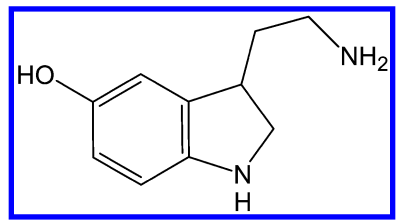

Figure 9. 5-Hydroxytriptamine

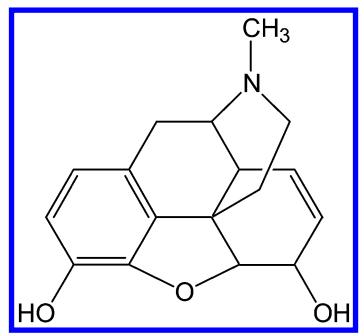

Figure 10. Morphine

In Oxidative Stress: Diagnostics, Prevention, and Therapy Volume 2; Hepel, et al.;
ACS Symposium Series; American Chemical Society: Washington, DC, 2015.

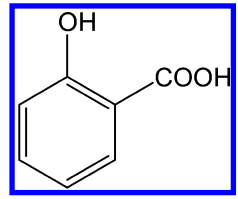

Figure 11. Salicylic acid

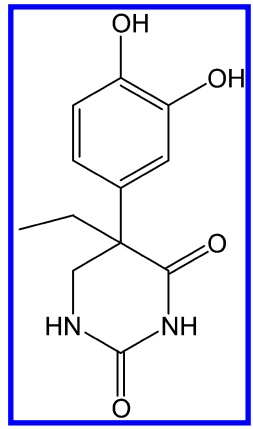

Figure 12. Catechol derivative\of phenobarbital

Publication Date (Web): October 13, 2015 | doi: 10.1021/bk-2015-1200.ch008

Toxicity

There is increasing concern about possible toxic effects of TCS. In relation to mode of action, the unifying mechanism can be applied involving attack by ROS leading to various adverse effects. Extensive prior literature exists that demonstrates a correlation between generation of ROS via quinone metabolites and harmful effects. Evidence involves lipid peroxidation, protein oxidation and cleavage, and attack of vital body organs.

Other representative examples can be cited. Benzene, a well-known carcinogen, generates ROS-OS via metabolism to phenol, diols and quinones. Uroshiol (poison ivy) contains 3-pentadecyl catechol (Fig. 13) as an important component (*26*). Toxicity has been related to metabolic oxidation to an o-quinone. GSH, an antioxidant (AO) inhibits the adverce effects which evidently arise from harmful oxidation. Redox cycling by ET o-quinone apparently generates ROS which deplete AOs, resulting in further increase in ROS.

In Oxidative Stress: Diagnostics, Prevention, and Therapy Volume 2; Hepel, et al.;
ACS Symposium Series; American Chemical Society: Washington, DC, 2015.

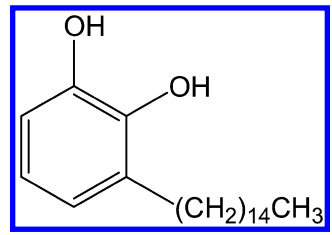

Figure 13. 3-Pentadecylcatechol

Abbreviations

TCS= triclosan; ET= electron transfer agent; ROS= reactive oxygen species; OS= Oxidative stress; AO= antioxidant; PCP= pentachlorophenol

Acknowledgments

Editorial assistance by Thelma Chavez is acknowledged.

References

1. Kovacic, P.; Becvar, L. E. *Curr. Pharm. Des* **2000**, *6*, 143–167.
2. Kim, Y.-M.; Murugesan, K.; Schmidt, S.; Bokare, V.; Jeon, J.-R.; Kim, E.-J.; Chang, Y.-S. *Biosource Technol.* **2011**, *102*, 2206–2212.
3. Kovacic, P.; Jacintho, J. D. *Curr. Med. Chem.* **2001**, *8*, 773–796.
4. Kovacic, P.; Jacintho, J. D. *Curr. Med. Chem.* **2001**, *8*, 863–892.
5. Kovacic, P.; Sacman, A.; Wu-Weis, M. *Curr. Med. Chem.* **2002**, *9*, 823–847.
6. Poli, G.; Cheeseman, K. H.; Dianzani, M. U.; Slater, T. F. *Free Radicals in the Pathogenesis of Liver Injury*; Pergamon: New York, 1989; pp 1−330.
7. Kovacic, P.; Thurn, L. A. *Curr. Vasc. Pharmacol.* **2005**, *3*, 107–117.
8. Kovacic, P.; Somanathan, R. *Curr. Med. Chem.: Cent. Nerv. Syst. Agents* **2005**, *5*, 249–258.
9. Kovacic, P.; Pozos, R. S.; Somanathan, R.; Shangari, R.; O'Brien, P. J. *Curr. Med. Chem.* **2005**, *5*, 2601–2623.
10. Kovacic, P.; Cooksy, A. L. *Med. Hypotheses* **2005**, *64*, 366–367.
11. Kovacic, P.; Somanathan, R. *J. Recept. Signal Transduction* **2003**, *28*, 323–346.
12. Kovacic, P.; Somanathan, R. In *Reviews of Environmental Contamination and Toxicology*; Whitacre, D. M., Ed.; Springer: New York, 2009; Vol. 201, pp 41−69.
13. Kovacic, P.; Somanathan, R. In *Reviews of Environmental Contaminations and Toxicology*; Whitacre, D. M., Ed.; Springer: New York, 2010; Vol. 203, pp 119−138.
14. Kovacic, P.; Somanathan, R. *Med. Hypotheses* **2009**, *70*, 914–923.
15. Kovacic, P.; Somanathan, R. *Cell Membr. Free Radical Res.* **2008**, *1*, 56–69.
16. Kovacic, P.; Edwards, C. *J. Recept. Signal Transduction* **2010**, *30*, 133–142.

Publication Date (Web): October 13, 2015 | doi: 10.1021/bk-2015-1200.ch008

17. Halliwell, B.; Gutteridge, J. M. C. *Free Radicals in Biology and Medicine*; Oxford University Press: New York, 1999; pp1−897.
18. Gutteridge, J. M. C.; Quinlan, G. J.; Kovacic, P. *Free Radical Res.* **1998**, *92*, 1–14.
19. Kemsley, J. *Chem. Eng. News* **2014**, *92*, 10–13.
20. Munoz, M.; De Pedro, Z. M.; Casas, J. A.; Rodriguez, J. J. *Chem. Eng. J.* **2012**, *198−199*, 275–281.
21. Zhang, H. C.; Huang, C. H. *Environ. Sci. Technol.* **2003**, *37*, 2421–2430.
22. Yu, J. C.; Kwong, T. Y.; Luo, Q.; Cai, Z. W. *Chemosphere* **2006**, *65*, 390–399.
23. Kovacic, P.; Somanathan, R. In *Systems Biology of Free Radicals and Antioxidants*; Laher, I., Ed.; Springer-Verlag: Berlin, 2014; Vol. 180, pp 4063−4083.
24. Kovacic, P.; Somanathan, R. *Nat. Prod. J.* **2014**, *4*, in press.
25. Kovacic, P.; Somanathan, R. In *Cell Signaling and Molecular Targets in Cancer*; Chatterjee, M., Kashfi, K., Eds.; Springer: 2012; Chapter 12, pp 273−298.
26. Schmidt, R. J.; Khan, L.; Chung, L. Y. *Arch. Dermatol. Res.* **1990**, *282*, 56–64.

Publication Date (Web): October 13, 2015 | doi: 10.1021/bk-2015-1200.ch008

Publication Date (Web): October 13, 2015 | doi: 10.1021/bk-2015-1200.ch009

Chapter 9

MTIP and Flavins: Alcoholism Drugs, Electron Transfer, and Reactive Oxygen Species

Peter Kovacic[1,*] and Ratnasamy Somanathan[1,2]

[1]Department of Chemistry and Biochemistry, San Diego State University, San Diego, California 92182-1030, United States
[2]Centro de Graduados e Investigación del Instituto Tecnológico de Tijuana, Apdo postal 1166, Tijuana, B.C. Mexico
[*]E-mail: pkovacic@mail.sdsu.edu

There are various drugs which combat alcoholism, a recent one being MTIP. The drug bears close structural resemblance to flavins, mainly in relation to the conjugated diimine moiety. With regard to mechanism involving electron transfer (ET), reactive oxygen species (ROS), and oxidative stress (OS), extensive literature from the flavins can be extrapolated to the MTIP analog. Other alcoholism drugs, namely β-carboline, benzodiazepines, naltrexone, and disulfiram are addressed based on the unifying mechanism of ET-ROS-OS.

Keywords: MTIP; flavin; β-carboline; benzodiazepines; naltrexone; disulfiram; electron transfer; reactive oxygen species; oxidative stress; diimine

Introduction

In the USA, alcohol is one of the most abused drugs, resulting in enormous economic and personal losses. Although advances have been made in treatment by drugs, there is considerable room for improvement. The earlier review (*1*) addresses this issue, as well as other relevant aspects. In the present case, the focus is on MTIP (Fig. 1), a drug of the imidazopyridazine class.

In Oxidative Stress: Diagnostics, Prevention, and Therapy Volume 2; Hepel, et al.;
ACS Symposium Series; American Chemical Society: Washington, DC, 2015.

Publication Date (Web): October 13, 2015 | doi: 10.1021/bk-2015-1200.ch009

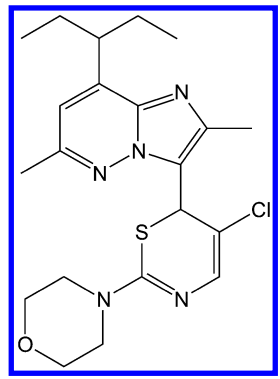

Figure 1. MTIP

"The preponderance of bioactive substances or their metabolites incorporate ET functionalities, which, we believe, play an important role in physiological responses (*2*). These main groups include quinones (or phenolic precursors), metal complexes (or complexors), aromatic nitro compounds (or reduced hydroxylamine and nitroso derivatives), and conjugated imines (or iminium species) (Scheme 1). *In vivo* redox cycling with oxygen can occur (Scheme 2) giving rise to oxidative stress (OS) through generation of reactive oxygen species (ROS), such as hydrogen peroxide, hydroperoxides, alkyl peroxides, and diverse radicals (hydroxyl, alkoxyl, hydroperoxyl, and superoxide (Scheme 3) . In some cases, ET results in interference with normal electrical effects, e.g., in respiration or neurochemistry. Generally, active entities possessing ET groups display reduction potentials in the physiologically responsive range, i.e., more positive than -0.5 V. Hence, ET *in vivo* can occur resulting in production of ROS which can be beneficial in cell signaling at low concentrations, but produce toxic results at high levels. Electron donors consist of phenols, N-heterocycles or disulfides in proteins which produce relatively stable radical cations. ET, ROS, and OS have been increasingly implicated in the mode of action of drugs and toxins, e.g., anti-infective agents (*3*), anticancer drugs (*4*), carcinogens (*5*), reproductive toxins (*6*), nephrotoxins (*7*), hepatotoxins (*8*), cardiovascular toxins (*9*), nerve toxins (*10*), mitochondrial toxins (*11*), abused drugs (*12*), pulmonary toxins (*13*), ototoxins (*14*), and various other categories (*15*).

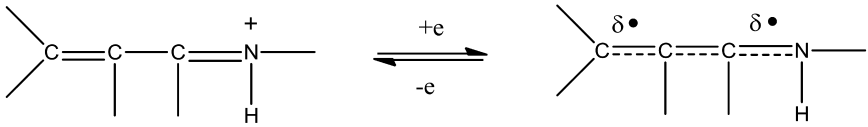

Scheme 1. Redox cycling by conjugated iminium

In Oxidative Stress: Diagnostics, Prevention, and Therapy Volume 2; Hepel, et al.;
ACS Symposium Series; American Chemical Society: Washington, DC, 2015.

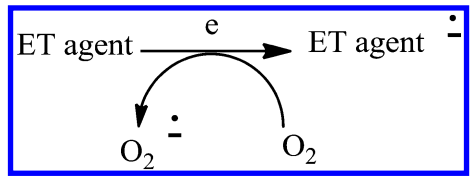

Scheme 2. Redox cycling with superoxide formation

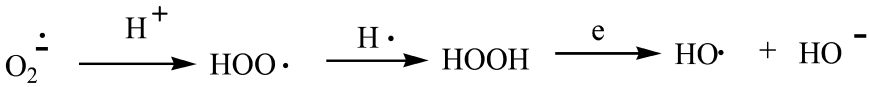

Scheme 3. Other ROS from superoxide

There is a plethora of experimental evidence supporting the OS theoretical framework, including generation of the common ROS, lipid peroxidation, degeneration products of oxidation, depletion of AOs, effect of exogenous AOs, DNA oxidation and cleavage products, as well as electrochemical data. This comprehensive, unifying mechanism is in keeping with the frequent observations that many ET substances display a variety of activities, e.g., multiple drug properties, as well as toxic effects.

It is important to recognize that mode of action in the biodomain is often multifaceted. In addition to the ET-ROS-OS approach, other aspects may pertain, such as enzyme inhibition, allosteric effects, receptor binding, metabolism and physical factors."

Flavin adenine dinucleotide (FAD), possessing a conjugated diimine structure and an important redox enzyme, can serve as a model for the vinylogous portion of MTIP. The redox properties of FAD support involvement of ET-ROS-OS in the action of MTIP.

FAD Model for MTIP

The conjugated diimine structure (Fig. 2) is the functional core for FAD ET in the form of the isoalloxazine (Fig. 3) prosthetic group. The MTIP molecule incorporates a vinylogous diimine (Fig 4) in a relationship with respect to flavin, which should facilitate electron uptake. In both cases, delocalization of the resulting radical anion is enhanced by the carbonyl, benzenoid or thiazole groups. Thus, it is reasonable to expect MTIP to exhibit electrochemical behavior similar to that of flavin. The extensive literature on flavin mode of action also can be applied to the MTIP analog. Other alcoholism drugs are also discussed from the standpoint of ET-ROS-OS.

Publication Date (Web): October 13, 2015 | doi: 10.1021/bk-2015-1200.ch009

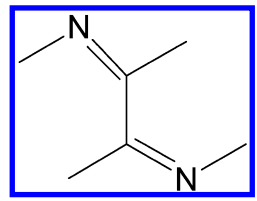

Figure 2. Conjugated diimine of FAD

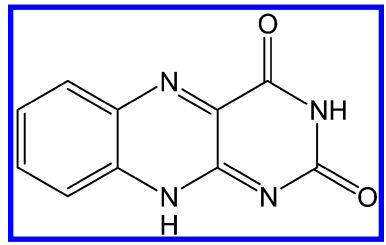

Figure 3. Isoalloxazine

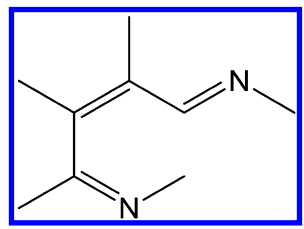

Figure 4. Vinylogous diimine of MTIP

MTIP (The Imidazopyridazine Class)

Corticotropin-releasing factor systems (CRF) are involved in behavioral stress response, mainly through their receptors (*16*). Alcohol withdrawal produces anxiety responses that are related to increased CRF levels. These responses are countered by CRF antagonists. CRF appears to play a major role in addiction by alcohol and other drugs. A "kindling/stress" hypothesis of alcohol dependence has been advanced. Hence, CRF antagonists provide a means for treatment of certain aspects of alcoholism. The imidazopyridazine class, an orally available, brain penetrant CRF antagonist, possesses favorable properties based on preclinical in vivo studies.

In preclinical models, MTIP blocks behavioral pathology in alcoholics, with alcohol metabolism unaffected (*16*). Reduction of excessive alcohol self-administration and prevention of relapse after abstinence are key objectives for any treatment. Both are effectively achieved by the drug in preclinical models. The therapeutic effects of MTIP in alcoholics may be possible to achieve with doses that do not adversely affect normal behavior. One aim of the research was to discover a compound with low toxicity and minimal liver accumulation. From initial investigations, MTIP appears to present a promising profile (*17*).

Publication Date (Web): October 13, 2015 | doi: 10.1021/bk-2015-1200.ch009

An important aspect of drug action involves interaction as a ligand with the receptor. MTIP inhibits binding of CRF to its receptor (*16*). CRF has been associated with alcoholism and other psychiatric conditions. The agent is able to enter the CNS and accomplish receptor docking.

Our approach addresses chemical aspects associated with binding process, e.g., the electrochemistry. Also of relevance is the nature of the interactions that pertain, some of which are electrostatic. As a prevalent occurrence in receptor interaction, it is reasonable to expect hydrogen-bonding or protonation which can influence electrochemical behavior (see below).

Hydrogen Bonding in FAD

References on ET functionalities in the Introduction reveal that conjugated iminium species are usually better electron acceptors in ET than their imine counterpart. Electrophilicity is also enhanced by hydrogen bonding on the imine. Various lines of evidence support the thesis in the case of the conjugated diimine moiety present in the isoalloxazine nucleus. Results reveal that the dynamic nature of ET flavoproteins cab be ascribed to hydrogen bonding of the heterocyclic ring with surrounding amino acids (*18*). NMR studies were made of this type of bonding (*19*). Hydrogen bonding has been implicated in the modulation of the redox properties of the flavin unit (*20*). The electrochemistry of H-bonded flavin complexes has been investigated (*21*, *22*). An important report involves a synthetic flavin receptor that binds 6-azaflavin through 5-7 hydrogen bonds (*23*). Redox potentials were considerably affected by such H-bonding involving a positive shift, $\Delta E_{1/2}$ of 220-317 mV. Similar results were reported in another investigation (*24*). A review addresses related systems leading to similar outcomes (*25*). Resonance Raman data are available dealing with H-bonding at nitrogens or carbonyl of the ring (*26*, *27*). The effect of H-bonding on scalar couplings was investigated (*28*). Specific H-donors in protein are reported to be tyr and protonated lysine (*29*). There are other relevant articles that address this general topic (*30*, *31*).

FAD Reduction Potential

The electrochemical property appears to have an important association with biochemical activity. Representative examples of the rather extensive literature are provided. The data clearly indicate that reduction potentials are well within the range permitting ET in vivo, namely -0.15 to -0.31 V (*32–39*).

At pH 7, the two-electron reduction for the FAD/$FADH_2$ couple is ~0.27 V, and ~0.23 V for free FAD (*39*). The values for various complexes of FAD with NAD+ analogs fall in the range of -0.15 to -0.22 V. Potentiometric studies show a figure of -0.24 V (*32*). The formal redox potential for FAD is -0.21 V (vs NHE, pH 7) (*33*). A value of-0.31 V is reported for the midpoint reduction potentials of the oxidized/semiquinone of the FMD-binding domain (*34*). For free FMN at pH 7, the midpoint potential for the quinone/semiquinone couple is -0.24 V at pH 7 (*35*). A similar study gave a figure of 0.15 V (*36*). The formal potential for

In Oxidative Stress: Diagnostics, Prevention, and Therapy Volume 2; Hepel, et al.;
ACS Symposium Series; American Chemical Society: Washington, DC, 2015.

Publication Date (Web): October 13, 2015 | doi: 10.1021/bk-2015-1200.ch009

FAD and FMN at pH 7 was ~ -0.25 V vs SCE (*37*). The pH dependence was explored (*35–37*). The coordination of flavins to zinc ion yields complexes which demonstrate facilitation of electrochemical reduction (*38*). Flavins are known to bind various metal ions. Enhanced electrophilicity of the complex favors electron uptake.

Electron Transfer by FAD

Many investigators in the life sciences are unaware that the diimine portion of the isoalloxazine nucleus is part of a broad class of conjugated imine ET functionalities discussed in the Introduction. Various articles report on the ET properties of the heterocyclic nucleus. A study was made of photoinduced ET by donor-acceptor pairs, involving triplet state acceptors of FMN and FAD, with donors, such as tryptophan, tyrosine and histidine (*40*). ET by diflavin reductases was examined in which the role of the binding sites of the isoalloxazine rings of the flavin cofactors is discussed (*41*). Interfalvin ET in human cytochrome P450 reductase is enhanced by coenzyme binding (*42*). There is a rate-limiting ET step during transfer of negative charge from reduced flavoprotein to oxygen (*43*). A hopping mechanism was invoked for flavoprotein (*44*).

Formation of ROS via ET by FAD

ROS can be generated by flavin enzymes either by ET to oxygen with the formation of superoxide (discussed first) or by reaction of the reduced flavin with oxygen to form flavin hydroperoxide (FlOOH).

Part of the chemical versatility of flavoenzymes is related to their reactivity towards oxygen which exhibits large variation among flavoproteins (*45*). In relation to factors that control reactivity with oxygen, a number have been proposed, including dipoles, charge distribution, dynamics and solvation. Detailed mechanistic aspects of superoxide production are reported (*46*). Chemically modified flavins bound to glucose oxidase were used in a study of oxygen isotope effects on ET to oxygen (*47*). Data indicate that pterins and flavins are efficient photosenzitizers of singlet oxygen production that may play a role in their biochemistry (*48*). Flavin photochemistry involves formation of flavin radicals which convert oxygen to superoxide by ET (*49*). Results support the contention that photoreduction of flavoproteins underlies light-induced formation of hydrogen peroxide in cells (*50*). Superoxide is a common precursor of the peroxide.

The alternate route for ROS generation entails conversion to FlOOH. All enzymes of the monooxygenase class form readily detectable flavin C(4a)-hydroperoxide intermediates (*46*). The hydroperoxide can undergo oxygen atom transfer or eliminate hydrogen peroxide. Mechanistic aspects are discussed. The hydroperoxides act as catalytic, mild oxidants for a variety of organic substrates in an environmentally friendly manner (*51*).

Publication Date (Web): October 13, 2015 | doi: 10.1021/bk-2015-1200.ch009

In Oxidative Stress: Diagnostics, Prevention, and Therapy Volume 2; Hepel, et al.;
ACS Symposium Series; American Chemical Society: Washington, DC, 2015.

Publication Date (Web): October 13, 2015 | doi: 10.1021/bk-2015-1200.ch009

Flavins and Cell Signaling

In recent years, novel flavoenzymes have been reported which are implicated in a variety of biological processes, including cell signaling (*52*). MICAL (molecule interacting with Cas L) is a protein which is involved in signaling events that guide axonal growth in the developing CNS. The essential N-terminal domain is a flavin-dependent monooxygenase. These recently discovered materials comprise a family of evolutionary-conserved signal transduction proteins that contain multiple domains which interact with the cytoskeleton, cytoskeletal adapter proteins, and other signaling entities (*53*). Studies suggest a role for MICAL flavoenzyme redox functions in axonal pathfinding events. The review summarizes a role for MICALs in semaphorin signaling. A study was made of light-mediated signal transduction in the flavin-binding plant photoreceptor structure (*54*). Phototropin consists of a C-terminal serine/threonine kinase and two upstream light, oxygen or voltage domains that each contain FMN.

A latter section deals with basic aspects of cell signaling.

B-Carbolines

These agents, recently developed, show promise based on early reports (*1*). Data do not unequivocally support the role for the GABA(A) receptor as the sole mediator of the antagonistic actions of β-carboline-3-carboxylate-tert-butyl ester (Fig. 5). The drug reduces alcohol drinking behavior, attenuates euphoigenic properties of the drug, while countering motor-impairing effects. The exact mechanism by which carboline selectively reduces alcohol-seeking behavior is unknown. The drug exhibits the greatest bibding selectively of the currently available ligands.

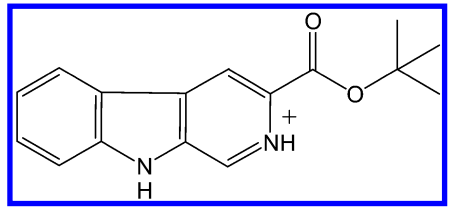

Figure 5. A protonated β-carboline

We propose a novel ET mechanism which may be involved in the neurochemical action of β-carbolines during alcoholism. A basis for the approach is structural similarity of the protonated Fig. 5 to N-methyl-4-phenypyridinium (MPP+, Fig. 6), a Parkinson-inducing substance. Theoretical studies on MPP+ demonstrate that ease of electron uptake is influenced by conformations of the phenyl ring (*55*). From quantum mechanical calculations, electron affinity is most favorable for the nearly coplanar arrangement. Site binding would be expected to alter conformation in comparison with situation in solution and hence, to influence reduction potential. Comparison of the $E_{1/2}$ values for biphenyl and fluorene (possessing a methylene bridge in the *ortho*-positions) reveals a dramatic

In Oxidative Stress: Diagnostics, Prevention, and Therapy Volume 2; Hepel, et al.;
ACS Symposium Series; American Chemical Society: Washington, DC, 2015.

enhancement of about 0.3 V in the reduction potential for the essentially coplanar conformation through restriction of rotation. Then electron uptake in vivo may be feasible for MPP+, accompanied by ET reactions and redox participation. Various reports support this contention. Evidence indicates that an important effect of MPP+ may involve inhibition of mitochondrial energy production via interference with the electron transport system. It is reasonable to hypothesize that agents which can participate in ET might interfere with electron transport chains essential for mitochondrial respiration. Thus, MPP+ may be acting as an ET shunt or block.

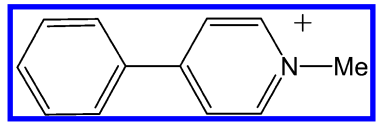

Figure 6. MPP+

Alternatively, redox cycling by MPP+ has been proposed for peroxyl radical and MPP radical by reaction with superoxide. In turn, MPP radical interacts with oxygen leading to SO and MPP+. There is considerable literature which documents involvement of MPP+ in the generation of ROS, and some deals with redox cycling.

In relation to mode of action at the molecular level, useful insight may be gained by comparison of protonated carboline with its structural analog MPP+. As in the case of biphenyl *vs* fluorene, a dramatic increase in reduction potential should be realized by the presence of the NH bridge which produces essential coplanarity in the molecular core. The ester group would further enhance electron uptake, whereas NH has somewhat negative effect. Salt formation might be realized intramolecularly by the 3-CO_2H group after ester hydrolysis. In the case of the related drug 3-propoxy-beta carboline hydrochloride, the agent is administered in the pyridinium (iminium-like) cationic form.

Benzodazepines

A problem that often accompanies alcoholism is anxiety and depression which are not affected by agents prescribed in therapy, e.g., maltrexone (*1*). This condition is frequently treated by anxiolytic drugs, mostly benzodiazepines (BDZs), such as valium (Fig. 7). Electrochemical studies provide evidence for participation of BDZ in ET reactions. The agents are highly conjugated imines which yield iminiums, ET functionalities, by protonation, e.g., Fig. 7. These drugs influence the activity of all major areas in the CNS, presumably through stereospecific binding to protein receptors, which result in various electrochemical phenomena. BDZs facilitate neurotransmission at synapses, and they enhance the effect of GABA on chloride channels, thus increasing ionic conductance. Also, charges are induced in the electrically excitable membrane properties of spinal neurons. Reduction potentials of various protonated BDZs fall within the physiologically active range. Hence, ET reactions might be a contributing

In Oxidative Stress: Diagnostics, Prevention, and Therapy Volume 2; Hepel, et al.;
ACS Symposium Series; American Chemical Society: Washington, DC, 2015.

Publication Date (Web): October 13, 2015 | doi: 10.1021/bk-2015-1200.ch009

Publication Date (Web): October 13, 2015 | doi: 10.1021/bk-2015-1200.ch009

factor to the physiological action. Correlations exists involving reduction potentials, structure, and drug activity. The structure of protonated valium, also called diazepam, (Fig. 7) incoporates a conjugated iminium functionality. According to theoretical calculations, electronic effects and ET play important roles in the chemical behavior (*1*). Our mechanistic approach is in accord with literature reports describing production of ROS by BDZs. Observed physiological effects may be in response to the reactive intermediates, or in many cases, ET alone could be involved. Findings demonstrate that antipsychotic clozapine produced oxidative damage in the rat brain. The drug can be activated by radical intermediates that cause OS. There is inhibition of mitochondrial respiration by BDZs, presumably by an ET process (*11*).

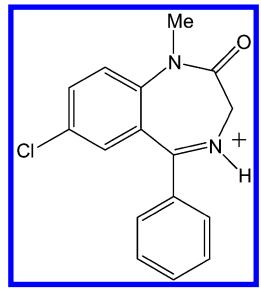

Figure 7. Protonated diazepam

Naltrexone

This drug (Fig. 8) is used to help addicts stay alcohol-free, but is not a cure (*1*). Treatment, involving a multi-component regimen, begins after dependency ends. The alkaloid can be intergrated into the basic mechanistic approach entailing ET-ROS-OS.

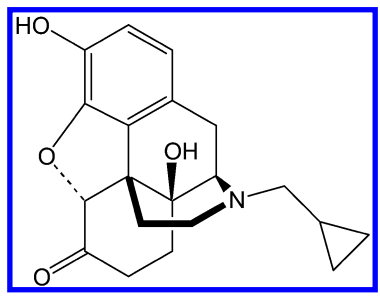

Figure 8. Naltrexone

Useful information is gained from metabolic investigations. Often a metabolite is the active form as appears to be the case with naltrexone. The two products most frequently cited are beta- naltrexol and 2-hydroxy-3-O-methyl-beta-naltrexol (*56–58*). The former, a principal metabolite, is designated the active form (*58*). It is instructive to consider a possible, important role for the

In Oxidative Stress: Diagnostics, Prevention, and Therapy Volume 2; Hepel, et al.;
ACS Symposium Series; American Chemical Society: Washington, DC, 2015.

catechol derivative. Although beta-naltrexol is a major product, its activity may be via the catechol ether which could be a derived metabolite. This substance could induce ET by means of generated phenoxyl radicals. Also, the catechol form can undergo redox transformations in conjunction with its o-quinone partner. This mechanistic perspective enjoys support from related alkaloids morphine and heroin. As in the case of naltrexone, morphine undergoes aromatic hydroxylation, yielding catechol-type product (*1*) which conceivably undergoes redox cycling with the corresponding o-quinone. Heroin undergoes in vivo hydrolysis of the diester to yield morphine. Also, the two alkaloids incorporate a tert-amine structure, as with naltrexone, which can undergo oxidation to ET iminium species.

Publication Date (Web): October 13, 2015 | doi: 10.1021/bk-2015-1200.ch009

Disulfiram (DSF) (Antabuse)

DSF (Fig. 9) is drug used in alcohol aversion therapy (*1*). Our approach deals mainly with metabolism in connection with mode of action. The drug inhibits aldehyde dehydrogenase, thereby causing a rise in acetaldehyde levels in alcoholics, with resultant unpleasant, toxic symptoms. Apparently, the sulfoxide metabolite (Fig. 10) is a key actor. Evidence suggests that DSF is a promising treatment for cocaine addiction. Sulfoxide **10**, evidently one of the active inhibitory agents in vivo, is related to α-dicarbonyl compounds, e.g., diacetyl and its monoxime derivatives (*59*), which possess reduction potentials favorable for ET in biosystems. A similar likeness pertains to α-iminocarboxylic acids which also electron affinic (*60*). A recent review provides a unifying mode of action for abused drugs centered on ET-ROS-OS (*12*).

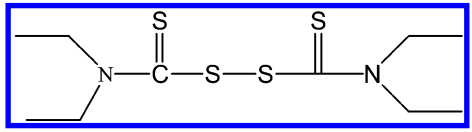

Figure 9. Disulfiram

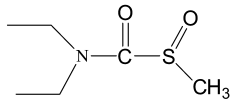

Figure 10. Sulfoxide metabolite of DSF

DSF displays various toxicities to body constituents, including the liver, CNS and mitochondria (*1*, *61*). It is relevant that reviews provide widespread evidence for a unifying theme of ET-ROS-OS. Supporting evidence is provided by the favorable effects of AOs (*1*).

Alcohol and Cell Signaling (*1*)

Chemical cell communication has attracted much attention in various areas of the life sciences. Although much research has been devoted to alcohol liver metabolism in this connection, there are reports dealing with effects on CNS (*62*). For example, ethanol exposure produced impaired insulin signaling associated with increased apoptosis and reduced mitochondrial function in neuronal cells. Cell signaling by nature is quite complicated. A simplified approach involving electrons, ROS and reactive nitrogen species (RNS) has been reported (*63–74*).

Abbreviations

ET= electron transfer agent; ROS= reactive oxygen species; OS= oxidative stress; AO= antioxidant; MTIP= 3-(4-chloro-2-morpholin-4-yl-thiazol-5-yl)-8-(1-ethylpropyl)-2,6-dimethylimidazo[1,2-b]pyridazine; FAD= Flavin adenine dinucleotide; BDZs= benzodiazepines; DSF= disulfiram

Publication Date (Web): October 13, 2015 | doi: 10.1021/bk-2015-1200.ch009

Acknowledgments

Editorial assistance by Thelma Chavez is acknowledged.

References

1. Kovacic, P.; Somanathan, R. In *New Research in Alcohol Abuse and Alcoholism*; Brozner, E. Y., Ed.; Nova: New York, 2006; pp 49−102.
2. Kovacic, P.; Somanathan, R. *Curr. Bioactive Compds.* **2010**, *6*, 46–59.
3. Kovacic, P.; Becvar, L. E. *Curr. Pharm. Des.* **2000**, *6*, 143–167.
4. Kovacic, P.; Osuna, J. A. *Curr. Pharm. Des.* **2000**, *6*, 277–309.
5. Kovacic, P.; Jacintho, J. D. *Curr. Med. Chem.* **2001**, *8*, 773–796.
6. Kovacic, P.; Jacintho, J. D. *Curr. Med. Chem.* **2001**, *8*, 863–892.
7. Kovacic, P.; Sacman, A.; Wu-Weis, M. *Curr. Med. Chem.* **2002**, *9*, 823–847.
8. Poli, G.; Cheeseman, K. H.; Dianzani, M. U.; Slater, T. F. *Free Radicals in the Pathogenesis of Liver Injury*; Pergamon: New York, 1989; pp 1−330.
9. Kovacic, P.; Thurn, L. A. *Curr. Vasc. Pharmacol.* **2005**, *3*, 107–117.
10. Kovacic, P.; Somanathan, R. *Curr. Med. Chem.* **2005**, *5*, 2601–2623.
11. Kovacic, P.; Pozos, R. S.; Somanathan, R.; Shangari, R.; O'Brien, P. J. *Curr. Med. Chem.* **2005**, *5*, 2601–2623.
12. Kovacic, P.; Cooksy, A. L. *Med. Hypotheses* **2005**, *64*, 366–367.
13. Kovacic, P.; Somanathan, R. In *Reviews of Environmental Contamination and Toxicology*; Whitacre, D. E., Ed.; Springer: New York, 2009; Vol. 201, pp 41−69.
14. Kovacic, P.; Somanathan, R. *Med. Hypotheses* **2008**, *70*, 914–923.
15. Halliwell, B.; Gutteridge, J. M. C. *Free Radicals in Biology and Medicine*; Oxford University Press: New York, 1999; pp 1−897.
16. Gehlert, D. R.; Cippitelli, A.; Thorsell, A.; Le, A. D.; Hipskind, P. A.; Hamdouchi, C.; Lu, J.; Hembre, E. J.; Cramer, J.; Song, M.; McKinzie, E. J.; Morin, M.; Ciccocioppo, R.; Heilig, M. *J. Neurosci.* **2007**, *27*, 2718–2716.

17. Rovner, S. *Chem. Eng. News* **2007**, *85*, 12.
18. Sato, K.; Nishina, Y.; Shiga, K.; Tanka, F. *J. Photochem. Photobiol.* **2003**, *B70*, 67–73.
19. Niemz, A.; Rotello, V. M. *J. Mol. Recognit.* **1996**, *9*, 158–162.
20. Cooke, G.; Dulclairoir, F. M. A.; John, P.; Polwart, N.; Rotello, V. M. *Chem. Commun.* **2003**, 2468–2469.
21. Carroll, J. B.; Cooke, G.; Garety, J. F.; Jordan, J. F.; Mabruk, S.; Rotello, V. M. *Chem. Commun.* **2005**, 3838–3840.
22. Boyd, A. S. F.; Carroll, J. B.; Cooke, G.; Garety, J. F.; Jordan, B. J.; Mabruk, S.; Rosair, G.; Rotello, V. M. *Chem. Commun.* **2005**, 2468–2470.
23. Kajiki, T.; Moriya, H.; Hoshino, K.; Kuroi, T.; Kondo, S-I.; Nabeshima, T.; Yano, Y. *J. Org. Chem.* **1999**, *64*, 9679–9689.
24. Chang, F.-C.; Bradley, L. H.; Swenson, R. P. *Biochim. Biophys. Acta* **2001**, *1504*, 319–328.
25. Tucker, J. H. R.; Collinson, S. R. *Chem. Soc. Rev.* **2002**, *31*, 147–156.
26. Lively, C. R.; McFarland, J. T. *J. Phys. Chem.* **1990**, *94*, 3980–3994.
27. Hazekawa, I.; Nishina, Y.; Sato, K.; Shichiri, M.; Miura, R.; Shiga, K. *J. Biochem.* **1997**, *121*, 1147–1154.
28. Löhr, F.; Yalloway, G. N.; Mayhew, S. G.; Rüterjans, H. *ChemBioChem* **2004**, *5*, 1523–1534.
29. Piacaud, T.; Desbois, A. *J. Biol. Chem.* **2002**, *277*, 31715–31721.
30. Niemz, A.; Rotello, V. M. *Acc. Chem. Res.* **1999**, *32*, 44–52.
31. Cooke, G. *Angew. Chem., Int. Ed.* **2003**, *42*, 4860–4870.
32. Robetrs, G. A.; Celik, A.; Hunter, D. J. B.; Ost, T. W. B.; White, J. H.; Chapman, S. K.; Turner, N. J.; Flitsch, S. L. *J. Biochem. Chem.* **2003**, *278*, 49914–48920.
33. Birss, V. I.; Elzanowska, H.; Turner, R. A. *Can. J. Chem.* **1988**, *66*, 86–96.
34. Finn, R. D.; Basram, J.; Roitel, O.; Wolf, C. R.; Munro, A. W.; Paine, M. J. I.; Scrutton, N. S. *Eur. J. Biochem.* **2003**, *270*, 1164–1175.
35. Steensma, E.; Heering, H. A.; Hagen, W. R.; Van Mierlo, C. P. M. *Eur. J. Biochem.* **1996**, *235*, 167–172.
36. Heeting, H. A.; Hagen, W. R. *J. Electoanal. Chem.* **1996**, *404*, 249–260.
37. Kubota, L. T.; Gorton, L.; Roddick-Lanzilotta, A.; McQuillan, A. J. *Bioenergetics* **1998**, *47*, 39–46.
38. König, B.; Pelka, M.; Reichenbach-Klinke, R.; Schelter, J.; Daub, J. *Eur. J. Org. Chem.* **2001**, 2297–2303.
39. Barber, M. J.; Trimboli, A. J.; Nomikos, S.; Smith, E. T. *Arch. Biochem. Biophys.* **1997**, *345*, 88–96.
40. Crovetto, L.; Braslavsky, S. E. *J. Phys. Chem. A* **2006**, *110*, 7307–7315.
41. Murataliev, M. B.; Feyereisen, R.; Walker, F. A. *Biochim. Biophys. Acta* **2004**, *1698*, 1–26.
42. Gutierrez, A.; Munro, A. W.; Grunau, A.; Wolf, C. R.; Scrutton, N. S. *J. Biochem.* **2003**, *270*, 2612–2621.
43. Roth, J. P.; Klinman, J. P. *Proc. Natl. Acad. Sci. U.S.A.* **2003**, *100*, 62–67.
44. Nöll, G.; Kozma, E.; Grandori, R.; Carey, J.; Schödl, T.; Hauska, G.; Daub, J. *Langmuir* **2006**, *22*, 2378–2383.
45. Mattevi, A. *Trends Biochem. Sci.* **2006**, *31*, 276–283.

In Oxidative Stress: Diagnostics, Prevention, and Therapy Volume 2; Hepel, et al.;
ACS Symposium Series; American Chemical Society: Washington, DC, 2015.

Publication Date (Web): October 13, 2015 | doi: 10.1021/bk-2015-1200.ch009

46. Massey, V. *J. Biol. Chem.* **1994**, *269*, 22459–22462.
47. Roth, J. P.; Wincek, R.; Nodet, G.; Edmondson, D. E.; McIntire, W. S.; Klinman, J. P. *J. Am. Chem. Soc.* **2004**, *126*, 15120–15134.
48. Egorov, S. Y.; Krasnovsky, A. A., Jr.; Bashtanov, M. Y.; Mironov, E. A.; Ludnikova, T. A.; Kritsky, M. S. *Biochemistry (Moscow)* **1999**, *64*, 1117–1121.
49. Laloraya, M. M.; Pradeep, K. G.; Laloraya, M. *Biochem. Mol. Biol. Int.* **1994**, *33*, 543–551.
50. Hockberger, P. E.; Skimina, T. A.; Centonze, V. E.; Lavin, C.; Chu, S.; Dadras, S.; Reddy, J. K.; White, J. G. *Proc. Natl. Acad. Sci. U.S.A.* **1999**, *96*, 6255–6260.
51. Imada, Y.; Naota, T. *Chem. Rev.* **2007**, *7*, 354–361.
52. De Colibus, L.; Mattevi, A. *Curr. Opin. Struct. Biol.* **2006**, *16*, 722–728.
53. Kolk, S. M.; Pasterkamp, R. J. *Adv. Exp. Med. Biol.* **2007**, *600*, 38–51.
54. Crosson, S.; Moffat, K. *Proc. Natl. Acad. Sci. U.S.A.* **2001**, *98*, 2995–3000.
55. Kovacic, P.; Edwards, W. D.; Ming, G. *Free Radical Res. Commun.* **1991**, *14*, 25–32.
56. Macgregor, T. R.; Drum, M. A.; Harrigan, S. E.; Wiley, J. N.; Reuning, R. H. *J. Pharmacol.* **1983**, *35*, 38–42.
57. Wall, M. E.; Brine, D. R.; Perez-Reyes, M. *Drug Metab. Dispos.* **1981**, *9*, 369–375.
58. Paudel, K. S.; Nalluri, B. N.; Hammel, D. C.; Valiveti, S.; Kiptoo, M. O.; Crooks, P. A.; Stinchcomb, A. L. *J. Pharm. Sci.* **2005**, *94*, 1965–1975.
59. Nierfar, N. N.; Haycock, F. L.; Wesermann, J. L.; Macstay, J. A.; Heasly, V. L.; Kovacic, P. *J. Mex. Chem. Soc.* **2002**, *46*, 307–312.
60. Kovacic, P.; Popp, W. J.; Timberlake, J. W.; Ryan, M. D. *Chem. Biol. Interact.* **1989**, *69*, 235.
61. Balakirev, M. Y.; Zimmer, G. *Chem. Biol. Interact.* **2001**, *138*, 299–311.
62. De la Monte, S. M.; Wands, J. R. *Cell. Mol. Life Sci.* **2002**, *59*, 882–893.
63. Forman, H. G., Cadenas, E., Eds. *Oxidative Stress and Signal Transduction.*; Chapman and Hall: New York, 1997.
64. Hancock, G. T. *Cell Signaling*; Oxford University Press: New York, 2005.
65. Demple, B. In *Handbook of Cell Signaling*; Bradshaw, R. A., Dennis, E. A., Eds.; Academic Press: New York, 2004; Vol. 3, pp 191−195.
66. Kovacic, P.; Pozos, R. S. *Birth Defects Res., Part C* **2006**, *78*, 333–344.
67. Hansen, J. M. *Birth Defects Res., Part C* **2006**, *78*, 293–307.
68. Jones, D. P. *Antioxid. Redox. Signaling* **2006**, *8*, 1865–1879.
69. Lee, N. K.; Choi, Y. G.; Baik, J. Y.; Han, S. Y.; Jeong, D. W.; Bae, Y. S.; Kim, N.; Lee, S. Y. *Blood* **2005**, *106*, 852–859.
70. Miller, A. A. *Antioxid. Redox. Signaling* **2006**, *8*, 1113–1120.
71. Bunik, V. I.; Schloss, J. V.; Pinto, J. T.; Gibson, G. E.; Cooper, A. J. *Neurochem. Res.* **2006**, *32*, 871–891.
72. Liu, L.-Z.; Hu, X.-W.; Xia, C.; He, J.; Shi, X.; Fang, J.; Jiang, B. H. *Free Radical Biol. Med.* **2006**, *41*, 1521–1533.
73. Shields, J. M.; Pruitt, K.; McFall, A.; Shaub, A.; Der, C. J. *Trends Cell Biol.* **2000**, *10*, 147–154.
74. Kovacic, P. *Med. Hypotheses* **2007**, *69*, 1105–1110.

Publication Date (Web): October 13, 2015 | doi: 10.1021/bk-2015-1200.ch009

Publication Date (Web): October 13, 2015 | doi: 10.1021/bk-2015-1200.ch010

Chapter 10

How Does Acetaminophen Function? Metabolite, Electron Transfer, Reactive Oxygen Species, Oxidative Stress and COX

Peter Kovacic[1,*] and Ratnasamy Somanathan[1,2]

[1]Department of Chemistry and Biochemistry, San Diego State University, San Diego, California 92182-1030, United States
[2]Centro de Graduados e Investigación del Instituto Tecnológico de Tijuana, Apdo postal 1166, Tijuana, B.C. Mexico
[*]E-mail: pkovacic@mail.sdsu.edu

A recent article presents mode of action by acetaminophen as an enigma involving various contributing factors. An alternative approach entails redox cycling by the N-acetyl benzoquinone imine metabolite. The resulting reaction oxygen species can play a role in both therapy and toxicity. The broader ramifications of the unifying mechanism are also addressed, including a multifaceted approach. Commonality with the widely accepted COX theory is treated.

Keywords: acetaminophen; N-acetyl benzoquinone imine; electron transfer; reactive oxygen species; oxidative stress; COX; toxicity

Introduction

A recent news item titled "The Enigma Pill" deals with action mode of acetaminophen (Fig 1) (Tylenol) (APAP), a widely used sedative and antipyretic (*1*). A 2013 article states that it is now generally accepted that cyclooxygenase (COX) enzymes play an important role (*2*). This chapter summarizes the numerous modes of action that have been proposed with contribution to the enigma. Also, focus is centered on an alternative approach involving metabolism, electron transfer (ET), reactive oxygen species (ROS), oxidative stress (OS) and

In Oxidative Stress: Diagnostics, Prevention, and Therapy Volume 2; Hepel, et al.;
ACS Symposium Series; American Chemical Society: Washington, DC, 2015.

COX. A leading actor is the N-acetyl benzoquinone imine (NAPQ1) (Fig 2) metabolite, which appears to function as an ET agent that generates ROS-OS.

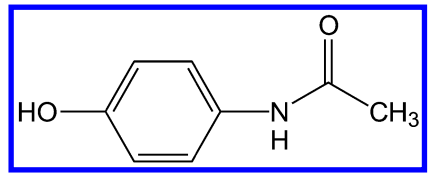

Figure 1. Acetaminophen (APAP)

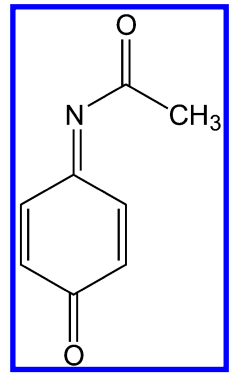

Figure 2. NAPQ1

The unifying mechanism applied here is an extension of prior work (*3*). "The preponderance of bioactive substances, usually as the metabolites, incorporate ET functionalities. We believe these play an important role in physiological responses. The main groups include quinones (or phenolic precursors), metal complexes (or complexors), aromatic nitro compounds (or reduced hydroxylamine and nitroso derivatives), and conjugated imines (or iminium species). The imine category is the main object of our review and is the least well known. Resultant redox cycling is illustrated in Scheme 1. Iminiums are usually better electron acceptors than imines, due partly to positive charge. In vivo redox cycling with oxygen can occur, giving rise to oxidative stress (OS) through generation of ROS, such as hydrogen peroxide, hydroperoxides, alkyl peroxides, and diverse radicals (hydroxyl, alkoxyl, hydroperoxyl, and superoxide) (Scheme 2).

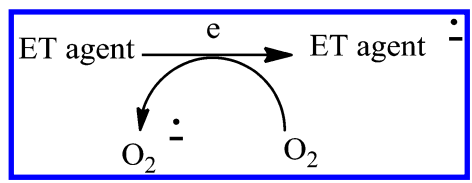

Scheme 1. Redox cycling with superoxide formation

In Oxidative Stress: Diagnostics, Prevention, and Therapy Volume 2; Hepel, et al.;
ACS Symposium Series; American Chemical Society: Washington, DC, 2015.

Publication Date (Web): October 13, 2015 | doi: 10.1021/bk-2015-1200.ch010

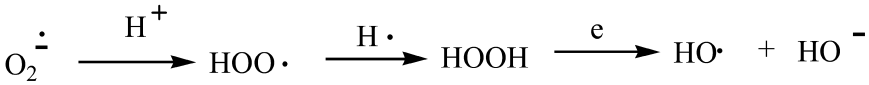

Scheme 2. Other ROS from superoxide

In some cases ET results in involvement with normal electrical effects (e.g., in respiration of neurochemistry). Generally, active entities possessing ET groups display reduction potentials in the physiologically responsive range, (i.e., more positive than about -0.5 V). Hence, ET in vivo can occur resulting in production of ROS which can be beneficial in cell signaling at low concentrations, but produce toxic results at high levels. Electron donors consist of phenols, N-heterocycles or disulfides in proteins which produce relatively stable radical cations. ET, ROS and OS have been increasingly implicated in the mode of action of drugs and toxins, (e.g., antiinfective agents (*4*), anticancer drugs (*5*), carcinogens (*6*), reproductive toxins (*7*), nephrotoxins (*8*) hepatotoxins (*9*), cardiovascular toxins (*10*), nerve toxins (*11*), mitochondrial toxins (*12*), abused drugs (*13*), pulmonary toxins (*14*), ototoxins (*15*), and various other categories (*16*). There is a plethora of experimental evidence supporting the ET-ROS theoretical framework. This evidence includes generation of the common ROS, lipid peroxidation, degradation products of oxidation, depletion of AOs, effect of exogenous AOs, and DNA oxidation and cleavage products, as well as electrochemical data. This comprehensive, unifying mechanism is consistent with the frequent observations that many ET substances display a variety of activities (e.g., multiple-drug properties), as well as toxic effects. It is important to recognize that mode of action in the biodomain is often multifaceted. In addition to the ET-ROS-OS approach, other aspects may pertain, such as, enzyme inhibition, allosteric effects, receptor binding, metabolism and physical factors. A specific example involves protein binding by quinones in which protein nucleophiles, such as amino or thiol, effect conjugate addition."

Enigma Mode of Action

When researchers are asked of knowledge about how APAP works, the responses ranged from "pretty clear" to "poorly" (*1*). The "mechanism seems messy enough to discourage even the most optimistic scientists". Various action modes have been proposed with differing degrees of evidence, including chemical messengers associated with inflammation and pain, as well as neurotransmission in the brain and spinal cord (*1*). Another proposal invokes blockage of prostaglandin formation in the central nervous system (CNS) (*17*, *18*). A focus was on COX inhibition with evidence that this could represent a primary central mechanism. The analgesic activity appears to be prevented by blockage of cannabinoid receptors (*19*, *20*). Serotonin (5-HT) transmission in the CNS may also play a role (*21*). There is the suggestion that the drug indirectly employs communication systems similar to those of opioids (*22*). However, acetaminophen is neither an opioid nor an NSAID.

In Oxidative Stress: Diagnostics, Prevention, and Therapy Volume 2; Hepel, et al.;
ACS Symposium Series; American Chemical Society: Washington, DC, 2015.

Publication Date (Web): October 13, 2015 | doi: 10.1021/bk-2015-1200.ch010

APAP, following deacetylation, undergoes acylation of the amine by the fatty acid arachidonic acid (*23*). The bioactive product, possessing enhanced lipid solubility, would be expected to undergo reactions similar to those of APAP. Another proposed mode of action consists of interaction at the brain or spinal cord in APAP-induced antinociception (*22*).

N-Acetyl p-Benzoquinone Imine (NAPQI) Metabolite

There is appreciable literature linking the NAPQI metabolite to physiological activity. Some of the reports relate to the ROS unifying theory. APAP is known to play a prominent role in inducing liver toxicity (*24*). The toxic metabolite NAPQ1 Is believed to be importantly involved, including effector of apoptosis and depletion of GSH which is commonly an oxidant effect. Increase in GSH peroxides following APAP administration and the beneficial effect of a SOD mimic pointed to generation of ROS. Direct evidence for ROS generation was provided by the flow cytometers. ROS production was also associated with mitochondrial damage characterized by collapse of transmembrane potential. The various lines of evidence point to a role for ROS in APAP-induced liver insult. Another report links APAP hepatotoxicity to lipid peroxidation and covalent binding to macromolecules leading to mitochondrial damage (*25*). The result is attributed to the NAPQI metabolite via sulfhydryl oxidation or addition. The adverse influences were countered by bicyclol which is believed to elicit a variety of biological effects through its AO and antiinflammatory properties (*25*, *26*). Another report associates NAPQ1 with the toxic side effects of the parent drug (*27*). Several other articles deal with reaction of NAPQ1 with thiol groups via conjugate addition which is likely involved in quinone binding to protein (*25*, *28–30*). A related example entails reaction of NAPQ1 with proline and the resultant biological ramifications (*31*). In addition to GSH depletion by the quinone imine, there is a role for reactive nitrogen species in APAP induced toxicity (*32*). p-Benzoquinone, an electrophile, is also reported as a metabolite (*29*), capable of functioning in a manner similar to NAPQ1.

In relation to basic chemistry, NAPQ1 is a close analog of p-benzoquinone which is well known ET agent (Scheme 3). Uptake of an electron to form a radical anion would be facilitated by the acetyl substituent of NAPQ1 in conjugation resulting in further, favorable delocalization as illustrated in Fig. 3.

Important light is cast upon the mechanism by comparison with the α-carbonylimine structure which has been investigated by means of electrochemistry (*33*). Reduction potentials fell within the range favorable for in *vivo* ET protonation or hydrogen bonding which form iminium type species enhanced electron affinity. Relationship to physiological activity was discussed. The acetaminophen metabolite is electronically related as a vinylog of the parent α-carbonylimine model. The vinylogous character bestows enhanced favorable stabilization via conjugation in the generated radical anion. The captodative effect is discussed as a beneficial contributing factor.

Publication Date (Web): October 13, 2015 | doi: 10.1021/bk-2015-1200.ch010

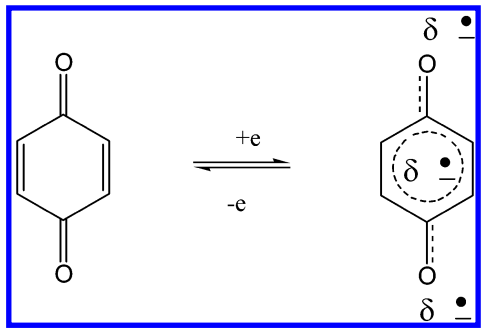

Scheme 3. p-Benzoquinone redox

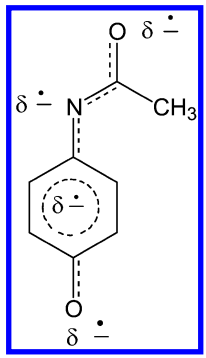

Figure 3. Delocalized radical anion of NAPQ1

Publication Date (Web): October 13, 2015 | doi: 10.1021/bk-2015-1200.ch010

Toxicity

This topic is also treated in other sections. Hepatotoxicity has been extensively investigated and presented as a serious threat in some cases. In addition, the Introduction presents numerous examples entailing application of ET-ROS-OS to toxicity, including that of the liver. There is substantial literature on the subject in more recent years. Hence, it should not be surprising that APAP fits the unifying theme via the ET iminoquinone metabolite leading to ROS-OS.

The advese reactions have been associated with OS and NAPQ1 metabolite, including ROS (*34*). Various systems may be responsible for ROS generation. Studies indicate that APAP and NAPQ1 are the primary ototoxic agents (*35*). Data indicate involvement of ROS overproduction.

Commonality Involving COX and ET-ROS-OS Mechanisms

There is wide acceptance that APAP operates by inhibition of COX enzymes which can function as peroxidases (*13*). In the process, the drug undergoes oxidation in which it functions as an AO, a common property of phenols (*36*), e.g., vitamin E. The phenols can also act as pro-oxidants (*36*), which applies to APAP via metabolism to a iminoquinone resulting in generation of ROS and OS. Oxidation of the drug leads to reduction or inhibition of the COX enzymes. Previously, the two mechanisms were regarded as separate and diverse pathways. This novel perspective reveals that the two are intimately associated with the COX enzyme acting as a peroxidase oxidant of the drug with conversion to the ET imnioquinone metabolite. This represents an expansion of the unifying feature. There has been extensive literature on COX enzymes. A book in 1998 addresses various aspects, including inhibition, mechanism of action, therapy, and drugs, e.g., aspirin (*37*).

Other Analgesics and Related Drugs

Aspirin

This related drug is treated in another Chapter in the book.

Benzodiazepines (BDZs)

The tranquilizers are widely involved in the CNS operating via electrical effects (*13*). The BDZs increase ionic conductance in connection with synapses and chloride ion channels. Electrical phenomena are observed in membrane neurons. Protonated BDZs display reduction potentials in the physiologically active range. There are correlations involving reduction potentials, structure and drug activity. A prominent member is Valium (Diazepam) (Fig. 4) which is a highly conjugated imine. Theoretical calculations support participation of ET and electronic effects. A report deals with activation of Clozapine to radical metabolites that produce OS and inhibit mitochondrial respiration, apparently by ET.

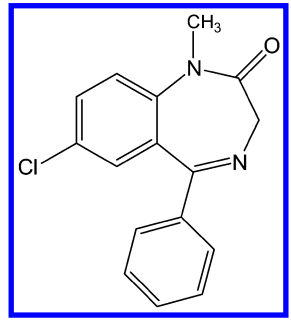

Figure 4. Valium

In Oxidative Stress: Diagnostics, Prevention, and Therapy Volume 2; Hepel, et al.;
ACS Symposium Series; American Chemical Society: Washington, DC, 2015.

Publication Date (Web): October 13, 2015 | doi: 10.1021/bk-2015-1200.ch010

Publication Date (Web): October 13, 2015 | doi: 10.1021/bk-2015-1200.ch010

Phenobarbital

Incorporation in the unifying theme has been previously addressed (*13*). Various modes of action are documented, including ion channel blockage, effect on membrane potentials and neurotransmission. An ET mechanism as anticonvulsant is reported, involving electrical phenomena. A key aspect entails aromatic hydroxylation leading to phenol and catechol metabolites (see Fig. 5) which can serve as precursors of ET quinone derivatives. o-Quinone are known to posses favorable reduction potentials making for facile participation in reductions in vivo.

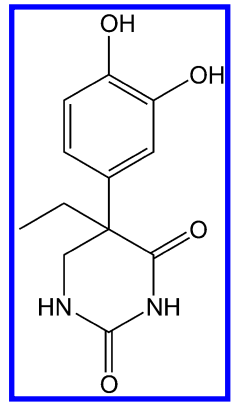

Figure 5. Phenobarbital catechol metabolite

Phenytoin

The hydantoin is used as an epileptic (*13*). OS is suggested as being involved in the neurotoxicity. Similar to Phenobarbital, the drug is converted metabolically to phenol and catechol products with subsequent oxidation to an ET o-quinone (Fig. 6). Subsequent binding to protein can occur. The drug can induce oxidative damage to DNA and proteins, apparently from ROS generated by ET redox cycling. Also, an epoxide metabolite has been discussed, which may generate ROS via alkylation of DNA.

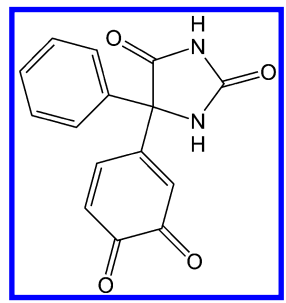

Figure 6. Phenytoin o-quinone metabolite

In Oxidative Stress: Diagnostics, Prevention, and Therapy Volume 2; Hepel, et al.;
ACS Symposium Series; American Chemical Society: Washington, DC, 2015.

Morphine and Heroin

These are among the earliest analgetic abused drugs. Various reports incorporate them within the unifying mechanism (*13*). With morphine, apoptosis was linked to superoxide, with protection by the thiol AO N-acetylcysteine. Redox cycling with oxygen occurs with production of superoxide and hydrogen peroxide. Since heroin is metabolized to morphine, the above results would also pertain. Levels of lipid peroxides were enhanced in heroin abusers. Relation between toxicity and ROS was reported. Oxidation and peroxidation pointed to the presence of ROS. There are other drugs related to morphine which may operate in a similar manner mechanistically.

Publication Date (Web): October 13, 2015 | doi: 10.1021/bk-2015-1200.ch010

Broad Ramifications of the Unifying Theme

The unifying theme of ET-ROS-OS emulates related aspects common in nature. For example, in living systems, one finds common structural threads in protein (amide), carbohydrate (acetal) and lipids (ester), as well as in reaction systems, such as enzymes (oxidases, esterases, hydrolases), electron transfer and electrochemistry. The ET-ROS-OS theme has found widespread application as exemplified in the Introduction. Many antibacterial agents appear to copy the immune systems in what is described as phagomimetic action (*38*). At high levels, ROS are commonly found as a unifying feature in toxicity, being associated with a wide variety of adverse reactions. It is notable that ROS at low concentrations can exert beneficial effects in a unifying aspect based on cell signaling (*39*). Another unifying aspect that lauds credence is the beneficial effect of AOs on deleterious processes supporting the common involvement of toxic ROS. Participation of ET agents (see Introduction) in ROS formation is a neglected aspect. Another case of unification applies to action mechanism of abused drugs, including banned ones and legal sedatives, such as APAP, aspirin and barbiturates (*13*).

Abbreviations

APAP= Acetaminophen; NAPQ1= N-acetyl benzoquinone imine; ET= electron transfer; ROS= reactive oxygen species; OS= oxidative stress; AO= antioxidant; COX= cyclooxygenase; CNS= central nervous system

Acknowledgments

Editorial assistance by Thelma Chavez and Bianca Aviña is acknowledged.

References

1. Drahl, C. *Chem. Eng. News* **2014**, *92* (29), 31–32.
2. Davies, M. J.; Day, R. O.; Mohamudally, A.; Scott, K F. *Inflammopharmacology* **2013**, *21*, 201–232.
3. Kovacic, P.; Somanathan, R. *Curr. Bioact. Compd.* **2010**, *6*, 46–59.

4. Kovacic, P.; Becvar, L. E. *Curr. Pharm. Des* **2000**, *6*, 143–167.
5. Kovacic, P.; Osuna, J. A. *Curr. Pharm. Des.* **2000**, *6*, 277–309.
6. Kovacic, P.; Jacintho, J. D. *Curr. Med. Chem.* **2001**, *8*, 773–796.
7. Kovacic, P.; Jacintho, J. D. *Curr. Med. Chem.* **2001**, *8*, 863–892.
8. Kovacic, P.; Sacman, A.; Wu-Weis, M. *Curr. Med. Chem.* **2002**, *9*, 823–847.
9. Poli, G.; Cheeseman, K. H.; Dianzani, M. U.; Slater, T. F. *Free Radicals in the Pathogenesis of Liver Injury*; Pergamon: New York, 1989; pp 1−330.
10. Kovacic, P.; Thurn, L. A. *Curr. Vasc. Pharmacol.* **2005**, *3*, 107–117.
11. Kovacic, P.; Somanathan, R. *Curr. Med. Chem.* **2005**, *5*, 2601–2623.
12. Kovacic, P.; Pozos, R. S.; Somanathan, R.; Shangari, R.; O'Brien, P. J. *Curr. Med. Chem.* **2005**, *5*, 2601–2623.
13. Kovacic, P.; Cooksy, A. L. *Med. Hypotheses* **2005**, *64*, 357–367.
14. Kovacic, P.; Somanathan, R. In *Reviews of Environmental Contamination and Toxicology*; Whitacre, D. E., Ed.; Springer: New York, 2009; Vol. 201, pp 41−69.
15. Kovacic, P.; Somanathan, R. *Med. Hypotheses* **2008**, *70*, 914–923.
16. Halliwell, B.; Gutteridge, J. M. C. *Free Radicals in Biology and Medicine*; Oxford University Press: New York, 1999; pp 1−897.
17. Flower, R. J.; Vane, J. R. *Nature* **1972**, *240*, 410–411.
18. Aronoff, D. M.; Oates, J. A.; Boutaud, O. *Clin. Pharmacol. Ther.* **2006**, *79*, 9–19.
19. Chandrasekharan, N. V.; Dai, H.; Roos, K. L. T.; Evanson, N. K.; Tomsik, J.; Elton, T. S.; Simmons, D. L. *Proc. Natl. Acad. Sci. U.S.A.* **2002**, *99*, 13926–13931.
20. Ottani, A.; Leone, S.; Sandrini, M.; Ferrari, A.; Bertolini, A. *Eur. J. Pharmacol.* **2006**, *531*, 280–281; DOI: 10.1016/j.ejphar.2005.12.015.
21. Pickering, G.; Loriot, M-A.; Libert, F.; Eschalier, A.; Beaune, P.; Dubray, C. *Clin. Pharmacol. Ther.* **2006**, *79*, 371–378.
22. Raffa, R. B.; Stone, D. J.; Tallarida, R. J. *J. Pharmacol. Exp. Ther.* **2000**, *295*, 291–294.
23. Högesätt, E. D.; Jönsson, B. A. G.; Ermund, A.; Andersson, D. A.; Böjork, H.; Alexander, J. P.; Cravatt, B. F.; Basbaum, A. I.; Zygmunt, P. M. *J. Biol. Chem.* **2005**, *280*, 31405–31412.
24. Ferret, P. J.; Hammoud, R.; Tulliez, M.; Tran, A.; Trébéden, H.; Jaffray, P.; Malassagne, B.; Calmus, Y.; Weill, B.; Batteux, F. *Hapatology* **2001**, *33*, 1173–1180.
25. Li, Y.; Dai, G. W.; Li, Y.; Liu, G. T. *Yao Xue Xue Bao* **2001**, *36*, 723–726.
26. Zhang, J.; Fu, B.; Zhang, X.; Zhang, L.; Bai, X.; Zhao, X.; Chen, L.; Cui, L.; Zhu, C.; Wang, L.; Zhao, Y.; Zhao, T.; Wang, X. *Brain Res. Bull.* **2014**, *100*, 38–40.
27. Simon, H.; Melles, D.; Jacquoilleot, S.; Sanderson, P.; Zazzeroni, R.; Karst, U. *Anal. Chem.* **2012**, *84*, 8777–8782.
28. Gumbrevičius, G.; Sveikata, A.; Sveikatiene, R.; Stankevičius, E. *Medicine (Kaunas)* **2012**, *48*, 379–381.
29. Andersson, D. A.; Gentry, C.; Alenmyr, L.; Killander, D.; Lewis, S. E.; Andersson, A.; Bucher, B.; Galzi, J-L.; Sterner, O.; Bevan, S.;

Högestätt, E. D.; Zygmunt, P. M. *Nat. Commun.* **2011**, *2*, 551; DOI: 10.1038/ncomms1559.
30. Madsen, K. G.; Olsen, J.; Skonberg, C.; Hansen, S. H.; Jurva, U. *Chem. Res. Toxicol.* **2007**, *20*, 821–831.
31. Senter, P. D.; Al-Abed, Y.; Metz, C. N.; Benigni, F.; Mitchell, R. A.; Chesney, J.; Han, J.; Gartner, C. G.; Nelson, S. D.; Todaro, G. J.; Bucala, R. *Proc. Natl. Acad. Sci. U.S.A.* **2002**, *99*, 144–149.
32. Burke, A. S.; MacMillan; Crow, L. A.; Hinson, J. A. *Chem. Res. Toxicol.* **2010**, *23*, 1286–1289.
33. Niufar, N. N.; Haycock, F. L.; Wesemann, J. L.; MacStay, J. A.; Heasley, V. L.; Kovacic, P. *J. Mex. Chem. Soc.* **2002**, *46*, 307–312.
34. Letelier, M. E.; López-Valladares, M.; Peredo-Silva, L.; Rojas-Sepúlveda, D.; Aracena, P. *Toxicol. In Vitro* **2011**, *25*, 1310–1313.
35. Kalinec, G. M.; Thein, P.; Parsa, A.; Yorgason, J.; Luxford, W.; Urrutia, R.; Kalinec, F. *Hear Res.* **2014**, *313*, 26–37.
36. Kovacic, P.; Somanathan, R. In *Frontiers in Antioxidants Research*; Panglossi, H. V., Ed.; Nova Science Publishers: Hauppauge, NY, 2006; pp 1−38.
37. Vane, J. R.; Botting, J. H. *Selective COX-2 inhibitors: pharmacology, clinical effects, and therapeutic potential*; Proceedings of a conference held on March 20-21, 1997, in Cannes, France; Kluwer Academic: Dordrecht, London, 1988; pp 1−150.
38. Gutteridge, G. M. C.; Quinlan, G. J.; Kovacic, P. *Free Radical Res.* **1998**, *28*, 1–14.
39. Kovacic, P.; Pozos, R. S. *Birth Defects Res., Part C* **2006**, *78*, 333–344.

Publication Date (Web): October 13, 2015 | doi: 10.1021/bk-2015-1200.ch010

Publication Date (Web): October 13, 2015 | doi: 10.1021/bk-2015-1200.ch011

Chapter 11

Aspirin (Analgesic) and Dicamba (Herbicide): Electron Transfer, Reactive Oxygen Species, Oxidative Stress, and Antioxidant

Peter Kovacic[1,*] and Ratnasamy Somanathan[1,2]

[1]Department of Chemistry and Biochemistry, San Diego State University, San Diego, California 92182-1030, United States
[2]Centro de Graduados e Investigación del Instituto Tecnológico de Tijuana, Apdo postal 1166, Tijuana, B.C. Mexico
[*]E-mail: pkovacic@mail.sdsu.edu

Although aspirin is an analgesic and dicamba is an herbicide, both are derivatives of salicylic acid and both undergo similar metabolic transformation. The salicylic acid type of metabolite can be regarded as the key to physiological action. Subsequent hydroxylation to catechol or hydroquinone derivatives would lead to o- or p- quinones. The quinones generate ROS which can be involved in therapy or toxic reactions. AO properties are attributed to phenolic metabolites. The existence of favorable and harmful effects of phenol is rationalized. The unifying mode of action can be applied generally to analgesics and herbicides. The CNS plays an important role. The phenol group of various analgesic drugs or their metabolites (acetaminophen, aleve, morphine and aspirin) represents a common feature of mechanistic significance.

Keywords: Aspirin; CNS; dicamba; electron transfer; oxidative stress; radicals

Introduction

This review deals with acetyl salicylic acid (aspirin) (ASA) (Fig 1), an analgesic, and dicamba (Fig. 2), an herbicide, in relation to similarities and

In Oxidative Stress: Diagnostics, Prevention, and Therapy Volume 2; Hepel, et al.;
ACS Symposium Series; American Chemical Society: Washington, DC, 2015.

physiological activity. A prior unifying, mechanistic theme is applied as follows (*1*).

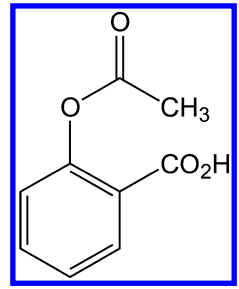

Figure 1. Aspirin

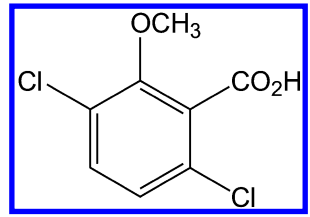

Figure 2. Dicamba

"The preponderance of bioactive substances, usually as the metabolites, incorporate ET functionalities. We believe these play an important role in physiological responses. The main groups include quinones (or phenolic precursors), metal complexes (or complexors), aromatic nitro compounds (or reduced hydroxylamine and nitroso derivatives), and conjugated imines (or iminium species). Resultant redox cycling is illustrated in Scheme 1. In vivo redox cycling with oxygen can occur, giving rise to oxidative stress (OS) through generation of reactive oxygen species (ROS), such as hydrogen peroxide, hydroperoxides, alkyl peroxides, and diverse radicals (hydroxyl, alkoxyl, hydroperoxyl, and superoxide) (Scheme 2).

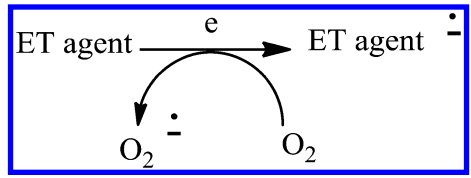

Scheme 1. Redox cycling with superoxide formation

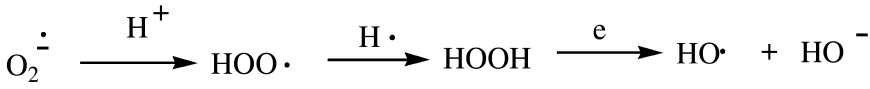

Scheme 2. Other ROS from superoxide

In Oxidative Stress: Diagnostics, Prevention, and Therapy Volume 2; Hepel, et al.;
ACS Symposium Series; American Chemical Society: Washington, DC, 2015.

Publication Date (Web): October 13, 2015 | doi: 10.1021/bk-2015-1200.ch011

In some cases ET results in involvement with normal electrical effects (e.g., in respiration of neurochemistry). Generally, active entities possessing ET groups display reduction potentials in the physiologically responsive range, (i.e., more positive than about -0.5 V). Hence, ET in vivo can occur resulting in production of ROS which can be beneficial in cell signaling at low concentrations, but produce toxic results at high levels. Electron donors consist of phenols, N-heterocycles or disulfides in proteins which produce relatively stable radical cations. ET, ROS and OS have been increasingly implicated in the mode of action of drugs and toxins, (e.g., antiinfective agents (*2*), anticancer drugs (*3*), carcinogens (*4*), reproductive toxins (*5*), nephrotoxins (*6*), hepatotoxins (*7*), cardiovascular toxins (*8*), nerve toxins (*9*), mitochondrial toxins (*10*), abused drugs (*11*), pulmonary toxins (*12*), ototoxins (*13*), and various other categories (*14*).

There is a plethora of experimental evidence supporting the ET-ROS theoretical framework. This evidence includes generation of the common ROS, lipid peroxidation, degradation products of oxidation, depletion of AOs, effect of exogenous AOs, and DNA oxidation and cleavage products, as well as electrochemical data. This comprehensive, unifying mechanism is consistent with the frequent observations that many ET substances display a variety of activities (e.g., multiple-drug properties), as well as toxic effects.

It is important to recognize that mode of action in the biodomain is often multifaceted. In addition to the ET-ROS-OS approach, other aspects may pertain, such as, enzyme inhibition, allosteric effects, receptor binding, metabolism and physical factors. A specific example involves protein binding by quinones in which protein nucleophiles, such as amino or thiol, effect conjugate addition."

It is interesting that ASA and dicamba possess related structures and undergo similar metabolism. The unifying modes of action are applicable to both agents in relation to activity and toxicity. The approach is a continuation of prior reports dealing with the unifying mechanism, including the central nervous system (CNS).

Publication Date (Web): October 13, 2015 | doi: 10.1021/bk-2015-1200.ch011

ET-ROS-OS-AO Mechanism for Aspirin

Various reports exist that support the unifying mode of action, as applied to ASA (*2*). "Some of the metabolic pathways have been quite well delineated, such as the first step entailing deacetylation of acetyl salicylic acid by esterase to yield salicylic acid (Fig. 3). Under appropriate conditions, oxidative metabolism gives rise to 2,5-dihydroxy-and 2,3-dihydroxybenzoic acids (Fig. 4 and 5). Quite plausibly, subsequent facile conversion to the o- and p- quinones (Fig. 6 and 7) can set the stage for redox cycling by ET with induction of OS. Alternatively, salicylic acid avidly chelates iron to furnish a complex with potential ET properties. The scenarios are buttressed by evidence for ROS and lipid peroxidation." Redox cycling by quinones is illustrated in Scheme 3.

In Oxidative Stress: Diagnostics, Prevention, and Therapy Volume 2; Hepel, et al.;
ACS Symposium Series; American Chemical Society: Washington, DC, 2015.

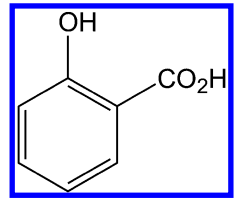

Figure 3. Salicylic acid

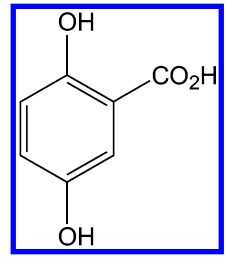

Figure 4. Hydroquinone metabolite of SA

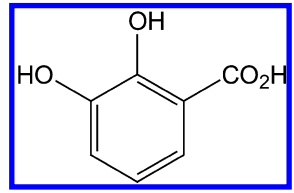

Figure 5. Catechol metabolite of SA

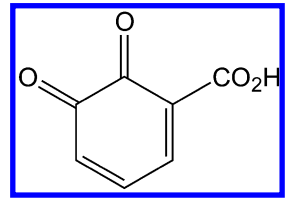

Figure 6. o-Benzoquinone-3-carboxyl

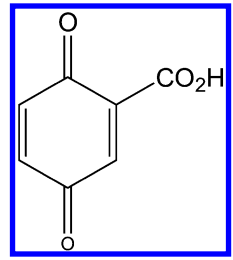

Figure 7. p-Benzoquinone-2-carboxyl

In Oxidative Stress: Diagnostics, Prevention, and Therapy Volume 2; Hepel, et al.;
ACS Symposium Series; American Chemical Society: Washington, DC, 2015.

Publication Date (Web): October 13, 2015 | doi: 10.1021/bk-2015-1200.ch011

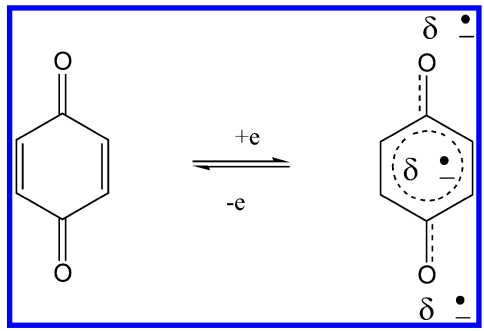

Scheme 3. Redox cycling by p-benzoquinone

Publication Date (Web): October 13, 2015 | doi: 10.1021/bk-2015-1200.ch011

A 2005 report deals with reaction of hydroxyl radicals with SA at the lead dioxide electrode (*15*). The radical is commonly generated in vivo from hydrogen peroxide, serving as an oxidant and hydroxylating agent. In the electrode reaction, the amount of 2,5-dihydroxybenzoic acid is much more than that of 2,3-isomer. Radical substitution reactions are apparently involved. SA induced OS in the form of hydrogen peroxide in root cultures (*16*). In more recent studies, ASA induces OS with associated complications, including mitochondrial dysfunction (*17*). We theorize that the dysfunction may involve ET interference with ET in the mitochondrial chain. Altered GSH redox metabolism plays a crucial role in ASA induced toxicity. Treatment of the cells with the thiol AO N-acetylcysteine attenuated the adverse effects which, we suggest might involve ROS.

SA is not only a metabolite of ASA, but it is also an anti-inflammatory drug (*18*). The metabolite induces formation of thiobarbituric acid reactive substances (TBARS) which is indicative of ROS. Antioxidants suppressed TBARS generation, suggesting involvemnent of ROS. Results indicate that SA induces lipid peroxidation which is related to oxidative metabolism. Findings point to triggering of mitochondrial dysfunction by SA leading to lethal liver cell injury by lipid peroxidation.

AO effects of ASA and SA were examined in rats (*19*). SA reduced OS, and large amounts of ASA are needed to produce an AO effect, apparently via liver generation of AOs. The effects of SA as AO were more intense than for ASA (*20*). ASA reduced OS, but only at high concentration. The AO effect may reflect metabolism to SA which could be the actual AO since phenols are well known AO agents, e.g., vitamin E. SA plays an important role in the cytoprotective effect in brain tissue. A review shows action as AOs and pro-oxidants, depending on condition (*21*).

Commonality Involving COX and ET-ROS-OS Mechansim

There is evidence that drugs that metabolize to phenols can operate by inhibition of COX enzymes which can function as peroxidases (*21*, *22*). In the process, the drug undergoes oxidation in which it functions as an AO, a common property of phenols (*23*), e.g., vitamin E. The phenols can also act as pro-oxidants, which applies to aspirin via metabolism to an ET quinone resulting in generation

of ROS and OS. Oxidation of the drug or metabolites leads to reduction or inhibition of the COX enzymes (*21*, *22*). Previously, the two mechanisms were regarded as separate and diverse pathways. This novel perspective reveals that the two are intimately associated with the COX enzyme acting as a peroxidase oxidant of the drug with conversion to the ET quinone metabolite. This represents an expansion of the unifying feature. There has been extensive literature on COX enzymes. COX appears to play a role in aspirin action.

ASA, CNS and COX

In addition to treatment of this aspect in other sections, some recent literature is presented. ASA impairs ganglion neurons by inducing an increase in superoxide resulting in apoptosis (*24*). After ASA administration, GABA and serotonin mediated neurotransmission in the CNS resulted in hyperactivity. A large amount of the drug produced increased current flow into the auditory cortex. Inhibition of COS produces many of the adverse reactions of NSAIDs, including aspirin, which reduce prostaglandin synthesis in the CNS (*25*).

Aspirin Toxicity

This topic has been reviewed recently (*26*). Salicylate ingestion in excess is a common cause of poisoning in children, which has improved in recent years. The adverse effects are characterized by many symptoms, including hyperventilation, dehydration, hypokalemia, acidosis, nausea, vomiting, diaphoris, tinnitus, vertigo, tachycardia, hyperactivity, agitation, delirium, hallucination, convulsions, lethargy, and stupor. Hyperthermia indicates severe toxicity, especially in children. When used properly, aspirin is not a dangerous drug, and is consumed in vast quantities.

Dicamba Metabolism

A key aspect involves demethylation of the ether resulting in the phenolic groups of the 2,5-dichloro SA derivative (Fig. 8) (*27*, *28*). Mechanistically, there are two possible routes for the transformation. One comprises hydrolysis which is depicted in Scheme 4. The other consists of radical oxidation that entails a hemiacetal metabolite in Scheme 5. Subsequent oxidation would lead to the hydroquinone (Fig. 9) and p-benzoquinone (Fig. 10) derivatives.

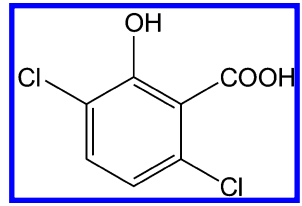

Figure 8. 2,5-Dichlorosalicylic acid

In Oxidative Stress: Diagnostics, Prevention, and Therapy Volume 2; Hepel, et al.;
ACS Symposium Series; American Chemical Society: Washington, DC, 2015.

Publication Date (Web): October 13, 2015 | doi: 10.1021/bk-2015-1200.ch011

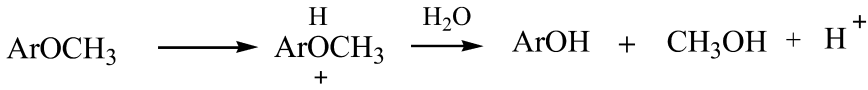

Scheme 4. Acid catalyzed hydrolytic demethylation of $ArOCH_3$

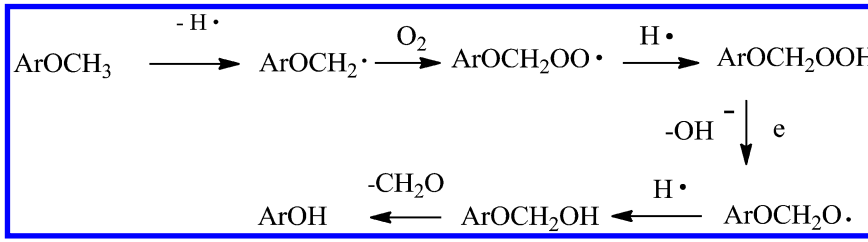

Scheme 5. Oxidative radical demethylation of $ArOCH_3$

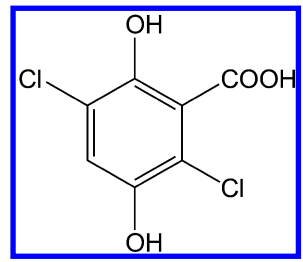

Figure 9. Hydroquinone derivative of Dicamba

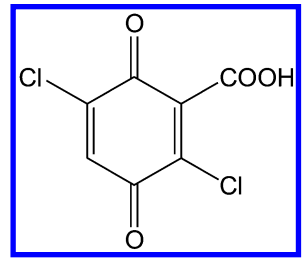

Figure 10. p-Benzoquinone-2-carboxyl-3,6-dichloro

Dicamba Toxicity

Data reveal that the herbicide is moderately to slightly toxic (*29*), In female, pregnant rabbits there was slightly reduced fetal weight and increased loss of fetuses. With dogs, some enlargement of liver cells occurred, but not in humans. Dicamba was found to be slightly toxic to cold water fish.

Publication Date (Web): October 13, 2015 | doi: 10.1021/bk-2015-1200.ch011

Unifying Mechanism of Herbicide Toxicity

The mode of toxicity described for dicamba fits into a broader scenario that has been proposed for other members of this general class involving the CNS (*30*). The bipyridyl herbicides, paraquat (Fig. 11) and diquat (Fig. 12), belong to this class for which the mode of action has been well established, in line with ET-ROS-OS. Extensive evidence supports redox cycling with formation of superoxide and other ROS, as illustrated in Scheme 1 and 2. It is well documented that ROS play a significant role in toxicity. The agents are conjugated iminiums which belong to the ET class (see Introduction).

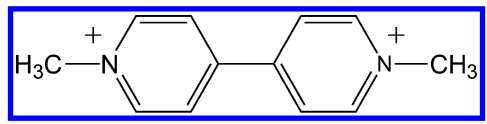

Figure 11. Paraquat

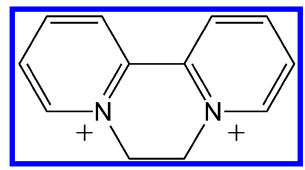

Figure 12. Diquat

The diphenylether herbicide, e.g., oxylluorfen (Fig. 13) and fluorodifen (Fig. 14), also fit the unifying theme since they are ET agents of the $ArNO_2$ type (see Introduction). In the case of oxyfluorfen, the structure also contains an ethyl ether group capable of dealkylation to a phenol, with potential for subsequent ET quinone formation via diol (see Introduction). This class appears to act by generating various ROS, resulting in lipid peroxidation and other oxidative damage. Another factor may involve ET during enzyme inhibition in the mitochondrial ET chain.

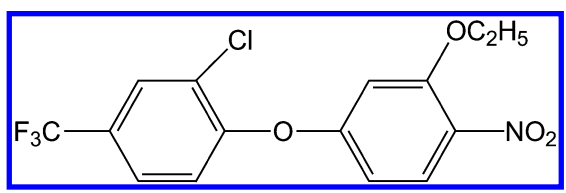

Figure 13. Oxyfluorfen

In Oxidative Stress: Diagnostics, Prevention, and Therapy Volume 2; Hepel, et al.;
ACS Symposium Series; American Chemical Society: Washington, DC, 2015.

Publication Date (Web): October 13, 2015 | doi: 10.1021/bk-2015-1200.ch011

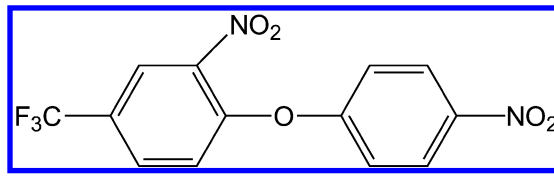

Figure 14. Fluorodifen

About 50% of the herbicide groups operate by inhibition of ET chains, in accord with the unifying theory, including diuron and atrazine. The process involves increased lipid peroxidation which may be caused by singlet oxygen.

Commonality of Aspirin and Dicamba

There are pronounced structural similarities. Both are benzoic acid and phenolic derivatives. In metabolism, salicylic acid or the dichloro derivative are the principal metabolites produced. The two agents are alike in displaying slight to moderate toxicity in humans and other animals. The differences can be attributed to effect of chlorine, different receptors, and different sites of action.

Other Analgesics and Related Drugs

Drugs that belong in this class include benzodiazepines (tranquilizers), phenobarbital (sedative painkiller), phenytoin (anti-epilepsy), and morphine and heroin (analgesics) which are treated in more details in the acetaminophen chapter.

Abbreviations

ET= electron transfer; ROS= Reactive oxygen species; OS= oxidative stress; AO= antioxidant; ASA= acetyl salicylic acid (aspirin); SA= salicylic acid; CNS= central nervous system

Acknowledgments

Editorial assistance by Thelma Chavez is acknowledged.

References

1. Kovacic, P.; Somanathan, R. *Curr. Bioact. Compd.* **2010**, *6*, 46–59.
2. Kovacic, P.; Becvar, L. E. *Curr. Pharm. Des* **2000**, *6*, 143–167.
3. Kovacic, P.; Osuna, J. A. *Curr. Pharm. Des.* **2000**, *6*, 277–309.
4. Kovacic, P.; Jacintho, J. D. *Curr. Med. Chem.* **2001**, *8*, 773–796.
5. Kovacic, P.; Jacintho, J. D. *Curr. Med. Chem.* **2001**, *8*, 863–892.
6. Kovacic, P.; Sacman, A.; Wu-Weis, M. *Curr. Med. Chem.* **2002**, *9*, 823–847.

Publication Date (Web): October 13, 2015 | doi: 10.1021/bk-2015-1200.ch011

7. Poli, G.; Cheeseman, K. H.; Dianzani, M. U.; Slater, T.F. *Free Radicals in the Pathogenesis of Liver Injury*; Pergamon: New York, 1989; pp 1−330.
8. Kovacic, P.; Thurn, L. A. *Curr. Vasc. Pharmacol.* **2005**, *3*, 107–117.
9. Kovacic, P.; Somanathan, R. *Curr. Med. Chem.* **2005**, *5*, 2601–2623.
10. Kovacic, P.; Pozos, R. S.; Somanathan, R.; Shangari, R.; O'Brien, P. J. *Curr. Med. Chem.* **2005**, *5*, 2601–2623.
11. Kovacic, P.; Cooksy, A. L. *Med. Hypotheses* **2005**, *64*, 357–367.
12. Kovacic, P.; Somanathan, R. In *Reviews of Environmental Contamination and Toxicology*; Whitacre, D. E., Ed.; Springer: New York, 2009; Vol. 201, pp 41−69.
13. Kovacic, P.; Somanathan, R. *Med. Hypotheses* **2008**, *70*, 914–923.
14. Halliwell, B.; Gutteridge, J. M. C. *Free Radicals in Biology and Medicine*; Oxford University Press: New York, 1999; pp1−897.
15. Ai, S.; Wang, Q; Li, H.; Jin, L. *J. Electroanal. Chem.* **2005**, *578*, 223–229; DOI:10.1016/j.jelechem.2005.01.002.
16. Ali, M. B.; Hahn, E.-J.; Paek, K.-Y. *Molecules* **2007**, *12*, 607–621.
17. Raza, H.; John, A. *PLOS ONE* **2012**; DOI: 10.137/journal.pone.0036325.
18. Hirokazu, D.; Toshiharu, H. *Chem.-Biol. Interact.* **2010**, *183*, 363–368.
19. Guerrero, A.; González-Correa, J. A.; Muńoz-Marìn, J.; Sánchez-De La Cuesta, F.; De La Cruz, J. P. *Neurosci. Lett.* **2004**, *358*, 153–156.
20. De La Cruz, J. P.; Guerrero, A.; González-Correa, J. A.; Arrebola, M. M.; Sánchez-De La Cuesta, F. *J. Neurosci. Res.* **2004**, *75*, 280–290.
21. Kovacic, P.; Somanathan, R. In *Frontires in Antioxidants Research*; Panglossi, H. V., Ed.; Nova: New York, 2006; Chapter 1, pp 1−38.
22. Davies, M. J.; Day, R. O.; Mohamudally, A.; Scott, K. F. *Inflammopharmacology* **2013**, *21*, 201–232.
23. Vane, J. R., Botting, J. H., Eds. In *Selective COX-2 inhibitors: Pharmacology, Clinical Effects and Therapeutic Potential*; Kluwar Academic: 1998, pp 1−150.
24. Sheppard, A.; Hayes, S. H.; Chen, G. D.; Ralli, M.; Salvi, R. *Acta Otorhinolaryngol. Ital.* **2014**, *34*, 79–93.
25. Bovill, J. G. *Eur. J. Anesthesiol.* **1997**, *15*, 9–15.
26. Waseem, M. *Medscape: Drugs, Diseases and Procedures*; Corden, T. E., Ed.; March 15, 2013.
27. Gu, J.-G.; Han, B.; Duan, S. *Int. Biodeterior. Biodegrad.* **2008**, *62*, 455–459.
28. Lin, C.; Gu, J.-G.; Qiao, C.; Duan, S.; Gu, J.-D. *Biol. Fertility Soil* **2006**, *42*, 395–401.
29. *Wikipedia*, Aug. 2014.
30. Halliwell, B.; Gutteridge, J. M. C. *Free Radicals in Biology and Medicine*; Oxford University Press: New York, 2000; pp 510−514.

Publication Date (Web): October 13, 2015 | doi: 10.1021/bk-2015-1200.ch011

Publication Date (Web): October 13, 2015 | doi: 10.1021/bk-2015-1200.ch012

Chapter 12

DNA Damage by Highly Oxidizing Environmental Pollutants

Anna M. Nowicka,[1,2,*] Agata Kowalczyk,[1,2] Edyta Matysiak,[2] and Maria Hepel[1,*]

[1]Department of Chemistry, State University of New York at Potsdam, Potsdam, New York 13676, United States
[2]Faculty of Chemistry, University of Warsaw, ul. Pasteura 1, PL 02-093 Warsaw, Poland
[*]E-mail: anowicka@chem.uw.edu.pl, hepelmr@potsdam.edu

Chromium(VI) compounds are strongly oxidizing carcinogenic pollutants causing severe DNA damage including strand brakes, oxidation of nitrogen bases, and others. The chromium genotoxicity involves a multitude of mechanisms associated with the reduction of Cr(VI) to Cr(III). This reduction is considered to be essential for DNA damage and thus the potentiation of carcinogenesis. Since Cr(VI) can be reduced to Cr(III) by antioxidants: glutathione (GSH), cysteine, or ascorbic acid (AA), and these antioxidants are known to otherwise prevent the oxidative stress-related cellular damage, it is intriguing to assess the role of these anti-oxidants in Cr(VI) effects on DNA. Therefore, in this work, we have investigated in detail the interactions of different Cr species with double-stranded DNA using electrochemical quartz crystal nanogravimetry (EQCN), linear scan voltammetry (LSV), AFM, and UV-Vis spectroscopy. The binding constant determined from EQCN measurements and Scatchard plot analysis for DNA-Cr associates were found to be: 626 ± 52 M^{-1} for DNA-Cr(VI) and $(9.60 \pm 0.90)\times10^3$ M^{-1} for DNA-Cr(III), with clear dominance of Cr(III) binding by DNA. The binding parameters determined were compared with the literature FTIR data. On the other hand, damages to DNA were caused by Cr(VI) and Cr(V). The observed effects have been evaluated in

In Oxidative Stress: Diagnostics, Prevention, and Therapy Volume 2; Hepel, et al.; ACS Symposium Series; American Chemical Society: Washington, DC, 2015.

Publication Date (Web): October 13, 2015 | doi: 10.1021/bk-2015-1200.ch012

view of Cr species influence on DNA interactions with model chemotherapeutic drug mitoxatrone studied earlier.

Introduction

Chromium compounds have long been recognised as the major carcinoges causing DNA damage, such as the strands breaks and oxidation of nitrogen bases. Chromium occurs in natural samples in two main valence states as Cr(III) and Cr(VI). These two environmentally relevant valence states of chromium have a contrasting impact on environment and health. Cr(VI) exerts mutagenic effects in most short-term mutagenicity test performed, whereas Cr(III) does not (*1*, *2*). The chromium genotoxicity involves a multiplicity of mechanisms associated with the reduction of Cr(VI) to Cr(III). This reduction of Cr(VI) to a lower valence is considered to be essential for DNA damage and thus the potentiation of carcinogenesis. Cr(VI) can be reduced by gluthatione (GSH), cysteine, or ascorbic acid (AA) into Cr(III) (*3*) which reacts with DNA to form Cr(III)-DNA adducts (*4–6*). Because Cr(III) is a final form of chromium within the cell, the interaction of Cr(III) with DNA my play crucial role in the carcinogenic action of Cr(VI) salts.

The mechanism of the Cr(VI) reduction has broadly been discussed in the literature (*7–10*). The first step of Cr(VI) reduction proceeds via one-electron and one-proton process to pentavalent chromium. At neutral pH in aqueous solution, Cr(V) rapidly disproportionates through a bimolecular mechanism producing Cr(VI) and reactive Cr(IV) intermediates (*11*) (see: Scheme 1), ultimately resulting in the final redox proportions of two Cr(VI) and one Cr(III) per three Cr(V). However, at more acidic pH's, disproportionation of this species is minimal and decomposition is slow and attributed to ligand oxidation. It is known that Cr(V) is considered by many to play a major role in the induction of cancer by the genotoxic and carcinogenic form of chromium, chromium (VI).

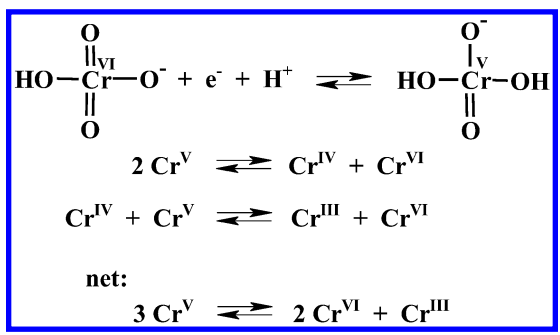

Scheme 1. Reduction mechanism of Cr(VI).

Because oxidation reactions of Cr(V) and (VI) with biological molecules, such as DNA, are likely to be important in the mechanism of Cr(VI) carcinogenesis, we have used electrochemical quartz crystal nanobalance (EQCN), UV-Vis spectroscopy, and linear voltammetry to investigate the interactions of Cr species

In Oxidative Stress: Diagnostics, Prevention, and Therapy Volume 2; Hepel, et al.;
ACS Symposium Series; American Chemical Society: Washington, DC, 2015.

with DNA. The observed effects are evaluated in view of Cr species influence on DNA interactions with model chemotherapeutic drug mitoxatrone studied earlier (*6*).

Experimental

Chemicals

The Cr(VI) source was K_2CrO_4, the Cr(III) source was $Cr(NO_3)_3 \cdot 9H_2O$. Ascorbic acid (AA) and disodium ethylenediamine tetraacetate (EDTA) were obtained from Sigma. The pK_a of ascorbic acid is 4.2, thus in 0.02 M PBS buffer (pH 7.4) AA exists as the ascorbate monoanion (*12*). Poly(allylamine hydrochloride) (PAH) was purchased from Fisher. The pK_a of PAH is 8.5, thus in 0.02 M PBS buffer (pH 7.4) PAH exist as the polycation (*13*). Calf thymus double stranded DNA (dsDNA) was purchased from Sigma. Only those dsDNA shipments were accepted for the measurements which gave the ratio of the DNA absorbances at λ = 260 and λ = 280 in the range 1.7 ÷ 2.0, and the ratio of the absorbances at λ = 260 and λ = 250 in the range 1.4 ÷ 1.7 (*14*). These absorbance ranges are a good criterion for the DNA purity, including the absence of protein. In fact, our ctDNA samples gave the absorbance ratio in the middle of the indicated ranges. The ctDNA solutions of 1 mg DNA per 1 mL of phosphate buffer (pH ≅ 7.4) were prepared at least 24 hours before experiments. The ctDNA concentration was determined from the value of the absorbance at λ = 260 nm; ε = 13,200 $M^{-1}cm^{-1}$ (*15*).

Instrumentation

UV-Vis spectra were recorded on Varian model 50 Bio spectrophotometer equipped with a quartz micro-colorimetric vessel of 1 cm path length. The spectra were recorded one hour after preparing the solutions. Linear voltammetry studies were performed by potentiostat Elchema model PS-1705. Voltammetric experiments were carried out in the three- electrode system: platinum wire - counter electrode, reference electrode (Ag/AgCl) and glassy carbon disc electrode (GCDE) of 3 mm in diameter as the working electrode. The working glassy carbon disc electrode was polished before each measurement with 0.3 and, at the end, 0.05 μm Al_2O_3 powders on a wet pad. After polishing, the aluminum oxide was removed by rinsing the electrode surface with a direct stream of ultrapure water (Mili-Q, Milipore, Billerica, MA, USA; conductivity of 0.056 μS/cm). During the voltammetric experiments, the electrochemical cell was kept in a Faraday cage to minimize the electrical noise. Finally, before experiments all analyzed solutions were deoxygenated with pure argon for 15 minutes. An electrochemical quartz crystal nanobalance model EQCN-700 (Elchema, Potsdam, NY) with 10 MHz AT-cut quartz crystal resonators was used in this study. The EQCN technique allowed us for simultaneous monitoring of voltamperometirc and nanogravimetric characteristics. The resonant frequency of the quartz crystal lattice vibrations in a thin quartz crystal wafer was measured as a function of the mass attached to the crystal interfaces. For thin rigid films, the interfacial mass changes $\triangle m$ are related

Publication Date (Web): October 13, 2015 | doi: 10.1021/bk-2015-1200.ch012

to the shift in series resonance oscillation frequency Δf of the EQCN through the Sauerbrey equation (*16*, *17*):

$$\Delta f = \frac{2\Delta m n f_0^2}{A\sqrt{\mu_q \rho_q}} \quad (1)$$

where f_0 is oscillation frequency in the fundamental mode, n is the overtone number, A is the piezoelectically active surface area, ρ_q is the density of quartz (ρ_q = 2.648 g cm^{-3}), and μ_q is the shear modulus of quartz ($\mu_q = 2.947\times10^{11}$ g cm^{-1}s^{-2}). The oscillator was tuned to the resonance frequency of working piezoelectrodes to minimize effects due to energy dissipation in protein films. All experimental variables influencing the resonant frequency (*17*) of the EQCN electrodes such as the temperature, pressure, viscosity and density of the solution, were kept constant in the apparent mass change measurements. The piezoelectrically active (geometrical) surface area of the working Au electrode was 0.196 cm^2 and the real surface area A = 0.255 cm^2 (roughness factor R = 1.3). A 200 nm thick Au film was deposited on a 14-mm diameter, 0.166-mm thick, AT-cut quartz resonator wafer with vacuum evaporated Ti adhesion interlayer (20 nm thick). The real surface area was determined for Au-EQCN electrodes by a standard monolayer oxide formation procedure (*18*). The resonator crystals were sealed to the side opening in a glass vessel of 50 mL capacity using high purity siloxane glue with intermediate viscosity (Elchema SS-431). The seal was cured for 24 h at room temperature. The working electrode was polarized using Pt wire counter electrode and its potential measured versus double-junction Ag/AgCl electrode.

Publication Date (Web): October 13, 2015 | doi: 10.1021/bk-2015-1200.ch012

Immobilization of DNA on Electrodes

The Au-piezoelectrode surface was cleaned by cycling in 0.1 M H_2SO_4 in the range 0 to +1.5 V until stable voltammogram was recorded, followed by immersing in piranha etching solution (30 % H_2O_2 : H_2SO_4 = 1 : 3) for 10 s, and rinsing with distilled water. The accumulation *Calf Thymus* double stranded DNA (ctDNA) on the gold electrode surface was done by adsorption at a constant potential. A freshly cleaned Au-EQCN electrode was immersed in DNA solution (4 μM) for 30 min. Since the DNA molecules are negatively charged in pH 7.0 (*19*), the immobilization of DNA on Au-EQCN surface was performed by holding the potential of the electrode at a constant positive value of E = +80 mV for 30 min. After that time the frequency change stabilized.

The ctDNA was also adsorbed on a GCDE surface from 4 μM DNA solution by applying the potential E = +200 mV for 20 min, then the electrode (GCDE/ctDNA) was rinsed with distilled water and kept in PBS buffer. In tests for DNA damage with Cr species, the electrode was treated in a solution containing Cr species on different oxidation state for 15 min, unless otherwise stated. After that, the electrode was rinsed with distilled water and immersed in pure 0.02 M PBS buffer. Fresh film of ctDNA was prepared before each experiment.

The ctDNA was also immobilized on a poly(allylamine hydrochloride) (PAH) film on Au. The Au/PAH films were formed by injection of 30 mL of 3 mg/mL PAH solution in 0.5 M NaCl (pH 5). In 3 mg/mL PAH aqueous solution, PAH

exists in the form of a polycation. By applying the potential E = –50 mV for 1 hour, the PAH film was formed on the gold electrode surface. Then, the electrode and cell were slowly rinsed with distilled water and DNA was adsorbed from a 20 mM PBS buffer (pH 7.4) containing ctDNA (100 μM bp (base pairs)) under the bias potential E = +50 mV for 1 h. Finally, such a modified electrode was ready for testing the DNA interactions with Cr species. The procedure for preparation of Au/PAH/ctDNA modified electrode is illustrated in Figure 1.

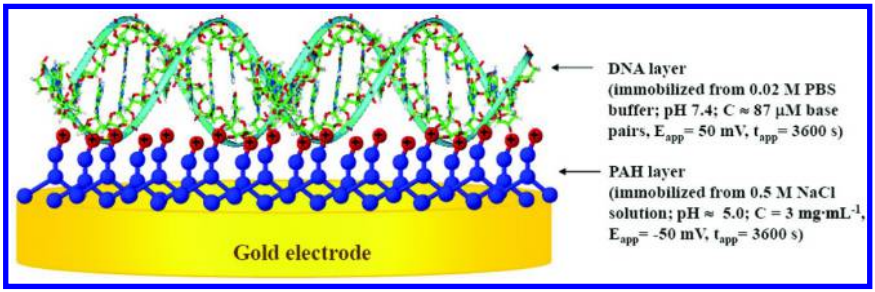

Figure 1. Scheme of preparing of the gold electrode to the EQCN measurements. (see color insert)

Atomic Force Microscopy (AFM) Measurements

Atomic force microscopy experiments were performed with a 5500 AFM instrument (Agilent Technologies, Santa Clara, CA, USA). Magnetic AC mode was used for imaging, and the data were obtained in the Fenton solution. Type VI MAC levers (Agilent Technologies, Santa Clara, CA, USA) were used for imaging. The typical resonance frequency of the cantilevers was 50 ÷ 60 kHz in air and it was reduced to 18 ÷ 24 kHz in the solution. The images were acquired at 20 °C. A small gold bead prepared by Clavilier method was utilized as a substrate (*20*). The bead was spot welded to gold foil and atomically flat (111) facets were used for image acquisition. The substrate as well as the teflon parts of the liquid cell were cleaned in piranha solution (concentrated H_2SO_4 / 30 % hydrogen peroxide 3:1) and thoroughly rinsed with Milli-Q water. *(CAUTION: piranha solution reacts violently with organics and should be handled with extreme care)*. Gold bead was flame-annealed and quenched in Milli-Q water before each experiment. The root-mean-square (RMS) surface roughness for DNA films was determined for 1×1 μm^2 images using Pico Image Basic software provided with 5500 AFM instrument.

Data Analysis

The binding parameters for the ctDNA interactions with Cr species were obtained for 20 mM PBS buffer (pH 7.4) which is close to the physiological pH. A useful tool to determine these parameters, regardless of the technique used, is the polymer model of McGhee and von Hippel (*21*). The following formula describes the interactions between the dsDNA strand and the ligand:

In Oxidative Stress: Diagnostics, Prevention, and Therapy Volume 2; Hepel, et al.;
ACS Symposium Series; American Chemical Society: Washington, DC, 2015.

Publication Date (Web): October 13, 2015 | doi: 10.1021/bk-2015-1200.ch012

$$\frac{r}{C_f} = K(1-nr)\left[\frac{1-nr}{1-(n-1)r}\right]^{n-1} \quad (2)$$

where K is the binding constant, n is the number of binding matrix units that are occupied by one molecule of the ligand, and $r = C_b/C_{\text{matrix unit}}$, where $C_b = C_0 - C_f$, C_b is the concentration of the ligand molecules bound to dsDNA, C_0 is the total concentration of the ligand, C_f is the concentration of the free molecules of the ligand in the solution, and $C_{\text{matrix unit}}$ is the analytical concentration of the binding unit in dsDNA. The assumptions of the model fit very well the experimental reality. The lattice is assumed to be homogeneous, is taken as a linear array of many repeating units, and the basic lattice residue corresponds to a nucleic acid base-pair. A ligand molecule is assumed to bind to the lattice and to cover n consecutive lattice residues. The occupied residue is inaccessible to another ligand. To determine K and n the concentrations of unbound and bound ligand should be known and then the Scatchard plot ($r/C_f = f(r)$) should be drawn. The extraction of K and n values has been done by the least-square fitting of equation (2) to the experimental data.

Results and Discussion

In the reactions with ctDNA, Cr(VI) creates a number of putative lesions including inter- and intra-strand cross-linked adducts, DNA-protein cross-links, DNA strand breaks, a basic sites, and oxidized nucleic acid bases (*22–24*). Oxidative damage and the formation of oxidized lesions in DNA is considered one of the critical steps in the induction of carcinogenesis by Cr(VI). Oxidation of DNA can occur at the deoxyribose sugar creating DNA strand breaks or at the nucleic acid bases creating oxidized base lesions (*25*, *26*). In this ongoing study we have investigated the effects of Cr species on the interactions of a model chemotherapeutic drug mitoxantrone with DNA (*6*) and, in this work, we present results of our investigations on direct interactions of variable chromium species with DNA in solution, as well as with DNA immobilized on an electrode surface.

Effects of Chromium Species on ctDNA in Solution

The UV-Vis spectroscopic measurements of ctDNA dissolved in 20 mM phosphate buffer solutions (pH 7.4), in the presence of Cr(VI) and Cr(III), were performed to compare the effects of chromium species. The results are presented in Figure 2.

Publication Date (Web): October 13, 2015 | doi: 10.1021/bk-2015-1200.ch012

Publication Date (Web): October 13, 2015 | doi: 10.1021/bk-2015-1200.ch012

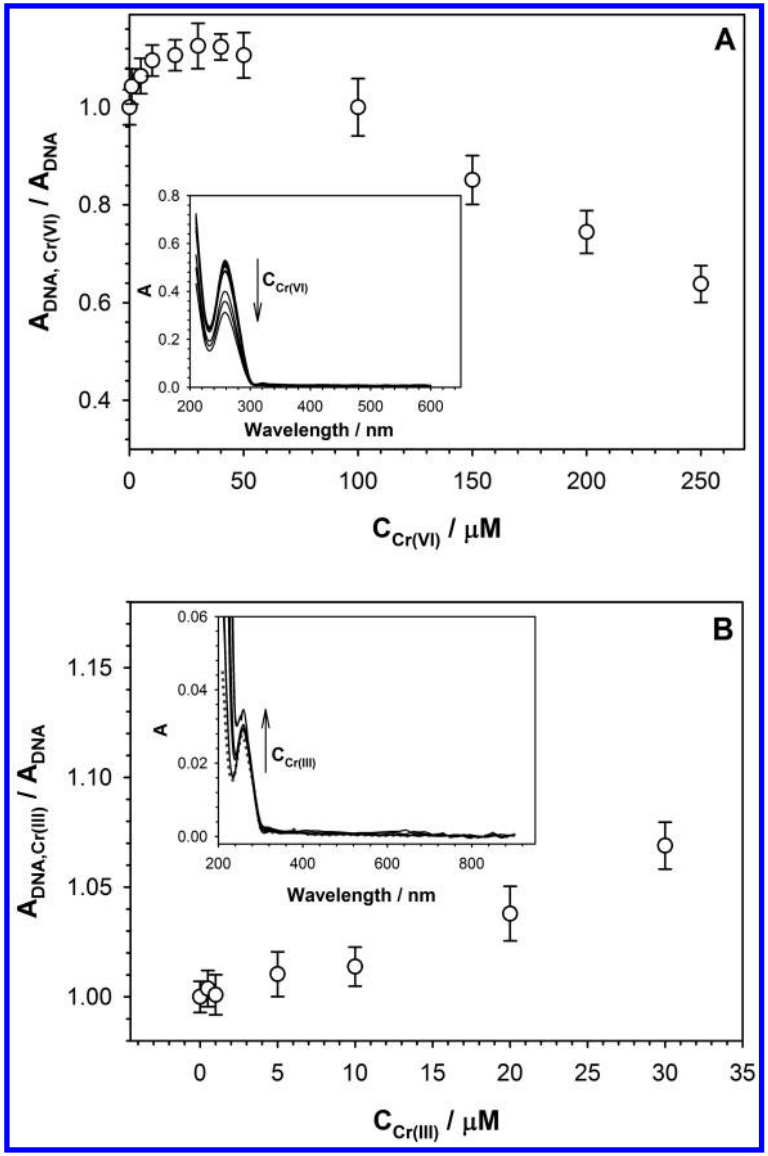

Figure 2. Dependence of the normalized DNA absorbance versus concentration of Cr(VI) (A) and Cr(III) (B). ctDNA concentration: 38.87 μM base pairs and 2.2 μM base pairs for Cr(VI) and Cr(III) experiments respectively. Data obtained one hour after preparing of the mixture. Insets: Background subtracted DNA UV-Vis spectra; pure ctDNA solution - dotted line.

The data were taken using the following procedure. After each addition of the chromium to the DNA solution, the mixture was stabilized for 1 h and the spectra were recorded. The absorbance changes observed after interactions of ctDNA with Cr(VI) and Cr(III) species were measured at λ = 260 nm. The reason for using small amounts of DNA in experiments with Cr(III) was the low solubility of Cr(III) in PBS buffer. The UV-Vis spectra obtained for solutions containing DNA with different concentrations of Cr(VI) have shown that the DNA absorbance initially increases (for $C_{Cr(VI)} < 50$ μM) and then decreases for Cr(VI) concentrations significantly higher than the DNA concentration. This means that the addition of Cr(VI) leads to the changes in DNA structure. In contrast to this, the addition of Cr(III) does not change the DNA absorbance.

Similar experiments have also been performed using the electrochemical LSV technique. An inspection of LSV characteristics for the guanine oxidation current changes during Cr(VI) titration of a ctDNA solution leads to the conclusion that Cr(VI) is causing considerable damage to the DNA. As seen in Figure 3, the addition of Cr(VI) results in diminished guanine oxidation current.

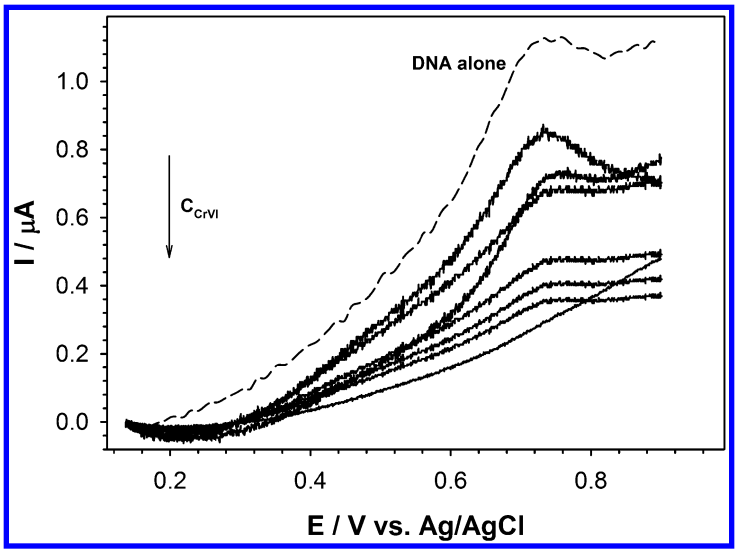

Figure 3. Background subtracted ctDNA voltammograms recorded in 0.02 M PBS solution for a bare glassy carbon disc electrode (GCDE) in the presence of Cr(VI). ctDNA was in the soluble state at the concentration 7.4 μM bp. Aliquots of Cr(VI) were added to the same solution. Data were obtained 15 minutes after each addition of Cr(VI); scan rate v = 100 mV/s.

This means that Cr(VI) causes a pronounced loss in the electrochemical activity of the participating guanine molecules. A major lesion formed in a DNA duplex by the attack of Cr(VI) consists of a 7,8-dihydro-8-oxoguanine (8-oxoG) which is formed by the oxidation of a guanine residue.

To check the influence of intermediate valence states of chromium on ctDNA, experiments *in* situ reduction of Cr(VI) by ascorbic acid were carried out. It is known (*27*) that the reduction of Cr(VI) with a 10-fold molar excess of ascorbate initially leads to a transient Cr(IV) species and the oxidized form of ascorbate, dehydroascorbate (DHA), followed by the second reduction reaction of Cr(IV) with AA to give rise to the acsorbyl radical, $AA^{\bullet-}$, and a kinetically inert Cr(III) species:

$$Cr(VI) + AA \rightarrow Cr(IV) + DHA \quad (3)$$

$$Cr(IV) + AA \rightarrow Cr(III) + AA^{\bullet-} \quad (4)$$

By decreasing of the AA concentration with respect to Cr(VI) concentration, to a ratio of 1:1, the time needed to reduce Cr(VI) to Cr(III) becomes longer than that for the excess of AA. During this prolonged reduction time, the intermediate valence states of chromium dominate. In the presence of ctDNA, the guanine oxidation process in DNA by Cr(VI) takes also place. The sequential one-electron oxidation of guanine in DNA by Cr(VI) in the presence of AA leads to the formation of a product spiroiminodihydantoin (Sp) (*27*). The possible mechanism of one-electron oxidation of guanine by Cr(VI) is shown in Scheme 2.

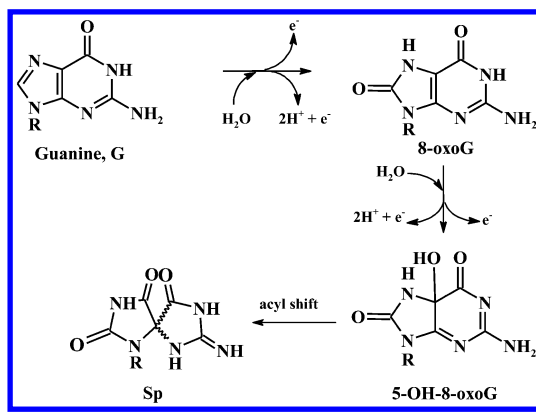

Scheme 2. Possible mechanism of one-electron oxidation of guanine by Cr(VI).

The Cr(VI) reduction by addition of AA was spectroscopically controlled by measuring the absorbance at 372 nm. The experiments were performed in the absence and in the presence of ctDNA in the solution. The ctDNA concentration was very similar to this adsorbed at the PAH layer or at the GCDE electrode (*ca.* 25.5 pmol bp/cm^2). Obtained results are presented in Figure 4.

In Oxidative Stress: Diagnostics, Prevention, and Therapy Volume 2; Hepel, et al.;
ACS Symposium Series; American Chemical Society: Washington, DC, 2015.

Publication Date (Web): October 13, 2015 | doi: 10.1021/bk-2015-1200.ch012

Publication Date (Web): October 13, 2015 | doi: 10.1021/bk-2015-1200.ch012

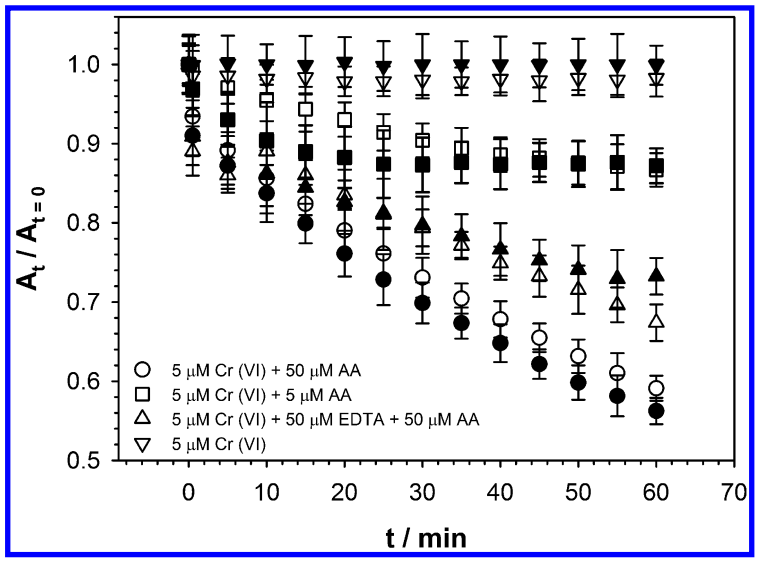

Figure 4. Effect of additions of AA and AA + EDTA on the absorbance of Cr(VI) at 372 nm. Open symbols correspond to the solutions with ctDNA, filled symbols correspond to the solutions without ctDNA.

The results in Figure 4 show that the efficiency of the Cr(VI) reduction by ascorbic acid is different in the absence and in the presence of ctDNA in the solution. In the presence of ctDNA, the reduction process of Cr(VI) by AA competes with the Cr(VI) binding reaction with ctDNA. The Cr(VI) bound to ctDNA is more resistant for the influence of AA.

ctDNA Immobilized on a Glassy Carbon Disc Electrode (GCDE)

The accumulation of ctDNA on the electrode surface was carried out by adsorption at a constant potential. The freshly polished glassy carbon electrode was immersed in a ctDNA solution (100 μM base pairs). Since the ctDNA molecules are negatively charged in 0.02 M phosphate buffer solution (pH 7.4) (*19*), the immobilization of ctDNA on the glassy carbon surface was performed by holding the potential of the electrode at a constant positive value of +200 mV for 20 min. Fresh film of ctDNA was prepared before each measurements. The influence of the presence of Cr(VI) on ctDNA electrochemistry is presented in Figure 5.

The increase of guanine oxidation current can be explained by unwinding of DNA double helix as a results of oxidation of nucleic bases by Cr(VI).

We also checked the influence of variable valence states of chromium for guanine oxidation process. The results are presented in Figure 6. The strongest effect (decrease of the guanine oxidation current) was observed after immersing the modified electrode (GCDE/ctDNA) to the Cr(III) solution. The reason of this

decrease is the attachment of Cr(III) by hydrogen bonding to N7-G. The behavior of Cr(III) versus DNA created in the reaction of Cr(VI) with the excess of AA is different. This effect can be explained by different coordination of Cr(III). The coordination of the final Cr(III) products varied with the concentration of AA in the solution.

EQCN Measurements of ctDNA-Chromium Binding

The interactions of chromium species with ctDNA were studied by applying the EQCN technique (Figure 7). The maximum binding of chromium to DNA was observed for a 1 : 1 reaction ratio of Cr(VI) to AA. This effect confirmed that intermediate valence states of chromium (Cr(V) and/or Cr(IV)) are more likely to react with ctDNA than Cr(III). At 10 : 1 ascorbic acid to Cr(VI) concentration ratio, the binding levels dropped significantly. Also, incubation of Cr (III) with AA resulted in low ctDNA-Cr binding, compared to the situation without AA. Similar behavior was observed for the mixture: 5 μM Cr(VI) + 5 μM AA + 50 μM mannitol compared to 1 : 1 ratio of Cr(VI) to AA. The decrease of the mass of Cr(V) bound to DNA can be explained by the reaction of Cr(V) with mannitol.

Publication Date (Web): October 13, 2015 | doi: 10.1021/bk-2015-1200.ch012

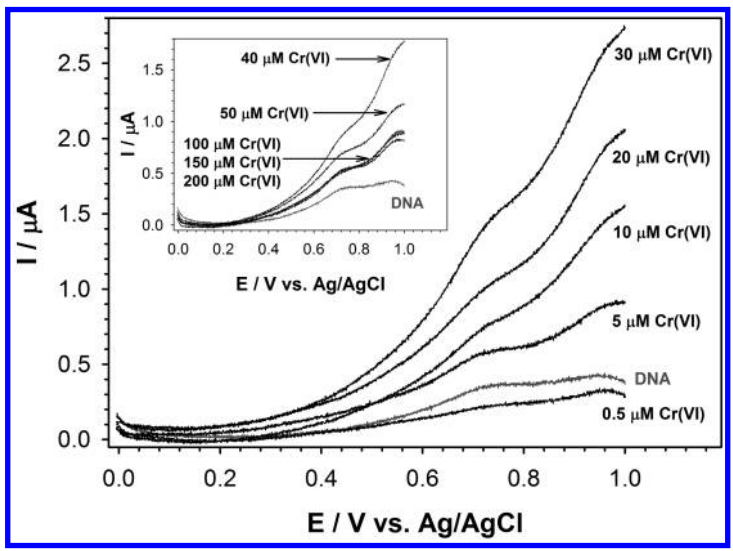

Figure 5. Background subtracted ctDNA voltammograms, recorded in pure 0.02 M PBS, for a ctDNA-modified glassy carbon disc electrode (GCDE/ctDNA), after 15 min treatment in solutions of Cr(VI). Fresh film of ctDNA was prepared before each experiment. Experimental conditions: scan rate v = 50 mV/s; the solution was degassed 20 min. before each measurement.

Publication Date (Web): October 13, 2015 | doi: 10.1021/bk-2015-1200.ch012

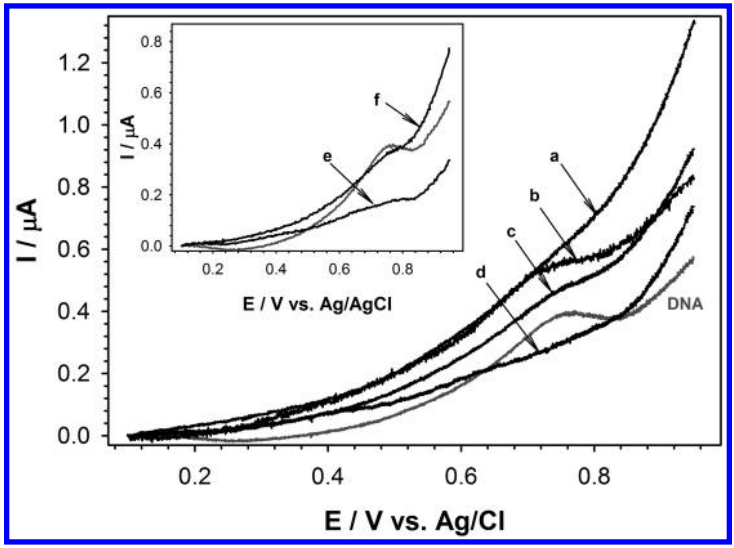

Figure 6. Background subtracted voltammograms for ctDNA adsorbed on a GCDE at E = 0.2 V, after 15 min treatment in: (a) 5 µM Cr(VI) + 50 M AA; (b) 5 µM Cr(VI); (c) 5 µM Cr(VI) + 50 µM EDTA + 50 µM AA; (d) 5 M Cr(VI) + 5 µM AA; (e) 5 µM Cr(III); (f) 5 µM Cr(III) + 50 µM AA, followed by washing and immersing in pure 0.02 M PBS buffer (pH 7.4); v = 50 mV/s; AA: ascorbic acid.

These experiments showed that the ability of Cr(III) to bind ctDNA is dependent on the Cr(III) coordination. Also, the Cr(III) complexes resulting from reactions of Cr(III) with AA are not necessarily the same as those formed in the reduction of Cr(VI) by AA.

The binding parameters of the interactions of the Cr(III) and Cr(VI) with DNA were also determined. To achieve this goal, the titration of the surface bound ctDNA (Au/PAH/ctDNA) with increasing concentrations of the chromium species in the solution was performed. The obtained results are presented in Figures 8 and 9.

The binding parameters: binding constant (K) and binding site size (n), were extracted by least-square fitting of equation (2) to the data in Scatchard plots presented in Figure 10. The binding constants for interactions of dsDNA with Cr(III) and Cr(VI) species determined from EQCN measurements were compared with the literature FTIR data (*5*), presented in Table 1. The difference between those data and ours may be related to the fact that the infrared spectral measurements do not provide any signals for base pairs not bound to the chromium.

Publication Date (Web): October 13, 2015 | doi: 10.1021/bk-2015-1200.ch012

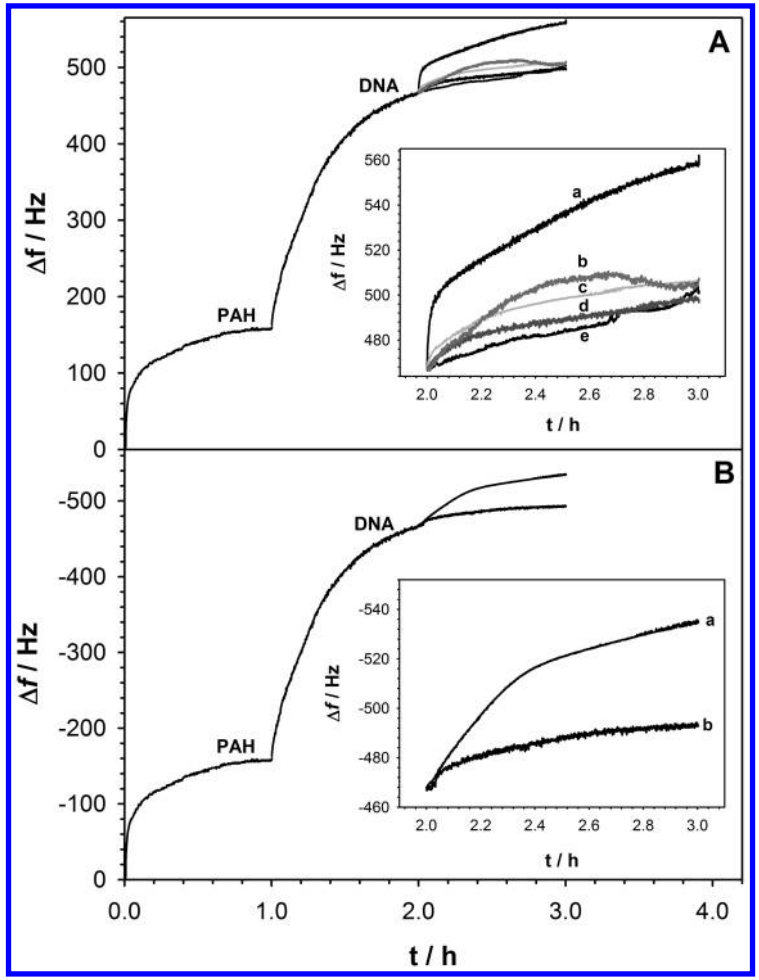

Figure 7. (A) Plot of frequency shifts during modification of a Au-EQCN electrode with PAH and ctDNA marked on the curve, followed by the treatment with various Cr(VI) solutions (curves magnified in Inset): (a) 5 μM Cr(VI) + 5 μM AA; (b) 5 μM Cr(VI) + 5 μM AA + 50 μM mannitol; (c)5 μM Cr(VI), (d) 5 μM Cr(VI) + 50 μM EDTA + 50 μM AA; (e) 5 μM Cr(VI) + 50 μM AA. (B) Same as (A) but the Au/PAH/ctDNA electrode treated with Cr(III) solutions: (a) 5 μM Cr(III); (b) 5 μM Cr(III) + 50 μM AA. Concentration of adsorbed ctDNA at PAH layer determined from UV-data of the ctDNA solution before after adsorption is ca. 21 pmol bp/cm².

In Oxidative Stress: Diagnostics, Prevention, and Therapy Volume 2; Hepel, et al.;
ACS Symposium Series; American Chemical Society: Washington, DC, 2015.

Publication Date (Web): October 13, 2015 | doi: 10.1021/bk-2015-1200.ch012

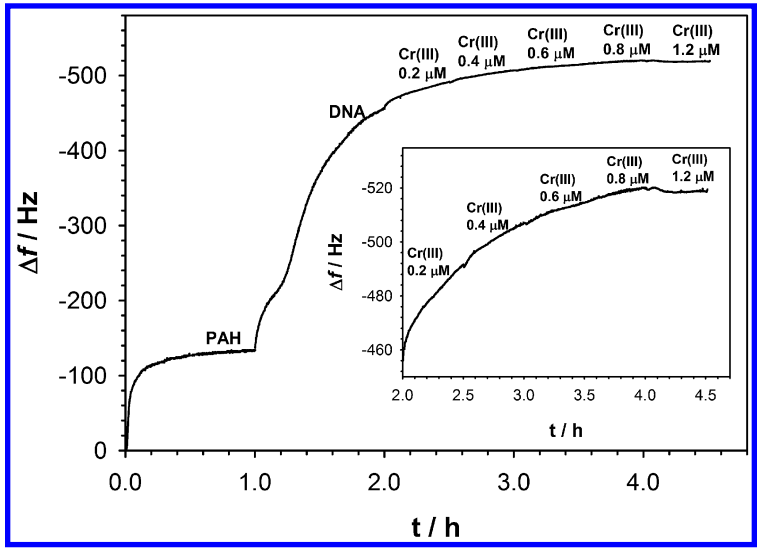

Figure 8. Frequency shifts observed during exposure of Au-EQCM/PAH/ctDNA to Cr(III) solutions. Concentration of adsorbed ctDNA at PAH layer determined from UV-data of the ctDNA solution before after adsorption is 28.3 pmol bp/cm².

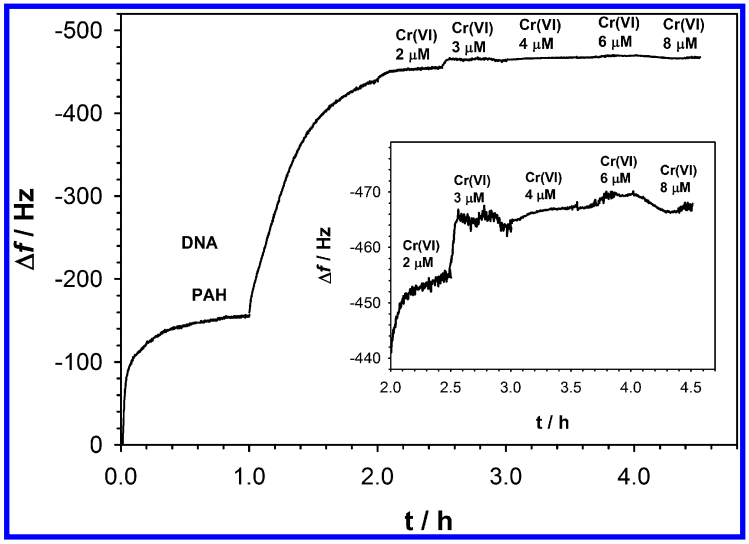

Figure 9. Frequency shifts observed during exposure of Au-EQCM/PAH/ctDNA to Cr(VI) solutions. Concentration of adsorbed ctDNA at PAH layer determined from UV-data of the ctDNA solution before after adsorption is 28.3 pmol bp/cm².

Publication Date (Web): October 13, 2015 | doi: 10.1021/bk-2015-1200.ch012

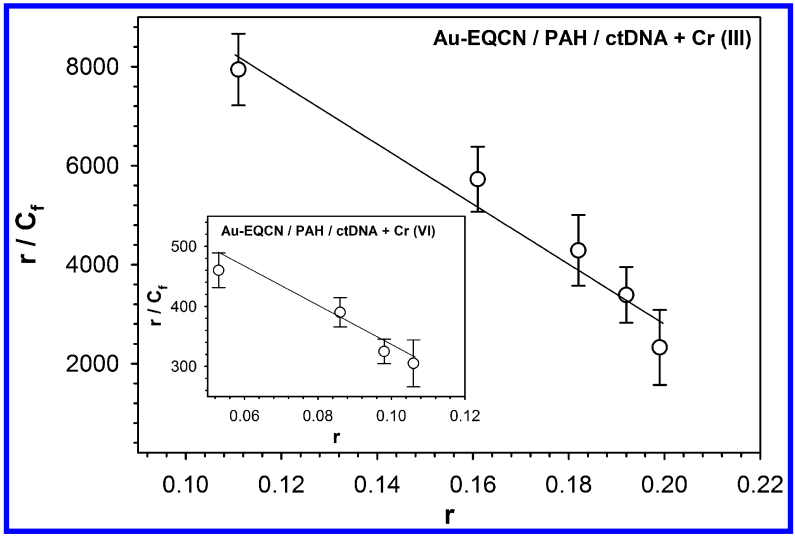

Figure 10. Scatchard plot obtained from EQCN results for the interaction Cr(III) and Cr(VI) with ctDNA.

Table 1. Binding parameters of interactions between ctDNA and Cr(III) and Cr(VI) species determined from EQCN data presented in this work and FTIR data from the literature (*5*).

	Cr species	*binding constant* (M^{-1})	*site size*
EQCN data	Cr(VI) Cr(III)	626 ± 52 (9.60 ± 0.90)×10³	4.71 ± 0.40 4.04 ± 0.38
FTIR data (*5*)	Cr(VI) Cr(III)	508 3.15 ×10³	— —

AFM Imaging

AFM imaging was performed to evaluate the ctDNA layer structure in the absence and the presence of different Cr species in the solution, see in Figure 10. The immobilization of ctDNA by electrostatic interactions resulted in the formation of large patches with the size ranging from 20 to 100 nm. Such behavior is consistent with previously reported results for amorphous DNA layers on hard and flat surfaces where the aggregated DNA formed lumps with the average diameter of 50 ÷ 60 nm (*28*, *29*). The formation of amorphous DNA layers is commonly observed for the films with high molecular density as well as for long DNA molecules (*30*). As seen in Figure 11, introduction of Cr species to the solution, has led to diminishing the ctDNA patches. Basically, all aggregates became smaller and thinner.

Publication Date (Web): October 13, 2015 | doi: 10.1021/bk-2015-1200.ch012

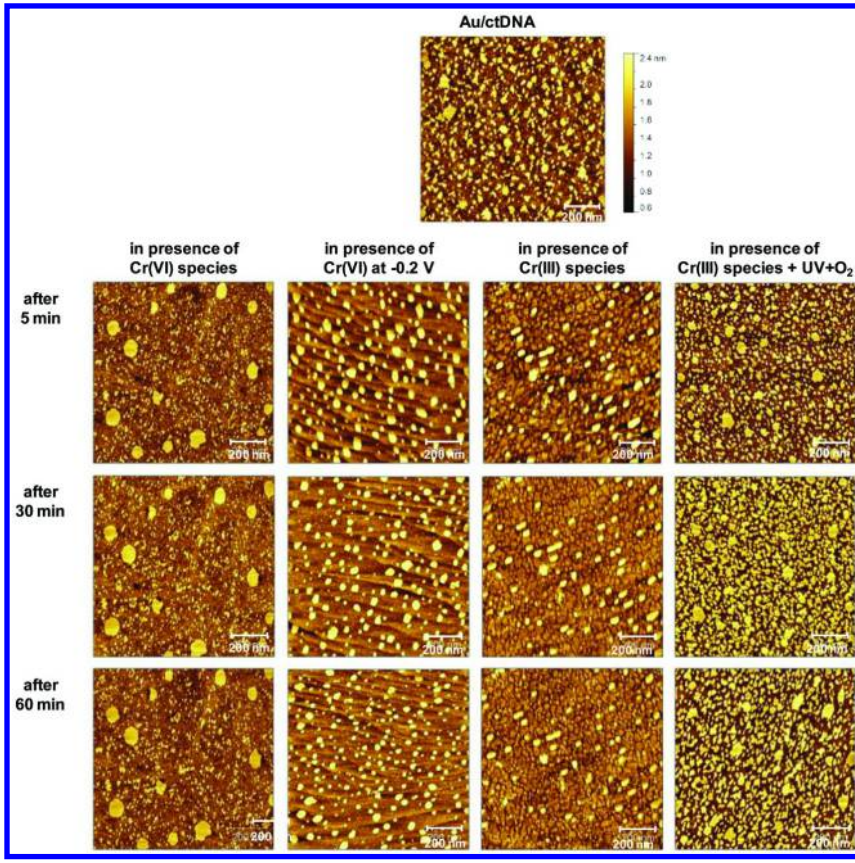

Figure 11. AFM images of ctDNA clusters on a Au(111) surface after contact with (columns left to right): Cr(VI) at open circuit, Cr(VI) at E = -0.2 V, Cr(III), and Cr(III) + O_2 + UV exposure, after treatment time: 5, 30 and 60 min (in rows top to bottom, respectively). (see color insert)

The effect of Cr(VI) is pronounced and increases with exposure time. Cr(III) does not affect the ctDNA film morphology if present alone. However, under UV illumination and with access of air, Cr(III) solutions also cause significant changes to the ctDNA film.

Effect of Chromium Species on ctDNA Molecules Contact-Adsorbed on Au-EQCN Electrode

In these experiments, ctDNA was immobilized on a Au-EQCN electrode surface by direct contact-adsorption, without any SAM basal film. The modified electrode (Au-EQCN/ctDNA) was carefully washed with water and exposed to Cr solutions. A typical frequency change during ctDNA immobilization process is shown in the inset in Figure 12.

Publication Date (Web): October 13, 2015 | doi: 10.1021/bk-2015-1200.ch012

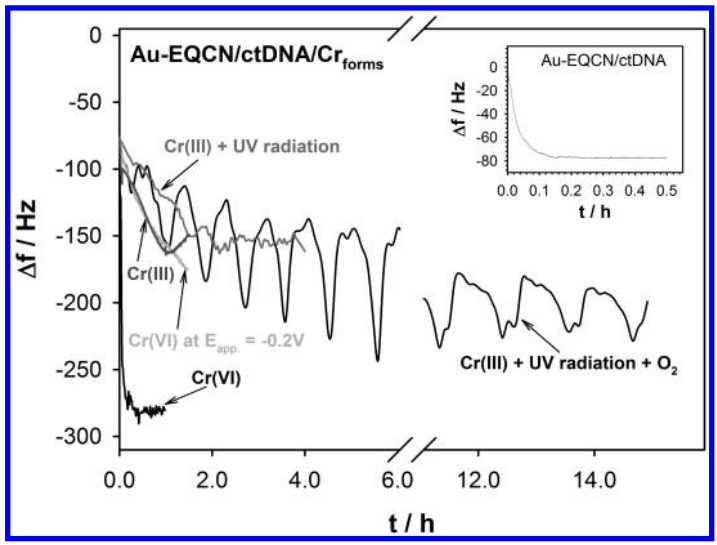

Figure 12. Frequency shifts observed during exposure of Au-EQCM/ctDNA to Cr solutions. Inset: Frequency shifts observed during accumulation of ctDNA at Au-EQCN electrode surface at +0.08 V. Experimental conditions: $C_{Cr(VI)}$= 1 μM (water solution); $C_{Cr(III)}$= 5 μM (water solution); 8 W UV lamp (95 % UV-A and 5 % UV-B).

The resonant frequency shift Δf (corresponding to the mass accumulation according to the Sauerbrey equation) was *ca.* 77 ± 10 Hz for the fundamental frequency f_0 = 6 MHz. The apparent mass increase related to the observed experimental frequency shift for ctDNA accumulation is: m_{ctDNA} = 4.3×77 = 331.1 ± 43 ng, which corresponds to 771.8 ± 100.2 ng/cm^2. In order to maintain a constant coverage of the electrodes with ctDNA, we kept the adsorption process until a steady state frequency was reached. This amounted to *ca.* 1800 s. In the next step, the modified electrode (Au-EQCN/ctDNA) was carefully washed with water and exposed to freshly prepared Cr solutions. To obtain the intermediate valence states of chromium (Cr (IV) and Cr(V)) in the solution, the Au-EQCN/ctDNA modified electrode was immersed in a Cr(VI) solution and hold at the potential E = –200 mV. The resonant frequency shifts recorded during binding of Cr species by DNA residues on Au-EQCN/ctDNA are presented in Figure 12. The interaction of Cr(VI) with ctDNA film leads to the oxidation of DNA components, mainly nitrogen bases. The Cr species at lower valency can oxidize DNA, as well as form high-affinity complexes. The molecular mass of oxidized DNA elements are significantly higher compared to those unoxidized. This fact is supported by the observed decrease in the resonant frequency. This considerable mass increase cannot be due just to the oxidation process or complex forming but rather mirrors the hydration of the changed nucleotides. An interesting result was observed in the case of exposure of ctDNA film to Cr(III) solution in the presence of dissolved oxygen and UV irradiation, see in Figure 12. The oscillations appeared after imposition of the UV radiation. The direct effect

of action of UV radiation on ctDNA is the formation of dimers of pyrimidine bases: C-C, C-T and T-T in the same DNA strand. It is known that UV radiation is also capable of generating radical oxygen species (ROS) such as superoxide anion ($O_2^{\bullet-}$), hydrogen peroxide (H_2O_2) and molecular singlet oxygen ($^1O_2$) (*31–35*). ROS are responsible for a number of mutagenic lesions to DNA (*26*). 8-Oxoguanine which misspairs with adenine and induces GC→AT transition is the most common DNA alteration. The explanation of the frequency oscillations is not straightforward. A possible explanation of the oscillation effect involves the following: first, due to UV irradiation, the DNA strands were excited leading to the ctDNA conformation change and its packing in the layer. This triggered the loss of the hydrating water molecules and caused a change in the viscoelasticity of the ctDNA layer and the corresponding frequency change (*36*). Next, the DNA chains released the excess energy, were hydrated again and the corresponding drop in frequency occurred. The drop in the frequency is related to the fact that Cr(III) under the condition of UV irradiation and the presence of molecular oxygen can be oxidized to the higher valency Cr species and this species can oxidize the DNA. In the case of no oxygen in the solutions the oscillations were not be observed.

Publication Date (Web): October 13, 2015 | doi: 10.1021/bk-2015-1200.ch012

Conclusions

We have investigated the interactions between Cr species on different oxidation state with ctDNA using electrochemical quartz crystal nanogravimetry (EQCN), linear scan voltammetry, AFM and UV-Vis spectroscopy. Most damage to ctDNA has been observed for Cr(VI), as expected, but also Cr(V) and Cr(IV) intermediates formed either by the reduction of Cr(VI) with ascorbic acid or by UV irradiation of Cr(III) in the presence of O_2.The binding constant determined from EQCN measurements and Scatchard plot analysis for ctDNA-Cr associates were found to be: 626 ± 52 M^{-1} for Cr(VI) and $(9.60 \pm 0.90)\times10^3$ M^{-1} for Cr(III), with clear dominance of Cr(III) binding by DNA.

Acknowledgments

This work was partially supported by the SUNY Research Foundation Collaborative Grant No. 66507.

References

1. Venitt, S.; Levy, L. Mutagenicity of chromates in bacteria and its relevance to chromate carcinogenesis. *Nature* **1974**, *250*, 493–495.
2. Bianchi, V.; Celotti, L.; Lanfranchi, G.; Majone, F.; Marin, G.; Montaldi, A.; Sponza, G.; Tarmino, G.; Venier, P.; Zantedeschi, A.; Levis, A. G. Genetic effects of chromium compounds. *Mutat. Res.* **1983**, *117*, 279–300.

3. Connett, P.; Wetterhahn, K. E. In vitro reaction of the carcinogen chromate with cellular thiols and carboxylic acids. *J. Am. Chem. Soc.* **1985**, *107*, 4282–4288.
4. Wolf, T.; Kasemann, R.; Ottenwälder, H. Molecular interaction of different chromium species with nucleotides and nucleic acids. *Carcinogenesis* **1989**, *10*, 655–659.
5. Arakawa, H.; Ahmad, R.; Naoui, M.; Tajmir-Riahi, H. A. A Comparative Study of Calf Thymus DNA Binding to Cr(III) and Cr(VI) Ions: evidence for the guanine N-7-chromium-phosphate chelate formation. *J. Biol. Chem.* **2000**, *275*, 10150–10153.
6. Nowicka, A. M.; Stojek, Z.; Hepel, M. Chromium(VI) but not chromium(III) species decrease mitoxantrone affinity to DNA. *J. Phys. Chem. B* **2013**, *117*, 1021–1030.
7. Krumpolc, M.; Roček, J. Chromium(V) oxidations of organic compounds. *Inorg. Chem.* **1985**, *24*, 617–621.
8. Gould, E. S. Redox chemistry of chromium (IV) complexes. *Coord. Chem. Rev.* **1994**, *135-136*, 651–684.
9. Sugden, K. D.; Wetterhahn, K. E. Reaction of chromium(V) with the EPR spin traps 5,5-dimethylpyrroline N-oxide and phenyl-N-tert-butylnitrone resulting in direct oxidation. *Inorg. Chem.* **1996**, *35*, 651–657.
10. Welch, C. M.; Nekrassova, O.; Compton, R. G. Reduction of hexavalent chromium at solid electrodes in acidic media: reaction mechanism and analytical applications. *Talanta* **2005**, *65*, 74–80.
11. Tong, J. Y.; Johnson, R. L. The dissociation equilibria of trioxochlorochromate(VI) and chromic acid. *Inorg. Chem.* **1966**, *5*, 1902–1906.
12. Buettner, G. R. In the absence of catalytic metals ascorbate does not autoxidize at pH 7: ascorbate as a test for catalytic metals. *J. Biochem. Biophys. Methods* **1988**, *16*, 27–40.
13. Bhatia, S. R.; Khattak, S. F.; Roberts, S. C. Polyelectrolytes for cell encapsulation. *Curr. Opin. Colloid Interface Sci.* **2005**, *10*, 45–51.
14. Carter, T. M.; Rodriguez, M.; Bard, A. J. Voltammetric studies of the interaction of metal chelates with DNA. 2. Tris-chelated complexes of cobalt(III) and iron(II) with 1,10-phenanthroline and 2,2′-bipyridine. *J. Am. Chem. Soc.* **1989**, *111*, 8901–8911.
15. McFadyen, W. D.; Sotirellis, N.; Denny, W. A.; Wakelin, P. G. The interaction of substituted and rigidly linked diquinolines with DNA. *Biochim. Biophys. Acta* **1990**, *1048*, 50–58.
16. Sauerbrey, G. The use of quartz oscillators for weighing thin films and for microweighing. *Z. Phys.* **1959**, *155*, 206–222.
17. Hepel, M. In *Interfacial electrochemistry. Theory, experiment, and applications*; Wieckowski, A., Ed.; Marcel Dekker: New York, 1999; pp 599−631.
18. Trasatti, S.; Petrii, O. A. Real surface area measurements inelectrochemistry. *Pure Appl. Chem.* **1991**, *63*, 711–734.

Publication Date (Web): October 13, 2015 | doi: 10.1021/bk-2015-1200.ch012

19. Brett, C. M. A.; Oliveira-Brett, A. M.; Serrano, S. H. P. On the adsorption and electrochemical oxidation of DNA at glassy carbon electrodes. *J. Electroanal. Chem.* **1994**, *366*, 225–231.
20. Clavilier, J. The role of anion on the electrochemical behaviour of a {111} platinum surface; an unusual splitting of the voltammogram in the hydrogen region. *J. Electroanal. Chem.* **1980**, *107*, 211–216.
21. McGhee, J. D.; von Hippel, P. H. Theoretical aspects of DNA-protein interactions: co-operative and non-co-operative binding of large ligands to a one-dimensional homogeneous lattice. *J. Mol. Biol.* **1974**, *86*, 469–489.
22. Cupo, D. Y.; Wetterhahn, K. E. Binding of chromium to chromatin and DNA from liver and kidney of rats treated with sodium dichromate and chromium(III) chloride *in vivo*. *Cancer Res.* **1985**, *45*, 1146–1151.
23. Hamilton, J. W.; Wetterhahn, K. E. Chromium (VI)-induced DNA damage in chick embryo liver and blood cells in vivo. *Carcinogenesis* **1986**, *7*, 2085–2088.
24. Miller, C. A.; Costa, M. Characterization of DNA-protein complexes induced in intact cells by the carcinogen chromate. *Mol. Carcinog.* **1988**, *1*, 125–133.
25. Pratviel, G.; Bernadou, J.; Meunier, B. You have full text access to this content carbon-hydrogen bonds of DNA sugar units as targets for chemical nucleases and drugs. *Angew. Chem., Int. Ed.* **1995**, *34*, 746–769.
26. Burrows, C. J.; Muller, J. G. Oxidative nucleobase modifications leading to strand scission. *Chem. Rev.* **1998**, *98*, 1109–1152.
27. Slade, P. G.; Hailer, M. K.; Martin, B. D.; Sugden, K. D. Guanine-specific oxidation of double-stranded DNA by Cr(VI) and ascorbic acid forms spiroiminodihydantoin and 8-oxo-2‘-deoxyguanosine. *Chem. Res. Toxicol.* **2005**, *18*, 1140–1149.
28. Casero, E.; Darder, M.; Diaz, D. J.; Pariente, F.; Martin-Gago, J. A.; Abruna, H.; Lorenzo, E. XPS and AFM characterization of oligonucleotides immobilized on gold substrates. *Langmuir* **2003**, *19*, 6230–6235.
29. Sawant, P. D.; Watson, G. S.; Nicolau, D., Jr.; Myhra, S.; Nicolau, D. V. Hierarchy of DNA immobilization and hybridization on poly-l-lysine using an atomic force microscopy study. *J. Nanosci. Nanotechnol.* **2005**, *5*, 951–957.
30. Nicolau, D. V.; Sawant, P. D. In *Immobilisation of DNA on Chips I*; Wittmann, C., Ed.; Springer-Verlag: Berlin, 2005; Vol. 260, pp 113−160.
31. Saito, I.; Inoue, K.; Matsuura, T. Occurrence of the singlet-oxygen mechanism in photodynamic oxidations of guanosine. *Photochem. Photobiol.* **1975**, *21*, 27–30.
32. Bradley, M. O.; Erickson, L. C. Comparison of the effect of hydrogen peroxide and x-ray irradiation on toxicity, mutation, and DNA damage/repair in mammalian cells (V79). *Biochim. Biophys. Acta* **1981**, *654*, 135–141.
33. Cunningham, M. L.; Krinsky, N. I.; Giovanazzi, S. M.; Peak, M. J. Superoxide anion is generated from cellular metabolites by solar radiation and its components. *Free Radical Biol. Med.* **1985**, *1*, 381–385.
34. Wei, H.; Ca, Q.; Rahn, R.; Zhang, X.; Wang, Y.; Lebwohl, M. DNA structural integrity and base composition affect ultraviolet light-induced oxidative DNA damage. *Biochemistry* **1998**, *37*, 6485–6490.

35. Blok, J.; Verhey, W. S. D. The attack of free radicals on biologically active DNA in irradiated aqueous solutions. *Radiat. Res.* **1968**, *34*, 689–703.
36. Nowicka, A. M.; Donten, M.; Stojek, Z. Repeated rearrangements of oligonucleotides immobilized on gold surface caused by UV irradiation in presence of dissolved oxygen. *Electrochim. Acta* **2013**, *110*, 133–138.

Publication Date (Web): October 13, 2015 | doi: 10.1021/bk-2015-1200.ch012

Publication Date (Web): October 13, 2015 | doi: 10.1021/bk-2015-1200.ch013

Chapter 13

Electrochemical Biosensors for Real-Time Monitoring of Reactive Oxygen and Nitrogen Species

Xiaobo Liu, Eduard Dumitrescu, and Silvana Andreescu*

Department of Chemistry & Biomolecular Science, Clarkson University, 8 Clarkson Avenue, Potsdam, New York 13699-5810
***E-mail: eandrees@clarkson.edu**

Oxidative and nitrosative stress has been associated with the pathophysiology and development of many diseases. Reactive oxygen and nitrogen species (ROS/RNS) have important physiological functions and play a critical role in redox regulation and oxidative and nitrosative stress. Quantification of ROS/RNS is essential for studying oxidative and nitrosative stress. This chapter provides a critical overview of the various electrochemical biosensors which can be used for *in vivo* and *in vitro* measurements of four primary ROS/RNS species: superoxide radicals, nitric oxide, hydrogen peroxide and peroxynitrite. The design, operational principle and applications of these sensors are described. Challenges and opportunities for real-time measurements of ROS/RNS species in biological systems and the translational aspects of this technology from chemistry and engineering laboratories to biology and clinical settings are discussed.

Introduction

Oxidative and nitrosative stress is involved in the development of aging (*1*), carcinogenesis (*2*), neurodegenerative disorders, such as Alzheimer's disease and Parkinson's disease (*3*, *4*), and some other health-related conditions (*5*–*8*). Under this physiological state, the generation of reactive oxygen/nitrogen species (ROS/RNS) overwhelms the limitation of the cells' antioxidant defense system (*9*, *10*).

In Oxidative Stress: Diagnostics, Prevention, and Therapy Volume 2; Hepel, et al.;
ACS Symposium Series; American Chemical Society: Washington, DC, 2015.

The deleterious impact of these conditions are a consequence of the high level of stress. Severe damage, including necrosis and apoptosis, is observed in cells exposed to oxidative stress conditions. Excessive ROS/RNS has been considered a sign of oxidative stress, while minor levels of oxidative and nitrosative stress merely trigger protective effects in the cell (*11*). Figure 1 shows the primary ROS and RNS and the interconversions between these species. Among ROS/RNS, hydroxyl (HO•), superoxide ($O_2^{\bullet-}$) and nitric oxide (NO) have been the most extensively studied. Hydrogen peroxide (H_2O_2) and peroxynitrite ($ONOO^-$) are not free radicals by themselves, but they can generate free radicals through various chemical reactions (*12*).

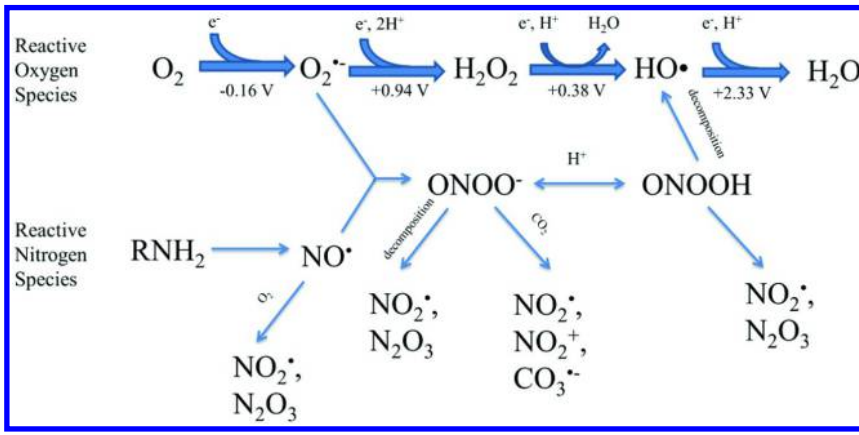

Figure 1. Primary reactive oxygen and nitrogen species (ROS/RNS) derived from the biological conversion of oxygen into superoxide ion ($O_2^{\bullet-}$) and nitric oxide (NO). (Reprinted with permissions from Reference (13, 14). Reference (13) Copyright 2008 American Chemical Society; Reference (14) Copyright 2013 Nature Publishing Group.)

Quantification of ROS/RNS species is critical for the study and understanding of oxidative and nitrosative stress. Most ROS/RNS species are difficult to detect due to their high reactivity and short life time. Various analytical methods, such as UV/Vis spectroscopy, fluorescence spectrometry and gas or liquid chromatography have been developed to quantify these species (*15*). However, most of these methods involve indirect quantification routes, require long assay time and do not provide a concentration profile of ROS/RNS species at their production site. These drawbacks limit the usefulness of such measurements. Customized microelectrodes or microbiosensors have demonstrated potential for real-time measurements in biological cells and tissues with high sensitivity and spatial resolution (*16*). Such devices can facilitate the study of the mechanism of action and role of ROS/RNS. Specifically designed microbiosensors can be used

Publication Date (Web): October 13, 2015 | doi: 10.1021/bk-2015-1200.ch013

in the biological and biomedical field to study how oxidative and nitrosative stress and ROS/RNS affect biological species and disease conditions. Compared to other transduction methods, electrochemical biosensors have attracted significant interest (*17*). Their advantages include: (1) high selectivity, (2) high sensitivity and low detection limit, (3) small size making these probes suitable for *in vivo* measurements and (4) inexpensiveness and relative ease of preparing and use (*18*). Electrochemical biosensors have been applied to quantify several essential biomolecules and ROS/RNS *in vitro* and *in vivo* (*19–22*). This chapter reviews the recent advances in electrochemical biosensors for the detection of ROS/RNS species and assessment of oxidative stress status, with a focus on the suitability and/or adaptability of these devices for real-time measurements in biological systems.

Publication Date (Web): October 13, 2015 | doi: 10.1021/bk-2015-1200.ch013

Electrochemical Sensors for the Detection of Nitric Oxide (NO)

From its initial discovery as an endothelial-derived relaxing factor (*23–25*), nitric oxide (NO) attracted a great deal of attention in biology and medicine. Studies carried out in the last 25 years linked this small molecule with many physiological processes. NO readily diffuses into cells where it can react with molecular targets. Compared to other ROS/RNS, NO by itself is not highly reactive. However, NO can interact with $O_2^{\bullet-}$ and form highly reactive oxidants like peroxynitrite ($ONOO^-$), nitrite (NO_2^-), and nitrate (NO_3^-) (*26*, *27*) that can cause damage to DNA, enzymes, proteins, lipids, etc. (*28*, *29*). It has been shown that the concentration of NO plays an important role in cardiovascular disease (*30*, *31*), hypertension (*32*, *33*), neuronal disease (*34*, *35*), respiratory disease (*36*), cancer (*37*) and diabetes (*38*). Due to its relevance in biological processes, analytical methods which provide fast, sensitive, selective and real-time quantification of NO in biological samples are of great interest. Several challenges need to be considered when designing NO detection methodologies. First, the NO concentration is usually very low. While some studies estimated a concentration of NO at μM level (*39*), others showed that the NO concentration could be as low as 100 pM (*40*), which requires improved detection sensitivity. Secondly, it is well-known that the stability of NO in biological media is reduced. The half-life of NO in tissues is in the order of seconds and can be as low as 0.1 seconds (*41*). Therefore, NO detection methods should have a short response time and provide a rapid, real-time measurement.

Several conventional methods have been used to measure NO, including the Griess assay (*42*), electron spin resonance (ESR) (*43*), quantum cascade laser (*44*), spectrophotometry (*45*, *46*), chemiluminescence (*47*) and fluorescence (*48*, *49*). The Griess assay is one of the common methods used to determine NO with a limit of detection of about 1 μM. The method, however, has limited applicability in complex biological matrices (*50*). Other methods such as quantum cascade laser based detection has been used for gaseous NO assessment (*44*), while chemiluminescence and spectrophotometric assays have been traditionally used

In Oxidative Stress: Diagnostics, Prevention, and Therapy Volume 2; Hepel, et al.;
ACS Symposium Series; American Chemical Society: Washington, DC, 2015.

for *in vitro* NO tests. These assays can also be adapted for measurements in cell cultures (*45*) and other biological samples (*47*). Electron spin resonance (*43*) and fluorescence with organic chromophores (*51*) allow investigation of NO concentration, but have limited temporal and spatial resolution and are not easy to use for quantitative analysis, especially in complex samples (*52*). Electrochemical methods using microelectrodes represent a powerful alternative to conventional methodologies for NO detection in biological systems. Electrochemistry is the only method that can provide real-time kinetic determination of NO at the production site and be adapted for *in vivo* measurements (*52*, *53*). Conventional strategies to fabricate NO selective electrochemical microsensors developed over the last 20 years have been reviewed (*52–60*). While significant advances in electrode materials and design characteristics have facilitated development of sensitive electrochemical probes, most NO measurements in biological systems still make use of "classical strategies."

The first example of a NO selective sensor was reported in 1990 by K. Shibuki (*61*), who used the initial O_2 sensor design reported by L. Clark (*62*), with a platinum wire working electrode and a thin gas-permeable rubber membrane. Electrode materials that are typically used to fabricate NO electrodes include platinum and its alloys (*63*, *64*), gold (*65*) and carbon fibers (*22*, *66*). Enhanced performances can be achieved on electrodes modified with different materials to increase surface area, catalytic properties and improve selectivity. For example, platinization improved the sensitivity of platinum electrodes by increasing the effective surface area (*67*). Deposition of platinum black particles on carbon fibers combined the properties of both materials, improving NO measurement capabilities (*66*, *68*). The electrochemical oxidation of NO takes place at a high potential (> 0.8 V), where other electrochemically active species that are present in the biological system respond. Therefore, electrochemical NO sensors based on direct oxidation of NO may suffer from selectivity problems. To ensure selectivity, many NO electrodes are modified with a hydrophobic membrane permeable to NO, but impermeable to usual interfering compounds in biological matrix such as ascorbate, nitrite, uric acid, H_2O_2 and serotonin (*59*). A common approach is to use multiple sequential layers, each with a different property for blocking interferences (*22*). The commonly used membranes are Nafion (*22*, *63*, *64*, *69*), *o*-phenylenediamine (*o*-PD) (*22*, *70*) or *m*-phenylenediamine (*m*-PD) (*63*), poly-phenol and poly-eugenol (*65*, *70*), resorcinol (*63*), chitosan (*71*) and aniline (*70*). A platinum-iridium alloy disk electrode modified with Nafion was used for *in vivo* NO detection in the prefrontal cortex and nucleus accumbens of freely moving rats (*72*). Interference studies confirmed the ability of Nafion to eliminate ascorbic acid signals. A similar microelectrode configuration was used for investigation of NO in the prefrontal cortex in an animal model of Schizophrenia in freely moving rats (*69*). We used single carbon fiber electrodes modified with Nafion and o-PD to determine zebrafish intestinal NO (*22*). The small dimension of carbon fibers (≈ 5 μm diameter) allowed a convenient implantation of the probe in the zebrafish intestine and enabled direct NO measurements with a detection limit of 1.43 nM. Figure 2 shows an example of NO measurements in the intestine of zebrafish using this electrode.

Publication Date (Web): October 13, 2015 | doi: 10.1021/bk-2015-1200.ch013

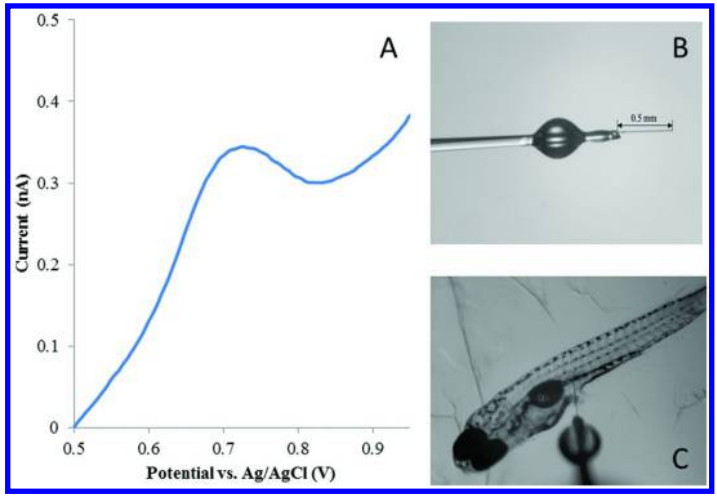

Figure 2. Typical differential pulse voltammogram (DPV) response of intestinal NO in a 5 dpf zebrafish embryo using a single carbon fiber NO selective sensor (A). Images showing a single carbon fiber NO selective sensor (B) and the implantation of the sensor in the middle section of zebrafish intestine (C).

Other strategies to fabricate NO microelectrodes involve catalytic oxidation of NO via electron mediators deposited directly on the electrode surface or incorporated within a membrane. The mediator is used to enhance the electrochemical signal and to further minimize the interferences from electroactive species by selectively catalyzing the oxidation or reduction of the NO (*55*). On the other hand, their catalytic activity also increases the electrochemical signal of interfering substances that are oxidized at or below the holding potential. Hence, these types of NO sensors may also suffer from reduced selectivity (*73*). To provide selectivity, catalytic layers can be used in conjunction with permselective membrane. Conventional mediators used for NO sensors are metalloporphyrins (*74–77*) and metallophtalocyanines (*78–80*). Other materials, such as salen complexes (*81*) and Meldola blue (*71*) are also used for the same purpose. The interaction of nitric oxide with porphyrins and phtalocyanines was intensively studied (*82–84*). While many electrochemical sensors based on porphyrins have been reported, their sensing mechanism for NO is still largely unknown (*53*). Most studies attribute the enhanced measurement capabilities to their affinity for NO and resistance to degradation (*55*). It was shown that other mediators might have comparable efficiency. J. Njagi, et al. used Meldola blue, a recognized mediator for NADH and H_2O_2 oxidation (*85*), to develop a sensitive sensor for NO monitoring in brain slices (*71*). The platinum-based electrode modified with Meldola blue, *o*-PD and chitosan exhibited a low detection limit of 1 nM, a broad linear range and good stability when used for measurements in brain slices. Figure 3 shows a general schematic representation of a metal-based sensor modified with a mediator and one or more permselective membranes.

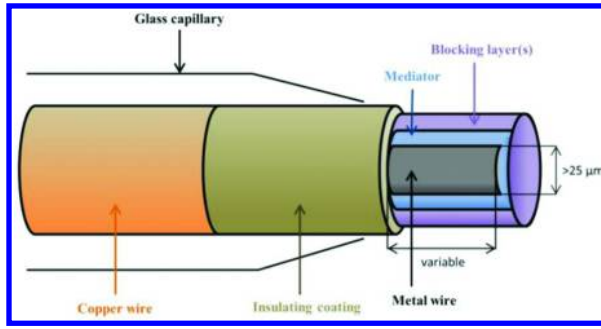

Figure 3. General design for a metal-based sensor modified with a mediator and blocking layer(s).

Publication Date (Web): October 13, 2015 | doi: 10.1021/bk-2015-1200.ch013

Giving the high interest for NO measurements in biological media, it is expected that new directions will be explored in order to expand the applicability of these probes into other areas in biology and medicine. Electrode designs are continuously improving with the use of new materials and probe configurations. In the last five years, there has been an exponential increase in the use of nanomaterials to improve the sensitivity of NO probes. These include carbon based materials (*86–88*) such as graphene (*89–93*) and carbon nanotubes (*94–97*), as well as metal nanoparticles (*98*). These materials have good electrical conductivity, a high surface to volume ratio and electrocatalytic properties which make them suitable for electrochemistry applications (*86*, *87*). A combination of multi-walled carbon nanotubes with cobalt porphyrin showed improved electrocatalytic activity towards NO oxidation (*99*). Wang, L. et al. developed a sensor using multi-walled carbon nanotubes functionalized with a polymeric film of ethylenediamine (EDA) (*97*). The sensor was used to monitor NO release from rat liver samples. Other sensors make use of the electrocatalytic properties of metal and metal oxide nanoparticles (*98*) such as nickel oxide (*94*) and ferric oxide (*100*). The use of gold nanoparticles incorporated in a sol-gel film (*101*) or deposited on a multi-walled carbon nanotubes film (*102*, *103*) has also been reported.

Electrochemical sensors offer an effective way for measuring NO in different biological samples. Figure 2 showed an example of measurement in zebrafish embryo. Figure 4 shows an example of electrochemical profiling of NO in cortical and hypocampal areas of the brain. This work demonstrated the potential of NO microelectrodes for studying NO release in diverse biological systems (*104*). Although many NO probes have been developed and some are commercially available, their implementation as routine measurement devices in biological and biomedical settings and in clinical diagnosis has not been fully realized. This might be due to problems related to electrode passivation, difficulties in calibration, cross-reactivity with other reactive species and biocompatibility of the probes. These issues, among with other translational aspects, will be discussed in the last section of this chapter.

Publication Date (Web): October 13, 2015 | doi: 10.1021/bk-2015-1200.ch013

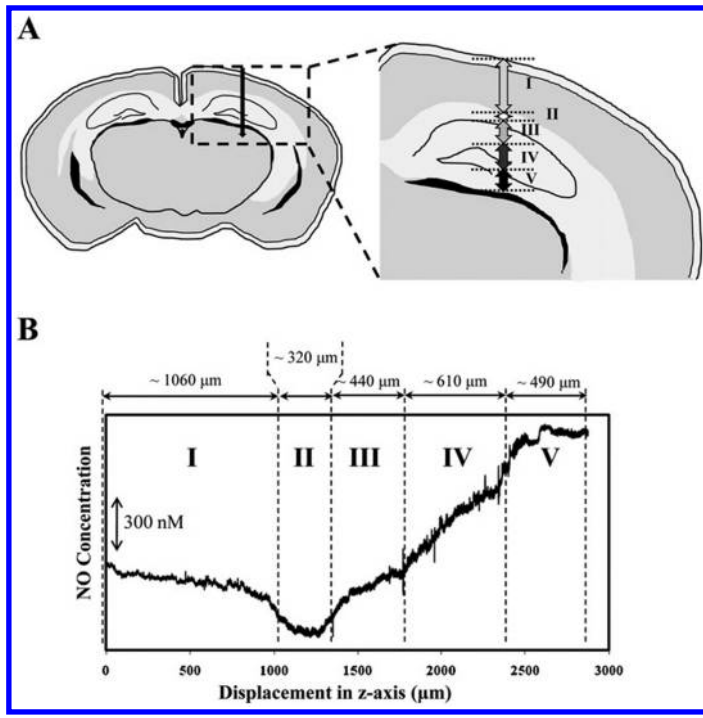

Figure 4. Electrochemical profiling of NO in cortical and hypocampal areas in different areas of the brain, showing penetration and monitoring site. (Reprinted with permission from Reference (104). Copyright 2011 Elsevier Ireland Ltd.)

Electrochemical Detection of Hydrogen Peroxide (H_2O_2)

H_2O_2 is an important molecule in molecular biology, pharmaceutical industry, biochemistry, food industry and clinical field (*105*). Quantification of H_2O_2 and understanding the mechanism of release are of particular importance in biomedical research (*106*). H_2O_2 is one of the most stable ROS. Moreover, H_2O_2 is also a side product of some biochemical reactions catalyzed by oxidase enzymes, such as glucose oxidase (GOx), alcohol oxidase (AlOx), lactate oxidase (LOx), urate oxidase (UOx), cholesterol oxidase (ChoOx), glutamate oxidase (GlOx), lysine oxidase (LyOx), etc. These features make the detection of H_2O_2 attractive in academic research and industrial applications. Conventional methods, including UV-Vis spectrophotometry (*107*, *108*) and fluorescence (*109–111*) methods have been the most widely used for the detection of H_2O_2, but have limitations when applied to biological systems. *In vivo* monitoring and real-time measurements are hard to achieve by these methods. Alternatively, electrochemical sensors are suitable candidates and can provide direct *in situ* measurements. Due to its versatility, electrochemical detection of H_2O_2 has been widely investigated. H_2O_2 can be detected electrochemically at its oxidation potential, between ~ 0.6 to 0.8 V *vs* standard Ag/AgCl reference electrode. The preferred working

electrode material is platinum. Monitoring H_2O_2 reduction is also possible, but this approach suffers from overlapping signals from molecular oxygen (*112*).

$$H_2O_2 \rightarrow O_2 + 2H^+ + 2e^-$$

With appropriate modification on the electrode surface, the sensitivity, selectivity and detection limit of electrochemical H_2O_2 sensors can be significantly improved (*113*). The common electrode materials are electron mediators such as metal hexacyanoferrates (*114*), heme proteins (*115*) and transition metals and their oxides (*116*). With the rapid development of nanotechnology, incorporation of nanomaterials in the surface modification process is an emerging trend in the design of H_2O_2 sensors. Such examples include functionalized graphene/graphene oxide (*117–119*), silicon nanomaterials (*120*) and metal and metal oxide nanoparticles (*117*, *121–124*).

However, due to the large overpotential required for oxidation, where most other electroactive species (i.e., ascorbic acid, uric acid) are oxidized, direct measurement of H_2O_2 suffers from limited specificity (*125*). Thus, most sensors are functionalized with permselective membranes that allow passage of H_2O_2 while preventing the access of other molecules (*126*). These membranes eliminate interferences by controlling the pore dimensions. Different polymers, multilayers and mixed layers of varying dimensions, charges or polarities have been used to restrict the access of some electroactive interfering compounds present in the sample. The use of such membranes, however, may decrease the response time of the sensor by inducing diffusion limitations, e.g. increasing the time to establish an equilibrium of the diffusional mass transport (*127*). Permselective membranes are, in general, polymeric non-conductive films (*127*). Electropolymerized coatings have also been used and have shown reduced susceptibility to biofouling (*128*). Films obtained by electropolymerization include over-oxidized polypyrrole (*129–131*), polyphenylenediamine (*132–135*) and polyion complex layer (i.e., poly-L-lysine and poly-4-styrenesulfonate) (*136*). Although electropolymerized films show excellent permselectivity, they are relatively unstable when used for long periods of time and their performance tends to fail rapidly when they are operated at 37 °C (*137*). Several works have reported that the maintenance of high permselectivity with repeated use is difficult for electropolymerized films (*138–140*). Other types of membranes reject interferences through an electrostatic repulsion mechanism. A widely used approach is to use negatively charged membranes of sulfonate type (Nafion or Eastman Kodak AQ pefluorinatedionomer, a negatively charged polymer coating that can eliminate interferences from negatively charged species (*141–143*)), or cellulose acetate (*144*), which can eliminate interferences from acetaminophen, ascorbate and urate.

Hamdi and collaborators (*131*) have shown that the selectivity of Pt electrodes coated with electrodeposited over-oxidized polypyrrole and polyphenylenediamine films display H_2O_2 selectivity relative to ascorbic acid of ≥130 and ≥240 respectively, and relative to dopamine of ≥100 and 80 respectively. By comparison, Nafion- and polyaniline-coated electrodes give inferior selectivity performance. Similarly, Hu et al (*145*) coated the electrode

In Oxidative Stress: Diagnostics, Prevention, and Therapy Volume 2; Hepel, et al.;
ACS Symposium Series; American Chemical Society: Washington, DC, 2015.

Publication Date (Web): October 13, 2015 | doi: 10.1021/bk-2015-1200.ch013

with layers of polypyrrole and Nafion, acting both as size and charge exclusion membranes. Brown and Lowry (*146*) have systematically investigated different coating procedures for depositing Nafion onto Pt microelectrodes and have found that the elimination of interference from ascorbic and uric acid was more effective by using a thermally annealing procedure involving 5 pre-coats and 2 subsequent dip-bake layers. This procedure was also successful in completely eliminating the response from the neurotransmitter dopamine and did not affect the permeability for oxygen. However, the sensitivity of the sensor for the detection of H_2O_2 also reduced after the deposition of membranes.

In addition to chemical sensors based on direct oxidation or reduction of H_2O_2, other strategies involving proteins, in their wide majority heme proteins possessing peroxidase activity, have been developed. These devices have attained extraordinary levels of sensitivity with detection limits in the nM range, enabling measurements of the release of H_2O_2 by mitochrondria. A horseradish peroxidase (HRP)-based H_2O_2 sensor with the enzyme crosslinked in a polymer matrix was used to monitor H_2O_2 bursts from isolated mitochondria at an operating potential of 0 V vs standard Ag/AgCl reference electrode (*147*). Another example of measurements from isolated mitochondria is a sensor based on carbon–maghemite nanocompsites (*124*). A successful application of these sensors has been demonstrated for measurements of H_2O_2 released from hepatocytes (*148*). The accurate measurement of H_2O_2 released from alcohol-injured hepatocytes demonstrates the potential of these probes in biological and clinical fields. This experimental setup is illustrated in Figure 5.

Publication Date (Web): October 13, 2015 | doi: 10.1021/bk-2015-1200.ch013

Electrochemical Detection of Superoxide ($O_2^{\bullet-}$)

$O_2^{\bullet-}$ is a short-lived reactive oxygen intermediate resulting from the one-electron reduction of oxygen and one of the primary components of ROS. $O_2^{\bullet-}$ is one of the most abundant radicals produced in biological systems and the precursor of most other ROS species. Due to its central role as a major contributor to oxidative stress, the measurement of $O_2^{\bullet-}$ is of significant importance. However, detection of $O_2^{\bullet-}$ is complicated due to its very short lifetime (i.e., in the order of miliseconds), high diffusion rate from the production site and the very low and variable concentration level. Moreover, in aqueous solution, $O_2^{\bullet-}$ will undergo a fast disproportionation to H_2O_2. This disproportionation makes it particularly difficult to differentiate signals and biological effects between the two species. Conventional methods used to quantify $O_2^{\bullet-}$ *in vitro* include spectrometry (*149*), liquid chromatography-mass spectrometry (LC-MS) combined with electron paramagnetic resonance (EPR) (*150*), fluorescence (*151*) and EPR (*152*, *153*). These methods can provide qualitative information, but they are not small enough to be used in situ at cell or tissue locations where suproxide is produced. Therefore, these methods do not provide a real-time concentration profile. Most biological studies to investigate $O_2^{\bullet-}$ are performed using ROS specific dyes. However, the specificity of these dyes has been questioned and such measurements have limited temporal and spatial resolution (*154*, *155*).

In Oxidative Stress: Diagnostics, Prevention, and Therapy Volume 2; Hepel, et al.;
ACS Symposium Series; American Chemical Society: Washington, DC, 2015.

Publication Date (Web): October 13, 2015 | doi: 10.1021/bk-2015-1200.ch013

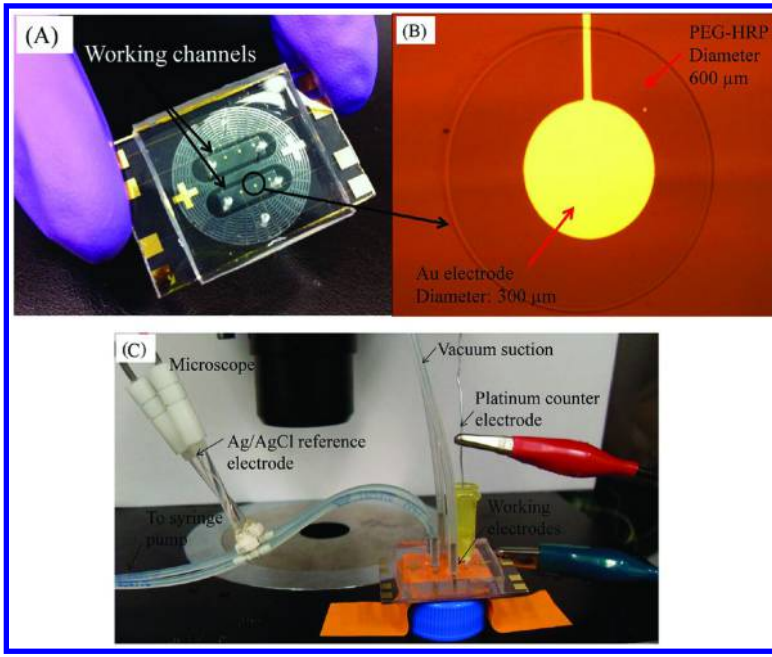

Figure 5. (A) PDMS covered sensing chip containing eight micropatterned Au electrodes (four in each working channel). (B) An image of a PEG−HRP polymerized Au electrode. (C) Microfluidic device for on-chip electrochemical experiments containing flow-through Ag/AgCl as reference (connected to the outlet), Pt wire as counter (in the inlet), and patterned Au as working electrodes. (Reprinted with permission from Reference (148). Copyright 2013 American Chemical Society.)

Electrochemistry is a powerful alternative that can provide rapid real-time measurements of ROS species in complex biological environments (*19–21*, *156*, *157*). Real-time measurements of the release kinetic of $O_2^{\bullet-}$ radicals can be conducted by using a cytochrome *c* biosensor (*158*). Two types of $O_2^{\bullet-}$ biosensors have been reported in literature, based on either cytochrome *c* or superoxide dismutase (SOD) (*159–162*). The sensing strategies involve direct or biocatalytic oxidations at the electrode surface, typically mediated by redox proteins. Depending on the design, the electrode can be coated with permselective membranes, redox relays or redox hydrogels to promote the electron transfer.

Sensors based on cytochrome *c* measure the reduction of the heme center of cytochrome *c* at the electrode surface by the $O_2^{\bullet-}$ radical. The reduced cytochrome *c* is then reoxidized at the electrode surface generating an anodic current which is correlated with the concentration of $O_2^{\bullet-}$. To fabricate the biosensor, cytochrome *c* is electrically "wired" on the electrode surface. Electron transfer between the electrode and the redox protein, cytochrome *c*, is typically achieved on a gold wire via a packed layer of self-assembled monolayers (SAMs) (*161*, *163*, *164*). The detection principle is shown in Figure 6. Typically, short-chain

thiols provide efficient electron transfer between cytochrome *c* and the electrode surface and are used in most configurations. However, short chain thiols are not effective agaist interferences. Electroactive interferences are significantly blocked by long-chain thiols used in SAM (*161*). Therefore, most cytochrome *c*-based sensors employ a mixed (long and short) SAM layer to achieve an efficient electron transfer and prevent interfering signals from the coexisting electroactive species. Other sensors are using multiple layers of cytochrome *c* immobilized between electroactive polymers. For example, a sensor fabricated by deposition of six cytochrome *c*/poly(aniline(sulfonic acid)) (PASA) layers on a gold electrode showed highest sensitivity among a series of sensors made of 2 to 15 layers (*165*). The reaction rate between the redox protein and the $O_2^{\bullet-}$ radicals is a determining factor in the sensitivity of cytochrome *c*-based biosensors. To increase the reaction rate, cytochrome *c* mutants prepared by site directed mutagenesis focusing on aminoacids near the heme edge were tested. The results indicated that the reaction rate, and therefore the sensitivity of the sensor, varies and can be modulated by using mutant forms of cytochrome *c* (*166*).

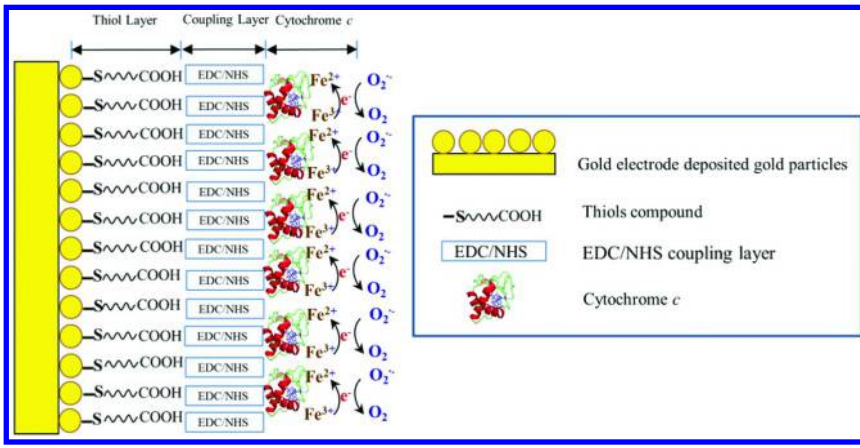

Figure 6. Design and sensing principle of cytochrome c-based $O_2^{\bullet-}$ biosensors based on self-assemble monolayer (SAM).

While many configurations of cytochrome *c* biosensors have been developed, few applications of these sensors to measure $O_2^{\bullet-}$ production in 'real' biological systems have been reported. Scheller and colleagues used a SAM-cytochrome *c* biosensor to determine the level of $O_2^{\bullet-}$ in the gastrocnemius muscle of a rat under artificially induced ischemic condition (*167*, *168*). Our group utilized a cytochrome *c* biosensor prepared from mixed thiols to determine $O_2^{\bullet-}$ radicals production from rat brain slice during ischemia (*158*). Figure 7 shows a typical current-time response of the biosensor showing continuous monitoring of $O_2^{\bullet-}$ in mouse hippocampal brain slice exposed to simulated ischemic conditions, created by exposing the slice to hypoglycemic, acidic and hypoxic conditions (glucose was lowered to 2 mM and the cell was bubbled with 15 % CO_2 and 1% oxygen). These sensors also can be used to study cellular mechanisms involved during

In Oxidative Stress: Diagnostics, Prevention, and Therapy Volume 2; Hepel, et al.;
ACS Symposium Series; American Chemical Society: Washington, DC, 2015.

Publication Date (Web): October 13, 2015 | doi: 10.1021/bk-2015-1200.ch013

mitochondrial $O_2^{\bullet-}$ generation (*169*) and they enable such measurements at single cell level. Rahman and colleagues used a conducting polymer to immobilize cytochrome *c* and lipid molecules to stabilize the catalytic activity of the heme center. This sensor was utilized to measure $O_2^{\bullet-}$ in rat brain (*170*).

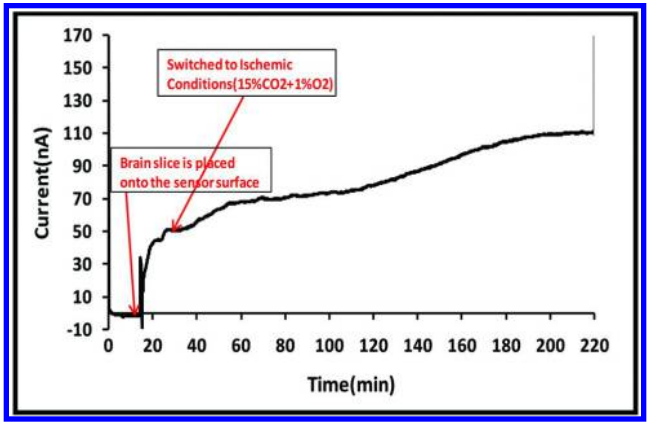

Figure 7. Real-time amperometric measurements of $O_2^{\bullet-}$ production in a brain slice model of cerebral ischemia. (Reprinted with permission from Reference (158). Copyright 2012 Elsevier Inc.)

$O_2^{\bullet-}$ sensors based on SOD involve the dismutation of the $O_2^{\bullet-}$ radical to O_2 and H_2O_2 catalyzed by SOD through a two electron transfer process. Several generations of this type of sensors have been designed (Figure 8). In the first generation, the enzymatically produced H_2O_2 is detected at the electrode surface at an applied potential corresponding to oxidation or reduction of H_2O_2. This type of sensors usually incorporates SOD immobilized on the electrode surface in a H_2O_2 permeable membrane (*171*, *172*). This design has two main limitations which restrain the applicability for measurements in biological systems: (1) $O_2^{\bullet-}$ can undergo rapid spontaneous dismutation and (2) the high applied potential (> 0.5 V vs. Ag/AgCl) required for the oxidation of H_2O_2 will also oxidize other electroactive substances that are typically present in biological samples such as ascorbic acid, uric acid, etc. The use of H_2O_2-impermeable membranes (*173*), self-referencing sensors (*174*) and permselective membranes like poly-*m*-phenylenediamine (PPD) (*175*) are effective strategies to remove such interferences. The second generation of SOD-based ($O_2^{\bullet-}$) biosensors is based on th use of electron transfer mediators (*176*) to enhance the electron transfer from SOD to the sensor surface. Immobilization of SOD on the electrode surface was achieved through SAM (*177*), sol-gel film (*178*) or through a genetically engineered cysteine (*179*, *180*). Endo and colleagues have successfully used a SOD-based biosensor to measure tissue-$O_2^{\bullet-}$ radicals generated from the heart tissue of endotoxin administered Wistar Kyoto rat in a flow cell system (*176*). In another work, $O_2^{\bullet-}$ derived from zymosan treated macrophage cells was detected using a biosensor made of SOD/sodium alginate sol-gel film (*178*). The third generation of SOD sensors involve direct electron transfer between the redox

In Oxidative Stress: Diagnostics, Prevention, and Therapy Volume 2; Hepel, et al.;
ACS Symposium Series; American Chemical Society: Washington, DC, 2015.

Publication Date (Web): October 13, 2015 | doi: 10.1021/bk-2015-1200.ch013

active center of SOD and the electrode surface (*181–183*). A SOD modified gold electrode functioning as a third generation $O_2^{\bullet-}$ biosensor with the SOD immobilized via a SAM of cysteine allowed monitoring of both the oxidation of ($O_2^{\bullet-}$) to O_2 at -0.2 V and its reduction to H_2O_2 at 0.3 V in the concentration range from 13 to 130 mM/min with a detection limit of 6 nM/min (*182*). A miniaturized probe based on this strategy was fabricated on a carbon fiber functionalized with gold nanoparticles (*181*), demonstrating potential for miniaturization.

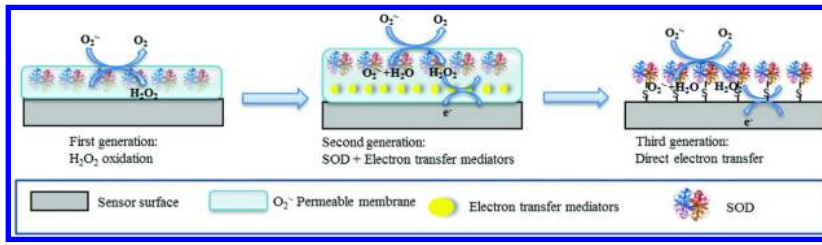

Figure 8. Sensing principle and evolvement of SOD-based $O_2^{\bullet-}$ biosensors.

In addition to sensors based on biological receptors, the use of biomimetic materials that mimic SOD or cytochrome *c* activity are gaining increasing acceptance. For example, a polymeric iron porphyrin complex which mimics cytochrome *c* activity used as a biomimetic sensing material enabled sensitive detection of $O_2^{\bullet-}$. The amperometric response was monitored at a potential of 0.5 V and showed a linear relationship with the $O_2^{\bullet-}$ concentration. Coordination of an imidazole ligand to the iron porphyrin complex enhanced selectivity against H_2O_2 (*184*, *185*). Fujita and colleagues have applied a sensor coated with a polymeric porphyrin complex to measure $O_2^{\bullet-}$ in the right atria of endotoxemic rats generated *in vivo* (*186*). More advanced applications of $O_2^{\bullet-}$ sensors were demonstrated for single living cell analysis (*13*). Bare carbon and/or platinized carbon electrode have been used to determine ROS/RNS induced by physical stress in a single fibroblast (*187–189*), mitochondria (*147*) and in different types of macrophage (*68*, *190*). Figure 9 shows an example of a single cell measurement conducted by Amatore and colleagues (*191*).

Electrochemical Detection of Peroxynitrite ($ONOO^-$)

$ONOO^-$ is the product of the reaction between $O_2^{\bullet-}$ and NO (*192*, *193*) (Figure 1). $ONOO^-$ is highly active and has a short half-life time under physiological conditions. Peroxynitrite has been involved in several pathological conditions such as Parkinson's disease (*194*), proteins and DNA damage (*195*), fatty liver disease (*196*) and acute ischemia-reperfusion injury (*197*), due to its nitration effect. Conventional methologies to study the role of $ONOO^-$ in biological systems involve fluorescence (*198–200*) and bioluminescence (*201*) probes. These methods provide a visual distribution of $ONOO^-$ in cells and tissues (*202*). However, they generally lack specificity and are unable to provide real-time quantitative assessment (*48*).

In Oxidative Stress: Diagnostics, Prevention, and Therapy Volume 2; Hepel, et al.;
ACS Symposium Series; American Chemical Society: Washington, DC, 2015.

Publication Date (Web): October 13, 2015 | doi: 10.1021/bk-2015-1200.ch013

Publication Date (Web): October 13, 2015 | doi: 10.1021/bk-2015-1200.ch013

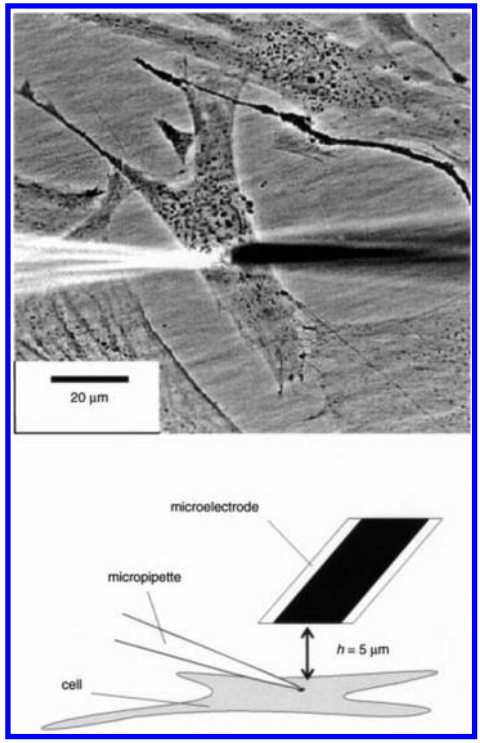

Figure 9. Optical microscopic view and schematic side view showing a human fibroblast in a Petri dish and the positioning of a microelectrode (black shadow on right) which constitute together a semiartificial synapse. A glass micropipette (white shadow on left) was used to trigger the oxidative stress response. (Reprinted with permission from Reference (191). Copyright 2001 WILEY-VCH.)

Few publications reported the development of electrochemical sensors for the detection of $ONOO^-$. Most sensors are based on the use of chemically modified electrodes containing catalytic materials. Manganese phthalocyanine (*203*, *204*) and manganese porphyrin (*205*) are commonly used as electrochemical mediators in these sensor designs. A sensor based on manganese-[poly-2,5-di-(2-thienyl)-1H-pyrrole)-1-(p-benzoicacid)] has been used to monitor $ONOO^-$ produced from phorbolmyristate acetate (PMA)-stimulated YPEN-1 glioma cells (*206*). A poly(cyanocobalamin) modified sensor provided suitable sensitivity and selectivity for the detectin of $ONOO^-$ (*207*). More recently, cobalt phthalocyanine tetracarboxylic acid modified reduced graphene oxide was used as en electrocatalyst for the detection of $ONOO^-$ and H_2O_2 demonstrating very low detection limits of 1.7 nM for $ONOO^-$ and 60 µM for H_2O_2 (*208*).

Publication Date (Web): October 13, 2015 | doi: 10.1021/bk-2015-1200.ch013

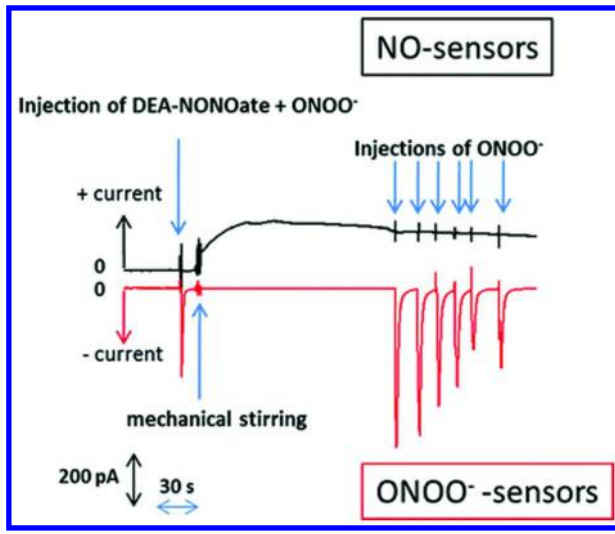

Figure 10. Example of simultaneous detection of NO and $ONOO^-$ by two amperometric measurements at +0.8 and −0.1 V vs Ag/AgCl using a multiplex array. (Reprinted with permission from Reference (209). Copyright 2011 Royal Society of Chemistry.)

While highly sensitive, these platforms suffer from reduced selectivity from the reduction of molecular oxygen or the oxidation of H_2O_2 and other electroactive analytes. Amatore and colleagues used a platinized carbon-fiber microelectrode to perform direct measurement of $ONOO^-$ in a single cell (*191*). A manganese phthalocyanine modified carbon fiber microelectrode has also been used to quantify $ONOO^-$ at single cell level (*203*).

Miniaturized and Multiplexed Platforms for ROS/RNS Sensing

Simultaneous detection of multiple ROS/RNS is of great biological interest. Multidetection combined with real-time kinetic analysis would allow study of the cross-reactivity of individual species and their interrelated processes, including production, chemical transformation and degradation pathways. Such measurements could provide a more comprehensive understanding of the contribution of individual radicals and their effects in biological systems. An interesting on-chip multiplexed platform was reported by Quinton and collab. This platform allows simultaneous amperometric detection of NO and $ONOO^-$ released by cultured cells (*209*). The device includes a set of gold ultramicroelectrodes (UMEs) of 50 µm diameter, Ag/AgCl reference electrode and gold counter electrode. The NO electrodes were electrochemically modified with poly(eugenol) and poly(phenol) to provide selectivity for NO. The detection was performed amperometrically at 0.8 V vs Ag/AgCl in PBS. The $ONOO^-$ electrodes were uncoated gold electrodes used without further chemical modification of the surface. Detection was performed at -0.1 V vs Ag/AgCl to

measure the reduction of ONOOH. The low applied potential eliminated most electroactive interferences. Figure 10 shows an example of dual NO and $ONOO^-$ measurement on the multiplexed microfabricated platform. The methodology was adapted by the same group to disposable UMEs (*210*) to increase sensitivity and allow detection of low concentrations of NO and $ONOO^-$ released by PMA (phorbol-12-myristate-13-acetate)-induced HL60 cells. These platforms were integrated within cell culture wells. Such devices have potential broad applicability in cell biology for studying real-time oxidative stress in cell cultures.

Translational Aspects: Measurement Challenges and Opportunities in Biological Systems

The studies summarized in the previous sections demonstrate the potential of electrochemical sensors as viable tools for measuring the temporal and spatial accumulation of ROS/RNS. These devices provide important information regarding the role of oxidative stress and facilitate quantitation of these species in biological systems. Advantages of this method include real-time detection at low cost with high spatial resolution, high sensitivity, inexpensive equipment and minimum disturbance of the sample. However, while a large number of electrochemical sensors have been reported in literature for the detection of ROS/RNS, few of these sensors have been actually used for measurements in "real" biological samples. Most reported studies are performed under "ideal" laboratory conditions in standard solutions of laboratory generated radicals. Translation of this technology to biological and biomedial labs is still challenging and has been hampered by several limitations. Many of the reported sensors still require miniaturization, full functionality in the biological environment (e.g. cell cuture medium, tissues), high sensitivity and selectivity as well as biocompatibility with minimum perturbation of the environment. The most critical issues are:

- The non-specific adsorption in biological environments remains problematic and requires engineering of more effective materials and electrode coatings to prevent biofouling. The complexity of the biological environment may compromise the integrity of the sensor surface, resulting in a decrease of response after *in vivo* measurements. This decrease introduces potential measurement errors (*71*, *170*). The post calibration can decrease by up to 40 % of the pre-measurement signal (*211*). Electrode fouling due to the non-specific adsorption of proteins has been identified as the main cause for this decrease (*212*). While several approaches have been reported to address this issue with varying degree of success (e.g. electrode coating with natural proteins such as bovine serum albumin (BSA) or with antifouling polymers such as polyethylene glycol (PEG)), biofouling is still problematic (*71*). By carefully designing the sequence of layers and the type of membrane material, it is possible to achieve pre- and post-calibration with a 5% deviation in the post-measurement calibration (*132*).

In Oxidative Stress: Diagnostics, Prevention, and Therapy Volume 2; Hepel, et al.;
ACS Symposium Series; American Chemical Society: Washington, DC, 2015.

Publication Date (Web): October 13, 2015 | doi: 10.1021/bk-2015-1200.ch013

- Elimination of interferences and overlapping signals from the many electroactive molecules requires better design of the electrode surface to incorporate separation membranes while still enabling detection of the target with high sensitivity. When this is not possible, pattern recognition techniques could be used to discriminate signals (*213*, *214*).
- Achieve and demonstrate selectivity of measurements for ROS/RNS. The various types of ROS/RNS species coexisting in the system are short lived and highly reactive, being involved in dynamically changing reactions. Validation of sensor response with other methods or biological manipulation to selectively suppress, enhance or overexpress the level of these species should be performed to define the nature of the ROS/RNS and confirm the identity of the observed signals. For example, specificity of $O_2^{\bullet-}$ measurements should be confirmed with addition of SOD. Biological manipulations can also be made to enhance NO release. Oxidative and nitrosative stress take place simultaneously and species like $O_2^{\bullet-}$ and NO coexist. $O_2^{\bullet-}$ is converted to peroxynitrate in the presence of NO, which may lead to errors in the determination of individual species. Simultaneous detection of multiple ROS/RNS species should be addressed in the future to study the individual roles, interrelated processes, the kinetics of release and inactivation of the various reactive species. Needle like and planar disk shape electrodes enabling detection of multiple species have been developed as preliminary attempts to build an automated multi-target analytical platform (*205*, *215–217*). Moreover, variation in the oxygen level, medium composition (e.g. some cell culture media may contain antioxidants), environmental conditions, temperature or pH may affect electrochemical signals. Careful evaluation of these variables and testing of interferences in real conditions is necessary before implementation of the device as an analytical tool for biological measurements.
- Many electrodes are still too bulky to be adapted to cell cultures or inserted in tissues. These probes, even if they showed excellent selectivity and sensitivity performance, still need further miniaturization. Nanostructured materials can be implemented in microsensor designs to enlarge the surface area and facilitate miniaturization.

Conclusion and Future Trends

In summary, electrochemical biosensors have demonstrated potential for rapid, sensitive and real-time measurements of a variety of ROS/RNS species. Given the wide range of physiological effects and their critical roles in redox regulation and oxidative stress, the development of fast and accurate methods for the detection of these species is of clinical importance. A variety of such sensors have been designed and some have been applied to biological relevant situations. Sensitive, dynamic and real-time measurement capabilities with possibilities for multiplexing and single cell detection are major advantages of the electrochemical methods over conventional spectrophotometric and fluorescent assays. Unlike

In Oxidative Stress: Diagnostics, Prevention, and Therapy Volume 2; Hepel, et al.;
ACS Symposium Series; American Chemical Society: Washington, DC, 2015.

optical methods, these sensors do not require addition of reagents for the detection of radicals, as the electron transfer is achieved by electrical means. They can also directly quantify ROS/RNS radicals with spatial resolution and can also be adapted for *in vivo* measurements. The main challenge for the future is to design more robust sensors that can be used in the complex biological environment and to enable translation of this technology from the sensing laboratories into the biology and clinical fields. An active cooperation between electroanalytical chemists, biologists and clinicians is needed to ensure successful translation of this technology into the biomedical field.

Future sensors require development of new materials and innovative engineering design of specific membranes with enhanced antifouling properties. There is also a need to improve selectivity and sensitivity of these probes. Recently developed nanopipettes and nanosensors (*218–220*) can potentially be adapted for real time investigations of ROS/RNS in single cells and neurons. Micro-electrochemical sensing arrays consisting of various functionalized UMEs and nanoscale sensors can also be developed in the future to obtain broader mechanistic understanding of the release characteristics of individual ROS/RNS species in biological systems and to determine their contribution to the development of disease. Improved electrochemical sensors with enhanced performance for $O_2^{\bullet-}$, H_2O_2 and $ONOO^-$ could also be obtained by the development of genetically engineered redox proteins (*221*) to enhance the molecular specificity and the electron transfer rate at the electrode surface.

Based on the growing interest in the study of oxidative stress and the growing evidence linking oxidative stress with many diseases, we envision that in the next few years we will see increased research activities in the development of customized microelectrodes designed for measurements in specific biological conditions and sample types. A broader adoption of these sensors by the biomedical community will be promoted through close collaborations beween analytical chemists, biologists, engineers and medical professionals.

Publication Date (Web): October 13, 2015 | doi: 10.1021/bk-2015-1200.ch013

Acknowledgments

This work was supported by NIH # R21NS078738-01 and NSF grants # 1200180, 1336493 and 0954919. Any opinions, findings, and conclusions or recommendations expressed in this material are those of the author(s) and do not necessarily reflect the views of the funding agencies.

References

1. Finkel, T.; Holbrook, N. J. *Nature* **2000**, *408*, 239–247.
2. Klaunig, J. E.; Kamendulis, L. M.; Hocevar, B. A. *Toxicol. Pathol.* **2010**, *38*, 96–109.
3. Jomova, K.; Vondrakova, D.; Lawson, M.; Valko, M. *Mol. Cell. Biochem.* **2010**, *345*, 91–104.
4. Uttara, B.; Singh, A. V.; Zamboni, P.; Mahajan, R. T. *Curr. Neuropharmacol.* **2009**, *7*, 65–74.

5. Reuter, S.; Gupta, S. C.; Chaturvedi, M. M.; Aggarwal, B. B. *Free Radical Biol. Med.* **2010**, *49*, 1603–1616.
6. Higashi, Y.; Noma, K.; Yoshizumi, M.; Kihara, Y. *Circ. J.* **2009**, *73*, 411–418.
7. Palmieri, B.; Sblendorio, V. *Eur. Rev. Med. Pharmacol. Sci.* **2007**, *11*, 383–399.
8. Palmieri, B.; Sblendorio, V. *Eur. Rev. Med. Pharmacol. Sci.* **2007**, *11*, 27–54.
9. Halliwell, B. *Lancet* **1994**, *344*, 721–724.
10. Rahman, K. *Clin. Interv. Aging* **2007**, *2*, 219–236.
11. Xia, T.; Kovochich, M.; Brant, J.; Hotze, M.; Sempf, J.; Oberley, T.; Sioutas, C.; Yeh, J. I.; Wiesner, M. R.; Nel, A. E. *Nano Lett.* **2006**, *6*, 1794–1807.
12. Gilgun-Sherki, Y.; Melamed, E.; Offen, D. *Neuropharmacology.* **2001**, *40*, 959–975.
13. Amatore, C.; Arbault, S.; Guille, M.; Lemaitre, F. *Chem. Rev.* **2008**, *108*, 2585–2621.
14. Imlay, J. A. *Nat. Rev. Microbiol.* **2013**, *11*, 443–454.
15. Prior, R. L.; Wu, X.; Schaich, K. *J. Agric. Food Chem.* **2005**, *53*, 4290–4302.
16. Özel, R. E.; Liu, X.; Alkasir, R. S. J.; Andreescu, S. *TrAC, Trends Anal. Chem.* **2014**, *59*, 112–120.
17. Mello, L. D.; Kubota, L. T. *Talanta* **2007**, *72*, 335–348.
18. Kissinger, P. T. *Biosens. Bioelectron.* **2005**, *20*, 2512–2516.
19. Andreescu, S.; Gheorghiu, M.; Özel, R. E.; Wallace, K. N. Methodologies for Toxicity Monitoring and Nanotechnology Risk Assessment. *Biotechnology and Nanotechnology Risk Assessment: Minding and Managing the Potential Threats around Us*; ACS Symposium Series; Ripp, S., Henry, T. B., Eds.; American Chemical Society: Washington, DC, 2011; Vol. 1079, pp 141−180.
20. Özel, R. E.; Wallace, K. N.; Andreescu, S. *Anal. Chim. Acta* **2011**, *695*, 89–95.
21. Özel, R. E.; Ispas, C.; Ganesana, M.; Leiter, J. C.; Andreescu, S. *Biosens. Bioelectron.* **2014**, *52*, 397–402.
22. Özel, R. E.; Hayat, A.; Wallace, K. N.; Andreescu, S. *RSC Adv.* **2013**, *3*, 15298–15309.
23. Khan, M. T.; Furchgott, R. F. Additional Evidence that Endothelium-Drived Relaxing Facotr is Nitric Oxide. In *Pharmacology: Proceedings of the Xth International Congress of Pharmacology (IUPHAR)*, Sydney, Australia, August 23−29, 1987;Rand, M. J., Raper, C., Eds.; Elsevier: Amsterdam, 1987.
24. Ignarro, L. J.; Buga, G. M.; Wood, K. S.; Byrns, R. E.; Chaudhuri, G. *Proc. Natl. Acad. Sci. U. S. A.* **1987**, *84*, 9265–9269.
25. Palmer, R. M. J.; Ferrige, A. G.; Moncada, S. *Nature* **1987**, *327*, 524–526.
26. Beckman, J. S.; Koppenol, W. H. *Am. J. Physiol.: Cell Physiol.* **1996**, *271*, C1424–C1437.
27. Kelm, M. *Biochim. Biophys. Acta, Bioenerg.* **1999**, *1411*, 273–289.
28. Knott, A. B.; Bossy-Wetzel, E. *Diabetes, Obes. Metab.* **2010**, *12*, 126–133.

Publication Date (Web): October 13, 2015 | doi: 10.1021/bk-2015-1200.ch013

29. Thomas, D. D.; Ridnour, L. A.; Isenberg, J. S.; Flores-Santana, W.; Switzer, C. H.; Donzelli, S.; Hussain, P.; Vecoli, C.; Paolocci, N.; Ambs, S.; Colton, C. A.; Harris, C. C.; Roberts, D. D.; Wink, D. A. *Free Radical Biol. Med.* **2008**, *45*, 18–31.
30. Flammer, A.; Lüscher, T. *Pfluegers Arch.* **2010**, *459*, 1005–1013.
31. Förstermann, U. *Pfluegers Arch.* **2010**, *459*, 923–939.
32. Wilcox, C. S. *Am. J. Physiol.: Regul., Integr. Comp. Physiol.* **2005**, *289*, R913–R35.
33. Kuklinska, A. M.; Mroczko, B.; Musial, W. J.; Usowicz-Szarynska, M.; Sawicki, R.; Borowska, H.; Knapp, M.; Szmitkowski, M. *Int. Heart J.* **2009**, *50*, 341–351.
34. Calabrese, V.; Mancuso, C.; Calvani, M.; Rizzarelli, E.; Butterfield, D. A.; Giuffrida Stella, A. M. *Nat. Rev. Neurosci.* **2007**, *8*, 766–775.
35. Steinert, J. R.; Chernova, T.; Forsythe, I. D. *Neuroscientist* **2010**, *16*, 435–452.
36. Baptist, A. P.; Khan, F. I.; Wang, Y.; Ager, J. J. *Asthma* **2008**, *45*, 670–674.
37. Mocellin, S.; Bronte, V.; Nitti, D. *Med. Res. Rev.* **2007**, *27*, 317–352.
38. Pitocco, D.; Zaccardi, F.; Di Stasio, E.; Romitelli, F.; Santini, S. A.; Zuppi, C.; Ghirlanda, G. *Rev. Diabet. Stud.* **2010**, *7*, 15–25.
39. Kirino, T. *J. Cereb. Blood Flow Metab.* **2002**, *22*, 1283–1296.
40. Hall, C. N.; Garthwaite, J. *Nitric Oxide* **2009**, *21*, 92–103.
41. Thomas, D. D.; Liu, X.; Kantrow, S. P.; Lancaster, J. R. *Proc. Natl. Acad. Sci. U. S. A.* **2001**, *98*, 355–360.
42. Green, L. C.; Wagner, D. A.; Glogowski, J.; Skipper, P. L.; Wishnok, J. S.; Tannenbaum, S. R. *Anal. Biochem.* **1982**, *126*, 131–138.
43. Xu, Y. C.; Cao, Y. L.; Guo, P.; Tao, Y.; Zhao, B. L. *Phytopathology* **2004**, *94*, 402–407.
44. Wojtas, J.; Bielecki, Z.; Stacewicz, T.; Mikolajczyk, J.; Medrzycki, R.; Rutecka, B. *Acta Phys. Pol., A.* **2011**, *120*, 794–797.
45. Ridnour, L. A.; Sim, J. E.; Hayward, M. A.; Wink, D. A.; Martin, S. M.; Buettner, G. R.; Spitz, D. R. *Anal. Biochem.* **2000**, *281*, 223–229.
46. Spasojević, I.; Batinić-Haberle, I.; Fridovich, I. *Nitric Oxide* **2000**, *4*, 526–533.
47. Hausladen, A.; Rafikov, R.; Angelo, M.; Singel, D. J.; Nudler, E.; Stamler, J. S. *Proc. Natl. Acad. Sci. U. S. A.* **2007**, *104*, 2157–2162.
48. McQuade, L. E.; Lippard, S. *J. Curr. Opin. Chem. Biol.* **2010**, *14*, 43–49.
49. Miao, R.; Mu, L.; Zhang, H.; Xu, H.; She, G.; Wang, P.; Shi, W. *J. Mater. Chem.* **2012**, *22*, 3348–3353.
50. Sun, J.; Zhang, X.; Broderick, M.; Fein, H. *Sensors* **2003**, *3*, 276–284.
51. Yang, Y.; Seidlits, S. K.; Adams, M. M.; Lynch, V. M.; Schmidt, C. E.; Anslyn, E. V.; Shear, J. B. *J. Am. Chem. Soc.* **2010**, *132*, 13114–13116.
52. Xu, T.; Scafa, N.; Xu, L.-P.; Su, L.; Li, C.; Zhou, S.; Liu, Y.; Zhang, X. *Electroanalysis* **2014**, *26*, 449–468.
53. Bedioui, F.; Griveau, S. *Electroanalysis* **2013**, *25*, 587–600.
54. Christodoulou, D.; Kudo, S.; Cook, J. A.; Krishna, M. C.; Miles, A.; Grisham, M. B.; Murugesan, R.; Ford, P. C.; Wink, D. A. *Methods Enzymol.* **1996**, *268*, 69–83.

Publication Date (Web): October 13, 2015 | doi: 10.1021/bk-2015-1200.ch013

55. Privett, B. J.; Shin, J. H.; Schoenfisch, M. H. *Chem. Soc. Rev.* **2010**, *39*, 1925–1935.
56. Trouillon, R. *Biol. Chem.* **2013**, *394*, 17–33.
57. Zhang, X. *Front. Biosci.* **2004**, *9*, 3434–3446.
58. Bedioui, F.; Villeneuve, N. *Electroanalysis* **2003**, *15*, 5–18.
59. Bedioui, F.; Quinton, D.; Griveau, S.; Nyokong, T. *Phys. Chem. Chem. Phys.* **2010**, *12*, 9976–9988.
60. Pekarova, M.; Lojek, A.; Hrbac, J.; Kuchta, R.; Kadlec, J.; Kubala, L. *Folia Biol.* **2014**, *60*, 8–12.
61. Shibuki, K. *Neurosci. Res.* **1990**, *9*, 69–76.
62. Severinghaus, J.; Astrup, P. *J. Clin. Monit. Comput.* **1986**, *2*, 125–139.
63. Huang, C.; Brisbois, E.; Meyerhoff, M. *Anal. Bioanal. Chem.* **2011**, *400*, 1125–1135.
64. Wynne, A. M.; Reid, C. H.; Finnerty, N. J. *J. Electroanal. Chem.* **2014**, *732*, 110–116.
65. Quinton, D.; Girard, A.; Thi Kim, L. T.; Raimbault, V.; Griscom, L.; Razan, F.; Griveau, S.; Bedioui, F. *Lab Chip.* **2011**, *11*, 1342–1350.
66. Wang, Y.; Noël, J.-M.; Velmurugan, J.; Nogala, W.; Mirkin, M. V.; Lu, C.; Collignon, M. G.; Lemaître, F.; Amatore, C. *Proc. Natl. Acad. Sci. U. S. A.* **2012**, *109*, 11534–11539.
67. Lee, Y.; Yang, J.; Rudich, S. M.; Schreiner, R. J.; Meyerhoff, M. E. *Anal. Chem.* **2003**, *76*, 545–551.
68. Amatore, C.; Arbault, S.; Koh, A. C. W. *Anal. Chem.* **2010**, *82*, 1411–1419.
69. Finnerty, N. J.; Bolger, F. B.; Pålsson, E.; Lowry, J. P. *ACS Chem. Neurosci.* **2013**, *4*, 825–831.
70. Quinton, D.; Porras-Gutiérrez, A. G.; Gutiérrez-Granados, S.; Griveau, S.; Bedioui, F. *ECS Trans.* **2010**, *25*, 39–46.
71. Njagi, J.; Erlichman, J. S.; Aston, J. W.; Leiter, J. C.; Andreescu, S. *Sens. Actuators, B* **2010**, *143*, 673–680.
72. Finnerty, N. J.; O'Riordan, S. L.; Palsson, E; Lowry, J. P. *J. Neurosci. Methods* **2012**, *209*, 13–21.
73. Ferreira, N. R.; Ledo, A.; Frade, J. G.; Gerhardt, G. A.; Laranjinha, J.; Barbosa, R. M. *Anal. Chim. Acta* **2005**, *535*, 1–7.
74. Brunet, A.; Privat, C.; Stepien, O.; David-Dufilho, M.; Devynck, J.; Devynck, M. A. *Analusis* **2000**, *28*, 469–474.
75. Diab, N.; Oni, J.; Schulte, A.; Radtke, I.; Blöchl, A.; Schuhmann, W. *Talanta* **2003**, *61*, 43–51.
76. Biesaga, M.; Pyrzyńska, K.; Trojanowicz, M. *Talanta* **2000**, *51*, 209–224.
77. Oliveira, T. I. S.; dos Santos, V. N.; Lomonaco, D.; Correia, A. N.; Mazetto, S. E.; de Lima-Neto, P. *J. Electrochem. Soc.* **2013**, *160*, B113–B118.
78. Vilakazi, S. L.; Nyokong, T. *J. Electroanal. Chem.* **2001**, *512*, 56–63.
79. Griveau, S.; Dumézy, C.; Séguin, J.; Chabot, G. G.; Scherman, D.; Bedioui, F. *Anal. Chem.* **2006**, *79*, 1030–1033.
80. Nyokong, T.; Vilakazi, S. *Talanta* **2003**, *61*, 27–35.
81. Mao, L.; Yamamoto, K.; Zhou, W.; Jin, L. *Electroanalysis* **2000**, *12*, 72–77.
82. Nguyen, T. Q.; Escaño, M. C. S.; Kasai, H. *J. Phys. Chem. C* **2010**, *114*, 10017–10021.

Publication Date (Web): October 13, 2015 | doi: 10.1021/bk-2015-1200.ch013

83. Vilakazi, S.; Nyokong, T. *Polyhedron* **2000**, *19*, 229–234.
84. Cárdenas-Jirón, G. I.; Gonzalez, C.; Benavides, J. *J. Phys. Chem. C* **2012**, *116*, 16979–16984.
85. Vasilescu, A.; Noguer, T.; Andreescu, S.; Calas-Blanchard, C.; Bala, C.; Marty, J.-L. *Talanta* **2003**, *59*, 751–765.
86. Pumera, M.; Ambrosi, A.; Bonanni, A.; Chng, E. L. K.; Poh, H. L. *TrAC, Trends Anal. Chem.* **2010**, *29*, 954–965.
87. Yáñez-Sedeño, P.; Pingarrón, J. M.; Riu, J.; Rius, F. X. *TrAC, Trends Anal. Chem.* **2010**, *29*, 939–953.
88. Chen, D.; Feng, H.; Li, J. *Chem. Rev.* **2012**, *112*, 6027–6053.
89. Gan, T.; Hu, S. *Microchim. Acta* **2011**, *175*, 1–19.
90. Li, W.; Geng, X.; Guo, Y.; Rong, J.; Gong, Y.; Wu, L.; Zhang, X. *ACS Nano* **2011**, *5*, 6955–6961.
91. Guo, C. X.; Ng, S. R.; Khoo, S. Y.; Zheng, X.; Chen, P.; Li, C. M. *ACS Nano* **2012**, *6*, 6944–6951.
92. Jiang, S.; Cheng, R.; Wang, X.; Xue, T.; Liu, Y.; Nel, A.; Huang, Y.; Duan, X. *Nat. Commun.* **2013**, *4*.
93. Liu, Y. M.; Punckt, C.; Pope, M. A.; Gelperin, A.; Aksay, I. A. *ACS Appl. Mater. Interfaces* **2013**, *5*, 12624–12630.
94. Wang, F.; Chen, X. W.; Chen, Z. L. *Microchim. Acta* **2011**, *173*, 65–72.
95. Zhao, L.; Zhu, S.; Zhou, J. *Sens. Actuators, B* **2012**, *171*, 563–571.
96. Santos, R. M.; Rodrigues, M. S.; Laranjinha, J.; Barbosa, R. M. *Biosens. Bioelectron.* **2013**, *44*, 152–159.
97. Wang, L.; Hu, P.; Deng, X.; Wang, F.; Chen, Z. *Biosens. Bioelectron.* **2013**, *50*, 57–61.
98. Luo, X.; Morrin, A.; Killard, A. J.; Smyth, M. R. *Electroanalysis* **2006**, *18*, 319–326.
99. Yan, Y.; Yao, P.; Mu, Q.; Wang, L.; Mu, J.; Li, X.; Kang, S.-Z. *Appl. Surf. Sci.* **2011**, *258*, 58–63.
100. Zhang, L.; Ni, Y.; Wang, X.; Zhao, G. *Talanta* **2010**, *82*, 196–201.
101. Kannan, P.; John, S. A. *Electrochim. Acta* **2010**, *55*, 3497–3503.
102. Deng, X.; Wang, F.; Chen, Z. *Talanta* **2010**, *82*, 1218–1224.
103. Maluta, J. R.; Canevari, T. C.; Machado, S. A. S. *J. Solid State Electrochem.* **2014**, *18*, 2497–2504.
104. Jo, A.; Do, H.; Jhon, G. J.; Suh, M.; Lee, Y. *Neurosci. Lett.* **2011**, *498*, 22–25.
105. Chen, W.; Cai, S.; Ren, Q.-Q.; Wen, W.; Zhao, Y.-D. *Analyst* **2012**, *137*, 49–58.
106. Nauseef, W. M. *Biochim. Biophys. Acta, Gen. Subj.* **2014**, *1840*, 757–767.
107. Sellers, R. M. *Analyst* **1980**, *105*, 950–954.
108. Eisenberg, G. *Ind. Eng. Chem., Anal. Ed.* **1943**, *15*, 327–328.
109. Lin, V. S.; Dickinson, B. C.; Chang, C. *J. Methods Enzymol.* **2013**, *526*, 19–43.
110. Liu, Y. A.; Liao, X. *Curr. Org. Chem.* **2013**, *17*, 654–669.
111. Oh, W.-K.; Jeong, Y. S.; Kim, S.; Jang, J. *ACS Nano* **2012**, *6*, 8516–8524.
112. Wilson, G. S.; Hu, Y. B. *Chem. Rev.* **2000**, *100*, 2693–2704.
113. Ispas, C.; Njagi, J.; Cates, M.; Andreescu, S. *J. Electrochem. Soc.* **2008**, *155*, F169–F176.

Publication Date (Web): October 13, 2015 | doi: 10.1021/bk-2015-1200.ch013

114. Zhang, Y.; Sun, X.; Zhu, L.; Shen, H.; Jia, N. *Electrochim. Acta* **2011**, *56*, 1239–1245.
115. Zhang, Q.; Qiao, Y.; Zhang, L.; Wu, S.; Zhou, H.; Xu, J.; Song, X.-M. *Electroanalysis* **2011**, *23*, 900–906.
116. Meng, F.; Yan, X.; Liu, J.; Gu, J.; Zou, Z. *Electrochim. Acta* **2011**, *56*, 4657–4662.
117. Huang, K.-J.; Niu, D.-J.; Liu, X.; Wu, Z.-W.; Fan, Y.; Chang, Y.-F.; Wu, Y.-Y. *Electrochim. Acta* **2011**, *56*, 2947–2953.
118. Liu, M.; Liu, R.; Chen, W. *Biosens. Bioelectron.* **2013**, *45*, 206–212.
119. Xi, F.; Zhao, D.; Wang, X.; Chen, P. *Electrochem. Commun.* **2013**, *26*, 81–84.
120. Yan, Q.; Wang, Z.; Zhang, J.; Peng, H.; Chen, X.; Hou, H.; Liu, C. *Electrochim. Acta* **2012**, *61*, 148–153.
121. Koposova, E.; Liu, X.; Kisner, A.; Ermolenko, Y.; Shumilova, G.; Offenhäusser, A.; Mourzina, Y. *Biosens. Bioelectron.* **2014**, *57*, 54–58.
122. Lee, Y. J.; Park, J. Y.; Kim, Y.; Ko, J. W. *Curr. Appl Phys.* **2011**, *11*, 211–216.
123. Gaynor, J. D.; Karakoti, A. S.; Inerbaev, T.; Sanghavi, S.; Nachimuthu, P.; Shutthanandan, V.; Seal, S.; Thevuthasan, S. *J. Mater. Chem. B* **2013**, *1*, 3443–3450.
124. Magro, M.; Baratella, D.; Pianca, N.; Toninello, A.; Grancara, S.; Zboril, R.; Vianello, F. *Sens. Actuators, B* **2013**, *176*, 315–322.
125. Palmisano, F.; Zambonin, P. G.; Centonze, D. *Fresenius' J., Anal. Chem.* **2000**, *366*, 586–601.
126. Vaidya, R.; Wilkins, E. *Med. Eng. Phys.* **1994**, *16*, 416–421.
127. Bridge, K. A.; Higson, S. P. *J. Electroanalysis* **2001**, *13*, 191–198.
128. Myler, S.; Eaton, S.; Higson, S. P. *J. Anal. Chim. Acta* **1997**, *357*, 55–61.
129. Walker, E.; Wang, J.; Hamdi, N.; Monbouquette, H. G.; Maidment, N. T. *Analyst* **2007**, *132*, 1107–1111.
130. Hamdi, N.; Wang, J. J.; Walker, E.; Maidment, N. T.; Monbouquette, H. G. *J. Electroanal. Chem.* **2006**, *591*, 33–40.
131. Hamdi, N.; Wang, J. J.; Monbouquette, H. G. *J. Electroanal. Chem.* **2005**, *581*, 258–264.
132. Killoran, S. J.; O'Neill, R. D. *Electrochim. Acta* **2008**, *53*, 7303–7012.
133. McAteer, K.; O'Neill, R. D. *Analyst* **1996**, *121*, 773–777.
134. Lowry, J. P.; Miele, M.; O'Neill, R. D.; Boutelle, M. G.; Fillenz, M. *J. Neurosci. Methods* **1998**, *79*, 65–74.
135. Clark, R. A.; Zerby, S. E.; Ewing, A. G. Electrochemistry in neuronal microenvironments; In *Electroanalytical Chemistry*; Bard, A. J., Rubinstein, I., Eds.; Marcel Dekker: New York, NY, 1998; Vol. 20, pp 227−294.
136. Mizutani, F.; Sato, Y.; Hirata, Y.; Sawaguchi, T.; Yabuki, S. *Anal. Chim. Acta* **1998**, *364*, 173–179.
137. Wilson, G. S.; Gifford, R. *Biosens. Bioelectron.* **2005**, *20*, 2388–2403.
138. Bartlett, P. N.; Cooper, J. M. *J. Electroanal. Chem.* **1993**, *362*, 1–12.
139. Cosnier, S. *Electroanalysis* **1997**, *9*, 894–902.
140. Christie, I. M.; Vadgama, P.; Loyd, S. *Anal. Chim. Acta* **1993**, *274*, 191–199.
141. Vaidya, R.; Atanasov, P.; Wilkins, E. *Med. Eng. Phys.* **1995**, *17*, 416–424.

Publication Date (Web): October 13, 2015 | doi: 10.1021/bk-2015-1200.ch013

142. Burmeister, J. J.; Palmer, M.; Gerhardt, G. A. *Biosens. Bioelectron.* **2005**, *20*, 1772–1779.
143. Matsumoto, T.; Furusawa, M.; Fujiwara, H.; Matsumoto, Y.; Ito, N. *Sens. Actuators, B* **1998**, *49*, 68–72.
144. Zhang, F.; Chan, S. W.; Spanier, J. E.; Apak, E.; Jin, Q.; Robinson, R. D.; Herman, I. P. *Appl. Phys. Lett.* **2002**, *80*, 127.
145. Hu, Y. B.; Mitchell, K. M.; Albahadily, F. N.; Michaelis, E. K.; Wilson, G. S. *Brain Res.* **1994**, *659*, 117–125.
146. Brown, F. O.; Lowry, J. P. *Analyst* **2003**, *128*, 700–705.
147. Suraniti, E.; Ben-Amor, S.; Landry, P.; Rigoulet, M.; Fontaine, E.; Bottari, S.; Devin, A.; Sojic, N.; Mano, N.; Arbault, S. *Angew. Chem., Int. Ed.* **2014**, *53*, 6655–6658.
148. Matharu, Z.; Enomoto, J.; Revzin, A. *Anal. Chem.* **2013**, *85*, 932–939.
149. Bartosz, G. *Clin. Chim. Acta* **2006**, *368*, 53–76.
150. Chen, R.; Warden, J. T.; Stenken, J. A. *Anal. Chem.* **2004**, *76*, 4734–4740.
151. Dwyer, D. J.; Belenky, P. A.; Yang, J. H.; MacDonald, I. C.; Martell, J. D.; Takahashi, N.; Chan, C. T. Y.; Lobritz, M. A.; Braff, D.; Schwarz, E. G.; Ye, J. D.; Pati, M.; Vercruysse, M.; Ralifo, P. S.; Allison, K. R.; Khalil, A. S.; Ting, A. Y.; Walker, G. C.; Collins, J. J. *Proc. Natl. Acad. Sci. U. S. A.* **2014**, *111*, E2100–E2109.
152. Roubaud, V.; Sankarapandi, S.; Kuppusamy, P.; Tordo, P.; Zweier, J. L. *Anal. Biochem.* **1998**, *257*, 210–217.
153. Rosen, G. M.; Pou, S.; Ramos, C. L.; Cohen, M. S.; Britigan, B. E. *FASEB J.* **1995**, *9*, 200–209.
154. Kalyanaraman, B.; Darley-Usmar, V.; Davies, K. J. A.; Dennery, P. A.; Forman, H. J.; Grisham, M. B.; Mann, G. E.; Moore, K.; Roberts, L. J., II; Ischiropoulos, H. *Free Radical Biol. Med.* **2012**, *52*, 1–6.
155. Murrant, C. L.; Reid, M. B. *Microsc. Res. Tech.* **2001**, *55*, 236–248.
156. Özel, R. E.; Wallace, K. N.; Andreescu, S. *Environ. Sci.: Nano* **2014**, *1*, 27–36.
157. Chen, W.; Ren, Q. Q.; Yang, Q.; Wen, W.; Zhao, Y. D. *Anal. Lett.* **2012**, *45*, 156–167.
158. Ganesana, M.; Erlichman, J. S.; Andreescu, S. *Free Radical Biol. Med.* **2012**, *53*, 2240–2249.
159. Manning, P.; McNeil, C. J.; Cooper, J. M.; Hillhouse, E. W. *Free Radical Biol. Med.* **1998**, *24*, 1304–1309.
160. Gobi, K. V.; Mizutani, F. *J. Electroanal. Chem.* **2000**, *484*, 172–181.
161. Ge, B.; Lisdat, F. *Anal. Chim. Acta* **2002**, *454*, 53–64.
162. Tian, Y.; Mao, L.; Okajima, T.; Ohsaka, T. *Anal. Chem.* **2002**, *74*, 2428–2434.
163. Cortina-Puig, M.; Muñoz-Berbel, X.; Rouillon, R.; Calas-Blanchard, C.; Marty, J. L. *Bioelectrochemistry* **2009**, *76*, 76–80.
164. Beissenhirtz, M. K.; Scheller, F. W.; Lisdat, F. *Electroanalysis* **2003**, *15*, 1425–1435.
165. Beissenhirtz, M. K.; Scheller, F. W.; Lisdat, F. *Anal. Chem.* **2004**, *76*, 4665–4671.

Publication Date (Web): October 13, 2015 | doi: 10.1021/bk-2015-1200.ch013

166. Wegerich, F.; Turano, P.; Allegrozzi, M.; Möhwald, H.; Lisdat, F. *Anal. Chem.* **2009**, *81*, 2976–2984.
167. Scheller, W.; Jin, W.; Ehrentreich-Förster, E.; Ge, B.; Lisdat, F.; Büttemeier, R.; Wollenberger, U.; Scheller, F. W. *Electroanalysis* **1999**, *11*, 703–706.
168. Büttemeyer, R.; Philipp, A. W.; Mall, J. W.; Ge, B.; Scheller, F. W.; Lisdat, F. *Microsurgery* **2002**, *22*, 108–113.
169. Henderson, J. R.; Swalwell, H.; Boulton, S.; Manning, P.; McNeil, C. J.; Birch-Machin, M. A. *Free Radical Res.* **2009**, *43*, 796–802.
170. Rahman, M. A.; Kothalam, A.; Choe, E. S.; Won, M. S.; Shim, Y. B. *Anal. Chem.* **2012**, *84*, 6654–6660.
171. Descroix, S.; Bedioui, F. *Electroanalysis* **2001**, *13*, 524–528.
172. Mesároš, Š.; Vaňková, Ž.; Grunfeld, S.; Mesárošová, A.; Malinski, T. *Anal. Chim Acta* **1998**, *358*, 27–33.
173. Song, M. I.; Bier, F. F.; Scheller, F. W. *Bioelectrochem. Bioenerg.* **1995**, *38*, 419–422.
174. Lvovich, V.; Scheeline, A. *Anal. Chem.* **1997**, *69*, 454–462.
175. Pernot, P.; Mothet, J. P.; Schuvailo, O.; Soldatkin, A.; Pollegioni, L.; Pilone, M.; Adeline, M. T.; Cespuglio, R.; Marinesco, S. *Anal. Chem.* **2008**, *80*, 1589–1597.
176. Endo, K.; Miyasaka, T.; Mochizuki, S.; Aoyagi, S.; Himi, N.; Asahara, H.; Tsujioka, K.; Sakai, K. *Sens. Actuators, B* **2002**, *83*, 30–34.
177. Tian, Y.; Mao, L.; Okajima, T.; Ohsaka, T. *Biosens. Bioelectron.* **2005**, *21*, 557–564.
178. Wang, X.; Han, M.; Bao, J.; Tu, W.; Dai, Z. *Anal. Chim. Acta* **2012**, *717*, 61–66.
179. Beissenhirtz, M. K.; Scheller, F. W.; Viezzoli, M. S.; Lisdat, F. *Anal. Chem.* **2005**, *78*, 928–935.
180. Kapp, A.; Beissenhirtz, M. K.; Geyer, F.; Scheller, F.; Viezzoli, M. S.; Lisdat, F. *Electroanalysis* **2006**, *18*, 1909–1915.
181. Tian, Y.; Mao, L. Q.; Okajima, T.; Ohsaka, T. *Biosens. Bioelectron.* **2005**, *21*, 557–564.
182. Ohsaka, T.; Tian, Y.; Shioda, M.; Kasahara, S.; Okajima, T. *Chem. Commun.* **2002**, 990–991.
183. Tian, Y.; Ariga, T.; Takashima, N.; Okajima, T.; Mao, L. Q.; Ohsaka, T. *Electrochem. Commun.* **2004**, *6*, 609–614.
184. Yuasa, M.; Oyaizu, K.; Yamaguchi, A.; Ishikawa, M.; Eguchi, K.; Kobayashi, T.; Toyoda, Y.; Tsutsui, S. *Polym. Adv. Technol.* **2005**, *16*, 287–292.
185. Yuasa, M.; Oyaizu, K.; Yamaguchi, A.; Ishikawa, M.; Eguchi, K.; Kobayashi, T.; Toyoda, Y.; Tsutsui, S. *Polym. Adv. Technol.* **2005**, *16*, 616–621.
186. Fujita, M.; Tsuruta, R.; Kasaoka, S.; Fujimoto, K.; Tanaka, R.; Oda, Y.; Nanba, M.; Igarashi, M.; Yuasa, M.; Yoshikawa, T.; Maekawa, T. *Free Radical Biol. Med.* **2009**, *47*, 1039–1048.
187. Arbault, S.; Pantano, P.; Jankowski, J. A.; Vuillaume, M.; Amatore, C. *Anal. Chem.* **1995**, *67*, 3382–3390.

Publication Date (Web): October 13, 2015 | doi: 10.1021/bk-2015-1200.ch013

188. Arbault, S.; Pantano, P.; Sojic, N.; Amatore, C.; Best-Belpomme, M.; Sarasin, A.; Vuillaume, M. *Carcinogenesis* **1997**, *18*, 569–574.
189. Arbault, S.; Sojic, N.; Bruce, D.; Amatore, C.; Sarasin, A.; Vuillaume, M. *Carcinogenesis* **2004**, *25*, 509–515.
190. Wang, Y.; Noël, J.-M.; Velmurugan, J.; Nogala, W.; Mirkin, M. V.; Lu, C.; Collignon, M. G.; Lemaître, F.; Amatore, C. *Proc. Natl. Acad. Sci. U. S. A.* **2012**, *109*, 11534–11539.
191. Amatore, C.; Arbault, S.; Bruce, D.; de Oliveira, P.; Erard, M.; Vuillaume, M. *Chem. - Eur. J.* **2001**, *7*, 4171–4179.
192. Szabo, C.; Ischiropoulos, H.; Radi, R. *Nat. Rev. Drug Discovery* **2007**, *6*, 662–680.
193. Pacher, P.; Beckman, J. S.; Liaudet, L. *Physiol. Rev.* **2007**, *87*, 315–424.
194. Mythri, R.; Harish, G.; Dubey, S.; Misra, K.; Srinivas Bharath, M. M. *Mol. Cell. Biochem.* **2011**, *347*, 135–143.
195. Ahmad, R.; Rasheed, Z.; Ahsan, H. *Immunopharmacol. Immunotoxicol.* **2009**, *31*, 388–396.
196. García-Ruiz, I.; Fernández-Moreira, D.; Solís-Muñoz, P.; Rodríguez-Juan, C.; Díaz-Sanjuán, T.; Muñoz-Yagüe, T.; Solís-Herruzo, J. A. *J. Proteome Res.* **2010**, *9*, 2450–2459.
197. Kim, J.; Seok, Y. M.; Jung, K. J.; Park, K. M. *Am. J. Physiol-Renal.* **2009**, *297*, F461–F470.
198. Yang, D.; Wang, H. L.; Sun, Z. N.; Chung, N. W.; Shen, J. G. *J. Am. Chem. Soc.* **2006**, *128*, 6004–6005.
199. Sun, Z. N.; Wang, H. L.; Liu, F. Q.; Chen, Y.; Tam, P. K. H.; Yang, D. *Org. Lett.* **2009**, *11*, 1887–1890.
200. Ueno, T.; Urano, Y.; Kojima, H.; Nagano, T. *J. Am. Chem. Soc.* **2006**, *128*, 10640–0641.
201. Sieracki, N. A.; Gantner, B. N.; Mao, M.; Horner, J. H.; Ye, R. D.; Malik, A. B.; Newcomb, M. E.; Bonini, M. G. *Free Radical Biol. Med.* **2013**, *61*, 40–50.
202. Lin, W.; Buccella, D.; Lippard, S. J. *J. Am. Chem. Soc.* **2013**, *135*, 13512–13520.
203. Xue, J.; Ying, X.; Chen, J.; Xian, Y.; Jin, L.; Jin, J. *Anal. Chem.* **2000**, *72*, 5313–5321.
204. Cortés, J. S.; Granados, S. G.; Ordaz, A. A.; Jiménez, J. A. L.; Griveau, S.; Bedioui, F. *Electroanalysis* **2007**, *19*, 61–64.
205. Kubant, R.; Malinski, C.; Burewicz, A.; Malinski, T. *Electroanalysis* **2006**, *18*, 410–416.
206. Koh, W. C. A.; Son, J. I.; Choe, E. S.; Shim, Y. B. *Anal. Chem.* **2010**, *82*, 10075–10082.
207. Wang, Y.; Chen, Z. *Talanta* **2010**, *82*, 534–539.
208. Hosu, S. I.; Wang, Q.; Vasilescu, A.; Peteu, S. F.; Raditoiu, V.; Railian, S.; Zaitsev, V.; Turcheniuk, K.; Wang, Q.; Li, M.; Boukherroub, R.; Szunerits, S. *RSC Adv.* **2015**, *5*, 1474–1484.
209. Quinton, D.; Girard, A.; Kim, L. T. T.; Raimbault, V.; Griscom, L.; Razan, F.; Griveaua, S.; Bedioui, F. *Lab Chip* **2011**, *11*, 1342–1350.

Publication Date (Web): October 13, 2015 | doi: 10.1021/bk-2015-1200.ch013

210. Kim, L. T. O. T.; Escriou, V.; Griveau, S.; Girard, A.; Griscom, L.; Razan, F.; Bedioui, F. *Electrochim. Acta* **2014**, *140*, 33–36.
211. Sardesai, N. P.; Ganesana, M.; Karimi, A.; Leiter, J. C.; Andreescu, S. *Anal. Chem.* **2015**, *87*, 2996–3003.
212. Behrend, C. E.; Cassim, S. M.; Pallone, M. J.; Daubenspeck, J. A.; Hartov, A.; Roberts, D. W.; Leiter, J. C. *J. Neurosci. Methods* **2009**, *180*, 278–289.
213. Sazonova, N.; Njagi, J. I.; Marchese, Z. S.; Ball, M. S.; Andreescu, S. Schuckers, S. Detection and Prediction of Concentrations of Neurotransmitters Using Voltammetry and Pattern Recognition. *Proceedings of the 31st Annual International Conference of the IEEE Engineering in Medicine and Biology Society*; Minneapolis, MN, September 3−6, 2009; IEEE: 2009.
214. Stefan-van Staden, R. I.; Moldoveanu, I.; van Staden, J. F. *J. Neurosci. Methods* **2014**, *229*, 1–7.
215. Isik, S.; Berdondini, L.; Oni, J.; Blöchl, A.; Koudelka-Hep, M.; Schuhmann, W. *Biosens. Bioelectron.* **2005**, *20*, 1566–1572.
216. Chang, S. C.; Pereira-Rodrigues, N.; Henderson, J. R.; Cole, A.; Bedioui, F.; McNeil, C. *J. Biosens. Bioelectron.* **2005**, *21*, 917–922.
217. Isik, S.; Castillo, J.; Blöchl, A.; Csöregi, E.; Schuhmann, W. *Bioelectrochemistry* **2007**, *70*, 173–179.
218. Actis, P.; Maalouf, M. M.; Kim, H. J.; Lohith, A.; Vilozny, B.; Seger, R. A.; Pourmand, N. *ACS Nano* **2013**, *8*, 546–553.
219. Clausmeyer, J.; Actis, P.; López Córdoba, A.; Korchev, Y.; Schuhmann, W. *Electrochem. Commun.* **2014**, *40*, 28–30.
220. Schrlau, M. G.; Dun, N. J.; Bau, H. H. *ACS Nano* **2009**, *3*, 563–568.
221. Prabhulkar, S.; Tian, H.; Wang, X.; Zhu, J. J.; Li, C. Z. *Antioxid. Redox Signaling* **2012**, *17*, 1796–1822.

Publication Date (Web): October 13, 2015 | doi: 10.1021/bk-2015-1200.ch013

Publication Date (Web): October 13, 2015 | doi: 10.1021/bk-2015-1200.ch014

Chapter 14

Redox Activity of Oxidative Stress-Damping Endogenous Thiol Biomolecules

Agata Chalupa and Maria Hepel*

Department of Chemistry, State University of New York at Potsdam, Potsdam, New York 13676
***E-mail: hepelmr@potsdam.edu**

The internal oxidative-stress control and prevention system in living organisms is based on homeostasis of redox potential. The main effector of this system is the redox couple: glutathione (GSH) and its disulfide (GSSG), with the support of NADPH and GSH reductase. GSH in this redox couple is a ubiquitous reducing agent responsible for neutralization of harmful radicals and reactive oxygen species. However, the processes of GSH oxidation and GSSG reduction on electrodes are strongly hindered. In this Chapter, we present results of our investigations of redox reactivity of endogenous thiols: GSH, cysteine (Cys), and homocysteine (Hcys) on electrocatalytic cobalt phthalocyanine (CoPc) monolayer film on glassy carbon electrode. We show that a strong competition between GSH, Cys, and Hcys exists similar to that observed in thiol-capped Au nanoparticle assembly processes. Detailed investigations indicate that the electroanalytical determination of thiols in multicomponent solutions must take into account the dependence of sensitivity on competitive charge-transfer complex formation.

Introduction

The cellular oxidative stress originates from various internal and external sources. Any process that acts to increase the production of reactive oxygen species (ROS) (*1*, *2*), including H_2O_2, $O_2^{\bullet-}$, and $HO^{\bullet}$, and biomolecular radicals, is causing the oxidative stress. The oxidative stress has a profound impact on

In Oxidative Stress: Diagnostics, Prevention, and Therapy Volume 2; Hepel, et al.;
ACS Symposium Series; American Chemical Society: Washington, DC, 2015.

Publication Date (Web): October 13, 2015 | doi: 10.1021/bk-2015-1200.ch014

life processes (*3*), including the metabolism, energy production, communication pathways, cell cycles, anti-pathogenic defences, and disease control. While the oxidative stress performs an outstanding life-supporting and cellular defense duties, it may also act toward organ damage and disease progression. In the latter category, oxidative stress-generating ROS radicals may participate in carcinogenesis and, for instance, by inducing inflamamtion of heart muscle leading to cardiomyopathy and coronary heart disease (*4*, *5*). The excess of ROS in the brain is damaging the central nervous system leading to such illnesses as the Parkinson's (*6–8*), Down syndrome (*9*, *10*), and autism (*11*, *12*). It has been found that the oxidative stress may cause a serious damage to DNA (*13*, *14*), proteins, and lipids (*3*). It contributes to many debilitating or fatal diseases, such as diabetes (*15*, *16*), Alzheimer's (*17–19*), cardiovascular (*4*, *5*, *20*, *21*), acute renal failure (*22*, *23*), cancer (*24*, *25*), and others, and plays an important role in accelerating the aging process (*3*).

The devastating effects of ROS overproduction can be counterbalanced by anti-oxidants, the compounds scavenging biomolecule radicals and ROS. There are many groups of exogeneous anti-oxidants that are consumed with foods, including flavonoids, polyphenols, phytochemicals, etc. The internal defence system of most living organisms against radical attacks is based on a small biothiol molecule, glutathione (GSH) (*26*) which is a strong reducing agent. GSH undergoes oxidation to glutathione disulfide (GSSG) giving up an electron to a radical, and thereby neutralizing it. The concentration ratio of GSH to GSSG determines the anti-oxidizing power of the couple (*27*, *28*). The depleted GSH can be replenished by the reaction of GSSG with NADPH catalyzed by GSH reductase participating in the redox level homeostasis (*29*, *30*). The sulfhydryl groups of proteins and other biothiol molecules, such as cysteine (Cys), can also participate in maintaining the low redox potential and thus prevent oxidative stress. Analytical determinations of biothiols can be carried out by different techniques. Excellent reviews on this subject have been published (*31*, *32*). The determination of GSH and Cys, as well as homocysteine (Hcys), can be performed using HPLC with fluorescence detection (*33*, *34*), liquid chromatography-mass spectroscopy (LC-MS) (*35*, *36*), gas chromatography-mass spectroscopy (GC-MS) (*35*, *37*) or B-doped diamond electrodes (*38*) but lower cost methods based on resonance elastic light scattering (*39–43*), UV-Vis absorption (*44*), fluorescence (*45–48*), electrochemical techniques (*49–52*) and on sensors (*53–61*) are also available. Lee et al. (*62*) have developed an electrochemical method for detection of GSH and homocysteine by expoiting differences in the rates of their reactions with an *in situ* formed oxidized catechol. The 1,4-Michael addition reaction leads to the formation of an adduct exhibiting a new voltammetric peak which was utilized for sensitive thiol determination. Unfortunately, many electroanalytical methods require extensive pretreatment procedures (*63–75*) to attain sufficient sensitivity. Often, different reagents have been used to either derivatize biothiols or modify their electrochemical activity to achieve better selectivity (*76–81*). Recently, a method for the determination of total concentration of antioxidants: GSH, cysteine, homocysteine, and ascorbic acid, has been developed by Compton et al. (*82*). Distinguishing between GSH, Cys, and Hcys has been attempted (*39*, *40*, *43*, *83–85*) but still remains a challenge, especially due to the structural similarity

of Cys and Hcys. The Au and Ag colloids have been widely used to study the interactions of biothiols with plasmonic nanoparticles (*39*, *40*, *86*, *87*) and to evaluate the ligand exchange processes in nanoparticle-shell self-assembling monolayers using colorimetric or RELS techniques.

The redox reactivity of GSH/GSSG couple in homogeneous biological media is fast due to the enzymatic lowering of activation energy barrier of electron transfer processes. However, on solid electrodes, both the oxidation of GSH and the reduction of GSSG are strongly hindered (*39*). In this Chapter, we present results of investigations of redox reactivity of glutathione, cysteine, and homocysteine on an electrocatalytic cobalt phthalocyanine (CoPc) monolayer film on a glassy carbon electrode (GCE). The studies of GSH oxidation of CoPc have earlier been carried out by Zagal and coworkers (*53*) on CoPc-coated graphite electrodes and polypyrrole-embedded CoPc sensors (*55*), and recently in our group on CoPc-modified glassy carbon and graphene electrodes. We show that a strong competition between GSH, Cys, and Hcys exists similar to that observed in thiol-capped Au nanoparticle assembly processes (*39*, *88*) which prevents a straightforward analysis of multicomponent mixtures of the thiols. Therefore, we have performed detailed investigations to develop a framework for the multicomponent analysis taking into account active matrix effects. The remarkable activity of CoPC acting as an artificial enzyme for oxidation of biothiols and their disulfide reduction may be utilized in future for developing sensitive, fast, and inexpensive biomimetic sensors for screening biomarkers of oxidative stress in doctors office and field health centers.

Publication Date (Web): October 13, 2015 | doi: 10.1021/bk-2015-1200.ch014

Experimental

Chemicals

All chemicals used for investigations were of analytical grade purity. Reduced L-glutathione (GSH), DL-homocysteine (Hcys), L-cysteine (Cys), N,N-Dimethylformamide (DMF), boric acid, acetic acid, and cobalt(II) phthalocyanine were purchased from Sigma-Aldrich Chemical Company (St. Louis, MO, U.S.A.). Sodium phosphate dibasic heptahydrate (Na_2HPO_4•7 H_2O), phosphoric acid and sodium phosphate monobasic dihydrate (NaH_2PO_4•2 H_2O) were obtained from J.T. Baker Chemical Co. Solutions were prepared using Millipore (Billerica, MA, U.S.A.) Milli-Q deionized water (conductivity σ = 55 nS/cm). They were deoxygenated by bubbling with purified nitrogen.

Instrumentation

Cyclic voltammetric (CV) measurements were performed with Elchema potentiostat/galvanostat Model PS-205 (Potsdam, NY, USA) with a three-electrode configuration. Potentials were measured versus the double-junction Ag/AgCl reference electrode, obtained from Elchema, with a 3 M KNO_3 external filling solution. A Pt wire was used as the counter electrode. The glassy carbon

In Oxidative Stress: Diagnostics, Prevention, and Therapy Volume 2; Hepel, et al.;
ACS Symposium Series; American Chemical Society: Washington, DC, 2015.

electrode (GCE) with an area of 7.1 mm^2, obtained from Elchema (Potsdam, NY, U.S.A.) was used as the working electrode. The program waveform was supplied and data acquisition performed by Voltscan 5.0 interactive software from Elchema with 16-bit precision. The measurements were carried out in 50 mM phosphate buffer solutions, pH 7.4, unless otherwise stated. The surface of GCE electrode was polished with 0.05 μm alumina slurry (Coating Service Department, Indianapolis, U.S.A.) on a flat pad and rinsed repeatedly with water to remove any alumina residue. The potential was scanned between -1.1 V and +0.4 V, unless otherwise noted. Subsequent measurements were carried out by polishing the surface of GCE and depositing a fresh electrocatalyst coating.

Publication Date (Web): October 13, 2015 | doi: 10.1021/bk-2015-1200.ch014

Molecular Dynamics Simulation and Quantum Mechanical Calculations

Quantum mechanical calculations of electronic structures for CoPc molecule and its interactions with GSH, cysteine and homocysteine were performed using modified Hartree-Fock methods with 6-31G* basis set and pseudopotentials, semi-empirical PM3 method, and density functional theory (DFT) with B3LYP functional and correlated methods (*89*, *90*). The molecular dynamics simulations and quantum mechanical calculations were carried out using procedures embedded in Wavefunction (Irvine, CA, U.S.A.) Spartan 6. The electron density and local density of states are expressed in atomic units, au^{-3}, where 1 au = 0.52916 Å and 1 au^{-3} = 6.7491 $Å^{-3}$.

Results and Discussion

Cobalt-Phthalocyanine-Coated Catalyst Sensor

The structures of main compounds studied are presented in Scheme 1, including cobalt phthalocyanine (CoPc), glutathione (GSH), homocysteine (Hcys), and cysteine (Cys). Note that Co cation in CoPc complex is formally on the +1 or +2 oxidation state. Upon adsorption or immobilization of CoPc on the electrode surface, it can be oxidized/reduced by appropriately adjusting the electrode potential.

Testing different catalysts for electrooxidation of GSH, Cys, and Hcys, as well as the GSSG reduction, has been performed using derivatives of coumarin, fluorone black, and cobalt phthalocyanine (CoPc) as the electron mediators. Here we present the results obtained with cobalt CoPc electrocatalyst (Scheme 1a and 2). CoPc has unique electron mediation properties and it works specifically with thiols and disulphides. In tests with this catalyst, several electrode materials and different sensor compositions have been prepared and their electroactivity was evaluated. We have found that, the substrates tested, including Au, Pt, and various forms of carbon, do not show any electrocatalytic activity toward thiol oxidation when tested alone. However, when exposed to CoPc, they gain catalytic activity which is then clearly due to the adsorbed CoPc molecules (*53*, *91*, *92*). For instance, carbon electrodes coated with CoPc offer much better catalytic

In Oxidative Stress: Diagnostics, Prevention, and Therapy Volume 2; Hepel, et al.;
ACS Symposium Series; American Chemical Society: Washington, DC, 2015.

activity than bare electrodes. Among different carbons, we have examined the following: glassy carbon (GCE), ordinary graphite (OGE), pyrolytic carbon (PCE), carbon nanotube (CNT) printed electrodes, covalently bound CNT (cbCNT), highly oriented pyrolytic graphite (HOPG), and graphene nanosheet substrates (GNS). Here, we present the results for GCE coated with CoPc. From these measurements, best potentials have been selected for each component to enable differentiation. Different levels of catalytic activity come from CoPC and its specific interactions with the carbon substrates.

Characterization of GCE/CoPC

The CoPC electrocatalyst layer was deposited by casting from a 50 mM CoPc solution in DMF. The adsorption was carried out for 30 min and after that time the drop of casting solution was dislodged and the sensor was washed several times with DMF and distilled water followed by drying in a stream of nitrogen. In Figure 1, cyclic voltammetry characteristics for a GCE/CoPc electrode is presented in the potential range from -1.15 to +0.4 V vs. Ag/AgCl reference. The electrode capacitance, determined at E = -0.5 V, is C = 209.5 μF/cm^2. The high value of differential capacitance is due to the extended real surface area and the catalyst film.

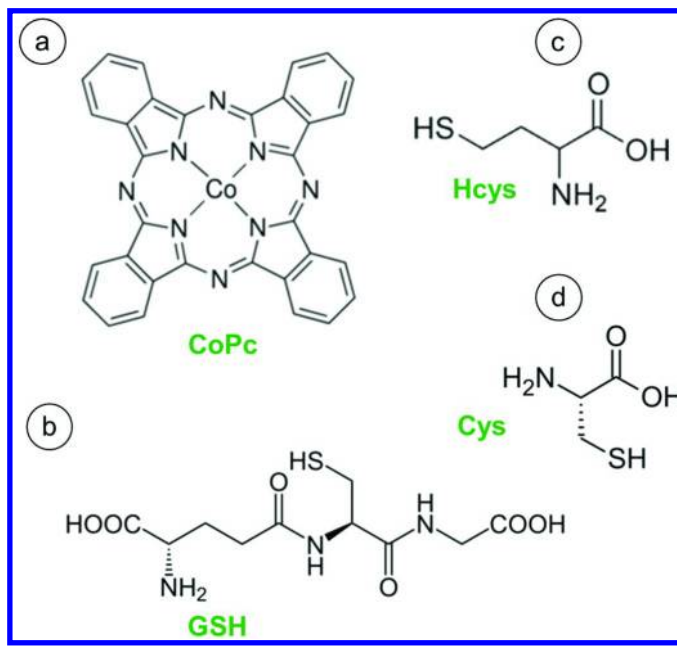

Scheme 1. Structure of the compounds used in the investigations: a) Cobalt phthalocyanine (CoPc); b) glutathione (GSH); c) homocysteine (Hcys), and (d) cysteine.

In Oxidative Stress: Diagnostics, Prevention, and Therapy Volume 2; Hepel, et al.;
ACS Symposium Series; American Chemical Society: Washington, DC, 2015.

Publication Date (Web): October 13, 2015 | doi: 10.1021/bk-2015-1200.ch014

Publication Date (Web): October 13, 2015 | doi: 10.1021/bk-2015-1200.ch014

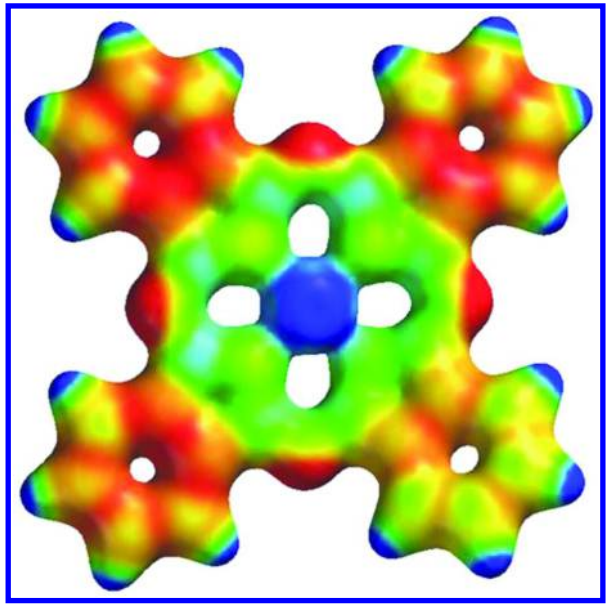

Scheme 2. Electronic density surface with electrostatic potential map of a CoPc molecule; σ = 0.08, potential color coded from high (blue) to low (red). (see color insert)

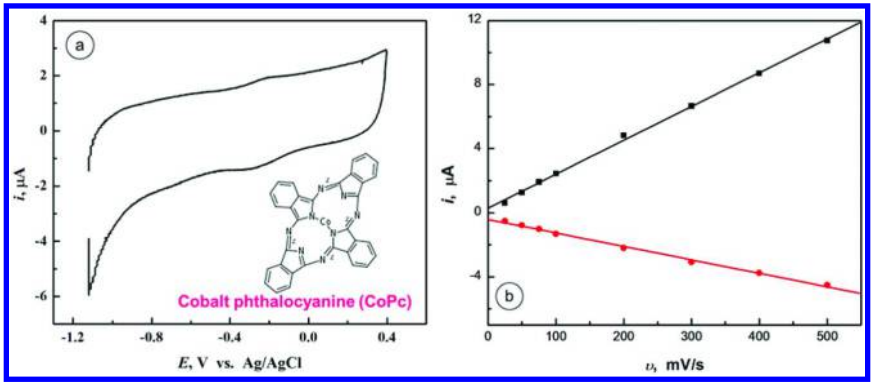

Figure 1. (a) Cyclic voltammogram of the cobalt phthalocyanine-modified glassy carbon electrode (GCE/CoPc); v = 100 mV/s, electrolyte: 50 mM phosphate buffer, pH 7.43; (b) Dependence of $i_{E=0}$ vs. v. The higher slope of the anodic curve (upper line) is due to the contribution of the oxidation current of CoPc.

Electrocatalytic Activity of GCE/CoPc toward GSH Oxidation

The catalytic properties of GCE/CoPc electrode are illustrated in Figure 2a. Voltammetric curve 1 was obtained in 3.85 mM GSH solution on bare

In Oxidative Stress: Diagnostics, Prevention, and Therapy Volume 2; Hepel, et al.;
ACS Symposium Series; American Chemical Society: Washington, DC, 2015.

GCE electrode and curve 2 on GCE/CoPc electrode. It is seen that there is no electrocatalytic activity of the GCE alone, but a pronounced catalytic GSH-oxidation current peak is observed on a GCE/CoPc electrode. On the return scan, a cathodic current peak at E = -0.96 V is observed. It is due to the reduction of GSSG formed during the forward scan at potentials E > -0.2 V. The background curve obtained on a bare GCE in buffer solution is presented in curve 3. There is no extensive background shift on adding GSH to the solution. This is important since the background stability contributes to the measurement accuracy at low analyte concentration.

Publication Date (Web): October 13, 2015 | doi: 10.1021/bk-2015-1200.ch014

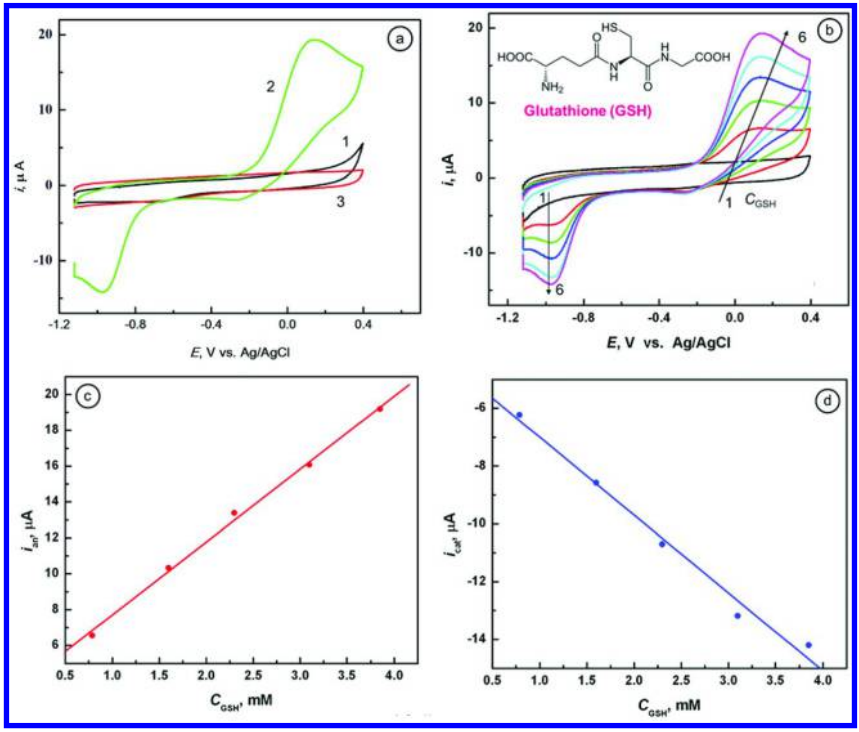

Figure 2. (a) Cyclic voltammograms obtained in 3.85 mM GSH solution for: (1) a bare glassy carbon electrode (GCE) and (2) a cobalt phthalocyanine-modified glassy carbon electrode (GCE/CoPc). Curve (3) was obtained for a bare GCE electrode in buffer solution. (b) Cyclic voltammograms obtained for a GCE/CoPc electrode in solutions with concentrations of GSH, C_{GSH} [mM]: (1) 0, (2) 0.79, (3) 1.6, (4) 2.3, (5) 3.1, (6) 3.85. (c) Dependence of anodic current peak for GSH oxidation (E_{pa} = +0.115 V) on C_{GSH}. (d) Dependence of cathodic peak current for GSSG reduction (E_{pc} = -0.97 V) on C_{GSH}. Other conditions: v = 100 mV/s; 50 mM phosphate buffer, pH 7.43. (see color insert)

In Oxidative Stress: Diagnostics, Prevention, and Therapy Volume 2; Hepel, et al.;
ACS Symposium Series; American Chemical Society: Washington, DC, 2015.

Publication Date (Web): October 13, 2015 | doi: 10.1021/bk-2015-1200.ch014

To confirm that the observed anodic and cathodic currents are due to the oxidation of GSH and reduction of GSSG, respectively, detailed GSH-conecntration studies have been performed. The obtained results are presented in Figures 2-3. A collection of CV curves obtained for a GCE/CoPc electrode in solutions with GSH concentration ranging from 0 to 3.85 mM are presented in Figure 2b. The dependence of anodic current peak at E_{pa} = +0.115 V for GSH oxidation on C_{GSH} is presented in Figure 2c and the dependence of cathodic peak current at E_{pc} = -0.97 V for GSSG reduction on C_{GSH} is presented in Figure 2d.

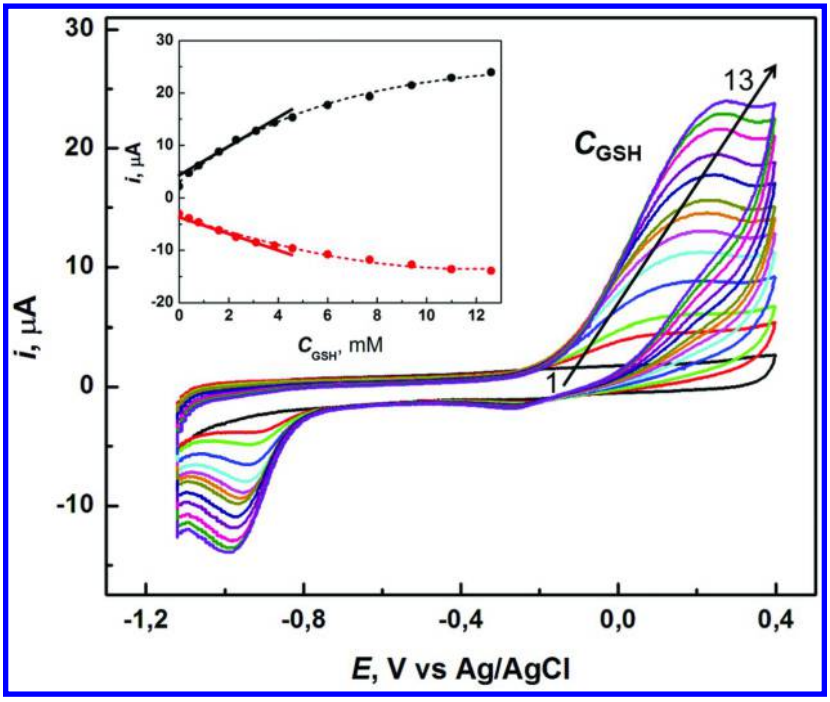

Figure 3. Cyclic voltammograms obtained for GSH solutions for a cobalt phthalocyanine-modified glassy carbon electrode (GCE/CoPc), C_{GSH} [mM]: (1) 0, (2) 0.4, (3) 0.79, (4) 1.6, (5) 2.3, (6) 3.1, (7) 3.85, (8) 4.5, (9) 6.0, (10) 7.7, (11) 9.4, (12) 11, (13) 12.6; 50 mM phosphate buffer, pH 7.43; v = 100 mV/s. INSET: Dependence of i_p vs. C_{GSH}.

The calibration plots in Figure 2 are linear. However, at higher GSH concentrations (C_{GSH} > 4 mM), a nonlinear behavior is clearly observed. It is illustrated in Figure 3.

The dependence of peak current for GSH oxidation and GSG reduction on square root of the scan rate is presented in Figure 4. The plots are linear which confirms that the processes in question involve solution species: GSH and GSSG.

Publication Date (Web): October 13, 2015 | doi: 10.1021/bk-2015-1200.ch014

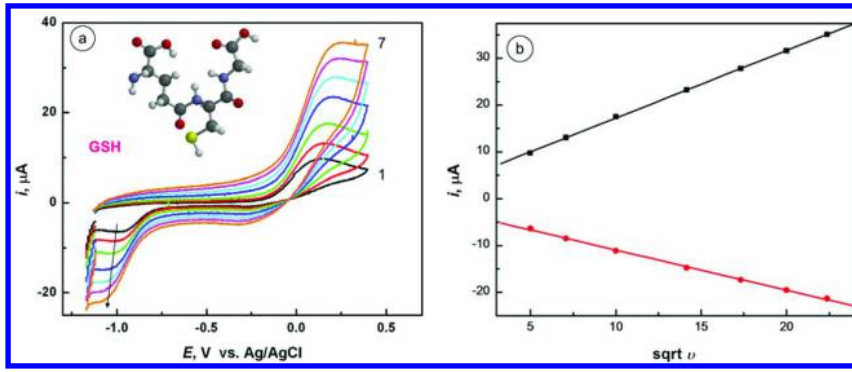

Figure 4. (a) Cyclic voltammograms for 3.85 mM GSH in 50 mM phosphate buffer, pH 7.43 on a cobalt phthalocyanine-modified glassy carbon electrode (GCE/CoPc), recorded at v [mV/s]: (1) 25, (2) 50, (3) 100, (4) 200, (5) 300, (6) 400, (7) 500; (b) dependence of i_p vs. sqrt(v). (see color insert)

Note that the redox potential of GSSG/GSH couple is given by:

$$GSSG + 2H^+ + 2e^- = 2\ GSH \tag{1}$$

$$E = E^{0'}_{GSSG/GSH,pH=7} + \frac{2.303RT}{nF}\log\left(\frac{C_{GSSG}}{C^2_{GSH}}\right) - \frac{2.303RT}{F}(pH - 7) \tag{2}$$

where the relative standard potential at pH = 7 is (*93*, *94*):

$$E^{0'}_{GSSG/GSH,pH=7} = -0.240V \tag{3}$$

where n = 2, R is the gas constant, T is the absolute temperature, and the Nernstian slope $2.302RT/F$ = 0.05916 V at 25 ^{0}C. This shows that even with the electrocatalyst film on GCE, the oxidation process of GSH is still irreversible.

Electrocatalytic Activity of GCE/CoPc toward Hcys Oxidation

The GCE/CoPc electrodes have also been tested for the response to homocysteine and cysteine. In Figure 5, the electrocatalytic properties of GCE and GCE/CoPc toward the oxidation of Hcys are compared. Voltammetric curve 1 was obtained in 3.85 mM Hcys solution on bare GCE electrode and curve 2 on GCE/CoPc electrode. It is seen that there is no electrocatalytic activity of the GCE alone, but pronounced catalytic Hcys-oxidation current peaks are observed on a GCE/CoPc electrode. In contrast to GSH, two anodic peaks for the oxidation of Hcys are observed. They likely correspond to the formation of a radical Hcys$^{\bullet}$ intermediate in the first step, followed by the formation of a disulphide in the second step. On the return scan, a cathodic current peak at E = -0.96 V is observed. It is due to the reduction of homocystine (a disulphide) formed during the forward scan at potentials E > +0.18 V. The background curve obtained on

In Oxidative Stress: Diagnostics, Prevention, and Therapy Volume 2; Hepel, et al.;
ACS Symposium Series; American Chemical Society: Washington, DC, 2015.

a bare GCE in buffer solution is presented in curve 3. There is no extensive background shift on adding Hcys to the solution.

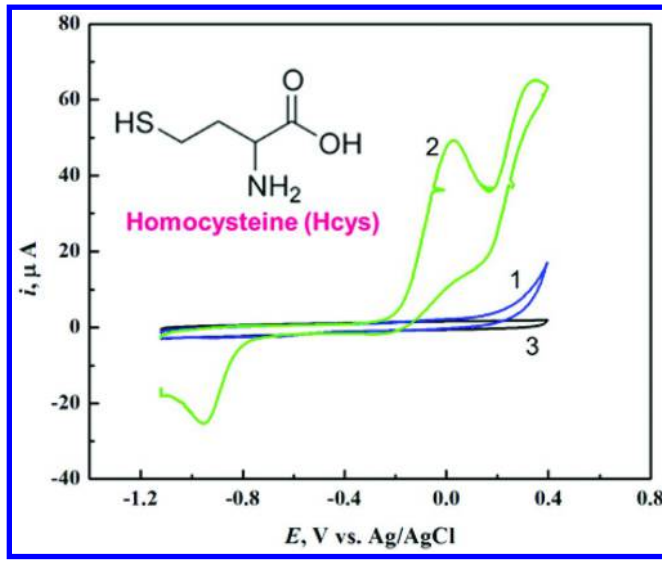

Figure 5. Cyclic voltammograms for homocysteine obtained on: (1) bare glassy carbon electrode (GCE) and (2) cobalt phthalocyanine-modified glassy carbon electrode (GCE/CoPc); C_{Hcys}, 3.85 mM. Curve (3) represents the background curve for a bare GCE in phosphate buffer. v = 100 mV/s, electrolyte: 50 mM phosphate buffer, pH 7.43.

To confirm that the observed anodic and cathodic currents are due to the oxidation of Hcys and reduction of homocystine, respectively, detailed Hcys-concentration studies have been performed. The obtained results are presented in Figure 6. A collection of CV curves obtained for a GCE/CoPc electrode in solutions with Hcys concentration ranging from 0 to 3.85 mM are presented in Figure 6. The linear dependence of anodic current peak at E_{pa} = +0.115 V for the first step of Hcys oxidation on C_{Hcys}, presented in Figure 6b (upper line), indicates that the reaction is first order with respect to Hcys. The dependence of cathodic peak current at E_{pc} = -0.97 V for homocystine reduction on C_{Hcys}, presented in Figure 6b (lower line) is also linear.

The scan dependence of anodic and cathodic peak currents has been analyzed in the range of scan rates from 25 to 500 mV/s, as illustrated in Figure 7. Both peak currents depend linearly on square root of scan rate. This confirms that the reactants originate from the solution phase rather than from a film on the electrode. This means that homocystine formed during the anodic oxidation at potentials $E >$ 0.3 V remains in the solution phase in the vicinity of the electrode surface and is available for backward reduction during the cathodic going scan, at potentials $E <$ -0.8 V. The separation between the anodic and cathodic waves is large, $\Delta E_p > 0.9$ V (taking into account the first anodic step), indicating on a high irreversibility of the oxidation/reduction processes of Hcys.

In Oxidative Stress: Diagnostics, Prevention, and Therapy Volume 2; Hepel, et al.;
ACS Symposium Series; American Chemical Society: Washington, DC, 2015.

Publication Date (Web): October 13, 2015 | doi: 10.1021/bk-2015-1200.ch014

Publication Date (Web): October 13, 2015 | doi: 10.1021/bk-2015-1200.ch014

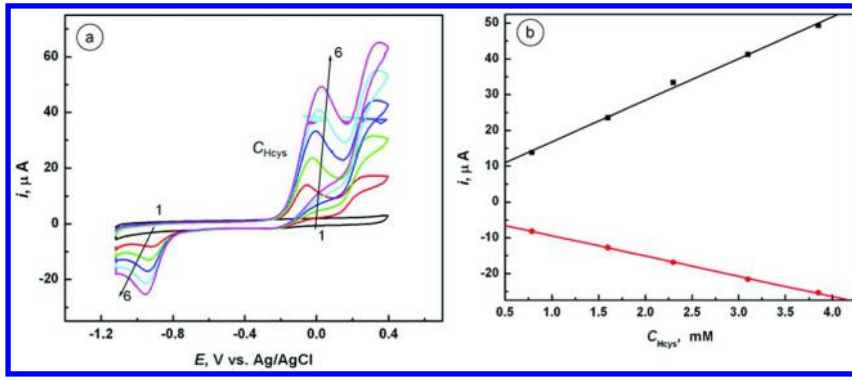

Figure 6. (a) Cyclic voltammograms for Hcys in 50 mM phosphate buffer, pH 7.43, recorded on a cobalt phthalocyanine-modified glassy carbon electrode (GCE/CoPc), for C_{Hcys} [mM]: (1) 0, (2) 0.79, (3) 1.6, (4) 2.3, (5) 3.1, (6) 3.85. (b) Dependence of i_p vs. C_{Hcys}; v = 100 mV/s. (see color insert)

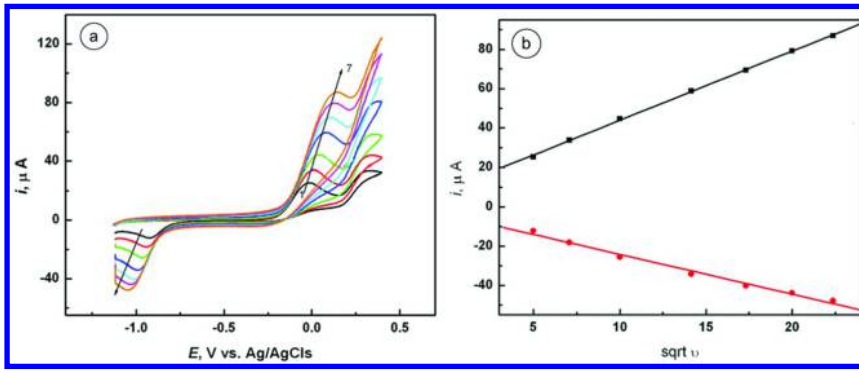

Figure 7. (a) Cyclic voltammograms for a 3.85 mM Hcys in 50 mM phosphate buffer, pH 7.43, obtained on a cobalt phthalocyanine modified-glassy carbon electrode (GCE/CoPc) with v [mV/s]: (1) 25, (2) 50, (3) 100, (4) 200, (5) 300, (6) 400, (7) 500; (b) Dependence of i_p vs. square root of v.

The homocysteine voltammetric fingerprint is different than that of GSH, although the reactivity of both compounds is similar. In Figure 8, two families of voltammograms for an increasing anodic reversal potential E_{ra} are presented. It is seen that the cathodic peak grows with increasing E_{ra}. The growth continues when E_{ra} increases in the potential range of the first Hcys oxidation peak and then remains largely invariant with E_{ra} when E_{ra} increases in the area of the second Hcys oxidation peak. This is likely due to the fact that the Hcys oxidation product, formed in the first stage (i.e. in the potential area of the first oxidation peak), adsorbs on the electrode surface while further oxidation leads to the product that is solution-soluble. These characteristics are important for the analysis of GSSG based on measurements of the rate of its reduction at $E < 0.9$ V vs Ag/AgCl.

In Oxidative Stress: Diagnostics, Prevention, and Therapy Volume 2; Hepel, et al.;
ACS Symposium Series; American Chemical Society: Washington, DC, 2015.

Publication Date (Web): October 13, 2015 | doi: 10.1021/bk-2015-1200.ch014

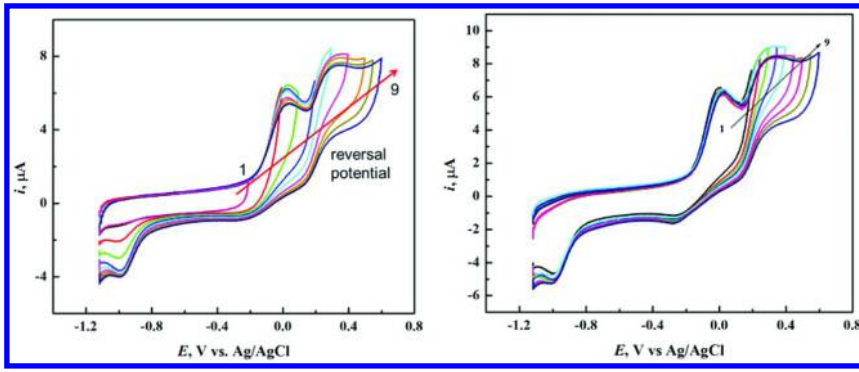

Figure 8. (a) Cyclic voltammograms of Hcys recorded on a cobalt phthalocyanine-modified glassy carbon electrode (GCE/CoPc) for increasing anodic reversal potential E_{ra} [mV]: (1) -200, (2) 0, (3) 100, (4) 200, (5) 300, (6) 400, (7) 500, (8) 550, (9) 600; v = 100 mV/s, C_{Hcys} = 400 μM in 50 mM phosphate buffer, pH 7.43; (b) same, but with E_{ra} changing only in the range of the second Hcys oxidation peak. (see color insert)

Electrocatalytic Activity of GCE/CoPc toward Cys Oxidation

The GCE/CoPc electrodes have also been tested for the response to cysteine. In Figure 9, the electrocatalytic properties of GCE and GCE/CoPc toward the oxidation of Cys are compared.

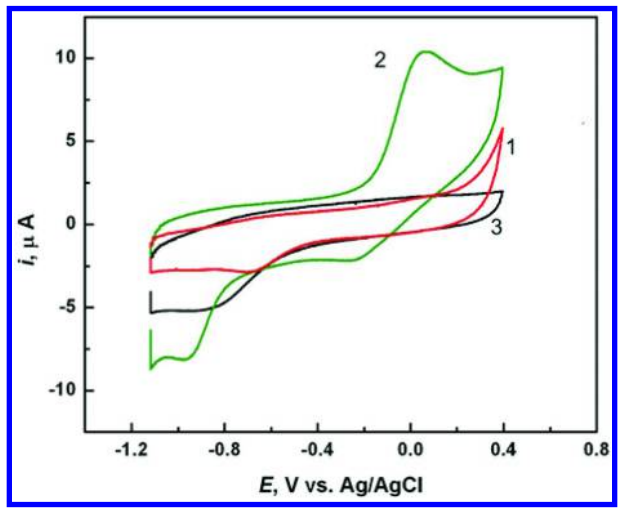

Figure 9. Cyclic voltammograms for cysteine (Cys)obtained on: (1) bare glassy carbon electrode (GCE) and (2) cobalt phthalocyanine-modified glassy carbon electrode (GCE/CoPc); C_{Cys} = 790 μM. Curve (3) represents the background curve for bare GCE electrode in phosphate buffer. v = 100 mV/s, electrolyte: 50 mM phosphate buffer, pH 7.43.

Publication Date (Web): October 13, 2015 | doi: 10.1021/bk-2015-1200.ch014

Voltammetric curve 1 was obtained in 3.85 mM Cys solution on bare GCE electrode and curve 2 on GCE/CoPc electrode. It is seen that there is no electrocatalytic activity of the GCE alone, but a pronounced catalytic Cys-oxidation current peak at E = +0.04 V vs. Ag/AgCl is observed on a GCE/CoPc electrode. In contrast to Hcys, only one anodic peak for the oxidation of Cys is observed, despite of the structural and functional similarity of Hcys and Cys (the only difference being one more CH_2 group in the Hcys carbon chain). The single Cys oxidation peak means that the disulphide (cystine) is formed in two consecutive overlapping steps. On the return scan, a cathodic current peak at E = -0.97 V is observed. It is due to the reduction of cystine formed during the forward scan at potentials E > -0.2 V. The background curve obtained on a bare GCE in buffer solution is presented in curve 3. There is no extensive background shift on adding Cys to the solution.

To confirm that the observed anodic and cathodic currents are due to the oxidation of Cys and reduction of cystine, respectively, detailed Cys-concentration studies have been performed. The obtained results are presented in Figure 10. A collection of CV curves obtained for a GCE/CoPc electrode in solutions with Cys concentration ranging from 0 to 3.85 mM are presented in Figure 10. The linear dependence of anodic current peak at E_{pa} = +0.04 V for the Cys oxidation on C_{Cys}, presented in Figure 10b (upper line), indicates that the reaction is first order with respect to Cys. The dependence of cathodic peak current at E_{pc} = -0.97 V for cystine reduction on C_{Cys}, presented in Figure 10b (lower line) is also linear.

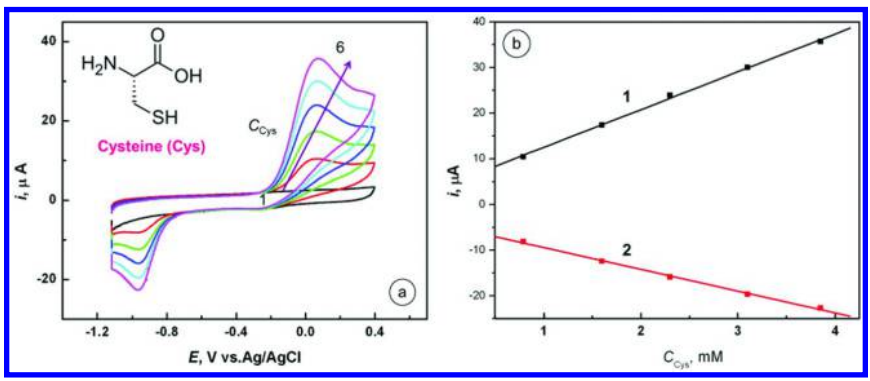

Figure 10. (a) Cyclic voltammograms, recorded on a cobalt phthalocyanine-modified glassy carbon electrode (GCE/CoPc), for Cys solutions with C_{Cys} [mM]: (1) 0, (2) 0.79, (3) 1.6, (4) 2.3, (5) 3.1, (6) 3.85; v = 100 mV/s; 50 mM phosphate buffer, pH 7.43; (b) dependence of i_p vs. C_{Cys}. (see color insert)

The scan dependence of anodic and cathodic peak currents has been analyzed in the range of scan rates from 25 to 500 mV/s, as illustrated in Figure 11. Both dependencies are linear with square root of scan rate, confirming that reactants from the solution are involved.

Publication Date (Web): October 13, 2015 | doi: 10.1021/bk-2015-1200.ch014

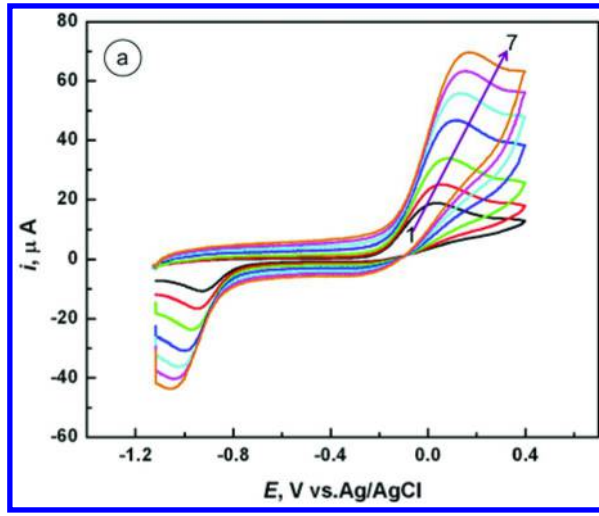

Figure 11. (a) Cyclic voltammograms for 3.85 mM Cys in 50 mM phosphate buffer, pH 7.43, on a cobalt phthalocyanine modified glassy carbon electrode (GCE/CoPc), recorded for v [mV/s]: (1) 25, (2) 50, (3) 100, (4) 200, (5) 300, (6) 400, (7) 500.

Selection of Characteristic Potentials for Differentiation of GSH, Hcys and Cys

Whereas GSH, Hcys, and Cys exhibit similar oxidation and reduction processes, their voltammetric characteristics differ in shape and the oxidation and reduction potentials. These differences can be exploited for differentiation between these thiols. Also, the analysis of mixed solutions can be readily performed provided that no appreciable interference between the thiols exists which, however, may not be the case due to the strong competition between thiols. The measurements described below have been carried out to address these issues.

In Figure 12, cyclic voltammograms for Hcys, Cys, and GSH have been compared. They were recorded on a cobalt phthalocyanine-modified glassy carbon electrode (GCE/CoPc) in 50 mM phosphate buffer, pH 7.43, for 790 μM thiols, at a scan rate of 100 mV/s.

It is seen that the anodic oxidation current onset is the lowest for Hcys, followed by Cys and GSH. At the same concentration level, Hcys exhibits two anodic peaks at $E_{pa,1}$ = +0.015 V and $E_{pa,2}$ = +0.340 V, Cys shows a single anodic peak at E_{pa} = +0.040 V, and GSH a wave with E_{pa} = +0.080 V. The Hcys valley observed in the potential range between the two anodic peaks shows a current minimum at E_{min} = +0.120 mV. By selecting the four peak potentials and E_{min}, the current-voltage profile can be analyzed. There are however, subtle problems with matrix effects which have to be addressed. Because of these effects, the standard addition method has to be applied in the analysis. In the following Figures, some of the matrix effects and interdependencies are presented.

Publication Date (Web): October 13, 2015 | doi: 10.1021/bk-2015-1200.ch014

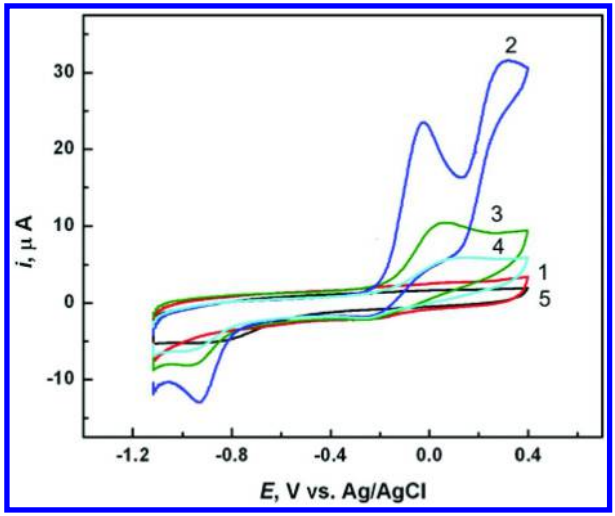

Figure 12. Cyclic voltammograms recorded on a cobalt phthalocyanine-modified glassy carbon electrode (GCE/CoPc) in 50 mM phosphate buffer, pH 7.43, for: (1) buffer only, (2-4) after addition of the 0.79 mM analyte: (2) Hcys, (3) Cys, and (4) GSH; curve (5) shows the background CV for a bare GCE electrode without catalyst; v = 100 mV/s.

The competition between GSH and Hcys is illustrated in Figure 13. It is seen that the anodic peak currents for oxidation of GSH and Hcys depend on the order in which the reagents (GSH and Hcys) are added. The concentration of Hcys is selected much lower than that of GSH so that the contribution of Hcys to the anodic current is negligible, as shown in curve 1. The experiments of Figure 13a have been performed for a high ratio of GSH to Hcys, C_{GSH}/C_{Hcys} = 385. GSH alone shows a high peak current (curve 2).

When GSH and Hcys are added to the buffer solution in a different sequence, the GSH peak current is seen to change markedly. Curve 3 shows that if Hcys, despite of its low concentration, is added before GSH, then the GSH peak is 30% lower than that for GSH alone. When GSH and Hcys are added together at the same time (i.e., when both reagents are present in the solution when the electrode is first immersed), the decrease of the GSH peak is smaller. There is clearly a strong competition between GSH and Hcys for the electrocatalytic redox centers in CoPc. These effects have not been described in the literature and this is the first investigation uncovering this competition. While the competitive adsorption of electroactive species and ligands is well known, here we deal rather with a slow-complexation competition since there is virtually no adsorption of reagents on a GCE surface.

Similar experiments have been performed for a lower ratio of GSH to Hcys, C_{GSH}/C_{Hcys} = 4. The obtained results are presented in Figure 13b, for C_{GSH} = 1.6 mM and C_{Hcys} = 400 μM. Curve 3 shows a GSH oxidation current in absence of Hcys and curve 4 shows the oxidation wave when GSH was added first, followed by the addition of Hcys. A higher anodic current is observed due to the additive effect of the oxidation of GSH and Hcys.

Publication Date (Web): October 13, 2015 | doi: 10.1021/bk-2015-1200.ch014

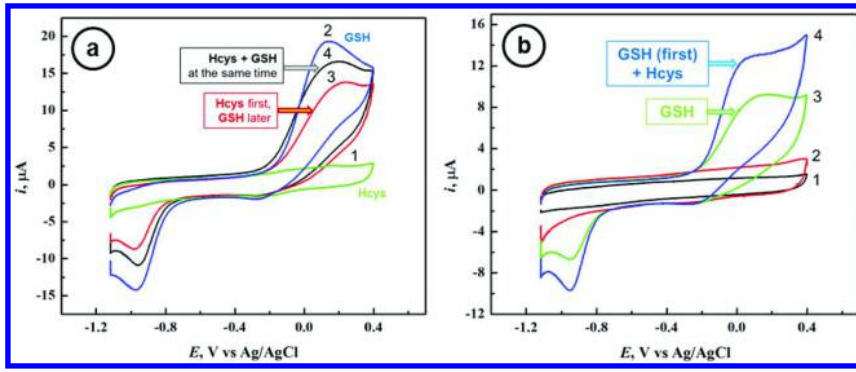

Figure 13. (a) Cyclic voltammograms for a cobalt phthalocyanine-modified glassy carbon electrode (GCE/CoPc) obtained after addition of: (1) 10 μM Hcys, (2) 3.85 mM GSH, (3) 3.85 mM GSH to a buffer containing 10 μM Hcys, (4) 10 μM Hcys + 3.85 mM GSH added at the same time. (b) Cyclic voltammograms for GCE and GCE/CoPc electrodes: (1) GCE in a buffer solution, (2) GCE/CoPc in a buffer solution, (3) GCE/CoPc in 1.6 mM GSH, (4) GCE/CoPc in 1.6 mM GSH after addition of 400 μM Hcys. Other conditions: 50 mM phosphate buffer solution, pH 7.43, v = 100 mV/s; all concentrations given are final concentrations.

The GSH-concentration dependence of voltammetric characteristics for a GCE/CoPc electrode obtained in the presence of 10 μM Hcys is presented in Figure 14.

The relationships $i_{pa} = f(C_{GSH})$ and $i_{pc} = f(C_{GSH})$ are linear in the lower concentration range ($C_{GSH} < 2$ mM) and show a decreased slope (sensitivity) $\partial i_p/\partial C_{GSH}$ at higher GSH concentrations.

Voltammograms for GSH solutions containing 10 μM Hcys, recorded for different potential scan rates, are presented in Figure 14b. In the presence of Hcys, the dependence of GSH oxidation peak current still is linear with square root of the scan rate v, indicating that the transport of GSH from solution is involved in the electrode process. The same concerns to GSSG-reduction peak current.

The experiments for GSH solutions containing 100 μM Hcys have also been performed. The GSH-concentration dependence of voltammetric characteristics for a GCE/CoPc electrode obtained in the presence of 100 μM Hcys is presented in Figure 15a. The relationships $i_{pa} = f(C_{GSH})$ and $i_{pc} = f(C_{GSH})$ are linear in the lower concentration range ($C_{GSH} < 2$ mM) and show a decreased slope (sensitivity) $\partial i_p/\partial C_{GSH}$ at higher GSH concentrations.

Voltammograms for GSH solutions containing 100 μM Hcys, recorded for different potential scan rates, are presented in Figure 15b. In the presence of Hcys, the dependence of GSH oxidation peak current is still linear with square root of the scan rate v, indicating that the transport of GSH from solution is involved in the electrode process. The same concerns to GSSG-reduction peak current.

Publication Date (Web): October 13, 2015 | doi: 10.1021/bk-2015-1200.ch014

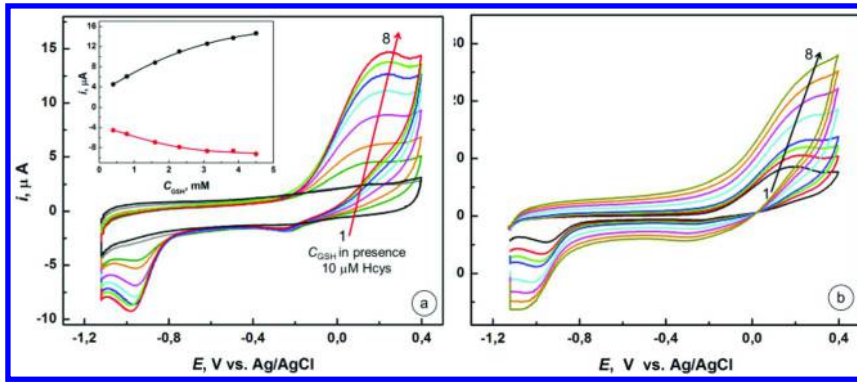

Figure 14. (a) Cyclic voltammograms for a GCE/CoPc electrode obtained for GSH solutions containing 10 μM Hcys, C_{GSH} [mM]: (1) 0, (2) 0.4, (3) 0.79, (4) 1.6, (5) 2.3, (6) 3.1, (7) 3.85; (8) 4.5; 50 mM phosphate buffer, pH 7.43; v = 100 mV/s. INSET: Dependence of i vs. C_{GSH}. (b) Cyclic voltammograms for a GCE/CoPc in 4.5 mM GSH solution containing 10 μM Hcys, obtained for different scan rates v [mV/s]: (1) 25, (2) 50, (3) 75, (4) 100, (5) 200, (6) 300, (7) 400, (8) 500; 50 mM phosphate buffer, pH 7.43. (see color insert)

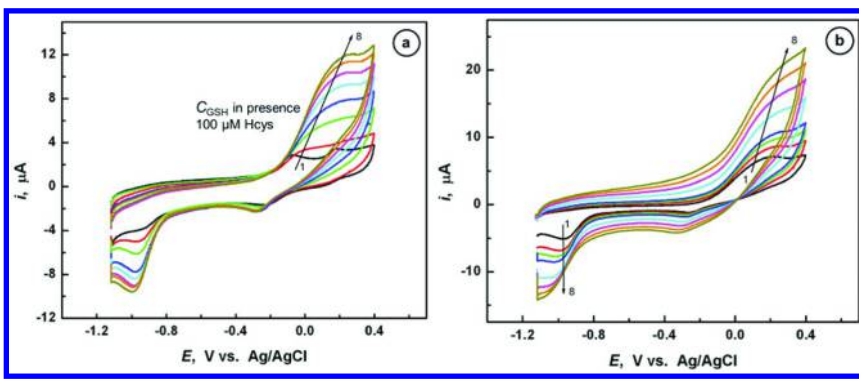

Figure 15. (a) Cyclic voltammograms for a GCE/CoPc electrode obtained for GSH solutions containing 100 μM Hcys, C_{GSH} [mM]: (1) 0, (2) 0.4, (3) 0.79, (4) 1.6, (5) 2.3, (6) 3.1, (7) 3.85; (8) 4.5; v = 100 mV/s. (b) Cyclic voltammograms for a GCE/CoPc in 4.5 mM GSH solution containing 100 μM Hcys, obtained for v [mV/s]: (1) 25, (2) 50, (3) 75, (4) 100, (5) 200, (6) 300, (7) 400, (8) 500. Other conditions: 50 mM phosphate buffer, pH 7.43.

In Oxidative Stress: Diagnostics, Prevention, and Therapy Volume 2; Hepel, et al.;
ACS Symposium Series; American Chemical Society: Washington, DC, 2015.

Since many oxidation processes of bioorganic compounds proceed faster in alkaline than in neutral solutions, we have tested the CoPc catalyst performance in Britton-Robinson buffer of pH 12. The results are presented in Figure 16 for a cobalt phthalocyanine-modified glassy carbon electrode (GCE/CoPc) in GSH solutions containing 10 μM Hcys. The anodic oxidation peak is better defined than that observed at lower pH and the peak potential E_{pa} = +0.06 V is also lower (E_{pa} = +0.20 V for pH = 7.43). The oxidation onset is seen at potentials as low as E = -0.26 V. However, the peak current values relative to the background capacitive current are lower than those at lower pH. As a consequence, the limit of detection is lower for neutral pH. For this reason, the neutral pH has been selected as better suited for the GSH analysis.

Publication Date (Web): October 13, 2015 | doi: 10.1021/bk-2015-1200.ch014

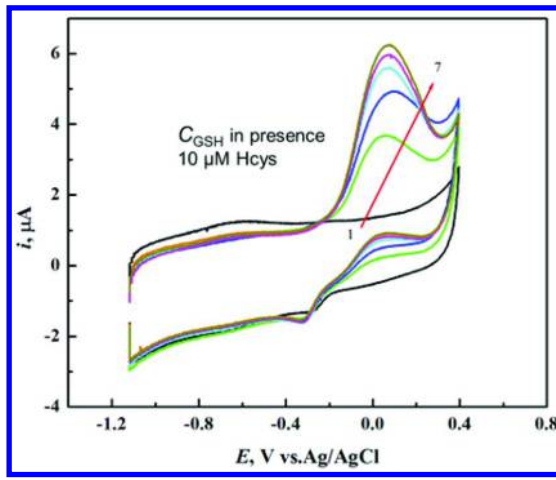

Figure 16. Cyclic voltammograms for a cobalt phthalocyanine-modified glassy carbon electrode (GCE/CoPc) obtained for GSH solutions containing 10 μM Hcys, C_{GSH} [mM]: (1) 0, (2) 0.79, (3) 1.6, (4) 2.3, (5) 3.1, (6) 3.85; (7) 4.5; 40 mM B-R buffer, pH 12; v = 100 mV/s.

The comparison of various calibration plots for GSH, Hcys and Cys is presented in Figure 17. The highest sensitivity is obtained for Hcys, followed by Cys, and the least sensitivity is observed for GSH. This is probably due to the larger size of GSH molecule and also its multiple local positive charges which are repelled by the $Co^{+1/+2}$ cation in CoPc core being the catalytic center of the electron exchange process. It is also seen that the competition from Hcys in GSH determination vanishes at lower GSH concentrations.

Publication Date (Web): October 13, 2015 | doi: 10.1021/bk-2015-1200.ch014

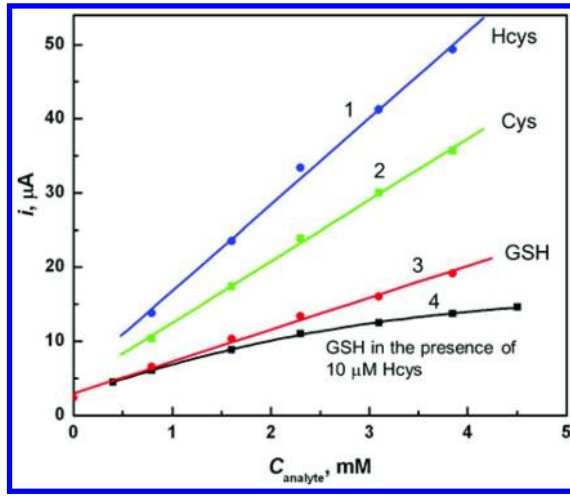

Figure 17. Dependence of i_{pa} vs. $C_{analyte}$ for different biomarkers of oxidative stress, obtained for a phosphate buffer pH 7.43, on a CoPC-modiefied GCE electrode, for: (1) Hcys, (2) Cys, (3) GSH, (4) GSH in the presence of 10 μM Hcys, v = 100 mV/s.

Conclusions

In the absence of biocatalytic effects, the redox reactivity of GSH/GSSG couple on solid electrodes is strongly hindered. We have shown that the rates of redox reactions of glutathione, as well as other biothiols: cysteine and homocysteine, can be enhanced on electrocatalytic cobalt phthalocyanine (CoPc) monolayer film electrodes, enabling voltammetric detection of these important biomarkers of oxidative stress. We have demonstrated that a strong competition between GSH, Cys, and Hcys exists due to the competitive charge-transfer complex formation. We have previously observed a strong ligand competion in thiol-capped Au nanoparticle assembly processes studied using UV-Vis and resonance elastic light scattering spectroscopies. While the strong competition of thiols prevents straightforward analysis of multicomponent mixtures, the detailed investigations indicate that the analysis can be carried out using the standard addition method taking into account active matrix effects which cannot be neglected.

Acknowledgments

This work was partially supported by the U.S. DoD grant No. AS073218.

Publication Date (Web): October 13, 2015 | doi: 10.1021/bk-2015-1200.ch014

References

1. Sen, S.; Chakraborty, R.; Sridhar, C.; Reddy, Y. S. R.; De, B. *Int. J. Pharm. Sci. Rev. Res.* **2010**, *3*, 91–100.
2. Hepel, M.; Stobiecka, M., Detection of Oxidative Stress Biomarkers Using Functional Gold Nanoparticles. In *Fine Particles in Medicine and Pharmacy*; Matijevic, E., Ed.; Springer Science Publ.: New York, 2012; pp 241-281.
3. Poljsak, B., *Decreasing Oxidative Stress and Retarding the Aging Process*; Nova Sci. Publishing: New York, 2010.
4. Tardif, J.-C. *Cardiology Rounds* **2003**, *7*, 9.
5. Lakshmi, S. V. V.; Padmija, G.; Kuppusamy, P.; Kutala, V. K. *Indian J. Biochem. Biophys.* **2009**, *46*, 421–440.
6. Krishnan, C. V.; Garnett, M.; Chu, B. *Int. J. Electrochem. Sci.* **2008**, *3*, 1348–1363.
7. Nikam, S.; Nikam, P.; Ahaley, S. K.; Sontakke, A. V. *Indian J. Clin. Biochem.* **2009**, *24*, 98–101.
8. Singh, R. P.; Sharad, S.; Kapur, S. *JIACM* **2004**, *5*, 218–25.
9. Perluigi, M.; Butterfield, D. A. *Expert Rev. Proteomics* **2011**, *8*, 427–429.
10. Zana, M.; Janka, Z.; Kalman, J. *Neurobiol. Aging* **2007**, *28*, 648–676.
11. James, S. J.; Cutler, P.; Melnyk, S.; Jernigan, S.; Janak, L.; Gaylor, D. W.; Neubrander, J. A. *Am. J. Clin. Nutr.* **2004**, *80*, 1611–1617.
12. James, S. J.; Melnyk, S.; Jernigan, S.; Cleves, M. A.; Halsted, C. H.; Wong, D. H.; Cutler, P.; Bock, K.; Boris, M.; Bradstreet, J. J.; Baker, S. M.; Gaylor, D. W. *Am. J. Med. Genet. B Neuropsychiatr. Genet.* **2006**, *141B*, 947–956.
13. Stobiecka, M.; Prance, A.; Coopersmith, K.; Hepel, M. Antioxidant effectiveness in preventing paraquat-mediated oxidative DNA damage in hte presence of H_2O_2. In *Oxidative Stress: Diagnostics, Prevention and Therapy*; Andreescu, S., Hepel, M., Eds.; Oxford University Press: Oxford, 2012; Vol. 1083, pp 211−233.
14. Hepel, M.; Stobiecka, M.; Peachey, J.; Miller, J. *Mutat. Res.* **2012**, *735*, 1–11.
15. Moussa, S. A. *Romanian J. Biophys.* **2008**, *18*, 225–236.
16. Wiernsperger, N. F. *Diabetes Metab.* **2003**, *29*, 579–585.
17. Markesbery, W. R. *Free Radical Biol. Med.* **1997**, *23*, 134–147.
18. Perry, G.; Cash, A. D.; Smith, M. A. *J. Biomed. Biotechnol.* **2002**, *2* (3), 120–123.
19. Yves, C. *Am. J. Clin. Nutr.* **2000**, *71*, 621S–9S.
20. Hamilton, C. A.; H. Miller, W. H.; Al-Benna, S.; Brosnan, M. J.; Drummond, R. D.; McBride, M. W.; Dominiczak, A. F. *Clin. Sci.* **2004**, *106*, 219–234.
21. Madamanchi, N. R.; Vendrov, A.; Runge, M. S. *Arterioscler. Thromb. Vasc. Biol.* **2005**, *25*, 29–38.
22. Galle, J. *Nephrol. Dial. Transplant.* **2001**, *16*, 2135–2137.
23. Himmelfarb, J.; McMonagle, E.; Freedman, S.; Klenzak, J.; McMenamin, E.; Le, P.; Pupim, L. B.; Ikizler, T. A.; PicardGroup. *J. Am. Soc. Nephrol.* **2004**, *15*, 2449–2456.

In Oxidative Stress: Diagnostics, Prevention, and Therapy Volume 2; Hepel, et al.;
ACS Symposium Series; American Chemical Society: Washington, DC, 2015.

24. Halliwell, B. *Biochem. J.* **2007**, *401*, 1–11.
25. Tandon, V. R.; Sharma, S.; Mahajan, A.; Bardi, G. H. *JK Science* **2005**, *7*, 1–3.
26. Masella, R.; Di Benedetto, R.; Vari, R.; Filesi, C.; Giovannini, C. *J. Nutr. Biochem.* **2005**, *16*, 577–586.
27. Kohen, R.; Nyska, A. *Toxicol. Pathol.* **2002**, *30*, 620–650.
28. Hepel, M.; Stobiecka, M. Detection of Oxidative Stress Biomarkers Using Novel Nanostructured Biosensors. In *New Perspectives in Biosensors Technology and Applications*; Serra, P. A., Ed.; INTECH: Vienna, 2011; pp 343−372.
29. Mansoor, M. A.; Svardal, A. M.; Ueland, P. M. *Anal. Biochem.* **1992**, *200*, 218–229.
30. Kleinman, W. A.; Richie, J. P. *Biochem. Pharmacol.* **2000**, *60*, 19–29.
31. Harfield, J. C.; Batchelor-McAuley, C.; Compton, R. G. *Analyst* **2012**, *137*, 2285–2296.
32. White, P. C.; Lawrence, N. S.; Davis, J.; Compton, R. G. *Electroanalysis* **2002**, *14*, 89–98.
33. Cereser, C.; Guichard, J.; Drai, J.; Bannier, E.; Garcia, I.; Boget, S.; Parvaz, P.; Revol, A. *J. Chromatogr. B* **2001**, *752*, 123–132.
34. Kusmierek, K.; Glowacki, R.; Bald, E. *Anal. Bioanal. Chem.* **2006**, *385*, 855–860.
35. Refsum, H.; Ueland, P. D.; Nygård, P.; Vollset, S. E. *Annu. Rev. Med.* **1998**, *49*, 31–62.
36. Tcherkas, Y. V.; Denisenko, A. D. *J. Chromatogr. A* **2001**, *913*, 309–313.
37. Stabler, S. P.; Marcell, P. D.; Rodell, E. R.; Allen, R. H.; Savage, D. G.; Lindenbaum, J. *J. Clin. Invest.* **1988**, *81*, 466–474.
38. Spătaru, N.; Sarada, B. V.; Popa, E.; Tryk, D. A.; Fujishima, A. *Anal. Chem.* **2001**, *73*, 514–519.
39. Stobiecka, M.; Deeb, J.; Hepel, M. *Biophys. Chem.* **2010**, *146*, 98–107.
40. Stobiecka, M.; Hepel, M. *Sens. Actuators, B* **2010**, *149*, 373–380.
41. Xiao, Q.; Zhang, L.; Lu, C. *Sens. Actuators, B* **2012**, *166-167*, 650–657.
42. Wang, J.; Li, Y. F.; Huang, C. Z.; Wua, T. *Anal. Chim. Acta* **2008**, *626*, 37–43.
43. Sun, S. K.; Wang, H. F.; Yan, X. P. *Chem. Commun.* **2011**, *47*, 3817–3819.
44. Leesutthiphonchai, W.; Dungchai, W.; Siangproh, W.; Ngamrojnavanich, N.; Chailapakul, O. *Talanta* **2011**, *85*, 870–876.
45. Hepel, M.; Stobiecka, M. *J. Photochem. Photobiol. A* **2011**, *225*, 72–80.
46. Xu, H.; Hepel, M. *Anal. Chem.* **2011**, *83*, 813–819.
47. Tan, H.; Chen, Y. *J. Biomed. Opt.* **2012**, *17*, 017001.
48. Stobiecka, M.; Molinero, A. A.; Chalupa, A.; Hepel, M. *Anal. Chem.* **2012**, *84*, 4970–4978.
49. Stobiecka, M.; Hepel, M. *Biosens. Bioelectron.* **2011**, *26*, 3524–3530.
50. Stobiecka, M.; Deeb, J.; Hepel, M. *Electrochem. Soc. Trans.* **2009**, *19*, 15–32.
51. Çubukçu, M.; Ertaş, F. N.; Anık, Ü. *Microchim. Acta* **2013**, *180*, 93–100.
52. Ndamanisha, J. C.; Bai, J.; Qi, B.; Guo, L. *Anal. Biochem.* **2009**, *386*, 79–84.

Publication Date (Web): October 13, 2015 | doi: 10.1021/bk-2015-1200.ch014

53. Pereira-Rodrigues, N.; Cofre, R.; Zagal, J. H.; Bedioui, F. *Bioelectrochem.* **2007**, *70*, 147–154.
54. Sehlotho, N.; Griveau, S.; Ruillé, N.; Boujtita, M.; Nyokong, T.; Bedioui, F. *Mater. Sci. Eng. C* **2008**, *28*, 606–612.
55. Guttierrez, A. P.; Argote, M. R.; Griveau, S.; Zagal, J. H.; Granados, S. G.; Ordas, A. A.; Bedioui, F. *J. Chil. Chem. Soc.* **2012**, *52*, 1244–1247.
56. Raoof, J. B.; Ojani, R.; Baghayeri, M. *Sens. Actuators, B* **2009**, *143*, 261–269.
57. Inoue, T.; Kirchhoff, J. R. *Anal. Chem.* **2000**, *72*, 5755–5760.
58. Joshi, K. A.; Pandey, P. C.; Chen, W.; Mulchandani, A. *Electroanalysis* **2004**, *16*, 1938–1943.
59. Han, H.; Tachikawa, H. *Front. Biosci.* **2005**, *10*, 931–939.
60. Lee, P. T.; Compton, R. G. *Electroanalysis* **2013**, *25*, 1613–1620.
61. Lee, P. T.; Ward, K. R.; Tschulik, K.; Chapman, G.; Compton, R. G. *Electroanalysis* **2014**, *26*, 366–373.
62. Lee, P. T.; Lowinsohn, D.; Compton, R. G. *Sensors* **2014**, *14*, 10395–10411.
63. Richie, J. P.; Lang, C. A. *Anal. Biochem.* **1987**, *163*, 9–15.
64. Gong, K.; Zhu, X.; Zhao, R.; Xiong, S.; Mao, L.; Chen, C. *Anal. Chem.* **2005**, *77*, 8158–8165.
65. Abiman, P.; Wildgoose, G. G.; Compton, R. G. *Electroanalysis* **2007**, *19*, 437–444.
66. Arduini, F.; Majorani, C.; Amine, A.; Moscone, D.; Palleschi, G. *Electrochim. Acta* **2011**, *56*, 4209–4215.
67. Gong, Z. X.; Li, H. *J. Electrochem. Soc.* **2000**, *147*, 238–241.
68. Houze, P.; Gamra, S.; Madelaine, I.; Bousquet, B.; Gourmel, B. *J. Clin. Lab. Anal.* **2001**, *15*, 144–153.
69. Carvalho, F. D.; Remião, F.; Valet, P.; Timbrell, J. A.; Bastos, M. I.; Ferreira, M. A. *Biomed. Chromatogr.* **2005**, *8*, 134–136.
70. Chen, J.; He, Z.; Liu, H.; Cha, C. *J. Electroanal. Chem.* **2006**, *588*, 324–330.
71. Pacsial-Ong, E. J.; McCarley, R. L.; Wang, W.; Strongin, R. M. *Anal. Chem.* **2006**, *78*, 7577–7581.
72. Vandeberg, P. J.; Johnson, D. C. *Anal. Chem.* **1993**, *65*, 2713–2718.
73. Winters, R. A.; Zukowski, J.; Ercal, N.; Matthews, R. H.; Spitz, D. R. *Anal. Biochem.* **1995**, *227*, 14–21.
74. Mazloum-Ardakani, M.; Sheikh-Mohseni, M. A.; Mirjalili, B. F. *Electroanalysis* **2013**, *25*, 2021–2029.
75. Salehzadeh, H.; Mokhtari, B.; Nematollahi, D. *Electrochim. Acta* **2014**, *123*, 353–361.
76. Nekrassova, O.; White, P. C.; Threlfell, S.; Hignett, G.; Wain, A. J.; Lawrence, N. S.; Davis, J.; Compton, R. G. *Analyst* **2002**, *127*, 797–802.
77. Scampicchio, M.; Lawrence, N. S.; Arecchi, A.; Mannino, S. *Electroanalysis* **2007**, *19*, 2437–2443.
78. Hignett, G.; Threlfell, S.; Wain, A. J.; Lawrence, N. S.; Wilkins, S. J.; Davis, J.; Compton, R. G.; Cardosi, M. F. *Analyst* **2001**, *126*, 353–357.
79. Seymour, E. H.; Wilkins, S. J.; Lawrence, N. S.; Compton, R. G. *Anal. Lett.* **2002**, *35*, 1387–1399.

Publication Date (Web): October 13, 2015 | doi: 10.1021/bk-2015-1200.ch014

80. White, P. C.; Lawrence, N. S.; Tsai, Y. C.; Davis, J.; Compton, R. G. *Mikrochim. Acta* **2001**, *137*, 87–91.
81. Liu, X.; Lv, H.; Sun, Q.; Zhong, Y.; Zhao, J.; , J.Fu; Lin, M.; Wang, J. *Anal. Lett.* **2012**, *45*, 2246–2256.
82. Lowinsohn, D.; Lee, P. T.; Compton, R. G. *Int. J. Electrochem. Sci.* **2014**, *9*, 3458–3472.
83. Wang, W. H.; Escobedo, J. O.; Lawrence, C. M.; Strongin, R. M. *J. Am. Chem. Soc.* **2004**, *126*, 3400.
84. Lu, C.; Zu, Y. B. *Chem. Commun.* **2007**, 3871.
85. Chen, H. L.; Zhao, Q.; Wu, Y. B.; Li, F. Y.; Yang, H.; Yi, T.; Huang, C. H. *Inorg. Chem.* **2007**, *46*, 11075.
86. Lim, I. I. S.; Ip, W.; Crew, E.; Njoki, P. N.; Mott, D.; Zhong, C. J.; Pan, Y.; Zhou, S. Q. *Langmuir* **2007**, *23*, 826.
87. Lim, I. I. S.; Mott, D.; Ip, W.; Njoki, P. N.; Pan, Y.; Zhou, S. Q.; Zhong, C. J. *Langmuir* **2008**, *24*, 8857.
88. Stobiecka, M.; Coopersmith, K.; Hepel, M. *J. Colloid Interface Sci.* **2010**, *350*, 168–177.
89. Atkins, P. W.; Friedman, R. S. *Molecular Quantum Mechanics*; Oxford University Press: Oxford, 2004.
90. Hehre, W. J.; Radon, L.; Schleyer, P. R.; Pople, J. A. *Ab-initio Molecular Orbital Theory*; Wiley: New York, 1985.
91. Santos da Silva, I.; Araújo, M. F. A.; Ferreira, H. A.; de Jesus Gomes Varela, J., Jr.; Tanaka, S. M. C. N.; Tanaka, A. A.; Angnes, L. *Talanta* **2011**, *83*, 1701–1706.
92. Luz, R. C. S.; Moreira, A. B.; Damos, F. S.; Tanaka, A. A.; Kubota, L. T. *J. Pharm. Biomed. Anal.* **2006**, *42*, 184–191.
93. Schafer, F. Q.; Buettner, G. R. *Free Radical Biol. Med.* **2001**, *30*, 1191–1212.
94. Hiroi, M.; Ogihara, T.; Hirano, K.; Hasegawa, M.; Morinobu, T.; Tamai, H.; Niki, E. *Free Radical Biol. Med.* **2005**, *38*, 1057–1072.

Publication Date (Web): October 13, 2015 | doi: 10.1021/bk-2015-1200.ch014

Publication Date (Web): October 13, 2015 | doi: 10.1021/bk-2015-1200.ch015

Chapter 15

Oxidative Stress Biomarkers and ROS Molecular Probes

Joanna Stanicka, William Landry, and Thomas G. Cotter*

School of Biochemistry and Cell Biology, University College Cork, Cork, Ireland
***E-mail: t.cotter@ucc.ie**

Reactive oxygen species (ROS) are short lived highly reactive molecular entities that are generated in cells and have the ability to rapidly oxidise target molecules such as proteins or lipids. The consequences of this oxidation is often a loss or change of function of the target molecules. The highly reactive nature of ROS and their sometime transient effects, can make their measurement challenging to say the least. Targets of ROS include DNA that can be readily oxidised with one the most common products being the nucleoside 8-hydroxydeoxyguanosine (8-OHdG) which in turn is a widely used marker of oxidative DNA damage. Lipid peroxidation is also a cellular hallmark of oxidative stress with polyunsaturated fatty acids being particularly susceptible.

Biomolecular Markers of Oxidative Stress

Biomarker can be defined as a characteristic that is objectively measured and evaluated as an indicator of a biological process, either normal or abnormal that can be found in blood, other body fluids, tissues or cells and can be used to diagnose or determine response to a treatment. With oxidative stress being increasingly associated with many diseases, much focus has been placed on identifying biomarkers linked to changes in the cellular redox environment in order to diagnose patients with redox associated diseases. Biomarkers which closely correlate with the pathophysiological process of a disease provide the most promise for diagnostic use.

In Oxidative Stress: Diagnostics, Prevention, and Therapy Volume 2; Hepel, et al.;
ACS Symposium Series; American Chemical Society: Washington, DC, 2015.

Publication Date (Web): October 13, 2015 | doi: 10.1021/bk-2015-1200.ch015

As a result of their transient nature directly examining ROS levels and their production is challenging, making the examination of the biomolecules which are altered downstream of ROS production an appealing approach. As ROS are highly reactive molecules and can interact with many biomolecules, it could be presumed that there is a large pool of potential biomarkers available to choose from. However, due to the highly reactive nature of ROS and sometimes transient nature of their effects, finding suitable biomarkers to identify oxidative damage can be a challenge. As a result of these limitations Giustarini et al. suggested a list of specific criteria a good biomarker of oxidative stress should satisfy to function as a suitable disease marker (*1*). This list in part suggested that it is critical that the products of oxidation are chemically stable, able to be quantified accurately and are linked to specific pathways of oxidation. Additionally, concentrations found in biological samples should directly correlate with the severity of the disease so it can be used for diagnosis and to monitor any therapeutic responses (*1*).

Unfortunately the majority of the biomarkers used to study oxidative stress do not meet all the criteria listed. As a result, here an overview will be given of some of the most commonly used biomarkers for ROS-induced oxidative damage, which best adhere to the list of specific criteria suggested by Giustarini *et al.* (*1*). Focus will be placed on three biomarkers which are produced as a direct result of ROS production and these are 8-hydroxydeoxyguanosine (8-OHdG), isoprostanes and gluthatione (GSH), representing biomarkers of the three main biomolecules affected by oxidative damage.

Oxidative DNA Damage: 8-Hydroxydeoxyguanosine (8-OHdG)

Oxidised bases, apurinic/apyrimidinic (AP) or abasic sites, single strand (SSB) and double strand breaks (DSBs) are the typical modifications which form on DNA as a result of ROS-induced oxidative damage. Of the many modifications possible, the nucleoside 8-hydroxydeoxyguanosine (8-OHdG) is one of the most commonly produced DNA base lesions, which can result during oxidative stress. The number of 8-OHdG lesions present in nuclear and mitochondrial cellular DNA is known to directly correlate with intracellular ROS levels making the quantification of 8-OHdG widely used biomarker for oxidative stress (*2*). 8-OHdG lesions are formed during oxidative stress when a hydroxyl radical ($OH\cdot$) reduces the C8 position of the guanine base ring producing 8-hydroxy-7,8-dihydroguanyl radical which is then oxidised (*3*). Although not directly lethal to the affected cell, 8-OHdG lesions are highly mutagenic, inducing DNA base substitutions and significantly contributing to the development and progression of cancers (*4*, *5*). Additionally, elevated levels of 8-OHdG have been associated with neurological disorders like Alzheimer's and Parkinson's disease as well as atherosclerosis and various conditions associated with diabetes (*6*–*8*).

A variety of techniques are utilised to quantify 8-OHdG levels. These include chromatography, mass spectrometry, electrophoretic, enzyme and immunological-based methods (*9*). Quantification of 8-OHdG DNA lesions following extraction of DNA from cells or tissues has been a common practise for many years. However, it is now known that unavoidable oxidative damage can occur during the extraction and handling of DNA, thereby producing

In Oxidative Stress: Diagnostics, Prevention, and Therapy Volume 2; Hepel, et al.;
ACS Symposium Series; American Chemical Society: Washington, DC, 2015.

Publication Date (Web): October 13, 2015 | doi: 10.1021/bk-2015-1200.ch015

artefacts (*10*). 8-OHdG quantification subsequent to DNA extraction can give an inaccurate representation of the level of oxidative DNA damage, bringing in to question the validity of results determined by this method. As a result of this, The European Standards Committee for Oxidative DNA Damage (ESCODD) was set up to identify and resolve methodological problems like artefacts of oxidation, which occurs during isolation, purification and handling of DNA products, by evaluating existing protocols and providing more reliable methods for sample preparation and analysis. The ESCODD studies confirmed that several of the methods used for detecting and quantifying 8-OHdG lesions in extracted cellular DNA gave rise to incorrect conclusions due to the generation of oxidative artefacts, with large discrepancies noted between the levels of lesions documented using different quantification methods (*10*, *11*). Two of the most extensively used 8-OHdG quantification methods for extracted DNA were high performance liquid chromatography (HPLC) with electrochemical detection (ECD) and the formamidopyrimidine DNA glycosylase (FPG) enzymatic approach used to digest DNA converting 8-OHdG to apurinic sites which are subsequently measured as DNA breaks using the electrophoresis-based comet assay. Although susceptible to the generation of 8-OHdG artefacts during preparation, HPLC-ECD was still chosen as the method of choice, affording satisfactory accuracy when quantifying 8-OHdG levels of extracted DNA. However with research groups recording fold differences in 8-OHdG levels after undertaking similar analyses in human cells it was clear that this method of quantification was far from ideal (*1*, *10*, *11*).

Interestingly, examination of 8-OHdG levels is not limited to extraction of cellular DNA. During DNA repair, 8-OHdG lesions are generally detected by cellular systems and excised before subsequently being excreted in urine without being metabolised further (*12*). This makes it possible to measure the level of 8-OHdG lesions from urinary samples, providing a more convenient and non-invasive way of measuring oxidative DNA damage. Examining urinary 8-OHdG levels has multiples benefits over methods which require DNA extraction, these include long-term stability of 8-OHdG in urine, no production of artefacts and the use of immunological-based methods like ELISA, allowing quicker high-throughput studies, reducing the need for expensive chromatography or mass-spectrometry equipment and trained personnel (*8*, *13*). Consequently, this approach continues to receive widespread attention, with multiple studies demonstrating that quantification of urinary levels of 8-OHdG can act as a good biomarker for oxidative DNA damage which has resulted in its extensive use when examining some degenerative diseases and numerous cancers (*14*, *15*).

Unfortunately, this method is not without its drawbacks either as levels of urinary 8-OHdG measured may not be entirely DNA-derived, but rather be from the deoxyGTP precursor pool, which can also give a false representation of the level of cellular oxidative damage (*16*). Furthermore, discrepancies are also noted between the different methods utilised for 8-OHdG quantification with the commonly used ELISA demonstrating a high degree of variability when compared to the more accurate chromatography-based methods (*17*). As a result of discrepancies between urinary 8-OHdG quantification methods, The European Standards Committee on Urinary (DNA) Lesion Analysis (ESCULA) was established to perform a similar function as ECSODD, identifying

HPLC-tandem mass spectrometry (MS/MS) as the gold standard for urinary 8-OHdG quantification (*17*). However, the high-throughput and inexpensive nature of ELISA still makes it a more favourable quantification method. As a result, there has been much aspiration to optimise this technique leading to a study by Rossner *et al.* which demonstrated that purification of urine using solid phase extraction (SPE) and the use of standardised calibrants like creatinine substantially improves ELISA quantification of urinary 8-OHdG and provides better accuracy with results more consistent with HPLC-MS/MS quantification (*18*). Although still not as accurate as HPLC-MS/MS this study demonstrated the potential for ELISA to be an accurate method of urinary 8-OHdG quantification, providing a more accessible approach to perform oxidative stress studies.

Publication Date (Web): October 13, 2015 | doi: 10.1021/bk-2015-1200.ch015

Lipid Peroxidation

Lipid peroxidation is a hallmark of oxidative stress, resulting when lipids interact with oxygen-derived oxidants such as ROS to produce highly reactive electrophilic aldehydes. Polyunsaturated fatty acids (PUFAs) in particular are very unstable lipids due to multiple reactive double bonds being present in their molecular structures and because of this are highly susceptible to lipid peroxidation under conditions of oxidative stress (*19*). Arachidonic acid, docosahexaenoic acid, linoleic acid and eicosapentaenoic acid are examples of biologically important PUFAs, all of which can be subject to ROS-initiated lipid peroxidation. The primary products of ROS-induced peroxidation of PUFAs are lipid hydroperoxides, with further chemical decomposition of these molecules potentially producing a diverse array of electorphilic aldehyde products such as Malondialdehyde (MDA), 4-hydroxy-2- nonenal (HNE) and acrolein (*20*). In addition, more complex secondary oxidation products such as isoprostanes (IsoPs) can also be generated from the non-enzymatic ROS-catalysed peroxidation of highly unsaturated PUFAs like arachidonic acid (*21*).

All these aldehydes can have multiple biological functions but are also highly reactive and can have harmful effects, readily reacting with DNA, phospholipids and proteins to which they can attach covalently to form stable adducts with the amino acid residues cysteine, lysine and histidine and can cause protein carbonylation, a common indicator of protein oxidative damage (*22*, *23*). As a result of their reactive nature lipid peroxidation products have been implicated in the pathogenesis of a number of diseases and are heavily associated with cardiovascular and neurodegenerative disorders (*24–26*). As stated lipid peroxidation is a hallmark of oxidative damage, making the many electrophilic aldehydes products produced potential biomarkers of oxidative stress. Although there are multiple products of lipid peroxidation few have the ideal properties to be utilised for this purpose. Acrolein, MDA and HNE have all seen use as biomarkers of lipid peroxidation and oxidative stress with varying degrees of success. However, IsoPs are considered the “gold standard” biomarker for examining endogenous lipid peroxidation, seeing significant attention for use as biomarkers of oxidative stress and will be discussed further.

In Oxidative Stress: Diagnostics, Prevention, and Therapy Volume 2; Hepel, et al.;
ACS Symposium Series; American Chemical Society: Washington, DC, 2015.

Publication Date (Web): October 13, 2015 | doi: 10.1021/bk-2015-1200.ch015

Isoprotanes

Isoprostanes (IsoPs) are prostaglandin-like molecules which are predominantly formed by non-enzymatic peroxidation of arachidonic acid, a ubiquitous PUFA present in phospholipids of the cell membrane (*27*, *28*). A diverse array of human disorders present with elevated levels of IsoPs in tissue and bodily fluids, examples include but are not limited to atherosclerosis (*29*), diabetes (*30*), neurodegenerative disease like Alzheimer's (*31*) and certain types of cancer (*32*, *33*). Interestingly, IsoPs are considered to be a reliable biomarker for oxidative stress and endogenous lipid peroxidation as they are stable oxidation products (*34*, *35*). IsoPs are chemically stable *in vivo* as well as *ex vivo* and once generated are released into circulation by phospholipases (*1*, *36*). Consequently, IsoPs are not only detectable in cell and tissues samples but also biological fluids including urine, plasma, bile, cerebrospinal and amniotic fluid (*27*, *28*, *37–39*). These characteristics make IsoPs an ideal biomarker for non-invasive diagnostic use.

There are many different IsoPs but following a study of 30 endogenous biomarkers of oxidative stress, it was determined that quantification of urinary or plasma F_2-IsoP levels from both animal and human samples was demonstrated to directly correlate with *in vivo* oxidative stress establishing this molecules diagnostic potential (*34*). In theory, 64 individual F_2-IsoP molecules can be produced and like prostaglandins can play roles in a host of cellular functions (*23*). One of most abundant of these F_2-IsoPs is 15-F_2t-IsoP (or 8-iso-PGF2R) which is also one of the most thoroughly investigated biomarkers for oxidative stress. There are multiple methods which have been developed to quantify the levels of this F_2-IsoP, these include gas chromatography-mass spectrometry (GC-MS), GC-tandem MS (GC-MS/MS), liquid chromatography-tandem MS (LC-MS/MS) and immunoassays. Quantification of F_2-isops by MS in particular GS-MS using electron capture negative ionisation is considered the "gold standard" as it offers high sensitivity, specificity yielding quantitative results and is the most accurate method with a marked advantage over immunoassays such as ELISA (*35*).

Although ELISA measurements allow high-throughput analysis of samples, are cheaper and relatively easy to perform when compared to MS, multiple studies have demonstrated variable performance between the commercially available F_2-IsoP ELISAs and poor correlation with MS results (*40*, *41*). These discrepancies are suggested in part to be a consequence of the polyclonal antibodies used to bind F_2-IsoPs which demonstrate cross-reactivity with other molecules of a similar structure (*42*). Additionally, antibody cross-reactivity can inflate quantification of IsoP concentrations and the presence of biological impurities can interfere further with antibody binding (*42*). All these factors demonstrate that immunoassay based analysis of IsoPs levels is a poor choice and to perform a reproducible and accurate study MS methods should be utilised. However, due to ease of use ELISA still remains a popular method for F_2-IsoP quantification.

Finally, there is some evidence to suggest that some F_2-IsoPs can also be produced independently of oxidative stress as a result of cyclooxygenase (COX) activity (*43*). The fact that COX activity has been linked to F_2-IsoP production highlights that quantified increases in F_2-IsoP levels may give false representation

of the levels of cellular oxidative stress if produced due to COX activity. As a result of this factor and the discussed problems with quantification, it is clear that using IsoPs as a biomarker for oxidative stress is not without its drawbacks, however these molecules still remain one of the most extensively studied and accurate biomarkers of oxidative stress currently available.

Glutathione (GSH) Antioxidant System

During oxidative stress, levels of GSH decrease due to oxidation and formation of GSH disulfides resulting in a decrease in the ratio of GSH to GSSG and PSSG. Consequently, the ratio of reduced to oxidised GSH (GSH:GSSG) is often used to examine redox status and is a well-established marker of oxidative stress. Alternatively, as the levels of protein s-glutathiolation are considerably higher during conditions of oxidative stress, its examination can also be used as a marker of protein oxidation and has also been utilised as a biomarker for oxidative stress (*24*, *44*).Changes in GSH concentrations and elevation of protein s-glutathiolation are known to be associated with Amyotrophic lateral sclerosis, AIDS, Alzheimer's Disease, cardiovascular disease, a range of cancers, diabetes, Friedreich's Ataxia, rheumatoid arthritis, hyperlipidaemia and renal failure among others (*24*, *44–49*).

Blood samples are the most frequently examined biological sample used to determine GSH levels. GSH is known to be present in blood samples at the milimolar level with its oxidised forms at micromolar levels. The average ratio of GSH to GSSG in blood is from 10:1 to 100:1 and as a result small changes in oxidation of GSH to GSSG or disulfide exchange will greatly affect ratio, making this method a sensitive method for determining oxidative stress. Interestingly, considerations need to be made when examining blood samples as erythrocytes can contain up to 500 times more GSH than plasma therefore haemolysis can result in an over estimation of GSH levels (*50*). Alternatively, s-glutathiolation has generally been investigated for diagnostic use by examining glutathiolation of proteins in circulating cells such as erythrocytes, with haemoglobin s-glutathiolation suggested to be a good biomarker of oxidative stress (*51*).

For many years, several different analytical methods have been utilised to determine GSH and GSSG concentrations from patient samples. For a long time the most commonly reported method was HPLC used in conjunction with various detection techniques which include ultraviolet and fluorescence detection as well as MS and electrochemical detection (ECD) (*50*). ECD was regarded as the most attractive method of detection due to its simplicity, high sensitivity and relatively low cost when compared to the others. However, Liquid Chromatography (LC)-tandem MS (MS/MS) has been shown to have improved selectivity, precision and accuracy as well as a higher sensitivity while still demonstrating a good agreement with studies which previously used HPLC-ECD (*52*). These added benefits of LC-MS/MS over HPLC-ECD have resulted in this method being more widely used for analysis of GSH and its related compounds in recent years. In contrast, although s-glutathiolation of susceptible proteins is also achieved using the same high resolution methods as those used to quantified total GSH, low resolution

In Oxidative Stress: Diagnostics, Prevention, and Therapy Volume 2; Hepel, et al.;
ACS Symposium Series; American Chemical Society: Washington, DC, 2015.

Publication Date (Web): October 13, 2015 | doi: 10.1021/bk-2015-1200.ch015

techniques like Western Blotting used under non-reducing conditions are more commonly used (*53*). Additionally, immunoassay methods like ELISA have also been used to quantify the level of glutathiolation of specific proteins, with some success demonstrated for its use for glutathiolated actin (*54*).

Unfortunately, like the other biomarkers discussed accurately measuring GSH, GSSG and PSSG levels can be difficult as GSH is easily oxidised non-enzymatically to GSSG by molecular oxygen and can react with disulfides resulting in thiol-disulfide exchange (*55*). Both these factors can greatly affect GSH:GSSG ratio in samples and therefore give false readings during quantification. In fact, different research groups have published differences in GSH, GSSG and PSSG concentrations of over 100 fold in healthy individuals as well as people with the same diseases, with some studies even showing increases in oxidation when others have shown decreases (*56*, *57*). These inconsistencies are now known to be due to artefact generation from poor specimen handling and preparation, as a result careful considerations are required to reduce risk (*57*). Studies have shown that artefact generation as a result of oxidation is pH and temperature dependent (*55*). Therefore, keeping samples at lower pH and temperatures during sample pre-treatment and storage in addition to adding the chelating agent Ethylenediaminetetraacetic acid (EDTA) produces an accurate quantification of GSH levels due to suppression of oxidation reactions (*55*, *56*). Furthermore, addition of the alkalying agent N-Ethylmaleimide (NEM) immediately after sample collection has been demonstrated to greatly decrease artefact generation (*57*). NEM freezes GSH redox status, blocking artificial GSH oxidation as well as preventing disulfide exchange which is achieved in part by inhibiting GSSG and PSSG reductases (*56*). Interestingly, if NEM is omitted artificially high GSSG and PSSG with lower GSH levels have been shown to be recorded (*57*).

In recent year's examination of GSH have become more far more accurate as a result of technological advancements in quantification, considerably improving reproducibility. Furthermore, the implementation of appropriate sample pre-treatment and storage which suppresses side reactions of GSH has ensured generation of artefacts is negligible allowing more accurate quantification of GSH, GSSG and PSSG. There is now much debate about the validity of previous studies which did not implement these pre-treatment methods and as such whether or not GSH, GSSG or PSSG levels are altered in patients with the diseases studied needs to be confirmed (*57*). However, if measured using artefact free methods, examining GSH and its oxidised forms is considered to be an extremely sensitive biomarkers of oxidative stress.

ROS Probes

Although the aforementioned oxidative stress markers are useful tools for the estimation of the levels of oxidative stress in samples, they may not directly correlate with the changes in the levels of ROS themselves. For example, cellular

In Oxidative Stress: Diagnostics, Prevention, and Therapy Volume 2; Hepel, et al.;
ACS Symposium Series; American Chemical Society: Washington, DC, 2015.

Publication Date (Web): October 13, 2015 | doi: 10.1021/bk-2015-1200.ch015

signalling induction of hydrogen peroxide (H_2O_2) generation can stimulate cellular effects without leading to biomolecular damage. In this case an increase in the H_2O_2 concentration is not followed by an accumulation of oxidative stress markers. Alternatively, an elevation in oxidative stress marker levels may not always correspond to an alteration in the oxidative state of the cell. For instance, it has been demonstrated that a reduction in transcriptional/translational fidelity leads to the carbonylation of proteins, a protein modification, often used as a marker of oxidative stress (*58*). This study has also proposed that protein carbonylation may operate as a tagging system for misfolded polypeptides (*58*). In conclusion, in order to comprehensively assess the oxidative state of samples, it is evident that the detection of the markers of oxidative stress should be accompanied by direct measurement of the ROS concentration.

Publication Date (Web): October 13, 2015 | doi: 10.1021/bk-2015-1200.ch015

However, ROS is a family of chemically heterogeneous molecules of different kinetics and oxidation activities, which in turn can cause distinctive cellular effects induced by specific oxidative reactions. For example, the unique chemistry of H_2O_2 allows it to reversibly oxidise sensitive cysteines of phosphatases, modulating the phosphorylation state of the cell. In contrast, while H_2O_2 is almost inert to DNA, $OH\cdot$ can irreversibly oxidise DNA bases leading to abasic sites, DNA adducts and DNA strand breaks (*59*). This diversity demonstrates that in order to study redox processes, along with the measurements of oxidative stress markers and ROS concentration, it is necessary to determine the type of ROS generated.

In contrast to the examination of more stable oxidative stress markers in lysed and processed samples, the direct detection of ROS carries certain difficulties. Due to the extremely short half-lives of ROS, their detection must occur in live samples, following minimal processing that could modulate ROS generation and detection. Furthermore, intracellularly generated ROS are immediately cleared by antioxidant enzymes that operate at the kinetic rates of up to 2×10^7 M^{-1} s^{-1} (*60*). Therefore, ROS detecting sensors should be able to successfully compete for the ROS with these antioxidant enzymes.

Most of the commercially available fluorescent dyes for ROS are based on the oxidation-reduction processes between the oxidative reactive species and reduced probes. Upon reaction between the sensor and the ROS, the oxidised probe becomes a highly fluorescent molecule. Generally the reduced forms of ROS probes are colourless (or display a minimal fluorescent signal) and the oxidised ones emit a coloured light upon excitation with a specific wavelength.

Along with an expanding field of redox biology, a considerable interest has been invested in the improvement of fluorescent ROS probes. In the next several paragraphs we will review the most common ROS probes and recent advancements in ROS measurements in cells both *in vitro* and *in vivo*.

DCF

The most widely used probe to detect ROS is 2′,7′-Dichlorodihydrofluorescein (DCF) (Figure 1). DCF was synthesised and used as a H_2O_2 probe for the first time in 1965 by Brandt *et al.* (*61*). While it was a breakthrough discovery

In Oxidative Stress: Diagnostics, Prevention, and Therapy Volume 2; Hepel, et al.;
ACS Symposium Series; American Chemical Society: Washington, DC, 2015.

for redox research at that time, the widespread usage of DCF since then has revealed several of its shortcomings: 1) it is not selective for H_2O_2; 2) it is easily photooxidised and photobleached; 3) it does not react directly with H_2O_2 but it requires peroxidise or metal catalysts; 4) it displays a non-linear relationship between concentration of ROS and fluorescent signal; 5) it is easily membrane diffusible (*62*). All of these caveats make DCF unsuitable for redox reaction studies. These points cannot be underestimated, given the plethora of research papers attempting to study intracellular signalling through DCF fluorescence, even in the recent literature (Figure 2).

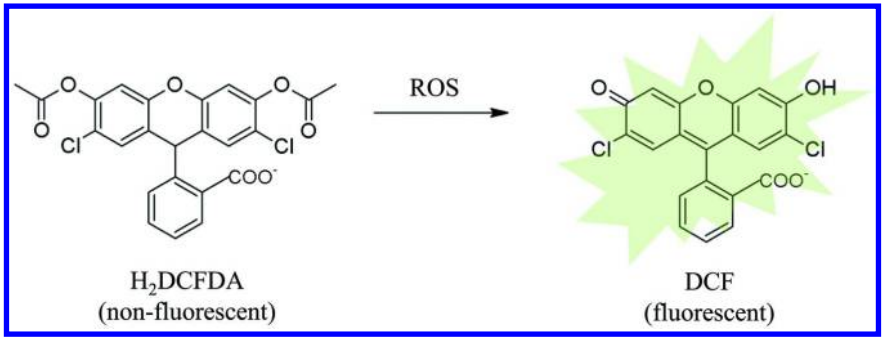

Figure 1. Reaction of H_2DCFDA with ROS yields green flourescent product.

DHE and MitoHE (MitoSOX)

Over the last 20 years of dihydroethidium (DHE) usage, many contradicting studies on its specificity have been reported. Some data suggested a specificity towards superoxide anion (*63*, *64*), while other studies show reactions between DHE and haeme proteins (*65*) or other ROS/ reactive nitrogen species (*66*, *67*). Finally, in 2010 Zielonka and Kalyanaraman wrote an extensive review summarising all work regarding DHE as a ROS-detecting probe (*68*). DHE fluorescent signals can be falsely enhanced by intercalation of the dye with DNA. Furthermore, DHE can be oxidised by various radicals to form differentially oxidised products. However, only product reaction with superoxide (2-OH-E) alters the signal so the probe can be excited by 396 nm wavelength (Figure 3). Therefore, in order to reveal the superoxide-induced signal, a 396 nm wavelength should be used as an excitation source (*68*, *69*).

In order to target the probe specifically to mitochondria, DHE was conjugated to the triphenylphosphonium (TPP+) moiety, resulting in the MitoSOX dye. Cationic TPP+ allows the probe to move through the mitochondrial membrane and accumulate in the mitochondrial matrix. While MitoSOX possesses the inherent disadvantages associated with DHE, it is a promising tool to investigate mitochondrial superoxide/ROS production (*70*).

Publication Date (Web): October 13, 2015 | doi: 10.1021/bk-2015-1200.ch015

Publication Date (Web): October 13, 2015 | doi: 10.1021/bk-2015-1200.ch015

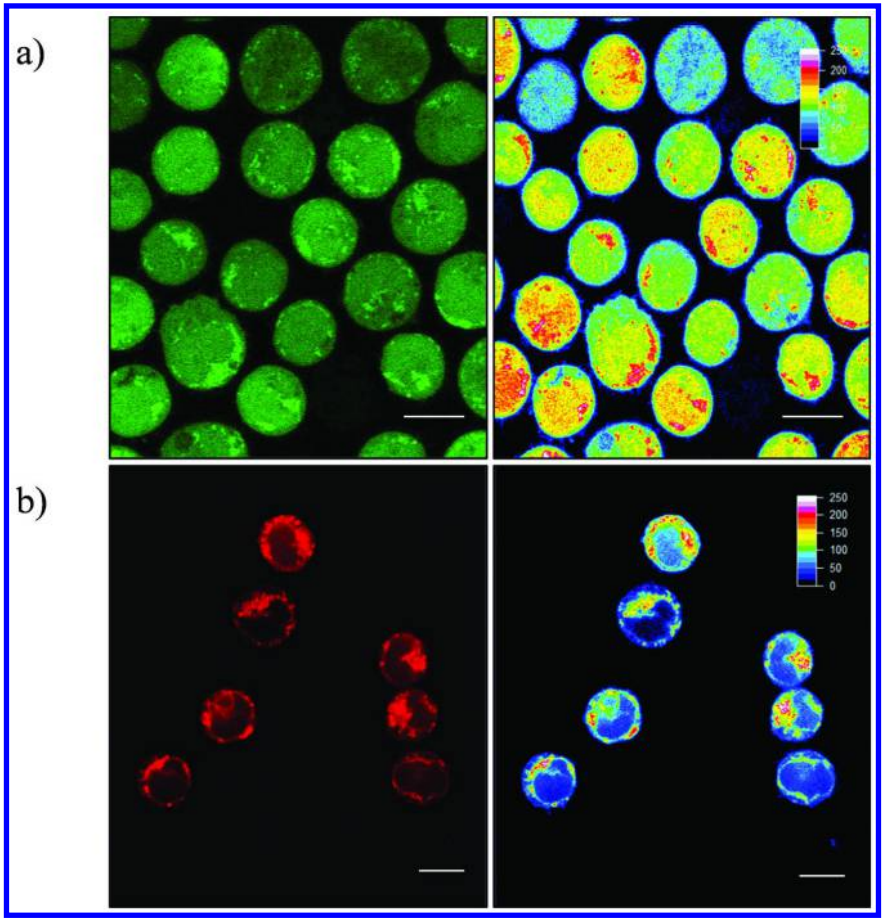

Figure 2. Confocal images of DCF (a)) and PO1 (b)) stained MV4-11 cells. Pseudo-coloured images on the right represent intensity distribution (from highest intensity indicated by white to the lowest designated by black).

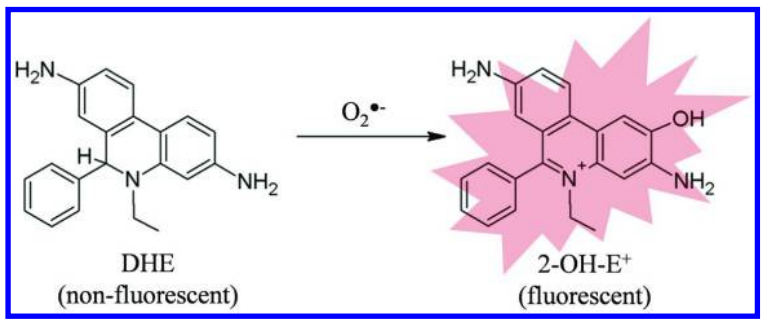

Figure 3. Reaction of DHE with superoxide anion yields red flourescent product 2-OH-E$^+$.

Publication Date (Web): October 13, 2015 | doi: 10.1021/bk-2015-1200.ch015

OxyBurst Family: SE, BSA and FC

The OxyBurst family of ROS dyes is composed of: FC OxyBurst, OxyBurst Green H_2HFF BSA and OxyBURST Green. FC OxyBurst is a DCF moiety linked to BSA and anti-BSA antibody complex that stimulates the FC receptor causing the internalization of the probe and the subsequent measurement of the oxidative burst in the phagovacuole. As FC OxyBurst is based on DCF moiety it possesses similar inherent problems, however owing to the specific internalization it may be a useful tool to study NADPH oxidase-induced ROS burst. On the other hand, BSA linked OxyBURST Green H_2HFF in (OxyBurst Green H_2HFF BSA) does not allow the probe to translocate into the cell, which makes the probe useful for the ROS measurement in the extracellular space. In fact, the probe was used for the detection of the extracellular release of the ROS in coronary arterial myocytes generated by Nox1 (*71*).

Boronate-Deprotection Probes

The specific reaction between H_2O_2 and boronate was employed in the development of the first H_2O_2 specific probes, important for examination of redox signalling processes (*72*) (Figure 4). The first developed probes (green peroxyfluor 1, red peroxyresorufin 1 and blue peroxyxanthone 1) were based on the fluorescence-emitting opening of the bis-boronate-originated lactone structure (*73*, *74*). This was successful in detecting H_2O_2 at the micromolar level, and as such was useful in measuring H_2O_2 relevant to oxidative stress. Further optimization of the probes relying on the removal of one of the boronates revealed substantial increase in H_2O_2 sensitivity. This chemical alteration allowed the monoboronate-based family of probes (Peroxyfluor-3, Peroxy Orange 1 and Peroxy Yellow 1) to detect physiological/signalling changes in H_2O_2 concentration upon phorbol 12-myristate 13-acetate (PMA), epidermal growth factor (EGF) stimulation (*75*). The colour palette of these probes allowed to simultaneously either colocalize the H_2O_2 generation in the cell with organelle-tracker or concurrent detection of H_2O_2 and other ROS probes e.g. APF (*75*, *76*) (Figure 2). The further modification of monoborate-possessing probes, namely addition of methyl –ester group increased cellular retention following cleavage by esterases, resulting in synthesis of Peroxy Yellow 1 Methyl-Ester (PY1-ME) (*77*). This probe has been used in the investigation of H_2O_2 uptake by aquaporins in HEK 293 cells (*78*). Interestingly, PY1-ME showed similar results to genetically encoded fluorescent H_2O_2 sensor – Hyper (*77*). The latest version of PF-1, Peroxy Fluor 6 acetoxymethyl ester (PF6-AM), was synthesized in order to explore mechanism of NOX regulation in the brain (*79*). The addition of the acetoxymethyl group gives the dye increased cellular retention and hence increased sensitivity to H_2O_2. The AM-esters aid in the translocation of the probe through the membrane and traps it there following the AM groups reaction with cellular esterases. This structural alteration made PF6-AM probe more sensitive than previous members of the Peroxy family. PF6-AM responded to concentrations as low as 10 μM exogenous H_2O_2, and signaling levels of H_2O_2 upon FGF-2 stimulation, which was not possible with Peroxy Green 1 (*79*).

In Oxidative Stress: Diagnostics, Prevention, and Therapy Volume 2; Hepel, et al.;
ACS Symposium Series; American Chemical Society: Washington, DC, 2015.

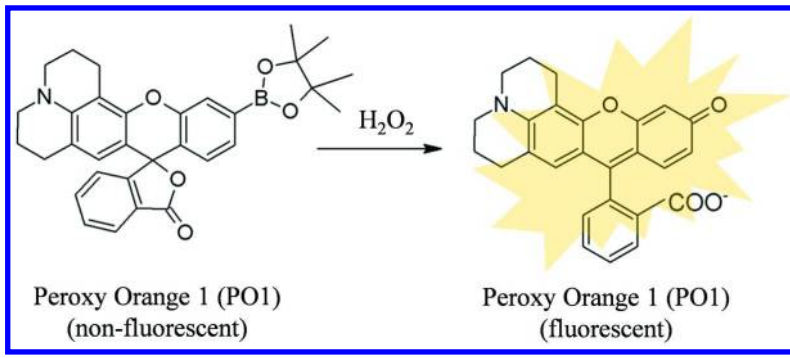

Figure 4. Reaction of PO1 with H_2O_2 yields an orange flourescent product.

Publication Date (Web): October 13, 2015 | doi: 10.1021/bk-2015-1200.ch015

Addition of the boronate moiety to the click-modified coumarin platform combined H_2O_2-chemoselectivity with the highly fluorescent characteristics of the coumarin dye (*80*). The coumarin moiety also allows possible tethering of the compound to other functional groups, to target it to different organelles or to improve some physico-chemical properties such as sensitivity, photostability, permeability. The probe responded with a 5-fold increase in the fluorescence intensity following 5 μM H_2O_2 treatment (*80*). Furthermore, the probe's emission intensity was shown to be dependent specifically on H_2O_2 concentration, and the concentration dependence does not occur in the presence of other ROS (*80*).

The boronate chemistry was also utilised in the synthesis of RS-BE probe that fluoresces upon presence of both H_2O_2 and iron/copper ions (*81*). The reaction with H_2O_2 unmasks the specific chelating region of the RS-BE that can react specifically with metal ions, yielding a fluorescent metal-coordinated product. RS-BE was demonstrated to specifically fluoresce in the presence of the Fe/Cu ions and H_2O_2 in neuroblastoma cells (*81*). Fe and H_2O_2 react with each other in the Fenton reaction that yields highly damaging $OH^{\bullet}$. Probes that offers specific detection of H_2O_2 in the presence of Fe/Cu, such as RS-BE, could aid in the localization of sites damaged by H_2O_2.

Ratiometric H_2O_2 Probes

While specific detection of H_2O_2 has been considerably improved by the development of boronate-based probes, quantification of the fluorescent signal upon the reaction with H_2O_2 has still remained a significant issue. Signal from the single-wavelength emitting probes can be affected by the concentration of the probe, which questions the quantification analysis of these probes. Ratiometric probes monitor changes in the fluorescence in ratio to the probe itself, which corrects the artifacts caused by the variable concentration of the probe or photobleaching. Ratio Peroxyfluor 1, a ratiometric monoboronate-based probe, overcomes these issues as the quantification of the change in the fluorescence is calculated as a ratio of the fluorescence upon reaction with H_2O_2 (λ_{517}) to the internal fluorescence of the probe (λ_{464}) (*82*). Following the reaction with H_2O_2,

In Oxidative Stress: Diagnostics, Prevention, and Therapy Volume 2; Hepel, et al.;
ACS Symposium Series; American Chemical Society: Washington, DC, 2015.

fluorescence resonance energy transfer (FRET) occurs between the coumarin moiety (donor) and boronate group (acceptor) in the two-fluorophore cassette that leads to an 8-fold increase in fluorescence intensity ratio (*82*).

Similar chemistry has been utilised in the synthesis of a ratiometric– Peroxy Lucifer 1 (PL1) - another H_2O_2-measuring ratiometric probe (*83*). Upon reacting with H_2O_2, internal charge transfers within the Lucifer platform result in a change in the emission colour of the dye. The key advantage of PL-1 is the fact that it allows the measurement of localized H_2O_2 generation with simultaneous monitoring of the H_2O_2 variation across the rest of the cell. The relative ratios of the green versus blue fluorescence intensity revealed changes in the local H_2O_2 changes in the vesicles versus the cytoplasm upon PMA stimulation of RAW 264.7 macrophages (*83*).

Similarly, dimethylaminocinnamaldehyde (DMACA), a ratiometric H_2O_2 probe demonstrates intra-molecular charge transfer upon the reaction with H_2O_2 (*84*). The transfer involves a change in the ratio of the absorption/emission at two wavelengths. Interestingly, the change in colour is also visible to the naked eye which could be useful in the synthesis of a simple H_2O_2 sensor in solutions. The probe demonstrated a significant responsiveness to 2μM H_2O_2 treatment in the prostate cancer cell line (PC3), resulting in a change in a probe colour from red to blue (*84*).

Publication Date (Web): October 13, 2015 | doi: 10.1021/bk-2015-1200.ch015

Deep-Tissue Penetrating Probes

All of the aforementioned probes are suitable for the detection and measurement of H_2O_2 in the cell samples. However, in the clinical environment it may be important to measure changes in the redox state of tissue samples, for example following patient biopsy.

There have been few probes reported utilising the boronate-phenol chemistry and allowing for H_2O_2 imaging in thicker tissue. Naphto-Peroxyfluor-1 (NPF1) is one such probe, in which the addition of a naphtofluorescein moiety results in emission in the visible far-red region of the spectrum (*85*). This change in the fluorescence profile has several benefits. Firstly, it avoids problems with background fluorescence from the specimen. Secondly, it enables imaging of thicker samples (>80um) e.g. tissue slices. While this probe presents the aforementioned advantages, it utilizes one-photon microscopy which carries a number of drawbacks. The short excitation wavelengths are quite damaging to live specimens, substantially shortening the time for accurate imaging. These shortcomings were overcome in Peroxy Naphthalene 1 (PN1), the first H_2O_2 specific two-photon fluorescent probe with the excitation profile in the near-infrared region (*86*). PN1 probe is applicable to deeper tissue imaging as it facilitates prolonged imaging without causing much damage to the specimen. Additionally, PN1 is a ratiometric dye that can be used for quantitative analysis of the H_2O_2 generation. The probe's fluorescence is not affected by changes in biological range of pH, and does not cause cytotoxicity (*86*). The combination of two-photon microscopy with ratiometric analysis makes PN1 a good candidate for examining H_2O_2 levels in tissue.

By combining the boronate chemoselectivity and the cationic triphenylphosphonium affinity for mitochonidria (TPP+), Masanta *et al.* synthesized a two-photon H_2O_2 probe targeted to mitochondria called (SHP-Mito) (*87*). The addition of 6-(benzo[d]thiazol-20-yl)-2-(N,N-dimethylamino)naphthalene (BTDAN) as a reporter allows for the ratiometric analysis of the probe oxidation. The probe was demonstrated to be unresponsive to other ROS/RNS and pH change. Due to two-photon excitation, the probe was useful for the deep tissue imaging ranging from 100-180 μm (*87*).

In Vivo H_2O_2 Detection

One of the most important characteristics of ROS fluorescent probes is their compatibility for studies in animal models. However, imaging of these probes in animals introduces some problems with the diffusion and tissue/organ penetration of these probes, and subsequent probe visualisation in the animals. Combination of the near-infrared detection of cyanine-7 (Cy-7) with the chemoselectivity of phenylboronic acid resulted in the synthesis of a quinone derivative QCy7 (*88*). The near-infrared (NIR) imaging of cyanine is an attractive tool in animal studies due to the deep penetration of the NIR photons and low background fluorescence of the tissue. The boronate group is linked through an ether-linkage to sulfonated derivative of QCy7, as sulfonation increases the solubility of the compound. The reaction between the phenylboronic acid and H_2O_2 results in the hydrolysis of the compound, yielding the fluorescing sulfo-QCy7. Importantly, Sulfo-QCy7 probe was used to non-invasively image exogenously administered H_2O_2 into mice. The change in the concentration of H_2O_2 following injection resulted in a change in the fluorescent signal. Moreover, the dye allowed for the monitoring of H_2O_2 signaling upon injection of LPS into mice. Study of the chemical stability of Sulfo-QCy7 found that the intensity of the fluorescence signal showed a minimal change over the first 5 hours. In conlusion, Sulfo-QCy7 offers a promising research tool for noninvasive intravital quantitative imaging of animals.

Bioluminescence possesses favourable properties for *in vivo* imaging. Connecting a boronate moiety to a firefly luciferin platform resulted in a synthesis of Peroxy Caged Luciferin-1 (PCL-1) (*89*). While maintaining the H_2O_2 selectivity, the probe has an ability to non-invasively measure H_2O_2 throughout the whole mouse body without removal of the fur or skin. Moreover, the signal received from the luciferin depends linearly on the concentration of the H_2O_2 within a range from 5-250 μM in both aqueous solutions and in the cell culture environment. The probe was used to detect increases in H_2O_2 upon testosterone stimulation that was attenuated by the combination of testosterone with N-acetylcysteine (NAC), a radical scavenger, in the FVB-luc+ mice. While PCL-1 offers an interesting tool to study the redox changes in animals, the animal needs to ubiquitously express the firefly luciferase in order to visualize the reaction of the probe.

The specific intracellular localisation of ROS can distinctly modify cellular responses and/or cell pathology. Therefore, there is considerable research interest in developing *in vivo* probes that detect ROS in cellular organelles, for instance mitochondria or nucleus. MitoBoronic acid (MitoB) is a ratiometric

Publication Date (Web): October 13, 2015 | doi: 10.1021/bk-2015-1200.ch015

mass spectroscopy probe that uses the boronate group conjugated to the cationic phosphonium moiety for mitochondrial accumulation (*90*). Upon reaction with H_2O_2, MitoB is converted to the phenol product (MitoP). Mass spectroscopy analysis of the MitoB/MitoP ratio allows it to accurately measure H_2O_2 in the whole organism, as well as in cells and tissues. MitoB responds to changes in mitochondrial ROS in mice, *Caenorhabditis elegans* and *Drosophila melanogaster*. The probe offers the measurement of H_2O_2 concentration H_2O_2 in the mitochondria with a nanomolar accuracy. Combination of specific mitochondrial targeting and H_2O_2 -chemoselective switch with mass spectroscopy analysis in MitoB proposes a unique candidate for H_2O_2 measurement in the mitochondria of cells and animals.

Nuclear Peroxy Emerald 1 (NucPE1) (*91*) is a monoboronate-based probe that localizes to the nucleus. NucPE1 was demonstrated to detect changes in H_2O_2 in the nucleus *in vivo* in *C. elegans* (*91*). The probe was also demonstrated to respond to nuclear H2O2 alterations in various leukaemic cell lines (*92*, *93*). Because of its excellent nuclear localization in a variety of cell, the probe offers a promising tool to study nuclear H_2O_2 (*94*). However, further studies need to be carried out to determine the mechanism of its nuclear accumulation, as well as its sensitivity/ dynamic range properties.

Publication Date (Web): October 13, 2015 | doi: 10.1021/bk-2015-1200.ch015

OH· Probes

The aforementioned OH· has got extremely short-life (10^{-9} s) and it is considered the most aggressive free radical. OH· is produced in the Fenton reaction, when iron (II) is oxidised by H_2O_2 to iron (III). It has been demonstrated that OH· readily reacts with amino acids, proteins, lipids and DNA, which can lead to cell damage and apoptosis. This makes OH· an important molecule to detect when examining oxidative stress.

One of the most commonly used OH·-detecting fluorescent probes is coumarin-3-carboxylic acid (3-CCA). Following the reaction with OH· 3-CCA becomes hydroxylated forming a fluorescent 7-OHCCA product (*95*) (Figure 5). 3-CCA was demonstrated to detect chemical and radiation sources of OH·. However, due to high pH sensitivity of the fluorescent product, pH must be carefully monitored (*95*).

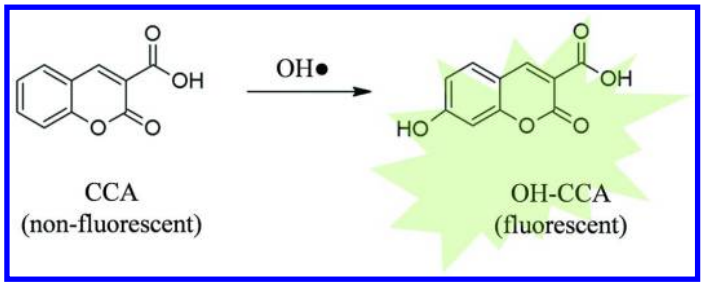

Figure 5. Reaction of CCA with OH· yields OH-CCA, a green flourescent product.

In Oxidative Stress: Diagnostics, Prevention, and Therapy Volume 2; Hepel, et al.;
ACS Symposium Series; American Chemical Society: Washington, DC, 2015.

The reactivity of 3-CCA with OH· was utilised in the synthesis of Coumarin-NEutral Red (CONER), which is a ratiometric nanoprobe composed of biocompatible nanoparticles and encapsulated neutral red with 3-CCA derivative (*96*). CONER probe quantifies the OH· levels as a fluorescence ratio of the reference Texas Red dye and the OH·-sensing 3-CCA moiety. It was demonstrated that CONER nanoprobe responded specifically to OH· in viable cancer cells exposed to oxidative stress (*96*).

Hydroxyphenyl fluorescein (HPF) has been commercially available to detect OH· for many years (Figure 6). However, similar to other intensity-based (non-ratiometric) fluorescent probes, HPF fluorescence is dependent on the pH, concentration of the probe and other environmental factors. Therefore, sensitivity of HPF for OH· has been used in the development of AuNC@HPF, a nanoprobe where the gold nanocluster (AuNC) protected by bovine serum albumin is employed as a reference fluorophore, and the HPF function as both a OH· sensor and the source of the response signal (*97*). The probe can be spectrophotometrically detected by a single emission peak at 637 nm, originating from AuNC reference fluorescence (*97*). Upon addition of OH·, a second HPF emission peak can be observed at 515 nm – which is strictly dependent on the concentration of OH·. The probe demonstrates a high selectivity for OH· over other ROS, as well as good water solubility, cell permeability and long-term stability (*97*).

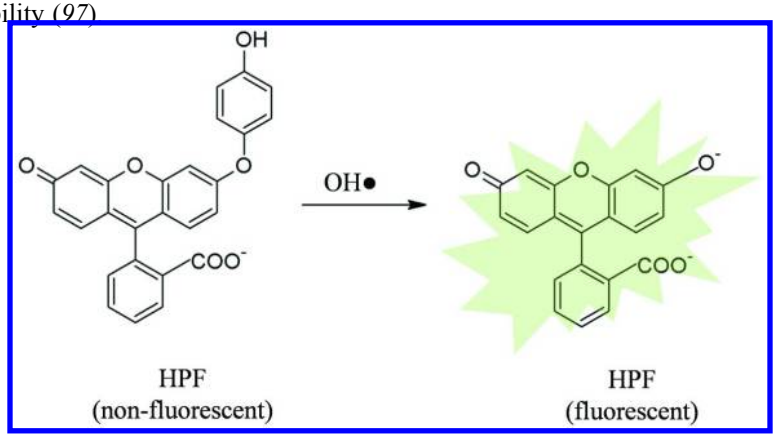

Figure 6. Reaction of HPF with OH· yields a green flourescent product.

Concluding Remarks

Some of ROS characteristics, such as a short half-life and extreme reactivity, make them difficult to detect, measure and analyse quantitatively. Furthermore, a high concentration of cellular antioxidant enzymes and great kinetic rates of their reactions with ROS result in a molecular competition between a probe and an antioxidant enzyme. With the expansion of redox biology, the number of newly synthesised ROS probes increased and while most of them still require some validation and optimisation, the progress has been made, especially in the advancements in the probes selective for a particular ROS (Figure 6).

In Oxidative Stress: Diagnostics, Prevention, and Therapy Volume 2; Hepel, et al.;
ACS Symposium Series; American Chemical Society: Washington, DC, 2015.

Publication Date (Web): October 13, 2015 | doi: 10.1021/bk-2015-1200.ch015

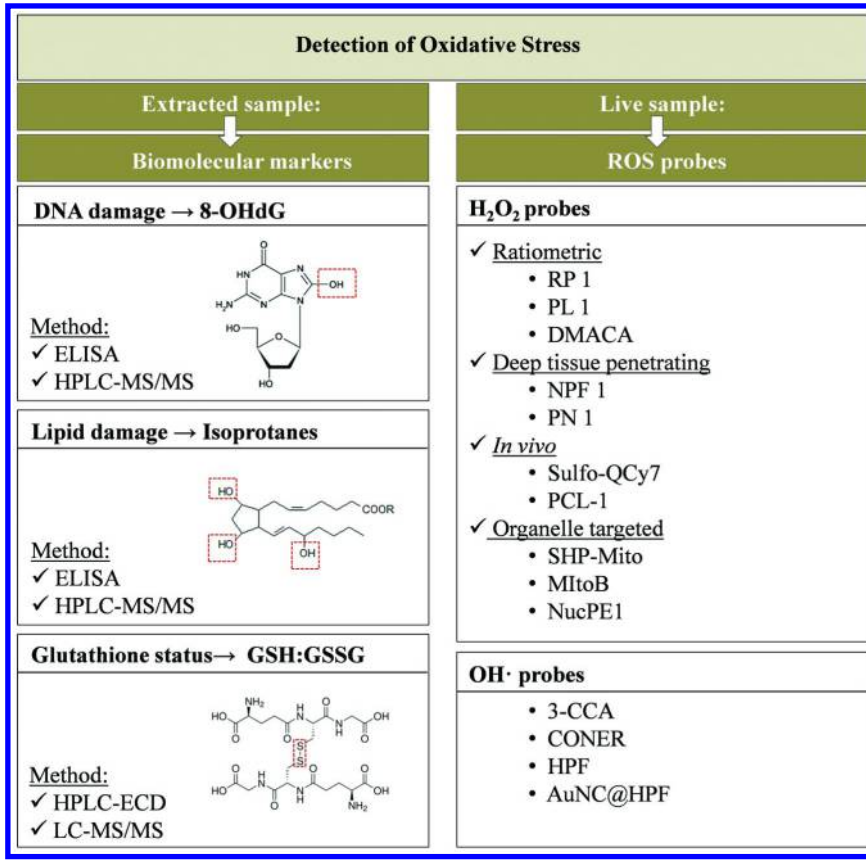

Figure 7. A schematic representing the choice of proposed probes and markers to detect oxidative stress in biological samples.

In order for ROS probes to be used in oxidative stress examination in clinical environment, the probes should be: 1) chemo-selective for the specific ROS; 2) easily distributed around cells and tissues; 3) sensitive to slight changes in ROS signaling; 4) photostable and retainable post-fixation to facilitate imaging or measurements; and 5) non-toxic to be used in humans in the future. While some of the novel probes fulfil some of these criteria, the utilisation of live ROS detection in clinical samples is still in its infancy.

With the onset and progression of many diseases being increasingly linked with changes in the cellular redox state, accurately examining these changes has become increasingly more important. Examining oxidative stress biomarkers has the potential to provide greater insight into the characteristics of redox-related disease as well as help identify new therapeutic and diagnostic methods (*98*, *99*). As discussed, major discrepancies have been noted between the various measurement methods used. However, the use of these biomarkers to examine oxidative stress has continued to grow and as a result much attention has been placed on increasing accuracy through improvement of all aspects of analysis,

from sample collection, processing and the standardisation of measurement procedures. Although there are many biomarkers of oxidative stress to choose from, the previously discussed biomarkers still remain some of the most utilised for the determination of oxidative stress both in the laboratory and clinic (Figure 7).

References

1. Giustarini, D.; Dalle-Donne, I.; Tsikas, D.; Rossi, R. *Crit. Rev. Clin. Lab. Sci.* **2009**, *46*, 241–281.
2. Wiseman, H.; Halliwell, B. *Biochem. J.* **1996**, *313* (Pt 1) (2), 17–29.
3. Altieri, F.; Grillo, C.; Maceroni, M.; Chichiarelli, S. *Antioxid. Redox Signal.* **2008**, *10* (5), 891–937.
4. Cheng, K. C.; Cahill, D. S.; Kasai, H.; Nishimura, S.; Loeb, L. A. *J. Biol. Chem.* **1992**, *267* (1), 166–72.
5. Wallace, S. S. *Free Radical Biol. Med.* **2002**, *33* (1), 1–14.
6. Mecocci, P.; MacGarvey, U.; Beal, M. F. *Ann. Neurol.* **1994**, *36* (5), 747–51.
7. Kikuchi, A.; Takeda, A.; Onodera, H.; Kimpara, T.; Hisanaga, K.; Sato, N.; Nunomura, A.; Castellani, R. J.; Perry, G.; Smith, M. A.; Itoyama, Y. *Neurobiol. Dis.* **2002**, *9* (2), 244–8.
8. Wu, L. L.; Chiou, C. C.; Chang, P. Y.; Wu, J. T. *Clin. Chim. Acta* **2004**, *339* (1−2), 1–9.
9. Kryston, T. B.; Georgiev, A. B.; Pissis, P.; Georgakilas, A. G. *Mutat. Res.* **2011**, *711* (1−2), 193–201.
10. Collins, A. R.; Cadet, J.; Möller, L.; Poulsen, H. E.; Viña, J. *Arch. Biochem. Biophys.* **2004**, *423* (1), 57–65.
11. Gedik, C. M.; Collins, A. *FASEB J.* **2005**, *19* (1), 82–4.
12. Cooke, M. S.; Evans, M. D.; Herbert, K. E.; Lunec, J. *Free Radical Res.* **2000**, *32* (5), 381–97.
13. Loft, S.; Svoboda, P.; Kasai, H.; Tjønneland, A.; Vogel, U.; Møller, P.; Overvad, K.; Raaschou-Nielsen, O. *Carcinogenesis* **2006**, *27* (6), 1245–50.
14. Cooke, M. S.; Olinski, R.; Loft, S. *Cancer Epidemiol. Biomarkers Prev.* **2008**, *17* (1), 3–14.
15. Valavanidis, A.; Vlachogianni, T.; Fiotakis, C. *J. Environ. Sci. Health, Part C: Environ. Carcinog. Ecotoxicol. Rev.* **2009**, *27* (2), 120–39.
16. Sakumi, K.; Furuichi, M.; Tsuzuki, T.; Kakuma, T.; Kawabata, S.; Maki, H.; Sekiguchi, M. *J. Biol. Chem.* **1993**, *268* (31), 23524–30.
17. Barregard, L.; Møller, P.; Henriksen, T.; Mistry, V.; Koppen, G.; Rossner, P.; Sram, R. J.; Weimann, A.; Poulsen, H. E.; Nataf, R.; Andreoli, R.; Manini, P.; Marczylo, T.; Lam, P.; Evans, M. D.; Kasai, H.; Kawai, K.; Li, Y.-S.; Sakai, K.; Singh, R.; Teichert, F.; Farmer, P. B.; Rozalski, R.; Gackowski, D.; Siomek, A.; Saez, G. T.; Cerda, C.; Broberg, K.; Lindh, C.; Hossain, M. B.; Haghdoost, S.; Hu, C.-W.; Chao, M.-R.; Wu, K.-Y.; Orhan, H.; Senduran, N.; Smith, R. J.; Santella, R. M.; Su, Y.; Cortez, C.; Yeh, S.; Olinski, R.; Loft, S.; Cooke, M. S. *Antioxid. Redox Signal.* **2013**, *18* (18), 2377–91.

Publication Date (Web): October 13, 2015 | doi: 10.1021/bk-2015-1200.ch015

18. Rossner, P.; Mistry, V.; Singh, R.; Sram, R. J.; Cooke, M. S. *Biochem. Biophys. Res. Commun.* **2013**, *440* (4), 725–30.
19. Porter, N. A.; Caldwell, S. E.; Mills, K. A. *Lipids* **1995**, *30* (4), 277–90.
20. Esterbauer, H.; Schaur, R. J.; Zollner, H. *Free Radical Biol. Med.* **1991**, *11* (1), 81–128.
21. Yin, H.; Porter, N. A. *Antioxid. Redox Signal.* **2005**, *7* (1-2), 170–84.
22. Dalle-Donne, I.; Giustarini, D.; Colombo, R.; Rossi, R.; Milzani, A. *Trends Mol. Med.* **2003**, *9* (4), 169–176.
23. Milne, G. L.; Yin, H.; Hardy, K. D.; Davies, S. S.; Roberts, L. J. *Chem. Rev.* **2011**, *111* (10), 5973–96.
24. Dalle-Donne, I.; Rossi, R.; Colombo, R.; Giustarini, D.; Milzani, A. *Clin. Chem.* **2006**, *52* (4), 601–23.
25. Reed, T. T. *Free Radical Biol. Med.* **2011**, *51* (7), 1302–19.
26. Ho, E.; Karimi Galougahi, K.; Liu, C.-C.; Bhindi, R.; Figtree, G. a. *Redox Biol.* **2013**, *1* (1), 483–91.
27. Morrow, J. D.; Hill, K. E.; Burk, R. F.; Nammour, T. M.; Badr, K. F.; Roberts, L. J. *Proc. Natl. Acad. Sci. U. S. A.* **1990**, *87* (23), 9383–7.
28. Morrow, J. D.; Awad, J. A.; Boss, H. J.; Blair, I. A.; Roberts, L. J. *Proc. Natl. Acad. Sci. U. S. A.* **1992**, *89* (22), 10721–5.
29. Morrow, J. D. *Arterioscler. Thromb. Vasc. Biol.* **2003**, *23* (3), 368–70.
30. Kaviarasan, S.; Muniandy, S.; Qvist, R.; Ismail, I. S. *J. Clin. Biochem. Nutr.* **2009**, *45* (1), 1–8.
31. Markesbery, W. R.; Kryscio, R. J.; Lovell, M. A.; Morrow, J. D. *Ann. Neurol.* **2005**, *58* (5), 730–5.
32. Dai, Q.; Gao, Y.-T.; Shu, X.-O.; Yang, G.; Milne, G.; Cai, Q.; Wen, W.; Rothman, N.; Cai, H.; Li, H.; Xiang, Y.; Chow, W.-H.; Zheng, W. *J. Clin. Oncol.* **2009**, *27* (15), 2482–8.
33. Barocas, D. A.; Motley, S.; Cookson, M. S.; Chang, S. S.; Penson, D. F.; Dai, Q.; Milne, G.; Roberts, L. J.; Morrow, J.; Concepcion, R. S.; Smith, J. A.; Fowke, J. H. *J. Urol.* **2011**, *185* (6), 2102–7.
34. Kadiiska, M. B.; Gladen, B. C.; Baird, D. D.; Germolec, D.; Graham, L. B.; Parker, C. E.; Nyska, A.; Wachsman, J. T.; Ames, B. N.; Basu, S.; Brot, N.; Fitzgerald, G. A.; Floyd, R. A.; George, M.; Heinecke, J. W.; Hatch, G. E.; Hensley, K.; Lawson, J. A.; Marnett, L. J.; Morrow, J. D.; Murray, D. M.; Plastaras, J.; Roberts, L. J.; Rokach, J.; Shigenaga, M. K.; Sohal, R. S.; Sun, J.; Tice, R. R.; Van Thiel, D. H.; Wellner, D.; Walter, P. B.; Tomer, K. B.; Mason, R. P.; Barrett, J. C. *Free Radical Biol. Med.* **2005**, *38* (6), 698–710.
35. Morrow, J. D. *Arterioscler., Thromb., Vasc. Biol.* **2005**, *25* (2), 279–86.
36. Stafforini, D. M.; Sheller, J. R.; Blackwell, T. S.; Sapirstein, A.; Yull, F. E.; McIntyre, T. M.; Bonventre, J. V.; Prescott, S. M.; Roberts, L. J. *J. Biol. Chem.* **2006**, *281* (8), 4616–23.
37. Morrow, J. D.; Awad, J. A.; Kato, T.; Takahashi, K.; Badr, K. F.; Roberts, L. J.; Burk, R. F. *J. Clin. Invest.* **1992**, *90* (6), 2502–7.
38. Morrow, J. D.; Zackert, W. E.; Yang, J. P.; Kurhts, E. H.; Callewaert, D.; Dworski, R.; Kanai, K.; Taber, D.; Moore, K.; Oates, J. A.; Roberts, L. J. *Anal. Biochem.* **1999**, *269* (2), 326–31.
39. Basu, S. *Antioxid. Redox Signal.* **2008**, *10* (8), 1405–34.

Publication Date (Web): October 13, 2015 | doi: 10.1021/bk-2015-1200.ch015

40. Proudfoot, J.; Barden, A.; Mori, T. A.; Burke, V.; Croft, K. D.; Beilin, L. J.; Puddey, I. B. *Anal. Biochem.* **1999**, *272* (2), 209–15.
41. Smith, K. A.; Shepherd, J.; Wakil, A.; Kilpatrick, E. S. *Ann. Clin. Biochem.* **2011**, *48* (Pt 2), 147–54.
42. Il'yasova, D.; Morrow, J. D.; Ivanova, A.; Wagenknecht, L. E. *Ann. Epidemiol.* **2004**, *14* (10), 793–7.
43. Tsikas, D.; Suchy, M.-T.; Niemann, J.; Tossios, P.; Schneider, Y.; Rothmann, S.; Gutzki, F.-M.; Frölich, J. C.; Stichtenoth, D. O. *FEBS Lett.* **2012**, *586* (20), 3723–30.
44. Giustarini, D.; Rossi, R.; Milzani, A.; Colombo, R.; Dalle-Donne, I. *J. Cell. Mol. Med.* **2004**, *8* (2), 201–12.
45. Navarro, J.; Obrador, E.; Carretero, J.; Petschen, I.; Aviñó, J.; Perez, P.; Estrela, J. M. *Free Radical Biol. Med.* **1999**, *26* (3−4), 410–8.
46. Pastore, A.; Federici, G.; Bertini, E.; Piemonte, F. *Clin. Chim. Acta* **2003**, *333* (1), 19–39.
47. Pastore, A.; Piemonte, F.; Locatelli, M.; Lo Russo, A.; Gaeta, L. M.; Tozzi, G.; Federici, G. *Clin. Chem.* **2001**, *47* (8), 1467–9.
48. Piemonte, F.; Pastore, A.; Tozzi, G.; Tagliacozzi, D.; Santorelli, F. M.; Carrozzo, R.; Casali, C.; Damiano, M.; Federici, G.; Bertini, E. *Eur. J. Clin. Investig.* **2001**, *31* (11), 1007–11.
49. Zitka, O.; Skalickova, S.; Gumulec, J.; Masarik, M.; Adam, V.; Hubalek, J.; Trnkova, L.; Kruseova, J.; Eckschlager, T.; Kizek, R. *Oncol. Lett.* **2012**, *4* (6), 1247–1253.
50. Santa, T. *Drug Discovery Ther.* **2013**, *7* (5), 172–177.
51. Bursell, S. E.; King, G. L. *Clinical Chem.* **2000**, *46* (2), 145–6.
52. Squellerio, I.; Caruso, D.; Porro, B.; Veglia, F.; Tremoli, E.; Cavalca, V. *J. Pharm. Biomed. Anal.* **2012**, *71*, 111–8.
53. Dalle-Donne, I.; Scaloni, A.; Giustarini, D.; Cavarra, E.; Tell, G.; Lungarella, G.; Colombo, R.; Rossi, R.; Milzani, A. *Mass Spectrom. Rev.* **2005**, *24* (1), 55–99.
54. Johansson, M.; Lundberg, M. *BMC Biochem.* **2007**, *8*, 26–26.
55. Santa, T.; Aoyama, C.; Fukushima, T.; Imai, K.; Funatsu, T. *Biomed. Chromatogr.* **2006**, *20* (6−7), 656–61.
56. Rossi, R.; Milzani, A.; Dalle-Donne, I.; Giustarini, D.; Lusini, L.; Colombo, R.; Di Simplicio, P. *Clinical Chem.* **2002**, *48* (5), 742–53.
57. Rossi, R.; Dalle-Donne, I.; Milzani, A.; Giustarini, D. *Clinical Chem.* **2006**, *52* (7), 1406–14.
58. Dukan, S.; Farewell, A.; Ballesteros, M.; Taddei, F.; Radman, M.; Nyström, T. *Proc. Natl. Acad. Sci. U. S. A.* **2000**, *97* (11), 5746–5749.
59. Cadet, J.; Delatour, T.; Douki, T.; Gasparutto, D.; Pouget, J.-P.; Ravanat, J.-L.; Sauvaigo, S. *Mutat. Res., Fundam. Mol. Mech. Mutagen.* **1999**, *424* (1–2), 9–21.
60. Mishina, N. M.; Tyurin-Kuzmin, P. A.; Markvicheva, K. N.; Vorotnikov, A. V.; Tkachuk, V. A.; Laketa, V.; Schultz, C.; Lukyanov, S.; Belousov, V. V. *Antioxid. Redox Signal.* **2011**, *14* (1), 1–7.
61. Brandt, R.; Keston, A. S. *Anal. Biochem.* **1965**, *11* (1), 6–9.

Publication Date (Web): October 13, 2015 | doi: 10.1021/bk-2015-1200.ch015

62. Chen, X.; Zhong, Z.; Xu, Z.; Chen, L.; Wang, Y. *Free Radical Res.* **2010**, *44*, 587–604.
63. Carter, W.; Narayanan, P. K.; Robinson, J. P. *J. Leukocyte Biol.* **1994**, *55* (0741-5400 (Print)), 253–8.
64. Bindokas, V. P.; Jordán, J.; Lee, C. C.; Miller, R. J. *J. Neurosci.* **1996**, *16*, 1324–36.
65. Papapostolou, I.; Patsoukis, N.; Georgiou, C. D. *Anal. Biochem.* **2004**, *332* (2), 290–298.
66. Bilski, P. J.; Karriker, B.; Chignell, C. F. *Chem. Phys. Lett.* **2009**, *475* (1–3), 116–119.
67. Palazzolo-Ballance, A. M.; Suquet, C.; Hurst, J. K. *Biochemistry* **2007**, *46*, 7536–48.
68. Zielonka, J.; Kalyanaraman, B. *Free Radical Biol. Med.* **2010**, *48*, 983–1001.
69. Robinson, K. M.; Janes, M. S.; Pehar, M.; Monette, J. S.; Ross, M. F.; Hagen, T. M.; Murphy, M. P.; Beckman, J. S. *Proc. Natl. Acad. Sci. U. S. A.* **2006**, *103*, 15038–43.
70. Robinson, K. M.; Janes, M. S.; Beckman, J. S. *Nat. Protoc.* **2008**, *3*, 941–7.
71. Zhang, G.; Zhang, F.; Muh, R.; Yi, F.; Chalupsky, K.; Cai, H.; Li, P.-L. *Am. J. Physiol.* **2007**, *292*, H483–95.
72. Lippert, A. R.; Van de Bittner, G. C.; Chang, C. J. *Acc. Chem. Res.* **2011**, *44*, 793–804.
73. Chang, M. C. Y.; Pralle, A.; Isacoff, E. Y.; Chang, C. J. *J. Am. Chem. Soc.* **2004**, *126*, 15392–3.
74. Miller, E. W.; Albers, A. E.; Pralle, A.; Isacoff, E. Y.; Chang, C. J. *J. Am. Chem. Soc.* **2005**, *127* (47), 16652–16659.
75. Dickinson, B. C.; Huynh, C.; Chang, C. J. *J. Am. Chem. Soc.* **2010**, *132*, 5906–15.
76. Woolley, J. F.; Naughton, R.; Stanicka, J.; Gough, D. R.; Bhatt, L.; Dickinson, B. C.; Chang, C. J.; Cotter, T. G. *PLoS One* **2012**, *7*, e34050.
77. Miller, E. W.; Dickinson, B. C.; Chang, C. J. *Proc. Natl. Acad. Sci. U. S. A.* **2010**, *107*, 15681–6.
78. Miller, E. D.; Bryan, C.; Chang, C. J. *Proc. Natl. Acad. Sci. U. S. A.* **2010**, *107* (36), 15681–6.
79. Dickinson, B. C.; Peltier, J.; Stone, D.; Schaffer, D. V.; Chang, C. J. *Nat. Chem. Biol.* **2011**, *7*, 106–12.
80. Du, L.; Ni, N.; Li, M.; Wang, B. *Tetrahedron Lett.* **2010**, *51* (8), 1152–1154.
81. Wei, Y.; Zhang, Y.; Liu, Z.; Guo, M. *Chem. Commun. (Cambridge, U. K.)* **2010**, *46*, 4472–4.
82. Albers, A. E.; Okreglak, V. S.; Chang, C. J. *J. Am. Chem. Soc.* **2006**, *128*, 9640–1.
83. Srikun, D.; Miller, E. W.; Domaille, D. W.; Chang, C. J. *J. Am. Chem. Soc.* **2008**, *130*, 4596–7.
84. Kumar, M.; Kumar, N.; Bhalla, V.; Sharma, P. R.; Qurishi, Y. *Chem. Commun. (Cambridge, U. K.)* **2012**, *48*, 4719–21.
85. Albers, A. E.; Dickinson, B. C.; Miller, E. W.; Chang, C. J. *Bioorg. Med. Chem. Lett.* **2008**, *18*, 5948–50.

Publication Date (Web): October 13, 2015 | doi: 10.1021/bk-2015-1200.ch015

86. Chung, C.; Srikun, D.; Lim, C. S.; Chang, C. J.; Cho, B. R. *Chem. Commun. (Cambridge, UK)* **2011**, *47*, 9618–20.
87. Masanta, G.; Heo, C. H.; Lim, C. S.; Bae, S. K.; Cho, B. R.; Kim, H. M. *Chem. Commun. (Cambridge, UK)* **2012**, *48*, 3518–20.
88. Karton-Lifshin, N.; Segal, E.; Omer, L.; Portnoy, M.; Satchi-Fainaro, R.; Shabat, D. *J. Am. Chem. Soc.* **2011**, *133*, 10960–5.
89. Van de Bittner, G. C.; Dubikovskaya, E. A.; Bertozzi, C. R.; Chang, C. J. *Proc. Natl. Acad. Sci. U. S. A.* **2010**, *107*, 21316–21.
90. Cochemé, H. M.; Quin, C.; McQuaker, S. J.; Cabreiro, F.; Logan, A.; Prime, T. A.; Abakumova, I.; Patel, J. V.; Fearnley, I. M.; James, A. M.; Porteous, C. M.; Smith, R. A. J.; Saeed, S.; Carré, J. E.; Singer, M.; Gems, D.; Hartley, R. C.; Partridge, L.; Murphy, M. P. *Cell Metab.* **2011**, *13* (3), 340–350.
91. Dickinson, B. C.; Tang, Y.; Chang, Z.; Chang, C. J. *Chem. Biol.* **2011**, *18* (8), 943–948.
92. Guida, M.; Maraldi, T.; Beretti, F.; Follo, M. Y.; Manzoli, L.; De Pol, A. *Biomed Res. Int.* **2014**, *2014*, 456937.
93. Stanicka, J.; Russell, E. G.; Woolley, J. F.; Cotter, T. G. *J. Biol. Chem.* **2015**.
94. Woolley, J. F.; Stanicka, J.; Cotter, T. G. *Trends Biochem. Sci.* **2013**, *38* (11), 556–65.
95. Manevich, Y.; Held, K. D.; Biaglow, J. E. *Radiat. Res.* **1997**, *148* (6), 580–91.
96. Ganea, G. M.; Kolic, P. E.; El-Zahab, B.; Warner, I. M. *Anal. Chem.* **2011**, *83* (7), 2576–81.
97. Zhuang, M.; Ding, C.; Zhu, A.; Tian, Y. *Anal. Chem.* **2014**, *86* (3), 1829–36.
98. Bardia, A.; Tleyjeh, I. M.; Cerhan, J. R.; Sood, A. K.; Limburg, P. J.; Erwin, P. J.; Montori, V. M. *Mayo Clin. Proc.* **2008**, *83* (1), 23–34.
99. Myung, S.-K.; Ju, W.; Cho, B.; Oh, S.-W.; Park, S. M.; Koo, B.-K.; Park, B.-J. *BMJ* **2013**, *346*, f10–f10.

Publication Date (Web): October 13, 2015 | doi: 10.1021/bk-2015-1200.ch015

Publication Date (Web): October 13, 2015 | doi: 10.1021/bk-2015-1200.ch016

Chapter 16

Impact of Artifactual *Ex Vivo* Oxidation on Biochemical Research

Chad R. Borges,* Joshua W. Jeffs, and Erandi P. Kapuruge

Department of Chemistry and Biochemistry, College of Liberal Arts and Sciences, Arizona State University, Tempe, Arizona 85287, and The Biodesign Institute, Arizona State University, Tempe, Arizona 85287
***E-mail: chad.borges@asu.edu**

Once exposed to the atmosphere all major classes of bio-organic molecules are susceptible to oxidation that they would not normally experience *in vivo*. Direct reactions with oxygen are spin forbidden, but frequently unavoidable trace quantities of redox-active transition metals are often thermodynamically positioned to facilitate formation of biomolecular radicals and/or formation of superoxide radicals, creating a stream of reactive oxygen species (ROS) that readily damage biomolecules. Generally the degree of damage depends on the availability of O_2, concentration of redox active metals, temperature, and the length of exposure above the freezing point of the specimen. Using examples from the biomedical literature, this chapter provides an overview of the ways in which DNA, proteins, and lipids can experience artifactual oxidation *ex vivo* and the potential impact these reactions may have on the goal(s) of an investigation.

At room temperature aqueous solutions exposed to air develop a dissolved oxygen concentration [$O_{2(aq)}$] of approximately 0.25 mM (*1*, *2*). Thermodynamically, this concentration of O_2 constitutes a more highly oxidizing environment relative to that of most cells and interstitial fluids in which oxidation-susceptible biomolecules such as protein, lipids and DNA normally reside. At face value, this suggests that investigators should be wary of potential oxidative artifacts every time an *in vitro* biochemical experiment is carried out.

In Oxidative Stress: Diagnostics, Prevention, and Therapy Volume 2; Hepel, et al.;
ACS Symposium Series; American Chemical Society: Washington, DC, 2015.

Publication Date (Web): October 13, 2015 | doi: 10.1021/bk-2015-1200.ch016

Fortunately, the formation of such artifacts is largely irrelevant to numerous *ex vivo* biomolecular systems that are transiently exposed to the atmosphere—especially when precautions such as the use of appropriate metal chelators and sample chilling/freezing are employed to minimize reaction rates. Even at elevated *in vitro* O_2 concentrations, the direct (single-electron) oxidation of most biomolecules by O_2 (including some of those with the purported capacity to "autoxidize" such as cysteine and ascorbate) remains thermodynamically unfavorable (*3*). Moreover, with two unpaired electrons, ground state O_2 resides in a triplet electronic spin state while ground state bio-organic molecules exist as singlet molecules. Thus direct reaction between O_2 and most biomolecules is spin forbidden, causing severe kinetic hindrance of even those multi-electron reactions that are thermodynamically favorable.

But the story of how atmospheric oxygen influences *in vitro* biochemical experiments does not end here. There are two major non-enzymatic routes by which O_2 can be made reactive with ordinary biomolecules:

1. Transition metals such as iron and copper can interact directly with biomolecules, abstracting electrons and forming biomolecular radicals, thereby providing an inroad for the reaction of O_2 and related reactive oxygen species (ROS) with common organic biomolecules (Scheme 1). In this pathway, the oxidized form of a transition metal such as iron or copper strips an electron from an organic molecule (RH_2) that has a single-electron-oxidized radical form with a reduction potential which *in that particular solution* (that is to say *E*, not necessarily $E°$ or $E°'$) is lower than that of the oxidized metal (reaction 1). Examples of such molecules are plentiful (*3*) and include small molecules such as ascorbic acid, cysteine, dopamine and other similar compounds that possess free thiols, catechols, or other electronically conjugated structures capable of stabilizing an unpaired electron.

In some cases the oxidized biomolecule may remain bound to the reduced metal as a chelation complex that effectively lowers the reduction potential of the metal couple below that for the reduction of O_2 to $O_2^{\bullet-}$; when this happens the metal can directly reduce O_2 to $O_2^{\bullet-}$ (reaction 2) even while remaining bound to the organic biomolecule (*3*–*5*). Alternatively (or additionally), the initial metal-mediated redox event will produce an organic radical ($^{\bullet}RH$) which, depending on its chemical nature, can directly reduce O_2 to $O_2^{\bullet-}$ while forming the two-electron oxidized form of the organic molecule R (reaction 3). This reaction is more common for R molecules with low single-electron reduction potentials (*3*). Alternatively, $^{\bullet}RH$ may react directly with O_2 to produce organic hydroperoxides that can initiate a chain-reaction of peroxidation (reactions 4a,b). This reaction is common for polyunsaturated conjugated dienyl radicals such as those that are generated from polyunsaturated fatty acids. (Autoxidation propagation rate constants (k_p) for several common fatty acids and sterols in benzene solution at 37 °C have been determined by Xu et al (*11*) and range from 11 M^{-1} s^{-1} for cholesterol to 197 M^{-1} s^{-1} for arachidonic acid to 2260 M^{-1} s^{-1} for 7-dehydrocholesterol (based on a k_p for linoleic acid of 62 M^{-1} s^{-1} (*12*)). The authors also reported mole fraction-based autoxidation propagation rate constants for various unsaturated phospholipids in mixed liposomes.) When formed, $O_2^{\bullet-}$ can either spontaneously dismutate into H_2O_2 with a rate constant of 8 x 10^4

In Oxidative Stress: Diagnostics, Prevention, and Therapy Volume 2; Hepel, et al.;
ACS Symposium Series; American Chemical Society: Washington, DC, 2015.

M^{-1} s^{-1} at pH 7.8 (*13*) (reaction 5) or, depending on relative reduction potentials, reduce more of the oxidized form of the metal to reform O_2 (reaction 6). At this point reduced transition metal ions and H_2O_2 have been produced in solution and can react to produce $^{\bullet}OH$ via Fenton chemistry (reaction 7). In the close proximity of myeloperoxidase (MPO), reactions 8-9 can generate $^{\bullet}OH$ from H_2O_2 and Cl^- (*9*, *10*).

$RH_2 + Me^{n+} \rightarrow {}^{\bullet}RH + Me^{(n-1)+} + H^+$ (1)

$O_2 + Me^{(n-1)+} \rightarrow O_2^{\bullet-} + Me^{n+}$ (2)

and/or

$^{\bullet}RH + O_2 \rightarrow R + O_2^{\bullet-} + H^+$ (3)

and/or

$^{\bullet}RH + O_2 \rightarrow HROO^{\bullet}$ (4a); Propagation: $HROO^{\bullet} + RH_2 \rightarrow {}^{\bullet}RH + HROOH$ (4b)

$2O_2^{\bullet-} + 2H^+ \rightarrow O_2 + H_2O_2$ (5)

and/or

$O_2^{\bullet-} + Me^{n+} \rightarrow O_2 + Me^{(n-1)+}$ (6)

$Me^{(n-1)+} + H_2O_2 \rightarrow Me^{n+} + OH^- + {}^{\bullet}OH$ (7)

Added together, reactions (6) and (7) constitute the Haber-Weiss reaction.

In the presence of myeloperoxidase (MPO)

$H_2O_2 + Cl^- \rightarrow HOCl + OH^-$ (Catalyzed by MPO) (8)

$HOCl + O_2^{\bullet-} \rightarrow Cl^- + O_2 + {}^{\bullet}OH$ (9)

Scheme 1. Common reactions that can lead to the spontaneous production of ROS in vitro / ex vivo. Reactions involving metals can take place while the biomolecule or other compound chelates the metal—a phenomenon that can dramatically alter the reduction potential of the metal redox couple. Whether or not a particular redox reaction occurs depends on its thermodynamic favorability, defined by $\Delta G = -nFE_{cell}$, where ΔG is the free energy of the reaction (negative for a spontaneous reaction), n is moles of electrons transferred, F is the Faraday constant and E_{cell} is the potential difference between the half-reactions. For biochemical systems, $E^{\circ\prime}$ values determined at physiologically relevant pH should be used with the Nernst equation for purposes of estimating thermodynamic feasibility. (For additional information and reference data see refs. (6–8)). Addition of reactions (6) and (7, the Fenton Reaction) constitute the Haber-Weiss reaction but are shown separately for the sake of clarity. Reactions 8 and 9 require the close proximity of MPO (9, 10). Additional reactions may occur (not shown), depending on the biochemical system under consideration.

Publication Date (Web): October 13, 2015 | doi: 10.1021/bk-2015-1200.ch016

Publication Date (Web): October 13, 2015 | doi: 10.1021/bk-2015-1200.ch016

Some of the common biomolecules represented by 'RH_2' in Scheme 1 are often described as those that "autoxidize" (*3*). As described (*3*), "autoxidation" is defined as the "… apparently uncatalyzed oxidation of a substance exposed to the oxygen of the air…", but the direct reaction of O_2 with nearly all biomolecules is spin forbidden and therefore not likely to occur at a significant rate, meaning that a catalyst such as a transition metal is required (*14*). Table I provides examples of how metal catalysts impact the rates of some well known "autoxidation" reactions.

As alluded to above, chelators can have a dramatic effect on the reduction potential of transition metals and thereby mediate increases or decreases in apparent rates of autoxidation. For example, chelation of the Fe(III)/Fe(II) redox couple by 1,10-phenanthroline at pH 7 increases E°′ from 0.110 V to 1.15 V, whereas chelation by diethylenetriaminepentaacetic acid (DETAPAC or DTPA) decreases the reduction potential to 0.030 V and chelation by ferritin drops it to -0.190 V (*7*). (As pointed out by Buettner (*7*), *E*° of Fe(III)/Fe(II) is 0.770 V *at pH 0.* For biochemical systems it is more meaningful to refer to E°′ of Fe(III)/Fe(II) at pH 7, which is 0.110 V.) Moreover, metals can be chelated by sample components that are not normally thought of as chelating reagents—including buffers. For example, in HEPES buffer at pH 6.5, Fe(II) shows a near-complete lack of autoxidation; but in phosphate buffer at pH 6.5, Fe(II) autoxidizes rapidly (*27*).

Table I. Impact of metals on the rates of autoxidation reactions.

Autoxidized Compound	***Metal-Relevant Parameter(s) Investigated***	***Summary Results***	***Ref.***
Ascorbate [a]	Conc. of Cu(II) on rate	Uncatalyzed "half-life": > 1,748 min. "Half-life" w/ 727 nM Cu(II): 1,748 min. "Half-life" w/ 7.27 µM Cu(II): 181 min. "Half-life" w/ 3.36 mM Cu(II): 6 min.	(*15*)
Ascorbate [b]	Conc. of Cu(II) on rate	50 nM Cu(II): 2 mAu/min 500 nM Cu(II): 50 mAu/min 1,000 nM Cu(II): 100 mAu/min	(*2*)
Ascorbate [b]	Conc. of Fe(III) and EDTA-Fe(III) on rate	1 µM Fe(III): 1.5 mAu/min 1 µM Fe(III)-EDTA: 4.5 mAu/min 5 µM Fe(III): 6 mAu/min 5 µM Fe(III)-EDTA: 23 mAu/min [m]	(*2*)
Cysteine (Cys) [c]	Catalytic rates facilitated by different metals (0.01 mol metal/mol Cys)	No added catalyst: 0.4 µL O_2/min Cu(II): 16.3 µL O_2/min Fe(III): 21.1 µL O_2/min Na_2SeO_3: 14 µL O_2/min Co(II): 2.1 µL O_2/min Mn(II): 1.0 µL O_2/min	(*16*)

Continued on next page.

In Oxidative Stress: Diagnostics, Prevention, and Therapy Volume 2; Hepel, et al.;
ACS Symposium Series; American Chemical Society: Washington, DC, 2015.

Table I. (Continued). Impact of metals on the rates of autoxidation reactions.

Autoxidized Compound	*Metal-Relevant Parameter(s) Investigated*	*Summary Results*	*Ref.*
Glutathione (GSH) [c]	Catalytic rates facilitated by different metals (0.01 mol metal/mol GSH)	No added catalyst: 0.3 μL O_2/min Cu(II): 2.4 μL O_2/min Fe(III): 0.9 μL O_2/min Na_2SeO_3: 18.2 μL O_2/min Co(II): 2.3 μL O_2/min Mn(II): 0.6 μL O_2/min	(*16*)
Dihydrolipoic acid [c]	Catalytic rates facilitated by different metals (0.01 mol metal/mol dihydrolipoic acid)	No added catalyst: 0 μL O_2/min Cu(II): 0 μL O_2/min Fe(III): 0 μL O_2/min Na_2SeO_3: 4.0 μL O_2/min Co(II): 4.6 μL O_2/min Mn(II): 1.5 μL O_2/min	(*16*)
Coenzyme A (CoA) [c]	Catalytic rates facilitated by different metals (0.01 mol metal/mol CoA)	No added catalyst: 0.2 μL O_2/min Cu(II): 0.9 μL O_2/min Fe(III): 0.3 μL O_2/min Na_2SeO_3: 1.1 μL O_2/min Co(II): 0.5 μL O_2/min Mn(II): 0.3 μL O_2/min	(*16*)
Cys [d] (and related derivatives)	Mechanism governing Cu(II)-catalyzed oxidation of Cys-related thiols to disulfides	Biphasic kinetics where $Rate_{Phase\ 1} = k_1[Cu^{2+}][CysS^-]/K_2(1+K_1/[CysS^-]) + [CysS^-]$ [n] Cysk_1 = 0.32 s^{-1} Cys ethyl ester k_1 = 0.37 s^{-1} Cysteamine k_1 = 0.13 s^{-1} N-Acetylcysteine k_1 = 0.013 s^{-1}	(*17*)
GSH [d]	Mechanism governing Cu(II)-catalyzed oxidation of GSH to GSSG	Biphasic kinetics (0.1 mM GSH): Phase 1: 5 μM Cu(II) spent 1 μM O_2/min Phase 1: 40 μM Cu(II) spent 2.8 μM O_2/min Phase 2: 5 μM Cu(II) spent 2.1 μM O_2/min Phase 2: 40 μM Cu(II) spent 4.1 μM O_2/min	(*18*)
Dithiothreitol (DTT) [e]	Mechanism governing Cu(II)-catalyzed oxidation of DTT	Biphasic kinetics (0.1 mM DTT): 10 μM Cu(II) spent 48 μM O_2 in Phase 1 90 μM Cu(II) spent 2 μM O_2 in Phase 1 •OH Production in Phase 2 No added Cu(II) gave 2.5×10^{-3} fluoresc. u/hr 10 μM Cu(II) gave 64×10^{-3} fluoresc. u/hr	(*19*)

Continued on next page.

Publication Date (Web): October 13, 2015 | doi: 10.1021/bk-2015-1200.ch016

Table I. (Continued). Impact of metals on the rates of autoxidation reactions.

Autoxidized Compound	*Metal-Relevant Parameter(s) Investigated*	*Summary Results*	*Ref.*
Cys [f]	Cu(II)-catalyzed oxidation of Cys by $[Mo(CN)_8]^{3-}$	Uncatalyzed $t_{1/2}$ = 0.21 s 5 μM Cu(II)-catalyzed $t_{1/2}$ = < 0.002 s	(*20*)
Glucose [g]	Effect of Fe(III), Cu(II), and phosphate (Pi) on oxidation rate	10 mM Pi: 0.54 fluoresc. u/9 days 100 mM Pi: 12.8 fluoresc. u/9 days 10 mM Pi + 20 μM Fe(III): 0.47 fluoresc. u/9 days 100 mM Pi + 10 μM Cu(II): 7.2 fluoresc. u/9 days	(*21*)
Fructose [g]	Effect of Fe(III), Cu(II), and phosphate (Pi) on oxidation rate	10 mM Pi: 11.8 fluoresc. u/9 days 100 mM Pi: 74.3 fluoresc. u/9 days 10 mM Pi + 20 μM Fe(III): 9.9 fluoresc. u/9 days 100 mM Pi + 10 μM Cu(II): 35 fluoresc. u/9 days	(*21*)
Arachidonate Micelles [h]	Effect of AMP-Fe(II)/AMP-Fe(III) on lipid peroxidation as measured by formation of malondialdehyde (MDA)	1.7:0.1 mM AMP-Fe(II)/0 added Fe(III): 0.58 nmol MDA/min*mL 1.7:0.1 mM AMP-Fe(II)/0 added Fe(III) & 3.4 mM extra AMP: 0.33 nmol MDA/min*mL AMP-Fe(II) & AMP-Fe(III) (1.7:0.1 mM ea): 1.16 nmol MDA/min*mL	(*22*)
Microsomal Phospholipid Liposomes [i]	Effect of Citrate-Fe(II) and/or Citrate-Fe(III) on lipid peroxidation	0.1:0.1 mM Citrate-Fe(II): 0 nmol MDA/min*mL 0.1:0.1 mM Citrate-Fe(III): 0 nmol MDA/min*mL 0.1:0.1 mM Citrate-Fe(II) & 0.1:0.1 mM Citrate-Fe(III): 0.85 nmol MDA/min*mL	(*23*)
3,5-Di-*t*-butyl pyrocatechol (3,5-DTBP) [j]	Relative reaction rates catalyzed by various metals	Times for rxn of 2.5 mmol O_2 by 50 mL soln contg 0.10 M 3,5-DTBP and 1 mM $MetalCl_2$ Co(II) & Mn(II): 15-20 min Zn(II) & Cu(II): 40-60 min Ni(II) ≈ No metal added: > 60 min Fe(II): Longer than No metal added	(*24*)

Continued on next page.

Publication Date (Web): October 13, 2015 | doi: 10.1021/bk-2015-1200.ch016

Table I. (Continued). Impact of metals on the rates of autoxidation reactions.

Autoxidized Compound	*Metal-Relevant Parameter(s) Investigated*	*Summary Results*	*Ref.*
Chlorogenic acid (CGA) [k]	Ability of different metals at 100 μM to enhance the rate of lipid peroxidation induced by oxidized CGA	Al(III) & Mg(II): 130% of Control (No metal) Ca(II): 125% of Control Cd(II): 115% of Control Zn(II): 108% of Control	(*25*)
Dopamine (DA) [l]	Effect of Fe(III) chelation with nitrilotriacetic acid (NTA) on rate of dopamine oxidation	No Metal Added: 0.4 nM H_2O_2/min 250 μM Fe(III): 12.5 nM H_2O_2/min 250 μM Fe(III) & NTA: 0.4 nM H_2O_2/min	(*26*)

[a] In 20 μM, citrate buffer pH 3.17. [b] In 125 μM in Chelex-100® treated phosphate buffer pH 7.0. [c] 5-50 μM thiols in 0.1-0.21 M phosphate buffer, pH 7-7.38. [d] In 40 mM phosphate buffer pH 7.4. [e] In 20 mM phosphate buffer pH 7.4. [f] 5 mM Cys in 2 mM acetate buffer pH 4.2 with 0.1 M sodium triflate. [g] In PBS (at phosphate concentration indicated) with 5 mM sodium benzoate and 10 mM sugar at 40 °C for 9 days. Detection based on fluorescence of hydroxylated benzoate products generated by hydroxyl radicals. [h] In 30 mM NaCl, pH 6. [i] In 50 mM NaCl, pH 7.0 at 37 °C. [j] In 80% MeOH containing 0.10 M $KHCO_3$. [k] In 0.2 M acetate pH 5.0. [l] In 50 mM Tris, pH 7.2; [DA], [Fe(III)], [NTA] = 250 μM. [m] EDTA *slowed* total oxidation due to other metals. [n] K_1 and K_2 are equilibrium constants for the ligation of 1 and 2 cysteine molecules to Cu^{2+}, respectively.

2. The second non-enzymatic route by which O_2 can be made reactive with ordinary biomolecules involves electronic excitation of ground state O_2 via light and a photosensitizer (which often contains a metal atom) to create singlet O_2 (namely, the $^1\Delta_g$ state). Singlet O_2 (or $^1O_2$) is capable of direct reaction with many organic biomolecules—in particular those containing carbon-carbon double bonds. This often leads to formation of unstable organic peroxides that decompose in ways that destroy the original biomolecule. Due to limited half-life in solution (described below), $^1O_2$ is much less important as a means for oxidatively damaging biomolecules than the ROS generated by the reactions portrayed in Scheme 1.

Thus despite the fact that O_2 cannot react directly with organic biomolecules, the ubiquitous presence of trace metals makes O_2-mediated damage of biomolecules an ever-looming threat—both biologically and, particularly, when biological systems are exposed to unnaturally high concentrations of dissolved O_2 supplied by the atmosphere. This chapter provides a synopsis of the role of *ex vivo* oxidation in producing experimental artifacts during *in vitro* research that involves DNA, proteins, and lipids.

Publication Date (Web): October 13, 2015 | doi: 10.1021/bk-2015-1200.ch016

What Can Go Wrong?

Two undesirable outcomes may arise from *ex vivo* biomolecular oxidation *that impacts experimental results whether investigators are aware of the impact or not* (pink ovals, Scheme 2); these include A) Outright Misinterpretation of Results, and B) No Mistakes in Interpretation, but Incomplete Understanding of Results. These undesirable conclusions may be arrived at by five separate paths: Path 1) Oxidation goes unnoticed but results are interpretable. This will lead to Outcome A; Path 2) Oxidation goes unnoticed and results are uninterpretable. This results in Outcome B; Path 3) Oxidation is noticed, but proper interpretation of results does not depend on parsing *ex vivo* oxidation from *in vivo* or non-artifactual *in vitro* oxidation, resulting in Outcome B; Path 4) Oxidation is noticed, proper interpretation of results depends on parsing *ex vivo* oxidation from *in vivo* or non-artifactual *in vitro* oxidation, and the possibility of *ex vivo* oxidation is recognized, but investigators are unable to distinguish *ex vivo* from *in vivo* oxidation. This results in Outcome B; Path 5) Oxidation is noticed and proper interpretation of results depends on parsing *ex vivo* oxidation from *in vivo* or non-artifactual *in vitro* oxidation—but the possibility that *ex vivo* oxidation has occurred is not considered. This leads to Outcome A. In summary, there are five paths leading to two undesirable outcomes, but only one path to completely understanding experimental results that involve biomolecular oxidation—and this path requires investigator awareness of potential pitfalls.

This chapter focuses on the *ex vivo* oxidation events that are most likely to generate misleading results in biochemical research. Though given brief mention in Table I, catechols (including neurotransmitters, epinephrine and related species) and related polyphenols are less prevalent in biochemical research than DNA, proteins, and lipids. Moreover, they are well known for their redox properties and tend not to be major/integral components of biochemical systems that are focused on other molecules.

As such, most investigators who work with these compounds routinely implement methodological precautions and experimental controls to minimize and eliminate artifactual redox effects. Thus there are few examples where lack of knowledge concerning their redox properties has led to misinterpretation of results and this trend is expected to be sustained into the future. Readers interested in additional information are referred to recent in-depth research articles on the metal binding characteristics of these compounds and the resulting anti-/pro-oxidant properties that such binding imparts (*28*, *29*).

Table II provides an overview of how sample handling can lead to artifactual oxidation of DNA, proteins, and lipids, why it matters, and the likelihood of serendipitously detecting an oxidative modification when one is not looking for it. Using examples from the biomedical literature, the sections that follow provide additional details on the types of *ex vivo* oxidation reactions that can occur, their potential impact on the main goal(s) of an investigation, and means by which they can be minimized.

Publication Date (Web): October 13, 2015 | doi: 10.1021/bk-2015-1200.ch016

Publication Date (Web): October 13, 2015 | doi: 10.1021/bk-2015-1200.ch016

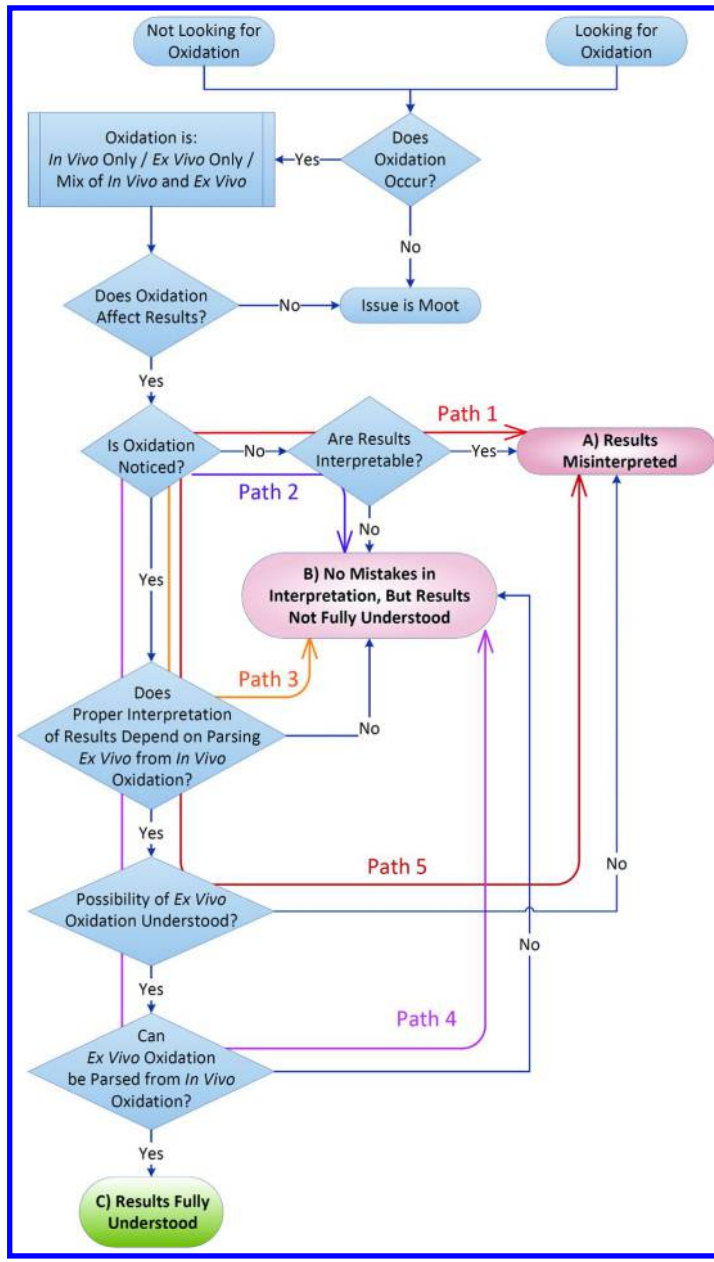

Scheme 2. Flow chart outlining the possibilities of how ex vivo oxidation may impact biochemical research.

Table II. Induction, impact, and likelihood of detecting artifactual oxidation of DNA, protein, and lipids.

Biomolecule	*Sample Handling-Based Causes of Oxidation*	*Why Artifactual Ex vivo Oxidation Matters*	*Likelihood of Detecting an Oxidative Modification when Not Looking for It*
DNA	Processing-mediated oxidation during preparation for analysis of oxidized DNA (*30*, *31*)	Leads to overestimation of *in vivo* oxidative damage	N/A
	Processing-mediated oxidation during preparation for DNA sequencing (*32*)	Causes mistakes in DNA sequencing (*33–35*). If undetected, flawed/inaccurate data may be reported (*32*)	Low
Proteins & Peptides	Handling & Storage-Induced Modifications - Handling or storing protein or peptide solution above its freezing point - Plasma/serum handling & storage above -30 °C (*36*)	[a] **1.** Results in non-specific formation of Cys-SOH at free Cys residues (*37*) **2.** May result in artifactual disulfide bonds (via Cys-SOH (*37*) or direct catalysis by trace metals (*5*)) including homo- and hetero- disulfide dimers (*36*, *37*) **3.** May result in formation of Met-sulfoxide **4.** May result in artifactually elevated protein glycation levels (Ref (*38*) & unpublished data described under *Oxidative Glycation* subsection)	Low for non-MS based techniques / High for MS-based techniques
	Instrument-Induced Modifications - ESI-MS source voltage too high [b] - Electrophoresis (*39*, *40*)	**1.** Unanticipated peptide *m/z* shifts may lead to undesirable signal splitting. **2.** Intact protein or peptide oxidation may be misinterpreted as an *in vivo* or other non-artifactual event.	High

Continued on next page.

Publication Date (Web): October 13, 2015 | doi: 10.1021/bk-2015-1200.ch016

Table II. (Continued). Induction, impact, and likelihood of detecting artifactual oxidation of DNA, protein, and lipids.

Biomolecule	*Sample Handling-Based Causes of Oxidation*	*Why Artifactual Ex vivo Oxidation Matters*	*Likelihood of Detecting an Oxidative Modification when Not Looking for It*
Lipids	Imperfections in sample collection, handling/processing and storage (*41*)	Leads to overestimation of *in vivo* oxidative damage	Medium - High
	Intentional exposure to air and light to facilitate characterization (*42*)	Employed intentionally for the purpose of molecular characterization	N/A

[a] Protein & Peptides: If **1-4** are detected, these events may be confused with *in vivo* oxidation and/or may be interpreted as relevant to *in vivo* processes when they are not; or may be inaccurately reported as a biomarker of disease. If **1-4** remain undetected, this may result in altered biomolecular interactions (e.g., see Methionine Sulfoxidation subsection), leading to erroneous interpretation of a wide variety of possible results. [b] Applicable to ESI source designs in which a high positive voltage is applied to the spray needle in positive ion mode (*43*).

Publication Date (Web): October 13, 2015 | doi: 10.1021/bk-2015-1200.ch016

DNA

Artifactual Oxidation During Sample Prep for the Analysis of Oxidized DNA

Oxidized DNA has been implicated as a causal factor in aging and nearly every chronic disease (*44–50*) including neurodegenerative diseases (*51*, *52*), cardiovascular disease (*53*, *54*) and cancer (*55*, *56*). Inflammation and ionizing radiation from the sun are major sources of the ROS and nitrogen (RNS) species produced *in vivo* that damage DNA. Hydroxyl radical (•OH)-mediated DNA damage is the most well-studied form of DNA damage. As described by Cadet et al (*30*), this has led to the characterization of at least 80 unique, oxidatively modified forms of purine and pyrimidine bases. Hydroxyl radicals are also the most common source of *ex vivo* damage to DNA, reacting with it at diffusion-controlled rates (*50*). Scheme 1 describes how hydroxyl radicals can be spontaneously generated in aqueous solution.

Impact on Main Goals of Analysis

Measurement of oxidized DNA is employed in a wide variety of efforts to find biomarkers of disease as well as to define its etiology and suggest new courses of therapy (reviewed in (*44–56*)). Numerous techniques for quantifying oxidized DNA have been developed over the past few decades and were critically reviewed by Cadet et al (*30*) in 2011. Available classes of techniques include

^{32}P-postlabeling assays, enzymatic methods that convert oxidized bases into strand breaks, immunoassays, and chromatographic techniques ranging from GC/MS, HPLC with electrochemical detection, LC/MS, and LC-MS/MS.

Regardless of the analytical technique employed, the prevention of artifactual *ex vivo* oxidation during sample storage and preparation is critical to ensuring the integrity of the final result. Some of the early approaches to measuring oxidized DNA were so fraught with accuracy problems that the European Standards Committee on Oxidative DNA Damage (ESCODD) was established in 1997 to find the sources of error and variability in the analysis of 8-oxo-7,8-dihydro-2′-deoxyguanosine (8-oxodG)—one of the most abundant forms of oxidized DNA. Perhaps the most severely flawed methods were found to be those based on GC/MS, due to the fact that sample heating during derivatization (silylation) resulted in artifactual generation of 8-oxo-7,8-dihydroguanine (8-oxoG) with an efficiency of about 0.01% over a heating period of 30 min at 130-140 °C (*30*, *57*, *58*) leading to dramatic overestimation of oxidized DNA quantities. Other purine and pyrimidine bases were found to be oxidized during derivatization as well (*59*). Workarounds such as pre-purification of oxidized bases prior to analysis achieved some degree of success, but have not been highly employed (*30*). Overall, the use of GC/MS techniques considered to be inaccurate by ESCODD has decreased dramatically since the turn of the century. Cadet et al (*30*) have recommended that "… all the measurements of oxidized bases in cellular DNA using the GC–MS assay that were made during almost 20 years have no pertinence and should be discarded. Therefore the use of these data for the assessment of the biological role of oxidation products of DNA (*50*) has no relevance."

Immunoassays based on antibodies generated against oxidized DNA bases have also been found to dramatically overestimate quantities of oxidized DNA (*60*). This is largely due to the lack of antibody specificity.

No matter what approach is employed, DNA samples must inevitably be stored and handled prior to endpoint analysis. Poor sample storage conditions and/or flawed extraction procedures and techniques will almost always lead to artificially high reports of oxidized DNA levels. Efforts to minimize artifactual oxidation during sample processing for measurement of 8-oxodG (which takes over an hour at various thawed-state temperatures) have found that the use of the iron chelator deferoxamine (DFO) (*31*, *61*) (cf. Scheme 1) and the chaotrope sodium iodide (*61*) are advantageous in preventing artifactual oxidation, but do not completely solve the problem (*62*). Increased quantities of extracted DNA also serve to minimize the fraction of DNA that is artifactually oxidized during sample preparation (*63*). DNA quantities of at least a few tens of micrograms were found necessary to reach the lower plateau region of this non-linear effect.

As with many other bioanalytical challenges, LC-MS/MS is considered to be the gold standard for the analysis of oxidized DNA (*30*, *64*). In particular, an approach that limited sample exposure to air by directly injecting crude DNA hydrolysates without final vacuum concentration or solid phase extraction steps was found to minimize artifactual DNA oxidation (*31*). Additionally, chromatographic separation of 8-oxodG from its precursor 2′-deoxyguanosine (dG) was found to be necessary to avoid the potential confounding effects of

In Oxidative Stress: Diagnostics, Prevention, and Therapy Volume 2; Hepel, et al.;
ACS Symposium Series; American Chemical Society: Washington, DC, 2015.

Publication Date (Web): October 13, 2015 | doi: 10.1021/bk-2015-1200.ch016

in-source oxidation that can take place in microseconds during the electrospray ionization (ESI) process (*65*, *66*) when a high positive voltage is applied to the post-column analyte solution or the spray needle in positive ion mode. Such artifactual oxidation in the ESI source is due to corona discharge which occurs upon dielectric breakdown of gas molecules in the ion source region at a critical applied voltage, generating a plasma consisting of free electrons and radical cations (*67*, *68*). The free electrons are accelerated toward the positively charged spray needle at high energies, resulting in the splitting of water molecules to produce hydroxyl radicals ($H_2O + e^- \rightarrow H^\bullet + {}^\bullet OH + e^-$) (*69*) and other ROS (*69–71*) that can readily oxidize organic components of the spray droplets in which they are dissolved (*72*). As described in additional detail in the *Proteins* section below, this problem can be avoided entirely by employing an ESI source design in which the spray needle is held at ground and the inlet of the mass spectrometer is held at a high negative voltage in positive ion mode.

Given the challenges described above, few if any methods are highly accurate with regard to absolute quantification of oxidized DNA, but this does not mean that conclusions drawn from studies that employ imperfect analytical approaches are necessarily flawed: If the analytical methodologies are reasonably precise (i.e., precise enough to provide adequate statistical power) and the study design is such that it does not introduce any systematic bias into one group vs. another, such studies are often able to reveal *relative differences* between experimental groups that can be relied upon to draw valid conclusions. The major limitation of such studies, however, is that results from different laboratories generally cannot be compared to one another, despite the fact that they may report results in the exact same units.

Artifactual Oxidation During Sample Preparation for DNA Sequencing

Most analyses of DNA are carried out with the goal of obtaining sequence information. In such cases investigators are not looking for oxidative damage to the DNA and in the majority of cases are not actively concerned about it. It has been known since 1992 that oxidative DNA base damage in the form of 8-oxoG causes G > T and A > C substitutions (*33*). Only recently, however, was the impact of artifactual oxidative DNA damage on the fidelity of low frequency mutation calling in Next Generation Sequencing (NGS) reported for the first time (*32*).

During deep coverage exome analyses of melanoma tumors and matched normal tissues, Costello et al (*32*) reported initially noticing an unexpectedly high number of variants at allelic fractions < 20% in *both* sample sets. They noticed that the G > T variants always presented in the first Illumina HiSeq instrument read and that the C > A variants always showed up in the second read. Additional investigation led them to pinpoint a nonbiological source for the variants, namely oxidation of G to 8-oxoG during acoustic shearing for 165 s to generate 150-bp fragments for exome sequencing. Despite being kept in a 10 °C water bath, the investigators observed that during shearing the actual sample temperature rose to about 30 °C. (Notably, the artifactual variants did not present themselves when DNA was sheared using a 500-bp protocol for whole genome sequencing.) Additional investigation revealed that inclusion of 0.1

In Oxidative Stress: Diagnostics, Prevention, and Therapy Volume 2; Hepel, et al.;
ACS Symposium Series; American Chemical Society: Washington, DC, 2015.

Publication Date (Web): October 13, 2015 | doi: 10.1021/bk-2015-1200.ch016

mM DFO and 1 mM EDTA in the shearing buffer were independently able to prevent oxidative damage but that DFO significantly decreased yields from the library construction process. Ultimately, the experience caused the investigators to alter their operating procedures such that before processing, all incoming DNA samples are now buffer exchanged into Tris buffer containing 1 mM EDTA.

In conclusion, Costello and colleagues expressed serious concern that other sample processing-related sequence misinterpretation errors may well be confounding efforts to discover and act upon true low frequency tumor mutations—and called upon the sequencing community to systematically review data from different protocols to determine if other rare sequencing anomalies caused by sample handling-induced molecular aberrations may be getting incorrectly attributed to a pathobiological source. Their seminal work has been recognized by other investigators and *ex vivo*-oxidized DNA is starting to become recognized as an important potential source of errors in DNA sequencing (*73*, *74*).

Publication Date (Web): October 13, 2015 | doi: 10.1021/bk-2015-1200.ch016

Proteins

Outside of specialized redox-active co-factors such as Fe-S clusters, the sulfur-containing amino acids within proteins are the most susceptible to spontaneous artifactual, *ex vivo* oxidation. For cysteine (Cys) residues this is in line with their roles as structural disulfides (which generally have reduction potentials below -300 mV (*75*, *76*)) and allosteric disulfides (*76*, *77*) / redox signaling mediators (reviewed in detail elsewhere (*75*, *78*, *79*) which have elevated reduction potentials in the range of -70 to -330 mV (*75*)—allowing them to control important biological processes by cycling back and forth between the oxidized and reduced forms.

It has been known for decades that reduced, unfolded proteins can spontaneously re-oxidize within about 20 hrs at room temperature, regenerating their native sets of intramolecular disulfide bonds when their solutions are exposed to air (*80–85*). Free thiol-containing peptides are well known for their propensity to spontaneously oxidize into disulfide-linked dimers within a similar time frame when dissolved in aqueous, neutral-pH solutions exposed to air and unavoidable quantities of redox-active transition metals.

Likewise, methionine (Met)-containing peptides are expected to undergo some degree of sulfoxidation during common sample preparation workflows for proteomic analyses that often expose samples to room temperature for several hours in addition to incubation at 37 °C overnight. This is evidenced by the ubiquitous practice of searching tandem mass spectra datasets for Met-sulfoxide as a variable modification of Met.

In short, when protein solutions are exposed to air, oxidation of solvent-exposed Cys and Met will proceed at any temperature above the freezing point of the solution. For biological samples with high concentrations of solutes, this temperature can be quite low. For example, blood plasma freezes at -30 °C (*86–89*) and despite the appearance of being frozen at -20 °C, proteins containing free-Cys and Met will oxidize when such specimens are stored at this temperature. In a recent study (*36*), the free thiol of albumin was found to reach maximal

S-cysteinylation after 60 days at -20 °C, while the onset of apolipoprotein A-I (apoA-I) oxidation occurred after about 150 days at -20 °C.

The growing prominence of mass spectrometry as a tool for protein analysis has resulted in increasing awareness of artifactual, *ex vivo* protein oxidation. Few if any other analytical tools are as capable of serendipitously revealing and, at the same time, qualitatively identifying oxidative protein modifications. Ironically, under certain circumstances mass spectrometers (*43*, *72*, *90*) and electrophoresis equipment (*39*, *40*) can themselves induce artifactual protein oxidation. These phenomena are described in greater depth in the *Instrument-Induced Oxidation* subsection below.

Ex vivo Formation of Cysteine Sulfenic Acid (Cys-SOH)

Cys-SOH has been found to serve in many different roles as an intermediate in redox-based processes. It plays an important role in regulating the activity of numerous different proteins including peroxidases, oxidoreductases, kinases, phosphatases, transcription factors, cysteine proteases, and ion channels (reviewed in (*91*)). *In vitro*, artifactual disulfides form readily through processes catalyzed by trace metals such as copper (cf. Table I) and do not necessarily require a stable intermediate such as Cys-SOH in which oxygen is bound to the thiol sulfur atom (*5*, *17–19*). But in a study published in 2010, Rehder and Borges (*37*) found that Cys-SOH can serve as an oxidative intermediate in the spontaneous formation of disulfide-based peptide dimers and in *in vitro*-based nonenzymatic oxidative protein folding.

These results, in combination with others that had hinted at the non-specific nature of Cys-SOH formation *in vitro* (*18*, *92*), demonstrated that Cys-SOH is ubiquitously present at low relative concentrations at all solution-accessible free Cys residues in protein and peptide solutions exposed to air. These findings are not in conflict with reports that have demonstrated the importance of Cys-SOH as an oxidative intermediate in specific enzymatic and redox-regulatory processes. The unique protein microenvironments that stabilize oxidative thiol intermediates determine the ultimate specificity of otherwise non-specific redox chemistry. That stated, the discovery of the ubiquitous existence of Cys-SOH *in vitro* (*37*) does suggest cautionary interpretation of shotgun proteomics-based studies that aim to identify all Cys-SOH functional groups in samples that have been exposed to air.

Mixed Disulfides

Whether formed via thiol/disulfide exchange, Cys-SOH intermediates, or trace metal catalyzed formation of self-reactive thiyl radicals (*5*, *17–19*), mixed disulfides are an inevitable long-term consequence of exposing to air solutions that contain multiple molecular forms of reduced, thiol containing Cys residues (Scheme 3). Initially, free thiol-containing species such as free cysteine or β-mercaptoethanol will reduce disulfide bonds via a thiol-exchange mechanism. But eventually, after hours of exposure to the atmosphere under thawed conditions, all solvent-accessible thiols will oxidize to disulfides, resulting in a mixture of homo- and heterodisulfide dimers. This holds true regardless of

In Oxidative Stress: Diagnostics, Prevention, and Therapy Volume 2; Hepel, et al.;
ACS Symposium Series; American Chemical Society: Washington, DC, 2015.

Publication Date (Web): October 13, 2015 | doi: 10.1021/bk-2015-1200.ch016

the nature of the thiol-containing species—whether they be small molecule free thiols mixed with proteins bearing solvent-accessible free Cys residues (*92*), only small molecules/peptides (*37*), or only full sized proteins whose thiol groups can make contact with one another (*93*, *94*). The key to observing this behavior is to let reactions proceed for a long enough period of time.

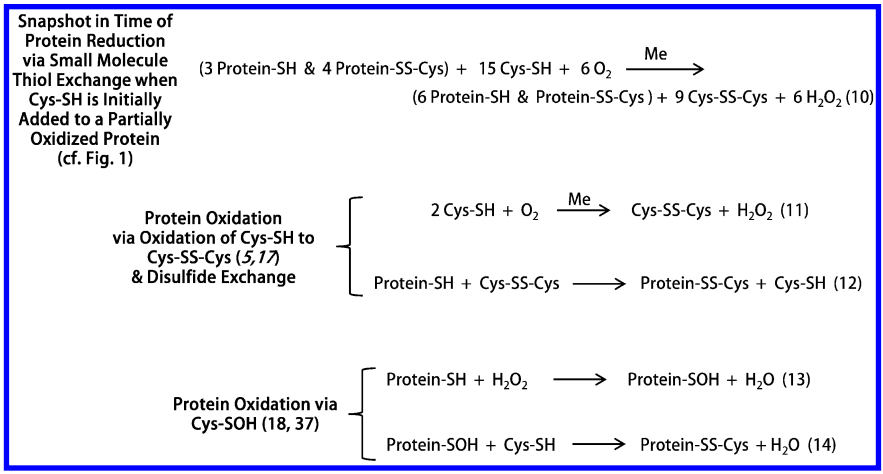

Scheme 3. Protein reduction by small molecule free thiols in vitro (using Cys-SH as an example reducing agent) and subsequent (re)oxidation of thiol groups in samples exposed to air. As shown (reactions 10-11), some of the thiol reducing agent "autoxidizes" in the presence of O_2 and redox active metals. Thus if the ratio of thiol reductant to oxidized protein is too low, reduction of the protein will be incomplete (cf. Figures 1-2). In the presence of oxygen and catalytically active trace metals, all solution-accessible thiols will eventually be converted to either Protein-SS-Cys or Cys-SS-Cys, (cf. Figure 2). For the sake of simplicity disulfide formation via minor reactions involving thiyl radicals are not shown (cf. refs. (5, 17–19)). Likewise, it is assumed that this particular protein cannot form a homodimer; if that were possible it would also be one of the final oxidation products and would take part in reactions analogous to those shown for Protein-SS-Cys and Cys-SS-Cys (reactions 11-14). Me indicates a redox active transition metal.

Publication Date (Web): October 13, 2015 | doi: 10.1021/bk-2015-1200.ch016

Publication Date (Web): October 13, 2015 | doi: 10.1021/bk-2015-1200.ch016

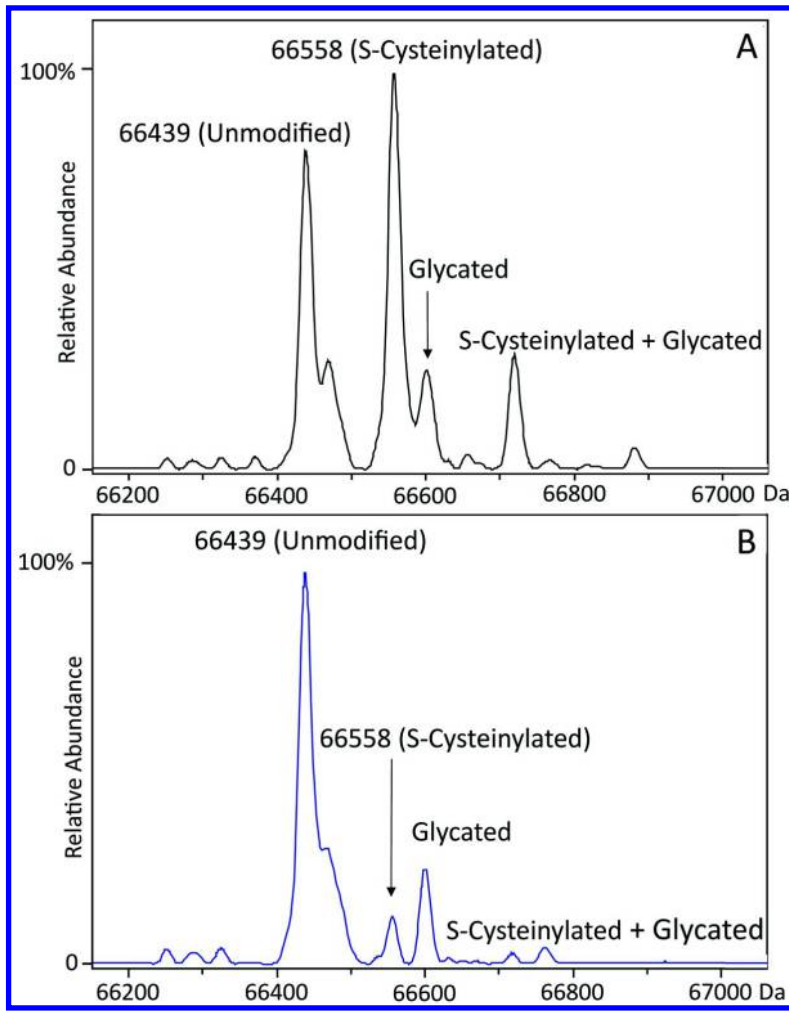

Figure 1. Charge deconvoluted ESI mass spectra of high purity, lipid-free human serum albumin isolated from human serum, shown as purchased from a commercial source (A), and following near-complete mixed-disulfide reduction with 2-fold molar excess of cysteine (B).

Publication Date (Web): October 13, 2015 | doi: 10.1021/bk-2015-1200.ch016

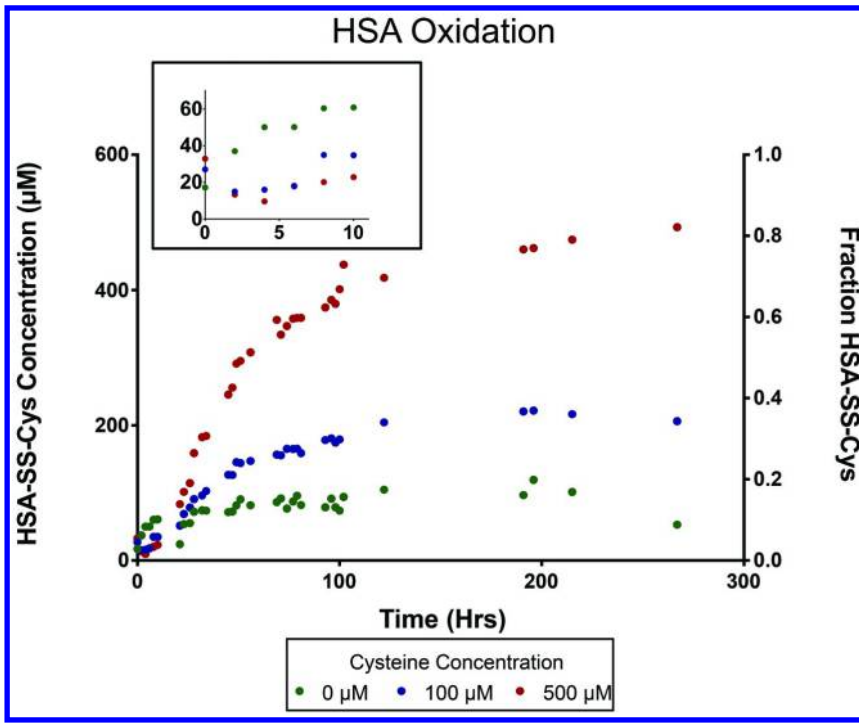

Figure 2. Time course for oxidative formation of the mixed disulfide between human serum albumin (HSA) and free cysteine (Cys) in vitro. The starting concentration of reduced HSA was 600 μM. Based on calculations of the dilution factor for purification of reduced HSA, approximately 100 μM of the original 4 mM Cys-SH added for initial reduction (cf. main text; now present as ~50 μM Cys-SS-Cys (Scheme 3, reaction 11)) had not been removed, accounting for the increase in HSA-SS-Cys in the sample with 0 added Cys. The initial decrease in HSA-SS-Cys for the samples with 100 μM and 500 μM added Cys (inset) corresponds to initial reduction followed by subsequent oxidation.

Human serum albumin (HSA) contains a single free cysteine residue (Cys34). As derived from fresh, healthy human serum, HSA is about 20% S-Cysteinylated (*36*). HSA purchased from vendors tends to display an elevated degree of S-Cysteinylation (Figure 1a), presumably due to oxidative processes that occur during protein purification. Upon adding 4 mM cysteine (Cys-SH) to 2 mM HSA, and incubation at room temperature for 2 hours, the reduction of HSA was nearly complete (Figure 1b). Notably, the reduction process did not reduce HSA structural disulfides as evidenced by the lack of a mass shift of the peak at 66,439 Da and by the fact that upon re-oxidation mass spectral peaks corresponding to di- or tri- S-Cysteinylated-HSA (HSA-SS-Cys) did not appear. Following reduction, excess Cys-SH and Cys-SS-Cys were removed from solution using a spin filter with a nominal molecular weight cutoff of 30 kDa. Cys-SH was then added at 0, 100 and 500 μM to three separate aliquots of 600 μM HSA, and the relative

fractional abundance of HSA-SS-Cys was monitored by mass spectrometric analysis of the intact protein over time (Figure 2). Initially, residual HSA-SS-Cys was reduced by the added Cys-SH (Figure 2, inset), but after several hours formation of HSA-SS-Cys began to occur (Scheme 3), reaching a maximum that correlated well with the total amount of Cys-SH added at the beginning of the time course.

The oxidation reactions operative in these experiments work the same way in complex biological samples. The authors' research group recently demonstrated that without the addition of any exogenous chemicals, the fraction of albumin in human blood plasma that is S-Cysteinylated increases rapidly when the plasma is stored above -30 °C—reaching a plateau of less than 100% S-Cysteinylation that is consistent with the total concentration of free cysteine plus molar equivalents of cysteine-within-cystine in plasma. This plateau was reached with 7 days at room temperature or 60 days at -20 °C (*36*).

The spontaneous formation of mixed disulfides *ex vivo* may impact *in vitro* biological systems under investigation. As such, *in vitro* data must be interpreted with caution; if extrapolation of results to conclusions about *in vivo* biochemistry is planned, experimental conditions should include a redox buffer (e.g., with a mixture of glutathione/oxidized glutathione (GSH/GSSG)) to mimic *in vivo* conditions. The fact that the simple, spontaneous redox chemistry that drives biologically less-interesting phenomena is responsible for or can recapitulate complex, biologically important biomolecular interactions does not diminish the reported importance or specificity of such interactions. As alluded to above, the unique protein microenvironments that stabilize oxidative thiol intermediates and guide/dock thiol-containing molecules to these sites determine the ultimate specificity of otherwise nonspecific redox chemistry.

Publication Date (Web): October 13, 2015 | doi: 10.1021/bk-2015-1200.ch016

Methionine Sulfoxidation

Methionine sulfoxidation is well known to the proteomics community as a largely artifactual modification (*95*) that may or may not be present on any given Met-containing peptide. It tends to be treated as a nuisance modification, but one that can readily be handled by routine proteomics workflows and data processing and analysis algorithms. Yet interestingly, when cultured cells are oxidized by direct exposure to a lethal dose of hydrogen peroxide (30% H_2O_2) for 2 hours at 37 °C, methionine sulfoxide (MetSO) tends to show up near neighboring polar residues (*96*), and the sequence specificity of methionine sulfoxide reductase enzymes appears to be a major factor in determining the balance of Met oxidation (*96*). Facilitated by its reversibility *in vivo*, MetSO has been found to serve as either a "molecular bodyguard" (*97*, *98*) and/or as an important mediator of redox regulation and signaling—including cross-talk with protein phosphorylation (reviewed in detail elsewhere (*99–101*)). Thus for studies involving detection or quantification of Met/MetSO, distinguishing between MetSO produced by biological processes *in vivo* vs. artifactual processes *ex vivo* can be critically important.

In most cases, the *in vitro*, artifactual formation of MetSO occurs as a result of ROS that are produced by the difficult-to-avoid combination of O_2 and trace

In Oxidative Stress: Diagnostics, Prevention, and Therapy Volume 2; Hepel, et al.;
ACS Symposium Series; American Chemical Society: Washington, DC, 2015.

metals outlined above (Scheme 1). The impact that artifactual formation of MetSO has on a particular experiment can vary widely; possible outcomes are diagrammed in Scheme 2. Because it is such a small molecular modification, the likelihood of serendipitously detecting protein methionine oxidation in most workflows (especially those that do not involve mass spectrometry) is very low—though it has happened (*102*)).

The limited ability to detect MetSO can have major consequences on experimental results. For example, MetSO has been documented to disrupt the following interactions: MetSO-antibody binding to protein A/G and Fc receptors (*103–105*), MetSO-calmodulin binding to plasma membrane Ca-ATPase (*106*, *107*) and CaMKII (*108*) (and a host of other consequences related to the impaired ability of MetSO-calmodulin to bind Ca^{2+} (*100*, *109*)), and MetSO-calcineurin binding to calmodulin (*110*). MetSO also alters the activity of parathyroid hormone (*111–114*), MetSO-antigenic peptide binding to the MHC and subsequent recognition by the T cell receptor (*115*), the binding of a MetSO C-type natriuretic peptide analog to its receptor (*116*), and the binding of the MetSO prion protein (PrP) to antibodies against its Helix-3 region (*117*). When modified by MetSO, phosphorylation of specific serine residues within nitrate reductase (*118*) is inhibited (additional examples of crosstalk between MetSO and protein phosphorylation are reviewed by Rao et al (*99*)). Furthermore, MetSO causes a general increase in protein surface hydrophobicity (*119*) and can lead to increased ubiquitination (*120*) and 20S proteasomal degradation (*121*). In a complicating twist, MetSO has also recently been shown to decrease 20S proteasomal degradation of alpha-synuclein (*122*). Perhaps even more interestingly, MetSO is emerging as an important *activator* of redox-signaling events (reviewed by (*100*)), including activation of CaMKII (which is reversed by methionine sulfoxide reductase A) (*123*), the *E. coli* transcription factor HypT (*124*), and f-actin disassembly (*125*, *126*).

Based on these reports, it is evident that the artifactual formation of MetSO in sub-optimally handled protein samples should not be dismissed as a relatively unimportant event that has no significant bearing on the outcome of research results or even, potentially, clinical assays that rely on protein-protein interactions.

It is common practice to characterize recombinant proteins or native proteins purified from a biological host using gels—which in general are not capable of revealing the presence of MetSO. It is common to think of the artifactual MetSO observed on peptides in bottom-up proteomics experiments as something that really only occurs during alkylation, proteolysis, and final sample work-up prior to analysis. As shown by Liu et al (*127*), this most certainly does occur—and they describe an isotopic labeling strategy to track oxidation that occurs during these steps. But artifactual, *ex vivo* oxidation of intact proteins can occur quite readily as well. For example, immediate analysis of intact beta-2-microglobulin (B2M) by MALDI mass spectrometry following extraction from human plasma or urine by antibody-based affinity capture reveals no oxidation of its single Met residue (*128–130*). Yet B2M obtained from a commercial source that had been purified from human urine contained approximately 50% MetSO (Figure 3a). Buffer exchange by spin filter in 0.1 M acetic acid over a time period of about 90 min at roughly 30 °C increased MetSO (Figure 3b), but reduction with

Publication Date (Web): October 13, 2015 | doi: 10.1021/bk-2015-1200.ch016

N-methylmercaptoacetamide (*131*) reduced MetSO back to Met (while also reducing the protein's disulfide bond (Figure 3c).

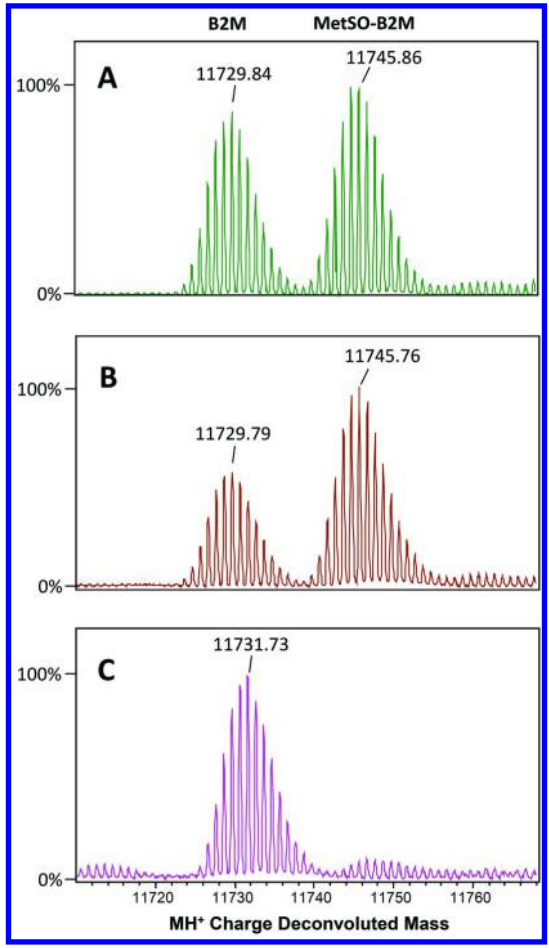

Figure 3. ESI-MS charge deconvoluted spectra of beta-2-microglobulin (B2M) protein purified from pooled human urine. Shown as obtained from the vendor (A). The calculated MH^+ mass of the 7th and most abundant isotope of B2M is 11729.80 Da (11745.79 Da for MetSO-B2M). Spin-filter purification in 0.1 M acetic acid resulted in additional formation of MetSO (B). Reduction with N-methylmercaptoacetamide resulted in reduction of MetSO as well as reduction of the disulfide bond with concomitant addition of two hydrogen atoms (C). Spectra were acquired on a Bruker maXis 4G equipped with an Agilent G1385A microflow ESI ion source that is held at ground while the instrument inlet was set at a high negative voltage (in positive ion mode). Settings: End plate offset -500 V, capillary -4,500 V, nebulizer nitrogen 2 bar, dry gas nitrogen 3 L/min at 210 ºC.

Publication Date (Web): October 13, 2015 | doi: 10.1021/bk-2015-1200.ch016

Publication Date (Web): October 13, 2015 | doi: 10.1021/bk-2015-1200.ch016

As proteins are purified away from their native biological environment, the risk of artifactual oxidation increases due to a loss of any natural redox buffering capacity that might accompany the unmodified biospecimen. For the same reason, the risk of substantial accumulation of MetSO relative to Met also increases at low protein concentrations. Recognizing the possibility that intact proteins may become artifactually oxidized *ex vivo*—even when they remain within their native biological environment can be critically important. Human apoA-I provides an illustrative example:

ApoAI is the major protein component of high density lipoprotein (HDL). Each protein molecule contains 3 Met residues at positions 86, 112, and 148. The first definitive evidence that these residues could be oxidized to MetSO was provided in 1988 (*132*). In this study, Anantharamaiah and colleagues showed that Met oxidation alters the secondary structure of apoAI and modifies the hydrophobicity of the nonpolar faces of the amphipathic helices that interact with HDL lipids—altering its lipid binding characteristics. As further research on the mechanism and functional impact of apoAI Met oxidation developed, it was suggested that MetSO-apoAI could potentially serve as a biomarker of conditions associated with cardiovascular-related oxidative stress, including atherosclerosis (*133–135*). But as published in 2009 (*136*), a large clinical study failed to show an association between MetSO-apoAI and coronary heart disease.

Several years later Borges et al (*36*) provided definitive evidence that MetSO-ApoAI can form spontaneously in human plasma that is stored above its freezing point of -30 °C (*86–89*), though this takes about 150 days to occur when specimens are stored at -20 °C. Moreover, this same report revealed a complete lack of apoAI MetSO (at least above 2-3% relative abundance) in all freshly collected plasma samples—including 24 specimens collected from patients during myocardial infarction. Though it clearly occurs, artifactual, *ex vivo* oxidation of apoAI in whole blood plasma may not be the definitive reason why no association between coronary heart disease and MetSO-apoAI was found (*136*), but it may well have contributed to the evidence that was built up over the years supporting a potential association between MetSO-apoAI and cardiovascular disease. The section on *Lipids* below describes the mechanism behind the artifactual oxidation of apoAI in plasma.

Oxidative Glycation

The excess oxygen and redox-active metals present in the *in vitro* environment can facilitate protein modification at residues other than Cys and Met. For example, enolization of the open-chain form of glucose followed by single-electron transfer to the oxidized form of a redox-active transition metal ion such as Fe(III), generates Fe(II) and the enediol radical glucose anion which can then directly react with O_2 to produce superoxide and the dicarbonyl form of glucose (*38*). Dismutation of the superoxide to H_2O_2 (Scheme 1, Reaction 5) provides the final necessary component for Fenton chemistry and production of hydroxyl radicals which (besides other forms of damage) ultimately contribute to additional production of the oxidized dicarbonyl form of glucose. This dicarbonyl form of glucose formed by the aforementioned “autoxidation” reactions is highly

reactive with protein amino groups and, *in vitro*, was found to be responsible for up to 45% of the attachment of glucose to bovine serum albumin that occurred within 10 hrs at 37 °C (*38*).

This reaction pathway constitutes a significant alternative to traditional Schiff base formation between glucose and protein amino groups followed by Amadori rearrangement. Theoretically, this "autoxidative glycation" pathway (*38*) could be activated in *ex vivo* blood specimens due to elevated $O_2(aq)$ concentration, creating the possibility of inaccurate protein glycation measurements. The glycated form of the human hemoglobin β-chain, HbA1c, is an important long-term clinical marker of blood glucose control. It provides a snapshot of overall blood glucose control over the past few months, according to the mean half-life of erythrocytes. When whole blood was stored at a series of temperatures above its freezing point for time frames of 1 to 57 days then analyzed by several commonly employed clinical assays, results demonstrated clear instabilities in the assays, primarily due to the unacceptable appearance of an extra chromatographic peak between the HbA1c and HbA0 chromatographic peaks (*137*, *138*). The chromatographic peak was not identified, but it was clearly attributable to artifactual, *ex vivo* processes.

In a recent study of the oxidative stability of HSA in human blood plasma (*36*), it was noticed that besides dramatic increases in the relative abundance of HSA-SS-Cys (determined by analysis of the intact protein by mass spectrometry), there appeared to be increases in the glycated form of albumin (Figure 4). Upon further inspection, these increases were found to be statistically significant when plasma aliquots from the healthy individual ($p < 0.01$) and from a poorly controlled diabetic ($p < 0.05$) were stored at -20 °C for 6 months. Further studies are underway to determine if oxidative, *ex vivo* processes were responsible for this result or if blood plasma protein glycation is simply not at equilibrium *in vivo*.

Publication Date (Web): October 13, 2015 | doi: 10.1021/bk-2015-1200.ch016

Instrument-Induced Oxidation

The *ex vivo* biochemical reactions discussed up to this point occur spontaneously when specimens are exposed to the atmosphere. It is also possible to artifactually oxidize proteins through the use of instrumentation that requires high voltages, which can facilitate reactions that are otherwise thermodynamically unfavorable.

Gel electrophoresis is perhaps the most widely employed method of protein analysis. It is often employed as a means of protein separation prior to analysis of proteins by mass spectrometry, constituting a classical method of proteomic analysis. It has been known since the 1960s that SDS-PAGE can cause artifactual protein oxidation (*139*) and loss of band resolution within gels. Some of the efforts to control it have been based on degassing the polymerization solution (*140*), photoinitiation of gel polymerization with flavin mononucleotide (*139*, *141*), and addition of the ROS scavenger thioglycolate into the cathode buffer reservoir (*142*). In 2004, Sun et al used MALDI-TOF mass spectrometry to show that a combination of all three of these steps resulted in no detectable oxidation of Met and Trp-containing tryptic peptides from equine heart cytochrome c (*39*).

In Oxidative Stress: Diagnostics, Prevention, and Therapy Volume 2; Hepel, et al.;
ACS Symposium Series; American Chemical Society: Washington, DC, 2015.

Publication Date (Web): October 13, 2015 | doi: 10.1021/bk-2015-1200.ch016

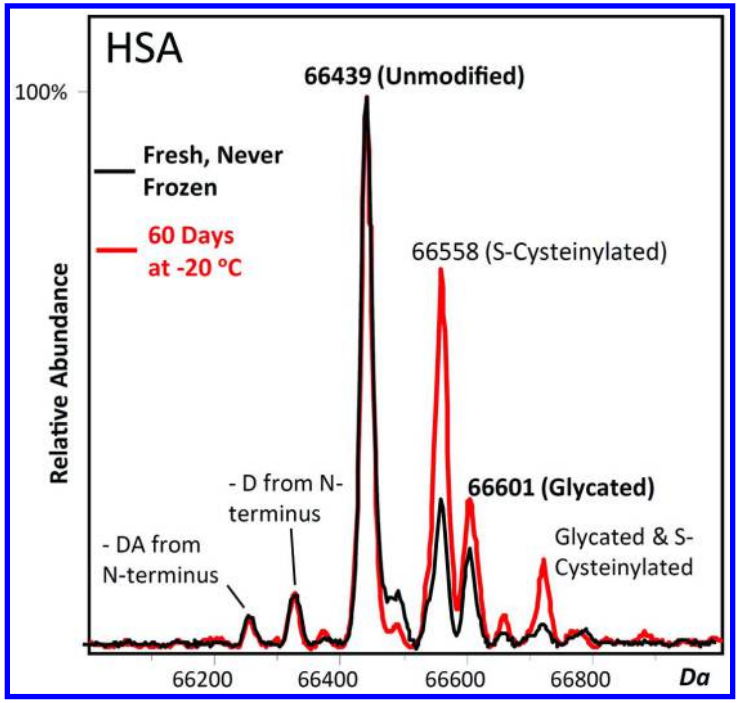

Figure 4. Charge deconvoluted electrospray ionization-mass spectra of albumin from a healthy donor showing an increase in the relative abundance of S-Cysteinylated albumin and glycated albumin when the plasma specimen was stored at -20 °C for 60 days. Red and black spectra are from the same individual sample, aged as indicated. Reproduced with permission from reference (36). Copyright 2014 The American Society for Biochemistry and Molecular Biology.

But these precautions are not universally applied by all investigators today. Using conventional proteomics practices, Froelich and Reid (*143*) have noted the artifactual oxidation of Met, Trp, and S-carboxyamidomethyl (iodoacetamide-alkylated Cys, S-CAM) that occurs under conditions of in-solution or in-gel tryptic digestion of the model protein bovine apotransferrin. MetSO formation was worse under in-gel conditions, but low-level artifactual oxidation of Trp and S-CAM were approximately equivalent under the two digestion conditions. Likewise, in a study focused on oxidation of Trp, Perdivara et al (*40*) demonstrated that tryptic and chymotryptic fragments of antibodies exhibited substantially greater formation of all forms of Trp oxidation when the proteins were first exposed to SDS-PAGE followed by in-gel proteolytic digestion vs. simple in-solution digestion.

As mentioned, proteomics approaches often employ mass spectrometry-based analysis of peptides following in-gel proteolytic digestion of proteins subjected to SDS-PAGE. Oxidation susceptible amino acid residues that remain reduced prior to analysis by electrospray ionization-mass spectrometry face one final hurdle: oxidation caused by the ESI process itself. The possibility of corona discharge

Publication Date (Web): October 13, 2015 | doi: 10.1021/bk-2015-1200.ch016

and subsequent generation of associated reactive species in the gas phase during ESI has been understood since the inception of ESI (*144*). Likewise, ESI inventor and Nobel Laureate John Fenn and his colleagues also understood early-on that charge-balancing electrochemical reactions (oxidation in positive ion mode and reduction in negative ion mode) take place in solution near the ESI spray needle during the ESI process—though Fenn admittedly took this fact for granted and did not discuss it much during the early days of ESI (*145*).

In 1993 a study of the impact of ESI-mediated oxidative processes on peptides revealed that even under normal operating conditions Met is particularly susceptible to being oxidized into MetSO (*72*). In 2009 Boys et al (*43*) reported a study in which they took it upon themselves to determine whether electrochemical processes within the spray needle or ROS generated by corona discharge during the desolvation/ionization process (*69–71*) (Figure 5) is responsible for protein oxidation that can occur during ESI. They found that corona discharge is solely responsible for this phenomenon and that it can occur under standard operating conditions that employ nitrogen as the nebulizer gas and a low capillary voltage.

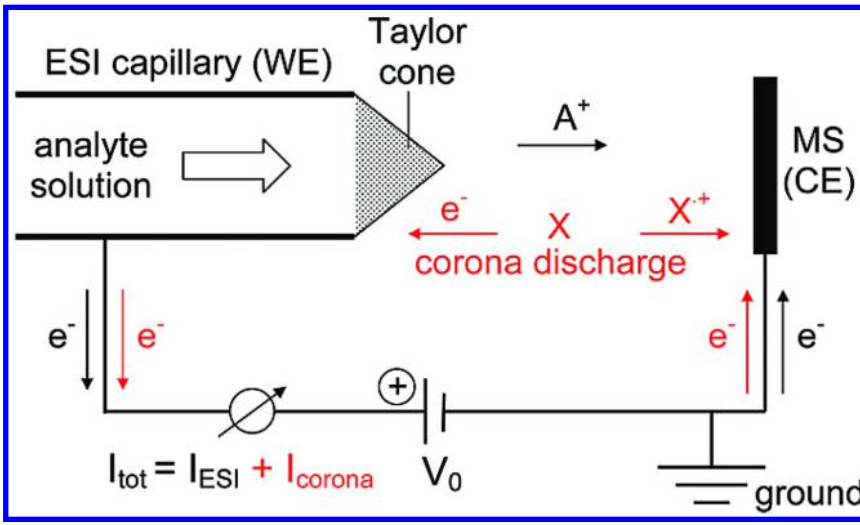

Figure 5. Schematic depiction of an ESI source in positive ion mode (black). Positively charged solvent droplets and analyte ions (A^+) are ejected from the tip of the Taylor cone. Flow directions of charge carriers are indicated by thin arrows. Shown in red are the additional current contributions under corona discharge conditions, where neutral gas molecules X break down to form X^+ and free electrons. MS, mass spectrometer; CE, counter electrode; WE, working electrode; V0, capillary voltage. Reproduced with permission from reference (43). Copyright 2009 The American Chemical Society.

Fortunately, rearrangement of the ESI source geometry such that the spray emitter is grounded and the inlet of the mass spectrometer is raised to a high negative voltage (in positive ion mode) prevents protein oxidation due to corona discharge. Corona discharge may still occur under this arrangement, but

electrons formed from the dielectric breakdown of neutral gas molecules are not back-attracted to the ESI emitter and accelerated toward it at high, ionizing energies. At present, Agilent and Bruker both employ this design. Notably, however, it is not possible to circumvent electrochemical reactions with this ion source geometry (*146*). In the author's experience with this source design (*36*, *37*, *147–152*), no ESI source-mediated artifactual protein oxidation has been observed (cf. Figure 3).

Lipids

Lipids are well-recognized in terms of their susceptibility to spontaneous, non-enzymatic *ex vivo* oxidation. The reaction of unsaturated lipids with oxygen to produce "autoxidizing", self-propagating lipid radicals, lipid peroxide radicals, and lipid hydroperoxides requires a mixture of Fe(II) & Fe(III) (*3*, *22*, *23*, *153–155*) (at an optimal ratio of 1:1 (*154*)) and can be initiated via the mechanisms described in the Introduction (Scheme 1), including photochemical / $^1O_2$-initiated peroxidation. These reactions can be useful in lipid characterization, but they can be problematic in lipid research when they are not monitored or controlled. As described below, they can also mediate the artifactual oxidation and covalent modification of proteins and nucleic acids.

Lipid Characterization

Mere exposure of unsaturated lipids to ambient conditions where air and light are available is enough to facilitate their oxidation and degradation. In a recently reported analytical method for characterization of double bond positions in unsaturated lipids (*42*), exposure to air and light served as requisite TLC-plate preparation parameters required to induce cleavage at double bonds with formation of chain-terminal aldehydes. In relatively pure samples, sufficient molecular alteration to facilitate characterization occurred within 1 hour exposure time to air and light at room temperature. The authors' results (*42*) demonstrated that singlet oxygen was more important than ozone (*156–159*) in mediating unsaturated lipid oxidation in the dry environment.

Interestingly, they pointed out that the radiative lifetime of $^1O_2$ (as the $^1\Delta_g$ state) is 45 min in the gas phase (*160*), but only 10^{-6} to 10^{-3} s in solution (*161*, *162*)—explaining why, in their study, oxidation of unsaturated lipids was observed on air-exposed surfaces, but not in solution. Under this mechanism of oxidation, $^1O_2$ would serve as the initial biomolecule oxidant rather than a metal ion (Scheme 1). Notably, reaction rates were found to differ for individual surfaces based on their roughness—with rougher surfaces leading to faster oxidation.

In concluding, the authors caution investigators to be wary of artifactual oxidation of lipids within dried biological samples that may occur due to ambient air exposure. Considering the popularity of lipid profiling by MALDI imaging and the growing interest in oxidative lipomics (*163*), the spontaneous *in vitro* oxidation of dry, surface-exposed lipids in tissue slices would seem to merit additional investigation with regard to the possibility of *ex vivo* artifacts arising

Publication Date (Web): October 13, 2015 | doi: 10.1021/bk-2015-1200.ch016

during sample preparation before introduction of tissue samples into the vacuum system of the mass spectrometer.

F_2-Isoprostanes as Representatives of Lipid-Based Markers of Oxidative Stress

F_2-isoprostanes (F2-IsoPs) are a molecular series of oxidized, largely phospholipid-derived forms of arachidonic acid (Scheme 4). They are released from phospholipids by phospholipase A2 and platelet activating factor acetylhydrolase. In circulation, HDL serves as their major lipoprotein carrier (*164*). In 1990 Morrow et al discovered that they can be produced spontaneously *in vitro* by enzyme-independent processes (*165*). Later that year, Morrow and colleagues also reported that F2-IsoPs are produced *in vivo* via a cyclooxygenase-independent mechanism involving free-radical mediated peroxidation of arachidonic acid (*166*).

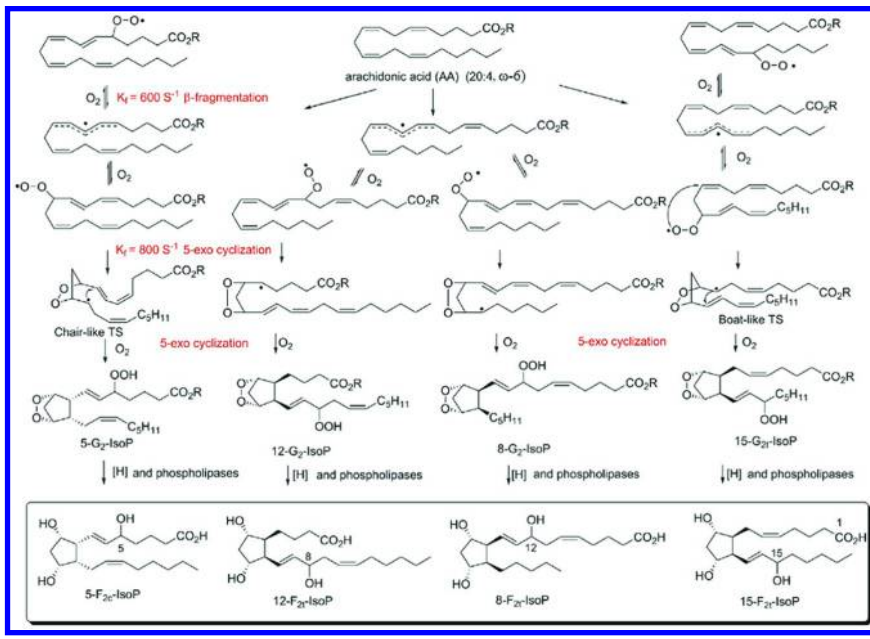

Scheme 4. Isoprostane formation from arachidonic acid. Reproduced with permission from reference (167). Copyright 2013 Elsevier.

Though there are other commonly employed lipid-based markers of *in vivo* oxidative stress such as malondialdehyde (MDA), 4-Hydroxy-2(E)-nonenal (HNE), 4-Hydroxy-2(E)-hexenal (HNE), and degree of LDL oxidation (reviewed elsewhere (*168–171*)), F2-IsoPs are widely considered to be the "gold standard" indicator of *in vivo* lipid oxidation as well as a general metric of physiological oxidative stress (*41*, *168*, *172–177*). They are frequently represented by measurement of 15-F_{2t}-IsoP in particular (also known as 8-*iso*-$PGF_{2\alpha}$ (*172*)).

In Oxidative Stress: Diagnostics, Prevention, and Therapy Volume 2; Hepel, et al.;
ACS Symposium Series; American Chemical Society: Washington, DC, 2015.

Publication Date (Web): October 13, 2015 | doi: 10.1021/bk-2015-1200.ch016

A few years ago, F2-IsoPs were validated as markers of oxidative damage in cardiovascular health by the European Food Safety Authority (EFSA) (*175*).

As established very early in the study of F2-IsoPs as markers of oxidative stress/damage (*165*), measurements of F2-IsoPs are highly susceptible to artifactual elevation due to non-enzymatic, free-radical mediated chemical reactions *in vitro* (Scheme 1). In particular, they found that storage of human blood plasma at -20 °C for several months resulted in an approximately 50-fold increase in these compounds.

Since that time, "best practices" have been established for the analysis of F2-IsoPs in plasma; they include collection into chilled tubes containing EDTA/butylated hydroxytoluene (BHT)/GSH with immediate centrifugation and storage at -80 °C for 1 month prior to analysis (*41*). Barden et al (*41*) recently carried out a systematic study on the effects of anticoagulants/antioxidants, storage temperature and storage time on F2-IsoP concentrations in plasma. They found that a 4-hr processing delay at 4 °C or room temperature followed by storage at -80 °C for 1 month did not cause results to deviate from those obtained using "best practices". However, storage of "best practice" samples for 6 months at -80 °C or any other deviation from "best practices" resulted in significantly elevated (often extremely elevated) measurements of F2-IsoPs. As pointed out by the study authors, the analysis of F2-IsoPs as markers of oxidative stress *in vivo* is on the rise—often being carried out as a part of multicenter studies where it may not always be feasible to carry out "best practices" when it comes to collection, immediate processing, cold storage (-80 °C), and analysis within one month. But their study proves that unless it is possible to guarantee execution of "best practices" for collection, processing, and storage of samples to be analyzed for F2-IsoPs, the results of such studies are likely to be dubious (at best) or even erroneous.

Considering that similar non-enzymatic free-radical mediated mechanisms are also behind the formation of other common markers of *in vivo* oxidative stress such as MDA, HNE, and HNA, similar precautions are also warranted with regard to their analysis and data interpretation. It is possible that artifactual, *ex vivo* lipid oxidation has contributed to confusion and conflicting reports on the role of polyunsaturated fatty acids in oxidative stress and chronic inflammatory diseases (*168*).

Publication Date (Web): October 13, 2015 | doi: 10.1021/bk-2015-1200.ch016

Oxidative Transfer from Lipids to Protein and DNA

Polyunsaturated lipids are highly prone to oxidation as described above and illustrated generically in Scheme 1 (esp. Rxns 4a,b). Interestingly, they do not always keep their oxidative damage to themselves; under the right conditions, they can readily pass their oxidative wounds to other classes of molecules, including proteins and DNA.

ApoAI is the most abundant protein component of HDL. As mentioned above, HDL is the major lipoprotein carrier of plasma F2-IsoPs. HDL is also the major carrier of all lipid hydroperoxides in human plasma (*178*). In 1998, two independent groups (*179–181*) reported that apoAI reduces lipid hydroperoxides in human HDL. Garner and colleagues (*179*, *180*) demonstrated that Met112 and

Met148 of apoAI (but not Met86) receive the oxidative insult immediately and are themselves converted to MetSO in the process. They additionally showed that the single Met residue of the apoAII polypeptide (Met26) can participate in the oxidative transfer from lipid hydroperoxides. Interestingly, incubation of Cu^{2+} with air-exposed isolated, lipid-free apoAI did not result in apoAI oxidation (*179*); moreover, dissociation of HDL by SDS inhibited reduction of lipid hydroperoxides (*180*).

These results proved the importance of the intact HDL particle in facilitating *in vitro* oxidation of apoAI and apoAII Met residues. Considering that HDL is the major carrier of plasma lipid hydroperoxides (*164*, *178*), these data suggest that among plasma proteins, apoAI and apoAII may be uniquely susceptible to Met oxidation.

Besides direct transfer of an oxidative insult, lipid peroxidation can result in lipid decomposition into a variety of reactive electrophiles (*169*, *182*, *183*). 1,3-propanedial (more commonly known as malondialdehyde (MDA)) and 4-hydroxy-2-nonenal (HNE) are two of the most abundant and well-studied examples. Following formation of initial lipid hydroperoxides and their rearrangement to endoperoxides (Scheme 4, rows 3-5), further oxidation and cleavage result in formation of MDA and HNE (*169*, *184*)—the latter occurring to completion within a few hours for dry samples at 37 °C (*184*). These species readily react and form covalent adducts with amino- and thiol-containing biomolecules—including both protein (*182*, *185*), and DNA (*183*, *186*, *187*). Within living cells this results in a plethora of mostly negative consequences. Because of this, numerous studies have sought to identify and quantify MDA, HNE and other lipid-based electrophile adducts of protein (reviewed in (*182*, *185*, *188*)) and DNA (reviewed in (*48*, *186*)), often with the goal of using these as biomarkers of disease or—in the case of DNA—promutagenic insult.

Since lipid oxidation and downstream protein and DNA adduct formation within biological samples can readily occur *ex vivo*, caution should always be taken with regard to study design, execution, and interpretation of data—including data already deposited in the literature.

Publication Date (Web): October 13, 2015 | doi: 10.1021/bk-2015-1200.ch016

Preventing Artifactual Oxidation

Minimize Oxygen Availability

Since artifactual *ex vivo* oxidation depends on molecular oxygen, the most effective way to prevent such oxidation reactions from occurring is to eliminate O_2 as a reactant. This can be done by working in a glovebox (or other oxygen-free environment) and degassing all solutions; but more often than not this approach is either impossible or creates excessive logistical difficulties and therefore, in most cases, does not represent a practical solution to the problem.

Remove or Chelate Catalytic Metals

The rate constant for the direct (catalyst-free) reaction of O_2 with ground state, singlet biomolecules has been calculated to be about 10^{-5} M^{-1} s^{-1} (*3*). This suggests

In Oxidative Stress: Diagnostics, Prevention, and Therapy Volume 2; Hepel, et al.;
ACS Symposium Series; American Chemical Society: Washington, DC, 2015.

that elimination of metals should be an effective means of preventing artifactual *ex vivo* oxidation. Indeed, removal and/or chelation of metals are the most common approaches to preventing artifactual oxidation because in most cases they are the most practical to implement without interfering with experimental constraints. Yet removal and chelation do not represent a perfect, "catch-all" solution to the problem (*3*). Miller et al (*3*) have provided a well-balanced discussion of common approaches and challenges involved in removing trace metals or neutralizing them via chelation. Several important aspects of the discussion include the following:

1) Trace quantities of metal contamination can be extremely difficult, if not impossible to eliminate because even the best metal-chelating resins rely on a competitive equilibrium between the resin and the experimental solution. Thus if the experimental solution contains a strongly-chelating buffer such as phosphate or Tris, treatment with a metal-exchange resin can actually deposit additional metals into solution by extracting them from the chelating resin (*3*, *189*).

2) Chelation (e.g., using EDTA, DFO, diethylene triamine pentacetic acid (DTPA)) can be an effective means to minimize autoxidation by curtailing biomolecular interactions and altering metal ion reduction potentials, but it is not guaranteed to render redox-active metals inert. In some cases—particularly those involving iron—chelation can actually *increase* the rate of autoxidation (cf. ascorbate in Table I) (*2*, *190*). Miller et al (*3*) provide a useful table of reduction potentials of complexed metals and illustrate a means by which to calculate (estimate) such potentials based on equilibrium binding constants of chelators with the reduced and oxidized forms of the same metal. They point out that chelators that use oxygen atoms to ligate the metal tend to prefer the oxidized form of the metal and generally decrease its reduction potential; conversely chelators that employ nitrogen for metal binding tend to prefer the reduced form of the metal and generally increase its reduction potential. Notably, many if not most buffers—including "Good's Buffers"—possess some capacity to ligate metals and alter their redox properties. The fact that most buffers (and biomolecules in general) ligate iron and copper is borne out by the fact that the solubilities of $Cu(II)_{aq}$ and $Fe(III)_{aq}$ at neutral pH are 10^{-9} M and 10^{-18} M, respectively (*3*). Thus their mere presence in solution at higher concentrations indicates that they have formed complexes with other ligands in solution—ligands that likely alter their reduction potentials and thus affect the rates at which they catalyze redox reactions.

3) If attempts to remove or chelate metals are made, a functional test to determine if the treated solution is indeed 'catalytic metal-free' should be employed before and after metal removal. A simple test designed by Buettner (*2*) based on the spectrophotometrically monitored autoxidation of ascorbate is recommended.

Scavenge Oxygen

Oxygen scavengers are commonly employed in the food and pharmaceutical packaging industries to keep products fresh that are intended for human consumption. These are often based on Fe(0) or Fe(II) and involve scavenging O_2 in the gas phase—e.g., from the headspace of a sealed container. Some

In Oxidative Stress: Diagnostics, Prevention, and Therapy Volume 2; Hepel, et al.;
ACS Symposium Series; American Chemical Society: Washington, DC, 2015.

Publication Date (Web): October 13, 2015 | doi: 10.1021/bk-2015-1200.ch016

oxygen and ROS scavengers, however, are based on ascorbate or other organic molecules (*191*) and in some limited-lifetime *in vivo*-like contexts where their pro-oxidant properties are not active, may be viable for practical application in biochemical experiments (*192*, *193*). Enzymes such as superoxide and catalase may be employed to scavenge superoxide and hydrogen peroxide, respectively; but as enzymes these have relatively short lifetimes in solution.

Avoid Singlet Oxygen

Production of singlet oxygen requires only air (O_2) and ambient light. As described in the *Lipids* section above, singlet oxygen is much more stable in the gas phase than in solution. Thus while it is impractical to work in the dark, it may often be prudent to avoid complete dehydration of samples being studied—particularly those containing unsaturated lipids.

Keep Archived Biological Samples Fully Frozen

While obviously not useful as a means of preventing artifactual oxidation while liquid-phase biochemical experiments are being conducted, freezing is the most common means of preserving liquid biospecimens. Logistically, it is a very simple means of preservation, but it is not fool-proof: Specimens must be stored below their freezing points to avoid artifactual, *ex vivo* oxidation (*36*); as pointed out above, biological specimens with high protein content can have severely depressed freezing points (e.g., -30 °C for blood plasma (*86–89*)). Moreover, freezers with auto-defrost features are often poorly suited for long term storage because of their propensity to dehydrate samples that are not perfectly sealed. Storage in liquid nitrogen (-196 °C) meets these criteria while simultaneously minimizing exposure to oxygen.

Conclusions

All major classes of biomolecules are susceptible to artifactual, *ex vivo* oxidation. Investigator awareness is the most important parameter in preventing the misinterpretation of results or the spread of erroneous conclusions stemming from this phenomenon (Scheme 2). Once investigators are aware of the potential problem, all possible steps during sample preparation and analysis should be taken to ensure that *ex vivo* oxidation is minimized. These generally include minimizing sample temperature and exposure to air, addition of appropriate metal chelators (*3*) and selection of a non-exacerbating buffer system (*27*), and, for lipids, minimizing exposure of dried samples to both air and light. In addition, investigators must remain aware that even though their analytical approach may not directly detect the oxidized form of the biomolecule of interest (and it may go undetected), artifactual oxidation can still directly impact results: For example, if detection or quantification simply involves densitometric analysis of a band of DNA or protein in a gel it is impossible to determine if that DNA or protein is oxidized—or if some upstream effector that produced that band was damaged

In Oxidative Stress: Diagnostics, Prevention, and Therapy Volume 2; Hepel, et al.;
ACS Symposium Series; American Chemical Society: Washington, DC, 2015.

Publication Date (Web): October 13, 2015 | doi: 10.1021/bk-2015-1200.ch016

by oxidation. Likewise, assays such as ELISAs that are based on biomolecular interaction with a photometric readout provide no direct information on whether the target analyte is oxidized and whether or not the oxidative modification might have had an impact on the results. In such cases where oxidative damage cannot be detected directly, the experimental design must include appropriate controls that will reveal whether or not artifactual oxidation is taking place and impacting results.

Additionally, biomarker studies require knowledge of biospecimen history including collection, processing and handling, final storage state, length of storage in that state, and details on any deviations from storage in that state. At a minimum it should be known that case and control samples were collected, processed and stored in parallel with one another with minimal deviation in sample handling variables. *Ex vivo*-variables that relate to the biospecimen can be as important as *in vivo*-variables and should be given as much attention during study design and development as biological variables. In the long run, time and effort invested in minimizing the misleading impact of artifactual *ex vivo* oxidation will provide a more direct route to bona fide biological discovery and its associated technological advances.

Publication Date (Web): October 13, 2015 | doi: 10.1021/bk-2015-1200.ch016

Acknowledgments

We are grateful to the College of Liberal Arts and Sciences, Department of Chemistry & Biochemistry at Arizona State University for providing faculty start-up funds that supported the writing of this manuscript. CB also acknowledges NIH grants R01DK082542 and R24DK090958 which supported acquisition of some of the data presented herein. The content is solely the responsibility of the authors and does not necessarily represent the official views of the National Institutes of Health.

References

1. Gevantman, L. H. In *CRC Handbook of Chemistry and Physics*, 95th ed.; Haynes, W. M., Ed.; CRC Press/Taylor and Francis: Boca Raton, FL, 2015; Section 5, pp 149−152.
2. Buettner, G. R. *J. Biochem. Biophys. Methods* **1988**, *16*, 27–40.
3. Miller, D. M.; Buettner, G. R.; Aust, S. D. *Free Radic. Biol. Med.* **1990**, *8*, 95–108.
4. Khan, M. M.; Martell, A. E. *J. Am. Chem. Soc.* **1967**, *89*, 4176–4185.
5. Pecci, L.; Montefoschi, G.; Musci, G.; Cavallini, D. *Amino Acids* **1997**, *13*, 355–367.
6. Skoog, D. A.; West, D. M.; Holler, F. J.; Crouch, S. R. *Fundamentals of Analytical Chemistry*, 9th ed.; Brooks/Cole: Belmont, CA, 2014.
7. Buettner, G. R. *Arch. Biochem. Biophys.* **1993**, *300*, 535–543.
8. Wardman, P. *J. Phys. Chem. Ref. Data* **1989**, *18*, 1637–1755.
9. Ramos, C. L.; Pou, S.; Britigan, B. E.; Cohen, M. S.; Rosen, G. M. *J. Biol. Chem.* **1992**, *267*, 8307–8312.

10. Britigan, B. E.; Ratcliffe, H. R.; Buettner, G. R.; Rosen, G. M. *Biochim. Biophys. Acta* **1996**, *1290*, 231–240.
11. Xu, L.; Davis, T. A.; Porter, N. A. *J. Am. Chem. Soc.* **2009**, *131*, 13037–13044.
12. Howard, J. A.; Ingold, J. A. *Can. J. Chem.* **1967**, *45*, 793.
13. Fridovich, I. *Annu. Rev. Pharmacol. Toxicol.* **1983**, *23*, 239–257.
14. Aust, S. D.; Morehouse, L. A.; Thomas, C. E. *J. Free Radic. Biol. Med.* **1985**, *1*, 3–25.
15. Barron, E. S. G.; DeMeio, R. H.; Klemperer, F. *J. Biol. Chem.* **1936**, *112*, 625–640.
16. Tsen, C. C.; Tappel, A. L. *J. Biol. Chem.* **1958**, *233*, 1230–1232.
17. Kachur, A. V.; Koch, C. J.; Biaglow, J. E. *Free Radic. Res.* **1999**, *31*, 23–34.
18. Kachur, A. V.; Koch, C. J.; Biaglow, J. E. *Free Radic. Res.* **1998**, *28*, 259–269.
19. Kachur, A. V.; Held, K. D.; Koch, C. J.; Biaglow, J. E. *Radiat. Res.* **1997**, *147*, 409–415.
20. Hung, M. L.; Stanbury, D. M. *Inorg. Chem.* **2005**, *44*, 3541–3550.
21. Lawrence, G. D.; Mavi, A.; Meral, K. *Carbohydr. Res.* **2008**, *343*, 626–635.
22. Bucher, J. R.; Tien, M.; Aust, S. D. *Biochem. Biophys. Res. Commun.* **1983**, *111*, 777–784.
23. Minotti, G.; Aust, S. D. *Chem. Phys. Lipids* **1987**, *44*, 191–208.
24. Grinstead, R. R. *Biochemistry* **1964**, *3*, 1308–1314.
25. Sakihama, Y.; Cohen, M. F.; Grace, S. C.; Yamasaki, H. *Toxicology* **2002**, *177*, 67–80.
26. La, M.; Chen, C. D.; Li, H.; Yang, C. Y. *Int. J. Electrochem. Sci.* **2014**, *9*, 6870–6879.
27. Welch, K. D.; Davis, T. Z.; Aust, S. D. *Arch. Biochem. Biophys.* **2002**, *397*, 360–369.
28. Garcia, C. R.; Angele-Martinez, C.; Wilkes, J. A.; Wang, H. C.; Battin, E. E.; Brumaghim, J. L. *Dalton Trans.* **2012**, *41*, 6458–6467.
29. Nkhili, E.; Loonis, M.; Mihai, S.; El Hajji, H.; Dangles, O. *Food Funct.* **2014**, *5*, 1186–1202.
30. Cadet, J.; Douki, T.; Ravanat, J. L. *Mutat. Res.* **2011**, *711*, 3–12.
31. Chao, M. R.; Yen, C. C.; Hu, C. W. *Free Radic. Biol. Med.* **2008**, *44*, 464–473.
32. Costello, M.; Pugh, T. J.; Fennell, T. J.; Stewart, C.; Lichtenstein, L.; Meldrim, J. C.; Fostel, J. L.; Friedrich, D. C.; Perrin, D.; Dionne, D.; Kim, S.; Gabriel, S. B.; Lander, E. S.; Fisher, S.; Getz, G. *Nucleic Acids Res.* **2013**, *41*, e67.
33. Cheng, K. C.; Cahill, D. S.; Kasai, H.; Nishimura, S.; Loeb, L. A. *J. Biol. Chem.* **1992**, *267*, 166–172.
34. McAuley-Hecht, K. E.; Leonard, G. A.; Gibson, N. J.; Thomson, J. B.; Watson, W. P.; Hunter, W. N.; Brown, T. *Biochemistry* **1994**, *33*, 10266–10270.
35. Beard, W. A.; Batra, V. K.; Wilson, S. H. *Mutat. Res., Gen. Toxicol. Environ. Mutagen.* **2010**, *703*, 18–23.

36. Borges, C. R.; Rehder, D. S.; Jensen, S.; Schaab, M. R.; Sherma, N. D.; Yassine, H.; Nikolova, B.; Breburda, C. *Mol. Cell. Proteomics: MCP* **2014**, *13*, 1890–1899.
37. Rehder, D. S.; Borges, C. R. *Biochemistry* **2010**, *49*, 7748–7755.
38. Wolff, S. P.; Dean, R. T. *Biochem. J.* **1987**, *245*, 243–250.
39. Sun, G.; Anderson, V. E. *Electrophoresis* **2004**, *25*, 959–965.
40. Perdivara, I.; Deterding, L. J.; Przybylski, M.; Tomer, K. B. *J. Am. Soc. Mass Spectrom.* **2010**, *21*, 1114–1117.
41. Barden, A. E.; Mas, E.; Croft, K. D.; Phillips, M.; Mori, T. A. *Anal. Biochem.* **2014**, *449*, 129–131.
42. Zhou, Y.; Park, H.; Kim, P.; Jiang, Y.; Costello, C. E. *Anal. Chem.* **2014**, *86*, 5697–5705.
43. Boys, B. L.; Kuprowski, M. C.; Noel, J. J.; Konermann, L. *Anal. Chem.* **2009**, *81*, 4027–4034.
44. Sampath, H. *Environ. Mol. Mutagen.* **2014**, *55*, 689–703.
45. Storr, S. J.; Woolston, C. M.; Zhang, Y.; Martin, S. G. *Antioxid. Redox Signaling* **2013**, *18*, 2399–2408.
46. Simonelli, V.; Mazzei, F.; D'Errico, M.; Dogliotti, E. *Mutat. Res.* **2012**, *731*, 1–13.
47. Berquist, B. R.; Wilson, D. M., 3rd .*Cancer Lett.* **2012**, *327*, 61–72.
48. Tudek, B.; Winczura, A.; Janik, J.; Siomek, A.; Foksinski, M.; Olinski, R. *Am. J. Transl. Res.* **2010**, *2*, 254–284.
49. Cooke, M. S.; Olinski, R.; Evans, M. D. *Clin. Chim. Acta* **2006**, *365*, 30–49.
50. Cooke, M. S.; Evans, M. D.; Dizdaroglu, M.; Lunec, J. *FASEB J.* **2003**, *17*, 1195–1214.
51. Sykora, P.; Wilson, D. M., 3rd; Bohr, V. A. *Mech. Ageing Dev.* **2013**, *134*, 440–448.
52. Mao, P.; Reddy, P. H. *Biochim. Biophys. Acta* **2011**, *1812*, 1359–1370.
53. Kroese, L. J.; Scheffer, P. G. *Curr. Atheroscler. Rep.* **2014**, *16*, 452.
54. Malik, Q.; Herbert, K. E. *Free Radic. Res.* **2012**, *46*, 554–564.
55. Bridge, G.; Rashid, S.; Martin, S. A. *Cancers* **2014**, *6*, 1597–1614.
56. Brierley, D. J.; Martin, S. A. *Antioxid. Redox Signaling* **2013**, *18*, 2420–2428.
57. Ravanat, J. L.; Turesky, R. J.; Gremaud, E.; Trudel, L. J.; Stadler, R. H. *Chem. Res. Toxicol.* **1995**, *8*, 1039–1045.
58. Hamberg, M.; Zhang, L. Y. *Anal. Biochem.* **1995**, *229*, 336–344.
59. Douki, T.; Delatour, T.; Bianchini, F.; Cadet, J. *Carcinogenesis* **1996**, *17*, 347–353.
60. Cooke, M. S.; Olinski, R.; Loft, S.; European Standards Committee on Urinary (DNA) Lesion Analysis. *Cancer Epidemiol., Biomarkers Prev.* **2008**, *17*, 3−14
61. Ravanat, J. L.; Douki, T.; Duez, P.; Gremaud, E.; Herbert, K.; Hofer, T.; Lasserre, L.; Saint-Pierre, C.; Favier, A.; Cadet, J. *Carcinogenesis* **2002**, *23*, 1911–1918.
62. Escodd; Gedik, C. M.; Collins, A. *FASEB J.* **2005**, *19*, 82−84.
63. Badouard, C.; Menezo, Y.; Panteix, G.; Ravanat, J. L.; Douki, T.; Cadet, J.; Favier, A. *Zygote* **2008**, *16*, 9–13.

Publication Date (Web): October 13, 2015 | doi: 10.1021/bk-2015-1200.ch016

64. Garratt, L. W.; Mistry, V.; Singh, R.; Sandhu, J. K.; Sheil, B.; Cooke, M. S.; Sly, P. D.; Arestcf. *Free Radic. Biol. Med.* **2010**, *48*, 1460−1464.
65. Dizdaroglu, M.; Jaruga, P.; Rodriguez, H. *Nucleic Acids Res.* **2001**, *29*, E12.
66. Matter, B.; Malejka-Giganti, D.; Csallany, A. S.; Tretyakova, N. *Nucleic Acids Res.* **2006**, *34*, 5449–5460.
67. Morrow, R. *J. Phys. D: Appl. Phys.* **1997**, *30*, 3099–3114.
68. Chen, J.; Davidson, J. H. *Plasma Chem. Plasma Proc.* **2002**, *22*, 199–224.
69. Wang, W. C.; Wang, S.; Liu, F.; Zheng, W.; Wang, D. Z. *Spectrochim. Acta, Part A* **2006**, *63*, 477–482.
70. Fehsenfeld, F. C.; Mosesman, M.; Ferguson, E. E. *J. Chem. Phys.* **1971**, *55*, 2115–2120.
71. Good, A.; Durden, D. A.; Kebarle, P. *J. Chem. Phys.* **1970**, *52*, 212.
72. Morand, K.; Talbo, G.; Mann, M. *Rapid Commun. Mass Spectrom.* **1993**, *7*, 738–743.
73. Supek, F.; Lehner, B. *Nature* **2015**.
74. Do, H.; Dobrovic, A. *Clin. Chem.* **2015**, *61*, 64–71.
75. Wouters, M. A.; Fan, S. W.; Haworth, N. L. *Antioxid. Redox Signaling* **2010**, *12*, 53–91.
76. Cook, K. M.; Hogg, P. J. *Antioxid. Redox Signaling* **2013**, *18*, 1987–2015.
77. Butera, D.; Cook, K. M.; Chiu, J.; Wong, J. W.; Hogg, P. J. *Blood* **2014**, *123*, 2000–2007.
78. Winterbourn, C. C.; Hampton, M. B. *Free Radic. Biol. Med.* **2008**, *45*, 549–561.
79. Wouters, M. A.; Iismaa, S.; Fan, S. W.; Haworth, N. L. *Int. J. Biochem. Cell Biol.* **2011**, *43*, 1079–1085.
80. White, F. H., Jr.; Anfinsen, C. B. *Ann. N. Y. Acad. Sci.* **1959**, *81*, 515–523.
81. Anfinsen, C. B.; Haber, E. *J. Biol. Chem.* **1961**, *236*, 1361–1363.
82. Anfinsen, C. B.; Haber, E.; Sela, M.; White, F. H., Jr. *Proc. Natl. Acad. Sci. U. S. A.* **1961**, *47*, 1309–1314.
83. White, F. H., Jr. *J. Biol. Chem.* **1961**, *236*, 1353–1360.
84. Haber, E.; Anfinsen, C. B. *J. Biol. Chem.* **1962**, *237*, 1839–1844.
85. Anfinsen, C. B. *Science* **1973**, *181*, 223–230.
86. Farrugia, A.; Hill, R.; Douglas, S.; Karabagias, K.; Kleinig, A. *Thromb. Res.* **1992**, *68*, 97–102.
87. MacKenzie, A. P. Presented at American Institute of Chemical Engineers Symposium: Processing and fractionation of blood plasma, Philadelphia, PA, June 8−12, 1980.
88. Bravo, M. I.; Grancha, S.; Jorquera, J. I. *Pharmeuropa Scientific Notes* **2006**, *2006*, 31–35.
89. Human plasma for fractionation. *PhEur Monograph 0853*, Suppl. 5.3; Council of Europe: Strasbourg, France, 2005.
90. Maleknia, S. D.; Chance, M. R.; Downard, K. M. *Rapid Commun. Mass Spectrom.* **1999**, *13*, 2352–2358.
91. Lo Conte, M.; Carroll, K. S. *J. Biol. Chem.* **2013**, *288*, 26480–26488.
92. Johansson, M.; Lundberg, M. *BMC Biochem.* **2007**, *8*, 26.
93. Zavialov, A. V.; Gaestel, M.; Korpela, T.; Zav'yalov, V. P. *Biochim. Biophys. Acta, Protein Struct. Mol. Enzymol.* **1998**, *1388*, 123–132.

Publication Date (Web): October 13, 2015 | doi: 10.1021/bk-2015-1200.ch016

94. Yusuf, S. N. H. M.; Bailey, U. M.; Tan, N. Y.; Jamaluddin, M. F.; Schulz, B. L. *Biochem. Biophys. Res. Commun.* **2013**, *432*, 438–443.
95. Potgieter, H. C.; Ubbink, J. B.; Bissbort, S.; Bester, M. J.; Spies, J. H.; Vermaak, W. J. *Anal. Biochem.* **1997**, *248*, 86–93.
96. Ghesquiere, B.; Jonckheere, V.; Colaert, N.; Van Durme, J.; Timmerman, E.; Goethals, M.; Schymkowitz, J.; Rousseau, F.; Vandekerckhove, J.; Gevaert, K. *Mol. Cell. Proteomics* **2011**, *10*, doi: 10.1074/mcp.M110.006866.
97. Levine, R. L.; Mosoni, L.; Berlett, B. S.; Stadtman, E. R. *Proc. Natl. Acad. Sci. U. S. A.* **1996**, *93*, 15036–15040.
98. Luo, S.; Levine, R. L. *FASEB J.* **2009**, *23*, 464–472.
99. Rao, R. S. P.; Moller, I. M.; Thelen, J. J.; Miernyk, J. A. *Cell Stress Chaperones* **2015**, *20*, 15–21.
100. Drazic, A.; Winter, J. *Biochim. Biophys. Acta* **2014**, *1844*, 1367–1382.
101. Kim, G.; Weiss, S. J.; Levine, R. L. *Biochim. Biophys. Acta* **2014**, *1840*, 901–905.
102. Kanayama, A.; Inoue, J.; Sugita-Konishi, Y.; Shimizu, M.; Miyamoto, Y. *J. Biol. Chem.* **2002**, *277*, 24049–24056.
103. Gaza-Bulseco, G.; Faldu, S.; Hurkmans, K.; Chumsae, C.; Liu, H. *J. Chromatogr. B: Anal. Technol. Biomed. Life Sci.* **2008**, *870*, 55–62.
104. Bertolotti-Ciarlet, A.; Wang, W. R.; Lownes, R.; Pristatsky, P.; Fang, Y. L.; McKelvey, T.; Li, Y. Z.; Li, Y. S.; Drummond, J.; Prueksaritanont, T.; Vlasak, J. *Mol. Immunol.* **2009**, *46*, 1878–1882.
105. Pan, H.; Chen, K.; Chu, L.; Kinderman, F.; Apostol, I.; Huang, G. *Protein Sci.* **2009**, *18*, 424–433.
106. Yao, Y.; Yin, D.; Jas, G. S.; Kuczer, K.; Williams, T. D.; Schoneich, C.; Squier, T. C. *Biochemistry* **1996**, *35*, 2767–2787.
107. Gao, J.; Yao, Y.; Squier, T. C. *Biophys. J.* **2001**, *80*, 1791–1801.
108. Snijder, J.; Rose, R. J.; Raijmakers, R.; Heck, A. J. *J. Struct. Biol.* **2011**, *174*, 187–195.
109. Bigelow, D. J.; Squier, T. C. *Mol. BioSyst.* **2011**, *7*, 2101–2109.
110. Carruthers, N. J.; Stemmer, P. M. *Biochemistry* **2008**, *47*, 3085–3095.
111. Galceran, T.; Lewis-Finch, J.; Martin, K. J.; Slatopolsky, E. *Endocrinology* **1984**, *115*, 2375–2378.
112. Horiuchi, N. *J. Bone Miner. Res.* **1988**, *3*, 353–358.
113. Nabuchi, Y.; Fujiwara, E.; Ueno, K.; Kuboniwa, H.; Asoh, Y.; Ushio, H. *Pharm. Res.* **1995**, *12*, 2049–2052.
114. Hocher, B.; Oberthur, D.; Slowinski, T.; Querfeld, U.; Schaefer, F.; Doyon, A.; Tepel, M.; Roth, H. J.; Gron, H. J.; Reichetzeder, C.; Betzel, C.; Armbruster, F. P. *Kidney Blood Pressure Res.* **2013**, *37*, 240–251.
115. Weiskopf, D.; Schwanninger, A.; Weinberger, B.; Almanzar, G.; Parson, W.; Buus, S.; Lindner, H.; Grubeck-Loebenstein, B. *J. Leukoc. Biol.* **2010**, *87*, 165–172.
116. Thibault, G.; Grove, K. L.; Deschepper, C. F. *Mol. Pharmacol.* **1995**, *48*, 1046–1053.
117. Canello, T.; Frid, K.; Gabizon, R.; Lisa, S.; Friedler, A.; Moskovitz, J.; Gasset, M.; Gabizon, R. *PLoS Pathog.* **2010**, *6*.

Publication Date (Web): October 13, 2015 | doi: 10.1021/bk-2015-1200.ch016

118. Hardin, S. C.; Larue, C. T.; Oh, M. H.; Jain, V.; Huber, S. C. *Biochem. J.* **2009**, *422*, 305–312.
119. Chao, C. C.; Ma, Y. S.; Stadtman, E. R. *Proc. Natl. Acad. Sci. U. S. A.* **1997**, *94*, 2969–2974.
120. Hershko, A.; Heller, H.; Eytan, E.; Reiss, Y. *J. Biol. Chem.* **1986**, *261*, 1992–1999.
121. Ferrington, D. A.; Sun, H.; Murray, K. K.; Costa, J.; Williams, T. D.; Bigelow, D. J.; Squier, T. C. *J. Biol. Chem.* **2001**, *276*, 937–943.
122. Alvarez-Castelao, B.; Goethals, M.; Vandekerckhove, J.; Castano, J. G. *Biochim. Biophys. Acta* **2014**, *1843*, 352–365.
123. Erickson, J. R.; Joiner, M. L.; Guan, X.; Kutschke, W.; Yang, J.; Oddis, C. V.; Bartlett, R. K.; Lowe, J. S.; O'Donnell, S. E.; Aykin-Burns, N.; Zimmerman, M. C.; Zimmerman, K.; Ham, A. J.; Weiss, R. M.; Spitz, D. R.; Shea, M. A.; Colbran, R. J.; Mohler, P. J.; Anderson, M. E. *Cell* **2008**, *133*, 462–474.
124. Drazic, A.; Miura, H.; Peschek, J.; Le, Y.; Bach, N. C.; Kriehuber, T.; Winter, J. *Proc. Natl. Acad. Sci. U. S. A.* **2013**, *110*, 9493–9498.
125. Hung, R. J.; Pak, C. W.; Terman, J. R. *Science* **2011**, *334*, 1710–1713.
126. Lee, B. C.; Peterfi, Z.; Hoffmann, F. W.; Moore, R. E.; Kaya, A.; Avanesov, A.; Tarrago, L.; Zhou, Y.; Weerapana, E.; Fomenko, D. E.; Hoffmann, P. R.; Gladyshev, V. N. *Mol. Cell.* **2013**, *51*, 397–404.
127. Liu, H.; Ponniah, G.; Neill, A.; Patel, R.; Andrien, B. *Anal. Chem.* **2013**, *85*, 11705–11709.
128. Tubbs, K. A.; Nedelkov, D.; Nelson, R. W. *Anal. Biochem.* **2001**, *289*, 26–35.
129. Niederkofler, E. E.; Tubbs, K. A.; Gruber, K.; Nedelkov, D.; Kiernan, U. A.; Williams, P.; Nelson, R. W. *Anal. Chem.* **2001**, *73*, 3294–3299.
130. Nedelkov, D.; Nelson, R. W. *Am. J. Kidney Diseases* **2001**, *38*, 481–487.
131. Houghten, R. A.; Li, C. H. *Anal. Biochem.* **1979**, *98*, 36–46.
132. Anantharamaiah, G. M.; Hughes, T. A.; Iqbal, M.; Gawish, A.; Neame, P. J.; Medley, M. F.; Segrest, J. P. *J. Lipid Res.* **1988**, *29*, 309–318.
133. Pankhurst, G.; Wang, X. L.; Wilcken, D. E.; Baernthaler, G.; Panzenbock, U.; Raftery, M.; Stocker, R. *J. Lipid Res.* **2003**, *44*, 349–355.
134. Panzenbock, U.; Stocker, R. *Biochim. Biophys. Acta* **2005**, *1703*, 171–181.
135. Wang, X. S.; Shao, B.; Oda, M. N.; Heinecke, J. W.; Mahler, S.; Stocker, R. *J. Lipid Res.* **2009**, *50*, 586–594.
136. Woodward, M.; Croft, K. D.; Mori, T. A.; Headlam, H.; Wang, X. S.; Suarna, C.; Raftery, M. J.; MacMahon, S. W.; Stocker, R. *Clin. Sci.* **2009**, *116*, 53–60.
137. Little, R. R.; Rohlfing, C. L.; Tennill, A. L.; Connolly, S.; Hanson, S. *Diabetes Technol. Ther.* **2007**, *9*, 36–42.
138. Rohlfing, C. L.; Hanson, S.; Tennill, A. L.; Little, R. R. *Diabetes Technol. Ther.* **2012**, *14*, 271–275.
139. Brewer, J. M. *Science* **1967**, *156*, 256–257.
140. Chidakel, B. E.; Ellwein, L. B.; Chrambach, A. *Anal. Biochem.* **1978**, *85*, 316–320.
141. Rabilloud, T.; Vincon, M.; Garin, J. *Electrophoresis* **1995**, *16*, 1414–1422.

Publication Date (Web): October 13, 2015 | doi: 10.1021/bk-2015-1200.ch016

142. Hunkapiller, M. W.; Lujan, E.; Ostrander, F.; Hood, L. E. *Methods Enzymol.* **1983**, *91*, 227–236.
143. Froelich, J. M.; Reid, G. E. *Proteomics* **2008**, *8*, 1334–1345.
144. Fenn, J. B.; Mann, M.; Meng, C. K.; Wong, S. F.; Whitehouse, C. M. *Science* **1989**, *246*, 64–71.
145. de la Mora, J. F.; Van Berkel, G. J.; Enke, C. G.; Cole, R. B.; Martinez-Sanchez, M.; Fenn, J. B. *J. Mass Spectrom.* **2000**, *35*, 939–952.
146. Van Berkel, G. J.; Kertesz, V. *Anal. Chem.* **2007**, *79*, 5510–5520.
147. Borges, C. R.; Jarvis, J. W.; Oran, P. E.; Nelson, R. W. *J. Proteome Res.* **2008**, *7*, 4143–4153.
148. Borges, C. R.; Jarvis, J. W.; Oran, P. E.; Rogers, S. P.; Nelson, R. W. *J. Biomol. Technol.* **2008**, *19*, 167–176.
149. Rehder, D. S.; Nelson, R. W.; Borges, C. R. *Protein Sci.* **2009**, *18*, 2036–2042.
150. Borges, C. R.; Rehder, D. S.; Jarvis, J. W.; Schaab, M. R.; Oran, P. E.; Nelson, R. W. *Clin. Chem.* **2010**, *56*, 202–211.
151. Rehder, D. S.; Borges, C. R. *BMC Biochem.* **2010**, *11*, 25.
152. Borges, C. R.; Oran, P. E.; Buddi, S.; Jarvis, J. W.; Schaab, M. R.; Rehder, D. S.; Rogers, S. P.; Taylor, T.; Nelson, R. W. *Clin. Chem.* **2011**, *57*, 719–728.
153. Minotti, G.; Aust, S. D. *J. Biol. Chem.* **1987**, *262*, 1098–1104.
154. Minotti, G.; Aust, S. D. *Free Radic. Biol. Med.* **1987**, *3*, 379–387.
155. Miller, D. M.; Aust, S. D. *Arch. Biochem. Biophys.* **1989**, *271*, 113–119.
156. Cohen, S. L. *Anal. Chem.* **2006**, *78*, 4352–4362.
157. Wisthaler, A.; Weschler, C. J. *Proc. Natl. Acad. Sci. U. S. A.* **2010**, *107*, 6568–6575.
158. Pavlaskova, K.; Strnadova, M.; Strohalm, M.; Havlicek, V.; Sulc, M.; Volny, M. *Anal. Chem.* **2011**, *83*, 5661–5665.
159. Ellis, S. R.; Hughes, J. R.; Mitchell, T. W.; Panhuis, M. I. H.; Blanksby, S. J. *Analyst* **2012**, *137*, 1100–1110.
160. Arnold, S. J.; Kubo, M.; Ogryzlo, E. A. *Adv. Chem. Ser.* **1968**, 133.
161. Merkel, P. B.; Kearns, D. R. *J. Am. Chem. Soc.* **1972**, *94*, 1029.
162. Wilkinson, F.; Helman, W. P.; Ross, A. B. *J. Phys. Chem. Ref. Data* **1995**, *24*, 663–1021.
163. Spickett, C. M.; Pitt, A. R. *Antioxid. Redox Signaling* **2015**.
164. Proudfoot, J. M.; Barden, A. E.; Loke, W. M.; Croft, K. D.; Puddey, I. B.; Mori, T. A. *J. Lipid Res.* **2009**, *50*, 716–722.
165. Morrow, J. D.; Harris, T. M.; Roberts, L. J., 2nd. *Anal. Biochem.* **1990**, *184*, 1–10.
166. Morrow, J. D.; Hill, K. E.; Burk, R. F.; Nammour, T. M.; Badr, K. F.; Roberts, L. J., 2nd. *Proc. Natl. Acad. Sci. U. S. A.* **1990**, *87*, 9383–9387.
167. Galano, J. M.; Mas, E.; Barden, A.; Mori, T. A.; Signorini, C.; De Felice, C.; Barrett, A.; Opere, C.; Pinot, E.; Schwedhelm, E.; Benndorf, R.; Roy, J.; Le Guennec, J. Y.; Oger, C.; Durand, T. *Prostaglandins Other Lipid Mediators* **2013**, *107*, 95–102.
168. Kelley, N. S.; Yoshida, Y.; Erickson, K. L. *Metab. Syndr Relat. Disord.* **2014**, *12*, 403–415.

Publication Date (Web): October 13, 2015 | doi: 10.1021/bk-2015-1200.ch016

169. Spickett, C. M.; Wiswedel, I.; Siems, W.; Zarkovic, K.; Zarkovic, N. *Free Radic. Res.* **2010**, *44*, 1172–1202.
170. Zarkovic, N. *Mol. Aspects Med.* **2003**, *24*, 281–291.
171. Long, E. K.; Picklo, M. J. *Free Radic. Biol. Med.* **2010**, *49*, 1–8.
172. Vigor, C.; Bertrand-Michel, J.; Pinot, E.; Oger, C.; Vercauteren, J.; Le Faouder, P.; Galano, J. M.; Lee, J. C.; Durand, T. *J. Chromatogr. B: Anal. Technol. Biomed. Life Sci.* **2014**, *964*, 65–78.
173. Milne, G. L.; Gao, B.; Terry, E. S.; Zackert, W. E.; Sanchez, S. C. *Free Radic. Biol. Med.* **2013**, *59*, 36–44.
174. Kadiiska, M. B.; Basu, S.; Brot, N.; Cooper, C.; Saari Csallany, A.; Davies, M. J.; George, M. M.; Murray, D. M.; Jackson Roberts, L., 2nd; Shigenaga, M. K.; Sohal, R. S.; Stocker, R.; Van Thiel, D. H.; Wiswedel, I.; Hatch, G. E.; Mason, R. P. *Free Radic. Biol. Med.* **2013**, *61*, 408–415.
175. European Food Safety Authority. *EFSA J.* **2011**, *9*, 2474–2486.
176. Basu, S. *Antioxid. Redox Signaling* **2008**, *10*, 1405–1434.
177. Kadiiska, M. B.; Gladen, B. C.; Baird, D. D.; Germolec, D.; Graham, L. B.; Parker, C. E.; Nyska, A.; Wachsman, J. T.; Ames, B. N.; Basu, S.; Brot, N.; Fitzgerald, G. A.; Floyd, R. A.; George, M.; Heinecke, J. W.; Hatch, G. E.; Hensley, K.; Lawson, J. A.; Marnett, L. J.; Morrow, J. D.; Murray, D. M.; Plastaras, J.; Roberts, L. J., 2nd; Rokach, J.; Shigenaga, M. K.; Sohal, R. S.; Sun, J.; Tice, R. R.; Van Thiel, D. H.; Wellner, D.; Walter, P. B.; Tomer, K. B.; Mason, R. P.; Barrett, J. C. *Free Radic. Biol. Med.* **2005**, *38*, 698–710.
178. Bowry, V. W.; Stanley, K. K.; Stocker, R. *Proc. Natl. Acad. Sci. U. S. A.* **1992**, *89*, 10316–10320.
179. Garner, B.; Witting, P. K.; Waldeck, A. R.; Christison, J. K.; Raftery, M.; Stocker, R. *J. Biol. Chem.* **1998**, *273*, 6080–6087.
180. Garner, B.; Waldeck, A. R.; Witting, P. K.; Rye, K. A.; Stocker, R. *J. Biol. Chem.* **1998**, *273*, 6088–6095.
181. Mashima, R.; Yamamoto, Y.; Yoshimura, S. *J. Lipid Res.* **1998**, *39*, 1133–1140.
182. Domingues, R. M.; Domingues, P.; Melo, T.; Perez-Sala, D.; Reis, A.; Spickett, C. M. *J. Proteom.* **2013**, *92*, 110–131.
183. Winczura, A.; Zdzalik, D.; Tudek, B. *Free Radic. Res.* **2012**, *46*, 442–459.
184. Schneider, C.; Tallman, K. A.; Porter, N. A.; Brash, A. R. *J. Biol. Chem.* **2001**, *276*, 20831–20838.
185. Jacobs, A. T.; Marnett, L. J. *Acc. Chem. Res.* **2010**, *43*, 673–683.
186. Nair, U.; Bartsch, H.; Nair, J. *Free Radic. Biol. Med.* **2007**, *43*, 1109–1120.
187. Schaur, R. J. *Mol. Aspects Med.* **2003**, *24*, 149–159.
188. Perluigi, M.; Coccia, R.; Butterfield, D. A. *Antioxid. Redox Signaling* **2012**, *17*, 1590–1609.
189. Borg, D. C.; Schaich, K. M. *Isr. J. Chem.* **1984**, *24*, 38–53.
190. Miller, D. M.; Spear, N. H.; Aust, S. D. *Arch. Biochem. Biophys.* **1992**, *295*, 240–246.
191. Kerry, J.; Butler, P. *Smart packaging technologies for fast moving consumer goods*; John Wiley: Chichester, U.K., Hoboken, NJ, 2008.
192. Niki, E. *Am. J. Clin. Nutrit.* **1991**, *54*, S1119–S1124.
193. Rehder, D. S.; Schaab, M. R.; Borges, C. R. U.S. Patent No. 8,669,111, 2014.

Publication Date (Web): October 13, 2015 | doi: 10.1021/bk-2015-1200.ch016

Publication Date (Web): October 13, 2015 | doi: 10.1021/bk-2015-1200.ch017

Chapter 17

Scanning Electrochemical and Fluorescence Microscopy for Detection of Reactive Oxygen Species in Living Cells

Sean E. Salamifar[1,2] and Rebecca Y. Lai[*,2]

[1]Streck Inc., 7002 S 109th Street, La Vista, Nebraska 68128, United States
[2]Department of Chemistry, University of Nebraska-Lincoln, Lincoln, Nebraska 68588, United States
[*]E-mail: rlai2@unl.edu

Understanding the complex nature of reactive oxygen species (ROS) requires the development of new analytical techniques that are rapid, sensitive, and capable of real-time detection of both intra- and extracellular ROS. In this regards, electrochemical techniques have shown to be promising when compared to conventional techniques used for ROS studies. The broad applicability of electrochemical techniques in quantifying ROS in living cells has resulted in the development of a wide range of electrochemical ROS sensors to date. However, relatively few of them have found applications in real biological studies; most have remained at the proof-of-concept stage. Hybrid optoelectrochemical approaches such as scanning electrochemical microscopy and fluorescence microscopy have shown to augment the detection capabilities of electrochemical techniques, rendering them suitable for studying complex biological systems.

Introduction

Roles and effects of reactive oxygen species (ROS) in biological systems have gained substantial attention in the past decades. However, despite the numerous research studies performed in this field, some aspects of ROS function are still disputed (*1–3*). ROS are byproduct of oxygen metabolism including species such as hydroxyl radicals ($OH\cdot$), superoxide anions ($O_2^{\cdot -}$), singlet oxygen

In Oxidative Stress: Diagnostics, Prevention, and Therapy Volume 2; Hepel, et al.;
ACS Symposium Series; American Chemical Society: Washington, DC, 2015.

($^1O_2$) and hydrogen peroxide (H_2O_2) etc., which are continuously produced at very low concentrations inside or within the membrane of living cells. ROS has long been known to be produced solely by phagocytic cells as a part of the defensive response of immune cells. Recent evidence has shown that ROS also play a key role as a messenger in normal cells and are responsible for regulating various cell functions, including gene expression, apoptosis, and the activation of cell signaling cascades. Inside cells, ROS concentrations are kept at certain levels via various detoxifying mechanisms. However, ROS could also diffuse out of the cell membrane and serve as both inter- and intracellular messengers (*4–8*).

Considering the above facts, it is clear that unraveling the complex dynamic nature of ROS requires analytical techniques that are rapid, sensitive, and capable of real-time detection of both intra- and extracellular ROS. In this regard, conventional optical techniques, which are the most commonly employed techniques for ROS detection, suffer from several drawbacks that limit the type of information attainable from complex biological studies. Fluorescence detection of ROS requires staining of the cells, which could result in an irreversible change in the cell environment; rendering real-time monitoring of ROS less feasible. The inability of the fluorescent dyes to accurately differentiate between various ROS is another existing challenge; relatively few fluorescent dyes are deemed suitable for ROS analysis, and the specificity of their response towards different types of ROS is still disputed. Last, despite being produced inside the cell, as previously stated, a portion of ROS can diffuse out of the cell. Most optical techniques can provide information about intracellular ROS activities, however, less quantitative information can be reliably obtained about extracellular ROS if analyzed using these techniques by themselves (*9–14*).

Taken into account some of the disadvantages associated with optical techniques, there is a need for analytical techniques that can provide more comprehensive information on ROS activities in complex biological systems. More recently, electrochemical techniques have emerged as promising alternatives to optical techniques for both intracellular and extracellular ROS studies. Electrochemical techniques for ROS analysis are relatively inexpensive, and more importantly, they are inherently non-invasive given that they do not entail various staining steps. The cells are less perturbed, enabling near real-time monitoring of their innate behavior. It is worth noting that the experimental conditions for electrochemical detection of ROS have been established for a long time (*15–20*). The applicability of electrochemical techniques to study ROS function in living cells have resulted in the development of a wide range of electrochemical ROS sensors in the past decade. These detection strategies have been reviewed elsewhere and will not be discussed in this chapter (*21*). However, despite the large number of electrochemical ROS sensors reported in the literature, relatively few have found applications in cell biology, and most have remained at proof-of-concept-level. This gap between innovations and applications in cell biology can be attributed to following factors.

First, the advantages of electrochemical techniques are not as well-known or well-documented among researchers in the field of cell biology. Thus, to encourage the use of electrochemical techniques in cell biology, these techniques should be designed in a way that will allow researchers to consistently evaluate

Publication Date (Web): October 13, 2015 | doi: 10.1021/bk-2015-1200.ch017

the reliability of the measurements. Ideally, this can be achieved by comparing the electrochemical data with data obtained from conventional analytical tools used in cell biology at real time. To bridge the gap between innovations in electrochemical ROS detection and real world applications, it is necessary to develop hybrid techniques that are based on the strategic combination of electrochemical and optical detection techniques. As such, the shortcomings of each technique could be circumvented to enable sensitive and accurate analysis of ROS in living cells at real time. Secondly, most currently available electrochemical ROS sensors measure ROS only at a single point above the cells; the amount of information attainable under this experimental condition is not comprehensive. Spatially resolved ROS activity cannot be obtained using this detection approach. To circumvent this potential problem, researchers have resorted to employing scanning electrochemical microscopy (SECM) for this application. In SECM imaging, rather than collecting electrochemical data at a single point, an activity image composed of a large number of data points is produced. The resultant image provides a more accurate picture of the ROS activity of the substrate surface under study (*22–24*). To date, SECM imaging has proven to be effective in analyzing ROS in complex biological systems, simultaneous use of an optical technique such as fluorescence microscopy (FM) will further enhance its applicability for real world analysis. This chapter summarizes the advantages of employing just such hybrid technique to detect ROS in PC3 human prostate cancer cells (PC3).

Publication Date (Web): October 13, 2015 | doi: 10.1021/bk-2015-1200.ch017

Combination of Scanning Electrochemical Microscopy and Optical Microscopy for Biological Applications

SECM, first introduced by Bard and co-workers in 1989, is a scanning technique that utilizes a miniaturized electrode such as an ultramicroelectrode (UME) as the scanning tip to examine topographical and surficial electrochemical properties of materials. In this technique, a high resolution (sub-micron) translational stage enables the SECM tip to move in the X, Y and Z planes within the vicinity of the substrate, while the electrochemical signal is simultaneously recorded. Depending on the SECM mode, the presence and type of the substrate affects the electrochemical signal, thereby creating a topographic or/and an activity image (*23*). Since its introduction, SECM has rapidly found applications in a large number of research areas including biological studies. Different modes of SECM and its applications in biological studies have been reviewed recently, and will not be discussed here in detail (*22*, *25–28*). In brief, the most common mode of SECM used in cellular studies is the "substrate generation/tip collection" (SG/TC) mode. The concept behind this mode of operation and the configuration of SECM for cellular studies, which includes the use of an optical microscope, are shown in Figure 1. In SG/TC mode, electroactive species that are generated by a substrate are electrochemically detected at the surface of an ultramicroelectrode, which is placed in the vicinity of the substrate surface. The ultramicroelectrode is set at a potential where the redox reaction of the electroactive species at its surface becomes thermodynamically favorable. The SECM tip, when properly positioned in the vicinity of a cell, can detect the electroactive species released

In Oxidative Stress: Diagnostics, Prevention, and Therapy Volume 2; Hepel, et al.;
ACS Symposium Series; American Chemical Society: Washington, DC, 2015.

from the cell. In this configuration, owing to the proximity between the cell and the SECM tip, the target of interest that is released from the cell can reach the electrode surface prior to diffusing out to the bulk solution. The tip potential has to be set at a value where the electrochemical reaction of the target becomes thermodynamically favorable. Thus, as soon as the target species reaches the electrode surface, a current that is proportional to the concentration of the target species is detected and recorded.

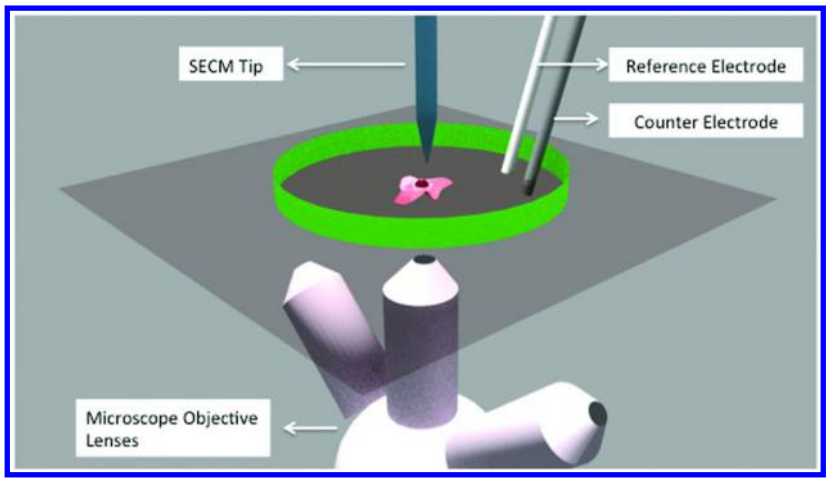

Figure 1. Schematic representation of an SECM instrument combined with an inverted optical microscope for cell analysis.

The aforementioned SECM setup and translucent properties of living cells allow coupling of SECM with most optical imaging techniques, including FM. As mentioned previously, FM is a complementary technique to SECM, and in most cases, an inverted fluorescence microscope is used. The space above the stage of most inverted microscopes has adequate room for proper arrangement of the SECM tip and other elements of an electrochemical cell, including the counter electrode and reference electrode. This strategic coupling enables the SECM tip to examine cell properties from above, while the microscope monitors cell behavior as well as movement of the tip from below. It is worth noting that the coupling of SECM with a conventional optical microscope, such as a compound microscope or a stereomicroscope, is relatively common in cell studies; however, there are very few studies that utilized the hybrid SECM-FM approach, in particular, for detection of ROS in cells. This hybrid optoelectrochemical technique is likely to be well-suited for analysis of biologically-relevant targets beyond ROS, these potentially impactful applications have yet to be fully explored.

In the following section, we briefly review reports in which SECM-FM was employed to study various processes in living cells. Next, we describe in detail an application of SECM-FM in the analysis of ROS in PC3 cells.

In Oxidative Stress: Diagnostics, Prevention, and Therapy Volume 2; Hepel, et al.;
ACS Symposium Series; American Chemical Society: Washington, DC, 2015.

Publication Date (Web): October 13, 2015 | doi: 10.1021/bk-2015-1200.ch017

Combination of Scanning Electrochemical Microscopy and Fluorescence Microscopy for Studying Living Cells

Kaya *et al.* first employed SECM-FM to study the respiratory activities of cultured adenocarcinoma cervical cancer cells (HeLa) cells at a single cell level (*29*). They monitored the respiration activity of the living cell both before and after exposure to toxic reagents using this hybrid technique. According to their observations, there is a decrease in cellular activity upon exposing the cells to toxic reagents. More importantly, SECM is capable of monitoring the decline in cellular activity more rapidly than FM; these results highlight the superiority of SECM in analyzing the influence of inhibitors on cellular activities.

Other reports by Kuss *et al.* showed the ability of SECM to quantitatively and noninvasively evaluate the effect of multidrug resistance-related protein 1 (MRP1) on multidrug resistance (MDR) in HeLa cells (*30*, *31*). Given that MDR in cells involves the overexpression of transmembrane proteins P-glycoprotein (P-gp) and MRP1, they first coclutured wild-type HeLa cells with MRP1 overexpressing HeLa cells (HeLa-R). They then used FM to prove the success of such coculture. Next, they used ferrocenemethanol, a water-soluble redox mediator, to quantify MRP1 activity of the aforementioned cell lines through its unique interaction with glutathione, a small molecule involved in MRP1-related transport. Last, by comparing the electrochemical signal intensities, they concluded that there is a difference in the response for the HeLa and HeLa-R cells, with the later showing an increase in MRP1 activity. SECM has proven to be suitable for evaluating risk of drug resistance in cells, screening different MDR inhibitors, as well as classifying the resistance signature of several cancer cell types.

In another study, Matsumae *et al.* quantitatively evaluated the differentiation status of a single live embryonic stem (ES) cell by monitoring the activity of alkaline phosphatase (ALP), an undifferentiation marker of ES cells, using SECM (*32*). They electrochemically measured the expression level of ALP in ES cells to evaluate their differentiation status. They observed an extremely low electrochemical response from the differentiated cells and attributed it to the decreased ALP activity in ES cells after differentiation. They concluded that SECM can distinguish the differentiation status of a single, live ES cell by simply analyzing the electrochemical signal. They also evaluated viability of the cells under the experimental conditions employed in SECM using a live/dead fluorescence technique. All ES cells were found to be alive after the experiment, indicating that the SECM measurements have no detectable side effects on cell viability. These measurements are minimally invasive, but useful in assessing cell differentiation, which is often difficult to recognize based purely on morphological changes.

In a more recent study, stamping of a petri dish with a microwell array for large-scale production of microtissues was introduced as a suitable platform for SECM cell studies (*33*). Sridhar *et al.* assessed the respiratory activity of different cell lines cultured into these microwell arrays under different conditions using SECM; they also used conventional live/dead fluorescent techniques in parallel to confirm the data obtained by SECM. They have, for the first time, demonstrated

Publication Date (Web): October 13, 2015 | doi: 10.1021/bk-2015-1200.ch017

In Oxidative Stress: Diagnostics, Prevention, and Therapy Volume 2; Hepel, et al.;
ACS Symposium Series; American Chemical Society: Washington, DC, 2015.

the use of SECM for non-invasive analysis of 3D cellular models and microtissue arrays formed in a stamped petri dish.

Combination of Scanning Electrochemical Microscopy and Fluorescence Microscopy for Detection of Reactive Oxygen Species in Living Cells

The application of SECM for ROS analysis was first reported by the group of Zhifeng Ding (*20*, *34–36*). More recently, Salamifar and Lai employed a hybrid SECM-FM approach to detect ROS in living cells. For the first time, they combined dual-potential SECM lateral scan and FM to analyze both extra- and intracellular ROS content in PC3 cells, a prostate cancer cell line known to have a high ROS content. In the following section, we provide a comprehensive summary of this specific study, including details of the instrumentation, experimental conditions, and data analysis (*37*).

Scanning Electrochemical Microscopy and Fluorescence Microscopy Setup

SECM measurements were performed on a PC-controlled CHI model 920C SECM (CH Instruments, Austin, TX) that uses a combination of stepper motors and an XYZ piezo block for tip positioning. A three-electrode cell configuration was used, with the 10-µm diameter Pt SECM tip as the working electrode, a 1-mm diameter platinum wire as the counter electrode and a Ag/AgCl (3 M KCl) electrode as the reference electrode. The SECM instrument was coupled to an inverted fluorescence microscope (Axio Vert.A1, Zeiss Co, Oberkochen, Germany) according to the arrangement described in the Introduction. A home-built extension arm was used to enable SECM imaging of the PC3 cells grown on a plastic petri dish. The petri dish was placed directly on top of the inverted fluorescence microscope objective.

Experimental Conditions for Fluorescence Imaging and Electrochemical Detection of ROS

A fluorescence-based viability assay kit (Image-iT ™ LIVE Green Reactive Oxygen Species Detection Kit (I36007)) was used to detect intracellular ROS. The assay utilized 5-(and-6)-carboxy-2′,7′-dichlorodihydrofluorescein diacetate (carboxy-H2DCFDA), a reliable green-fluorescent stain to detect ROS in living cells (Ex/Em: 495/529 nm). In addition to carboxy-H2DCFDA, a blue-fluorescent and cell-permeant nucleic acid stain, Hoechst 33342, was used to stain the cells' nucleus (Ex/Em: 350/461 nm).

After the staining procedure, the cells were washed again with 1X PBS for three times. Next, the petri dish was placed on the SECM stage, the cap was removed and the buffer solution was replaced with the appropriate solution for

In Oxidative Stress: Diagnostics, Prevention, and Therapy Volume 2; Hepel, et al.;
ACS Symposium Series; American Chemical Society: Washington, DC, 2015.

Publication Date (Web): October 13, 2015 | doi: 10.1021/bk-2015-1200.ch017

electrochemical experiments. The Pt wire counter and Ag/AgCl reference (3M KCl) electrodes were placed inside of the petri dish close to the inner sidewall. The SECM tip was mounted on the SECM stage and was slowly brought in contact with the solution with the help of SECM moving motors. By monitoring the tip position with the help of the microscope, the tip was placed in close proximity to the cells. Prior to ROS detection, tip current (i_T) *vs.* one-directional (1-D) lateral distance scans (lateral scans) were collected using $Ru(NH_3)_6^{3+}$ as the redox mediator, where the tip potential (E_T) was held at -0.3 V (*vs.* Ag/AgCl). Electrochemical detection of the two main ROS species, O_2 and H_2O_2, occurs at potentials more negative than -0.60 V under the experimental conditions used in this study; thus, to detect extracellular ROS, the lateral scans were recorded in 1X PBS with E_T set at potentials more negative than -0.6 (e.g., -0.65 V and -0.85 V). With E_T set at -0.65 V, the tip current should be affected mostly by the release of the two main ROS species from the cells, thereby producing an activity image of the cell surface. However, with E_T set at a more negative potential (-0.85 V), the resultant image should be dependent on both surface ROS activity and topography of the cells. The electrochemical responses recorded at the two potentials are described in detail in following sections.

Publication Date (Web): October 13, 2015 | doi: 10.1021/bk-2015-1200.ch017

Topographical Study of PC3 Cells

Prior to detecting ROS release, to maintain the distance between SECM tip and cell surface, a topographical image of the cell was first recorded with lateral scanning in the Y direction using $Ru(NH_3)_6^{3+}$ as the solution mediator. In brief, 2 mM of $Ru(NH3)_6^{3+}$ was first added to the cell media and E_T was set at -0.3 V to reduce $Ru(NH_3)_6^{3+}$. The approach curve was recorded by moving the tip in a vertical direction towards the bottom of the petri dish. Using the negative approach curved obtained in this way, the distance between tip and petri dish was set at ~ 8 μm. The tip was stopped and was scanned laterally in the Y direction. Figure 2A shows the phase contrast image of the PC3 cells relative to the SECM tip. The two chosen scan paths used to obtain the 1-D lateral scans are marked by arrows B and C (Figure 2 B). The chosen paths were located at 10 μm from each other, and the tip was moved from one path to another by moving 10 μm in the X direction. Figure 2B and C show the resultant tip currents during two subsequent lateral scans along paths B and C, respectively, in a cell medium containing 2 mM $Ru(NH_3)_6^{3+}$ with E_T set at -0.3 V. In both cases i_T decreased significantly from its initial value when the tip moved above the cells, resulting in two dips in the lateral scans.

The concept behind this interpretation is described in detail elsewhere (*38*). In brief, given $Ru(NH_3)_6^{3+/2+}$ is hydrophilic and cannot move across the hydrophobic cell membrane, the cell surface acts just like an inert substrate, which blocks the diffusion of $Ru(NH_3)_6^{3+/2+}$ to the tip at very short tip-cell distances. Thus, any decrease in i_T during the lateral scan is attributed to the decrease in the tip-cell distance, which corresponds to the increase in cell height. Similarly, any decrease in the tip-cell distance due to the increase of cell height will result in a decrease in the corresponding i_T.

Publication Date (Web): October 13, 2015 | doi: 10.1021/bk-2015-1200.ch017

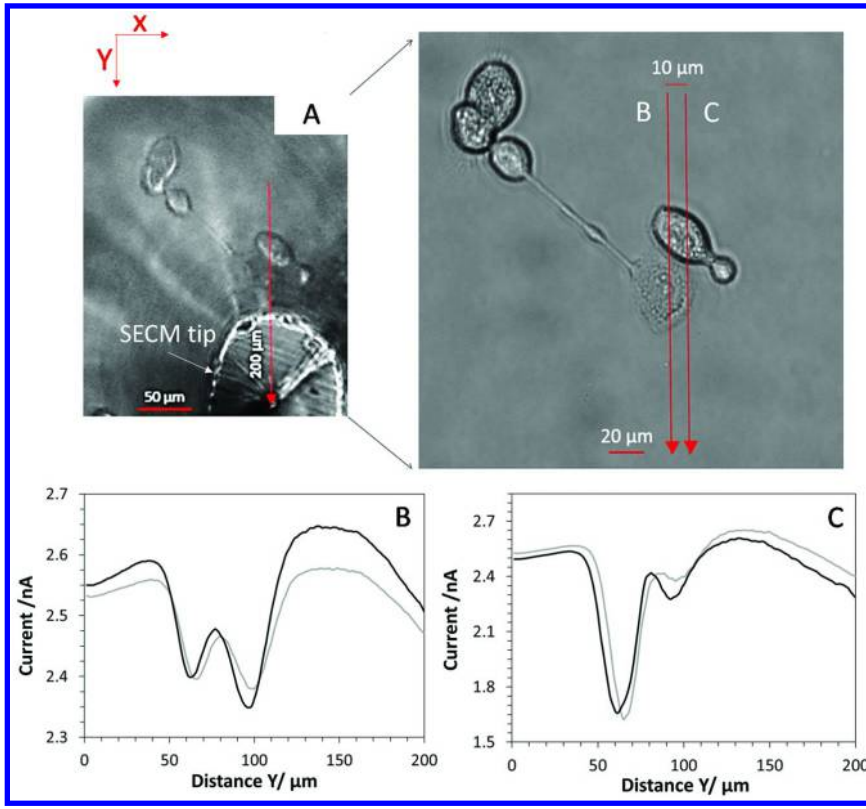

Figure 2. Phase contrast image of the PC3 cells and 10-µm Pt SECM tip position (A). The resultant lateral scans along marked paths B (B) and C (C). The red arrow shows the scan direction. The scans were collected in F-12K medium containing 2 mM $Ru(NH_3)_6^{3+}$ (pH=7.4) with E_T set at -0.3 V. Reproduced with permission from reference (37). Copyright 2013 American Chemical Society.

The two successive dips in the lateral scan were comparable in amplitude, suggesting similarity in both the height and morphology between the two cells along path B. The lateral scan across path C showed a similar trend, the amplitude of the dips, however, was noticeably different. A large decrease in i_T was observed above the first cell; the decrease in i_T was much smaller when the tip was positioned above the second cell. These results imply higher height for the first cell when compared to the second cell along path C. Additional lateral scans along paths B and C (gray curves in Figure 2B and C) were collected to demonstrate the technique's reproducibility. The resultant scans were very similar to the ones recorded previously, confirming the reproducibility of this method for topographic mapping at cellular dimensions. The maximum cell height across the two lateral scan paths was calculated from the maximum change in i_T during each scan. A maximum change of 11% and 16% in i_T was determined along paths B and C, respectively, by simply comparing the initial i_T value to its minimum value recorded on the top of the cells. Employing standard negative feedback SECM

theory for a 10-μm tip located at 8 μm from an insulating substrate, the maximum topographical change in cell height was found to be 2.2 μm and 3.1 μm along B and C paths, respectively.

Detection of ROS Released from PC3 Cells

The main focus of their study was to determine the flux of O_2 and H_2O_2, the two main ROS species released from the cells, using SECM. Prior to the experiment, 1X PBS was added to the petri dish after removal of the F-12K medium; E_T was set at a potential capable of reducing both O_2 and H_2O_2. As mentioned previously, electrochemical detection of the two main ROS species, O_2 and H_2O_2, requires a potential more negative than -0.60 V. Figure 3A shows the phase contrast image of the PC3 cells superimposed on the fluorescence image obtained in the presence of Hoechst 33342. The fluorescence image resulted from carboxy-H2DCFDA staining superimposed on the Hoechst 33342 fluorescence image is shown in Figure 3B. The lateral scans recorded above the cell, along the marked path (red arrow in Figure 3A), under different experimental conditions are shown in Figure 3C, D and E. A decrease in i_T above the cell was observed in the lateral scan collected in F-12K medium containing 1 mM $Ru(NH_3)_6^{3+}$ with E_T set at -0.3 V; this change in current is likely due to a topographical change as previously described (Figure 3C). However, when the same scan was recorded in 1X PBS with E_T set at -0.65 V, the profile of the scan changed significantly (Figure 3D). The recorded i_T decreased, reaching a minimum value above the cell, and increased sharply right above the center of the cell, reaching a maximum, followed by a decrease back to the initial baseline value. This unique profile can be explained; when the SECM tip is directly above the cell, the i_T is a summation of the background current from the reduction of dissolved electroactive species such as O_2, and the current from the reduction of ROS species (i.e., O_2, H_2O_2) released from the cells. The magnitude of the background current is dependent on the distance between the SECM tip and the cell, in addition to the respiratory function of the cell which is known to deplete nearby O_2. Thus, the decrease in i_T in the earlier portion of the lateral scan is likely ascribed to the decrease in the tip-cell distance, which suggests an increase in topographical height (i.e., SECM tip was on top of the cell). The background current decreases at shorter tip-cell distances because of the limited diffusion of dissolved O_2. Respiratory function of the cell and the reduction of O_2 at the SECM tip further deplete O_2 within the tip-cell gap, creating a concentration gradient of O_2 between the intracellular medium and the electrolyte solution close to the cell surface. This concentration gradient could assist in driving ROS from inside the cell towards the SECM tip (*39*).

If no extra ROS is released from the cell, the compounded effect generally results in a sharp decrease in the i_T. But in this case, as the distance between the tip and cell decreases, higher flux of ROS could reach the tip before diffusing into the bulk solution. Thus, at short tip-cell distances, the ROS current increases as the background current decreases. At the maximum height of the cell (i.e., shortest distance between the tip and the cell), the background current and ROS current should reach their corresponding minimum and maximum. Based on this

Publication Date (Web): October 13, 2015 | doi: 10.1021/bk-2015-1200.ch017

theory, the sharp increase in i_T seen in the latter portion of the scan suggests that the decrease in background current originating from the change in the tip-cell distance is outcompeted by the increase in ROS current. It also alludes to the diffusion of ROS from inside the cell due to the depletion of O_2 within the tip-cell gap, which could occur very rapidly. Reproducibility of this trend was substantiated by repeating the same scan after allowing the cell to reach equilibrium for about ~1 min (gray line in Figure 3D). It is worth noting that the SECM results agree well with the fluorescence data; the cell under investigation showed strong green fluorescence, indicating high ROS content (Figure 3B). The peak current obtained from the lateral scan at $E_T \leq$ -0.65 V should be proportional to the amount of ROS released by the cell and thus can be used for quantification of ROS in living cells.

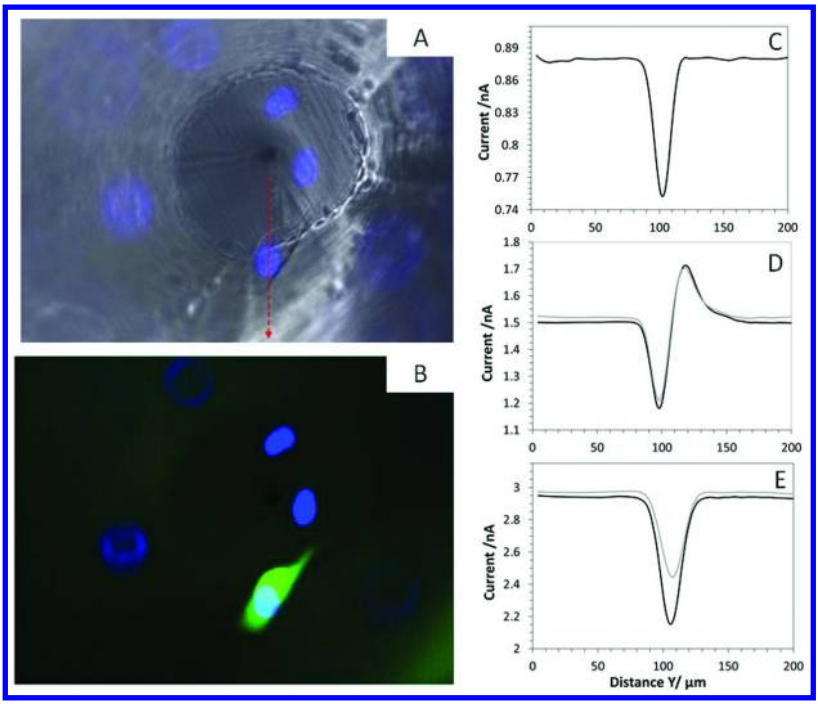

Figure 3. Phase contrast image superimposed on the fluorescence image resulted from Hoechst 33342 staining (blue fluorescence) (A). Superimposed fluorescence images resulted from carboxy- H2DCFDA (green fluorescence) and Hoechst 33342 staining (B). Lateral scans collected along the marked path (red arrow) shown in Panel A in F-12K medium containing 1 mM $Ru(NH_3)_6^{3+}$ with E_T set at -0.3 V (C), in 1X PBS with E_T at -0.65 V (D) and -0.85 V (E). Reproduced with permission from reference (37). Copyright 2013 American Chemical Society.

Publication Date (Web): October 13, 2015 | doi: 10.1021/bk-2015-1200.ch017

A separate scan along the same path with E_T set at -0.85 V was collected to further confirm this theory (Figure 3E). Owing to the increase in the background current, the i_T was two times larger even at the beginning of scan. However, unlike the scan recorded with E_T set at -0.65 V (Figure 3D), no increase in i_T was observed throughout the scan. This behavior could be explained; with E_T set at -0.85 V, the effect of ROS current on the total i_T is minimized because of the large background current. The trend reported here is reasonably reproducible, as verified by the gray line in Figure 3E, which represents the second scan recorded at the same location ~1 min after the first scan (black line). This further supports the above interpretation of the i_T change during the lateral scan. The use of two different E_T is critical in this study; it enables clear differentiation between i_T originated from the release of ROS and that attributed to the differences in cell topography and cellular respiration. Although most experiments were conducted under ambient physiological conditions, the effect of dissolved O_2 on the experimental results was also evaluated. Figure 4A shows the phase contrast image superimposed on the fluorescence image of the cells after Hoechst 33342 staining (blue fluorescence). The superimposed fluorescence image of the cells after carboxy-H2DCFDA (green fluorescence) and Hoechst 33342 staining is shown in Figure 4B. SECM images resulting from scanning the tip in the X-Y plane above the marked area in Panel A in a nitrogen-purged 1X PBS solution with E_T held at -0.65 V and -0.85 V are shown in Figure 4C and D, respectively. In the absence of dissolved O_2, the effect of ROS release from cells was more pronounced because of the decrease in the background current. Nevertheless, a noticeable decrease in i_T prior to a sharp increase was evident. When E_T was set to -0.85 V, a decrease in i_T over the entire cell surface was observed (Figure 4D).

Overall, the SECM results obtained in an O_2-free environment are similar to that observed under an ambient condition. Furthermore, there is a strong correlation between the SECM and fluorescence results. It is worth mentioning that when the SECM tip moved across two neighboring cells, a large increase in i_T was only seen with the cell exhibiting strong green fluorescence (i.e., high ROS content). The second cell did not show considerable fluorescence, thus only a slight increase in i_T over the cell surface was evident. The consistency between the 1-D scan data in the Y-axis and the 2-D scan data in the X-Y plane further emphasizes the advantages of using lateral scan for this study. The 1-D method is fast, simple, and effective, it also reduces the chance of fouling or crashing the SECM tip into the cell. Contrastingly, 2-D scanning is more time consuming; for this type of study, the use of repetitive tip rastering could prevent the cells from returning to their equilibrium state, which could affect the accuracy of the results owing to the differences in the diffusion layer.

Publication Date (Web): October 13, 2015 | doi: 10.1021/bk-2015-1200.ch017

Publication Date (Web): October 13, 2015 | doi: 10.1021/bk-2015-1200.ch017

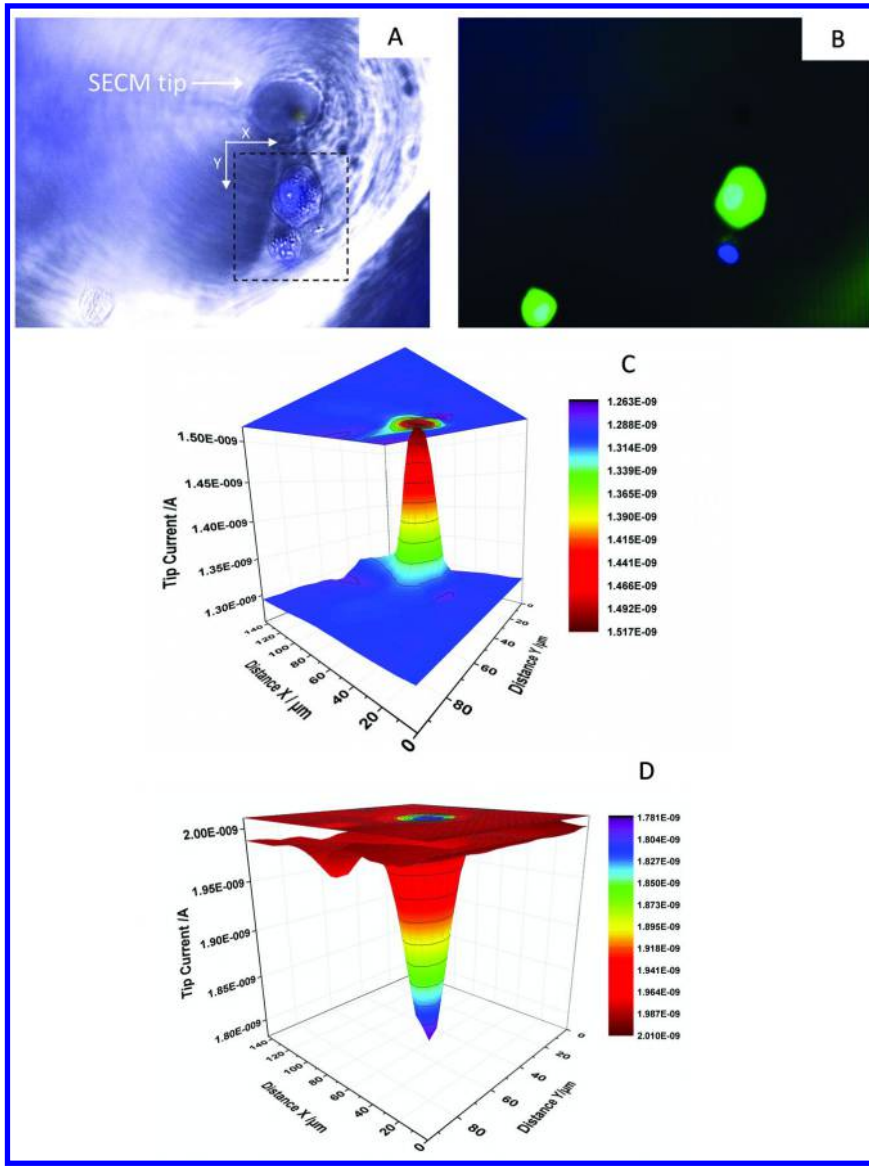

Figure 4. Phase contrast image superimposed on the fluorescence image of the cells after Hoechst 33342 staining (blue fluorescence) (A). A superimposed fluorescence image resulted from carboxy-H2DCFDA (green fluorescence) and Hoechst 33342 staining (B).SECM images resulting from scanning the tip in the X-Y plane above the marked area in Panel A in a nitrogen-purged 1X PBS solution with E_T held at -0.65 V (C) and -0.85 V (D). Reproduced with permission from reference (37). Copyright 2013 American Chemical Society.

Publication Date (Web): October 13, 2015 | doi: 10.1021/bk-2015-1200.ch017

Positive Control Experiments

The cells were incubated in tert-butyl hydroperoxide (TBHP), a known ROS inducer, to further demonstrate this method's applicability in cell ROS analysis (*40*). As can be seen in Figure 5, stronger fluorescence was observed from the cells post-TBHP treatment. The two peaks shown in the lateral scan when E_T was set at -0.65 V suggest substantial release of ROS from both cells. However, unlike results from experiments where TBHP was not employed, no decrease in i_T was recorded prior to the sharp increase in i_T above the cells (Figure 5C). This behavior could be attributed to the enhanced release of ROS from the cells after being treated with TBHP; the increase in current from the electrochemical reduction of ROS outcompetes the decrease in background current. The change in membrane properties and cell topography could be, in part, responsible for the drastic change in the lateral scan profile. Two dips were observed in the lateral scan when E_T was set at -0.85 V, reflecting the topographical image of the cells. The fluorescence results were found to be consistent with the SECM results; for the cell that showed weaker fluorescence (Y ~ 40 µm), the i_T minimum was lower than the cell that displayed stronger fluorescence (Y ~ 65 µm) (Figure 5D).

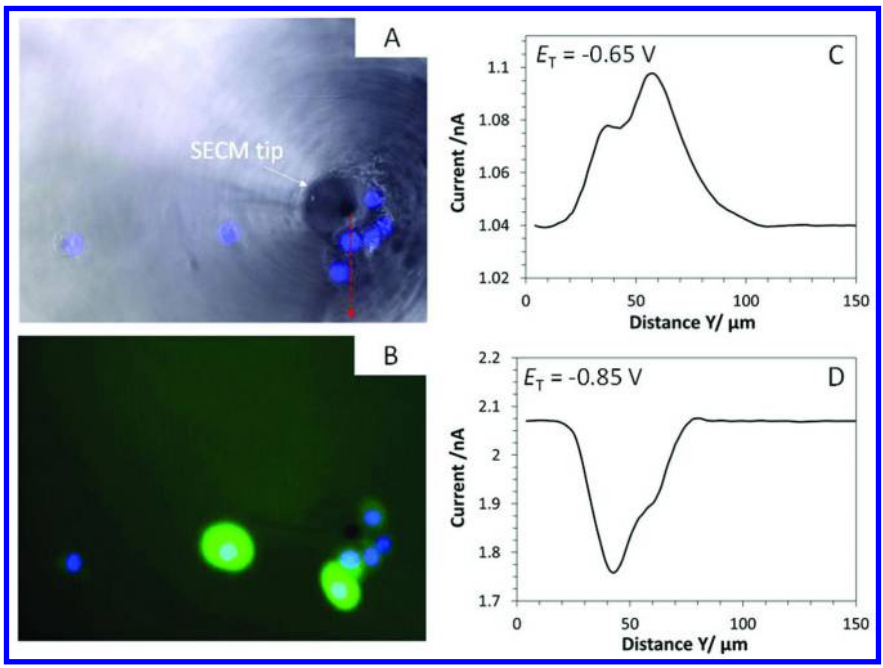

Figure 5. Phase contrast image of the cells superimposed on a fluorescence image resulted from Hoechst 33342 staining after a 90-min incubation in 100 µM TBHP (A). Superimposed fluorescence images resulted from carboxy-H2DCFDA and Hoechst 33342 staining (B).Lateral scans collected along the marked path (red arrow) in Panel A in 1X PBS with E_T set at -0.65 V (C) and -0.85 V (D). Reproduced with permission from reference (37). Copyright 2013 American Chemical Society.

Conclusion and Outlook

Like most hybrid techniques, SECM-FM detection approaches are more advantageous than using the two techniques separately, in particular, for studying ROS in living cells. Recently, the combination of dual-potential SECM lateral scan and FM has found application in the analysis of both extra- and intracellular ROS content in PC3 cells. Although still in its infancy, this hybrid optoelectrochemical technique has potential for future use in accurate quantification of ROS in complex biological systems. The main advantage of this detection approach is that it is non-invasive, yet capable of real time extra- and intracellular analysis at the single-cell level. But like all new techniques, there are challenges to be overcome. In this case, instrument complexity arisen from combining two rather different techniques is an impeding factor that could limit its popularity among researchers. Other technical issues such as electrode fouling and precise control of the tip-cell distance have to be addressed to improve its applicability in cell biology. If the above challenges can be adequately addressed, its range of applications could be quite broad. And with proper experimental design and optimization, more challenging problems such as ROS speciation could be addressed using this analytical approach. Considering recent advances in the fabrication and use of nanoelectrodes, this hybrid technique, if compatible with nanoelectrodes, will find new uses in studying cellular behavior inside a single living cell (*41*, *42*).

Publication Date (Web): October 13, 2015 | doi: 10.1021/bk-2015-1200.ch017

Acknowledgments

This research was supported by the National Science Foundation (CHE-0955439) and Army Research Office (W911NF-09-2-0039).

References

1. Apel, K.; Hirt, H. *Annu. Rev. Plant Biol.* **2004**, *55*, 373–399.
2. Droge, W. *Physiol. Rev.* **2002**, *82*, 47–95.
3. Finkel, T.; Holbrook, N. J. *Nature* **2000**, *408*, 239–247.
4. Circu, M. L.; Aw, T. Y. *Free Radic. Biol.* **2010**, *48*, 749–762.
5. Halliwell, B. *J. Neurochem.* **1992**, *59*, 1609–1623.
6. Jacobson, M. D. *Trends Biochem. Sci.* **1996**, *21*, 83–86.
7. Murphy, M. P. *Biochem. J.* **2009**, *417*, 1–13.
8. Nordberg, J.; Arner, E. S. J. *Free Radic. Biol.* **2001**, *31*, 1287–1312.
9. Gomes, A.; Fernandes, E.; Lima, J. L. F. C. *J. Biochem. Biophys. Methods* **2005**, *65*, 45–80.
10. Gomes, A.; Fernandes, E.; Lima, J. *J. Biochem. Biophys. Methods* **2005**, *65*, 45–80.
11. Halliwell, B.; Whiteman, M. *Br. J. Pharmacol.* **2004**, *142*, 231–255.
12. Setsukinai, K.; Urano, Y.; Kakinuma, K.; Majima, H. J.; Nagano, T. *J. Biol. Chem.* **2003**, *278*, 3170–3175.

13. Zhao, H. T.; Joseph, J.; Fales, H. M.; Sokoloski, E. A.; Levine, R. L.; Vasquez-Vivar, J.; Kalyanaraman, B. *Proc. Natl. Acad. Sci. U. S. A.* **2005**, *102*, 5727–5732.
14. Zhao, H. T.; Kalivendi, S.; Zhang, H.; Joseph, J.; Nithipatikom, K.; Vasquez-Vivar, J.; Kalyanaraman, B. *Free Radic. Biol.* **2003**, *34*, 1359–1368.
15. Nyska, A.; Kohen, R. *Toxicol. Pathol.* **2002**, *30*, 620–650.
16. Cheah, L.-T.; Dou, Y.-H.; Seymour, A.-M. L.; Dyer, C. E.; Haswell, S. J.; Wadhawan, J. D.; Greenman, J. *Lab Chip* **2010**, *10*, 2720–2726.
17. Chen, W.; Ren, Q.-Q.; Yang, Q.; Wen, W.; Zhao, Y.-D. *Anal. Lett.* **2012**, *45*, 156–167.
18. Hu, R.; Guille, M.; Arbault, S.; Lin, C. J.; Amatore, C. *Phys. Chem. Chem. Phys.* **2010**, *12*, 10048–10054.
19. Yuasa, M.; Oyaizu, K. *Curr. Org. Chem.* **2005**, *9*, 1685–1697.
20. Zhao, X.; Lam, S.; Jass, J.; Ding, Z. *Electrochem. Commun.* **2010**, *12*, 773–776.
21. Gaspar, S. Detection of Superoxide and Hydrogen Peroxide from Living Cells Using Electrochemical Sensors. In *Oxidative Stress: Diagnostics, Prevention, and Therapy*; Andreescu, S., Hepel, M., Eds.; ACS Symposium Series 1083; American Chemical Society: Washington, DC, 2011; pp 289–309.
22. Amemiya, S.; Bard, A. J.; Fan, F.-R. F.; Mirkin, M. V.; Unwin, P. R. *Annu. Rev. Anal. Chem.* **2008**, *1*, 95–131.
23. Bard, A. J.; Fan, F. R. F.; Kwak, J.; Lev, O. *Anal. Chem.* **1989**, *61*, 132–138.
24. Sun, P.; Laforge, F. O.; Mirkin, M. V. *Phys. Chem. Chem. Phys.* **2007**, *9*, 802–823.
25. Schulte, A.; Nebel, M.; Schuhmann, W. *Annu. Rev. Anal. Chem.* **2010**, *3*, 299–318.
26. Ebejer, N.; Gueell, A. G.; Lai, S. C. S.; McKelvey, K.; Snowden, M. E.; Unwin, P. R. *Annu. Rev. Anal. Chem.* **2013**, *6*, 329–351.
27. Beaulieu, I.; Kuss, S.; Mauzeroll, J.; Geissler, M. *Anal. Chem.* **2011**, *83*, 1485–1492.
28. Gyurcsanyi, R. E.; Jagerszki, G.; Kiss, G.; Toth, K. *Bioelectrochemistry* **2004**, *63*, 207–215.
29. Kaya, T.; Torisawa, Y. S.; Oyamatsu, D.; Nishizawa, M.; Matsue, T. *Biosens. Bioelectron.* **2003**, *18*, 1379–1383.
30. Kuss, S.; Cornut, R.; Beaulieu, I.; Mezour, M. A.; Annabi, B.; Mauzeroll, J. *Bioelectrochemistry* **2011**, *82*, 29–37.
31. Kuss, S.; Polcari, D.; Geissler, M.; Brassard, D.; Mauzeroll, J. *Proc. Natl. Acad. Sci. U. S. A.* **2013**, *110*, 9249–9254.
32. Matsumae, Y.; Arai, T.; Takahashi, Y.; Ino, K.; Shiku, H.; Matsue, T. *Chem. Commun.* **2013**, *49*, 6498–6500.
33. Sridhar, A.; de Boer, H. L.; van den Berg, A.; Le Gac, S. *PLoS One* **2014**, *9*, e93618.
34. Zhang, M. M. N.; Long, Y.-T.; Ding, Z. *J. Inorg. Biochem.* **2012**, *108*, 115–122.
35. Zhao, X.; Zhang, M.; Long, Y.; Ding, Z. *Can. J. Chem.* **2010**, *88*, 569–576.
36. Zhu, R. K.; Macfie, S. M.; Ding, Z. F. *J. Exp. Bot.* **2005**, *56*, 2831–2838.

In Oxidative Stress: Diagnostics, Prevention, and Therapy Volume 2; Hepel, et al.;
ACS Symposium Series; American Chemical Society: Washington, DC, 2015.

37. Salamifar, S. E.; Lai, R. Y. *Anal. Chem.* **2013**, *85*, 9417–9421.
38. Koley, D.; Bard, A. J. *Proc. Natl. Acad. Sci. U.S.A.* **2010**, *107*, 16783–16787.
39. Nebel, M.; Grützke, S.; Diab, N.; Schulte, A.; Schuhmann, W. *Angew. Chem., Int. Ed.* **2013**, *52*, 6335–6338.
40. Hardman, R. A.; Afshari, C. A.; Barrett, J. C. *Cancer Res.* **2001**, *61*, 1392–1397.
41. Wang, Y.; Noel, J.-M.; Velmurugan, J.; Nogala, W.; Mirkin, M. V.; Lu, C.; Collignon, M. G.; Lemaitre, F.; Amatore, C. *Proc. Natl. Acad. Sci. U. S. A.* **2012**, *109*, 11534–11539.
42. Salamifar, S. E.; Lai, R. Y. *Anal. Chem.* **2014**, *86*, 2849–2852.

Publication Date (Web): October 13, 2015 | doi: 10.1021/bk-2015-1200.ch017

Publication Date (Web): October 13, 2015 | doi: 10.1021/bk-2015-1200.ch018

Chapter 18

Toward a Synthetic View of the Therapeutic Use of Cerium Oxide Nanoparticles for the Treatment of Neurodegenerative Diseases

A. Y. Estevez,[*,1,2] W. E. DeCoteau,[2] K. L. Heckman,[1] and J. S. Erlichman[1]

[1]Biology Department, St. Lawrence University, Canton, New York 13617
[2]Psychology Department, St. Lawrence University, Canton, New York 13617
[*]E-mail: aestevez@stlawu.edu

Cerium oxide nanoparticles (nanoceria; CeNPs) are potent catalytic antioxidants that are being studied as a potential therapeutic intervention for diseases where free radicals and reactive oxygen and nitrogen species play an important pathological role. However, there are also reports of toxic properties of CeNPs in biological settings, demonstrating that not all CeNPs behave the same way. An understanding of the chemical and biological factors that underlie these disparate findings is imperative if the ultimate goal is to translate the use of these nanoparticles to a clinical setting. This review will attempt to synthesize some recent data relevant to the use of CeNPs for therapeutic purposes, starting with a general discussion of the role of reactive oxygen and nitrogen species in physiological and pathological states. We will then describe the mechanism of action of CeNPs, integrate published data that provide insight into the physiochemical parameters that influence CeNP pharmacokinetics and efficacy/toxicity in biological systems. Finally, we will highlight some recent studies from our group that use CeNPs as neuroprotective agents in animal models of neurodegenerative disease. We suggest that further progress in this field will require an iterative analysis of how the biological identity of CeNPs changes upon traversing distinct biological environments and that there are no simple surrogates for intact animal studies.

In Oxidative Stress: Diagnostics, Prevention, and Therapy Volume 2; Hepel, et al.;
ACS Symposium Series; American Chemical Society: Washington, DC, 2015.

Publication Date (Web): October 13, 2015 | doi: 10.1021/bk-2015-1200.ch018

Introduction

Reduction-Oxidation (redox) reactions are involved in a growing number of important biological and physiological processes. The signaling agents in these systems are often reactive oxygen and nitrogen species (ROS/RNS), some of which can be classified as free radicals due to the presence of an odd number of electrons in their outer orbital shell. In biological systems, the primary, first-order ROS/RNS signaling molecules associated with normal physiological processes are hydrogen peroxide (H_2O_2), superoxide ($O_2^{\bullet -}$) and nitric oxide (NO). Second order species such as hydroxyl ($^{\bullet}OH$) and peroxynitrite ($ONOO^-$) may also be involved in physiologic redox signaling, although this has not been tested directly given the lack of tools to directly measure these molecules in vivo.

ROS/RNS that are produced by a local, cellular source in small enough quantities to be confined to cellular microdomains can function as a 'rheostat' for discrete, spatial signaling pathways in that location (e.g., electron transport chain regulation by NADPH). This notion is supported by studies that have demonstrated discrete localization of different isoforms of both pro- (e.g., NADPH oxidase) and anti-oxidant enzyme systems (e.g., superoxide dismutase) in discrete cellular compartments. On a larger scale and working together, these systems may be able to coordinate global redox signaling in the cell for more integrative, complex cellular functions. The cellular and molecular targets of ROS/RNS are ubiquitous in living systems and include phosphatases, a myriad of kinases including tyrosine and serine/threonine kinases, transcription factors, metabolic regulators and ion channels (*1*, *2*). Such broad-ranging effects suggest that these molecules are critical regulators of fundamental physiological function (*3*). Indeed, moderate levels of ROS/RNS function as signals to promote cell proliferation, regulation, and survival (*4*), whereas increased levels of ROS/RNS can induce cell death (*5–13*). Although this conceptual framework is useful in delineating the nuances of ROS/RNS on physiologic function, quantitative estimates for these levels are not currently known. Development of new methods to measure the accumulation of ROS/RNS in living tissue which retained both good spatial resolution, selectivity and sensitivity would be invaluable to parsing the relative contributions of each to biologic function.

Energy metabolism is tightly linked with the production of reactive oxygen species in most eukaryotic cells (*14–16*). Mitochondria are not only the powerhouses for ATP generation in cells, they are also the major site of free radical generation (*17*). The electron transport chain (ETC) localized in the inner membrane of mitochondria is a major source of superoxide, particularly Complexes I and III. In contrast, the outer mitochondrial membrane, produces hydrogen peroxide resulting from the activation of monoamine oxidase important for the oxidative deamination of monoamines (such as the catecholamines). This pathway represents one of the major sources for hydrogen peroxide generation in neurons (*18*, *19*). Aside from an unavoidable by-product of cellular respiration (*20*), other endogenous sources of ROS in mammals include seven isoforms of NADPH oxidases (NOXs) (*21–23*) that are differentially expressed in diverse cells and species; the flavoenzymes in the endoplasmic reticulum; xanthine oxidase;

In Oxidative Stress: Diagnostics, Prevention, and Therapy Volume 2; Hepel, et al.;
ACS Symposium Series; American Chemical Society: Washington, DC, 2015.

lipoxygenases; cyclooxygenases; cytochrome P450s; and myeloperoxidase (*24*, *25*).

Although ROS/RNS play important roles in normal cellular physiology, the highly reactive nature of these molecules makes them potentially harmful to cellular processes beyond the intended signaling targets. To minimize unwarranted interactions of ROS/RNS, cells posses endogenous systems to neutralize them (*26*). Enzymes including catalase, superoxide dismutase and the thio/peroxiredoxins as well as small molecules such as glutathione, coenzyme Q and vitamins A, C and E are all important contributors to cellular antioxidant defenses. However, when the levels of ROS/RNS exceed the ability of these systems to neutralize them, the result is a condition known as oxidative stress. For example, mitochondrial dysfunction coupled with a high metabolic rate and pathologic changes in enzyme activities of oxidases leads to the accumulation of ROS/RNS and induces oxidative injury in affected tissues.

Owing to its high metabolic rate and abundance of lipids, the brain is particularly susceptible to oxidative injury. Accumulating evidence has implicated oxidative stress as a central mechanism in stroke (*27*) and a growing number of chronic neurodegenerative diseases including Alzheimer's disease, Parkinson's disease, amyotrophic lateral sclerosis (ALS), and multiple sclerosis (MS) (*28–30*). The mechanism of ROS/RNS induction may vary in a particular disease state and the response and loss of neurons to chronic oxidative stress is also not uniform in the brain. While many brain neurons can cope with a rise in oxidative stress, there are select populations of neurons in the brain that are particularly vulnerable. Because of their selective vulnerability, these neurons are usually the first to exhibit functional decline and cell death during normal aging, or in neurodegenerative diseases (*31*). While the selective vulnerability of particular neuronal pools in neurodegenerative diseases has only begun to be studied with respect to oxidative stress, much more is known about the effects of oxidative injury in the hippocampus, a primary target of stroke, which we will consider later in this chapter.

Despite the knowledge of involvement of ROS/RNS in neurodegenerative diseases, there is still a lack of suitable antioxidant pharmacological treatment that has been successful in slowing down or halting the progression of cell death in these disorders. Human studies with various antioxidant therapies have yielded mixed results. For example, Vitamin E has been tested in trials for Parkinson's Disease (PD), Alzheimer's Disease (AD) and amyotrophic lateral sclerosis (ALS) and the results have ranged from lowering the risk of disease progression (*32–34*) to lack of efficacy (*35–42*). This general lack of success of antioxidant therapy could be due to many reasons including the animal models used, unsuitable penetration across the blood brain barrier, timing of antioxidant administration (production of free radicals sometimes occurs very early in the disease process) and failure to achieve adequate concentrations at the target site to neutralize the reactive oxygen and nitrogen species produced (*43–46*). Due to their unique chemistry and potent antioxidant capabilities, cerium oxide nanoparticles (nanoceria, CeNPs) have recently emerged as a promising option for the treatment of neurodegenerative diseases.

Publication Date (Web): October 13, 2015 | doi: 10.1021/bk-2015-1200.ch018

Mechanism of Action of Cerium Oxide Nanoparticles

During the past decade, nanomaterials of many types have attracted increasing interest in different fields, such as material science, chemistry, biology, and therapeutics (*47–51*). The development of nanotechnology products may play an important part in adding a new armamentarium of therapeutics to the treatment of diseases whose etiology derives from oxidative stress. Recent studies have shown that several nanoscale metal oxides such as Pt, Au, 'nanojewels' (Au and Pt on nanodiamonds) and nanoceria are potent antioxidants that have catalytic activities that often greatly exceed endogenously produced superoxide dismutase and catalase enzymatic activity. Thus far, the most intensively studied of the metal oxides in biological systems has been nanoceria. Both the toxicology and physiology of this material has been examined in biological systems including *C. elegans* (*52*), zebrafish (*53*), cell cultures (*54*, *55*), rodent brain slices (*56*) and intact rodent models (*57*, *58*).

Publication Date (Web): October 13, 2015 | doi: 10.1021/bk-2015-1200.ch018

Unique Chemistry of Cerium Oxide Nanoparticles

Cerium is a lanthanide series rare earth metal. In nanparticle form (1-100 nm scale), cerium is combined with oxygen and adopts a crystalline structure. CeNPs have potent antioxidant activity – both superoxide dismutase- and catalase-mimetic activities have been described (*59–62*). Cerium can reversibly bind oxygen and shift oxidation states (Ce^{4+}/Ce^{3+}), giving the nanoparticle the ability to regenerate depending on the redox environment (*58*, *63*). Thus, the small size, antioxidant capability and regenerative nature of CeNPs are all advantageous for treating neurodegenerative diseases.

Although the exact mechanisms whereby nanoceria scavenge ROS/RNS are not completely understood, there are two working hypotheses that could account for the catalytic activity of the nanoparticles (*64*). The first is that the Ce^{3+}/Ce^{4+} ions interact directly with the ROS/RNS to neutralize both superoxide and hydrogen peroxide. The second hypothesis postulates that both reactions proceed by oxygen vacancy creation and annihilation (filling), with the cerium ionic states cycling between Ce^{3+} and Ce^{4+}. Interested readers are referred to an excellent review of this chemistry with all the attendant theoretical underpinnings (*64*). From a biologist's perspective, the oxygen vacancy hypothesis is more appealing because it provides a mechanism for selective binding and destruction of oxygen containing free radicals. The ionic hypothesis does not provide for any such selectivity mechanism that fits with the biological data that clearly suggests selective neutralization of ROS/RNS (*56*). For example, the ability of nanoceria to operate as a SOD/catalase/peroxidase mimetic has been demonstrated in a variety of cell free systems (*59*, *61*, *65–67*). Depending on the species, ROS/RNS were reduced between ~15-70% in an oxidative brain injury model (*56*). If there was no selective destruction of ROS/RNS molecules we should observe

In Oxidative Stress: Diagnostics, Prevention, and Therapy Volume 2; Hepel, et al.;
ACS Symposium Series; American Chemical Society: Washington, DC, 2015.

relatively promiscuous oxidation of many cellular molecules which would not be surprising given that Ce^{4+} is a very potent oxidizer with a half-cell potential of ~1.5 V. By comparison, hydrogen peroxide has a half-cell potential of ~1.7 V and is consequently a very electrophilic species. In contrast, most biological molecules/tissues have negative half-cell potentials. Thus, in the absence of selective interactions with ROS/RNS, the addition of nanoceria (Ce^{4+}) would be expected to oxidize many cellular proteins and lipids in a manner similar to the addition of peroxide. Unfortunately, the role of oxygen vacancies has not been well studied. Attempts have been made to increase oxygen vacancy formation with the addition of dopants, however, convincing evidence that dopant assimilation and oxygen formation was achieved is still lacking (*64*). Nevertheless, this represents a good conceptual framework until additional studies either refine or refute this hypothesis.

To provide further support for selective neutralization of ROS/RNS we examined the catalase and oxidase activity of our custom-synthesized particles (2.5 nm hydrodynamic radius, approximately -24 mV zeta potential) utilizing a commercially available Amplex red catalase kit (Life Technologies; Grand Island, NY). We incubated 60 μM of CeNPs with 10 μM H_2O_2 in individual wells of 96-well plates for 30 minutes. The Amplex red reagent was then added to each well and incubated for another 30 minutes. In the presence of horseradish peroxidase, the Amplex reagent reacts with any unused H_2O_2 to generate the fluorescent product resorufin. Thus, the level of fluorescence at the end of the experiment is inversely related to the catalase activity present in the sample. It has also been demonstrated that nanoparticles can oxidize the Amplex red reagent in the absence of H_2O_2, albeit with different kinetics (*68*). Thus, to measure this oxidase activity using the same kit, we incubated a higher concentration of CeNPs (6.5 mM) for 5 hours with the Amplex reagent and horseradish peroxidase in the absence of H_2O_2. To compare the level of oxidase activity in each of our samples, the fluorescence values obtained were normalized to separate wells containing only 10 μM H_2O_2 and the Amplex red reagent incubated for the same length of time. Two important findings arose from this work. First, catalase activity is much higher in our smaller particles compared to larger (4-5 times larger) commercially available CeNPs (Estevez et al., unpublished observations). Second, the oxidase activity is approximately 1800 times less compared to the same concentration of H_2O_2 demonstrating that there is not a high level of non-selective oxidation occurring with the CeNPs. This approach has helped us correlate CeNP enzyme-mimetic activities with outcomes in our biological test beds as well as examine aspects of synthesis and stabilization that helps us 'tune' the kinetics of these enzyme activities in an iterative fashion. For example, even though the core of the particle was synthesized and stabilized the same way, changes in the final wash steps where some stabilizer components were 'added back' led to considerable differences in the oxidase-mimetic activity of the particles (Figure 1). We are currently in the process of developing a similar ex-vivo assay for assessing SOD-mimetic activity of our nanoparticles in order to compare the activities of various nanoparticles, noting that care must be exercised when using commercial kits that often use redox sensitive indicators that could interact directly with the CeNPs.

Publication Date (Web): October 13, 2015 | doi: 10.1021/bk-2015-1200.ch018

Publication Date (Web): October 13, 2015 | doi: 10.1021/bk-2015-1200.ch018

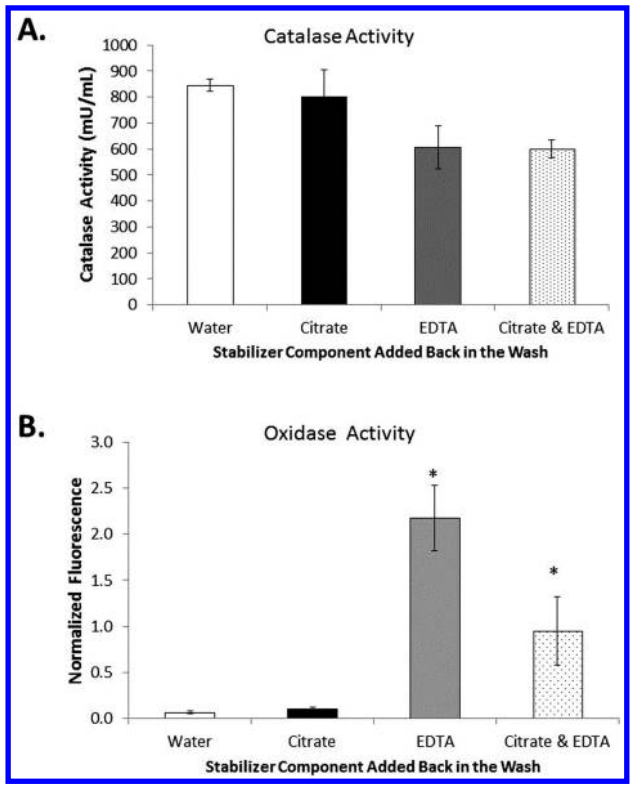

*Figure 1. Catalase (A) and oxidase (B) activities for various formulations of CeNPs measured using the Amplex red catalase kit (Life Technologies; Grand Island, NY). In each formulation, the core particle was the same; the difference was in the particular stabilizer component (citrate, EDTA or citrate & EDTA) added back during the post-synthesis wash. The water wash had no stabilizers added back. Data are presented as mean ± SEM of n=3-4 assays performed in triplicate for each sample. The catalase activity was calculated based on a standard curve using bovine catalase as a reference. The oxidase data were normalized to 10 μM H_2O_2. Statistical significance was determined using a one-way ANOVA followed by Dunnett's test comparing each formulation to the water wash. *p<0.001*

The measured catalase activity of our particles is significantly higher compared to brain catalase activities, which range between 10-70 mU/mg tissue (*69*, *70*), providing further mechanistic support for their potent antioxidant activity. Using a superoxide cytochrome c-based microsensor in our oxidative injury based brain slice assay, we have previously shown that ~6 μM (1 μg/ml) nanoceria is equivalent to 580 U of SOD (*71*) a remarkably high level of enzymatic activity given brain levels have been measured to be less than 1 U/mg tissue (*72*, *73*). This suggests that normally in the brain, the higher turnover rate

of SOD would lead to an accumulation of H_2O_2 in tissue if catalase was the sole enzyme involved in its destruction. However, it is difficult to translate these activities to the in vivo context since there are multiple routes of degradation for H_2O_2 and many coupled reactions that can 'siphon' superoxide (e.g., formation of peroxynitrite generated by the reaction of superoxide and nitric oxide).

Pharmacokinetics of Cerium Oxide Nanoparticles

Based on our in vitro work, the addition of CeNPs to cells would be expected to greatly reduce their ROS/RNS load given the very high catalytic activity of the particles. This is particularly true given the ability of CeNPs to continue neutralizing ROS/RNS as long as they are resident in the tissue (*58*, *74*, *75*). The key to harnessing the potential of nanoceria is being able to get the chemistry to the biological target of interest. This is no easy task given the interactions of particles with plasma proteins and the numerous biological membranes that need to be crossed to enter the cells of interest (*75*). The pharmacokinetic properties of a compound can therefore completely compromise its potential biomedical application. Material not able to bring its chemistry to the target will either not be biologically active or potentially generate off-target effects. This section will address some of the pharmacokinetic factors that influence the ability of the CeNPs to reach their intended target.

Importance of the Nano-Bio Interface

Nanoparticle surfaces in biological environments are modified by the adsorption of biomolecules such as proteins and lipids. This leads to generation of the "hard" (protein-particle interaction) and "soft" (protein-protein/particle interactions) coronas. The 'hard' corona has a relatively high affinity for the particle surface and dissociates slowly. In contrast, the 'soft' corona is labile, and formed principally through protein-protein/particle interactions (*76*, *77*). In a typical biological environment, many biomolecules (e.g., plasma proteins, RNA/DNA aptamers, enzymes) compete for the limited surface of nanoparticles. With administration of nanoparticles intravenously, the CeNPs will first encounter blood plasma that contains several thousand proteins whose abundance varies by 12 orders of magnitude. The surface area of the particle, radius of curvature, surface reactivity and surface charge can influence not only the complement and density of proteins adsorbed to the surface but also the ultimate structure and biological effects of the particle (*78–81*). Typically, for a fixed core size, nanoparticles modified with anionic or cationic ligands adsorbed more protein than those modified with neutral ligands, reflecting a greater propensity for proteins to associate with charged nanoparticles via electrostatic interactions (*82–84*). Assuming similar surface effects/functionalization, particles with smaller radii typically adsorbed a higher density of serum protein than those

Publication Date (Web): October 13, 2015 | doi: 10.1021/bk-2015-1200.ch018

with larger diameters. Although this may seem counter-intuitive, it appears that 'flatter' particle surfaces (i.e., lower radius of curvature) allow for greater steric hindrance between adjacent adsorbed proteins than smaller particles with greater curvature.

Recent work by Walkey et al. (*85*) has shown that there are specific protein fingerprints which closely correlate with cell association. In this study they developed a quantitative model that used the serum protein corona fingerprint to predict cell association using a suite of compositionally diverse gold nanoparticles. To evaluate cell association, they used inductively coupled plasma-atomic emission spectroscopy (ICP-AES) in immortalized, human lung epithelial carcinoma (A549) cells in culture. This was the first study to develop a statistical model to identify the most important proteins and physical characteristics that correlated highly with cell association. They demonstrated that the protein corona encodes more biologically relevant information about the association of the nanoparticle with a cell than its physical properties. In addition, they identified specific proteins that correlated negatively with cell association (e.g., complement). It is important to note, however, that this study was not designed to study cellular uptake or trafficking of particles per sé; the association observed could simply reflect the particle binding to the plasma membrane.

The results from Walkey et al. (*85*) showed that the serum protein fingerprint's role in cell association depended primarily on the size and composition of the particle, suggesting that specific fingerprints would need to be established for particles with varying composition and sizes. If this were not complicated enough, it is also likely that there will be differences in cellular uptake/trafficking depending on the cell type studied (see subsequent section). Given the number of variables involved, it may be a good approach to utilize a similar modeling method developed by Walkey et al. (*85*) and apply it to in vivo systems which have many different cell types and cellular compartments that vary in both ionic composition and protein content. In adopting such an approach, the investigator is simply interested in the physiological endpoint (i.e. improved performance, increased survival, etc.). However, while this will help correlate outcome to the physical and chemical characteristics of the material (synthetic identity), it does not elucidate which proteins are ultimately responsible for the downstream biology (biological identity). To address the latter issue, we must replicate the dynamic milieu the particles are exposed to as they traverse from one biological compartment to the next and study how the biological identitity of the particle changes over time. This could be done by washing the particles in a serial fashion through solutions that mimic plasma, extracellular fluid and intracellular fluid, each with its own unique ionic composition and protein content. Nanoparticles could then be recovered from these solutions and tested in in vitro test beds. If successful (i.e., we see dramatically different biological outcomes in our in vitro target cells), this experimental design would be enormously productive in translating the 'synthetic identity' of the particle with its 'biological identity' and subsequent physiological effects (*86*). While we may be able to get estimates of alterations in the hard corona using ex vitro and in vitro approaches, understanding the protein-protein interactions between the particle-adsorbed proteins and free proteins in solution will be more difficult, especially if they greatly contribute

Publication Date (Web): October 13, 2015 | doi: 10.1021/bk-2015-1200.ch018

to the terminal biological effects. In summary, while the work of Walkey et al. (*85*) is an excellent start and provides a conceptual framework for designing in vivo experiments, the modeling paradigm will need to be adapted to correlate the material science aspects with the biological outcomes in intact animals.

Plasma Half-Life and Biodistribution of Cerium Oxide Nanoparticles

In rodent models, bare particles are prone to aggregate and accumulate in reticulendothelial organs (i.e. liver and spleen) (*87–90*) where they are phagocytized by tissue-resident macrophages (*86*, *91*). Not surprisingly, the plasma half-life of these formulations of nanoceria are also quite short, between ~ 7 minutes to 1 hour depending on the formulation. In general, the addition of stabilizers improves plasma half-life and tissue deposition (*87*, *90*, *92*). Stabilizers are often added to prevent aggregation of CeNPs in the high ionic strength of biological solutions such as plasma or reduce removal by resident macrophages in the liver and spleen. PEGylation has been used successfully to increase plasma circulation times, reducing scavenging by tissue-resident or circulating monocytes and reducing deposition in the liver and spleen (*93*). Although the characteristics imparted by PEG are an advantage in improving biocompatibility and increasing target tissue accumulation associated with increased circulation times compared to other more labile stabilizers, these benefits can be offset by diminished catalytic activity of nanoceria with high density PEG coating in which the surface chemistry dominates chemical reactivity. For example, we found that increasing the amount of PEG decorating the surface of CeNPs (increased molar ratio of PEG) enhanced CeNP deposition in the brain of healthy mice (Figure 2A). However, this increase in biodistribution imparted by PEG is counterbalanced by a reduction in the catalytic activity of the particle. When tested in an in vitro hippocampal brain slice model of ischemia, CeNPs decorated with a higher molar ratio of PEG displayed lower neuroprotective redox activity (Figure 2B). In addition, PEG decreases cellular uptake which may be associated, in part, with an increase in particle size.

We have developed a stabilizer package that includes both citrate and the metal chelator EDTA on a 2.5 nm ceria nanoparticle (*58*) with minimal effects on hydrodynamic radii. The combination of citric acid and EDTA results in highly monodispersed particles that resist agglomeration in high salt solutions and cannot be pelleted out using ultracentrifugation (436,000 x g, 4 degrees Celsius). Removal of the citrate or EDTA from the stabilizer formulation or altering the molar ratio of citrate to EDTA in the synthesis increases aggregation and diminishes ROS neutralizing activity of the particles and their deposition in the brain (Erlichman et al., unpublished observations). Pharmacokinetic studies of these particles administered intravenously in the rat revealed that the half-life of citrate/EDTA nanoceria was ~4 hours, considerably longer than ceria stabilized with citrate alone and far longer than 'bare' particles, with much lower deposition in the reticulondothelial organs (*58*) than other comparably sized CeNPs.

In Oxidative Stress: Diagnostics, Prevention, and Therapy Volume 2; Hepel, et al.;
ACS Symposium Series; American Chemical Society: Washington, DC, 2015.

Publication Date (Web): October 13, 2015 | doi: 10.1021/bk-2015-1200.ch018

Publication Date (Web): October 13, 2015 | doi: 10.1021/bk-2015-1200.ch018

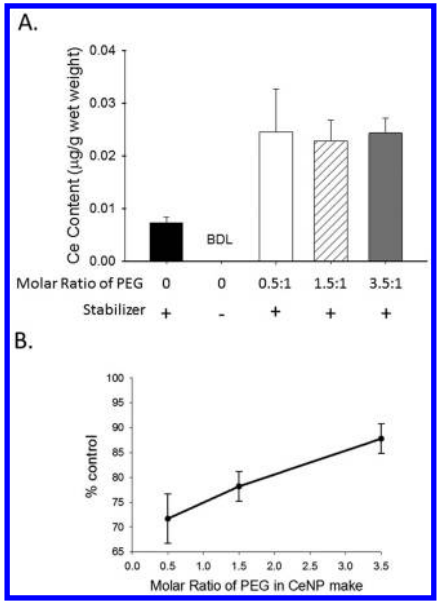

Figure 2. Effects of PEG on CeNP biodistribution and antioxidant activity. (A) PEGylation increases brain deposition of CeNPs. Healthy CD-1 mice were exposed to a single 20 mg/kg dose of CeNPs via tail vein injection. The PEGylated CeNPs were synthesized using our citric acid/EDTA stabilizer package and increasing molar ratios of PEG (0 PEG; 0.5 PEG:1 CeNP; 1.5 PEG; 1 CeNP; 3.5 PEG:1 CeNP). Brains were harvested 3 days after injection and CeNPs were detected with inductively-coupled mass spectroscopy. The addition of PEG increased brain deposition of the CeNPs compared to the control CeNPs (with stabilizer only). When the stabilizer was washed out (- stabilizer), the CeNPs were not detectable in the brain (BDL = below detectable limit), demonstrating the importance of stabilization in particle biodistribution. Data are shown as mean ± SEM of n = 3 brains for each condition. (B) PEGylated CeNPs have decreased antioxidant activity. Neuroprotective redox activity of CeNPs was measured using an in vitro hippocampal brain slice model of cerebral ischemia as reported previously (56). Mouse hippocampal brain slices were exposed to 30 min of ischemia and 5.8 µM CeNPs (added at the time of ischemic insult). Cell death was assessed with SYTOX green nucleic acid stain (Life Technologies; Grand Island, NY) 24 hr later. Cell death in CeNP-treated brain slices is expressed as % control cell death where controls were matched slices prepared in parallel and exposed to 30 minutes of ischemia without CeNP treatment. A higher molar ratio of PEG decreases the neuroprotective properties of the CeNPs (r^2 =0.99; p = 0.05). (Note that 100% control is equivalent to no neuroprotection). Data are shown as mean ± SEM of n = 10 – 15 matched pairs of brain slices in each condition.

Publication Date (Web): October 13, 2015 | doi: 10.1021/bk-2015-1200.ch018

Cellular Uptake and Localization of Cerium Oxide Nanoparticles

Nanoparticles with hydrodynamic radii less than 5 nm appear to equilibrate much more rapidly with the extracellular space than larger particles due slower transport across the vascular endothelium. Although this has not been rigorously tested for a variety of nanoparticle sizes, charge and composition, the limited studies that have been done have shown that 11 nm immunoglobulin molecules require ~24 hours to equilibrate between the vascular compartment and the extracllular space (*94*). In contrast, smaller molecules such as the dextran-Technetium (radii < 4 nm), rapidly cross the capillary fenestrae and enter the extracellular space. The physiologic upper limit of pore size for allowing the transcapillary passage of lipid-insoluble macromolecules via most non-sinusoidal blood capillaries ranges between 5 and 12 nm (*95*). Therefore, macromolecules larger than the physiologic upper limits of pore size in the non-sinusoidal blood capillary types generally do not accumulate within the respective tissue interstitial spaces and their lymphatic drainages unless they are actively transcytosed across endothelial cells (*95*). The lymphatic vessel endothelial layer is more permeable than that of the vascular endothelium because of its role in clearance of macromolecules from the extracellular space; particles less than 6 nm in diameter can flow easily into and out of the lymphatic vessels (*94*).

It is clear that the cellular uptake of nanoparticles in reduced, in vitro preparations is dependent on many factors including size, shape, net charge, charge density/distribution and ligand density (if functionalized), and this has been discussed in detail in several excellent reviews (*96–99*). Thus far, there appear to be few conserved rules regarding how these factors impact cellular uptake that are predictive for all nanoparticles. Previous studies have shown that nanoparticles can be transcytosed into cells by pinocytosis, endocytosis and direct membrane interactions (*99*). In general, larger particles (~30 nm) are taken up more avidly than smaller particles (~1 nm), and very small particles (< 6 nm) are thought to be quickly cleared by the renal system, resulting in very short half-lives (*79*). It has been observed with other, non-ceria nanoparticles, that larger, negatively charged particles are taken up primarily by cells of the immune system, whereas little of the material is transcytosed into non-phagocytic cells. In contrast, positively charged nanoparticles are often translocated rapidly into cells. It is thought that the net negative charge on cells imparted by proteins enhances the electrostatic attraction of cationic particles, thus improving membrane interactions, whereas anionic particles are repelled. Although this may appear intuitive, uptake by cells depends on the net effect of both physical and chemical properties, and thus charge alone does not uniquely correlate with cellular uptake for all particles.

Using non-stabilized nanoceria, Patil et al. 2007 showed that in vitro uptake by immortalized cancer cells was increased in particles with more negative zeta potentials (-30 mV to -40 mV) (*100*). Utilizing cultured keratinocytes, Singh et al. 2010 showed wide cellular distribution of negatively charged CeNPs (~-18 mV) in lysosomes, endoplasmic reticulum, mitochondria, cytoplasm and the nucleus (*101*). Asati et al. 2010 showed that polymer-coated cerium oxide nanoparticles with a positive or neutral charge were more readily taken up by non-transformed cell lines (HEK293 and H9C2), whereas nanoceria with a

negative surface charge internalized mostly in the cancer cell lines (A549 and MCF-7) (*102*), which recapitulated the work of Patil et al. 2007, who used the same lung carcinoma cell line. In the cancer cell lines studied by Asati et al., surface charge directed cellular localization. They found that positively charged nanoceria accumulated in lysosomes and decreased viability by ROS-mediated mechanisms, whereas neutral polymeric coated particles resided in the cytosol and demonstrated no apparent cellular toxicity. These effects appeared to be dependent on the composition of the core; repeating the experiment with iron core particles eliminated toxicity, but not cellular uptake, suggesting that the ceria core mediated the toxic effects of these particles. Walkey and Chan (*85*) have recently shown that changing the core while controlling for other factors has profound effects on the composition of the protein corona, raising the possibility that the biological effects may not be directly related to core composition per sé. Dowding et al. 2013, demonstrated that the uptake of positively charged particles (~+30 mV) could be enhanced with the addition of hexamethylenetetramine (HMT) on the surface (*103*). The increase in cellular accumulation of these nanoparticles in human embryonic endothelial cells was associated with decreased viability, suggesting that either the HMT is toxic by itself or the particles may have co-localized to the lysosomes (*104*). Importantly, these particles become negatively charged once they are passivated in serum.

In intact brain slices, negatively charged nanoceria (~-20 mV) decreased ROS levels and tissue damage following ischemia (*56*). Although mechanisms of cellular entry were not studied, TEM analysis showed the presence of CeNPs throughout the cell including mitochondria, neurofilaments, lipid membranes and myelin sheaths. Based on these findings, the initial surface charge, influenced both by the core composition and stabilizer, may dictate the proteins that comprise the corona and the downstream, biological effects. Thus, the net charge of the particle becomes secondary to the proteins that contribute to the charge. Moreover, these data suggest that uptake may also be dependent on the cell type studied. There is a large body of literature that shows that activity of pinocytotic and endocytotic mechanisms vary widely between cell types (*105*, *106*). Consequently, some organs may take up more ceria than others, and this is supported by studies that have used mass spectrometry data to measure ceria deposition in tissues in vivo. These data show that there is enormous variability in nanoceria accumulation between organs, a finding that may reflect the aggregate activity of uptake mechanisms of this material by cells comprising the tissue (*58*, *88*, *90*, *107*, *108*).

Given the complexity of the factors that regulate cellular uptake, this is an enormously important area of research that needs to be intensively studied in the future. Having a better understanding of the cellular localization of nanoceria may unify the disparate biological findings (i.e., ROS scavenger versus ROS generator) that have appeared in the literature over the past 5 years.

Clearance of Nanoceria

The clearance of nanoparticles also reflects how the body views the material as a biological entity. Renal clearance of negatively charged particles is thought to occur quickly with particles less than 6 nm in size, but nanomaterial larger than

Publication Date (Web): October 13, 2015 | doi: 10.1021/bk-2015-1200.ch018

6 nm is likely to end up in the liver and the spleen (*79*). In addition to size, surface charge is also an important determinant of the renal handling of nanomaterials. The effect of molecular charge on renal filtration is due to at least two factors. First, there are changes in size following the surface adsorption of proteins (*86*, *109*, *110*), and second, there are electrostatic interactions between the particles and the fixed, negative charges within the glomerular capillary wall and filtration slits (*111*). Studies evaluating the effect of molecular charge on glomerular filtration of similarly sized molecules have shown that filtration is greatest for cationic molecules, followed by neutral molecules, while anionic molecules are least readily filtered through the glomerular capillary wall, which is not surprising given the anionic filtration slits.

The hepatobiliary system represents the primary route of excretion for nanoparticles that do not undergo renal clearance (*94*). The liver provides the critical function of catabolism and biliary excretion of blood-borne particles and also serves as an important site for the elimination of foreign substances and particles through phagocytosis (*94*, *112*). Nanomaterials that are excreted by the biliary system, are first degraded via the hepatocytes. Phagocytic Kupffer cells are critical for the removal of pathogenic substances from the blood including foreign colloidal materials such as nanoparticles (*94*, *112*). Kupffer cells possess numerous scavenger receptors as well as receptors for selective endocytosis of opsonized particles (receptors for complement proteins and for the Fc region of immunoglobins). Kupffer cells are capable of internalizing nanoparticles of various diameters and composition, regardless of their coating (*113–116*). Hepatocytes also play an important role in liver clearance through endocytosis and enzymatic breakdown of foreign particles. Although the phagocytic capacity of hepatocytes is much less than that of Kupffer cells, these cells represent an important physiologic pathway for foreign particle processing and are a potential site for toxicity (*94*, *112*). There are, however important differences between these two systems. Hepatocytes contribute to the biliary pathway and, as a result, particles processed by these cells are excreted into the bile and represent a means for clearance. In contrast, Kupffer cells are part of the reticuloendothelial system (RES) and rely exclusively on intracellular degradation for particle removal. Similar to all phagocytic cells of the RES, particles that are not broken down by intracellular processes will remain within the cell and will therefore be retained in the body.

High levels of 'bare' or citrate-stabilized nanoparticles are retained in the liver in rodents up to 90 days post-administration, and importantly little decrement is observed over time (*90*). The high concentration and long duration of residence may likely contribute to the observed toxicity in the liver and the spleen associated with these formulations of nanoceria (*90*, *117*). In the Tseng et al. 2012 study (*117*), nanoceria endocytosed by the hepatocytes were often present as large cytoplasmic agglomerates ~150 nm in size. In day 30 liver samples, nanoceria-containing Kupffer cells together with mononucleated cells formed sinusoidal granulomata. Electron dense nanoceria agglomerates were most abundant in Kupffer cells, and the size of these agglomerates exceeded 2 μm in diameter.

In contrast to these findings, citrate/EDTA stabilized nanoceria showed much lower deposition to RES organs and good dose-dependent deposition in the brain

In Oxidative Stress: Diagnostics, Prevention, and Therapy Volume 2; Hepel, et al.;
ACS Symposium Series; American Chemical Society: Washington, DC, 2015.

Publication Date (Web): October 13, 2015 | doi: 10.1021/bk-2015-1200.ch018

(*58*). Moreover, progressive clearance from the brain, liver and spleen over a twelve month period was apparent with large decreases in organ deposition being observed after 2 months in the tissues we examined (Figure 3). To-date, the mechanism(s) of ceria clearance in intact animals have not been well studied and are not currently known. Although decreases in nanoceria content were noted, low levels of nanoceria in the liver, spleen and brain persists for months regradelss of formulation (*88*, *90*, *107*, *108*, *118*).

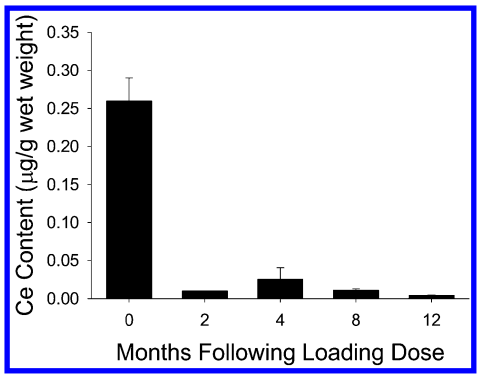

Figure 3. Clearance of CeNPs from mouse brains after a single 20 mg/kg tail vein injection. CeNPs brain deposition was determined via inductively-coupled mass spectroscopy 24 hours after the loading dose (0 month), then bimonthly. Data are shown as mean ± SEM of N= 12 total animals with 2-3 animals per time point.

Publication Date (Web): October 13, 2015 | doi: 10.1021/bk-2015-1200.ch018

Example of Off-Target Effects of Cerium Oxide Nanoparticles: Modulation of General Immune Cell Function & Inflammation

CeNPs, like any foreign material introduced into an organism, have the potential to affect tissue homeostasis whether they reach the target organ site or not. Of particular importance is the ability of immune cells to detect this "foreignness" and subsequently mount specific immune responses and/or generate general inflammation (*119*). Thus, unintended, non-ROS related effects of the CeNPs on the immune system pose a significant drawback to the use of these nanomaterials for therapeutic purposes. Respiratory tract exposure is a common focus of CeNP immunomodulatory/immunotoxicity studies (*120–124*), since this is the most likely route of accidental, occupational exposure. Intratracheal exposure to aggregation-prone CeNPs induce increases in alveolar macrophage populations in the bronchoalveolar lavage (BAL) fluid (*121*), while head and nose exposure to slightly different CeNPs decreased populations of the same cells (*123*). Similarly, variable effects in cytokine production were observed in these two scenarios. Intratracheal exposure resulted in the production of increased levels of IL-12 (*121*) and TGF-β (*124*) from ex vivo stimulated alveolar macrophages. These observations provide a conflicting picture of how the macrophages are impacted by CeNP exposure, since IL-12 favors the generation

of pro-inflammatory T helper (TH) 1 cells (*125*), while TGF-β is considered to be immunosuppressant (*126*). Though not directly attributable to macrophage cells, the head/nose administration of CeNPs resulted in increased levels of the pro-inflammatory cytokines IL-1beta, IL-6, and TNF-α in the blood of exposed rats (*123*). Different manufacturers synthesized the CeNPs for these studies, and size and agglomeration status were reportedly different, suggesting that such characteristics drive distinct immune effects. Further, the in vivo vs in vitro nature of experimentation can contribute to observed effects, as a murine macrophage cell line exhibited no change in TNF-α production upon exposure to CeNPs (*127*), in contrast to the results of the in vivo exposure (*123*). At this point, these observations fail to support a clear consensus as to whether the CeNPs induce a pro-inflammatory or anti-inflammatory phenotype from macrophages. More systematic study of separate CeNP variables (size, zeta potential, surface modification) will be necessary in order for more broad conclusions to be drawn regarding macrophage effects.

While macrophages are distinct due to their ability to produce high levels of pro-inflammatory cytokines, dendritic cells play a critical role in bridging the innate and adaptive immune responses, by responding to foreign antigens and displaying them along with additional cell-surface signals to activate T cells (*128*). Assessment of the effects of CeNPs on dendritic cells has thus far been limited to in vitro study (*129*). Human dendritic cells exposed to CeNPs responded with some upregulation of the co-stimulatory molecule CD86 as well as elevated production of the immunosuppressive cytokine IL-10 and the pro-inflammatory cytokine IL-6, compared to control treatment (*129*). However, despite increased CD86 expression (which should promote T cell activation and secondary proliferation), the CeNP-treated dendritic cells did not affect T cell proliferation in co-cultures. In co-cultures with allogeneic TH cells, however, CeNP-treated dendritic cells elicited increased production of IL-4, -5, and -10 from the TH cells, indicative of a TH2 polarized immune response (*129*). When mitogenic stimuli were added to this co-culture of CeNP-treated dendritic cells and allogeneic T cells, levels of these TH2 cytokines were decreased, while levels of the TH1 cytokines IL-2, IFN-γ, and TNF-α were slightly elevated (*129*). Thus, these in vitro results suggest that a TH2 T cell polarity would be generated in response to dendritic cell exposure to CeNPs outside the context of other immune-activating stimuli, but that a pro-inflammatory TH1 polarization would be achieved with simultaneous immune activation and CeNP-dendritic cell exposure. While this study does utilize co-cultures of immune cells to mimic somewhat more realistically in vivo cellular interactions, the in vivo administration of CeNPs is far superior in gauging their biological effects due to the complex interplay that occurs between cells within the immune system as a whole. As previously noted, it is difficult to predict whether the same degree of CeNP exposure to either dendritic cells or T cells would occur in vivo, which may render these in vitro results interesting, but perhaps less informative than more physiologically relevant in vivo studies that are certainly the gold standard.

Identifying universal trends of how immune cells respond to CeNP exposure (whether considering antioxidant or more broad immunomodulatory properties of CeNPs) is not possible at this point, given the paucity of studies as well

Publication Date (Web): October 13, 2015 | doi: 10.1021/bk-2015-1200.ch018

as the variability in CeNP formulations investigated. Examination of basic immune functions such as T cell responses to CeNP exposure simultaneous with vaccination, virus/bacteria exposure, or allergic responses will provide an understanding of whether CeNPs would unfavorably influence these responses. For example, pre-allergy induction, repeated exposure to iron nanoparticles reduced the severity of the immune response including production of allergen-specific IgE antibodies (a TH2 polarized response) (*130*). (Interestingly, this result correlates with the observation that immune stimuli plus CeNP exposure can decrease TH2 responses (*129*).) In contrast to the repeated exposure (*130*), a single exposure to iron nanoparticles one hour prior to antigen (allergen) sensitization, elicited decreased production of both TH1 and TH2 cytokines seven days later (*131*), demonstrating that a more complete picture of responses to CeNP exposure requires examination of differing doses, timing of doses, and frequencies of exposure. Certainly, this application of CeNPs to animals undergoing basic immune responses is beyond what is examined in standard accidental exposure analysis. However, if CeNPs are to soon be applied therapeutically for some of the diseases under investigation, their impact on standard immune function (beyond any antioxidant properties!) must be more completely characterized.

Publication Date (Web): October 13, 2015 | doi: 10.1021/bk-2015-1200.ch018

Cerium Oxide Nanoparticles as Neuroprotective Agents in Animal Models of Neurodegenerative Disease

The differences in the biodistribution and physiological effects between different formulations of nanoceria need to be further explored so that the biological behaviors of these nanomaterials can be tuned to enhance desirable properties while dampening off-target interactions. Currently, nanoceria research labs test the biological aspects of their material empirically and then try to generate structure-function relationships based on the biological models they have used. This approach is time-consuming and often offers predictability only in the systems in which it was tested. In our view, given the complexities associated with the nano-bio interface, there may be no simple surrogate for intact animal studies. Reduced, simpler preparations may be used successfully once you have established the biological effects in intact animals and then correlated them back with responses in more reduced systems. Once you have identified simpler models that reflect behavior in vivo, using in vitro systems for subsequent CeNP development becomes more fruitful. We have used this approach to develop our CeNPs for treatment of neurodegenerative diseases. Below we review several of these models.

Cerebral Ischemia

Cerebral ischemia is defined as the lack of blood flow to the brain. Global ischemia occurs during cardiac arrest when the entire brain is deprived of blood.

In Oxidative Stress: Diagnostics, Prevention, and Therapy Volume 2; Hepel, et al.;
ACS Symposium Series; American Chemical Society: Washington, DC, 2015.

Focal ischemia, or stroke, occurs when a clot or a bleed disrupts blood flow to a specific region of the brain. Stroke was the fifth leading cause of death in 2013 (*132*) and is a leading cause of long-term disability in the United States (American Stroke Association). Reduced glucose and oxygen delivery to the brain quickly disrupts transmembrane ionic gradients in neurons and leads to a series of events, known as the ischemic cascade, that culminate in cell death via necrosis or apoptosis (*133*). It has been estimated that every minute of a stroke leads to the loss of millions of neurons and billions of synaptic connections (*134*).

Oxidative stress plays a prominent role in ischemic cell death. Reactive oxygen species are produced during the ischemic period and even more so during the reperfusion period when blood flow is restored (*135*). As illustrated in Figure 4, sources of ROS/RNS during ischemia include the disrupted electron transport chain, glutatmate excitotoxicity, xanthine oxidase, and neuronal nitric oxide synthase. In addition, the reaction of nitric oxide with superoxide yields the highly reactive peroxynitrite anion. During reperfusion, restoration of oxygen delivery generates a big burst of ROS, primarily superoxide, via Complex I of the electron transport chain. NADPH oxidases in neurons and microglial cells invading the site of injury also contribute to further ROS production (*135–137*).

To date, the only FDA approved drug for the treatment of stroke is recombinant tissue plasminogen activator (rt-PA), a clot-busting drug used to restore blood flow. Thus, development of therapies aimed at protecting neurons from dying upon an ischemic insult as well as the development of ways to get these drugs to the target site are very active areas of investigation in stroke research (*138*).

Because of the prominent role of ROS/RNS and ischemic injury, we were interested in studying the potential of CeNPs for therapeutic use in stroke. We used a cultured, organotypic hippocampal brain slice model of ischemia for our studies. Due to its highly conserved neural architecture, the hippocampus is an ideal brain area to study oxidative injury. The majority of neurons in this important brain area are densely packed into a single layer, which is divided into several distinct anatomical regions (CA1 through CA4). The hippocampal regions CA1 and CA3 are adjacent to each other and are composed of morphologically similar neurons, pyramidal neurons. Despite their physical proximity and morphological similarity, CA1 and CA3 neurons respond to oxidative stress very differently. Pyramidal neurons in the CA1 region suffer massive cell death while those in CA3 mostly survive following oxidative injury regardless of the agent used or the type of ROS/RNS generated (*139–142*). This pattern of selective sensitivity of CA1 neurons to oxidative stress parallels the selective vulnerability of CA1 neurons to other pathologic conditions, such as hypoxia, ischemia, and neurodegeneration. Following ischemia, hippocampal astrocytes display selective loss of glutamate transport activity, increased mitochondrial ROS/RNS generation, and reduced mitochondrial membrane potential. This selective dysfunction of hippocampal astrocytes has been suggested as being important in determining the selective loss of CA1 neurons under ischemia and other oxidizing insults (*143*).

Publication Date (Web): October 13, 2015 | doi: 10.1021/bk-2015-1200.ch018

Publication Date (Web): October 13, 2015 | doi: 10.1021/bk-2015-1200.ch018

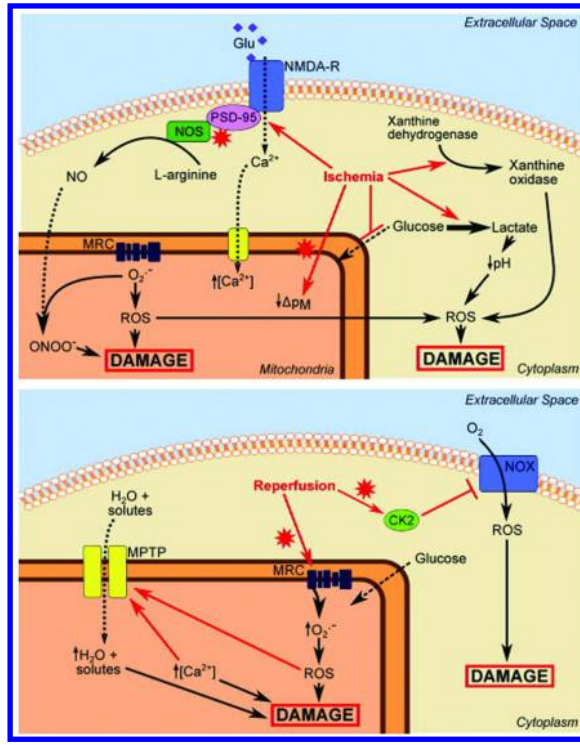

Figure 4. Overview of ROS production in brain ischemia and reperfusion. Top: ROS production in ischemia. Lack of oxygen promotes the interruption of oxidative phosphorylation at the mitochondrial respiratory chain (MRC). Mitochondrial depolarization (↓ΔpM) together with intracellular acidification (↓pH) caused by an accumulation of lactate as an anaerobic product of glycolysis, result in increased levels of superoxide ($O_2^{\bullet -}$) conversion to other ROS. Activation of the NMDA receptor by glutamate increases Ca^{2+} influx as well as the activation (via the adaptor protein postsynaptic density (PSD)-95) of neuronal nitric oxide synthase (nNOS), which generates nitric oxide (NO) from L-arginine. Xanthine oxidase, which results from the conversion of xanthine dehydrogenase under these conditions, contributes to the production of ROS. NO reacts with $O_2^{\bullet -}$ to generate the harmful reactive species peroxynitrite ($ONOO^-$). Bottom: ROS production in reperfusion. In addition to the pathways initiated during ischemia, oxygen availability after ischemia resets the MRC resulting in a large increase in $O_2^{\bullet -}$ mostly from complex I. Oxidative stress and increased Ca^{2+} cause opening of the mitochondrial permeability transition pore (MPTP). This allows entry of water and solutes from the cytoplasm resulting in mitochondrial swelling and damage. Generation of ROS also occurs in the cytoplasm through the action of NADPH-oxidase (NOX). Upon reperfusion, the inhibitory enzyme casein kinase 2 (CK2) is downregulated contributing to activation of NOX. The resulting oxidative stress outweighs antioxidant defenses and leads to cell damage, necrosis or apoptosis. Figure and legend reproduced (with minor modification) with permission from reference (135). Copyright Elsevier 2013.

In our study we showed that addition of 1 μg/mL commercial CeNPs (Sigma-Aldrich; St. Louis, MO) at the time of the ischemic insult reduced hippocampal cell death by about 50% (*56*). In addition, using fluorescent indicator dyes we were able to show that CeNPs modestly reduced superoxide and nitric oxide levels, but had a very profound effect on ischemia-induced 3-nitrotyrosine formation as measured using ELISA. Taken together, these data suggest that the protective effects of CeNPs were likely mediated by a reduction of the downstream effects of peroxynitrite. This brain slice model continues to be of immense use in our laboratory as we investigate how alterations of the physiochemical parameters of novel CeNPs influences the neuroprotective efficacy of the nanoparticles (Figure 2B).

Publication Date (Web): October 13, 2015 | doi: 10.1021/bk-2015-1200.ch018

Multiple Sclerosis

Multiple sclerosis (MS) is an autoimmune disease (*144*) characterized in affected patients by motor (*145*) and even cognitive deficits (*146*) resulting from loss of the myelin sheath surrounding neurons in the CNS (*147*). A number of factors have been linked to the incidence of MS, including genetics (*148*), environmental factors such as sunlight exposure (*149*), and even the similarity of neuronal antigens to pathogenic antigens (molecular mimicry) (*150*). At the cellular level, a variety of immune cells have been implicated in disease pathology, ranging from antibody-mediated neuronal damage to targeting of neurons by cytotoxic T lymphocytes to pro-inflammatory events orchestrated by T helper (TH) cells of the TH1 and TH17 polarity (*151*). The distinct contributions of these immune effectors likely accounts for the different patterns of disease progression observed in MS patients (*152*).

The complex interplay of cellular events involves disruption of the blood brain barrier and entry into the brain of auto-reactive lymphocytes as well as bone-marrow derived macrophages (*151*). Activated macrophages produce not only pro-inflammatory cytokines (*153*), but also contribute ROS to the milieu in the brain (*154*). As electron scavengers, ROS disrupt biomolecule constituents of neurons, in particular the lipid components of the myelin sheath. Damaged myelin impairs the efficiency of nerve impulse transmission between neurons as well as to the neuromuscular junction (*147*). Therapeutics to treat MS currently on the market target aspects of immune cell infiltration into the blood stream and brain as well as the total lymphocyte populations in general by hindering cell proliferation and triggering DNA damage-induced cell death (*155*, *156*). Still other drugs focus on skewing the polarity of TH cells away from those involved in MS pathology or shifting the balance of cytokine production from pro-inflammatory to anti-inflammatory (*155*, *156*). However, none of the currently approved drugs target the ROS generated by macrophages during pathogenesis.

Experimental autoimmune encephalomyelitis (EAE) is a rodent model of multiple sclerosis that has long been used to investigate MS pathogenesis as well as to test potential therapeutic agents (*157*). Disease induction can be accomplished by the administration of a myelin peptide combined with Complete Freund's Adjuvant to activate self-reactive T cells along with injections of pertussis toxin or the adoptive transfer of autoreactive T cells generated in this

manner to naïve animals (*158*). The EAE model involving the use of a peptide from myelin oligodendrocyte protein generates a chronic progressive disease pattern in affected animals (*158*) with a pathology that involves ROS (*159*). Intravenous administration of CeNPs to EAE animals in prophylactic (before disease induction) and therapeutic (after disease induction) treatment regimens alleviated disease severity (assessed by clinical scores) and slowed disease progression compared to control animals; in fact, this protection was similar to that afforded by the currently prescribed drug fingolimod (*58*). Motor function on rotarod, balance beam, and hanging wire tasks was also preserved more effectively in CeNP-treated animals. This efficacy appeared to be related to the ability of CeNPs to neutralize free radicals, as less total ROS was detected in brain slices harvested from CeNP-treated mice compared to controls (*58*). The application of CeNPs to the MS model represents a therapeutic approach not currently fulfilled by any of the drugs currently on the market. As yet, it has been difficult to translate the efficacy observed with potential antioxidant-based drugs in animal models (*160–162*) to clinical trials, in part due to the difficulty in delivering adequate therapeutic doses to the brain as well as the consumable antioxidant nature of these materials (*58*, *163*). Even with these limitations, interest in antioxidants persists. Currently, six antioxidants are in various stages of clinical trials. These compounds include: lipoic acid, inosine, vitamin A, idebdenone, melatonin and n-acetyl cysteine. The advantages CeNPs have over these other potential therapies are their small size (and secondary ability to penetrate the blood brain barrier) and their regenerative antioxidant capacity (*58*), that appears, at this point, to be the predominant mechanism of action.

Macrophages that contribute to ROS production are a potential cellular target of the CeNPs in the EAE model, though in vivo studies have not yet definitively pinpointed these cells as specifically targeted by CeNPs. However, in vitro studies have demonstrated the ability of various CeNP formulations to reduce the production of ROS by activated human (*164–166*) or murine macrophage (*127*, *167*) cell lines, with the degree of reduction varying by particle size (*165*). Direct demonstration of the translatability of this observation is lacking, with co-staining of macrophages and ROS and analysis via immunohistochemistry in tissues sections or via flow cytometry being the most convincing evidence needed. Even upon activation or maturation stimuli, dendritic cells are not significant producers of ROS, so it is not surprising that CeNP exposure alone induced only slight ROS production; however, true to their classification as antioxidants, the CeNPs reduced ROS levels elicited from dendritic cells cultured with H_2O_2 (*129*). The disadvantage of such in vitro studies is that CeNPs are placed directly in culture with the macrophages, a scenario that is not necessarily replicated in vivo. Delivery of nanomaterials through intravenous or even subcutaneous routes, for example, requires that the particles traverse through multiple barriers to reach a destination that could include the presence of macrophage cells. The size of the particle certainly impacts the ability of the CeNPs to penetrate tissues and cells, but the protein corona acquired during this passage could also limit the transportation of the nanoparticles as well as their potential antioxidant function upon reaching that site. Thus, in vitro results support the antioxidant effects of CeNPs on macrophages, though a lack of definitive evidence of the same effect

Publication Date (Web): October 13, 2015 | doi: 10.1021/bk-2015-1200.ch018

in vivo limits the ability to convincingly extrapolate these observations to disease models mediated by these immune cells.

Amyotrophic Lateral Sclerosis

Amyotrophic lateral sclerosis (ALS), commonly known as "Lou Gehrig's Disease," is a progressive, fatal, neurodegenerative disease that affects upper and lower motor neurons in the brain and the spinal cord (*168*). Approximately 90-95% of the cases of ALS are sporadic (SALS; unknown cause) with the remaining 5-10% classified as familial (FALS; genetic). The majority of the familial cases, ~20%, are due to mutations in the Cu/Zn superoxide dismutase 1 (SOD1) gene (*169*, *170*). Transgenic mice bearing a $SOD1^{G93A}$ point mutation, which replicates a common mutation in FALS, have a toxic gain of function related to the expression of the mutant SOD1 gene (*170*, *171*). The $SOD1^{G93A}$ mice display many of the biochemical, clinical and pathological features of both familial and sporadic ALS in humans. Given the similar pathology between sporadic and familial human and transgenic murine diseases, the transgenic $SOD1^{G93A}$ animals are often the first model system in which potential ALS therapies are tested (*172–174*).

Oxidative stress plays a prominent role in ALS pathology (*175–178*). There is also abundant evidence of excess ROS/RNS and their associated damage to DNA, RNA, lipids and proteins in $SOD1^{G93A}$ mice (*179–184*). Mitochodrial dysfunction (*185*, *186*) and glutamatergic excitotoxicity (*187*, *188*) are putative sources of oxidative stress. Furthermore, dysregulation in the Rac/Nox pathway leading to redox dysregulation is also linked to $SOD1^{G93A}$ mice (*189*) as are defects in redox regulated-tumor protein1, ubiquitin carboxyl-terminal hydrolase isoenzyme L1, and αB crystallin (*190*). Antioxidant drugs have shown some efficacy in animal studies of ALS (*191–197*). In addition, a meta-analysis of multiple preclinical drug trials indicates that drugs with combined anti-inflammatory and anti-oxidant properties are among the most promising candidates for further investigation in ALS (*198*). There is still no cure or treatment today that halts or reverses ALS (*198*). There is one FDA approved drug, riluzole, that modestly slows the progression of ALS (*197*). Riluzole interferes with glutamatergic neurotransmission and might therefore mitigate downstream ROS production by reducing excitotoxicity (*187*).

CeNPs mimic the activity of both catalase and superoxide dismutase (*59–62*) and, therefore, may have therapeutic value for those suffering from ALS. A number of compounds have been shown to be effective in animal models of ALS. Unfortunately, with the lone exception of rizuole, all have shown poor translation to human clinical trials (*196*, *198*). These disappointing results may be tied to the pharmacology of the drugs. For example, the drugs may not adequately penetrate the human blood-brain-barrier, they may not target the proper human nervous system tissue, or, even if they succeed in reaching the proper target, they may be unable to sustain their therapeutic effectiveness for a sufficient length of time. The poor translation from animal model to human trials may also be related to poor experimental design. ALS animal model studies have endured a number of criticisms ranging from their failure to use age- and litter-matched animals,

Publication Date (Web): October 13, 2015 | doi: 10.1021/bk-2015-1200.ch018

Publication Date (Web): October 13, 2015 | doi: 10.1021/bk-2015-1200.ch018

to their failure to use the proper statistical models when analyzing mortality data, to a publication bias toward studies with positive results (*198–200*). As a means to improve the translational power of animal studies in ALS, a set of consensus guidelines for preclinical testing in ALS was developed (*199*). Abiding by these guidelines, we have assessed the therapeutic efficacy of CeNPs in a mouse model of ALS. Specifically we tested the hypothesis that treatment with CeNPs (20 mg/kg, injected twice a week through the tail vein), begun at the onset of motor weakness, would protect $SOD1^{G93A}$ transgenic mice from further muscle weakness and, ultimately, prolong their survival. Motor function was monitored by measuring the latency to fall from a hanging wire grip strength test. The overall decline in forelimb grip strength averaged across the first 25 days of treatment was significantly worse in control animals compared to the mice treated with CeNPs (Figure 5). Further, Kaplan-Meier analysis indicated that $SOD1^{G93A}$ mice receiving CeNPs from the onset of motor signs survived significantly longer than the control animals (DeCoteau et al., in preparation). Together, these results suggest CeNPs hold promise as an anti-oxidant therapy for the treatment of ALS and other neurodegenerative disorders.

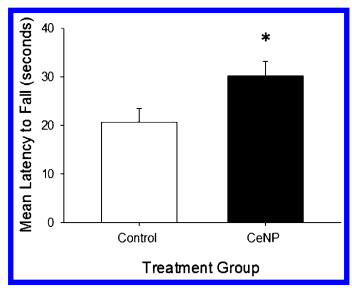

*Figure 5. Cerium oxide nanoparticles ameliorate motor deficits in $SOD1^{G93A}$ mice. Motor strength was assessed by measuring the latency to fall from a hanging wire apparatus. Decreases in hanging wire performance marked the onset of disease for individual mice. CeNPs (20 mg/kg, n= 20) or vehicle control (n=27) treatment was delivered intravenously at disease onset and twice weekly thereafter. Mean latency to fall from the hanging wire apparatus was calculated for the first 25 days of treatment. A T-test for ranks revealed a significant difference between treatment groups (*p=0.031). Error bars reflect the standard error of the mean.*

Conclusions

Cerium oxide nanoparticles have many properties that make them potentially useful for treating neurodegenerative diseases. They display both catalase- and superoxide dismutase-mimetic activities and are able to neutralize many different types of ROS/RNS without promiscuous oxidation of important cellular constituents. CeNPs are not consumed in the process of neutralizing ROS/RNS because the ceria atoms can cycle between Ce^{3+} and Ce^{4+} states depending on the redox conditions. Their small size also facilitates the crossing of biological

barriers. Despite these advantageous characteristics, there are mixed reports in the literature regarding the biological effects of CeNPs; they have been reported to be helpful antioxidants in some cases but also mediators of toxicity in others. As outlined in this review, a multitude of factors could be at the root of these disparate reports. In particular, it is important to recognize that the synthetic identity of the particle is not necessarily the same as the biological identity. That is, the properties of the particles measured in vitro (e.g., size, zeta potential, enzymatic activity) could change under physiological conditions due to particle agglomeration and/or adsorption of proteins onto the particle surface. Addition of a stabilizer (such as citric acid) can limit agglomeration, but the this stabilizer can change or even be lost in physiological milieu. Moreover, the proteins that adsorb onto the particle surface can profoundly influence the pharmacokinetics of the particle such that CeNP biodistribution and clearance can be completely different even if the core particle (cerium oxide) remains the same. This could subsequently influence whether or not the particles reach their intended target site or have off-target effects (e.g., accumulate in reticuloendothelial organs or provoke an immune response). An important implication of these findings is that experiments in reduced biological preparations (cell culture) or in model systems such as zebrafish and *C. elegans* may not necessarily recapitulate the effects of CeNPs in an intact rodent (or ultimately in humans), as multiple biological barriers with varying protein composition must be crossed to reach the intended target (i.e., the nervous system). Although some recent studies have shed insight into factors that influence the protein fingerprint of nanoparticles, there are currently no unifying principles for predicting the proteins that comprise these fingerprints nor their ultimate effect on nanoparticle pharmacokinetics. Despite this seemingly unsurmoutable experimental barriers, we have seen success of our citric acid-EDTA stabilized 2.5 nm CeNPs in rodent models of MS and ALS. However, further progress in this field will require an iterative analysis of how the biological identity of CeNPs changes upon traversing distinct biological environments and then coupling this information to the biological efficacy or toxicity of such particles in intact animals.

Publication Date (Web): October 13, 2015 | doi: 10.1021/bk-2015-1200.ch018

References

1. Bogeski, I.; Niemeyer, B. A. *Antioxid. Redox Signaling* **2014**, *21*, 859–862.
2. Nathan, C.; Cunningham-Bussel, A. *Nat. Rev. Immunol.* **2013**, *13*, 349–361.
3. Forman, H. J.; Ursini, F.; Maiorino, M. *J. Mol. Cell. Cardiol.* **2014**, *73*, 2–9.
4. Nishida, M.; Sawa, T.; Kitajima, N.; Ono, K.; Inoue, H.; Ihara, H.; Motohashi, H.; Yamamoto, M.; Suematsu, M.; Kurose, H.; van der Vliet, A.; Freeman, B. A.; Shibata, T.; Uchida, K.; Kumagai, Y.; Akaike, T. *Nat. Chem. Biol.* **2012**, *8*, 714–724.
5. Kamata, H.; Hirata, H. *Cell. Signaling* **1999**, *11*, 1–14.
6. Nathan, C.; Ding, A. *Cell* **2010**, *140*, 951–951.e2.
7. Cross, A. R.; Jones, O. T. *Biochim. Biophys. Acta* **1991**, *1057*, 281–298.
8. Haddad, J. J. *Cell. Signaling* **2002**, *14*, 879–897.
9. Turpaev, K. T. *Biochemistry (Moscow)* **2002**, *67*, 281–292.

10. Green, R. M.; Graham, M.; O'Donovan, M. R.; Chipman, J. K.; Hodges, N. J. *Mutagenesis* **2006**, *21*, 383–390.
11. Rahman, I.; Marwick, J.; Kirkham, P. *Biochem. Pharmacol.* **2004**, *68*, 1255–1267.
12. England, K.; Cotter, T. G. *Redox Report* **2005**, *10*, 237–245.
13. Trachootham, D.; Lu, W.; Ogasawara, M. A.; Valle, N. R.; Huang, P. *Antioxid. Redox Signaling* **2008**, *10*, 1343–1374.
14. Feng, W.; Liu, G.; Allen, P. D.; Pessah, I. N. *J. Biol. Chem.* **2000**, *275*, 35902–35907.
15. Karisch, R.; Fernandez, M.; Taylor, P.; Virtanen, C.; St-Germain, J.; Jin, L. L.; Harris, I. S.; Mori, J.; Mak, T. W.; Senis, Y. A.; Östman, A.; Moran, M. F.; Neel, B. G. *Cell* **2011**, *146*, 826–840.
16. Figueira, T. R.; Barros, M. H.; Camargo, A. A.; Castilho, R. F.; Ferreira, J. C. B.; Kowaltowski, A. J.; Sluse, F. E.; Souza-Pinto, N.; Vercesi, A. E. *Antioxid. Redox Signaling* **2013**, *18*, 2029–2074.
17. Wang, X.; Michaelis, E. K. *Front. Aging Neurosci.* **2010**, *2*, 12.
18. Cadenas, E.; Davies, K. J. A. *Free Radical Biol. Med.* **2000**, *29*, 222–230.
19. Balaban, R. S.; Nemoto, S.; Finkel, T. *Cell* **2005**, *120*, 483–495.
20. Fischer, M. T.; Sharma, R.; Lim, J. L.; Haider, L.; Frischer, J. M.; Drexhage, J.; Mahad, D.; Bradl, M.; van Horssen, J.; Lassmann, H. *Brain* **2012**, *135*, 886–899.
21. Jiang, F.; Zhang, Y.; Dusting, G. J. *Pharmacol. Rev.* **2011**, *63*, 218–242.
22. Aguirre, J.; Lambeth, J. D. *Free Radical Biol. Med.* **2010**, *49*, 1342–1353.
23. Lambeth, J. D. *Nat. Rev. Immunol.* **2004**, *4*, 181–189.
24. Imlay, J. A. *Annu. Rev. Biochem.* **2008**, *77*, 755–776.
25. Leto, T. L.; Morand, S.; Hurt, D.; Ueyama, T. *Antioxid. Redox Signaling* **2009**, *11*, 2607–2619.
26. Lenaz, G. In *Advances in Experimental Medicine and Biology*; Scatena, R., Bottoni, P., Giardina, B., Eds.; Springer: 2012; Vol. 942, pp 93−136.
27. Lin, H.; Chen, S.; Wu, H.; Hsu, H.; Chen, M.; Lee, Y.; Wu, K.; Chien, K. *Int. J. Cardiol.* **2015**, *183*, 214–220.
28. Rodrigo, R.; Fernandez-Gajardo, R.; Gutierrez, R.; Matamala, J. M.; Carrasco, R.; Miranda-Merchak, A.; Feuerhake, W. *CNS Neurol. Disord.: Drug Targets* **2013**, *12*, 698–714.
29. Gao, H.; Zhou, H.; Hong, J. *Trends Pharmacol. Sci.* **2012**, *33*, 295–303.
30. Zhou, C.; Huang, Y.; Przedborski, S. *Ann. N. Y. Acad. Sci.* **2008**, *1147*, 93–104.
31. Stranahan, A. M.; Mattson, M. P. *Neural Plast.* **2010**, *2010*, 108190.
32. Ascherio, A.; Weisskopf, M. G.; O'Reilly, E. J.; Jacobs, E. J.; McCullough, M. L.; Calle, E. E.; Cudkowicz, M.; Thun, M. J. *Ann. Neurol.* **2005**, *57*, 104–110.
33. Sano, M.; Ernesto, C.; Thomas, R. G.; Klauber, M. R.; Schafer, K.; Grundman, M.; Woodbury, P.; Growdon, J.; Cotman, C. W.; Pfeiffer, E.; Schneider, L. S.; Thal, L. J. *N. Engl. J. Med.* **1997**, *336*, 1216–1222.
34. Morris, M. C.; Beckett, L. A.; Scherr, P. A.; Hebert, L. E.; Bennett, D. A.; Field, T. S.; Evans, D. A. *Alzheimer Dis. Assoc. Disord.* **1998**, *12*, 121–126.

Publication Date (Web): October 13, 2015 | doi: 10.1021/bk-2015-1200.ch018

35. Kieburtz, K.; McDermott, M.; Como, P.; Growdon, J.; Brady, J.; Carter, J.; Huber, S.; Kanigan, B.; Landow, E.; Rudolph, A. *Neurology* **1994**, *44*, 1756–1759.
36. Shoulson, I. *Ann. Neurol.* **1998**, *44*, S160–6.
37. Zhang, S. M.; Hernan, M. A.; Chen, H.; Spiegelman, D.; Willett, W. C.; Ascherio, A. *Neurology* **2002**, *59*, 1161–1169.
38. Luchsinger, J. A.; Tang, M. X.; Shea, S.; Mayeux, R. *Arch. Neurol.* **2003**, *60*, 203–208.
39. Zandi, P. P.; Anthony, J. C.; Khachaturian, A. S.; Stone, S. V.; Gustafson, D.; Tschanz, J. T.; Norton, M. C.; Welsh-Bohmer, K. A.; Breitner, J. C. *Arch. Neurol.* **2004**, *61*, 82–88.
40. Yaffe, K.; Clemons, T. E.; McBee, W. L.; Lindblad, A. S. *Neurology* **2004**, *63*, 1705–1707.
41. Desnuelle, C.; Dib, M.; Garrel, C.; Favier, A. *Amyotrophic Lateral Scler. Other Mot. Neuron Disord.* **2001**, *2*, 9–18.
42. Graf, M.; Ecker, D.; Horowski, R.; Kramer, B.; Riederer, P.; Gerlach, M.; Hager, C.; Ludolph, A. C.; Becker, G.; Osterhage, J.; Jost, W. H.; Schrank, B.; Stein, C.; Kostopulos, P.; Lubik, S.; Wekwerth, K.; Dengler, R.; Troeger, M.; Wuerz, A.; Hoge, A.; Schrader, C.; Schimke, N.; Krampfl, K.; Petri, S.; Zierz, S.; Eger, K.; Neudecker, S.; Traufeller, K.; Sievert, M.; Neundorfer, B.; Hecht, M. *J. Neural Transm.* **2005**, *112*, 649–660.
43. Steinhubl, S. R. *Am. J. Cardiol.* **2008**, *101*, S14–S19.
44. Kamat, C. D.; Gadal, S.; Mhatre, M.; Williamson, K. S.; Pye, Q. N.; Hensley, K. *J. Alzheimer's Dis.* **2008**, *15*, 473–493.
45. Saso, L.; Firuzi, O. *Curr. Drug Targets* **2014**, *15*, 1177–1199.
46. Danta, C. C.; Piplani, P. *Expert Opin. Drug Discovery* **2014**, *9*, 1205–1222.
47. Kim, B. Y. S.; Rutka, J. T.; Chan, W. C. W. *N. Engl. J. Med.* **2010**, *363*, 2434–2443.
48. Martin, R.; Menchon, C.; Apostolova, N.; Victor, V. M.; Alvaro, M.; Herance, J. R.; Garcia, H. *ACS Nano* **2010**, *4*, 6957–6965.
49. Nie, Z.; Petukhova, A.; Kumacheva, E. *Nat. Nanotechnol.* **2010**, *5*, 15–25.
50. Wang, J.; Byrne, J. D.; Napier, M. E.; DeSimone, J. M. *Small* **2011**, *7*, 1919–1931.
51. Lavik, E.; von Recum, H. *ACS Nano* **2011**, *5*, 3419–3424.
52. Scharf, A.; Piechulek, A.; von Mikecz, A. *ACS Nano* **2013**, *7*, 10695–10703.
53. Powers, C. M.; Slotkin, T. A.; Seidler, F. J.; Badireddy, A. R.; Padilla, S. *Neurotoxicol. Teratol.* **2011**, *33*, 708–714.
54. Joris, F.; Manshian, B. B.; Peynshaert, K.; De Smedt, S. C.; Braeckmans, K.; Soenen, S. J. *Chem. Soc. Rev.* **2013**, *42*, 8339–8359.
55. Schubert, D.; Dargusch, R.; Raitano, J.; Chan, S. W. *Biochem. Biophys. Res. Commun.* **2006**, *342*, 86–91.
56. Estevez, A. Y.; Pritchard, S.; Harper, K.; Aston, J. W.; Lynch, A.; Lucky, J. J.; Ludington, J. S.; Chatani, P.; Mosenthal, W. P.; Leiter, J. C.; Andreescu, S.; Erlichman, J. S. *Free Radical Biol. Med.* **2011**, *51*, 1155–1163.
57. Chen, J.; Patil, S.; Seal, S.; McGinnis, J. F. *Nat. Nanotechnol.* **2006**, *1*, 142–150.

Publication Date (Web): October 13, 2015 | doi: 10.1021/bk-2015-1200.ch018

58. Heckman, K. L.; DeCoteau, W.; Estevez, A.; Reed, K. J.; Costanzo, W.; Sanford, D.; Leiter, J. C.; Clauss, J.; Knapp, K.; Gomez, C.; Mullen, P.; Rathbun, E.; Prime, K.; Marini, J.; Patchefsky, J.; Patchefsky, A. S.; Hailstone, R. K.; Erlichman, J. S. *ACS Nano* **2013**, *7*, 10582–10596.
59. Korsvik, C.; Patil, S.; Seal, S.; Self, W. T. *Chem. Commun. (Cambridge)* **2007** (10), 1056–1058.
60. Heckert, E. G.; Seal, S.; Self, W. T. *Environ. Sci. Technol.* **2008**, *42*, 5014–5019.
61. Pirmohamed, T.; Dowding, J. M.; Singh, S.; Wasserman, B.; Heckert, E.; Karakoti, A. S.; King, J. E.; Seal, S.; Self, W. T. *Chem. Commun. (Cambridge)* **2010**, *46*, 2736–2738.
62. Lee, S. S.; Song, W.; Cho, M.; Puppala, H. L.; Nguyen, P.; Zhu, H.; Segatori, L.; Colvin, V. L. *ACS Nano* **2013**, *7*, 9693–9703.
63. Karakoti, A.; Singh, S.; Dowding, J. M.; Seal, S.; Self, W. T. *Chem. Soc. Rev.* **2010**, *39*, 4422–4432.
64. Reed, K.; Cormack, A.; Kulkarni, A.; Mayton, M.; Sayle, D.; Klaessig, F.; Stadler, B. *Environ. Sci.: Nano* **2014**, *1*, 390–405.
65. Nolan, M.; Parker, S. C.; Watson, G. W. *Phys. Chem. Chem. Phys.* **2006**, *8*, 216–218.
66. Heckert, E. G.; Karakoti, A. S.; Seal, S.; Self, W. T. *Biomaterials* **2008**, *29*, 2705–2709.
67. Karakoti, A. S.; Monteiro-Riviere, N. A.; Aggarwal, R.; Davis, J. P.; Narayan, R. J.; Self, W. T.; McGinnis, J.; Seal, S. *JOM (1989)* **2008**, *60*, 33–37.
68. Lee, C. W.; Chen, Y. C.; Ostafin, A. *J. Biomed. Nanotechnol.* **2009**, *5*, 477–485.
69. Mailer, K.; Del Maestro, R. F. *Mol. Cell. Biochem.* **1991**, *107*, 47–54.
70. Ward, R. J.; Kest, W.; Bruyeer, P.; Lallemand, F.; De Witte, P. *Alcohol Alcohol.* **2001**, *36*, 39–43.
71. Ganesana, M.; Erlichman, J. S.; Andreescu, S. *Free Radical Biol. Med.* **2012**, *53*, 2240–2249.
72. Alper, G.; Sozmen, E. Y.; Kanit, L.; Mentes, G.; Ersoz, B.; Kutay, F. *Turk. J. Med. Sci.* **1998**, *28*, 491–494.
73. Khan, J. Y.; Black, S. M. *Pediatr. Res.* **2003**, *54*, 77–82.
74. Estevez, A. Y.; Erlichman, J. S. *Nanomedicine* **2014**, *9*, 1437–1440.
75. Walkey, C.; Das, S.; Seal, S.; Erlichman, J.; Heckman, K.; Ghibelli, L.; Traversa, E.; McGinnis, J. F.; Self, W. T. *Environ. Sci.: Nano* **2015**, *2*, 33–53.
76. Lundqvist, M.; Stigler, J.; Elia, G.; Lynch, I.; Cedervall, T.; Dawson, K. A. *Proc. Natl. Acad. Sci. U.S.A.* **2008**, *105*, 14265–14270.
77. Monopoli, M. P.; Aberg, C.; Salvati, A.; Dawson, K. A. *Nat. Nanotechnol.* **2012**, *7*, 779–786.
78. Lynch, I.; Dawson, K. A. *Nano Today* **2008**, *3*, 40–47.
79. Albanese, A.; Tang, P. S.; Chan, W. C. W. *Annu. Rev. Biomed. Eng.* **2012**, *14*, 1–16.
80. Gao, H.; He, Q. *Expert Opin. Drug Delivery* **2014**, *11*, 409–420.
81. Huang, R.; Carney, R. P.; Ikuma, K.; Stellacci, F.; Lau, B. L. T. *ACS Nano* **2014**, *8*, 5402–5412.

Publication Date (Web): October 13, 2015 | doi: 10.1021/bk-2015-1200.ch018

Publication Date (Web): October 13, 2015 | doi: 10.1021/bk-2015-1200.ch018

82. Cho, E. C.; Xie, J.; Wurm, P. A.; Xia, Y. *Nano Lett.* **2009**, *9*, 1080–1084.
83. Yuan, H.; Li, J.; Bao, G.; Zhang, S. *Phys. Rev. Lett.* **2010**, *105*, 138101.
84. Hirsch, V.; Kinnear, C.; Moniatte, M.; Rothen-Rutishauser, B.; Clift, M. J. D.; Fink, A. *Nanoscale* **2013**, *5*, 3723–3732.
85. Walkey, C. D.; Olsen, J. B.; Song, F.; Liu, R.; Guo, H.; Olsen, D. W.; Cohen, Y.; Emili, A.; Chan, W. C. W. *ACS Nano* **2014**, *8*, 2439–2455.
86. Walkey, C. D.; Olsen, J. B.; Guo, H.; Emili, A.; Chan, W. C. W. *J. Am. Chem. Soc.* **2012**, *134*, 2139–2147.
87. Yokel, R. A.; Florence, R. L.; Unrine, J. M.; Tseng, M. T.; Graham, U. M.; Wu, P.; Grulke, E. A.; Sultana, R.; Hardas, S. S.; Butterfield, D. A. *Nanotoxicology* **2009**, *3*, 234–248.
88. Hardas, S. S.; Butterfield, D. A.; Sultana, R.; Tseng, M. T.; Dan, M.; Florence, R. L.; Unrine, J. M.; Graham, U. M.; Wu, P.; Grulke, E. A.; Yokel, R. A. *Toxicol. Sci.* **2010**, *116*, 562–576.
89. Kong, L.; Cai, X.; Zhou, X.; Wong, L. L.; Karakoti, A. S.; Seal, S.; McGinnis, J. F. *Neurobiol. Dis.* **2011**, *42*, 514–523.
90. Yokel, R. A.; Au, T. C.; MacPhail, R.; Hardas, S. S.; Butterfield, D. A.; Sultana, R.; Goodman, M.; Tseng, M. T.; Dan, M.; Haghnazar, H.; Unrine, J. M.; Graham, U. M.; Wu, P.; Grulke, E. A. *Toxicol. Sci.* **2012**, *127*, 256–268.
91. Rodriguez, P. L.; Harada, T.; Christian, D. A.; Pantano, D. A.; Tsai, R. K.; Discher, D. E. *Science* **2013**, *339*, 971–975.
92. Dan, M.; Wu, P.; Grulke, E. A.; Graham, U. M.; Unrine, J. M.; Yokel, R. A. *Nanomedicine (London)* **2012**, *7*, 95–110.
93. Karakoti, A. S.; Singh, S.; Kumar, A.; Malinska, M.; Kuchibhatla, S. V. N. T.; Wozniak, K.; Self, W. T.; Seal, S. *J. Am. Chem. Soc.* **2009**, *131*, 14144–14145.
94. Longmire, M.; Choyke, P. L.; Kobayashi, H. *Nanomedicine* **2008**, *3*, 703–717.
95. Sarin, H. *J. Angiog. Res.* **2010**, *2*, 14-2384–2-14.
96. Frohlich, E. *Int. J. Nanomed.* **2012**, *7*, 5577–5591.
97. Verma, A.; Stellacci, F. *Small* **2010**, *6*, 12–21.
98. Han, H.; Martin, J. D.; Lee, J.; Harris, D. K.; Fukumura, D.; Jain, R. K.; Bawendi, M. *Angew. Chem., Int. Ed.* **2012**, *52*, 1414–1419.
99. Ding, H.; Ma, Y. *Small* **2015**, *11*, 1055–1071.
100. Patil, S.; Sandberg, A.; Heckert, E.; Self, W.; Seal, S. *Biomaterials* **2007**, *28*, 4600–4607.
101. Singh, S.; Kumar, A.; Karakoti, A.; Seal, S.; Self, W. T. *Mol. BioSyst.* **2010**, *6*, 1813–1820.
102. Asati, A.; Santra, S.; Kaittanis, C.; Perez, J. M. *ACS Nano* **2010**, *4*, 5321–5331.
103. Dowding, J. M.; Das, S.; Kumar, A.; Dosani, T.; McCormack, R.; Gupta, A.; Sayle, T. X. T.; Sayle, D. C.; von Kalm, L.; Seal, S.; Self, W. T. *ACS Nano* **2013**, *7*, 4855–4868.
104. Hirst, S. M.; Karakoti, A.; Singh, S.; Self, W.; Tyler, R.; Seal, S.; Reilly, C. M. *Environ. Toxicol.* **2013**, *28*, 107–118.
105. Doherty, G. J.; McMahon, H. T. *Annu. Rev. Biochem.* **2009**, *78*, 857–902.

106. Vercauteren, D.; Vandenbroucke, R. E.; Jones, A. T.; Rejman, J.; Demeester, J.; De Smedt, S.C.; Sanders, N. N.; Braeckmans, K. *Mol. Ther.* **2010**, *18*, 561–569.
107. Yokel, R. A.; Tseng, M. T.; Dan, M.; Unrine, J. M.; Graham, U. M.; Wu, P.; Grulke, E. A. *Nanomedicine* **2013**, *9*, 398–407.
108. Yokel, R. A.; Hussain, S.; Garantziotis, S.; Demokritou, P.; Castranova, V.; Cassee, F. R. *Environ. Sci.: Nano* **2014**, *1*, 406–428.
109. Lück, M.; Paulke, B.; Schröder, W.; Blunk, T.; Müller, R. H. *J. Biomed. Mater. Res.* **1998**, *39*, 478–485.
110. Casals, E.; Pfaller, T.; Duschl, A.; Oostingh, G. J.; Puntes, V. F. *Small* **2011**, *7*, 3479–3486.
111. Boron, W. F.; Boulpaep, E. L. In *Medical Physiology: a cellular and molecular approach*, 2nd ed.; Saunders: Philadelphia, PA, 2009; p 1352.
112. Lenaerts, V.; Nagelkerke, J. F.; Van Berkel, T. J.; Couvreur, P.; Grislain, L.; Roland, M.; Speiser, P. *J. Pharm. Sci.* **1984**, *73*, 980–982.
113. Ogawara, K.; Yoshida, M.; Higaki, K.; Kimura, T.; Shiraishi, K.; Nishikawa, M.; Takakura, Y.; Hashida, M. *J. Controlled Release* **1999**, *59*, 15–22.
114. Sadauskas, E.; Wallin, H.; Stoltenberg, M.; Vogel, U.; Doering, P.; Larsen, A.; Danscher, G. *Part Fibre Toxicol.* **2007**, *4*, 10.
115. Cho, W.; Cho, M.; Jeong, J.; Choi, M.; Cho, H.; Han, B. S.; Kim, S. H.; Kim, H. O.; Lim, Y. T.; Chung, B. H.; Jeong, J. *Toxicol. Appl. Pharmacol.* **2009**, *236*, 16–24.
116. Choi, C. H. J.; Alabi, C. A.; Webster, P.; Davis, M. E. *Proc. Natl. Acad. Sci. U.S.A.* **2010**, *107*, 1235–1240.
117. Tseng, M. T.; Lu, X.; Duan, X.; Hardas, S. S.; Sultana, R.; Wu, P.; Unrine, J. M.; Graham, U.; Butterfield, D. A.; Grulke, E. A.; Yokel, R. A. *Toxicol. Appl. Pharmacol.* **2012**, *260*, 173–182.
118. Heckman, K. L.; DeCoteau, W.; Estevez, A.; Reed, K. J.; Costanzo, W.; Sanford, D.; Leiter, J. C.; Clauss, J.; Knapp, K.; Gomez, C.; Mullen, P.; Rathbun, E.; Prime, K.; Marini, J.; Patchefsky, J.; Patchefsky, A. S.; Hailstone, R. K.; Erlichman, J. S. *ACS Nano* **2013**, *7*, 10582–10596.
119. Dobrovolskaia, M. A.; McNeil, S. E. *Nat. Nanotechnol* **2007**, *2*, 469–478.
120. Cho, W. S.; Duffin, R.; Poland, C. A.; Howie, S. E.; MacNee, W.; Bradley, M.; Megson, I. L.; Donaldson, K. *Environ. Health Perspect.* **2010**, *118*, 1699–1706.
121. Ma, J. Y.; Zhao, H.; Mercer, R. R.; Barger, M.; Rao, M.; Meighan, T.; Schwegler-Berry, D.; Castranova, V.; Ma, J. K. *Nanotoxicology* **2011**, *5*, 312–325.
122. Nalabotu, S. K.; Kolli, M. B.; Triest, W. E.; Ma, J. Y.; Manne, N. D.; Katta, A.; Addagarla, H. S.; Rice, K. M.; Blough, E. R. *Int. J. Nanomed.* **2011**, *6*, 2327–2335.
123. Srinivas, A.; Rao, P. J.; Selvam, G.; Murthy, P. B.; Reddy, P. N. *Toxicol. Lett.* **2011**, *205*, 105–115.
124. Ma, J. Y.; Mercer, R. R.; Barger, M.; Schwegler-Berry, D.; Scabilloni, J.; Ma, J. K.; Castranova, V. *Toxicol. Appl. Pharmacol.* **2012**, *262*, 255–264.
125. Raphael, I.; Nalawade, S.; Eagar, T. N.; Forsthuber, T. G. *Cytokine* **2014**.

Publication Date (Web): October 13, 2015 | doi: 10.1021/bk-2015-1200.ch018

126. Oh, S. A.; Li, M. O. *J. Immunol.* **2013**, *191*, 3973–3979.
127. Xia, T.; Kovochich, M.; Liong, M.; Madler, L.; Gilbert, B.; Shi, H.; Yeh, J. I.; Zink, J. I.; Nel, A. E. *ACS Nano* **2008**, *2*, 2121–2134.
128. Mildner, A.; Jung, S. *Immunity* **2014**, *40*, 642–656.
129. Schanen, B. C.; Das, S.; Reilly, C. M.; Warren, W. L.; Self, W. T.; Seal, S.; Drake, D. R., 3rd. *PLoS One* **2013**, *8*, e62816.
130. Ban, M.; Langonne, I.; Huguet, N.; Guichard, Y.; Goutet, M. *Toxicol. Lett.* **2013**, *216*, 31–39.
131. Shen, C. C.; Wang, C. C.; Liao, M. H.; Jan, T. R. *Int. J. Nanomed.* **2011**, *6*, 1229–1235.
132. Kochanek, K. D.; Murphy, S. L.; Xu, J. Q.; Arias, E. *NCHS Data Brief*; Centers for Disease Control and Prevention: 2014; Vol. 178.
133. Estevez, A. Y.; Erlichman, J. S. In *Oxidative Stress: Diagnostics, Prevention and Therapy*; Andreescu, E. S., Hempel, M., Eds.; American Chemical Society: 2011; Vol. 1083, pp 255−288.
134. Saver, J. L. *Stroke* **2006**, *37*, 263–266.
135. Manzanero, S.; Santro, T.; Arumugam, T. V. *Neurochem. Int.* **2013**, *62*, 712–718.
136. Thiel, A.; Heiss, W. D. *Stroke* **2011**, *42*, 507–512.
137. Nayernia, Z.; Jaquet, V.; Krause, K. H. *Antioxid. Redox Signaling* **2014**, *20*, 2815–2837.
138. Thompson, B. J.; Ronaldson, P. T. *Adv. Pharmacol.* **2014**, *71*, 165–202.
139. Wilde, G. J. C.; Pringle, A. K.; Wright, P.; Iannotti, F. *J. Neurochem.* **1997**, *69*, 883–886.
140. Vornov, J. J.; Park, J.; Thomas, A. G. *Exp. Neurol.* **1998**, *149*, 109–122.
141. Sarnowska, A. *Folia Neuropathol.* **2002**, *40*, 101–106.
142. Wang, X.; Pal, R.; Chen, X.; Limpeanchob, N.; Kumar, K. N.; Michaelis, E. K. *Mol. Brain Res.* **2005**, *140*, 120–126.
143. Ouyang, Y.; Voloboueva, L. A.; Xu, L.; Giffard, R. G. *J. Neurosci.* **2007**, *27*, 4253–4260.
144. Weiner, H. L. *Ann. Neurol.* **2009**, *65*, 239–248.
145. Zeller, D.; Classen, J. *Neuroscience* **2014**, *283*, 222–230.
146. Rocca, M. A.; Amato, M. P.; De Stefano, N.; Enzinger, C.; Geurts, J. J.; Penner, I. K.; Rovira, A.; Sumowski, J. F.; Valsasina, P.; Filippi, M. *Lancet Neurol.* **2015**, *14*, 302–317.
147. Lassmann, H. *J. Neurol. Sci.* **2013**, *333*, 1–4.
148. Sawcer, S.; Franklin, R. J.; Ban, M. *Lancet Neurol.* **2014**, *13*, 700–709.
149. Acheson, E. D.; Bachrach, C. A.; Wright, F. M. *Acta Psychiatr. Scand. Suppl.* **1960**, *35*, 132–147.
150. Chastain, E. M.; Miller, S. D. *Immunol. Rev.* **2012**, *245*, 227–238.
151. Gonzalez, H.; Pacheco, R. *J. Neuroinflammation* **2014**, *11*, 201-014–0201-8.
152. Iwanowski, P.; Losy, J. *J. Neurol. Sci.* **2015**, *349*, 10–14.
153. Raivich, G.; Banati, R. B. *Brain Res. Brain Res. Rev.* **2004**, *46*, 261–281.
154. Friese, M. A.; Schattling, B.; Fugger, L. *Nat. Rev. Neurol.* **2014**, *10*, 225–238.
155. Du Pasquier, R. A.; Pinschewer, D. D.; Merkler, D. *CNS Drugs* **2014**, *28*, 535–558.

Publication Date (Web): October 13, 2015 | doi: 10.1021/bk-2015-1200.ch018

156. Kim, W.; Zandona, M. E.; Kim, S. H.; Kim, H. J. *J. Clin. Neurol.* **2015**, *11*, 9–19.
157. Duffy, S. S.; Lees, J. G.; Moalem-Taylor, G. *Mult. Scler. Int.* **2014**, *2014*, 285245.
158. Constantinescu, C. S.; Farooqi, N.; O'Brien, K.; Gran, B. *Br. J. Pharmacol.* **2011**, *164*, 1079–1106.
159. Nikic, I.; Merkler, D.; Sorbara, C.; Brinkoetter, M.; Kreutzfeldt, M.; Bareyre, F. M.; Bruck, W.; Bishop, D.; Misgeld, T.; Kerschensteiner, M. *Nat. Med.* **2011**, *17*, 495–499.
160. Aktas, O.; Waiczies, S.; Smorodchenko, A.; Dorr, J.; Seeger, B.; Prozorovski, T.; Sallach, S.; Endres, M.; Brocke, S.; Nitsch, R.; Zipp, F. *J. Exp. Med.* **2003**, *197*, 725–733.
161. Hendriks, J. J.; Alblas, J.; van der Pol, S. M.; van Tol, E. A.; Dijkstra, C. D.; de Vries, H. E. *J. Exp. Med.* **2004**, *200*, 1667–1672.
162. Moriya, M.; Nakatsuji, Y.; Miyamoto, K.; Okuno, T.; Kinoshita, M.; Kumanogoh, A.; Kusunoki, S.; Sakoda, S. *Neurosci. Lett.* **2008**, *440*, 323–326.
163. Schreibelt, G.; van Horssen, J.; van Rossum, S.; Dijkstra, C. D.; Drukarch, B.; de Vries, H. E. *Brain Res. Rev.* **2007**, *56*, 322–330.
164. Celardo, I.; De Nicola, M.; Mandoli, C.; Pedersen, J. Z.; Traversa, E.; Ghibelli, L. *ACS Nano* **2011**, *5*, 4537–4549.
165. Lord, M. S.; Jung, M.; Teoh, W. Y.; Gunawan, C.; Vassie, J. A.; Amal, R.; Whitelock, J. M. *Biomaterials* **2012**, *33*, 7915–7924.
166. Ting, S. R.; Whitelock, J. M.; Tomic, R.; Gunawan, C.; Teoh, W. Y.; Amal, R.; Lord, M. S. *Biomaterials* **2013**, *34*, 4377–4386.
167. Hirst, S. M.; Karakoti, A. S.; Tyler, R. D.; Sriranganathan, N.; Seal, S.; Reilly, C. M. *Small* **2009**, *5*, 2848–2856.
168. Barber, S. C.; Shaw, P. J. *Free Radical Biol. Med.* **2010**, *48*, 629–641.
169. Rosen, D. R.; Siddique, T.; Patterson, D.; Figlewicz, D. A.; Sapp, P.; Hentati, A.; Donaldson, D.; Goto, J.; O'Regan, J. P.; Deng, H. X. *Nature* **1993**, *362*, 59–62.
170. Robberecht, W. *J. Neurol.* **2000**, *247*, 2–6.
171. Cluskey, S.; Ramsden, D. B. *Mol. Pathol.* **2001**, *54*, 386–392.
172. Gurney, M. E.; Fleck, T. J.; Himes, C. S.; Hall, E. D. *Neurology* **1998**, *50*, 62–66.
173. Snow, R. J.; Turnbull, J.; da Silva, S.; Jiang, F.; Tarnopolsky, M. A. *Neuroscience* **2003**, *119*, 661–667.
174. Ryu, H.; Smith, K.; Camelo, S. I.; Carreras, I.; Lee, J.; Iglesias, A. H.; Dangond, F.; Cormier, K. A.; Cudkowicz, M. E.; Brown, R. H., Jr.; Ferrante, R. J. *J. Neurochem.* **2005**, *93*, 1087–1098.
175. Parakh, S.; Spencer, D. M.; Halloran, M. A.; Soo, K. Y.; Atkin, J. D. *Oxid. Med. Cell. Longevity* **2013**, *2013*, 408681.
176. Ferrante, R. J.; Browne, S. E.; Shinobu, L. A.; Bowling, A. C.; Baik, M. J.; MacGarvey, U.; Kowall, N. W.; Brown, R. H., Jr.; Beal, M. F. *J. Neurochem.* **1997**, *69*, 2064–2074.
177. Shaw, P. J.; Ince, P. G.; Falkous, G.; Mantle, D. *Ann. Neurol.* **1995**, *38*, 691–695.

In Oxidative Stress: Diagnostics, Prevention, and Therapy Volume 2; Hepel, et al.;
ACS Symposium Series; American Chemical Society: Washington, DC, 2015.

Publication Date (Web): October 13, 2015 | doi: 10.1021/bk-2015-1200.ch018

178. Shibata, N.; Nagai, R.; Uchida, K.; Horiuchi, S.; Yamada, S.; Hirano, A.; Kawaguchi, M.; Yamamoto, T.; Sasaki, S.; Kobayashi, M. *Brain Res.* **2001**, *917*, 97–104.
179. Barber, S. C.; Mead, R. J.; Shaw, P. J. *Biochim. Biophys. Acta* **2006**, *1762*, 1051–1067.
180. Beal, M. F. *Ann. Neurol.* **1995**, *38*, 357–366.
181. Goodall, E. F.; Morrison, K. E. *Expert Rev. Mol. Med.* **2006**, *8*, 1–22.
182. Reynolds, A.; Laurie, C.; Mosley, R. L.; Gendelman, H. E. *Int. Rev. Neurobiol.* **2007**, *82*, 297–325.
183. Casoni, F.; Basso, M.; Massignan, T.; Gianazza, E.; Cheroni, C.; Salmona, M.; Bendotti, C.; Bonetto, V. *J. Biol. Chem.* **2005**, *280*, 16295–16304.
184. Drechsel, D. A.; Estevez, A. G.; Barbeito, L.; Beckman, J. S. *Neurotox. Res.* **2012**, *22*, 251–264.
185. Palomo, G. M.; Manfredi, G. *Brain Res.* **2014**.
186. Vehvilainen, P.; Koistinaho, J.; Gundars, G. *Front. Cell. Neurosci.* **2014**, *8*, 126.
187. Blasco, H.; Mavel, S.; Corcia, P.; Gordon, P. H. *Curr. Med. Chem.* **2014**, *21*, 3551–3575.
188. Menon, P.; Kiernan, M. C.; Vucic, S. *Curr. Med. Chem.* **2014**, *21*, 3535–3550.
189. Carter, B. J.; Anklesaria, P.; Choi, S.; Engelhardt, J. F. *Antioxid. Redox Signaling* **2009**, *11*, 1569–1586.
190. Poon, H. F.; Hensley, K.; Thongboonkerd, V.; Merchant, M. L.; Lynn, B. C.; Pierce, W. M.; Klein, J. B.; Calabrese, V.; Butterfield, D. A. *Free Radical Biol. Med.* **2005**, *39*, 453–462.
191. Crow, J. P.; Calingasan, N. Y.; Chen, J.; Hill, J. L.; Beal, M. F. *Ann. Neurol.* **2005**, *58*, 258–265.
192. Golden, T. R.; Patel, M. *Antioxid. Redox Signaling* **2009**, *11*, 555–570.
193. Jung, C.; Rong, Y.; Doctrow, S.; Baudry, M.; Malfroy, B.; Xu, Z. *Neurosci. Lett.* **2001**, *304*, 157–160.
194. Traynor, B. J.; Bruijn, L.; Conwit, R.; Beal, F.; O'Neill, G.; Fagan, S. C.; Cudkowicz, M. E. *Neurology* **2006**, *67*, 20–27.
195. Neymotin, A.; Calingasan, N. Y.; Wille, E.; Naseri, N.; Petri, S.; Damiano, M.; Liby, K. T.; Risingsong, R.; Sporn, M.; Beal, M. F.; Kiaei, M. *Free Radical Biol. Med.* **2011**, *51*, 88–96.
196. Orrell, R. W. *Br. Med. Bull.* **2010**, *93*, 145–159.
197. Habib, A. A.; Mitsumoto, H. *Expert Opin. Emerg. Drugs* **2011**.
198. Benatar, M. Lost in translation. *Neurobiol. Dis.* **2007**, *26*, 1–13.
199. Ludolph, A. C.; Bendotti, C.; Blaugrund, E.; Chio, A.; Greensmith, L.; Loeffler, J. P.; Mead, R.; Niessen, H. G.; Petri, S.; Pradat, P. F.; Robberecht, W.; Ruegg, M.; Schwalenstocker, B.; Stiller, D.; van den Berg, L.; Vieira, F.; von Horsten, S. *Amyotrophic Lateral Scler.* **2010**, *11*, 38–45.
200. Solomon, J. A.; Tarnopolsky, M. A.; Hamadeh, M. J. *PLoS One* **2011**, *6*, e20582.

Publication Date (Web): October 13, 2015 | doi: 10.1021/bk-2015-1200.ch018

Publication Date (Web): October 13, 2015 | doi: 10.1021/bk-2015-1200.ch019

Chapter 19

Nanomaterials Induced Cell Damage

S. Bashir,[1] T. Wang,[2] Y.-P. Chen,[3] and J. Louise Liu[1,2,3,*]

[1]Chemical Biology Research Group, Texas A&M University-Kingsville, MSC 161, 700 University Blvd., Kingsville, Texas 78363, United States
[2]Department of Chemistry, Texas A&M University-Kingsville, MSC 161, 700 University Blvd., Kingsville, Texas 78363, United States
[3]Department of Chemistry, Texas A&M University, PO Box 30012, College Station, Texas 77842-3012, United States
[*]E-mail: jingbo.liu@chem.tamu.edu and kfjll00@tamuk.edu

Certain biochemical tests are necessary for high throughput evaluation of nanomaterial toxicity. Recent advances in structured or engineered surfaces on nanomaterials (NMs) have shown ultrahigh surface area and enabled rapid biochemical evaluation by using metal organic frameworks (MOFs) as biological probes in diagnosis and therapy in cells. MOFs not only offer the same advantages as colloids but also possess ultra-high surface area, biocompatibility and ultra-low doses, which can be practically applied toward treatments of diseases. To demonstrate the rapid bioassay, nitrogen monoxide (NO) was used to be a "diagnostic marker" of general cell health. These trends in NO as a function of either time (kinetic scan) or concentration in retinal pigmented epithelium (RPE) cells was compared and contrasted to more traditional bioassays such as lactate dehydrogenase (LDH), caspase or determination of reactive oxygen species (ROS). The bioassays suggest that NO can be used in cells and adopted as a global marker of toxicity for a wide variety of systems. In the current research, iron-ABBT MOFs of varying formulations were evaluated and had varying toxicities. The mechanism of toxicity was inferred using standard biomarkers, such as SN-38 (anti-topoisomerase I inhibitor), cyanide (inhibitor of cytochrome c oxidase) or sodium nitroprusside (vasodilator) and effectiveness appears to

In Oxidative Stress: Diagnostics, Prevention, and Therapy Volume 2; Hepel, et al.; ACS Symposium Series; American Chemical Society: Washington, DC, 2015.

be via oxidative stress and lesser inhibition of cell proliferation or cytochrome c oxidase.

Prelog: Nanomaterial Toxicological Science

The motivations for this book chapter are two-fold. First, the exponential boost in the applications of nanomaterials in the community and environment had led to increased awareness of the beneficial/harmful effects of nanomaterials on cells. Second are strategies or conceptual approaches required for high throughput assays; current assays are based on a standard cell or animal assays, which are usually run for 24 to 72 h to examine one biochemical metric, for example potential genotoxicity of a compound. It is interesting that in the early 1980s, a similar problem for combinatorial drug arose and was addressed in the Microtox ™ test (*1*). It had demonstrated that the test was an excellent predictor of general toxicity for all classes of compounds. The test was rapid, cheap and high throughput, although the test did not predict which specific genes/proteins were altered in cytotoxicity. A similar test, known as Mutatox™ test (*2*) was developed to assess genotoxicity in the laboratory. Both tests involved changes in microorganism absorbance/fluorescence upon addition of 'agent', whose toxicity needs to be evaluated. In the current research synopsis, changes in fluorescence of nitrogen monoxide (NO) were evaluated and compared/contrasted with other standard tests to investigate whether NO was a reliable and general predictor of agent (metal-organic framework) toxicity in retinal pigmented epithelium (RPE) cells. It is our content that this approach would provide rapid high throughput screening in any cell system capable of generating NO.

We give a very brief review of metal-organic frameworks (MOFs, section one), followed by detailed experimental protocols (in section two) of common bioassays undertaken to assess cell health are nitrogen monoxide (NO), and membrane integrity via lactate dehydrogenase (LDH). Other specific tests include the mitochondrial membrane potential (MMP) assay, assessment of the degree of apoptosis (caspase 3/7-assay), and oxidative stress using dichloro-dihydrofluorescein diacetate (CM H2DCFDA). These selective fluorescent probes were used in retinal pigmented epithelium (RPE) cell cultures with other standard chemical agents or controls such as sodium nitrite, sodium cyanide or sodium nitroprusside. The results for each bioassay using standard agents and the different MOF formulations of Iron 2-amino-3,6-bis(4-carboxyphenyl)benzoate are summarized in section three. In section four, the results are compared and contrasted, including the mode of potential cytotoxicity of the formulated MOFs in cell culture. A brief summary is given in section five and future trends/research is offered in the last section (six) followed by appropriate citations in APA format. The data was collected in our laboratory and the intent was demonstrated that where NO may be used appropriately as a high throughput marker in screening of MOFs in biological systems for initial gento-, cytotoxicity.

In Oxidative Stress: Diagnostics, Prevention, and Therapy Volume 2; Hepel, et al.;
ACS Symposium Series; American Chemical Society: Washington, DC, 2015.

Publication Date (Web): October 13, 2015 | doi: 10.1021/bk-2015-1200.ch019

Brief Introduction to Metal-Organic Frameworks in Biological Research

Publication Date (Web): October 13, 2015 | doi: 10.1021/bk-2015-1200.ch019

Metal-organic frameworks are coordinative compounds with metal nodes and organic linkers, giving rise to topologically complex structures as well as repeating three-dimensional patterns (*3*). These structures have an internal volume, which was historically used to adsorb gas molecules, such as hydrogen or carbon dioxide (*4*). However, since these materials can be designed to be a desired architecture with certain pore sizes, acidity, or affinity for water (hydrophobic/hydrophilic), it has allowed diverse uses as drug carriers or storage materials (*5*). In recent years, they have shown great potential in biomedical applications such as release of nitrogen monoxide (*6*), generation of reactive species, hyperthermia in treatment of cancer cells or slow release of anticancer or useful drugs (*7*).

For example it was shown that MOFs can store ibuprofen (greater than 1g of drug per gram of MOF) with a release time of almost one month (*8*). This approach has been extended to other therapeutic drugs related to antitumor, antiviral areas, as well as cosmetic agents. Iron trimesate has been shown to trap busulfan with a greater degree than polymers (*9*), suggesting Fe-MOFs be used in drug-delivery vehicles. Since the MOFs are three dimensional in nature with organic linkers and metal coordinative sites (*10*), MOFs have been used in imaging and therapy, a new field known as theranostics. Iron terephthalate can be modified to incorporate aminoterephthalate groups (*11*), with both anticancer and imaging properties within the framework (*12*). Other approaches include use of iron carboxylates with non-toxic paramagnetic iron, with internally bound water, in which the metals behave as Lewis acids and bound water as Lewis bases, allowing imaging to occur (*13*). MOFs have also been directly injected into animals such as rats without any toxicity and aggregation within biological fluids, although their internal stability is unknown. To increase stability, some MOFs are coated with polyethylene glycon, silica, rhodamine end groups and cyclic pent peptide (integrin) for targeting, imaging and therapy (*14*).

In summary, MOFs are a new type of highly porous materials that has numerous applications beyond pure gas storage. Due to their internally porous structure, these systems can be employed as nanocarriers of drug molecules. Due to the interconnectivity and periodicity, MOFs are crystalline, and easily characterized using X-ray crystallographic technique, which is helpful to understand the structure-property relationship. Since these systems incorporate functionalized linkers within the framework, biologically important drugs, or short peptides can also be implanted inside. The literature about their bio toxicity has not been completely studied; however, considerable reviews pointed out that MOFs can be stable in biological fluids without aggregating in the body. MOFs can release the target molecules, such as NO either quickly or slowly, with high drug loading capability, as well as potentially tagging and imaging depending on the presence of other heavy metals such as Gd or iron centers. The main structural features in MOFs needed to consider are 1) proper particle size to prevent agglomeration in biological fluids or in solution; 2) minimization of active sites on the surface to stop unwanted side reactions. This may be accomplished

In Oxidative Stress: Diagnostics, Prevention, and Therapy Volume 2; Hepel, et al.;
ACS Symposium Series; American Chemical Society: Washington, DC, 2015.

through encapsulation with polyethylene glycol; 3) ability of the MOFs to cross the blood brain barrier for biomedical treatment applications; 4) their long term toxicity in living bodies. Studies have shown that iron carboxylates are non-toxic, but it is unclear whether other metal centers or co-centers would exhibit low toxicity; and 5) stability of formulations in creams or gels that can be topically applied (e.g. hormone replacement therapy).

Experimental

Materials and Methods

All chemicals were obtained from either VWR International (Atlanta, GA) or Sigma-Aldrich (St. Louis, MO). Doubly distilled water was used in the buffers, sterilized waters in cell cultures. Other reagents not obtained from the above were:5-(and-6)-chloromethyl-2, 7-dichlorodihydrofluorescein diacetate (CM-H2DCFDA, (abbreviated as ROS) to measure reactive oxygen species (*15*), DAF-FM Diacetate (D23842, to measure NO (*16*) and Singlet Oxygen Sensor dye (S36002, for determination of singlet oxygen (*17*) were purchased from Invitrogen/Molecular Probes (Eugene, OR).Tetramethyl rhodamine methyl ester (MMP, to measure mitochondrial membrane potential (*18*), the CytoTox-ONE™ Homogeneous Membrane Integrity Assay (LDH, to determine cell viability (*19*), and the Caspase 3/7 Assay is a fluorescence assay that measures caspase-3 and -7 activities (*20*) were purchased from Promega (Madison, WI). The bicinchoninic acid assay for protein determination (*21*) was obtained from Pierce (Rockford, IL).

Cell Cultures

Human hTERT-RPE cell cultures (*22*) were maintained in a buffer consisting of essential medium with Earle's salts (Invitrogen/GIBCO Life Technologies, Inc., Carlsbad, CA) supplemented with 10% heat-inactivated fetal bovine serum, 100 units/ml penicillin, 100 μg/mL streptomycin, 1.4 mM L-glutamine, maintained at 35°C in an incubator having an atmosphere of 95% air and 5% CO_2 and 75% humidity. The cells used were in log-phase growth. The cells were examined by microscopy and a random selection of a membrane integrity assay for lactate dehydrogenase.

Bottom-Up Preparation of MOF Probes

Metal-organic framework compounds were synthesized using hydro-solvothermal methodology to obtain crystalline materials with varying geometries, depending on the metal/ ligand species, molar ratios and fabrication temperatures. The synthesis variables might introduc possibilities in terms of physical, optical,

Publication Date (Web): October 13, 2015 | doi: 10.1021/bk-2015-1200.ch019

magnetic or electrical properties. The transition metal, iron (Fe), and the organic linker, carboxyphenyl benzoate ligand were selected to crystalize our target MOFs here. The nucleation of MOF crystals occurred at elevated temperatures. The ligands are summarized in table 1 and synthesis route is summarized in figure 1. The advantages of the solvothermal synthesis approach are relatively short reaction time and lower reaction temperature.

Monitoring of nitrogen monoxide (NO), reactive oxygen species (ROS), singlet oxygen sensing (SOS), lactate dehydrogenase (LDH), mitochondrial membrane potential (MMP) and Caspase Activity

Publication Date (Web): October 13, 2015 | doi: 10.1021/bk-2015-1200.ch019

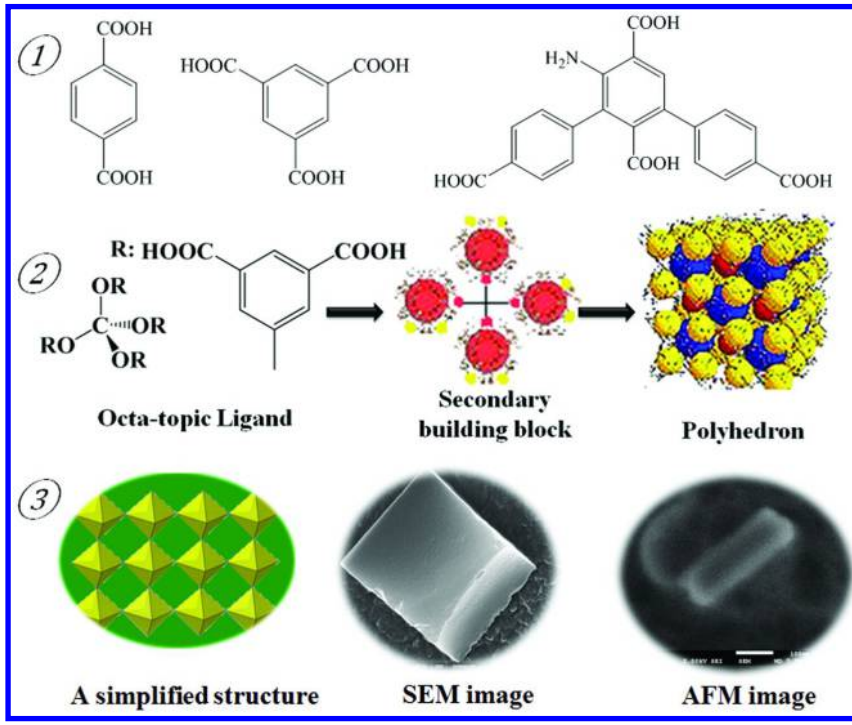

Figure 1. Schematic of metal-organicframework synthesis using flexible approach with iron (as coordinative metal) and carboxyphenyl)benzoate (as ligand) to generate a coordinative framework with defined porosity, dimension, reflectivity, permittivity and conductivity. (1) shows three selected ligands; (2) the hydro-solvothermal chemistry of MOFs synthesis; and (3) SEM images of MOF's typical morphology. (Adopted with permission from (23). Copyright (2012) American Chemical Society)

Table 1. Summary of chemical names and ligand ratios for the L-series of the MOFs evaluated for cytotoxicity.[a]

Label	*Metal (M)*	*Ligand (L)*	*Ratio (M:L)*	*IUPAC Name*
L1	Fe(III)	ABBT Ester	1:1	Iron 1,4-dimethyl-3-amino-2,5-bis(4methoxycarbonyl)phenyl]benzene-1,4-dicarboxylate (**)
L2	Fe(III)	ABBT	1:1	Iron 2-amino-3,6-bis(4-carboxyphenyl)benzoate (***)
L1′	Fe(III)	ABBT Ester	1:2	**
L2,*	Fe(III)	ABBT	1:2	***
L11	Fe(III)	ABBT Ester	1:2	**
L1"	Fe(III)	ABBT Ester	1:3	**
L12	Fe(III)	ABBT Ester	1:3	**
L11,*	Fe(III)	ABBT Ester	1:4	**
L11′	Fe(III)	ABBT Ester	1:4	**
L1,2	Fe(III)	ABBT Ester	2:1	**
L2′	Fe(III)	ABBT	2:1	***

[a] Composition formed at two broad temperatures, < 150 °C and (*) > 150 °C.

Publication Date (Web): October 13, 2015 | doi: 10.1021/bk-2015-1200.ch019

The appropriate kits were used with following manufacture protocols. Briefly to measure the protein content, the cells were harvested from the culture plate and suspended in lysis buffer, using a procedure described by Zhang (*24*). The cells were centrifuged at x1000g for 10 min at 4 °C. The resulting pellet was re suspended in phosphate buffered saline (phosphate buffered saline, (PBS), pH 7.4) to a volume ranged from 4 mL to 22 mL. The final volume was chosen to yield between 100,000 - 150,000 cells per well or measurement (*25*). For protein content determination, approximately 1:8 ratios of cells to Bradford reagent (*v/v*) were added in the dark, with bovine serum albumin (BSA) calibration (100 mg/mL-2000 mg/mL (*26*)) was added to the cuvette or 96-well plate. The samples were incubated at 37 °C for 30 min in the dark and then the absorption (Aλ=562 nm) measured. For the bioassay activity, a 1:1 v/v ratio was used between sample and reagent and fluorescence measured (*27*). For the NO (Excitationλ 495/ Emission$_{\lambda}$ 515 nm), ROS (Ex 492/ Em 517 nm), LDH (Aλ 490 nm - Aλ 680nm), SOS (Ex 504/ Em 525 nm) or MMP (Ex 549/ Em 575 nm), the samples were also added in the dark and the samples incubated for 45 minutes and fluorescence measured. For inhibitor comparison, the whole cells (WC) were resuspended in phosphate buffered saline supplemented with 8 mM pyruvate (*28*) and between 1 μM to 900 mM of the specific inhibitor or additive.

The actual concentration is stated on the graphs. Where the compounds were water soluble, they were mixed in phosphate buffered saline or deionized water, else they were mixed in dimethylsulfoxide (DMSO). The concentration of the

stock was high enough such that only 0.5-25 µL of sample was added to the whole cells, such that the volume was always less than 10% to eliminate the possibility of DMSO toxicity on the cells (*29*). The cells could be supplemented with additional 80 mM pyruvate dropped as a rich top-layer before mixing (+RL) or without (-RL).

Results

Cytotoxicity Evaluation: Lactate Dehydrogenase Assay

To investigate whether the nanomaterials or metal-organic frameworks were toxic to cells, two specific end-point experiments were carried out. One was to determine the cell membrane homogeneity using the lactate dehydrogenase as a marker of cell viability.

Lactate dehydrogenase (LDH) is an extracellular cytosolic protein which was found upon plasma membrane damage. The amount of LDH is determined by a dual enzymatic reaction between lactate (converted to pyruvate by LDH) and tetrazolium salt (INT) reduction to formazan (determined by measurement of absorbance at 490 nm, figure 2). The level of LDH in the extracellular matrix is an indicator of cell damage and indirectly cytotoxicity. In our experimental setup the reaction was prolonged by addition of pyruvate to the medium to support retinal pigment epithelium (RPE) growth and under these circumstances, a comparison between whole RPE cells (WC) without (control group) and with (experimental group) was carried out. Higher values to that of the WC control were indicative of cellular damage and cytotoxicity.

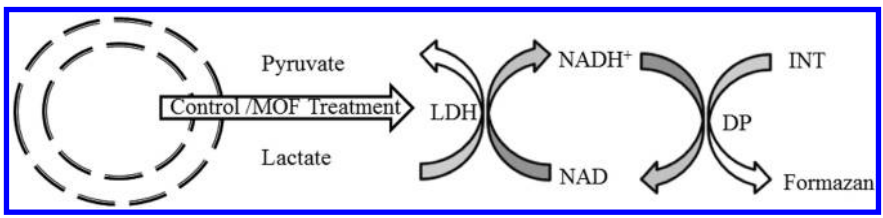

Figure 2. Schematic of lactate dehydrogenase (LDH) cytotoxicity assay mechanism generating a colorimetric product via diaphorase (DP) catalysis of 2-(4-Iodophenyl)-3-(4-nitrophenyl)-5-phenyl-2H-tetrazolium chloride (INT) reduced by nicotinamide adenine dinucleotide hydride (NADH) to cherry red formazan. (© 2015 Thermo Fisher Scientific, Inc. Used under permission. www.lifetechnologies.com)

The relationship between addition of our nanomaterials/metal-organic frameworks (NMs/MOFs) and Whole Cell (WC) without pre-conditioning (-RL) is shown in figure 3. For simplicity the NM MOFS were called there "L-series", in which various ligands to metal was varied. The numbers in brackets such as A1, E3, are the sample well locations. For example, the second column in the bar graph below represents whole cells without any additional preconditioning with 212 micromolar drug SN-38 in well E6. Also see Table 1 for name of ligands used.

Publication Date (Web): October 13, 2015 | doi: 10.1021/bk-2015-1200.ch019

Publication Date (Web): October 13, 2015 | doi: 10.1021/bk-2015-1200.ch019

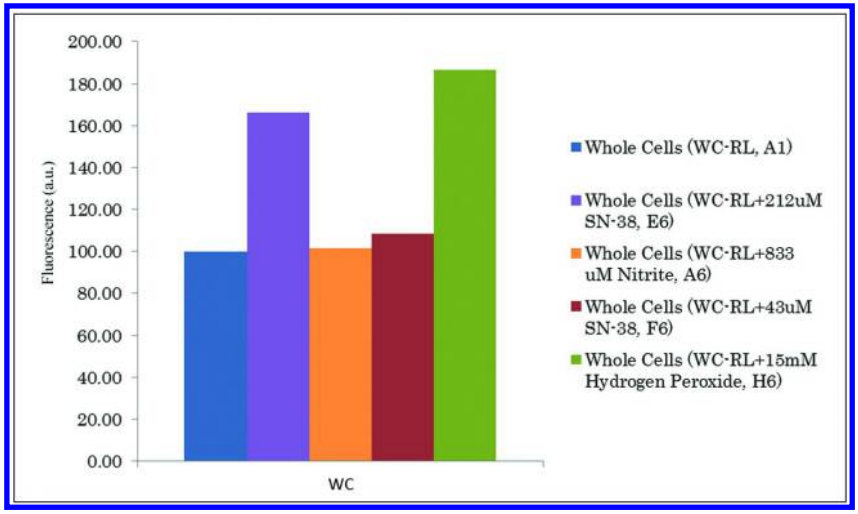

Figure 3. Measurement of Lactate dehydrogenase (LDH fluorescence, a.u.) activity difference between the normalized averages of the first readings (at 0.16 h, W 0.16 h=100%) from retinal pigment epithelium whole cells (WC) treated with various co-factors and without (-)a rich layer of supplemental pyruvate (RL).

The assay was run from 10 minutes to 14 hours (30 min data shown above) and it can be seen that most of the metal-organic framework nanomaterials (NMs) induce an equal or lower absorbance than whole cells treated with phosphate buffered saline (PBS). MOF "L2, 1:2" exhibited the lower absorbance, whilst MOF "L1, 2:1" exhibited the highest absorbance (approximately 112% relative to 100% of the control). The above results strongly suggest the NMs are not cytotoxic to RPE cells.

To put some context to the above experiments, a second comparison experiment was carried out with 7-Ethyl-10-hydroxy-camptothecin (SN-38), a topoisomerase I inhibitor used in anticancer treatment (*30*), nitrite an electron donor shown to be important in the production of nitrogen monoxide (*31*), and hydrogen peroxide, a strong oxidizer that is known to cause lipid peroxidation in cells and alteration in NO levels (*32*). Addition of higher doses of SN-38 gave rise to higher cytotoxicity, as well as hydrogen peroxide (positive control) whereas nitrite (negative control) was not cytotoxic to cells, even at high concentration (figure 4). Comparison between the figures would place the L-series of MOFs to exhibit similar cytotoxicity to low doses of SN-38.

Publication Date (Web): October 13, 2015 | doi: 10.1021/bk-2015-1200.ch019

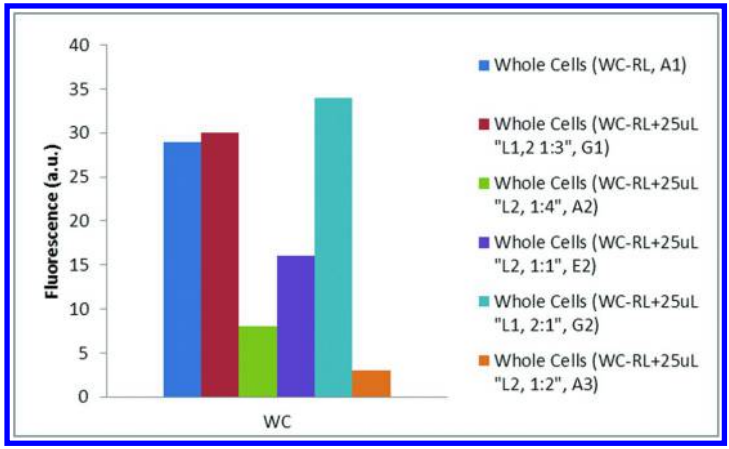

Figure 4. Measurement of Lactate dehydrogenase (LDH fluorescence, a.u.) activity difference between the normalized averages of the first readings (at 0.16 h, W 0.16 h=100%) from retinal pigment epithelium whole cells (WC) treated with various co-factors and without (-)a rich layer of supplemental pyruvate (RL) treated with various metal organic-framework-Series "L". [The numbers in brackets such as A1, E3, are the sample well locations. For example, the second column in the bar graph above represents whole cells without any additional preconditioning with 25 microliters of MOF-L2 with a metal to ligand ratio of 1:1. See Table 1 for name of ligands used.]

Cytotoxicity Evaluation: Caspase 3/7 Assay

Cellular insult or stress can induce p53 which can interact with a number of intermediates such as p53-induced protein with a death domain (PIDD (*33*)). PIDD in turn activate caspase-2, which in turn activates a pro-apoptotic protein BH3 interacting domain death agonist (BID). BID is a pro-apoptotic protein (BID (*34*)) which induces cytochrome c release from the mitochondrial to the cytoplasm. Once in the cytoplasm, cytochrome c activate caspase 3 and caspase 7 resulting in apoptosis (*35*). A simplified scheme is illustrated below in figure 5 and the basis of the bioassay in figure 6.

Figure 5. A simplified scheme where cytochrome c (Cyt c), 2'-deoxyadenosine 5'-triphosphate (dATP) allow Caspase 9 to activate Caspase 3/7 leading to cell death.

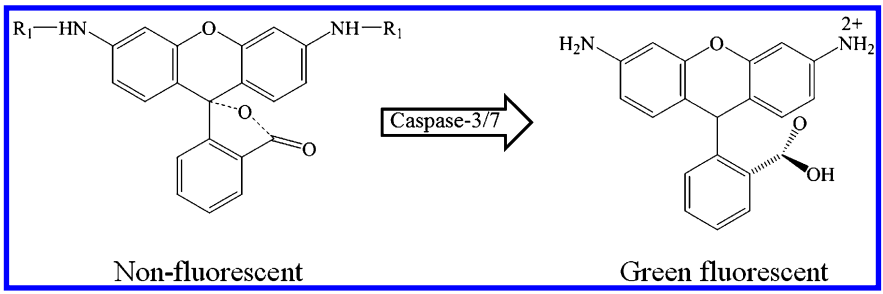

Figure 6. Cleavage of the Caspase substrate DEVD (R1) based on 3',6'-diaminospiro[2-benzofuran-1,9'-xanthene]-3-One structure, which upon excision of the dipeptide by the caspase 3/7 enzyme yields a fluorescent complex based on a [6-amino-9-(2-carboxyphenyl)-9H-xanthen-3-yl]-λ^5-azanebis(ylium) structure. The magnitude of the fluorescence from the complex is used to estimate the degree of caspase activity. (© 2015 Thermo Fisher Scientific, Inc. Used under permission. www.lifetechnologies.com)

Publication Date (Web): October 13, 2015 | doi: 10.1021/bk-2015-1200.ch019

Caspase-3/7 is cysteine and aspartic acid rich proteases that belong to a family of enzymes that regular cell death. Through addition of a pro-fluorescence substrate peptide (Asp-Glu-Val-Asp, DEVD, denoted as R1), the caspase activity can be estimated by measurement of the fluorescence by virtue of cleavage at the C-terminal side of the aspartate residue.

The LDH assay indicates level of cytotoxicity not necessarily apoptosis, whereas the caspase 3 assay is more specific to apoptosis. Both assays yield similar results suggesting that the nanomaterials do not spontaneously induce apoptosis relative to whole cells (WC) treated with PBS (figure 7).

Comparing the results with nitrite and anti-cancer drug SN-38 suggests that both induce cytotoxicity and apoptosis (figure 8). SN38 has suggested earlier by interacting with DNA (*36*) and high doses of nitrite either interfere with the bioassay or suggest that high dose of nitrogen monoxide (NO) induce cell death (*37*, *38*), with hydrogen peroxide causing immediate plasma wall oxidation and lysis (*39*).

Changes in Intracellular Nitrogen Monoxide

The high fluorescence after addition of nitrite, facilitate investigation of intracellular NO concentrations using 4,5-diaminofluorescein diacetate analog to bind to NO and form a benzotriazole compounds which is measured. The scheme is illustrated in figure 9.

Publication Date (Web): October 13, 2015 | doi: 10.1021/bk-2015-1200.ch019

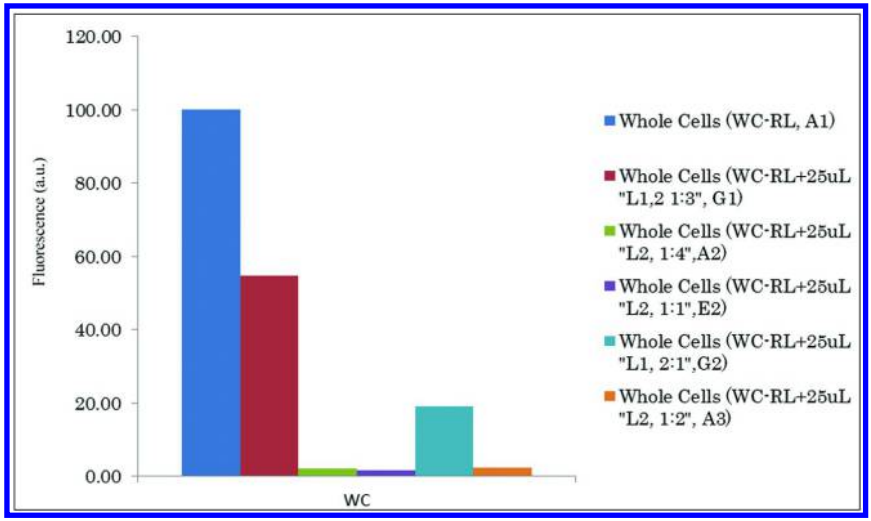

Figure 7. Measurement of Caspase 3/7 activity difference between the normalized first readings (at 0.16 h, W 0.16 h=100%) from retinal pigment epithelium whole cells (WC) treated with various co-factors and without (-)a rich layer of supplemental pyruvate (RL) treated with metal organic framework compounds-Series "L". [The number in brackets such as A1, E3, are the sample well locations, thus the second column represents whole cells without any additional preconditioning with 25 microliters of MOF-L2 with a metal to ligand ratio of 1:4. See Table 1 for name of ligands used.]

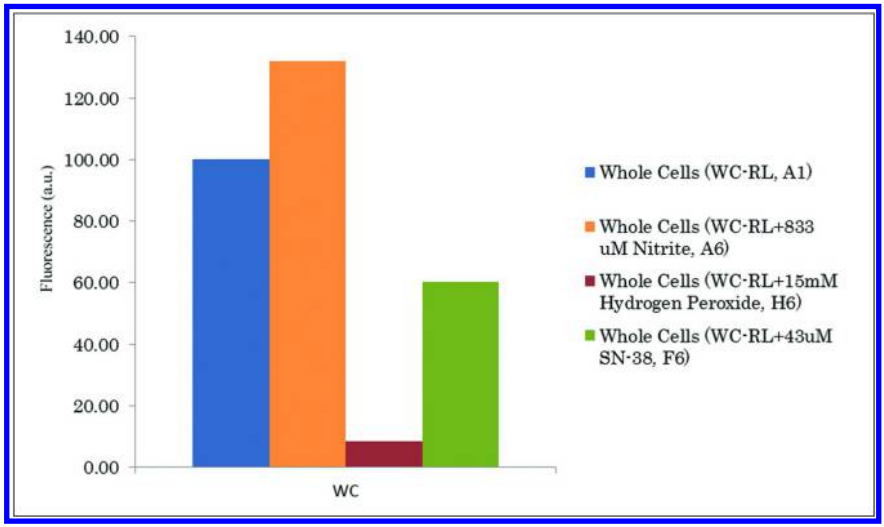

Figure 8. Measurement of Caspase 3/7 activity difference between the normalized averages of the first readings (at 0.16 h, W 0.16 h=100%) from retinal pigment epithelium whole cells (WC) treated with various co-factors and without (-)a rich layer of supplemental pyruvate (RL) treated with various co-factors.

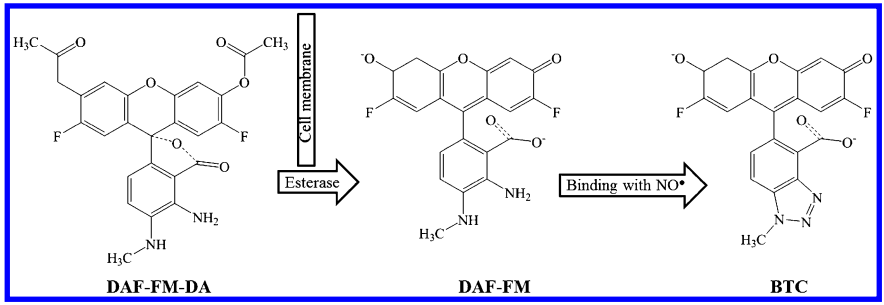

Figure 9. Reaction scheme for the detection of nitric oxide (NO) by 6'-(acetyloxy)-4-amino-2',7'-difluoro-5-(methylamino)-3-oxospiro[2-benzofuran-1,9'-xanthene]-3'-yl acetate based on 4,5-diaminofluorescein diacetate (DAF-FM-DA) to the weakly fluorescent 2-amino-6-(2,7-difluoro-3-oxido-6-oxoxanthen-9-yl)-3-(methylamino)benzoate or 4,5-diaminofluorescein, (DAF-FM) upon binding with nitrogen monoxide yields the strongly fluorescent 5-(2,7-difluoro-3-oxido-6-oxoxanthen-9-yl)-1-methyl-1,2,3-benzotriazole-4-carboxylate (BTC) dye. (© 2015 Thermo Fisher Scientific, Inc. Used under permission. www.lifetechnologies.com)

Publication Date (Web): October 13, 2015 | doi: 10.1021/bk-2015-1200.ch019

To evaluate the bioassay nitrogen monoxide (NO) was measured in whole RPE cells (WC) with a number of co-factors (figure 10). The cells were treated with PBS (control), sodium nitrite (positive control) which was expected to yield a higher NO fluorescence, sodium cyanide (negative control) which is known as an irreversible binding agent to complex IV, shutting down respiration (*40*) and thereby indirectly affecting NO production. Sodium nitroprusside was used as a "slow-release" of NO, as opposed to nitrite which generates NO within an hour (incubation time of assay was between 30-60 minutes), whereas with nitroprusside (same incubation time) but less NO is measured within minutes of the assay (*41*), potassium ferrocyanide was used as a redox couple (*42*) and also as an heme oxidant (*43*), with the expectation that NO synthase (one of the enzymes that generates NO) would be inhibited if the active heme site was oxidized Fe(III) with NO-Fe(II) being the bioactive form (*44*).

As anticipated addition of nitrite gave the highest fluorescence for NO and addition of sodium prusside and ferrocyanide the least, in the case of prusside as a NO source, this may inhibition further biosynthesis and for ferro cyanide, inactivation of the binding site of NO synthase, a major source of biosynthesis in the cell. In comparison to our NMs/MOFs, shown in figure 11, several trends were observed and summarized below.

Publication Date (Web): October 13, 2015 | doi: 10.1021/bk-2015-1200.ch019

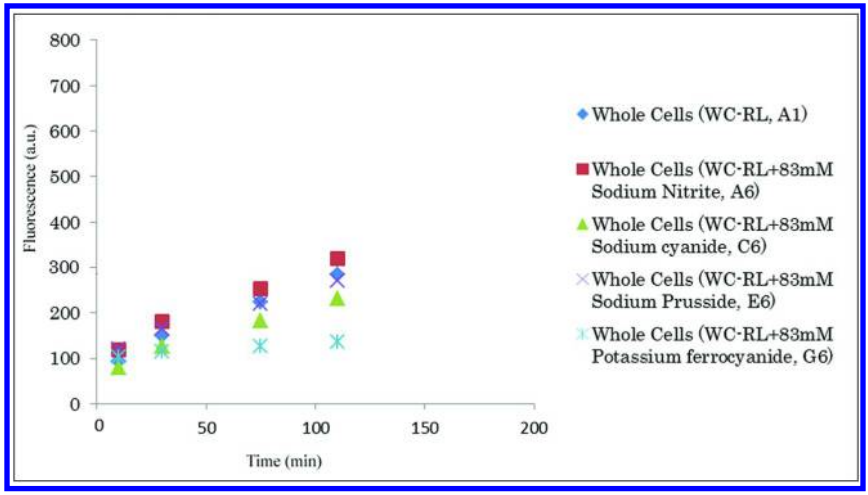

Figure 10. Measurement of nitrogen monoxide (NO) from retinal pigment epithelium whole cells (WC) treated with various co-factors and without (-)a rich layer of supplemental pyruvate (RL) treated with various co-factors.

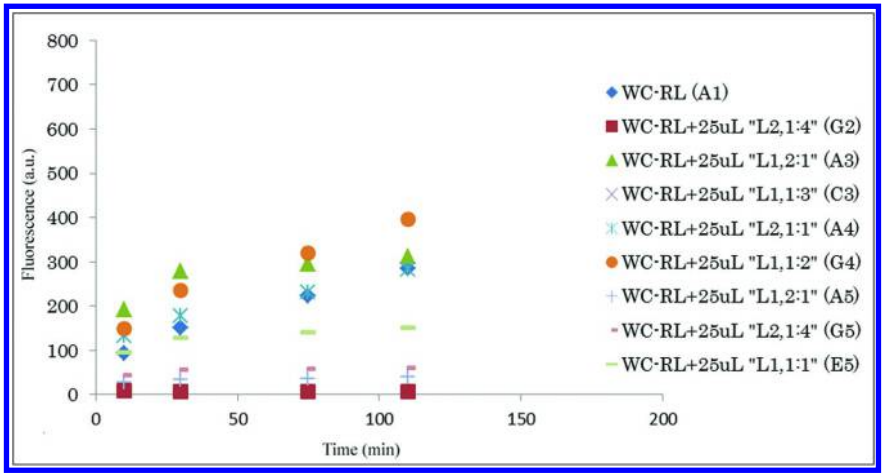

Figure 11. Measurement of nitrogen monoxide (NO) from retinal pigment epithelium whole cells (WC) treated with various co-factors and without (-) a rich layer of supplemental pyruvate (RL) treated with various metal organic framework compounds- Series "L". [The number in brackets such as A1, E3, are the sample well locations, thus the second column represents whole cells without any additional preconditioning with 25 microliters of MOF-L2 with a metal to ligand ratio of 1:4. See Table 1 for name of ligands used.]

Publication Date (Web): October 13, 2015 | doi: 10.1021/bk-2015-1200.ch019

Relative to WC with buffer (control), some MOFs exhibit lowers NO fluorescence. This may be due to a number of possible reasons. This maybe that the MOF are toxic to the NO biosynthesis enzymes, in a manner similar to potassium ferrocyanide, but to a greater degree, or that the MOFs captured and trapped the NO within the MOF framework, with little or no release, giving a small response. MOF "L2, 1:4", gives a flat response, almost immediately, with almost no nitric oxide signal, however since the Caspase and LDH bioassays indicate the MOF is not bio toxic, it may suggest NO trapping or that the MOF is not cytotoxic but inactivated the bio enzymes responsible for NO generation. "L1, 2:1" and "L1, 1:1" [only ligand-to-metal ratio varied] give low linear signal, suggesting either cytotoxicity to the cell, inactivation of the enzyme or NO trapping. MOF "L2, 1:1" gave a response similar to WCs and "L1,2:1", and "L1,1:2"gave higher NO attributed fluorescence than WC. Since the L-series of MOF have similar metal centers and some structures give higher NO signal, it supports the possibility that the low NO signal of "L2, 1:4" is likely due to NO trapping, although the other MOF could inactivate the enzymes as previously speculated. The above indicate that metal-to-ligand ratio (1:1 to 1:2 to 1:4 to 2:1) do influence the efficiency and degree of NO trapping and measured NO fluorescence. See table 1 for name of ligands used].Further examination suggests a rate change around the hour, with a similar trend to that of potassium ferrocyanide. To examine this trend further the assay was run to 14 hours and the average of the last few readings minus the first few readings relative to controls for each group were plotted. The reference or control plot (figure 12). As anticipated the NO levels are lesser at 14 hour mark, than at the first hour mark (WC values were divided by themselves WC 1 h/WC 1 h and WC 14 h/WC 14 and the respective co-factors divided by the appropriate WC, and then substrate WC 14-WC 1 and so on). As expected the control would have a value of zero percent and all values would give a negative percent, suggesting a slowdown in NO production as a function of time. This is expected for two reasons, one that high levels of NO are inhibitory to further NO generation and that NO required energy and metabolites, which are consumed over the 14h time period. As previously stated potassium ferrocyanide inactivates the binding sites and with greater time, more of the sites are inactivated leading to less NO generation, although it is not clear whether the inactivation is direct, indirect, competitive, non-competitive or uncompetitive, although work by Wink suggests this may be competitive in nature (*45*). A similar analysis for the L-series of MOFs (figure 13) suggest the most MOFs yield a slowdown, similar to that observed for sodium nitroprusside (~ 60%) with MOFs "L1, 2:1" and "L1, 1:3" exhibiting greater slowdown that to what potassium ferrocyanide (~ 85% versus ~136% versus ~ 159%). This may be to the reasons given above (inhibition of NO, inactivation of NO synthase) or trapping of NO by the MOF, with the trapping becoming more efficient with assay time. The MOFs which gave the highest NO signal are also the ones which give the greater retardation, suggest a feedback loop whether high NO levels generated by, for example "L1, 2:1" over time lead to slower and slower generation of No by NO synthase due to competitive inhibition of NO by itself or other factors (*46*). Analysis of the rate within the first hour relative to WC (control) is shown in figure 14. Whereas figures 12 and 13 compare the difference at the last time-point

with the first time-point, figure 14 compares the rates within the first hour. The advantages of such as comparison are that cells have energy and nutrients and relative NO generation to WC (set at 100%) can be examined.

As anticipated addition of sodium cyanide yields less NO than the control (whole cells in PBS), but both sodium nitrite (fast acting) and sodium nitroprusside (slow acting) give the highest fluorescence attributed to NO generation within the cell (*47*). Potassium ferrocyanide gives an intermediate value suggesting that inactivation of the iron center is not immediate that the ferrocyanide (*48*) is assisting generation of NO by an NO independent pathways (*49*) as opposed to nitrite which is assisting the generation of NO through a NO-dependent pathways, for example via cyclic guanine monophosphate (*50*). The various interactions are summarized in figure 15, based on a review by Ortuño-Sahagún (*51*). Evaluation of the L-series of MOFs (in figure 16) is discussed.

The results suggest the initial NO production of MOFs "L2, 1:4", "L1, 2:1", and "L2, 1:4" is less than whole cells (WC), whereas MOF "L1, 1:1" is similar and MOFs "L1, 2:1", "L1, 1:3", "L2, 1:1" and "L1, 1:2" yield greater fluorescence than the control.

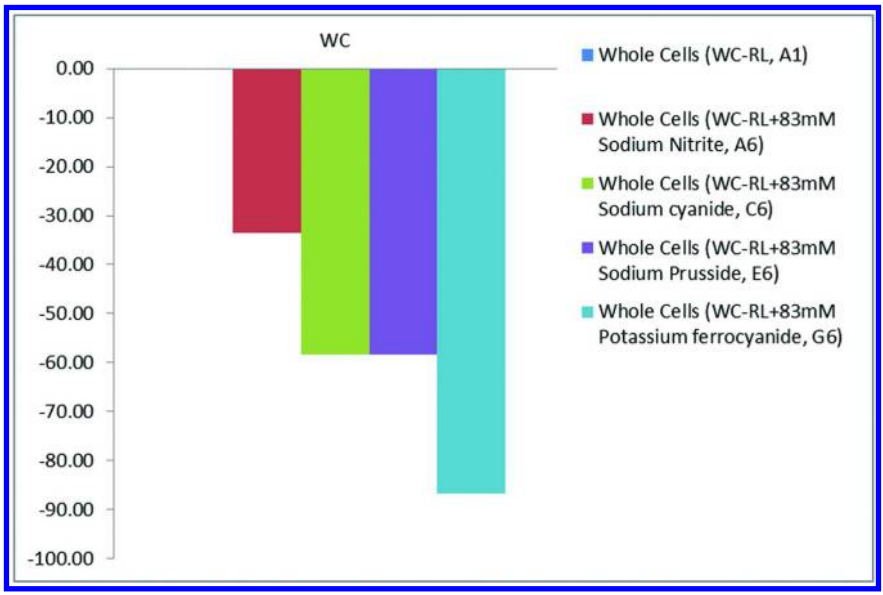

Figure 12. Measurement of nitrogen monoxide (NO) difference between the normalized average of the last readings (at 14 h, WC 14 h=100%) and the normalized first readings (at 0.16 h, W 0.16 h=100%) from retinal pigment epithelium whole cells (WC) treated with various co-factors and without (-)a rich layer of supplemental pyruvate (RL) treated with various co-factors. WC set at 0% difference.

Publication Date (Web): October 13, 2015 | doi: 10.1021/bk-2015-1200.ch019

Publication Date (Web): October 13, 2015 | doi: 10.1021/bk-2015-1200.ch019

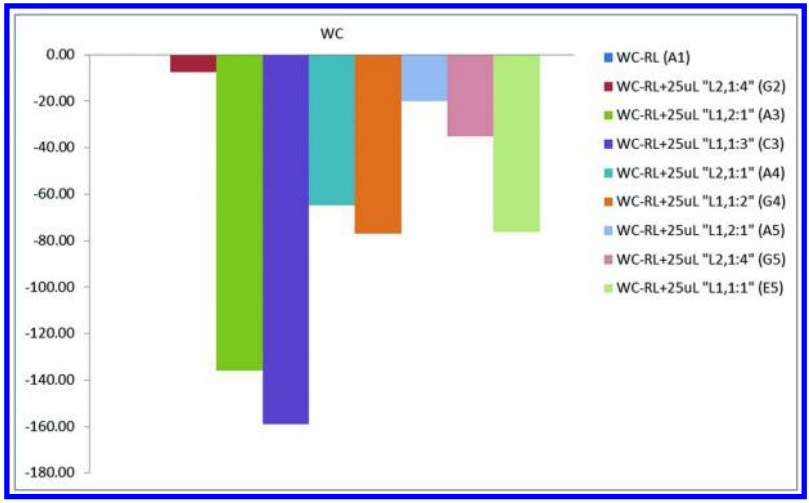

Figure 13. Measurement of nitrogen monoxide (NO) difference between the normalized average of the last readings (at 14 h, WC14 h=100%) and the normalized first readings (at 0.16 h, WC 0.16 h=100%) from retinal pigment epithelium whole cells (WC) treated with various co-factors and without (-)a rich layer of supplemental pyruvate (RL) treated with various metal organic framework compounds- Series "L". WC set at 0% difference. [The number in brackets such as A1, E3, are the sample well locations, thus the second column represents whole cells without any additional preconditioning with 25 microliters of MOF-L2 with a metal to ligand ratio of 1:4. See Table 1 for name of ligands used.]

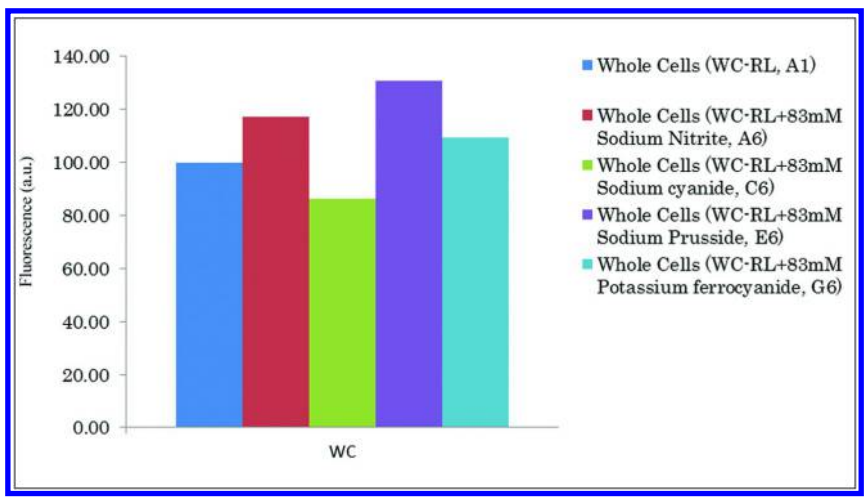

Figure 14. Measurement of nitrogen monoxide (NO) difference between the normalized average of the first readings (at 0.16 h, WC 0.16 h=100%) and the average MOF readings (at 0.16 h) from retinal pigment epithelium whole cells (WC) treated with various co-factors and without (-)a rich layer of supplemental pyruvate (RL) treated with various co-factors.

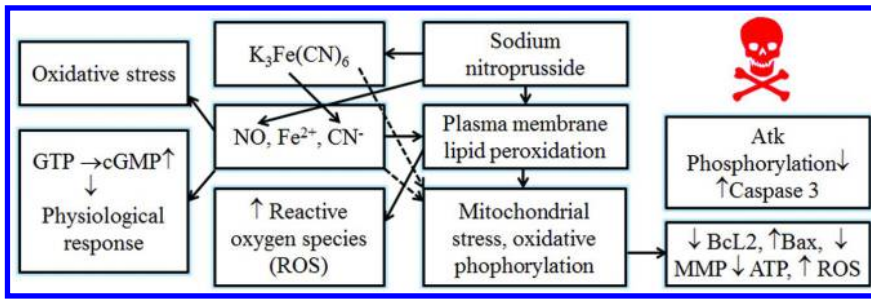

Figure 15. Summary of observed effects of sodium nitroprusside (based on our observation and literature publications) on NO generation and RPE cell survival. SNP has a number of non-synthetic functions such as nitric oxide (NO) production, oxidation and reduction or formation of iron, cyanide anions, hydroxyl radicals, intermediates. These intermediates in turn carry out oxidative and nitrosative stress, in addition to proteins, nucleic acids, and lipids inactivation by means of oxidation and nitrosylation. Iron, via the Fenton-like reactions, generates hydroxyl and other reactive species (superoxide), damaging membranes by lipid peroxidation with decreased cellular viability, measured by the LDH assay. Stress is relieved by addition of NO, although NO may trigger NO-dependent biochemical pathways , which through phosphorylation may lead to an reduction of Bcl2 and an increase in BID, through mitochondrial stress and triggering of apoptotic pathways. Sodium nitroprusside also acts upon the mitochondria, at low levels stimulates vasodilation, but at high levels is inhibitory to NO synthase and may cause mitochondrial membrane damage, release of cytochrome c and subsequent activation of caspases, as well as decreasing the phosphorylation of Atk. cyanide, potassium ferrocyanide and sodium nitroprusside also affect the functioning of the mitochondrial respiratory chain, thereby lowering the mitochondrial membrane potential (MMP), reducing ATP production and assisting in the generation of singlet oxygen and reactive oxygen species.

Publication Date (Web): October 13, 2015 | doi: 10.1021/bk-2015-1200.ch019

Changes in Mitochondrial Membrane Potential

In the summary figure 14, it was speculated that NO levels if damaging to the mitochondrial may lower the mitochondrial membrane potential (MMP), if lowered to zero or higher than control values, this may indicate mitochondrial stress and a possibility of triggering caspase 3 via cytochrome c release. Figure 17 represents the profile with the regular controls. The mitochondrial potential values drop, due to tetramethylrhodamine ethyl ester, that accumulates in active mitochondria due to electrostatic attraction. Depolarization of inactivation of mitochondrial will lower the membrane potential and result in lower dye accumulation (*52*). In the above figure, the values drop until 100 minutes when they rise again, suggesting final burst of activity. Sodium prusside and nitrite give similar profiles suggesting they do not directly affect the mitochondrial membrane potential, while sodium cyanide has values higher than control, suggesting direct

interaction and mitochondrial stress. Figure 18 is the figure with the L-series of MOFs.

Only MOF "L2, 1:4" has a lower MMP (at 40 min), all the other MOFs have higher MMP values, the highest values are attributed to MOFs "L1, 2:1", "L1, 1:2", "L2, 1:1" with MOFs "L1, 1:1"; "L1, 1:2" and "L1, 2:1" having values higher than what were observed for sodium cyanide. This may mean they exhibit greater stress on the mitochondria than sodium cyanide or that the dye accumulates and preferentially binds to, or is captured by the MOFs. A comparison of the difference between the first last value and first value is shown in figure 19. The control has a value of zero, a positive value suggests that as time increases so does the rate or accumulation of the dye, with the MMP dye, this suggests mitochondrial stress and potential onset of apoptosis, except with potassium ferrocyanide, which has previously suggested indicates potential enzyme inactivation and decreases with time.

MOFs "L1, 2:1" (low dose and high dose, same volume), "L1, 1:1" have positive values (figure 20), slightly greater than what was observed for sodium prusside (~ 27%; 33%; and 53% versus 20% for sodium prusside), MOFs "L1, 1:3" and "L2, 1:1" have a small net change and MOF "L1, 1:2" has a greater negative change than potassium ferrocyanide (~ 75% versus 6% for potassium ferrocyanide). Assuming the mechanism of action is similar to the standards, they may act in a similar manner, or the dye may be captured by the MOFs.

An analysis within one hour is shown in figure 21, indicates that initial NO generation as measured by the fluorescence of the dye is similar, although potassium ferrocyanide gave the highest value, indicating that, greater than one hour may be required fir appreciable enzyme inactivation to be observed, or that there are other NO biosynthetic enzymes that are not inactivated by potassium ferrocyanide. Examination of the L-series of MOFs like the controls, show greater NO generation than the control for all MOFs except MOFs "L2, 1:4", "L1, 2:1" and "L2, 1:4", which are slightly less than the control and MOFs "L1, 2:1","L1, 1:3", and "L1, 1:2", values much higher than the control (~150%). It is not possible to give a reason for these differences, but it appears that the L-series of MOFs can be used as probes to understand certain biochemical state of the chemical, are themselves not cytotoxic and under certain circumstances can induce generation of NO and facilitate apoptosis (figure 22).

Publication Date (Web): October 13, 2015 | doi: 10.1021/bk-2015-1200.ch019

Changes in Reactive Oxygen Species

Finally the reactive oxygen species for a smaller subset of L-series of MOFs was carried our relative to WC in PBS and is shown in figure 23. This was done, because in the earlier NO and MMP experiment it appeared that oxidative stress may be one factor that might contribute to mitochondrial stress. Here a non-fluorescent dichlorofluorescein derivative dye was used (figure 24), which upon deacetatylation by intracellular esterases becomes highly fluorescent as an *in vitro* measure of cellular oxidation occurs (*53*), as shown in figure 23.

Publication Date (Web): October 13, 2015 | doi: 10.1021/bk-2015-1200.ch019

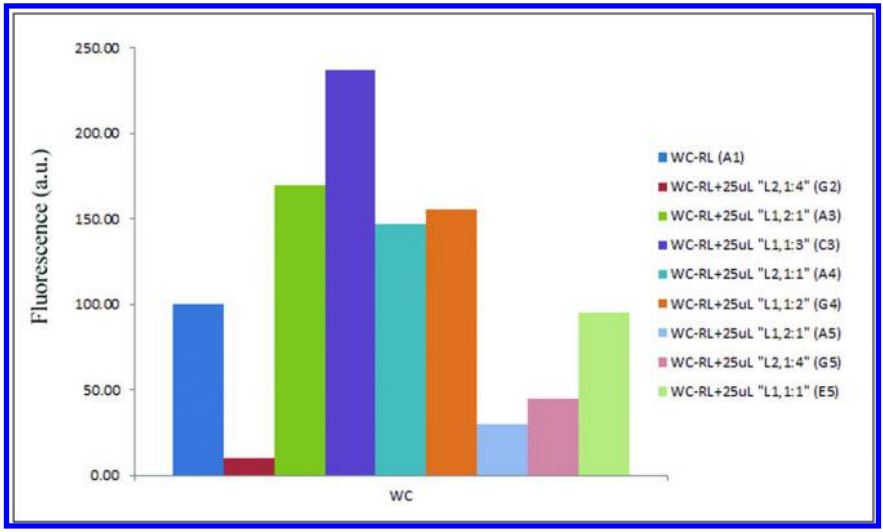

Figure 16. Measurement of nitrogen monoxide (NO) difference between the normalized average of the first readings (at 0.16 h, WC 0.16 h=100%) and the average MOF readings (at 0.16 h) from retinal pigment epithelium whole cells (WC) treated with various co-factors and without (-)a rich layer of supplemental pyruvate (RL) treated with various metal organic framework compounds- Series "L". [The number in brackets such as A1, E3, are the sample well locations, thus the second column represents whole cells without any additional preconditioning with 25 microliters of MOF-L1 with a metal to ligand ratio of 2:1. See Table 1 for name of ligands used.]

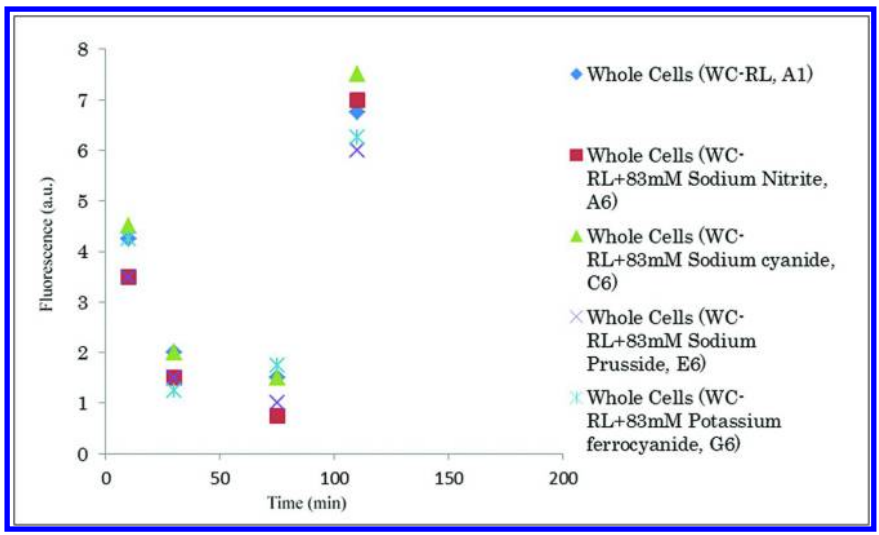

Figure 17. Measurement of mitochondrial membrane potential (MMP) from retinal pigment epithelium whole cells (WC) treated with various co-factors and without (-) a rich layer of supplemental pyruvate (RL) treated with various co-factors.

Publication Date (Web): October 13, 2015 | doi: 10.1021/bk-2015-1200.ch019

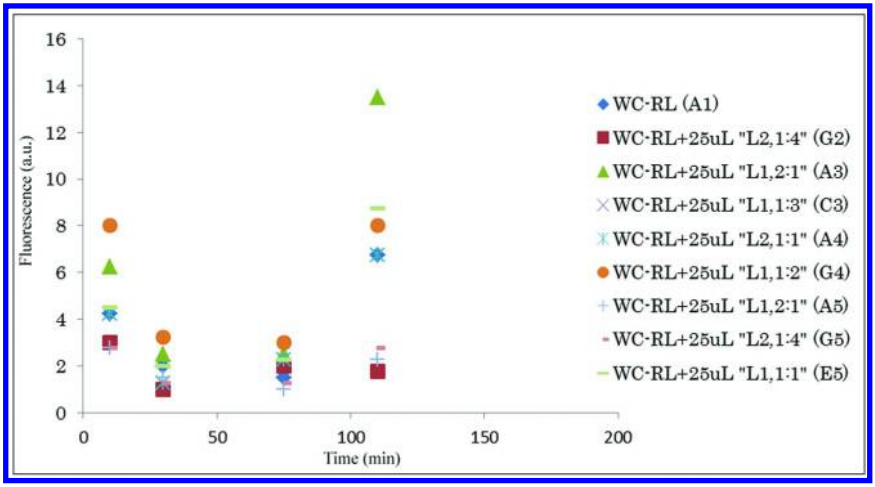

Figure 18. Measurement of mitochondrial membrane potential (MMP) from retinal pigment epithelium whole cells (WC) treated with various co-factors and without (-) a rich layer of supplemental pyruvate (RL) treated with various metal organic framework compounds- Series "L". [The number in brackets such as A1, E3, are the sample well locations, thus the second column represents whole cells without any additional preconditioning with 25 microliters of MOF-L2 with a metal to ligand ratio of 1:4. See Table 1 for name of ligands used.]

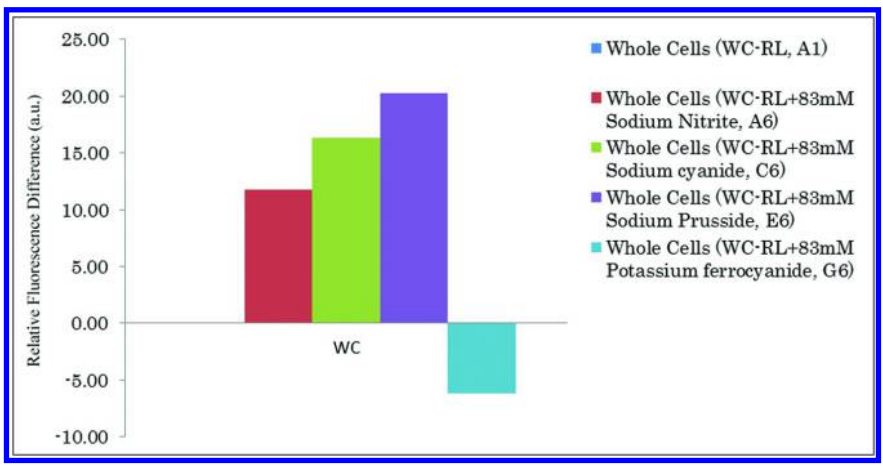

Figure 19. Measurement of mitochondrial membrane potential (MMP) difference between the normalized average of the last readings (at 14 h, WC 14 h=100%) and the normalized first readings (at 0.16 h, W 0.16 h=100%) from retinal pigment epithelium whole cells (WC) treated with various co-factors and without (-)a rich layer of supplemental pyruvate (RL) treated with various co-factors. WC set at 0% difference.

Publication Date (Web): October 13, 2015 | doi: 10.1021/bk-2015-1200.ch019

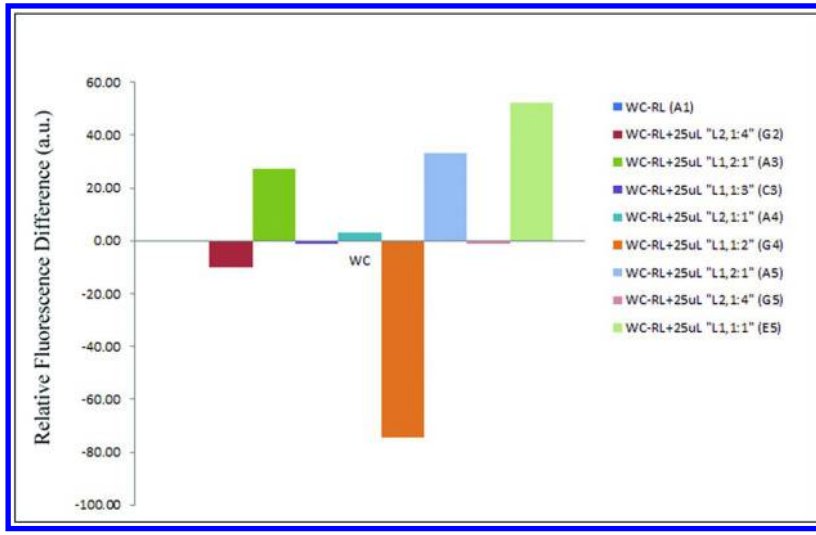

Figure 20. Measurement of mitochondrial membrane potential (MMP) Difference between the normalized average of the last readings (at 14 h, WC 14 h=100%) and the normalized first readings (at 0.16 h, W 0.16 h=100%; WC set at 0% difference.) from retinal pigment epithelium whole cells (WC) treated with various co-factors and without (-) a rich layer of supplemental pyruvate (RL) treated with various metal organic framework compounds- Series "L". [The number in brackets such as A1, E3, are the sample well locations, thus the second column represents whole cells without any additional preconditioning with 25 microliters of MOF-L2 with a metal to ligand ratio of 1:4. See Table 1 for name of ligands used.]

Examination of the ROS fluorescence, relative to control (set to 100%) suggest that MOF "L1, 2 1:3" had a higher di-chlorofluorescein derivative dye fluorescence of approximately 160% to 190% (for control) suggesting that ROS mediate damage may not be a major source of cellular stress, unlike Co-MOF that is highly oxidizing in bacterial cells (summarized in figure 25).

Discussion

There is minimal information on the cytotoxicity of MOFs, although in a few studies iron carboxylate MOFs were injected into rats with no side-effects or measured toxicity (*54*). The three general phases can be characterized as activation of the MOF (figure 26), loading of drug or gas storage and either catalysis or interaction with or at the guest interface (*55*).

Publication Date (Web): October 13, 2015 | doi: 10.1021/bk-2015-1200.ch019

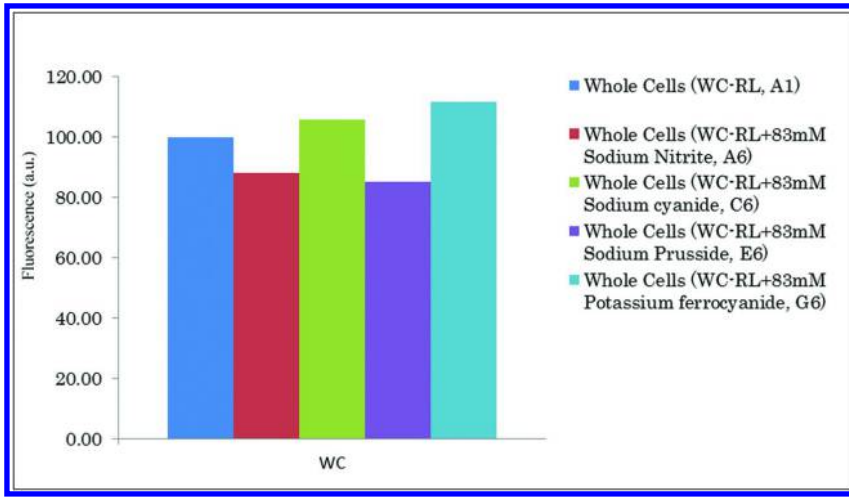

Figure 21. Measurement of mitochondrial membrane potential (MMP) difference between the normalized average of the first readings (at 0.16 h, WC 0.16 h=100%) and the average MOF readings (at 0.16 h) from retinal pigment epithelium whole cells (WC) treated with various co-factors and without (-) a rich layer of supplemental pyruvate (RL) treated with various co-factors.

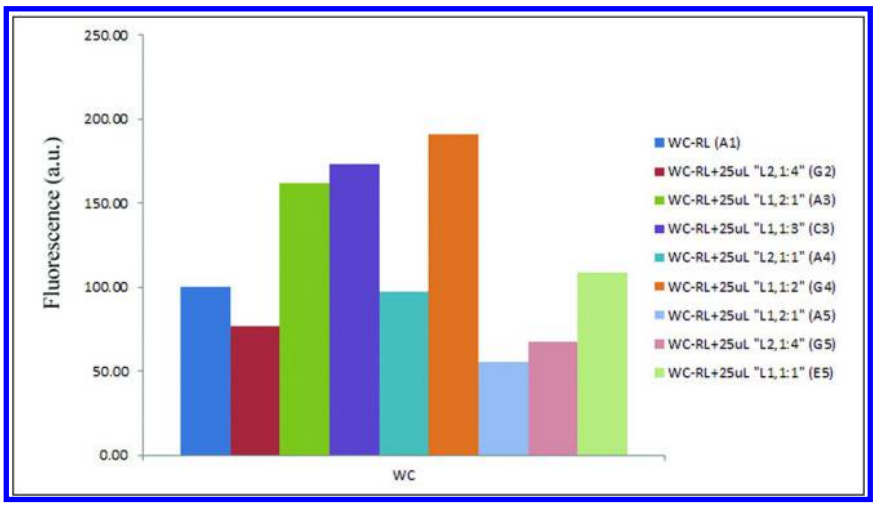

Figure 22. Measurement of mitochondrial membrane potential (MMP) difference between the normalized average of the first readings (at 0.16 h, WC 0.16 h=100%) and the average MOF readings (at 0.16 h) from retinal pigment epithelium whole cells (WC) treated with various co-factors and without (-) a rich layer of supplemental pyruvate (RL) treated with various metal organic framework compounds- Series "L". [The number in brackets such as A1, E3, are the sample well locations, thus the second column represents whole cells without any additional preconditioning with 25 microliters of MOF-L2 with a metal to ligand ratio of 1:4. See Table 1 for name of ligands used.]

Publication Date (Web): October 13, 2015 | doi: 10.1021/bk-2015-1200.ch019

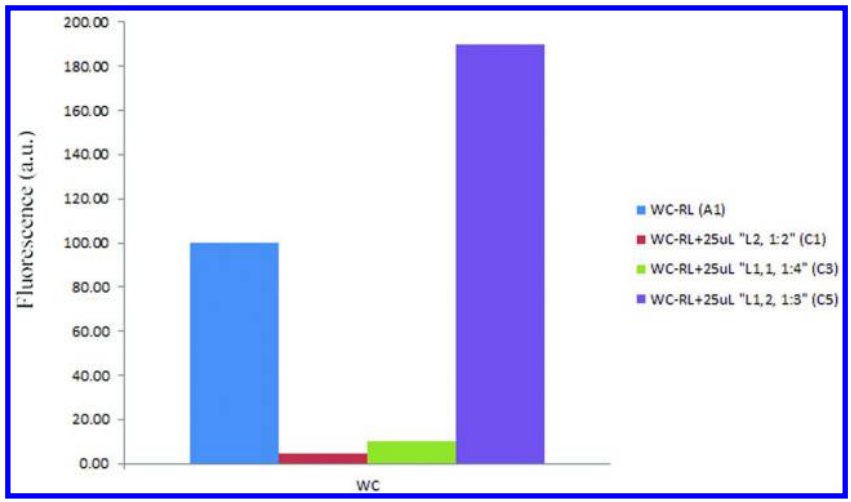

Figure 23. Measurement of Reactive Oxygen Species (ROS) difference between the normalized average of the first readings (at 0.16 h, WC 0.16 h=100%) and the average MOF readings (at 0.16 h) from retinal pigment epithelium whole cells (WC) treated with various co-factors and without (-) a rich layer of supplemental pyruvate (RL) treated with various metal organic framework compounds- Series "L". [The number in brackets such as A1, E3, are the sample well locations, thus the second column represents whole cells without any additional preconditioning with 25 microliters of MOF-L2 with a metal to ligand ratio of 1:2. See Table 1 for name of ligands used.]

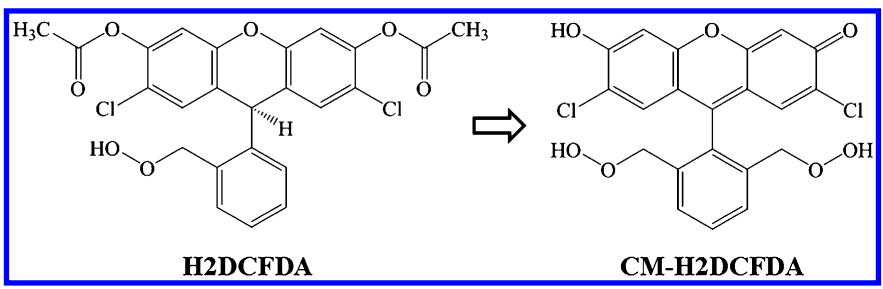

Figure 24. The structure of 6-(acetyloxy)-2,7-dichloro-9-[2(hydroperoxymethyl) -phenyl]-9H-xanthen-3-yl acetate (H2DCFDA) that is non-fluorescent upon interaction with reactive oxygen forms a 5-(and-6)-chloromethyl-2, 7-dichloro-dihydrofluorescein diacetate (CM H2DCFDA) structure based on 9-[2,6-bis(hydroperoxymethyl)- phenyl]-2,7-dichloro-6-Hydroxyxanthen-3-one which is highly fluorescent di-chlorofluorescein derivative. (© 2015 Thermo Fisher Scientific, Inc. Used under permission. www.lifetechnologies.com)

Publication Date (Web): October 13, 2015 | doi: 10.1021/bk-2015-1200.ch019

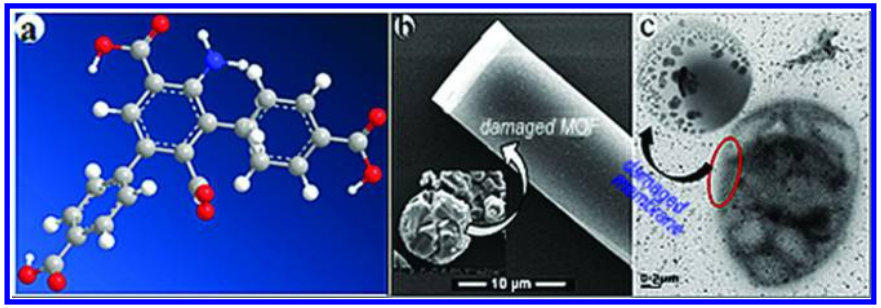

Figure 25. Co-based MOFs used as disinfectant, a: The structure determined by single crystal X-ray diffraction; b: SEM morphological image of Co-MOFs; and c: Bacteria cell wall of E. coli using Co-MOF disinfectant. (figure modified from figure 8 of (23))

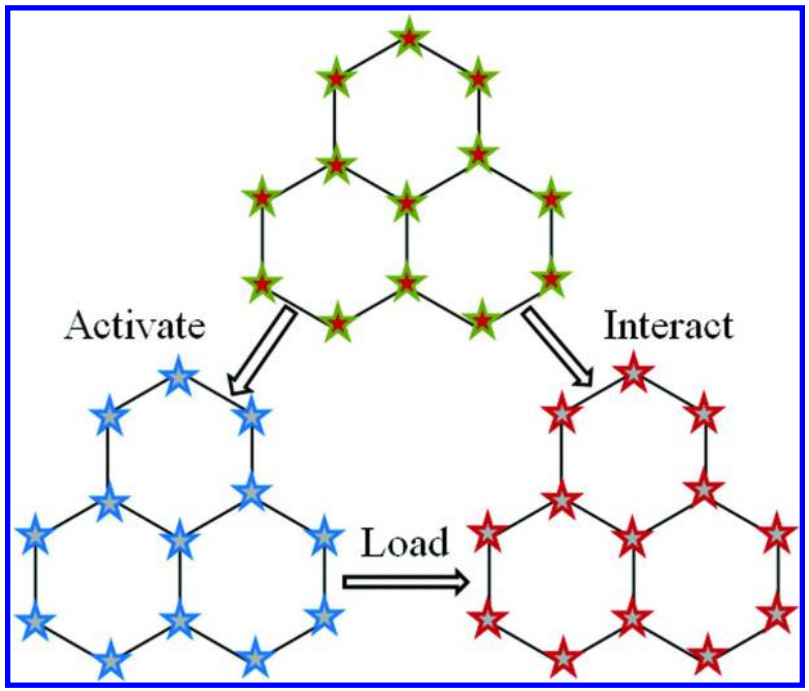

Figure 26. Simplified scheme of MOF activation and interaction in biological systems

Table 2. Summary of the relative results to whole cells in PBS (WC), which were set to 100%.

Assay	*Value (min.)*	*Value (max.)*	*System*
Caspase	9%		HP
Caspase		132%	NIT
Caspase	2%		"L2, 1:1"
Caspase		54%	"L12, 1:3"
LDH	100%		WC (PBS)
LDH		186%	HP
LDH	12%		"L2, 1:2"
LDH		112%	"L1, 2:1"
MMP	88%		CN
MMP		113%	PFC
MMP	56%		"L1, 2:1"
MMP		190%	"L1, 1:2"
NO	86%		CN
NO		130%	PFC
NO	10%		"L2, 1:4"
NO		140%	"L1, 1:3"
ROS	77%		NitroP
ROS		140%	PFC
ROS	2%		"L2, 1:2"
ROS		160%	"L12, 1:3"
CN	Sodium cyanide		
HP	Hydrogen peroxide		
LDH	Lactate dehydrogenase assay		
MMP	Mitochondrial membrane potential		
NIT	Sodium nitrite		
NitroP	Sodium Nitroprusside		
NO	Nitrogen monoxide		
PFC	Potassium ferrocyanide		
ROS	Reactive oxygen species		
WC	Whole cells (phosphate buffered saline)		

Publication Date (Web): October 13, 2015 | doi: 10.1021/bk-2015-1200.ch019

Table 3. Summary of NO donors and study in ischemia using Rat animal model for cerebral ischemia.[a]

Animal	*Disease Model*	*Ischemia/ reperfusion time (h)*	*NO Source*	*Dose, administration method*	*Select Notes*	*Ref*
Goat	MCAO	0.33/168	DEAN	1 nmol/L, 3h prior, IV	Relaxation of MCA	(*83*)
Rat	MCAO	20/24	GSNO	1mg/kg on reperfusion	Reduced caspase-3-activity, iNOS expression was reduced.	(*84*)
Rabbit	MCAO	0.5/2	ProliNO	1umol/L, onset of reperfusion for 1h, IA	Reduced ROS levels	(*85*)
Rat	PMCAO	24/-	SIN-1	1.5 mg/kg/h trans-ischemia, IV	*In vitro* platelet aggregration decreased	(*86*)
Rat	MCAO	20/24	SNAP	2 umol/kg/10 min on reperfusion, IV	Reduced lipid peroxidation, plasma NO levels increased.	(*87*)
Rat	4-VO	15/6	NitroP	5mg/kg 0.5h prior to ischemia, IP	Reduced cytochrome c in cytoplasma, nNOS expression was reduced.	(*88*)
Rat	MCAO	1.5/1.5	Sodium nitrite	480 nmol/min, 1.5 post-ischemia, IV	Reduced ROS/RNS	(*89*)
Rat	MCAO	2/168	Sperm-ineN	0.36 mg/kg/120 min trans-ischemia, IV	Cerebral perfusion was increased	(*90*)
Rat	MCAO	1.5/24	NBP	0.1 mmol/kg, 1h prior to ischemia, IV	Reduced nNOS expression, Increased cGMP levels	(*91*)

[a] DEAN = Diethylamine NONOate; MCA = Middle cerebral artery; GSNO = S-nitroso-glutathionine; IA = Intraarterial; iNOS = inducible nitric oxide synthase; IP = Intraperitoneal; IV = Intravenous; (P)MCAO = (Permanent) middle cerebral artery occlusion; NBP = 3-n-butylphthalide derivative; NitroP = Sodium nitroprusside; nNOS = neuronal nitric oxide synthase; NO = Nitric oxide; SIN-1 = 3-morpholinosydnonimine; ProliNO = 1-[2-(carboxylato)pyrrolidin-1-yl]diazen-1-ium-1,2-diolate;SNAP = S-nitroso-N-acetyl-penicillamine; SperminineN = (Z)-1-[N-[3-aminopropyl]-N-[4-(3-aminopropylammonio)butyl]-amino]diazen-1-ium-1,2-diolate; 4-VO = Four vessel occlusion model.

Publication Date (Web): October 13, 2015 | doi: 10.1021/bk-2015-1200.ch019

The L-series of MOFs primarily ligand template is structurally similar to iron fumarate (*56*), an iron supplement. MOF have a number of advantages which can be used to lower potential toxicity. These include, variation on the pore size to trap, smaller or larger molecules, use of organic linkers that will allow biodegradability to occur, use of different organic linkers to vary the hydrophobic-hydrophilic internal space and interactions, and charging of certain ligands, to stabilize biological molecules. A summary of results is shown in table 2.

Other positive or negative controls were used and are also listed. Where a number of MOFs gave similar values, the lowest of the representative sample is shown. All results are values obtained within the first hour (0.16 h) with the same volume of buffer, co-factor or L-series MOF.

Nitrogen monoxide is a signaling molecule, which can facilitate both would-healing, vasodilation and cell death, depending on dose and other pro-/anti-apoptotic factors (*57*). Since the molecule is a neutral gas, it is unlikely to travel a great distance and its effects are local (*58*). A number of materials have been used in NO storage, and release, such as silica nanoparticles (*59*), zeolites, (*60*), polymers (*61*), and MOFs (*62*). A few reports indicate that NO trapped MOFs induced apoptosis (*63*). MOF CPO-27 has been used to release large amounts of NO for vasodilation (*64*), other MOFs include copper trimesate, and iron terephthalate based MIL-101 (*11*). These reports suggest that MOFs can be designed to store and release either quickly (CPO-27) or slowly (HKUST-1).

The use of inorganic or organic nitrogen monoxide (NO) in the treatment of Ischemia (*65*) either cerebral or cardiac is another attractive feature of the NO storing MOFs, in that they can be used to examine cellular toxicity and where appropriate as neuroprotective agents (*66*). Nitrogen monoxide thus can paradoxically be toxic or protective depending on its concentration, cellular location and the cellular hemostasis of the cell (*67*). Nitrogen monoxide is biological synthesized by NO synthase (NOS, with three isoforms, eNOS, nNOS and iNOS (*68*)) which is expressed in most cells and can be upregulated by changes in intracellular calcium (*69*). In the brain, it is generated in the endothelium and plexus and is protective of the endothelium from oxidative stress and inflammation, promoting cellular communication and adhesion (*70*), platelet aggregation (*71*). During cardiac or cerebral insult, oxygen is deprived and upon reperfusion, potential damage can occur. The paradoxical effects of NOS are attributed to its isoforms; eNOS is generally protective in ischemia (*72*), whereas nNOS contributes to early injury (*73*), with iNOS contributing to late injury (*74*). High NO levels due to iNOS also contribute to protein nitrosylation and neural damage ("bad effect" (*75*)), although NO from eNOS are protective ("good effect" (*76*)), requiring NO donors as a potential treatment regime (*77*). External NO can be released as the nitrosonium cation (*78*) or nitroxyl anion (*79*) from organic nitrates, such as nitroglycerin (*80*); sulfur conjugated nitrosothiols such as S-nitroso-glutathione (*81*) or sodium nitroprusside (*82*). Metal organic-frameworks offer another attractive feature, as NO storage. Table 3 is a summary of select NO agents used in treatment of ischemia.

Publication Date (Web): October 13, 2015 | doi: 10.1021/bk-2015-1200.ch019

Publication Date (Web): October 13, 2015 | doi: 10.1021/bk-2015-1200.ch019

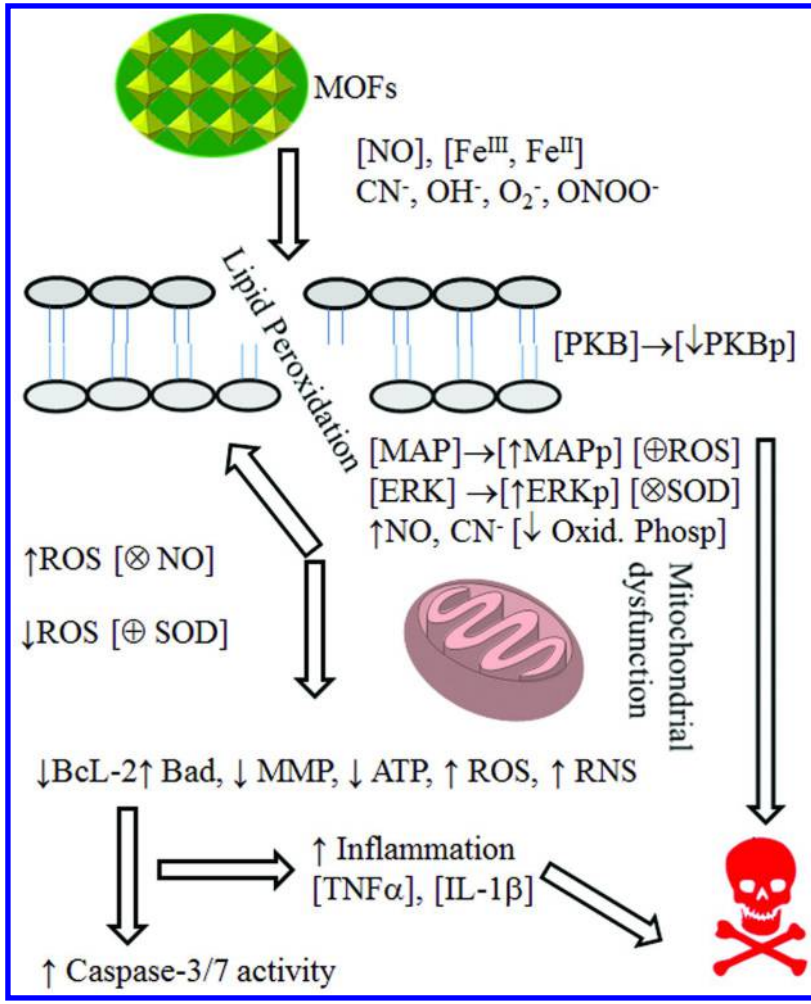

Figure 27. Summary of the various biochemical altered that were measured directly or inferred through analysis of published literature, that are consistent with our observations. The mode of cell death is related to a number of biochemical pathways some of which are activated towards cytotoxicity or deactivated towards cell protection by the various MOF formulations. For example, the interaction with the cell membrane and MOF can lead to lipid peroxidation and cell disruption. In addition the MOF can change the redox state of iron-proteins found in the mitochondria that are responsible for respiration. Similar reactive oxygen/nitrogen species may be generated contributed towards oxidative stress or binding of cyanide ion with respiratory proteins. The consequence of oxidative/ nitrosative stress are numerous and may lead to covalent modification of lipids, proteins or nucleic acids. Change of redox state of iron may further promote Fenton catalysis of hydroxyl radicals or anions that in consort with superoxide or peroxynitrite further contributes to lipid peroxidation and membrane disassembly. These effects are countered (Ä) by

In Oxidative Stress: Diagnostics, Prevention, and Therapy Volume 2; Hepel, et al.;
ACS Symposium Series; American Chemical Society: Washington, DC, 2015.

supplemental nitrogen monoxide (NO) which can bind with iron, potentiating (Å) its protective effectiveness. Mitogen-activated protein kinase 2 (MAP) and triggers the activation of extracellular signal-regulated kinases (ERKs), upon phosphorylation (p) that initiate cellular signaling contributing to oxidative stress. These enzymes can be down regulated through the action of superoxide dismutase (SOD) that acts upon superoxide (O_2^-), which in turn may be generated from peroxynitrite ($ONOO^-$). Expression of ERK is known to act upon the mitochondria and decrease B-cell lymphoma 2 (BcL-2) a protein known to promote cell survival by blocking apoptosis and an increase in Bcl-2-associated X protein (Bax) that is known to promote apoptosis. The differential regulation of BcL-2/Bax would promote cell death (☠) via mitochondrial apoptotic pathways that would also contribute to release of cytochrome c and activation of caspase 3/7. Addition of sodium nitroprusside (without or with cyanide anion, CN-) would promote mitochondrial dysfunction such as alternations in adenosine triphosphate (ATP), mitochondrial membrane potential (MMP), reactive oxygen species (ROS), reactive nitrogen species (RNS) in addition to activation of pro-apoptotic factors and regulation of anti-apoptotic factors, collecting slowing down oxidative phosphorylation (Oxid. Phosp.) Superoxide dismutase (SOD) is known to slow down mitochondrial dysfunction by scavenging RNS that can contribute to ROS and lipid peroxidation. The catalysis of SOD and catalase can be diminished by decreased phosphorylation of protein kinase B (PKB), which is potentiated by sodium nitroprusside (NitroP). Release of cytochrome c to the cytoplasm can also increase pro-inflammation factors, such as tumor necrosis factor-alpha and interleukin 1 beta, which further contribute to cytokine-induced oxidative stress and cell death. It can be seen that metal-organic frameworks (MOF) and monitoring of nitric oxide (NO) is an example of how a high throughput screen may be utilized to estimate general cellular toxicity. Cell death thus could be from a number of different biochemical pathways based either in the cytoplasm or mitochondria or cell/plasma membrane that can be target using nanomaterial based chemical agents; conversely MOFs can be used as NO release agents through selective storage and release or direct release using iron metal coordinative with NO releasing ligands. (Figure Modified with via Creative Commons Attribution License from (51). Copyright (2013) Hindawi Publishing Corporation).

Publication Date (Web): October 13, 2015 | doi: 10.1021/bk-2015-1200.ch019

It can be seen from a brief summary in table 3, that utilization of NO donors for cerebral protection is expensive, lengthy and cumbersome, since the dose-per-mass of NO donor is not always known, nor is their kinetic profiles (*92*). For evaluation of new chemical agents, NO can be monitored to determine toxicity of the chemical agent and the MOF can be used for NO storage, release in a manner similar to the role played by nNOS, thereby promoting protection.

The L-series of MOFs have been shown to exhibit low cytotoxicity as determined using the lactate dehydrogenase assay, relative to whole cells in phosphate buffered saline (figure 4), as well as the caspase-3 bioassay to determine whether the cells undergo apoptosis (figure 5). Biological cells also undergo a range of changes often through mediators, receptors, or through messenger

molecules (*93*), one major indicator was nitrogen monoxide (NO). Our assay using a NO specific fluorescent dye indicates that, NO increases with time up to at least one hour, when there is a slow-down (the NO slope is less steep) and NO production was observed until approximately 800 minutes, after which there was a drop and eventual cell death. Analysis suggests some MOFs may trap NO, or inactivate the enzyme after the hour mark, giving rise to very low NO signal, such as MOF "L2, 1:4". Since the biochemistry of NO is complex, it is difficult to make any generalizations, however, assuming the MOFs are not inactivating, it would suggest the with additional linkers, NO is trapped and not released and with less linkers, "L1, 1:3" NO is trapped and released to a much greater degree, similar to what was observed for nitrite addition. The likely mechanism was summarized in figure 15 and includes, interaction with NO synthase, possibility of redox changes to Fe^{II} to Fe^{III} and limited mitochondrial stress leading to generation of reactive oxygen species, although the fluorescence was lower than controls for most MOFs evaluated. The source of the reactive oxygen species (ROS) is unknown (*94*), it is likely to originate from the mitochondria (*28*) but since whole cells were tested and not mitochondrial fractions, it is not possible to link ROS to a specific cellular source, although it is known that oxidative phosphorylation can generate reactive oxygen species (*95*) as well as oxidation within the cell (*96*), plasma membrane (*97*) and surrounding media, used in the incubation of the cells (*98*). This allows the possibility of use of MOF "L1 2, 1:3" as a potential anti-cancer agent in inducing oxidation in rapidly dividing cells. The potential mode of action is summarized in figure 27.

Publication Date (Web): October 13, 2015 | doi: 10.1021/bk-2015-1200.ch019

Summary

A number of linkers with benzene-1,4-dicarboxylate were generated (L-series) and evaluated for cytotoxicity. Two assays were carried out. In both assays (lactate dehydrogenase and Caspase 3/7), the fluorescence ratio between the whole cell with MOFs and WC with phosphate buffered saline was less than the MOFs, suggesting that the L-series of MOFs do not damage the plasma membrane of RPE cells. A similar trend was observed for the caspase assay, where the positive controls (hydrogen peroxide and SN-38) gave higher fluorescence. To determine whether the MOF changes the biochemical function of the cells, nitrogen monoxide levels were measured within an hour and after 14 hours and a comparison made. The results are more complicated; some MOFs gave very low fluorescence values, whilst some gave much higher values, similar to measured fluorescence upon addition of nitrite, suggesting increased electron availability or transport. Through comparison with nitrite, sodium nitroprusside and potassium ferrocyanides (used as controls), it may suggest that MOFs interact in a similar manner, or that they trap NO, giving rise to low signals, or that they modify the active metal iron in NO synthase, like potassium ferrocyanide but in a much quicker fashion. The fact that other members of the L-series of MOFs gave high NO signal, indicate that MOFs trapped NO, giving rise to low NO values. Finally, reactive oxygen species and mitochondrial membrane potential was also measured, using specific dyes, for ROS, most MOFs gave low ROS

values, except "1 2, 1:3" (~160% to 100% for control). For the MMP, MOFs "L1, 1:2" and "L1, 2:1" gave the highest values, suggesting that these MOFs may stress the mitochondria, or that the charged dye preferentially binds to the MOFs. In summary the biological evaluation suggests that the L-series of MOFs are not cytotoxicity, have limited NO storage capacity and under certain environments become oxidizing, stressing the mitochondria and leading to cell death, which can be applied towards treatment of certain cancer cell types.

Brief Future Prospects and Guidelines

Any general high throughput screening tools such as Mutatox™ (*2*) or Microtox™ (*1*) suffer from lack of precision of specific genes/proteins or protein-receptor that are target by chemical agents, in addition to potential occurrence of false positives and lack of sensitivity of agents in the low parts-per-billion. The utilization of NO as a general marker of 'cell health' would also exhibit the same drawbacks. In the context of MOFs, another complication was that it was not possible quantify of degree of NO trapping by the MOF or release. Additional experiments are required to delineate whether MOFs trap or trap-and release nitric oxide (NO storage). These can be addressed through MOF co-incubation with cells and separate Brunauer–Emmett–Teller (BET) MOF experiments. If the MOFs are toxic, the cells will not grow. Lastly, the sensitivity limitation is the limitation imposed by the 4,5-diaminofluorescein fluorescent probe, which would put chemical agents concentrations in the low part-per-million range (ppm).

Evaluation of MOFs with other cell lines or different cell types is required to assess both their anti-cancer properties and their long term biological stability, over months, not days or weeks. The advantages of utilization of MOFs are the tailorable selectivity to bind or release NO to treat cellular dysfunction. The advantages are that in intermediate ppm range, MOFs can be directly and quickly evaluated in any cell system that is capable of generating NO under chemical stress, as MOF utilization becomes more ubiquitous, their cytotoxicity will need to be evaluated using a common benchmark and as a first approximation. Measurement of NO offers a relatively quick general benchmark in toxicity assessment.

Publication Date (Web): October 13, 2015 | doi: 10.1021/bk-2015-1200.ch019

Acknowledgments

The authors wish to thank the College of Arts & Sciences (CoA&S, Dr. Bashir, 160336-00002), SFFP (Bashir), DOEd PPHOA (Dr. Torres) and Welch Departmental Grant (AC-0006, Dr. Houf) at Texas A&M University-Kingsville (TAMUK) for funding and student support respectfully. The Microscopy and Imaging Center (MIC) at TAMU and the Department of Chemistry at TAMUK are also duly acknowledged for their technical support and nanostructure characterization. The Welch Foundation (AC-006) is further acknowledged in providing financial support to T. Wang in pursuance of her graduate studies. Dr. J. Wigle (RHDO, TX) is also thanked for the use of his laboratory space, reagents

and equipment to complete all the bioassays using RPE cells, as well as Ms. C. Castellanos, (RHDO) with assistance with cell culture reagents and Dr. E. Holwitt (USAF Academy, CO) for discussion relating to role of NO in stress.

Authors' Contribution

The research work referred to in part in the Results Section was undertaken by S. Bashir. Y.-P. Chen (acquired microscopy related data and analysis), T. Wang (wrote first draft, partial experimental design, partial and data analysis) and J. Liu (who conceived the research idea, scope, aims and thrust of the current book chapter as invited by the editor, completed the remaining experimental design, all other experimental work and analysis, editing of subsequent drafts and on-line submission) cited as (*23*).

Publication Date (Web): October 13, 2015 | doi: 10.1021/bk-2015-1200.ch019

Abbreviations

-	Without
Atk	Gene product initially from AK[R] mice were injected with transforming [t] retrovirus [Akt-8], from which the viral oncogene, [v-akt] and human homologues [Akt1 and Akt2] were isolated. Dysfunction of [Atk] can lead to cancer. Usually called protein kinase B (PHB) signalling pathway.
ATP	Adenosine triphosphate
Bax	Bcl-2-associated X protein
BcL-2	B-cell lymphoma 2
CN	Sodium cyanide
DAF-FM	4-Amino-5-Methylamino-2′,7′-Difluorofluorescein
Diacetate	Diacetate
DMSO	Dimethylsulfoxide
ERK	Extracellular signal-regulated kinases
H2DCFDA	6-(acetyloxy)-2,7-dichloro-9-[2(hydroperoxymethyl) -phenyl]-9H-xanthen-3-yl acetate
HP	Hydrogen Peroxide (also listed as H_2O_2)
hTERT	Immortilized with human Telomerase reverse transcriptase
IL-1β	Interleukin-*1 beta*
LDH	Lactate dehydrogenase assay
MAP	Mitogen-activated protein kinase 2
MMP	Mitochondrial membrane potential
MOF	Metal-organic framework
☠	Cell Death
NIT	Sodium nitrite
NitroP	Sodium nitroprusside
NO	Nitric Oxide
O_2^-	Superoxide

$ONOO^-$	Peroxynitrite
Oxid. Phosp	Oxidative phosphorylation
PBS	Phosphate buffered saline
PFC	Potassium ferrocyanide
PKB	Protein kinase B
RL	Rich layer of Pyruvate
RNS	Reactive nitrogen species
ROS	Reactive oxygen species
RPE	Retinal pigment epithelium
SEM	Scanning electron microscopy
SN-38	7-Ethyl-10-hydroxy-camptothecin
SOD	Superoxide dismutase
TEM	Transmission electron microscopy
TNFα	Tumor necrosis factor alpha
WC	Whole Cells

Publication Date (Web): October 13, 2015 | doi: 10.1021/bk-2015-1200.ch019

References

1. Ribo, J. M.; Kaiser, K. L. *Environ. Toxicol. Water Qual.* **1987**, *2* (3), 305–323.
2. Kwan, K. K.; Dutka, B. J.; Rao, S. S.; Liu, D. Mutatox test: a new test for monitoring environmental genotoxic agents. *Environ Pollut.* **1990**, *65* (4), 323–332.
3. Peer, D.; Karp, J. M.; Hong, S.; Farokhzad, O. C.; Margalit, R.; Langer, R. Nanocarriers as an emerging platform for cancer therapy. *Nat. Nanotech.* **2007**, *2* (12), 751–760.
4. Collins, D. J.; Zhou, H. C. Hydrogen storage in metal–organic frameworks. *J. Med. Chem.* **2007**, *17* (30), 3154–3160.
5. Kim, J.; Kim, H. S.; Lee, N.; Kim, T.; Kim, H.; Yu, T.; Hyeon, T. *Angew. Chem., Int. Ed.* **2008**, *47* (44), 8438–8441.
6. McKinlay, A. C.; Eubank, J. F.; Wuttke, S.; Xiao, B.; Wheatley, P. S.; Bazin, P.; Morris, R. E. Nitric Oxide Adsorption and Delivery in Flexible MIL-88 (Fe) Metal–Organic Frameworks. *Chem. Mater.* **2013**, *25* (9), 1592–1599.
7. Zhou, H. C.; Long, J. R.; Yaghi, O. M. Introduction to metal–organic frameworks. *Chem. Rev.* **2012**, *112* (2), 673–674.
8. An, J.; Geib, S. J.; Rosi, N. L. High and selective CO2 uptake in a cobalt adeninate metal−organic framework exhibiting pyrimidine-and amino-decorated pores. *J. Am. Chem. Soc.* **2009**, *132* (1), 38–39.
9. Chalati, T.; Horcajada, P.; Couvreur, P.; Serre, C.; Ben Yahia, M.; Maurin, G.; Gref, R. Porous metal organic framework nanoparticles to address the challenges related to busulfan encapsulation. *Nanomedicine* **2011**, *6* (10), 1683–1695.
10. Jhung, S. H.; Lee, J. H.; Yoon, J. W.; Serre, C.; Férey, G.; Chang, J. S. Microwave Synthesis of Chromium Terephthalate MIL-101 and Its Benzene Sorption Ability. *Adv. Mater.* **2007**, *19* (1), 121–124.

11. Taylor-Pashow, K. M.; Rocca, J. D.; Xie, Z.; Tran, S.; Lin, W. Postsynthetic modifications of Iron-Carboxylate nanoscale Metal-Organic frameworks for imaging and drug delivery. *J. Am. Chem. Soc.* **2009**, *131* (40), 14261–14263.
12. Miller, S. R.; Heurtaux, D.; Baati, T.; Horcajada, P.; Grenèche, J. M.; Serre, C. Biodegradable therapeutic MOFs for the delivery of bioactive molecules. *Chem. Commun.* **2010**, *46* (25), 4526–4528.
13. Yang, X.; Hong, H.; Grailer, J. J.; Rowland, I. J.; Javadi, A.; Hurley, S. A.; Gong, S. cRGD-functionalized, DOX-conjugated, and ^{64}Cu-labeled superparamagnetic iron oxide nanoparticles for targeted anticancer drug delivery and PET/MR imaging. *Biomaterials* **2011**, *32* (17), 4151–4160.
14. Taylor, K. M.; Rieter, W. J.; Lin, W. Manganese-Based Nanoscale Metal-Organic Frameworks for Magnetic Resonance Imaging. *J. Am. Chem. Soc.* **2008**, *130* (44), 14358–14359.
15. Kristiansen, K. A.; Jensen, P. E.; Møller, I. M.; Schulz, A. Monitoring reactive oxygen species formation and localisation in living cells by use of the fluorescent probe CM-H_2DCFDA and confocal laser microscopy. *Physiol. Plant.* **2009**, *136* (4), 369–383.
16. Itoh, Y.; Ma, F. H.; Hoshi, H.; Oka, M.; Noda, K.; Ukai, Y.; Toda, N. Determination and bioimaging method for nitric oxide in biological specimens by diaminofluorescein fluorometry. *Anal. Biochem.* **2000**, *287* (2), 203–209.
17. Lin, H.; Shen, Y.; Chen, D.; Lin, L.; Wilson, B. C.; Li, B.; Xie, S. Feasibility study on quantitative measurements of singlet oxygen generation using singlet oxygen sensor green. *J Fluoresc.* **2013**, *23* (1), 41–47.
18. Floryk, D.; Houek, J. Tetramethyl rhodamine methyl ester (TMRM) is suitable for cytofluorometric measurements of mitochondrial membrane potential in cells treated with digitonin. *Biosci. Rep.* **1999**, *19* (1), 27–34.
19. Riss, T. L.; Moravec, R. A. Use of multiple assay endpoints to investigate the effects of incubation time, dose of toxin, and plating density in cell-based cytotoxicity assays. *Assay Drug Dev. Technol.* **2004**, *2* (1), 51–62.
20. Ojrien, M. H. A.; Moravec, R.; Riss, T. Caspase-glo · 3/7 assay: use fewer cells and spend less time with this homogeneous assay. *Luminescence* **2003**, *200*, 0–1.
21. Wiechelman, K. J.; Braun, R. D.; Fitzpatrick, J. D. Investigation of the bicinchoninic acid protein assay: identification of the groups responsible for color formation. *Anal. Biochem.* **1988**, *175* (1), 231–237.
22. Wigle, J. C.; Castellanos, C. C.; Denton, M. L.; Holwitt, E. A. In *Mechanisms for Low-Light Therapy*; Hamblin, M. R., Carroll, J. D., Arany, P., Eds.; IX, Proceedings of the International Society for Optics and Photonics (SPIE) Biomedical Optics and Biophotonics Symposium (BiOS); SPIE: Washington, DC, 2014; Vol. 8932, pp 89320D−89320D.
23. Liu, J.; Chamakura, K.; Perez-Ballestero, R.; Bashir, S. In *Nanomaterials for Biomedicine*; Nagarajan, R.; ACS Symposium Series; ACS:Washington, DC, 2012; Vol. 1119, pp 129−154.
24. Zhang, Q.; Raoof, M.; Chen, Y.; Sumi, Y.; Sursal, T.; Junger, W.; Hauser, C. J. Circulating mitochondrial DAMPs cause inflammatory responses to injury. *Nature* **2010**, *464* (7285), 104–107.

Publication Date (Web): October 13, 2015 | doi: 10.1021/bk-2015-1200.ch019

25. Rieck, P.; Peters, D.; Hartmann, C.; Courtois, Y. A new, rapid colorimetric assay for quantitative determination of cellular proliferation, growth inhibition, and viability. *J. Tissue Cult Methods* **1993**, *15* (1), 37–41.
26. Zor, T.; Selinger, Z. Linearization of the Bradford protein assay increases its sensitivity: theoretical and experimental studies. *Anal. Biochem.* **1996**, *236* (2), 302–308.
27. Koresawa, M.; Okabe, T. High-throughput screening with quantitation of ATP consumption: a universal non-radioisotope, homogeneous assay for protein kinase. *Assay Drug Dev. Technol.* **2004**, *2* (2), 153–160.
28. Yang, D.; Elner, S. G.; Bian, Z. M.; Till, G. O.; Petty, H. R.; Elner, V. M. Pro-inflammatory cytokines increase reactive oxygen species through mitochondria and NADPH oxidase in cultured RPE cells. *Exp. Eye Res.* **2007**, *85* (4), 462–472.
29. Öz, E. S.; Aydemir, E.; Fışkın, K. DMSO exhibits similar cytotoxicity effects to thalidomide in mouse breast cancer cells. *Oncol. Lett.* **2012**, *3* (4), 927–927.
30. Barth, S. W.; Briviba, K.; Watzl, B.; Jäger, N.; Marko, D.; Esselen, M. *In vivo* bioassay to detect irinotecan-stabilized DNA/topoisomerase I complexes in rats. *Biotechnol J.* **2010**, *5* (3), 321–327.
31. Zech, J. C.; Pouvreau, I.; Cotinet, A.; Goureau, O.; Le Varlet, B.; De Kozak, Y. *Invest. Ophthalmol. Vis. Sci.* **1998**, *39* (9), 1600–1608.
32. Ballinger, S. W.; Van Houten, B; Conklin, C. A.; Jin, G. F.; Godley, B. F. Hydrogen peroxide causes significant mitochondrial DNA damage in human RPE cells. *Exp. Eye Res.* **1999**, *68* (6), 765–772.
33. Telliez, J. B.; Bean, K. M.; Lin, L. L. LRDD, a novel leucine rich repeat and death domain containing protein. *Biochim. Biophys. Acta, Protein Struct. Mol. Enzymol.* **2000**, *1478* (2), 280–288.
34. Wang, K.; Yin, X. M.; Chao, D. T.; Milliman, C. L.; Korsmeyer, S. J. BID: a novel BH3 domain-only death agonist. *Genes Dev.* **1996**, *10* (22), 2859–2869.
35. Sparrow, J. R.; Cai, B. Blue light–induced apoptosis of A2E-containing RPE: involvement of caspase-3 and protection by Bcl-2. *Invest. Ophthalmol. Vis. Sci.* **2001**, *42* (6), 1356–1362.
36. Russo, P.; Catassi, A.; Malacarne, D.; Margaritora, S.; Cesario, A.; Festi, L.; Granone, P. Tumor necrosis factor enhances SN38-mediated apoptosis in mesothelioma cells. *Cancer* **2005**, *103* (7), 1503–1518.
37. Wang, Z.; Paik, D. C.; Del Priore, L. V.; Burch Scholar, R. L., III; Gaillard, E. R. Nitrite-modified extracellular matrix proteins deleteriously affect retinal pigment epithelial cell function and viability: a comparison study with nonenzymatic glycation mechanisms. *Curr. Eye Res.* **2005**, *30* (8), 691–702.
38. Brüne, B. Nitric oxide: NO apoptosis or turning it ON? *Cell Death Differ.* **2003**, *10* (8), 864–869.
39. Cai, J.; Nelson, K. C.; Wu, M.; Sternberg, P., Jr; Jones, D. P. Oxidative damage and protection of the RPE. *Prog. Retin. Eye Res.* **2000**, *19* (2), 205–221.

Publication Date (Web): October 13, 2015 | doi: 10.1021/bk-2015-1200.ch019

40. Leavesley, H. B.; Li, L.; Prabhakaran, K.; Borowitz, J. L.; Isom, G. E. Interaction of cyanide and nitric oxide with cytochrome c oxidase: implications for acute cyanide toxicity. *Toxicol. Sci.* **2008**, *101* (1), 101–111.
41. Bates, J. N.; Baker, M. T.; Guerra, R., Jr.; Harrison, D. G. Nitric oxide generation from nitroprusside by vascular tissue: evidence that reduction of the nitroprusside anion and cyanide loss are required. *Biochem. Pharmacol.* **1991**, *42*, S157–S165.
42. Kiedrowski, L.; Manev, H.; Costa, E.; Wroblewski, J. T. Inhibition of glutamate-induced cell death by sodium nitroprusside is not mediated by nitric oxide. *Neuropharmacology* **1991**, *30* (11), 1241–1243.
43. Dulak, J.; Józkowicz, A.; Dembinska-Kiec, A.; Guevara, I.; Zdzienicka, A.; Zmudzinska-Grochot, D.; Cooke, J. P. Nitric oxide induces the synthesis of vascular endothelial growth factor by rat vascular smooth muscle cells. *Arterioscler. Thromb. Vasc. Biol.* **2000**, *20* (3), 659–666.
44. Griscavage, J. M.; Fukuto, J. M.; Komori, Y.; Ignarro, L. J. Nitric oxide inhibits neuronal nitric oxide synthase by interacting with the heme prosthetic group. Role of tetrahydrobiopterin in modulating the inhibitory action of nitric oxide. *J. Biol. Chem.* **1994**, *269* (34), 21644–21649.
45. Wink, D. A.; Darbyshire, J. F.; Nims, R. W.; Saavedra, J. E.; Ford, P. C. Reactions of the bioregulatory agent nitric oxide in oxygenated aqueous media: Determination of the kinetics for oxidation and nitrosation by intermediates generated in the nitric oxide/oxygen reaction. *Chem. Res Toxicol.* **1993**, *6* (1), 23–27.
46. Stout, A. K.; Woodward, J. J. Differential effects of nitric oxide gas and nitric oxide donors on depolarization-induced release of ^{3}[H] norepinephrine from rat hippocampal slices. *Neuropharmacology* **1994**, *33* (11), 1367–1374.
47. Ignarro, L. J.; Lippton, H.; Edwards, J. C.; Baricos, W. H.; Hyman, A. L.; Kadowitz, P. J.; Gruetter, C. A. Mechanism of vascular smooth muscle relaxation by organic nitrates, nitrites, nitroprusside and nitric oxide: evidence for the involvement of S-nitrosothiols as active intermediates. *J. Pharmacol. Exp. Ther.* **1981**, *218* (3), 739–749.
48. Garry, M. G.; Richardson, J. D.; Hargreaves, K. M. Sodium nitroprusside evokes the release of immunoreactive calcitonin gene-related peptide and substance P from dorsal horn slices via nitric oxide-dependent and nitric oxide-independent mechanisms. *J. Neurosci.* **1994**, *14* (7), 4329–4337.
49. Messmer, U.; Brune, B. Nitric oxide-induced apoptosis: p53-dependent and p53-independent signalling pathways. *Biochem. J.* **1996**, *319*, 299–305.
50. Ignarro, L. J.; Bush, P. A.; Buga, G. M.; Wood, K. S.; Fukuto, J. M.; Rajfer, J. Nitric oxide and cyclic GMP formation upon electrical field stimulation cause relaxation of corpus cavernosum smooth muscle. *Biochem. Biophys. Res. Commun.* **1990**, *170* (2), 843–850.
51. Ortuño-Sahagún, D. Nitric oxide donors as neuroprotective agents after an ischemic stroke-related inflammatory reaction. *Oxid. Med. Cell. Longevity* **2013**, 297357-1–297357-17.
52. Labeed, F. H.; Coley, H. M.; Hughes, M. P. Differences in the biophysical properties of membrane and cytoplasm of apoptotic cells revealed using dielectrophoresis. *Biochim. Biophys. Acta* **2006**, *1760* (6), 922–929.

Publication Date (Web): October 13, 2015 | doi: 10.1021/bk-2015-1200.ch019

53. Chung, H.; Hwang, J. J.; Koh, J. Y.; Kim, J. G.; Yoon, Y. H. Triamcinolone acetonide-mediated oxidative injury in retinal cell culture: comparison with dexamethasone. *Invest. Ophthalmol. Vis. Sci.* **2007**, *48* (12), 5742–5749.
54. Horcajada, P.; Chalati, T.; Serre, C.; Gillet, B.; Sebrie, C.; Baati, T.; Gref, R. Porous metal-organic-framework nanoscale carriers as a potential platform for drug delivery and imaging. *Nat. Mater.* **2010**, *9* (2), 172–178.
55. Della Rocca, J.; Liu, D.; Lin, W. Nanoscale metal–organic frameworks for biomedical imaging and drug delivery. *Acc. Chem. Res.* **2011**, *44* (10), 957–968.
56. Chalati, T.; Horcajada, P.; Gref, R.; Couvreur, P.; Serre, C. Optimisation of the synthesis of MOF nanoparticles made of flexible porous iron fumarate MIL-88A. *J. Med. Chem.* **2011**, *21* (7), 2220–2227.
57. Hinks, N. J.; McKinlay, A. C.; Xiao, B.; Wheatley, P. S.; Morris, R. E. Metal organic frameworks as NO delivery materials for biological applications. *Microporous Mesoporous Mater.* **2010**, *129* (3), 330–334.
58. Fox, S.; Wilkinson, T. S.; Wheatley, P. S.; Xiao, B.; Morris, R. E.; Sutherland, A.; Rossi, A. G. NO-loaded Zn^{2+}exchanged zeolite materials: A potential bifunctional anti-bacterial strategy. *Acta Biomater.* **2010**, *6* (4), 1515–1521.
59. Shin, J. H.; Schoenfisch, M. H. Inorganic/organic hybrid silica nanoparticles as a nitric oxide delivery scaffold. *Chem. Mater.* **2007**, *20* (1), 239–249.
60. Wheatley, P. S.; Butler, A. R.; Crane, M. S.; Fox, S.; Xiao, B.; Rossi, A. G.; Morris, R. E. NO-releasing zeolites and their antithrombotic properties. *J. Am. Chem. Soc.* **2006**, *128* (2), 502–509.
61. Parzuchowski, P. G.; Frost, M. C.; Meyerhoff, M. E. Synthesis and characterization of polymethacrylate-based nitric oxide donors. *J. Am. Chem. Soc.* **2002**, *124* (41), 12182–12191.
62. Reynolds, M. M.; Frost, M. C.; Meyerhoff, M. E. Nitric oxide-releasing hydrophobic polymers: preparation, characterization, and potential biomedical applications. *Free Radic. Biol. Med.* **2004**, *37* (7), 926–936.
63. Kröncke, K. D.; Suschek, C. V. Adulterated effects of nitric oxide–generating donors. *J. Invest. Dermatol.* **2008**, *128* (2), 258–260.
64. McKinlay, A. C.; Xiao, B.; Wragg, D. S.; Wheatley, P. S.; Megson, I. L.; Morris, R. E. Exceptional Behavior over the Whole Adsorption- Storage-Delivery Cycle for NO in Porous Metal Organic Frameworks. *J. Am. Chem. Soc.* **2008**, *130* (31), 10440–10444.
65. Guix, F. X.; Uribesalgo, I.; Coma, M.; Munoz, F. J. The physiology and pathophysiology of nitric oxide in the brain. *Prog. Neurobiol.* **2005**, *76* (2), 126–152.
66. Schulz, R.; Kelm, M.; Heusch, G. Nitric oxide in myocardial ischemia/reperfusion injury. *Cardiovasc Res.* **2004**, *61* (3), 402–413.
67. Ferdinandy, P.; Schulz, R. Nitric oxide, superoxide, and peroxynitrite in myocardial ischaemia-reperfusion injury and preconditioning. *Br. J. Pharmacol.* **2003**, *138* (4), 532–543.
68. Adachi, N.; Lei, B.; Soutani, M.; Arai, T. Different roles of neuronal and endothelial nitric oxide synthases on ischemic nitric oxide production in gerbil striatum. *Neurosci. Lett.* **2000**, *288* (2), 151–154.

Publication Date (Web): October 13, 2015 | doi: 10.1021/bk-2015-1200.ch019

69. Szydlowska, K.; Tymianski, M. Calcium, ischemia and excitotoxicity. *Cell Calcium* **2010**, *47* (2), 122–129.
70. Kuhlencordt, P. J.; Rosel, E.; Gerszten, R. E.; Morales-Ruiz, M.; Dombkowski, D.; Atkinson, W. J.; Huang, P. L. Adulterated effects of nitric oxide–generating donors. *Am. J. Physiol. Cell Physiol.* **2004**, *286* (5), C1195–C1202.
71. Moore, C.; Sanz-Rosa, D.; Emerson, M. Distinct role and location of the endothelial isoform of nitric oxide synthase in regulating platelet aggregation in males and females *in vivo*. *Eur. J. Pharmacol.* **2011**, *651* (1), 152–158.
72. Iadecola, C.; Zhang, F.; Casey, R.; Nagayama, M.; Ross, M. E. Delayed reduction of ischemic brain injury and neurological deficits in mice lacking the inducible nitric oxide synthase gene. *J. Neurosci.* **1997**, *17* (23), 9157–9164.
73. Bayır, H.; Kagan, V. E.; Clark, R. S.; Janesko-Feldman, K.; Rafikov, R.; Huang, Z.; Kochanek, P. M. Neuronal NOS-mediated nitration and inactivation of manganese superoxide dismutase in brain after experimental and human brain injury. *J. Neurochem.* **2007**, *101* (1), 168–181.
74. Wildhirt, S. M.; Weismueller, S.; Schulze, C.; Conrad, N.; Kornberg, A.; Reichart, B. Inducible nitric oxide synthase activation after ischemia/reperfusion contributes to myocardial dysfunction and extent of infarct size in rabbits: evidence for a late phase of nitric oxide-mediated reperfusion injury. *Cardiovasc. Res.* **1999**, *43* (3), 698–711.
75. Samdani, A. F.; Dawson, T. M.; Dawson, V. L. Nitric oxide synthase in models of focal ischemia. *Stroke* **1997**, *28* (6), 1283–1288.
76. Endres, M.; Laufs, U.; Liao, J. K.; Moskowitz, M. A. Targeting eNOS for stroke protection. *Trends Neurosci.* **2004**, *27* (5), 283–289.
77. Aliev, G.; Palacios, H. H.; Lipsitt, A. E.; Fischbach, K.; Lamb, B. T.; Obrenovich, M. E.; Bragin, V. Nitric oxide as an initiator of brain lesions during the development of Alzheimer disease. *Neurotox Res.* **2009**, *16* (3), 293–305.
78. Shiva, S.; Wang, X.; Ringwood, L. A.; Xu, X.; Yuditskaya, S.; Annavajjhala, V.; Gladwin, M. T. Ceruloplasmin is a NO oxidase and nitrite synthase that determines endocrine NO homeostasis. *Nat. Chem. Biol.* **2006**, *2* (9), 486–493.
79. Switzer, C. H.; Flores-Santana, W.; Mancardi, D.; Donzelli, S.; Basudhar, D.; Ridnour, L. A.; Wink, D. A. The emergence of nitroxyl (HNO) as a pharmacological agent. *Biochim. Biophys. Acta, Bioenerg.* **2009**, *1787* (7), 835–840.
80. Borer, J. S.; Redwood, D. R.; Levitt, B.; Cagin, N.; Bianchi, C.; Vallin, H.; Epstein, S. E. Reduction in myocardial ischemia with nitroglycerin or nitroglycerin plus phenylephrine administered during acute myocardial infarction. *New Engl. J. Med.* **1975**, *293* (20), 1008–1012.
81. Nadtochiy, S. M.; Burwell, L. S.; Brookes, P. S. Cardioprotection and mitochondrial S-nitrosation: effects of S-nitroso-2-mercaptopropionyl glycine (SNO-MPG) in cardiac ischemia–reperfusion injury. *J. Mol. Cell. Cardiol.* **2007**, *42* (4), 812–825.

Publication Date (Web): October 13, 2015 | doi: 10.1021/bk-2015-1200.ch019

82. Miller, R. R.; Vismara, L. A.; Zelis, R; Amsterdam, E. A.; Mason, D. T. Clinical use of sodium nitroprusside in chronic ischemic heart disease. Effects on peripheral vascular resistance and venous tone and on ventricular volume, pump and mechanical performance. *Circulation* **1975**, *51* (2), 328–336.
83. Salom, J. B.; Barberá, M. D.; Centeno, J. M.; Ortı, M.; Torregrosa, G.; Alborch, E. Relaxant Effects of Sodium Nitroprusside and NONOates in Goat Middle Cerebral Artery: Delayed Impairment by Global Ischemia-Reperfusion. *Nitric Oxide* **1999**, *3* (1), 85–93.
84. Khan, M.; Sekhon, B.; Giri, S.; Jatana, M.; Gilg, A. G.; Ayasolla, K.; Singh, I. Nitrosoglutathione reduces inflammation and protects brain against focal cerebral ischemia in a rat model of experimental stroke. *J. Cereb. Blood Flow Metab.* **2005**, *25* (2), 177–192.
85. Pluta, R. M.; Rak, R.; Wink, D. A.; Woodward, J. J.; Khaldi, A.; Oldfield, E. H.; Watson, J. C. Effects of nitric oxide on reactive oxygen species production and infarction size after brain reperfusion injury. *Neurosurgery* **2001**, *48* (4), 884–893.
86. Zhang, F.; White, J. G.; Iadecola, C. Effect of cytokines and nitric oxide on tight junctions in cultured rat retinal pigment epithelium. *J. Cereb. Blood Flow Metab.* **1994**, *14* (2), 217–226.
87. Khan, M.; Jatana, M.; Elango, C.; Paintlia, A. S.; Singh, A. K.; Singh, I. Cerebrovascular protection by various nitric oxide donors in rats after experimental stroke. *Nitric Oxide* **2006**, *15* (2), 114–124.
88. Pei, D. S.; Song, Y. J.; Yu, H. M.; Hu, W. W.; Du, Y.; Zhang, G. Y. Exogenous nitric oxide negatively regulates c-Jun N-terminal kinase activation via inhibiting endogenous NO-induced S-nitrosylation during cerebral ischemia and reperfusion in rat hippocampus. *J. Neurochem.* **2008**, *106* (4), 1952–1963.
89. Jung, K. H.; Chu, K.; Lee, S. T.; Park, H. K.; Kim, J. H.; Kang, K. M.; Roh, J. K. Microwave Synthesis of Chromium Terephthalate MIL-101 and Its Benzene Sorption Ability. *Biochem. Biophys. Res. Commun.* **2009**, *378* (3), 507–512.
90. Salom, J. B.; Ortı, M.; Centeno, J. M.; Torregrosa, G.; Alborch, E. Reduction of infarct size by the NO donors sodium nitroprusside and spermine/NO after transient focal cerebral ischemia in rats. *Brain Res.* **2000**, *865* (2), 149–156.
91. Zhuang, P.; Ji, H.; Zhang, Y. H.; Min, Z. L.; Ni, Q. G.; You, R. ZJM-289, a novel nitric oxide donor, alleviates the cerebral ischaemic-reperfusion injury in rats. *Clin. Exp. Pharmacol. Physiol.* **2010**, *37* (3), e121–e127.
92. Moncada, S.; Higgs, E. A. Molecular mechanisms and therapeutic strategies related to nitric oxide. *FASEB J.* **1995**, *9* (13), 1319–1330.
93. Huxford, R. C.; Della Rocca, J.; Lin, W. Metal-organic frameworks as potential drug carriers. *Curr. Opin. Chem. Biol.* **2010**, *14* (2), 262–268.
94. Lutz, D. A.; Guo, Y.; McLaughlin, B. J. *Exp. Eye Res.* **1995**, *61* (4), 487–493.
95. King, A.; Gottlieb, E.; Brooks, D. G.; Murphy, M. P.; Dunaief, J. L. Mitochondria-derived Reactive Oxygen Species Mediate Blue Light-induced Death of Retinal Pigment Epithelial Cells. *Photochem. Photobiol.* **2004**, *79* (5), 470–475.

Publication Date (Web): October 13, 2015 | doi: 10.1021/bk-2015-1200.ch019

96. Sreekumar, P. G.; Kannan, R.; Yaung, J.; Spee, C. K.; Ryan, S. J.; Hinton, D. R. Protection from oxidative stress by methionine sulfoxide reductases in RPE cells. *Biochem. Biophys. Res. Commun.* **2005**, *334* (1), 245–253.
97. Molday, R. S. Photoreceptor membrane proteins, phototransduction, and retinal degenerative diseases. The Friedenwald Lecture. *Invest. Ophthalmol. Vis. Sci.* **1998**, *39* (13), 2491–2513.
98. Hall, M. O.; Abrams, T. A.; Mittag, T. W. ROS ingestion by RPE cells is turned off by increased protein kinase C activity and by increased calcium. *Exp. Eye Res.* **1991**, *52* (5), 591–598.

Publication Date (Web): October 13, 2015 | doi: 10.1021/bk-2015-1200.ch019

Publication Date (Web): October 13, 2015 | doi: 10.1021/bk-2015-1200.ch020

Chapter 20

Free Radicals in Mycobacterial Disease

John E. Pearl*

The Trudeau Institute, 154 Algonquin Ave, Saranac Lake, New York 12983
***E-mail: jpearl@trudeauinstitute.org**

This chapter will discuss the role of the well-defined free radicals nitric oxide and superoxide in the context of mycobacterial disease and experimental animal models in order to summarize their essential roles in inflammation and immunity. Research articles and reviews will be discussed based on their citation index and placed within the context of immunity to mycobacterial disease in humans and experimental animal models. The final portion of this chapter will be devoted to descriptions of some of the assays used to define the roles and sources of these free radicals within the context of mycobacterial disease.

Introduction and Scope

Free radicals underlie many fundamental physiological mechanisms in biological organisms; these free radicals have been described in detail with their electrochemical characteristics and reactive behaviors well-defined to the immense benefit of the scientific community. The reactivities of free radicals have been investigated under a wide variety of conditions leading to a revolution in our understanding of their essential contribution to organism homeostasis, immunity, neurological and disease. Yet, our understanding of the functional effects and biological context of these free radicals is much less clear. This lack of clarity arises from the difficultly in bridging our fine-grained knowledge of free radical physical chemistry with the biochemical diversity inherent in cells, tissues and organisms.

This chapter discusses the role of these well-defined free radicals in the context of the staggering biochemical diversity of vertebrates using mycobacterial disease and experimental animal models to summarize their essential roles in inflammation and immunity. Research articles and reviews are discussed based on

In Oxidative Stress: Diagnostics, Prevention, and Therapy Volume 2; Hepel, et al.;
ACS Symposium Series; American Chemical Society: Washington, DC, 2015.

their impact on research (i.e., their citation index) and placed within the context of immunity to mycobacterial disease in humans and experimental animal models. The final portion of this chapter is devoted to descriptions of some of the assays used to define the roles and sources of these free radicals within the context of mycobacterial disease.

Tuberculosis and Non-Tuberculous Mycobacterial Disease (NTM)

The taxon Mycobacteriaceae encompasses a number of clinically significant pathogens, many of which cause severe pulmonary infections and debilitating chronic diseases. Among these organisms are the causative agents of tuberculosis (TB) and nontuberculous mycobacteria (NTM) disease. TB is caused by *M. tuberculosis*, a single species divided into a range of monophyletic clades reflecting its geographic and co-evolutionary origins with its principal host, humans (*1*). In contrast to TB, pulmonary NTM disease is caused by infection by one or more slow-growing environmental mycobacterial species including *M. avium* and *M. intracellulare* which together constitute the *M. avium* Complex (MAC) (*2*). Both infections are notoriously difficult to treat, often requiring long multidrug chemotherapeutic courses. While TB garners much public health attention and multidrug-resistant tuberculosis is considered a global health threat (*3*), MAC (*4*) and other opportunistic mycobacterial diseases (*5*) also constitute a growing public health concern. Taken as an aggregate, these pulmonary pathogens represent a uniquely pernicious group of bacteria. Clinical TB, especially cases featuring drug-resistant bacilli are well-reviewed in the literature (*6*), as are the efforts to dissect the correlates of disease, protective immunity and vaccine-mediated protection (*7*). While MAC infection does not kill as many people annually as *M. tuberculosis,* it is capable of producing a constellation of a diverse diseases, many of which are chronic and often fatal. These diseases are characterized by progressive infections refractory to commonly prescribed antibiotics which may clinically present as pulmonary infection in healthy adults (*8*), lymphadenitis in children (*9*, *10*) and disseminated infection in immunocompromised individuals (*11*). Less commonly, MAC is found to colonize the skin and may cause soft tissue infections (*12*). *M. avium* is an important opportunistic pathogen (*11*) and much clinical research into the pathogenesis of *M. avium* infection has been focused on co-infection in Human Immunodeficiency Virus (HIV) and Acquired Immunodeficiency Disease Syndrome (AIDs) patients (*13*, *14*). In those immunocompromised patients with a defective $CD4^+$ T cell compartment, especially those infected with HIV (*15*) suffering from AIDS, infection by either *M. tuberculosis* (*16*) or MAC (*17*) are predictors of rapid decline and mortality.

Immunity to mycobacterial infection is founded on the interplay between bacteria-intrinsic capabilities and those strategies used by the host to rid itself of the bacilli. Factors important in the development of host immunity include the route of inoculation, the infectious (*18*) and antigenic (*19*) dose received, and the specific strain or isolate of mycobacteria (*20*). The age of the host (*21*), their

Publication Date (Web): October 13, 2015 | doi: 10.1021/bk-2015-1200.ch020

overall health status, and prior immunological experience with mycobacteria (*22–24*) are among some of the host-intrinsic features that determine the quality, type and effectiveness of resulting immunity (*25*). In addition, genetic determinants influence susceptibility to mycobacterial disease (*26–28*). From the perspective of the bacilli, it must survive aerosol transport (*29*) and deposition into the lung of the host, evade host mechanisms of innate immunity (*30*), establish an intracellular niche (*31*, *32*) and most importantly for humankind, the bacilli must sense and manipulate their microenvironment (*33*). Following initial immune recognition of infection (*34*, *35*), the host will mobilize its entire armamentarium in an attempt to limit bacterial growth and contain infection, a battle it wins in ~90% of human TB cases (*21*, *36*). In the remaining 10% of human TB infections where the containment of the bacteria fails, the host will attempt to limit the spread of infection resulting in cellular and tissue damage associated with ongoing immune defense (*34*, *35*). Part of this defense is to sequester the bacilli (*37*) and limit its access to oxygen (*38*) and to deprive the bacteria of nutrients (*39*) and energy sources (*40*).

In context of pulmonary MAC infection, the proportion of environmental MAC exposures leading to active infections is not known. It is known, however, that the prevalence pulmonary MAC infections requiring treatment is increasing with case rates that vary depending on the population group and their geography (*41*). In all groups, an increased risk of pulmonary disease correlates with existing lung disease and/or impaired immunity (*2*).

In either context, these slow-growing mycobacteria colonize individual cells and begin growing in the pulmonary tissue. Once the host detects the presence of invading bacteria, a pitched combat between host and pathogen arises with the formation of the distinctive mycobacterial granuloma, a unique pathophysiological structure that is formed to isolate the mycobacteria, restrict their access to oxygen and stop their growth (*42*, *43*). Among the few effective host-derived means of killing the mycobacteria is the generation of toxic free radicals including nitric oxide, superoxide, hydrogen peroxide and peroxynitrate (*2*) which are produced by cells of the innate response under the direction of the cell-mediated acquired immune response. The cellular sources of these free radicals include neutrophils and activated macrophages (*44*). In both humans and experimental systems using murine models of infection, immunity to mycobacteria is known to rely on innate mechanisms elicited and facilitated by the acquired response (*45*). Especially relevant to this discussion is the restriction of available oxygen within the mycobacterial lesion which suggests the possibility of biochemical equilibria not normally favored in other normoxic host tissues.

In Mycobacterial Disease, Free Radical Production Is Triggered by Cytokines

Among the most-cited research articles involving mycobacteria and free radicals are studies investigating the link between the consequences to mycobacteria of activation of macrophages. This activation induces the production of antimycobacterial free radicals, including nitric oxide and superoxide. These studies are important because they provide a basis for understanding the context

Publication Date (Web): October 13, 2015 | doi: 10.1021/bk-2015-1200.ch020

within which the host produces these especially toxic and damaging free radicals to combat mycobacterial infection. In our collective attempt to better understand human disease, various murine models of TB and pulmonary mycobacterial disease have been used extensively (*46–48*). These models have defined essential cells (*49*, *50*) and mechanisms of protective immunity (*51*, *52*) which correspond to those required for protective immunity in humans (*53–55*). In the most general terms, immunity to pulmonary mycobacterial infection is quite distinct to that for other bacterial pathogens in that mycobacteria are obligate intracellular pathogens (*56*) infecting professional phagocytes, most often macrophages (*57*, *58*), which effectively shields them from the activity of immunoglobulins (*59*, *60*) and complement (*61*). Depending on the species of mycobacteria, some inhibit acidification of their intracellular compartment by blocking the molecular machinery used by the host to kill and degrade the contents of the endosomes prior to fusion with the infected phagosome (*62–64*). In contrast to other infectious diseases, while prior infection by mycobacteria can generate immunological memory, this response is not always protective (*65*) and previous infection can alter a patients susceptibility to environmental mycobacteria (*66*). One of the most important consequences of mycobacterial infection for those who develop pulmonary tuberculosis is the chronic nature of disease. Latent TB, as defined by the World Health Organization (WHO), is a state of persistent immune response to stimulation by *M. tuberculosis* antigens without evidence of clinically manifested active TB (*67*). The elapsed time between infection and abatement of the active immunological response resulting in the formation of a granuloma containing long-term persisting bacteria (*68*), which is often months to years in duration, qualifies TB as a chronic infectious disease. Indeed, TB can survive in a dormant or metabolically quiescent state (*69*, *70*) within the pulmonary granuloma for the lifetime of the patient, often recrudescing in later life (*71*) and infecting household or other close contacts (*72*). Although not compared directly in the literature, pulmonary MAC disease progression is generally more gradually continuous as it appears that *M. avium* lack the ability to enter into an analogous dormant or metabolically quiescent state.

Besides their tenacious ability to infect and survive within the immunocompetent host, mycobacterial infection poses chemotherapeutic challenges as well. With their lipid-rich cell wall, both *M. tuberculosis* and MAC resist the actions of many common antibacterial drugs (*73*), and those few drugs that are effective *in vitro* must be delivered to the intracellular endosome within which the bacterial resides at therapeutic concentrations (*74*). To underscore this difficulty, human drug therapy for mycobacterial disease is always lengthy, often requiring multiple drugs administered over 3-12 months which may be accompanied by severe side effects, including hepatic toxicity (*75*). Globally, effective chemotherapy, especially in context of multidrug-resistant (MDR) tuberculosis is expensive and requires significant supervision which is beyond the means of many patients and public health services (*76*, *77*).

In experimental murine models of tuberculosis, the generation of antimycobacterial immunity is known to depend on a number of essential host cytokines including Interferon-gamma (IFN-γ) (*78*, *79*) and its signaling components such as Interferon Regulatory Factor 1 (IRF-1) (*80*), Tumor Necrosis

In Oxidative Stress: Diagnostics, Prevention, and Therapy Volume 2; Hepel, et al.;
ACS Symposium Series; American Chemical Society: Washington, DC, 2015.

Publication Date (Web): October 13, 2015 | doi: 10.1021/bk-2015-1200.ch020

Factor-alpha (TNF-α) (*81*) and Interleukin-12 (IL-12) (*82*). The essentiality of these signaling molecules for mycobacterial immunity has been demonstrated by various methods, but the main experimental proof involves comparing immunologically intact control mice to those in which a specific gene(s), gene product(s) or cellular population(s) have been reduced or functionally eliminated, thereby allowing the comparison of the number of viable bacteria residing in various organs, such as the lung, liver and spleen.

Considered individually, IFN-γ is a cytokine produced by T and NK cells and is essential along with TNF-α for limiting mycobacterial growth within infected macrophages by triggering the production of reactive nitrogen intermediates (RNI) (*83*) and reactive oxygen intermediates (ROI) (*84*).

TNF-α is a cytokine involved in a diverse range of biological responses; among its more notable functions, it plays a protective role in the immunopathology of mycobacterial infection where its depletion is linked to caseous necrosis, altered distribution of bacilli within the granuloma and increased bacterial load (*81*). It is produced by a large number of distinct cell types of both the immune system as well as other non-immune cells while its primary immunological receptor, TNFR2, is expressed only on cells of the immune system. When *M. tuberculosis*- or *M. avium*-infected macrophages are exposed to TNF-α and IFN-γ, antimycobacterial concentrations of nitric oxide are produced (*85–87*).

Protective antimycobacterial immunity is known to depend on nitric oxide, which has been shown to result from the stimulation of macrophage Toll-like receptor 2 by a 19-kD *M. tuberculosis* lipoprotein leading to the induction of IL-12 which in turn triggers intracellular NK-kB and induction of the inducible nitric oxide synthase (iNOS) promoter (*82*).

Many reports of nitric oxide in mycobacterial disease do not directly measure nitric oxide production or concentration, but instead report indirect evidence of nitric oxide production. In some, the activity of the iNOS promoter was used to infer nitric oxide production while in others, the presence of reaction products such as nitrite/nitrate are assayed. In many studies involving murine models of disease, authors used genetic knockout mice in which the functional activity of the iNOS promoter is genetically disrupted. Indeed, very few techniques can directly assay the amount of nitric oxide produced and none could quantify NO in a complex mechanistic biological context. This last aspect is an essential point – even today, few if any methods commonly available to the bench scientist exist to directly assay free radical produced from living cells in biological models of disease.

Mycobacterial Killing Is Dependent on Reactive Nitrogen and Oxygen Intermediates

The body of research literature encompassing nitric oxide and superoxide represents a rich tapestry of systematic investigation, brilliant insight and multidisciplinary work. This effort has produced research articles relating to nitric oxide and mycobacteria (as keywords) in excess of 1700 reports beginning in 1991 and peaking in 2013 with 125 articles and for superoxide and mycobacteria, 542 research articles have been published since 1976, peaking in 2012 with 32

In Oxidative Stress: Diagnostics, Prevention, and Therapy Volume 2; Hepel, et al.;
ACS Symposium Series; American Chemical Society: Washington, DC, 2015.

Publication Date (Web): October 13, 2015 | doi: 10.1021/bk-2015-1200.ch020

articles. This rich body of literature accompanies the discovery that the killing of mycobacteria by the infected host is dependent on both reactive nitrogen and oxygen intermediates and that these separate mechanisms (*83*) are triggered by a complex network of host immune factors and cellular interactions (*65*, *88–90*).

RNI and ROI in the Oxygen-Restricted Granuloma

The reactivity of nitric oxide in the absence of oxygen has been examined in detail from the context of anaerobic nitrification (*91*) and anaerobic ammonium oxidation (*92*) in soils and water, which is the same environmental niche as *M. avium* and other environmental pathogenic Mycobacteriaceae are known to inhabit (*93*). Both of these biological processes generate nitric oxide, to which *M. avium* and other environmental mycobacteria are likely exposed (*94*). The best studied example of the generation of nitric oxide under conditions of little or no oxygen involves nitrite decomposition, a process termed denitrification, which produces nitric oxide (*95*) among other nitrogen species, most often in anaerobic soil and water. Such soils and waters include those found in wetlands, which are generally anoxic and thus support the production of trace gases, including nitric oxide by anaerobic denitrifies (*96*). Thus it appears environmental mycobacteria are likely exposed to nitric oxide within their natural biome and therefore have been selected to develop strategies to mitigate the potential damage of such toxic radicals.

In contrast to environmental mycobacteria, those bacilli that cause tuberculosis, i.e. *M. tuberculosis* ssp. have no environmental reservoir yet have also been selected to develop strategies to abate the potential damage caused by immune-mediated generation of RNI and ROI (*97*) under conditions of oxygen limitation (*98*). In the infected human or murine host, this state of limited oxygen availability is broadly termed hypoxia.

Free Radicals in Situ

Since the supply of bioavailable oxygen to individual RNI- or ROI-producing cells varies by tissue type, organ structure, the physiological state of the host and the severity of disease or redox dysfunction, the amount of commensurate radical production can vary as well (*99*). While many tissues have broadly similar resting concentrations of oxygen, the rate of oxygen resupply through hemoglobin-mediated transfer can limit the respiratory capacity of resident cells (*100*). Under conditions of elevated rates of oxygen consumption, restricted vascular supply or pathological conditions, hypoxia is known to occur. Both normal physiological variation in the local concentration of oxygen and in pathological states influences the production and functional results of free radical generation (*101*, *102*).

While the reactivities of nitric oxide and superoxide in air under standard temperature and pressure are precisely defined, their reactivities in context of cells, tissue and organs are complex (*103*). This complexity is compounded by the dynamic and selectively isolated environment found within the mycobacterial granuloma (*32*, *104–106*). Both nitric oxide and superoxide possess very short bioactive half-lives (*103*, *107*) which can be influenced by the formation of adducts and through buffering properties of biological fluids (*108*). Thus,

Publication Date (Web): October 13, 2015 | doi: 10.1021/bk-2015-1200.ch020

it follows that the biochemistry of nitric oxide and superoxide within the mycobacterial granuloma is strongly influenced by local conditions, especially pH and available molecular oxygen.

Nitric Oxide

Nitric oxide (NO) plays a pivotal role in eukaryotic physiology, immunology and cell signaling (*109*). It is a freely diffusible gaseous radical possessing one free electron that readily forms covalent bonds with a variety of reactants. The 1-10 second biological half-life of nitric oxide reflects this reactivity (*107*). While nitric oxide is the preferred International Union of Pure and Applied Chemistry (IUPAC) name for the molecule, other synonyms are used within the biological literature, including nitrogen monoxide, nitrogen oxide and nitrosyl radical.

The discovery of nitric oxide, its production and associated synthases represents a large body of research by many groups all working toward a comprehensive understanding of the sources, functions and roles of this important signaling and effector molecule (*110*, *111*). The import of nitric oxide is such that it was famously named "Molecule of the Year" in 1992 (*112*). Nitric oxide is an important physiological regulator in the nervous, immune, and cardiovascular systems where its production is correlated with nitrite concentrations which is both a nitric oxide precursor and a degradation product (*113*). Its cellular source arises from three distinct nitric oxide synthase isoenzymes in humans: neuronal nitric oxide synthase (nNOS or NOS1) (*114*), inducible nitric oxide synthase (iNOS or NOS2) (*115*) and endothelial nitric oxide synthase (eNOS or NOS3) (*116*). The canonical reaction of these isoenzymes is shown in Equation 1. This reaction is categorized by the Enzyme Commission as Reaction 1.14.13.39 as NADPH-dependent nitric-oxide synthase (*117*).

$$2\ \text{L-arginine} + 3\ \text{NADPH} + 4\ O_2 \rightharpoonup 2\ \text{L-citrulline} + 2\ NO\cdot + 3\ NADP^+ + 4\ H_2O \qquad \text{[Equation 1]}$$

Constitutively expressed neuronal nitric oxide synthase, NOS1, is found in central and peripheral neuronal cells and some epithelial cells where it functions to regulate synaptic transmission within the central nervous system as well as to regulate blood pressure, smooth muscle relaxation, and vasodilation via peripheral nitrergic nerves (*118*). It has also been found to be expressed in skeletal muscle cells where nitric oxide functions to counter muscle contraction (*119*). Inducible nitric oxide synthase, NOS2, is one of the primary antibacterial free radical generators involved in the killing of mycobacteria (*120*). It has been identified in a variety of immune cells as well as those cells that are responsive to elements of the innate or acquired immune response, including macrophages, hepatocytes, chondrocytes, epithelial cells and smooth muscle cells (*121*, *122*). NOS2 activity has been shown to lessen the inflammatory response in a feedback mechanism (*123*). Constitutively expressed endothelial nitric oxide synthase, NOS3, is found in endothelial and epithelial cells (*124*). In endothelial cells the presence of

Publication Date (Web): October 13, 2015 | doi: 10.1021/bk-2015-1200.ch020

varying levels of nitric oxide aids in vasodilation which plays an important role in the regulation of blood pressure (*125*).

In work by Ding, et al, the term RNI was used to describe a number of nitrogen oxides having biological origins, including the radical nitric oxide (NO), nitrogen dioxide (NO_2) and the anions nitrite (NO_2^-) and nitrate (NO_3^-) (*83*). Interestingly, the use of the term 'RNI' as a somewhat loose description of these few molecules appears to have developed independently from the other scientific domains as a consequence of the study of nutritional intake of nitrate in people and other mammals (*126*, *127*). Other scientific domains also use the term 'RNI,' but its usage may encompass different species of nitrogen oxides.

Nitric oxide synthases (NOSs) synthesize the metastable free radical nitric oxide. The inducible isoform (NOS2) is calcium-independent and produces large amounts of gas that can be cytotoxic. NOS oxidizes the guanidine group of L-arginine (*128*) in a process that consumes five electrons and results in the generation of nitric oxide accompanied by the stoichiometric formation of L-citrulline. The process involves the oxidation of NADPH and the reduction of molecular oxygen.

Nitric oxide exists in a pH-dependent equilibrium with nitrite, (NO_2) and dinitrogen oxide (N_2O) (*129*). Under conditions where gaseous dioxygen is available, nitric oxide forms highly reactive peroxynitrate, $ONOO^-$, which has been shown to interact with tyrosine residues involved in regulatory protein phosphorylation (*130*). In addition to these regulatory activities, nitric oxide can also function as a terminal electron acceptor for bacterial anaerobic respiration (*131*). The ability to metabolize nitric oxide is not limited to obligate anaerobes, as an environmental *Pseudomonas* species has been identified that can oxidize nitric oxide to nitrite under a range of oxygen concentrations (*132*). Importantly, nitric oxide has been shown to play a key role in the killing of *M. tuberculosis* resident within the activated macrophage (*133*). In contrast, some strains of *M. avium* are highly resistant to the effect of bactericidal effects of nitric oxide (*134*).

Publication Date (Web): October 13, 2015 | doi: 10.1021/bk-2015-1200.ch020

Superoxide

Superoxide is produced in humans and in murine models of mycobacterial disease in two distinct contexts. The first context involves superoxide production as a byproduct of mitochondrial respiration (*135*); the second context occurs when superoxide produced as an inducible component of the antibacterial response by cells of the innate (*136*) and acquired immune responses (*137*). In addition, the presence of superoxide is thought to provide redox regulatory signaling (*138*) for homeostatic maintenance (*139*). While the radical superoxide is not especially damaging on its own, it can serve as a reactant to form the basis for the generation of number of more toxic radicals including hydrogen peroxide and hydroxyl radicals via the Haber-Weiss reaction, shown as its net reaction in Equation 2 (*140*). This panoply of reactive oxygen radicals can, if left unchecked, inactivate a number of essential enzymes (*141*), oxidize DNA (*142*) or damage other intracellular molecules (*143*).

$$O_2^{\cdot -} + H_2O_2 \rightharpoonup O_2 + OH^- + OH^{\cdot} \qquad \text{[Equation 2]}$$

The enzyme superoxide dismutase largely prevents damage associated with superoxide through its conversion to hydrogen peroxide (*144*). This resulting hydrogen peroxide is degraded by either catalase or glutathione peroxidase.

The inducible production of superoxide by immune cells is involved in mycobacterial killing (*144*). Superoxide is produced by the NADPH oxidase complex (*145*, *146*), which is assembled proximal to the plasma membrane of neutrophils (*147*) or in an orientation that delivers superoxide into the phagolysosome in macrophages (*148*). This enzyme is classified as an NAD-dependent dehydrogenase, whose generic reaction is shown in Equation 3.

$$NADPH + 2O_2 \rightleftharpoons NADP^+ + 2O_2^{\cdot -} + H^+ \qquad \text{[Equation 3]}$$

NADPH oxidase is a multimeric complex composed of subunits whose specific composition differs in each of the cell types capable of generating superoxide (*149*, *150*). In human phagocytes capable of producing superoxide, the NADPH oxidase complex is composed of a membrane-associated flavocytochrome b559, itself a heterodimer subunits, gp91phox and p22phox, and four cytosolic subunits, including p47phox, p67phox, p40phox, and the GTPase Rac. Superoxide is generated by electron transfer from NADPH to oxygen via gp91phox (*151*). In human neutrophils the NADPH oxidase complex consists of structural homologs to those listed above which differ primarily in the GTPase which acts as a means of activating the enzymatic complex and linking chemokines with superoxide production (*152*, *153*). Reactive oxygen species generated by the different isoforms of the complex are proposed to function in signal transduction (*154*) related to cell growth and cancer (*155*, *156*), angiogenesis (*157*) and both innate (*158*) and acquired immunity (*159*).

Key Contributions to the Role of Free Radicals in Mycobacterial Disease

In order to gain an unbiased overview of the approaches used to define the key role of free radicals in mycobacterial disease, a literature review was performed using the Web of Science (Thomson Reuters.) The following Table 1 through Table 3 list the most highly cited research articles identified by combinations of these keywords; Table 1 lists the works containing the keywords “mycobacterium” and “nitric oxide”, Table 2, “mycobacterium” and “superoxide” and Table 3, “mycobacterium” and “nitric oxide” and “superoxide”. The methods column identifies the primary assays by which the authors performed their work. The language for each entry is paraphrased from the research article and thus illustrates the common description of these assays. In some cases, for example those involving the Griess reaction, many authors describe it as a nitric oxide assay; while this may be technically imprecise as the reaction actually converts nitrite to its colorimetric azo- form, description of it as a nitric oxide assay is in fact more descriptive due to the well-known chemical relationship between nitrate, nitrite and nitric oxide.

Publication Date (Web): October 13, 2015 | doi: 10.1021/bk-2015-1200.ch020

Table 1. Highly cited research articles "mycobacterium" and "nitric oxide."

Topic Keywords: mycobacterium AND nitric oxide. Number of articles matching search criteria = 1849.	
Ref	*Method(s)*
(*79*) Flynn, 1993	Serological RNI assayed using the Griess reaction for nitrite. Splenic NOS2 mRNA.
(*160*) Liu, 2006	None, discussion only.
(*161*) Dalton, 1993	Nitric oxide production in adherent peritoneal exudate cells (PECs) using the Griess reaction for nitrite; inhibited by N^G-2′-monomethyl-L-arginine (NNMA.)
(*82*) Brightbill, 1999	NOS2 promoter activity was measured using a reporter plasmid containing chloramphenicol acetyltransferase (*162*). NOS2 mRNA production in RAW264.7 cell line.
(*81*) Flynn, 1995	Nitric oxide produced by splenic macrophages assayed in the supernatant by the Griess reagent. Immunohistochemical detection of iNOS in frozen lung sections using a rabbit polyclonal antibody.
(*163*) Nathan, 2000	Review in which the generation of toxic ROI and RNI in host defense against pathogens is considered and necessity for both in response to mycobacterial infection is proposed.
(*80*) Kamijo, 1994	Nitric oxide produced by adherent peritoneal macrophages assayed in the supernatant by the Griess reagent. Peritoneal macrophage iNOS mRNA is assayed.
(*86*) Chan, 1992	Nitric oxide produced by cultured primary murine macrophages and cell lines D9 and J774.16 using the Griess reagent. *M. tuberculosis* strain Erdman was exposed to various concentrations of nitric oxide produced as an equilibrium product by acidified nitrite and assayed for [^{3}H]uracil incorporation.
(*164*) Schnappinger, 2003	Both wildtype and NOS2-deficient murine bone-marrow-derived macrophages were infected with M. tuberculosis clinical isolate 1254 activated with exogenous IFN-γ and gene expression microarray run on bacilli.
(*165*) Darrah, 2007	Referenced only.

Publication Date (Web): October 13, 2015 | doi: 10.1021/bk-2015-1200.ch020

Table 2. Highly cited research articles "mycobacterium" and "superoxide."

Topic keywords: mycobacterium AND superoxide. Number of articles matching search criteria = 748.	
Ref	*Method*
(*166*) Zhang, 1992	*M. tuberculosis* H37Rv gene *katG,* encoding catalase and peroxidase activity, was deleted and shown to confer sensitivity to isoniazid when present in the bacterial genome; subsequently *katG* was found to be a source of intrabacterial nitric oxide upon treatment with isoniazid (*167*).
(*168*) McCord, 1971	Various *Mycobacterium* species were shown to possess superoxide dismutase and catalase activity using the reduction of cytochrome c by superoxide assayed spectrophotometrically at 550 nm (*169*).
(*86*) Chan 1992	O_2- was produced by IFN-γ- and LPS-treated murine cell lines D9 and J774.16 and was assayed by the reduction of cytochrome c reduction assay (*170*) H_2O_2 was assayed using the horseradish peroxidase-catalyzed oxidation of fluorescent scopoletin (*171*).
(*172*) Nathan 1979	Showed that *M. bovis Bacille Calmette-Guérin* (BCG)-infected macrophages and phorbol myristate acetate (PMA)-activated granulocytes trigger hydrogen peroxide production assayed by horseradish peroxidase-catalyzed oxidation of fluorescent scopoletin (*171*, *173*)
(*174*) Bryk, 2000	Showed the mycobacterial peroxiredoxin alkylhydroperoxide reductase subunit C (*aphC)* was capable of catalytically converting peroxynitrite, the product of nitric oxide and superoxide, to nitrate.
(*175*) Pabst, 1980	O_2^- production by adherent murine peritoneal macrophages infected with M. bovis BCG was assayed using superoxide dismutase-inhibitable reduction of ferricytochrome c (*176*).
(*177*) Orme 1993	Review linking superoxide production as a potent antibacterial response to acquired T cell immunity.
(*178*) Denis, 1991	O_2^- production was assayed via the SOD-inhibitable reduction of ferricytochrome c spectrophotometrically quantified at OD_{500} nm (*179*)

Continued on next page.

Publication Date (Web): October 13, 2015 | doi: 10.1021/bk-2015-1200.ch020

Table 2. (Continued). Highly cited research articles "mycobacterium" and "superoxide."

Topic keywords: mycobacterium AND superoxide. Number of articles matching search criteria = 748.	
Ref	*Method*
(*180*) Garbe, 1996	*M. tuberculosis* expresses heat shock proteins in response to intracellular superoxide elicited by menadione but not to exogenous hydrogen peroxide as demonstrated by incorporation of radiolabeled metabolites ^{35}S-methionine and ^{35}S-cysteine and visualized by autoradiography of two-dimensional gels.
(*179*) Bermudez, 1988	O_2^- production was assayed via the SOD-inhibitable reduction of ferricytochrome c spectrophotometrically quantified at OD_{500} nm.

Table 3. Highly cited research articles "mycobacterium," "superoxide" and "nitric oxide."

Topic keywords: mycobacterium AND nitric oxide AND superoxide. Number of articles matchng search criteria = 115.	
Ref	*Method*
(*86*) Chan, 1992	Nitric oxide: see Table 1. Superoxide and hydrogen peroxide: see Table 2
(*174*) Bryk, 2000	See note in Table 2.
(*178*) Denis, 1991	Cell-free culture supernatants from human macrophages were assayed for nitrite by the Greiss reaction (*181*). Superoxide: see Table 2.
(*180*) Garbe, 1996	*M. tuberculosis* expresses heat shock proteins in response to nitric oxide elicited using the nitric oxide donor SNAP (S-nitroso-N-acetyl-D,L-penicillamine) as demonstrated by incorporation of radiolabeled metabolites ^{35}S-methionine and ^{35}S-cysteine and visualized by autoradiography of two-dimensional gels. Superoxide: see Table 2.

Continued on next page.

Publication Date (Web): October 13, 2015 | doi: 10.1021/bk-2015-1200.ch020

Table 3. (Continued). Highly cited research articles "mycobacterium," "superoxide" and "nitric oxide."

Topic keywords: mycobacterium AND nitric oxide AND superoxide. Number of articles matchng search criteria = 115.	
Ref	*Method*
(*182*) Vazquez-Torres, 2000	Nitric oxide production was inhibited using N^G-monomethyl-L-arginine and was confirmed by the loss of nitrite production assayed using the Griess reagent. The presence of hydrogen peroxide was visualized in electron micrographs using cerium chloride, which reacts with H_2O_2 to form an electrodense cerium perhydroxide precipitate (*183*). Macrophage superoxide production was estimated by the reduction of lucigenin (bis-*N*-methylacridinium) and quantified using a chemiluminometer (*184*). The p22phox or p47phox subunits of NADPH oxidase from murine macrophages were visualized using indirect immunofluorescent microscopy using rabbit anti-p22phox or p47phox polyclonal antibodies followed by a rhodamine-conjugated goat anti-rabbit polyclonal antibodies.
(*185*) Denis, 1991	Showed that RNI rather than ROI was responsible for the bactericidal activity against *M. tuberculosis* by murine macrophages. Nitrite concentration in the culture supernatants was determined spectrophotometrically at 543 nm using the Griess reaction (*181*). In addition, RNI production was inhibited by N^G-monomethyl-L-arginine acetate as well as arginase. Showed that the number of *M. tuberculosis* bacilli infecting IFN-γ activated murine macrophages was unaffected by the addition of either superoxide dismutase and/or catalase.
(*186*) Shi, 2003	Showed that NOS2 expression in the lungs of *M. tuberculosis*-infected mice correlated with bacterial load using real-time PCR to determine the copy number of the mRNA. Sections of *M. tuberculosis*-infected lungs were stained for NOS2 using immunocytochemistry. Used molecular beacon real-time PCR to assay the effect of nitric oxide on the expression of the mycobacterial *acr* gene (*187*). Used molecular beacon real-time PCR to assay the effect of superoxide on the expression of the mycobacterial *sodA* and *sodC* genes; these were found to be downregulated in this model which suggested to the authors that superoxide dismutase does not play an essential role in the protection of *M. tuberculosis* against host immunity.

Continued on next page.

Publication Date (Web): October 13, 2015 | doi: 10.1021/bk-2015-1200.ch020

Table 3. (Continued). Highly cited research articles "mycobacterium," "superoxide" and "nitric oxide."

Topic keywords: mycobacterium AND nitric oxide AND superoxide. Number of articles matchng search criteria = 115.	
Ref	*Method*
(*188*) Ng, 2004	Showed the primary function of *M. tuberculosis* KatG is to catabolize the peroxides generated by the murine phagocyte NADPH oxidase and plays a role in pathogenesis. Nitric oxide was removed from the experimental system using congenic $NOS2^{-/-}$ (deficient) mice; superoxide generated by $gp91^{Phox-/-}$. Neither nitric oxide nor superoxide were explicitly assayed, except through the increased susceptibility of genetic knockout strains to presence of exogenous hydrogen peroxide.
(*189*) Piddington, 2001	Showed that *M. tuberculosis* superoxide dismutase, SodC, enhances the resistance to the murine antimycobacterial oxidative burst generated by activated macrophages. The production of superoxide was quantified by detecting the reduction of nitroblue tetrazolium (NBT) within the macrophages and quantified at OD_{550} nm (*190*). The production of RNS was detected by quantitating the amount of nitrite released by macrophages, using the Griess reagent (*191*).
(*192*) Hurdle, 2011	This thoughtful review discusses the electronic and functional characteristics of the mycobacterial membrane in the context of energy metabolism and chronic bacterial persistence in pulmonary disease. It considers the enhanced effects of nitric oxide and superoxide in the presence of ionophores and on various key enzymes of bacterial metabolism, including cytochrome oxidases.

Publication Date (Web): October 13, 2015 | doi: 10.1021/bk-2015-1200.ch020

Direct Assays for the Detection of Nitric Oxide

Ozone-Based Chemiluminescent Detection of Nitric Oxide

The ability to directly quantify nitric oxide and its adducts in biological samples represents a significant advance in redox research. Despite this, the number of research articles referencing chemiluminescent detection of nitric oxide in the context of mycobacterial disease is actually quite small, less than 30.

Predicated on the complex biochemical interactions between nitric oxide and its many potential redox partners, a method of ozone-based chemiluminescent detection has been developed to directly quantify nitric oxide and it's adducts. This methodology requires a supply of gaseous ozone (O_3) as well as a non-reactive carrier gas such as nitrogen or helium and so is not commonly used in research laboratories; nevertheless, it has been commercialized by at least two laboratory instruments manufacturers for use in both the clinic and by more specialized

research groups (the Sievers Nitric Oxide Analyzer NOA 280i, GE Analytical Instruments and the CLD 88 sp NO Analyzer, Eco Physics.) This assay quantifies nitric oxide based on its reaction with ozone (O_3) where it forms an electronically excited molecule of nitrogen dioxide (NO_2) which then spontaneously emits a photon as it returns to its ground state. A photomultiplier or other light detector is used to measure the intensity of this infra-red chemiluminescent signal which is spectrally isolated using 600 nm long-pass filter. The intensity of the chemiluminescent signal is proportional to the amount of nitric oxide present in the sample. Importantly, pretreatment of the analyte with a strong reducing agent, such as a tri-iodide (I_3), has the potential to convert various adducts such as nitrate, nitrosothiols and nitrosoamines among others to nitric oxide which is then chemiluminescently quantified. Nitrite is not reduced to nitric oxide by I_3 treatment, however, alternate reducing agents have been used to liberate nitric oxide from nitrite and thus detect nitric oxide.

The Sievers Nitric Oxide Analyzer NOA 280i is marketed for both liquid and gaseous nitric oxide measurements with the stated liquid sample range "Nanomolar to millimolar" and a sensitivity of 1 pmol detected as 1 nM in a 1 mL sample injection; the gas sample ranges from 0.5 parts per billion (ppb) to 500 parts per million (ppm) with a sensitivity of 0.5 ppm. The Eco Physics CLD 88 sp NO Analyzer, is reported to measure nitric oxide concentrations from 0.1 –5000 (ppb) with a minimal detectable concentration of 0.06 ppb, depending on the gaseous sample flow rate into the instrument.

Publication Date (Web): October 13, 2015 | doi: 10.1021/bk-2015-1200.ch020

Electron Paramagnetic Resonance Spectroscopy

Electron paramagnetic resonance spectroscopic detection of nitric oxide and other radicals is a fundamentally important assay because it is one of the few methods that can quantify the instantaneous amount of nitric oxide or nitrosyl within a biological sample (*193*). This characteristic can distinguish chronic nitric oxide production (i.e., long term, low level) from acute production (i.e., short term, high concentration) which would produce very similar amounts of nitrate and nitrite, a circumstance that is further complicated by dietary intake of nitrates and nitrites that also contribute to variation in serum or plasma concentrations (*194*).

To summarize a rich and vibrant body of literature (*193*), electron paramagnetic resonance (EPR) detects the presence of unpaired electrons by subjecting a cryogenically frozen biological sample to an intense varying magnetic field while irradiated it with microwaves at a fixed frequency. The spin states of unpaired electrons associated with nitric oxide will cause variation of the magnetic field strength leading to the generation of an absorption spectrum with peak absorption measured at a given microwave frequency. Since biological samples will contain many different paramagnetic molecules and generally low concentrations of nitric oxide, various spin-trapping or spin-labeling molecules can be used to amplify the absorption spectra of nitric oxide. Despite the obvious advantages of EPR detection of nitric oxide in mycobacterial research, only five research publications have used this approach.

In stark contrast to the previously described assays, direct fluorescent detection of nitric oxide is a comparatively simple laboratory method using a variety of non- or minimally-fluorescent substrates that react with nitric oxide to form fluorescent molecules. The advantages to such compounds are their relatively low cost and their minimal instrumentation requirements.

A second key advantage arises from the biological aspects of RNI production in context of mycobacterial disease in that it is not generated by most cells of the assayed tissue, for instance the lung or spleen, and of those cells that do produce nitric oxide, they are easily identified as strong producers (*90*). Nitric oxide is typically detected at a very low concentration within a population of primary cells isolated from infected hosts, for example cells isolated from whole murine lungs or spleens; this concentration reflects the vigorous production of nitric oxide by only a few cells among millions of non-producing cells. Despite this low overall or organ-level concentration, the local nitric oxide concentration may be quite high within the mycobacterial lesion due to its small size which contains most of the nitric oxide-producing cells found within the infected organ. Since nitric oxide has a very short bioactive half-life and it diffuses from its point source into the surrounding tissue, most of the cells in a given specimen will have little to no fluorescence signal while those relatively rare cells generating nitric oxide will be highly fluorescent. The many dimly or non-fluorescent cells present which constitute the fluorescent background from which the rare population of highly fluorescent cells contributes to an assay with a high dynamic range.

The disadvantage to this approach is often a lack of specificity for nitric oxide and relatively insensitive detection methods based on the stoichiometric accumulation of fluorescent signal, also termed an ‘endpoint dosimetric’ assay rather than the instantaneous amount of nitric oxide present. The lack of specificity is especially important in the context of murine models of mycobacterial disease because RNI and ROI are often coexpressed within the local lesion and may in fact be generated by the same cell.

The rationale that drove the development of these fluorescent probes was a clear understanding of the need to localize the production of nitric oxide to individual or clusters of viable cells in situ. This need was especially important in the field of mycobacterial disease research where the antibacterial properties of inducible nitric oxide had been discovered only a few years earlier.

DAF (4,5-diaminofluorescein)-Based Fluorescent Probes

One of the primary advantages of fluorescent probes based on 4,5-diaminofluorescein and related molecules are their ability to be formulated to facilitate diffusion across cellular membranes where the molecule is converted to its highly fluorescent triazolofluorescein form by non-specific intracellular esterases that render the probe much less able to diffuse out of the cell. The relative cell-permanence of nitric oxide-associated fluorescent signal is an important aspect of the utility of these probes, lending itself to assays suitable

In Oxidative Stress: Diagnostics, Prevention, and Therapy Volume 2; Hepel, et al.;
ACS Symposium Series; American Chemical Society: Washington, DC, 2015.

Publication Date (Web): October 13, 2015 | doi: 10.1021/bk-2015-1200.ch020

for fluorescent microscopy, flow cytometry and plate-based fluorimetry (*195*, *196*). While many of the commercially available preparations of DAF-based fluorescent probes are marketed as detectors of nitric oxide, they in fact react with peroxynitrate ($ONOO^-$) (*197*) or dinitrogen trioxide (N_2O_3); despite this imprecision, it is generally agreed that this class of fluorescent probes does quantify cumulative nitric oxide exposure, albeit indirectly. DAF-based fluorescent probes are slightly sensitive to variation in pH (*198*), although most kits supply sufficiently buffered reagents to minimize this effect. In most commercial kits, their stated limits of nitric oxide [*sic*] detection are ~3 nM for DAF-FM (4-amino-5-methylamino-2′,7′-difluorofluorescein) and ~5 nM for DAF-2.

Publication Date (Web): October 13, 2015 | doi: 10.1021/bk-2015-1200.ch020

Indirect Assays for Nitric Oxide

Hemoglobin and Myoglobin-Based Oxidation Assays

Nitric oxide is known to strongly interact with a number of heme-containing molecules, including ferrous deoxyhemoglobin and myoglobin among others. This interaction is understood to represent the primary mechanism for nitric oxide catabolism in vivo (*199*, *200*). Historically, these reactions helped to define some of the basic biological characteristics of nitric oxide in blood and plasma; at the time, literature suggested this type of reaction, i.e., the conversion of oxygenated hemoglobin to methemoglobin, could be used as a direct means for assaying nitric oxide in biological samples by quantifying spectrophotometric absorbance changes to solutions of heme-containing molecules (*201*). Mechanistically, it was later discovered that these seemingly simple catabolic reactions were complicated by the presence of oxygen and its reactive intermediates (*202*, *203*). Few if any commercially produced nitric oxide assay kits based on the oxidation of hemoglobin or myoglobin are available.

Enzymatic Assays

Among the oldest methods for indirectly quantifying nitric oxide production is through the use of enzymatic assays that measure the two-step nitric oxide synthase-mediated conversion of L-arginine to L-citrulline, a process that requires NADPH and yields a molecule of nitric oxide (*204*). Separation of reactants is accomplished by a number of techniques including ion-exchange chromatography. Historically, this assay was performed with radiolabeled L-arginine which was followed by liquid scintillation counting to demonstrate the source of nitric oxide (*205*). The advantage of this and other similar enzymatic assays is that the stoichiometric properties of the enzymes and their required cofactors are often well-known, such as NADPH in the example above. Furthermore, well-designed enzymatic assays can yield a precise quantitative outcome through the judicious use of stable isotopically labelled reactants, competitors and enzymatic antagonists, such as L-NG-monomethyl arginine (L-NMMA) and other controls. One potential limitation of the radiolabeled enzymatic assay

is that radioactive L-arginine, when processed by nitric oxide synthase, can generate radiolabeled gaseous nitric oxide whose quantification may be quite difficult due to its highly reactive nature, short half-life and tissue diffusibility (*206*). The primary advantage of enzymatic assays is their high precision and low background.

Griess-Reaction Based Assays

One of the oldest and most widely used assays of nitric oxide generation is the Griess reaction, which is the formation of colored diazonium compounds from that occurs in the presence of nitrite (*207*). Implicit in this and many other 'nitric oxide' assays is the relationship between nitric oxide production and the accumulation of nitrite (NO_2^-) and nitrate (NO_3^-) anions which defines a complex biochemical pathway producing, consuming and acting on a wide range of metabolites (*199*, *208*). In this context, it is well-understood that nitric oxide is produced enzymatically through the oxidation of L-arginine (*87*, *114*).

The reaction itself typically uses sulphanilamide in a dilute phosphoric acid solution with an analyte containing nitrite (NO_2^-) that forms a yellow diazonium salt. Upon the addition of naphthylethylenediamine dihydrochloride, this salt turns salmon or pink/purple with an absorbance at 520-550 nm which is proportional to the amount of nitrite in the analyte. In most assays, nitrite is quantified in the analyte and then total nitrate is determined using the enzyme nitrate reductase to convert all nitrate into nitrite.

The success of this assay depends on good experimental design and appropriate controls. For example, experimental design may require several distinct biological controls, perhaps lacking the induction of nitric oxide or those that are treated with an enzymatic inhibitors, such as those targeting essential cofactors or substrates as well as small molecule inhibitors (*209*). Examples of these inhibitors include N^G- 2′-monomethyl-L-arginine (N^GMMA) and aminoguanidine (*210*). Cell-free or nitric oxide-free media may also be useful to establish a lower level of quantification. Various standard curves are necessary as well. As one of many excellent examples, Ding and colleagues assayed anionic nitrite as a proxy for nitric oxide (*83*) where the analyte was standardized against a serial dilution of sodium nitrite with a reported background value of 0.2 to 0.3 nmol of nitrite detected.

For many years, commercially available Griess assay kits have provided the non-redox specialist with a "good enough" means of measuring nitric oxide. Despite not directly assaying nitric oxide, these kits provide a simple, cheap and arguably essential approach to quantifying nitric oxide. Several variations to this general approach have been developed including fluorescent probes such as (2,3-diaminonaphthalene); these assays offer an increase in assay sensitivity which lowers their limit of detection to ~500 nM in such volumes as 50 µL. Griess reaction-based assay kits are available from a number of vendors which generally claim appropriate use on such biological specimens as serum, plasma, urine, saliva, lysates, and media. Most demonstrate detection sensitivities of around 2 µM in a small, often 50 µL samples. While Griess-type assays are

In Oxidative Stress: Diagnostics, Prevention, and Therapy Volume 2; Hepel, et al.;
ACS Symposium Series; American Chemical Society: Washington, DC, 2015.

Publication Date (Web): October 13, 2015 | doi: 10.1021/bk-2015-1200.ch020

technically simple and quick to perform, they can generate false positive results in the presence of microbial contaminants such as *E. coli*, *Kelbsiella* ssp. or *Pseudomonas* ssp., which are known to be strong nitrate reducers which can replicate quickly in some analytes (*211*).

NOS2 mRNA Assays

Polymerase chain reaction, PCR, and reverse transcriptase-PCR form the basis of the molecular biology revolution that began in 1985 and continues today (*212*). Quantitative messenger RNA-based assays for the detection of altered gene expression of NOS2 have demonstrated that the number of mRNA copies correlates with amount of nitric oxide generated (*213*). These assays, while not directly quantifying nitric oxide, can effectively establish a link between the environment or signaling milieu which trigger the generation of nitric oxide and the necessary synthesis of inducible nitric oxide synthase molecular components. Importantly, this technique is relatively simple and requires instrumentation that is commonly available in labs or core facilities.

Immunohistochemical Detection of iNOS

Immunohistochemical detection of iNOS in formalin-fixed or frozen tissue is an excellent approach to localizing the possible cells and tissue regions from which nitric oxide may originate. Importantly, this technique offers a unique perspective in that the presence of iNOS within cells distributed through infected or diseased heterogeneous tissue can be identified (*214*). Antibody-medicated immunohistochemical detection of iNOS is often combined with other phenotypic markers to show that specific cellular populations in complex tissue (*90*).

Direct Assays for Superoxide

Electron Paramagnetic Resonance Spectroscopy

The detection and quantification of superoxide generated in biological systems is a daunting endeavor due to its high reactivity and short half-life. In a current and thorough review, various detection methodologies are summarized and their relative strengths assessed (*215*). Within the context of this chapter, however, direct quantification of superoxide is challenging for many of the same reasons direct quantification as nitric oxide is difficult. As a free radical, superoxide exhibits a strong EPR signal and it is possible to detect superoxide directly using electron paramagnetic resonance spectroscopy when its abundance is high. For practical purposes, however, this can be achieved only *in vitro* under non-physiological conditions (*193*). EPR used with the spin trap 5,5-dimethyl-1-pyrrolidine-N-oxide (DMPO) has been reported to detect intrabacterial superoxide production in *M. tuberculosis* treated with the

In Oxidative Stress: Diagnostics, Prevention, and Therapy Volume 2; Hepel, et al.;
ACS Symposium Series; American Chemical Society: Washington, DC, 2015.

Publication Date (Web): October 13, 2015 | doi: 10.1021/bk-2015-1200.ch020

chemotherapeutic rifampin (*216*). Despite the obvious advantages to direct quantification, little application of EPR to the production of superoxide in mycobacterial disease has been reported.

Chemiluminescent Detection of Superoxide

Other methods have been developed for the direct detection and quantification of superoxide, including a widely used chemiluminescent assay based on lucigenin (10,10′-dimethyl-9,9′-biacridinium dinitrate) (*217*) in which a photon is emitted when the probe is reduced. This chemiluminescence generates a quantifiable signal when measured over time. Successful use of this probe is dependent on careful baseline measurements and equilibration of the luminometer as well as selection of appropriate, high-purity reagents. Furthermore, good assay design may include enzymatic controls, such as catalase and/or superoxide dismutase, or other free radical scavengers in order to aid in the identification the chemical species reducing the chemiluminescent probe. luminol (5-amino-1,2,3,4-tetrahydro-1,4-phthalazinedione, 3-aminophthalic acid hydrazide) represents a complementary chemiluminescent probe for the direct detection of hydrogen peroxide is (*218*). Very little research has been performed using the chemiluminescent probes to assay superoxide production in mycobacterial disease.

Fluorescent Detection of Superoxide

Direct detection of superoxide by various fluorescent molecules has been rigorously reviewed with careful attention paid to the chemical specificities of the various probes (*219*). While many manufacturers market their probes for superoxide detection and quantification, the biochemistry of these molecules is quite complex; therefore, additional analytical methods including LC–MS or HPLC are required to define the fluorescent product resulting from their reaction with superoxide or other electron donors (*220*). Since most of these fluorescent probes are non-specific for various ROI species, appropriate enzymatic controls are necessary, including superoxide dismutase and catalase, whose presence will reduce superoxide- or hydrogen peroxide-associated fluorescent signal. Often, however, one may observe both species and perhaps others contributing to the probe's fluorescence.

Ferricytochrome c Reduction Assay for Detection of Superoxide

One of the most widely used assays for superoxide detection is uses the reduction of ferricytochrome c (Fe^{3+}) to ferrocytochrome c (Fe^{2+}) by superoxide which is quantified spectrophotometrically as increased absorbance at 550 nm (*221*). This assay is similar to the other direct detection methods for superoxide in that ferricytochrome c can accept an unpaired electron from any source and

In Oxidative Stress: Diagnostics, Prevention, and Therapy Volume 2; Hepel, et al.;
ACS Symposium Series; American Chemical Society: Washington, DC, 2015.

Publication Date (Web): October 13, 2015 | doi: 10.1021/bk-2015-1200.ch020

therefore it is essential that superoxide dismutase- and catalase-treated controls are included in the experimental design.

Indirect Assays for Superoxide

As noted earlier, indirect assays often quantify side reactants, products or adducts. This is especially true in the case of superoxide in which most biological systems have enzymatic pathways for the elimination of these radicals. It is well known that superoxide dismutase converts superoxide to hydrogen peroxide (*222*, *223*) which can be assayed in order to estimate the amount and rate of production of superoxide.

Publication Date (Web): October 13, 2015 | doi: 10.1021/bk-2015-1200.ch020

Fluorescent Detection of Superoxide Using Scopoletin

While many probes has fluorescently using a number of reported were measured using the product of horseradish peroxidase oxidation of fluorescent scopoletin. This assay quantifies the loss of fluorescence at 460 nm caused by the presence of hydrogen peroxide in the presence of horseradish peroxidase (*224*, *225*).

Fluorescent Detection of Alkyl Hydroperoxidase (AhpC) Activity

The function of the mycobacterial gene alkyl hydroperoxidase (*ahpC*) has been associated with enhanced resistance to hydrogen peroxide in tuberculosis (*226*) and was shown to be a member of the peroxiredoxin family whose function is to protect organisms from oxidative stress (*97*). The assay used to define this function involved the addition of the purified protein AhpC to solutions of fluorescent dihydrorhodamine or supercoiled DNA to which peroxynitrite was added. The amount of protection that AhpC against peroxynitrate-mediated fluorescent quenching or open-circle DNA was quantified (*174*).

Conclusion

Free radicals play an important role in mycobacterial disease and represent an essential component of antimycobacterial defense. In addition to their direct effects on mycobacteria, the presence of nitric oxide and superoxide provide signals that help modulate the host immune response. Despite our increasing understanding of the role these molecules play in mycobacterial disease, at least three important questions remain. These questions include: what are the *in vivo* cellular sources of nitric oxide and superoxide in the diseased lung? What are the signaling and regulatory requirements necessary for their generation? Can free radical production be modulated to more effectively treat mycobacterial disease?

Considering the broad direction of research involving nitric oxide and superoxide over the previous decades, future work will further define the *in vivo*

cellular sources of these molecules during pulmonary disease. This in itself will be an important observation, as there is no clear consensus regarding the source of free radical production or whether these molecules are generated by infected macrophages or by non-infected bystander cells. It seems likely that the source of free radical production shifts from cells of the innate response early during the infection, perhaps neutrophils and monocytes, to strong production bt macrophages within and around the highly dynamic granuloma found during latent TB (*68*). It follows that the source, rate of production and amount of nitric oxide and superoxide will vary over the course of disease and that these characteristics may be predictive for clinical complications such as cavitation or recrudescence for TB or dissemination for pulmonary MAC disease. The details regarding the source(s) of free radical production represent a rich but as-yet undiscovered country.

Of the various cellular sources of nitric oxide and superoxide in pulmonary mycobacterial disease, much remains unknown about the larger signaling milieu within which these cells function and how their products influence the local microenvironment. In addition, we know little about how the cells that generate nitric oxide and superoxide integrate multiple cytokine, chemokine and ligand signals. Notably, one aspect of nitric oxide and superoxide signaling has enjoyed considerable progress, in which we are now beginning to understand the effect of these radicals on the mycobacteria themselves (*227*).

The targeted modulation of nitric oxide and/or superoxide represents the culmination of applied research into their role in pulmonary mycobacterial disease. Once a clear understanding of the interrelated host and mycobacterial biology is gained, and the sources and roles of free radicals in TB and pulmonary MAC disease defined, modulation of these species may be achievable. The purpose of such modulation may include approaches to more effectively kill mycobacteria, perhaps to reduce the severity of immunopathology or to enhance the effectiveness current drug treatment regimens.

The wide range of methods and approaches used to explore the important relationship between free radical production and mycobacterial disease, of which only a few are summarized here, attest to the innovation and insight of the research community. Unfortunately, no method currently exists for the real-time simultaneous quantification of the wide variety of radicals that are currently known to play a role in mycobacterial disease caused by TB or pulmonary MAC infection. A number of approaches, however, are improving our ability to detect and quantify these free radicals, including novel combinations of existing techniques such as those that combine fluorescence and confocal microscopy with electrochemical quantification of nitric oxide and superoxide (*228*).

Publication Date (Web): October 13, 2015 | doi: 10.1021/bk-2015-1200.ch020

References

1. Parwati, I.; van Crevel, R.; van Soolingen, D. Possible underlying mechanisms for successful emergence of the Mycobacterium tuberculosis Beijing genotype strains. *Lancet Infect. Dis.* **2010**, *10* (2), 103–11.

2. Turenne, C. Y.; Wallace, R., Jr.; Behr, M. A. Mycobacterium avium in the postgenomic era. *Clin. Microbiol. Rev.* **2007**, *20* (2), 205–29.
3. Raviglione, M. *Gear up to end TB: Introducing the end TB Strategy*; World Health Organization: 2015.
4. Pedley, S.; Bartram, J. *Pathogenic mycobacteria in water: A guide to public health consequences, monitoring and management*; IWA Publishing: 2004.
5. *Management of Buruli ulcer–HIV coinfection: technical update*; World Health Organization: 2015.
6. Park, C. K.; Kwon, Y. S. Respiratory review of 2014: tuberculosis and nontuberculous mycobacterial pulmonary disease. *Tuberc. Respir. Dis.* **2014**, *77* (4), 161–6.
7. Bhatt, K.; Verma, S.; Ellner, J. J.; Salgame, P. Quest for correlates of protection against tuberculosis. *Clin. Vaccine Immunol.* **2015**, *22* (3), 258–66.
8. Chitty, S. A.; Ali, J. Mycobacterium avium complex pulmonary disease in immunocompetent patients. *South Med. J.* **2005**, *98* (6), 646–52.
9. Esther, C. R., Jr.; Henry, M. M.; Molina, P. L.; Leigh, M. W. Nontuberculous mycobacterial infection in young children with cystic fibrosis. *Pediatr. Pulmonol.* **2005**, *40* (1), 39–44.
10. Pierre-Audigier, C.; Ferroni, A.; Sermet-Gaudelus, I.; Le Bourgeois, M.; Offredo, C.; Vu-Thien, H.; Fauroux, B.; Mariani, P.; Munck, A.; Bingen, E.; Guillemot, D.; Quesne, G.; Vincent, V.; Berche, P.; Gaillard, J. L. Age-related prevalence and distribution of nontuberculous mycobacterial species among patients with cystic fibrosis. *J. Clin. Microbiol.* **2005**, *43* (7), 3467–70.
11. Corti, M.; Palmero, D. Mycobacterium avium complex infection in HIV/AIDS patients. *Expert Rev. Anti-Infect. Ther.* **2008**, *6* (3), 351–63.
12. Wagner, D.; Young, L. S. Nontuberculous mycobacterial infections: a clinical review. *Infection* **2004**, *32* (5), 257–70.
13. Bermudez, L. E. Immunobiology of Mycobacterium avium infection. *Eur. J. Clin. Microbiol. Infect. Dis.* **1994**, *13* (11), 1000–6.
14. Mycobacterioses and the acquired immunodeficiency syndrome. Joint Position Paper of the American Thoracic Society and the Centers for Disease Control. *Am. Rev. Respir. Dis.* **1987**, *136* (2), 492–6.
15. Mamishi, S.; Pourakbari, B.; Marjani, M.; Mahmoudi, S. Diagnosis of latent tuberculosis infection among immunodeficient individuals: review of concordance between interferon-gamma release assays and the tuberculin skin test. *Br. J. Biomed. Sci.* **2014**, *71* (3), 115–24.
16. Bruchfeld, J.; Correia-Neves, M.; Kallenius, G. Tuberculosis and HIV Coinfection. *Cold Spring Harbor Perspect. Med.* **2015**, *5* (7).
17. Henkle, E.; Winthrop, K. L. Nontuberculous mycobacteria infections in immunosuppressed hosts. *Clin. Chest Med.* **2015**, *36* (1), 91–9.
18. Power, C. A.; Wei, G.; Bretscher, P. A. Mycobacterial dose defines the Th1/Th2 nature of the immune response independently of whether immunization is administered by the intravenous, subcutaneous, or intradermal route. *Infect. Immun.* **1998**, *66* (12), 5743–50.
19. Aagaard, C.; Hoang, T. T.; Izzo, A.; Billeskov, R.; Troudt, J.; Arnett, K.; Keyser, A.; Elvang, T.; Andersen, P.; Dietrich, J. Protection

Publication Date (Web): October 13, 2015 | doi: 10.1021/bk-2015-1200.ch020

and polyfunctional T cells induced by Ag85B-TB10.4/IC31 against Mycobacterium tuberculosis is highly dependent on the antigen dose. *PLoS One* **2009**, *4* (6), 0005930.
20. Hernandez-Pando, R.; Marquina-Castillo, B.; Barrios-Payan, J.; Mata-Espinosa, D. Use of mouse models to study the variability in virulence associated with specific genotypic lineages of Mycobacterium tuberculosis. *Infect. Genet. Evol.* **2012**, *12* (4), 725–31.
21. Salgame, P.; Geadas, C.; Collins, L.; Jones-Lopez, E.; Ellner, J. J. Latent tuberculosis infection - Revisiting and revising concepts. *Tuberculosis* **2015**, *95* (4), 373–84.
22. Andrews, J. R.; Noubary, F.; Walensky, R. P.; Cerda, R.; Losina, E.; Horsburgh, C. R. Risk of progression to active tuberculosis following reinfection with Mycobacterium tuberculosis. *Clin. Infect. Dis.* **2012**, *54* (6), 784–91.
23. Cardona, P. J. A dynamic reinfection hypothesis of latent tuberculosis infection. *Infection* **2009**, *37* (2), 80–6.
24. Chiang, C. Y.; Riley, L. W. Exogenous reinfection in tuberculosis. *Lancet Infect. Dis.* **2005**, *5* (10), 629–36.
25. Cooper, A. M. Host versus pathogen: two sides of the same challenge in the TB world. *Eur. J. Immunol.* **2009**, *39* (3), 632–3.
26. Bellamy, R. Susceptibility to mycobacterial infections: the importance of host genetics. *Genes Immun.* **2003**, *4* (1), 4–11.
27. Bellamy, R. Genetic susceptibility to tuberculosis. *Clin. Chest Med.* **2005**, *26* (2), 233–46.
28. Levin, M.; Newport, M. Understanding the genetic basis of susceptibility to mycobacterial infection. *Proc. Assoc. Am. Physicians* **1999**, *111* (4), 308–12.
29. Clark, S. O.; Hall, Y.; Kelly, D. L.; Hatch, G. J.; Williams, A. Survival of Mycobacterium tuberculosis during experimental aerosolization and implications for aerosol challenge models. *J. Appl. Microbiol.* **2011**, *111* (2), 350–9.
30. Schorey, J. S.; Cooper, A. M. Macrophage signalling upon mycobacterial infection: the MAP kinases lead the way. *Cell. Microbiol.* **2003**, *5* (3), 133–42.
31. Zuniga, J.; Torres-Garcia, D.; Santos-Mendoza, T.; Rodriguez-Reyna, T. S.; Granados, J.; Yunis, E. J. Cellular and humoral mechanisms involved in the control of tuberculosis. *Clin. Dev. Immunol.* **2012**, *193923* (10), 17.
32. Saunders, B. M.; Britton, W. J. Life and death in the granuloma: immunopathology of tuberculosis. *Immunol. Cell Biol.* **2007**, *85* (2), 103–11.
33. Huynh, K. K.; Grinstein, S. Regulation of vacuolar pH and its modulation by some microbial species. *Microbiol. Mol. Biol. Rev.* **2007**, *71* (3), 452–62.
34. Dorhoi, A.; Kaufmann, S. H. Perspectives on host adaptation in response to Mycobacterium tuberculosis: modulation of inflammation. *Semin. Immunol.* **2014**, *26* (6), 533–42.
35. Philips, J. A.; Ernst, J. D. Tuberculosis pathogenesis and immunity. *Annu. Rev. Pathol.* **2012**, *7*, 353–84.

Publication Date (Web): October 13, 2015 | doi: 10.1021/bk-2015-1200.ch020

36. Getahun, H.; Matteelli, A.; Chaisson, R. E.; Raviglione, M. Latent Mycobacterium tuberculosis infection. *N. Engl. J. Med.* **2015**, *372* (22), 2127–35.
37. Ehlers, S. Lazy, dynamic or minimally recrudescent? On the elusive nature and location of the mycobacterium responsible for latent tuberculosis. *Infection* **2009**, *37* (2), 87–95.
38. Gupta, S.; Chatterji, D. Stress responses in mycobacteria. *IUBMB Life* **2005**, *57* (3), 149–59.
39. Banerjee, S.; Farhana, A.; Ehtesham, N. Z.; Hasnain, S. E. Iron acquisition, assimilation and regulation in mycobacteria. *Infect. Genet. Evol.* **2011**, *11* (5), 825–38.
40. Somashekar, B. S.; Amin, A. G.; Rithner, C. D.; Troudt, J.; Basaraba, R.; Izzo, A.; Crick, D. C.; Chatterjee, D. Metabolic profiling of lung granuloma in Mycobacterium tuberculosis infected guinea pigs: ex vivo 1H magic angle spinning NMR studies. *J. Proteome Res.* **2011**, *10* (9), 4186–95.
41. Mirsaeidi, M.; Machado, R. F.; Garcia, J. G.; Schraufnagel, D. E. Nontuberculous mycobacterial disease mortality in the United States, 1999-2010: a population-based comparative study. *PLoS One* **2014**, *9* (3).
42. Cambier, C. J.; Falkow, S.; Ramakrishnan, L. Host evasion and exploitation schemes of Mycobacterium tuberculosis. *Cell* **2014**, *159* (7), 1497–509.
43. Orme, I. M.; Basaraba, R. J. The formation of the granuloma in tuberculosis infection. *Semin. Immunol.* **2014**, *26* (6), 601–9.
44. Filipe-Santos, O.; Bustamante, J.; Chapgier, A.; Vogt, G.; de Beaucoudrey, L.; Feinberg, J.; Jouanguy, E.; Boisson-Dupuis, S.; Fieschi, C.; Picard, C.; Casanova, J. L. Inborn errors of IL-12/23- and IFN-gamma-mediated immunity: molecular, cellular, and clinical features. *Semin. Immunol.* **2006**, *18* (6), 347–61.
45. Pelletier, M.; Forget, A.; Bourassa, D.; Gros, P.; Skamene, E. Immunopathology of BCG infection in genetically resistant and susceptible mouse strains. *J. Immunol.* **1982**, *129* (5), 2179–85.
46. Beamer, G. L.; Turner, J. Murine models of susceptibility to tuberculosis. *Arch. Immunol. Ther. Exp.* **2005**, *53* (6), 469–83.
47. Cooper, A. M.; Appelberg, R.; Orme, I. M. Immunopathogenesis of Mycobacterium avium infection. *Front. Biosci.* **1998**, *5* (3), e141–8.
48. Shi, C.; Shi, J.; Xu, Z. A review of murine models of latent tuberculosis infection. *Scand. J. Infect. Dis.* **2011**, *43* (11−12), 848–56.
49. Kaufmann, S. H. Cell-mediated immunity: dealing a direct blow to pathogens. *Curr. Biol.* **1999**, *9* (3), R97–9.
50. Prendergast, K. A.; Kirman, J. R. Dendritic cell subsets in mycobacterial infection: control of bacterial growth and T cell responses. *Tuberculosis* **2013**, *93* (2), 115–22.
51. Rowe, J. H.; Ertelt, J. M.; Way, S. S. Foxp3(+) regulatory T cells, immune stimulation and host defence against infection. *Immunology* **2012**, *136* (1), 1–10.
52. Torrado, E.; Cooper, A. M. IL-17 and Th17 cells in tuberculosis. *Cytokine Growth Factor Rev.* **2010**, *21* (6), 455–62.

Publication Date (Web): October 13, 2015 | doi: 10.1021/bk-2015-1200.ch020

53. Flynn, J. L. Lessons from experimental Mycobacterium tuberculosis infections. *Microbes Infect.* **2006**, *8* (4), 1179–88.
54. Fletcher, H. A. Correlates of immune protection from tuberculosis. *Curr. Mol. Med.* **2007**, *7* (3), 319–25.
55. Goldsack, L.; Kirman, J. R. Half-truths and selective memory: Interferon gamma, CD4(+) T cells and protective memory against tuberculosis. *Tuberculosis* **2007**, *87* (6), 465–73.
56. Cosma, C. L.; Sherman, D. R.; Ramakrishnan, L. The secret lives of the pathogenic mycobacteria. *Annu. Rev. Microbiol.* **2003**, *57*, 641–76.
57. Bermudez, L. E.; Wagner, D.; Sosnowska, D. Mechanisms of Mycobacterium avium pathogenesis. *Arch. Immunol. Ther. Exp.* **2000**, *48* (6), 521–7.
58. Russell, D. G. Mycobacterium tuberculosis: here today, and here tomorrow. *Nat. Rev. Mol. Cell Biol.* **2001**, *2* (8), 569–77.
59. Achkar, J. M.; Casadevall, A. Antibody-mediated immunity against tuberculosis: implications for vaccine development. *Cell Host Microbe* **2013**, *13* (3), 250–62.
60. Kozakiewicz, L.; Phuah, J.; Flynn, J.; Chan, J. The role of B cells and humoral immunity in Mycobacterium tuberculosis infection. *Adv. Exp. Med. Biol.* **2013**, *783*, 225–50.
61. Hossain, M. M.; Norazmi, M. N. Pattern recognition receptors and cytokines in Mycobacterium tuberculosis infection--the double-edged sword? *Biomed. Res. Int.* **2013**, *179174* (10), 12.
62. Rohde, K.; Yates, R. M.; Purdy, G. E.; Russell, D. G. Mycobacterium tuberculosis and the environment within the phagosome. *Immunol. Rev.* **2007**, *219*, 37–54.
63. Soldati, T.; Neyrolles, O. Mycobacteria and the intraphagosomal environment: take it with a pinch of salt(s)! *Traffic* **2012**, *13* (8), 1042–52.
64. Steinberg, B. E.; Grinstein, S. Pathogen destruction versus intracellular survival: the role of lipids as phagosomal fate determinants. *J. Clin. Invest.* **2008**, *118* (6), 2002–11.
65. Khader, S. A.; Cooper, A. M. IL-23 and IL-17 in tuberculosis. *Cytokine* **2008**, *41* (2), 79–83.
66. Marras, T. K.; Daley, C. L. Epidemiology of human pulmonary infection with nontuberculous mycobacteria. *Clin. Chest Med.* **2002**, *23* (3), 553–67.
67. Organization, W. H. *Guidelines on the management of latent tuberculosis infection*, Geneva, 2015; WHO/HTM/TB: 2015.
68. Mack, U.; Migliori, G. B.; Sester, M.; Rieder, H. L.; Ehlers, S.; Goletti, D.; Bossink, A.; Magdorf, K.; Holscher, C.; Kampmann, B.; Arend, S. M.; Detjen, A.; Bothamley, G.; Zellweger, J. P.; Milburn, H.; Diel, R.; Ravn, P.; Cobelens, F.; Cardona, P. J.; Kan, B.; Solovic, I.; Duarte, R.; Cirillo, D. M. LTBI: latent tuberculosis infection or lasting immune responses to M. tuberculosis? A TBNET consensus statement. *Eur. Respir. J.* **2009**, *33* (5), 956–73.
69. Cardona, P. J. New insights on the nature of latent tuberculosis infection and its treatment. *Inflammation Allergy: Drug Targets* **2007**, *6* (1), 27–39.

Publication Date (Web): October 13, 2015 | doi: 10.1021/bk-2015-1200.ch020

70. Garton, N. J.; Waddell, S. J.; Sherratt, A. L.; Lee, S. M.; Smith, R. J.; Senner, C.; Hinds, J.; Rajakumar, K.; Adegbola, R. A.; Besra, G. S.; Butcher, P. D.; Barer, M. R. Cytological and transcript analyses reveal fat and lazy persister-like bacilli in tuberculous sputum. *PLoS Med.* **2008**, *5* (4), 0050075.
71. Cardona, P. J. Revisiting the natural history of tuberculosis. The inclusion of constant reinfection, host tolerance, and damage-response frameworks leads to a better understanding of latent infection and its evolution towards active disease. *Arch. Immunol. Ther. Exp.* **2010**, *58* (1), 7–14.
72. Lee, S. J.; Lee, S. H.; Kim, Y. E.; Cho, Y. J.; Jeong, Y. Y.; Kim, H. C.; Lee, J. D.; Kim, J. R.; Hwang, Y. S.; Kim, H. J.; Menzies, D. Risk factors for latent tuberculosis infection in close contacts of active tuberculosis patients in South Korea: a prospective cohort study. *BMC Infect. Dis.* **2014**, *14* (566), 014–0566.
73. Rodrigues, L.; Viveiros, M.; Ainsa, J. A. Measuring efflux and permeability in mycobacteria. *Methods Mol. Biol.* **2015**, 2450–9_13.
74. Dartois, V. The path of anti-tuberculosis drugs: from blood to lesions to mycobacterial cells. *Nat. Rev. Microbiol.* **2014**, *12* (3), 159–67.
75. Blumberg, H. M.; Burman, W. J.; Chaisson, R. E.; Daley, C. L.; Etkind, S. C.; Friedman, L. N.; Fujiwara, P.; Grzemska, M.; Hopewell, P. C.; Iseman, M. D.; Jasmer, R. M.; Koppaka, V.; Menzies, R. I.; O'Brien, R. J.; Reves, R. R.; Reichman, L. B.; Simone, P. M.; Starke, J. R.; Vernon, A. A. American Thoracic Society/Centers for Disease Control and Prevention/Infectious Diseases Society of America: treatment of tuberculosis. *Am. J. Respir. Crit. Care Med.* **2003**, *167* (4), 603–62.
76. Abubakar, I.; Zignol, M.; Falzon, D.; Raviglione, M.; Ditiu, L.; Masham, S.; Adetifa, I.; Ford, N.; Cox, H.; Lawn, S. D.; Marais, B. J.; McHugh, T. D.; Mwaba, P.; Bates, M.; Lipman, M.; Zijenah, L.; Logan, S.; McNerney, R.; Zumla, A.; Sarda, K.; Nahid, P.; Hoelscher, M.; Pletschette, M.; Memish, Z. A.; Kim, P.; Hafner, R.; Cole, S.; Migliori, G. B.; Maeurer, M.; Schito, M. Drug-resistant tuberculosis: time for visionary political leadership. *Lancet Infect. Dis.* **2013**, *13* (6), 529–39.
77. Veron, L. J.; Blanc, L. J.; Suchi, M.; Raviglione, M. C. DOTS expansion: will we reach the 2005 targets? *Int. J. Tuberc. Lung Dis.* **2004**, *8* (1), 139–46.
78. Cooper, A. M.; Dalton, D. K.; Stewart, T. A.; Griffin, J. P.; Russell, D. G.; Orme, I. M. Disseminated tuberculosis in interferon gamma gene-disrupted mice. *J. Exp. Med.* **1993**, *178* (6), 2243–7.
79. Flynn, J. L.; Chan, J.; Triebold, K. J.; Dalton, D. K.; Stewart, T. A.; Bloom, B. R. An essential role for interferon-gamma in resistance to mycobacterium-tuberculosis infection. *J. Exp. Med.* **1993**, *178* (6), 2249–2254.
80. Kamijo, R.; Harada, H.; Matsuyama, T.; Bosland, M.; Gerecitano, J.; Shapiro, D.; Le, J.; Koh, S. I.; Kimura, T.; Green, S. J.; Mak, T. W.; Taniguchi, T.; Vilcek, J. Requirement for transcription factor IRF-1 in NO synthase induction in macrophages. *Science* **1994**, *263* (5153), 1612–1615.
81. Flynn, J. L.; Goldstein, M. M.; Chan, J.; Triebold, K. J.; Pfeffer, K.; Lowenstein, C. J.; Schreiber, R.; Mak, T. W.; Bloom, B. R. Tumor-

Publication Date (Web): October 13, 2015 | doi: 10.1021/bk-2015-1200.ch020

necrosis-factor-alpha is required in the protective immune-response against mycobacterium-tuberculosis in mice. *Immunity* **1995**, *2* (6), 561–572.
82. Brightbill, H. D.; Libraty, D. H.; Krutzik, S. R.; Yang, R. B.; Belisle, J. T.; Bleharski, J. R.; Maitland, M.; Norgard, M. V.; Plevy, S. E.; Smale, S. T.; Brennan, P. J.; Bloom, B. R.; Godowski, P. J.; Modlin, R. L. Host defense mechanisms triggered by microbial lipoproteins through toll-like receptors. *Science* **1999**, *285* (5428), 732–736.
83. Ding, A. H.; Nathan, C. F.; Stuehr, D. J. Release of reactive nitrogen intermediates and reactive oxygen intermediates from mouse peritoneal macrophages. Comparison of activating cytokines and evidence for independent production. *J. Immunol.* **1988**, *141* (7), 2407–12.
84. Weiss, G.; Schaible, U. E. Macrophage defense mechanisms against intracellular bacteria. *Immunol. Rev.* **2015**, *264* (1), 182–203.
85. Tomioka, H.; Saito, H. Characterization of immunosuppressive functions of murine peritoneal macrophages induced with various agents. *J. Leukocyte Biol.* **1992**, *51* (1), 24–31.
86. Chan, J.; Xing, Y.; Magliozzo, R. S.; Bloom, B. R. Killing of virulent mycobacterium-tuberculosis by reactive nitrogen intermediates produced by activated murine macrophages. *J. Exp. Med.* **1992**, *175* (4), 1111–1122.
87. Bermudez, L. E. Differential mechanisms of intracellular killing of Mycobacterium avium and Listeria monocytogenes by activated human and murine macrophages. The role of nitric oxide. *Clin. Exp. Immunol.* **1993**, *91* (2), 277–81.
88. Cooper, A. M.; Adams, L. B.; Dalton, D. K.; Appelberg, R.; Ehlers, S. IFN-gamma and NO in mycobacterial disease: new jobs for old hands. *Trends Microbiol.* **2002**, *10* (5), 221–6.
89. Khader, S. A.; Pearl, J. E.; Sakamoto, K.; Gilmartin, L.; Bell, G. K.; Jelley-Gibbs, D. M.; Ghilardi, N.; deSauvage, F.; Cooper, A. M. IL-23 compensates for the absence of IL-12p70 and is essential for the IL-17 response during tuberculosis but is dispensable for protection and antigen-specific IFN-gamma responses if IL-12p70 is available. *J. Immunol.* **2005**, *175* (2), 788–95.
90. Pearl, J. E.; Torrado, E.; Tighe, M.; Fountain, J. J.; Solache, A.; Strutt, T.; Swain, S.; Appelberg, R.; Cooper, A. M. Nitric oxide inhibits the accumulation of CD4+CD44hiTbet+CD69lo T cells in mycobacterial infection. *Eur. J. Immunol.* **2012**, *42* (12), 3267–79.
91. Zumft, W. G. Cell biology and molecular basis of denitrification. *Microbiol. Mol. Biol. Rev.* **1997**, *61* (4), 533–616.
92. Kartal, B.; Maalcke, W. J.; de Almeida, N. M.; Cirpus, I.; Gloerich, J.; Geerts, W.; Op den Camp, H. J.; Harhangi, H. R.; Janssen-Megens, E. M.; Francoijs, K. J.; Stunnenberg, H. G.; Keltjens, J. T.; Jetten, M. S.; Strous, M. Molecular mechanism of anaerobic ammonium oxidation. *Nature* **2011**, *479* (7371), 127–30.
93. Falkinham, J. O., 3rd. Environmental sources of nontuberculous mycobacteria. *Clin. Chest Med.* **2015**, *36* (1), 35–41.

Publication Date (Web): October 13, 2015 | doi: 10.1021/bk-2015-1200.ch020

94. McKenney, D. J.; Shuttleworth, K. F.; Vriesacker, J. R.; Findlay, W. I. Production and loss of nitric oxide from denitrification in anaerobic brookston clay. *Appl. Environ. Microbiol.* **1982**, *43* (3), 534–41.
95. Delwiche, C. C.; Bryan, B. A. Denitrification. *Annu. Rev. Microbiol.* **1976**, *30*, 241–62.
96. Conrad, R. Soil microorganisms as controllers of atmospheric trace gases (H2, CO, CH4, OCS, N2O, and NO). *Microbiol. Rev.* **1996**, *60* (4), 609–40.
97. Trivedi, A.; Singh, N.; Bhat, S. A.; Gupta, P.; Kumar, A. Redox biology of tuberculosis pathogenesis. *Adv. Microb. Physiol.* **2012**, *60*, 263–324.
98. Rustad, T. R.; Sherrid, A. M.; Minch, K. J.; Sherman, D. R. Hypoxia: a window into Mycobacterium tuberculosis latency. *Cell. Microbiol.* **2009**, *11* (8), 1151–9.
99. Koskenkorva-Frank, T. S.; Weiss, G.; Koppenol, W. H.; Burckhardt, S. The complex interplay of iron metabolism, reactive oxygen species, and reactive nitrogen species: insights into the potential of various iron therapies to induce oxidative and nitrosative stress. *Free Radic. Biol. Med.* **2013**, *65*, 1174–94.
100. Dranka, B. P.; Hill, B. G.; Darley-Usmar, V. M. Mitochondrial reserve capacity in endothelial cells: The impact of nitric oxide and reactive oxygen species. *Free Radic. Biol. Med.* **2010**, *48* (7), 905–14.
101. Strehl, C.; Fangradt, M.; Fearon, U.; Gaber, T.; Buttgereit, F.; Veale, D. J. Hypoxia: how does the monocyte-macrophage system respond to changes in oxygen availability? *J. Leukocyte Biol.* **2014**, *95* (2), 233–41.
102. Wiese, M.; Gerlach, R. G.; Popp, I.; Matuszak, J.; Mahapatro, M.; Castiglione, K.; Chakravortty, D.; Willam, C.; Hensel, M.; Bogdan, C.; Jantsch, J. Hypoxia-mediated impairment of the mitochondrial respiratory chain inhibits the bactericidal activity of macrophages. *Infect. Immun.* **2012**, *80* (4), 1455–66.
103. Beckman, J. S.; Koppenol, W. H. Nitric oxide, superoxide, and peroxynitrite: the good, the bad, and ugly. *Am. J. Physiol.* **1996**, *271* (5) (Pt 1), C1424–37.
104. Fitzgerald, L. E.; Abendano, N.; Juste, R. A.; Alonso-Hearn, M. Three-dimensional in vitro models of granuloma to study bacteria-host interactions, drug-susceptibility, and resuscitation of dormant mycobacteria. *Biomed. Res. Int.* **2014**, *623856* (10), 21.
105. Hunter, R. L. Pathology of post primary tuberculosis of the lung: an illustrated critical review. *Tuberculosis* **2011**, *91* (6), 497–509.
106. Reece, S. T.; Kaufmann, S. H. Floating between the poles of pathology and protection: can we pin down the granuloma in tuberculosis? *Curr. Opin. Microbiol.* **2012**, *15* (1), 63–70.
107. Sies, H. Strategies of antioxidant defense. *Eur. J. Biochem.* **1993**, *215* (2), 213–9.
108. Lundberg, J. O.; Gladwin, M. T.; Ahluwalia, A.; Benjamin, N.; Bryan, N. S.; Butler, A.; Cabrales, P.; Fago, A.; Feelisch, M.; Ford, P. C.; Freeman, B. A.; Frenneaux, M.; Friedman, J.; Kelm, M.; Kevil, C. G.; Kim-Shapiro, D. B.; Kozlov, A. V.; Lancaster, J. R., Jr.; Lefer, D. J.; McColl, K.; McCurry, K.; Patel, R. P.; Petersson, J.; Rassaf, T.; Reutov, V. P.; Richter-Addo, G. B.; Schechter, A.; Shiva, S.; Tsuchiya, K.; van Faassen, E. E.; Webb, A. J.;

Publication Date (Web): October 13, 2015 | doi: 10.1021/bk-2015-1200.ch020

Zuckerbraun, B. S.; Zweier, J. L.; Weitzberg, E. Nitrate and nitrite in biology, nutrition and therapeutics. *Nat. Chem. Biol.* **2009**, *5* (12), 865–9.
109. Dejam, A.; Hunter, C. J.; Schechter, A. N.; Gladwin, M. T. Emerging role of nitrite in human biology. *Blood Cells Mol. Dis.* **2004**, *32* (3), 423–9.
110. Ignarro, L. J. Nitric oxide. A novel signal transduction mechanism for transcellular communication. *Hypertension* **1990**, *16* (5), 477–83.
111. Nathan, C. F.; Hibbs, J. B., Jr. Role of nitric oxide synthesis in macrophage antimicrobial activity. *Curr. Opin. Immunol.* **1991**, *3* (1), 65–70.
112. Culotta, E.; Koshland, D. E., Jr. NO news is good news. *Science* **1992**, *258* (5090), 1862–5.
113. Piknova, B.; Schechter, A. N. Measurement of nitrite in blood samples using the ferricyanide-based hemoglobin oxidation assay. *Methods Mol. Biol.* **2011**, *704*, 39–56.
114. Geller, D. A.; Billiar, T. R. Molecular biology of nitric oxide synthases. *Cancer Metastasis Rev.* **1998**, *17* (1), 7–23.
115. Nussler, A. K.; Billiar, T. R. Inflammation, immunoregulation, and inducible nitric oxide synthase. *J. Leukocyte Biol.* **1993**, *54* (2), 171–8.
116. Vanhoutte, P. M. Inducible nitric oxide synthase and vascular smooth muscle. *Jpn. J. Pharmacol.* **1992**, *58* (Suppl. 2), 192P–199P.
117. Fleischmann, A.; Darsow, M.; Degtyarenko, K.; Fleischmann, W.; Boyce, S.; Axelsen, K. B.; Bairoch, A.; Schomburg, D.; Tipton, K. F.; Apweiler, R. IntEnz, the integrated relational enzyme database. *Nucleic Acids Res.* **2004**, *32*, D434–7 (Database issue).
118. Vizzard, M. A.; Erdman, S. L.; Roppolo, J. R.; Forstermann, U.; de Groat, W. C. Differential localization of neuronal nitric oxide synthase immunoreactivity and NADPH-diaphorase activity in the cat spinal cord. *Cell Tissue Res.* **1994**, *278* (2), 299–309.
119. Nakane, M.; Schmidt, H. H.; Pollock, J. S.; Forstermann, U.; Murad, F. Cloned human brain nitric oxide synthase is highly expressed in skeletal muscle. *FEBS Lett.* **1993**, *316* (2), 175–80.
120. Blackwell, J. M.; Barton, C. H.; White, J. K.; Roach, T. I.; Shaw, M. A.; Whitehead, S. H.; Mock, B. A.; Searle, S.; Williams, H.; Baker, A. M. Genetic regulation of leishmanial and mycobacterial infections: the Lsh/Ity/Bcg gene story continues. *Immunol. Lett.* **1994**, *43* (1-2), 99–107.
121. Liew, F. Y. Nitric oxide in infectious and autoimmune diseases. *Ciba Found. Symp.* **1995**, *195*, 234–9.
122. Denis, M. Human monocytes/macrophages: NO or no NO? *J. Leukocyte Biol.* **1994**, *55* (5), 682–4.
123. Pfeilschifter, J.; Eberhardt, W.; Hummel, R.; Kunz, D.; Muhl, H.; Nitsch, D.; Pluss, C.; Walker, G. Therapeutic strategies for the inhibition of inducible nitric oxide synthase--potential for a novel class of anti-inflammatory agents. *Cell Biol. Int.* **1996**, *20* (1), 51–8.
124. Ortiz, P. A.; Garvin, J. L. Trafficking and activation of eNOS in epithelial cells. *Acta Physiol. Scand.* **2003**, *179* (2), 107–14.
125. Kimura, H.; Esumi, H. Reciprocal regulation between nitric oxide and vascular endothelial growth factor in angiogenesis. *Acta Biochim. Pol.* **2003**, *50* (1), 49–59.

Publication Date (Web): October 13, 2015 | doi: 10.1021/bk-2015-1200.ch020

126. Tannenbaum, S. R.; Fett, D.; Young, V. R.; Land, P. D.; Bruce, W. R. Nitrite and nitrate are formed by endogenous synthesis in the human intestine. *Science* **1978**, *200* (4349), 1487–9.
127. Green, L. C.; Ruiz de Luzuriaga, K.; Wagner, D. A.; Rand, W.; Istfan, N.; Young, V. R.; Tannenbaum, S. R. Nitrate biosynthesis in man. *Proc. Natl. Acad. Sci. U. S. A.* **1981**, *78* (12), 7764–8.
128. Hibbs, J. B.; Taintor, R. R.; Vavrin, Z. Macrophage cytotoxicity: role for L-arginine deiminase and imino nitrogen oxidation to nitrite. *Science* **1987**, *235*, 473–476.
129. Gladwin, M. T.; Grubina, R.; Doyle, M. P. The new chemical biology of nitrite reactions with hemoglobin: R-state catalysis, oxidative denitrosylation, and nitrite reductase/anhydrase. *Acc. Chem. Res.* **2009**, *42* (1), 157–67.
130. Brennan, M. L. A tale of two controversies: defining both the role of peroxidases in nitrotyrosine formation in vivo using eosinophil peroxidase and myeloperoxidase-deficient mice, and the nature of peroxidase-generated reactive nitrogen species. *J. Biol. Chem.* **2002**, *277*, 17415–17427.
131. Kwiatkowski, A. V.; Shapleigh, J. P. Requirement of nitric oxide for induction of genes whose products are involved in nitric oxide metabolism in Rhodobacter sphaeroides 2.4.3. *J. Biol. Chem.* **1996**, *271* (40), 24382–8.
132. Koschorreck, M.; Moore, E.; Conrad, R. Oxidation of nitric oxide by a new heterotrophic Pseudomonas sp. *Arch. Microbiol.* **1996**, *166* (1), 23–31.
133. MacMicking, J. D.; North, R. J.; LaCourse, R.; Mudgett, J. S.; Shah, S. K.; Nathan, C. F. Identification of nitric oxide synthase as a protective locus against tuberculosis. *Proc. Natl. Acad. Sci. U. S. A.* **1997**, *94* (10), 5243–8.
134. Lousada, S.; Florido, M.; Appelberg, R. Virulence of Mycobacterium avium in mice does not correlate with resistance to nitric oxide. *Microb. Pathog.* **2007**, *43* (5-6), 243–8.
135. Hirst, J. Mitochondrial complex I. *Annu. Rev. Biochem.* **2013**, *82*, 551–75.
136. Winterbourn, C. C.; Kettle, A. J. Redox reactions and microbial killing in the neutrophil phagosome. *Antioxid. Redox Signaling* **2013**, *18* (6), 642–60.
137. Minakami, R.; Sumimotoa, H. Phagocytosis-coupled activation of the superoxide-producing phagocyte oxidase, a member of the NADPH oxidase (nox) family. *Int. J. Hematol.* **2006**, *84* (3), 193–8.
138. Bae, Y. S.; Oh, H.; Rhee, S. G.; Yoo, Y. D. Regulation of reactive oxygen species generation in cell signaling. *Mol. Cells* **2011**, *32* (6), 491–509.
139. Nickel, A.; Kohlhaas, M.; Maack, C. Mitochondrial reactive oxygen species production and elimination. *J. Mol. Cell. Cardiol.* **2014**, *73*, 26–33.
140. Kehrer, J. P. The Haber-Weiss reaction and mechanisms of toxicity. *Toxicology* **2000**, *149* (1), 43–50.
141. Dean, R. T.; Fu, S.; Stocker, R.; Davies, M. J. Biochemistry and pathology of radical-mediated protein oxidation. *Biochem. J.* **1997**, *324* (Pt 1), 1–18.
142. Helbock, H. J.; Beckman, K. B.; Ames, B. N. 8-Hydroxydeoxyguanosine and 8-hydroxyguanine as biomarkers of oxidative DNA damage. *Methods Enzymol.* **1999**, *300*, 156–66.
143. Kwiecien, S.; Jasnos, K.; Magierowski, M.; Sliwowski, Z.; Pajdo, R.; Brzozowski, B.; Mach, T.; Wojcik, D.; Brzozowski, T. Lipid peroxidation,

Publication Date (Web): October 13, 2015 | doi: 10.1021/bk-2015-1200.ch020

reactive oxygen species and antioxidative factors in the pathogenesis of gastric mucosal lesions and mechanism of protection against oxidative stress - induced gastric injury. *J. Physiol. Pharmacol.* **2014**, *65* (5), 613–22.
144. Auchere, F.; Rusnak, F. What is the ultimate fate of superoxide anion in vivo? *J. Biol. Inorg. Chem.* **2002**, *7* (6), 664–7.
145. Bustamante, J.; Picard, C.; Boisson-Dupuis, S.; Abel, L.; Casanova, J. L. Genetic lessons learned from X-linked Mendelian susceptibility to mycobacterial diseases. *Ann. N. Y. Acad. Sci.* **2011**, *1246*, 92–101.
146. Fazal, N. The role of reactive oxygen species (ROS) in the effector mechanisms of human antimycobacterial immunity. *Biochem. Mol. Biol. Int.* **1997**, *43* (2), 399–408.
147. Yang, C. T.; Cambier, C. J.; Davis, J. M.; Hall, C. J.; Crosier, P. S.; Ramakrishnan, L. Neutrophils exert protection in the early tuberculous granuloma by oxidative killing of mycobacteria phagocytosed from infected macrophages. *Cell Host Microbe* **2012**, *12* (3), 301–12.
148. Cooper, A. M.; Segal, B. H.; Frank, A. A.; Holland, S. M.; Orme, I. M. Transient loss of resistance to pulmonary tuberculosis in p47(phox-/-) mice. *Infect. Immun.* **2000**, *68* (3), 1231–4.
149. Kleniewska, P.; Piechota, A.; Skibska, B.; Goraca, A. The NADPH oxidase family and its inhibitors. *Arch. Immunol. Ther. Exp.* **2012**, *60* (4), 277–94.
150. Henderson, L. M. NADPH oxidase subunit gp91phox: a proton pathway. *Protoplasma* **2001**, *217* (1-3), 37–42.
151. Mizrahi, A.; Berdichevsky, Y.; Ugolev, Y.; Molshanski-Mor, S.; Nakash, Y.; Dahan, I.; Alloul, N.; Gorzalczany, Y.; Sarfstein, R.; Hirshberg, M.; Pick, E. Assembly of the phagocyte NADPH oxidase complex: chimeric constructs derived from the cytosolic components as tools for exploring structure-function relationships. *J. Leukocyte Biol.* **2006**, *79* (5), 881–95.
152. Quinn, M. T.; Gauss, K. A. Structure and regulation of the neutrophil respiratory burst oxidase: comparison with nonphagocyte oxidases. *J. Leukocyte Biol.* **2004**, *76* (4), 760–81.
153. Panday, A.; Sahoo, M. K.; Osorio, D.; Batra, S. NADPH oxidases: an overview from structure to innate immunity-associated pathologies. *Cell. Mol. Immunol.* **2015**, *12* (1), 5–23.
154. Spencer, N. Y.; Engelhardt, J. F. The basic biology of redoxosomes in cytokine-mediated signal transduction and implications for disease-specific therapies. *Biochemistry* **2014**, *53* (10), 1551–64.
155. Meitzler, J. L.; Antony, S.; Wu, Y.; Juhasz, A.; Liu, H.; Jiang, G.; Lu, J.; Roy, K.; Doroshow, J. H. NADPH oxidases: a perspective on reactive oxygen species production in tumor biology. *Antioxid. Redox Signaling* **2014**, *20* (17), 2873–89.
156. Weyemi, U.; Redon, C. E.; Parekh, P. R.; Dupuy, C.; Bonner, W. M. NADPH Oxidases NOXs and DUOXs as putative targets for cancer therapy. *Anticancer Agents Med. Chem.* **2013**, *13* (3), 502–14.
157. Ushio-Fukai, M.; Urao, N. Novel role of NADPH oxidase in angiogenesis and stem/progenitor cell function. *Antioxid. Redox Signaling* **2009**, *11* (10), 2517–33.

Publication Date (Web): October 13, 2015 | doi: 10.1021/bk-2015-1200.ch020

158. Karlsson, A.; Dahlgren, C. Assembly and activation of the neutrophil NADPH oxidase in granule membranes. *Antioxid. Redox Signaling* **2002**, *4* (1), 49–60.
159. Cachat, J.; Deffert, C.; Hugues, S.; Krause, K. H. Phagocyte NADPH oxidase and specific immunity. *Clin. Sci.* **2015**, *128* (10), 635–48.
160. Liu, P. T.; Stenger, S.; Li, H. Y.; Wenzel, L.; Tan, B. H.; Krutzik, S. R.; Ochoa, M. T.; Schauber, J.; Wu, K.; Meinken, C.; Kamen, D. L.; Wagner, M.; Bals, R.; Steinmeyer, A.; Zugel, U.; Gallo, R. L.; Eisenberg, D.; Hewison, M.; Hollis, B. W.; Adams, J. S.; Bloom, B. R.; Modlin, R. L. Toll-like receptor triggering of a vitamin D-mediated human antimicrobial response. *Science* **2006**, *311* (5768), 1770–1773.
161. Dalton, D. K.; Pittsmeek, S.; Keshav, S.; Figari, I. S.; Bradley, A.; Stewart, T. A. Multiple defects of immune cell-function in mice with disrupted interferon-gamma genes. *Science* **1993**, *259* (5102), 1739–1742.
162. Xie, Q. W.; Whisnant, R.; Nathan, C. Promoter of the mouse gene encoding calcium-independent nitric oxide synthase confers inducibility by interferon gamma and bacterial lipopolysaccharide. *J. Exp. Med.* **1993**, *177* (6), 1779–84.
163. Nathan, C.; Shiloh, M. U. Reactive oxygen and nitrogen intermediates in the relationship between mammalian hosts and microbial pathogens. *Proc. Natl. Acad. Sci. U. S. A.* **2000**, *97* (16), 8841–8848.
164. Schnappinger, D.; Ehrt, S.; Voskuil, M. I.; Liu, Y.; Mangan, J. A.; Monahan, I. M.; Dolganov, G.; Efron, B.; Butcher, P. D.; Nathan, C.; Schoolnik, G. K. Transcriptional adaptation of Mycobacterium tuberculosis within macrophages: Insights into the phagosomal environment. *J. Exp. Med.* **2003**, *198* (5), 693–704.
165. Darrah, P. A.; Patel, D. T.; De Luca, P. M.; Lindsay, R. W. B.; Davey, D. F.; Flynn, B. J.; Hoff, S. T.; Andersen, P.; Reed, S. G.; Morris, S. L.; Roederer, M.; Seder, R. A. Multifunctional T(H)1 cells define a correlate of vaccine-mediated protection against Leishmania major. *Nat. Med.* **2007**, *13* (7), 843–850.
166. Zhang, Y.; Heym, B.; Allen, B.; Young, D.; Cole, S. The catalase peroxidase gene and isoniazid resistance of *Mycobacterium tuberculosis*. *Nature* **1992**, *358* (6387), 591–593.
167. Timmins, G. S.; Master, S.; Rusnak, F.; Deretic, V. Nitric oxide generated from isoniazid activation by KatG: source of nitric oxide and activity against Mycobacterium tuberculosis. *Antimicrob. Agents Chemother.* **2004**, *48* (8), 3006–9.
168. McCord, J. M.; Keele, B. B. J.; Fridovich, I. An enzyme based theory of obligate anaerobiosis the physiological function of super oxide dismutase. *Proc. Natl. Acad. Sci. U. S. A.* **1971**, *68* (5), 1024–1027.
169. McCord, J. M.; Fridovich, I. Superoxide Dismutase: an enzymic function for erythrocuprein (hemocuprein). *J. Biol. Chem.* **1969**, *244* (22), 6049–6055.
170. Chan, J.; Fujiwara, T.; Brennan, P.; McNeil, M.; Turco, S. J.; Sibille, J. C.; Snapper, M.; Aisen, P.; Bloom, B. R. Microbial glycolipids: possible virulence factors that scavenge oxygen radicals. *Proc. Natl. Acad. Sci. U. S. A.* **1989**, *86* (7), 2453–7.

In Oxidative Stress: Diagnostics, Prevention, and Therapy Volume 2; Hepel, et al.;
ACS Symposium Series; American Chemical Society: Washington, DC, 2015.

Publication Date (Web): October 13, 2015 | doi: 10.1021/bk-2015-1200.ch020

171. De la Harpe, J.; Nathan, C. F. A semi-automated micro-assay for H2O2 release by human blood monocytes and mouse peritoneal macrophages. *J. Immunol. Methods* **1985**, *78* (2), 323–36.
172. Nathan, C. F.; Silverstein, S. C.; Brukner, L. H.; Cohn, Z. A. Extracellular cytolysis by activated macrophages and granulocytes. II. Hydrogen-peroxide as a mediator of cytotoxicity. *J. Exp. Med.* **1979**, *149* (1), 100–113.
173. Nathan, C. F.; Brukner, L. H.; Silverstein, S. C.; Cohn, Z. A. Extracellular cytolysis by activated macrophages and granulocytes. I. Pharmacologic triggering of effector cells and the release of hydrogen peroxide. *J. Exp. Med.* **1979**, *149* (1), 84–99.
174. Bryk, R.; Griffin, P.; Nathan, C. Peroxynitrite reductase activity of bacterial peroxiredoxins. *Nature* **2000**, *407* (6801), 211–215.
175. Pabst, M. J.; Johnston, R. B. Increased production of superoxide anion by macrophages exposed invitro to muramyl dipeptide or lipopolysaccharide. *J. Exp. Med.* **1980**, *151* (1), 101–114.
176. Johnston, R. B., Jr.; Godzik, C. A.; Cohn, Z. A. Increased superoxide anion production by immunologically activated and chemically elicited macrophages. *J. Exp. Med.* **1978**, *148* (1), 115–27.
177. Orme, I. M.; Andersen, P.; Boom, W. H. T-cell response to Mycobacterium tuberculosis. *J. Infect. Dis.* **1993**, *167* (6), 1481–1497.
178. Denis, M. Tumor-necrosis-factor and granulocyte macrophage-colony stimulating factor stimulate human macrophages to restrict growth of virulent mycobacterium-avium and to kill avirulent mycobacterium-avium - killing effector mechanism depends on the generation of reactive nitrogen intermediates. *J. Leukocyte Biol.* **1991**, *49* (4), 380–387.
179. Bermudez, L. E. M.; Young, L. S. Tumor necrosis factor, alone or in combination with IL-2, but not IFN-gamma, is associated with macrophage killing of mycobacterium-avium complex. *J. Immunol.* **1988**, *140* (9), 3006–3013.
180. Garbe, T. R.; Hibler, N. S.; Deretic, V. Response of Mycobacterium tuberculosis to reactive oxygen and nitrogen intermediates. *Mol. Med.* **1996**, *2* (1), 134–142.
181. Green, L. C.; Wagner, D. A.; Glogowski, J.; Skipper, P. L.; Wishnok, J. S.; Tannenbaum, S. R. Analysis of nitrate, nitrite, and [15N]nitrate in biological fluids. *Anal. Biochem.* **1982**, *126* (1), 131–8.
182. Vazquez-Torres, A.; Xu, Y. S.; Jones-Carson, J.; Holden, D. W.; Lucia, S. M.; Dinauer, M. C.; Mastroeni, P.; Fang, F. C. Salmonella pathogenicity island 2-dependent evasion of the phagocyte NADPH oxidase. *Science* **2000**, *287* (5458), 1655–1658.
183. Briggs, R. T.; Drath, D. B.; Karnovsky, M. L.; Karnovsky, M. J. Localization of NADH oxidase on the surface of human polymorphonuclear leukocytes by a new cytochemical method. *J. Cell Biol.* **1975**, *67* (3), 566–86.
184. Li, Y.; Zhu, H.; Kuppusamy, P.; Roubaud, V.; Zweier, J. L.; Trush, M. A. Validation of lucigenin (bis-N-methylacridinium) as a chemilumigenic probe for detecting superoxide anion radical production by enzymatic and cellular systems. *J. Biol. Chem.* **1998**, *273* (4), 2015–23.

Publication Date (Web): October 13, 2015 | doi: 10.1021/bk-2015-1200.ch020

185. Denis, M. Interferon-gamma-treated murine macrophages inhibit growth of tubercle-bacilli via the generation of reactive nitrogen intermediates. *Cell. Immunol.* **1991**, *132* (1), 150–157.
186. Shi, L. B.; Jung, Y. J.; Tyagi, S.; Gennaro, M. L.; North, R. J. Expression of Th1-mediated immunity in mouse lungs induces a Mycobacterium tuberculosis transcription pattern characteristic of nonreplicating persistence. *Proc. Natl. Acad. Sci. U. S. A.* **2003**, *100* (1), 241–246.
187. Garbe, T. R.; Hibler, N. S.; Deretic, V. Response to reactive nitrogen intermediates in Mycobacterium tuberculosis: induction of the 16-kilodalton alpha-crystallin homolog by exposure to nitric oxide donors. *Infect. Immun.* **1999**, *67* (1), 460–5.
188. Ng, V. H.; Cox, J. S.; Sousa, A. O.; MacMicking, J. D.; McKinney, J. D. Role of KatG catalase-peroxidase in mycobacterial pathogenesis: countering the phagocyte oxidative burst. *Mol. Microbiol.* **2004**, *52* (5), 1291–1302.
189. Piddington, D. L.; Fang, F. C.; Laessig, T.; Cooper, A. M.; Orme, I. M.; Buchmeier, N. A. Cu,Zn superoxide dismutase of Mycobacterium tuberculosis contributes to survival in activated macrophages that are generating an oxidative burst. *Infect. Immun.* **2001**, *69* (8), 4980–4987.
190. Absolom, D. R. Basic methods for the study of phagocytosis. *Methods Enzymol.* **1986**, *132*, 95–180.
191. Stuehr, D. J.; Marletta, M. A. Mammalian nitrate biosynthesis: mouse macrophages produce nitrite and nitrate in response to Escherichia coli lipopolysaccharide. *Proc. Natl. Acad. Sci. U. S. A.* **1985**, *82* (22), 7738–42.
192. Hurdle, J. G.; O'Neill, A. J.; Chopra, I.; Lee, R. E. Targeting bacterial membrane function: an underexploited mechanism for treating persistent infections. *Nat. Rev. Microbiol.* **2011**, *9* (1), 62–75.
193. Hawkins, C. L.; Davies, M. J. Detection and characterisation of radicals in biological materials using EPR methodology. *Biochim. Biophys. Acta* **2014**, *2*, 708–21.
194. Green, L. C.; Ruiz de Luzuriaga, K.; Wagner, D. A.; Rand, W.; Istfan, N.; Young, V. R.; Tannenbaum, S. R. Nitrate biosynthesis in man. *Proc. Natl. Acad. Sci. U. S. A.* **1981**, *78* (12), 7764–8.
195. Tiscornia, A.; Cairoli, E.; Marquez, M.; Denicola, A.; Pritsch, O.; Cayota, A. Use of diaminofluoresceins to detect and measure nitric oxide in low level generating human immune cells. *J. Immunol. Methods* **2009**, *342* (1-2), 49–57.
196. Kojima, H.; Nakatsubo, N.; Kikuchi, K.; Kawahara, S.; Kirino, Y.; Nagoshi, H.; Hirata, Y.; Nagano, T. Detection and imaging of nitric oxide with novel fluorescent indicators: diaminofluoresceins. *Anal. Chem.* **1998**, *70* (13), 2446–53.
197. Roychowdhury, S.; Luthe, A.; Keilhoff, G.; Wolf, G.; Horn, T. F. Oxidative stress in glial cultures: detection by DAF-2 fluorescence used as a tool to measure peroxynitrite rather than nitric oxide. *Glia* **2002**, *38* (2), 103–14.
198. Kojima, H.; Urano, Y.; Kikuchi, K.; Higuchi, T.; Hirata, Y.; Nagano, T. Fluorescent Indicators for Imaging Nitric Oxide Production. *Angew. Chem., Int. Ed.* **1999**, *38* (21), 3209–3212.

Publication Date (Web): October 13, 2015 | doi: 10.1021/bk-2015-1200.ch020

199. Yoshida, K.; Kasama, K.; Kitabatake, M.; Okuda, M.; Imai, M. Metabolic fate of nitric oxide. *Int. Arch. Occup. Environ. Health* **1980**, *46* (1), 71–7.
200. Wennmalm, A.; Benthin, G.; Petersson, A. S. Dependence of the metabolism of nitric oxide (NO) in healthy human whole blood on the oxygenation of its red cell haemoglobin. *Br. J. Pharmacol.* **1992**, *106* (3), 507–8.
201. Murphy, M. E.; Noack, E. Nitric oxide assay using hemoglobin method. *Methods Enzymol.* **1994**, *233*, 240–50.
202. Gow, A. J.; Luchsinger, B. P.; Pawloski, J. R.; Singel, D. J.; Stamler, J. S. The oxyhemoglobin reaction of nitric oxide. *Proc. Natl. Acad. Sci. U. S. A.* **1999**, *96* (16), 9027–32.
203. Joshi, M. S.; Ferguson, T. B., Jr.; Han, T. H.; Hyduke, D. R.; Liao, J. C.; Rassaf, T.; Bryan, N.; Feelisch, M.; Lancaster, J. R., Jr. Nitric oxide is consumed, rather than conserved, by reaction with oxyhemoglobin under physiological conditions. *Proc. Natl. Acad. Sci. U. S. A.* **2002**, *99* (16), 10341–6.
204. Boughton-Smith, N. K.; Evans, S. M.; Laszlo, F.; Whittle, B. J.; Moncada, S. The induction of nitric oxide synthase and intestinal vascular permeability by endotoxin in the rat. *Br. J. Pharmacol.* **1993**, *110* (3), 1189–95.
205. Knowles, R. G.; Merrett, M.; Salter, M.; Moncada, S. Differential induction of brain, lung and liver nitric oxide synthase by endotoxin in the rat. *Biochem. J.* **1990**, *270* (3), 833–6.
206. Yoshida, K.; Kasama, K.; Kitabatake, M.; Imai, M. Biotransformation of nitric oxide, nitrite and nitrate. *Int. Arch. Occup. Environ. Health* **1983**, *52* (2), 103–15.
207. Griess, P. Bemerkungen zu der Abhandlung der HH. Weselsky und Benedikt „Ueber einige Azoverbindungen". *Ber. Dtsch. Chem. Ges.* **1879**, *12* (1), 426–428.
208. Lundberg, J. O.; Weitzberg, E.; Gladwin, M. T. The nitrate-nitrite-nitric oxide pathway in physiology and therapeutics. *Nat. Rev. Drug Discovery* **2008**, *7* (2), 156–67.
209. Southan, G. J.; Szabo, C. Selective pharmacological inhibition of distinct nitric oxide synthase isoforms. *Biochem. Pharmacol.* **1996**, *51* (4), 383–94.
210. Chan, J.; Tanaka, K.; Carroll, D.; Flynn, J.; Bloom, B. R. Effects of nitric oxide synthase inhibitors on murine infection with Mycobacterium tuberculosis. *Infect. Immun.* **1995**, *63* (2), 736–40.
211. Roy, J. B.; Wilkerson, R. G. Fallibility of Griess (nitrite) test. *Urology* **1984**, *23* (3), 270–1.
212. Garcia, J. G.; Ma, S. F. Polymerase chain reaction: a landmark in the history of gene technology. *Crit. Care Med.* **2005**, *33* (Suppl. 12), S429–32.
213. MacMicking, J. D.; Taylor, G. A.; McKinney, J. D. Immune control of tuberculosis by IFN-gamma-inducible LRG-47. *Science* **2003**, *302* (5645), 654–9.
214. Beesley, J. E. Histochemical methods for detecting nitric oxide synthase. *Histochem. J.* **1995**, *27* (10), 757–69.
215. Nauseef, W. M. Detection of superoxide anion and hydrogen peroxide production by cellular NADPH oxidases. *Biochim. Biophys. Acta* **2014**, *2*, 757–67.

Publication Date (Web): October 13, 2015 | doi: 10.1021/bk-2015-1200.ch020

216. Piccaro, G.; Pietraforte, D.; Giannoni, F.; Mustazzolu, A.; Fattorini, L. Rifampin induces hydroxyl radical formation in Mycobacterium tuberculosis. *Antimicrob. Agents Chemother.* **2014**, *58* (12), 7527–33.
217. Dikalov, S.; Griendling, K. K.; Harrison, D. G. Measurement of reactive oxygen species in cardiovascular studies. *Hypertension* **2007**, *49* (4), 717–27.
218. Vladimirov, Y. A.; Proskurnina, E. V. Free radicals and cell chemiluminescence. *Biochemistry* **2009**, *74* (13), 1545–66.
219. Kalyanaraman, B.; Darley-Usmar, V.; Davies, K. J.; Dennery, P. A.; Forman, H. J.; Grisham, M. B.; Mann, G. E.; Moore, K.; Roberts, L. J., 2nd; Ischiropoulos, H. Measuring reactive oxygen and nitrogen species with fluorescent probes: challenges and limitations. *Free Radic. Biol. Med.* **2012**, *52* (1), 1–6.
220. Zielonka, J.; Kalyanaraman, B. Hydroethidine- and MitoSOX-derived red fluorescence is not a reliable indicator of intracellular superoxide formation: another inconvenient truth. *Free Radic. Biol. Med.* **2010**, *48* (8), 983–1001.
221. Maghzal, G. J.; Krause, K. H.; Stocker, R.; Jaquet, V. Detection of reactive oxygen species derived from the family of NOX NADPH oxidases. *Free Radic. Biol. Med.* **2012**, *53* (10), 1903–18.
222. Fridovich, I. Superoxide dismutases. *Adv. Enzymol. Relat. Areas Mol. Biol.* **1974**, *41* (0), 35–97.
223. Saltzman, H. A.; Fridovich, I. Editorial: Oxygen toxicity. Introduction to a protective enzyme: superoxide dismutase. *Circulation* **1973**, *48* (5), 921–3.
224. Root, R. K.; Metcalf, J.; Oshino, N.; Chance, B. H2O2 release from human granulocytes during phagocytosis. I. Documentation, quantitation, and some regulating factors. *J. Clin. Invest.* **1975**, *55* (5), 945–55.
225. Root, R. K.; Metcalf, J. A. H2O2 release from human granulocytes during phagocytosis. Relationship to superoxide anion formation and cellular catabolism of H2O2: studies with normal and cytochalasin B-treated cells. *J. Clin. Invest.* **1977**, *60* (6), 1266–79.
226. Sherman, D. R.; Mdluli, K.; Hickey, M. J.; Barry, C. E., 3rd; Stover, C. K. AhpC, oxidative stress and drug resistance in Mycobacterium tuberculosis. *Biofactors* **1999**, *10* (2-3), 211–7.
227. Green, J.; Rolfe, M. D.; Smith, L. J. Transcriptional regulation of bacterial virulence gene expression by molecular oxygen and nitric oxide. *Virulence* **2014**, *5* (8), DOI: 10.4161/viru.27794.
228. Ganesana, M.; Erlichman, J. S.; Andreescu, S. Real-time monitoring of superoxide accumulation and antioxidant activity in a brain slice model using an electrochemical cytochrome c biosensor. *Free Radic. Biol. Med.* **2012**, *53* (12), 2240–9.

Publication Date (Web): October 13, 2015 | doi: 10.1021/bk-2015-1200.ch020

Subject Index

In Oxidative Stress: Diagnostics, Prevention, and Therapy Volume 2; Hepel, et al.;
ACS Symposium Series; American Chemical Society: Washington, DC, 2015.

C

D

In Oxidative Stress: Diagnostics, Prevention, and Therapy Volume 2; Hepel, et al.;
ACS Symposium Series; American Chemical Society: Washington, DC, 2015.

Publication Date (Web): October 13, 2015 | doi: 10.1021/bk-2015-1200.ix002

E

L

In Oxidative Stress: Diagnostics, Prevention, and Therapy Volume 2; Hepel, et al.;
ACS Symposium Series; American Chemical Society: Washington, DC, 2015.

Publication Date (Web): October 13, 2015 | doi: 10.1021/bk-2015-1200.ix002

M

N

In Oxidative Stress: Diagnostics, Prevention, and Therapy Volume 2; Hepel, et al.;
ACS Symposium Series; American Chemical Society: Washington, DC, 2015.

Publication Date (Web): October 13, 2015 | doi: 10.1021/bk-2015-1200.ix002

In Oxidative Stress: Diagnostics, Prevention, and Therapy Volume 2; Hepel, et al.; ACS Symposium Series; American Chemical Society: Washington, DC, 2015.

Publication Date (Web): October 13, 2015 | doi: 10.1021/bk-2015-1200.ix002

O

P

In Oxidative Stress: Diagnostics, Prevention, and Therapy Volume 2; Hepel, et al.;
ACS Symposium Series; American Chemical Society: Washington, DC, 2015.

R

In Oxidative Stress: Diagnostics, Prevention, and Therapy Volume 2; Hepel, et al.;
ACS Symposium Series; American Chemical Society: Washington, DC, 2015.

Publication Date (Web): October 13, 2015 | doi: 10.1021/bk-2015-1200.ix002

T

V

Publication Date (Web): October 13, 2015 | doi: 10.1021/bk-2015-1200.ix002

In Oxidative Stress: Diagnostics, Prevention, and Therapy Volume 2; Hepel, et al.;
ACS Symposium Series; American Chemical Society: Washington, DC, 2015.